VOL. 697 NOS. 1 + 2 21 APRIL 1995
COMPLETE IN ONE ISSUE

20th International Symposium on Chromatography Bournemouth, 19–24 June 1994

JOURNAL OF CHROMATOGRAPHY A

INCLUDING ELECTROPHORESIS AND OTHER SEPARATION METHODS

ELSEVIER

JOURNAL OF CHROMATOGRAPHY A

INCLUDING ELECTROPHORESIS AND OTHER SEPARATION METHODS

Scope. The *Journal of Chromatography A* publishes papers on all aspects of **chromatography, electrophoresis** and related methods. Contributions consist mainly of research papers dealing with chromatographic theory, instrumental developments and their applications. In the *Symposium volumes*, which are under separate editorship, proceedings of symposia on chromatography, electrophoresis and related methods are published. *Journal of Chromatography B: Biomedical Applications* —This journal, which is under separate editorship, deals with the following aspects: developments in and applications of chromatographic and electrophoretic techniques related to clinical diagnosis or alterations during medical treatment; screening and profiling of body fluids or tissues related to the analysis of active substances and to metabolic disorders; drug level monitoring and pharmacokinetic studies; clinical toxicology; forensic medicine; veterinary medicine; occupational medicine; results from basic medical research with direct consequences in clinical practice.

Submission of Papers. The preferred medium of submission is on disk with accompanying manuscript (see *Electronic manuscripts* in the Instructions to Authors, which can be obtained from the publisher, Elsevier Science B.V., P.O. Box 330, 1000 AH Amsterdam, Netherlands). Manuscripts (in English; *four* copies are required) should be submitted to: Editorial Office of *Journal of Chromatography A*, P.O. Box 681, 1000 AR Amsterdam, Netherlands, Telefax (+31-20) 485 2304, or to: The Editor of *Journal of Chromatography B: Biomedical Applications*, P.O. Box 681, 1000 AR Amsterdam, Netherlands. Review articles are invited or proposed in writing to the Editors who welcome suggestions for subjects. An outline of the proposed review should first be forwarded to the Editors for preliminary discussion prior to preparation. Submission of an article is understood to imply that the article is original and unpublished and is not being considered for publication elsewhere. For copyright regulations, see below.

Publication information. *Journal of Chromatography A* (ISSN 0021-9673): for 1995 Vols. 683–714 are scheduled for publication. *Journal of Chromatography B: Biomedical Applications* (ISSN 0378-4347): for 1995 Vols. 663–674 are scheduled for publication. Subscription prices for *Journal of Chromatography A*, *Journal of Chromatography B: Biomedical Applications* or a combined subscription are available upon request from the publisher. Subscriptions are accepted on a prepaid basis only and are entered on a calendar year basis. Issues are sent by surface mail except to the following countries where air delivery via SAL is ensured: Argentina, Australia, Brazil, Canada, China, Hong Kong, India, Israel, Japan, Malaysia, Mexico, New Zealand, Pakistan, Singapore, South Africa, South Korea, Taiwan, Thailand, USA. For all other countries airmail rates are available upon request. Claims for missing issues must be made within six months of our publication (mailing) date. Please address all your requests regarding orders and subscription queries to: Elsevier Science B.V., Journal Department, P.O. Box 211, 1000 AE Amsterdam, Netherlands. Tel.: (+31-20) 485 3642; Fax: (+31-20) 485 3598. Customers in the USA and Canada wishing information on this and other Elsevier journals, please contact Journal Information Center, Elsevier Science Inc., 655 Avenue of the Americas, New York, NY 10010, USA, Tel. (+1-212) 633 3750, Telefax (+1-212) 633 3764.

Abstracts/Contents Lists published in Analytical Abstracts, Biochemical Abstracts, Biological Abstracts, Chemical Abstracts, Chemical Titles, Chromatography Abstracts, Current Awareness in Biological Sciences (CABS), Current Contents/Life Sciences, Current Contents/Physical, Chemical & Earth Sciences, Deep-Sea Research/Part B: Oceanographic Literature Review, Excerpta Medica, Index Medicus, Mass Spectrometry Bulletin, PASCAL-CNRS, Referativnyi Zhurnal, Research Alert and Science Citation Index.

US Mailing Notice. *Journal of Chromatography A* (ISSN 0021-9673) is published weekly (total 52 issues) by Elsevier Science B.V., (Sara Burgerhartstraat 25, P.O. Box 211, 1000 AE Amsterdam, Netherlands). Annual subscription price in the USA US$ 5389.00 (US$ price valid in North, Central and South America only) including air speed delivery. Second class postage paid at Jamaica, NY 11431. **USA POSTMASTERS**: Send address changes to *Journal of Chromatography A*, Publications Expediting, Inc., 200 Meacham Avenue, Elmont, NY 11003. Airfreight and mailing in the USA by Publications Expediting.

See inside back cover for Publication Schedule, Information for Authors and information on Advertisements.

0021-9673/95/$09.50

Printed in the Netherlands

For Contents see p. VII.

JOURNAL OF CHROMATOGRAPHY A

VOL. 697 (1995)

JOURNAL OF CHROMATOGRAPHY A

INCLUDING ELECTROPHORESIS AND OTHER SEPARATION METHODS

ELSEVIER

Amsterdam – Lausanne – New York – Oxford – Shannon – Tokyo

0021-9673/95/$09.50

SYMPOSIUM VOLUME

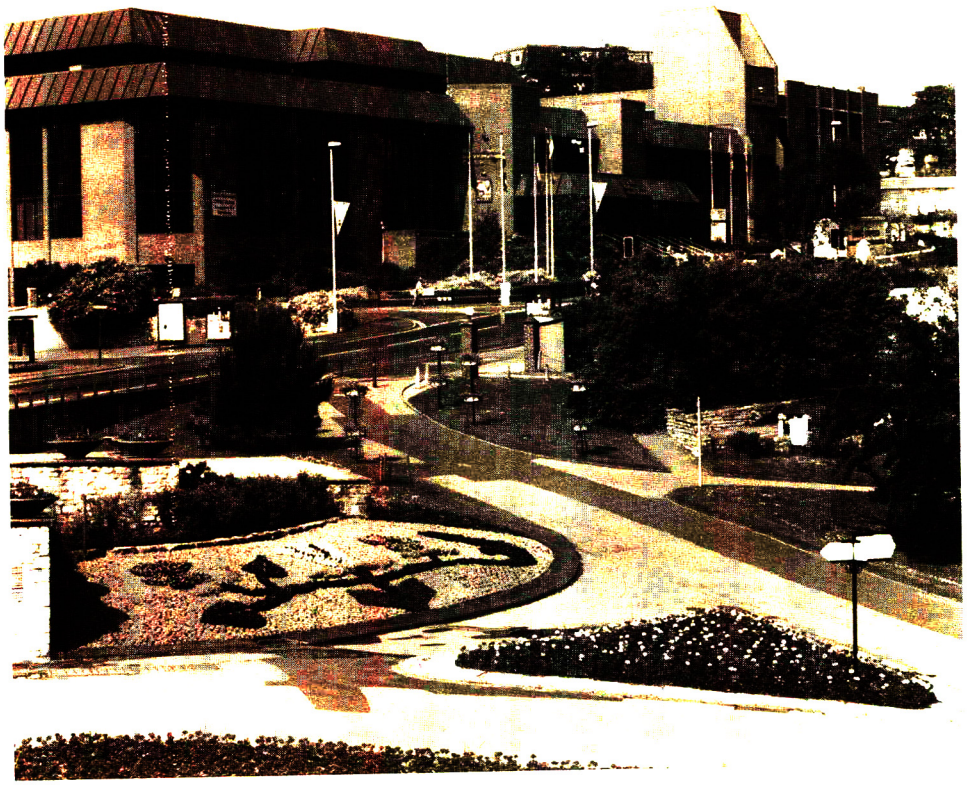

20TH INTERNATIONAL SYMPOSIUM ON CHROMATOGRAPHY

Bournemouth (UK), 19–24 June 1994

Guest Editors

M.B. EVANS
(Hatfield, UK)

A.F. FELL
(Bradford, UK)

VOL. 697, NOS. 1 + 2 JOURNAL OF CHROMATOGRAPHY A 21 APRIL 1995

CONTENTS

(Abstracts/Contents Lists published in Analytical Abstracts, Biochemical Abstracts, Biological Abstracts, Chemical Abstracts, Chemical Titles, Chromatography Abstracts, Current Awareness in Biological Sciences (CABS), Current Contents/Life Sciences, Current Contents/Physical, Chemical & Earth Sciences, Deep-Sea Research/Part B: Oceanographic Literature Review, Excerpta Medica, Index Medicus, Mass Spectrometry Bulletin, PASCAL-CNRS, Referativnyi Zhurnal, Research Alert and Science Citation Index)

20TH INTERNATIONAL SYMPOSIUM ON CHROMATOGRAPHY, BOURNEMOUTH, 19–24 JUNE 1994

LIQUID CHROMATOGRAPHY

Theoretical and general

Sample preparation

GAS CHROMATOGRAPHY

MISCELLANEOUS SEPARATION METHODS

ELSEVIER

Journal of Chromatography A, 697 (1995) 1–2

JOURNAL OF CHROMATOGRAPHY A

Foreword

The *20th International Symposium on Chromatography* (20th ISC) took place at the International Centre in Bournemouth (BIC) from 19 to 24 June 1994. The meeting organised by the Chromatographic Society, in association with the GDCh of Germany and GAMS of France, was attended by almost 500 delegates representing 37 countries world-wide. The scientific programme consisted of 44 oral and 278 poster papers covering the full spectrum of separation science. Forty-three companies took part in a scientific exhibition of equipment and accessories organised by Reed International. Councillor Dr. John Millward, the Mayor of Bournemouth, welcomed delegates and highlighted the important role of chromatography in the life and physical sciences. Also, during the Opening Ceremony, the Society's Martin and Jubilee Medals were presented to Professor Pat Sandra and Dr. Ian Wilson, respectively.

The high quality of the scientific contributions of the formal programme and informal discussions in the relaxing atmosphere of the BIC overlooking the sea, resulted in a rewarding experience for delegates. In particular, the integration of the exhibition and poster sessions through the provision of a central Poster Court proved to be a most successful innovation. Likewise, the presentation of the symposium abstracts in a unified form as the Chromatography Year Book contributed to a quality meeting that maintained the high scientific standards of previous symposia in the ISC series. Support was received from a number of companies that enabled the Organising Committee to assist students and young scientists, particularly from East European countries, to participate in the symposium. We gratefully acknowledge such generosity at a time of economic recession.

Delegates and their partners enjoyed a varied social programme, the highlight of which was the symposium banquet held in the Pavilion Ballroom at which the Mayor and Mayoress were the guests of honour. During the evening a Rose Bowl was presented to Mrs. Jennifer Challis, the retiring Executive Secretary, in recognition of her many years of dedicated service to the Society.

As the Chairmen of the 20th ISC we wish to express our appreciation to the members of the Organising Committee: Dr. Chris Bevan, Dr. Derek Stevenson, Mr. Peter Wall and Dr. Stephen Westwood, whose hard work and intellectual input assured the logistic and scientific success of the meeting. Special votes of thanks are due to Dr. Roly Jones whose indefatigable efforts were essential in coordinating the business aspects of the enterprise, to Anita Howard who effectively managed the exhibition and to Ian Dougall and Nick Clark of Event Media who produced the Chromatography Year Book. Also, we are pleased to acknowledge the substantial efforts of the members of the Society's Secretariat and the staff of the BIC in ensuring a smooth running event.

We are greatly indebted to the members of the Scientific Committee and, in particular, our colleagues from France and Germany: Dr. Henri Colin, Professor Michel Martin, Professor Karlheinz Ballschmiter and Dr. Günter Kraus, for

SSDI 0021-9673(94)01145-1

their efforts in devising an excellent scientific programme and for their encouragement and helpful advice. Also, we wish to thank all the delegates for their active participation which helped to make the 20th ISC a successful and enjoyable symposium.

This volume contains a selection of the papers presented at the meeting, which are representative of the high scientific standard of the symposium. We are indebted to Dr. Erich Heftmann and to the editorial staff of the *Journal of Chromatography A* for their efforts in the rapid publication of this special issue.

Hatfield, UK Michael B. Evans
Symposium Chairman

Bradford, UK Anthony F. Fell
Chairman of Scientific Committee

ELSEVIER

Journal of Chromatography A, 697 (1995) 3–16

JOURNAL OF CHROMATOGRAPHY A

Criteria for developing rugged high-performance liquid chromatographic methods

Pascale F. Vanbel[a,*], Bernard L. Tilquin[a], Peter J. Schoenmakers[b]

[a]*Pharmaceutical School, Université Catholique de Louvain, UCL 7230, Av. E. Mounier 72, B-1200 Brussels, Belgium*

[b]*Analytical Department, Royal Dutch/Shell Laboratory (Shell Research), Badhuisweg 3, NL-1031 CM Amsterdam, Netherlands*

Abstract

An approach is described that allows the ultimate ruggedness of chromatographic methods to be rigorously included as an objective from the outset of systematic method development. Ruggedness criteria are defined as derivatives of other (typically resolution-based) criteria. Numerical estimates of ruggedness criteria can readily be obtained during selectivity optimization. It is necessary to consider ruggedness simultaneously with other objectives of the separation using multi-criteria decision making (MCDM) procedures. Three MCDM methods were considered in this work, viz., Pareto-optimality (PO) plot, Derringer's desirability function and the multiple-threshold approach (MTA). The characteristics of these three methods are discussed and the feasibility of developing rugged separations by systematically varying the pH and solvent composition is demonstrated.

1. Introduction

Owing to the widespread use of HPLC in routine analysis, it is very important that good HPLC methods are developed and that these are thoroughly validated. Many systematic methods exist for method development and optimization. The ruggedness or robustness of a method is typically evaluated independently at a much later stage as part of the method validation process. Full or fractional factorial experimental designs are used extensively for this purpose [1–5]. Developing rugged HPLC separations is of great practical importance. By considering ruggedness at an early stage of method development, both the amount of work required and the chance of failure during the method validation stage can be greatly reduced.

In this paper, we describe an original approach for evaluating the ruggedness of a predicted optimum (and of all experimental points in the parameter space) without the need to perform additional experiments. The defined ruggedness criteria (R_u) are based on numerical estimates of the derivatives of a specific criterion (e.g., minimum effective resolution) with respect to the optimized parameters (pH and solvent composition).

However, it is difficult to envisage ruggedness as a goal in itself in method development procedures. Obviously, highly rugged methods that are inadequate in terms of other criteria (e.g., resolution, analysis time) are unacceptable. Therefore, quality of separation (resolution) and robustness criteria represent a good example of a set of goals to be considered in a multi-criteria decision making (MCDM) process. Recently, several MCDM methods were reviewed [6,7].

* Corresponding author.

0021-9673/95/$09.50
SSDI 0021-9673(94)00933-3

Simultaneous optimization of both types of criteria (resolution and robustness) is achieved here by using three MCDM strategies. The first is based on the pareto-optimality concept, which was introduced into chromatography by Smilde et al. [8]. An experiment is called pareto-optimal if there is no other experiment that has a better result on one criterion without having a worse result on another. The second procedure uses Derringer's desirability function, which has been applied to the optimization of several chromatographic performance goals by Bourguignon and Massart [9]. It is based on the transformation of the measured properties to a dimensionless desirability scale for each criterion, so that values of several properties, obtained from different scales of measurement, may be combined. The desirability scale ranges between $d = 0$ (undesirable level of quality) and $d = 1$ (target value). The geometric mean of the desirability values for all criteria is then used to compare different experiments. The third method defines a threshold value for one criterion (generally resolution) and optimizes the other criterion for all situations in which the threshold for the first criterion is reached. A multiple-threshold approach (MTA) can also be used.

Although an MCDM process involving the pareto-optimality concept and a robustness coefficient has already been described in the field of pharmaceutical formulations [10–14], this concept is new in chromatography. By way of example, we shall apply our method for optimizing RP-HPLC separations by varying simultaneously the pH and solvent composition.

2. Theory

2.1. Resolution criteria

Optimization procedures require adequate response criteria to assess the quality of each chromatogram obtained during the process.

When pH is one of the optimization parameters, variations in efficiency and peak symmetry occur during the optimization procedure. The effective resolution defined by Schoenmakers et al. [15] is then the logical and recommended choice for characterizing the quality of the separation between two peaks [16]. It takes into account the individual widths of the two peaks, the asymmetry factors and peak heights. Considering the separation of a pair of peaks, two values of the resolution exist for each peak. The first, R_n, describes the extent to which a peak i is separated from the next peak (j), and the second value, R_p, reflects the extent to which peak i is separated from the previous peak. Generally, the lowest of these two values is kept.

R_n and R_p are calculated by using the following equations:

$$R_n = \frac{(t_j - t_i)(1 + A_{s,i})(1 + A_{s,j})\sqrt{N_i N_j}}{4A_{s,i}t_i(1 + A_{s,j})\sqrt{N_j} + 4t_j(1 + A_{s,i})\sqrt{N_i}\sqrt{1 + \frac{1}{2}\ln\left(\frac{h_j}{h_i}\right)}} \quad (1)$$

$$R_p = \frac{(t_j - t_i)(1 + A_{s,i})(1 + A_{s,j})\sqrt{N_i N_j}}{4A_{s,i}t_i(1 + A_{s,j})\sqrt{N_j}\sqrt{1 + \frac{1}{2}\ln\left(\frac{h_i}{h_j}\right)} + 4t_j(1 + A_{s,i})\sqrt{N_i}} \quad (2)$$

where t is the retention time, A_S is the asymmetry factor, N is the number of theoretical plates and h is the peak height.

However, using effective resolution implies that not only retention data, but also data on efficiency (or peak areas), peak heights and peak symmetry need to be recorded. Schoenmakers et al. [16] recently demonstrated the feasibility of simultaneously optimizing separations with regard to selectivity, efficiency and peak shape. The optimization procedure requires the modelling of retention time, peak height, peak area and peak asymmetry. From these chromatographic characteristics, effective resolution can be calculated at each point in the parameter space.

2.2. Ruggedness criteria

Considering the optimization of two independent parameters such as pH and solvent composition (volume fraction of methanol = φ_{MeOH}), robustness can be evaluated by using the numeri-

cal estimates of the derivatives of a selected criterion (basically minimum effective resolution, $R_{l,\min}$) with respect to the optimized parameters. Robustness criteria [$R_u(\varphi)$ and $R_u(\mathrm{pH})$] are then described by the equations

$$R_u(\varphi) = \Delta_\varphi \cdot \frac{dR_{l,\min}}{d\varphi} \quad (3)$$

$$R_u(\mathrm{pH}) = \Delta_{\mathrm{pH}} \cdot \frac{dR_{l,\min}}{d\mathrm{pH}} \quad (4)$$

where $dR_{l,\min}/d\varphi$ and $dR_{l,\min}/d\mathrm{pH}$ are the variation of the minimum effective resolution with solvent composition and with pH, respectively, Δ_φ and Δ_{pH} are the permitted variations of solvent composition (e.g., 0.01) and pH (e.g., 0.05), respectively, which are defined by the user according to the instrumental errors. Notice that $dR_{l,\min}/d\varphi$ and $dR_{l,\min}/d\mathrm{pH}$ provide information on the impact of small variations in the optimization parameters on the separation. These values can be used to determine limits between which these parameters must be maintained in order to obtain reproducible results. R_u (pH) [or $R_u(\varphi)$] gives an indication of how much the minimum effective resolution will vary if we are able to control pH (or φ) within Δ_{pH} (or Δ_φ) units.

By adding Eq. 3 to Eq. 4, we obtain a global robustness criterion. The following equation is then obtained:

$$R_u = \Delta_\varphi \cdot \frac{dR_{l,\min}}{d\varphi} + \Delta_{\mathrm{pH}} \cdot \frac{dR_{l,\min}}{d\mathrm{pH}} \quad (5)$$

R_u has to be minimized during the optimization process. However, greater values of the robustness criterion can be accepted when the minimum resolution increases. Similarly, when the minimum resolution value is only marginally acceptable, the requirements for the ruggedness of the method will be much stricter. Another ruggedness criterion (R_u^*), which is related to the actual resolution value, is then expressed by

$$R_u^* = \frac{R_u}{R_{l,\min}} \quad (6)$$

Inversing Eq. 6 leads to

$$[R_u^*]^{-1} = \frac{R_{l,\min}}{R_u} \quad (7)$$

$[R_u^*]^{-1}$ has to be maximized. Using this last criterion avoids the occurrence of mathematical problems when the minimum resolution is zero. However, in a computer program, a provision is needed to deal with the case in which R_u is zero (when the minimum resolution is essentially constant).

Similarly, Eqs. 3 and 4 can also be modified separately to give

$$[R_u^*(\varphi)]^{-1} = \frac{R_{l,\min}}{R_u(\varphi)} \quad (8)$$

$$[R_u^*(\mathrm{pH})]^{-1} = \frac{R_{l,\min}}{R_u(\mathrm{pH})} \quad (9)$$

Considering the definition of $R_u(\varphi)$ and $R_u(\mathrm{pH})$, $R_u^*(\varphi)$ and $R_u^*(\mathrm{pH})$ are indications of the relative error at a given value of the minimum resolution.

3. Experimental

3.1. Instrumentation

The HPLC system consisted of two Waters Model 6000A pumps (Millipore–Waters, Milford, MA, USA), which were controlled by a Waters system controller. The system was equipped with an injection valve (Model 7125; Rheodyne, Cotati, CA, USA) fitted with a 20-μl injection loop and a variable-wavelength UV–visible detector from Waters (Model 481). The apparatus was connected to an IBM-compatible computer and chromatographic data (retention times, peak heights, peak areas and asymmetry factors) were collected by chromatographic integration software (PC Integration Pack; Kontron Instruments, Milan, Italy).

3.2. Chromatographic conditions

A reversed-phase system was chosen for this study. We used a 5-μm C_{18} LiChrospher column (125 × 4 mm I.D.) and a 5-μm C_{18} LiChrospher

precolumn (4 × 4 mm I.D.) from Merck (Darmstadt, Germany) at ambient temperature (the laboratory temperature is maintained at 22 ± 1°C by the ventilation system). The hold-up time (t_0) was estimated to be 1.28 min, by using replicate injections of 10^{-4} *M* KI. The flow-rate was 1.0 ml/min and UV detection was set at 254 nm.

Mixtures of methanol (MeOH) and citrate–phosphate buffers constituted the different mobile phases. Methanol was of HPLC grade (UCB, Leuven, Belgium). The volume fraction of MeOH was varied between 0.30 and 0.40. Water was obtained from a Milli-Q purification system (Millipore, Milford, MA, USA). Citrate–phosphate buffers (pH ranging from 2.76 to 6.83) were prepared by mass at a total ionic strength of 0.05 *M* according to Ref. [17]. Constant ionic strength was obtained by the addition of the appropriate amount of potassium chloride. Potassium chloride, citric acid and disodium hydrogenphosphate (all of the highest purity) were purchased from Merck. Reported pH values are those of the aqueous solution, before mixing with methanol. The mixture injected into the HPLC system consisted of four acids: salicylic acid (0.2 mg/ml), benzoic acid (0.1 mg/ml), 3,5-dinitrobenzoic acid (0.02 mg/ml) and *m*-nitrobenzoic acid (0.02 mg/ml). Salicylic acid was purchased from UCB. The other solutes were supplied by Merck. All solutes were of the highest available purity. Stock standard solutions of the investigated compounds were prepared in methanol and then diluted as required in water–methanol (90:10). Peak recognition was performed by the injection of each individual solute.

3.3. Software

Different in-house software programs were developed or improved to model the different chromatographic parameters (retention time, peak height, peak area and asymmetry factor) and to generate response surfaces. All the programs were written in Pascal (Turbo Pascal 7.0; Borland International, Scotts Valley, CA, USA) and implemented on an IBM-compatible computer. Data generated by Pascal programs were imported directly in Excel software (version 4.0) in a Windows environment (Microsoft).

3.4. Optimization procedure

A 4 × 3 experimental design (three levels of methanol volume fraction and four levels of pH) was used to realize the simultaneous optimization of pH and solvent composition (Fig. 1). Eq. 10 was used to model the capacity factor (k) as a function of pH and φ (volume fraction of organic modifier):

$$k = \frac{\left[k^0_{HA}\, e^{S_{HA}\varphi + T_{HA}\varphi^2} \cdot 10^{-pH} + k^0_{A^-} K^0_a\, e^{(S_{A^-}+Q_1)\varphi + (T_{A^-}+Q_2)\varphi^2} \right]}{10^{-pH} + K^0_a\, e^{(Q_1\varphi + Q_2\varphi^2)}} \quad (10)$$

where k^0_{HA} and $k^0_{A^-}$ are extrapolated capacity factors of the protonated and the dissociated forms, respectively, of the solute in pure water, K^0_a is the extrapolated acid-dissociation constant in pure water, S_{HA} and T_{HA} are parameters describing the variation of retention with φ for protonated species, S_{A^-} and T_{A^-} are corresponding parameters for dissociated species and Q_1 and Q_2 are coefficients describing the variation of the acid-dissociation constant with φ.

The use of a 4 × 3 experimental design and the use of Eq. 10 were recommended by Lopes Marques and Schoenmakers [18] in a previous study on the modelling of retention as a function

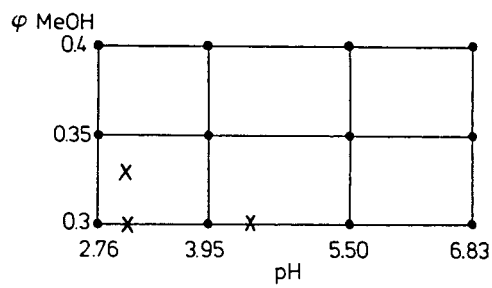

Fig. 1. The 3 × 4 experimental design used for the separation of a mixture of four acids; × refers to additional experiments.

of pH and solvent composition. Eq. 10 is also suitable to model peak height and peak area [16]. For the asymmetry factor (A_S), the following quadratic equation was found to give a reasonable description (see also Ref. [16]):

$$A_S = A_{S,HA}\, e^{S_{HA}\varphi + T_{HA}\varphi^2} + A_{S,A^-}\, e^{(S_{A^-}\varphi + T_{A^-}\varphi^2)}\mathrm{pH} + K_a^0\, e^{(Q_1\varphi + Q_2\varphi^2)}(\mathrm{pH})^2 \quad (11)$$

4. Results and discussion

The values for pH and solvent composition corresponding to the experimental design in Fig. 1 are listed in Table 1. Experiments 1–12 are the initial experiments defined by the experimental design; 13–15 are three additional experiments that were added to the data set to yield an improved description of the response surface. Table 2 gives retention times, peak heights, peak areas and asymmetry factors for the four solutes at the fifteen experimental locations. The coefficients describing these data for retention (capacity factors), peak height and peak area in terms of Eq. 10 and asymmetry factors in terms of Eq. 11 are listed in Table 3. Table 4 provides some idea on the accuracy of the model descriptions. Two criteria are listed, the sum of squares (SSQ) of the absolute deviations between calculated (by the model) and experimental data and the average relative deviation between calculated and experimental data (ARD). Generally, Eq. 10 provides accurate descriptions of experimental data. ARD values are between 2.5% and 5.3% for capacity factors (average absolute deviation ≤ 0.1 capacity factor units), between 2.7% and 9.5% for peak heights and between 0.4% and 2.7% for peak areas. Asymmetry data are described reasonably well by Eq. 11 (average absolute deviation ≤ 0.1), except for salicylic acid at $\varphi_{MeOH} = 0.30$, where larger deviations were observed (average absolute deviation 0.18; maximum absolute deviation 0.34). Note that large SSQ values for the height and area models are largely caused by the magnitude of the parameters (see Table 2). Conversely, large values for ARD occur for parameters with low values (k, A_S).

Table 1
pH and volume fraction of methanol (φ_{MeOH}) corresponding to the fifteen experimental locations

No.[a]	pH	φ_{MeOH}
1	2.76	0.30
2	2.76	0.35
3	2.76	0.40
4	3.95	0.30
5	3.95	0.35
6	3.95	0.40
7	5.50	0.30
8	5.50	0.35
9	5.50	0.40
10	6.83	0.30
11	6.83	0.35
12	6.83	0.40
13	3.07	0.30
14	3.07	0.33
15	4.39	0.30

[a] Nos. 1–12 are the initial experiments defined by the experimental design; Nos. 13–15 are three additional experiments.

Fig. 2 shows the response surface of the minimum effective resolution obtained during the simultaneous optimization of pH and mobile phase composition for a mixture of four acidic solutes. This response surface is complex owing to the occurrence of peak cross-overs during the optimization process. Consequently, this practical example is appropriate to study the use and usefulness of robustness criteria.

Figs. 3 and 4 give the response surfaces of the individual robustness criteria [$R_u(\varphi)$ and $R_u(\mathrm{pH})$] calculated by Eqs. 3 and 4, respectively. The response surface of the global robustness criterion (R_u) expressed by Eq. 5 is shown in Fig. 5.

In this study, the permitted variations of solvent composition and pH were set at 0.01 and 0.05, respectively. For each point in the parameter space, minimum effective resolution and ruggedness factors are provided by the optimization software. These values constitute the response surfaces.

MCDM procedures combining minimum effective resolution and robustness criteria were ap-

Table 2
Experimental data for 3,5-dinitrobenzoic acid, benzoic acid, salicylic acid and *m*-nitrobenzoic acid at fifteen experimental locations indicated in Table 1

Acid	No.	Retention time (min)	Area (mV s)	Height (mV)	Asymmetry
3,5-Dinitrobenzoic	1	12.49	1697	53.1	1.53
	2	8.76	1685	71.8	1.41
	3	6.59	1759	88.5	1.55
	4	5.32	1966	97.7	1.25
	5	4.17	1956	103.6	1.19
	6	3.36	1946	139.9	1.46
	7	4.43	1882	122.7	1.28
	8	3.55	1899	149.4	1.43
	9	2.93	1889	164.1	1.59
	10	4.36	1858	125.7	1.39
	11	3.41	1866	145.8	1.53
	12	2.83	1859	164.1	1.60
	13	8.59	1875	75.9	1.37
	14	7.02	1939	97.0	1.45
	15	4.57	1950	119.0	1.35
Benzoic	1	14.55	1219	36.2	1.30
	2	9.94	1186	48.9	1.29
	3	6.89	1144	61.1	1.42
	4	10.47	1095	36.7	1.07
	5	7.67	1102	38.9	1.04
	6	5.68	1091	59.0	1.16
	7	2.47	1038	96.6	1.61
	8	2.15	1045	102.1	1.73
	9	1.92	1022	107.3	1.92
	10	2.00	980	93.6	1.84
	11	1.78	938	93.1	1.96
	12	1.67	991	101.5	2.08
	13	13.74	1109	32.5	1.29
	14	10.87	1153	46.5	1.30
	15	6.69	1060	50.8	0.97
Salicylic	1	13.89	1558	48.3	1.59
	2	9.57	1500	60.9	1.45
	3	6.84	1520	79.2	1.43
	4	4.08	920	60.4	1.22
	5	3.23	908	61.1	1.22
	6	2.64	907	72.5	1.34
	7	2.62	879	70.7	1.83
	8	2.24	857	75.8	1.89
	9	1.94	858	82.8	1.98
	10	2.56	868	67.2	1.80
	11	2.14	863	77.2	1.95
	12	1.88	854	85.9	2.06
	13	9.24	1266	51.7	1.13
	14	7.54	1217	61.0	1.09
	15	3.02	896	69.8	1.81

Table 2 (*continued*)

Acid	No.	Retention time (min)	Area (mV s)	Height (mV)	Asymmetry
m-Nitrobenzoic	1	13.89	1161	34.2	1.57
	2	9.53	1301	52.5	1.52
	3	6.68	1204	61.6	1.59
	4	5.45	1132	55.7	1.41
	5	4.18	1147	61.0	1.33
	6	3.31	1143	81.5	1.49
	7	2.67	1110	98.9	1.53
	8	2.28	1129	111.6	1.72
	9	2.00	1157	121.5	1.86
	10	2.57	1118	97.9	1.65
	11	2.17	1111	105.5	1.82
	12	1.93	1125	120.3	1.92
	13	11.22	1132	36.6	1.48
	14	8.87	1192	50.7	1.53
	15	3.57	1163	81.2	1.54

plied to a selection of 115 grid points, each representing a specific combination of pH and φ_{MeOH}. The number of grid points selected can easily be increased, but some clarity will be lost in the presentation. Fig. 6 shows the pareto-optimality plot for the minimum effective resolution, $R_{l,min}$, and the overall ruggedness criterion, R_u (Eq. 5). Resolution has to be maximized and R_u has to be minimized. Pareto-optimal (PO) points are given in Table 5. The MCDM plot (Fig. 6) visualizes directly the pay-off between the two criteria. Information with respect to both criteria is available, so we can decide which of the points is preferable. No preselection of weighting factors or threshold values for the criteria is needed. The PO points 11, 12 and 13 (from Table 5) represent favourable choices. Indeed, good resolution is achieved at acceptable values of the ruggedness criterion. Each PO point in Table 5 represents a potential optimum. The chromatographer may opt for a good separation with $R_{l,min} = 1.74$ and $R_u = 0.21$ (corresponding to conditions of pH 4.31 and $\varphi_{MeOH} = 0.30$; see Table 5) or one may prefer a worse separation with a greater robustness (i.e., lower R_u value), such as $R_{l,min} = 1.4$ and $R_u = 0.09$ (at pH 4.27 and $\varphi_{MeOH} = 0.34$). In MCDM procedures using PO plots, this kind of decision can be made after inspection of the figure and predicted chromatograms at the various PO points. Fig. 7 represents a chromatogram obtained at one of the PO points (i.e., at pH 4.31 and $\varphi_{MeOH} = 0.30$).

The combination of the pareto-optimality method with a robustness coefficient appears to be a powerful tool for selecting the "best" conditions in pH optimization studies. As mentioned by Bourguignon and Massart [9], the pareto-optimality method loses much of its simplicity when more than two criteria are optimized.

Although total ruggedness factors, in which the total variation of the minimum resolution is taken into account, appear to be more relevant than partial ruggedness coefficients, it can be interesting to consider separate ruggedness criteria [R_u(pH) and $R_u(\varphi)$]. Indeed, by calculating the global ruggedness criterion R_u, a high value of R_u(pH) can be compensated by a low value of $R_u(\varphi)$ (or vice versa). Derringer's desirability function can easily be applied to the optimization of more than two criteria. The application of this method requires the definition of the minimum [$Y^{(-)}$] and maximum [$Y^{(+)}$] acceptable values of the response criteria. $Y^{(-)}$ and $Y^{(+)}$ have to be defined according to the objectives of the chromatographer. By way of example, to transform the minimum effective

Table 3
Coefficients describing retention (capacity factor, k), peak height (h), and peak area (A) in terms of Eq. 10 and asymmetry factors (A_S) in terms of Eq. 11

Acid	Parameter	k^0_{HA} [a]	$k^0_{A^-}$	K^0_a	S_{HA}	S_{A^-}	Q_1	T_{HA}	T_{A^-}	Q_2
3,5-Dinitro-benzoic	k	$5.50 \cdot 10^7$	12.07	$5.44 \cdot 10^{-2}$	−59.66	−4.00	13.98	49.45	−4.21	−57.86
	h	$7.84 \cdot 10^{-4}$	11.98	$3.75 \cdot 10^{19}$	63.60	11.71	$-3.16 \cdot 10^2$	−87.67	−12.92	$4.58 \cdot 10^2$
	A	17.26	$1.33 \cdot 10^3$	$3.40 \cdot 10^{13}$	25.45	2.24	$-2.13 \cdot 10^2$	−35.80	−3.34	$3.00 \cdot 10^2$
	A_S	$4.79 \cdot 10^5$	$-3.69 \cdot 10^{10}$	$6.48 \cdot 10^5$	−68.89	$-1.38 \cdot 10^2$	−88.88	94.26	$1.81 \cdot 10^2$	$1.14 \cdot 10^2$
Benzoic	k	$2.53 \cdot 10^2$	49.19	$2.01 \cdot 10^{-2}$	−12.19	−21.92	−30.01	5.32	21.44	35.92
	h	2.10	$2.61 \cdot 10^2$	$2.90 \cdot 10^{-4}$	11.75	−6.20	−17.64	−8.83	9.93	27.74
	A	$5.98 \cdot 10^2$	$2.68 \cdot 10^3$	$1.15 \cdot 10^{-1}$	4.26	−5.61	−31.91	−6.58	7.88	32.67
	A_S	$2.36 \cdot 10^7$	$-2.41 \cdot 10^{12}$	$2.45 \cdot 10^7$	−89.84	$-1.60 \cdot 10^2$	$-1.08 \cdot 10^2$	$1.22 \cdot 10^2$	$2.15 \cdot 10^2$	$1.45 \cdot 10^2$
Salicylic	k	$5.00 \cdot 10^2$	1.50	$2.73 \cdot 10^{-5}$	−6.13	4.54	38.04	−11.80	−18.58	−72.69
	h	3.65	51.01	$5.80 \cdot 10^7$	11.46	$2.72 \cdot 10^{-1}$	$-1.25 \cdot 10^2$	−9.69	2.63	$1.24 \cdot 10^2$
	A	$2.38 \cdot 10^5$	$1.30 \cdot 10^3$	$1.18 \cdot 10^{-1}$	−24.51	−2.18	−18.76	35.82	2.83	28.89
	A_S	$6.96 \cdot 10^2$	$-6.70 \cdot 10^{-3}$	1.42	−30.62	39.34	−15.86	37.21	−88.49	13.85
m-Nitro-benzoic	k	75.44	1.28	$8.21 \cdot 10^{-7}$	−3.74	4.72	42.01	−7.68	−17.64	−67.56
	h	$8.50 \cdot 10^{-4}$	60.72	$3.38 \cdot 10^{11}$	56.60	1.44	$-2.08 \cdot 10^2$	−71.83	78.05	$2.94 \cdot 10^2$
	A	1.30	$2.18 \cdot 10^3$	$2.14 \cdot 10^{11}$	39.56	−3.91	$-1.74 \cdot 10^2$	−56.04	5.70	$2.29 \cdot 10^2$
	A_S	$2.37 \cdot 10^4$	$-2.05 \cdot 10^{10}$	$8.77 \cdot 10^4$	−51.82	$-1.35 \cdot 10^2$	−80.05	69.89	$1.76 \cdot 10^2$	$1.05 \cdot 10^2$

[a] Or equivalent parameters, i.e., h^0_{HA} and $h^0_{A^-}$, A^0_{HA} and $A^0_{A^-}$, or $A^0_{S,HA}$ and A^0_{S,A^-}.

Table 4
Accuracy of model descriptions

Parameter	3,5-Dinitrobenzoic acid		Benzoic acid		Salicylic acid		*m*-Nitrobenzoic acid	
	SSQ	*ARD* (%)	*SSQ*	*ARD* (%)	*SSQ*	*ARD* (%)	*SSQ*	*ARD* (%)
k	0.13	2.5	0.23	5.3	0.14	4.4	0.35	4.0
h	660.9	5.5	612.4	9.5	79.9	2.7	143.3	3.1
A	49752.9	2.7	12192.9	2.1	363.2	0.4	2780.0	1.0
A_S	0.049	3.4	0.32	9.1	0.61	12.4	0.083	4.0

SSQ = sum of squares of the absolute deviations between calculated and experimental data; *ARD* = average relative deviation between calculated and experimental data.

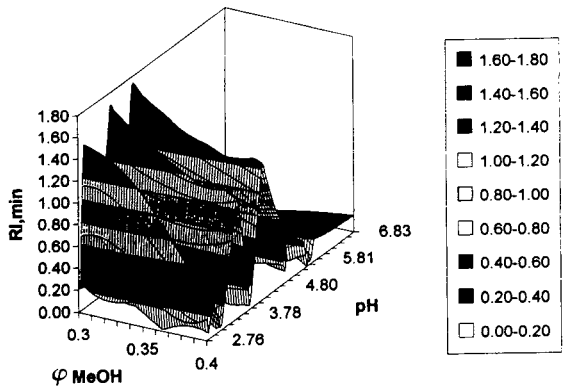

Fig. 2. Response surface of the minimum effective resolution obtained during the optimization of the separation of four solutes.

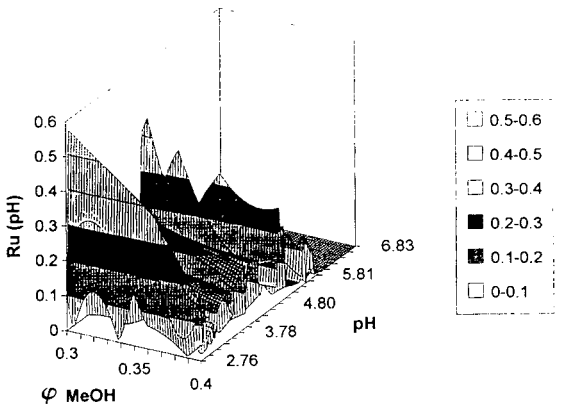

Fig. 4. Response surface of the individual robustness criterion R_u(pH) obtained during the optimization of the separation of four solutes.

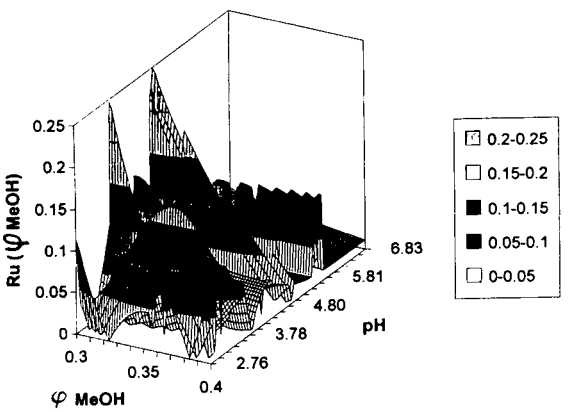

Fig. 3. Response surface of the individual robustness criterion $R_u(\varphi)$ obtained during the optimization of the separation of four solutes.

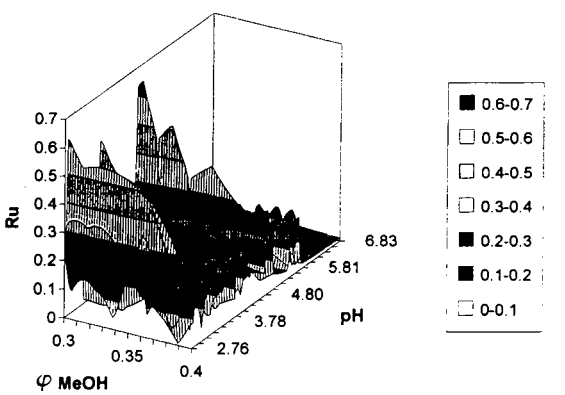

Fig. 5. Response surface of the global robustness criterion R_u obtained during the optimization of the separation of four solutes.

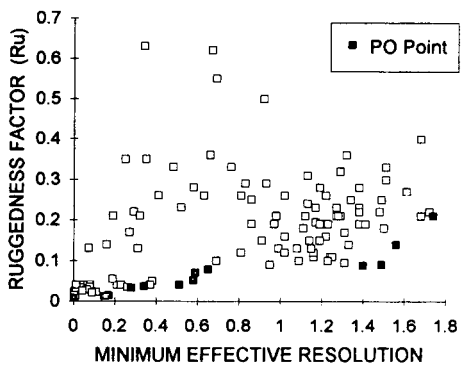

Fig. 6. Pareto-optimality plot for the minimum effective resolution and the ruggedness criterion R_u.

resolution into desirability values, $Y^{(-)}$ is set to 0.5 and $Y^{(+)}$ to 1.5. For the global ruggedness factor (R_u), we define a target value of 0.2 [for individual ruggedness factors $R_u(\varphi)$ and R_u(pH), this value is set to 0.1]. Values $\geq$0.4 [or 0.2 for R_u(pH) and $R_u(\varphi)$] have a desirability equal to 0. Reasonable target values of 0.1 for $R_u(\varphi)$ and R_u(pH) were defined by assuming that the variation of the minimum effective resolution with solvent composition and with pH should not exceed 0.1 for a variation of φ of 0.01 and for a variation of pH of 0.05 (Δ_φ and Δ_{pH} are set at 0.01 and 0.05, respectively). R_u, $R_u(\varphi)$ and R_u(pH) have to be minimized during the process. However, as mentioned in the theoretical

Table 5
Pareto-optimal points and corresponding pH and φ_{MeOH} values

No.	φ_{MeOH}	pH	$R_{l,min}$	R_u
1	0.30	3.30	0.003	0.010
2	0.40	6.83	0.15	0.012
3	0.40	6.14	0.17	0.014
4	0.36	5.20	0.28	0.033
5	0.40	5.20	0.34	0.037
6	0.30	4.88	0.51	0.040
7	0.36	4.75	0.58	0.052
8	0.34	4.75	0.59	0.070
9	0.40	4.75	0.65	0.078
10	0.34	4.27	1.40	0.089
11	0.32	3.65	1.49	0.090
12	0.32	4.27	1.56	0.14
13	0.30	4.31	1.74	0.21

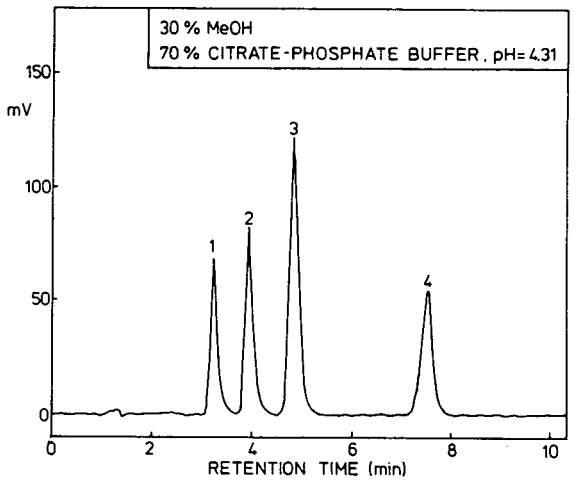

Fig. 7. Chromatogram selected as a possible optimum (φ_{MeOH} = 0.30; pH = 4.31). Peaks: 1 = salicylic acid; 2 = *m*-nitrobenzoic acid; 3 = 3,5-dinitrobenzoic acid; 4 = benzoic acid.

section, higher values of the robustness criterion can be accepted when the minimum resolution increases. Conversely, when the minimum resolution value is (very) low, the requirements for the ruggedness factor are stricter. To this end, we developed a total ruggedness criterion corrected according to the resolution value, $[R_u^*]^{-1}$, calculated from Eq. 7. The corresponding individual ruggedness criteria are $[R_u^*(\varphi)]^{-1}$ and $[R_u^*(\text{pH})]^{-1}$ expressed by Eqs. 8 and 9. These three criteria have to be maximized.

By analogy with the values defined for R_u, the target value is set to 5 for $[R_u^*]^{-1}$. The minimum acceptable value for this criterion is 2.5. Minimum and maximum acceptable values for the corresponding individual ruggedness criteria are set to 5 and 10, respectively.

One-sided transformations of the response criteria into desirability values (d) are shown in Fig. 8. Four different global desirability values (D_1–D_4) are calculated by using the geometric mean of the desirability values on all criteria. These four global desirabilities correspond to the combination of the minimum effective resolution ($R_{l,min}$) with four different expressions of the robustness factor. D_1 combines the minimum effective resolution ($R_{l,min}$) with $[R_u^*]^{-1}$. D_2

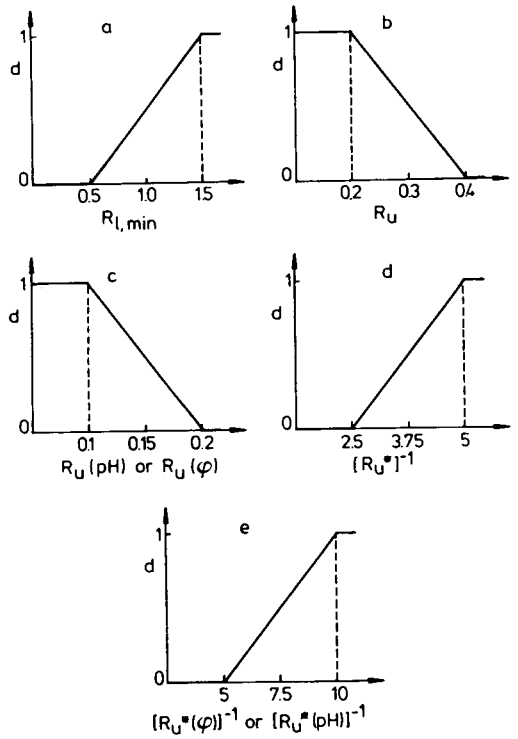

Fig. 8. One-sided transformations of response criteria into desirability values, d. (a) Minimum effective resolution; (b–e) robustness criteria.

takes into account the desirability of $R_{l,min}$ and separate desirabilities for the individual robustness criteria $[R_u^*(pH)]^{-1}$ and $[R_u^*(\varphi)]^{-1}$. D_3 is the combination of $R_{l,min}$ and the robustness factor R_u. Like D_2, D_4 considers three criteria: $R_{l,min}$ and the individual robustness criteria $R_u(pH)$ and $R_u(\varphi)$ separately. Table 6 gives the experimental conditions yielding the best values of the overall desirabilities D_1, D_2, D_3 or D_4, from the 115 selected sets of data. Some of them lead to an overall desirability of 1. This ideal value is obtained when the target value is reached for each criterion. The optimization can then be considered to be completely successful with regard to the objectives defined by the chromatographer.

The overall desirabilities including separate robustness factors in terms of pH and φ_{MeOH} (D_2 or D_4) can be lower than those considering a global robustness criterion (D_1 or D_3). For example, considering experiment 1 from Table 6, the value of D_3 is 0.71, but $D_4 = 0$ because $R_u(pH)$ exceeds 0.2 ($d = 0$; see Fig. 8c). In contrast, R_u has an intermediate value between the minimum and maximum acceptable values (see Fig. 8b). However, the overall ruggedness factors appear to be more relevant, because

Table 6
Experimental conditions and corresponding values of the criteria [$R_{l,min}$; R_u; $R_u(pH)$; $R_u(\varphi)$] yielding the best values of the overall desirabilities D_1, D_2, D_3 or D_4

No.	pH	φ_{MeOH}	k_{max}	$R_{l,min}$	R_u	$R_u(\varphi)$	$R_u(pH)$	D_1	D_2	D_3	D_4
1	3.61	0.30	8.47	1.51	0.30	0.092	0.21	1	0.77	0.71	0
2	4.27	0.30	5.14	1.72	0.22	0.085	0.135	1	1	0.95	0.87
3	4.31	0.30	4.90	1.74	0.21	0.14	0.072	1	1	0.97	0.85
4	4.35	0.30	4.67	1.61	0.27	0.12	0.15	1	1	0.81	0.74
5	4.39	0.30	4.45	1.49	0.25	0.11	0.14	0.99	0.99	0.86	0.81
6	4.43	0.30	4.22	1.38	0.23	0.098	0.13	0.94	0.96	0.86	0.84
7	2.92	0.30	10.04	1.50	0.18	0.030	0.15	1	1	1	0.79
8	3.65	0.30	8.31	1.68	0.21	0.10	0.11	1	1	0.97	0.97
9	4.27	0.32	4.63	1.56	0.14	0.076	0.064	1	1	1	1
10	4.31	0.32	4.43	1.48	0.22	0.11	0.11	0.99	0.99	0.94	0.93
11	4.35	0.32	4.23	1.38	0.22	0.10	0.12	0.94	0.96	0.89	0.89
12	3.65	0.32	7.17	1.49	0.090	0.078	0.012	0.99	0.99	0.99	0.99
13	4.27	0.34	4.12	1.40	0.089	0.063	0.026	0.95	0.97	0.94	0.97

these values refer to the total variation of the minimum resolution.

For seven experimental conditions, D_1 reaches the ultimate value of 1. This value is only obtained twice for D_3. This fact can be easily explained because D_1 takes into account the global ruggedness factor corrected for the resolution, $[R_u^*]^{-1}$. "Higher" values of R_u are then accepted when the minimum resolution increases. In our opinion, using $[R_u^*]^{-1}$ is recommended when Derringer's desirability method is used. In contrast to the pareto-optimality procedure, this method does not permit the visualization of the pay-off between the two types of criteria (minimum resolution and robustness).

Selecting D_1 as the best overall desirability function gives seven optimum experiments (see Table 6). We can choose experiment 3 which corresponds to the best resolution and leads to a short analysis time (7.56 min). This experiment is also a pareto-optimal point (see Table 5) and the corresponding chromatogram (at pH 4.31 and $\varphi_{MeOH} = 0.30$) is shown in Fig. 7.

A multiple-threshold approach (MTA) can also be applied for optimizing several chromatographic goals. Fixed thresholds for any given criterion can be visualized as a step function (see Fig. 9a and b). A single number to assess optimization quality is then obtained by maximizing or minimizing a final criterion, the value of which is not required to meet a specified target. Analysis time is an obvious choice for this purpose. The hyperbolic curve in Fig. 9c for retention (capacity factor of the last peak, k_{max}) corresponds to the use of $1/k_{max}$ as the final optimization criterion. The total desirability can be expressed as the product of all individual values. This function is equal to the value of the final criterion if all thresholds are reached and equal to zero if the latter is not the case. From the analogy between Figs. 8 and 9, the MTA can be seen as a special case of the Derringer method. The advantage of using firm thresholds is the transparency and the obvious correctness of the method. There is no compromise involved in the MTA process, so that the chromatographer may trust the results more easily

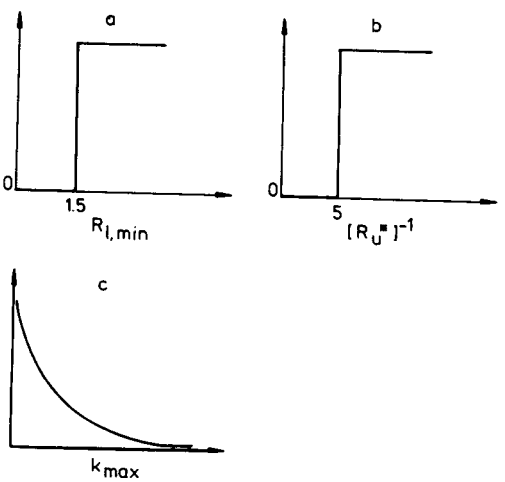

Fig. 9. Example of multiple-threshold approach: (a) and (b) step functions for the minimum effective resolution and $[R_u^*]^{-1}$; (c) hyperbolic curve for retention (k_{max}).

than those obtained in a less transparent manner. A disadvantage is the black-and-white nature of firm thresholds. If the thresholds are not reached, all information on the separation is lost and "grey" (almost optimum) areas on a response surface are discarded. A typical approach in practice is to set ideal targets and lower these stepwise if all targets cannot be met simultaneously. Although this method is not unattractive in case of a single threshold, potential problems arise when several thresholds need to be established and iteratively optimized.

Conventionally, a compromise between time and separation quality is achieved with this strategy. When the threshold resolution value is reached, the optimum analysis time is selected. If the threshold value is not reached, the criterion value is zero. In this study, this method was used for optimizing the minimum effective resolution and a ruggedness criterion. Other combinations of (multiple) threshold criteria are obviously possible. The threshold value of the minimum effective resolution is set at 1.5. Among the experiments reaching this minimum resolution (Nos. 1, 2, 3, 4, 7, 8 and 9 in Table 6), the highest ruggedness factor, $[R_u^*]^{-1}$, is selected. Experiment 9 then represents the optimum (pH 4.27 and $\varphi_{MeOH} = 0.32$) with $[R_u^*]^{-1} = 11.1$.

A multiple-threshold approach can also be used. For example, target values for the minimum resolution (typically 1.5) and for the ruggedness factor $[R_u^*]^{-1}$ (typically 5) can first be defined. Subsequently, and only if both threshold values are reached, the analysis time can be minimized. In this case, experiment 9 is again selected (see Table 6).

Having established the possibility of including ruggedness criteria in selectivity optimization procedures, many other possibilities arise. We have concentrated in this study on the ruggedness of chromatographic resolution, but various other ruggedness criteria can be envisaged. Particularly relevant may be a concentration ruggedness parameter ($R_{u,c}$). In the case in which concentration is obtained from the area (A_i) of a solute peak relative to that of an internal standard (A_{st}), a definition may read

$$R_{u,c} = \sum_x \left(\Delta_x \cdot \frac{d(A_i/A_{st})}{dx} \right) \quad (12)$$

where x denotes the optimization parameters (solvent composition, pH, etc.).

Analogous equations for peak height and other quantification methods can be readily derived. This will be part of future work.

5. Conclusions

It is of great potential benefit to consider the ruggedness of chromatographic separations at an early stage of method development. This greatly reduces the risk of major disappointments when seemingly good methods fail a ruggedness test.

Ruggedness criteria can be elegantly defined as partial or total derivatives of resolution-based criteria with respect to the parameters to be optimized. However, ruggedness cannot be a goal in itself and it must be incorporated in multi-criteria decision making (MCDM) strategies. Three such approaches have been applied in the present study, each showing certain advantages.

Pareto-optimality plots are a highly informative and convenient tool, provided that a trade-off is sought between not more than two different criteria (e.g., resolution and ruggedness). Derringer's desirability function allows the incorporation of many different criteria to yield a single number for the overall quality of a separation. However, the chromatographer sacrifices control of the optimization process, as various compromises between the different criteria will lead to identical desirability values. Using a multiple-threshold approach (MTA), well defined targets can be achieved. MTA is the most easily applied MCDM method, provided that the initial targets can be met. When this is not the case and several thresholds need to be reconsidered, a more complex situation arises, in which other MCDM methods become more attractive.

Acknowledgements

P.F.V. thanks the academic authorities of the Catholic University of Louvain for making possible her working period in Amsterdam and Shell Research for financial support.

References

[1] M. Mulholland and J. Waterhouse, *Chromatographia*, 25 (1988) 769.
[2] M. Mulholland, P.J. Naish, D.R. Stout and J. Waterhouse, *Chemometr. Intell. Lab. Syst.*, 5 (1989) 263.
[3] J.A. van Leeuwen, L.M.C. Buydens, B.G.M. Vandeginste, G. Kateman, P.J. Schoenmakers and M. Mulholland, *Chemometr. Intell. Lab. Syst.*, 10 (1991) 337.
[4] C. Vandenbosch, C. Vannecke and D.L. Massart, *J. Chromatogr.*, 592 (1992) 37.
[5] Y. Vander Heyden, M.S. Khots and D.L. Massart, *Anal. Chim. Acta*, 276 (1993) 189.
[6] S.N. Deming, *J. Chromatogr.*, 550 (1991) 15.
[7] M.W.B. Hendriks, J.H. de Boer, A.K. Smilde and D.A. Doornbos, *Chemometr. Intell. Lab. Syst.*, 16 (1992) 175.
[8] A.K. Smilde, A. Knevelman and P.M.J. Coenegracht, *J. Chromatogr.*, 369 (1986) 1.
[9] B. Bourguignon and D.L. Massart, *J. Chromatogr.*, 586 (1991) 11.
[10] J.H. de Boer, A.K. Smilde and D.A. Doornbos, *Chemometr. Intell. Lab. Syst.*, 7 (1990) 223.
[11] J.H. de Boer, A.K. Smilde and D.A. Doornbos, *Chemometr. Intell. Lab. Syst.*, 10 (1991) 325.

[12] J.H. de Boer, A.K. Smilde and D.A. Doornbos, *Chemometr. Intell. Lab. Syst.*, 15 (1992) 13.
[13] J.H. de Boer, *Ph.D. Thesis*, University of Groningen, Groningen, 1992, Ch. 11.
[14] J.H. de Boer, *Pharm. World Sci.*, 15 (1993) 180.
[15] P.J. Schoenmakers, J.K. Strasters and A. Bartha, *J. Chromatogr.*, 458 (1988) 355.
[16] P.J. Schoenmakers, N. Mackie and R.M. Lopes Marques, *Chromatographia*, 35 (1993) 18.
[17] P.J. Elving, J.M. Markowitz and I. Rosenthal, *Anal. Chem.*, 28 (1956) 1179.
[18] R.M. Lopes Marques and P.J. Schoenmakers, *J. Chromatogr.*, 592 (1992) 157.

ELSEVIER

Journal of Chromatography A, 697 (1995) 17–29

JOURNAL OF CHROMATOGRAPHY A

Systematic method development in hydrophobic interaction chromatography
I. Characterization of the phase system and modelling retention

Géza Rippel[a,*], Ágota Bede[b], László Szepesy[b]

[a]*Department of Agricultural Chemical Technology, Technical University of Budapest, Gellért tér 4, H-1521 Budapest, Hungary*
[b]*Department of Chemical Technology, Technical University of Budapest, Budafoki u. 8, H-1521 Budapest, Hungary*

Abstract

In order to rationalize the selection of the phase system (the stationary phase and the mobile phase) applicable for the separation of some proteins, gradient measurements were carried out on three columns of different types using three salts as eluent constituents. The slope and intercept of the ln k–salt concentration relationship for proteins varied with the different phase systems. The hydrophobicity index (c^*) showed how the alteration of the type of phase system affects the selectivity of separation. Two-dimensional mapping along the parameters of the slope–intercept relationship revealed the extent of the difference among the phase systems. In addition, the effect of solutions of binary and ternary salt mixtures on the retention of proteins was investigated. Measurements were carried out according to a mixture design and the retention time was modelled with the predictive method of Jandera and by fitting a polynomial to the data according to the Sentinel method. The accuracy of the former method were dependent on the type of phase system. The fit of second-order polynomial gave very good results but a first-order model was also acceptable.

1. Introduction

The separation of bio-macromolecules is currently of major interest. Reversed-phase chromatography (RPC) is now the most commonly used technique for HPLC separations. Numerous reports [1–4] have shown that RPC has very high resolving power for proteins and peptides. However, the strong interaction between the highly hydrophobic stationary phase and the protein, on the one hand, and the use of organic modifiers as eluent constituents, on the other, can be very detrimental to the native structure of the proteins. As a consequence of these interactions, most of the proteins are subjected to unfolding and denaturation, and can lose some or all of their biological activity.

Hydrophobic interaction chromatography (HIC) has developed into a real alternative to RPC for the separation and purification of proteins. In HIC the proteins are retained by a weakly hydrophobic stationary phase at high salt concentration and are eluted by a decreasing salt gradient [5–7]. The main advantage of HIC over RPC for separating proteins is that because of the milder interaction between the proteins and

* Corresponding author.

0021-9673/95/$09.50
SSDI 0021-9673(94)01031-5

the phase system, most biomolecules retain their activity and suffer very little denaturation.

Retention and selectivity in HIC can be modulated by means of several operating parameters such as the type and characteristics of the stationary phase, type of salt, parameters of the gradient (initial and final salt concentration, gradient time), flow-rate, pH, temperature and addition of organic modifiers [7].

The retention behaviour of proteins in HIC can be described in general by the thermodynamic model of Horváth and co-workers [8–10]. The solvophobic theory relates the retention of proteins to the molar surface tension increment of the salt [11–13]. The validity of the model requires that there be no specific binding of the salt to the protein molecule and no change in the protein structure under different operating conditions. Although it has been found that the molar surface tension argument is an oversimplification of the process and cannot be generally applied because of the unpredictable specific salt-binding effects [14–16], the solvophobic theory provides a good theoretical basis for understanding the basic processes of HIC, and the molal surface tension increment can be used to give a first guess of the effectiveness of a salt.

In contrast to RPC, where the stationary phases show only minor differences as regards the retention and selectivity of separation for various solutes, in HIC the stationary phases may show different effects depending on the type of support and ligand applied. It has been also demonstrated that the various salts affect differently the retention of proteins on the different stationary phases [17,18]. In addition, it has been found that the salts have different effects on the retention of the hydrophilic and hydrophobic proteins [18,19]. For these reasons, the selection of an appropriate stationary phase is of great importance in the design and optimization of HIC separations. Notwithstanding, few studies on the characterization and influence of the stationary phase have been published [20–22]. The above results also imply that the effect of a salt cannot be predicted in advance but should always be determined experimentally in the given phase system for all the proteins to be investigated.

The selective variations of retention of the individual proteins due to salt exchange in the eluents [16,18,19] indicate that by using binary or ternary salt gradients of different kinds and compositions, fine tuning of the selectivity of separations can be accomplished. However, the effect of the salt mixtures in the eluent has only been studied recently by El Rassi et al. [23]. One of our aims was to explore the potential of the application of salt compositions.

Within the past few years, a new generation of products for computer-assisted HPLC method development has emerged. The results have been summarized in several books and in many publications [24–29]. Because RPC is the most frequently used technique of HPLC, most of the softwares was released for optimization of separations of this type under isocratic or gradient conditions. Some methods developed for small molecules have been successfully applied also for peptide and protein samples [30–34]. Nevertheless, no publication has appeared on the application of computer-assisted method development for HIC separations.

Despite the results of intensive investigations revealing the effect of many factors that influence the retention of proteins under HIC conditions, the design and optimization of HIC separations are not trivial. At present, the selection of the phase system and the operating conditions is established on the basis of subjective preferences and local experience, and the optimization, if at all, is carried out mainly by trial and error. The other objective of our study was the application of some methods, originally developed and generally applied for RPC separations, in the design and optimization of HIC separations.

In this paper we discuss the possibilities of modelling the retention of proteins on different columns using single and multiple salt solutions as eluent constituents; in the next part the rational selection of the phase system and the systematic optimization of HIC separations will be discussed.

2. Experimental

2.1. Apparatus

A Merck–Hitachi (Merck, Darmstadt, Germany) LiChrograph, consisting of an L-6200 programmable pump with accessories for low-pressure eluent mixing, a Rheodyne Model 7125 injector with a 10-μl loop and an L-4250 UV–Vis programmable detector operated at 280 nm, was used. System control and data acquisition and evaluation were performed with a D-6000 HPLC Manager running on an IBM PC AT compatible computer.

2.2. Columns

The main characteristics of the columns used are listed in Table 1.

2.3. Materials

Analytical-reagent grade ammonium sulphate, sodium acetate and sodium sulphate were purchased from Reanal (Budapest, Hungary). Distilled water was prepared by double distillation and ion-exchange.

Cytochrome *c* (CYT), ribonuclease A (RNA), ovalbumin (OVA), lysozyme (LYS) and α-chymotrypsinogen A (CHY) were obtained from Sigma (St. Louis, MO, USA).

2.4. Procedures

For the scanning exercises, measurements were carried out at three different gradient times (15, 30 and 45 min) using linear inverse gradients from 2 to 0 *M* ammonium sulphate and sodium sulphate and from 4 to 0 *M* sodium acetate in 0.05 *M* sodium phosphate buffer adjusted to pH 7 with 0.1 *M* NaOH. The flow-rate was 0.5 ml/min for sodium acetate and 1 ml/min for the other two salts. For the binary (2:1 and 1:2) and ternary (1:1:1) salt systems, the above solutions were mixed volumetrically in advance, and the measurements were carried out with 30-min gradients generated by the above buffer at a flow-rate of 1 ml/min.

Samples were prepared by dissolving about 2 mg of each protein in 1 ml of water. All the measurements were repeated at least twice and the average data are used throughout this paper.

3. Results and discussion

A systematic method development process must consist of some or all of the following steps [24,27]: initial exercises, retention optimization,

Table 1
Characteristics of the columns used

Material	Source	Ligand type	Support	Dimensions (mm × mm I.D.)	Particle size (μm)	Pore size (Å)
Synchropak Propyl	Synchrom (Linden, IN, USA)	Propyl	Silica	250 × 4.1	6.5	300
Hema-BIO 1000 Phenyl	Tessek (Prague, Czech Republic)	Phenyl	HEMA[a]	80 × 8.0	10	1000
POROS PH	PerSeptive Biosystems (Cambridge, MA, USA)	Phenyl	PSDVB[b]	100 × 4.6	10	8000/1000 (bimodal)

[a] Hydroxyethyl methacrylate.
[b] Styrene–divinylbenzene copolymer.

selectivity optimization, kinetic optimization, i.e., the optimization of the efficiency of the separation, and validation. All of these steps can be further divided. The initial exercises involve, among others, the precise formulation of the goal of separation, the selection of the phase system that is appropriate for the separation and the definition of the parameter space within which the optimum is presumed to be located. The last steps means the identification of the parameters affecting the retention of components to be separated and the definition of their range relevant to a practicable optimization of the separation. A method or algorithm must be also selected that provides an efficient and rapid way to find the optimum.

For RPC separations, most of the above steps can be considered as "standardized". There are some sort of stationary phases (octadecyl, octyl and, to a lesser extent, phenyl or cyano types) which are used very frequently, and the organic modifiers are almost always methanol, acetonitrile or in some instances tetrahydrofuran, used alone or in mixtures. In contrast, in HIC neither the type of stationary or mobile phase nor the range of the eluent strength can be selected in this way. Recently, a wide variety of stationary phases suitable for HIC separations have become available [7,10,22] and, theoretically, all the salts having "salting-out" properties can be considered as modifiers [8–10]. This, on the one hand, provides great flexibility for the selection of the phase system but, on the other, this means "too much freedom", because at present there is no method either for rational selection or even for reliable characterization of the phase system.

It has been found [17–19] that the combination of different salt solutions and columns of different types leads to unique phase systems, i.e., by varying the type of salts in the eluents and/or the type of the stationary phase, not only the retention of the components changes but also the selectivity of the separations.

In a recent study [35], we investigated some RPC methods suggested for the characterization of stationary phases. The results obtained for columns used in RPC and in HIC showed that the overall strength of the stationary phases can be evaluated fairly well but the results regarding polarity and/or hydrophobicity are misleading, especially for the HIC columns. It was also found that not only the type of ligand but also the type of support may have a significant effect on the retention.

Three widely differing stationary phases were selected for this study. The strength of HEMA fell in the range of that of the RPC columns, PRO was the weakest column in the RPC mode [35] but one of the strongest in HIC mode [18], and on POROS no retention could have been obtained under RPC conditions but excellent separations were reported under HIC conditions. However, these stationary phases differ not only in the overall strength but also in the type of ligand and the type and geometry of the support. Here we postulate that the more different the characteristics of the columns are, the greater the effect on retention and selectivity would be.

As regards salts, the above rule of thumb was applied again. Ammonium sulphate is the most commonly used salt in HIC [5,6]. In another study [19], we found that compared with ammonium sulphate, sodium acetate exerted selective effects on the proteins, i.e., it increased the retention of the hydrophobic proteins but decreased that of the hydrophilic proteins.

On the basis of our earlier results [7,17–19], sodium citrate should have been the third candidate but it was left out because some solubility problems occurred during the preparation of the multiple salt solutions. Instead, sodium sulphate was selected, because a special effect (deviation from the predictions of the solvophobic theory) was found also for this salt [5].

This kind of experimental design (using three different columns and three different modifiers) can be considered as an adaptation of that used in RPC when, in addition to an alkyl-type stationary phase, phenyl and cyano types are also tested for tuning the selectivity of separations [36–38]. This approach is especially recommended for samples with which more common methods of adjusting selectivity (modifier type and/or strength, pH, temperature, etc.) are impossible, problematic or inconvenient.

The HIC separations are always performed

under gradient conditions. The theory and practice of gradient elution has been well developed, and it has been discussed and summarized in many books and other publications [30–33]. It was found [19,39] that the so-called linear solvent strength (LSS) model of gradient elution is a good approximation under HIC conditions. When using only one salt in the eluent, it makes possible, on one hand, the estimation of the parameters of the retention profiles of the proteins and, on the other, the systematic and efficient optimization of HIC separations.

In RPC, there are two ways of modelling the retention of the components in multi-solvent eluents. The first is the Sentinel method, which was introduced originally for the optimization of selectivity under isocratic conditions and was later extended to the optimization of gradient separations [40–42]. First, "iso-eluotropic" binary eluents are designed that provide more or less the same retention for the components. Next, each of these gradients represents one "mixture variable" in a mixture design technique approximating the retention of components in multi-solvent systems by a second-order polynomial. In the other method [43–46], the parameters of the retention profiles of components in the binary systems are estimated, and then the retention of components in ternary and quaternary eluents can be calculated from these parameters in an iterative way.

In HIC, the logarithmic retention factor of components (ln k) can be well approximated as

$$\ln k = \ln k_w + Sc \quad (1)$$

where c is the concentration of the salt used in the eluent, and ln k_w (the extrapolated ln k value to pure water) and S are constants characteristic of the phase system applied. If a linear gradient of salt is used, the net retention time of the components can be given as

$$t'_g = \ln (Smt_m k_0 + 1)/Sm \quad (2)$$

where m is the slope of the gradient, t_m is the hold-up time and k_0 is the retention of component at the initial eluent composition (c_0). From data for two gradient runs, the parameters of Eq. 1 can be estimated. If more than two gradient data are available, the validity of Eq. 1 can also be checked. The method has been described in details elsewhere [19].

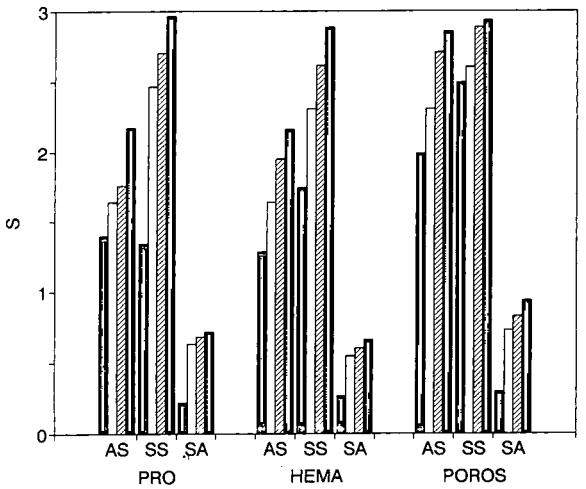

Fig. 1. Slope of retention profiles (S in Eq. 1) obtained in the different phase systems. The bars represent RNA (grey), OVA (white), LYS (hatched) and CHY (black).

The slope (S) and intercept (ln k_w) values obtained with the different systems are shown in Figs. 1 and 2, respectively. (In most instances the data for CYT could not be evaluated because of

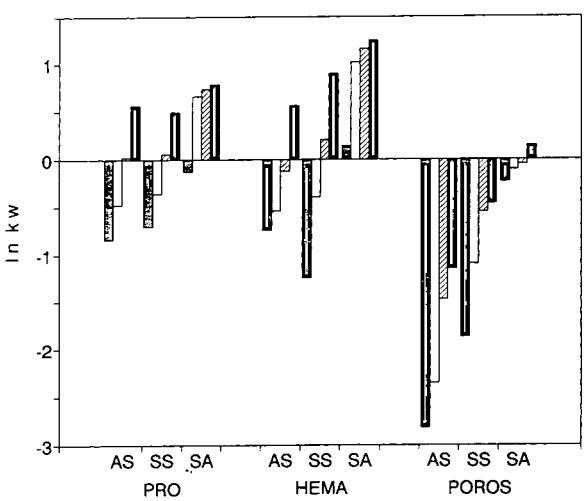

Fig. 2. Intercept of retention profiles (ln k_w in Eq. 1) obtained in the different phase systems. The bars represent RNA (grey), OVA (white), LYS (hatched) and CHY (black).

pre-elution or because of the serious overlap with the system peak, so this component was omitted from the evaluation, but not from the later optimization.) It is immediately seen that the differences between the columns are not as large as would have been expected from characterization in the RPC mode [35]. This is a direct confirmation of our earlier presumption that the tested methods provide reliable characteristics for the RPC columns but misleading results for the HIC columns.

The S parameters (Fig. 1) are similar on PRO and HEMA and are higher on POROS, but the order of columns cannot be established unambiguously on the basis of this parameter. The rates of alterations generated by the salt exchange in the eluent are also very similar. The use of sodium sulphate (SS) instead of ammonium sulphate (AS) increases slightly and replacing ammonium sulphate with sodium acetate (SA) decreases significantly the values of this characteristic, i.e., the salt type had a much larger effect on S than the type of stationary phase.

Larger differences can be observed in the values of $\ln k_w$ (Fig. 2). In general, this characteristic is the lowest in ammonium sulphate (AS) and the highest in sodium acetate (SA), but it is clear that here the type of stationary phase is the dominant factor, i.e., a change in the type of stationary phase exerts a larger effect on $\ln k_w$ than that of the salt type.

As the retentions of proteins as reflected by the above parameters are affected by the type of stationary phase and by the type of salt, a complete characterization of the phase systems must take into account both of them. Recently, a new hydrophobicity index of solutes under RPC conditions was suggested [47] which we adapted to HIC conditions [18]. It can be calculated as

$$c^* = -\ln k_w / S \qquad (3)$$

where c^* is the salt molality at which $\ln k = 0$ (cf., Eq. 1), i.e., the molar concentrations of the related compounds are identical in the stationary and mobile phases. (It must be noted that earlier we designated this parameter m_0, but this is a confusing term because in the literature m is used for the slope of the gradient and the subscript zero relates to the initial conditions of the gradient.)

The calculated values for the proteins in the different phase systems are shown in Fig. 3. The course of the data seems to be some sort of mirror image of the $\ln k_w$ values but as c^* involves both $\ln k_w$ and S, it can be considered as a measure of the overall strength of the phase system. The lower is c^* the larger is the "retentive strength" of the phase system. Related to ammonium sulphate (AS), sodium acetate increases c^* on all the stationary phases, but the extent of the changes varies from column to column. The effect of sodium sulphate seems to be specific to the stationary phase. The range of c^* values decreases on PRO and increases on HEMA, but the average values are more or less the same. On POROS the range and the absolute values also decreased. It is also seen that the order of the columns relating to strength cannot be established; it depends greatly on the type of salts. The order obtained in sodium acetate (SA) is consistent, but in sodium sulphate there are considerable differences between the stationary phases.

As regards the individual proteins, the changes in the difference between the c^* values corre-

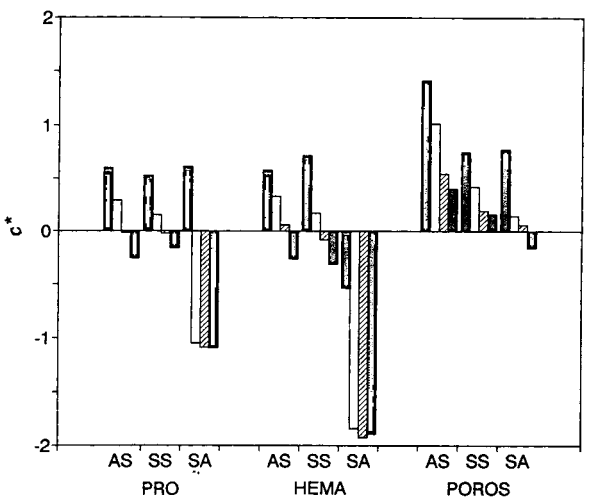

Fig. 3. Hydrophobicity index (c^*) calculated for the proteins. The bars represent RNA (grey), OVA (white), LYS (hatched) and CHY (black).

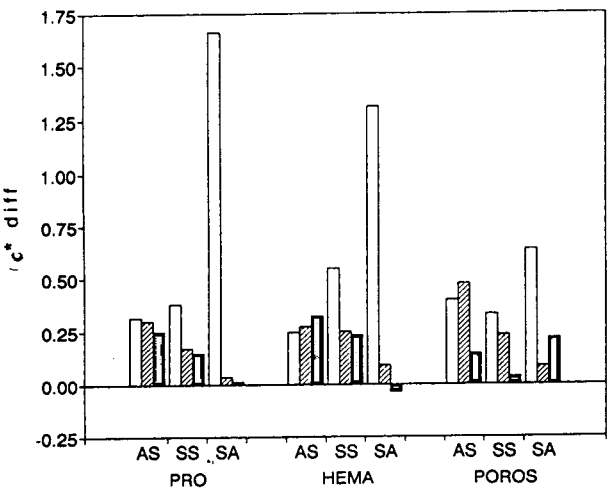

Fig. 4. Difference in c^* for pairs of proteins. The bars represent RNA–OVA (white), OVA–LYS (hatched) and LYS–CHY (black).

spond to the changes in the selectivity of the phase systems. The calculated differences are shown in Fig. 4. It is seen that neither the extent nor the order of these values are the same in the different systems. This means that changes in the type of the stationary phase and/or the salt type always modifies the selectivity of the phase system.

Under RPC conditions, S and $\ln k_w$ are not independent but show a good correlation [35]. Earlier we found a similar relationship between these two parameters also under HIC conditions [21], which can be formulated as

$$S = q + p \ln k_w \quad (4)$$

where q and p are constants. The characterization of a series of stationary phases that were different with respect to the type and surface concentration of the ligands and also the material and geometry of the support showed that these parameters are not constant but are specific to the phase system [35]. When mapping the columns with regard to these parameters obtained under RPC conditions, the RPC and HIC columns formed two distinct clusters, indicating the different strengths of the stationary phases.

On applying Eq. 4 to the data obtained in this study, good correlations were obtained ($r > 0.981$). The two-dimensional mapping of the phase system investigated is shown in Fig. 5. The values obtained in ammonium sulphate (AS) and in sodium sulphate (SS) on all the columns fall in or near the region of that of the RPC columns obtained for low-molecular-mass (LMM) components under RPC conditions (cf. Fig. 9 in Ref. [35]). This means that the HIC columns exhibit more or less the same strength for proteins under HIC conditions as the RPC columns for the LMM components in the RPC mode.

The smaller effect of changing from ammonium sulphate (AS) to sodium sulphate (SS) is clearly seen. The points relating to HEMA almost coincide and those for PRO are very close to each other. The difference on POROS is greater. Using sodium acetate (SA) instead of ammonium sulphate (AS) decreases all the q values and spreads the points over a wider range of p. As at present the meaning of these parameters under HIC conditions is not clear, further evaluation of changing the type of phase system cannot be accomplished, but the similarities and differences are clearly seen.

Having evaluated the gradient data obtained in single-salt systems, all the parameters are

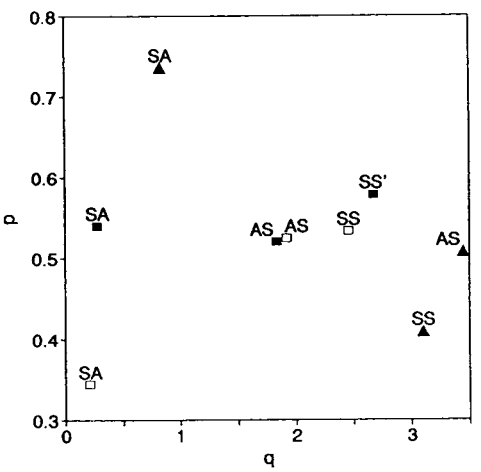

Fig. 5. Two-dimensional mapping of the phase systems using the parameters of Eq. 4 obtained in ammonium sulphate (AS), sodium sulphate (SS) and sodium acetate (SA). ■ = PRO; □ = HEMA; ▲ = POROS.

present for checking the applicability of the equation proposed by Jandera [43–46] for calculating retention in multi-solvent gradients under RPC conditions. The net retention time of a component can be given as

$$t'_g = \ln (t_m S_g k_{0g} + 1)/S_g \quad (5)$$

where

$$S_g = \sum S_i m_i$$

$$k_{0g} = \exp\left(\sum S_i c_{0i} + \sum c_{gi} \ln k_{wi} \Big/ \sum c_{gi}\right)$$

$$c_{gi} = c_{0i} - m_i t'_g/2$$

where t_m is the hold-up time of the system and i refers to the ith modifier (here salt). This iterative or recursive equation was applied for calculating the retention times of proteins in binary and ternary salt systems listed under Experimental. In addition, measurements were also carried out using these eluents.

The retention times obtained on the columns are shown in Fig. 6 and are listed in the third columns in Tables 2–4. Note that the figures correspond to the (unfolded) edges of the triangular mixture design. For a better overview, the apex corresponding to ammonium sulphate (AS) is put at both ends. MIX refers to the 1:1:1 solution. It is clearly seen that the gradient time of components changes according to a smooth function as the eluent composition changes from the solution of one pure salt to another. In most binary solutions this function seems to be a straight line.

The possibility of modelling retention was investigated in three ways. First, according to Eq. 5 the retention times were calculated from the parameters (S, ln k_w) obtained from the evaluation of the gradient data. The results are summarized in the fourth columns (calcd.) of Tables 2–4. Next, a first-order polynomial of the form

$$t_g = a_0 + a_1 c_{01} + a_2 c_{02} + a_3 c_{01} c_{02} \quad (6)$$

was fitted to the data, where c_{01} and c_{02} are the initial concentrations of ammonium sulphate (AS) and sodium sulphate (SS) and a_0–a_3 are

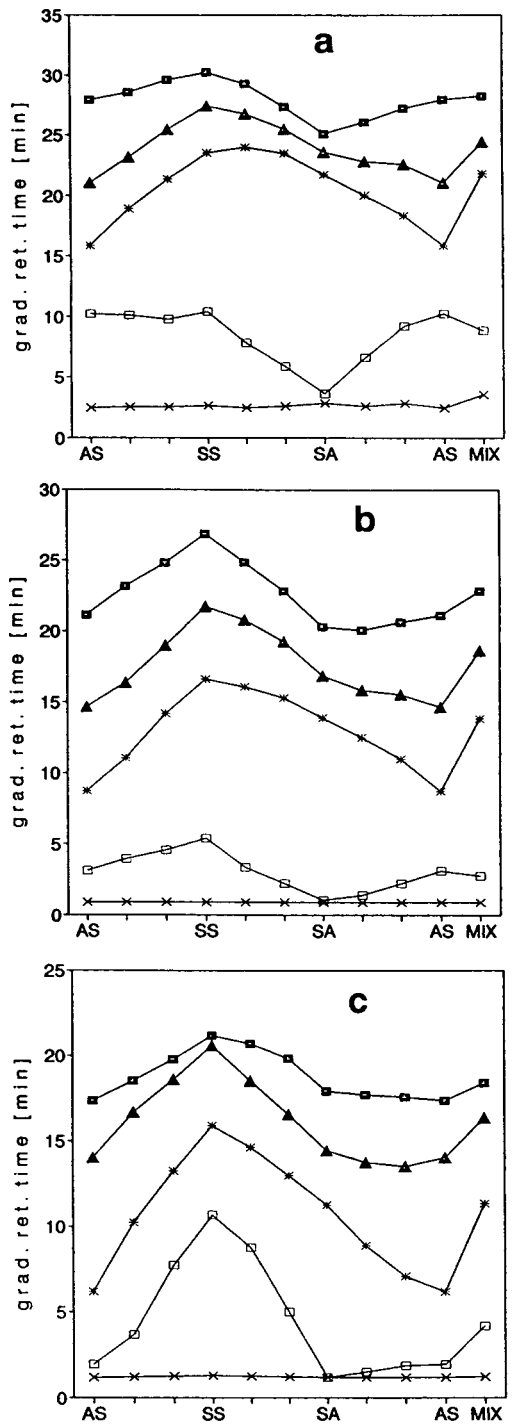

Fig. 6. Retention times obtained experimentally on (a) PRO, (b) HEMA and (c) POROS. ◘ = CHY; ▲ = LYS; ∗ = OVA; □ = RNA; × = CYT.

Table 2
Gradient retention times obtained experimentally (measd.) on HEMA and calculated from Eq. 5 (calcd.), from Eq. 6 (fit1) and from Eq. 7 (fit2)

Compound	Salt	Measd.	Calcd.	Fit1	Fit2
RNA	AS	3.09	3.29	3.08	3.15
		3.95	4.91	3.78	3.87
		4.55	4.55	4.48	4.60
	SS	5.38	5.19	5.18	5.33
		3.38	4.76	3.70	3.49
		2.21	2.90	2.22	2.07
	SA	1.04	0.91	0.93	1.06
		1.40	2.04	1.52	1.46
		2.25	3.04	2.30	2.16
	AS	3.09	3.29	3.08	3.15
	MIX	2.77	3.87	3.00	2.82
OVA	AS	8.69	8.14	8.81	8.61
		11.00	10.95	11.45	11.30
		14.13	13.57	14.10	13.96
	SS	16.57	15.88	16.74	16.59
		16.04	16.96	15.93	16.17
		15.25	15.92	15.12	15.24
	SA	13.87	12.99	14.30	13.82
		12.50	12.80	12.47	12.66
		10.97	11.40	10.64	10.93
	AS	8.69	8.14	8.81	8.61
	MIX	13.81	14.36	13.28	13.56
LYS	AS	14.62	14.42	14.35	14.64
		16.37	17.20	16.87	16.64
		18.95	19.58	19.39	18.97
	SS	21.70	21.59	21.91	21.63
		20.77	21.59	20.36	20.96
		19.24	19.78	18.80	19.34
	SA	16.83	15.85	17.25	16.77
		15.81	16.78	16.28	16.06
		15.50	16.48	15.32	15.35
	AS	14.62	14.42	14.35	14.64
	MIX	18.59	19.27	17.84	17.99
CHY	AS	21.08	20.94	20.93	21.06
		23.09	23.18	22.95	23.07
		24.77	25.01	24.96	24.97
	SS	26.82	26.51	26.97	26.74
		24.82	25.43	24.72	24.87
		22.83	22.96	22.47	22.67
	SA	20.25	19.30	20.22	20.14
		20.01	20.27	20.46	20.25
		20.59	21.20	20.70	20.55
	AS	21.08	20.94	20.93	21.06
	MIX	22.83	23.56	22.71	22.77

Table 3
Gradient retention times obtained experimentally (measd.) on PRO and calculated from Eq. 5 (calcd.), from Eq. 6 (fit1) and from Eq. 7 (fit2)

Compound	Salt	Measd.	Calcd.	Fit1	Fit2
RNA	AS	10.24	10.11	10.66	10.28
		10.08	10.20	10.43	10.02
		9.75	10.29	10.20	10.01
	SS	10.39	10.39	9.97	10.24
		7.78	8.51	8.00	8.01
		5.85	5.88	6.04	5.78
	SA	3.60	3.43	4.07	3.55
		6.60	5.92	6.27	6.87
		9.19	8.51	8.46	9.12
	AS	10.24	10.11	10.66	10.28
	MIX	8.84	8.51	8.23	8.44
OVA	AS	15.88	15.84	16.16	15.87
		18.89	18.98	18.84	18.94
		21.35	21.52	21.51	21.46
	SS	23.52	23.52	24.18	23.44
		23.97	24.37	23.57	24.11
		23.47	23.63	22.95	23.50
	SA	21.69	21.23	22.34	21.61
		20.00	20.59	20.28	20.22
		18.35	19.01	18.22	18.31
	AS	15.88	15.84	16.16	15.87
	MIX	21.81	22.04	20.89	21.48
LYS	AS	21.07	20.97	21.22	21.09
		23.20	23.63	23.37	23.25
		25.48	25.60	25.52	25.37
	SS	27.41	27.08	26.67	27.44
		26.72	27.18	26.43	26.74
		25.47	26.01	25.18	25.39
	SA	23.61	23.19	23.94	23.40
		22.79	23.25	23.03	23.14
		22.57	22.66	22.12	22.37
	AS	21.07	20.97	21.22	21.09
	MIX	24.45	25.29	24.28	24.58
CHY	AS	27.95	27.90	27.90	28.01
		28.55	28.88	28.78	28.72
		29.57	29.62	29.66	29.48
	SS	30.24	30.19	30.55	30.29
		29.23	29.55	28.82	29.17
		27.29	27.87	27.09	27.43
	SA	25.05	24.47	25.36	25.08
		26.05	26.24	26.21	26.05
		27.17	27.37	27.05	27.03
	AS	27.95	27.90	27.90	28.01
	MIX	28.25	28.62	27.93	28.08

Table 4
Gradient retention times obtained experimentally (measd.) on POROS and calculated from Eq. 5 (calcd.), from Eq. 6 (fit1) and from Eq. 7 (fit2)

Compound	Salt	Measd.	Calcd.	Fit1	Fit2
RNA	AS	1.96	1.80	1.32	1.49
		3.70	4.33	4.46	4.95
		7.75	7.37	7.60	8.20
	SS	10.68	10.57	10.74	11.25
		8.77	9.08	7.60	8.00
		5.00	5.06	4.46	4.74
	SA	1.16	1.12	1.32	1.49
		1.51	2.58	1.32	1.49
		1.86	3.20	1.32	1.49
	AS	1.96	1.80	1.32	1.49
	MIX	4.18	5.93	4.46	4.85
OVA	AS	6.19	6.36	6.16	6.19
		10.25	9.44	9.59	10.16
		13.25	12.62	13.01	13.39
	SS	15.91	15.74	16.44	15.88
		14.65	15.54	14.60	14.60
		12.95	13.77	12.76	13.05
	SA	11.25	10.70	10.92	11.23
		8.89	10.92	9.34	8.85
		7.07	9.71	7.75	7.16
	AS	6.19	6.36	6.16	6.19
	MIX	11.35	12.64	11.18	11.25
LYS	AS	14.05	14.47	13.94	14.06
		16.68	16.54	16.24	16.58
		18.59	18.54	18.53	18.75
	SS	20.61	20.48	20.83	20.58
		18.53	19.38	18.61	18.55
		16.57	17.09	16.38	16.52
	SA	14.43	13.54	14.16	14.49
		13.76	15.27	14.09	13.74
		13.52	15.71	14.02	13.60
	AS	14.05	14.47	13.94	14.06
	MIX	16.37	17.57	16.31	16.25
CHY	AS	17.37	17.24	17.15	17.35
		18.51	18.58	18.55	18.38
		19.81	19.91	19.95	19.67
	SS	21.17	21.22	21.35	21.22
		20.67	20.92	20.30	20.66
		19.83	19.66	19.25	19.56
	SA	17.91	17.48	18.20	17.91
		17.71	18.56	17.85	17.73
		17.59	18.59	17.50	17.54
	AS	17.37	17.24	17.15	17.35
	MIX	18.41	19.77	18.90	18.97

constants. The results (fit1) are summarized in the fifth columns of Tables 2–4. Finally, a second-order polynomial of the form

$$t_g = b_0 + b_1c_{01} + b_2c_{02} + b_3c_{01}c_{02} + b_4c_{01}^2 + b_5c_{02}^2 \quad (7)$$

was also fitted, where c_{01} and c_{02} are the same as above and b_0–b_5 are constants. The results (fit2) are summarized in the last columns of Tables 2–4. For demonstration, some selected results are shown in Fig. 7.

As regards retention times predicted by Eq. 5, the fit is always very good in the ammonium sulphate–sodium sulphate (AS–SS) system, acceptable in the sodium sulphate–sodium acetate (SS–SA) mixtures but weak in the sodium acetate–ammonium sulphate (SA–AS) solutions. The model always predicts concave surfaces in the phase systems investigated which sometimes results in local maxima (cf., SS–SA mixtures in Fig. 7b) not indicated by the measurements, or in opposite curvature (concave instead of convex as in SA–AS mixtures in Fig. 7a). As the error of measurements was fairly high (±1 min), sometimes the values are erratic (cf., SA–AS mixtures in Fig. 7b), and hence it cannot be established how significant is the curvature indicated by these values. With this technique the smallest errors were obtained in the AS–SS mixtures on PRO and the largest in the SA–AS system on POROS. For the latter case the difference between the measured and the calculated retention times exceeds 2 min in some solutions. It seems that the closer are two systems on the p–q plot (Fig. 4), the better is the prediction.

In single-salt solutions, Eq. 5 reduces to Eq. 2, hence the data are applicable for checking the accuracy of the parameters of Eq. 1 obtained from the evaluation of the gradient data. It is seen that the largest error occurs in sodium acetate (SA) where, in most instances, Eq. 5 underestimates the retention times. This inaccuracy can be attributed to the error of measurements being the highest in this solution. It is also possible that the LSS conditions do not hold true in this instance, i.e., Eq. 2 is only an approxi-

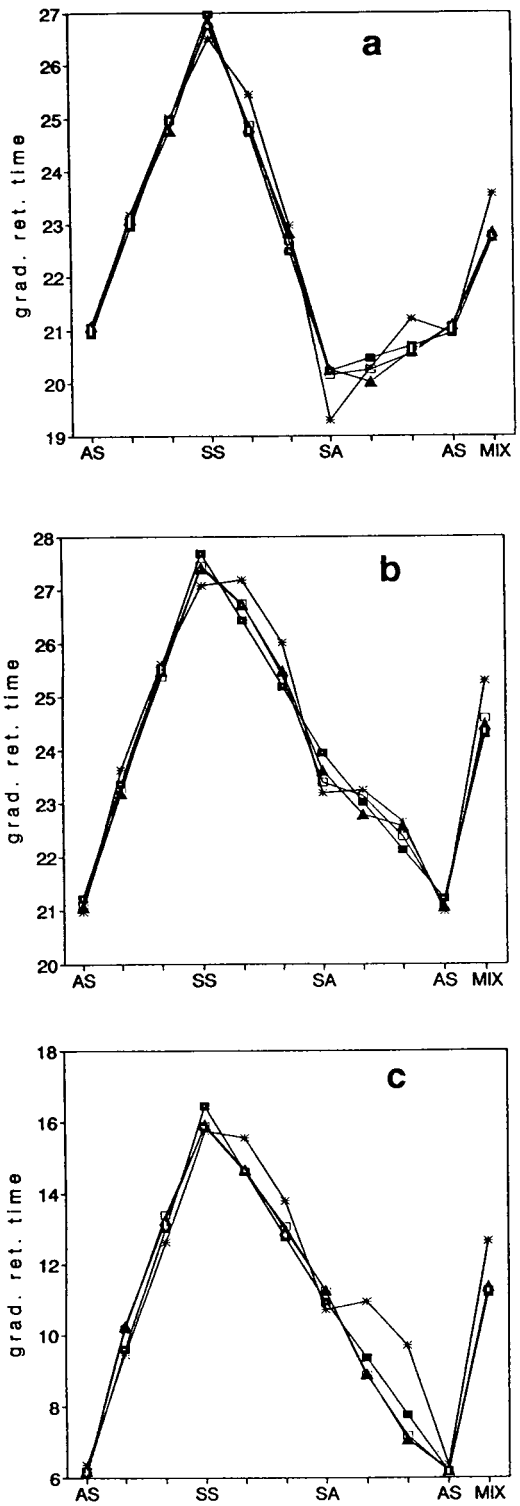

mation of the retention time. However, further investigation is needed to reveal the full reason for this systematic error.

In order to fit the underlying model of the mixture design, one of the single-salt solutions must be regarded as a diluter and the other two as modifiers. For the former sodium acetate (SA) was selected, because the retention time was always the lowest in this system under the conditions applied.

The fit of the first-order polynomial (Eq. 6) is much better ($r > 0.957$) than that of the results provided by the predictive model (Eq. 5); however, the statistical evaluation of the parameters (a_0–a_3) showed that the fourth term on the right-hand side (the so-called cross-effect term) is almost always negligible. This means that simple interpolation gives retention times with good accuracy in multiple salt solutions under gradient conditions. This is supported by the fact that the retention time in MIX is always very close to the average of that measured in the single-salt solutions.

The second-order polynomial (Eq. 7) gave the best estimate of retention time ($r > 0.988$); however, the full polynomial was always redundant, i.e., some terms of the model were insignificant in all instances.

The above results could indicate that the second-order polynomial should always be used for modelling, but this kind of approach has some shortcomings. First, it is applicable only for the prediction of retention in "solvent strength gradients", i.e., when the amount of modifiers decreases during the gradient but their ratio remains constant. However, it is only one of the possible designs. The predictive model can estimate retention in gradients where only or also the ratio of the modifiers changes [43–46], hence, we consider that the advantages and

Fig. 7. Gradient retention times obtained experimentally (▲) and calculated from Eq. 5 (*), Eq. 6 (■) and Eq. 7 (□) for (a) CHY on HEMA (the values correspond to the respective columns in Table 3), (b) LYS on PRO. (the values correspond to the respective columns in Table 2) and (c) OVA on POROS (the values correspond to the respective columns in Table 2).

limitations of this model should be further investigated.

Another deficiency of the mixture design technique is that it tells nothing about the effect of the third salt. A complete investigation must take into account all the combinations of "diluters" and "modifiers", i.e., which selection of the salt solutions entered in the model of Eq. 7 (or Eq. 6) gives the most adequate description of the effect of salt compositions.

4. Conclusions

A systematic method development must include the selection of the phase system (the stationary phase and mobile phase) which is appropriate for the separation. At present this step is carried out by trial and error in HIC. The rationalization of the choice can be accomplished by characterization of the phase system. For this purpose, gradient measurements were carried out at three different gradient times on three columns of different kinds using three salts as eluent constituents.

First, the slope and intercept values of the ln k–salt concentration relationship of proteins were calculated according to the LSS model of gradient elution. Although alterations of the selectivity of the phase systems such as changing the type of salt and/or that of the stationary phases was indicated, a clear characterization could not have been made with these values. Next, the hydrophobicity index (c^*) characteristic of the protein and of the phase system used was calculated. These parameters and even their differences showed how the variation of the type of phase system affected the selectivity of separation. Finally, two-dimensional mapping with regard to the parameters (p, q) of the slope–intercept relationships revealed the similarities and differences among the systems.

Another step in the optimization process is the selection of the model describing the retention in the phase system chosen. The effect of salt compositions on retention was investigated using solutions of binary and ternary salt mixtures. For describing the retention in these systems, three models were applied and compared.

The accuracy of the predictive model developed by Jandera was dependent on the type of phase system. The distance on the p–q plot seemed to be an indication of the applicability.

According to the Sentinel method, a second-order polynomial was fitted to the retention times and very good correlations were obtained. On the other hand, the effect of all the salts used could not be evaluated. The application of a first-order model also gave acceptable results, which makes the description the retention of proteins in binary and ternary salt solutions under gradient conditions very easy.

Acknowledgements

We gratefully acknowledge the financial support given by the Hungarian Academy of Sciences under grants OTKA No. 1998/1991 and OTKA No. F7634/1993. Special thanks are due to Dr. Jan Plicka (UVVVR, Prague, Czech Republic) and Dr. László Várady (PerSeptive Biosystems, Cambridge, MA, USA) for donating the Separon HEMA and the POROS PH columns, respectively. The technical assistance of Mrs. Katalin Fazekas is greatly appreciated.

References

[1] M.T.W. Hearn, in Cs. Horváth (Editor), *High Performance Liquid Chromatography —Advances and perspectives*, Vol. 3, Academic Press, New York, 1983, p. 87.

[2] M.A. Stadalius and L.R. Snyder, in Cs. Horváth (Editor), *High Performance Liquid Chromatography —Advances and Perspectives*, Vol. 3, Academic Press, New York, 1986, p. 195.

[3] F.E. Regnier, *Science*, 238 (1987) 319.

[4] C.T. Mant and R.S. Hodges, in K. Gooding and F.E. Regnier (Editors), *High Performance Liquid Chromatography of Biological Macromolecules: Methods and Applications*, Marcel Dekker, New York, 1989, p. 1101.

[5] J.L. Fausnaugh, L.A. Kennedy and F.E. Regnier, *J. Chromatogr.*, 317 (1984) 141.

[6] R.E. Shansky, S.L. Wu, A. Figueroa and B.L. Karger, in K. Gooding and F.E. Regnier (Editors), *High Performance Liquid Chromatography of Biological Macromolecules: Methods and Applications*, Marcel Dekker, New York, 1989, p. 95.

[7] L. Szepesy and G. Rippel, *LC·GC Int.*, 5, No. 11 (1992) 24.
[8] Cs. Horváth, W.R. Melander and I. Molnár, *J. Chromatogr.*, 469 (1989) 3.
[9] W.R. Melander and Cs. Horváth, *Arch. Biochem. Biophys.*, 183 (1977) 200.
[10] W.R. Melander, D. Corradini and Cs. Horváth, *J. Chromatogr.*, 317 (1984) 67.
[11] J.L. Fausnaugh and F.E. Regnier, *J. Chromatogr.*, 359 (1986) 131.
[12] W.R. Melander, Z. El Rassi and Cs. Horváth, *J. Chromatogr.*, 469 (1989) 3.
[13] A. Katti, Y.F. Maa and Cs. Horváth, *Chromatographia*, 24 (1987) 646.
[14] N.T. Miller and B.L. Karger, *J. Chromatogr.*, 326 (1985) 45.
[15] S.L. Wu, A. Figueroa and B.L. Karger, *J. Chromatogr.*, 371 (1986) 3.
[16] L. Szepesy and Cs. Horváth, *Chromatographia*, 26 (1988) 13.
[17] L. Szepesy and G. Rippel, *Chromatographia*, 34 (1992) 391.
[18] L. Szepesy and G. Rippel, *J. Chromatogr. A*, 668 (1994) 337.
[19] G. Rippel and L. Szepesy, *J. Chromatogr. A*, 664 (1994) 27.
[20] D.L. Gooding, M.N. Schmuck and K.M. Gooding, *J. Chromatogr.*, 296 (1984) 107.
[21] Z. El Rassi and Cs. Horváth, *J. Liq. Chromatogr.*, 2 (1986) 3245.
[22] N. Cooke, P. Shieh and N. Miller, *LC·GC Int.*, 3, No. 1 (1990) 9.
[23] Z. El Rassi, L.F. De Ocampo and M.D. Bacolod, *J. Chromatogr.*, 499 (1990) 141.
[24] J.C. Berridge, *The Techniques for the Automated Optimization of HPLC Separation*, Wiley, New York, 1985.
[25] P.J. Schoenmakers, *Optimization of Chromatographic Selectivity —a Guide to Method Development*, Elsevier, Amsterdam, 1986.
[26] Sz. Nyiredy (Editor), special issue on Optimization of Mobile Phase, *J. Liq. Chromatogr.*, 12, Nos. 1 and 2 (1989).
[27] J.L. Glajch and L.R. Snyder (Editors), Special volume on Computer-Assisted Method Development for High-Performance Liquid Chromatography, *J. Chromatogr.*, 485 (1989); reprinted as a book, Elsevier, Amsterdam, 1990.
[28] L.R. Snyder and J.W. Dolan, *LC·GC Int.*, 3, No. 10 (1990) 28.
[29] A. Drouen, J.W. Dolan, L.R. Snyder, A. Poile and P.J. Schoenmakers, *LC·GC Int.*, 5, No. 2 (1992) 28.
[30] B.F.D. Ghrist, B.S. Cooperman and L.R. Snyder, *J. Chromatogr.*, 459 (1988) 1.
[31] B.F.D. Ghrist and L.R. Snyder, *J. Chromatogr.*, 459 (1988) 25.
[32] B.F.D. Ghrist and L.R. Snyder, *J. Chromatogr.*, 459 (1988) 43.
[33] B.F.D. Ghrist, L.R. Snyder and B.S. Cooperman, in K. Gooding and F.E. Regnier (Editors), *High Performance Liquid Chromatography of Biological Macromolecules: Methods and Applications*, Marcel Dekker, New York, 1989, p. 403.
[34] R.C. Chloupek, W.S. Hancock and L.R. Snyder, *J. Chromatogr.*, 594 (1992) 65.
[35] G. Rippel, A. Alattyani and L. Szepesy, *J. Chromatogr.*, 668 (1994) 301.
[36] J.L. Glajch, J.J. Kirkland, K.M. Squire and J.M. Minor, *J. Chromatogr.*, 199 (1980) 57.
[37] J.L. Glajch, J.C. Gluckman, J.G. Charikofsky, J.M. Minor and J.J. Kirkland, *J. Chromatogr.*, 318 (1985) 23.
[38] P.E. Antle, A.P. Goldberg and L.R. Snyder, *J. Chromatogr.*, 321 (1985) 1.
[39] L.R. Snyder and M.A. Stadalius, in Cs. Horváth (Editor), *High Performance Liquid Chromatography —Advances and Perspectives*, Vol. 4, Academic Press, New York, 1986, p. 195.
[40] J.L. Glajch and J.J. Kirkland, *Anal. Chem.*, 54 (1982) 2593.
[41] J.J. Kirkland and J.L. Glajch, *J. Chromatogr.*, 255 (1983) 27.
[42] J.L. Glajch and J.J. Kirkland, *J. Chromatogr.*, 485 (1989) 51.
[43] P. Jandera, J. Churacek and H. Colin, *J. Chromatogr.*, 214 (1981) 35.
[44] P. Jandera, *J. Liq. Chromatogr.*, 12 (1989) 117.
[45] P. Jandera, *J. Chromatogr.*, 485 (1989) 421.
[46] P. Jandera, *J. Liq. Chromatogr.*, 14 (1991) 3125.
[47] K. Valkó and P. Slégel, *J. Chromatogr.*, 631 (1993) 49.

ELSEVIER

Journal of Chromatography A, 697 (1995) 31–43

JOURNAL OF CHROMATOGRAPHY A

Expert system for the ion chromatographic determination of alkali and alkaline earth metals in mineral waters

N. Gros, B. Gorenc*

Department of Chemistry and Chemical Technology, University of Ljubljana, 61000 Ljubljana, Slovenia

Abstract

The main limiting factors (the highest concentration that may be injected, the lowest concentrations that can be determined, attainable quality of results and limitations arising from the interfering effects of ions in much higher concentrations) that could prevent the successful suppressed ion chromatographic determination of lithium, sodium, ammonium, potassium, magnesium, calcium and strontium in any particular mineral water were obtained experimentally and organized into three databases supporting the operation of an expert system. The expert system permits the planning of appropriate dilutions, the prediction of suitable detector output ranges, the planning of the appropriate standard additions or concentrations of calibration solutions necessary for the successful quantitative analysis and predicts interferences for the determination of individual ions in particular real samples. The predictions of the expert system were checked experimentally on two different natural samples. All the predictions were realistic and, although very simple calculations were used by the expert system, appropriate distinction between different extents of interferences was achieved. The described expert system works well and offers significant support to the planning of the analysis of different natural mineral waters.

1. Introduction

In contrast to the suppressed ion chromatographic determination of anions, there are relatively few applications for the determination of both alkali and alkaline earth cations in natural waters. However, the development of a cation self-regenerating suppressor [1] and a novel Dionex IonPac CS12 column which permits the simultaneous isocratic determination of lithium, sodium, ammonium, potassium, magnesium, calcium and strontium and shows better sodium–ammonium and ammonium–potassium selectivity than previous columns [2,3] promises good opportunities also for more diverse and more complicated samples such as mineral waters. Mineral waters from central Europe [4] represent an extensive group of natural samples with very different total concentrations of dissolved solids (at least 1 g/l) and different concentrations and concentration proportions between individual ions. Sodium, potassium, magnesium and calcium can be present at concentrations up to several grams per litre. In an individual mineral water, one or a few of these cations usually predominate significantly, the others being present at concentrations from a few to several orders of magnitude lower. In the analysis of such samples with any analytical technique, the question of how the constituents present at

* Corresponding author.

0021-9673/95/$09.50
SSDI 0021-9673(94)0952-X

higher concentrations affect the determination of those present at lower concentrations plays a very important role and determines the extent to which a particular mineral water can be analysed with a selected analytical method.

Our previous computer programs [5,6], which were intended to facilitate the determination of anions in different natural waters, can also be helpful in the planning of the determination of cations in mineral waters, provided that an adequate experimentally based database for cations is first added. However, in these procedures each ion is considered as being the only one in the solution, and the answer to the question of the extent to which a particular mineral water can be analysed using suppressed ion chromatography cannot be given.

The aim of this work was to establish the limiting factors that could prevent the successful determination of all seven cations (lithium, sodium, ammonium, potassium, magnesium, calcium and strontium) in natural mineral waters and to develop the structure of an expert system that would consider these limiting factors in the planning of the most appropriate dilutions and other experimental conditions and that would be able to predict the extent to which any particular mineral water can be successfully analysed using suppressed ion chromatography.

2. Experimental

2.1. Apparatus and experimental conditions

The Dionex (Sunnyvale, CA, USA) Model 4000i ion chromatographic apparatus consisted of an IonPac CG12 guard column and IonPac CS12 separation column (diameter of macroporous particles 8.0 μm, ethylvinylbenzene cross-linked with 55% divinylbenzene, carboxylic functionality, capacity 2800 μequiv. per column), a cation self-regenerating suppressor (4 mm) and a Dionex conductimetric detector II (CMD). The injection volume was 25 μl and the eluent flow-rate was 1.0 ml/min. A spectra-Physics (San Jose, CA, USA) SP 4290 integrator was used.

2.2. Reagents and procedures

Stock standard solutions of cations were prepared at a concentration of 1 g/l from analytical-reagent grade chemicals using deionized water obtained from a Milli-Q water-purification system (Millipore, Bedford, MA, USA). A stock standard solution of the eluent with a concentration of 1 mol/l was prepared from 98% methanesulphonic acid purchased from Merck-Schuchardt (Hohenbrunn bei München, Germany) and an eluent containing 20 mmol/l methanesulphonic acid was prepared daily from it.

Hydrochloric acid (Titrisol) of concentration 100 mmol/l was purchased from Merck (Darmstadt, Germany) and was used for the neutralization of hydrogencarbonate in mineral waters.

2.3. Basic experiment

We intended to build up an experimentally based database that would enable one to estimate how, in different mineral waters, the predominant ions (sodium, potassium, calcium or magnesium) would affect the determination of other cations. In order to cover the many different concentration proportions with the smallest possible number of experimental steps, the experiment was divided into two separate parts. The results of the first part simulate chromatographic peaks that could interfere with the chromatographic peaks of analyte ions (simulated in the second part of the experiment).

Detector output ranges between 0.1 and 10 μS were used in the first part of the experiment. The solutions of potentially interfering cations (sodium, potassium, magnesium and calcium) were injected not only with the detector output range suitable for the determination of individual cations but also at lower detector output ranges. About 380 experiments were carried out; the concentration ranges of individual ions are summarized in Table 1 (experiment A).

The second experiment covered all six useful detector output ranges between 0.03 and 10 μS. For each detector output range a solution with

Table 1
Concentration ranges of ions in individual experiments

Ion	c (mg/l)			
	Experiment A	Experiment B	Experiment C	Experiment D
Li^+	–	0.0054–1.17	1.00–9.40	4.00–39.0
Na^+	0.018–9.20	0.011–3.73	4.00–32.0	16.0–142
NH_4^+	–	0.016–7.50	6.00–24.0	10.0–150
K^+	0.053–15.6	0.033–10.6	12.0–82.0	10.0–360
Mg^{2+}	0.013–8.89	0.072–2.50	2.00–20.0	8.00–106
Ca^{2+}	0.030–15.9	0.006–8.74	2.00–16.0	5.00–180
Sr^{2+}	–	0.069–22.9	17.0–136	60.0–620

appropriate concentrations of all seven cations was prepared. The concentration ranges of individual ions covered with these experiments are summarized in Table 1 (experiment B).

2.4. Linearity for lower concentrations of cations

Some preliminary investigations [7] of the repeatability of the measurements of peak areas and peak heights of all seven cations at detector output ranges from 0.03 to 10 μS showed higher relative standard deviations for the results obtained at the lowest two detector output ranges. Experiments carried out previously with anions showed that only five out of seven anions can be determined at a detector output range of 0.1 μS and only two at a detector output range of 0.03 μS. Therefore, the existence of the linear relationship between peak area or peak height and the concentrations of all seven cations had to be checked for the two lowest detector output ranges. Each experiment was carried out with at least eight solutions with different concentrations and each solution was injected at least twice. The concentration ranges of individual ions are summarized in Table 1 (experiment C was performed at a detector output range of 0.03 μS and experiment D at a detector output range of 0.1 μS). Although some correlation factors (r) were not extremely high (between 0.9541 and 0.9982 for a detector output range of 0.03 μS and between 0.9866 and 0.9996 for 0.1 μS), linear relationships between peak area or peak height and concentration were realized in all instances (in contrast to the experience with anions).

3. Results and discussion

3.1. Limiting factors and databases

There are mostly four types of limiting factors that determine the extent to which a particular mineral water can be successfully analysed: the highest concentration that can be injected, the lowest concentrations that can be determined, the expected quality of results and limitations arising from the interfering effects of ions in much higher concentrations. Limiting factors and the data necessary for the planning of quantitative analyses are collected in the database QUANTDET. The databases INTERFER and SPECIALC are useful for the estimation of interfering effects.

The database QUANTDET contains six different parameters. Following the producer's recommendation not to inject more than 10 nmol of any one analyte [8], the upper concentration limits (cmax) for all seven ions were calculated (Table 2). Other parameters given in Table 2 are the highest concentrations (cmaxDOR) that can

Table 2
Main limiting factors for the planning of quantitative analysis of mineral waters: maximum concentrations that may be injected (*c*max), the highest concentrations (*c*maxDOR) for individual DOR (μS), the lowest concentrations that were successfully injected (*c*min) and the limits of detection (LOD) (all concentrations are in mg/l)

Parameter	Li^+	Na^+	NH_4^+	K^+	Mg^{2+}	Ca^{2+}	Sr^{2+}
*c*max	2.78	9.20	7.22	15.6	9.72	16.0	35.1
*c*min	0.0010	0.0040	0.0060	0.0120	0.0020	0.0020	0.01
LOD	0.0005	0.0047	0.0052	0.0130	0.0041	0.0021	0.01
DOR (μS)	*c*maxDOR						
10	4.23[a]	12.5[a]	24.3[a]	35.0[a]	8.67	30.5[a]	79.3[a]
3	1.26	4.16	6.02	11.0	2.65	8.80	23.2
1	0.43	2.35	2.30	3.72	0.73	2.84	7.24
0.3	0.14	0.38	0.48	1.15	0.24	0.81	2.26
0.1	0.039	0.142	0.17	0.36	0.106	0.18	0.62
0.03	0.0094	0.032	0.030	0.082	0.020	0.016	0.136

[a] Only theoretically (higher than *c*max).

be successfully detected in individual detector output ranges (DOR), the lowest concentrations that were successfully injected (*c*min) and limits of detection (LOD), calculated as proposed in the statistical literature [9], from standard errors of the estimate ($s_{y/x}$) and from the slopes of regression lines obtained on the lowest detector output range (0.03 μS). These data are essential for the planning of appropriate dilutions and for the estimation of their effects on the possibility of the determination of ions at lower concentrations, and they offer the possibility of the prediction of detector output ranges and of the planning of the appropriate standard additions or concentrations of calibration solutions necessary for successful quantitative analysis. The data on the relative standard deviations for the repeated measurement of peak area (RSDarea) and peak heights (RSDheight) [7] can serve to give an approximate orientation about the quality of results that can be expected for each individual ion in each particular case.

The database INTERFER contains ten different parameters:

t(begin) = time at which the chromatographic peak of the analyte ion starts;

t(rt) = retention time of the chromatographic peak of the analyte ion;

t(end) = time at which the chromatographic peak of the analyte ion ends;

c-interf = concentration of potentially interfering ion;

*t*l(0) = time at which potentially interfering chromatographic peak begins;

*t*r(0) = time at which potentially interfering chromatographic peak ends;

*t*r(1) = time at which the right edge of potentially interfering chromatographic peak reaches 2.35% of total scale (PTS);

*t*r(2) = time at which the right edge of potentially interfering chromatographic peak reaches 10% of total scale (PTS);

*t*r(3) = time at which the right edge of potentially interfering chromatographic peak reaches 50% of total scale (PTS);

*t*r(4) = time of the last point at which potentially interfering chromatographic peak extends over 100% of total scale.

This database contains about 1000 data. The essential parameters describing the chromatographic peak of the analyte ion and the interfering chromatographic peak are represented in

Fig. 1. Five additional parameters can be calculated:

PTS(begin) = percentage of total scale at which the analyte chromatographic peak begins;

PTS(rt) = percentage of total scale at which the analyte chromatographic peak appears;

PTS(end) = percentage of total scale at which the analyte chromatographic peak ends;

NOVERLAP = percentage of peak width of the analyte ion that is not overlapped with the chromatographic peak of the interfering ion;

RTNOVERL = percentage of peak width between the end of the chromatographic peak of the interfering ion and the retention time of the chromatographic peak of the analyte ion.

The relationships for their calculation are as follows:

$$\mathrm{PTS}(x) = \mathrm{PTS}(j) - \frac{[\mathrm{PTS}(j) - \mathrm{PTS}(j-1)][t(x) - tr(j)]}{tr(j-1) - tr(j)} \quad (1)$$

$j = 0,1,2,3,4$; (a) x = begin, PTS(begin) = PTS(x); (b) x = rt, PTS(rt) = PTS(x) + PTS,

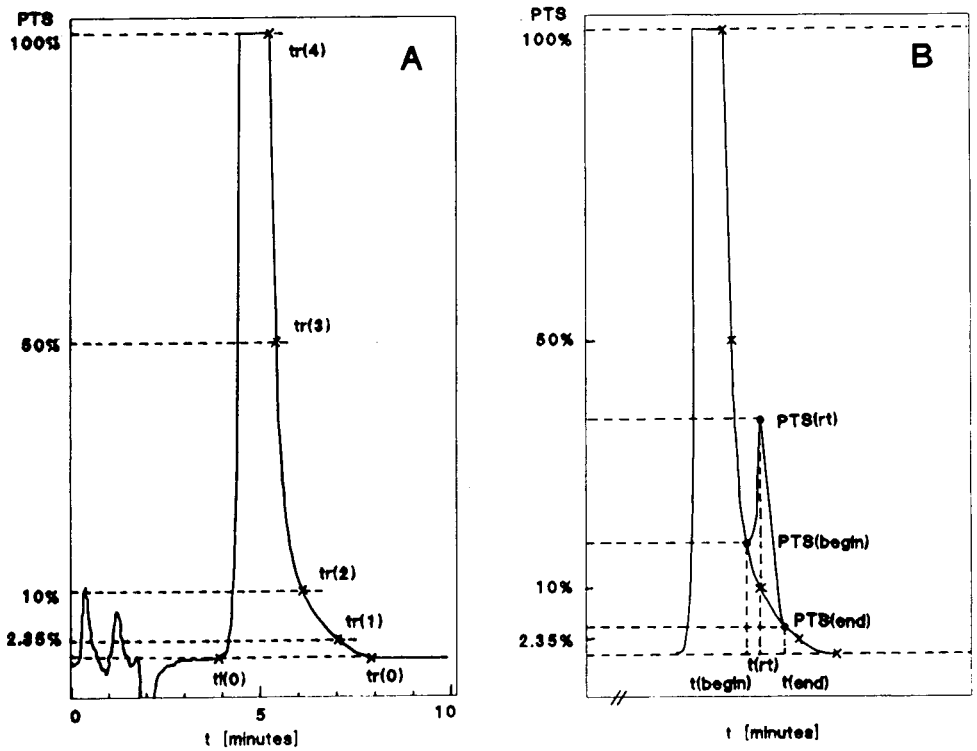

Fig. 1. Graphical representation of the main data collected in the database INTERFER that permit the calculation of the parameters PTS(begin), PTS(rt), PTS(end), NOVERLAP and RTNOVERL for the distinction between different extents of interference between ions. PTS = percentage of total scale; $tl(0)$ = time at which interfering chromatographic peak begins; $tr(0)$ = time at which interfering chromatographic peak ends; $tr(1)$ = time at which the right edge of the chromatographic peak reaches 2.35% of the total scale (PTS); $tr(2)$ = time at which the right edge of the chromatographic peak reaches 10% of the total scale (PTS); $tr(3)$ = time at which the right edge of the chromatographic peak reaches 50% of the total scale (PTS); $tr(4)$ = time at the last point at which the chromatographic peak extends over 100% of the total scale; t(begin) = time at which the analyte chromatographic peak starts; t(rt) = retention time of the analyte chromatographic peak; t(end) = time at which the analyte chromatographic peak ends; PTS(rt) = percentage of total scale at which the chromatographic peak appears; PTS(begin) and PTS(end) = percentage of total scale at which the chromatographic peak begins or ends.

PTS = 100 c/cmaxDOR, c = concentration of ion in injected sample; (c) x = end, PTS(end) = PTS(x).

$$\text{NOVERLAP} = 100 \cdot \frac{t(\text{end}) - tr(0)}{t(\text{end}) - t(\text{begin})} \quad (2)$$

$$\text{RTNOVERL} = 100 \cdot \frac{t(\text{rt}) - tr(0)}{t(\text{end}) - t(\text{begin})} \quad (3)$$

These five parameters were introduced in order to permit the simple distinction between different extents of overlapping between an interfering ion and the ion of interest in any real sample. A = related algorithm is described later (Figs. 5 and 6), but in order to facilitate understanding, the roles of individual parameters are explained here. In each particular case, t(begin) of the analyte ion is selected from the database on the basis of a previously predicted DOR suitable for the determination of this cation. The end of the potentially interfering chromatographic peak $tr(0)$ relating to c-interfer that is the nearest to the concentration expected in the sample is also selected from the database. The comparison of these two parameters [t(begin) and $tr(0)$] shows if there is any interference between the two chromatographic peaks, otherwise an interval for the switching of the detector output ranges can be given. The comparison of t(end) of the analyte chromatographic peak and $tr(0)$ shows if the peak width of the analyte ion at the baseline partially or completely overlaps with the interfering ion. If the former is true, parameter NOVERLAP (Eq. 2), describing the extent of interference, can be calculated. The comparison of t(rt) and $tr(0)$ shows if an interfering ion affects the measurement of the peak height of the analyte ion. If not, then calculation of RTNOVERL (Eq. 3) gives the percentage of the peak width of the analyte ion between the end of the interfering peak and the retention time of the determining ion. Calculation of PTS(begin), PTS(rt) and PTS(end) ensures additional insight into the extent of interfering effects. The largest extent can be expected if PTS(begin) exceeds PTS(rt). In this instance determining ion cannot even be observed and overlap with the interfering ion is complete. Appropriate data for the calculation of these parameters (Eq. 1) are selected from the database: the first time that it is lower and the first time that it is higher [tr(j) and $tr(j-1)$; j =

Table 3
Database SPECIALC

Conditions	Parameter	DOR (μS)						
		0.03		0.1	0.3		1	3
A[a]	PTS(begin) (%)	7.75		–	–		–	–
	NOVERLAO (%)	68.2		–	–		–	–
	RTNOVERL (%)	15.2		–	–		–	–
B[b]	PTS(end) (%)	2.35		6.18	21.7	(13.2)[c]	–	1.42
	NOVERLAP (%)	99.0		88.3	83.6	(82.1)[c]	–	91.5
	RTNOVERL (%)	47.5		41.1	40.3	(38.9)[c]	–	50.8
C[d]	PTS(begin) (%)	69.7	(27.1)[e]	1.48	–		–	–
	PTS(end) (%)	15.1		–	–		–	–
	NOVERLAP (%)	–	(58.8)[e]	86.6	–		–	–
	RTNOVERL (%)	–		33.0	–		–	–

[a] $K^+ \rightarrow Ca^{2+}$; c-interf = 15.6 mg/l.
[b] $Mg^{2+} \rightarrow K^+$; c-interf = 8.89 mg/l.
[c] c-interf = 7.46 mg/l.
[d] $Mg^{2+} \rightarrow Sr^{2+}$; c-interf = 8.89 mg/l.
[e] c-interf = 7.46 mg/l.

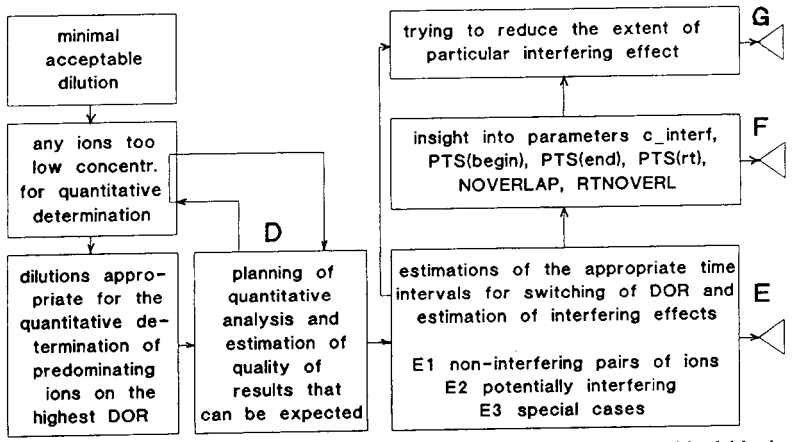

Fig. 2. Structure of the expert system and the main functions of individual blocks.

0,1,2,3,4] than t(begin) or t(rt) or t(end) are used.

Each of the four potentially interfering ions (sodium, potassium, magnesium and calcium) most significantly interferes with ions that follow immediately, e.g., sodium interferes with ammonium, potassium with magnesium, magnesium with calcium and calcium with strontium. The interferences that have a very limited extent (only a few c-interf and only a few DOR) are covered as special cases. This significantly reduced the size of the database INTERFER. A much smaller database (SPECIALC) with already calculated parameters PTS(begin), PTS(end), NOVERLAP and RTNOVERL was introduced. It is summarized in Table 3.

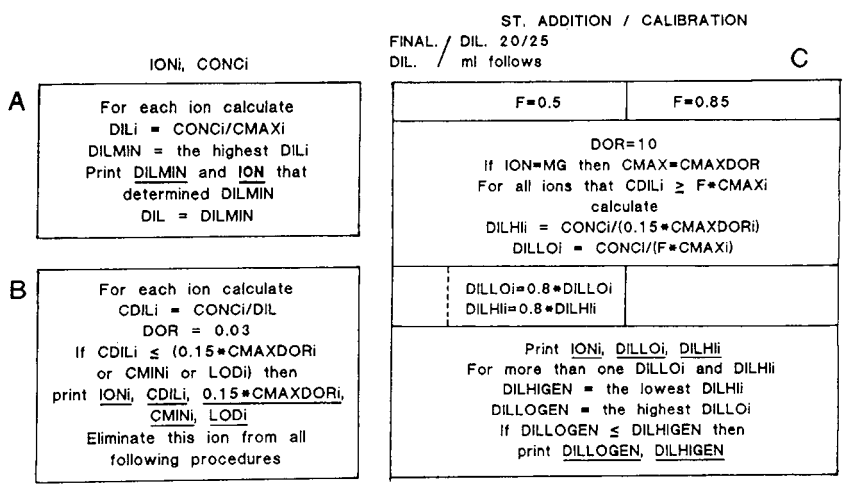

Fig. 3. Main operations of blocks A, B and C. The input data for block A are approximate concentrations (CONCi) of individual ions (IONi). For the operation of block C, selection between method of standard additions and method of calibration function (ST. ADDITION/CALIBRATION) has to be done first. If the first option was selected there is also the distinction between the case in which dilution means the final dilution (FINAL. DIL) and the case in which further dilution connected with standard additions follows (DIL. 20/25 ml follows; 20 ml of already diluted sample introduced into a 25-ml volumetric flask). All other data necessary for the operation of these three blocks are obtained from the database QUANTDET.

3.2. Expert system

Operations relating to experimentally obtained data collected in the three databases QUANTDET, INTERFER and SPECIALC were already briefly considered above, but the complete structure of the expert system and the main functions of individual blocks are represented in Fig. 2. The detailed structure and operation of the seven blocks are represented in Figs. 3–6. Input data are represented at the top of an individual block and other data are selected from the appropriate databases. The database necessary for the operation of an individual block is specified below each figure. In the structure of each block, output data are underlined. In order to allow an understanding of the operation of the expert system, the meanings of some additional variables are given as follows:

c1 = minimal concentration of calibration solution (mg/l),

*c*dil = concentration of ion after dilution (mg/l);

*c*n = maximum concentration of calibration solution (mg/l);

conc = approximate concentration of the ion in the sample (mg/l);

DIL = dilution;

DILHI = highest possible dilution for determination of ion on DOR = 10;

DILHIGEN = highest general dilution appropriate for all ions that have to be determined on DOR = 10;

DILLO = lowest possible dilution for determination of ion on DOR = 10;

DILLOGEN = lowest general dilution appropriate for all ions that have to be determined on DOR = 10;

DILMAX = maximum acceptable dilution for determination of an ion;

F = factor that determines the maximum concentration that can be successfully determined in a selected detector output range;

MINDIL = minimum dilution that does not cause overloading of the column;

MIX = maximum possible increase in concentration (mg/l) for the determination of an ion by the method of standard additions;

SWITCHIN = time interval (minutes) for switching of DOR between two ions.

The main function of block A is to find the ion that most significantly exceeds the maximum allowed concentration (*c*max) and to calculate minimum dilution (DILMIN) that appropriately decreases its concentration. Block B offers the possibility of checking whether the concentration of any ion after dilution became too low for determination and excludes such an ion from all further procedures. Dilutions (DILLO, DILHI) appropriate for the determination of the predominant ions on the highest DOR are predicted using block C. If there are more ions that have to be determined on DOR = 10 μS, block C also

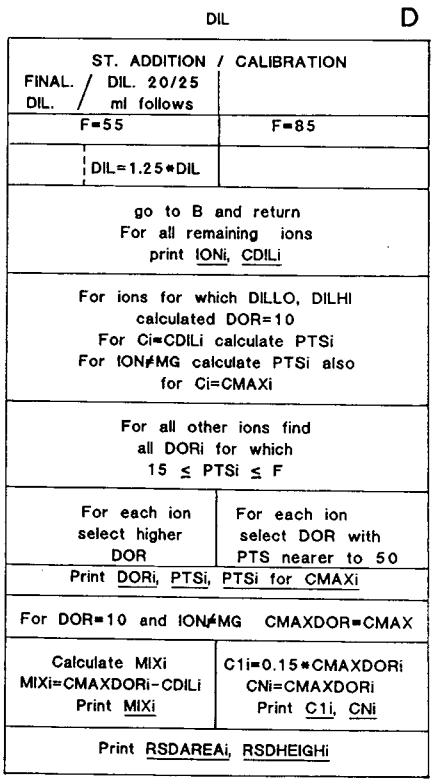

Fig. 4. Main operations of block D. Dilution has to be selected first. Other data are introduced from the database QUANTDET. The relationship PTS = 100*c*/*c*maxDOR is used for the calculation of the percentage of total scale at which the chromatographic peaks of individual ions appear using selected detector output ranges; *c* means the concentration of an ion in the injected sample.

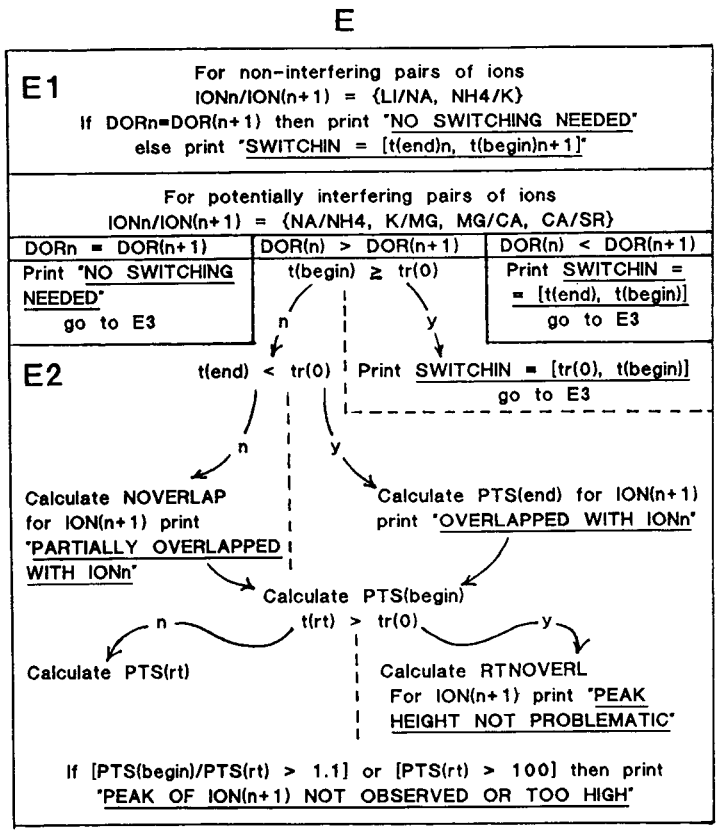

Fig. 5. Main operations of the first two parts (E1, E2) of block E. The database INTERFER is used. Eqs. 1–3 for the calculation of the parameters PTS(begin), PTS(rt), PTS(end), NOVERLAP and RTNOVERL were described in Section 3.1.

tries to find general dilutions (DILLOGEN, DILHIGEN) appropriate for all of them. There is a distinction between the method of calibration function and the method of standard additions. For the method of standard additions the specification of dilution means final dilution or if there is another step in which the concentration of ions is further reduced [20 ml of diluted sample introduced into a volumetric flask (25 ml), standard additions for individual ions added and then diluted with deionized water to 25 ml]. On the basis of the suggestions about suitable dilutions, the most appropriate dilution (DIL) can be selected and introduced into block D. This block finds the most suitable detector output ranges for the determination of individual ions, suggests appropriate standard additions (MIX) or concentrations of calibration solutions ($c1$, cn), and reports the relative standard deviations for the measurement of areas or heights of chromatographic peaks of individual ions in selected detector output ranges (RSDarea, RSDheigh). Block E permits the prediction of time intervals useful for switching between different detector output ranges during elution and estimates if there are any interfering effects caused by large differences in concentrations of individual ions. It classifies the interferences of different extents. Block F offers an insight into parameters that were calculated in the previous block and that permitted classification. The main function of block G is to check if increased dilution reduces a particular interfering effect.

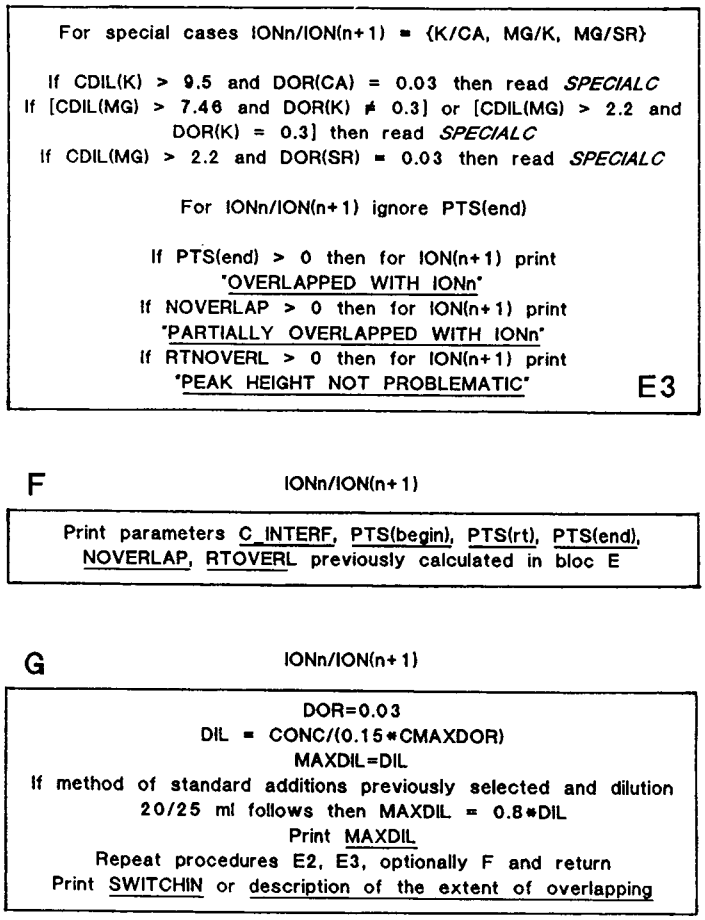

Fig. 6. Main operations of blocks E3, F and G. Blocks F and G are optional and pairs of ions in which one is interested have to be defined first. The database SPECIALC permits the operation of block E3. Block F utilizes data calculated in block E. Data for the operation of block G are obtained from the database QUANTDET.

3.3. Real mineral water samples

Two real samples, mineral water with the trade-name Petanjski Vrelec and mineral water from the bore-hole V-P (both from the health resort Radenska, Radenci, Slovenia), with different compositions and different total mineralization were selected, in order to illustrate the operation of the described expert system. We tried to cover all functions of the expert system so at the beginning of block C the method of calibration function was selected for Petanjski Vrelec and the method of standard additions (with dilution from 20 to 25 ml) for sample V-P. Approximate concentrations of individual ions (input data) and predictions for Petanjski Vrelec are summarized in Table 4. Table 5 gives the data for sample V-P. There are significant differences between the two predictions. In the former instance, sodium determines the necessary minimum dilution (DILMIN), in the latter calcium. DILMIN for sample V-P is more than ten times lower than DILMIN for Petanjski Vrelec. After minimum dilution the concentrations of all ions in sample V-P are high enough for determination. At the unavoidable minimum dilution strontium cannot be detected in Petanjski Vrelec mineral water.

Table 4
Predictions for natural mineral water Petanjski Vrelec obtained by the expert system

(A) DILMIN = 70 *Ion = Na*

(B) Concentration of Sr too low
cdil(Sr) = 0.014 mg/l 0.15cmax = 0.020 mg/l
cmin = 0.017 mg/l LOD = 0.016 mg/l

(C) Dilutions appropriate for quantitative determination of predominant ions at DOR 10 μS
Ion = Na DILLO = 83 DILHI = 345

(D) Dilution DIL = 200

Parameter	Li	Na	NH_4	K	Mg	Ca
cdil (mg/l)	0.002	3.23	0.012	0.33	0.25	0.78
DOR (μS)	0.03	10	0.03	0.3	1	1
PTS (%)	21.3	25.8	40.0	28.7	34.2	27.5
PTS (cmax) (%)	–	73.6	–	–	–	–
c1 (mg/l)	0.0014	1.38	0.005	0.17	0.11	0.43
cn (mg/l)	0.0094	9.20	0.03	1.15	0.73	2.84
RSDarea (%)	12.1	0.6	11.3	4.8	1.1	1.1
RSDheigh (%)	4.6	0.4	10.5	4.7	0.5	0.7

(E)

SWITCHIN (min)	(3.55, 3.67)	(5.20, 5.36)	(6.70, 6.70)	No switching needed
Ion	(Lower c-interf)	(Higher c-interf)		
NH_4	Partially overlapped with NA	Overlapped with Na, peak of NH_4 not observed or too high		

(F) ION = NH_4

c-interf	PTS(begin)	PTS(rt)	PTS(end)	NOVERLAP	RTOVERL
1.80	36.7	45.0	–	25.0	–
3.30	108	86.8	7.7	–	–

The main input data for the operation of the expert system were approximate concentrations of individual ions 0.41 mg/l for lithium, 646 mg/l for sodium, 2.30 mg/l for ammonium, 65.0 mg/l for potassium, 49.5 mg/l for magnesium, 155 mg/l for calcium and 1.00 mg/l for strontium.

Dilutions appropriate for the determination of sodium in Petanjski Vrelec water in the detector output range 10 μS extend from 83- to 345-fold and for further predictions we decided to use a 200-fold dilution (input data for block D). In the mineral water V-P two ions, calcium and magnesium, have to be determined at DOR = 10 μS. General dilutions appropriate for both of them are between 8.9- and 16-fold; we selected a tenfold dilution for further work. Only for the determination of lithium predicted in block D was the detector output range the same (0.03 μS) for both samples; for all others it differed.

Block E reports time intervals for switching of the detector output ranges between lithium and sodium, between ammonium and potassium and between potassium and magnesium for Petanjski Vrelec mineral water and between lithium and sodium and between potassium and magnesium for sample V-P. In both instances no switching is needed between magnesium and calcium and for sample V-P also between ammonium and potassium. Block E estimates that ammonium in sample V-P partially overlaps with sodium. The greatest interference with calcium is observed for strontium and there is also interference with

Table 5
Predictions for natural mineral water V-P obtained by expert system

(A) *DILMIN = 5.6* *Ion = Ca*

(C) *Dilutions appropriate for quantitative determination of predominant ions at DOR 10 μS*

Ion = Mg	DILLO = 6.2	DILHI = 21
Ion = Ca	DILLO = 8.9	DILHI = 16
	DILLOGEN = 8.9	DILHIGEN = 16

(D) *Dilution DIL = 10*

Parameter	Li	Na	NH_4	K	Mg	Ca	Sr
cdil (mg/l)	0.0048	0.88	0.04	0.16	2.69	7.11	0.036
DOR (μS)	0.03	3	0.1	0.1	10	10	0.03
PTS (%)	52.1	21.2	23.5	40.4	31.0	23.3	26.5
PTS (cmax) (%)	–	–	–	–	–	51.8	–
MIX (mg/l)	0.0046	3.28	0.13	0.20	5.98	8.89	0.100
RSDarea (%)	12.1	1.2	11.0	4.6	0.8	0.8	9.4
RSDheigh (%)	4.6	1.0	6.7	2.7	0.4	0.5	7.1

(E)

SWITCHIN (min)	(3.55, 3.67)	No switching needed	(6.58, 6.68)	No switching needed
Ion	(Lower *c* interf)		(Higher *c*-interf)	
NH_4	Partially overlapped with NA		Partially overlapped with NA	
Sr	Overlapped with Ca, peak of Sr not observed or too high Overlapped with Mg		Overlapped with Ca, peak of Sr not observed or too high Overlapped with Mg	

(G)

Sr	Overlapped with Ca, peak of SR not observed or too high		Overlapped with Ca, peak of Sr not observed or too high	
MAXDIL = 17.6				

The main input data for the operation of the expert system were approximate concentrations of individual ions 0.06 mg/l for lithium, 11.0 mg/l for sodium, 0.5 mg/l for ammonium, 2.0 mg/l for potassium, 33.6 mg/l for magnesium, 88.9 mg/l for calcium and 0.45 mg/l for strontium.

magnesium (one of the few special cases from the database SPECIALC).

In order to estimate the possibility of decreasing these interfering effects, block G was activated. However, although at the maximum dilution acceptable for the determination of strontium, the extent of interference remains the same. Also in mineral water V-P strontium could not be detected, although its concentration is not below the limit of detection as it is in Petanjski Vrelec mineral water.

The estimates of the extent of the interfering effect of sodium on ammonium obtained from two *c*-interfer, the closest to the approximate concentration of sodium in diluted Petanjski Vrelec sample (the next higher and the next lower concentration), do not agree. In order to find out which one represents a better approximation of real situation, block F was used. The value *c*-interfer = 3.30 is very close to cdil = 3.23, so it is more realistic to expect greater interference that would certainly prevent the determination of ammonium.

The predictions for both mineral waters were checked in the experiments under predicted conditions. The chromatograms are shown in

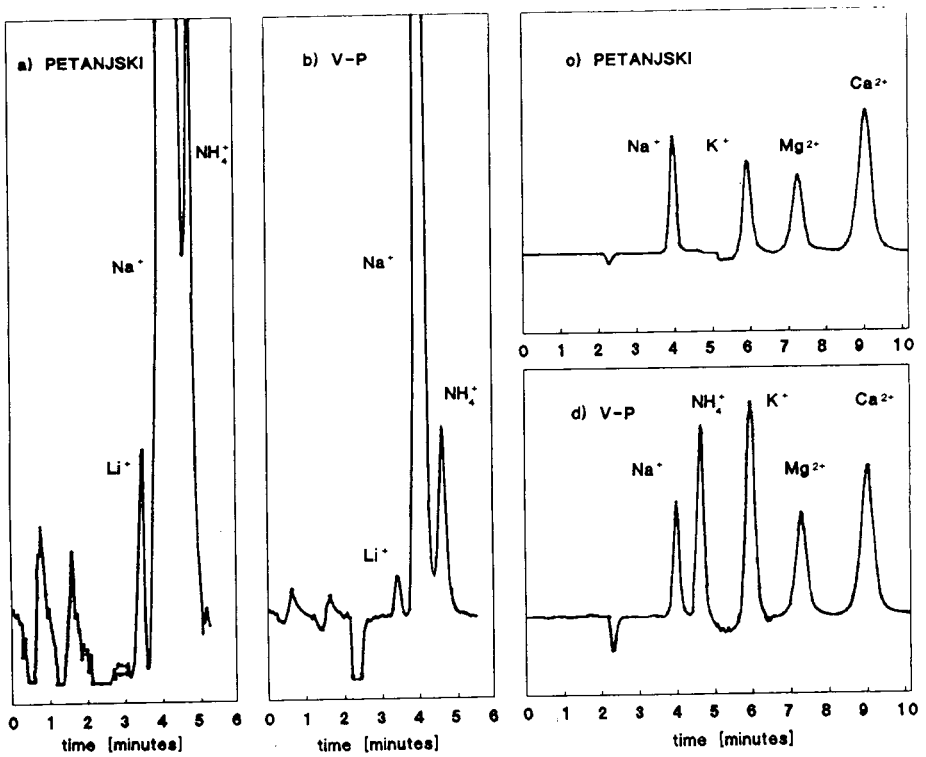

Fig. 7. Chromatograms of two different natural mineral waters obtained under conditions predicted by the expert system. Sample Petanjski Vrelec was diluted 200-fold and sample V-P 10-fold. The eluent was methanesulphonic acid at a concentration of 20 mmol/l. Chromatograms (a) and (b) were obtained with detector output ranges (DOR) 0.03 and 0.1 μS, respectively; in the other two cases DOR was switched during elution in accordance with the predictions summarized in Tables 4 and 5. The sequence was DOR = 10 μS for sodium, 0.3 μS for potassium and 1 μS for magnesium and calcium in (c) and DOR = 3 μS for sodium, 0.1 μS for ammonium and potassium and 10 μS for magnesium and calcium in (d).

Fig. 7. All the predictions were realistic and although very simple calculations were used [parameters PTS(begin), PTS(rt), PTS(end), NOVERLAP, RTNOVERL], appropriate distinctions between different extents of interferences were achieved.

The described expert system works well and offers significant support to the planing of the analysis of different natural mineral waters and prevents wastage of time and efforts to find solutions in situations that are unresolvable under the conditions involved.

References

[1] S. Rabin, J. Stillian, V. Barreto, K. Friedman and M. Toofan, *J. Chromatogr.*, 640 (1993) 97.

[2] D. Jensen, J. Weiss, M.A. Rey and C.A. Pohl, *J. Chromatogr.*, 640 (1993) 65.

[3] *Dionex Ion Exchange Columns: IonPac CS12 Sales manual*, Dionex, Sunnyvale, CA, 1992.

[4] W. Carlé, *Die Mineral und Thermalwasser von Mittel Europa*, Wissenchaftliche Verlagsgeselschaft, Stuttgart, 1975.

[5] N. Gros and B. Gorenc, *Chromatographia*, 36 (1993) 251.

[6] N. Gros and B. Gorenc, *J. Chromatogr. A*, 668 (1994) 385.

[7] N. Gros and B. Gorenc, *Chromatographia*, 39 (1994) 448.

[8] *Installation Instructions and Troubleshooting Guide for the IonPac CG12 Guard Column and IonPac CS12 Analytical Column*, Dionex, Sunnyvale, CA, 1992, Document 034657, p. 12.

[9] J.C. Miller and J.N. Miller, *Statistics for Analytical Chemistry*, Ellis Horwood, Chichester, 3rd ed., 1993, p. 115.

ELSEVIER

Journal of Chromatography A, 697 (1995) 45–52

JOURNAL OF CHROMATOGRAPHY A

Performance of reversed-phase parallel-current open-tubular liquid chromatography columns and comparison with theory

Marie Horká*, Vladislav Kahle, Miloš Krejčí, Karel Šlais

Institute of Analytical Chemistry, Academy of Sciences of the Czech Republic, Veveří 97, 611 42 Brno, Czech Republic

Abstract

The capillary column performance in reversed-phase parallel-current open-tubular liquid chromatography (RP-PC-OTLC) was studied with the use of cyclohexanol–water. The reduced retention and the height equivalent to a theoretical plate were studied as a function of the liquid velocity and the content of cyclohexanol in the capillary at constant column temperature. The effect of microemulsion formation on band broadening and retention is discussed. The plate heights obtained were compared with the Golay equation.

1. Introduction

In conventional capillary columns used widely in GC, LC or SFC, the inner surface of open capillaries of circular cross-section is coated with a uniform film of stationary phase. There is only one flow conduit in the tube. For an idealized model, the separation efficiency can be expressed with the help of the Golay equation [1]. For real capillaries, the stationary phase film tends to distribute non-uniformly on the wall, which causes some deviation from the simple theory [2].

In parallel-current open-tubular liquid chromatography (PC-OTLC) [3–6], both the mobile phase and the surface layer move in the same direction, but with different velocities. According to the idealized model [3], the ratios of the flow-rates and viscosities of the two phases determine the thickness and the velocity of the retentive layer. Further, it was found [4] that some minimum average velocity of the mobile phase is necessary for the maintenance of annular flow of the retentive liquid. The magnitude of this minimum velocity, termed here the critical velocity, is dependent on the interfacial tension between the two liquids. In PC-OTLC experiments [3–6], a two-phase flow was generated by a decrease in the solubility of the retentive liquid at the capillary inlet. This can be conveniently achieved by having a difference in the temperature of the liquid entering the capillary and the capillary temperature.

As the reversed-phase (RP) mode of LC is frequently used, we have examined [4] the relevant properties of some partially water–soluble organic liquids potentially suitable as retentive phases in RP-PC-OTLC. Of the compounds examined, cyclohexanol appeared to be the most promising retentive liquid.

Finally, the properties of the capillary inner surface also influence the thickness and distribution of the retentive layer on the inner surface and, consequently the separation efficiency [4]. According to the model used [3], varying the concentration of retentive liquid and/or the solution temperature should be useful for controlling the phase ratio in the capillary. How-

* Corresponding author.

0021-9673/95/$09.50
SSDI 0021-9673(94)00931-7

ever, temperature variations in the solution containing partially water-soluble organic liquids can generate dispersion systems, including microemulsions [7,8]. Further, one of the most commonly encountered complications affecting the homogeneity of capillary flow is that arising from variations in the solid–liquid interfacial tension in the system [8]. Liquid flow at a surface arising from surface tension gradients is commonly refered as Marangoni flow [7–9]. In multicomponent systems, surface tension gradients usually arise as a result of adsorption-related phenomena [8].

In order to evaluate the possibilities of controlling the method performance, we studied here the solute retention and dispersion characteristics in RP-PC-OTLC as a function of the mobile phase velocity and concentration of cyclohexanol in the liquid entering the capillary. A method for calculation of the axial zone dispersion in a cylindrical capillary with two flowing concentric annular layers was suggested by Gill [10]. However, this approach leads to equations that are too complicated for practical use. As, under the conditions examined here, the retentive layer is thin and its average velocity is only a small fraction of the mobile phase velocity, the contribution to the dispersion in the retentive phase caused by its flow was neglected for the first approximation. Therefore, the plate height found was compared with the Golay equation, in which actual solute retention characteristics and layer thickness were incorporated.

2. Calculations

In open-tubular chromatography with an immobile, uniformly distributed retentive layer, the capillary performance can be described with help of the Golay equation [1]:

$$H = 2D_M/u_M + [(1 + 6k + 11k^2)R^2/24(1 + k)^2 D_M + 2kd_f^2/3(1 + k)^2 D_R]u_M \quad (1)$$

where H is the height equivalent to a theoretical plate, R is the inner radius of the capillary column, u_M is the linear velocity of the mobile phase, D_M and D_R are the diffusion coefficients of solutes in the mobile and retentive phase, respectively, d_f is the thickness of the retentive phase film and k is the capacity ratio of the solute for the immobile retentive layer. The plate height is related to the width of the Gaussian zone by the equation $H = L/(t_{ri}/\sigma_i)^2$, which can be used for the calculation of H from the chromatogram. The capacity ratio can be related to the retention time of the analyte, i, in a capillary with an immobile retentive phase, t_i, and the elution time of the unretained compound, t_0, as $k = t_i/t_0 - 1$. On the other hand, k is related to the analyte distribution constant, K_i, and phase ratio, $\phi = S_R/S_M$, as $k = \phi K_i$, where S_R and S_M are the cross-sections of the retentive and mobile phase, respectively.

As the retentive phase flow influences the analyte retention, the term reduced retention, k_i^*, was introduced for the description of retention in PC-OTLC [3]. For practical reasons, it can be related, similarly to k, to the retention time of the solute in the capillary with a mobile retentive phase, t_{ri}, and t_0 as

$$k_i^* = t_{ri}/t_0 - 1 \quad (2)$$

The relation of k_i^* to the phase cross-section ratio, ϕ, and to the liquid–liquid distribution constant of the solute, K_i, was found as [3]

$$k_i^* = (\phi - q)/(1/K_i + q) \quad (3)$$

where q is the flow ratio of the retentive and mobile phases, $q = F_R/F_M$. As long as the temperature-induced changes in the liquid solubility are used for the generation of the two-phase flow, q may be related to the difference between the mass fraction of the retentive phase dissolved in the liquid entering the capillary, w, and the mass fraction of the dissolved retentive liquid in the mobile phase saturated by this liquid at the capillary temperature, w_T. Provided that F_R is less than 1% of F_M, q can be written simply as

$$q = F_R/F_M = \Delta w/(1 - \Delta w) \quad (4)$$

where

$$\Delta w = w - w_T \quad (5)$$

It can be seen from Eqs. 4 and 5 that both w determined by the composition of the inlet liquid and w_T determined by the column temperature can be used for the control of q. As the capillary temperature also influences other important parameters, including the viscosity and the surface tension [4,6], the variation in w seems to have the simplest relation to the capillary performance.

Based on the solubility and viscosity values, the phase ratio can be calculated as [3]

$$\phi = S_R/S_M = (1 - t + 1/\Delta w)/\{1/\Delta w - [1 + t(1/\Delta w - 1)]^{1/2}\} - 1 \quad (6)$$

where t is the viscosity ratio of the retentive and the mobile phases, respectively, $t = \eta_R/\eta_M$. Alternatively, the phase ratio can be calculated from Eq. 3 when k_i^*, K_i and q are known. The amount of the retentive phase in the capillary can also be visualized as the thickness of the retentive layer, d_f, which can be expressed with the help of Eq. 3 as

$$d_f = R\{1 - 1/[1 + k_i^*/K_i + q(k_i^* + 1)]^{1/2}\} \quad (7)$$

Alternatively to the description of the retention in terms of k_i^*, the capacity factor, k_i', defined similarly as in micellar electrokinetic capillary chromatography (MECC), was suggested [11]. Thus, $k_i' = \phi K_i$, which is simpler than Eq. 3. However, when calculating k_i' from the chromatogram, the following equation should be used [11]:

$$k_i' = (t_{ri} - t_o)/t_o(1 - t_{ri}/t_r) \quad (8)$$

which indicates the need to know the retention time of the compound completely dissolved in the retentive phase, t_r. The relationship of the last variable to other characteristics may be expressed as [11,12]

$$u_R/u_M = q/\phi = t_o/t_r \quad (9)$$

where u_R and u_M are the average linear velocities of the retentive and the mobile phase, respectively. Thus, the smaller q/ϕ is, the larger is the t_r value obtained and k_i' is closer to both k and k_i^*. On the other hand, reading t_r from the chromatogram becomes more difficult owing to the dispersion of the zone of the compound used as the tracer of u_R.

3. Experimental

3.1. Capillary preparation

Fused-silica capillaries of 0.2 mm O.D. and 35 μm I.D. were purchased from Laboratory of Chemistry of Glass and Ceramic Materials (Academy of Sciences of the Czech Republic, Prague, Czech Republic). A Simax-type glass tube (Kavalier, Sázava, Czech Republic) of 7 mm O.D. and 0.6 mm I.D. was drawn using a glass-drawing machine to obtain a glass capillary of 0.7 mm O.D. and 17 μm I.D. The internal surface of capillaries were twice modified with D_4 reagent [4]. The length of the capillaries used in PC-OT-LC experiments was 4–5 m.

3.2. Chromatograph

The chromatographic system used has been described previously [13]. A VCM 300 micropump (Development Works, Czechoslovak Academy of Sciences, Prague, Czech Republic) was used. The sample was injected using a laboratory-made six-port valve with a 20-μl loop and a flow splitter. The splitting ratio was 1:3500 or 1:7500. The capillary column was immersed in a water-bath connected with a U8 thermostat (MLW Prüfgeräte-Werk, Medingen/Sitz Freital, Germany). The column was maintained at 50.0°C. For on-column fluorimetric detection we adapted [6] a Kratos FS 950 fluorimeter (Schoeffel Instruments). The excitation wavelength was 254 nm and the emission wavelength was 320 nm. An EMD 10 electrochemical detector (Laboratory Instruments, Prague, Czech Republic) was equipped with a thin-layer microcell similar to that described previously [14]. The detector signal was monitored with a TZ 4100 line recorder (Laboratory Instruments).

3.3. Mobile phase

The pumped liquid was water with a known concentration of cyclohexanol. The solubility difference between the concentration of the retentive phase in the mobile phase in the pumped liquid and the concentration of the retentive phase in the mobile phase at the column temperature, Δw, was in the range 0.01–0.96 wt.%.

3.4. Chemicals and test solutes

The model analytes were salicylic acid (marker of the dead time, t_o), hydroquinone, phenol and carbazole. The test solutes and other chemicals used were purchased from Lachema (Brno, Czech Republic). D_4 reagent was obtained from VCHZ Synthezia (Kolín, Czech Republic). The viscosity ratio of coexisting liquids in the cyclohexanol–water system at 50°C, $t = 7.0$, was taken from Ref. [3]. The solute distribution constant K_i between coexisting cyclohexanol and water phases was taken from Ref. [3]. The K_i values for phenol and hydroquinone at 50°C were 16.7 and 4.9, respectively. The logarithm of the octanol–water distribution constant of carbazole is reported to be 3.29 [15]; a similar value is expected for the cyclohexanol–water system. The diffusion coefficients of solutes in the retentive and mobile phases, D_R and D_M, respectively, for phenol are $D_M = 4.5 \cdot 10^{-3}$ mm^2 s^{-1} and $D_R = 4.4 \cdot 10^{-4}$ mm^2 s^{-1} [4].

3.5. Measurements

The measurements were carried out in a linear velocity range from 1.0 up to 37 mm s^{-1}. The linear velocity of the mobile phase was determined from the retention time of salicylic acid (t_o) and the capillary length. The test solutes for the determination k_i^* and H were hydroquinone and phenol. The k_i^* values used in place of k in the Golay equation were determined from Eq. 2. The value of d_f was calculated from K_i, k_i^* and q with the use of Eq. 7. The values of u_c and d_f used are the averages from the values obtained with both test solutes [4]. Care was taken to use an arrangement of the instrumentation that does not affect the measurements owing to the extra-column band broadening [13,16]. Thus, the observed peak widths and calculated plate heights can be considered as the result of the processes within the capillary.

4. Results and discussion

4.1. Retention phase velocity

The average linear velocity of the retentive layer was determined both from the dead time, viscosity and solubility data and from the retention of carbazole. Carbazole was chosen owing to its suitable detection characteristics and high hydrophobicity. Therefore, Eq. 9 can be used for the estimation of u_R with sufficient precision. For the fused-silica capillary and the pumped liquid with $\Delta w = 0.81$ wt.% and $u_M = 8.33$ mm s^{-1}, $u_R = 0.31$ mm s^{-1} was found from the evaluation of t_o and t_r. Similarly, $u_R = 0.35$mm s^{-1} was found for $\Delta w = 0.51$ wt.% and $u_M = 12.5$ mm s^{-1}. These values of u_R are comparable with the u_R values 0.28 and 0.33 mm s^{-1}, respectively, which were obtained from q and ϕ values calculated from the solubility and viscosity data using Eqs. 4–6. Together with the previously reported values of ϕ and q [3], the values presented here indicate that, in the system studied, the contribution of the retentive layer to the total flow in the capillary is less than 1%. Thus, when using the Golay equation for the calculation of the theoretical plate height, the error due to neglecting the retentive layer flow can be expected to be within a few per cent of the calculated value. Further, the similar values obtained in different ways support the assumption of the existence of a flowing annular retentive layer under the conditions specified.

4.2. Retention and the plate height in RP-PC-OTLC

The performance of the system studied was evaluated from the k_i^* vs. u_M and H vs. u_M dependences for several values of Δw and for

phenol as solute (Figs. 1–5). In the graphs shown, line 1 (○) represents plate height, H_1, values calculated from the observed retention time of the peak, the peak variance and the capillary length, line 2 (●) represents H_2 values calculated from Golay equation for immobile films with the use of actual k_i^* and d_f values and line 3 (▽) corresponds to k_i^* calculated from the retention times. In all of the figures, a marked decrease in k_i^* can be observed at certain u_M values. This phenomenon was also observed previously [4,6] and was ascribed to the disturbance of the flow of the retentive layer due to the predominance of the surface tension forces over the viscous flow. The velocity at which the decrease in k_i^* occurs was termed the critical velocity, u_c [4]. The observed u_c values and k_i^* corresponding to u_c, k_{ic}^*, are summarized in Table 1. It can be seen that the solute retention

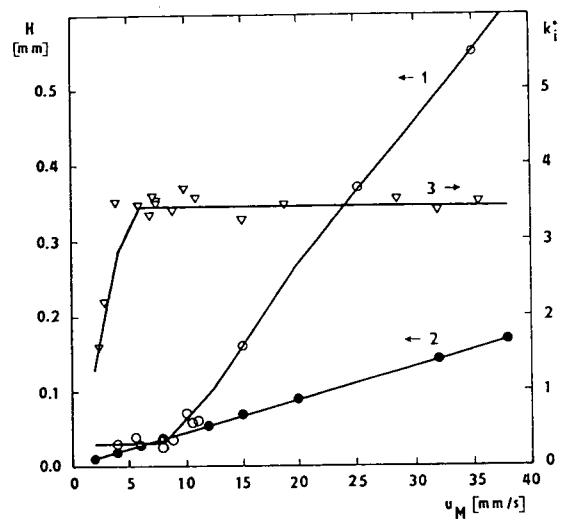

Fig. 1. Dependence of H_1, H_2 and k_i^* on u_M for phenol in RP-PC-OTLC in a glass capillary column. Conditions: 4 m × 0.017 mm I.D. glass capillary modified using D_4 reagent; column temperature, 50°C; pumped liquid, 100 mmol l^{-1} $NaClO_4$ and 1 mmol l^{-1} acetic acid in water saturated at 20°C with cyclohexanol ($\Delta w = 0.96$ wt.%); solutes, salicylic acid (dead time marker) and phenol; splitting ratio, 1:7500; mobile phase velocity, $u_M = 2$–38 mm s^{-1}; electrochemical detection. Line 1 (○) = H_1 values calculated from observed retention time of the peak, variance of the peak and capillary length; line 2 (●) = H_2 values calculated from the Golay equation for immobile films from k_i^* and d_f; line 3 (▽) = reduced retention k_i^* for phenol calculated from retention time.

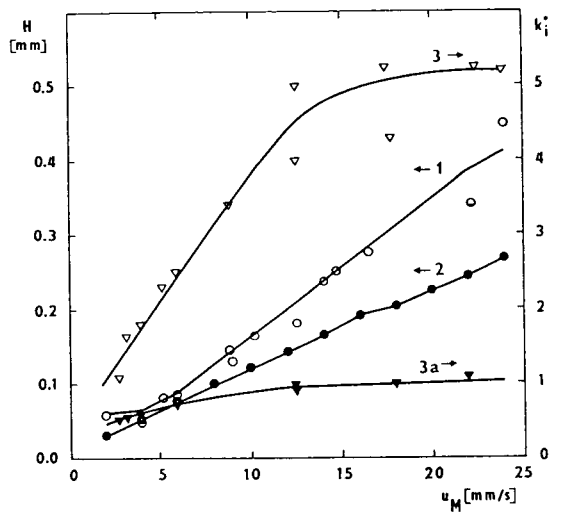

Fig. 2. Dependence of H_1, H_2 and k_i^* for phenol on u_M in RP-PC-OTLC in a fused-silica capillary column. Conditions: 5 m × 0.035 mm I.D. fused-silica capillary modified with D_4 reagent; column temperature, 50°C; pumped liquid, water saturated with cyclohexanol at 20°C, corresponding to $\Delta w = 0.96$ wt.%; solutes, salicylic acid (dead time marker), hydroquinone and phenol; splitting ratio, 1:3500; linear velocity of mobile phase flow, $u_M = 1$–38 mm s^{-1}; fluorimetric detection. Line 3a (▼) = reduced retention k_i^* for hydroquinone calculated from retention time. Other symbols as in Fig. 1.

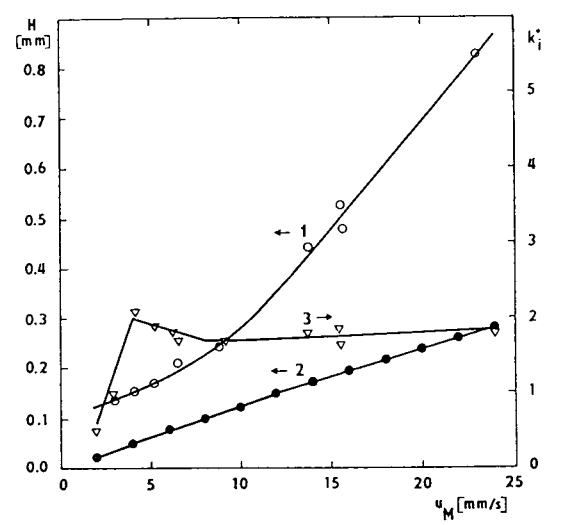

Fig. 3. Dependence of H_1, H_2 and k_i^* for phenol on u_M with $\Delta w = 0.31$ wt.%. Other conditions and symbols as in Fig. 2.

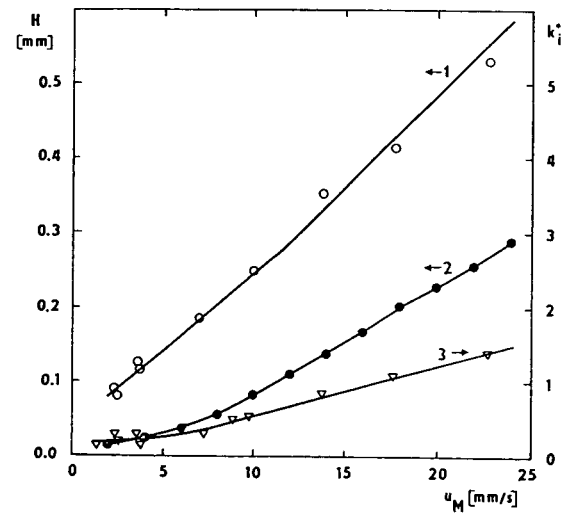

Fig. 4. Dependence of H_1, H_2 and k_i^* for phenol on u_M with $\Delta w = 0.11$ wt.%. Other conditions and symbols as in Fig. 2.

can be efficiently controlled by the amount of the retentive phase introduced at the capillary inlet.

Based on the comparison of u_c, k_{ic}^* and d_f values in Table 1, and also from the dependence of k_i^* and H on u_M, it can be concluded that the flow pattern depends strongly on Δw. As indicated in the Introduction, cyclohexanol is partially soluble in water [3,17] and may form a

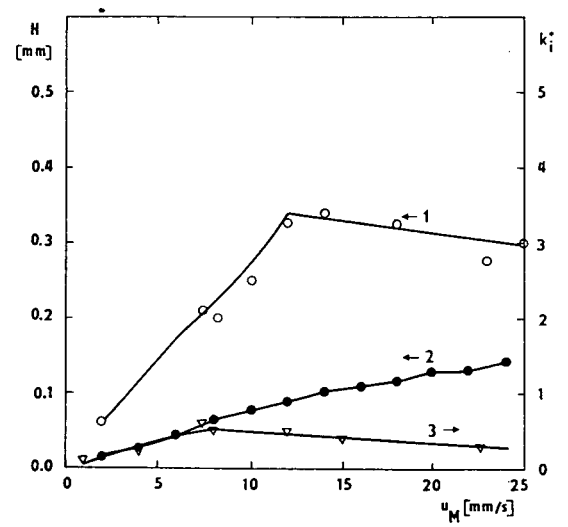

Fig. 5. Dependence of H_1, H_2 and k_i^* for phenol on u_M with $\Delta w = 0.01$ wt.%. Other conditions and symbols as in Fig. 2.

Table 1
Dependence of u_c and k_{ic}^* for phenol, ϕ and d_f for glass and fused-silica capillaries on the concentration of cyclohexanol in the pumped liquid

Capillary column	Δw (wt.%) (Eq. 5)	u_c (mm s^{-1})	k_i^* (Eq. 2)	ϕ (Eq. 6)	d_f (μm) (Eq. 7)
Glass	0.96	4.8	3.40	0.235	0.8
Fused silica	0.96	12.2	4.40	0.315	2.2
	0.51	7.5	3.10	0.206	1.6
	0.31	3.0	1.30	0.084	0.7
	0.11	5.7	0.30	0.019	0.2
	0.01	7.9	0.52	0.031	0.2

dispersion system with water [7,8]. Therefore, we examined the properties of the dispersion of cyclohexanol–water in macroscopic volume (cylinder 100 ml) at the temperature of the capillary (Fig. 6). The time dependence of the amount of the fraction of cyclohexanol in the emulsion droplets, w_e, is shown. This quantity was evaluated from w_T, the amount of the sedimented cyclohexanol-rich layer, and several values w in the range 0.01–0.96 wt.%. An increase in temperature from 20 to 50°C leads to

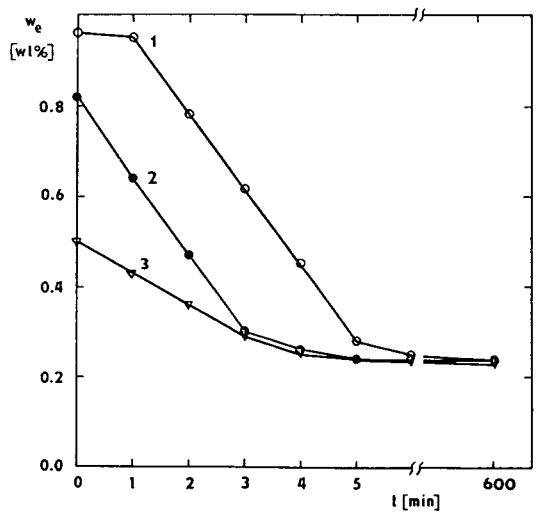

Fig. 6. Characterization of cyclohexanol–water solutions at a column temperature of 50°C. w_e (wt.%) = Concentration of cyclohexanol in the microemulsion at 50°C (macrovolume experiment); t = time (min). Δw = (1) 0.96, (2) 0.81 and (3) 0.51 wt.%. For explanation, see text.

a decrease in the solubility of cyclohexanol [17] and an emulsion appears. The amount corresponds to Δw given by Eq. 5. Then, the emulsion content decreases, which can be followed from the amount of sedimented layer. It follows from Fig. 6 that a microemulsion can exist for up to 10 h. After that time, the amount of cyclohexanol in the form of microemulsion droplets is w_e = 0.24 wt.% (see Fig. 6). Similar behaviour can also be expected in the capillary. However, the time for the sedimentation of the cyclohexanol liquid layer should be expected to decrease according to the characteristic dimension, which is about 1000 times smaller in the capillary. For $\Delta w = 0.11$ and 0.01 wt.%, the amount of cyclohexanol in the solution appears to be insufficient for the formation of a long-term stable microemulsion.

In order to visualize the departure of the observed H_1 from the calculated H_2 as a function of u_M around u_c, the relative values of the height equivalent to a theoretical plate, $h_r (= H_1/H_2)$, on the relative velocity of the mobile phase, $v_r (= u_M/u_c)$, were plotted in Fig. 7. At $v_r > 2.5$, $h_r = 2$–3 for all Δw values studied. Hence the capillary performance is not very different from the proposed model. At $v_r < 2.5$, h_r is in the range 1–2 for $\Delta w = 0.96$ wt.% (open circles) and $\Delta w = 0.51$ wt.% (closed circles). Similarly to the above conditions, a regular annular layer should be present. For $\Delta w = 0.31$, 0.11 and 0.01% (squares and open and closed triangles in Fig. 7, respectively) and $v_r < 2.5$, h_r increases markedly with decrease in v_r. Hence, the dispersion is far greater than predicted by Golay equation and a regular surface layer can no longer be expected. Additionally, k_{ic}^* decreases with decrease in Δw, but for the lowest Δw examined it is higher than for $\Delta w = 0.11$ wt.% (see Table 1).

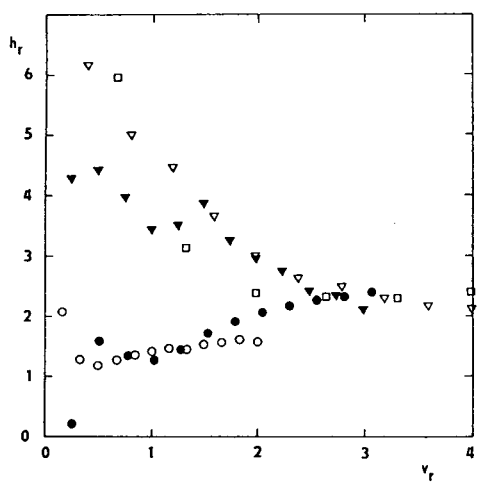

Fig. 7. Dependence of the relative height equivalent to a theoretical plate, h_r, on relative mobile phase velocity, v_r. Δw = (●) 0.96, (○) 0.51, (□) 0.31, (▽) 0.11 and (▼) 0.01 wt.%.

The above observations can probably be explained as follows. Above u_c, the mobile phase velocity is sufficient to maintain the regular annular shape of the retentive layer with cross-section determined by Eqs. 4–6. For u_M close to u_c and lower, the retentive layer becomes unstable so that the amount of retentive liquid in the layer decreases [3]. Depending on Δw, two limiting cases may occur:

(1) When Δw is large enough for the existence of the microemulsion (i.e., more then about 0.24 wt.% here), the part of the retentive liquid that is above the amount remaining in the layer can move as microemulsion droplets. Both the microemulsion and a decrease in the annular cross-section lead to a considerable decrease in k_i^*. On the other hand, the contact of the microemulsion droplets with the surface continuously smooths the irregularities in the surface layer. Similarly to the transport of the solute in the micellar systems [18], the existence of microemulsion droplets does not seriously impair the diffusion transport of the analyte. Thus, with decrease in v_M, h_r remains constant or decreases to approach unity.

(2) When Δw is small so that an appreciable amount of microemulsion cannot appear, the part of the retentive liquid that is not retained on the surface moves in the form of large droplets or, at very low velocities, in the form of segments. As mentioned previously [3], such conditions approach close to segmented liquid–liquid flow analysis. Simultaneously, owing to the capillary surface irregularities, the retentive liquid remaining on the surface is no longer in the form of a regular annular layer. Naturally, the zone dispersion increases markedly owing to both phenomena. The absence of a microemul-

sion also decreases the transport of the solute by the mobile phase so that the decrease in k_i^* is smaller. Additionally, as the surface coverage is low, the properties of the inner capillary surface strongly influence the regularity of the surface film of the retentive liquid.

As the liquid system within the capillary is under continuous movement, the microemulsion content probably differs from that observed under the stationary conditions. Nevertheless, the suggested model should be useful for the qualitative explanation of the discussed phenomena.

5. Conclusions

Above the critical velocity of the mobile phase, the performance of RP-PC-OTLC can be explained in terms of the model comprising the regular flowing surface layer of the retentive liquid. While the plate height is comparable to the values given by the Golay equation, the solute retention can be controlled by the amount of the retentive phase introduced at the top of the capillary column.

The behaviour of PC-OTLC with the mobile phase velocity below its critical value can be explained in terms of the suggested model involving the formation of a microemulsion. Owing to the high retention and efficiency, the system examined with a larger amount of the retentive liquid promises a better capillary performance.

References

[1] M.J. Golay, in D.H. Desty (Editor), *Gas Chromatography*, (Butterworths, London, 1958), p. 36.
[2] J.C. Giddings, *Unified Separation Science*, Wiley, New York, 1991.
[3] K. Šlais, M. Horká and K. Klepárník, *J. Chromatogr.*, 605 (1992) 167.
[4] K. Šlais and M. Horká, *J. Microcol. Sep.*, 5 (1993) 63.
[5] K. Šlais and M. Horká, *J. High Resolut. Chromatogr.*, 16 (1993) 194.
[6] M. Horká, V. Kahle and K. Šlais, *J. Chromatogr. A*, 660 (1994) 187.
[7] L.M. Prince, *Microemulsions Theory and Practice*, Academic Press, New York, 1977.
[8] D. Myers, *Surfaces, Interfaces, and Colloids, Principles and Applications*, VCH, New York, 1991.
[9] M. Krejčí, *Trace Analysis with Microcolumn Liquid Chromatography (Chromatographic Science Series*, Vol. 59), Marcel Dekker, New York, 1992.
[10] W.N. Gill, *AIChE J.*, 15 (1969) 745.
[11] P.G.H.M. Muijselaar and C.A. Cramers, *J. Microcol. Sep.*, 5 (1993) 187.
[12] K. Šlais, M. Horká and K. Klepárník, *J. Microcol. Sep.*, 5 (1993) 189.
[13] K. Janák, M. Horká and M. Krejčí, *J. Microcol. Sep.*, 3 (1991) 203.
[14] K. Šlais and M. Krejčí, *J. Chromatogr.*, 235 (1982) 21.
[15] A. Leo, C. Hansch and D. Elkins, *Chem. Rev.*, 71 (1971) 525.
[16] K. Janák, M. Horká and M. Krejčí, *J. Microcol. Sep.*, 3 (1991) 115.
[17] R. Stephenson and J. Stuart, *J. Chem. Eng. Data*, 31 (1986) 56.
[18] S. Terabe, K. Otsuka and T. Ando, *Anal. Chem.*, 61 (1989) 251.

ELSEVIER

Journal of Chromatography A, 697 (1995) 53–58

JOURNAL OF CHROMATOGRAPHY A

Effect of some mobile phase additives on the retention characteristics of different solute types on reversed-phase media. II

S.D. McCrossen[a], C.F. Simpson[b,*]

[a] *Analytical Sciences, SmithKline Beecham Pharmaceuticals, Old Powder Mills, Tonbridge, Kent TN11 9AN, UK*
[b] *Department of Chemistry, Birkbeck College, Gordon House, 29 Gordon Square, London WC1H 0PP, UK*

Abstract

In this paper, the use of aliphatic additives for mediating the retention characteristics of general solutes on reversed-phases using high-performance liquid chromatography is described. Aliphatic nitrile compounds have been investigated as potential mobile phase additives in simple mobile phases consisting of organic modifier–water mixtures. A range of amine solutes have been chromatographed at various levels of additive concentration on commercial bonded reversed-phases and their retention characteristics compared. Satisfactory separations were only obtained when additives such as valeronitrile and hexanenitrile were used in the mobile phase. The additives were effective in dramatically reducing peak tailing using a range of mobile phase compositions and commercial reversed-phases. The results obtained show that relatively small amounts of additive can cause significant changes in retention and can significantly improve the chromatography of organic amines.

1. Introduction

Reversed-phase high-performance liquid chromatography on bonded-phase silica is the preferred means of separating polar and non-polar solutes. The most common form of bonded-phase is silica covalently bonded with alkyl ligands. The retention characteristics of a reversed-phase are governed by the number of ligands bonded to the silica and the number of non-bonded surface silanol groups. The relative number of bonded-phase to silanol groups is dependent on the nature of the silica substrate, the chemical structure of the alkyl ligand and the chemistry of the bonding process.

Large differences in chromatographic retention can be observed between commercial columns and between different batches of the same brand of column packing. Marked differences were noted between some commercial C_{18} columns in a recent comparative investigation [1].

In particular, polar compounds, e.g. acids and amines, have been shown to be difficult to chromatograph satisfactorily on reversed-phases which have a high proportion of residual silanol groups [2,3]. The choice of a suitable column for any application is a difficult one and still relies on the experience and judgement of the analyst. However, some chromatographic tests can be carried out to ascertain the nature and retention character of reversed-phases [4–6].

Methods of circumventing the problem of column irreproducibility have been sought, e.g. the method of dynamically modifying silica. An

* Corresponding author.

0021-9673/95/$09.50
SSDI 0021-9673(94)00953-8

in-situ coating of stationary phase can be created on the silica surface by using mobile phase additives, usually polar long-chain aliphatic compounds, that are adsorbed on to the silica surface. The column takes on the retention characteristics of a reversed-phase. A reproducible 'reversed' phase can thus be created on any type of silica provided that equilibrium is achieved [7]. An analogous approach to eliminate column variability by using mobile phase additives to modify bonded-phases has been investigated by Lau and Simpson [8]. Aliphatic compounds having different functional groups may be used to modify the retention characteristics of the bonded-phase and has been demonstrated by a number of applications [8–11].

This investigation focuses on the use of aliphatic nitrile compounds as additives in reversed-phase high-performance liquid chromatography and supplements investigations previously carried out by the authors [10].

2. Experimental

A Hewlett-Packard 1090M HPLC system (Stockport, UK) was used. Data were collected at 10 points per second and reduced using the Waters 860 Expert Ease data system (Millipore, Watford, UK). HPLC grade methanol, acetonitrile and tetrahydrofuran (Romil Chemicals, Loughborough, UK) and purified water were used for the investigations. All chemicals were of analytical grade (Aldrich, Gillingham, UK). Chromatographic separations were performed on Spherisorb C_8, 3 μm, 3 cm × 4.6 mm I.D. columns (Phase Separations, Deeside, UK); Ultrasphere C_{18}, C_8, and CN 3 μm, 7.5 cm × 4.6 mm I.D. columns (Beckman, Fullerton, USA); and a Brownlee Velosep C_8, 4 cm × 3.2 mm I.D. column (Applied Biosystems, San Jose, CA, USA) thermostatted at 40°C. The flow-rate was 1.00 ± 0.02 ml/min and detection was UV at 254 nm (6 mm pathlength flow-cell). An Erma CR Model ERC-7515A refractive index detector (Tokyo, Japan) was used to determine retention time of the additives. The injection volume was 1.0 μl and replicates performed as necessary. Base-solvents consisting of organic modifier–water mixtures were prepared in fixed weight ratios. Mobile phases were then prepared from known weights of base-solvents and additive. Mobile phases were degassed with helium before use. The test solutes aniline, N-methylaniline, and N,N-dimethylaniline (pK_a values 4.6, 4.8 and 5.2, respectively) were prepared in methanol, acetonitrile and tetrahydrofuran at 0.5 mg/ml concentration. For refractive index measurements solutes were prepared in mobile phase at ca. 1 mg/ml concentration. Dead volume measurements were determined with sodium nitrate dissolved in base-solvent (ca. 0.02 mg/ml) at 220 nm for UV detection and ca. 1 mg/ml for refractive index detection. All separations were carried out isocratically after equilibrium had been established.

3. Results and discussion

3.1. Chromatography of amine solutes using alkylnitrile additives in methanol–water

Valeronitrile was found to be an effective mobile phase additive for improving peak shapes in the reversed-phase chromatography of some organic amines using aqueous methanol mobile phases [10]. As a corollary to this study other aliphatic nitrile compounds (butyronitrile and hexanenitrile) were tested as potential additives under the same chromatographic conditions. Aniline test compounds were separated using mobile phases consisting of mixtures of methanol–water containing additive on a commercial C_8 reversed-phase column. Fig. 1 shows the separation of the aniline test mixture using increasing amounts of hexanenitrile in the mobile phase. Excellent chromatography is obtained when the concentration of hexanenitrile is 0.05% (w/w). Fig. 2 shows a comparison of the separations obtained using butyronitrile, valeronitrile and hexanenitrile as additives (at the 0.05% w/w level) in methanol–water. The separations show the relative efficacy of the additives under the same experimental conditions and clearly demonstrate a trend, i.e. efficacy in-

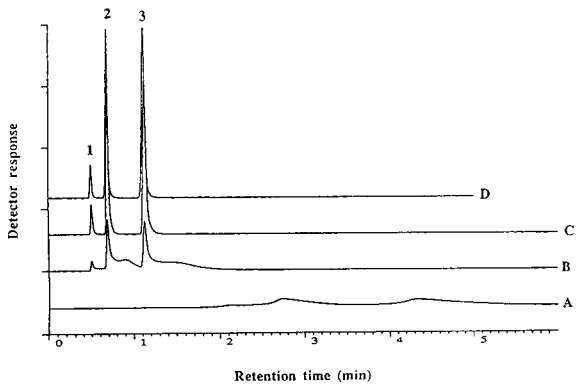

Fig. 1. Separation of anilines using methanol–water (50:50, w/w) with added hexanenitrile. Column: Spherisorb C_8, 3 μm, 3 cm × 4.6 mm I.D. Peaks: 1 = aniline; 2 = N-methylaniline; 3 = N,N-dimethylaniline. (A) No additive; (B) hexanenitrile at 0.01% (w/w); (C) hexanenitrile at 0.02% (w/w); (D) hexanenitrile at 0.05% (w/w).

creases with increasing chain-length of the additive, $C_5H_{11}CN > C_4H_9CN > C_3H_7CN$. For valeronitrile, approximately 0.2% (w/w) is required in the mobile phase to give good separation and peak shapes; for butyronitrile, up to 2% (w/w) was added but even so poor peak shapes were observed. The affinity of the additive for the stationary phase is controlled by the distribution coefficient of the additive between the stationary and mobile phases in the same way as general solutes behave. As the additive chain-length is increased its adsorption strength is increased and its efficacy as a moderator enhanced. It is not possible to chromatograph anilines satisfactorily without the use of valeronitrile and hexanenitrile additives in methanol–water. Butyronitrile is not an effective additive owing to its high solubility in methanol–water. Similar improvements in chromatography using valeronitrile as the mobile phase additive have also been observed for isomeric toluidines and pyridine separations [10].

3.2. Chromatography of amine solutes using alkylnitrile additives in acetonitrile–water and tetrahydrofuran–water

Hexanenitrile was used as an additive in mobile phases consisting of water and other organic modifiers having different properties to methanol. Mobile phases of acetonitrile–water and tetrahydrofuran–water were prepared on a weight basis with small amounts of hexanenitrile added. The separations of anilines using acetonitrile and tetrahydrofuran as organic modifiers are shown in Fig. 3 and Fig. 4, respectively. Good peak shape is realised at about the 0.05% (w/w) level added hexanenitrile. The results demonstrate that hexanenitrile is an effective additive in common aqueous mobile phases. Further work showed that similar additive efficacy is

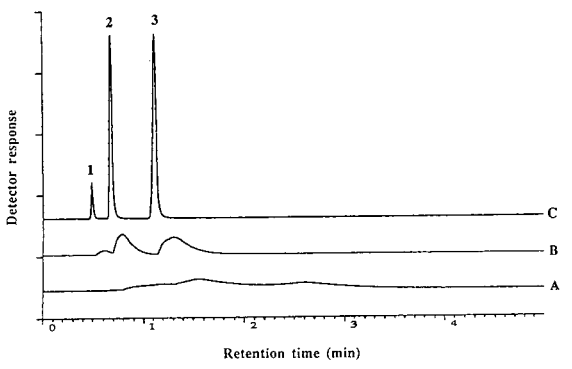

Fig. 2. Separation of anilines using methanol–water (50:50, w/w) with added butyronitrile, valeronitrile and hexanenitrile at the 0.05% (w/w) level. Peaks and column as in Fig. 1. (A) Butyronitrile; (B) valeronitrile; (C) hexanenitrile.

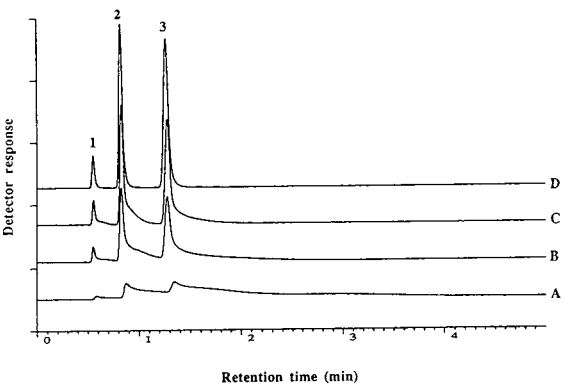

Fig. 3. Separation of anilines using acetonitrile–water (40:60, w/w) with added hexanenitrile. Peaks and column as in Fig. 1. (A) No additive; (B) hexanenitrile at 0.01% (w/w); (C) hexanenitrile at 0.02% (w/w); (D) hexanenitrile at 0.05% (w/w).

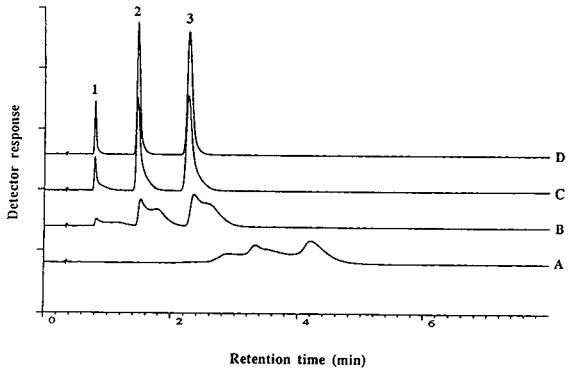

Fig. 4. Separation of anilines using tetrahydrofuran–water (30:70, w/w) with added hexanenitrile. Peaks and column as in Fig. 1. (A) No additive; (B) hexanenitrile at 0.01% (w/w); (C) hexanenitrile at 0.02% (w/w); (D) hexanenitrile at 0.05% (w/w).

obtained when using different ratios of water to organic modifier in the mobile phase (Fig. 5).

3.3. Chromatography of amine solutes using alkylnitrile additives in methanol–water on commercial reversed-phase columns

The chromatography of the anilines on different reversed-phase columns was studied. A second C_8 commercial column was tested with and without hexanenitrile added to a methanol–water mobile phase. Fig. 6 shows the chromatography when hexanenitrile is added to the mobile

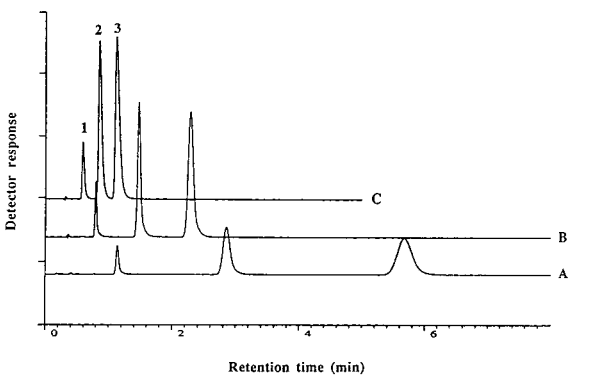

Fig. 5. Separation of anilines using tetrahydrofuran–water (20:80), (30:70) and (40:60, w/w) with added 0.05% (w/w) hexanenitrile. Peaks and column as in Fig. 1. (A) 20:80; (B) 30:70; (C) 40:60.

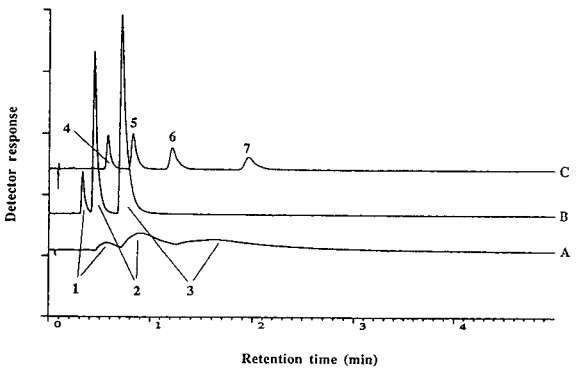

Fig. 6. Separations using methanol–water (50:50, w/w). Column: Brownlee Velosep C_8, 3 μm, 4 cm × 3.2 mm I.D. Peaks 1–3 as in Fig. 1; 4 = benzene; 5 = toluene; 6 = ethylbenzene; 7 = *n*-propylbenzene. (A) Anilines separation no additive; (B) anilines separation using hexanenitrile at 0.05% (w/w); (C) benzenes separation no additive.

phase at the 0.05% (w/w) level. The anilines peak shapes are improved though some tailing is still observed but this is due to the column performance as shown by the separation of some aromatic carbons (Fig. 6).

The study was extended to include C_{18} and cyano columns. Fig. 7 is a comparison of aniline separations performed on two reversed-phases (C_8 and C_{18}) and a cyano phase from the same manufacturer. Good separations are obtained on

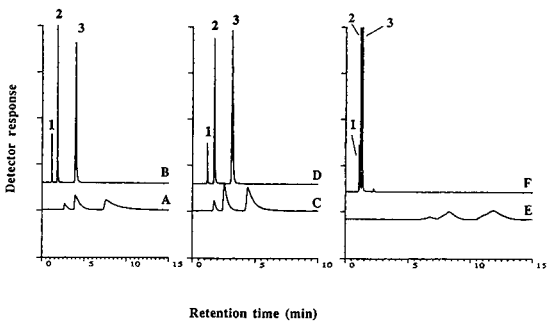

Fig. 7. Separation of anilines on Ultrasphere XL, 3 μm, 7.5 cm × 4.6 mm I.D. columns using methanol–water (50:50, w/w) and methanol–water (50:50, w/w) with added hexanenitrile. Peaks as in Fig. 1. (A) C_{18} column no additive; (B) C_{18} column 0.05% (w/w) hexanenitrile; (C) C_8 column no additive; (D) C_8 column 0.05% (w/w) hexanenitrile; (E) CN column no additive; (F) CN column 0.1% (w/w) hexanenitrile.

all three of the stationary phases when hexanenitrile is added to the mobile phase.

3.4. Adsorption of alkylnitrile additives and their mechanism of action

The chromatography of amines on reversed-phase media has always been problematical owing to amine molecules interacting with residual silanol groups. Many ways of eliminating these interactions have been devised; use of ion suppression [2]; competing amines [12] and speciality base-deactivated columns [13]. However the use of ion-pairing necessitates the use of careful pH control, competing amines destroy the column with continued use and the speciality base-deactivated columns have not been shown to perform adaquately in other reports [14,15] necessitating the inclusion of additives (e.g. N,N-dimethyloctylamine and tetrabutylammonium hydrogensulphate) to obtain adaquate performance.

The work described in this paper demonstrates that the presence of small quantities of alkylnitrile additives can afford many advantages over other common approaches for chromatographing amines. The alkyl additives act by either presenting a new stationary phase to the solute molecules or by preventing access to residual silanol groups. The effect of the additive on the mobile phase strength might also be a contributing factor. These effects are currently being investigated.

The chromatography of the anilines clearly involves two mechanisms at hexanenitrile concentrations below about 0.02% (w/w) as is shown by examining the amine peak shapes in Figs. 1, 3 and 4. The solute molecules may undergo dispersive interactions with the C_8 ligands and also hydrogen bonding interactions with the residual silanol groups which produces the distorted peak shape.

In an effort to determine the mechanism of action of the additives the retention of hexanenitrile was measured in methanol–water mobile phase containing added hexanenitrile. A composition of methanol–water base mobile phase (20:80) was required so that the retention time of hexanenitrile could be measured accurately using a 3 cm long column. The hexanenitrile retention decreases as the hexanenitrile concentration of the mobile phase increases (Fig. 8). This decrease in retention is also observed for the anilines chromatographed in this study and in previous work [10] when pyridine and the isomeric toluidines were studied. This observation suggests that a more polar in-situ stationary phase is being formed. The orientation of the hexanenitrile molecules at the stationary phase surface is thought to be akin to the adsorption of common ion-pairing agents such as alkyl sulphonates, i.e. the hydrocarbon alkyl chain of the molecule is partitioned into the C_8 ligands while the polar group is oriented toward the mobile phase. This has been supported by some recent spectroscopic evidence for the orientation of long-chain (C_7–C_{10}) *n*-alcohols adsorbed onto a C_{18} reversed-phase [16]. The retention of hexanenitrile passes through a minimum and then increases ($>0.2\%$ w/w hexanenitrile in the mobile phase). At this point there is a reversal of the retention character of the in-situ stationary phase, i.e. it becomes less polar and is possibly caused by the formation of hexanenitrile multilayers. Further, it was possible that the critical micelle concentration for hexanenitrile may have been exceeded at the minimum of the curve leading to a micellar mechanism for retention

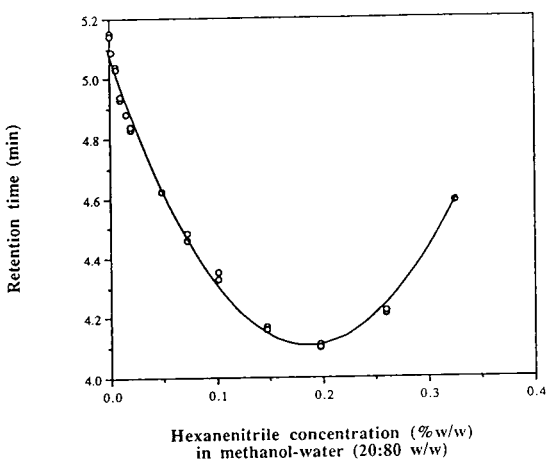

Fig. 8. Retention of hexanenitrile in methanol–water (20:80, w/w) with added hexanenitrile. Column as Fig. 1.

but NMR experimentation gave no evidence for this hypothesis. However, the possibility of micelle formation cannot be excluded. It is thought that the nitrile groups of the second layer of hexanenitrile molecules are oriented toward the nitrile groups of the monolayer. This could account for the increase in retention observed and has been suggested by Daucik et al. in their paper describing the use of hexanenitrile to influence the separation of some isomeric substituted tributylphenols [9]. Further work is in hand to provide a rationale for these effects and will be reported in a subsequent paper.

4. Conclusions

It has been shown that valeronitrile and hexanenitrile are effective mobile phase additives for the reversed-phase separations of amines but butyronitrile is ineffective. The efficacy of the additive is dependent on the alkyl chain-length and hexanenitrile was shown to be the most efficacious. Good chromatographic separations for amines were obtained using aqueous mobile phases having methanol, acetonitrile or tetrahydrofuran organic modifiers and containing hexanenitrile at low concentration. Equivalent effects were realised on reversed-phase columns from different sources when using the additives. To eliminate the undesired effects of silanol groups in reversed-phase chromatography these simple mobile phase additives offer several advantages over standard practices of separating organic amines in that the column performance does not deteriorate with use and the UV cut-off is of the same order as acetonitrile. Hexanenitrile is insoluble in pure water but is soluble up to about 0.5% (w/w) in aqueous–organic solvents.

References

[1] H.A. Claessens, E.A. Vermeer and C.A. Cramers, *LC·GC Int.*, 6 (1993) 692.
[2] M.A. Stadalius, J.S. Berus and L.R. Snyder, *LC·GC Mag.*, 6 (1988) 194.
[3] G.B. Cox, *J. Chromatogr. A*, 656 (1993) 353.
[4] H. Engelhardt, H. Löw and W. Götzinger, *J. Chromatogr.*, 544 (1991) 371.
[5] K. Kamata, K. Iwaguchi, S. Onishi, K. Jinno, R. Eksteen, K. Hosaya, M. Araki and N. Tanaka, *J. Chromatogr. Sci.*, 27 (1989) 721.
[6] L.C. Sander, *J. Chromatogr. Sci.*, 26 (1988) 381.
[7] S.H. Hansen, P. Helboe and M. Thomsen, *J. Chromatogr.*, 544 (1991) 53.
[8] Y. Lau and C.F. Simpson, *Anal. Proc.*, 25 (1988) 25.
[9] P. Daucik, A.M. Rizzi and J.F.K. Huber, *J. Chromatogr.*, 442 (1988) 53.
[10] S.D. McCrossen and C.F. Simpson, *Anal. Proc. incl. Anal. Comm.*, 31 (1994) 9.
[11] S.R. Cole and J.G. Dorsey, *J. Chromatogr.*, 635 (1993) 177.
[12] T. Hamoir, Y. Verlinden and D.L. Massart, *J. Chromatogr. Sci.*, 32 (1994) 14.
[13] D.V. McCalley, *J. Chromatogr.*, 636 (1993) 213.
[14] J. Verne-Mismer, M. Lamard and J. Wanger, *J. Chromatogr.*, 645 (1993) 251.
[15] J. Paesen, P. Claeys, E. Roets and J. Hoogmartens, *J. Chromatogr.*, 630 (1993) 117.
[16] M.E. Montogomery and M.J. Wirth, *Anal. Chem.*, 66 (1994) 680.

ELSEVIER

Journal of Chromatography A, 697 (1995) 59–69

JOURNAL OF CHROMATOGRAPHY A

Effect of various organic modifiers on the determination of the hydrophobicity parameters of non-homologous series of anticancer drugs

Esther Forgács*, Tibor Cserháti

Central Research Institute for Chemistry, Hungarian Academy of Sciences, P.O. Box 17, 1525 Budapest, Hungary

Abstract

The lipophilicities and specific hydrophobic surface areas of 21 commercial anticancer drugs were determined by means of reversed-phase thin-layer chromatography using methanol, ethanol, 1-propanol, 2-propanol, acetonitrile, dioxane and tetrahydrofuran as organic modifiers at various concentrations. The data were evaluated by various multivariate mathematical–statistical methods such as the spectral mapping technique and principal component analysis followed by two-dimensional non-linear mapping, varimax rotation and cluster analysis. The results indicate that the solvent strength and selectivity of organic modifiers are strongly related to the steric characteristics of the solvent molecule, suggesting competition between the anticancer drugs and solvent molecules for the hydrophobic surface of the stationary phase. It was established that for the evaluation of large retention data matrices the use of principal component analysis followed by two-dimensional non-linear mapping provides more information than one-dimensional cluster analysis.

1. Introduction

Quantative structure–activity relationship (QSAR) methods have been widely accepted and applied in the design of new bioactive compounds [1,2]. To find the best relationship between chemical structure and biological activity, many molecular parameters have been introduced and tested in QSAR studies [3]. Most of these parameters can easily be determined by various chromatographic methods [4]. Chromatographic techniques have some advantages: they are rapid and relatively simple; very small amounts of the substances are required and the compounds need not be very pure as the impurities separate during the chromatographic processes. Lipophilicity is one of the physicochemical parameters frequently applied in QSAR studies [5,6]. Lipophilicity can be determined by the classical partition method between water and *n*-octanol [7], by reversed-phase high-performance liquid chromatography (RP-HPLC) [8–10] and by reversed-phase thin-layer chromatography (RP-TLC) [11]. The lipophilicity values determined with RP-HPLC or RP-TLC generally show excellent correlation [12]. RP-TLC has been extensively applied to determine the lipophilicity of bioactive compounds [13]. To increase the accuracy of the lipophilicity determination, linear correlations have been calculated between the R_M values and the concentration of organic component in the mobile phase; the R_M value extrapolated to zero organic

* Corresponding author.

0021-9673/95/$09.50
SSDI 0021-9673(94)00807-8

phase concentration (R_{M0}) was regarded as the most accurate estimate of lipophilicity [14]. However, chromatographic methods have some drawbacks. The supports may partially retain their original adsorptive characteristics even after impregnation [15] and the R_M value changes with the amount [16]) and quality [17] of coating substance.

Much effort has been devoted to the elucidation of the mode of action of various anticancer drugs. They can bind to different biomolecules such as model and native membranes [18], DNAs [19,20] and various proteins [21]. The binding of anticancer drugs to proteins may modify protein structures [22] and can increase or decrease enzyme activity [23,24], resulting in modified biological efficiency of the drugs [25]. It is reasonable to assume that the hydrophobicity parameters (lipophilicity and specific hydrophobic surface area) of drugs may have a significant impact on their various biological effects.

Multivariate mathematical–statistical methods such as principal component analysis (PCA) [26], factor analysis [27] and the spectral mapping technique [28] have been successfully used for the extraction of maximum information from large retention data matrices.

The objectives of our work were the determination of the lipophilicity and specific hydrophobic surface area of non-homogeneous series of anticancer drugs under various RP-TLC conditions, to find the relationships between retention characteristics and physico-chemical parameters by the use of multivariate mathematical–statistical methods and to compare the information content of the methods. The drugs studied are listed in Table 1.

2. Experimental

2.1. Reversed-phase thin-layer chromatography

Polygram UV 254 plates (Macherey–Nagel, Düren, Germany) were impregnated by overnight predevelopment in *n*-hexane–paraffin oil (95:5, v/v). The IUPAC nomenclature for the anticancer drugs used is shown in Table 1. Anticancer drugs were separately dissolved in methanol at a concentration of 3 mg/ml and 2 μl of the solutions were spotted on the plates. Methanol–water, ethanol–water, 1-propanol–water, 2-propanol–water, acetonitrile–water, dioxane–water and tetrahydrofurane–water mixtures were used as eluents, the concentration of organic modifiers ranging from 10 to 75 vol.-% in steps of 5 vol.-%. The application of this wide range of organic modifier concentrations was motivated by the highly different hydrophobicities of anticancer drugs. Developments were carried out in sandwich chambers ($22 \times 22 \times 3$ cm) at room temperature, the distance of development being about 16 cm. After development the plates were dried at 105°C and the spots of anticancer drugs were revealed by their visible and UV spectra, with iodine vapour and with phosphomolybdic acid reagent. Each experiment was run in quadruplicate. The R_M values of the anticancer drugs were determined by

$$R_M = \log (1/R_F - 1) \quad (1)$$

Linear correlations between the R_M values of anticancer drugs and the concentration of organic modifiers in the eluent were calculated separately for each drug:

$$R_M = R_{M0} + bC \quad (2)$$

The intercept and slope values of Eq. 2 were considered as the best estimation of the hydrophobicity and specific hydrophobic surface area [29] of the drugs, respectively. It has been stated [29] that this slope perhaps reflect hydrocarbonaceous surface area but only for a set of solutes of closely similar electrostatic properties (dipole moments, polarizabilities). Obviously this set of compounds did not comply with the requirements mentioned above. However, it has recently been reported that the assumption also holds for non-homologous series of solutes [30,31]. In the case of a given drug the slope values are also related to the solvent strength of the organic modifiers (decrease in the R_M value caused by a 1% (v/v) increase in the concentration of the organic modifier [32]).

Table 1
Anticancer drugs studied

No.	Common name	IUPAC name	Source
1	Ftorafur	N-(2-Furanidyl)-5-fluorouracil	Medexport (Russia)
2	Bicnu	N,N-Bis(2-chloroethyl)-N-nitrosourea	Laboratoire Bristol (France)
3	Vincristin	22-Oxo-(3α,14β,16α)-14,15-dihydro-14-hydroxy-eburnamenine-14-carbocyclic acid methyl ester	Gedeon Richter (Hungary)
4	Vinblastine	(3α,14β,16α)-14,15-Dihydro-14-hydroxyeburnamenine-14-carbocyclic acid methyl ester	Gedeon Richter (Hungary)
5	Vumon	4′-O-Demethyl-1-O-(4,6-O-2-thenylidene-β-D-glucopyranosyl)epipodophyllotoxin	Bristol-Arzneimittel (Germany)
6	Provera	17-α-Acetoxy-6-α-(methyl)progesterone	Upjohn (UK)
7	Bleogin	N^1-[3-Dimethyl(sulfonio)propyl]bleomycinamide	Nippon Kayaku (Japan)
8	Paraplatin	9,11,15-Trihydroxy-15-methylprosta-5,13-dienoic acid	Bristol-Arzneimettel (Germany)
9	Zitazonium	2-[4-(2-Chloro-1,2-diphenylethynyl)phenoxy]-N,N-diethylethamine citrate	EGIS Pharmaceutical Works (Hungary)
10	Farmorubicin	(8*S-cis*)-10-[(3-Amino-2,3,6-trideoxy-α-L-*arabino*-hexopyranosyl)oxy]7,8,9,10-tetrahydro-6,8,11-trihydroxy-8-(hydroxyacetyl)-1-methoxy-5,12-naphthacenedione	Farmitalia (Italy)
11	Adriblastine (Doxorubicin)	10-[3-(Amino-2,3,6-trideoxy-α-L-hexapyranosyl)oxy]-7,8,9-tetrahydro-6,8,11-trihydroxy-8-(hydroxyacetyl)-1-methoxy-5,12-naphthacenedione	Farmitalia (Italy)
12	Natulan	*N*-(1-Methylethyl)4-[(2-methylhydrazino)methyl]-benzamide	Roche (Switzerland)
13	Alexan	4-Amino-1-β-D-arabifuranosyl-2(14)-pyrimidine	Mack (Germany)
14	Mitomycin C Kyowa	[1-a*R*]-6-Amino-8-[(aminocarbonyl)oxymethyl]-1,1a,2,8,8a,8b-hexahydro-8a-methoxy-5-methyl azirino-[2′,3′:3,4]pyrrolo[1,1*a*]indole-4,7-dione	Kyowa (Japan)
15	Cytoxan	2-[Bis(2-chloroethyl)amino]tetrahydro-2*H*-1,3,2-oxazaphosphorine 2-oxide monohydrate	Bristol-Myers (Germany)
16	Estracyt	Estra-1,3,5-(10)-triene-3,17-diol-3-[bischloroethyl)carbamate	Aktiebolaget (Sweden)
17	Deticene	5-(3,3-Dimethyl-1-triazenyl)-1*H*-imidazole-4-carboxamide	Rhone-Poulenc (France)
18	Methotrexate	2,4,-Diamino-10-methylpteroylglutamic acid	Lachema (Czech Republic)
19	Myelobromol	1,6-Dibromo-1,6-bis(desoxy)-D-mannitol	Chinoin (Hungary)
20	Zitostop	1,2,5,6-Tetramethylsulfon-D-mannitol	EGIS Pharmaceutical Works (Hungary)
21	Elobromol	1,6-Dibromo-1,6-bis(desoxy)-D-galactitol	Chinoin (Hungary)
22	Taxol	{2a*R*-[2aα,4β,4aβ,6β,9α(a*R**,β*S**),11α,12α,12aα,12bα}-β-(Benzoylamino)-α-hydroxybenzenepropanoic acid 6,12b-bis(acetyoxy)-12-(benzoyloxy)-2a,3,4,4a,5,6,9,10,11,12,12a,12b-dodecahydro-4,11-dihydroxy-4a,8,13,13-tetramethyl-5-oxo-7,11-methano-14-cyclodeca[3,4]benz[1,2-*b*]oxet-9-yl ester	Sigma Chemie (Germany)

2.2. *Multivariate mathematical–statistical methods*

Spectral mapping technique [33]

In order to separate the elution strength and elution selectivity of organic modifiers, the spectral mapping technique was applied. The *b* values of Eq. 2 and the anticancer drugs were the variables and observations, respectively. The dimensions of the spectral map were reduced to two by the non-linear mapping technique [34]. Stepwise regression analysis [35] was used for the

elucidation of the impact of the physico-chemical parameters of organic modifiers on their elution strength and selectivity. We should stress that the elution strength probably depends on the solutes specifically used in the experiments, therefore the conclusions drawn are valid only for this set of solutes and any extrapolation may lead to severe misinterpretation of the results. Stepwise regression analysis was used three times, the elution strength and the two coordinates of the spectral map being the dependent variables. The independent variables were in each instance the following physico-chemical parameters of organic modifiers:

π	Hansch–Fujita substituent constant characterizing hydrophobicity [36,37];
H-Ac and *H-Do*	indicator variables for proton acceptor and proton donor properties, respectively [38];
M-RE	molar refractivity [39];
F and *R*	electronic parameters characterizing the inductive and resonance effect, respectively [40];
σ	Hammett's constant, characterizing the electron-withdrawing power of the substituent [41];
Es	Taft's constant, characterizing steric effects of the substituent [42];
B_1, B_4 and B_1/B_4	Sterimol width parameters determined by the distance of substituents at their maximum point perpendicular to attachment [43,44].

The two equations used in stepwise regression analysis were the following:

Elution strength

$$= a + b_1\pi + b_2H\text{-}Do + b_3M\text{-}RE + b_4F + b_5R + b_6\sigma + b_7Es + b_8B_1 + b_9B_4 + b_{10}B_1/B_4 \quad (3)$$

First coordinate of the spectral map

$$= a + b_1\pi + b_2H\text{-}Do + b_3M\text{-}RE + b_4F + b_5R + b_6\sigma + b_7Es + b_8B_1 + b_9B_4 + b_{10}B_1/B_4 \quad (4)$$

The acceptance level for the individual independent variables was set to the 95% significance level.

Principal component analysis [45] followed by two-dimensional non-linear mapping, cluster analysis and varimax rotation [46]

The data matrix consisted of the parameters of Eq. 2 (intercept = R_{M0} and slope = b values determined with the seven organic modifiers) and various physico-chemical characteristics of drugs (altogether 23 variables) were considered as variables and the anticancer drugs were the observations. The data matrix is compiled in Table 2. As compounds **19–21** were very near to the front these data were omitted from the calculations. The physico-chemical parameters included in the calculation were as listed above. The limit of the variance explained was set to 99.9%. To facilitate the evaluation of the results of PCA, both two-dimensional non-linear mapping and cluster analysis were carried out on the principal component loadings and variables. To compare the information content of the two-dimensional non-linear map and that of varimax rotation, varimax rotation around two axes was carried out on the principal component loadings. As it was assumed that PCA can cause some data distortion, cluster analysis was also applied to the original data matrix. Cluster analysis, the non-linear mapping technique and varimax rotation are theoretically similar: each method calculates and visualizes the relative distances between the members of data matrix (in our cases physico-chemical and chromatographic parameters of drugs). To compare their information content, linear correlations were calculated between the corresponding distances on the non-linear map and cluster dendogram:

$$Y = a + bX_{1-2} \quad (5)$$

Table 2
Retention characteristics and physico-chemical parameters of anticancer drugs

Parameter	Anticancer drug																		
	1	**2**	**3**	**4**	**5**	**6**	**7**	**8**	**9**	**10**	**11**	**12**	**13**	**14**	**15**	**16**	**17**	**18**	**22**
$R_{M0(MeOH)}$	0.33	1.45	2.20	1.97	1.73	2.33	1.35	−0.32	3.81	2.13	1.90	1.24	0.99	1.17	1.33	4.55	0.94	0.88	4.08
$b_{(MeOH)}$	1.57	2.14	2.47	2.24	1.81	2.85	1.31	1.26	3.18	3.00	2.39	2.83	6.27	3.00	2.59	6.39	1.82	2.53	6.29
$R_{M0(EtOH)}$	0.32	1.04	2.26	2.14	2.20	3.42	1.30	−0.36	3.57	1.95	1.71	1.18	0.58	1.23	1.25	3.16	0.84	1.00	2.72
$b_{(EtOH)}$	2.87	2.19	3.91	3.71	4.88	6.63	4.70	1.94	6.14	4.28	3.70	3.92	10.00	5.01	3.48	5.11	2.46	6.12	5.16
$R_{M0(1\text{-}PROP)}$	0.09	1.01	1.48	1.77	1.81	2.28	1.29	−0.49	2.34	1.38	1.20	0.98	0.48	0.70	0.92	1.86	0.63	1.06	1.94
$b_{(1\text{-}PROP)}$	2.06	3.46	4.41	5.22	6.28	6.96	2.19	1.91	6.21	4.80	4.24	4.12	10.59	3.61	3.60	5.03	2.22	10.02	5.27
$R_{M0(2\text{-}PROP)}$	0.27	1.03	1.50	1.67	1.77	2.90	1.21	−0.52	3.18	1.51	1.38	0.96	0.43	0.72	0.98	2.70	0.61	0.77	2.41
$b_{(2\text{-}PROP)}$	4.06	2.61	3.22	3.52	4.70	6.95	4.85	1.57	7.39	4.27	3.96	3.67	9.81	3.49	3.26	5.59	2.14	6.28	5.56
$R_{M0(MeCN)}$	0.33	1.16	2.15	2.20	2.33	3.44	1.44	−0.59	2.71	1.75	1.55	1.16	1.24	1.24	1.24	2.86	0.72	0.99	2.98
$b_{(MeCN)}$	2.85	2.90	4.23	4.30	5.59	7.16	6.54	0.93	5.34	4.57	3.89	3.55	15.53	5.62	3.36	6.52	2.32	6.36	6.56
$R_{M0(DIOX)}$	0.19	0.96	1.63	1.82	2.01	2.64	1.26	−0.90	2.38	1.47	1.41	0.76	0.42	0.46	1.02	2.20	0.50	0.48	2.65
$b_{(DIOX)}$	2.91	2.24	2.86	3.09	4.71	4.86	6.19	0.50	3.76	3.93	4.30	2.79	10.70	2.70	3.69	3.66	1.91	3.77	5.41
$R_{M0(THF)}$	0.24	1.11	1.43	1.53	1.71	2.39	1.35	−0.04	1.89	1.02	0.99	0.31	−0.89	0.18	0.87	2.90	0.12	−0.12	2.33
$b_{(THF)}$	5.83	1.31	2.59	2.51	3.19	4.41	8.24	3.83	2.98	2.45	2.45	1.47	1.17	1.64	2.63	6.40	0.71	2.72	3.64
π	−0.81	0.37	16.72	17.93	7.44	8.76	−16.29	7.98	3.84	−1.56	−1.56	−1.07	−6.11	−1.43	0.38	13.76	2.28	−5.23	9.11
H-Do	0	1	1	1	1	1	1	0	1	1	1	1	1	1	1	1	1	1	1
M-Re	103.24	52.63	267.87	266.14	248.32	158.54	487.04	117.98	127.44	213.16	213.16	72.25	99.21	154.62	43.88	152.82	41.67	146.51	865.81
F	1.01	0.50	1.25	0.90	1.96	−0.06	4.01	0.51	1.37	1.52	1.52	0.06	0.05	−1.77	0.63	−0.56	0.68	−0.69	1.88
R	−2.13	−0.72	−0.13	−0.39	−4.54	−0.63	−15.28	−3.93	−1.29	−2.91	−2.91	−2.08	−4.38	−3.58	0.27	−0.89	−1.77	−6.97	−5.44
σ	1.44	1.43	0.86	0.44	2.38	0.76	3.94	−0.26	0.78	−0.69	−0.69	−0.47	0.34	−3.18	0.74	−0.59	0.56	1.35	3.33
Es	−7.16	−7.24	−30.09	−29.80	−26.19	−19.97	−82.19	−28.80	−21.83	−27.46	−27.46	−9.30	−10.84	−23.21	−6.21	−17.82	−8.02	−34.05	−5.34
B_1	10.00	9.90	27.67	27.59	27.10	16.20	79.43	30.73	13.66	29.61	29.61	9.24	16.78	22.45	7.42	19.32	6.18	60.56	62.49
B_4	13.24	14.68	56.59	56.27	40.89	26.30	92.28	41.23	21.10	39.58	39.58	16.86	23.74	31.94	10.92	34.16	12.07	43.76	79.08

where Y = relative distances between anticancer drugs on the non-linear map X_1 = relative distances between anticancer drugs on the cluster dendogram calculated from the original data matrix and X_2 = relative distances between anticancer drugs on the cluster dendogram after PCA. To facilitate the calculations only the distances between the nearest neighbour drugs on the maps were included in the equations. The comparison of distances was hampered by the fact that their absolute values depend on the dimensions of the plots. We overcame this difficulty by data normalization: the greatest distances on each map were considered to be 100% and the other distance were calculated accordingly.

To compare the information content of non-linear mapping and varimax rotation techniques, linear correlations were calculated between their corresponding coordinates:

$$Y_{1-2} = a + bX_{1-2} \quad (6)$$

where Y_{1-2} = first and second coordinates of the varimax rotation and X_{1-2} = first and second coordinates of the non-linear map.

3. Results and discussion

Compounds **19–21** were near to the front in each eluent system, which means that these drugs are highly hydrophilic and their hydrophobicity parameters cannot be determined under the experimental conditions used. Eq. 2 was significant for each anticancer drug in each eluent system, that is, these solutes do not show anomalous retention behaviour which can inhibit the calculation of their hydrophobicity and specific hydrophobic surface area (see retention data in Table 2).

The solvent strength and solvent selectivity of organic modifiers are compiled in Table 3. The solvent strength was calculated taking into consideration simultaneously the slope value of Eq. 2 for each anticancer drug. It is a dimensionless number without a concrete physico-chemical meaning, giving the order of solvent strengths of the organic modifiers relative to each other. The data clearly show that the solvent strengths of organic modifiers differ considerably; for alcohols they increase with increasing number of methylene groups in the molecule. The results further indicate that not only the solvent strengths but also the solvent selectivities are markedly different. Stepwise regression analysis selected two equations describing the relationship between the chromatographic parameters of organic modifiers and their physico-chemical parameters. The chromatographic parameters of each anticancer drug except compounds **19–21** were included in the calculations, and therefore the terms solvent strength and solvent selectivity (coordinates of the spectral map) refer to the solutes mentioned above:

Solvent strength

$$= -286.9 + 1003.6B_1/B_4 - 814.1(B_1/B_4)^2$$

$$F_{calc.} = 22.65\ ;\ r^2 = 0.9189$$

Table 3
Solvent strength and selectivity of organic modifiers: results of spectral mapping technique

Organic modifier	Solvent strength (arbitrary units)	Selectivity map	
		First coordinate	Second coordinate
Methanol	12.84	101.52	114.90
Ethanol	19.78	154.12	99.75
1-Propanol	21.15	113.44	63.09
2-Propanol	19.93	164.83	80.87
Acetonitrile	22.51	174.23	148.17
Dioxane	16.97	199.07	108.26
Tetrahydrofuran	13.80	212.79	4.42

First coordinate of spectral map

$$= 457.0 - 487.3B_1/B_4$$

$$F_{calc.} = 21.73\ ;\ r^2 = 0.8129$$

Good relationships were found between the derived retention parameters (solvent strength and the first coordinate of the spectral map) and the physico-chemical parameters of the anticancer drugs, the significance level being over 99% (see $F_{calc.}$ values). The steric parameter (molecular shape) accounts for 91 and 81% of the change in elution strength and elution selectivity of organic modifiers, respectively.

The results of PCA are summarized in Table 4. Six principal components explain the majority (91.67%) of the total variance. This result indicates that the 23 physico-chemical and chromatographic parameters can be substituted by six background variables without a substantial loss of information. Unfortunately, PCA does not prove the existence of such background variables

Table 4
Relationship between retention characteristics and physico-chemical parameters for anticancer drugs: results of principal component analysis

No. of principal component	Eigenvalue	Variance explained (%)	Total variance explained (%)
1	7.69	33.42	33.42
2	4.89	21.24	54.66
3	4.27	18.57	73.23
4	2.18	9.49	82.72
5	1.14	4.97	87.69
6	0.92	3.98	91.67

Parameter	Principal component loadings: No. of principal component				
	1	2	3	4	5
$R_{M0(MeOH)}$	−0.18	−0.01	0.13	0.87	0.28
$b_{(MeOH)}$	0.55	0.36	−0.38	0.05	0.50
$R_{M0(EtOH)}$	0.83	0.36	0.37	−0.01	−0.16
$b_{(EtOH)}$	0.61	0.17	−0.73	0.06	−0.08
$R_{M0(1\text{-}PROP)}$	0.86	0.23	0.32	−0.06	−0.23
$b_{(1\text{-}PROP)}$	0.51	0.30	−0.66	−0.08	−0.08
$R_{M0(2\text{-}PROP)}$	0.85	0.32	0.35	0.07	−0.16
$b_{(2\text{-}PROP)}$	0.67	0.16	−0.63	0.29	−0.08
$R_{M0(MeCN)}$	0.90	0.32	0.23	−0.04	−0.05
$b_{(MeCN)}$	0.56	0.07	0.78	0.03	0.06
$R_{M0(DIOX)}$	0.88	0.23	0.37	0.01	−0.06
$b_{(DIOX)}$	0.58	−0.11	−0.71	0.13	0.05
$R_{M0(THF)}$	0.71	0.13	0.64	0.01	0.01
$b_{(THF)}$	0.34	−0.53	0.25	0.42	−0.01
π	0.18	0.50	0.54	−0.20	0.34
H-Do	0.04	−0.12	−0.12	−0.88	0.11
M-Re	0.61	−0.49	0.18	−0.11	0.49
F	0.30	−0.66	0.30	0.23	−0.05
R	−0.20	0.89	0.29	0.01	0.10
σ	0.40	−0.56	0.12	0.28	0.15
Es	−0.23	0.77	−0.03	0.14	0.45
B_1	0.42	−0.80	−0.06	−0.20	0.11
B_4	0.51	−0.72	0.14	−0.28	0.20

as concrete physico-chemical entities but only indicates its mathematical possibility. The majority of retention parameters (hydrophobicity = R_{M0} and specific hydrophobic surface area = b values) have high loadings in the first PC, indicating that this principal component can be regarded as related to the molecular hydrophobicity. The second PC contains only the calculated physico-chemical parameters of drugs. The specific hydrophobic surface area values and the calculated hydrophobicity (π) values have high loadings in the third PC, suggesting a more or less strong relationship between these parameters.

Neither the retention characteristics nor the physico-chemical parameters of anticancer drugs

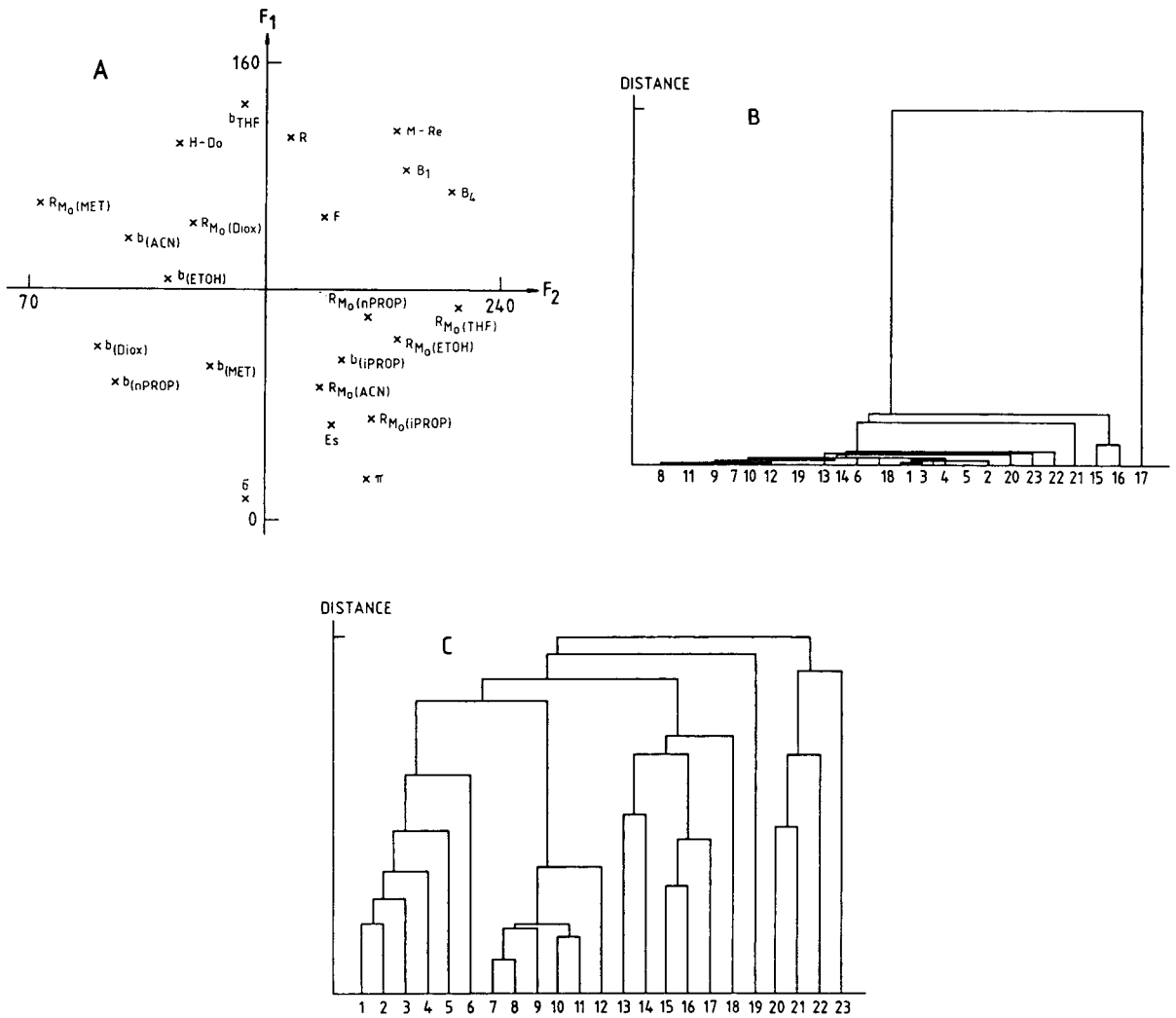

Fig. 1. Similarities and dissimilarities between the retention characteristics and physico-chemical parameters of anticancer drugs. (A) Two-dimensional non-linear map of PC loadings. Number of iterations, 90; maximum error $2.2 \cdot 10^{-3}$. (B) Cluster dendogram calculated from the original data matrix. (C) Cluster dendogram calculated from the PC loadings. Numbers on abscissa: 1 = $R_{M0(MeOH)}$; 2 = $b_{(MeOH)}$; 3 = $R_{M0(EtOH)}$; 4 = $b_{(EtOH)}$; 5 = $R_{M0(1\text{-}PROP)}$; 6 = $b_{(1\text{-}PROP)}$; 7 = $R_{M0(2\text{-}PROP)}$; 8 = $b_{(2\text{-}PROP)}$; 9 = $R_{M0(MeCN)}$; 10 = $b_{(MeCN)}$; 11 = $R_{M0(DIOX)}$; 12 = $b_{(DIOX)}$; 13 = $R_{M0(THF)}$; 14 = $b_{(THF)}$; 15 = π; 16 = *H-Do*; 17 = *M-RE*; 18 = *F*; 19 = *R*; 20 = σ; 21 = *Es*; 22 = B_1; 23 = B_4.

form distinct clusters on the two-dimensional non-linear map of PCA loadings and on the cluster dendograms (Fig. 1). These results indicate that each measured and calculated parameter has a different information content, they cannot be replaced by each other and they can be used separately in quantitative structure–activity relationship calculations. The findings discussed above are supported by the fact that only one significant linear correlation was found between the distances on the various maps (two-dimensional non-linear map and cluster analysis carried out on PC loadings: $r_{calc.} = 0.9884$, $r_{99\%} = 0.6524$). Although cluster analysis and non-linear mapping give theoretically similar results, we strongly advocate the application of the two-dimensional non-linear mapping technique instead of cluster analysis because on the two-dimensional non-linear map the observations or variables are distributed in a plane whereas they are along a line in the cluster analysis.

Significant linear correlations were found between the rotated PC loadings and the coordi-

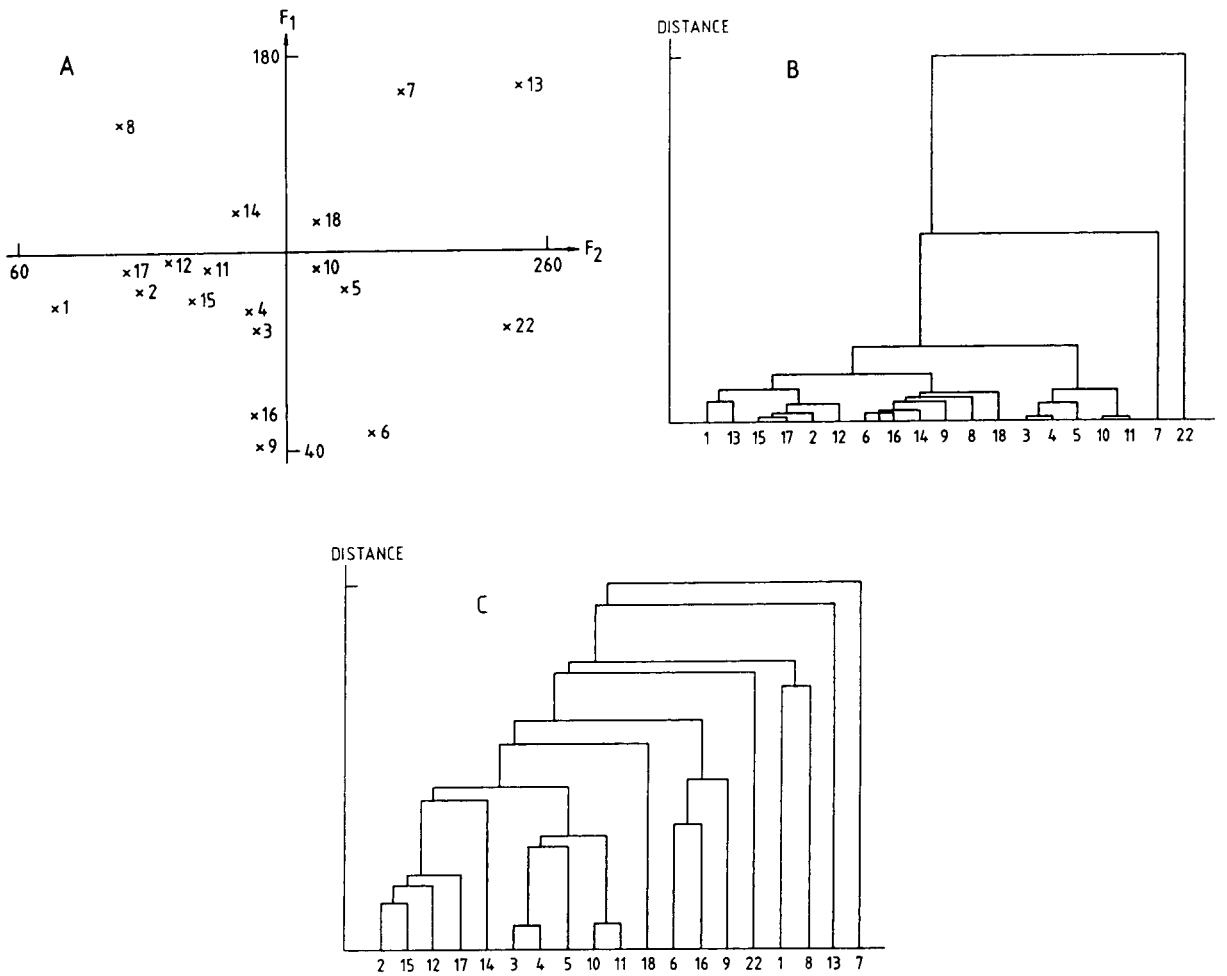

Fig. 2. Distribution of anticancer drugs according to their retention characteristics and physico-chemical parameters. (A) Two-dimensional non-linear map of PC variables. Number of iterations, 178; maximum error, $5.3 \cdot 10^{-3}$. (B) Cluster dendogram calculated from the original data matrix. (C) Cluster dendogram calculated from the PC variables. Numbers refer to anticancer drugs in Table 1.

nates of two-dimensional non-linear map of PC loadings ($n = 22$):

$$\text{varimax}_1 = 2.45 - (2.22 \pm 0.28) \cdot 10^{-3} \cdot \text{nlmap}_1$$

$$r_{\text{calc.}} = 0.9765\ ;\ r_{99.9\%} = 0.6524$$

$$\text{varimax}_2 = 1.43 - (9.21 \pm 5.89) \cdot 10^{-3} \cdot \text{nlmap}_2$$

$$r_{\text{calc.}} = 0.9431\ ;\ r_{99.9\%} = 0.6524$$

These data indicate that the information contents of varimax rotation and two-dimensional non-linear mapping (nlmap) are similar but not identical and both methods can be used to decrease the dimensionality of complicated data matrices.

The distribution of anticancer drugs according to their retention characteristics and physico-chemical parameters on the various maps is shown in Fig. 2. Compounds with similar retention characteristics and physico-chemical parameters are near to each other on the map whereas compounds with different characteristics are far from each other.

Acknowledgement

This work was supported by grant OTKA 7340 of the Hungarian Academy of Sciences.

References

[1] J. Andrew, W.E. Stuper, P. Brugger and S. Jurs, *Computer Assisted Studies of Chemical Structure and Biological Function*, Wiley, New York, 1979.
[2] C.J. Cavallito, *Structure–Activity Relationships*, Vol. 1, Pergamon Press, New York, 1973.
[3] R. Franke, in J.K. Seydel (Editor), *QSAR and Strategies in the Design of Bioactive Compounds*, VCH, Weinheim, 1985, p. 59.
[4] R. Kaliszan, *Quantitative Structure–Chromatographic Retention Relationships*, Wiley, New York, 1987.
[5] A. Fini, A. Roda, A.M. Bellini, E. Mencini and M. Guarneri, *J. Pharm. Sci.*, 79 (1990) 603.
[6] M. Vaara, W.Z. Plachya and H. Nikaido, *Biochim. Biophys. Acta*, 1042 (1990) 152.
[7] C. Hansch and S.M. Anderson, *J. Org. Chem.*, 32 (1967) 2583.
[8] A. Siwek and J. Sliwiok, *J. Chromatogr.*, 506 (1990) 109.
[9] W.J. Lambert, L.A. Wright and J.K. Stevens, *J. Pharm. Res.*, 7 (1990) 577.
[10] C. Yamagami, T. Ogura and N. Takao, *J. Chromatogr.*, 514 (1990) 123.
[11] C.B.C. Boyce and B.V. Milborrow, *Nature*, 208 (1965) 537.
[12] G.L. Biagi, M.C. Guerra, A.M. Barbaro, S. Barbieri, M. Recanatini and P.A. Borea, *J. Liq. Chromatogr.*, 13 (1990) 913.
[13] T. Cserháti and K. Magyar, *J. Biomed. Biophys. Methods*, 24 (1992) 249.
[14] J. Draffehn, B. Schonecker and K. Ponsold, *J. Chromatogr.*, 205 (1980) 113.
[15] W.F. Giesen and L.H.M. Janssen, *J. Chromatogr.*, 237 (1982) 199.
[16] T. Cserháti, Y.M. Darwish and Gy. Matolcsy, *J. Chromatogr.*, 270 (1983) 97.
[17] L. Ogierman and A. Silovecki, *J. High Resolut. Chromatogr. Chromatogr. Commun.*, 4 (1981) 357.
[18] J.B.A. Custodio, L.M. Almeida and V.M.C. Madeira, *Biochim. Biophys. Acta*, 1150 (1993) 123.
[19] T. Araka, T. Kusakabe, J. Kuwahara, M. Otsuka and Y. Sugiura, *Biochem. Biophys. Res. Commun.*, 190 (1993) 362.
[20] G.J. Finlay, E. Marshall, J.H.L. Matthews, K.D. Paull and B.C. Baguley, *Cancer Chemother. Pharmacol.*, 31 (1993) 401.
[21] M. Kimura, *Yakugaku Zasshi*, 112 (1992) 914.
[22] J.A. Broomhead, L.M. Rendina and L.K. Webster, *J. Inorg. Biochem.*, 49 (1993) 221.
[23] D.W. Fry, T.J. Boritzki, R.C. Jackson, P.D. Cook and W.R. Leopold, Mol. Pharmacol., 44 (1993) 479.
[24] C. Leguellec, B. Lacarelle, J. Catalin and A. Durand, *Cancer Chemother. Pharmacol.*, 32 (1993) 491.
[25] G.N. Kumar, U.K. Walle, K.N. Bhalla and T. Walle, *Res. Commun. Chem. Pathol. Pharmacol.*, 80 (1993) 337.
[26] R. Kaliszan and K. Osmialowski, *J. Chromatogr.*, 506 (1990) 3.
[27] B. Walczak, M. Dreux, J.R. Chretien, L. Morin-Allory, M. Lafosse and G. Felix, *J. Chromatogr.*, 464 (1989) 237.
[28] T. Cserháti, *J. Chromatogr. Sci.*, 29 (1991) 210.
[29] C. Horváth, W. Melander and I. Molnár, *J. Chromatogr.*, 125 (1976) 129.
[30] T. Cserháti and E. Forgács, *J. Chromatogr. A*, 665 (1994) 17.
[31] Y. Darwish, T. Cserháti and E. Forgács, *J. Chromatogr. A*, 668 (1994) 485.
[32] T. Cserháti, *J. Chromatogr. Sci.*, 31 (1993) 220.
[33] P.J. Lewi, *Arzneim.-Forsch.*, 26 (1976) 1295.
[34] J.W. Sammon, Jr., *IEEE Trans. Comput.*, C18 (1969) 401.
[35] H. Mager, *Moderne Regressionsanalyse*, Salle, Säuerlander, Frankfurt am Main, 1982, p. 135.
[36] T. Fujita, J. Iwasa and C. Hansch, *J. Am. Chem. Soc.*, 86 (1964) 5175.
[37] A. Leo, C. Hansch and M. Ames, *J. Pharm. Sci.*, 64 (1975) 559.

[38] C. Hasch and A. Leo, *Substituent Constants for Correlation Analysis in Chemistry and Biology*, Wiley, New York, 1979, p. 1.
[39] L. Pauling and D. Pressman, *J. Am. Chem. Soc.*, 67 (1945) 1003.
[40] R.W. Taft and I.C. Lewis, *J. Am. Chem. Soc.*, 80 (1958) 2436.
[41] L.P. Hammett, *Chem. Rev.*, 17 (1935) 125.
[42] R.W. Taft, *J. Am. Chem. Soc.*, 74 (1952) 3120.
[43] A. Verloop and J. Tipker, *Pestic. Sci.*, 7 (1976) 379.
[44] A. Verloop, W. Hoogenstraaten and J. Tipker, in J. Ariens (Editor), *Drug Design*, Vol. VII, Academic Press, New York, 1976, p. 165.
[45] K.V. Mardia, J.T. Kent and J.M. Bibby, *Multivariate Analysis*, Academic Press, London, 1979, p. 213.
[46] P. Willett, *Similarity and Clustering in Chemical Information Systems*, Research Studies Press, New York, 1987.

ELSEVIER

Journal of Chromatography A, 697 (1995) 71–80

JOURNAL OF CHROMATOGRAPHY A

Prediction of retention for substituted and unsubstituted polycyclic aromatic hydrocarbons in micellar liquid chromatography in the presence of organic modifiers

M.A. Rodríguez Delgado, M.J. Sánchez, V. González, F. García Montelongo*

Department of Analytical Chemistry, Food Science and Toxicology, University of La Laguna, 38071 La Laguna, Spain

Abstract

Statistical and factor analysis have been used to establish some general equations relating retention parameters to molecular descriptors of substituted and unsubstituted polycyclic aromatic hydrocarbons. They allow the determination of the retention behaviour of these solutes in micellar liquid chromatography using "hybrid" sodium dodecyl sulphate–water–alcohol micellar mobile phases and a Nova-Pak C_{18} column.

1. Introduction

In the past years several models have been published in the context of quantitative structure–retention relationships (QSSRs) in order to predict the retention behaviour in liquid and gas chromatography, and even though linear and non-linear models have been proposed and different statistics have been used, the practical significance of a model depends mostly on the coincidence between the calculated and the experimental data. Critical reviews of many of these efforts have been published by Kaliszan [1] and Lochmüller et al. [2].

Numerous solute-related physicochemical characteristic, descriptors, such as molecular connectivity (χ) [3–6], octanol–water partition coefficient (log P) [7,8], Van der Waals volume (V_{vw}) [9–11], length-to-breadth ratio of the molecule (L/B) [12–14], dipole moment (μ) [15,16], etc. or combinations of several descriptors [3,16,17] have been used in QSSRs, but in chromatographic practice a model is preferable if the descriptors have a clear physicochemical meaning.

It has been suggested that an adequate model should include as many descriptors as possible in order to take all types of interactions in the chromatographic system into account [18]. However, a great number of descriptors in the model can complicate the calculation, even with the use of computers, without ameliorating the model [19]. According to Kaliszan [20] observing all the statistical rules and recommendations, one must select the minimum number of descriptors to produce an equation with good predictive ability.

Polycyclic aromatic hydrocarbons (PAHs) are a unique group of compounds whose mutagenic and carcinogenic properties makes it necessary to develop accurate methods for their separation and identification. Reversed-phase high-performance liquid chromatography (RP-HPLC), with UV and/or fluorescence detection and acetonitrile–water or methanol–water as mobile phases,

* Corresponding author.

0021-9673/95/$09.50
SSDI 0021-9673(94)00870-1

has become increasingly popular among researchers for analysis of PAHs.

Micellar liquid chromatography (MLC) which uses aqueous surfactant solutions, at concentrations above the critical micelle concentration, as mobile phases in RP-HPLC, can be considered as an alternative to classical partition chromatography with hydro–organic phases. Some advantages of the technique are the low cost and the non-flammability, non-toxicity and easy disposal of the solvent. However, the low efficiency of these mobile phases has been well established mainly due to the slow mass transfer [21], but raising temperature and adding small amounts of alcohols, giving rise to the so-called "hybrid" mobile phases, enhances the efficiency of the separation and improves retention control [22]. The presence of the alcohol modifier in the system can alter the configuration of the stationary phase, and its incorporation in the micelle can result in additional interaction with solute.

In this paper multiple linear regression models are established between MLC retention parameters, using an anionic micellar system, in the presence of methanol, 2-propanol and *n*-butanol as the modifier, and several molecular descriptors of PAHs.

2. Experimental

2.1. Apparatus

All measurements were made with a Waters 600 multisolvent delivery system equipped with an U6K sample injector, a Waters Lambda-Max 481 LC variable-wavelength spectrophotometric detector operating at 254 nm, and a Baseline Workstation 810. The analytical column was a Waters (Milford, MA, USA) Nova-Pak C_{18}, 150×3.9 mm I.D., 4 μm particle diameter. A silica precolumn was employed to saturate the mobile phase with silicate to protect the analytical column and to avoid hydrolysis of the bonded stationary phase. The analytical column and the mobile phase reservoir were water-jacketed and temperature-controlled with a circulating bath.

2.2. Reagents

The surfactant sodium dodecyl sulfate (SDS) of electrophoresis grade was obtained from Aldrich (Milwaukee, WI, USA) and used as received. Methanol (MeOH), ethanol, 2-propanol (PrOH) and *n*-butanol (BuOH) were Merck (Darmstadt, Germany) analytical-reagent grade products. Naphthalene (1), acenaphthylene (2), fluorene (3), anthracene (4), phenanthrene (5), fluoranthene (6), pyrene (7), chrysene (8), benz[*a*]anthracene (9), benzo[*b*]fluoranthene (10), benzo[*a*]pyrene (11), benzo[*e*]pyrene (12), perylene (13), dibenz[*a,c*]anthracene (14), dibenz[*a,h*]anthracene (15), benzo[*ghi*]perylene (16), 1-methylanthracene (17), 2-methylanthracene (18), 9-methylanthracene (19), 9,10-dimethylanthracene (20), 2-methylphenanthrene (21) and 3,6-dimethylphenanthrene (22) were Aldrich products. Numbers identify the compound in tables.

2.3. Procedure

The appropriate mass of SDS was dissolved in Milli-Q (Millipore, Bedford, MA, USA) water containing the desired alcohol content, and the solution filtered through a 0.45-μm nylon membrane filter (Whatman, Kent, England). The mobile phase was degassed under vacuum in an ultrasonic bath prior to use. Stock solutions of PAHs were prepared in ethanol, and diluted with the same solvent when necessary.

The void volume of the system was measured by multiple injections of water or sodium nitrate solution and found to be 0.81 ml, and was used for all k' calculations. The k' values were measured at 60 ± 0.1°C, injections of 20 μl were made. All measurements were made at least five times. Calculated log k' are shown in Table 1.

2.4. Descriptors generation

The descriptors considered in this paper were

Table 1
Log k' values for the PAHs studied

PAH	Log k'														
	Methanol (%)					2-Propanol (%)					*n*-Butanol (%)				
	3	5	10	15	20	3	5	10	15	20	2	4	6	8	10
Naphthalene	1.322	1.314	1.272	1.229	1.183	1.252	1.208	1.113	1.022	0.936	1.202	1.115	1.030	0.959	0.875
Acenaphthylene	1.362	1.351	1.312	1.272	1.231	1.287	1.246	1.147	1.056	0.970	1.238	1.147	1.059	0.985	0.898
Fluorene	1.484	1.471	1.436	1.396	1.358	1.405	1.360	1.265	1.177	1.098	1.346	1.249	1.158	1.081	0.991
Anthracene	1.520	1.508	1.470	1.434	1.398	1.440	1.394	1.295	1.209	1.130	1.380	1.279	1.185	1.106	1.018
Phenanthrene	1.498	1.491	1.450	1.415	1.370	1.417	1.369	1.273	1.182	1.117	1.358	1.263	1.173	1.089	0.998
Fluoranthene	1.565	1.556	1.516	1.481	1.437	1.477	1.425	1.348	1.235	1.171	1.413	1.311	1.219	1.132	1.039
Pyrene	1.574	1.560	1.523	1.484	1.449	1.481	1.434	1.331	1.246	1.171	1.420	1.312	1.218	1.138	1.049
Chrysene	1.679	1.669	1.623	1.590	1.548	1.584	1.527	1.429	1.340	1.277	1.509	1.401	1.305	1.215	1.120
Benz[*a*]anthracene	1.685	1.670	1.633	1.591	1.557	1.588	1.536	1.433	1.347	1.275	1.516	1.399	1.299	1.214	1.122
Benzo[*b*]fluoranthene	1.742	1.733	1.689	1.654	1.611	1.637	1.580	1.477	1.388	1.329	1.564	1.444	1.346	1.256	1.158
Benzo[*a*]pyrene	1.749	1.733	1.696	1.653	1.621	1.645	1.590	1.485	1.402	1.332	1.567	1.445	1.346	1.263	1.171
Benzo[*e*]pyrene	1.706	1.692	1.648	1.614	1.580	1.609	1.553	1.445	1.358	1.288	1.531	1.411	1.310	1.227	1.136
Perylene	1.711	1.699	1.656	1.616	1.581	1.610	1.554	1.446	1.363	1.293	1.534	1.411	1.312	1.232	1.139
Dibenz[*a*,*c*]anthracene	1.815	1.807	1.760	1.721	1.677	1.703	1.640	1.537	1.444	1.383	1.612	1.491	1.387	1.294	1.192
Dibenz[*a*,*h*]anthracene	1.796	1.776	1.728	1.690	1.658	1.679	1.624	1.512	1.428	1.360	1.602	1.469	1.363	1.284	1.197
Benzo[*ghi*]perylene	1.854	1.837	1.793	1.759	1.723	1.746	1.691	1.582	1.497	1.426	1.654	1.526	1.419	1.330	1.235
1-Methylanthracene	1.620	1.606	1.565	1.526	1.493	1.534	1.484	1.382	1.293	1.218	1.467	1.354	1.253	1.168	1.075
2-Methylanthracene	1.641	1.626	1.586	1.550	1.518	1.554	1.503	1.410	1.320	1.248	1.485	1.373	1.275	1.191	1.100
9-Methylantracene	1.683	1.669	1.629	1.591	1.560	1.595	1.544	1.440	1.350	1.278	1.525	1.407	1.301	1.213	1.117
9.10-Dimethylantracene	1.616	1.601	1.563	1.523	1.491	1.532	1.478	1.387	1.294	1.219	1.463	1.354	1.255	1.171	1.081
2-Methylphenanthrene	1.707	1.691	1.648	1.609	1.576	1.615	1.559	1.457	1.363	1.289	1.538	1.415	1.307	1.217	1.120
3,6-Dimethylphenanthrene	1.605	1.598	1.556	1.516	1.482	1.518	1.468	1.368	1.281	1.206	1.451	1.342	1.244	1.161	1.069

Standard deviation ≤ 0.0012.

obtained from the bibliography {log P = logarithm of the octanol–water partition coefficient [3], χ = molecular connectivity index [12], L/B: the ratio of the maximalized length-to-breadth [12], F = correlation factor, calculated for each PAH as (number of double bonds) + (number of primary and secondary carbon atoms) − 0.5 for a non-aromatic ring) or calculated using the PC Model V4.0 approach (Serena Software, Bloomington, IN, USA) }. This program was used to determine the three-dimensional structure of compounds based on energy minimization. After setting up the geometrics of the molecules having the smallest minimized-energy, the stretching energy (STR), bond energy (BND), stretch bend constants (SB), torsional energy (TOR), Van der Waals volume (V_{vw}), dipole moment (DPMON), heat of formation (HF), fraction of non-polar surface area (NSSA/TSA), fraction of non-polar unsaturated surface area (NUSA/TSA) are calculated by the program. These data are shown in Table 2.

3. Results and discussion

In a previous work [19] equations such as log $k' = f(F,L/B)$ were established to explain the behaviour of unsubstituted PAHs when using SDS micellar mobile phases.

These kinds of equations can also be developed for unsubstituted PAHs when alcohol-modified SDS mobile phases are used and regression coefficients are even better in the presence of these modifiers (Table 3). Furthermore, while the relevance of the hydrophobicity of the

Table 2
Descriptors

PAH	*F*	*L/B*	Log *P*	χ	STR	BND	SB	TOR	V_{vw}	DPMON	HF	NSSA/TSA	NUSA/TSA
Naphthalene	5.0	1.24	3.35	3.408	0.17	0.07	0.00	12.00	5.39	0.00	35.00	0.6091	0.3972
Acenaphthylene	5.5	1.08	3.82	4.149	0.68	14.40	0.07	17.00	3.83	0.90	64.88	0.5629	0.4391
Fluorene	6.5	1.57	3.99	4.612	0.27	9.06	−0.08	13.70	3.76	0.32	48.22	0.6278	0.3734
Anthracene	7.0	1.57	4.63	4.809	0.28	0.15	0.01	18.00	8.14	0.01	55.79	0.5845	0.4195
Phenanthrene	7.0	1.46	4.63	4.815	0.47	0.68	0.03	19.00	9.34	0.16	49.35	0.5776	0.4224
Fluoranthene	8.0	1.22	5.22	5.565	0.59	15.29	0.02	25.00	6.02	0.44	70.69	0.5508	0.4519
Pyrene	8.0	1.27	5.22	5.559	0.32	0.19	0.01	24.00	9.74	0.00	57.59	0.5707	0.4298
Chrysene	9.0	1.72	5.91	6.226	0.85	1.41	0.07	26.00	13.70	0.00	66.15	0.5540	0.4485
Benz[*a*]anthracene	9.0	1.58	5.92	6.220	0.58	0.80	0.04	25.00	12.20	0.24	68.44	0.5694	0.4335
Benzo[*b*]fluoranthene	10.0	1.40	6.62	6.976	0.79	15.07	0.02	32.00	9.40	0.61	83.39	0.5404	0.4609
Benzo[*a*]pyrene	10.0	1.50	6.50	6.970	0.62	0.79	0.04	31.00	13.84	0.15	76.03	0.5571	0.4435
Benzo[*e*]pyrene	10.0	1.12	6.50	6.976	0.96	1.42	0.07	32.00	15.80	0.19	73.00	0.5401	0.4633
Perylene	10.0	1.27	6.58	6.976	0.96	1.52	0.06	32.00	15.71	0.00	79.94	0.5292	0.4750
Dibenz[*a,c*]anthracene	11.0	1.24	7.19	7.637	1.37	2.42	0.12	33.00	19.35	0.10	85.85	0.5504	0.4500
Dibenz[*a,h*]anthracene	11.0	1.12	6.85	7.720	0.82	1.43	0.06	32.00	16.19	0.00	81.58	0.5471	0.4546
Benzo[*ghi*]perylene	11.0	1.79	7.18	7.631	0.71	0.76	0.03	37.00	15.63	0.39	77.33	0.5372	0.4641
1-Methylanthracene	8.0	1.41	5.14	5.226	0.42	0.43	0.03	17.01	9.04	0.17	49.43	0.6306	0.3730
2-Methylanthracene	8.0	1.74	5.14	5.220	0.32	0.25	0.02	17.28	8.48	0.35	48.11	0.6398	0.3602
9-Methylantracene	9.0	1.23	5.65	5.655	0.71	1.41	0.07	16.74	10.71	0.18	53.59	0.6317	0.3725
9,10-Dimethylantracene	8.0	1.58	5.14	5.226	0.89	1.60	0.08	17.66	12.36	0.01	51.51	0.6814	0.3191
2-Methylphenanthrene	9.0	1.26	5.65	5.637	0.49	0.81	0.04	18.28	9.64	0.34	41.52	0.6291	0.3719
3,6-Dimethylphenanthrene	8.0	1.38	5.14	5.232	0.55	0.91	0.05	17.56	9.98	0.40	33.37	0.6911	0.3131

molecule remains almost constant (*a* coefficient), the shape (*b* coefficient) increases its relevance as methanol and propanol concentrations increase, when butanol is the modifier the relevance of both factors decreases on increasing its concentration which can be related to its hydrophobicity.

However, when log k' values for the methyl-substituted PAHs are included in these equations, the corresponding regression coefficients decrease in both normal and "hybrid" mobile phases. Moreover, when using, i.e., the equation log $k' = f(c,F,L/B)$ with hybrid mobile phases two straight lines can be observed on comparing calculated and experimental values (Fig. 1), one of them enclosing the unsubstituted PAHs ($R^2 = 0.997$) and the other enclosing the methyl-substituted PAHs ($R^2 = 0.926$), if the whole set of data are regressed all together the regression coefficient decreases even more ($R^2 = 0.985$). This effect has already been reported in RP-HPLC [23,24] and related to the non-planarity of the methyl-PAHs due to the presence of the methyl group in the so-called "bay-region" of the PAH structure.

Thus, it is necessary to establish a new model which can explain the behaviour of both unsubstituted and methyl-substituted PAHs. In this way the thirteen starting descriptors in Table 2 were subjected to factor analysis and the results are shown in Table 4. If the number of factors is chosen with the ordinary rule of selecting the ≥ 1 "eigenvalues", then four factors (F) are extracted, which account for the 93% of the total variance; thus only four factors were selected for further calculations.

Taking into consideration the factor loadings for the thirteen descriptors in the varimax rotated factor matrix (Table 4), one can see that descriptors F and NUSA/TSA explain 96% of the variance on F_1 and F_2, respectively, DPMON explains 92% of the variance of F_3 and L/B the 84% of F_4. That is, the retention behaviour of PAHs in this hybrid micellar mobile phase can be explained as a function of these four descriptors namely: F and L/B, geometric descriptors whose

Table 3
Regression equation for the retention of unsubstituted PAHs with a 0.15 *M* SDS mobile phase containing several concentration of alcohols

Statistical parameter	Log $k' = aF + bL/B + c$[a]									
	Fraction of alcohol in the mobile phase (%, v/v)									
	2	3	4	5	6	8	10	15	20	25	30
Methanol											
a		0.0791		0.0782			0.0770	0.0775	0.0786	0.0830	0.0880
b		0.0892		0.0887			0.0934	0.0964	0.0972	0.1020	0.1058
c		0.8231		0.8195			0.7816	0.7367	0.6867	0.6296	0.5662
R^2		0.997		0.997			0.996	0.997	0.996	0.995	0.995
S.D.		0.0083		0.0084			0.0094	0.0091	0.0096	0.0119	0.0124
F		2725.6		2650.5			2026.3	2197.5	2059.5	1483.5	1523.8
2-Propanol											
a		0.0721		0.0695			0.0669	0.0678	0.0708	0.0758	0.0808
b		0.0940		0.0941			0.0956	0.1022	0.1047	0.1059	0.1077
c		0.7825		0.7538			0.6729	0.5672	0.4671	0.3391	0.2125
R^2		0.998		0.997			0.994	0.997	0.997	0.997	0.997
S.D.		0.0071		0.0081			0.0105	0.0080	0.0083	0.0077	0.0083
F		3162.0		2251.3			1257.0	2217.6	2234.7	2958.4	2910.5
n-Butanol											
a	0.0662		0.0592		0.0561	0.0540	0.0526				
b	0.0842		0.0866		0.0850	0.0769	0.0722				
c	0.7780		0.7241		0.6569	0.6027	0.5296				
R^2	0.997		0.996		0.996	0.997	0.997				
S.D.	0.0074		0.0072		0.0076	0.0056	0.0062				
F	2462.9		2059.8		1681.1	2858.5	2219.9				

[a] $R^2 = 0.990$ when no alcohol modifier is present [19].

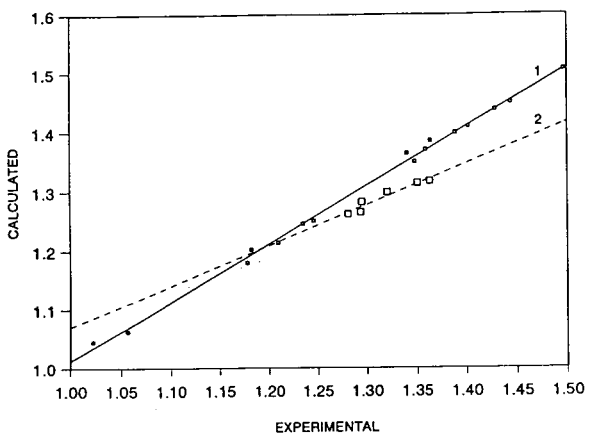

Fig. 1. Plot of calculated vs. experimental values according to the equation log $k' = f(F,L/B)$, with a 0.15 *M* SDS and 15% 2-propanol in water mobile phase. 1 = Unsubstituted PAHs; 2 = methyl-substituted PAHs.

relevance in the factor analysis reveals the importance of the size and shape of the molecule; NUSA/TSA, giving information about the electron delocalization along the aromatic rings, and DPMON, an electronic descriptor giving information about the dispersive forces. The relevance of these latter descriptors is in agreement with the idea that polarity can play an important role in the retention behaviour of PAHs. Although the total dipole moment has occasionally been reported as a significant parameter in QSRR equations, it has been shown that it can not be used to describe all specific polar features of the compounds [25]. However, one can see in Table 2 how DPMON acquires importance in describing the electronic properties of isomers (i.e., 1-methylanthracene 0.17 D, 2-methylanthracene 0.35 D).

Table 4
Factor analysis of the thirteen molecular descriptors

Eigenvalue	7.141	2.486	1.469	0.916	0.570				
% variance	54.9	74.1	85.4	92.4	96.8				
Variable	Unrotated matrix				Estimated communality	Varimax rotated			
	F_1	F_2	F_3	F_4		F_1	F_2	F_3	F_4
Log P	0.93849	0.19255	−0.03566	0.25065	0.98194	0.95240	0.25381	−0.09965	−0.02276
χ	0.95486	0.09643	0.02802	0.23145	0.97541	0.91864	0.35596	−0.05505	−0.04199
L/B	−0.09302	0.37045	0.62115	0.49676	0.77848	0.07518	−0.10550	−0.22455	−0.84337
F	0.90699	0.23686	−0.05548	0.29255	0.96740	0.95901	0.18660	−0.10396	−0.04563
STR	0.82766	0.00809	−0.44345	−0.03855	0.88322	0.78825	0.18964	0.03632	0.47392
BND	−0.05362	−0.88977	−0.17547	0.27000	0.89825	−0.12448	0.24647	0.90374	0.07256
SB	0.59479	0.23867	−0.57807	−0.21859	0.79268	0.60937	−0.05366	−0.17477	0.62284
TOR	0.95970	−0.14575	0.13001	0.03257	0.96024	0.75512	0.62298	0.00164	0.04388
V_{vw}	0.88862	0.43646	−0.05847	−0.07392	0.98903	0.84636	0.21472	−0.44805	0.16079
DPMON	−0.16525	−0.73507	−0.38094	0.39862	0.87165	−0.07825	−0.05621	0.92270	0.10480
HF	0.89256	−0.36217	0.13504	0.01360	0.94625	0.63353	0.71518	0.16787	0.07237
NSSA/TSA	−0.68906	0.50732	−0.40844	0.29187	0.98419	−0.23582	−0.96027	−0.05825	−0.05533
NUSA/TSA	0.68276	−0.50696	0.40794	−0.30712	0.98391	0.22450	0.96269	0.05085	0.06448

In order to check the latter conclusion, regression analysis was carried out on log k', F, L/B, NUSA/TSA and DPMON and the resulting equations are shown in Table 5. As can be seen, for a 0.15 M SDS mobile phase and for each percentage of alcohol modifier, the equation obtained shows a high correlation coefficient, a low standard deviation and a high Fisher F value, as well as a small number of independent variables [20].

Furthermore, from these equations it can be deduced that the retention of a PAH in MLC increases as: (1) F and L/B, size and shape of the molecule increase; we must remember that hydrophobicity increases with the size of the molecule as F and log P are highly correlated ($R^2 = 0.993$, $n = 22$) and appear on F_1 with high factor loadings; (2) as the dipole moment DPMOM increases, however, the loading of this descriptor is small when compared with F and L/B and serves mainly to differentiate between methyl-substituted isomers; and (3) as the NUSA/TSA ratio decreases, this descriptor gives information about the electron delocalization on the aromatic rings, thus retention increases as electrons are more localized. This effect can be clearly seen taking anthracene, 2-methylanthracene and 9,10-dimethylanthracene, which elute in this order, as an example. In their electronic maps (Fig. 2), one can see that the presence of a methyl substituent increases the electron localization (δ^-), this effect being more relevant for 9,10-dimethylanthracene, due to the inductive effect (δ^+) of the methyl group.

The results in Table 5 show that the coefficients of the independent variables change with the alcohol modifier and its percentage in the mobile phase (Fig. 3). In general, as the alcohol hydrophobicity increases the solute hydrophobicity becomes less important, due to competitivity of both alcohol and solute for the micelles. The same effect is observed as the alcohol percentage increases, until ca. 20% for methanol and propanol and ca. 6% for *n*-butanol, which can be related to the micelles losing their integrity at the higher modifier percentages [26,27] and to the formation of mixed micelles [28,29].

Given that the coefficients for the independent

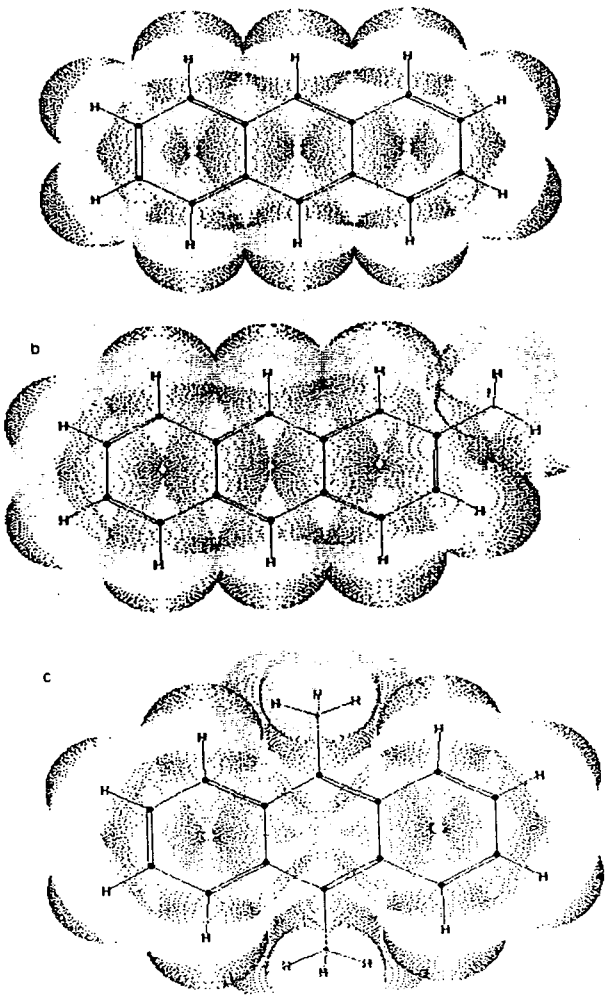

Fig. 2. The three-dimensional structure of (a) anthracene, (b) 2-methylanthracene and (c) 9,10-dimethylanthracene obtained by molecular modeling. The darker dots indicate the polar surface region on the molecules.

variables change as the percentage of the alcohol modifier in the mobile phase changes, it will be possible to develop a more general equation where this percentage will be taken into account, and valid up to ca. 20% methanol or 2-propanol or ca. 6% *n*-butanol in the mobile phase. The results are shown in Table 6.

Furthermore, as previously shown [30] the best selectivity for this group of PAHs on a C_{18} column is obtained with a 15% 2-propanol and ca. 0.15 *M* SDS in water mobile phase; an

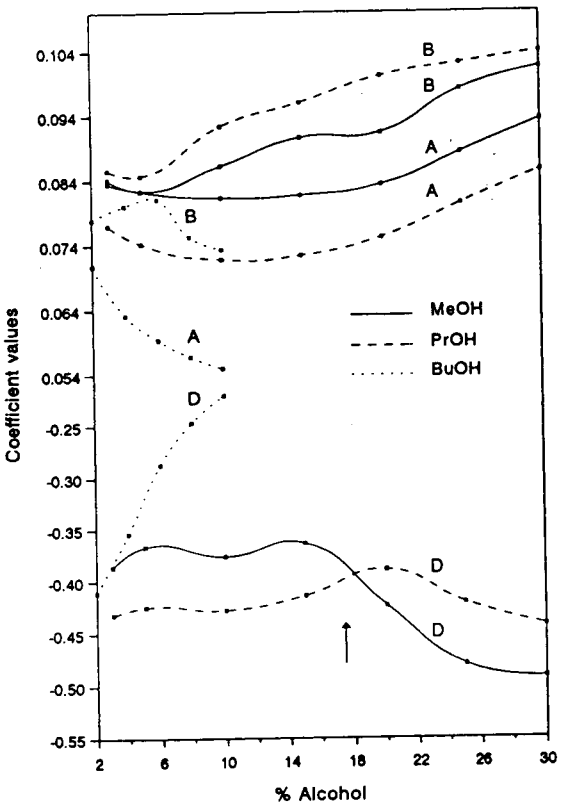

Fig. 3. Plot of the coefficients of the independent variables in the equations in Table 5 as a function of the alcohol percentage.

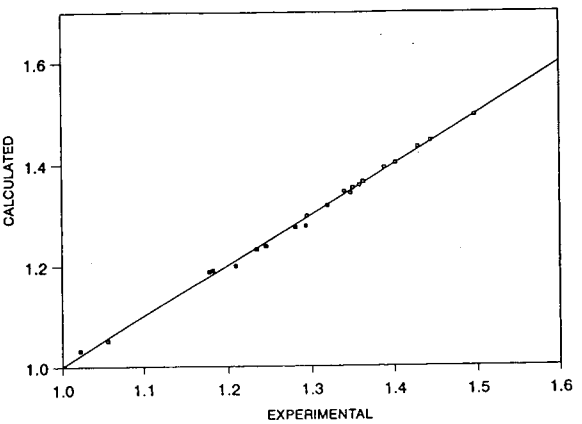

Fig. 4. Plot of calculated vs. experimental values according to Eq. b in Table 6, for a 0.15 *M* SDS and 15% 2-propanol in water mobile phase.

Table 5
Regression equation for the prediction of the retention of substituted and unsubstituted PAHs using a 0.15 *M* SDS mobile phase in the presence of alcohol modifier

Statistical parameter	Log $k' = aF + bL/B + c$DPMON $+ d$NUSA/TSA $+ e$										
	Fraction of alcohol in the mobile phase (%, v/v)										
	2	3	4	5	6	8	10	15	20	25	30
Methanol											
a		0.08349		0.08232			0.08130	0.08165	0.08328	0.08825	0.09328
b		0.08412		0.08239			0.08623	0.09057	0.09134	0.09809	0.10148
c		0.02076		0.01868			0.01874	0.02080	0.02067	0.02577	0.02355
d		−0.38637		−0.36638			−0.37651	−0.36369	−0.42398	−0.47994	−0.49158
e		0.95818		0.95027			0.91665	0.86354	0.83691	0.79629	0.73895
R^2		0.998		0.997			0.997	0.996	0.996	0.993	0.993
S.D.		0.00716		0.00768			0.00784	0.00805	0.00858	0.01178	0.01246
F		1896.7		1610.5			1506.9	1445.7	1313.4	776.4	779.2
2-Propanol											
a		0.07696		0.07419			0.07174	0.07229	0.07509	0.08033	0.08546
b		0.08555		0.08472			0.09236	0.09605	0.10016	0.10212	0.10384
c		0.01773		0.01690			0.02422	0.01727	0.01957	0.01901	0.01726
d		−0.43211		−0.42466			−0.42786	−0.41415	−0.38960	−0.42126	−0.44240
e		0.93966		0.90970			0.81941	0.71596	0.60378	0.48718	0.36937
R^2		0.997		0.996			0.994	0.996	0.997	0.997	0.997
S.D.		0.00717		0.00783			0.00929	0.00710	0.00755	0.00728	0.00794
F		1596.3		1246.6			825.5	1452.5	1394.2	1709.1	1625.9
n-Butanol											
a	0.07077		0.06315		0.05933	0.05672	0.05493				
b	0.07791		0.08008		0.08106	0.07525	0.07328				
c	0.02017		0.01661		0.01636	0.01270	0.0112				
d	−0.41099		−0.35420		−0.28759	−0.24710	−0.22116				
e	0.92414		0.85165		0.75760	0.68840	0.60393				
R^2	0.996		0.995		0.995	0.997	0.996				
S.D.	0.00721		0.00696		0.00683	0.00499	0.00563				
F	1329.2		1148.4		1067.6	1843.7	1366.2				

equation has been developed for this mobile phase (Table 6). Obviously a more general equation could be established as a simultaneous function of X, percentage of propanol, and C, concentration of surfactant, in the mobile phase which allows the prediction of the retention for this group of PAHs for any given chromatographic conditions using such a mobile phase. However, much more experimental work would be necessary for this objective.

The calculated log k' values according to Eq. b in Table 6, are plotted in Fig. 4 against the experimental values for the twenty two unsubstituted and methyl-substituted PAHs. The equation of the fitted straight line (linear least squares) was: $\log k'_{calc} = 0.0038 + 0.997 \log k'_{exp}$ ($R^2 = 0.997$, standard error of estimate = 0.00653). The high correlation coefficient, the proximity of the slope to unity and the low intercept revealed the absence of systematic errors.

4. Conclusions

Equations previously developed for the prediction of the retention of unsubstituted PAHs in micellar SDS mobile phases, can be also used for

Table 6
General regression equation for the prediction of the retention of substituted and unsubstituted PAHs using X (%) alcohol and C (M) SDS in water mobile phase

$$\text{Log } k' = a(X)F + b(X)L/B + c(X)\text{DPMON} + d(X)\text{NUSA/TSA} + e(X)$$

Eq. a: methanol (≤20%)

$$\begin{aligned}\text{Log } k' = {} & (8.57\cdot10^{-2} - 9.15\cdot10^{-4}X + 5.35\cdot10^{-5}X^2 - 6.94\cdot10^{-7}X^3)F \\ & + (8.89\cdot10^{-2} - 2.53\cdot10^{-3}X + 3.12\cdot10^{-4}X^2 - 8.96\cdot10^{-6}X^3)L/B \\ & + (2.64\cdot10^{-2} - 2.59\cdot10^{-3}X + 2.46\cdot10^{-4}X^2 - 6.58\cdot10^{-6}X^3)\text{DPMON} \\ & + (4.29\cdot10^{-1} + 1.66\cdot10^{-2}X - 8.20\cdot10^{-4}X^2)\text{NUSA/TSA} \\ & + (9.45\cdot10^{-1} + 8.34\cdot10^{-3}X - 1.59\cdot10^{-3}X^2 + 4.50\cdot10^{-5}X^3)\end{aligned}$$

Eq. b: 2-propanol (≤20%)

$$\begin{aligned}\text{Log } k' = {} & (8.24\cdot10^{-2} - 2.25\cdot10^{-3}X + 1.39\cdot10^{-4}X^2 - 2.24\cdot10^{-6}X^3)F \\ & + (8.26\cdot10^{-2} + 1.04\cdot10^{-3}X - 8.18\cdot10^{-6}X^2)L/B \\ & + (1.71\cdot10^{-2} - 5.77\cdot10^{-4}X + 3.00\cdot10^{-5}X^2)\text{DPMON} \\ & + (-4.28\cdot10^{-1} - 1.97\cdot10^{-3}X + 1.94\cdot10^{-4}X^2)\text{NUSA/TSA} \\ & + (9.86\cdot10^{-1} - 1.42\cdot10^{-2}X - 2.44\cdot10^{-4}X^2)\end{aligned}$$

Eq. c: n-butanol (≤6%)

$$\begin{aligned}\text{Log } k' = {} & (8.30\cdot10^{-2} - 7.58\cdot10^{-3}X + 7.87\cdot10^{-4}X^2 - 3.09\cdot10^{-5}X^3)F \\ & + (7.23\cdot10^{-2} + 3.34\cdot10^{-3}X - 3.24\cdot10^{-4}X^2)L/B \\ & + (2.40\cdot10^{-2} - 2.14\cdot10^{-3}X + 8.77\cdot10^{-5}X^2)\text{DPMON} \\ & + (-4.60\cdot10^{-1} + 1.92\cdot10^{-2}X + 3.00\cdot10^{-3}X^2 - 2.54\cdot10^{-4}X^3)\text{NUSA/TSA} + (1.01 - 4.02\cdot10^{-2}X)\end{aligned}$$

$$\text{Log } k' = a(C)F + b(C)L/B + c(C)\text{DPMON} + d(C)\text{NUSA/TSA} + e(C)$$

Eq. d: SDS (15% 2-propanol)

$$\begin{aligned}\text{Log } k' = {} & (1.46\cdot10^{-1} - 1.230C + 7.88C^2 - 19.60C^3)F \\ & + (1.77\cdot10^{-1} - 1.118C + 3.86C^2)L/B \\ & + (5.70\cdot10^{-2} - 5.66\cdot10^{-1}C + 2.027C^2)\text{DPMON} \\ & + (-1.72\cdot10^{-1} - 6.547C + 32.86C^2)\text{NUSA/TSA} \\ & + (1.209 - 6.263C + 41.00C^2 - 140.52C^3)\end{aligned}$$

X = Volume fraction of alcohol modifier, at 0.15 M SDS; C = concentration of SDS in presence of 2-propanol.

"hybrid" alcohol–SDS–water mobile phases with even better regression coefficients, showing that in both cases retention is mainly a function of size and shape of the molecules. However the prediction is no longer valid when dealing with methyl-substituted PAHs.

In the new equations developed for both unsubstituted and methyl-substituted PAHs, electronic parameters are included to take into account the electron distribution in the molecules. The coefficient of the independent variables in these equations show a quite different behaviour of the hybrid mobile phases containing methanol or 2-propanol from those containing butanol, which is related to their different hydrophobicity.

Furthermore, for ca. 20% methanol or propanol and ca. 6% butanol a changing behaviour is also observed and related to the micelles losing their integrity and to the formation of mixed micelles.

The equations developed to model the retention behaviour of both unsubstituted and methyl-substituted PAHs are useful for the optimization of the resolution in their separation using the elution data for a reduced number of compounds. However, more work is necessary on the optimum prediction equation.

Acknowledgement

This work was supported by DGICYT (Spain) grant PB88-0427.

References

[1] R. Kaliszan, *J. Chromatogr. A*, 656 (1993) 417.
[2] C.H. Lochmüller, C. Reese, A.J. Aschman and S.J. Breiner, *J. Chromatogr. A*, 656 (1993) 3.
[3] K. Jinno and K. Kawasaki, *Chromatographia*, 17 (1983) 445.
[4] W. Markowski, T. Dziso and T. Wawrszynowicz, *Pol. J. Chem.*, 52 (1978) 2063.
[5] R. Kaliszan and H. Lamparczyk, *J. Chromatogr. Sci.*, 16 (1978) 246.
[6] L.B. Kier and L.H. Hall, *Molecular Connectivity in Chemistry and Drug Research*, Academic Press, New York, 1976.
[7] C. Hansch and A. Leo, *Substituent Constant for Correlation Analysis in Chemistry and Biology*, Wiley, New York, 1979.
[8] H. Hanai, *J. Chromatogr.*, 161 (1978) 1.
[9] R.B. Hermann, *J. Phys. Chem.*, 76 (1972) 596.
[10] F.S. Calixto and A.G. Raso, *Chromatographia*, 14 (1981) 596.
[11] K. Jinno and A. Ishigaki, *J. High Resolut. Chromatogr. Chromatogr. Commun.*, 5 (1982) 668.
[12] S.A. Wise, W.J. Bonnett, F.R. Gunther and W.E. May, *J. Chromatogr. Sci.*, 19 (1981) 457.
[13] A. Radecki, H. Lamparczyk and R. Kaliszan, *Chromatographia*, 12 (1979) 595.
[14] M. Randic, *J. Chromatogr.*, 161 (1978) 1.
[15] R. Kaliszan and H.D. Höltje, *J. Chromatogr.*, 234 (1982) 303.
[16] K. Ong and R. Hites, *Anal. Chem.*, 63 (1991) 2829.
[17] K. Jinno and K. Kawasaki, *Chromatographia*, 17 (1983) 337.
[18] S.N. Lanin and Yu.S. Nikitin, *Chromatographia*, 25 (1988) 272.
[19] M.A. Rodríguez Delgado, M.J. Sánchez, V. González and F. García Montelongo, *Fresenius' J. Anal. Chem.*, 345 (1993) 748.
[20] R. Kaliszan, *Anal. Chem.*, 64 (1992) 619A.
[21] P. Yarmchuk, R. Weinberger, R. Hirsch and L.J. Cline-Love, *J. Chromatogr.*, 283 (1984) 47.
[22] J. Dorsey, M. DeEchegaray and J.S. Landy, *Anal. Chem.*, 55 (1983) 924.
[23] R.H. Rohrbaugh and P.C. Jurs, *Anal. Chem.*, 59 (1987) 1048.
[24] S.A. Wise, L.C. Sander, R. Lapouyade and P. Garrigues, *J. Chromatogr.*, 514 (1990) 111.
[25] V.S. Ong and R.A. Hites, *Anal. Chem.*, 63 (1991) 2829.
[26] M.G. Khaledi, E. Peuler and J.Ngeh-Ngwainbi, *Anal. Chem.*, 59 (1987) 2738.
[27] J.K. Strasters, E.D. Breyer, A.H. Rodgers and M.G. Khaledi, *J. Chromatogr.*, 511 (1990) 17.
[28] E. Aircart, D.J. Jobe, B Skalski and R.E. Verrall, *J. Phys. Chem.*, 96 (1992) 2348.
[29] D.J. Jobe, R.E. Verrall, B. Skalski and E. Aircart, *J. Phys. Chem.*, 96 (1992) 6811.
[30] M.A. Rodríguez Delgado, M.J. Sánchez, V. González and F. García Montelongo, *Anal. Chim. Acta*, in press.

ELSEVIER

Journal of Chromatography A, 697 (1995) 81–88

JOURNAL OF CHROMATOGRAPHY A

Evaluation of different techniques for peak purity assessment on a diode-array detector in liquid chromatography

H. Fabre*, A. Le Bris, M.D. Blanchin

Laboratoire de Chimie Analytique, Faculté de Pharmacie, 15 Avenue Charles Flahaut, 34060 Montpellier Cédex 01, France

Abstract

The efficiencies of nine different techniques implemented on a diode-array detector in liquid chromatography for peak homogeneity determination were compared at a concentration level of a drug that can be found in biological samples. Solutions of cefotaxime sodium (analyte) spiked with various amounts of a model impurity (theophylline) were injected under chromatographic conditions giving severe overlap of the peaks ($R_s = 0.14$). Under the conditions used, the most efficient techniques implemented in the instrument were spectral suppression (ca. 0.5%), derivative spectrum (<1%), followed by spectral overlay, absorbance ratio plot (<5%), multiple-wavelength chromatograms overlay and purity parameter (ca. 5%). The numerical value of the absorbance ratio could also be exploited statistically to detect 0.5% of impurity. Theophylline at levels up to 10% could not be detected using three-dimensional plots, contour diagrams and derivative chromatograms.

1. Introduction

Since the introduction of diode-array detectors (DAD), many approaches, the advantages and limits of which have been widely discussed in the literature ([1–6] and references cited therein), have been proposed for peak purity determination in liquid chromatography. Several techniques are generally used in conjunction to ensure the selectivity of an analytical procedure in research and development. Their selection is guided by their sensitivity for detecting the impurity and the spectral information available on both the analyte and impurity. A comparison of the performances, under the same chromatographic conditions, of several techniques implemented on a commercial instrument may be of interest to the analyst faced with the problem of peak homogeneity assessment.

In a previous study [7], we had compared the sensitivity of spectral suppression, spectral overlay and absorbance ratio techniques using a bench-top diode-array detector with a spectral bandwidth of 5 nm. We have now evaluated the efficiency of nine different techniques on a diode-array detector presenting a higher resolution and set at a spectral bandwidth of 1.3 nm. The study was carried out on the same compounds (cefotaxime sodium as analyte and theophylline as model impurity), under chromatographic conditions giving severe overlap of the peaks and at a concentration level of the analyte that can be found in biological samples (20 mg l^{-1}), with a view to biological applications.

* Corresponding author.

0021-9673/95/$09.50
SSDI 0021-9673(94)00979-1

2. Experimental

2.1. Chemicals

Cefotaxime (Roussel UCLAF) and theophylline (Cetrane Unicet) were used as received. Other chemicals were of analytical-reagent or HPLC grade.

2.2. Solutions

Stock standard aqueous solutions (100 mg l^{-1}) of cefotaxime and theophylline were prepared. From these solutions, working standard solutions of theophylline (20 mg l^{-1}), cefotaxime (20 mg l^{-1}), and cefotaxime (20 mg l^{-1}) spiked with 10%, 5%, 1% and 0.5% of theophylline with respect to cefotaxime, were prepared by suitable dilution with the mobile phase.

2.3. Apparatus and experimental conditions

The chromatographic system consisted of a Waters Model 510 pump fitted with a Rheodyne injection valve provided with a 20-μl loop, a Waters Model 991 diode-array detector, a Waters Model 5200 printer and a Powermate SX Plus Nec information system. The cartridge used (25 cm × 4.5 mm I.D.) was packed with LiChrosorb RP-18 (7 μm) (Merck). The mobile phase was 0.025 *M* potassium dihydrogenophosphate (pH 4)–methanol (85:15, v/v). The flow-rate was set

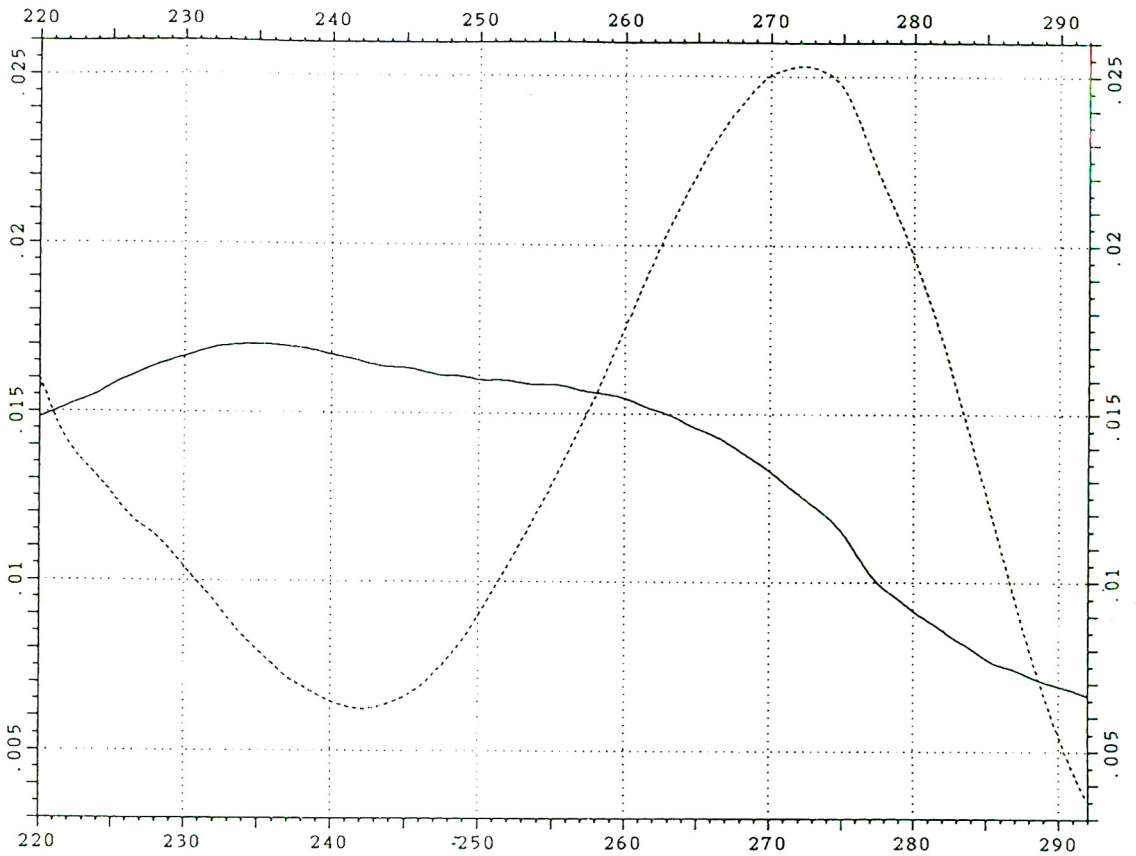

Fig. 1. Spectra of cefotaxime (20 mg l^{-1}) and theophylline (20 mg l^{-1}) recorded with the diode-array detector. Solid line, cefotaxime; dashed lines, theophylline. For operating conditions, see text.

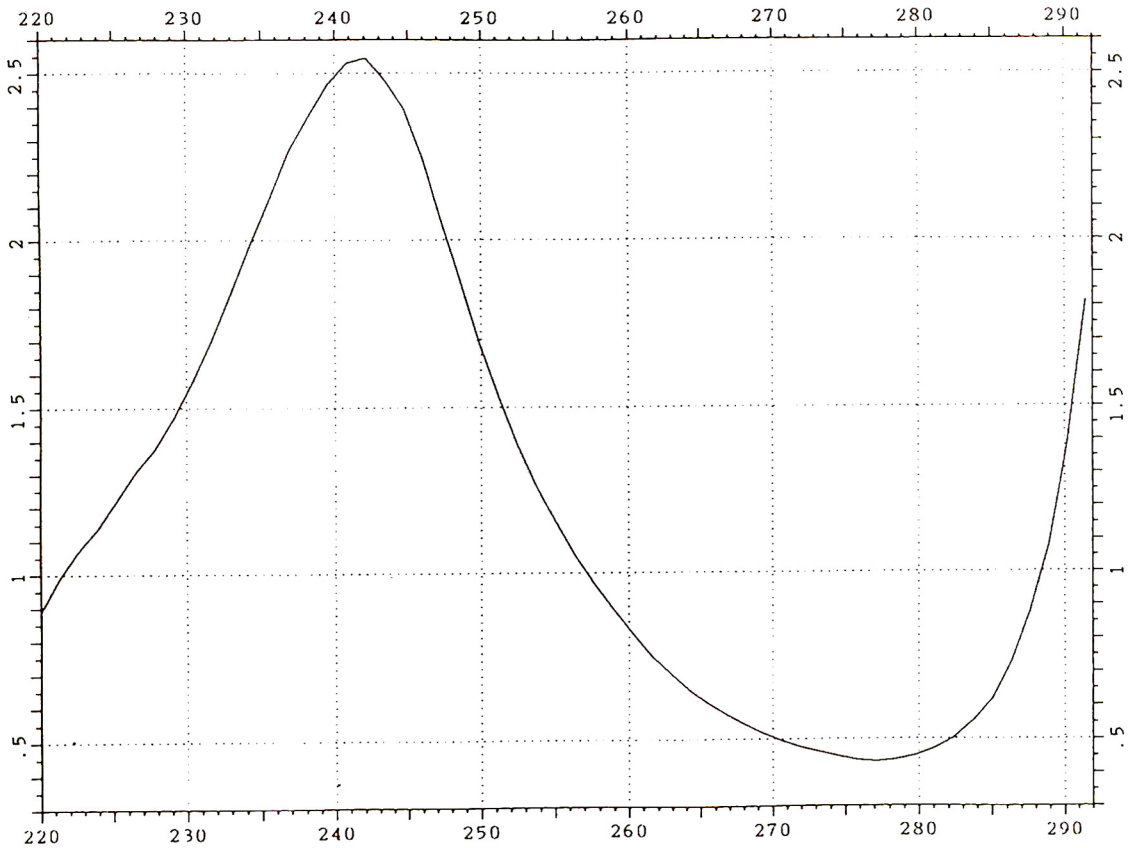

Fig. 2. C/T absorbance ratio as a function of wavelength.

at 1.3 ml min^{-1}. Each solution was injected six times successively in order to assess the repeatability of the results given by the different techniques. The spectral information was recorded in the range 220–300 nm with a spectral resolution of 1.3 nm. The sampling time was 26.64 ms.

The three-dimensional (3-D) plot of absorbance–time–wavelength was examined under 45° and 90° right and left viewing angles. The contour plot was analysed with 0.01 and 0.05 absorbance steps. Chromatograms were overlaid at 236.0, 242.2, 261.0, 276.2 and 290.0 nm. The derivative chromatograms (first to fourth) in the time domain were examined at the same wavelengths. Absorbance ratio and spectral suppression were investigated using 242 and 276 nm as selected wavelengths. For the absorbance ratio, the threshold values were set at 0.005 $\mu V\ s^{-1}$. Spectral overlay was carried out by collecting two spectra upslope, one at the apex and two downslope. The peak purity function was used with three threshold values (900, 950 and 980).

The first- and second-derivative spectra in the wavelength domain were recorded at the apex of the chromatographic peaks for the spiked and unspiked solutions. The derivative spectrum of the "impure" peak was overlaid with that of "pure" cefotaxime. Derivative spectra were recorded with an average number of eleven and fifteen points, respectively.

All the spectra were corrected for background absorbance using an interpolated baseline correction between peak start and peak end spectra.

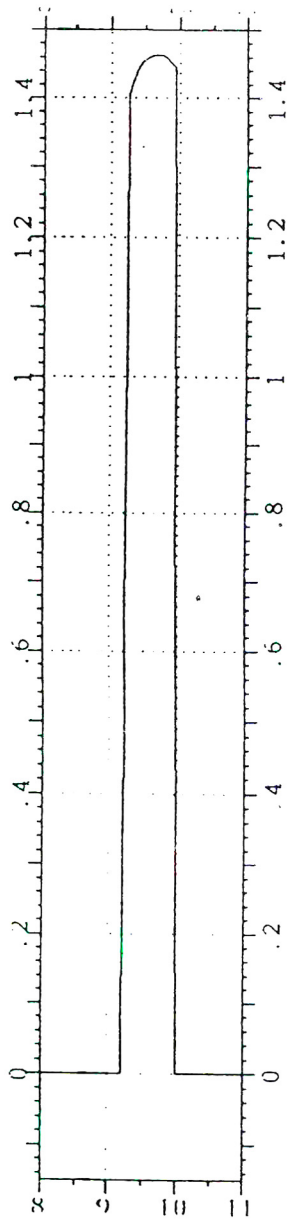

Fig. 3. Plot of absorbance ratio at 242 and 276 nm for a solution of C spiked with 5% of T (with respect to C).

3. Results and discussion

Under the chromatographic conditions used, the retention times were 9.37 min for theophylline (T) and 9.52 min for cefotaxime (C). The chromatographic resolution, calculated [8] from separate injections of the reference solutions of C and T, was found to be 0.14.

In all the techniques applied, the detection limit for the impurity in the analyte peak was evaluated by comparison to the results obtained on a pure peak of analyte.

The spectra of C and T (Fig. 1) were recorded with the diode-array detector from reference solutions of C and T. The plot of their ratio as a function of wavelength (Fig. 2) showed a maximum and a minimum at 242 and 276 nm which corresponded to a maximum spectral difference between the two compounds; these results are similar to those obtained previously [7]. This pair of wavelengths was selected for spectral suppression and absorbance ratio techniques [9].

The 3-D plots and the contour plots showed no difference between solutions of C spiked with T (even at a 10% level) and a reference solution of C. The first to fourth derivatives of the chromatograms also showed no difference. These results were as expected, owing to the extent of co-elution [2,4] and the low concentrations of T used in this study.

The overlay of chromatograms recorded at selected wavelengths showed a slight shift in the retention times of the chromatographic peaks for a solution of C spiked with 10% of T.

An absorbance ratio plot at 242 and 276 nm allowed 5% of T to be easily detected visually (Fig. 3) but failed for a 1% concentration. The insensitivity we found for this technique using a graphical format has been mentioned elsewhere [4,7]. When the chromatographic peaks of the analyte and an impurity are strongly overlapped and a pure standard is available, a numerical format that allows a statistical objective comparison between the absorbance ratio values for the "pure" and "impure" peaks should be preferred. It was not implemented in the instrument used. However, we collected the ratio values for the "pure" and "impure" peaks across the chromatographic peaks and performed a statistical comparison of their mean. The ratio values were collected every 4 s across the chromatographic peaks. Statistical evaluation showed that the variances between injections for the same solu-

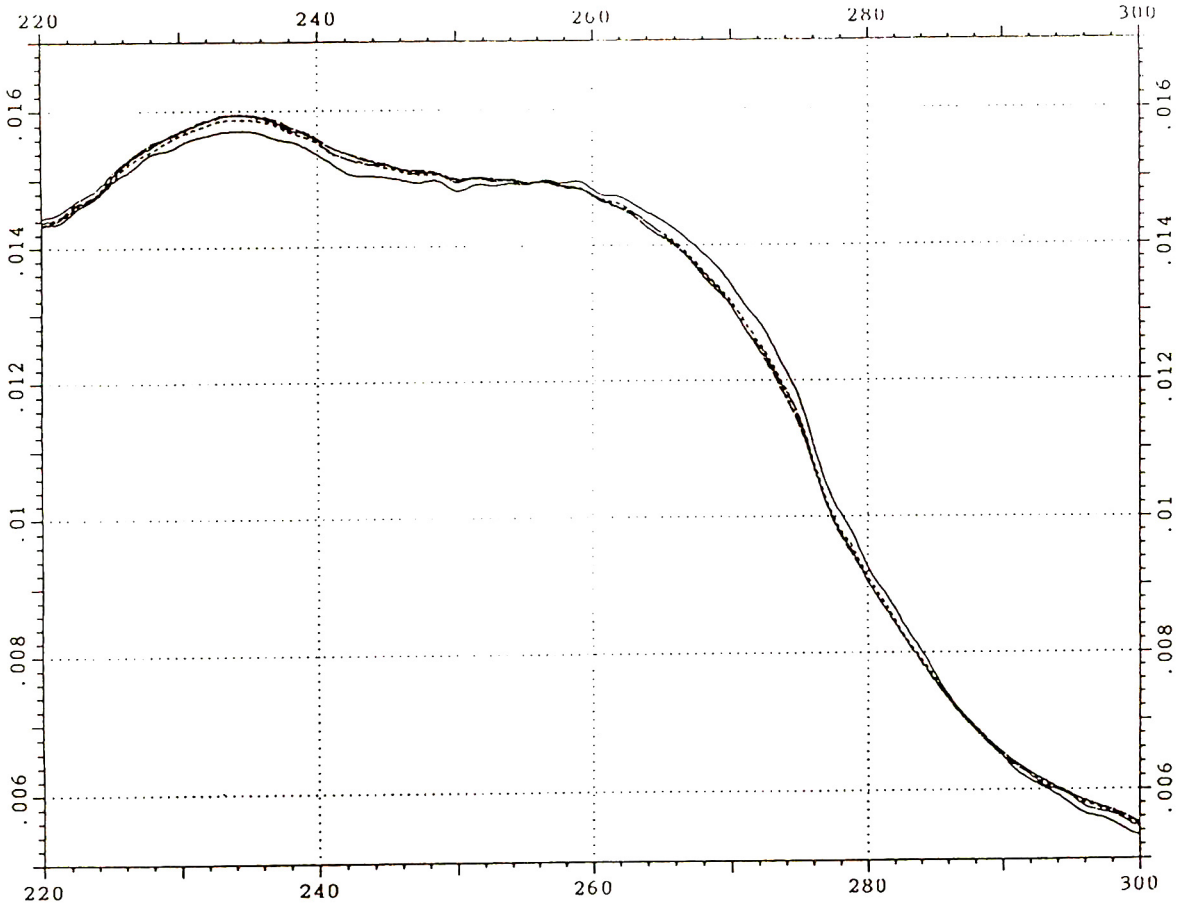

Fig. 4. Spectral overlay (apex, upslope, downslope) for a solution of C spiked with 5% of T (with respect to C).

Table 1
Evaluation of peak homogeneity by the peak purity function for a cefotaxime solution (C) and cefotaxime solutions spiked with different concentrations of theophylline (T)

No. of injection	T concentration added (%)[a]				
	0	10	5	1	0.5
1	99.41	88.89	97.82	99.54	99.55
2	99.31	88.99	98.05	99.47	99.47
3	99.38	87.67	96.54	99.39	99.44
4	99.93	88.16	97.72	99.32	99.35
5	99.50	87.41	97.97	98.90	98.79
6	99.52	86.42	96.94	99.61	99.02
Average	99.34	88.01[b]	97.51[b]	99.37	99.27

[a] Results are expressed as match percentage and are given for six successive injections of each solution.
[b] Significantly different from 0% ($\alpha = 0.05$).

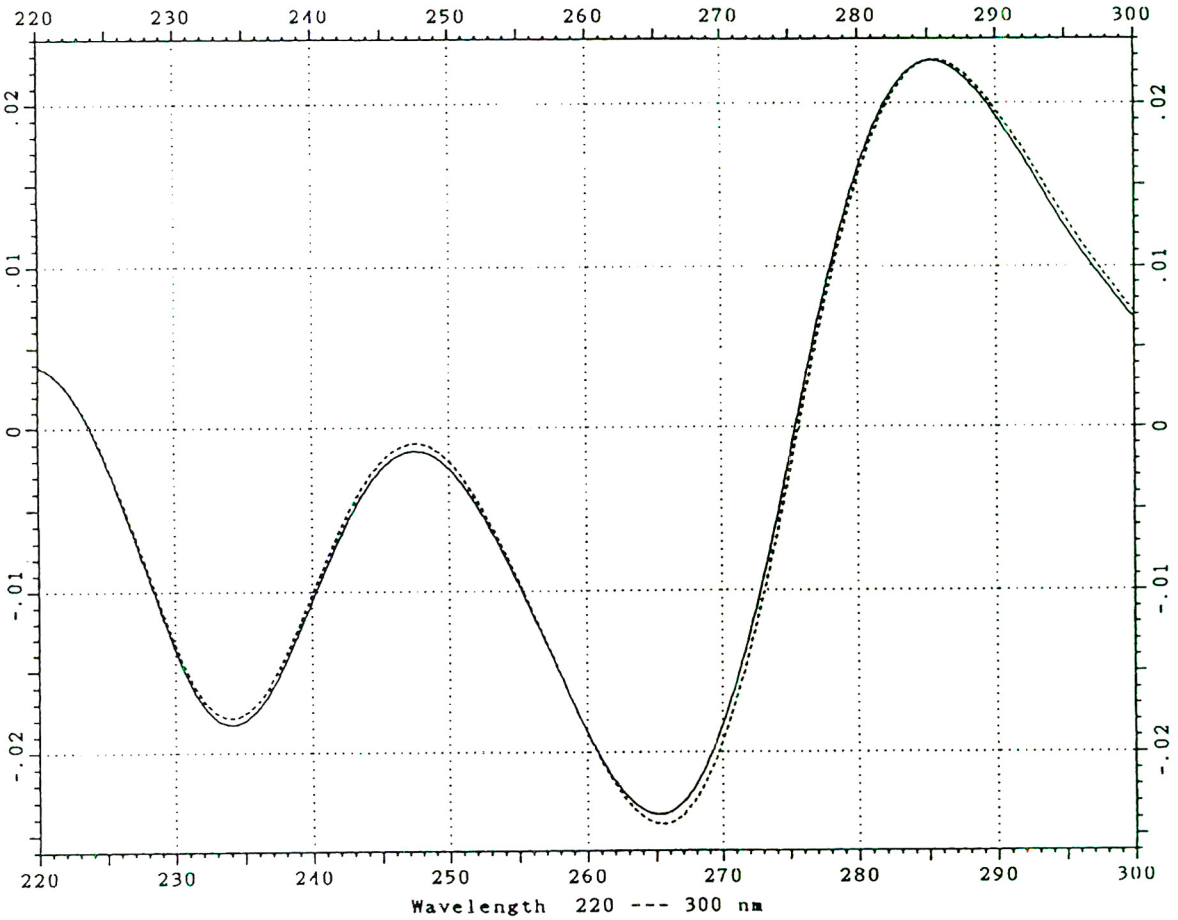

Fig. 5. Overlay of the second-derivative spectra recorded at the apex of the chromatographic peak for C spiked with 1% of T (with respect to C) and reference C.

tion were not significantly different ($\alpha = 5\%$). Therefore, the ratio values from a set of injections could be pooled for pure and impure peaks. The mean values for a peak spiked at the 0.5% level and an unspiked peak were significantly different ($\alpha = 5\%$). This shows that a statistical analysis of a large number of numerical ratio values across the peaks is a time-consuming but sensitive technique.

The overlay of spectra captured at the apex, upslope and downslope could detect easily less than 5% of impurity (Fig. 4), but failed at a 1% concentration. This low sensitivity, compared with the results obtained in previous studies [7], is due to the wavelength range used (220–300 nm instead of 190–300 nm). At about 210 nm, T presents a dramatic difference in absorptivity relative to C (see Fig. 1 in Ref. [7]), which explains the lower detection limits previously obtained. However, wavelengths higher than 220 nm should be adopted in routine use, owing to the absorbance of the mobile phase at low wavelengths.

The values of the purity parameter (expressed as match percentage) obtained from six successive injections of spiked and unspiked solutions (Table 1) were statistically compared. A one-way analysis of variance (ANOVA) and a Dunnett test showed that the mean value of the purity parameter calculated for 5% of T at a

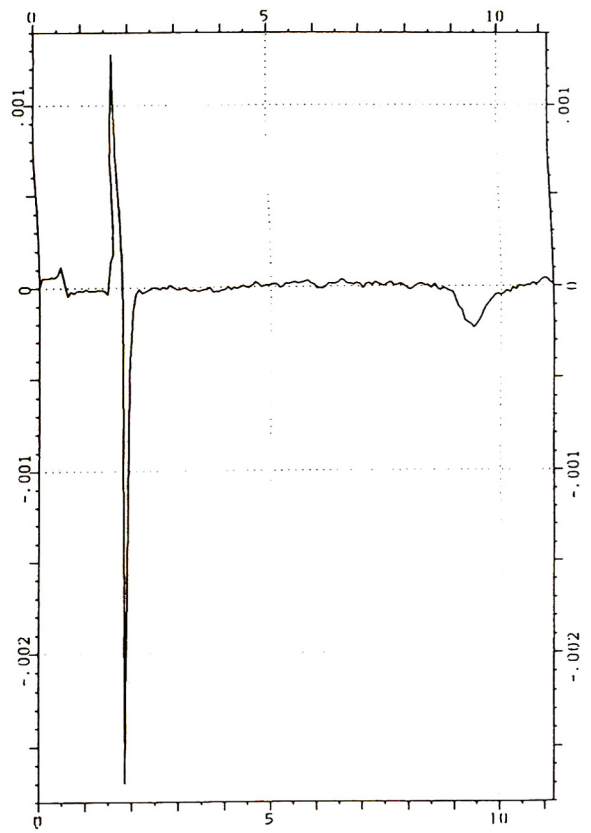

Fig. 6. Signal of T after suppression of C. Chromatogram from a solution of C spiked with 1% of T (with respect to C).

threshold value of 980 was significantly different ($\alpha = 0.05$) from that of C. No significant difference was found for 1% of theophylline.

The presence of 1% of T in the peak of C could easily be detected by recording the second-derivative spectrum captured at the apex of the peak. The derivative spectrum presents a significant difference to that of C (Fig. 5), showing the efficiency of the second derivative to enhance small spectral differences.

Spectral suppression was applied by measuring the difference absorbance ΔA at 242 and 276 nm and using the equation $\Delta A_{242,276} = A_{242} - 1.550A_{276}$. The constant for the suppression of the signal of C (1.550) was calculated from the ratio of the absorbances at 242 and 276 nm for a pure solution of C (100 mg l^{-1}). The efficiency of the analyte suppression was checked by injecting this solution and using the above equation. No signal was observed. Under the same conditions, the detection limit for T in C (signal-to-noise ratio = 2) was close to 0.5% and 1% of T in the peak of C could easily be detected (Fig. 6). Such a low detection limit could be obtained because the pair of wavelengths was fully optimized. An advantage of this technique over the absorbance ratio is that it can be successfully applied even if peaks are totally co-eluted and the response is related to the concentration [3,7,9].

4. Conclusions

The purpose of this work was to compare the efficiency of different techniques to evaluate the homogeneity of a chromatographic peak of an analyte at a concentration level of biological interest. The importance of performing an adequate background correction for the techniques comparing spectra or using ratios across the chromatographic peaks should be emphasized. An unspiked solution of the analyte should give a perfect match of the spectra collected at different time intervals across the chromatographic peak if the correction is properly carried out.

Among the different techniques investigated which have been shown to be sensitive under the selected conditions and with the specific instrument used, some of them (spectral overlay at the apex, upslope and downslope, peak purity parameter, multiple-wavelength chromatogram overlay) do not require any spectral information; others require a knowledge of the analyte spectra (spectral suppression, overlay of derivative spectra from the test and reference solutions). Some techniques cannot be fully optimized without a knowledge of the spectra of both the analyte and the impurity (spectral suppression and absorbance ratio); the performances obtained for the latter two in this study have been fully optimized with respect to the selection of the wavelengths used. The use of the peak purity function under the conditions used was not a very efficient technique, in contrast to the results

reported on some commercial instruments [6,10], which use different algorithms.

It should be noted that in our study we used a low concentration of analyte (20 mg l^{-1}), corresponding to a level of analyte that can be found in biological samples; lower detection limits of impurity should be obtained by using higher concentrations of analytes, e.g., for peak purity assessment for raw materials.

References

[1] A.F. Poile and R.D. Conlon, *J. Chromatogr.*, 204 (1981) 149.
[2] A.F. Fell, H.P. Scott, R. Gill and A.C. Moffat, *J. Chromatogr.*, 273 (1983) 3.
[3] B.J. Clark, A.F. Fell, H.P. Scott and D. Wersterlund, *J. Chromatogr.*, 286 (1984) 261.
[4] A.F. Fell, B.J. Clark and H.P. Scott, *J. Chromatogr.*, 297 (1984) 203.
[5] T.V. Alfredson, T.L. Sheehan, T. Lenert, S. Aamodt and L. Correia, *J. Chromatogr.*, 385 (1987) 213.
[6] H.K. Chan and G.P. Carr, *J. Pharm. Biomed., Anal.*, 8 (1990) 271.
[7] H. Fabre and A.F. Fell, *J. Liq. Chromatogr.*, 15 (1992) 3031.
[8] *Pharmacopée Européenne*, Maisonneuve, Sainte Ruffine, 2nd ed., 1987, p. V-6-20-4.
[9] E. Owino, B.J. Clark and A.F. Fell, *J. Chromatogr. Sci.*, 29 (1991) 298.
[10] *Product Note*, Hewlett-Packard, Avondale, PA, 1993.

ELSEVIER

Journal of Chromatography A, 697 (1995) 89–99

JOURNAL OF CHROMATOGRAPHY A

Retention characteristics of octadecylsiloxane-bonded silica and porous polymer particle-loaded membranes for solid-phase extraction

Mary L. Mayer, Salwa K. Poole, Colin F. Poole*

Department of Chemistry, Wayne State University, Detroit, MI 48202, USA

Abstract

Forced-flow planar chromatography was used to determine the kinetic and retention properties of an octadecylsiloxane-bonded, silica-based, particle-loaded membrane used for solid-phase extraction. The sorbent was heavily loaded with bonded phase resulting in a small intraparticle porosity. The large plate height and flow resistance indicates a heterogeneous particle size distribution for the membrane with a significant fraction of below average size particles. The hydrophobicity and silanophilic indexes and system constants in the solvation parameter model indicate similar retention properties to a common octadecylsiloxane-bonded silica cartridge sorbent under identical mobile phase conditions. The dimensional instability of a porous polymer particle-loaded membrane prevented its evaluation by forced-flow planar chromatography using the overpressured development chamber. Breakthrough volumes were determined for the porous polymer membrane under typical sample processing conditions for a number of solutes with varied properties and fitted to a solvation parameter model. A comparison to data previously obtained for an octadecylsiloxane-bonded, silica- based, particle-loaded membrane (Bakerbond) indicated that ease of cavity formation favors retention by the octadecylsiloxane-bonded silica particle-loaded membrane for non-polar and weakly polar analytes compared to the porous polymer particle-loaded membrane. Significantly larger breakthrough volumes, however, are obtained on the porous polymer particle-loaded membrane for polar analytes. The porous polymer sorbent competes more effectively with water in dipole-type interactions and as a hydrogen-bond acid. A solvent effect is speculatively suggested as the origin of the porous-polymer sorbent's favorable retention of hydrogen-bond bases compared to the octadecylsiloxane-bonded, silica-based, material.

1. Introduction

Solid-phase extraction (SPE) using sorbent cartridges is a widely accepted technique for the concentration and isolation of analytes from solution prior to chromatographic analysis [1–4].

In 1990 Hagen et al. [5] described a new approach to SPE employing particle-loaded membranes consisting of sorbent particles of about 8 μm diameter immobilized in a web of poly(tetrafluoroethylene) microfibrils. These membranes, in the form of flexible disks of various diameters and 0.5 mm thickness, are now commercially available. The practical advantages claimed for the disk format are related to the improved packing homogeneity of the membrane and its

* Corresponding author. Present address: Department of Chemistry, Imperial College of Science, Technology and Medicine, South Kensington, London SW7 2AY, UK.

0021-9673/95/$09.50
SSDI 0021-9673(94)01004-8

shorter height and greater cross-sectional area compared to typical cartridge devices. In turn these lead to shorter sample processing times, decreased plugging by particles, reduced channeling, and reduced non-specific matrix adsorption. There has been considerable interest in this new technology resulting in a significant number of reported applications to environmental, industrial and pharmaceutical samples. The literature is now too great to review in its entirety and we direct the reader to a few recent articles and reviews for a complete bibliography [6–10].

The physicochemical basis of the extraction mechanism using particle-loaded membranes is not well understood. The kinetic properties of an octadecylsiloxane-bonded silica particle-loaded membrane were studied by forced-flow planar chromatography [11]. From a consideration of kinetic and thermodynamic factors it was shown that the most important parameter in determining breakthrough volumes was retention. This led to the development of a solvation parameter model to characterize retention in terms of solute and sorbent characteristics based on Eq. 1 [12],

$$\log V_B = c + mV_X/100 + rR_2 + s\pi_2^H + a\alpha_2^H + b\beta_2^H \quad (1)$$

where V_B is the breakthrough volume, V_X the solute's characteristic volume, R_2 the solute's excess molar refraction, π_2^H is a measure of the solute's ability to stabilize a neighboring dipole by virtue of its capacity for orientation and induction interactions, and α_2^H and β_2^H are parameters characterizing the solute's hydrogen-bond acidity and hydrogen-bond basicity, respectively. The system coefficients m, r, s, a, b and c are solute independent and are characteristic of the sampling system (sorbent and sample solvent). These parameters are evaluated by multiple linear regression analysis by determining the breakthrough volume for a series of solutes with known explanatory variables. Once established, the breakthrough volume can be estimated for any solute in the same sampling system for which the solute explanatory variables are known or can be reasonably estimated from empirical combining rules. The solvation parameter model has been applied with great success to explain other solubility-related properties including retention in gas and liquid chromatography, octanol–water partition coefficients, and to characterize coatings for sensors [13–16].

2. Experimental

Organic solvents and water were Omnisolv grade from EM Science (Gibbstown, NJ, USA). Other chemicals were reagent grade or better and obtained from several sources. The Impress II sealant was obtained from Factory for Laboratory Instruments (Budapest, Hungary). Empore sheets cut to 20×10 cm, containing octadecylsiloxane-bonded silica particles and poly(styrene)–divinylbenzene porous polymer particles of the same composition used to prepare Empore extraction disks from Varian Sample Preparation Products (Harbor City, CA, USA) and J.T. Baker (Phillipsburgh, NJ, USA), respectively, were a gift from 3M Co. (St. Paul, MN, USA). Empore extraction disks, 47 mm diameter, containing poly(styrene)–divinylbenzene porous polymer particles were obtained from J.T. Baker.

2.1. Forced-flow chromatography

The apparatus used to determine the kinetic and thermodynamic properties of the particle-loaded membranes is described in detail elsewhere [11,17]. It consists of a Chrompres 25 overpressured development chamber (Factory of Laboratory Instruments) operated at a cushion pressure of 20 bar, a Model 2350 reciprocating-piston pump (ISCO, Lincoln, NE, USA), a Supco DPG-500 high-pressure transducer (Cole-Parmer, Chicago, IL, USA), a Rheodyne 7125 valve injector with a 20-μl sample loop (Anspec, Ann Arbor, MI, USA), and a UV-50 variable-wavelength detector (Varian Instruments, Walnut Creek, CA, USA) operated at 270 nm and 0.1 AU full scale. A Nelson Analytical 9000 series A/D interface (PE Nelson, Cupertino, CA,

USA) and an Epson Apex 200 computer running under PE Nelson 2100 PC integrator software (revision 5.1) were used for data acquisition and calculation of peak variance using the Dorsey–Foley peak shape model. A microburette was used to accurately calibrate the flow-rate.

The Empore sheets were supported by and immobilized onto a sheet of 20×10 cm aluminum using a light coating of Impress II sealant. The edges of the membrane were sealed with paraffin wax. A scalpel was used to cut inlet and outlet troughs in the Empore sheets at positions corresponding to the troughs in the cushion insert used to direct the eluent flow.

2.2. Direct measurement of breakthrough volumes

The porous polymer particle-loaded membrane disks were mounted in the usual way on the fritted glass support of a standard vacuum filtration apparatus (Millipore, Bedford, MA, USA) connected to a water aspirator via a flow metering valve as described previously [5,6,12]. Prior to use the membranes were washed by sucking 10 ml of acetonitrile through them and subsequently dried by pulling air through the membrane for about 10 min. The disk was then conditioned with methanol, 10 ml, by allowing the solvent to permeate the disk for a few minutes, followed by sucking the solvent through the membrane and releasing the vacuum before the last drop of methanol had passed through the membrane. The disk was then washed with water, 10 ml, followed by application of the sample without allowing the disk to become dry. The samples were sucked through the membrane at a flow-rate of 40 ± 3 ml/min. After the sample had been processed, the receiver was changed for elution of the standards with two 5-ml volumes of acetonitrile. Prior to elution of the standards the disk was allowed to dry for about 30 s under suction. The combined aliquots of acetonitrile were then transferred to a 10-ml volumetric flask, an internal standard added, and the solution adjusted to the mark. The internal standard was used to correct for injection volume differences in gas chromatography and was selected to have similar volatility to the analytes in solution and to be easily separated from them on the column. Suitable internal standards are 2-alkanones and fatty acid methyl esters.

Standard compounds selected to represent a varied range of intermolecular interactions and acceptable water solubility, taken from Table 1, were prepared in methanol and added to water containing 0.5% (v/v) methanol to give a known amount of standard, 10–20 μg, in an aqueous solution containing a total of 1% (v/v) methanol. Standards were processed in groups of three to five components per experiment (with representative compounds run in different mixtures to ensure that there was no significant interactions between compounds that affected the breakthrough volume measurements). Initially, samples were screened using decade changes in the sample volume to estimate the approximate breakthrough volumes, followed by a more systematic experimental design. For compounds with a breakthrough volume between 0 and 50 ml, measurements were made at 2.5-ml volume increments, 50 and 100 ml at 5-ml increments, 100 and 1000 ml at 10-ml increments, and greater than 1000 ml at 100-ml increments. The data were subsequently plotted as breakthrough curves. Since it is impossible to interpolate between experimental points to find the breakthrough volume, the difference between the amount of analyte recovered between two points and the general trend in the experimental breakthrough curves was used to establish the breakthrough volume.

2.3. Calculation of membrane properties

The experimental protocol and theoretical relationships used to calculate porosity, specific permeability, flow resistance, apparent particle size, plate height as a function of solvent velocity, hydrophobicity index, silanophilic index, and solute capacity factors in methanol–water mixtures were as reported previously [11,17–19].

The explanatory variables used in the solvation parameter model, Eq. 1, were taken from Refs. [13,14,20,21]. For convenience they are

Table 1
Explanatory variables for use in the solvation parameter model (Eq. 1)

Solute	$V_x/100$	R_2	π_2^H	α_2^H	β_2^H
Naphthalene	1.085	1.340	0.92		0.20
Anthracene	1.454	1.340	0.92		0.20
Benzene	0.716	0.610	0.52		0.14
Toluene	0.857	0.601	0.52		0.14
n-Propylbenzene	1.139	0.604	0.50		0.15
Chlorobenzene	0.839	0.718	0.65		0.07
1,2-Dichlorobenzene	0.961	0.872	0.78		0.04
1,4-Dichlorobenzene	0.961	0.825	0.75		0.02
Bromobenzene	0.891	0.882	0.73		0.09
1,2-Dibromobenzene	1.066	1.190	0.96		0.04
Iodobenzene	0.975	1.188	0.82		0.12
1,2,4-Trichlorobenzene	1.083	0.980	0.81		
Pentan-2-one	0.828	0.143	0.68		0.51
Hexan-2-one	0.969	0.136	0.68		0.51
Heptan-2-one	1.111	0.123	0.68		0.51
Nitrobenzene	0.891	0.871	1.11		0.28
Acetophenone	1.014	0.818	1.01		0.48
Anisole	0.916	0.708	0.75		0.29
Benzonitrile	0.871	0.742	1.11		0.33
Benzaldehyde	0.873	0.820	1.00		0.39
1-Nitropentane	1.057	0.212	0.95		0.29
4-Chloroacetophenone	1.136	0.955	1.09		0.44
Heptanal	1.111	0.140	0.65		0.45
Methyl benzoate	1.073	0.733	0.85		0.46
Phenyl acetate	1.073	0.661	1.13		0.54
3-Nitrotoluene	1.032	0.874	1.10		0.25
1,1,2,2-Tetrachloroethane	0.880	0.595	0.76	0.16	0.12
1,1,2-Trichloroethylene	0.715	0.524	0.37	0.08	0.03
Hexan-1-ol	1.013	0.210	0.42	0.37	0.48
Benzyl alcohol	0.916	0.803	0.87	0.33	0.56
1-Phenylethanol	1.057	0.784	0.83	0.30	0.66
Acetanilide	1.113	0.870	1.40	0.50	0.67
Benzamide	0.973	0.990	1.50	0.49	0.67
Phenol	0.775	0.805	0.89	0.60	0.30
2-Chlorophenol	0.898	0.853	0.88	0.32	0.31
4-Chlorophenol	0.896	0.915	1.08	0.67	0.20
2-Hydroxytoluene	0.916	0.840	0.86	0.52	0.30
3-Hydroxytoluene	0.916	0.820	0.88	0.57	0.34
4-Hydroxytoluene	0.916	0.820	0.87	0.57	0.31

assembled in Table 1. The characteristic molecular volumes were calculated using the incremental constants and method described by Abraham and McGowan [22]. Multiple linear regression analysis was performed using the program SPSS V4.0 (SPSS, Chicago, IL, USA) on an Epson Apex 200 personal computer.

3. Results and discussion

An earlier report provided a series of values for the kinetic and thermodynamic properties of octadecylsiloxane-bonded silica Bakerbond Empore membranes [11]. These can be compared to the values for a similar material using octa-

Table 2
Characteristic properties of octadecylsiloxane-bonded silica particle-loaded membranes

Property	Bakerbond	Varian Sample Preparation Products
Total porosity	0.52	0.54
Interparticle porosity	0.37	0.48
Intraparticle porosity	0.15	0.06
Specific permeability ($m^2 \times 10^{14}$)	2.50	2.21
Flow resistance parameter	1000–1250	1040
Apparent particle size (μm)	7.7	5.8
Minimum plate height (μm)	56	<120
Optimum velocity (mm/s)	0.13	<0.045
Hydrophobicity index	1.55	1.51
Silanophilic index	1.34	1.14

decylsiloxane-bonded silica from Varian Separation Products determined in this study (Table 2). Notionally, both membranes contain irregular 8-μm diameter particles with an average pore diameter of 6 nm. Their total porosity values are similar but the Varian product has a higher interparticle porosity and a lower intraparticle porosity than the Bakerbond material. For the Varian material most of the pore volume is either filled or the pore entrances blocked by the bonded phase. Given the intended use of the material in SPE this need not be detrimental. The larger interparticle porosity would suggest a more heterogeneous structure for the membrane compared to the Bakerbond material. The apparent particle size for the Varian product at 5.8 μm is significantly below the value indicated by the manufacturer. This combined with the poor plate height values for the Varian product compared to the Bakerbond material suggest a broader particle size distribution with a larger fraction of fine particles. A considerably higher pressure was required to obtain a given mobile phase velocity through the layer for the Varian membrane than was needed for the Bakerbond material. The overpressured development chamber is restricted to a maximum inlet pressure of about 20 bar so that the range of interparticle mobile phase velocities that could be used to study the kinetic properties of the Varian material was limited to 0.2 to 0.04 mm/s, corresponding to sample flow-rates for a 47-mm disk with a 38-mm active sampling area of about 3 to 16 ml/min. Within this flow-rate range the plate height for the membrane is controlled by the rate of mass transfer and a linear relationship between the plate height (H, μm) and the interparticle mobile phase velocity (u_e, mm/s) was observed:

$$H = 81.2 + 905u_e \quad R^2 = 1.000, n = 6$$

The minimum plate height for the Bakerbond material was 56 μm obtained at an optimum interparticle mobile phase velocity of 0.13 mm/s [11]. The optimum mobile phase velocity for the Varian product is at least an order of magnitude smaller and corresponds to a sample flow-rate that would not be useful in practice. The membrane is more likely to be used within the flow-rate range of the experiments or at higher values in which the chromatographic efficiency of the membrane is limited by contributions from the resistance to mass transfer and flow anisotropy. In terms of their kinetic characteristics the Bakerbond material is clearly superior but, as demonstrated elsewhere [12,19], the most important property of a particle-loaded membrane in judging its effectiveness for SPE is its retention characteristics. It is probable that a

minimum chromatographic efficiency is needed for the device to function without instantaneous breakthrough, but once this requirement is met, breakthrough is only weakly dependent on the chromatographic efficiency, at least for the low plate numbers associated with SPE devices.

An indication of the retention properties of the sorbent can be obtained from the relative retention of test solutes determined under specified conditions. A hydrophobicity index [23] and a silanophilic index [24] have been developed for the comparison of the retention characteristics of reversed-phase column packings in high-performance liquid chromatography and can be usefully applied to the comparison of SPE sorbents [11,19]. The normal range observed for the hydrophobicity index for column packings is 1.3 to 1.52 indicating that both the Bakerbond material (1.55) and the Varian material (1.51) are synthesized with a high volume of bonded phase material. Given their intended use in extraction this is desirable and there is little to choose between the two materials in this respect. The silanophilic index has values of 0.9 to 1.2 for intermediate activity and a value >1.2 for high activity. On this scale the Bakerbond material has a high silanophilic activity (1.34) while the Varian product is in the intermediate range (1.14). The difference in the silanophilic index between the two materials will be important in the relative retention of hydrogen-bonding solutes but should not significantly influence the retention of neutral solutes.

Particle-loaded membranes containing octadecylsiloxane-bonded silica particles are used predominantly with aqueous solutions containing 1% (v/v) methanol to ensure adequate wetting of the membrane, reasonable flow-rates, and useful breakthrough volumes for low-molecular-weight analytes [6]. Breakthrough volumes can be measured directly for use in Eq. 1 but this is a slow process. Alternatively, retention measurements can be made at more convenient mobile phase compositions and the value of the capacity factor at 1% (v/v) methanol obtained by a short extrapolation [19]. This process is generally faster when information for a large number of varied solutes is required to determine the system coefficients in Eq. 1. Data for the first-order or second-order fit of log k, where k is the capacity factor, against the volume fraction of methanol in the mobile phase (%, v/v) for the Varian material are given in Table 3. Data were generated in the range 100 to 50% (v/v) methanol. Increasing mobile phase viscosity combined with the poor chromatographic efficiency of the membrane restricted the measurements to a less than desirable range of mobile phase compositions. This range is not as wide as that available for the Bakerbond material [11]. The system coefficients for the experimental data, the extrapolated data for 1% (v/v) methanol, and the statistics for the fits are summarized in Table 4. There is a smooth change in the system coefficients as a function of mobile phase composition (Fig. 1), in line with expectations from previous studies. The results obtained by extrapolation of the capacity factor values to 1% (v/v) methanol provide a poor fit to Eq. 1. Consequently the system constants obtained are unreliable and should be considered no better than qualitative values and used accordingly.

For the present purposes a direct comparison of the retention properties of the Varian material can be made to a Bakerbond sorbent used in SPE cartridges at a composition of 70% (v/v) methanol in water [19]. The system constants for the Bakerbond cartridge sorbent for these conditions are: $m = 2.12$ (± 0.23), $r = 0.16$ (± 0.13), $s = -0.44$ (± 0.14), $a = -0.32$ (± 0.11), $b = -1.59$ (± 0.18) and $c = -0.71$ (± 0.21). The system constants, in this case, represent the contribution of defined intermolecular interactions to the transfer of a solute from a solution of 30% (v/v) water in methanol to an octadecylsiloxane-bonded silica sorbent in equilibrium with the solvent. Only the m and the r coefficients are positive and therefore favor transfer to the solvated sorbent. The r coefficient is barely significant so the most important contribution to retention is the cavity contribution represented by the m coefficient. The m coefficient is larger for the Bakerbond cartridge sorbent indicating that forming a cavity for the solute is easier for this material than for the Varian product. Neutral polar molecules have

Table 3
Relationship between the capacity factor and the volume fraction of methanol (φ) in the mobile phase determined by forced-flow planar chromatography

Solute	a_0	$a_1 \times 10^2$	$a_2 \times 10^4$	Composition range (%, v/v, methanol)
Naphthalene	2.070	−2.11		100–60
Benzene	1.887	−2.21		100–50
Toluene	2.523	−2.92		100–50
Anthracene	6.645	−1.271	6.35	100–70
Chlorobenzene	2.049	−2.22		100–50
Pentan-2-one	1.548	−1.96		100–50
Hexan-2-one	4.813	−1.002	4.82	100–50
4-Hydroxytoluene	2.550	−3.07		100–60
2-Hydroxytoluene	2.214	−3.85	1.28	100–50
Acetanilide	2.612	−5.53	2.53	100–50
Benzamide	0.597	−1.03		100–50
1,2-Dibromobenzene	2.803	−2.90		100–70
2-Chlorophenol	2.508	−4.29	1.40	100–50
1-Phenylethanol	2.664	−5.45	2.41	100–50
Benzyl alcohol	1.409	−1.86		100–50
Phenol	1.477	−2.08		100–50
Nitrobenzene	2.153	−2.45		100–60
n-Propylbenzene	2.703	−2.83		100–60
Anisole	2.138	−2.38		100–60
Acetophenone	1.473	−1.83		100–50
Benzonitrile	2.359	−4.42	1.75	100–50
Bromobenzene	2.268	−2.45		100–60
Benzaldehyde	2.257	−5.08	2.47	100–50
1,2-Dichlorobenzene	4.487	−7.64	3.09	100–60

Log $k_s = a_0 + a_1\varphi + a_2\varphi^2$ (in all cases $R^2 = 1.000$ for the fit). k_s = capacity factor for solute s.

about the same dipole type interactions with both sorbents and hydrogen-bond bases are marginally better retained on the Bakerbond sorbent and hydrogen-bond acids on the Varian sorbent. The difference in properties between the two sorbents are not large enough to reach any substantive conclusions about one material being superior to the other. They are slightly different in retention properties and both sorbents should function acceptably in SPE.

Particle-loaded membranes containing porous polymer sorbents were recently introduced to obtain improved retention of weak acids like phenols and to eliminate undesirable ion-exchange interactions of the silanol groups present in silica-based bonded phases with bases, such as amines [25]. The porous polymer particle-loaded membranes, unfortunately, were too dimensionally unstable to allow measurements to be made by forced-flow planar chromatography. Even after applying an overpressure of only 10 bar the membranes visibly changed shape and lifted from its aluminum support. It was impossible to obtain any useful information concerning the kinetic properties of these membranes and the direct method of determining breakthrough volumes had to be used to characterize their retention properties.

The breakthrough volumes for a series of solutes with a wide variation in solute properties for a sample solvent containing 1% (v/v) methanol in water are summarized in Table 5. The fit to Eq. 1 is as follows: $m = 3.520$ (± 0.2), $r = 0.336$ (± 0.09), $s = -0.265$ (± 0.11), $a = -2.306$ (± 0.08), $b = -0.761$ (± 0.12) and $c = -0.400$ (± 0.19). Statistically the fit to the data is good with a multiple correlation coefficient = 0.994, standard error = 0.08, and F-statistic =

Table 4
System coefficients and statistics for the fit to the solvation parameter model for the data obtained by forced-flow planar chromatography

Mobile phase composition (%, v/v, methanol)	System coefficients						Statistics			
	m	*r*	*s*	*a*	*b*	*c*	*R*	S.E.	*F*	*n*
100	0.343 (0.11)	0.120 (0.09)		−0.711 (0.10)	−0.379 (0.12)	−0.785 (0.09)	0.958	0.079	47	22
90	0.888 (0.09)	0.108 (0.07)	−0.183 (0.07)	−0.624 (0.06)	−0.717 (0.09)	−0.779 (0.07)	0.991	0.048	204	26
80	1.270 (0.12)	0.119 (0.09)	−0.391 (0.10)	−0.478 (0.07)	−1.072 (0.12)	−0.609 (0.10)	0.990	0.064	186	24
70	1.632 (0.14)	0.114 (0.10)	−0.365 (0.11)	−0.523 (0.08)	−1.402 (0.13)	−0.605 (0.11)	0.992	0.070	210	25
60	1.747 (0.21)	0.268 (0.09)	−0.454 (0.09)	−0.629 (0.07)	−1.491 (0.15)	−0.437 (0.15)	0.992	0.058	163	18
50	1.931 (0.23)	0.193 (0.09)	−0.504 (0.09)	−0.526 (0.07)	−1.567 (0.16)	−0.207 (0.16)	0.988	0.052	84	17
1	2.930 (0.57)	−1.702 (0.60)	−1.557 (0.57)	−0.681 (0.40)	−3.365 (0.79)	−0.313 (0.47)	0.830	0.079	6	20

R = Multiple linear regression coefficient; S.E. = standard error in the estimate; F = Fischer F-statistic; n = number of solutes. Values in parentheses are the uncertainty values (standard deviation) in the identified coefficient.

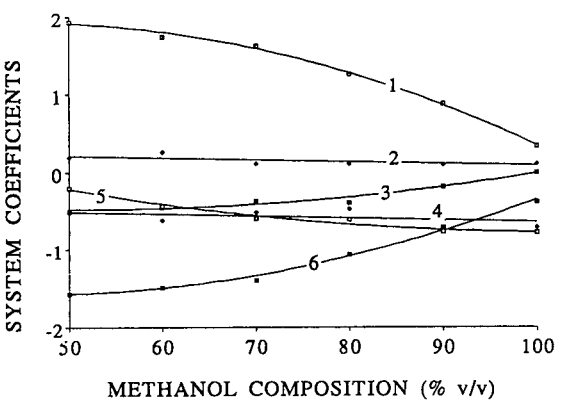

Fig. 1. Variation of the system constants as a function of the mobile phase composition for the octadecylsiloxane-bonded silica particle-loaded membrane from Varian Sample Preparation Products. Identification: 1 = m; 2 = r; 3 = s; 4 = a; 5 = c; 6 = b.

360. The system constants are reliable and can be quantitatively compared with the results for the Bakerbond octadecylsiloxane-bonded, silica-based, particle-loaded membranes [12] for which $m = 5.14$ (± 0.17), $s = -0.92$ (± 0.08), $a = -1.05$ (± 0.08), $b = -2.24$ (± 0.10) and $c = -1.23$ (± 0.17). In making a comparison between the two membrane types it is necessary to keep in mind that the stationary phase into which the solutes are extracted is comprised of the sorbent material and those sample solvent molecules selectively localized at the sorbent surface in the stagnant solvent interface region. With some certainty we can state that the solvent composition of the interfacial region and the sample solvent are different, but it is no simple matter to assign a composition to this region [1].

There are significant differences in the system constants for the two types of particle-loaded membranes indicating different characteristic extraction properties. Cavity formation is signifi-

Table 5
Breakthrough volumes for the porous polymer particle-loaded membrane (solvent 1%, v/v, methanol)

Solute	Log V_B
Heptan-2-one	3.070
1-Nitropentane	2.875
3-Nitrotoluene	2.942
Acetophenone	2.780
Anisole	2.544
Chlorobenzene	2.574
Benzaldehyde	2.477
Benzonitrile	2.477
Iodobenzene	3.130
1,2-Dichlorobenzene	3.070
Phenol	0.700
Nitrobenzene	2.477
2-Chlorophenol	1.929
4-Chloroacetophenone	3.176
1,1,2,2-Tetrachloroethane	2.146
Heptanal	2.041
1,4-Dichlorobenzene	3.079
1,1,2-Trichloroethylene	2.000
Benzyl alcohol	1.653
1-Phenylethanol	2.097
Hexan-1-ol	1.875
3-Hydroxytoluene	1.397
4-Hydroxytoluene	1.397
Methyl benzoate	3.114
Phenyl acetate	3.041
4-Chlorophenol	1.000

cantly easier for the solvated octadecylsiloxane-bonded silica sorbent than is the case for the solvated porous polymer. Since, within reason, the m coefficient can not be too large, the octadecylsiloxane-bonded silica sorbent is expected to provide larger breakthrough volumes for non-polar solutes. There is a favorable contribution from the r coefficient for extraction by the porous polymer (the r coefficient is not significant for the octadecylsiloxane-bonded silica sorbent) indicating weak selectivity for the retention of π- and n-electron acceptor solutes by the porous polymer sorbent. This effect, however, is generally small and in no way can compensate for differences in the ease of cavity formation for solutes lacking polar functional groups.

All polar interactions favor solubility in the sample solvent and result in a general decrease in the breakthrough volume. The extent to which the polar interactions affect the breakthrough volume are significantly influenced by properties of the solvated sorbent. The greater polarizability of the aromatic rings of the porous polymer results in a more favorable interaction with dipolar compounds and larger breakthrough volumes compared to the silica-based material. Neither material is competitive with water as a reservoir of hydrogen-bonding interactions but their capacity to retain hydrogen-bond acids and bases are complementary. The large negative a coefficient for the porous polymer probably reflects the strong hydrogen-bond basicity of water and the lack of competing interactions offered by the solvated sorbent. In which case the smaller negative a coefficient for the silica-based material is an indication that it can more effectively compete with water as a hydrogen-bond base than can the porous polymer, most likely due to the lone pair electrons on the oxygen of the siloxane and silanol groups of the silica-based sorbent. The larger negative b coefficient for the silica-based material compared to the porous polymer was unanticipated. It suggests that the solvated porous polymer is a stronger hydrogen-bond acid than the solvated silica-based material. Given that the porous polymer contains no obvious hydrogen-bond acid sites that could compete with the sample solvent then the differences in properties must be due to differences in composition of the stagnant interfacial solvent associated with the sorbent. Water is a moderate hydrogen-bond acid and methanol should be able to effectively compete with it. The porous polymer is effectively hydrophobic and should take up methanol in preference to water in a more selective manner than the structurally heterogeneous silica-based sorbent with its significant proportion of polar groups. The silanol groups of the silica-based material must be effectively involved in internal hydrogen bonding and hydrogen bonding to sorbed components of the sample solvent, and are unavailable to solutes entering the sorption layer. From this we infer that the difference in relative concentration of methanol, and possibly the thickness of the sorption layer, is responsible for

the greater apparent hydrogen-bond acidity of the porous-polymer sorbent compared to the silica-based material. This we admit is speculation but no other obvious explanation seems to fit the facts.

The difference in extraction properties of the two materials can be highlighted by considering the contribution of individual intermolecular interactions to the breakthrough volume. These are broken out as the contribution of solute size and non-polar interactions represented by $mV_X/100$, with possibly a contribution from the equation constant c, and individual polar interactions described by rR_2, $s\pi_2^H$, $a\alpha_2^H$ and $b\beta_2^H$ for a few select solutes in Table 6. For non-polar compounds and weakly polar compounds like *n*-butylbenzene the octadecylsiloxane-bonded silica sorbent is preferred because of its more favorable cavity term. Most dipolar compounds are also hydrogen-bond bases and for these compounds retention on the porous polymer is more favorable. The difference in contributions from $s\pi_2^H$ and $b\beta_2^H$ between the two materials for compounds like benzonitrile, acetophenone, anisole, and hexan-2-one is sufficient to offset the more favorable cavity term for the octadecylsiloxane-bonded silica sorbent. Most hydrogen-bond acids are also dipolar and significant hydrogen-bond bases. When the $a\alpha_2^H$ term is considered it strongly favors retention by the octadecylsiloxane-bonded silica sorbent for compounds like phenol and 1-phenylethanol but this advantage is more than compensated for by the less favorable $s\pi_2^H$ and $b\beta_2^H$ terms. Again the porous polymer provides more favorable breakthrough volumes for these compounds.

For the retention of low-molecular-mass polar solutes the porous polymer sorbent provides larger breakthrough volumes because it more effectively competes with water in dipolar and solute hydrogen-bond base interactions. The octadecylsiloxane-bonded sorbent has a more favorable cavity term and competes more effectively with water for solutes that are hydrogen-bond acids but, in general, for polar solutes the balance of all intermolecular interactions still favors retention by the porous polymer. Since solute size and the capacity for polar interactions are not expected to be correlated this picture could change for larger solutes which might well be preferentially retained by the octadecylsiloxane-bonded silica sorbent in those

Table 6
Contribution of different intermolecuar interactions to the breakthrough volume (log V_B) of some typical solutes (solvent 1%, v/v, methanol)

Solute	Membrane type[a]	Intermolecular interaction						Estimated breakthrough volume
		$mV_X/100$	rR_2	$s\pi_2^H$	$a\alpha_2^H$	$b\beta_2^H$	c	
n-Butylbenzene	ODS	6.579		−0.469		−0.336	−1.23	4.544
	PS–DVB	4.496	0.202	−0.135		−0.114	−0.40	4.058
Benzonitrile	ODS	4.477		−1.021		−0.805	−1.23	1.421
	PS–DVB	3.066	0.249	−0.294		−0.251	−0.40	2.370
Acetophenone	ODS	5.212		−0.929		−1.075	−1.23	1.978
	PS–DVB	3.569	0.275	−0.268		−0.365	−0.40	2.811
Phenol	ODS	3.984		−0.819	−0.630	−0.672	−1.23	0.624
	PS–DVB	2.728	0.271	−0.236	−1.384	−0.228	−0.40	0.751
1-Phenylethanol	ODS	5.433		−0.764	−0.315	−1.478	−1.23	1.646
	PS–DVB	3.721	0.263	−0.220	−0.692	−0.502	−0.40	2.170
Anisole	ODS	4.708		−0.690		−0.650	−1.23	2.138
	PS–DVB	3.224	0.238	−0.199		−0.221	−0.40	2.642
Hexan-2-one	ODS	4.981		−0.626		−1.142	−1.23	1.983
	PS–DVB	3.411	0.046	−0.180		−0.388	−0.40	2.489

[a] ODS = Octadecylsiloxane-bonded silica sorbent; PS–DVB = poly(styrene)–divinylbenzene porous polymer.

cases where the more favorable cavity term exceeds the difference in contributions from the polar interaction terms.

The addition of a small amount of organic solvent to the sample to obtain adequate flow through the membrane and stable sampling conditions over time is not an optional step [6]. The above results suggest that the selectivity of the sorbent for specific intermolecular interactions is significantly influenced by the choice of organic solvent employed. Methanol is almost always used for this purpose but solvents with a contra selectivity may be capable of significant changes in breakthrough volumes. The experimental protocol in combination with the solvation parameter model provides an experimental framework to study these effects quantitatively.

References

[1] C.F. Poole and S.K. Poole, *Chromatography Today*, Elsevier, Amsterdam, 1991, pp. 777–793.
[2] S.K. Poole, T.A. Dean, J.W. Oudsema and C.F. Poole, *Anal. Chim. Acta*, 236 (1990) 3.
[3] I. Liska, J. Krupcik and P.A. Leclercq, *J. High Resolut. Chromatogr.*, 12 (1989) 577.
[4] I. Liska, *J. Chromatogr. A*, 655 (1993) 163.
[5] D.R. Hagen, C.G. Markell, G. Schmitt and D.B. Blevins, *Anal. Chim. Acta*, 236 (1990) 157.
[6] M.L. Mayer and C.F. Poole, *Anal. Chim. Acta*, 294 (1994) 113.
[7] D. Barcelo, S. Chiron, S. Lacorte, E. Martinez and J.S. Salau and M.C. Hennion, *Trends Anal. Chem.* 13 (1994) 352.
[8] J. Hodgeson, J. Collins and W. Bashe, *J. Chromatogr. A*, 659 (1994) 395.
[9] J. Beltran, F.J. Lopez and F. Hernandez, *J. Chromatogr. A*, 283 (1993) 297.
[10] C. Markell, D.F. Hagen and V.A. Bunnelle, *LC·GC*, 9 (1991) 332.
[11] W.P.N. Fernando, M.L. Larrivee and C.F. Poole, *Anal. Chem.*, 65 (1993) 588.
[12] M.L. Larrivee and C.F. Poole, *Anal. Chem.*, 66 (1994) 139.
[13] M.H. Abraham, *Chem. Soc. Rev.*, 22 (1993) 73.
[14] M.H. Abraham, J. Andonian-Haftvan, G.S. Whiting, A. Leo and R.S. Taft, *J. Chem Soc., Perkin Trans. 2*, (1994) 1777.
[15] C.F. Poole, T.O. Kollie and S.K. Poole, *Chromatographia*, 34 (1992) 281.
[16] P.W. Carr, *Microchem. J.*, 48 (1993) 4.
[17] W.P.N. Fernando and C.F. Poole, *J. Planar Chromatogr.*, 3 (1990) 389.
[18] W.P.N. Fernando and C.F. Poole, *J. Planar Chromatogr.*, 4 (1991) 278.
[19] K.G. Miller and C.F. Poole, *J. High Resolut. Chromatogr.*, 17 (1994) 125.
[20] M.H. Abraham, *J. Phys. Org. Chem.*, 6 (1993) 660.
[21] M.H. Abraham, *J. Chromatogr.*, 644 (1993) 95.
[22] M.H. Abraham and J.C. McGowan, *Chromatographia*, 23 (1987) 243.
[23] K. Kimata, F. Iwaguchi, S. Onishi, K. Jinno, R. Eksteen, K. Hosoya, M. Araki, and N. Tanaka, *J. Chromatogr. Sci.*, 27 (1989) 721.
[24] M.J. Walters, *J. Assoc. Off. Anal. Chem.*, 70 (1987) 465.
[25] L. Schmidt, J.J. Sun, J.S. Fritz, D.F. Hagen, C.G. Markell and E.E. Wisted, *J. Chromatogr.*, 641 (1993) 57.

ELSEVIER

Journal of Chromatography A, 697 (1995) 101–105

JOURNAL OF CHROMATOGRAPHY A

Development of a binary solid-phase extraction cartridge for use in screening water samples for organic pollutants

Mark William Powell

Anglian Water Services Ltd., Milton Keynes Laboratory, P.O. Box 1500, Pineham, Milton Keynes MK15 9PG, UK

Abstract

Two chemically modified resins and a range of commercially available material were evaluated for use as solid-phase sorbents in an analytical procedure designed to screen water samples for trace level organic contamination. A binary cartridge, comprising acetyl-derivatised resin and an anion-exchange phase, was found to perform better for most compounds than conventional liquid–liquid extraction using dichloromethane.

1. Introduction

Liquid–liquid extraction (LLE) using dichloromethane is used in the water industry to extract and concentrate organic compounds from aqueous samples in a process designed to screen for trace level contamination. Dichloromethane is the solvent of choice owing to the tendency of most organic compounds possessing medium or low polarity to partition into the organic phase. The high volatility of the solvent enables its removal at ambient temperature; this is important if volatile analytes are not to be lost.

There are, however, a number of drawbacks associated with LLE in general and the use of dichloromethane in particular. Firstly, LLE is not amenable to automation; this is an important consideration, since automation reduces labour costs and improves turnaround time. The technique also generates a large volume of waste solvent, the disposal of which adds significantly to the cost of analysis. The use of dichloromethane is not favoured owing to its narcotic properties [1], on environmental grounds [2], and the potential for background levels in the laboratory to interfere with volatile organics analysis.

An ideal solution to these problems would be solid-phase extraction (SPE), a technique that is easily automated and requires the use of relatively low volumes of organic solvents. One of the principal characteristics of SPE is its selectivity; by judicious choice of bonded phase, sample pH, ionic strength and elution conditions, the analyst can control the classes of compounds that are isolated from the matrix [3]. In order to replace dichloromethane extraction, however, the SPE sorbent would have to be capable of retaining (and subsequently releasing to the elution solvent) a wide range of different compound types.

Solid-phase sorbents for trace enrichment using bonded silica chemistries have gained popularity owing to their dimensional stability; resin-based sorbents tend to swell or shrink according to the sample matrix and eluting solvent composition. A number of workers have successfully used resin sorbents for the extraction of organic compounds from water [4,5]. Recently, Sun and Fritz [6] reported the synthesis and

0021-9673/95/$09.50
SSDI 0021-9673(94)00958-9

use of chemically modified resins for SPE. These modified resins were more hydrophilic than the virgin material, and this was thought to promote extraction of the more polar compounds that might not be retained by non-polar interactions alone. Mills et al. [7] testify to the increasing popularity of mixed-mode SPE sorbents for extracting a greater range of compound classes than previously possible using a single mode of interaction. In the present work, modified resins, along with commercially available sorbents, including mixed-mode material, were evaluated for use in a broadly-based screening method.

2. Experimental

2.1. Reagents

All reagents and standard materials were of analytical-reagent quality or better. Hydroxymethyl and acetyl derivatives of Amberchrom 161M resin (Supelco, Poole, UK) were prepared using the method of Sun and Fritz [6]. The following commercial sorbents were used: 1 g activated carbon (Envi Carb, Supelco); 1 g mixed C_8/anion exchange (Certify II; Varian, Walton-on-Thames, UK); and amino and diamino bonded silicas (J.T. Baker, Reading, UK).

2.2. Equipment

Loading, drying and elution of SPE cartridges was performed on a spe-12G vacuum manifold (J.T. Baker) attached to a filter pump. The extracts were analysed using a Model 3400 GC (Varian) equipped with an on-column injector, open-split coupled to an ion trap detector (Finnigan MAT, Hemel Hempstead, UK) scanning from 49 to 449 u in 1 s. The column used was a J & W 30 m × 0.32 mm DB-1, film thickness 0.25 μm (Jones Chromatography, Hengoed, UK). The column temperature was programmed from 30 to 260°C at 8°C min^{-1}, and held for 10 min. The injector temperature was programmed from 30 to 260°C at 300°C min^{-1}, and held for 3 min. Helium carrier gas was used at an inlet pressure of 0.90 bar.

2.3. SPE methods

Two SPE procedures were used during the study, details of which are given below. The organic compounds spiked into the water were selected to give a wide range of polarities. They are representative of the types of compound required to show up on screening.

Procedure A

Three 1-l aliquots of an uncontaminated bore water were spiked with the organic compounds listed in Table 1 to a concentration of 1 $\mu g\ l^{-1}$. Methanol (20 ml) was added to each spiked sample and the bottles shaken to mix. Each extraction cartridge was conditioned with 3 × 3 ml methanol and washed with 3 ml HPLC-grade water. The samples were loaded at a flow-rate of approximately 5 ml min^{-1} and the cartridge rinsed with 3 ml HPLC-grade water. The sorbent beds were dried under vacuum for 45 min and the analytes eluted with 3 × 1 ml dichloromethane. The eluate was blown down to approximately 300 μl in a graduated vial, spiked with internal standard (1 μl of a 1 g l^{-1} solution of 1-chloroundecane in dichloromethane) and 1 μl injected for GC–MS analysis.

Procedure B

Sample pretreatment, loading and drying conditions were identical to procedure A, except that five replicate analyses were performed on each cartridge. The elution step was performed with 2 × 1 ml dichloromethane followed by 2 × 1 ml 2% trifluoroacetic acid (TFA) in methanol. The methanolic TFA eluate was collected separately, blown down to dryness and made up with 1 ml dichloromethane. The extracts were combined, blown down to volume and analysed according to the details given for procedure A.

2.4. LLE extraction method

A LLE procedure was adopted to enable a comparison to be made between existing meth-

Table 1
Recoveries of test compounds on the two modified resin types

Compound	Recovery (%)		
	Quantitation mass	Acetyl resin	Hydroxymethyl resin
Ethylbenzene	106	64 (0.4)	34 (27)
Phenol	94	6 (63)	8 (20)
1,4-Dichlorobenzene	146–150	67 (2)	26 (31)
n-Decane	57	38 (1)	33 (44)
2,6-Dimethylphenol	122	29 (25)	15 (28)
Naphthalene	128	59 (9)	75 (21)
2,4,5-Trichlorophenol	196–200	6 (59)	13 (81)
Atrazine	215	75 (16)	14 (86)
Pentachlorophenol	266	11 (115)	30 (75)
Linuron	61	128 (31)	83 (38)
Fluoranthene	202	91 (43)	65 (43)

R.S.D. (%, $n = 3$) in parentheses.

ods and the SPE techniques. Aliquots of 1 l of bore water were spiked at 1 $\mu g\ l^{-1}$ and shaken with 80 ml dichloromethane in a separating funnel. The organic layer was collected and the bulk of the solvent removed in a rotary evaporator. The remaining dichloromethane solution was transferred to a graduated vial, blown down and analysed according to the details given for procedure A.

2.5. SPE cartridge preparation

An initial study was conducted to determine which derivatised resin (hydroxymethyl or acetyl) would give the best recoveries of the compounds of interest. Two 6-ml polypropylene syringe barrel cartridges were packed with 600 mg of each resin and evaluated according to procedure A.

As a result of this initial work, the acetyl-modified resin was selected for further evaluation in a binary system with anion exchange phases. Two 6-ml polypropylene syringe barrel cartridges were packed as follows: 300 mg resin with 500 mg diamino-bonded silica; and 300 mg resin with 500 mg amino-bonded silica. The two phases were separated by a porous polyethylene frit. The mass of resin was selected to give a surface area equivalent to 500 mg silica-based material. The Supelco Envi Carb and Varian Certify II cartridges, also selected for study, were used as received, and all cartridges were processed according to procedure B.

For both trials, an unextracted portion of the spiking solution was used to calculate absolute recoveries.

3. Results

The results of the first study, which compared the two resin types, are given in Table 1 and the data produced by the second trial are given in Table 2.

4. Discussion

The acetyl resin was favoured over the hydroxymethyl-modified material owing to the poor yield of atrazine from the latter under the conditions of the test (Table 1). The reason for this might be strong hydrogen-bonding interactions between the hydroxyl groups on the resin and the secondary amine functionalities of atrazine. Since atrazine and some other triazine herbicides are ubiquitous in surface waters, and also because recoveries for most test compounds were higher from the acetyl phase, it was de-

Table 2
Recoveries of test compounds with SPE and LLE techniques

Compound	Recovery (%)[a]				
	a	b	c	d	e
Ethylbenzene	76 (72)	72 (18)	121 (18)	1 (20)	54 (12)
Phenol	21 (33)	75 (16)	0	0	18 (14)
1,4-Dichlorobenzene	50 (24)	100 (11)	69 (22)	3 (13)	56 (13)
n-Decane	20 (45)	62 (9)	32 (15)	32 (18)	36 (9)
2,6-Dimethylphenol	34 (10)	77 (12)	0	5 (15)	67 (11)
Naphthalene	53 (35)	99 (5)	42 (19)	20 (16)	64 (16)
2,4,5-Trichlorophenol	4 (86)	6 (33)	0	32 (9)	77 (14)
Atrazine	101 (23)	95 (10)	91 (11)	99 (6)	86 (15)
Pentachlorophenol	0	8 (31)	0	0	68 (22)
Linuron	117 (28)	99 (30)	79 (20)	126 (14)	96 (21)
Fluoranthene	69 (16)	87 (12)	0	82 (4)	84 (13)

R.S.D. (%, $n = 5$) in parentheses. For quantitation masses, see Table 1.
[a] a = Diamino/acetyl binary cartridge; b = amino/acetyl binary cartridge; c = Envi Carb cartridge; d = Certify II cartridge; e = dichloromethane extraction.

cided to concentrate development effort on the acetyl material.

The other problem with the derivatised phases used in isolation was poor recovery of more polar, anionic species (see recovery data for phenols in Table 1). Recovery of phenol was significantly lower on both modified resins than the values given by Sun and Fritz [6]. These authors reported phenol recoveries of 94 and 100% on hydroxymethyl- and acetyl-modified resin respectively. This difference can be explained by noting that Sun and Fritz used a sample volume of 20 ml and a sorbent mass of 100 mg compared to a sample volume of 1 l and a sorbent mass of 600 mg in the present work. It is reasonable to assume that breakthrough was responsible for the poor recoveries for phenol reported here. The recoveries of phenol and 2,6-dimethylphenol improved significantly with the incorporation of an anion-exchange phase (Table 2).

The best recoveries for six out of the eleven test compounds were obtained with the acetyl resin/amino-bonded silica combination. This combination of sorbents gave acceptable recoveries and precision for all test compounds with the exception of 2,4,5-trichlorophenol and pentachlorophenol, for which dichloromethane extraction gave the best recovery data. The recoveries of the chlorinated phenols from the acetyl/aminopropyl cartridge were unexpectedly low considering the relatively good recoveries observed for phenol and 2,6-dimethylphenol and may be caused by a stronger sorbent–analyte interaction, possibly involving both polar and non-polar bonding, than with the non-chlorinated phenols, rendering elution more difficult. Different elution conditions, perhaps using a base-modified solvent, might result in better performance.

The activated carbon cartridge gave low recoveries for most of the trial compounds, particularly for the phenols. The reason for this is unclear, although activated carbon is capable of retaining some organic compounds so strongly that desorption by the elution solvent becomes difficult [8]. The performance of the acetyl resin/diamino cartridge was poorer than that of the resin/amino combination. This cartridge contained a mixture of primary and secondary amine functionalities $[-(CH_2)_3NH(CH_2)_2NH_2]$; the amino phase contained only primary amine (aminopropyl) bonded silica. The primary phase has a more polar character than the mixed

primary/secondary material, which probably promotes a stronger interaction with anionic organic species such as the phenols.

The mixed-mode Certify II material gave very good recovery and precision performance for atrazine; otherwise, the performance of the Certify II sorbent was generally inferior to that of the binary resin phases. Dichloromethane extraction gave better recoveries only for the chlorinated phenols. Since these are environmentally important compounds, the relatively poor performance of the binary resin/ion-exchange cartridges will have to be improved before their routine use is possible.

5. Conclusions

SPE offers a viable alternative to the use of dichloromethane LLE for the screening of water samples for organic micropollutants. The use of SPE resulted in improved recoveries for all but two of the eleven compounds studied compared to dichloromethane extraction. Pressure is being placed upon analytical chemists to replace chlorinated solvents as analytical reagents; this work shows the potential of SPE to replace these chemicals in the analytical laboratory.

Further work needs to be undertaken to improve the reproducibility of the extraction, to assess the use of elution solvents other than dichloromethane, and to improve the performance of the technique with respect to chlorinated phenols. It would also be desirable to extend the range of compounds to which the technique can be applied.

Acknowledgements

The author would like to thank Dr. Janet Watson, Colin Jump, Chris Land and Ruud Schiffer (J.T. Baker Ltd.) and Dr. Mike Pinchin (Anglian Water) for supporting the work. I am also grateful to Bob Price, Director of Water Quality, Anglian Water, for permission to publish. The views expressed are those of the author, and not necessarily of Anglian Water.

References

[1] S. Budavari (Editor), *The Merck Index*, Merck & Co, Rahway, NJ, 11th ed., 1989.
[2] P. Ciccioli, in H.J. Th. Bloemen and J. Burn (Editors), *Chemistry and Analysis of Volatile Organic Compounds in the Environment*, Chapman & Hall, London, 1993, Ch. 3, p. 92.
[3] A. Newman, *Environ. Sci. Technol.*, 26 (1992) 1294.
[4] A.P. Infante, N.C. Guajardo, J.S. Alonso, M.C.M. Navascues, M.P.O. Melero, M.S.M. Cortabitarte and J.L.O. Narvion, *Wat. Res.*, 27 (1993) 1167.
[5] G.C. Mattern, J.B. Louis and J.D. Rosen, *J. Assoc. Off.Anal. Chem.*, 74 (1991) 982.
[6] J.J. Sun and J.S. Fritz, *J. Chromatogr.*, 590 (1992) 197.
[7] M.S. Mills, E.M. Thurman and M.J. Pedersen, *J. Chromatogr.*, 629 (1993) 11.
[8] A.M. Robertson and J.N. Lester, *Wat. Environ. Management*, in press.

ELSEVIER

Journal of Chromatography A, 697 (1995) 107–114

JOURNAL OF CHROMATOGRAPHY A

Studies on trapping efficiencies of various collection devices for off-line supercritical fluid extraction

Norbert Hüsers[a], Wolfgang Kleiböhmer[b,*]

[a]*Westfälische Wilhelms-Universität, Lehrstuhl für Analytische Chemie, Wilhelm-Klemm-Strasse 8, D-48149 Münster, Germany*
[b]*Institut für Chemo- und Biosensorik, Mendelstrasse 7, D-48149 Münster, Germany*

Abstract

Analyte collection in supercritical fluid extraction can be difficult, especially for relatively volatile substances. Losses of polycyclic aromatic hydrocarbons (PAHs) of up to 30% are observed with different liquid collection devices. A solid–liquid trap can minimize these trapping problems. Silica gel and two different octadecylsilanes were tested as solid sorbents. Good recoveries were found with pure carbon dioxide as the extraction fluid. Higher flow-rates did not increase analyte losses. The analytes were trapped on the solid surface. The use of modified carbon dioxide was also no problem. The analytes were eluted from the solid matrix after extraction by the modifier in the liquid phase. In the extraction of PAHs from real samples, further clean-up may be unnecessary when silica gel is used as a solid trapping material.

1. Introduction

Supercritical fluid extraction (SFE) is a modern alternative to Soxhlet extraction. The advantages of this extraction method are the shorter extraction times and smaller amounts of organic solvents required. The acceptance of SFE by the regulatory authorities has already started, as was demonstrated when the US Environmental Protection Agency (EPA) approved the first SFE method as a replacement for the conventional Soxhlet extraction of total petroleum hydrocarbons [1].

Generally there are two important steps in supercritical fluid extraction. First, the extraction parameters have to be correctly chosen to overcome solute–matrix interactions and to transport the analytes properly out of the extraction cell. The second step is the trapping of the analytes after the extraction process. Inefficient trapping leads to inaccurate results with low reproducibility. Hence the first step in developing any SFE method should be the testing of quantitatively efficient collection methods and, if necessary, the development of a new collection device [2].

In the case of "off-line" supercritical fluid extraction several trapping techniques are possible, e.g., solvent traps [3–5], solid-phase traps [6,7] and cryogenically cooled traps [8]. Collection will occur after depressurizing the compressed fluid. The resulting flow-rates of the expanded gas may reach 1000 ml/min and more. In this case, it is obvious that the trapping of the analytes, especially of volatile substances, can be difficult.

For collection using a liquid trap, the efficiency depends on the solubility of the analyte in the collection solvent, the flow-rates and the temperature of the solvent. Langenfeld et al. [3] investigated the collection efficiencies of differ-

* Corresponding author.

0021-9673/95/$09.50
SSDI 0021-9673(94)00830-2

ent solvents for semi-volatile pollutants [e.g., polycyclic aromatic hydrocarbons (PAHs)]. They used 2–10 ml of liquid solvent and a flow-rate of 500 ml/min. They found a dependence of the extraction results on the volatility of the analytes: the more volatile the substances, the poorer were the recoveries. Different solvents gave different collection efficiencies. Methylene chloride was the solvent with the best trapping efficiency. Acetone gave recoveries similar to those with methylene chloride. Methanol and *n*-hexane gave the highest losses. Cooling methylene chloride to 5°C increased the collection efficiency for the investigated PAHs.

In another study, the influence of flow-rate on solvent collection was investigated [9]. Higher flow-rates are problematic for solvent collection. Losses during the extraction process are possible. Even the restrictor temperature has an influence on the trapping efficiencies.

Solid-phase traps are an alternative for analyte trapping. Several traps have been investigated, e.g., μBondapack C_{18} for PCBs [10] and or phenyl-, octyl-, diol-, cyano- and amino-bonded silica for a polar test mixture containing acetophenone, N,N-dimethylaniline, *n*-decanoic acid, 2-naphthol and tetracosane [6]. After the extraction the analytes have to be eluted from the sorbent with an organic solvent. For solid traps, flow-rates of up to ca. 2000 ml/min of expanded fluid are usual [6]. The use of modified carbon dioxide, which generally in SFE is necessary to increase the extraction results, is difficult for solid traps. The organic solvents used as modifiers may elute the collected analytes from the solid sorbents during the extraction. Mulcahey and Taylor [7] investigated the effect of methanol as modifier on stainless steel and on octadecylsilane traps for the polar test mixture mentioned above. Here the trap temperature and the amount of modifier are very important for minimizing analyte losses.

The aim of this investigation was to determine the collection efficiencies for PAHs of a combined solid–liquid trap. Our first results with the solid–liquid trap have been published elsewhere [11,12]. The extraction results with different solvent traps and the solid–liquid trap were compared. Silica gel and octadecylsilane solid phases (ODS) were used. The extractions were performed with pure carbon dioxide and modified CO_2. The influence of the flow-rate of the expanded fluid on the recoveries was also investigated.

2. Experimental

2.1. Chemicals

Acetonitrile (HPLC grade) was obtained from Baker (Gross Gerau, Germany). Acetone, *n*-hexane, methylene chloride and toluene, which were of purity for residual analysis, were obtained from Merck (Darmstadt, Germany). Carbon dioxide (purity 4.5) was purchased from Westfalen AG (Münster, Germany).

Silica gel (40 μm) (Baker) was heated at 105°C for 1 h and cooled to room temperature before adding 10% (w/w) of water. After shaking for 1 h, the matrix was ready to use. ODS-modified silica (Chromabond) was obtained from Macherey–Nagel (Düren, Germany).

2.2. Supercritical fluid extraction

All extractions were carried out using a Dionex SFE-system (SFE-703). For extraction with modified carbon dioxide the system was equipped with a Dionex SFE-703M module. The extraction cells (3.5 ml, 5 cm × 9.4 mm I.D.) (Keystone Scientific) were filled with silanized glass-fibre wadding (Macherey–Nagel) and 1 g of ODS. A solution of sixteen EPA PAHs in benzene–methylene chloride (2000 μg/ml)(Sigma and Aldrich) was diluted in toluene (2 μg/ml). A 100-μl volume of this solution (total 3.2 μg of PAHs) was spiked on ODS. The extractions were performed in a dynamic mode at 40 MPa, oven temperature 90°C and restrictor temperature 150°C for 30 min with pure CO_2 or with CO_2 modified with 5% toluene. These parameters were selected because the same conditions were used for real sample extractions [11]. All extractions were performed in triplicate.

Two different linear restrictors (A and B) from Dionex (restrictor wafer, 250 and 1200 ml/min) were used. Restrictor A gave a flow-rate of ca. 300 ml/min and restrictor B ca. 1200 ml/min under the selected extraction conditions.

For analyte collection a dual-chamber trapping vial (Fig. 1a) [4] with 10 or 15 ml of different organic solvents was used. In case of the solid–liquid trap, the transfer tube was modified (Fig. 1b). The tube was filled with 0.3 g of silica gel or ODS material. A new transfer tube from Dionex with a disc of C_{18} material (octadecyl-modified glass-fiber matrix), fixed at the bottom end of the tube, was also tested. In the solid–liquid trap 10 ml of *n*-hexane were used as organic solvent. The collection vial with the trapping device was cooled to ca. 5°C.

After extraction with the modified dual-chamber trapping vial, the collected analytes were eluted from the solid traps. For silica gel 4 ml of toluene–light petroleum (1:2, v/v) and for ODS material 4 ml of methylene chloride were used. The Dionex solid trap was eluted with 3 ml of *n*-hexane.

To minimize evaporation losses, 50 μl of diethyl phthalate were added to each extract prior to evaporation of the solvent under a gentle stream of nitrogen. A 950-μl volume of acetonitrile was added and the extracts were analysed by HPLC.

2.3. HPLC analysis

For HPLC analysis an HP Series 1050 liquid chromatograph (Hewlett-Packard) equipped with an autosampler, quaternary pump, degasser, HP 1046A programmable fluorescence detector and HP ChemStation for data acquisition and data analysis was used. The PAHs were separated on a Bakerbond PAH 16-Plus column (250 × 3 mm I.D.) with a 20 mm precolumn at a column temperature of 30°C. Acetonitrile and water were used as the mobile phase at a flow-rate of 0.5 ml/min. The composition gradient of the mobile phase started with 50% acetonitrile and 50% water for 6 min, then the acetonitrile content was increased to 99% in 29 min with a linear gradient. This content was held constant for 10 min until the end of the analysis. For equilibration, the initial conditions were maintained for 15 min. For detection, the following excitation (Ex) and emission (Em) wavelength programme was used; naphthalene and acenaphthene (Ex 210 nm, Em 320 nm), phenanthrene and anthracene (Ex 248 nm, Em 384 nm), fluorene and pyrene (Ex 236 nm, Em 430 nm),

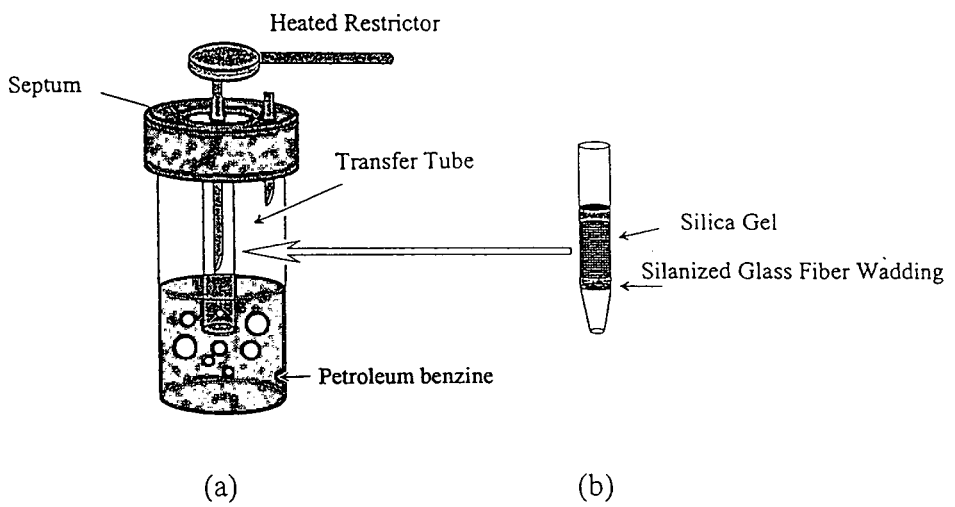

Fig. 1. (a) Dual-chamber trapping vial; (b) modified transfer tube.

benz[*a*]anthracene and chrysene (Ex 270 nm, Em 390 nm), benzo[*b*]fluoranthene, benzo[*k*]-fluoranthene and benzo[*a*]pyrene (Ex 250 nm, Em 440 nm), dibenz[*a*,*h*]anthracene and benzo[*ghi*]perylene (Ex 296 nm, Em 405 nm) and indeno[123-*cd*]pyrene (Ex 245 nm, Em 480 nm). For identification the retention times were compared and for quantification an external calibration with SRM 1647c solution in acetonitrile (Promochem, Wesel, Germany) was performed.

3. Results and discussion

The extraction yields in SFE depend on the solubility of the analytes in the supercritical fluid, the flow-rate, the extraction time, the interaction between analytes and the matrix and the trapping efficiency of the collection device. The aim of this investigation was to test several collection devices. Therefore, the PAH solution was spiked on ODS material. It is known that the interaction between PAHs and ODS material is low so that the selected extraction parameters, 90°C and 40 MPa, are sufficient to remove the analytes from the matrix and to sweep them out of the extraction cell.

3.1. Solvent collection

Influence of solvents

The trapping efficiencies of solvent collection in SFE depend on several parameters, such as the geometry of the trapping device, the solubility of the analytes in the solvent, the restrictor temperature, the solvent temperature and the flow-rate of the expanded fluid.

First the collection efficiencies of different organic solvents for PAHs were compared. The results with the dual-chamber trapping vial, restrictor A (flow-rate 300 ml/min) and different organic solvents (*n*-hexane, methylene chloride, acetone) are given in Table 1. The best results were found with acetone as collection solvent. Excluding the anomalous anthracene and benzo[*a*]pyrene, the recoveries of the low- to high-molecular-mass PAHs varied from 95% to 83% with standard deviations of 3.5 and 1.0%. The recoveries for methylene chloride were slightly lower (Table 1). The results for anthracene and benzo[*a*]pyrene with methylene chloride and acetone indicate that there may be a systematic error. *n*-Hexane gave recoveries of ca. 90% for the analytes with high volatility and ca. 70% for analytes with low volatility (Table 1). It was

Table 1
Recoveries (with standard deviations; $n = 3$) for PAHs of different liquid traps and of the purge studies with collection solvent *n*-hexane and flow-rates of gaseous CO_2 of 300 and 1200 ml/min

No.	Compound	*n*-Hexane		Methylene chloride	Acetone	Purge studies	
		300 ml/min	1200 ml/min	300 ml/min	300 ml/min	300 ml/min	1200 ml/min
1	Naphthalene	78.0 ± 3.3	72.2 ± 6.8	78.1 ± 7.2	83.1 ± 3.4	92.0 ± 5.4	96.0 ± 4.2
2	Acenaphthene	88.4 ± 6.6	76.1 ± 7.8	80.0 ± 3.4	89.4 ± 2.2	95.4 ± 1.8	96.4 ± 0.6
3	Fluorene	89.5 ± 7.5	76.0 ± 8.1	78.1 ± 1.5	90.0 ± 1.6	97.4 ± 1.2	97.7 ± 0.5
4	Phenanthrene	92.4 ± 8.8	84.9 ± 9.1	82.9 ± 1.0	95.3 ± 1.0	100.7 ± 0.2	111.1 ± 1.5
5	Anthracene	85.9 ± 2.7	70.0 ± 8.0	69.1 ± 2.4	80.0 ± 3.6	104.2 ± 1.9	102.6 ± 0.9
6	Fluoranthene	86.7 ± 11.2	81.5 ± 10.1	83.1 ± 4.2	90.6 ± 1.7	97.3 ± 0.5	112.0 ± 1.8
7	Pyrene	88.6 ± 11.6	78.7 ± 10.1	85.2 ± 4.1	91.5 ± 1.7	99.8 ± 0.3	107.8 ± 1.2
8	Benz[*a*]anthracene	78.0 ± 14.8	68.4 ± 8.9	77.2 ± 5.4	82.2 ± 0.7	100.4 ± 0.4	100.0 ± 0.3
9	Chrysene	78.9 ± 17.3	66.6 ± 8.1	80.3 ± 5.9	84.7 ± 1.1	98.8 ± 0.3	99.3 ± 0.3
10	Benzo[*b*]fluoranthene	73.2 ± 18.3	68.2 ± 10.5	78.1 ± 3.1	83.2 ± 1.3	97.9 ± 0.6	100.4 ± 0.5
11	Benzo[*k*]fluoranthene	75.1 ± 18.4	67.6 ± 7.7	78.9 ± 3.9	83.3 ± 0.9	97.8 ± 0.5	99.7 ± 0.5
12	Benzo[*a*]pyrene	70.7 ± 7.9	58.9 ± 9.1	66.7 ± 5.6	74.0 ± 3.4	106.3 ± 3.1	105.5 ± 1.6
13	Dibenz[*a*,*h*]anthracene	72.0 ± 19.4	70.3 ± 8.4	78.6 ± 3.5	83.9 ± 1.1	98.4 ± 0.4	100.0 ± 0.5
14	Benzo[*ghi*]perylene	70.5 ± 18.4	72.4 ± 11.7	79.4 ± 2.8	84.8 ± 2.0	98.3 ± 0.8	100.2 ± 0.6
15	Indeno[1,2,3-*cd*]pyrene	69.1 ± 18.7	75.7 ± 9.4	77.7 ± 2.7	83.1 ± 1.8	97.9 ± 1.2	99.7 ± 0.6

expected that the collection efficiencies of analytes with lower volatility would be better because of their higher molecular mass. This agrees with the results of Langenfeld et al. [3]. In contrast, with methylene chloride and acetone we observed a slight decrease in collection efficiencies from the less to the more volatile analytes. We have no reasonable explanation for this effect.

Langenfeld et al. [3] achieved quantitative recoveries with methylene chloride by keeping the solvent vial at 5°C (flow-rate ca. 500 ml/min).

Thompson et al. [5] reported recoveries for naphthalene of >90% with acetone and *n*-hexane and 83% with methylene chloride. They used the same dual-chamber trapping vial as we did but with different extraction parameters.

These three examples show the difficulties in trapping analytes in SFE with liquid solvents. It can be concluded that the collection parameters have to be optimized for each extraction problem.

Influence of flow-rates

The influence of higher flow-rates was investigated with restrictor B, which gives flow-rates of about 1200 ml/min (Table 1). *n*-Hexane was used as the collection solvent. For higher molecular mass analytes the recoveries were similar to those with restrictor A (Table 1), but for the more volatile substances the recoveries were lower. An influence of the flow-rate on the recoveries is obvious for the volatile substances, but surprisingly the recoveries for the more volatile analytes are better than those for the lower less volatile compounds. Although the flow-rate had been increased fourfold, the influence of this parameter on the recoveries was very low.

Losses of analytes while trapping with liquid solvents depend on either insufficient collection or the analytes being purged from the solvent with the gas flow. The purge losses of analytes from the collection solvent were tested by spiking the standard solution into the collection solvent, here *n*-hexane, and performing the normal extraction procedure. The extraction was performed with restrictors A and B to investigate the influence of different flow-rates. The recoveries were about 100% for both restrictors (Table 1). Analytes collected in the organic solvent were not purged from the solvent by the expanded fluid. This leads to the conclusion that poor recoveries are due to insufficient collection capacities of the trapping system.

3.2. The solid–liquid trap

ODS and silica gel–liquid trap

To increase the trapping efficiency of the dual-chamber vial, different solid–liquid traps were investigated. The transfer tube was filled with silica gel or ODS material (Fig. 1b). In Fig. 2 the recoveries with the silica gel–*n*-hexane trap, the ODS–*n*-hexane trap and the *n*-hexane solvent trap are compared. The collection efficiency of the solid–liquid trap is clearly better than that of the liquid trap. The recoveries increased by 10–30% for each analyte and reached more than 90%. Silica gel and ODS material showed no difference in adsorbing the analytes during extraction. Separate analyses of the organic solvent and the solid traps (silica gel and ODS material) after the extraction with pure carbon dioxide showed no PAHs in the organic solvent. After the extraction, the analytes were trapped on the solid matrix, while the expanded gas flowed through the solid phase. After the extraction the collected substances have to be eluted with a few millilitres of an appropriate organic solvent.

The same experiment was carried out with CO_2 modified with 5% of toluene. Again, the organic solvent and the solid matrix were analysed individually (Fig. 3). In this case the analytes were found in the organic solvent. This shows that the substances were eluted by the organic modifier. Elution of the analytes after the extraction with an organic solvent may no longer be necessary.

In contrast to the solid trap, the extraction with modified carbon dioxide did not reduce the collection efficiencies. When the new solid–liquid

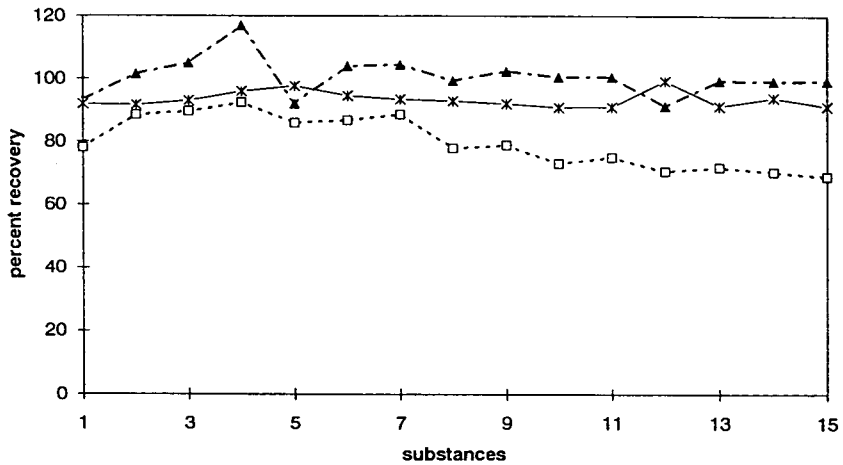

Fig. 2. Comparison of solid–liquid and liquid traps. Flow-rate of gaseous CO_2, 300 ml/min. □ = *n*-hexane; ▲ = silica gel–*n*-hexane; * = ODS = *n*-hexane. For substance identification, see Table 1.

trapping device was used, the eluted analytes were collected in the liquid.

Influence of flow-rates

The solid–liquid trap was tested with restrictor B (flow-rate 1200 ml/min). Silica gel was used as solid sorbent. The results are given in Table 2. In contrast to the liquid trap, there was no influence of the flow-rate on the recovery. All analytes were collected with good recoveries.

Dionex transfer tube

Extractions with restrictors A and B were performed with the C_{18} transfer tube. This solid–

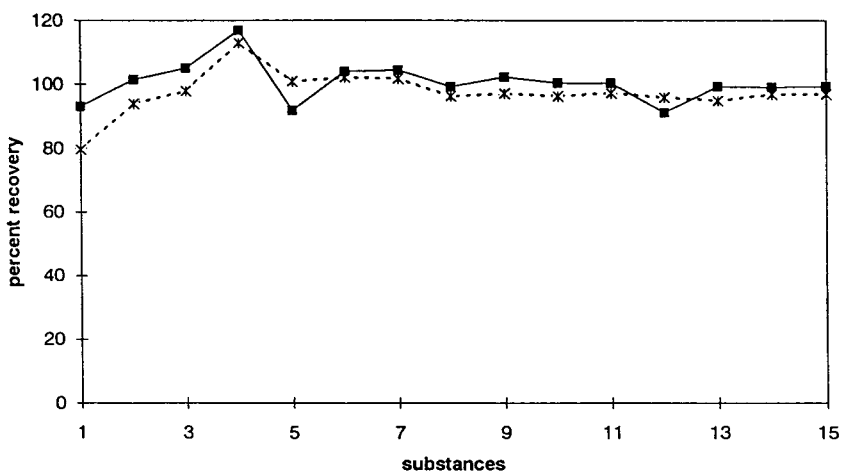

Fig. 3. Collection efficiencies with the silica gel–*n*-hexane trap for (■) carbon dioxide and (*) carbon dioxide modified with 5% of toluene. Flow-rate of gaseous CO_2, 300 ml/min. For substance identification, see Table 1.

Table 2
Collection efficiencies (recoveries with standard deviations; $n = 3$) for PAHs with different solid–liquid traps and flow-rates of gaseous CO_2 of 300 and 1200 ml/min

No.	Compound	Silica gel–*n*-hexane		ODS–*n*-hexane 300 ml/min	Dionex tubes–*n*-hexane	
		300 ml/min	1200 ml/min		300 ml/min	1200 ml/min
1	Naphthalene	93.2 ± 9.8	89.2 ± 24.0	91.8 ± 2.5	82.9 ± 10.0	95.1 ± 5.7
2	Acenaphthen	101.5 ± 8.5	89.9 ± 8.0	91.6 ± 0.1	86.8 ± 5.8	98.6 ± 0.8
3	Fluorene	105.0 ± 8.1	87.3 ± 6.6	93.0 ± 0.1	89.1 ± 6.5	98.7 ± 0.6
4	Phenanthrene	116.9 ± 6.6	94.8 ± 6.2	95.9 ± 1.3	92.4 ± 5.5	112.8 ± 0.7
5	Anthracene	92.0 ± 6.2	90.7 ± 6.9	97.6 ± 1.4	89.6 ± 4.2	95.4 ± 2.0
6	Fluoranthene	104.0 ± 5.5	99.7 ± 6.0	94.6 ± 1.8	97.8 ± 2.5	113.9 ± 0.8
7	Pyrene	104.5 ± 8.6	116.1 ± 11.0	93.4 ± 4.3	93.6 ± 2.2	110.1 ± 0.7
8	Benz[*a*]anthracene	99.4 ± 5.6	98.2 ± 2.6	92.8 ± 2.0	93.1 ± 1.4	99.0 ± 0.3
9	Chrysene	102.4 ± 5.8	96.0 ± 3.3	92.0 ± 1.4	93.6 ± 1.4	96.3 ± 0.2
10	Benzo[*b*]fluoranthene	100.5 ± 4.9	97.0 ± 3.0	90.8 ± 1.8	96.4 ± 0.8	99.1 ± 0.0
11	Benzo[*k*]fluoranthene	100.5 ± 4.9	95.0 ± 3.0	91.0 ± 1.8	94.8 ± 3.1	97.4 ± 0.5
12	Benzo[*a*]pyrene	91.3 ± 5.5	90.7 ± 4.7	99.3 ± 3.7	94.6 ± 8.1	85.8 ± 1.6
13	Dibenz[*a,h*]anthracene	99.4 ± 4.7	96.3 ± 4.9	91.2 ± 2.2	92.8 ± 5.6	98.0 ± 2.7
14	Benzo[*ghi*]perylene	99.2 ± 4.9	99.7 ± 4.9	94.0 ± 2.2	91.8 ± 4.8	102.0 ± 0.1
15	Indeno[1,2,3-*cd*]pyrene	99.4 ± 4.6	98.9 ± 4.5	91.2 ± 2.6	99.0 ± 7.4	107.9 ± 0.9

liquid trap gave the same results as the other two traps tested (Table 2). The collection efficiencies were much better than with the liquid trap and there was also no dependence on the flow-rate.

4. Conclusions

Combined solid–liquid traps clearly show advantages over liquid or solid traps. The recoveries were increased by ca. 20% by using the solid–liquid traps. There were no losses of the less volatile analytes, and we found no dependence on the flow-rate of the extraction fluid. Variations of the extraction parameters seem not to influence the trapping efficiencies. The use of modified carbon dioxide caused no problems, because the analytes that were trapped on the solid surface were washed out by the organic solvent and collected in the liquid phase. As can be seen, the solid–liquid trap is easy to handle and usable under different extraction conditions.

Our experiments have shown that the use of silica gel as a solid trap in real sample extraction minimizes the clean-up procedures. In many instances an additional clean-up is no longer necessary because it is integrated in the extraction process.

Acknowledgements

The financial support of the German Bundesministerium für Forschung und Technologie (01 VQ 9003) and the Ministerium für Wissenschaft und Forschung des Landes Nordrhein-Westfalen is gratefully acknowledged.

References

[1] B. Lesnick, US Environmental Protection Agency, Office of Solid Waste, announcement at the *EPA Workgroup Meeting, Washington, DC, 17 July 1992.*
[2] S.B. Hawthorne, D.J. Miller, M.D. Burford, J.J. Langenfeld, S. Eckert-Tilotta and P.K. Louie, *J. Chromatogr.*, 642 (1993) 301–317.
[3] J.J. Langenfeld, M.D. Burford, S.B. Hawthorne and D.J. Miller, *J. Chromatogr.*, 594 (1992) 297–307.
[4] N.L. Porter, A.F. Rynaski, E.R. Campbell, M. Saunders and B.E. Richter, *J. Chromatogr. Sci.*, 30 (1992) 367–373.

[5] P.G. Thompson, L.T. Taylor, B.E. Richter, N.L. Porter and J.L. Ezzell, *J. High Resolut. Chromaogr.*, 16 (1993) 713–716.
[6] L.J. Mulcahey, J.H. Hendrick and L.T. Taylor, *Anal. Chem.*, 63 (1991) 2225–2232.
[7] L.J. Mulcahey and L.T. Taylor, *Anal. Chem.*, 64 (1992) 2352–2358.
[8] M. Ashraf-Khorassani, R.K. Houck and J.M. Levy, *J. Chromatogr. Sci.*, 30 (1992) 361–366.
[9] S. Reindl and F. Höfler, *Anal. Chem.*, 66 (1994) 1808–1816.
[10] M.M. Schantz and S.N. Chesler, *J. Chromatogr. Sci.*, 363 (1986) 397–401.
[11] A. Meyer, W. Kleiböhmer and K. Cammann, *J. High Resolut. Chromatogr.*, 16 (1993) 491.
[12] A. Meyer and W. Kleiböhmer, *J. Chromatogr.*, 657 (1993) 327.

ELSEVIER

Journal of Chromatography A, 697 (1995) 115–122

JOURNAL OF CHROMATOGRAPHY A

High-performance liquid chromatography comparison of supercritical-fluid extraction and solvent extraction of microbial fermentation products

Simon Cocks[a], Stephen K. Wrigley[a,*], M. Inês Chicarelli-Robinson[a], Roger M. Smith[b]

[a]*Xenova Ltd, 240 Bath Road, Slough, Berkshire SL1 4EQ, UK*

[b]*Department of Chemistry, Loughborough University of Technology, Loughborough, Leics LE11 3TU, UK*

Abstract

The use of supercritical fluids for the extraction of biologically active compounds from the biomass of microbial fermentations has been compared with extraction using the organic solvents methanol and dichloromethane. Compounds representing a range of structural types were selected for investigation. All the extracts obtained were examined using reversed-phase high-performance liquid chromatography. The extractability of metabolites using unmodified and methanol-modified supercritical-fluid carbon dioxide was examined in particular detail for six microbial metabolites: chaetoglobosin A, mycolutein, luteoreticulin, 7,8-dihydro-7,8-epoxy-1-hydroxy-3-hydroxymethylxanthone-8-carboxylic acid methyl ester, sydowinin B and elaiophylin. The extraction strength of supercritical-fluid carbon dioxide alone appeared to be lower than that of dichloromethane. All the components of interest that were extractable with dichloromethane and methanol were also extractable with methanol-modified carbon dioxide.

1. Introduction

A number of natural products and natural product derived compounds have proved to be extremely useful as drugs for the treatment of a range of medical conditions [1]. Screening programmes directed at the discovery of low-molecular-mass compounds with useful biological properties from natural sources continue to constitute an important and expanding interest throughout the pharmaceutical industry [1–3]. New naturally-produced compounds with interesting biological activities are reported regularly and these often provide the basis for pharmaceutical or agrochemical development projects.

The most widely explored sources of natural products to date have been plants, marine organisms and micro-organisms, in particular actinomycetes and fungi. Large numbers of cell (biomass) associated microbial fermentation products are routinely screened in a variety of assays after extraction using a sequence of organic solvents of increasing polarity, to produce several extracts from each organism. The method of preparation of these samples is critical to the efficiency and success of the screening process [3,4] and there is a constant search for new extraction techniques and sample separation procedures. Once samples containing potentially

* Corresponding author.

0021-9673/95/$09.50
SSDI 0021-9673(94)00817-5

useful substances are detected, the active components are isolated chromatographically.

It has been suggested that supercritical fluids can be used as an alternative to organic solvents for the extraction of natural products [5–8], improving the purification process by achieving a selective extraction [9,10] of the desired sample components through careful control of the extraction conditions. The parameters which can be used to vary the extraction conditions are temperature, pressure, modifier or mobile phase [11]. Supercritical-fluid extraction (SFE) can thus reduce the overall time required for the separation and characterisation of particular metabolites from within complex mixtures [12–14].

Reports in the literature on the SFE of microbial natural products from various samples are relatively sparse. Most studies have described the extraction of plant products such as taxanes [15], parthenolide [16] or the constituents of Chinese herbal medicines [17]. The extraction of lipids from lyophilised microalgae has also been investigated [18]. While studies have been performed on the extraction of compounds from microbial sources such as carboxylic acids [19], and ergosterol [20] from mushrooms and aflatoxin B_1 from infected corn [21], there have been very few reports concerning microbial fermentation samples. A detailed account of the extraction of cyclosporin from the fungus *Beauveria nivea* is one of the more thoroughly investigated examples [22]. The use of SFE to remove a sterol from dry mouldy bran produced by solid-state fermentation with *Gibberella fujikuroi*, without extracting any gibberellic acid, has also been described [23].

The aim of this study is to investigate the structural types of compounds that are extractable from microbial fermentation samples using SFE. A subsequent publication will examine the quantitative extraction of a range of microbial fermentation products. We report here a comparative study of the use of supercritical-fluid carbon dioxide, with and without methanol modification, with that of the organic solvents dichloromethane (DCM) and methanol for the extraction of known metabolites from biomass samples obtained by microbial fermentation. This paper will concentrate on the extraction of chaetoglobosin A, **1**; from *Penicillium expansum*; mycolutein, **2**; and luteoreticulin, **3**; from an unidentified actinomycete; 7,8-dihydro-7,8-epoxy-1-hydroxy-3-hydroxymethylxanthone-8-carboxylic acid methyl ester, **4**; and sydowinin B, **5**, from *Aspergillus fumigatus*; and elaiophylin, **6**, from a *Streptomyces sp.* The structures of these compounds are shown in Fig. 1. Chaetoglobosin A is a member of the cytochalasin group of fungal metabolites and has previously been reported as a product of *Chaetomium globosum* [24]. The γ-pyrone derivative mycolutein and its α-pyrone analogue luteoreticulin are *Streptomyces* sp. metabolites [25,26]. Compound **4** has recently been isolated by us [27] and also reported separately as an *Aspergillus* sp. metabolite [28]. Sydowinin B is co-produced with **4** [27,28]. Elaiophylin is a glycosylated macrodiolide reported to be produced by *Streptomyces* sp. [29]. The extracts obtained by SFE and with organic solvents were compared by reversed-phase high-performance liquid chromatography (HPLC) analysis.

2. Experimental

2.1. Chemicals

The carbon dioxide was industrial grade (99.98%) from British Oxygen Company (Brentford, UK) and methanol and dichloromethane were HPLC grade from FSA Scientific Apparatus (Loughborough, UK).

2.2. Instrumentation for supercritical-fluid extraction

Supercritical fluid extractions were performed using a Jasco SFE system, (Hachiojo City, Tokyo, Japan), consisting of two Model 980 pumps, one for delivery of carbon dioxide and the other for addition of modifier. The pump head used for carbon dioxide delivery was cooled with an ethylene glycol–water mixture at −15°C. Extraction temperature was controlled in a Jasco 860-CO oven and the extraction was monitored

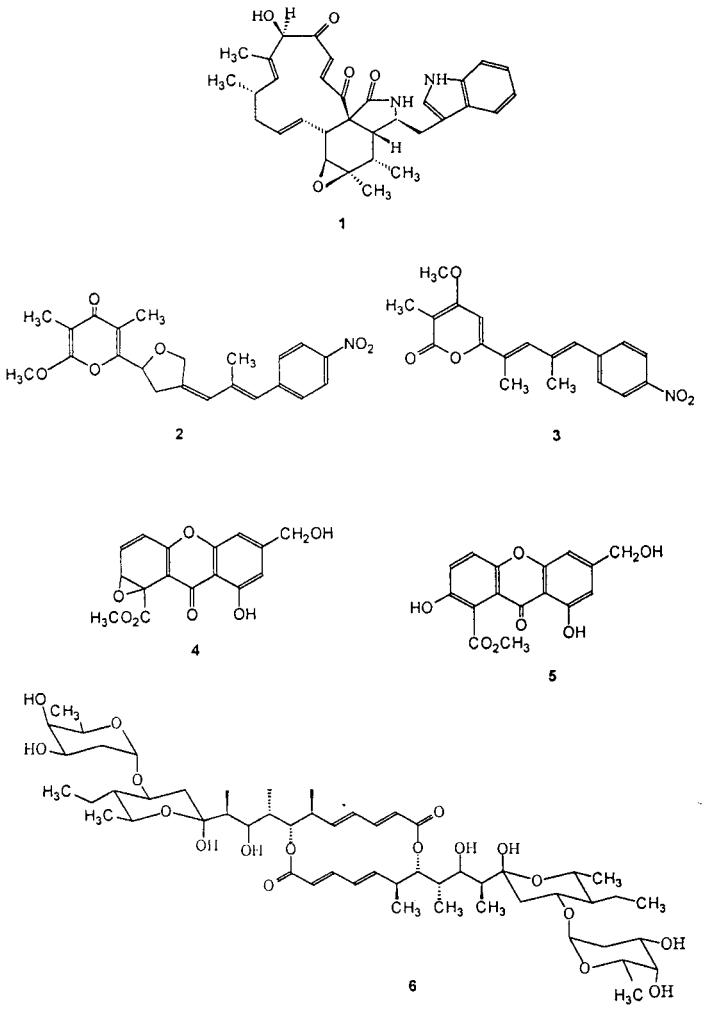

Fig. 1. The structures of: **1**, chaetoglobosin A, $C_{23}H_{36}N_2O_5$, molecular mass (M_r) 528; **2**, mycolutein, $C_{22}H_{23}NO_6$, M_r 397; **3** luteoreticulin, $C_{19}H_{19}NO_5$, M_r 341; **4**, 7,8-dihydro-7,8-epoxy-1-hydroxy-3-hydroxymethylxanthone-8-carboxylic acid methyl ester, $C_{16}H_{12}O_7$, M_r 316; **5**, sydowinin B, $C_{16}H_{12}O_7$, M_r 316; **6**, elaiophylin, $C_{54}H_{88}O_{18}$, M_r 1025.

on a Jasco UV975 variable-wavelength detector. Pressure regulation was performed using a Jasco 880-81 back pressure regulator. Data were captured using Borwin (Mettler-Toledo, Leicester, UK) software on an Elonex 486 computer, (Elonex London, UK).

2.3. High-performance liquid chromatography

HPLC separations were performed using a Waters (Watford, UK) system comprising a Waters 600E multisolvent delivery system, a Waters 996 photodiode array detector and a Waters 717 WISP sample injection unit. Peak detection and integration were obtained using a Waters Millennium 2010 Chromatography Manager. All chromatographic separations were performed in a temperature controlled room at 21°C.

The column used for the chromatographic analysis was a Waters Nova-Pak C_{18} Radial Pak cartridge (100 mm × 8 mm I.D.) contained in a

Waters radial compression module. All the extracts produced were analysed using the same linear water–acetonitrile gradient, increasing from 0 to 100% acetonitrile over a period of 15 min, after an initial delay of 2 min, at a flow-rate of 2 ml/min. Analysis of each sample was repeated, in some cases up to four times. The compounds of interest were identified by their retention times and comparison of their UV–visible spectra with those in Xenova's in-house spectral library on a Waters 996 photodiode array detector. Each compound had previously been isolated from its producing organism and its structure determined by a combination of spectroscopic techniques including mass spectrometry and nuclear magnetic resonance.

2.4. Microbial biomass sample production and preparation for extraction

The microbial biomass samples were harvested by centrifugation from fermentations produced by inoculation of each organism into 300 ml of an appropriate growth medium contained in a two litre conical flask and incubated with shaking at an appropriate temperature for seven days. The cells were then lyophilised and placed in sealed containers and stored at −20°C until required. Prior to extraction each sample was milled to a fine powder and separated into a minimum of five aliquots in the weight range 0.2–0.5 g, depending on the amount of biomass produced in the fermentation. The metabolites of interest were identified by their UV–visible spectra and HPLC retention times.

2.5. Solvent extraction

One of the pre-weighed aliquots was taken and sequentially extracted with dichloromethane (2×50 ml) and then methanol (2×50 ml). Extraction involved ultrasonication for 30 min. The extracts for each solvent were combined and filtered before being reduced to dryness on a rotary evaporator. The extracted material was redissolved in a known amount of methanol and transferred to a vial for HPLC analysis. All the extracts from one organism were dissolved in the same volume of the appropriate organic solvent.

2.6. Supercritical-fluid extraction procedure

An aliquot of the biomass sample was placed in a 3 ml extraction vessel which was placed into the SFE system. All the extractions were performed using a flow-rate of 2 ml/min at 40°C and 300 kg cm^{-2}.

Each sample was extracted for 30 min with carbon dioxide and then for 30 min with 20% (v/v) methanol-modified carbon dioxide. The unmodified and modified extracts were collected separately. In the case of the unmodified fraction the sample was dissolved in methanol. For the modified fraction, the methanol collected during the extraction was first removed under a stream of nitrogen. The dry extracts were redissolved in a known amount of methanol. Both fractions were then analysed by HPLC.

The SFE system was washed with methanol after each individual extraction and dried using carbon dioxide to ensure that no residue was left within the system which could carry over into subsequent extractions.

After each supercritical-fluid extraction the extraction vessel was switched out of line and removed from the system. The biomass was then removed from the vessel and sequentially extracted using the same procedure as detailed in the *Solvent extraction* section, to determine the quantities of the metabolites of interest not extracted using the SFE procedure. All supercritical fluid and residual extracts from one organism were dissolved in the same volume of methanol as the solvent extracts for that organism.

3. Results and discussion

The aim of the study was to establish a SFE protocol to fractionate and purify components from microbial fermentation biomass samples. The experiments detailed here are a qualitative comparison of organic solvent extraction versus SFE of microbial fermentation biomass samples.

Sequential solvent extraction using dichloro-

methane and methanol was first performed on a biomass sample from each fermentation. A fresh sample of the biomass was then taken and extracted using SFE. The SFE extraction conditions were not optimised for a particular sample but were chosen to maximise the extraction potential of the technique utilising a low extraction temperature with a high solvent density. A total time constraint of one hour was also placed upon the SFE extractions in order to facilitate a high number of extractions per day. Each sample was extracted sequentially with supercritical-fluid carbon dioxide and methanol-modified carbon dioxide. The residual biomass was then extracted with dichloromethane and methanol in order to give an indication of the completeness of the SFE extraction. Direct comparisons of the SFE and residual organic solvent extracts with the standard method of organic solvent extraction were made using reversed-phase HPLC. A detailed examination of six microbial metabolites is described. Each of these extractions was repeated at least once. The extracts obtained in each case were equivalent.

3.1. Chaetoglobosin A

The reversed-phase HPLC separations of the dichloromethane and methanol extracts of the biomass of *Penicillium expansum* are shown in Fig. 2. Most of the chaetoglobosin A was extracted by dichloromethane with a small amount of residual chaetoglobosin A observed in the methanol extract. Generally the methanol extract contained more polar components than the dichloromethane extract although there was no clear distinction. The chromatograms obtained by reversed-phase HPLC analysis of the SFE extracts of the biomass of this fungus are shown in Fig. 3. Chaetoglobosin A was found predominantly in the modified CO_2 extract (Fig. 3b) with small amounts present in the unmodified extract (Fig. 3a). Trace amounts of the compound remained after SFE and were observed in the dichloromethane extract (Fig. 3c). The subsequent methanol extract (Fig. 3d) contained very few metabolites. Chaetoglobosin A was extracted successfully using SFE with the majority of the metabolite of interest being extracted with methanol-modified carbon dioxide. A more selective, preparative extraction could perhaps

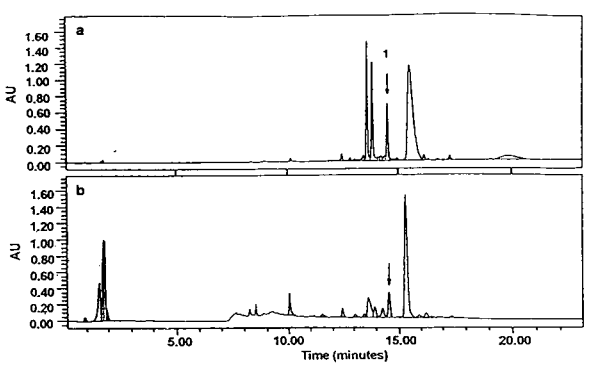

Fig. 2. Chromatograms of (a) dichloromethane and (b) methanol extracts of *Penicillium expansum*. The injection volumes were (a) 30 μl and (b) 50 μl.

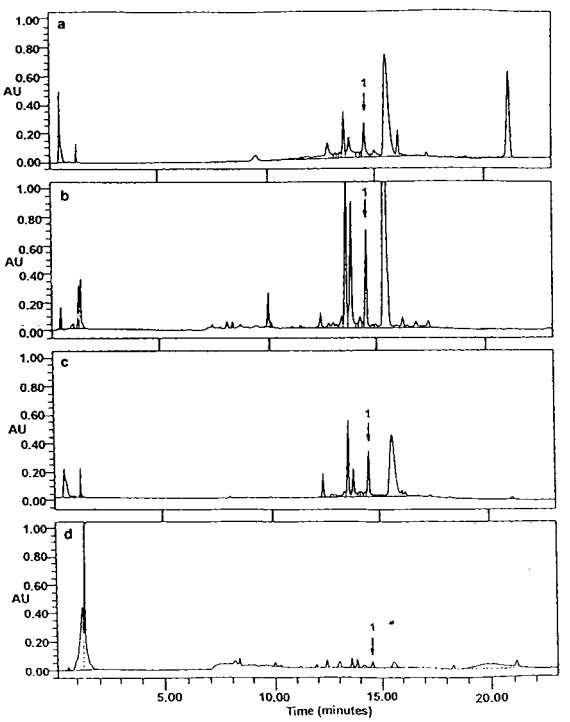

Fig. 3. Chromatograms of SFE and residual extracts of *Penicillium expansum*: (a) unmodified extract (180 μl); (b) methanol-modified extract (50 μl); (c) residual dichloromethane extract (180 μl) and (d) residual methanol extract (180 μl).

have been achieved by varying the concentration of methanol modifier and/or increasing the length of the extraction.

3.2. Mycolutein and luteoreticulin

The dichloromethane and supercritical-fluid extracts of the biomass of an unidentified actinomycete known to produce mycolutein and luteoreticulin were examined by HPLC (Fig. 4). The compounds were identified as being present in these extracts by their UV–visible spectra. Mycolutein is the more polar of the metabolites with a retention time of 15.2 min whilst luteoreticulin has a retention time of 15.8 min. On organic solvent extraction, these compounds were found predominantly in the dichloromethane extract with lesser amounts of both compounds also present in the methanol extract. On SFE, both compounds were extracted in small quantities with unmodified carbon dioxide (Fig. 4b) and in much larger amounts with methanol-modified carbon dioxide (Fig. 4c). Only trace amounts of both compounds were found in the organic solvent extracts of the biomass sample after SFE (Fig. 4d). Again successful extraction of the compounds of interest has been achieved by SFE in 1 h.

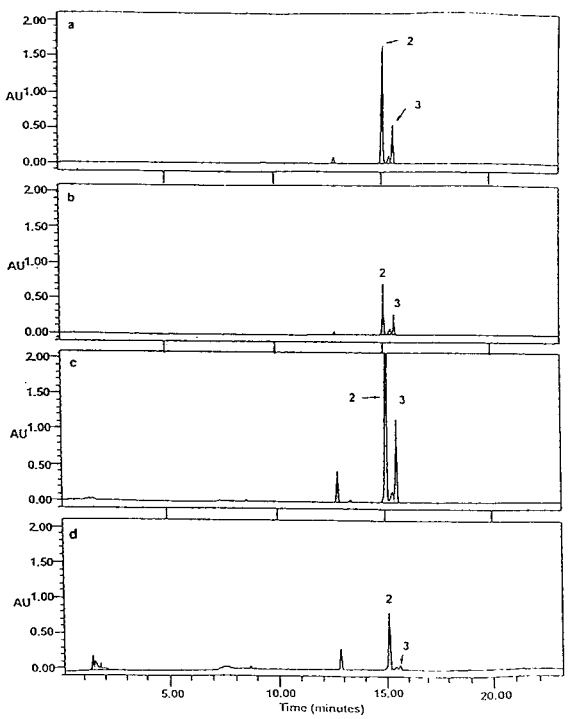

Fig. 4. Chromatograms of extracts containing mycolutein and luteoreticulin: (a) dichloromethane extract (5 μl); (b) unmodified CO_2 extract (5 μl); (c) methanol-modified extract (5 μl of sample diluted 1:9 with methanol) and (d) residual dichloromethane extract (5 μl).

3.3. 7,8-Dihydro-7,8-epoxy-1-hydroxy-3-hydroxymethylxanthone-8-carboxylic acid methyl ester and sydowinin B

The chromatograms obtained by reversed-phase HPLC analysis of the dichloromethane and supercritical-fluid extracts of the biomass of *Aspergillus fumigatus* are shown in Fig. 5. The chromatogram of the dichloromethane extract (Fig. 5a) shows the presence of **4** and sydowinin B (**5**) as peaks with retention times of 11.2 and 11.0 min, respectively. The methanol extract contained some sydowinin B but compound 4 was not present in detectable amounts.

The extract obtained with carbon dioxide alone (Fig. 5b) contained **4** and a small quantity of **5**. The methanol-modified extract (Fig. 5c) contained no detectable amount of **4** and large

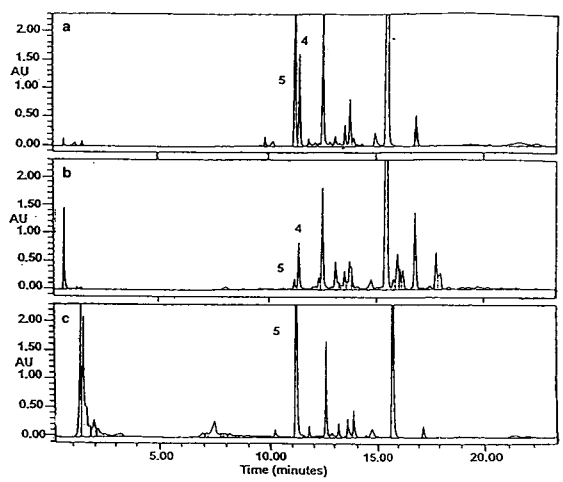

Fig. 5. Chromatograms of the dichloromethane and SFE extracts of *Aspergillus fumigatus*: (a) dichloromethane extract (50 μl); (b) unmodified CO_2 extract (80 μl) and (c) methanol-modified CO_2 extract (30 μl).

peak for **5**, now with a retention time of 11.1 min. The identification of the sydowinin B peak in these extracts was confirmed by HPLC analysis of the extracts after addition of a solution of a sample of sydowinin B, which had been previously purified and characterised spectroscopically, as an internal standard. The organic solvent extracts of the supercritical-fluid extracted biomass did not contain any detectable amounts of the two compounds of interest. The short retention times of **4** and sydowinin B indicate that these compounds are more hydrophilic than the other metabolites described so far. The results show that compound **4** was extracted well by dichloromethane and by unmodified supercritical-fluid carbon dioxide. The supercritical carbon dioxide extract, however, contained a relatively small quantity of sydowinin B compared to the dichloromethane extract. Extraction with supercritical carbon dioxide was thus more selective for compound **4** over sydowinin B than extraction with dichloromethane. Compound 4 was the metabolite of greater pharmaceutical interest in this fermentation [27,28] and these results demonstrate the utility of SFE as a selective preliminary fractionation step. Similar results have been obtained for the extraction of turmeric [30].

3.4. Elaiophylin

Elaiophylin was the largest compound studied with a molecular mass of 1025. The reversed-phase HPLC chromatograms of the organic solvent extracts of the biomass of a *Streptomyces sp.* known to produce elaiophylin are shown in Fig. 6. The chromatogram of the dichloromethane extract contained elaiophylin as its major component with a retention time of 13.8 min. Several other peaks with retention times in the range 13 to 18 min were also identified by UV–visible spectral matching as analogues of elaiophylin. The methanol extract of the biomass contained similar quantities of the elaiophylin components with the additional presence of many more polar, unrelated metabolites.

None of the elaiophylin components were extracted by SFE using carbon dioxide alone.

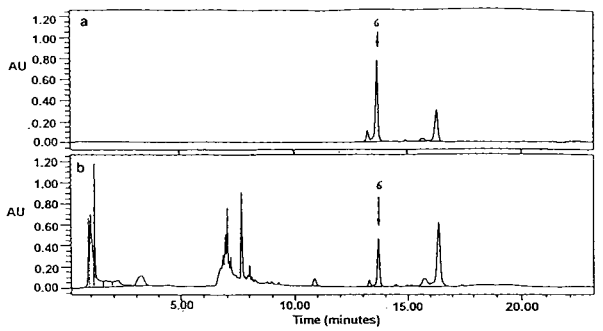

Fig. 6. Chromatograms of solvent extracts containing elaiophylins: (a) dichloromethane extract (50 μl) and (b) methanol extract (13 μl).

The chromatogram of the methanol-modified carbon dioxide extract (Fig. 7a) shows significant quantities of elaiophylin and its analogues. The chromatogram of the methanol extract of the biomass after SFE (Fig. 7b) contained lesser amounts of elaiophylin components. Successful but incomplete extraction of the elaiophylins was thus achieved using methanol-modified carbon dioxide.

4. Conclusions

These studies have demonstrated that microbial metabolites representing a range of structural classes and having molecular masses ranging

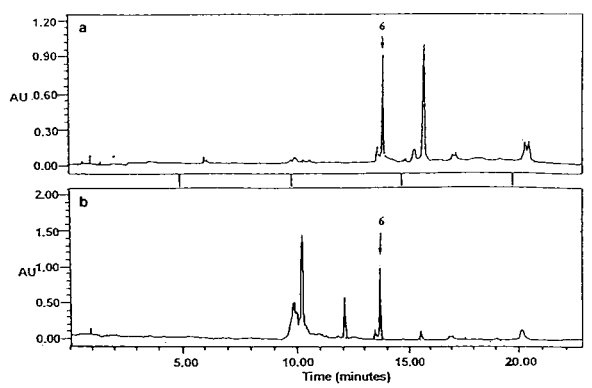

Fig. 7. Chromatograms of samples containing elaiophylins: (a) methanol-modified SFE extract (10 μl) and (b) residual methanol extract (50 μl).

from 316 to 1025 can be efficiently extracted from microbial fermentation biomass samples using supercritical-fluid carbon dioxide. In most cases supercritical-fluid carbon dioxide alone extracted slightly less of the compounds of interest than dichloromethane. Subsequent extraction with supercritical-fluid carbon dioxide modified by the addition of methanol achieved virtually complete extraction of most of these compounds. The efficiency of SFE is thus similar to that of organic solvent extraction for these metabolites. SFE has the advantage, however, that it has the potential to be controlled more finely to obtain a more selective, cleaner extract. The carbon dioxide and methanol modified extracts of **4** and sydowinin B from *Aspergillus fumigatus* also show how unmodified carbon dioxide can be used as a preliminary fractionation step with the more polar material being extracted only when methanol modifier is present. The compounds reported here are all of low to medium polarity and have good solubility in organic solvents.

Acknowledgements

SC would like to thank SERC and the Teaching Company Directorate for financial support. The authors would also like to thank the staff of the Ecology and Fermentation Departments at Xenova in particular Werner Katzer and Rewa Isherdass for the supply of the fermentation samples studied and Carol McNicholas, Mekonen Hagos and Neil Robinson of the Natural Products Chemistry Department who were involved in the initial identification of the compounds produced in these fermentations. Thanks also to Jackie Johnson for assistance with the chromatographic Figures and Debbie Armstrong for help in production of this manuscript.

References

[1] L.J. Nisbet and N. Porter, in S. Baumberg, I. Hunter and M. Rhodes (Editors), *Symp. Soc. Gen. Microbiol.*, 44 (1989) 309.
[2] S. Omura, *J. Ind. Microbiol.*, 10 (1992) 135.
[3] G.C. Yarborough, D.P. Taylor, R.T. Rowlands, M.S. Crawford and L.L. Lasure, *J. Antibiot.*, 46 (1993) 535.
[4] C.M.M. Franco and L.E.L. Coutinho, *Crit. Rev. Biotechnol.*, 11 (1991) 193.
[5] T.J. Bruno, C.A. Nieto de Castro, J.F.P. Hamel and A.M.F. Palavra, in J.F. Kennedy, J.M.S. Cabral (Editors), *Recovery Processes of Biological Materials*, Wiley, Chichester, 1993, p. 303.
[6] J.A. Hyatt, *J. Org. Chem.*, 49 (1984) 5097.
[7] M. Kane, J.R. Dean, S.M. Hitchen, C.J. Dowle and R.L. Tranter, *Anal. Proc.*, 29 (1992) 31.
[8] J.M. Wong and K.P. Johnston, *Biotechnol. Prog.*, 2 (1986) 29.
[9] K.P. Johnston, in M. Grayson and D. Eckroth (Editors), *Kirk - Othmer Concise Encyclopedia of Chemical Technology*, Wiley, New York, 1985.
[10] S.B. Hawthorne, *Anal. Chem.*, 62 (1990) 633A.
[11] M.E. McNally and J.R. Wheeler, *J. Chromatogr.*, 447 (1988) 53.
[12] M. Cygnarowicz-Provost, D.J. O'Brien, R.J. Maxwell and J.W. Hampson, *J. Supercrit. Fluids*, 5 (1992) 24.
[13] M.A. Schneiderman, A.K. Sharma and D.C. Locke, *J. Chromatogr.*, 409 (1987) 343.
[14] M.E. McNally and J.R. Wheeler, *J. Chromatogr.*, 410 (1987) 343.
[15] D.M. Heaton, K.D. Bartle, C.M. Rayner and A.A. Clifford, *J. High Resolut. Chromatogr.*, 16 (1993) 666.
[16] R.M. Smith and M.D. Burford, *J. Chromatogr.*, 627 (1992) 255.
[17] X. Ma, X. Yu, Z. Zheng and J. Mao, *Chromatographia*, 32 (1991) 40.
[18] J.T. Polak, M. Balaban, A. Peplow and A.J. Phlips, in *Supercritical Fluid Science Technology (ACS Symp. Ser.*, Vol. 406), American Chemical Society, Washington, DC, 1989, p. 449.
[19] M.I. Abdullah, J.C. Young and D.E. Games, *J. Agric. Food Chem.*, 42 (1994) 718.
[20] J.C. Young and D.E. Games, *J. Agric. Food Chem.*, 41 (1993) 577.
[21] M.I. Selim and M.H. Tsuei, *Am. Ind. Hyg. Assoc. J.*, 54 (1993) 135.
[22] D.W. Te Bokkel, *PhD Thesis*, Univ. West Ontario, 1990.
[23] P.K.R. Kumar, K.U. Sankar and B.K. Lonsane, *Chem. Eng. J.*, 46 (1991) B53.
[24] S. Sekita, K. Yoshihara and S. Natori, *Tetrahedron Lett.*, (1973) 2109.
[25] J.L. Schwatz, M. Tishler, B.H. Arison, H. Shafer and S. Omura, *J. Antibiot.*, 29 (1976) 236.
[26] E. Suzuki and S. Inoue, *J. Chem. Soc. Perkin Trans. I*, (1976) 404.
[27] *UK Patent*, Application No. 9312462.6 (1993).
[28] S. Nakanishi, K. Ando, I. Kawamoto and Y. Matsuda, *J. Antibiot.*, 46 (1993) 1775.
[29] H.P. Fiedler, W. Worner, H. Zahner, H.P. Kaiser, W. Keller-Schierlein and A. Muller, *J. Antibiot.*, 34 (1981) 1107.
[30] M.M. Sanagi, U.K. Ahmad and R.M. Smith, *J. Chromatogr. Sci.*, 31 (1993) 20.

ELSEVIER

Journal of Chromatography A, 697 (1995) 123–129

JOURNAL OF CHROMATOGRAPHY A

Solid-phase extraction of polycyclic aromatic hydrocarbons from soil samples

P.R. Kootstra[a,*], M.H.C. Straub[a], G.H. Stil[a], E.G. van der Velde[a], W. Hesselink[b], C.C.J. Land[b]

[a]*Laboratory of Organic-Analytical Chemistry, National Institute of Public Health and Environmental Protection (RIVM), P.O. Box 1, 3720 BA Bilthoven, Netherlands*

[b]*Research and Development Department, J.T. Baker B.V., P.O. Box 1, 7400 AA Deventer, Netherlands*

Abstract

A new solid-phase extraction (SPE) method was developed for the analysis of 16 polyaromatic hydrocarbons (PAHs) on the US Environmental Protection Agency priority list, in soil samples. Different types of SPE columns were tested and conditioning and elution steps were optimised. In the final procedure, soil samples are extracted with acetone and, after dilution with HPLC-grade water, loaded on a C_8 SPE column. After washing, all PAHs are eluted with tetrahydrofuran (THF). The final THF extract is analysed on an HPLC system for PAHs.

Recoveries of the volatile PAHs, naphthalene, acenaphthylene and acenaphthene were 80–90%. All other recoveries are comparable with standard liquid–liquid extraction (LLE) and range from 75 to 90%.

The method is compared with the conventional LLE method for different types of real soil samples of a Dutch monitoring programme. Results indicate that SPE is a good method for the sample preparation for the analysis of PAHs in soil samples. Compared with LLE, correlation coefficients are better than 0.9 with relative standard deviations for SPE between 0.8 and 9.1%. LLE standard deviations ranged from 1.1 to 15.1%.

1. Introduction

Polyaromatic hydrocarbons (PAHs) are widespread environmental contaminants and suspected to be carcinogenic [1,2]. The determination of PAHs in soil samples requires a good clean-up while aqueous samples need concentration because of low concentration levels. Today, sample preparation of soil is routinely done by liquid–liquid extraction (LLE) or Soxhlet extraction [3] in combination with column chromatography or solid-phase extraction (SPE) clean-up, as described by Kicinski [4]. In that paper a double-phase SPE method is described with an amino and a C_{18} SPE column. Unfortunately, this method also involves an evaporation step so only 11 of the 16 US Environmental Protection Agency (EPA) priority PAHs can be analysed. Supercritical fluid extraction (SFE) is also used for sample pretreatment [5–7]. SPE for the analysis of PAHs is mainly used for water samples, as described by the EPA (see [8]). In combination with an automated SPE system [9,10], good results can be obtained for both water or soil samples, but high investments are needed. Several laboratories in the Netherlands involved in environmental control and monitoring are routinely using this automated SPE

* Corresponding author.

0021-9673/95/$09.50
SSDI 0021-9673(94)01051-X

method. Summarised, column chromatography and evaporation steps in the clean-up procedures of the sample pretreatment might cause low recoveries for all PAHs and this will result in a loss of the volatile PAHs like naphthalene. In this paper, the development of a simple and cost-effective SPE method is described to replace the laborious and time-consuming LLE method used in our laboratory.

2. Experimental

2.1. Reagents and samples

Bakerbond SPE columns C_8 [200 mg 3 ml-LD (low displacement) 200 or 500 mg, 40 μm] and C_{18} (3 ml LD, 500 mg, 40 μm), HPLC-grade methanol, HPLC-grade acetonitrile and "Baker analysed" HPLC-grade water, Baker analysed tetrahydrofuran (THF), Baker analysed 2-propanol and a Bakerbond PAH 16 plus HPLC column (250 × 3 mm I.D.) were purchased from J.T. Baker (Deventer, Netherlands). LC-grade water was obtained by purifying demineralised water with a Milli-Q system (Millipore, Bedford, MA, USA). The EPA PAH standard reference material SRM 1647C of the National Institute of Standards and Technology (USA) was used (range 1–20 μg/ml for the different PAHs). All other reagents were of analytical grade and purchased from several local distributors.

Soil samples were collected for a Dutch monitoring programme on soil, to determine background levels of PAHs in the Netherlands. A selection was made of different types of soil (grass land, agriculture and orchard soil, including sand, peat and clay) and covered a wide concentration range of PAHs. For optimisation experiments, blank OECD soil [11,12] was used.

2.2. Apparatus

SPE columns were manually eluted on a Baker SPE-12 vacuum system. The high-pressure gradient LC system consisted of a Gynkotec (Germening, Germany) dual-piston low-pressure gradient LC pump. All LC solvents were degassed with a Separations GT-103 degasser (Separations, H.I. Ambacht, Netherlands). For detection of PAHs a Perkin-Elmer LS-4 fluorescence spectrometer was used in combination with an ABI 757 UV detector (Applied Biosystems, Foster City, CA, USA). Both detectors were wavelength programmed (described later). Data acquisition was performed on an HP 3365 Series II ChemStation equipped with an HP35900 A/D converter, running on an HP Vectra QS/20 personal computer (Hewlett-Packard, Rockville, USA).

2.3. Sample pretreatment SPE method

A 10-g amount of soil is placed into a 150-ml tube with 20 ml of acetone and the mixture is shaken for 30 min. After centrifugation at 1000 *g* for 5 min, exactly 10 ml of the acetone are pipetted in a 100-ml volumetric flask together with 5 ml of 2-propanol. The sample is brought to 100 ml with HPLC-grade water.

C_8 cartridges are conditioned with 1 × 3 ml of methanol, followed by two times 3 ml of water–2-propanol (9:1, v/v). The 100 ml sample solution are loaded onto the SPE column under vacuum. Then the column is washed with 3 ml of methanol–water (50:50, v/v). The PAHs are eluted with two times 1.5 ml of THF. The first 1.5 ml have to soak the cartridge for some minutes before eluting. After elution, the final THF extract is ready for injection. All flows through the cartridge are about 2 ml/min. For samples with fines in solution, after centrifugation, a filtration step is necessary.

2.4. Liquid–liquid extraction

A soil sample of 20 g is shaken with 25 ml of acetone for 10 min, 50 ml of light petroleum (b.p. 30–60°C) are added and the resulting solution is shaken for 20 min. After centrifugation (10 min at 1000 *g*), the extract is put into a separation funnel. The soil is extracted for a second time with 75 ml of acetone–light petroleum (1:3, v/v) and shaken for 30 min. The two extracts are combined and washed twice with 500 ml of Milli-Q water. The organic layer is sepa-

rated and dried over anhydrous sodium sulphate. The extract is reduced to 10 ml by evaporation (Kuderna Danish) and to 1 ml with a stream of nitrogen. The extract is purified over a 30-cm chromatography column, packed with 10 g of alumina. Light petroleum is used as eluent. The volume of this extract is reduced to 10 ml by evaporation (Kuderna Danish). This extract, with 50 μl 1-butanol as holder, is reduced at 50°C to dryness with a stream of nitrogen. The residue is dissolved in 1 ml of acetonitrile and the sample is ready for injection.

2.5. HPLC analysis

Mobile phase A consists of water and mobile phase B consists of acetonitrile. All flows are 0.5 ml/min. After equilibration, 5 min at acetonitrile–water (50:50, v/v), a linear gradient from 50 to 100% acetonitrile in 30 min is used for the elution of the PAHs. Both fluorescence and UV detection were used for all analyses. Fluorescence was wavelength programmed as indicated on the chromatogram. Details of the analytical conditions are described by Hesselink et al. [13].

3. Results and discussion

3.1. SPE method development

SPE method development was based on the selection of a SPE column type, followed by the optimisation of the conditioning and elution parameters. During method development the EPA mixture was in all cases 1:20 diluted in acetone–water. Primarily, the double phase SPE method according to Kicinski [4] was followed, although this method involves evaporation of organic solvent. The PAHs could not be eluted from the cartridge with only 6 ml of methanol or acetonitrile. Only a small percentage ($< 15\%$) of the three most polar compounds (naphthalene, acenaphthylene and acenaphthene) was recovered.

Secondly, Bakerbond C_8 cartridges (200 and 500 mg) were selected because of the good results with C_8 materials on automated SPE systems. Recoveries, with 3 ml of acetonitrile as eluent, were improved (20–40% for 200 mg C_8 and 30–50% for a 500-mg C_8 cartridge), but not sufficient. With 3 ml THF as eluent, recoveries increased to 60–70%. These partial recoveries can be explained by losses due to volatility, losses due to differences of binding capacity or losses due to interactions of PAHs with the wall of the cartridge.

According to Kicinski [4] and others, PAHs may interact with the wall. To prevent this kind of interaction, 2-propanol (10%, v/v) is frequently used in conditioning of the cartridge. With this modification, elution with 3 ml of THF lead to recoveries up to 90%.

To select the best SPE column type, C_8 or C_{18}, experiments were carried out to compare these two materials. In Table 1, results are summarised. From these results, it is clear that C_8 material (recoveries 73–90%) is better than C_{18} (recoveries 51–88%). Probably, the binding of the PAHs to the C_{18} material is too strong for complete elution with a small amount of solvent. Also the standard deviations on the C_8 cartridges are better. A typical HPLC chromatogram of a standard mixture using clean-up with SPE is shown in Fig. 1. With these conditions, the SPE method has been tested on real samples and the influence of the matrix has been investigated. No differences were found with four different batches of C_8 cartridges.

3.2. Comparison of the SPE method with LLE

First, a blank soil sample was shaken with acetone for 30 min. The extract was spiked with 200 μl EPA standard, resulting in PAH concentrations between 10–200 ng/ml, and treated as described in the Experimental section.

Table 2 shows the results of the experiments with the spiked extracts. It is clear that volatile PAHs like naphthalene, acenaphthylene and acenaphthene, fluorene and phenanthrene, have better recoveries using the SPE method. This is due to the evaporation steps in the LLE procedure. There is also a slight improvement in the recoveries of dibenz[*a*,*h*]anthracene, benzo[*ghi*]perylene and indeno[1,2,3-*cd*]pyrene. For

Table 1
Comparison of C_8 (500 mg) and C_{18} (500 mg) SPE columns ($n = 3$)

Compound	C_8		C_{18}	
	Recovery (%)	R.S.D. (%)	Recovery (%)	R.S.D. (%)
Naphthalene[a]	82	3.5	88	4.2
Acenaphthylene[a]	81	4.2	82	6.1
Acenaphthene	88	2.1	81	3.5
Fluorene	84	6.1	84	4.6
Phenanthrene	90	4.2	83	6.4
Anthracene	86	3.4	77	10.1
Fluoranthene	83	5.1	71	1.6
Pyrene	79	3.8	69	4.2
Benz[*a*]anthracene	80	2.1	68	3.8
Chrysene	80	4.2	75	4.9
Benzo[*b*]fluoranthene	82	5.0	64	3.8
Benzo[*k*]fluoranthene	77	4.9	66	6.0
Benzo[*a*]pyrene	73	4.2	51	5.8
Dibenz[*a*,*h*]anthracene	84	2.8	64	2.4
Benzo[*ghi*]perylene	87	6.9	65	5.2
Indeno[1,2,3-*cd*]pyrene	90	1.6	58	8.2

[a] UV detection.

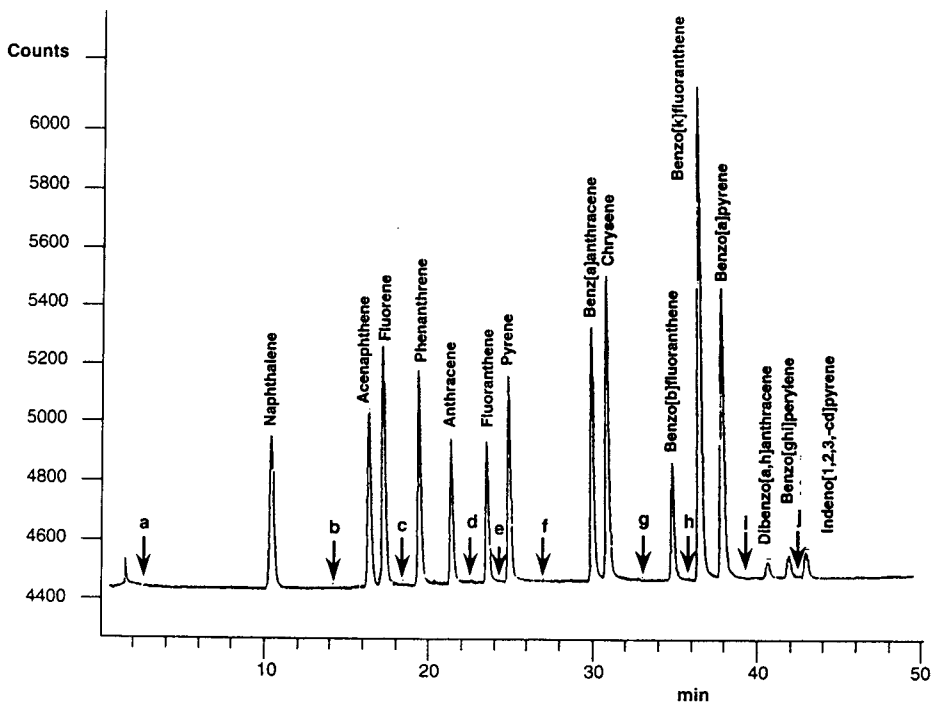

Fig. 1. Typical chromatogram of standard mixture with solid-phase extraction. Fluorescence detection with the following wavelength program (excitation/emission): a = 275 nm/325 nm; b = 253 nm/333 nm; c = 253 nm/373 nm; d = 285 nm/470 nm; e = 340 nm/395 nm; f = 270 nm/382 nm; g = 300 nm/440 nm; h = 300 nm/400 nm; i = 345 nm/420 nm; j = 300 nm/500 nm. Conditions: acetonitrile–water (50:50, v/v) to 100% acetonitrile in 30 min; Bakerbond PAH 16 plus column, 250 × 3 mm.

Table 2
Comparison between LLE and SPE of a spiked extract

Compound	LLE		SPE	
	Recovery (%)	R.S.D. (%)	Recovery (%)	R.S.D. (%)
Naphthalene[a]	70	–	102	0.9
Acenaphthylene[a]	–	–	89	3.1
Acenaphthene	76	–	89	2.1
Fluorene	81	1.1	91	0.8
Phenanthrene	86	3.0	96	2.0
Anthracene	88	3.6	92	4.0
Fluoranthene	95	3.2	97	2.6
Pyrene	99	12.2	87	2.4
Benz[*a*]anthracene	104	8.0	85	3.1
Chrysene	105	8.3	90	2.6
Benzo[*b*]fluoranthene	105	4.7	91	4.5
Benzo[*k*]fluoranthene	106	1.7	86	3.2
Benzo[*a*]pyrene	106	6.5	93	6.0
Dibenz[*a,h*]anthracene	77	6.6	89	5.7
Benzo[*ghi*]perylene	81	15.1	105	3.1
Indeno[1,2,3-*cd*]pyrene	93	1.4	91	9.1

For details see text ($n = 3$).
[a] UV detection.

all the other components, recoveries are comparable.

Secondly the method was compared with the LLE of different types of real soil samples of a Dutch monitoring programme on soil. A total of 12 samples was analysed with both methods. In Fig. 2, the correlation between SPE and LLE is shown for 12 soil samples. A good correlation

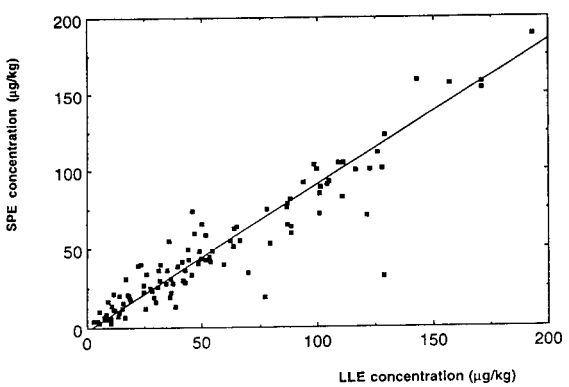

Fig. 2. Comparison of liquid–liquid extraction with solid-phase extraction of PAHs from 12 different type of soil samples.

($r^2 = 0.935$) exists between the two methods. However, above concentrations of 200 μg/kg, some deviation is possible. This may be due to a binding capacity of the C_8 material or due to the matrix. During the extraction procedure, some soil samples will clog the SPE column. Prefiltering over an empty SPE column or purified sand may be required. A typical HPLC chromatogram of a real soil sample using clean-up with SPE is shown in Fig. 3. Table 3 gives a summary of the characteristic differences between LLE and SPE as sample preparation method.

Preliminary results indicate that the method can be adapted to water samples. Further experiments are in progress.

4. Conclusions

A method for SPE of PAHs in field samples has been developed using a general stepwise approach for SPE. Starting with a standard mixture and several types of solid phases a suitable adsorbent was selected. Then the conditioning and elution parameters were optimised

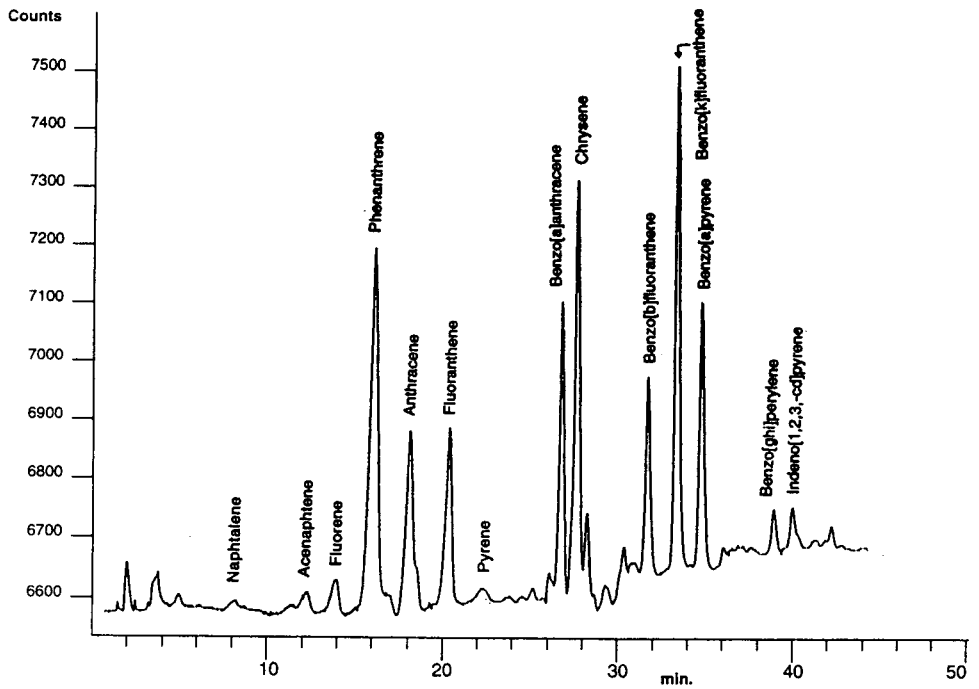

Fig. 3. Typical HPLC (fluorescence) chromatogram of peaty soil. SPE sample preparation as described in text. Conditions as in Fig. 1.

and finally these conditions were used to analyse real soil samples. Comparable results were found for PAH concentrations using SPE or LLE as sample preparation method. The SPE method showed improved recoveries for the volatile PAHs as expected, due to the omission of an evaporation step.

Table 3
Comparison between the characteristics of LLE and SPE

Characteristic	LLE	SPE
Sample preparation time	8 h	2.5 h
Amount of organic solvent	220 ml	35 ml
Recovery (all PAHs)	Good	Good
Recovery (volatile PAHs)	Poor	Good
Automation potential	No	Yes
Purity of extract	Good	Very good

The method is easy to use and has a good reproducibility.

References

[1] R.G. Harvey (Editor), *Polycyclic Hydrocarbons and Carcinogenesis*, American Chemical Society, Washington, DC, 1985.
[2] A. Bjørseth (Editor), *Handbook of Polycyclic Aromatic Hydrocarbons*, Vol. 1, Marcel Dekker, New York, 1983.
[3] S.R. Wild, S.P. McGrath and K.C. Jones, *Chemosphere*, 20 (1990) 703–716.
[4] H.G. Kicinski, *Z. Wasser-Abwasser-Forsch.*, 25 (1992) 289–298.
[5] A. Gratzfeld-Hüsgen, R. Schuster and H. Schulenberg-Schell, *Application Note 12-5091-726E*, Hewlett-Packard, Waldbronn, 1993.
[6] J. Dankers, M. Groenenboom, L.H.A. Scholtis and C. van der Heiden, *J. Chromatogr.*, 641 (1993) 357–362.
[7] T. Paschke, S.B. Hawthorne, D.J. Miller and B. Wenclawiak, *J, Chromatogr.*, 609 (1992) 333–340.

[8] S.A. Wise, L.C. Sander and W.E. May, *J. Chromatogr.*, 642 (1993) 329–349.
[9] G.S.J. Haak and M. Ham, *Int. Lab. News*, July (1994) 14.
[10] C. Klok, *Application Note No. 31*, Separations Analytical Instruments, H.I. Ambacht, 1992.
[11] *Earthworm Acute Toxicity Test; OECD Guideline for Testing Chemicals No. 207*, Organisation for Economic Cooperation and Development, Paris, 4 April 1984.
[12] *Toxicity for Earthworms —Artificial Soil Test; EEC Directive 79/831, Annex V, Part C: Methods for the Determination of Ecotoxicity-Level*, European Economic Community, Brussels, 14 June 1985.
[13] W. Hesselink, R.H.N.A. Schiffer and P.R. Kootstra, *J. Chromatogr. A*, 697 (1995) 165.

ELSEVIER

Journal of Chromatography A, 697 (1995) 131–136

JOURNAL OF CHROMATOGRAPHY A

Development and optimisation of an immunoaffinity-based solid-phase extraction for chlortoluron

S.J. Shahtaheri, M.F. Katmeh, P. Kwasowski, D. Stevenson*

Robens Institute, University of Surrey, Guildford, Surrey GU2 5XH, UK

Abstract

The determination of trace organics such as pesticides in biological and environmental samples require rapid, easy-to-use, reliable sample preparation procedures. Solid-phase extraction using silica or bonded silicas has proven useful for broad-range screening. We have used antisera to chlortoluron immobilised onto silica as a "tailor-made" solid-phase extraction system. The chlortoluron can be selectively retained and eluted using a simple phosphate buffered saline/ethanol mixture. Preliminary studies have demonstrated that the immuno column has a high volume breakthrough (at least 1 l of water) and can retain up to 500 ng of chlortoluron. Quantitative recovery from tap water, river water, drinking water, plasma and urine is achieved along with an HPLC trace free from co-eluting compounds at the chlortoluron retention time.

1. Introduction

The measurement of trace levels of organic chemicals such as drugs, metabolites, pesticides and other pollutants in biological and environmental samples is a challenging and exacting task. Growing concern about the risk to human health posed by toxic chemicals has led to an increase in the need for simple, reliable analytical methods. Although there are now many elegant separations on highly sophisticated instrumentation the rate-limiting step (and that most prone to errors) in most assays is during sample extraction and trace enrichment [1].

Many analytical methods use liquid–liquid extraction or solid-phase extraction techniques to perform sample clean-up [2]. Liquid–liquid methods cannot easily be automated and use large volumes of solvents that present environmental concerns. Solid-phase extraction methods using silica or bonded silicas have proven useful in simplifying sample preparation. Trace enrichment and clean-up can be achieved in a single step and only low volumes of solvents are used.

The use of commercially available low cost vacuum manifolds allows many samples to be processed simultaneously. Furthermore, complete automation of procedures based on solid-phase extraction is now possible using commercially available instrumentation. A wide range of phases from many suppliers based on silicas are available including reversed-phase, normal-phase, ion-exchange and mixed-mode phases. Although useful for broad-range screening, these phases do not actually have good selectivity and there is continued interest in the development of alternative sample preparation procedures. Recently there has been growing interest in the use of antibody mediated extractions since in principle highly selective analyte–antibody interactions

* Corresponding author.

0021-9673/95/$09.50
SSDI 0021-9673(94)01088-9

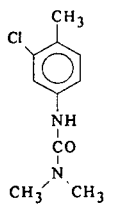

Fig. 1. Structure of chlortoluron.

are possible [3–7]. Immunoassays have long been used in clinical chemistry/biochemistry laboratories but more recently these techniques have become popular for monitoring toxic chemicals (such as pesticides) in the environment [8]. The antisera developed for such immuno methods provides the key reagent for antibody columns (also termed immunoaffinity columns).

This paper describes how we have successfully used antibodies to the herbicide chlortoluron (see Fig. 1) to develop a simple solid-phase extraction procedure for chlortoluron. The aims of the work were to develop a simple protocol for the retention and elution (in a small volume) of chlortoluron from an immunoaffinity column and to carry out a preliminary evaluation of the capability with respect to enrichment and clean-up.

2. Experimental

2.1. Chemicals

Chlortoluron reference standard was obtained from Greyhound, Birkenhead, UK. Methanol, ethanol, hydrochloric acid, disodium hydrogenorthophosphate, potassium dihydrogenorthophosphate, potassium chloride and sodium chloride were analytical-reagent grade from BDH–Merck, Poole, UK. Phosphate-buffered saline (PBS) pH 7.4 was prepared by adding 8.0 g sodium chloride, 0.2 g of potassium chloride, 0.2 g of potassium dihydrogenorthophosphate and 2.9 g disodium hydrogenorthophosphate to 1 l of distilled water.

2.2. Chromatographic conditions

The pump was a Beckman 110B (Beckman Instruments, High Wycombe, UK), operated at 1.0 ml/min. Detection was by UV at 244 nm using a Pye LC–UV spectrophotometer (Unicam, Cambridge, UK). The mobile phase consisted of methanol–water (70:30). Injection volumes of up to 100 μl were delivered using a WISP 710A (Waters Associates, Northwich, UK). The column was a Bondaclone 10 C_{18} (Phenomenex, Macclesfield, UK).

2.3. Immuno extraction

The immuno-extraction column was prepared by adding chlortoluron antisera to aldehyde activated porous silica (Clifmar Associates, Guildford, UK). The chlortoluron antisera had been raised in sheep and was used unpurified. Unbound aldehyde groups were deactivated using glycine. Columns contained approx. 1 g of solid phase and approx. 200 μl of antisera. The basic protocol for the immuno extraction was: (a) wash the column with 0.3% hydrochloric acid; (b) wash the column with 10 ml phosphate-buffered saline (PBS) at pH 7.4; (c) load the sample typically 1 ml (this fraction is labelled breakthrough in tables); (d) wash with 5×1 ml PBS (these fractions are labelled W in tables); (e) elute analyte with 2×1 ml PBS–ethanol (50:50) (these fractions are labelled E in tables).

3. Results and discussion

Initial results showed that chlortoluron was retained by the antibody column using a simple extraction procedure shown earlier. When applying 1 ml of 1 μg/ml chlortoluron to the column quantitative elution of analyte was achieved in five fractions of PBS, pH 8–ethanol (50:50), it was not possible to elute in one 1-ml fraction. It should be noted that recovery values are only approximate as no internal standard is used to allow for small volume changes.

Experiments using PBS–ethanol at different pH values have shown that pH could be used to

Table 1
Recovery of chlortoluron (1 ml of 1 μg/ml) in immuno-column fractions using different pH values to elute

Eluent pH	Fractions												Total
	BT	W1	W2	W3	W4	W5	E1	E2	E3	E4	E5	E6	
2	0	0	0	5	16	7	0	74	0	0	0	0	102
3	0	0	0	0	0	0	0	120	0	0	0	0	120
4	0	0	0	0	0	0	0	62	18	0	0	0	80
5	0	0	0	0	0	0	0	25	23	9	5	0	62
6	0	0	0	0	0	0	0	83	21	7	2	0	113
8	0	0	0	0	0	0	0	2	53	22	12	7	96

optimise the elution of chlortoluron (see Table 1) from the columns. At low pH it was possible to elute the chlortoluron in one × 1 ml fraction. Further experiments using 1 ml of chlortoluron over the range 0.1–0.5 μg/ml gave quantitative recovery in one 1-ml fraction even after retaining the chlortoluron through up to five wash steps. This suggested that the column has a capacity to retain up to 500 ng of chlortoluron. Optimum elution was achieved using 1 ml of pH 2 PBS–ethanol (50:50).

The effect of sample pH on chlortoluron retention in the immuno column was evaluated by monitoring the pH of all samples (distilled water, tap water, river water, plasma and urine). The pH varied over the range 5.7 to 8.3 and had no effect on the retention and elution profile of chlortoluron.

In order to evaluate the water volume breakthrough of the immuno-extraction cartridge 1-ml samples of 0.5 μg/ml chlortoluron were diluted into different volumes and added to the column. The results are shown in Table 2 demonstrating that up to at least 1000 ml of sample could be applied, without loss of recovery. In all cases the chlortoluron eluted in one 1-ml fraction. This allowed accurate measurement as low as at least 0.5 μg/l, though this is dependent on the detection system rather that the extraction procedure. A limit of detection as low as 0.1 μg/l was possible using 3 × baseline noise. It clearly demonstrated that the breakthrough of chlortoluron was due to the capacity of the column for chlortoluron, not due to the volume of water it was contained in. Trace enrichment from a large volume is thus possible. These experiments have shown that the columns we describe could retain up to 500 ng of chlortoluron. This is clearly very compatible with current chromatography detection systems.

In order to demonstrate that the retention was due to the immobilised antibody the elution profile of the antibody column was compared with that of activated silica and an immobilised non-immune antibody from the same sheep before it was injected with chlortoluron. The results are shown in Table 3 and clearly demonstrate that the chlortoluron is hardly retained by the activated silica but is retained and then selectively eluted by the chlortoluron antibody column.

Preliminary experiments to look at the effect of different matrices (drinking water, tap water, river water, urine and plasma) have also been

Table 2
Recovery of chlortoluron using different sample volumes (500 μg applied)

Volume (ml)	1	10	20	30	40	50	70	100	150	300	500	1000
Recovery (%)	116	127	105	102	89	105	115	118	102	89	103	119

Table 3
Recovery of chlortoluron from activated silica, a non-immune antibody column and a chlortoluron antibody column

Column	Fractions													
	BT	W1	W2	W3	W4	W5	W6	W7	W8	W9	W10	E1	E2	E3
Activated silica	0	0	0	5	26	29	18	9	5	3	2	0	0	0
Non-immune antibody	0	0	0	2	23	29	22	11	7	3	1	0	0	0
Chlortoluron antibody	0	0	0	0	0	0	0	0	0	0	0	0	91	0

carried out. The results showed that quantitative recovery (>91%) in one fraction was obtained from all matrices. The highly efficient clean-up that was obtained for all matrices is shown in Fig. 2 for urine and plasma. Very large interfering peaks eluted in wash fraction 1, getting less with fraction 2 and 3. By wash fraction 4 and 5 and the elution fractions no interference was seen at the chlortoluron retention time. For plasma the E2 fraction shows that unspiked plasma contained no interfering peak at the chlortoluron retention time. It should also be noted that all the experiments described in this paper have been carried out on the same column after appropriate regeneration, demonstrating the reusability of the immuno columns.

The reproducibility that might be achieved using this immuno-extraction procedure was evaluated by analysis of six 1-ml samples of distilled water spiked with 0.5 μg/ml. These results showed a within-day relative standard deviation (R.S.D.) of $\pm$ 6.9%. The results in Table 2 using the same mass of chlortoluron but in different volumes of water gave a mean recovery of 108% with an R.S.D. of $\pm$ 10.9%.

The work described here demonstrates the feasibility of using antibody–antigen interactions for trace enrichment and clean-up prior to chromatography. Although primarily aimed at isolation from the matrix antibodies can show cross-reactivity to structurally similar compounds, though in many cases they are separated by the chromatographic technique. Preliminary experiments with the chlortoluron immunoaffinity column showed that there was some cross-reactivity with linuron, chlorbromuron and chloroxuron but very little with isoproturon and methoxuron. Cross-reactivity could however be seen as an advantage when there was the need to isolate a class of compounds (such as phenylureas) which could then be separated by instrumental chromatography. Further experiments to investigate this interesting possibility are being carried out.

4. Conclusions

This work demonstrates that antibodies to chlortoluron can be successfully immobilised onto activated silica, without loss of immune response. The immuno columns can selectively extract chlortoluron from a variety of matrices, and give a clean sample for HPLC using a simple protocol involving PBS and ethanol at different pH values. Using water as an example it is possible to preconcentrate chlortoluron from up to 1000 ml of sample. The capacity of immunoaffinity columns for mass of chlortoluron is limited (approx. 500 ng) but this is compatible with chromatographic detection limits, and it is low values that potentially cause problems not such high concentrations. As the procedures are based on solid-phase extraction, both on and off-line automation should be possible. Immunobased solid-phase extraction offers a new sample preparation approach using "tailor-made" columns either alone or in combination with other clean-up steps. Now a very simple protocol has been developed this ought to be evaluated for a

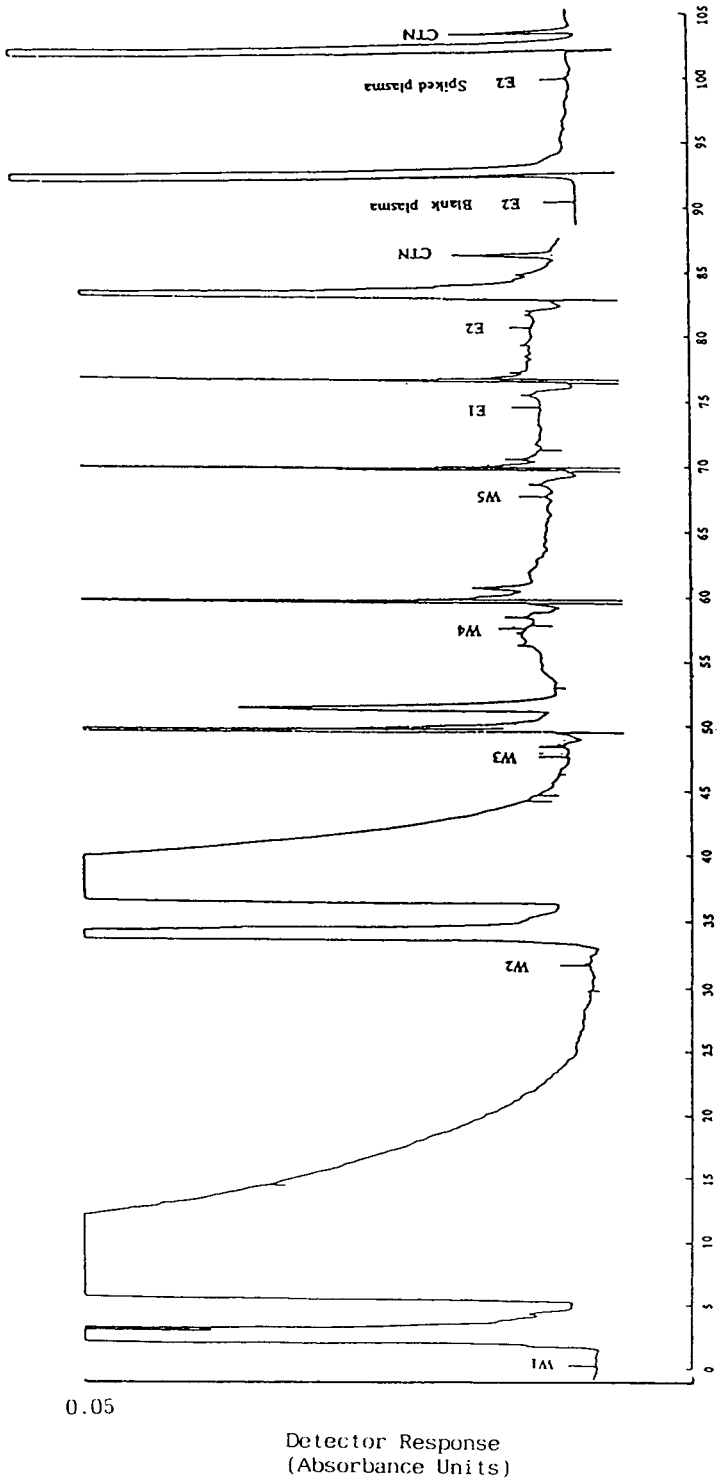

Fig. 2. Chlortoluron (CTN) immuno extraction from urine and plasma. HPLC conditions as in Experimental section.

wider range of analytes for which antisera is available, e.g. drugs and other pesticides.

Acknowledgements

This programme of work has received financial support from the Health and Safety Executive (to support M.F.K.) and the Iranian Ministry of Health (to support S.J.S.).

References

[1] U.A.Th. Brinkman, *J. Chromatogr. A*, 665 (1994) 217.
[2] D. Barceló, *Analyst*, 116 (1991) 681.
[3] C. van de Water and N. Haagsma, *J. Chromatogr.*, 411 (1987) 415.
[4] A. Farjam, A.E. Bragman, H. Lingeman and U.A.Th. Brinkman, *Analyst*, 116 (1991) 891.
[5] A. Farjam, A.E. Bragman, A. Soldaat, P. Timmerman, H. Lingeman, G.J. de Jong, R.W. Frei and U.A.Th. Brinkman, *Chromatographia*, 31 (1991) 469.
[6] M. Sharman, S. MacDonald and J. Gilbert, *J. Chromatogr.*, 603 (1992) 285.
[7] G.S. Rule, A.V. Mordehai and J. Henion, *Anal. Chem.*, 66 (1994) 230.
[8] G.W. Aherne, *Anal. Proc.*, 24 (1987) 140.

ELSEVIER

Journal of Chromatography A, 697 (1995) 137–143

JOURNAL OF CHROMATOGRAPHY A

Trace enrichment by solid-phase extraction for the analysis of heavy metals in water

V. Leepipatpiboon

Department of Chemistry, Faculty of Science, Chulalongkorn University, Bangkok 10330, Thailand

Abstract

A combination of chelating heavy metals such as Ag(I), Cd(II), Cu(II), Ni(II) and Pb(II) with 4-(2-pyridylazo)resorcinol (PAR) and extraction on C_{18} cartridges prior to atomic absorption spectrometry was developed for trace metal analysis. Various factors, e.g., pH, PAR concentration, amount of C_{18} and flow-rate, were investigated in order to optimize the enrichment procedure. Water samples with an enrichment factor of 20 were analyzed. Results obtained gave a precision of 1–5%, and a recovery of 81–100%. The errors were in the range of 0.5–0.7% at the μg/l level.

1. Introduction

The determination of trace amounts of metals in water requires inevitably a concentration step prior to atomic absorption spectrometric (AAS) analysis. Conventional solvent extraction is mostly used for preconcentration, but it has many practical and technical limitations. Solid-phase extraction (SPE) has gained increased attention as a replacement for solvent extraction. The principles and methods of SPE have previously been published [1–6]. This technique is widely used [7,8]. Even though C_{18} SPE cartridges have been used previously for the separation of metal chelates, the application to the preconcentration of trace metals from aqueous solution is new. The complexation of the metal ions with 8-hydroxyquinoline followed by adsorption on C_{18} chemically bonded silica gel has been reported [9].

In the present paper, SPE has been developed to analyze trace amounts of Ag^+, Cd^{2+}, Cu^{2+}, Ni^{2+}, and Pb^{2+} in water. These metals formed metal–PAR chelates with 4-(2-pyridylazo)resorcinol (PAR) and their chelates can be trapped on a C_{18} SPE cartridge and then eluted with a suitable solvent. In this study, nitric acid is used as an eluent. The aim of these experiments is to study the effect of variables on the recovery of heavy metals. Several experimental variables have been evaluated: the eluent volume and concentration, the pH of the extracted solution, the flow-rate for the retention and elution steps, the concentration of PAR, and the sorbent mass. To achieve these objectives, Cd–PAR and Cu–PAR chelates were employed as models for this study. Suitable conditions were used for the determination of Ag^+, Ni^{2+}, and Pb^{2+} as single components in water and then to determine the five metals as mixtures in water. In addition, the accuracy and precision of this technique were also studied.

0021-9673/95/$09.50
SSDI 0021-9673(94)00930-9

2. Experimental

2.1. Reagents

For flash chromatography octadecyl bulk packing of 40 μm average particle diameter (J.T. Baker, Phillipsburg, NJ, USA) was used without further purification. 4-(2-Pyridylazo)resorcinol (PAR) was purchased as the monosodium monohydrate salt (Merck, Darmstadt, Germany). Standard solutions for AAS (BDH) with concentrations of 1000 mg/l were used for the preparation of the working standard solutions and doubly distilled water was used throughout. All reagents were of analytical reagent grade.

The concentrations of the standard solutions of Cd and Cu used as models for this study were 0.05 mg/l and 0.02 mg/l, respectively.

2.2. Apparatus

The AAS measurements were carried out on a Shimadzu AA-670 (air–acetylene flame) instrument. Hollow-cathode lamps were employed as radiation sources. The operational conditions were those recommended by the manufacturer. A Baker-10 extraction system was used.

2.3. Procedure

Each C_{18} SPE cartridge for the evaluation of the variables was prepared by using a 4-ml polypropylene column. The steps for packing each cartridge were as follows: (1) put one piece of 10-mm glass fibre prefilter in a column, (2) pour 500 mg of octadecyl bulk packing into the cartridge, and (3) put another piece of 10-mm glass fibre prefilter over the packing.

Each cartridge must be activated before use by passing 3.0 ml of absolute methanol through the C_{18} SPE cartridge. To push the methanol downward, a vacuum pump must be used at 1333.22 N/m^2 pressure for ca. 30 s and then the pressure is decreased to 666.61 N/m^2. After the absolute methanol reaches ca. 2 mm above the top of the packing, 2.0 ml deionized water is passed through the column.

A C_{18} SPE cartridge was equipped with a Baker-10 extraction system. A 100-ml metal–PAR chelate solution was passed through the cartridge that had been activated before use. A vacuum pump was used to draw the solution down. For elution, dilute nitric acid was passed through the cartridge. The recovery of each metal under various conditions of sample preparation was calculated by comparing the sample absorbance of each metal with the standard solution. The results of the effect on the recovery are based on duplicate determinations.

The procedure for the precision study for each metal as a single component in water has been prepared by using the conditions that are summarized in Table 1. A series of solutions of each metal has been prepared for six determinations.

For the precision study of the five metals as mixtures in water the same conditions as for the study of the single components were used. Ten determinations were made for this study.

For the study of the accuracy a synthetic unknown mixture solution was used. Triplicate determinations were performed under the conditions mentioned earlier. The percent errors of each determination have been calculated on the assumption of 100% recovery of the metals (i.e., a concentration factor of 20) and has also been calculated using the recovery factor of each metal from the results of the precision study of the mixture components.

3. Results and discussion

3.1. The effect of nitric acid concentration

The results of the effect of nitric acid concentration on the recovery are presented in Table 2. The results show that the most suitable concentration of nitric acid is 1.0 *M* for both metals. Therefore, this concentration is chosen as the optimal concentration for the study of each metal.

3.2. The effect of nitric acid volume

The results of the effect of the nitric acid volume on the recovery are presented in Table 3. The results show that the minimal volume of 1.0 *M* nitric acid employed in this study to obtain the

Table 1
Conditions for the determination of cadmium and copper as Cd–PAR and Cu–PAR chelates

Conditions	Cd	Cu	Conditions selected for both metals
HNO_3 conc.	1.0 *M*	1.0 *M*	1.0 *M*
HNO_3 volume	3.0 ml	4.0 ml	4.0 ml
pH of extraction	Increases in the basic solution	Decreases in the basic solution	7–8
Flow-rate in the retention step	3.0 ml/min	6.0 ml/min	6.0 ml/min
Flow-rate in the retention step	0.1 ml/min	0.5 ml/min	6.0 ml/min
Excess of PAR concentration over metal	50 fold	20 fold	50 fold
Sorbent mass	50 mg	400 mg	500 mg

maximal percentage recovery is 4.0 ml for cadmium and 3.0 ml for copper. Hence, 4.0 ml of nitric acid is chosen as the optimal volume for the study of each metal.

3.3. The effect of pH

The results of the effect of the pH of the extracted solution on the recovery are presented in Table 4. The results show that the recovery of cadmium increases in the basic solution (above pH 8.0) while the recovery of copper decreases in the basic solution. The pH of the extracted solution should be ca. 7.0–8.0 to prevent the formation and precipitation of metal–hydroxide complexes in basic solution, which causes loss of analyte species.

3.4. The effect of flow-rate in the retention step

The results of the effect of the flow-rate in the retention step on the recovery are presented in Table 5. The results show that the optimal flow-rate obtained is 3.0 ml/min for cadmium and 6.0 ml/min for copper. To reduce the analysis times,

Table 2
Effect of nitric acid concentration on the recovery by using Cd–PAR and Cu–PAR chelates as models

Element	Conc. of HNO_3 (*M*)	Recovery (%)
Cd	0.1	63.80
	0.5	73.50
	1.0	75.80
	2.0	62.20
	4.0	60.30
Cu	0.1	94.50
	0.5	101.50
	1.0	102.75
	2.0	102.50
	4.0	101.10

Table 3
Effect of volume of nitric acid solution on the recovery by using Cd–PAR and Cu-PAR chelates as models

Element	Volume of 1.0 *M* HNO_3 (ml)	Recovery (%)
Cd	1.0	68.10
	2.0	70.30
	3.0	71.60
	4.0	74.20
	5.0	73.80
Cu	1.0	87.25
	2.0	96.75
	3.0	99.75
	4.0	99.75
	5.0	99.75

Table 4
Effect of pH of extracted solution on the recovery by using Cd–PAR and Cu–PAR chelates as models

Element	pH of extracted solution	Recovery (%)
Cd	5.0	69.60
	6.0	74.70
	7.0	73.90
	8.0	81.20
	9.0	85.20
	10.0	87.70
Cu	1.0	101.00
	2.0	102.75
	3.0	100.51
	4.0	101.00
	5.0	94.75
	10.0	51.00

the fastest flow-rate is the best choice to select. By using the instrument in this laboratory, a flow-rate of 6.0 ml/min is chosen for the study of each metal; higher flow-rates cannot be used due to the overload of the motor.

3.5. The effect of flow-rate in the elution step

The results of the effect of the flow-rate in the elution step on the recovery are presented in Table 6. The results show that the optimal flow-rate in this study is 0.1 ml/min for cadmium and 0.5 ml/min for copper. When the flow-rate changes to higher values, the recovery does not change significantly. In order to reduce the analysis times, a flow-rate of 6.0 ml/min is chosen for the study of each metal.

Table 5
Effect of flow-rate in the retention step on the recovery by using Cd–PAR and Cu–PAR chelates as models

Element	Flow-rate in retention step (ml/min)	Recovery (%)
Cd	2.0	78.60
	3.0	80.40
	4.0	76.20
	6.0	78.70
	8.0	78.60
	10.0	78.00
Cu	2.0	97.75
	3.0	98.25
	4.0	99.00
	6.0	100.50
	8.0	99.00
	10.0	99.25

Table 6
Effect of flow-rate in the elution step on the recovery by using Cd–PAR and Cu–PAR chelates as models

Element	Flow-rate in elution step (ml/min)	Recovery (%)
Cd	0.1	80.90
	0.5	78.00
	1.5	80.50
	3.0	76.00
	6.0	74.50
	9.0	73.10
Cu	0.1	94.25
	0.5	96.50
	1.5	91.25
	3.0	93.00
	6.0	92.25
	9.0	90.25

3.6. The effect of PAR concentration

The results of the effect of the PAR concentration on the recovery are presented in Table 7. The results show that the concentration of PAR at 50-fold excess over concentration of cadmium and 20-fold excess over concentration of copper are preferred. For the analysis of these metals as mixtures in water, the large excess of PAR concentration (over 50-fold) is recommended.

3.7. The effect of sorbent mass

The results of the effect of sorbent mass on the recovery are presented in Table 8. The results show that the minimal sorbent mass obtained from this study is 500 mg for cadmium and 400

Table 7
Effect of concentration of PAR on the recovery by using Cd–PAR and Cu–PAR chelates as models

Element	Conc. of PAR excess over conc. of metal (fold)	Recovery (%)
Cd	5	76.30
	10	77.90
	20	77.10
	50	82.80
	100	81.20
Cu	5	99.55
	10	98.75
	20	104.00
	50	100.25
	100	99.75

Table 8
Effect of sorbent mass on the recovery by using Cd–PAR and Cu–PAR chelates as models

Element	C_{18} SPE mass (mg)	Recovery (%)
Cd	100	33.70
	200	48.50
	300	67.30
	400	80.40
	500	82.80
Cu	100	76.00
	200	96.50
	300	97.75
	400	102.00
	500	98.75

mg for copper. Hence, the sorbent mass at 500 mg is chosen as the optimal mass for the study of each metal.

The suitable conditions for determination each metal can be performed by using the selected conditions that are summarised in Table 1.

The results of the precision on C_{18} SPE cartridges for determining each metal as a single component in water are shown in Table 9. The average recoveries and the relative standard deviations for Ag^+, Cd^{2+}, Cu^{2+}, Ni^{2+}, and Pb^{2+} are 81.82 ± 3.11, 84.81 ± 3.47, 96.08 ± 1.53, 95.36 ± 1.48 and $81.64 \pm 1.01\%$, respectively. The average recoveries with relative standard deviations for these metals as mixture components in water for Ag^+ Cd^{2+}. Ni^{2+} and Pb^{2+} are 81.05 ± 4.97, 89.41 ± 3.88, 100.86 ± 1.15, 98.62 ± 1.93 and $83.57 \pm 4.35\%$, respectively for $n = 10$. This technique can be used as an efficient sample preparation procedure for the determination of each metal as a single component in water or as mixtures of metals in water. Recoveries of these metals in both cases show insignificant differences.

The accuracy of this technique was also evaluated by the determination of a mixture of metals in an unknown synthetic solution and the results are shown in Table 10. The errors of Ag^+, Cd^{2+}, Cu^{2+}, Ni^{2+}, and Pb^{2+} are 15.98, 4.34, 0.29, 5.0 and 13.40% (by using the assumption of 100% recovery). The large value of the errors can be reduced by taking into account the recovery factors of these metals. Then the errors of Ag^+, Cd^{2+}, Cu^{2+}, Ni^{2+} and Pb^{2+} are 3.64, 6.98, 0.59, 3.69 and 3.63%, respectively. It is indicated that

Table 9
Precision for the determination of each metal as single components in water on a C_{18} SPE cartridge

Metal	mg/l	Detection limit (mg/l)	Average recovery[a] (%)	Relative standard deviation (%)
Ag	0.05	0.06	81.82	3.11
Cd	0.05	0.03	84.81	3.47
Cu	0.02	0.09	96.08	1.53
Ni	0.20	0.05	95.36	1.48
Pb	0.05	0.30	81.64	1.01

[a] The average recovery for these metals were obtained from six determinations.

Table 10
Precision for the determination each metal as mixture components in water on a C_{18} SPE cartridge

Metal		1	2	3	4	5	6	7	8	9	10	Average recovery (%)	Relative standard deviation (%)
Ag	Absorbance	0.163	0.174	0.183	0.172	0.168	0.175	0.161	0.157	0.161	0.163		
	Concentration	1.572	1.683	1.770	1.666	1.626	1.695	1.552	1.516	1.552	1.578		
	Recovery (%)	78.60	84.15	88.50	83.30	81.30	84.75	77.60	75.80	77.60	78.90	81.50	4.97
Cd	Absorbance	0.142	0.144	0.149	0.140	0.146	0.138	0.132	0.142	0.143	0.137		
	Concentration	0.897	0.912	0.949	0.884	0.929	0.868	0.827	0.899	0.909	0.867		
	Recovery (%)	89.70	91.20	94.90	88.40	92.90	86.80	82.70	89.90	90.90	86.70	89.41	3.88
Cu	Absorbance	0.235	0.235	0.232	0.233	0.232	0.229	0.237	0.236	0.232	0.232		
	Concentration	4.061	4.075	4.006	4.027	4.014	3.945	4.103	4.083	4.019	4.012		
	Recovery (%)	101.52	101.88	100.15	100.68	100.35	98.62	102.58	102.08	100.48	100.30	100.86	1.15
Ni	Absorbance	0.212	0.223	0.215	0.211	0.215	0.209	0.211	0.213	0.215	0.211		
	Concentration	3.914	4.126	3.978	3.892	3.985	3.859	3.897	3.930	3.973	3.896		
	Recovery (%)	97.85	103.15	99.45	97.30	99.62	96.48	97.42	98.25	99.32	97.40	98.62	1.93
Pb	Absorbance	0.229	0.240	0.230	0.220	0.234	0.234	0.230	0.241	0.234	0.232		
	Concentration	8.041	8.514	8.078	7.666	8.250	8.848	8.362	8.821	8.548	8.441		
	Recovery (%)	80.41	85.14	80.78	76.66	82.50	88.48	83.62	88.21	85.48	84.41	83.57	4.35

this technique is suitable for determining of trace levels of these metals with good results.

4. Conclusion

An efficient sample preparation method using solid-phase extraction for enhancing the concentration of some heavy metals in water was developed. High percent recoveries are obtained because there is no formation of emulsion, only a small amount of sample transfer, and using small volumes of extraction solvent results in little or no evaporation. It is also a simple, rapid, economical and safe method.

For future work, larger extraction volumes should be studied in order to give a better enrichment factor of the metals in the final volume. The design of a new apparatus can be improved by increasing the flow-rate of solutions studied. The detection limit and sensitivity of other metals can be determined by using this sample preparation technique with other instruments, i.e., graphite furnace or inductively-coupled plasma atomic absorption spectroscopy. Other ligands are also interesting to study for improving sensitivity and selectivity. The investigation of other heavy metals in water and various environmental samples should be also considered.

References

[1] R.E. Majors, *LC·GC Int.*, 4 (1991) 10.
[2] B.L. Tippins, *Nature*, 334 (1988) 273.
[3] B.L. Tippins, *Am. Lab.*, 19 (1987) 8.
[4] K.C. Van Horne, *Sorbent Extraction Technology*, Analytichem International, Harbor City, CA, 1985.
[5] M. Zief and R. Kiser, *Am. Lab.*, 22 (1990) 70.
[6] M. Zief and R. Kiser, *Solid Phase Extraction for Sample Preparation*, J.T. Baker, Phillipsburg, NJ, 1988.
[7] *Baker-10 SPE Application Guide Vol. 1*, J.T. Baker, Phillipsburg, NJ, 1982.
[8] *Baker-10 SPE Application Guide Vol. 2*, J.T. Baker, Phillipsburg, NJ, 1982.
[9] H. Watanabe, K. Goto, S. Taguchi, J.W. Mclaren, S.S. Berrnan and D.S. Russell, *Anal. Chem.*, 53 (1981) 739.

ELSEVIER

Journal of Chromatography A, 697 (1995) 145–152

JOURNAL OF CHROMATOGRAPHY A

Simplified clean-up for the determination of benzimidazolic fungicides by high-performance liquid chromatography with UV detection

A. Di Muccio*, I. Camoni, M. Ventriglia, D. Attard Barbini, M. Mauro, P. Pelosi, T. Generali, A. Ausili, S. Girolimetti

Istituto Superiore di Sanità, Laboratorio Tossicologia Applicata, Viale Regina Elena 299, 00161 Rome, Italy

Abstract

A method was developed that allows the determination of benomyl, carbendazim (MBC), thiophanate methyl (TFM) as carbendazim and thiabendazole (TBZ) by HPLC with UV detection. After extraction and cyclization of TFM into MBC, the conversion of benomyl into MBC is carried out by absorbing the raw extract on a ready-to-use, disposable column of a macroporous Kieselghur-type material and percolating 0.1 *M* HCl through it. Benzimidazolic residues are partitioned into the acid solution whereas most of the co-extractives are retained on the column. The final clean-up is performed on a strong cation-exchange (SCX) cartridge. The determination of MBC and TBZ is carried out by HPLC–UV detection on a polymeric reversed-phase column eluted with a water–acetonitrile (70 : 30). Recoveries of MBC and TBZ from pear, apple, orange, grape, kiwi, tomato and lettuce, spiked at levels of 0.22 and 0.88 mg/kg, were satisfactory (>70%). The main features of the method include high selectivity towards MBC and TBZ, reduced consumption of reagents and solvents, reduced handling operations, lack of emulsions and the use of disposable items.

1. Introduction

Benzimidazolic compounds are widely used in agriculture as both field and post-harvest fungicides. The main compounds in use are thiabendazole (TBZ), benomyl, carbendazim (MBC) and thiophanate methyl (TFM). As the last three compounds are intercorrelated, having MBC as common metabolite and major fungitoxic principle, a single maximum residue limit (MRL) is generally set for this group of three compounds.

The problems associated with the analysis of this class of compounds have been dealt with in two reviews [1,2].

In almost all methods, benomyl is readily converted during the analytical procedure into MBC by dilute acid treatment, either in the extraction stage [3], when hydrophilic extraction solvent is used, or later in the procedure by shaking the solvent containing the analyte with a dilute acid solution in a separating funnel.

TFM is not so easily converted into MBC and two approaches have been pursued, i.e., determination of TFM per se [3,4] or conversion into MBC with a dedicated step. Two main reactions have been reported: (i) treatment with 20% ammonia solution in dimethylformamide (DMF) at 80°C for 1 h [5] and (ii) treatment with 50% acetic acid solution and copper(II) acetate [6].

After conversion of benomyl and TFM into MBC, a clean-up for the two main species that

* Corresponding author.

0021-9673/95/$09.50
SSDI 0021-9673(94)01089-7

remain, i.e., MBC and TBZ, has to be set up. However, irrespective of the approach followed, the methods for the four compounds consist of lengthy, complex procedures, in which, taking advantage of the ionizable structure of MBC and TBZ, the clean-up is mostly based on a series of solvent–basic solution and solvent–acidic solution partitions carried out in separating funnels [4,5,7–9].

Although TBZ can be determined as such by gas chromatography (GC) with nitrogen–phosphorus detection (NPD) on capillary columns [10] and MBC by GC with NPD after acetylation [8] or with electron-capture detection (ECD) after trifluoroacetylation [11] or pentafluorobenzylation [7], high-performance liquid chromatography (HPLC) with UV detection [6] or UV followed by fluorescence detection [3,9] is advisable for analysing ionizable species and setting a single procedure for both MBC and TBZ.

However, the reported HPLC conditions require solvent modifiers such as a buffer [12] or ion-pairing reagent [9] in reversed-phase or acid [4] or ammonia solution [3] in normal-phase operation to improve the peak shape and/or resolution.

The aim of this work was to develop a simplified procedure, in which the clean-up is shortened and uses reduced amounts of reagents and glassware and the determination is based on simpler HPLC conditions.

2. Experimental

2.1. Reagents and materials

Ethyl acetate, dimethylformamide (DMF), ammonium formate, 20% ammonia solution (0.92 g/ml) and anhydrous sodium sulphate were of analytical-reagent grade. Hydrochloric acid (0.1 *M*) and sodium hydroxide solution (1 *M*) were used. Acetonitrile, methanol and water were of HPLC grade. Ammonium formate buffer (pH 6.8) was prepared as 0.1 and 5 *M* solutions. Celite 545 was obtained from BDH (Poole, UK). An Extrelut-3 column with an exit needle was supplied by Merck (Darmstadt, Germany). Bakerbond SPE aromatic sulphonic acid was purchased from Baker (Phillipsburg, NJ, USA). Acetone-washed glass-wool was used.

Pesticide reference standards from the collection in this laboratory were kindly supplied by the main manufacturer of the pesticides and were >99% pure.

2.2. Apparatus

HPLC analyses were carried out on a Hewlett-Packard Model 1050 instrument consisting of an autosampler (set to inject 20 μl), a pumping unit, a UV spectrophotometric detector and, in series, a Hewlett-Packard Model 1046A spectrofluorimetric detector. Chromatograms were recorded on Hewlett-Packard Model 3396 II integrators.

The HPLC conditions were as follows: HPLC column Asahipak ODP-50 (125 × 4.0 mm I.D.) (Hewlett-Packard) with a precolumn (Merck) (30 × 4 mm I.D.) filled with Perisorb RP-18, 30–40 μm (Merck); eluent, water–acetonitrile (70 : 30, v/v); column oven temperature, 40 °C; UV detector, set at 280 nm; spectrofluorimetric detector, excitation at 280 nm, emission at 310 nm, cut-off filter 280 nm.

An Omni-Mixer homogenizer was obtained from Sorvall (Norwalk, CT, USA) and a rotary evaporator from Büchi (Switzerland).

2.3. Procedure

Extraction

Weigh into the homogenization vessel 50 g of vegetable and add, in this order, 5 g of Celite, 5 ml of ammonia solution and 150 ml of ethyl acetate. Mix with a glass rod and add 25 g of Na_2SO_4 in small portions while stirring. Homogenize at medium speed for 20 min. Filter through glass-wool into a 500-ml erlenmeyer flask. Repeat the extractions with ethyl acetate (2 × 75 ml), filter, combine the ethyl acetate phases and concentrate almost to dryness with a rotary evaporator.

Cyclization of TFM into MBC

Transfer the crude extract to a 50-ml round-bottomed flask, using small portions of ethyl acetate to wash the erlenmeyer flask. Concentrate to dryness, dissolve the residue in 10 ml of DMF and add 1 ml of ammonia solution. Attach a water-cooled condenser and keep in a water-bath at 80°C for 1 h. Cool to room temperature, then pour the contents into a 250-ml separating-funnel containing 10 ml of 1 *M* NaOH. Wash the flask three times with 30, 30 and 10 ml of water, collecting the washings in the separating funnel. Mix and carry out three extractions with 75, 50 and 50 ml of ethyl acetate. Wash the combined ethyl acetate phases with 10 ml of water and discard the water. Collect the ethyl acetate in a 300-ml erlenmeyer flask and concentrate almost to dryness.

Conversion of benomyl into MBC

Dissolve the crude extract resulting at the end of either the extraction or cyclization step with 3 ml of ethyl acetate. Transfer the solution on to an Extrelut-3 column, allow the solvent to be absorbed into the bed and wait for 10 min to obtain an even distribution. Pass nitrogen through the cartridge, from bottom to top, at 0.5 l/min for 20 min, then disconnect the nitrogen.

Clean-up

Precondition a sulphonic acid cartridge by passing 2 × 1-ml portions of methanol and 2 × 1-ml portions of 0.1 *M* HCl (use a vacuum manifold). Position the Extrelut-3 column over the sulphonic acid cartridge and elute the column by passing 6 × 5-ml portions of 0.1 *M* HCl, using each portion to wash the erlenmeyer flask that had contained the ethyl acetate extract. Allow the acid solution draining from the Extrelut-3 column to pass through the cartridge so as to maintain the SCX cartridge wet.

Remove the Extrelut-3 column, wash the sulphonic acid cartridge with 2 × 1 ml of water, 3 × 2 ml of CH_3OH–H_2O (75 : 25, v/v) and 3 × 2 ml of CH_3OH–0.1 *M* ammonium formate buffer (pH 6.8) (50 : 50, v/v) and discard all the washings.

Elute the SCX cartridge with 1 × 2 ml of CH_3OH–5 *M* ammonium formate buffer (pH 6.8) (75 : 25, v/v) at ca. 0.4–0.5 ml/min to recover the MBC and TBZ residues.

Determination

Inject the solution resulting from the clean-up into the HPLC apparatus. Compare the chromatographic response (peak retention times, heights or areas) with that of standard solutions of MBC and TBZ and calculate residue amount.

2.4. Recovery experiments

Recovery trials were carried out by adding known amounts of the analytes to the selected vegetables and comparing the amounts found with the amount added.

3. Results and discussion

Most of current methodologies for benzimidazolic fungicides in vegetables rely on complex procedures based on separating funnel partitions. The main aim of this work was to develop a simplified method composed of steps carried out on disposable items. The extraction and cyclization steps were taken from the work by Gnaegi et al. [5] and no attempt was made to improve them.

Steps that have been improved are the conversion of benomyl into MBC, clean-up and determination. Based on our previously reported [13] application of a solid-matrix column in the clean-up of vegetable extracts for fungicide residue determination, we have developed a procedure for the conversion of benomyl into MBC in a single step by treating with dilute acid the raw extract dispersed on a macroporous Kieselghur-type material contained in a ready-to-use, disposable glass column.

This step offers substantial advantages over the classical separating funnel partitioning of the extract between ethyl acetate and 0.1 *M* HCl. These advantages include a straightforward operation with lack of emulsions, reduced consumption of solvents, reduced handling operations and the use of disposable items. After dispersing

the raw extract solution over the Extrelut material, most of ethyl acetate is removed by passing nitrogen through the column, from bottom to top. In this way, the co-extractives adhere to the solid particles and the major part is retained on the column because the co-extracted material is poorly soluble in diluted HCl.

On the other hand, the high surface area of the material ensures a high degree of dispersion and, hence, good efficiency of transfer of MBC and TBZ into the dilute HCl. Thus, in a single step, the Extrelut-3 column performs the conversion of benomyl into MBC and effects a partial clean-up of the extract without any possibility of emulsions, such as those frequently occurring in separating funnel operations. In Fig. 1 is shown the rate of removal of ethyl acetate from the Extrelut-3 column with different nitrogen flow rates. With the parameters chosen (0.5 l/min for 20 min) ca. 20% of the ethyl acetate remains on the column.

Although with complete removal (say 1 l/min for 20 min) of ethyl acetate the recoveries of MBC and TBZ were satisfactory, we preferred to leave some ethyl acetate on the column so that a thin film of solution, rather than a thin film of hydrophobic waxy material, surrounds the solid particles and, being more wettable, offers less resistance to the partition of the analytes into the dilute HCl.

The yield of conversion of benomyl into MBC was determined by applying 2 ml of standard solution containing 5.25 μg/ml of benomyl in ethyl acetate to the Extrelut-3 column and running the method as described from conversion to clean-up and determination. The conversion yields were between 80% and 85% ($n = 3$). Recoveries of benomyl added alone to green-red tomatoes and cucumber homogenates at levels of 0.22 and 0.88 mg/kg and analysed according to the whole procedure were in the range 83–88% ($n = 3$).

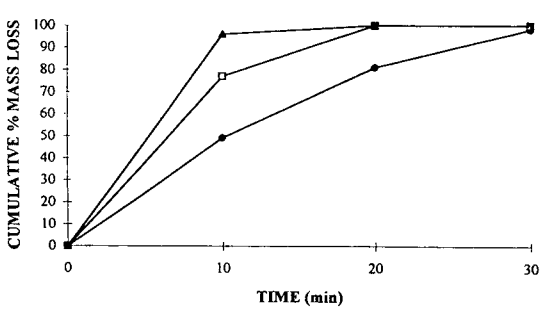

Fig. 1. Cumulative percentage mass loss of Extrelut-3 cartridges loaded with 3 ml of acetate using different nitrogen flow-rates: ○ = 0.5; □ = 1.0; ◆ = 2 ml/min.

As both MBC and TBZ are in cationic form at low pH, we thought that this could offer a fairly good way to isolate the analytes of interest from the majority of other co-extracted material. We therefore used a strong cation-exchange (SCX) cartridge to reconcentrate MBC and TBZ residues from the volume of diluted acid used to elute them from Extrelut-3 column in a manner similar to that reported by Leenheers et al. [14].

As the SCX we chose is a silica–propylphenylsulphonic acid, in addition to the cation-exchange properties it also shows a mechanism of retention based on hydrophobic interaction. Hence neutral lipophilic material can be washed out of the cartridge by increasing the methanol content of water–methanol mixtures, while cationic species can be eluted by increasing the salt concentration of the buffer solution.

At least 30 ml of 0.1 *M* HCl are necessary to elute MBC and TBZ from the Extrelut-3 column. By passing this solution through the SCX cartridge and analysing the draining acid, we proved that the analytes are completely retained. After washing with water to remove the excess acid, the SCX cartridge was washed with a methanol–water (75 : 25, v/v) to remove unwanted lipophilic material.

Attempts to increase further the methanol content proved unsuccessful as the subsequent elution scheme is altered, perhaps because the ionic environment of the SCX particles is upset. We therefore applied a wash with a buffer of low ionic strength [methanol–0.1 *M* ammonium formate buffer (pH 6.8) (50 : 50, v/v)] to remove slightly retained ionic species; the content of methanol and the ionic strength were increased to the point where MBC and TBZ were still retained on the cartridge.

At a 0.1 *M* buffer concentration, MBC and TBZ start to elute on increasing the methanol

content of the eluting mixture to 75%. However, as can be seen in Fig. 2, under these conditions three 2-ml fractions are needed to elute the analytes completely. Therefore, we gradually increased the NH_4^+ concentration to 5 *M* in order to elute MBC and TBZ in only one 2-ml fraction and have better sensitivity.

To establish the performance of the described method, some vegetables, including pears, apples, oranges, grapes, kiwis, red tomatoes and lettuce, were spiked at levels of 0.22 and 0.88 mg/kg with both MBC and TBZ and processed according to the procedure. Recoveries are reported in Table 1 and are considered satisfactory.

Further, a few samples with incurred residues of benzimidazolic fungicides were analysed according to Ref. [5] (extraction with ethyl acetate, cyclization, acid–base partitioning, spectro-

Table 1
Mean recoveries values of MBC and TBZ added at different levels to different crops analysed according to the proposed method (without cyclization) and determined by HPLC–UV detection

Crop	Mean recovery (%)[a]			
	0.22 mg/kg[b]		0.88 mg/kg[b]	
	MBC	TBZ	MBC	TBZ
Pear	84	90	81	88
Apple	73	93	75	90
Orange	73	95	77	91
Grape	84	79	85	87
Kiwi	83	75	83	78
Red tomato	89	84	87	85
Lettuce	84	80	82	83

[a] $n = 3$.
[b] Spiking levels.

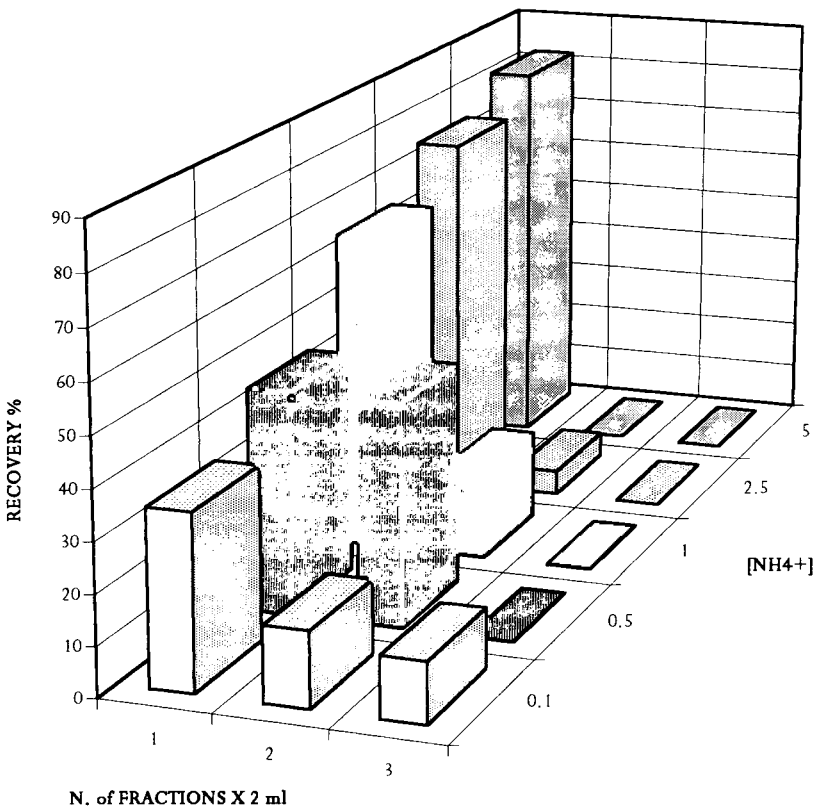

Fig. 2. Recovery of MBC from silica–aromatic sulphonic acid cartridge eluted with methanol–ammonium formate buffer (pH 6.8) (75 : 25, v/v) with increasing ionic strengths.

photometric determination, i.e., the method used previously in our laboratory) and the present HPLC–UV method. The results reported in Table 2 show reasonable agreement between the two series of determinations; where the values obtained by the present method are lower, this may be attributed to the more critical removal of the interferences in the reference method based on separating funnel partitioning and to the lower selectivity of spectrophotometry compared with HPLC–UV determination.

Although we did not determine specifically the maximum concentration levels for the different analytes to be retained on the SCX cartridge, the data reported in Table 2 show that the present method gave comparable results to the reference method up to 6 mg/kg, thus indicating that at least up to 300 μg of MBC can be retained by the SCX cartridge.

We also tried some C_{18} HPLC columns, but with unsatisfactory results for peak shape and recovery. We subsequently found that with a polymeric reversed-phase column MBC and TBZ could be eluted isocratically as symmetrical peaks with water–acetonitrile (70 : 30) without a solvent modifier, thus simplifying the chromatographic conditions. More recently we tried a Phenomenex Ultracarb 5 ODS column eluted with water–acetonitrile (50 : 50, v/v) and obtained good peak shapes similar to those reported by Lòpez et al. [15] with a Spherisorb ODS-1 column. Fig. 3 shows representative chromatograms of pear "blank", spiked pear sample and standard compounds, which show the good quality of the clean-up. In the unspiked vegetables matrices analysed, a small interfering peak was observed only with pear samples at the retention time of TBZ and at a level equivalent to ca. 0.03 mg/kg.

Table 2
Comparison of results obtained on analysing samples with incurred residues of benzimidazolic fungicides according to Ref. [5] and the present method

Crop	MBC content (mg/kg)	
	Ref. [5]	Present method
Courgette	0.36	0.21
Grape	1.20	1.10
Grape	2.90	1.80
Grape	6.00	5.40
Grape	2.40	0.60
Grape	2.00	1.70
Grape	2.90	3.00

Although the method may not appear simple, one should consider that it has the unique feature that it covers simultaneously four compounds, i.e., benomyl, MBC, TFM and TBZ. If the determination of TFM is not sought (cyclization omitted), the present method is simplified in comparison with the previous methods that mostly use time-consuming separating funnel separations. The preparation of a single sample takes ca. 4 h if cyclization is omitted. However, owing to the solid-phase operation, several samples can be processed in parallel.

Quantification was carried out via the UV detector response with reference to an external standard of comparable concentration. The HPLC–UV response was found to be linear between 0.69 and 44 μg/ml for both MBC and TBZ ($r^2 = 0.996$ and 0.995, respectively), corresponding to a range of quantification of 0.01–0.88 mg/kg. Higher concentrations were not assayed as more concentrated solutions are not readily prepared in acetonitrile. Hence, if needed, it is advisable to dilute the final extract to have the analytes in this range of concentration. Although widely different levels of the analytes can occur in field samples (say 5–6 mg/kg in the case of misuse), the most interesting range to explore is up to 1 mg/kg (i.e., the most frequently accepted MRL) in order to have the possibility of either assessing the compliance of the sample with the MRL or ruling out the presence of residues.

The spectrofluorimetric detector was added as a confirmatory technique and gave chromatograms and quantitative results similar to those with the UV detector.

As the aim of this work was to develop a clean-up procedure, the parameters for the fluorimetric detector were chosen as a compromise between MBC and TBZ and were set to give the same response as the UV detector.

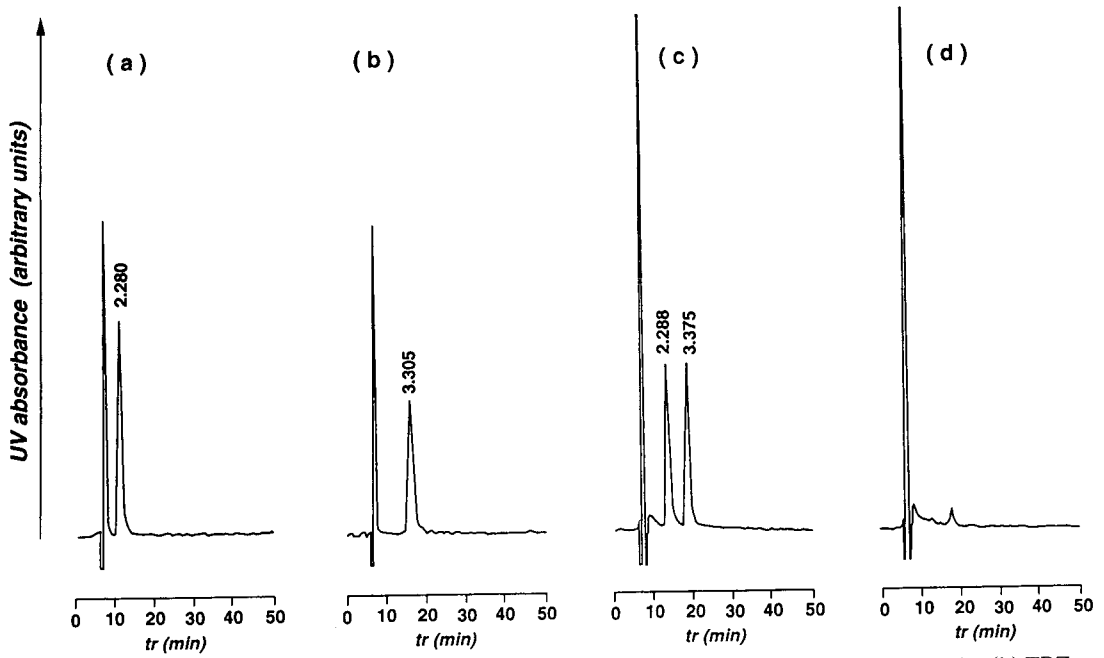

Fig. 3. Chromatograms with UV detection at 280 nm of (a) MBC standard solution, 5.5 μg/ml, t_R = 2.280 min; (b) TBZ standard solution, 5.5 μg/ml, t_R 3.305 min; (c) pear sample spiked with MBC and TBZ, 0.2 mg/kg each; (d) pear sample, same as (c) but not spiked. For conditions, see text.

Also, the UV wavelength was the optimum for MBC, not for TBZ. However, we chose this wavelength to have the same response at the same spiking level for the two compounds.

4. Conclusions

A method has been developed that allows the simultaneous determination of four benzimidazolic fungicide residues in several vegetables. The method involves ethyl acetate extraction under basic conditions, cyclization of TFM into MBC (which can be omitted if TFM is not sought), conversion of benomyl into MBC by dilute acid treatment of the raw extract adsorbed on a column of macroporous siliceous material, where also a partial clean-up occurs, a final clean-up by strong cation-exchange chromatography and HPLC–UV determination on a reversed-phase polymeric column simply eluted with water–acetonitrile (70 : 30, v/v).

The main features of the method include a clean-up based on simple operations and the use of disposable cartridges, with substantial savings of glassware, reagents and time compared with most existing methods. The clean-up is very selective towards MBC and TBZ and virtually no interfering peaks were observed in the chromatograms of the analysed crops. The recoveries values of MBC and TBZ from representative crops (pear, apple, orange, grape, kiwi, tomato and lettuce) were satisfactory (>70%) at spiking levels between 0.22 and 0.88 mg/kg.

Acknowledgements

This work was funded partly by the Italian Minister of Agriculture, "Research Program on Biological and Integrated Pest Management" (Contract No. D.M. 380/7240/90), and partly by the National Research Council (CNR), targeted project "Prevention and Control of Disease

Factors", subproject "Quality of the Environment and Health", research line "Toxicological Risk from Pesticides: Development and Integration of Methodologies" (Contract CNR/FAT. MA.93.00766.PF41).

References

[1] J. Sherma, *J. Chromatogr.*, 113 (1975) 97.
[2] S. Gorbach, *Pure Appl. Chem.*, 52 (1980) 2567.
[3] C. Bicchi, F. Belliardo, L. Cantamessa, G. Gasparini, M. Icardi and E. Sesia, *Pestic. Sci.*, 25 (1989) 355.
[4] C. Lazzarini, A. Caleffi and A. Del Re, *Chim. Ind. (Milan)*, 64 (1982) 315.
[5] F. Gnaegi, R. Mestres, J. Tourte and M. Campo, *Trav. Soc. Pharm. Montpellier*, 34 (1974) 91.
[6] C.F. Aten, J.B. Bourke and R.A. Marafioti, *J. Agric. Food Chem.*, 30 (1982) 610.
[7] G.H. Tjan and J.T.A. Jansen, *J. Assoc. Off. Anal. Chem.*, 62 (1979) 769.
[8] H. Pyysalo, *J. Agric. Food Chem.*, 25 (1977) 995.
[9] D.M. Gilvydis and S.M. Walters, *J. Assoc. Off. Anal. Chem.*, 73 (1990) 753.
[10] M.T. Lafuente, J.L. Tadeo and J.J. Tuset, *J. Chromatogr. Sci.*, 25 (1987) 84.
[11] J.P. Rochaud and J.R. Decallone, *J. Agric. Food Chem.*, 22 (1974) 259.
[12] C.H. Marvin, I.D. Brindle, R.P. Singh, C.D. Hall and M. Chiba, *J. Chromatogr.*, 518 (1990) 242.
[13] A. Di Muccio, R. Dommarco, D. Attard Barbini, A. Santilio, S. Girolimetti, A. Ausili, M. Ventriglia, T. Generali and L. Vergori, *J. Chromatogr.*, 643 (1993) 363.
[14] L.H. Leenheers, R. Engel, W.E.T. Spruit, W.J.A. Meuling and M.J.M. Jongen, *J. Chromatogr.*, 613 (1993) 89.
[15] L.F. Lòpez, A.G. Lòpez and M.V. Riba, *J. Agric. Food Chem.*, 37 (1989) 684.

ELSEVIER

Journal of Chromatography A, 697 (1995) 153–158

JOURNAL OF CHROMATOGRAPHY A

Effect of calcium-modified silica on retention and selectivity in normal-phase liquid chromatography

Mitsuyoshi Okamoto[a,*], Kazunori Nobuhara[b], Daido Ishii[c]

[a]*Gifu Prefectural Tajimi Hospital, 5-161, Maehata cho, Tajimi, Gifu 507, Japan*
[b]*Fuji Silysia Chemical Ltd., 2 Chome, Kozoji cho, Kasugai, Aichi 487, Japan*
[c]*Kumamoto Institute of Technology, 4-22-1, Ikeda cho, Kumamoto 860, Japan*

Abstract

Modification of a silica surface by calcium ions was studied by high-performance liquid chromatography. After treatment at pH 7.0 and 9.0 with calcium hydroxide, the calcium-modified silicas were subjected to physical and chemical analysis. From calcium measurement with a flame atomic absorption spectrometer, the extent of calcium adsorption was determined as 650 ppm on calcium-modified silica at pH 7.0 and 4800 ppm on calcium-modified silica at pH 9.0. The amount of calcium on the original silica was 58 ppm. The separation factor (α) for N-methylaniline versus N,N-dimethylaniline was measured to be 5.1 on calcium-modified silica at pH 9.0, but could not measured on calcium-modified silica at pH 7.0 or the original silica, using methanol–*n*-hexane (1:99, v/v) as the eluent. By comparison of calcium and amino-modified silica, the separation factors were measured under the same HPLC conditions and was found to be 9.0 on amino-modified silica. The results show that calcium-modified silicas are able to separate some basic model compounds as well as amino-modified silica.

1. Introduction

The surface of silica and adsorption on it have been the subject of many investigations. It has been shown that specific adsorption occurs on the surface silanol groups [1,2]. On the other hand, as the acidic silanol groups are responsible for the cation-exchange properties of silica, the theoretical specific capacity, Q_0, in aqueous solution was shown to be equivalent to the concentration of surface hydroxy groups, which is about 8 μmol/m^2 for a totally hydroxylated silica [3]. For strongly hydrated multivalent cations, the sorption capacities enhanced considerably on increasing the pH, as was shown by Vydra and co-workers [4,5].

Depending on pH, metal ions, for example, may exist in their non-hydrated or their hydrated form. As a consequence of the above considerations, one can expect a very complex ion-exchange behaviour of silica in electrolyte solution. Whereas water and aqueous solutions reduce the activity and acidity of the surface sites of silica, these properties are considerably enhanced in anhydrous media. In the special case of silica catalysts used for various heterogeneous reactions, such as hydration–dehydration and isomerization, the acidity can be measured with the aid of Hammett and arylcarbinol indicators by titration with amines in organic solvents [6].

On the other hand, flash chromatography [7]

* Corresponding author.

0021-9673/95/$09.50
SSDI 0021-9673(94)00869-8

provides a rapid and inexpensive general method for the preparative separation of mixtures requiring only moderate resolution. However, there are a few reports on the effect of silica surface modification by calcium ions on the chromatographic properties of the packing [8–15]. Therefore, we have studied the preparation and evaluation of inexpensive calcium-modified silica for the large-scale preparative separation and routine purification of organic compounds, in comparison with the expensive high-performance liquid chromatographic (HPLC) column gels.

2. Experimental

2.1. Reagent and materials

Benzene, N,N-dimethylaniline, N-methylaniline, 2-ethylpyridine, aniline, pyridine, dimethylphthalate, di-*n*-butyl phthalate, phenol and calcium hydroxide were obtained from Wako (Osaka, Japan). The other reagents and organic solvents were of analytical-reagent grade.

2.2. Porous silicas

Porous silica were prepared in our laboratories (Table 1, Ca-0). The particle size was 9.8 μm.

2.3. Calcium hydroxide solution

Calcium hydroxide solution (1 g per 100 ml) was prepared by dissolving calcium hydroxide in distilled, deionized water. After standing for 24 h at room temperature, the calcium hydroxide solution was filtered with a membrane filter (0.5 μm).

2.4. Calcium-modified silica

A 10-g amount of dried silica (original, Ca-0, Table 1) was immersed in 100 ml of distilled, deionized water. The silica suspension was then carefully adjusted to pH 7.0 (4.8 ml of the calcium hydroxide solution were added), boiled for 2 min, filtered with a membrane filter (0.5 μm), washed several times with methanol and dried in vacuo at 70°C for 1 day, finally producing Ca-I-modified silica, the properties of which are given in Table 1.

Also, the silica suspension was adjusted to pH 9.0 (78.6 ml of the calcium hydroxide solution were added), and the same procedure as with the Ca-I-modified silica series in Table 1 was then carried out, producing Ca-II-modified silica (Table 1).

The calcium contents of the Ca-0, Ca-I and Ca-II materials were determined with a Seiko (Tokyo, Japan) SAS-727 atomic absorption spectrometer, giving the data in Table 1. The specific surface areas were determined with a Shibata SA-1000 surface area pore volume analyser and are also given in Table 1. The conductivities were measured for suspensions of Ca-0, Ca-I or Ca-II, but not for solid material. The concentrations of the suspensions (5% slurry of Ca-0, Ca-I or Ca-II) were determined with a Kyoto Electronics (Kyoto, Japan) CM-117 conductivity meter, giving the data in Table 1.

The pK_a values of the surface sites were measured with the aid of Hammett and arylcarbinol indicators by titration with amines in or-

Table 1
Characteristics of calcium-modified silica

Modified silica	Specific surface area (m^2/g)	Mean pore diameter (Å)	Pore volume (ml/g)	pH[a]	Conductivity[a] (μS)	Calcium adsorption* (ppm)	Surface acidity (pK_a)
Ca-0 (original)	279	176	1.23	5.8	5	58	3.3
Ca-I	274	184	1.26	6.6	96	650	4.0
Ca-II	252	174	1.22	8.9	168	4800	4.8

[a] 5% Slurry solution.

Table 2
Chromatographic data for di-*n*-butyl phthalate (DBP) and dimethyl phthalate (DMP) (as neutral model compounds) on Ca-0-, Ca-I-, Ca-II- and NH_2-modified silica

Modified silica	Separation factor, $\alpha = k'_A/k'_B$ (DMP vs. DBP)
Ca-0	2.94
Ca-I	2.86
Ca-II	2.79
NH_2	2.53

Eluent, methanol–*n*-hexane (1:99, v/v); other conditions as in Fig. 1.

ganic solvents. The results are given in Table 1 [8].

2.5. Stability of distilled water-washed Ca-II-modified silica

Ca-II-modified silica was washed off the column with distilled water for 1000 min at 1 ml/min, finally producing Ca-III-modified silica.

2.6. Apparatus

The HPLC measurements were carried out on a Twincle instrument (Jasco, Tokyo, Japan), equipped with a Uvidec-100 IV variable-wavelength detector (Jasco) and a column of 250 × 4.6 mm I.D., packed with Ca-0-, Ca-I-, Ca-II- and Ca-III-modified silica.

3. Results and discussion

As shown in Table 2, the model neutral compounds could be separated on Ca-0-, Ca-I- and Ca-II-modified silica as well as NH_2-modified silica [16,17] with the same eluent [methanol–*n*-hexane (1:99, v/v)]. Table 2 shows the separation of dimethyl phthalate versus dibutyl phthalate. Owing to the influence of calcium no separation effect was seen on Ca-0-, Ca-I- and Ca-II-modified silica.

Fig. 1 shows the chromatographic behaviour of N,N-dimethylaniline and N-methylaniline, as basic model compounds, compared with NH_2-modified silica. As can be seen, N,N-dimethylaniline and N-methylaniline could be separated on Ca-II-modified silica, and also NH_2-modified silica, but not on Ca-0- and Ca-I-modified silica with the same eluent [methanol–*n*-hexane (1:99, v/v)]. It was presumed that the effect of ion-exchange sorption on Ca-II controlled the separation effect in the presence of calcium ions.

The number of theoretical plates (N) and the peak asymmetry factor (A_s) for basic model

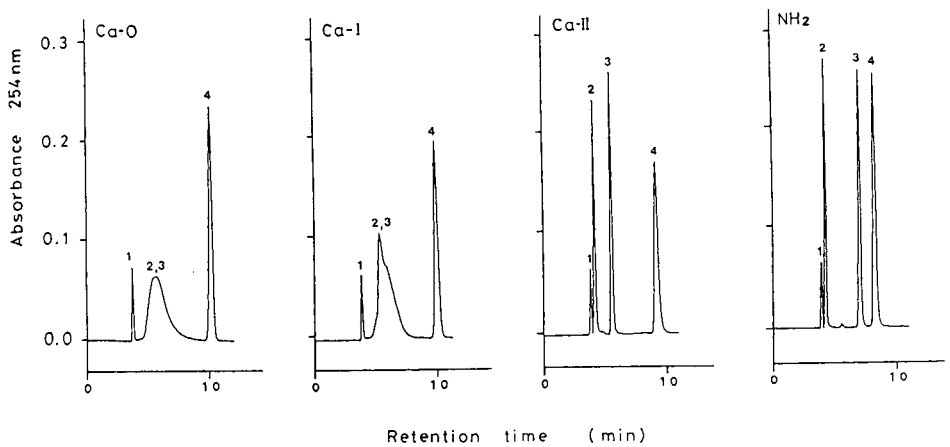

Fig. 1. Chromatographic behaviour of N,N-dimethylaniline and N-methylaniline (as basic model compounds) on Ca-0-, Ca-I- and Ca-II-modified silica, compared with NH_2-modified silica. Column, 250 × 4.6 mm I.D.; eluent, methanol–*n*-hexane (1:99, v/v); flow-rate, 1.0 ml/min; detection, UV at 254 nm. Peaks: 1 = benzene; 2 = N,N-dimethylaniline; 3 = N-methylaniline; 4 = dimethyl phthalate.

compounds (N,N-dimethylaniline, N-methylaniline, 2-ethylpyridine, aniline and pyridine) were measured on Ca-0-, Ca-I- and Ca-II-modified silica, with the same eluent as above. As the amount of calcium on the modified silica increases from Ca-0 to Ca-I to Ca-II, N and A_s can be expected to increase dramatically, as shown in Table 3 and Fig. 1.

The separation factors, α, were measured under the same HPLC conditions using Ca-0-, Ca-I- and Ca-II-modified silicas in comparison with NH_2-modified silica. Table 4 shows that the separation of phenol vs. dimethyl phthalate, owing to the influence of calcium ions, was worse on Ca-II- and NH_2-modified silica than on Ca-0- and Ca-I-modified silica.

Fig. 2 shows the relationship between the amount of calcium adsorbed (ppm) on Ca-0 and the calcium equilibrium concentration (ppm), as the calcium adsorption isotherms for silica at 25°C, using batch adsorption experiments. It can be seen that the extent of calcium adsorption on Ca-0 increases on elevating the calcium equilibrium concentration (ppm).

By increasing the extent of calcium adsorption, the conductivity (S) and pH, basic model compounds could be separated on Ca-0-, Ca-I- and Ca-II-modified silica (Tables 1 and 3 and Fig. 1). Fig. 3 shows the relationship between the extent of calcium adsorption on Ca-0 from a 5% slurry solution for each silica treated at different pH values. As can be seen, the extent of calcium adsorption increases as the pH of treatment increases.

Table 5 shows the separation factors, α, for basic model compounds (N,N-dimethylaniline

Table 4
Chromatographic data for phenol (as acidic model compound) on Ca-0-, Ca-I-, Ca-II- and NH_2-modified silica

Modified silica	Separation factor, $\alpha = k'_A/k'_B$ (phenol vs. DMP)
Ca-0	3.06
Ca-I	2.86
Ca-II	–
NH_2	–

DMP = dimethyl phthalate. Other conditions as in Fig. 1.

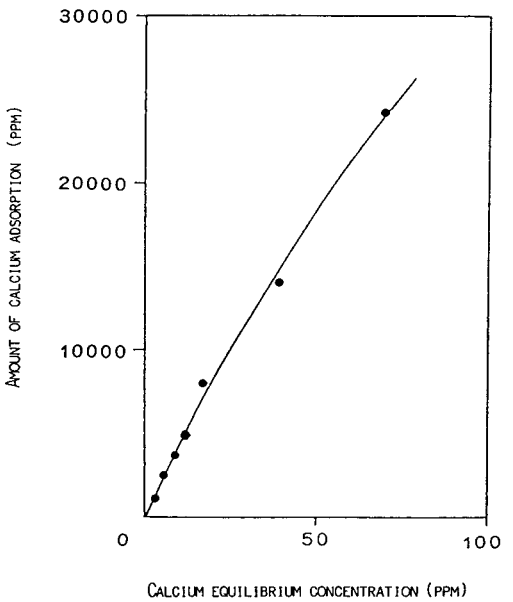

Fig. 2. Relationship between the extent of calcium adsorption and the calcium equilibrium concentration, as calcium adsorption isotherms for silica at 25°C.

Table 3
Capacity factor (k'), number of theoretical plates (N) and peak asymmetry factor (A_s) on Ca-0-, Ca-I- and Ca-II-modified silica

Modified silica	N,N-Dimethylaniline			N-Methylaniline			2-Ethylpyridine			Aniline			Pyridine		
	k'	N	A_s	k'	N	A_s	k'	N	A_s	k'	N	A_s	k'	N	A_s
Ca-0	0.13	4190	2.5	0.61	2516	5.4	1.93	152	21.3	2.49	1888	9.8	3.57	342	11.0
Ca-I	0.10	4962	2.0	0.58	3442	3.7	1.86	189	26.1	2.39	2874	5.7	3.56	487	20.1
Ca-II	0.02	4884	1.2	0.42	5784	1.3	0.83	5780	1.5	1.30	6310	1.4	1.61	4805	1.7
Ca-III	0.07	4410	1.2	0.50	5507	1.4	1.19	3150	2.1	2.62	6202	1.3	3.00	1070	4.0

N: per 25 cm. Other conditions as in Fig. 1.

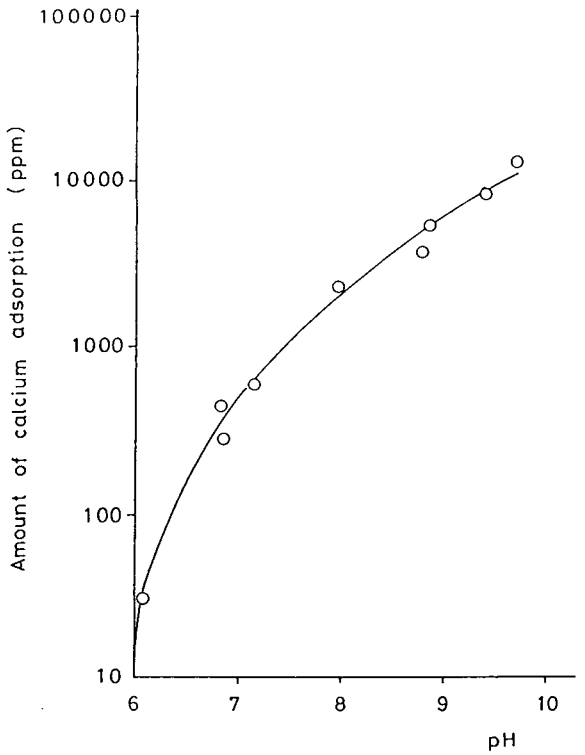

Fig. 3. Relationship between the extent of calcium adsorption from a 5% slurry solution for silica treated at different pH values.

and N-methylaniline) using NH_2-modified silica. As shown in Table 5 and Fig. 1 (Ca-II), Ca-II-modified silica could be also separate some basic model compounds as well as NH_2-modified silica.

Fig. 4 shows comparative chromatograms of some basic model compounds on Ca-II- and Ca-III-modified silica. It is interesting that the Ca-III-modified silica washed with distilled water could also separate some basic model compounds, as well as non-washed Ca-II-modified silica. The stabilities of the calcium columns were obtained under the conditions used in this study. N and A_s were measured on Ca-II- and Ca-III-modified silica, giving the data in Table 3.

Table 5
Chromatographic data for N,N-dimethylaniline and N-methylaniline (as basic model compounds) on Ca-0-, Ca-I-, Ca-II- and NH_2-modified silica

Modified silica	Separation factor, $\alpha = k'_A/k'_B$ (N-methylaniline vs. N,N-dimethylaniline)
Ca-0	1.00
Ca-I	1.25
Ca-II	5.62
NH_2	9.75

Conditions as in Table 4.

It is suggested that the separation mechanism is due mainly to Ca–Si bonds on the silica surface and that the silanol groups on the silica surface undergo an ion-adsorption interaction with the retention of some basic model compounds.

From studies on liquid chromatography with silica as sorbent, it is generally known that the interaction of the silica surface with the solute depends on the silanol groups. In previous papers [18,19], we assumed that the hydrogen-bonded silanol groups on the silica surface have an inhibitory effect on the retention of the solute and that the retention effect was due mainly to free silanol groups on the silica surface. Moreover, we assumed that the silanol groups which reacted with chemical reagents [hexamethyldisilazane (HMDS) or octadecyldimethylchlorosilane (ODS)], were mainly the free silanol groups on the silica surface. It was also shown that the silanol group concentration, $\alpha_{OH(s)}$, of the reactive silanols is almost constant at about 2 groups per 100 Å^2 (1 nm^2, mean pore diameter 116 Å, specific surface area 298 m^2/g, pore volume 1.22 ml/g, mean particle size 5.0 μm). According to our methods [18,19], the amount of calcium on the calcium-modified silica was suggested to be 0.574 groups per 100 Å^2 (1 nm^2) at pH 9.0.

These experimental results showed that calcium-modified silicas resulted in a drastic improvement in the separation of basic compounds, and a relatively small amount of calcium was needed to improve the separation of basic compounds.

In conclusion, the inexpensive Ca-II-modified silica seem to be more suitable for large-scale preparative separations of some basic model compounds, with easy preparation of the gels,

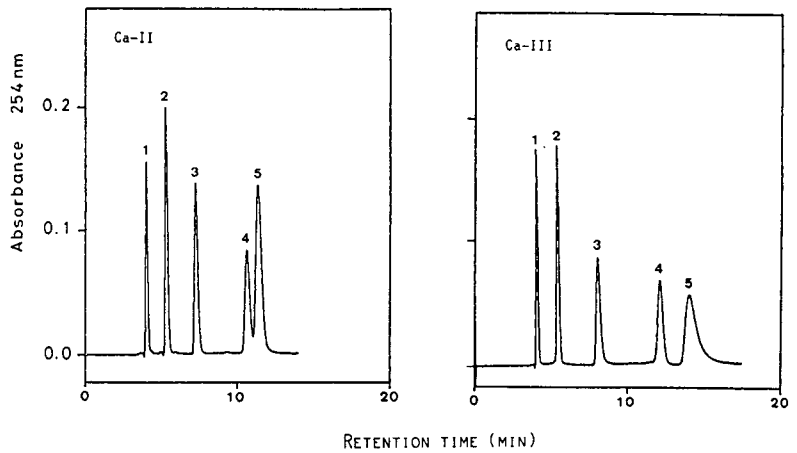

Fig. 4. Stability of calcium modified silica columns washed with distilled water. Other conditions as in Fig. 1. Ca-II = Ca-II-modified silica column not washed with distilled water; Ca-III = Ca-III-modified silica column washed with distilled water (1 ml/min, 1000 min). Eluent: Peaks; 1 = N,N-dimethylaniline; 2 = N-methylaniline; 3 = 2-ethylpridine; 4 = aniline; 5 = pyridine. methanol–*n*-hexane (1:99, v/v).

and health and safety and financial advantages for normal-phase LC packings in the laboratory.

It is concluded from the present investigation that it is not sufficient to evaluate column gels solely with regard to the amount of calcium on the calcium-modified silica. The relationship between the extent of calcium adsorption and the specific surface area of the silica supports must be considered further.

References

[1] A.V. Liselev, *Q. Rev. Chem. Soc.*, 15 (1961) 99.
[2] M.R. Basila, *J. Chem. Phys.*, 35 (1961) 1151.
[3] K.K. Unger, *Porous Silica*, Elsevier, Amsterdam, 1979.
[4] F. Vydra and J. Galba, *Collect. Czech. Chem. Commum.*, 32 (1967) 3530.
[5] F. Vydra and V. Stara, *Collect. Czech. Chem. Commum.*, 34 (1969) 3471.
[6] S.R. Morrison, *The Chemical Physics of Surfaces*, Plenum Press, New York, 1977.
[7] W.C. Still, M. Kahn and A. Mitra, *J. Org. Chem.*, 43 (1978) 2923.
[8] E. Heftmann, *Chromatography*, Part A, Elsevier, Amsterdam, 5th ed., 1992.
[9] E. Heftmann, *Chromatography*, Part B, Elsevier, Amsterdam, 5th ed., 1992.
[10] Y. Tanaka and G. Muto, *Anal. Chem.*, 45 (1973) 1864.
[11] W. Brown, *J. Chromatogr.*, 63 (1971) 478.
[12] W.A. Lada, *J. Radioanal. Chem.*, 50 (1979) 169.
[13] W.A. Lada and W. Smulek, *Radiochem. Radioanal. Lett.*, 34 (1978) 41.
[14] M.D. Arguello and J.S. Fritz, *Anal. Chem.*, 49 (1977) 1595.
[15] M. Okamoto, K. Nobuhara and D. Ishii, *Chromatographia*, in press.
[16] M. Okamoto, *J. Chromatogr.*, 202 (1980) 55.
[17] M. Okamoto and H. Kishimoto, *J. Chromatogr.*, 212 (1981) 251.
[18] M. Okamoto, K. Nobuhara and K. Jinno, *J. Chromatogr.*, 556 (1991) 407.
[19] M. Okamoto, K. Nobuhara, M. Masatani and K. Jinno, *Chromatographia*, 33 (1992) 203.

ELSEVIER

Journal of Chromatography A, 697 (1995) 159–164

JOURNAL OF CHROMATOGRAPHY A

Stability of high-performance liquid chromatography columns packed with C_1 and C_8 polysiloxanes sorbed into porous silica particles

Tania A. Anazawa, Francisco Carraro, Kenneth E. Collins, Isabel C.S.F. Jardim*

Instituto de Química, Universidade Estadual de Campinas, Caixa Postal 6154, 13083-970, Campinas, S.P., Brazil

Abstract

Columns, packed with 10 μm diameter porous silica particles (15 nm diameter pores) containing polydimethylsiloxane (20%, w/w) or polymethyloctylsiloxane (40%, w/w) sorbed into the pores, were tested for chromatographic stability as a function of elution volume. No significant changes in efficiency, retention factor or separation factor were observed following extended washing (up to 5000 column volumes) of either stationary phase with methanol–water mobile phases.

1. Introduction

Liquid–liquid chromatography (LLC) underwent considerable development from its introduction in 1941 [1] to the 1970s [2]. During this period liquid stationary phases became widely used for both normal- and reversed-phase chromatography. Packing materials having chemically bonded stationary phases have since displaced LLC: only a few specialized applications make use of LLC today. This is true despite the unique and potentially important characteristics of liquid-based stationary phases. To put this into perspective the advantages and disadvantages of these stationary phases should be considered.

Bonded phases have one great advantage over conventional liquid stationary phases: the structural groups (C_8, C_{18}, phenyl, etc.) are anchored to the silica support surface by covalent bonds which give a relatively high stability to these phases when used with conventional mobile phases. In contrast, most of the liquid stationary phases used in LLC since 1970 have consisted of small molecules ($M_r \leq 200$) which are retained in the pores of the support particles by much weaker dipolar (Van der Waals) attractive forces. Hence, these molecules are much more susceptible to loss (wash-out) in typical mobile phases. Indeed, to maintain the stationary liquid phase normally involves replacement of the molecules which are lost. This requires the presence of replacement stationary phase molecules in the mobile phase and very careful control of column temperature [2,3].

Two advantages of LLC over bonded-phase chromatography are equally impressive. Without the burden of chemical synthesis of a bonded phase, many different liquid materials, covering an enormous range of properties, can be considered. This can, in principle, open up HPLC to separations with a vast array of specific-interaction stationary phases. Another advantage is

* Corresponding author.

0021-9673/95/$09.50
SSDI 0021-9673(94)00810-8

the high reproducibility which can be achieved in routine separations with LLC columns [4], the reason being that the silica–stationary phase interface in LLC does not affect the chromatographic separation as much as in the case of bonded-phase HPLC. In addition, LLC stationary phases, but not bonded phases, can be repaired —or even replaced— to restore the initial separation properties of a column.

To decrease the stability (wash-off) problem in LLC, polymeric liquids can be considered. In this way the molecules which constitute the stationary phase can have very many weak (physical) bonds to the support surfaces and to

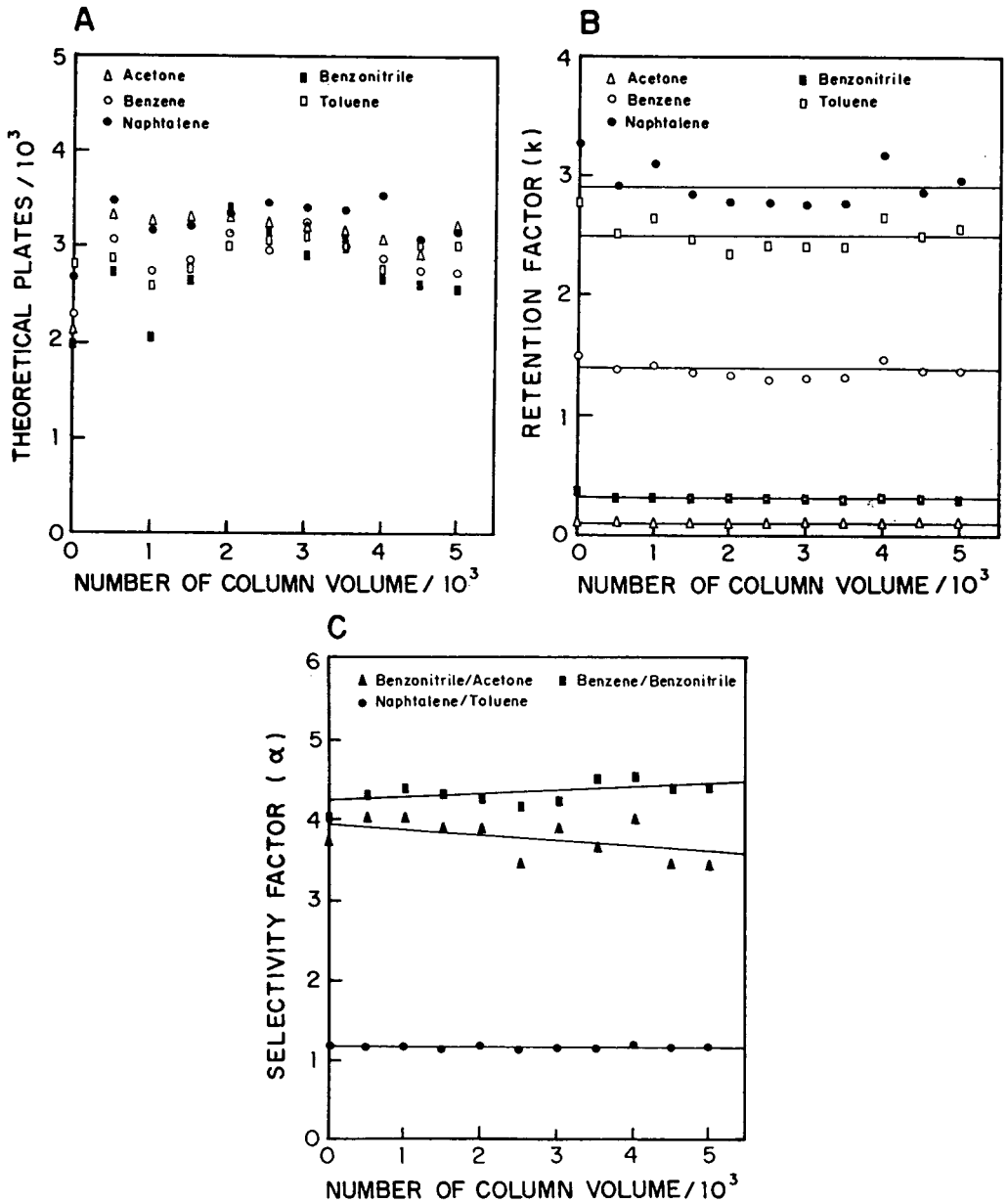

Fig. 1. (A) Column efficiency (theoretical plates, N); (B) retention factor (k) and (C) selectivity factor (α) as functions of volume of mobile phase passing a column packed with 20% (w/w) PDMS-loaded silica support.

each other, resulting in a degree of general stability of the phase even in the presence of moderately strong mobile phases. A number of polymeric materials were tested as possible LLC stationary phases prior to 1970 [5]. This work, largely with polyethylene glycols (Carbowaxes) with molecular masses in the range 200–20 000, led to the conclusion that column efficiency decreases with increasing molecular mass [5]. An explanation was that the viscosity of the polymer, which increases with its molecular mass, affects the diffusive mobility of solutes in the pores of porous supports and thus leads to increased band dispersion in the column.

However, we have recently shown [6] that separations carried out with a polymethyloctylsiloxane (PMOS) liquid phase on silica has a chromatographic behaviour remarkably similar to that obtained with conventional C_8 bonded phases.

In the present paper we show that high-molecular-mass polydimethylsiloxane (PDMS) and PMOS stationary phases are quite stable to extended washing with methanol–water mobile phases and that good chromatographic efficiency is achieved and maintained with these viscous liquid phases.

2. Experimental

2.1. Materials

Methanol (LiChrosolv), dichloromethane (LiChrosolv) and carbon tetrachloride (analytical-reagent grade) were obtained from Merck (Rio de Janeiro, Brazil).

The chromatographic test substances (acetone, benzonitrile, benzene, toluene and naphthalene) were analytical-reagent grade and not further purified.

Davisil silica having a mean particle diameter of 10 μm, a 15 nm mean pore diameter and a 240 $m^2\ g^{-1}$ specific surface area was obtained from Alltech (USA).

PDMS (product PS-048; M_r 139 000) and PMOS (product PS-140; M_r 6200) were obtained from Hüls America (USA).

2.2. Preparation of packing materials

Following drying at 150°C for 24 h, weighed quantities of the silica were added to solutions containing weighed quantities of polysiloxane (PDMS or PMOS) in 60 ml of dichloromethane. The mixtures were gently stirred for 3 h at room temperature and then the solvent was allowed to evaporate, without stirring, at room temperature.

2.3. Preparation of columns

Columns of 125 × 2.9 mm (PDMS) or 125 × 3.4 mm (PMOS) were made from type 316L stainless-steel tubing with highly polished interior surfaces. The columns were slurry packed at 38 MPa using a 10% (w/v) slurry of the prepared packing material in carbon tetrachloride.

2.4. Instrumentation

Two medium dispersion chromatographic systems were used. System 1 (PDMS column) used an Altex Model 110A pump, a Rheodyne Model 7125 injector with a 10-μl loop, and a Schoeffel Model SF 770 spectrophotometric detector (254 nm; 8 μl cell volume), coupled to an ECB Model RB 102 recorder. System 2 (PMOS column) consisted of a Waters Model 510 pump, SSI Model 3XL pneumatic injector with a 10-μl loop and a Waters Model 481 spectrophotometric

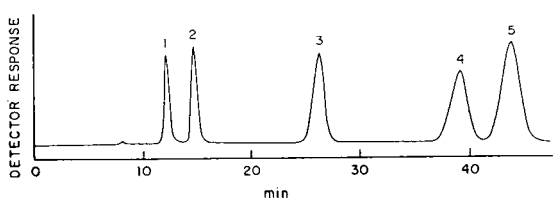

Fig. 2. Chromatogram obtained with a column packed with 20% (w/w) PDMS-loaded silica support at the end of the washing test. Peaks: 1 = acetone; 2 = benzonitrile; 3 = benzene; 4 = toluene; 5 = naphthalene. Column: 125 × 2.9 mm, mobile phase: methanol–water (50:50, v/v), flow-rate: 0.1 ml min^{-1}, detection: UV at 254 nm.

detector (254 nm; 14 μl cell volume), coupled to a Waters Model 740 integrator.

2.5. Stability testing

Methanol–water mobile phases (50:50 or 70:30, v/v) were passed through the columns at 2 ml min^{-1} to a total of 5000 column volumes. Chromatograms of a mixture of test compounds were obtained periodically with the same mobile phases as used for washing, at flow-rates of 0.1 and 0.2 ml min^{-1}, with the columns containing PDMS and PMOS, respectively. Efficiency (N), retention factor (k) and selectivity factor (α)

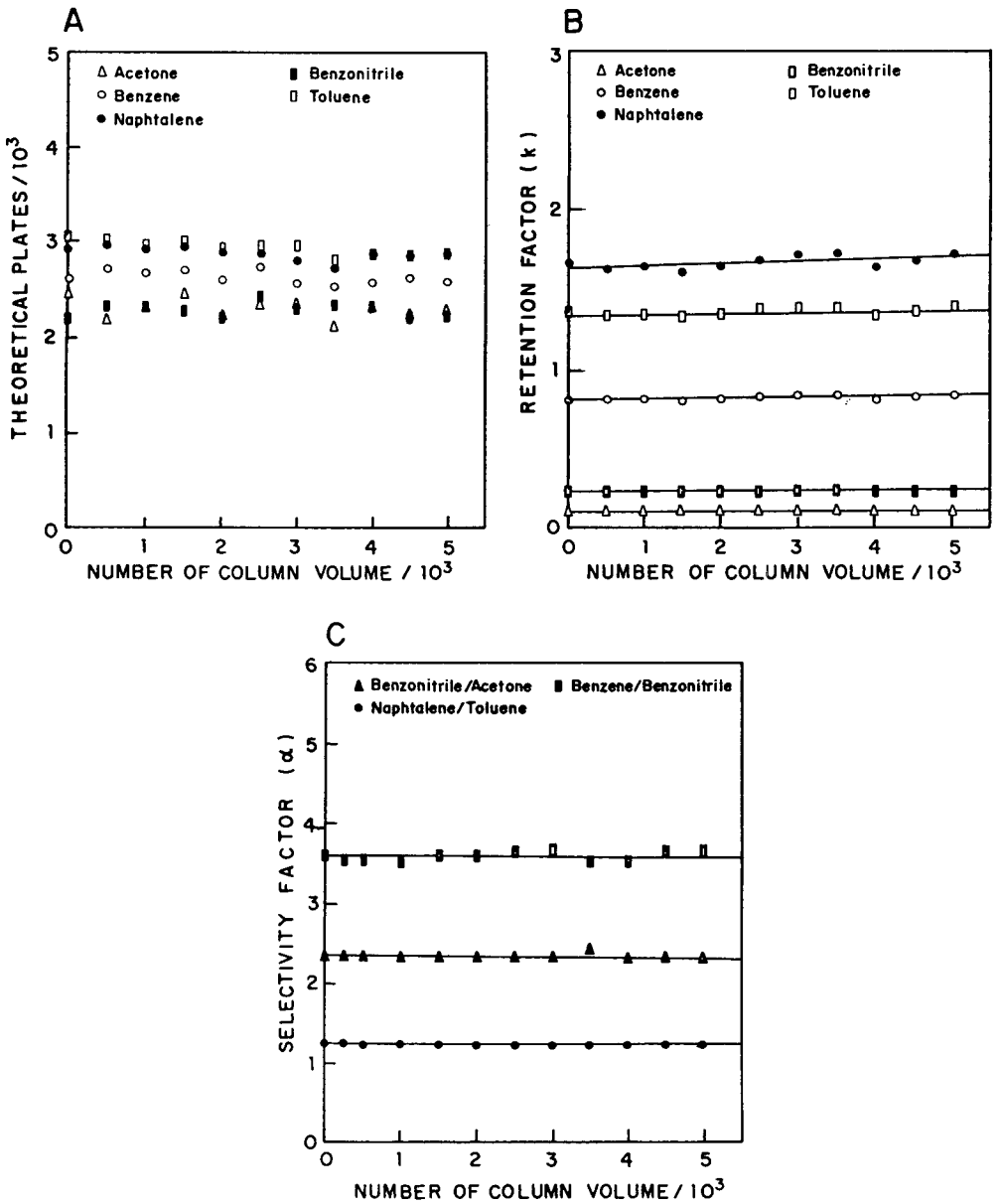

Fig. 3. (A) Column efficiency (theoretical plates, N); (B) retention factor (k) and (C) selectivity factor (α) as functions of volume of mobile phase passing a column packed with 40% (w/w) PMOS-loaded silica support.

values were determined from the chromatograms. The high flow-rate (2 ml min^{-1}) was used for the column washing so that the total time for the 5000 column volumes would not be excessive and to have somewhat stronger "wash-out" conditions. The lower flow-rates (0.1 and 0.2 ml min^{-1}) were near optimal for separations made with the two columns.

3. Results and discussion

Fig. 1 shows measurements of N, k and α for a column packed with 20% (w/w) PDMS-loaded packing material during column washing with a methanol–water (50:50) mobile phase. The column efficiency values fluctuate, reflecting the fact that the column temperature (and perhaps other experimental parameters) were not constant during the different chromatographic tests. Nevertheless, no general trend is apparent as evidence of column deterioration. The retention and selectivity factors, being relative parameters, show much less fluctuation and serve as indicators that no significant changes in column structure or function have taken place. The chromatogram obtained at the end of the washing test for this column is shown in Fig. 2.

Fig. 3 shows the corresponding chromatographic results for a column packed with 40% PMOS-loaded packing material. With no apparent changes in retention or selectivity factors resulting from the extended washing treatment, there is no indication of significant changes in this column. Chromatograms taken at the beginning and the end of the washing test (Fig. 4) likewise show that no significant changes have occurred.

The efficiencies obtained for the columns packed with PDMS and PMOS were ca. 26 000 and ca. 23 000 plates/m, respectively, for the naphthalene solute. Thus, the efficiencies of the two packings are similar. A comparison of the separations obtained with the five test solutes on the two packings can be made from ratios of corresponding retention factors (Figs. 1B and 3B). These k_{PDMS}/k_{PMOS} ratios are 0.91, 0.69, 0.55, 0.52 and 0.55 for acetone, benzonitrile, benzene, toluene and naphthalene, respectively.

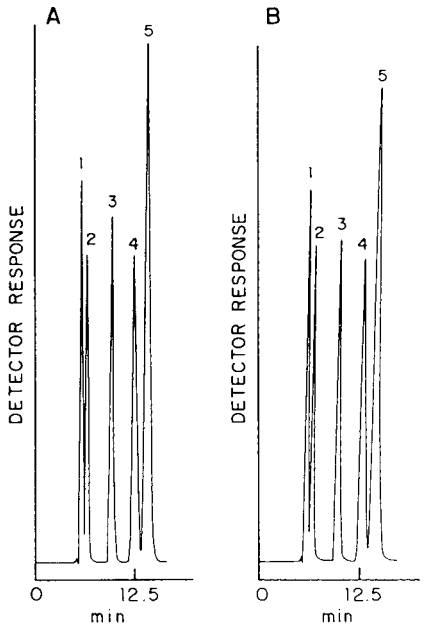

Fig. 4. Chromatograms obtained with a column packed with 40% (w/w) PMOS-loaded silica support at the beginning (A) and the end (B) of the washing test. Peaks as in Fig. 2. Column: 125 × 3.4 mm, mobile phase: methanol–water (70:30, v/v), flow-rate: 0.2 ml min^{-1}, detection: UV at 254 nm.

Thus, the more polar solutes (acetone and benzonitrile) behave differently than the less polar solutes on the two packings, with the residence time of the more polar solutes longer in the PDMS stationary phase than in the PMOS one. We can only speculate on the mechanistic basis for these chromatographic differences but, presumably, geometric differences in the "packing" of the long-chain polysiloxane molecules in the pores, as well as the viscosity differences, are controlling factors.

4. Conclusions

Moderately high viscosity (ca. 10^3–10^5 cSt) polysiloxane liquids, and presumably many other large-molecule liquids, can be used as stationary phases for reversed-phase HPLC. The polysiloxane phases are remarkably stable to wash-off by typical mobile phases such as methanol–water solutions. The efficiencies of columns prepared

with polysiloxane-loaded packing materials are similar to those obtained with conventional bonded-phase packing materials of the same pore diameter.

Thus, LLC with large-molecule stationary phases should be considered for chromatographic applications in which exotic functional group properties, long-term reproducibility or packing material economy are especially important.

References

[1] A.J.P. Martin and R.L.M. Synge, *Biochem. J.*, 35 (1941) 1358.
[2] L.R. Snyder and J.J. Kirkland, *Introduction to Modern Liquid Chromatography*, Wiley, New York, 2nd ed., 1979, Ch. 8, p. 323.
[3] J.P. Crombeen, S. Heemsta and J.C. Kraak, *J. Chromatogr.*, 286 (1984) 119.
[4] S.H. Hansen, P. Helboe and M. Thomsen, *J. Chromatogr.*, 544 (1991) 53.
[5] J.A. Schmit, in J.J. Kirkland (Editor), *Modern Practice of Liquid Chromatography*, Wiley, New York, 1971, Ch. 11, p. 375.
[6] T.A. Anazawa and I.C.S.F. Jardim, *J. Liq. Chromatogr.*, 17 (1994) 1265.

ELSEVIER

Journal of Chromatography A, 697 (1995) 165–174

JOURNAL OF CHROMATOGRAPHY A

Separation of polycyclic aromatic hydrocarbons on a wide-pore polymeric C_{18} bonded phase

Willy Hesselink[a,*], Ruud H.N.A. Schiffer[a], Peter R. Kootstra[b]

[a]*Research and Development Department, J.T. Baker, P.O. Box 1, 7400 AA Deventer, Netherlands*

[b]*Laboratory of Organic-Analytical Chemistry, National Institute of Public Health and Environmental Protection (RIVM), P.O. Box 1, 3720 BA Bilthoven, Netherlands*

Abstract

This paper presents a novel wide-pore C_{18} bonded phase. This bonded phase has polymeric properties and can separate a broad range of polycyclic aromatic hydrocarbons (PAHs) in different matrices. A column selectivity test mixture containing three well known chosen PAHs was used to evaluate the selectivity ($\alpha_{TBN/BaP}$ value) of the bonded phase under sub-ambient, ambient and elevated temperatures. The variation of the column selectivity with temperature was studied. The results showed that the separation of critical PAH isomers increased with decreasing temperatures. The separation of the 16 US Environmental Protection Agency PAH priority pollutants was found to vary continuously with temperature and $\alpha_{TBN/BaP}$ value. The effect of the slope of the gradient was also investigated and it was proved that a steeper gradient increased the separation of dibenz[*a*,*h*]anthracene and benz[*ghi*]perylene. Due to the fact that the column has a relative small internal diameter (3.0 mm), reduction of the mobile phase consumption was found to be almost 50% compared to the standard-size (4.6 mm) HPLC columns.

1. Introduction

Polycyclic aromatic hydrocarbons (PAHs) are environmental pollutants formed at high temperatures and under pyrolytic conditions during the incomplete combustion of organic matter. They are found in air, water and soil. Sources of PAHs are widespread including coal/oil-burning power plants, coke oven plants and exhaust gases from traffic. The World Health Organization has issued a guide value maximum of 10 mg/ml for the single PAH benzo[*a*]pyrene [1].

Because certain PAH isomers exist and because many of these PAHs are toxic or even carcinogenic/mutagenic [2], the development of an accurate and sensitive separation method is needed. Recommended analytical procedures are documented or proposed in several USA and European guidelines including the US Environmental Protection Agency (EPA) methods [3–5], International Standard Organization (ISO) method [6], German Standard (DIN) method [7] and Dutch Standard (NEN) method [8].

The EPA methods comprises a list of 16 PAH priority pollutants; the German and Dutch standard methods only specify 6 and 10 PAHs, respectively.

Because more and more PAHs are identified and investigated on their toxicity it can be expected that the list will be extended in the near

* Corresponding author.

0021-9673/95/$09.50
SSDI 0021-9673(94)01050-1

future. All of these methods specify reversed-phase chromatography using octadecyl (C_{18}) bonded phases in combination with either fixed or wavelength-programmed ultraviolet (UV) and fluorescence (FL) detection techniques.

Several extraction techniques including liquid–liquid extraction (LLE) and solid-phase extraction (SPE) procedures [9], are used to clean-up or/and pre concentrate low levels of PAHs in various

matrices. SPE is recommended in EPA method 550.1 using either C_{18} cartridges or extraction disks [3]. It is well known that differences in retention and selectivity for the separation of this important group of compound exist among commercial available C_{18} columns [10]. These differences result from variation in a number of parameters in the manufacturing of the bonded phase, including alkyl chain length [11], phase coverage [12,13], pore size [14] and the type of surface modification chemistry employed [15]. Selectivity differences among "PAH columns" have been reported by a number of workers [16–18]. These differences have been pronominal related to the nature of the bonded phase. Bonded phases that are prepared using silane modification can be produced in two different ways depending on the reagents and reaction conditions used in the bonded phase synthesis resulting in either monomeric or polymeric stationary phases [19]. Column selectivity is found to vary continuously with temperature, regardless of the type of bonded phase used [20]. A simple test with three carefully chosen PAH solutes {phenanthro[3,4-*c*]phenanthrene (PhPh), 1,2:3,4:5,6:7,8-tetrabenzonaphthalene (TBN) and benzo[*a*]pyrene (BaP) } can be used to discriminate between both phase types [21]. This test also provides useful information about the selectivity towards critical PAH pairs. This paper presents a novel wide-pore polymeric C_{18} bonded phase which can be used for the separation of a broad range of PAHs. The separation of both the six Borneff PAHs and the already stated 16 priority pollutants will be demonstrated using either isocratic or gradient elution. Also the effect of the column temperature and the slope of the gradient will be discussed. The differences in selectivity will be shown on the basis of chromatograms obtained from wide-pore polymeric C_{18} prepared with different $\alpha_{TBN/BaP}$ values.

2. Experimental

2.1. Chemicals

HPLC-gradient grade acetonitrile and water were from J.T. Baker (Deventer, Netherlands). Standard reference material (SRM) 1647c consists of an acetonitrile solution of 16 PAHs identified by the EPA as priority pollutants. SRM 869 was used to perform a selectivity test and contains BaP, TBN and PhPh. SRM 1597, a neutral, combustion-related mixture of PAHs isolated from coal tar is used to evaluate the performance of the chromatographic column. All SRMs were obtained from the National Institute of Standards and Technology (NIST, Gaithersburg, MD, USA) and were diluted to appropriate concentrations using HPLC-grade solvents. The six Borneff PAHs including perylene were used from a premixed (7 PAH mixture) standard (J.T. Baker).

2.2. Instrumentation

The HPLC gradient system (Perkin-Elmer, Norwalk, CT, USA) consisted of a Model LC-250 binary pump, a Model LC-290 UV–Vis variable-wavelength spectrophotometer and a Model LC 240 fluorescence detector. Data from this system were collected and evaluated using a Model 1020 LC integrator or a Model BD 111 flatbed recorder (Kipp and Zonen, Delft, Netherlands). Injections were done using a Model 7125 injector (Rheodyne, Cotati, USA) with a 20-μl sample loop. The HPLC column (Bakerbond PAH-16 Plus, 250 × 3.0 mm I.D. + integrated guard column, 20 × 3.0 mm I.D.) was filled with wide-pore (300 Å) polymeric C_{18} with a particle size of 5 μm (J.T. Baker).

A Mistral column thermostat (Spark Holland, Emmen, Netherlands) was used to obtain reproducible data between 10 and 45°C.

2.3. HPLC method

The selectivity of different batches of bonded phases was evaluated using SRM 869 test mixture under isocratic conditions with acetonitrile–water (85:15, v/v) at a flow-rate of 0.8 ml/min and at 25 ± 1°C. The peaks were monitored at 254 nm. SRM 1647c and SRM 1597 were both analyzed using different gradients (as described along the figures) at a flow-rate of 0.5 ml/min and temperature controlled. Both UV and fluorescence detection (either fixed or wavelength programmed) were used to monitor the PAHs. The six Borneff PAHs including perylene were separated isocratically using acetonitrile at a flow-rate of 0.5 ml/min and under sub-ambient conditions at 254 nm.

3. Results and discussion

3.1. Bonded phase design and column dimensions

The separation of PAHs is greatly influenced by the type of synthesis that is used for the preparation of C_{18}. In reversed-phase chromatography two types of silane modification can be distinguished that resulted in either monomeric or polymeric bond linkages. Monomeric phases are distinct greatly from polymeric phases when considering the selectivity of PAHs. The polymeric phases provided significantly enhanced selectivity characteristics, particularly for isomeric PAHs.

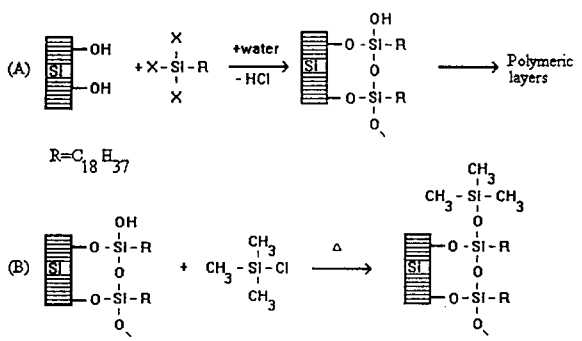

Fig. 1. Synthesis of polymeric C_{18} bonded phase using (A) trifunctional silane, (B) end-capping procedure.

Table 1
Physical properties of Bakerbond wide-pore polymeric C_{18} bonded phase synthesised under polymer-forming conditions

Physical property	Value
Mean particle diameter	5.0 μm
Pore diameter	17.3 nm
Pore volume	0.37 ml/g
Surface area	80 m^2/g
Carbon loading	7.0% C
Bonded phase coverage	4.5 μmol/m^2

Tests (e.g. mercury porosimetry technique) were performed using standard analytical procedures developed at J.T. Baker.

The Bakerbond PAH-16 plus column contains a wide-pore C_{18} bonded phase synthesised under polymer-forming conditions [22]. Polymeric

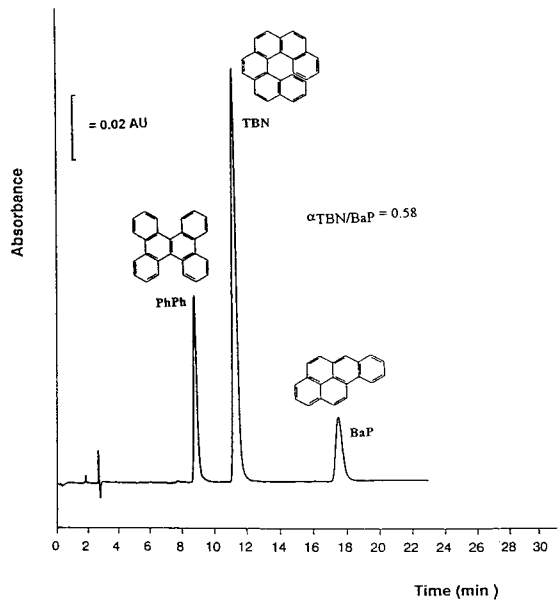

Fig. 2. Separation of SRM 869 on Bakerbond wide-pore (300 Å) C_{18} bonded phase. Conditions: column: 250 × 3.0 mm I.D., 5-μm particles; mobile phase: acetonitrile–water (85:15) at a flow-rate of 0.5 ml/min; temperature: 25 ± 1°C; UV detection at 254 nm; injection of 20 μl SRM 869 [5-fold dilution in acetonitrile–water (85:15, v/v)]. PhPh = Phenanthro[3,4-*c*]phenanthrene (0.49 μg/ml); TBN = tetrabenzonaphthalene (1.74 μg/ml); BaP = benzo[*a*]pyrene (0.33 μg/ml).

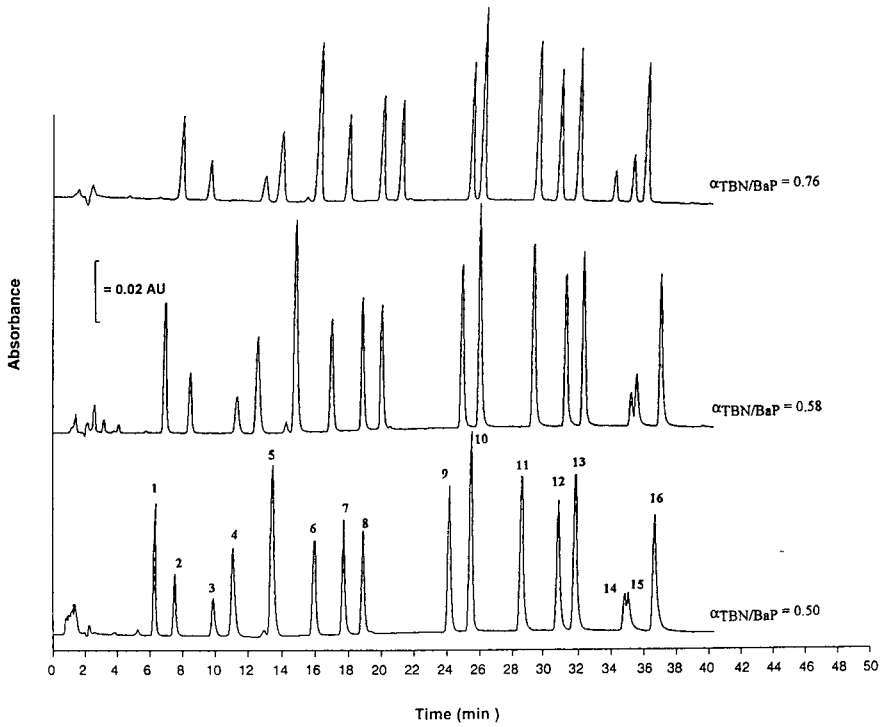

Fig. 3. Separation of SRM 1647c on three different batches Bakerbond wide-pore (300 Å) C_{18} bonded phase with different $\alpha_{TBN/BaP}$ values. Conditions: column: 250 mm × 3.0 mm I.D., 5-μm particles; mobile phase: acetonitrile–water (50:50) during 5 min, then linear gradient to 100% acetonitrile in 25 min at a flow-rate of 0.5 ml/min; temperature: 25 ± 1°C; UV detection at 254 nm; injection of 10 μl SRM 1647c [two-fold dilution in acetonitrile–water (50:50, v/v)]. Peaks: 1 = naphthalene (9.98 μg/ml); 2 = acenaphthalene (7.71 μg/ml); 3 = acenaphthene (10.28 μg/ml); 4 = fluorene (2.38 μg/ml); 5 = phenanthrene (1.74 μg/ml); 6 = anthracene (0.40 μg/ml); 7 = fluoranthene (3.83 μg/ml); 8 = pyrene (4.26 μg/ml); 9 = benz[*a*]anthracene (2.04 μg/ml); 10 = chrysene (1.85 μg/ml); 11 = benzo[*b*]fluoranthene (2.10 μg/ml); 12 = benzo[*k*]fluoranthene (2.34 μg/ml); 13 = benzo[*a*]pyrene (2.46 μg/ml); 14 = dibenz[*a,h*]anthracene (1.80 μg/ml); 15 = benzo[*ghi*]perylene (1.84 μg/ml); 16 = indeno[1,2,3-*cd*]pyrene (2.15 μg/ml).

phases can be prepared in two distinct ways, either by adsorbing a known quantity of water onto dry silica before reacting with the polyfunctional silane or in which the water is added directly into the reaction slurry to initiate polymerisation reaction. In the first method polymerisation of the silane is initiated by the adsorbed water at the silica surface. Bonded phases that are prepared using trifunctional silanes in the presence of water results in the formation of silane silanols, which can subsequently react with other silane molecules (cross-linking reactions) to form a silane polymer structure as illustrated in Fig. 1. The resulting hydrophobic surfaces are known to be hydrolytically stable [23]. For every silanol group that disappears during the reaction, two new ones are potentially formed once the product is brought in contact with water. These silanol groups can subsequently be removed (end-capped) by reaction with a small monofunctional silane, e.g. trimethylchlorosilane (TMCS). Higher retention and slightly better resolution of compounds were obtained with end-capped polymeric C_{18} bonded phases. The access of small polar molecules to any "free" silanols within or underlying such polymer bonded phase has been shown to be lower than for bonded phase prepared from monofunctional silanes [24]. Consequently, the rate of equilibration of a polymer phase with mobile phase is more rapid than with

a monomeric phase [25]. Some important physical properties of the wide-pore polymeric C_{18} bonded phase, used in this study, are illustrated in Table 1. It is important to control the ligand density, because this property may influence the chromatographic selectivity and binding capacity of the bonded phase. Shape selectivity for PAH isomers increases with increasing phase density [26]. The pore size of the bonded phase also plays an important role in the phase selectivity. On narrow-pore (<100 Å) polymeric bonded phases isomers may coelute, whereas on wide-pore (e.g. 300 Å) material complete resolution can be achieved [19].

The flow-rate of the mobile phase is proportional to the square of the column diameter [27]. This means that the mobile phase consumption can be reduced by half when using a medium-bore (3.0 mm I.D.) column instead of one of 4.6 mm I.D. (standard-size column).

When the sample size is limited; this is sometimes the case when small elution volumes are used to elute the PAHs during the sample preparation step; the use of narrower columns result in better sensitivity due to the fact that the minimum detectable mass (not concentration!) is lower.

3.2. Bonded phase PAH selectivity test

All wide-pore C_{18} batches are subjected (internal quality control) to a characterization method developed by Wise and May [12,28]. This test is based on the retention of three carefully chosen PAH solutes as shown in Fig. 2. The test is intended primarily for predicting the potential selectivity for complex PAH mixtures and to discriminate between monomeric and polymeric type of C_{18} stationary phases. The selectivity factor $\alpha_{TBN/BaP}$ (k'_{TBN}/k'_{BaP}) correlates with the retention characteristic of PAHs and the bonded phase chemistry.

The elution order for polymeric type C_{18} should be PhPh, TBN and then BaP, as shown in Fig. 2. A classification scheme has been proposed, based on measurement of $\alpha_{TBN/BaP}$ values for experimental and commercial C_{18} columns [30]. Generally, column selectivity is enhanced with lower $\alpha_{TBN/BaP}$ values. It is of extremely important to control the $\alpha_{TBN/BaP}$ during the C_{18} production. It should be noted that a small variation in this value will improve the precision of the PAH analysis. The $\alpha_{TBN/BaP}$ test is used by J.T. Baker to verify column reproducibility and assist in the adjustment of the bonding process. The influence of the $\alpha_{TBN/BaP}$ value is demonstrated in Fig. 3 in which the separation of SRM 1647c on three different batches (with variable $\alpha_{TBN/BaP}$ values) of wide-pore polymeric C_{18} is illustrated. Separation of all 16 PAHs can be achieved on bonded phases with $\alpha_{TBN/BaP}$ values between 0.6 and 0.8. At lower $\alpha_{TBN/BaP}$ values retention times of peaks 1–10 are decreased significantly. The resolution between the four-ring isomers benz[*a*]anthracene and chrysene is increased when the $\alpha_{TBN/BaP}$ value is decreased. The six-ring isomers benzo[*ghi*]perylene and indeno[1,2,3-*cd*]pyrene are better resolved at lower $\alpha_{TBN/BaP}$ values, but it should be noted that dibenz[*a,h*]anthracene and benzo[*ghi*]-perylene will coelute or even reversed when bonded phases with too low $\alpha_{TBN/BaP}$ values are used.

3.3. Fluorescence programmed-wavelength detection of PAHs

Two of the difficulties in the analysis of PAHs are the low levels in which they have to be determined (low- to sub-μg/l levels) and the relative complexity of the matrices of natural mixtures of PAHs from environmental extracts. Interfering compounds may coelute with the PAHs to be determined due to similar physical and chemical properties. Therefore a selective and sensitive detection technique is required. Fluorescence detection is the most sensitive and selective technique used for the measurement of PAHs in the picogram range. The EPA prescribes the use of both UV detection at 255 nm (for the first four PAHs) and fluorescence detection [excitation wavelength (λ_{ex}) 280 nm; emission wavelength (λ_{em}) >390 nm with cut-off filter).

To apply maximum selectivity and sensitivity in quantification, the proper fluorescence excita-

tion and emission wavelengths must be chosen. Retention times must be perfectly reproducible and the baseline segment between two peaks must be long enough in order to change the $\lambda_{ex}/\lambda_{em}$ wavelength accurately.

It is well known that due to the lack of native fluorescence acenaphthylene must be detected with UV detection techniques (e.g. diode array detector).

The analysis of SRM 1647c and SRM 1597, which is a complex natural pyrolytic mixture of PAHs from coke oven tar, is depicted in Fig. 4 and demonstrates the use of wavelength-programmed fluorescence detection.The tar standard contains 12 certified PAHs and 18 non-certified PAHs/polycyclic aromatic compounds and was injected without any sample preparation procedure (only diluted a factor 200 with mobile phase). Due to the high selectivity of both the stationary phase and the fluorescence detector 13 peaks were identified by comparison of the retention times. The first peak in the chromatogram comes from toluene that was used as dissolvation solvent for the standard material. The excellent resolution of the stationary phase permits switching the $\lambda_{ex}/\lambda_{em}$ wavelengths 9 times which results in a very clean baseline.

3.4. Effect of the temperature

Reversed-phase separations are commonly carried out under ambient conditions, although temperature can have significant effect on the resolution of compounds in particular for PAHs [20].

The separation of six methylchrysene isomers

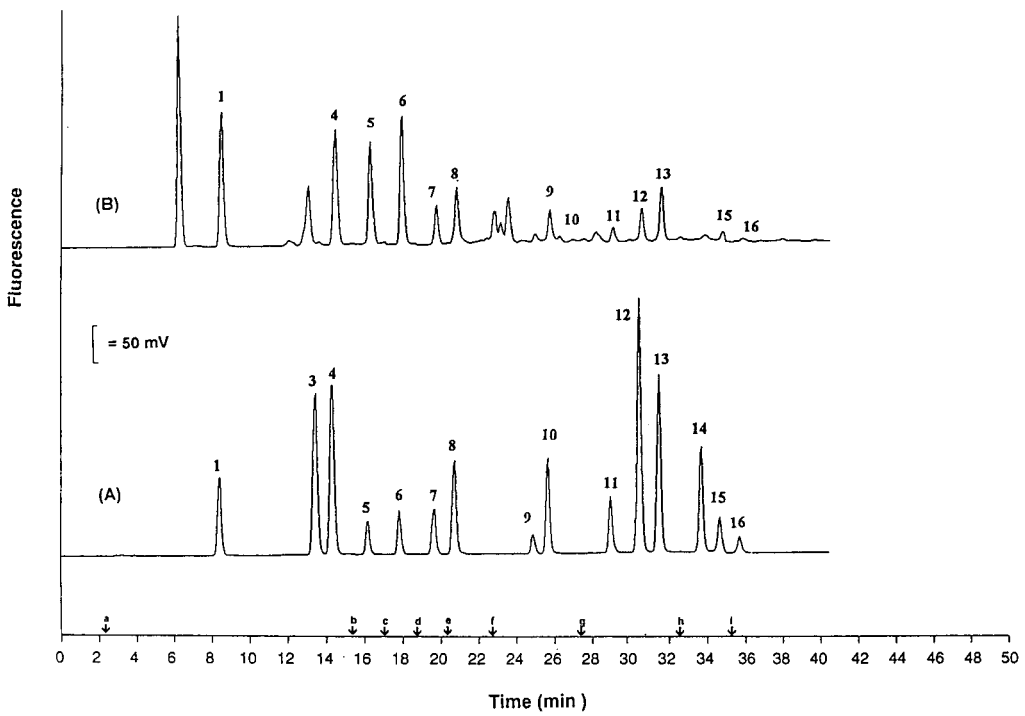

Fig. 4. Separation of (A) SRM 1647c and (B) SRM 1597, a complex mixture of PAHs from coal tar performed on Bakerbond wide-pore (300 Å) C_{18} bonded phase ($\alpha_{TBN/BaP,20°C} = 0.66$) using wavelength-programmed fluorescence detection. Conditions: mobile phase: acetonitrile–water (50:50) during 5 min, then linear gradient to 100% acetonitrile in 25 min and hold during 20 min; flow-rate: 0.5 ml/min; temperature: 20 ± 1°C; injection of 5 μl SRM 1647c [two-fold dilution in acetonitrile–water (50:50, v/v)] and injection of 5 μl SRM 1597 [200-fold dilution in acetonitrile–water (50:50, v/v)]; fluorescence program ($\lambda_{ex}/\lambda_{em}$ in nm): a = 280/330; b = 250/370; c = 250/405; d = 280/450; e = 270/390; f = 265/380; g = 290/430; h = 290/410; i = 300/500. Peaks as in Fig. 3.

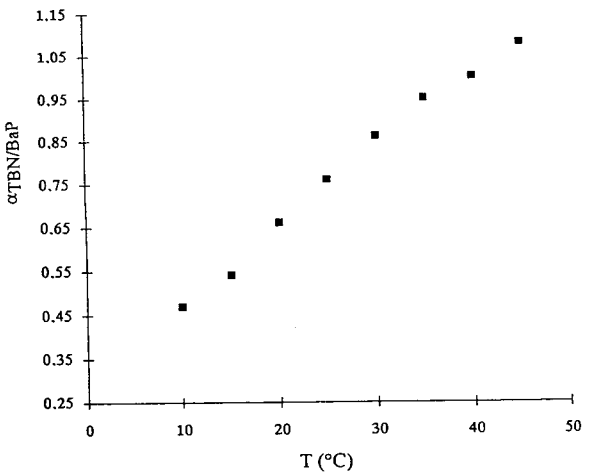

Fig. 5. Influence of the temperature on the selectivity factor $\alpha_{TBN/BaP}$. Conditions as in Fig. 2; temperatures: 10, 15, 20, 25, 30, 35, 40, 45 ± 1°C.

at ambient and sub-ambient temperatures has been described in Ref. [20]. All six isomers were resolved with Bakerbond wide-pore C_{18} under isocratic conditions using sub-ambient temperature program. The separation demonstrates the enhancement of shape selectivity for polymeric C_{18} at lower temperatures.

The dependence of selectivity on temperature for Bakerbond wide-pore C_{18} is illustrated in a plot of $\alpha_{TBN/BaP}$ vs. temperature in Fig. 5. At elevated temperatures, the relative retention of BaP (planar shaped molecule) decreased relative to TBN (non-planar shaped molecule) which means that the $\alpha_{TBN/BaP}$ increased. At lower temperatures $\alpha_{TBN/BaP}$ decreased.

In previous studies [11,13] it was suggested that non-planar or more compact PAHs elute earlier than planar or long narrow PAHs due to differences in penetration capability into the

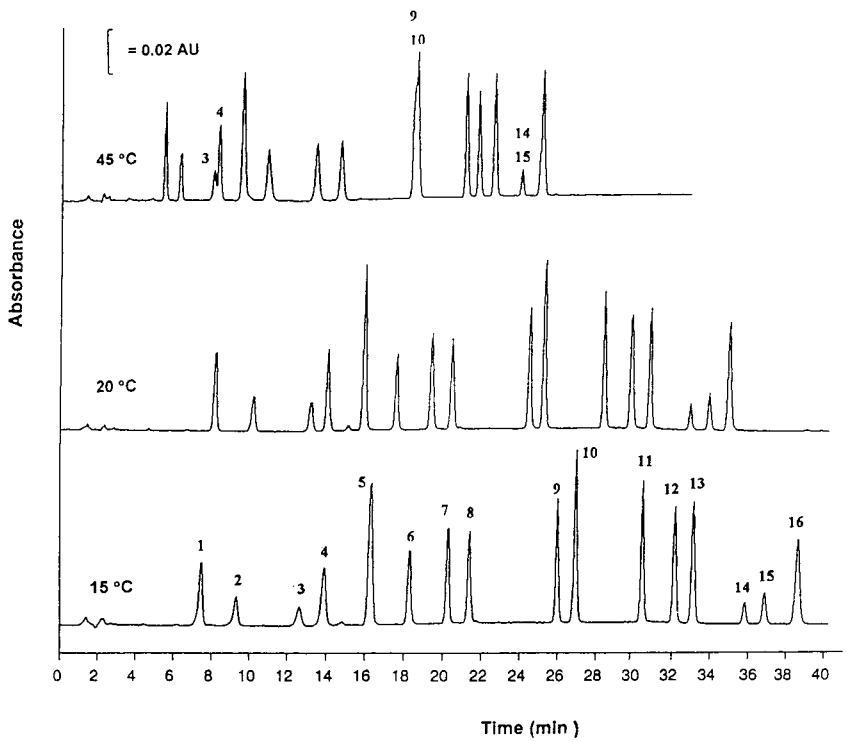

Fig. 6. Influence of the temperature on the separation of SRM 1647c. Conditions as in Fig. 3; temperatures: 15, 20, 45 ± 1°C.

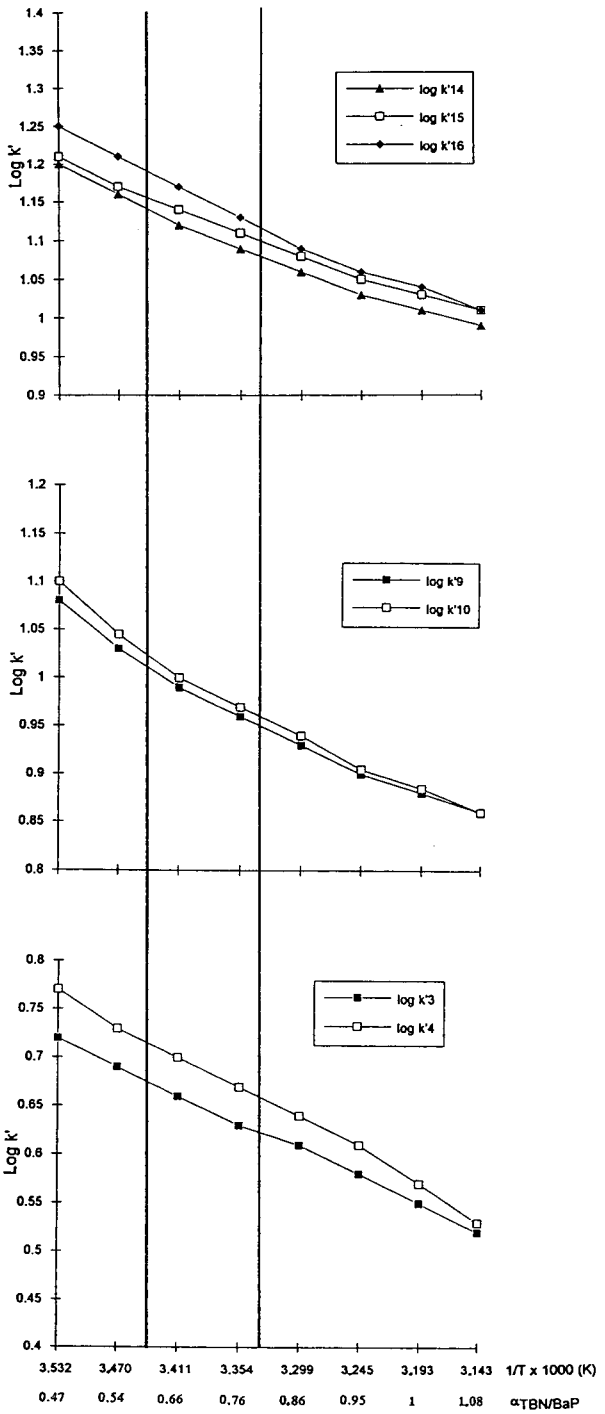

Fig. 7. Van't Hoff plots for monitoring the selectivity of some critical PAH isomers. Conditions as in Fig. 3; temperatures: 10, 15, 20, 25, 30, 35, 40, 45 ± 1°C.

stationary phase. The results obtained here agreed with these statements.

The separation of the 16 priority pollutant PAHs is also very sensitive to temperature variations as illustrated in Fig. 6. These chromatograms illustrates clearly that the selectivity changes dramatically with the temperature.

Three Van't Hoff plots, in which the log k' of some critical PAH pairs are plotted against $1/T$, are illustrated in Fig. 7. The figure also contains temperature related $\alpha_{TBN/BaP}$ values.

The enthalpy effect ($\Delta H_{m\rightarrow s}$) of the retention process can be determined from the slope of the curve. Non-linear plots points to an existence of

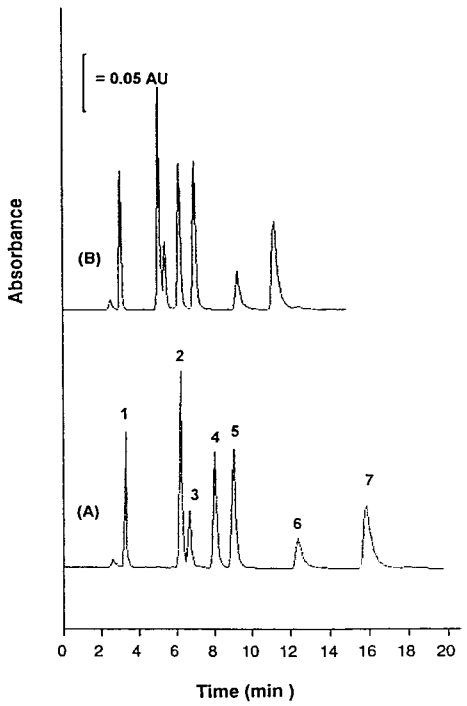

Fig. 8. Isocratic separation of seven PAHs (Borneff PAHs, including perylene) specified in DIN method 38407, Part 8, using Bakerbond wide-pore (300 Å) bonded phase. Conditions: 250 × 3.0 mm I.D. column, 5-μm particles; mobile phase: 100% acetonitrile at a flow-rate of 0.5 ml/min; temperature: (A) 15°C; (B) 20°C; UV detection at 254 nm; injection of 5.0 μl PAH-7 mixture (5-fold dilution in acetonitrile). Peaks: 1 = fluoranthene (10.0 μg/ml); 2 = benzo[*b*]fluoranthene (10.0 μg/ml); 3 = perylene (5.0 μg/ml); 4 = benzo[*k*]fluoranthene (10.0 μg/ml); 5 = benzo[*a*]pyrene (10.0 μg/ml); 6 = benzo[*ghi*]perylene (10.0 μg/ml); 7 = indeno[1,2,3-*cd*]pyrene (10.0 μg/ml).

phase transition within the bonded phase [29,30]. The presence of a transition is not observed for the wide-pore C_{18} polymeric bonded phase used in this study. Fig. 7 shows that at sub-ambient temperatures the separation of acenaphthene (peak 3) and fluorene (peak 4) is significantly enhanced (diverging curves). This is also the case for benzo[*ghi*]perylene (peak 15) and indeno-[1,2,3-*cd*]pyrene (peak 16).

Two vertical lines indicate the dynamic range of the bonded phase that gives complete separation of all 16 PAHs at a given temperature and $\alpha_{TBN/BaP}$ value.

At elevated temperatures, the relative retention of dibenz[*a*,*h*]anthracene (slope of the curve is greater) is decreasing relative to benzo[*ghi*]perylene (peak 15); thus $\alpha_{15/14}$ is increased.

Consequently, the enthalpy effect for benzo[*ghi*]perylene is greater than for peak 14 and 16.

This deviating retention behaviour of benzo[*ghi*]perylene may be due to differences in shape selectivity (benzo[*ghi*]perylene is also a planar shaped compound) towards the stationary phase.

The effect of the temperature on the phase selectivity is also demonstrated in Fig. 8 in which the separation of the six well known Borneff PAHs including perylene is shown. The separation between benzo[*b*]fluoranthene and perylene is enhanced at lower temperatures.

3.5. Effect of the gradient steepness on the separation of SRM 1647C

The influence of the slope of the gradient on the separation of SRM 1647c is illustrated in Fig. 9. Interestingly, using a steeper gradient results in a better separation of dibenz[*a*,*h*]anthracene (peak 14) and benzo[*ghi*]perylene (peak 15).

This selectivity enhancement is probably a result of a better solvation of the stationary

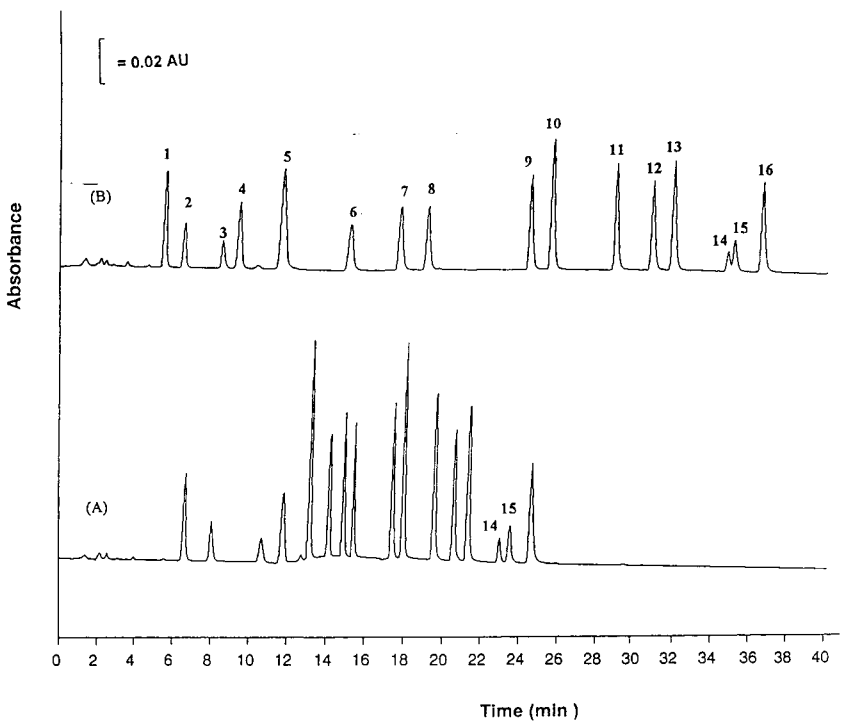

Fig. 9. Influence of the gradient steepness on the separation of SRM 1647c. Conditions as in Fig. 3. Acetonitrile–water (50:50) to 100% acetonitrile in (A) 5 min, (B) 25 min.

phase by acetonitrile compared to water/acetonitrile so that the interaction between the solute and the bonded phase layer is better. More study is necessary to proof this statement.

4. Conclusions

A novel silica based polymeric wide-pore C_{18} bonded phase is described for the separation of complex mixtures of PAHs. A selectivity test mixture is proved very useful to assess the phase selectivity. The $\alpha_{TBN/BaP}$ test is routinely used by us to verify column reproducibility and assist in the adjustment of the bonding process.

Complete separation of the 16 PAHs, identified by the EPA as priority pollutants, can only be achieved using bonded phases with $\alpha_{TBN/BaP}$ values in a well defined range ($0.6 < \alpha_{TBN/BaP} < 0.8$).

The high selectivity of the bonded phase enables the use of fluorescence programmed-wavelength detection.

The effect of the temperature on phase selectivity is far from negligible.

The column temperature is an important parameter that can be used to modify the selectivity for PAH separations. It has been demonstrated that the selectivity parameter $\alpha_{TBN/BaP}$ changes continuously with the temperature. At lower temperatures the selectivity of critical PAH isomer pairs is enhanced. The opposite trend occurs at elevated temperatures.

The slope of the gradient has a significant effects the resolution of dibenz[*a*,*h*]anthracene (peak 14) and benzo[*ghi*]perylene (peak 15). The separation of six Borneff PAHs inclusive perylene could be achieved under isocratic conditions using acetonitrile.

References

[1] *Guidelines for Drinking Water Quality*, Vols. 1 and 2, World Health Organization, Geneva, 1984.
[2] J. Borneff, presented at the *Symposium on Drinking Water Quality and Public Health, Water Research Centre, Medmenham, Marlow, UK, 4–6 November 1975.*
[3] J.W. Hodgeson, *Method 550.1*, Environmental Monitoring System Laboratory, US Environmental Protection Agency, Cincinnati, OH, 1990, pp. 143–167.
[4] *Method 8310, Test Methods for Evaluation of Solid Waste: Physical and Chemical Methods, SW-846*, US Environmental Protection Agency, Washington, DC, 1986, pp. 8310-1–8310-13.
[5] *Method 610, Test Methods: Methods for Organic Chemical Analysis of Municipal and Industrial Wastewater*, US Environmental Protection Agency, Cincinnati, OH, 1992, pp. 441–454.
[6] *ISO/TC 147/SC 2 Draft International Standard 7981-2*, International Organisation for Standardization, Vienna, 1989.
[7] *Draft German Standard Method, DIN Method 38407*, Part 8, Beuth Verlag, Berlin, 1993.
[8] *Draft Dutch Standard Method NEN 5731*, Nederlands Normalisatie-Instituut, Delft, 1992.
[9] P.R. Kootstra, M.H.C. Straub, G.H. Stil, E.G. van der Velde, W. Hesselink and C.C.J. Land, *J. Chromatogr. A*, 697 (1995) 123.
[10] L.C. Sander and S.A. Wise, *LC·GC Int.*, 3 (1990) 24
[11] L.C. Sander and S.A. Wise, *Anal. Chem.*, 59 (1987) 2309.
[12] S.A. Wise and W.E. May, *Anal. Chem.*, 55 (1983) 1479.
[13] S.A. Wise and L.C. Sander, *J. High Resolut. Chromatogr. Chromatogr. Commun.*, 8 (1985) 248.
[14] L.C. Sander and S.A. Wise, *J. Chromatogr.*, 316 (1984) 163.
[15] L.C. Sander and S.A. Wise, *Anal. Chem.*, 56 (1984) 504.
[16] R. Amos, *J. Chromatogr.*, 204 (1981) 469.
[17] K. Ogan and E. Katz, *J. Chromatogr.*, 188 (1980) 115.
[18] S.A. Wise, W.J. Bonnet, F.R. Guenther and W.E. Way, *J. Chromatogr. Sci.*, 19 (1981) 457.
[19] L.C. Sander and S.A. Wise, *CRC Crit. Rev. Anal. Chem.*, 18 (1987) 299.
[20] L.C. Sander and S.A. Wise, *Anal. Chem.*, 61 (1989) 1749.
[21] *NIST Certificate Standard Reference Material 869 (Column Selectivity Test Mixture for Liquid Chromatography of Polycyclic Aromatic Hydrocarbons)*, National Institute of Standards and Technology, Gaithersburg, MD, 1994.
[22] M.P. Henry, *J. Chromatogr.*, 544 (1991) 413.
[23] T.G. Waddel, D.E. Leyden and M.T. DeBello, *J. Am. Chem. Soc.* 103 (1981) 5303.
[24] L. Nedek, B. Buszewski and B. Berek, *J. Chromatogr.*, 360 (1986) 241.
[25] R.P.W. Scott and C.F. Simpson, *J. Chromatogr.*, 197 (1980) 11.
[26] K.B. Sentell and J.G. Dorsey, *J. Chromatogr.*, 461 (1989) 193.
[27] V.R. Meyer, *J. Chromatogr.*, 334 (1985) 197.
[28] L.C. Sander and S.A. Wise, *J. High Resolut. Chromatogr. Commun.*, 11 (1988) 383.
[29] D.J. Morel, *J. Chromatogr.*, 248 (1982) 231.
[30] S.A. Wise, L.C. Sander and W.E. May, *J. Chromatogr.*, 642 (1993) 329.

ELSEVIER

Journal of Chromatography A, 697 (1995) 175–184

JOURNAL OF CHROMATOGRAPHY A

Separation of metronidazole, its major metabolites and their conjugates using dynamically modified silica

Ulla Grove Thomsen*, Claus Cornett, Jette Tjørnelund, Steen Honoré Hansen

Department of Analytical and Pharmaceutical Chemistry, The Royal Danish School of Pharmacy, Universitetsparken 2, DK-2100 Copenhagen, Denmark

Abstract

Metronidazole has previously been used as a probe when investigating cytochrome P450 isoenzymes and thus the pattern of metabolism of this drug has been extensively studied. However, in previous investigations the conjugates were determined by indirect methods. In this paper we present a high-performance liquid chromatographic (HPLC) system for the simultaneous determination of metronidazole, its major metabolites and their glucuronic acid conjugates in biological fluids. The separation is performed using bare silica dynamically modified with N-cetyl-N,N,N-trimethylammonium bromide contained in the mobile phase. The separation of the acidic metabolites of metronidazole is greatly improved with this system compared to other published reversed-phase HPLC systems intended for the same purpose. Glucuronides of metronidazole and its hydroxy metabolites have been synthesized in vitro using rat liver microsomes and preparative HPLC. The method developed makes it possible to determine the intact glucuronic acid conjugates of metronidazole and the hydroxy metabolite in human urine.

1. Introduction

Metronidazole [1-(hydroxyethyl)-2-methyl-5-nitroimidazole] is a drug used for the treatment of protozoal infections (*Trichomoniasis vaginalis*) and infections caused by anaerobic micro-organisms [1–3]. The therapeutically active plasma concentration is about 5 μg/ml [3]. The drug is further used as a radio sensitiser of hypoxic cells (cancer therapy) [2]. Pharmacokinetic studies (in humans) using radioactive tracers have shown that about 77% of drug is excreted in the urine and about 14% is excreted in faeces (bilary excretion) within 5 days [2]. About 5% of the drug is excreted as CO_2 due to reductive metabolism by the gut flora leading to a breakdown of the imidazole ring [4,5] (Fig. 1); the latter studies were performed in rats.

Oxidative metabolism is the major route for biotransformation of metronidazole in humans and three major oxidative metabolites are found: the hydroxy metabolite, 1-(hydroxyethyl)-2-hydroxymethyl-5-nitroimidazole (HM); the acetic acid metabolite, 2-methyl-5-nitroimidazole-1-acetic acid (MAA) and the 2-carboxy metabolite, 1-(hydroxyethyl)-2-carboxy-5-nitroimidazole (MOOH). In rat the predominant route of biotransformation is conjugation with glucuronic acid and sulphuric acid [2,6,7]. In man the

* Corresponding author.

0021-9673/95/$09.50
SSDI 0021-9673(94)00750-0

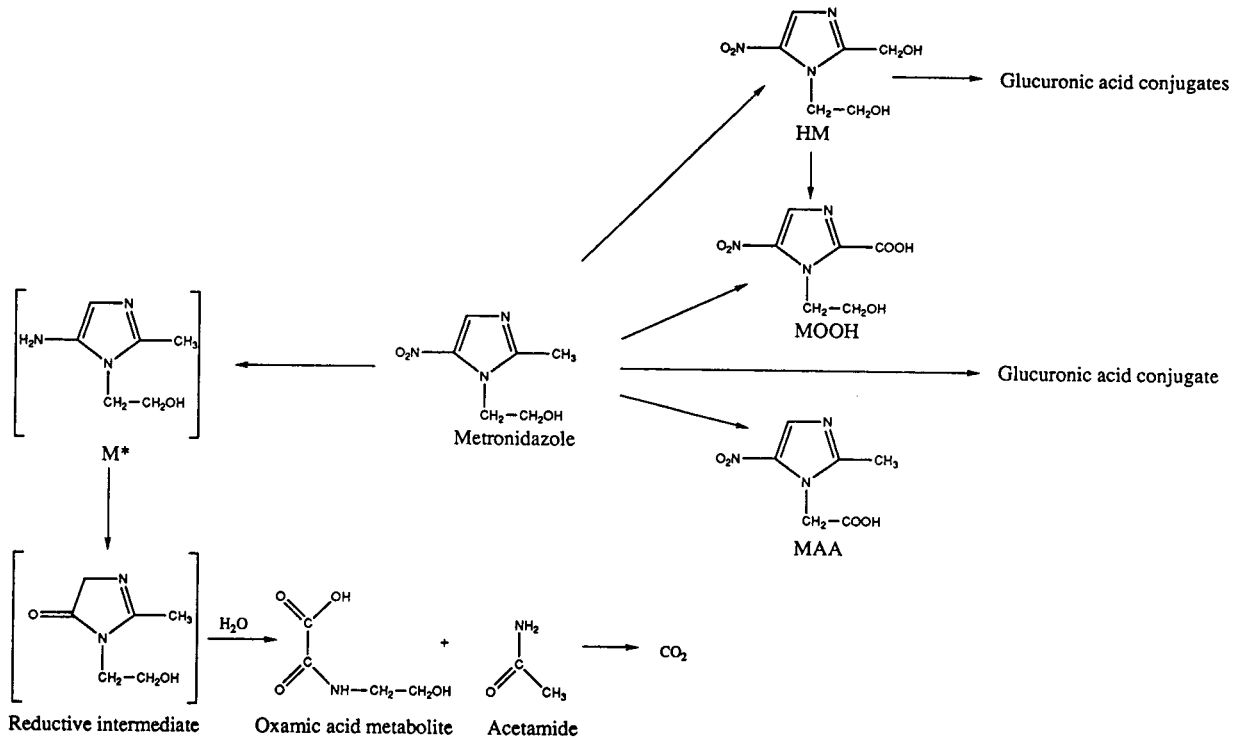

Fig. 1. Metabolic pattern of metronidazole.

parent drug as well as the metabolites are conjugated with glucuronic acid [1,2,6,8] (Fig. 1).

Metronidazole has previously been used as a probe when investigating cytochrome P450 isoenzymes. Thus the pattern of metabolism of this drug has been extensively studied [5,6,9] and a number of reversed-phase HPLC systems have been developed [9–16]. However, in these investigations the conjugates were determined by indirect methods (increase in concentration of mother substance before and after treatment with β-glucuronidase) because of lack of reference compounds and lack of a sufficiently selective separation method.

In this paper we present a HPLC system for the simultaneous determination of metronidazole, its major metabolites as well as their glucuronic acid conjugates in biological fluids. The separation is performed using bare silica dynamically modified with N-cetyl-N,N,N-trimethylammonium (CTMA) bromide dissolved in the mobile phase. The retention and separation of the acidic metabolites of metronidazole is greatly improved with this system compared to the earlier published HPLC systems used in studies of the metabolism of metronidazole [9–16].

2. Experimental

2.1. Chemicals

Metronidazole and the metabolites HM, MAA and MOOH were kindly donated by Steffen Loft, Department of Pharmacology, University of Copenhagen, Copenhagen, Denmark and Dumex (Copenhagen, Denmark). Disodium UDP-glucuronate (UDP-GA) and β-glucuronidase (*Escherichia coli*) (200 U/ml) were purchased from Boehringer (Mannheim, Germany). CTMA bromide (analytical grade) was purchased from Merck (Darmstadt, Germany). All other chemicals were of analytical-reagent grade.

2.2. Apparatus

Analytical chromatography

A Waters (Milford, MA, USA) liquid chromatographic system consisting of a Model 6000 A pump, a 715 Ultra WISP autoinjector, a 490E programmable multiwavelength detector was used and data were collected using Maxima 820 software. A Shimadzu (Kyoto, Japan) CTO-6A oven was used for thermostating the columns.

Preparative chromatography

A Merck–Hitachi (Darmstadt, Germany) 655A-12 liquid chromatographic system pump, a 655A variable-wavelength monitor and a D2000 integrator were used. A Rheodyne (Cotati, CA, USA) 7125 injection module with a 1.5-ml loop was used for sample introduction.

NMR spectroscopy

A 400 MHz Bruker (Rheinstetten, Germany) AMX 400 WB instrument was used.

2.3. Enzymatic synthesis of glucuronides

Liver microsomes were prepared as previously described [17]. The liver from 9-weeks-old male Sprague-Dawley rats were used. The protein content of the prepared microsomes was measured by the method of Lowry et al. [18] UDP-glucuronosyl transferase (UDP-GT) activity was measured by the method described earlier [19] except that the change in *p*-nitrophenol concentration was measured by HPLC instead of by spectrophotometry.

The optimal incubation mixture for the two substrates metronidazole and the hydroxy metabolite was found to be the following: rat microsomal protein, 35 mg/ml; substrate, 75 m*M*; potassium phosphate buffer (pH 7.4), 50 m*M*; $MgCl_2$, 5 m*M*; Triton X, 0.01%; UDP-GA, 12 m*M*; water to a total volume of 50 ml. This mixture was incubated in ten vials each containing 5 ml at 37°C for 8 h on a gyratory shaker. If 50 ml were incubated in a single vial the yield of the synthesis was significantly lower due to diffusion problems in the incubation vial.

The synthesis was stopped by adding 10 ml methanol to each vial, the proteins were allowed to precipitate and the mixture was centrifuged 30 min at 5000 *g*. The supernatants were pooled and the methanol removed by rotary evaporation. Finally the water phase was freeze dried. The glucuronides were isolated from this freeze-dried product using preparative HPLC. Identification and purity of the final products were determined by ^1H NMR (400 MHz) in ^2H_2O and by quantitative cleavage with β-glucuronidase followed by HPLC analysis of the parent drug towards a reference standard.

The ether glucuronide of metronidazole

Maximum yield was 0.09 mmol (31 mg) of the metronidazole glucuronide and the purity of the final product was 84%. The ^1H NMR spectrum confirmed the structure of the glucuronic acid conjugate of metronidazole (M-glcU) (Fig. 2A).

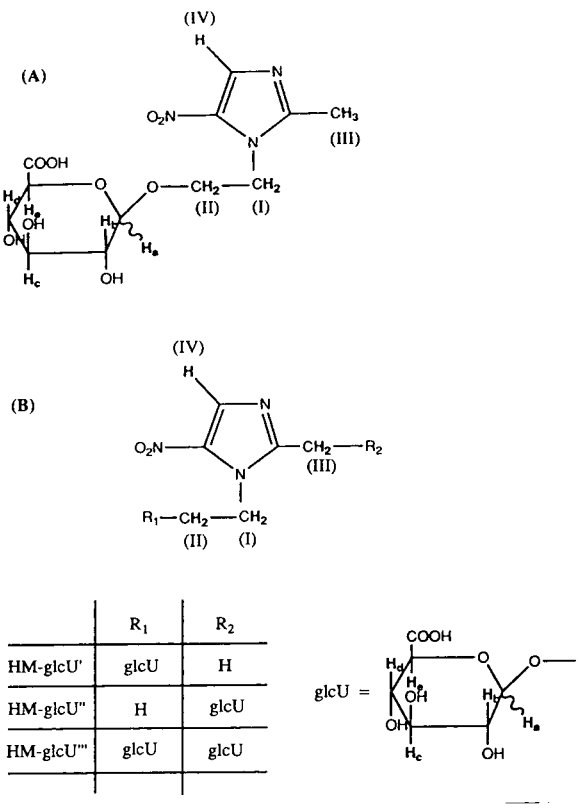

	R_1	R_2
HM-glcU'	glcU	H
HM-glcU''	H	glcU
HM-glcU'''	glcU	glcU

Fig. 2. (A) The glucuronic acid conjugate of metronidazole (M-glcU). (B) The glucuronic acid conjugates of the hydroxy metabolite.

δ = 2.51 ppm [$-CH_3$(III), s], 3.18 ppm (H_b, t), 3.38–3.45 ppm (H_c, H_d, m), 3.66 ppm (H_e, d), 4.04 ppm [$-CH_2$(I), m], 4.15 ppm [$-CH_2$(II), m], 4.31 ppm (H_a, d), and 8.09 ppm [H(IV), s].

The ether glucuronides of the hydroxy metabolite

As shown in Fig. 3. three conjugates of HM were formed in the incubation mixture (t_R = 7.93, 8.99 and 10.22 min). This fact was confirmed by cleavage with β-glucuronidase. The maximum yield of the synthesis was 0.12 mmol

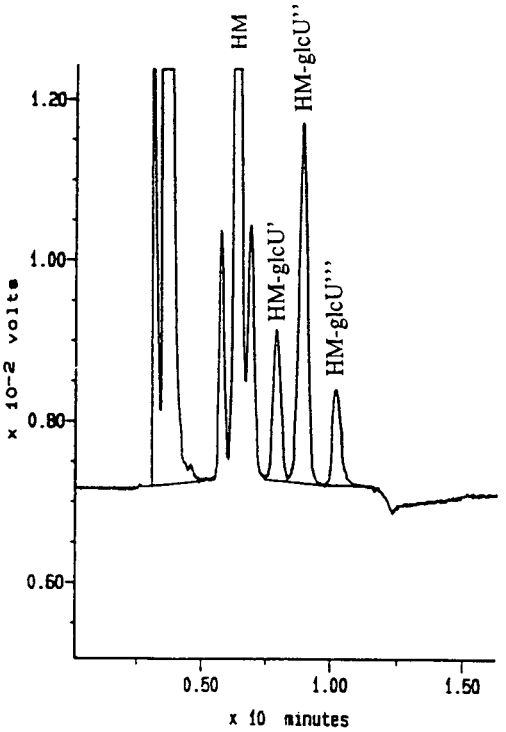

Fig. 3. Chromatogram of a sample from the incubation mixture during in vitro synthesis of conjugates of the hydroxy metabolite of metronidazole (HM). Retention times (min) for the conjugates are: HM-glcU' (7.93), HM-glcU'' (8.99), HM-glcU''' (10.22). Chromatographic conditions: saturation column (150 × 4.6 mm I.D.), dry packed with LiChroprep Si 60 (15–25 μm) placed between pump and injector. Analytical column, Knauer column (120 × 4.6 mm I.D.), slurry packed with LiChrosorb Si 60 (5 μm), thermostated at 35°C; eluent, methanol–0.2 *M* potassium phosphate (pH 7.0)–water (25:30:45, v/v/v) with 2.5 m*M* CTMA added. The flow-rate was initially 0.5 ml/min, after 9 min it was increased to 1.0 ml/min. UV detection at 312 nm.

of a mixture of glucuronides. The purity of the final products was poor (about 20%) for all three conjugates but an identification by ^{1}H NMR of the metabolites was performed.

The ^{1}H NMR spectrum of the first conjugate (t_R = 7.93 min) confirmed the structure of a mono sugar conjugate (HM-glcU') (see Fig. 2B). δ = 3.10 ppm (H_b, t), 3.29–3.39 ppm (H_c, H_d, m), 3.62 ppm (H_e, d), 3.95 ppm [$-CH_2$(I), m], 4.10 ppm [$-CH_2$(II), m], 4.22 ppm (H_a, d), 4.62 [$-CH_2$(III), t] and 8.10 ppm [H(IV), s].

The ^{1}H NMR spectrum of the second conjugate (t_R = 8.99 min) confirmed the structure of mono sugar conjugate (HM-glcU'') (see Fig. 2B). δ = 3.09 ppm (H_b, t), 3.25–3.45 ppm (H_c, H_d, m), 3.50 ppm (H_e, d), 3.95 ppm [$-CH_2$(I), m], 4.02 ppm (H_a, d), 4.50 ppm [$-CH_2$(II), m], 4.59 [$-CH_2$(III), t] and 8.00 ppm [H(IV), s].

The ^{1}H NMR spectrum of the last conjugate (t_R = 10.22 min) confirmed that the substance contains two glucuronic acid moieties (HM-glcU''') (Fig. 2B). The glucuronic acid protons show a complex pattern δ = 3.41–4.39 ppm. δ = 4.20 ppm [$-CH_2$(I), m], 4.30 ppm [$-CH_2$(II), m], 4.60 [$-CH_2$(III), t] and 8.05 ppm [H(IV), s].

2.4. Preparative HPLC

The isolation procedure for the glucuronide of metronidazole (M-glcU) was performed in two steps. A Knauer column (Berlin, Germany) packed with LiChrosorb NH_2 (Merck), 5 μm, was used (250 mm × 16 mm I.D.), with an eluent consisting of methanol–0.2 *M* ammonium carbonate (pH 7.8)–water (90:2:8, v/v/v). The flow-rate was 5 ml/min. Further clean up was performed on a polystyrene–divinylbenzene polymer column (PRPL-S 100A 8 μm; Polymer Labs., Shropshire, UK; 300 mm × 7.5 mm I.D.), with a mobile phase consisting of acetonitrile–water (5:95, v/v) containing 0.1% trifluoracetic acid and a flow-rate of 6 ml/min.

The glucuronides of the hydroxy metabolite were separated on a bare silica column, a Knauer column (120 × 4.6 mm I.D.) packed with LiChrosorb Si 60 (Merck) (5 μm), with a saturation column (150 × 4.6 mm I.D.) dry packed

with LiChroprep Si 60 (Merck) (15–25 μm) installed between the pump and the autoinjector. The mobile phase was methanol–0.2 *M* potassium phosphate (pH 7.0)–water (25:30:45, v/v/v) with 2.5 m*M* CTMA added. The flow-rate was 0.5 ml/min. The isolated glucuronides were finally purified on a PRPL-S 100A column, 8 μm, 300 mm × 7.5 mm I.D., using a mobile phase of acetonitrile–water (5:95, v/v) containing 0.1% trifluoracetic acid with a flow-rate of 5 ml/min.

2.5. Sample preparation

The urine samples were diluted 1:2 with methanol and after 1 h centrifuged for 12 min (5000 *g*). The supernatant was diluted 1:1 with water and 20 μl were injected into the liquid chromatograph.

Samples from the incubation mixtures containing liver microsomes were diluted 1:2 with methanol to stop the reactions and to precipitate the proteins. After centrifugation for 12 min (5000 *g*) 20 μl of the supernatant were injected into the HPLC system.

Cleavage of glucuronides with β-glucuronidase was performed as follows: 5 μl β-glucuronidase were added to 200 μl of the sample (pH 7.4) and the mixture was incubated at 37°C. After 18 h 400 μl methanol were added and the sample was centrifuged for 12 min (5000 *g*). If a urine sample was tested the supernatant was further diluted 1:1 with water before analysis.

2.6. Analytical chromatography

A saturation column (150 × 4.6 mm I.D.) drypacked with LiChroprep Si 60 (15–25 μm) was installed between the pump and the autoinjector. The analytical column was a Knauer column (120 × 4.6 mm I.D.) packed with LiChrosorb Si 60 (5 μm). Both columns were thermostated at 35°C. The final mobile phase developed for the assay of metronidazole, its metabolites and their conjugates was methanol–0.2 *M* potassium phosphate (pH 7.0)–water (25:30:45, v/v/v) with 2.5 m*M* CTMA added. The flow-rate was initially 0.5 ml/min and after 9 min increased to 1.0 ml/min. The UV detector was operated at 312 nm.

For the assay of *p*-nitrophenol the mobile phase was methanol–0.2 *M* potassium phosphate (pH 6.0)–water (60:5:35, v/v/v) containing 1.25 m*M* CTMA, with a flow-rate of 1.0 ml/min, the UV detector was operated at 405 nm.

3. Results and discussion

3.1. Enzymatic synthesis of glucuronides

The enzyme activities for the formation of glucuronic acid conjugates of *p*-nitrophenol in freeze-dried rat liver microsomes compared to non-freeze-dried liver microsomes were 25.9 ± 5 nmol/min · mg protein and 31.5 ± 5 nmol/min · mg protein, respectively. An activity in fresh rat liver microsomes of 28 nmol/min · mg protein was reported earlier [19]. It is favourable to use the freeze-dried product when synthesizing glucuronic acid conjugates because of the possibility for long-term storage (− 18°C for up to 6 months) [20]. Furthermore, higher protein concentrations may be used.

The development of optimal conditions for the synthesis of ether glucuronides of metronidazole and its hydroxy metabolite (HM) was based on the method previously described [21].

Metronidazole was found to be a poor substrate in vitro for the glucuronosyl transferase enzymes as the yield of glucuronic acid conjugates using standard conditions [21] for enzymatic synthesis was low. One of the reasons may be the high hydrophilicity of the drug itself decreasing the need for glucuronic acid conjugation. Even though the substrate specificity of the UDP-GT enzymes is broad, higher affinity of the enzymes towards the more lipophilic compounds is seen [22]. However, it was possible to increase the yield of the synthesis by increasing the substrate and protein concentration. The yield of the incubation was further optimized changing pH of the incubation mixture as well as the temperature during incubation. A maximum yield (evaluated as the area of the chromatographic peak from the glucuronic acid conjugate

formed) was observed after 8 h using an incubation mixture with pH 7.4 and a temperature of 37°C. The same yield could be observed after 24 h incubating at 25°C (pH 7.4). The incubation conditions that were used for synthesis M-glcU were found to be optimal for the synthesis of glucuronides of the hydroxy metabolite as well. In this study only the ether glucuronides of metronidazole and HM were synthesized for the identification of unknown peaks in the chromatograms. These were the only glucuronides observed in urine obtained from humans. No detectable amounts of acyl glucuronides of the acidic metabolites could be observed. This was determined using β-glucuronidase tests of urine samples, examining the concentration of the phase I metabolites before and after incubation with β-glucuronidase.

3.2. Chromatography

The separation methods for metronidazole and its major oxidative metabolites described in the literature are all based on reversed-phase chromatography performed on chemically bonded phases using mobile phases with a very low content of organic modifier (5–10%) [6,9,11,12,15,23]. However, these systems were not well suited for separation of the very polar acidic metabolites of metronidazole (MOOH, MAA) or the glucuronides. Instead we used bare silica dynamically modified with a long-chain quaternary ammonium compound (CTMA bromide). This results in a reversed-phase HPLC system where metronidazole and HM are retained by a reversed-phase mechanism. Anions such as the acidic metabolites (MAA, MOOH) and glucuronides (M-glcU, HM-glcU′, HM-glcU″, HM-glcU‴) form hydrophobic ion pairs with the CTMA ions which are separated by reversed-phase chromatography.

The chromatographic system was evaluated with respect to pH, amount of methanol, ionic strength and concentration of CTMA in the eluent to obtain satisfactory separation of metronidazole, its metabolites and the conjugates.

Organic modifier

When the amount of organic modifier was increased in the eluent the separation of metronidazole and HM was lost (Fig. 4A). Substituting acetonitrile for methanol or using combinations of the two modifiers was not successful as metronidazole and HM could not be separated. The final eluent was chosen to contain 25% (v/v) of methanol. Lower amounts were not used as the retention of the acidic metabolites would then be unnecessarily long.

pH

The effect of changing pH in the mobile phase can be rather complex in a HPLC system based on dynamically modified silica. The silanol groups have a pK_a value of 6.5–7.0 and when the pH of the mobile phase is increased the adsorption of CTMA to the silica surface increases. Thus, the increase in pH should lead to an increase in retention.

The observed decrease in retention times of the acidic metabolites results (Fig. 4B) from a combination of equilibrium states. As the pH increases the concentration of potassium ions increases and thereby the ionic strength in the system. The potassium ions will compete with CTMA for the solute as well as for the silanol groups of the column (resulting in lower retention as the pH increases). The negative charge of the phosphate ions increase as the pH increases and the phosphate ions might compete with the acids for CTMA interaction. The pH value of the system did not significantly influence the retention of metronidazole and HM. To keep retention of the acids as short as possible a pH of 7.0 was used in the eluent.

Ionic strength

The acidic metabolites have fairly long retentions while metronidazole and HM elute early in the chromatogram. A high ionic strength in the eluent has previously been proven to be able to selectively reduce the retention of anionic solutes [24]. Concomitantly, the increase in ionic strength will not change the retention of non-

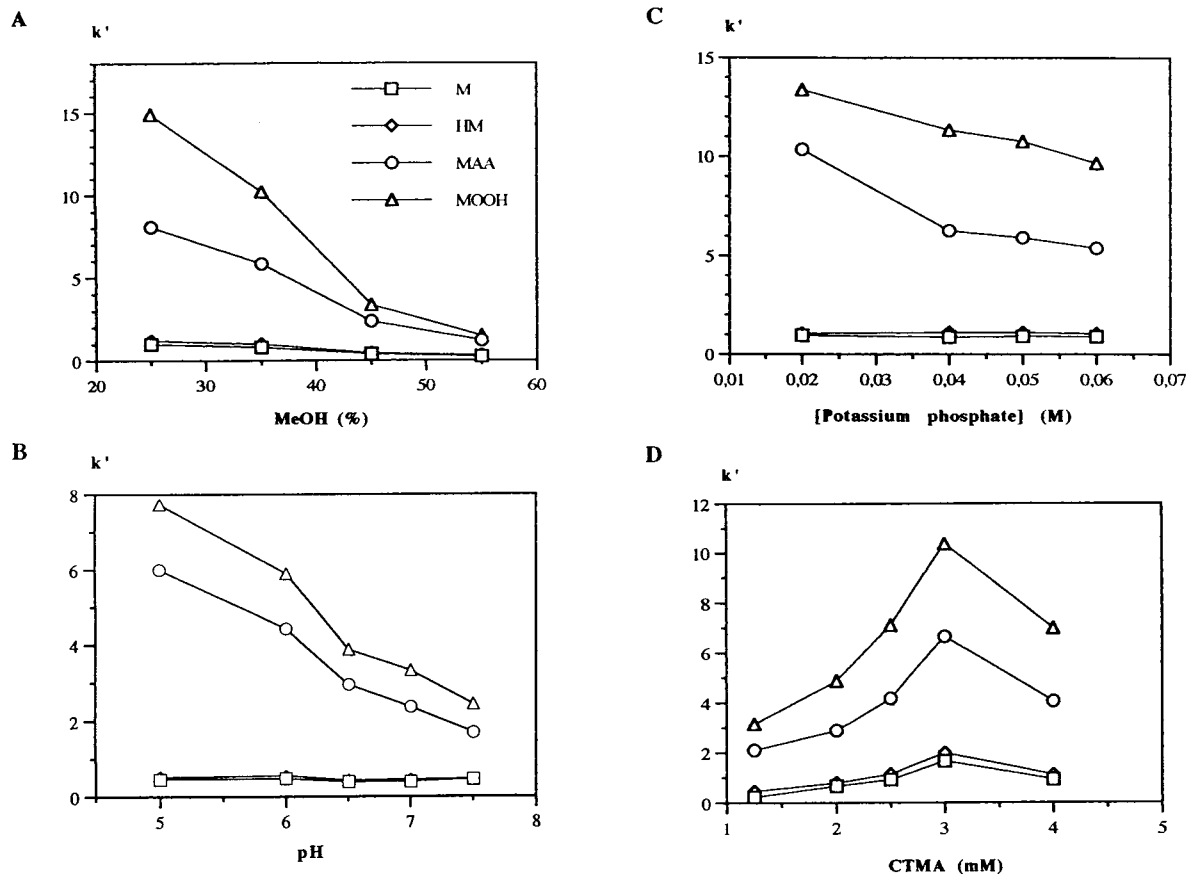

Fig. 4. (A) Relationship between the concentration of methanol and the capacity factor (k') for metronidazole (□) and its three major metabolites (◇ = HM; ○ = MAA; △ = MOOH). Columns as in Fig. 3; eluent, methanol–0.2 *M* potassium phosphate (pH 7.0)–water [(25–55):30:(15–45), v/v/v], with 2.5 m*M* CTMA added. (B) Relationship between pH of the buffer and k' for metronidazole and its three major metabolites. Columns as in Fig. 3; eluent, methanol–0.2 *M* potassium phosphate (pH 5.0–7.5)–water (25:30:45, v/v/v), with 2.5 m*M* CTMA added, symbols as in (A). (C) Relationship between potassium phosphate concentration in the buffer added and k' for metronidazole and its three major metabolites. Columns as in Fig. 3; eluent, methanol–0.2 *M* potassium phosphate (pH 7.0)–water [25:(10–30):(45–65), v/v/v], with 2.5 m*M* CTMA added, symbols as in (A). (D) Relationship between the concentration of CTMA and k' for metronidazole and its three major metabolites. Columns as in Fig. 3; eluent, methanol–0.2 *M* potassium phosphate (pH 7.0)–water (25:30:45, v/v/v), with 1.25–4.0 m*M* CTMA added, symbols as in (A). The hold-up time t_0 was determined as the retention time of deuterium oxide.

ionic solutes. Keeping the methanol concentration low favours the separation of metronidazole and HM. A combination of the parameters low methanol concentration and high ionic strength would thus be favourable. The result of increasing the ionic strength in the eluent with a methanol concentration of 25% is seen in Fig. 4C.

CTMA

The CTMA concentration was varied in the final system with 25% (v/v) methanol and 0.06 *M* potassium phosphate pH 7.0. The results are seen in Fig. 4D. In the evaluation of the optimal amount of CTMA separation of metronidazole and its metabolites as well as their conjugates were investigated. The retention of met-

ronidazole and its metabolites increases until a concentration of 3 m*M* is reached as more CTMA adsorbs to the silica surface. At 4 m*M* CTMA the critical micellar concentration (CMC) was most likely exceeded [25] and the capacity factors decreased. When CMC is exceeded a "secondary lipophilic phase" which migrate with the speed of the eluent is formed. Some of the solute molecules migrate into the micelles instead of interacting with the stationary phase and thus the retention decreases.

3.3. Assay validation

The detection limits for metronidazole, its metabolites and the conjugates in urine were determined to be the following: metronidazole 2 ng/ml, HM 9 ng/ml, M-glcU 8 ng/ml, MAA 20 ng/ml and MOOH 37 ng/ml. This was estimated as three times the standard deviation (σ) of the peak-to-peak noise ($N_{p\text{-}p}$), where $\sigma = N_{p\text{-}p}/5$ which is a good estimate when the noise is assumed to be normal distributed. The limit of quantitation was 5 ng/ml for metronidazole, 28 ng/ml for HM, 25 ng/ml for M-glcU, 65 ng/ml for MAA and 120 ng/ml for MOOH. The limit of quantitation was estimated as 10σ of the peak-to-peak noise. The calibration curves in urine of metronidazole (0.01–50 μg/ml), its phase I metabolites (0.1–50 μg/ml) and the conjugates (0.05–50 μg/ml) were linear within the concentration ranges specified ($r^2 > 0.99$).

Recovery studies of metronidazole and its metabolites in human urine were done by adding known amounts of the reference compounds to drug-free urine ($n = 6$). The recoveries for all solutes were found to be 87–103% and are seen in Table 1. The intra-assay relative standard deviations (R.S.D.s) are sufficiently low for the method to be used for routine analysis.

3.4. Applications

The metabolism of metronidazole in vivo was investigated in a single dose experiment. A 500-mg amount of metronidazole was given orally to two healthy volunteers (female, 23 years old,

Table 1
Analysis of samples of urine spiked with metronidazole and metabolites of metronidazole

Sample	Added (μg/ml)	Found (μg/ml)[a]	Recovery (%)	R.S.D. (%)
Metronidazole	2.76	2.57	93.5	3.4
	5.88	6.03	102.6	1.5
	62.66	57.96	92.5	3.0
HM	2.43	2.47	101.6	6.6
	5.50	5.30	96.7	2.2
	30.67	29.75	97.0	2.7
MAA	2.91	2.50	86.2	4.2
	7.14	6.78	95.8	1.4
	30.67	30.03	97.9	1.7
MOOH	2.67	2.72	102.4	7.7
	7.00	6.20	88.9	5.2
	28.00	27.65	98.8	0.8
M-glcU	1.85	1.85	100.0	1.6
	4.00	3.67	91.8	5.3
	10.08	9.77	87.1	1.8

[a] Mean, $n = 6$.

mass 55 kg and female, 25 years old, mass 62 kg) and urine was properly collected for 72 h.

Three metabolites and two conjugates were identified in the urine: HM, MAA, MOOH and the glucuronic acid conjugates of metronidazole (M-glcU) and one of the conjugates of the hydroxy metabolites (HM-glcU″). The two other conjugates of HM (HM-glcU′ and HM-glcU‴) could not be detected. The conjugate of HM has not been assayed directly in earlier published work regarding metabolism of metronidazole [9–16]. An example of a chromatogram of an authentic urine sample from one of the volunteers is shown in Fig. 5A along with a blank urine sample Fig. 5B. None of the acyl glucuronides of the acidic metabolites could be detected, not even indirectly using β-glucuronidase tests.

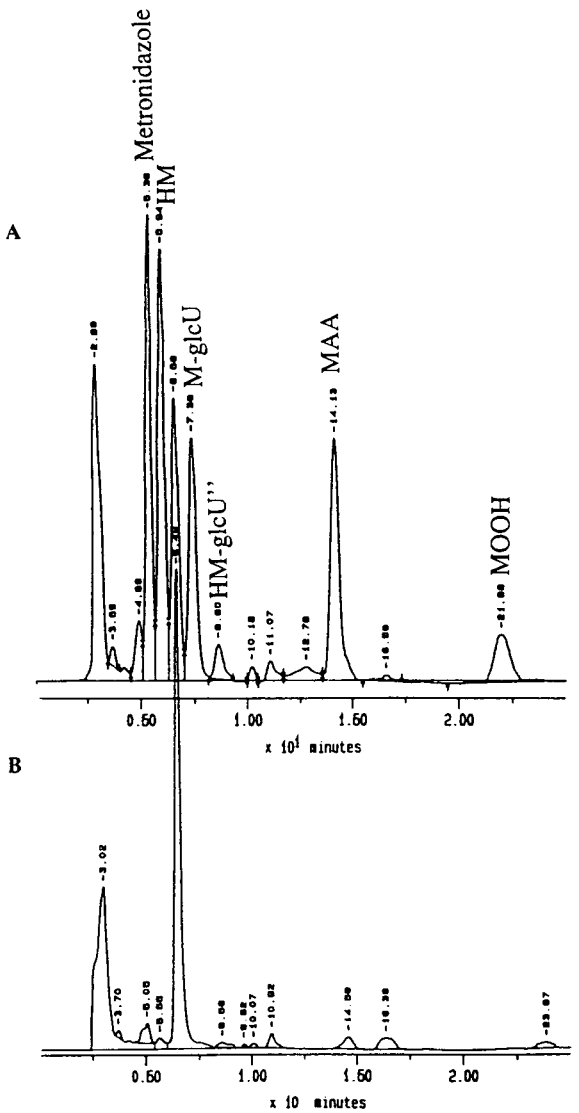

Fig. 5. Chromatograms of urine samples from (A) a volunteer 4 h after oral intake of 500 mg metronidazole and (B) the same volunteer before intake of 500 mg metronidazole. Chromatographic conditions were as described in Fig. 3.

The totally excreted amount of the given dose was 82% in the urine from the first volunteer and 74% from the second, which corresponds to the 77% earlier found [7]. The cumulated amounts of metronidazole, the three major metabolites and the glucuronic acid conjugates excreted over 72 h from the two volunteers are compared in Table 2. There are some differences between the metabolic profiles of the two volunteers especially with respect to excretion of metronidazole, its hydroxy metabolite and the acetic acid metabolite. One could speculate in polymorphism of the P450 isoenzymes but this would require extended investigations.

The single-dose study of metronidazole in human volunteers emphasizes the applicability of the chromatographic method in biological fluids. The HPLC system based on dynamically modified silica is very suitable for the separation and quantitation of compounds which differ in

Table 2
Cumulated urinary excretion of metronidazole and its metabolites and conjugates after oral administration of 500 mg metronidazole to two volunteers (1 and 2)

Compound	Excretion (% of dose)-within 72 h	
	1	2
Metronidazole	9.6	16.4
HM	28.7	22.0
MAA	10.1	19.5
MOOH	17.9	15.6
M-glcU	5.0	6.3
HM-glcU″	2.4	2.0
Total% of dose excreted	73.7	81.8

chemical properties such as drugs and their phase I and phase II metabolites.

Acknowledgements

The Alfred Benzon Foundation and the Danish Technology Council are kindly acknowledged for donating the NMR apparatus.

References

[1] K.W. Bock, B. Burchell, G.J. Dutton, O. Hänninen, G.J. Mudler, I.S. Owens, G. Siest and T.R. Tephly, *Biochem. Pharmacol.*, 32 (1983) 953.
[2] H. Allars, D. Coleman and R.S. Norton, *Eur. J. Drug Met. Pharmacokin.*, 10 (1985) 253.
[3] R. Tempelton, *Int. Congr. Ser.-Excerpta Med.*, 438 (1977) 28.
[4] R.M.J. Ings, J.A. McFadzean and W.E. Ormerod, *Biochem. Pharmacol.*, 23 (1974) 1421.
[5] R.L. Koch and P. Goldman, *J. Pharmacol. Exp. Ther.*, 208 (1979) 406.
[6] S. Loft, *Pharmacol. Toxicol.*, 66 (Suppl. 6) (1990) 1.
[7] N.L. LaRusso, D.G. Lindmark and M. Muller, *Biochem. Pharmacol.*, 27 (1978) 2247.
[8] S. Loft and H.E. Poulsen, *Xenobiotica*, 20 (1989) 185.
[9] S. Loft, S.V. Otton, M.S. Lennard, G.T. Tucker and H.E. Poulsen, *Biochem. Pharmacol.*, 41 (1991) 1127.
[10] M. Chacko, J. Nair and S.V. Bhide, *Indian J. Biochem. Biophys.*, 23 (1986) 220.
[11] B. Davis, D.D. Glover and B. Larsen, *Am. J. Obestet. Gynecol.*, 149 (1984) 802.
[12] I. Nilsson-Ehle, B. Ursing and P. Nilsson-Ehle, *Antimicrob. Agents Chemother.*, 19 (1981) 754.
[13] C.M. Kaye, M.G. Sankey and L.A. Thomas, *Br. J. Clin. Pharmacol.*, 9 (1980) 528.
[14] K. Lanbeck and B. Lindström, *J. Chromatogr.*, 162 (1979) 117.
[15] S. Loft, M. Døssing, H.E. Poulsen, J. Sonne, K.-L. Olesen, K. Simonsen and P.B. Andreasen, *Eur. J. Clin. Pharmacol.*, 30 (1986) 467.
[16] L.A. Wheeler, M. De Meo, M. Halula, L. George and P. Heseltine, *Antimicrob. Agents Chemother.*, 13 (1978) 205.
[17] R. Kalman and B. Gachalyi, *J. Chromatogr.*, 420 (1987) 228.
[18] O.H. Lowry, N.J. Rosebrough, A.L. Farr and R.J. Randall, *J. Biol. Chem.*, 193 (1951) 265.
[19] J.V. Andersen and S.H. Hansen, *J. Chromatogr.* 577 (1992) 325.
[20] J.V. Andersen, *Thesis*, Royal Danish School of Pharmacy, Copenhagen, 1990.
[21] W.H. Siddiqui and H.S. Buttar, *Arch. Int. Pharmacodyn.*, 239 (1979) 4.
[22] B. Burchell and W.G. Coughtrie, in W. Kalow (Editor), *Pharmacogenetics of Drug Metabolism*, Pergamon Press, New York, 1992, p. 195.
[23] L.P. Hackett and L.J. Dusci, *J. Chromatogr.*, 175 (1979) 347.
[24] S.H. Hansen, *J. Chromatogr.*, 491 (1989) 175.
[25] S.H. Hansen, *Bare Silica*, Chrompress, Snekkersten, Denmark, 1990.

ELSEVIER

Journal of Chromatography A, 697 (1995) 185–190

JOURNAL OF CHROMATOGRAPHY A

Qualitative, semi-quantitative and spectrophotometric determination of ruthenium(III) by solid-phase extraction with 3-hydroxy-2-methyl-1,4-naphthoquinone-4-oxime-loaded polyurethane foam columns

M.S. El-Shahawi*, M. Almehdi

Chemistry Department, Faculty of Science, UAE University, P.O. Box 17551, Al-Ain, United Arab Emirates

Abstract

A sensitive and selective extraction method was developed for the detection, semi-quantitative and spectrophotometric determination of ruthenium(III) in aqueous media. The method is based on the sorption of the ruthenium(III) complex of 3-hydroxy-2-methyl-1,4-naphthoquinone-4-oxime on a porous polyurethane foam membrane. In batch experiments, it was possible to detect as low as 0.1 and 0.02 ppm of ruthenium(III) with unloaded foam and foam loaded with reagent, respectively. The method was also employed for the detection of 10 ppb of ruthenium using the reagent foam column mode. The selectivity of the method for the detection of 1 ppm of ruthenium(III) in the presence of high concentrations of diverse ions was achieved. Preconcentration of ruthenium(III) from large sample volumes was carried out on a loaded foam column at pH 5–7, eluted with acetone and determined spectrophotometrically at 450 nm. The sorbed complex species on the foam showed an absorption maximum at 460 nm with a molar absorptivity of 2.8×10^4 dm^3 mol^{-1} cm^{-1}. On this basis, a method for the direct spectrophotometric determination of ruthenium(III) based on liquid–solid extraction of the Ru(III)–reagent complex on thin-layer parallelepiped foam was developed. The proposed methods were applied for the determination of ruthenium(III) in water and in its complexes.

1. Introduction

Compared with most other elements, ruthenium has a limited influence on the biosphere [1]. The amount of ruthenium readily introduced into rivers, lake and oceans through industrial wastes, catalyst application and material sciences [2–4] is minute. Sensitive, reliable and practicable methods are required for the determination of the element at trace levels [5].

The most common reported spectrophotometric procedures include the use of thioridazine hydrochloride [6], 9,10-phenanthrenequinone monoxime [7], sulphochlorophenolazorhodamine [8], *o*-mercaptoacetanilide in the presence of picaline [9], a catalytic method with periodate oxidation [10], ion-pair formation [11] and 3-hydroxy-2-methyl-1,4-naphthoquinone 4-oxime [12]. However, most of these reagents suffer from the lack of selectivity and sensitivity and

* Corresponding author. Permanent address: Chemistry Department, Faculty of Science at Damiatta, Damiatta, Egypt.

0021-9673/95/$09.50
SSDI 0021-9673(94)01071-4

usually require laborious enrichment steps. Several polarographic and voltammetric methods have been developed for the determination of ruthenium [13–16], but neither their sensitivity nor selectivity is very satisfactory.

Recently, several workers have proposed open-cell polyurethane foam as an inexpensive solid extractor for many organic and inorganic species [17–19]. Direct spectrophotometric measurements of the absorbance of a thin layer of solid polyurethane foam, reported as a new trend [20,21], have markedly improved the sensitivity of determination and avoided the tedious preconcentration step that is necessary in trace analysis. This paper reports the application of polyurethane foam loaded with 3-hydroxy-2-methyl-1,4-naphthoquinone-4-oxime reagent for the detection and semi-quantitative and direct spectrophotometric determination of trace levels of ruthenium in aqueous solution.

2. Experimental

2.1. Reagents and materials

Analytical-reagent grade chemicals and doubly distilled water were used throughout. Britton–Robinson (BR) buffer solution (pH 2.5–12) containing sodium hydroxide, glacial acetic acid, orthophosphoric acid and boric acid was prepared with distilled water. A stock standard solution (1 mg ml^{-1}) of ruthenium(III) (atomic absorption standard, BDH) was used and diluted with water for standard addition whenever required. Tributyl phosphate (TBP) (pure grade) was used without further purification. Polyurethane foam (PUF), an open-cell, polyether type (bulk density 30 kg m^{-3}), was supplied by Greiner (Schaumstoff-Werk-Kremsmunster, Austria). The foam materials (cubes of 5-mm edge and a parallelepiped of $10 \times 35 \times 2$ mm dimensions were washed as reported previously [22]. 3-Hydroxy-2-methyl-1,4-naphthoquinone-4-oxime (HMNQO) was prepared by the method of Sharma [12]. A $1 \cdot 10^{-3} M$ solution of HMNQO was prepared by dissolving the required mass of HMNQO in 100 ml of ethanol.

2.2. Reagent foam preparation

About 1 g of the dried white foam cubes and parallelepiped foam were equilibrated with 10 ml of HMNQO in ethanol followed by the addition of 1 ml of TBP with efficient stirring. The foam material was then allowed to remain in contact with the solution for 1 h and dried as reported previously [22].

2.3. Apparatus

A Pye Unicam SP8-400 double-beam UV–Vis spectrometer with a quartz cell of 10-mm path length and a Philips Model 9418 pH meter were used for absorbance and pH measurements, respectively. Glass columns of length 10 and 15 cm and I.D. 20 and 5 mm were used in the dynamic experiments.

2.4. Detection and semi-quantitative determination of ruthenium(III)

Batch experiments

To 3–5 ml of the aqueous solution of ruthenium(III) at 60°C and pH 7 in a normal test-tube was added one cube of unloaded, HMNQO-loaded or HMNQO–TBP-treated foam and the mixture was shaken for 3–5 min. The change in the colour of the foam cube from white to red-violet due to the coloured Ru(III)–HMNQO complex collected on the reagent foam is evidence for the detection of ruthenium(III).

Column experiments

A foam column detection test was carried out by percolating 100 ml of the aqueous solution of ruthenium(III) at 60°C and pH 5–7 through the HMNQO–TBP-loaded foam bed in the column (10 cm × 5 mm I.D.) at 5 ml min^{-1}. The developed red-violet colour on the foam bed is evidence for the detection of ruthenium(III).

2.5. Direct spectrophotometric determination of ruthenium by liquid–solid extraction on thin-layer parallelepiped polyurethane foam

Standard ruthenium(III) solutions (1–10 ml) containing 1–50 μg of ruthenium(III) were

pipetted into a 100-ml erlenmeyer flask, followed by 10 ml of buffer (pH 7) and 10 ml of 0.001 *M* HMNQO solution and the solution was heated at 60°C for 0.5 h. The volume of each solution was made up to 50 ml with distilled water, a piece of thin-layer parallelepiped foam was added and the solution was shaken for 10 min. The parallelepiped foam was then removed from the solution by decantation, washed thoroughly by squeezing twice with water, placed in a 10-mm quartz cell containing ethanol and set in the light path of the spectrometer. The absorbance of the coloured complex sorbed into the foam was measured at 460 nm against the HMNQO–thin-layer parallelepiped foam in ethanol. The net absorbance of the Ru–HMNQO chelate in the foam, A_F^*, was calculated from the equation

$$A_F^* = A_{F(Ru)} - A_{F(B)}$$

where $A_{F(Ru)}$ and $A_{F(B)}$ are the absorbances of the ruthenium complex on foam and blank, respectively.

2.6. Determination of Ru(III) in its complexes

The ruthenium(III) complexes were prepared as described previously [4] and digested employing the oxygen flask method as reported [11]. The resultant solution was reduced with 10 ml of 5% sodium sulphite solution followed by adding 5 ml of concentrated HCl. After boiling to remove the excess of SO_2 and transfer into a 50-ml volumetric flask, the solution was diluted to volume with water and the procedure in Section 2.5 was followed. The concentration was determined by reference to a calibration graph prepared under the same experimental conditions.

3. Results and discussion

The reaction of ruthenium(III) with HMNQO represents one of the most recent sensitive and selective approaches to the spectrophotometric determination of ruthenium after solid-phase extraction into microcrystalline *p*-dichlorobenzene [12]. The coloured product is formed rapidly and the equilibrium between the two phases is attained in a few seconds.

3.1. Qualitative and semi-quantitative determination of ruthenium(III)

The solution of ruthenium(III) was coloured (red-violet) by the addition of HMNQO at pH 5–7 [12]. This colour reaction was tested for the detection of ruthenium(III) with unloaded, HMNQO-loaded and HMNQO–TBP-treated foams. The surface area of the foam cube acts as an efficient collector for Ru(III)–HMNQO from aqueous solution at low concentration. The characteristic colour of the reaction product on the thin membranes of the foam material also allowed the detection of ruthenium(III) in extremely dilute aqueous solution.

On shaking one cube of the unloaded foam with 3–5 ml of hot Ru(III)–HMNQO at pH 7, it was possible to detect as little as 0.1 ppm of ruthenium(III). On shaking one cube of each HMNQO-loaded and HMNQO–TBP-treated foam with 3–5 ml of a hot aqueous solution of ruthenium, it was possible to detect as little as 0.05 and 0.02 ppm of ruthenium, respectively. The colour density on the foam cubes was found to depend on the concentration of Ru(III) in the aqueous solution. Hence it was possible to determine Ru(III) semi-quantitatively by comparison of the colour of the foam cubes with a standard colour scale (0.1–10 ppm) of ruthenium(III) employing HMNQO–TBP-treated foams under the same experimental conditions. The results obtained with HMNQO–TBP-treated foams are far better than those obtained with unloaded foams and HMNQO-loaded foams. The added TBP acts as a plasticizer of the foam material and enhances the diffusion of the species through the solid membrane and allows the collection of ruthenium(III) on the foam matrix [17,18,22].

The proposed HMNQO-loaded foam cubes can be easily packed in columns, producing a foam bed suitable for the detection and semi-quantitative determination of ruthenium in extremely dilute aqueous solutions. This was achieved by percolating 100 ml of the test ruthenium(III) solution through the foam col-

umn at a reasonable flow-rate (5 ml min^{-1}). The detection limit was found to be 10 ppb. The length of the coloured zone is proportional to the concentration of ruthenium. Semi-quantitative determination was possible using a colour scale covering concentrations from 5 to 50 ppb ruthenium(III).

Effect of diverse ions

The selectivity of the proposed HMNQO-loaded foam method was examined by detecting 1 μg of Ru(III) in the presence of a relatively high excess (10 mg) of each of Ba^{2+}, Cd^{2+}, La^{3+}, Zn(II), Al(III), Cr(III), Hg(II), Pt(IV), Ca^{2+}, Sr^{2+}, HPO_4^{2-}, $C_2O_4^{2-}$, NO_3^-, VO_3^-, SeO_3^{2-}, SeO_4^{2-}, acetate and formate ions. No interferences were observed using the straightforward procedures; V^{4+}, Pd^{2+}, Pt^{2+} and Os^{3+} interfered seriously. In the presence of some other ions, e.g., permanganate, copper(II), nickel(II), cobalt(II) and iron(III), simple modifications to the aqueous solution were introduced to eliminate their interferences in the proposed method. The results obtained are summarized in Table 1.

3.2. Quantitative determination of ruthenium(III)

Colourless polyurethane foam showed that the absorbance of the foam matrix is consistently lower than the absorbance of the corresponding thin layer of ion-exchange resin and has no absorption peaks in the range 400–800 nm [20]. The electronic spectrum of the parallelepiped thin-layer HMNQO-loaded foams showed no bands and the absorbance was negligible in the visible region, whereas the spectrum of Ru(III)–HMNQO sorbed on a thin layer of foam showed a well defined absorption peak at 460 nm (Fig. 1). This peak was tentatively assigned to ligand (π) $\rightarrow$ metal (d) charge transfer [23]. The electronic spectrum of the reagent HMNQO showed no absorption in the visible region (Fig. 1). Preliminary experiments showed that Ru(III) is quantitatively extracted by the HMNQO-loaded foam and a 3–5-min shaking time is sufficient to reach equilibrium for 100 ml of aqueous Ru(III) solution at pH 7 and 60°C. Lower or higher acidity gives incomplete extraction, as indicated by the decrease in the absorbance at 460 nm.

Validity of Beer's law

The absorbance of the HMNQO-loaded foam was measured against the concentration of Ru(III). A good linear relationship between the absorbance of the Ru(III) complex species in the foam and ruthenium(III) concentration was obtained under the experimental conditions used. Beer's law was obeyed up to 20 ppm of ruthenium. The molar absorptivity obtained from Beer's law and the Sandell sensitivity [23] for Ru(III)–HMNQO sorbed on the foam at 460 nm were found to be $2.8 \cdot 10^4$ dm^3 mol^{-1} cm^{-1} and 0.0022 μg cm^{-2}, respectively. A detection limit of 0.02 ppm of ruthenium was found. Reproducibility tests with five measurements of 10 ppm of ruthenium in the thin-layer foam showed a standard deviation of 0.2 μg cm^{-3}.

Table 1
Effect of foreign ions on the detection of 1 μg of ruthenium(III)

Foreign ion	Added as	Amount added (mg)	Masking agent
Fe^{3+}	$FeCl_3$	0.05	Add one crystal of KF
Ni^{2+}	$NiCl_2$	0.05	Add a few drops of 1% KCN solution
V^{5+}	NH_4VO_3	0.05	Add one crystal of NaF
MnO_4^-	$KMnO_4$	0.01	Add a few drops of 1% NaN_3 solution
MoO_4^{2-}	Na_2MoO_4	0.01	Shake the solution with diethyl ether–carbon tetrachloride (1:1, v/v) followed by addition of Ag_2SO_4

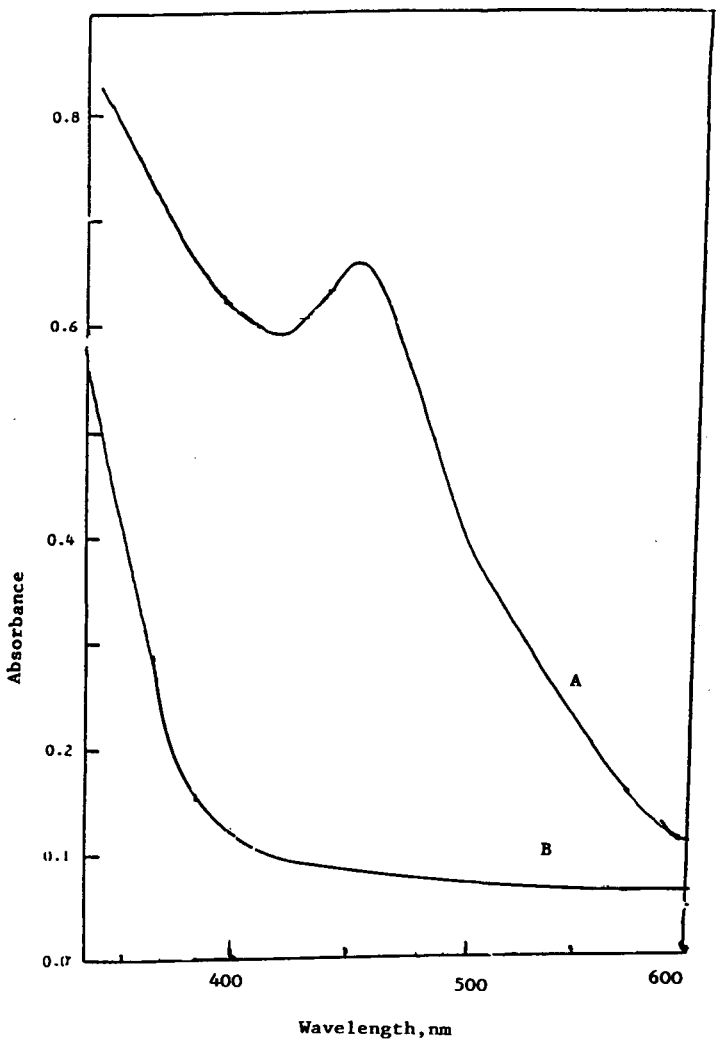

Fig. 1. Absorption spectra of ruthenium–HMNQO complex on thin-layer foam (A) against reagent blank HMNQO-loaded foam and (B) in aqueous solution at pH 7.

These results are better than those reported by Sharma [12].

The sensitivity of the method is better than or comparable to those of well known methods for ruthenium determination [12,13,24].

3.3. Analytical applications of the method

Determination of ruthenium(III) in water

The proposed extraction procedure was been applied for the determination of ruthenium in tap and sea waters employing the procedure in Section 2.5. Negative results were obtained, indicating the absence of ruthenium. Tap water (0.5 dm^3) samples containing various amounts of Ru(III) were added to the natural water and analysed by the proposed method; a 98–99% recovery of the added Ru(III) was obtained. The applicability of the method to the determination of lower than nanomolar levels of Ru(III) in water is also possible by filtration of the sample solution through a 0.45-μm membrane followed

Table 2
Results for the foam extractive spectrophotometric determination of Ru in its complexes

Complex[a]	Ru calculated (%)	Ru found (%)[b]	Standard deviation (%)
$RuCl_2(PPh_3)_2$ (koj)	24.52	24.8	0.26
$RuCl_2(PPh_3)_2$ (malt)	24.46	24.60	0.20
$RuCl_2(PPh_3)_2$ (trop)	24.7	24.4	0.20
$RuCl_2(PPh_3)_2$ (acac)	25.32	24.7	0.20

[a] Abbreviations: kojic acid (koj), maltol (malt), tropolone (trop) and acetylacetone (acac).
[b] Average of three determinations.

by extraction of the element with the HMNQO-loaded foam column (15 cm × 2 cm I.D.) at 5 ml min^{-1}. The sorbed complex is then eluted with acetone as reported [25] and analysed either by the procedure in Section 2.5 at 460 nm or by measuring the absorbance of the effluent solution of acetone containing the Ru(III)–HMNQO complex at 350 nm.

Determination of ruthenium(III) in its complexes

The microdetermination of ruthenium(III) in its complexes employing the proposed spectrophotometric procedures after digestion of the complexes was carried out. The results of these determinations are given in Table 2. The results obtained are in good agreement with the calculated values.

References

[1] E. Merian, *Metals and Their Compounds in the Environment, Occurrence, Analysis and Biological Relevance*, VCH, Weinheim, 1981.
[2] M.M. Taquikhan and R.S. Shukla, *J. Mol. Catal.*, 34 (1986) 19.
[3] R. Palaniappan and T.A. Kumar, *Analyst*, 118 (1993) 293, and references cited therein.
[4] A.M. El-Hendawy and M.S. El-Shahawi, *Polyhedron*, 8 (1989) 2813.
[5] Z. Marczenko, *Separation and Spectrophotometric Determination of Elements*, Ellis Horwood, Chichester, 1986.
[6] H.S. Gowda, J.B. Raji and S.A. Ahmed, *Indian J. Chem.*, 23A (1984) 621.
[7] A. Wasey, R.K. Bansal, M. Sataka and B.K. Puri, *Bull. Chem. Soc. Jpn.*, 56 (1983) 3603.
[8] R.F. Gurive, L.M. Trutneva, S.B. Savvin and N.N. Chalisova, *Zh. Anal. Khim.*, 39 (1984) 1653.
[9] A.K. Das and J. Das, *Indian J. Chem.*, 23A (1984) 359.
[10] A.M. Almuaibed and A. Townshend, *Microchem. J.*, 48 (1993) 210.
[11] M.S. El-Shahawi, A.Z. Abu-Zuhri and S.M. Aldaheri, *Fresenius' J. Anal. Chem.*, in press.
[12] R.K. Sharma, *Bull. Chem. Soc. Jpn.*, 66 (1993) 1084.
[13] M.S. El-Shahawi, A.Z. Abu-Zuhri and M.M. Kamal, *Fresenius' J. Anal. Chem.* (1994) 348.
[14] R. Palaniappan and V. Revathy, *Analyst*, 114 (1989) 517.
[15] R. Palaniappan, *Bull. Electrochem. Soc. India*, 39 (1991) 367.
[16] E.P. Medyansteva, G.K. Budinkov, O.N. Romanova and I.V. Zhivolup, *Zh. Anal. Khim*, 42 (1989) 639.
[17] M.S. El-Shahawi, *Talanta*, in press, and references cited therein.
[18] M.S. El-Shahawi, A.B. Farag and M.R. Mostafa, *Sep. Sci. Technol.*, 29 (1994) 289.
[19] A.B. Farag, M.S. El-Shahawi and S. Farrag, *Talanta*, in press.
[20] A.M. El-Wakil, M.S. El-Shahawi and A.B. Farag, *Anal. Lett.*, 23 (1990) 703.
[21] Y.A. Gawargious, M.N. Abbas and H.N.A. Hassan, *Anal. Lett.*, 21 (1988) 1477.
[22] A.B. Farag, A.M. El-Wakil and M.S. El-Shahawi, *Analyst*, 106 (1981) 809.
[23] E.B. Sandell, *Colorimetric Determination of Trace Metals*, Interscience, New York, 1959.
[24] G. Dinst and F. Hecht, *Mikrochim. Acta*, (1963) 895.
[25] S.J. Al-Bazi and A. Chow, *Talanta*, 31 (1984) 189.

ELSEVIER

Journal of Chromatography A, 697 (1995) 191–201

JOURNAL OF CHROMATOGRAPHY A

Application of a comparative evaluation of several reversed-phase columns to the automated analysis of candidate pharmaceuticals

I.M. Mutton

Structural Chemistry Department, Glaxo Research and Development Ltd., Greenford Road, Greenford, Middlesex UB6 0HE, UK

Abstract

This report discusses the evaluation of several modern reversed-phase chromatographic packing materials, and describes the application of a selected column in a method used to screen the purities of pharmaceutical candidates and intermediates. Columns are first evaluated with an acetonitrile gradient using a test mixture containing acids, bases and compounds of widely differing polarities. Selected phases are further assessed by analysing many typical samples. Finally, the use of the chosen column and method are described and discussed.

1. Introduction

Reversed-phase HPLC analysis is subject to well-known problems with unwanted retention mechanisms due to reactions of certain analytes with the siliceous support [1]. Ion exchange and hydrogen bonding with residual silanols can occur, as well as participation from residual trace metals in the base silica. Our laboratory has employed a large number of methods for analysis of acids, bases and other highly polar compounds. Many different mobile phases were necessary to chromatograph these diverse compounds on commonly used columns such as Spherisorb ODS-2. Method selection was time-consuming and results often disappointing. Recently, several deactivated reversed-phase packing materials have become commercially available. A comparative study of some of these materials was made so that a single method for this work could be adopted.

2. Experimental

2.1. Instrumentation

Hewlett-Packard (Bracknell, UK) 1090 Series M liquid chromatographs were used. They were equipped with 90-position autosamplers, DR5 pumps, ovens operated at 40°C, and diode array detectors. HP 79988A Revision 5.3 foreground/background operating software (Pascal Series) or HPLC^{3D} ChemStation (DOS Series) software was used. One autosampler was cooled to 8°C by air blown from a heat-exchange unit through which ethylene glycol coolant at 4°C was passed using a Julabo (Leighton Buzzard, UK) F10 recirculating bath.

2.2. Columns

Columns evaluated had dimensions of 150 × 4.6 mm and were packed with 5-μm particle size

0021-9673/95/$09.50
SSDI 0021-9673(94)01219-9

reversed-phase silicas. The columns were: Spherisorb ODS-2 (Phase Separations, Deeside, UK), Hypersil BDS C_{18} (Shandon, Runcorn, UK), Inertsil ODS-2 and 250 mm Kromasil C_{18} (Capital HPLC, Broxburn, UK); Suplex pKb 100 and Supelcosil ABZ (Supelco, Saffron Walden, UK); Ultracarb 5 ODS 20 and Ultracarb 5 ODS 30 (Phenomenex, Macclesfield, UK); and Zorbax SB-C_{18} (Hichrom, Reading, UK).

2.3. Test mixture

The test mix used for initial column screening was prepared in acetonitrile–deionised water (1:1). Its composition is shown in Table 1. The components of this mix were purchased from BDH (Poole, UK) (Component Nos. 1, 2, 4 and 5) and Aldrich (Gillingham, UK) (Components Nos. 3, 6, 8 and 9) and were of at least general-purpose grade. 2-Hydroxy-5-methylbenzaldehyde was available within Glaxo Research and Development.

2.4. Compound library for detailed column screening

A collection was made of 86 RP-HPLC candidates providing a representative range of polarities, pK values and chemistries. These were all proprietary compounds prepared within Glaxo Research and Development during various research programmes.

Table 1
Composition of test mixes

No.	Component	Concentration (μg/ml)
1	Pyridine	690
2	Benzylamine	110
3	N-Acetylprocainamide · HCl	85
4	Benzyl alcohol	155
5	Phenol	120
6	4-Nitrobenzoic acid	220
7	2-Hydroxy-5-methylbenzaldehyde	65
8	4-Chlorocinnamic acid	105
9	Phenyl ether	100

2.5. Analysis conditions

The mobile phases were: *system 1*: A = 0.1% (v/v) phosphoric acid, B = 95% (v/v) acetonitrile + 0.1% (v/v) phosphoric acid; *system 2*: A = water, B = 95% (v/v) acetonitrile; *system 3*: A = 50 mM, pH 2.3 ammonium dihydrogenphosphate, B = 95% (v/v) acetonitrile.

These were prepared with deionised water, HPLC-grade acetonitrile, and analytical-reagent grade phosphoric acid. System 3 was filtered to remove salt particulates. To avoid the possibility of introducing contaminants, systems 1 and 2 were not filtered. All mobile phases were thoroughly degassed with high-grade helium before use.

The test gradients employed were: B = 0% (2 min) to 100% over either 20 or 40 min, then held at 100% for 10 min before returning to B = 0% over 2 min. A post time of 6 min was added, giving a total cycle time of either 40 or 60 min. Measurements were made at 215 nm and 40°C, using a flow-rate of 1.0 ml/min. Aliquots of 10 μl were injected. UV spectra were used to confirm peak identities.

2.6. Peak evaluation criteria

Peak width values at half-height (w_h) and symmetry (SYM) values reported by the HP1090 data system [2,3] were recorded for each of the main component peaks. A perfectly symmetrical peak has a SYM value of unity. Successful chromatography (a "hit") was arbitrarily defined by a w_h value of <0.25 min.

2.7. Analytical protocol

Research compounds were analysed as $\leq 0.1\%$ (m/v) solutions in acetonitrile–water mixtures. Inertsil columns, protected with 20 mm guard cartridges, were used with the longer gradient to generate purity profiles. Many compounds only absorb at low wavelengths; thus for screening purposes the detector is set at 215 nm with a bandwidth of 10 nm to provide rapid initial purity assessments. This approach requires that the acid chosen (phosphoric) is UV trans-

parent and that all mobile phase components are of the highest quality. Quality control is maintained by running blanks and test mixes so that artefacts or column deterioration may be flagged rapidly.

3. Results and discussion

3.1. Initial column screening

Each column was evaluated by analysing the test mix using system 1 with the longer gradient. The results are shown in Fig. 1. The columns exhibit different activities towards bases, acids and metal chelators. Three columns having generally lower activities in this test (Inertsil, Kromasil C_{18} and ABZ) were selected for a more rigorous comparative evaluation with Spherisorb ODS-2.

3.2. Detailed column screening

The three selected columns were compared by analysing each of the 86 library compounds using 20-min gradients with mobile phase systems 1–3. The results are summarised in Table 2.

The w_h and SYM figures were only included for those compounds recorded as "hits" according to the peak evaluation criteria. The three selected materials each performed significantly better than Spherisorb ODS-2, which failed to satisfactorily chromatograph approximately 40% of the test compounds. In contrast, provided the mobile phase was acidified (system 1), Inertsil and Kromasil had a 99% success rate, and ABZ also performed very well. The single failure on Inertsil was due solely to the lipophilicity of the compound concerned and a slight extension of the isocratic period at 100% B resulted in satisfactory elution. It therefore does not indicate activity of the column towards the analyte. Compounds failing on Spherisorb ODS-2 generally had highly basic, acidic, ionic or polar natures; this observation agrees with our long-term experience of this material used with systems 2 and 3. The poor symmetry values of peaks recorded for "hits" are a further indication of its activity. Some residual activity is still apparent on the other three phases, and for each column an acidic mobile phase (system 1) is essential to maximise the chance of successfully running a novel compound. Inertsil provided significantly better w_h and SYM values than Kromasil and was therefore selected as the analytical packing material of choice from amongst those tested.

An independent comparison of several modern reversed-phase columns was published by McCalley [4] after completion of this work. In this case too, Inertsil was the best of the materials evaluated.

3.3. Selection of gradient conditions

We required a rugged, simple, high-throughput single procedure giving high information content and high-quality information. These criteria can be best met by a gradient approach if the method is to be capable of addressing the wide polarity range of samples and their (unknown) impurities [5]. This approach maximises the proportion of novel samples that can be successfully analysed.

A brief examination was made of the effect of different gradients on the resolution. Formal optimisation using computer simulation [6] was not attempted since each sample represents a potential set of unknown compounds. The test mix was run on an Inertsil ODS-2 column with system 1 using different gradient (GT) and cycle (CT) times, and the apparent resolution (R_s) between benzyl alcohol and phenyl ether was noted:

$$R_s = 1.177(t_{R1} - t_{R2})/(w_{h1} + w_{h2})$$

where t_{R1} and t_{R2} are the retention times in minutes of benzyl alcohol and phenyl ether, respectively, and w_{h1} and w_{h2} the corresponding peak widths at half height.

Table 3 demonstrates the loss of resolution with decreasing gradient time. Long gradient times produce a 4-fold increase in resolution, although less resolution per unit GT. However, because it is necessary to maintain realistic isocratic and re-equilibration periods, a more

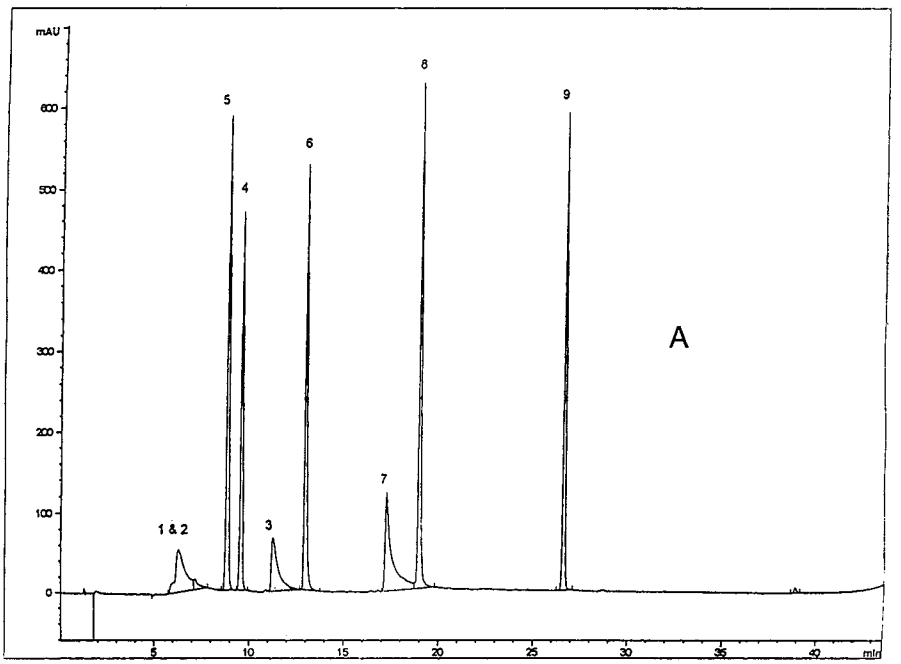
mAU
600
500
400
300
200
100
0
1 & 2
3
4
5
6
7
8
9
A
5
10
15
20
25
30
35
40
min

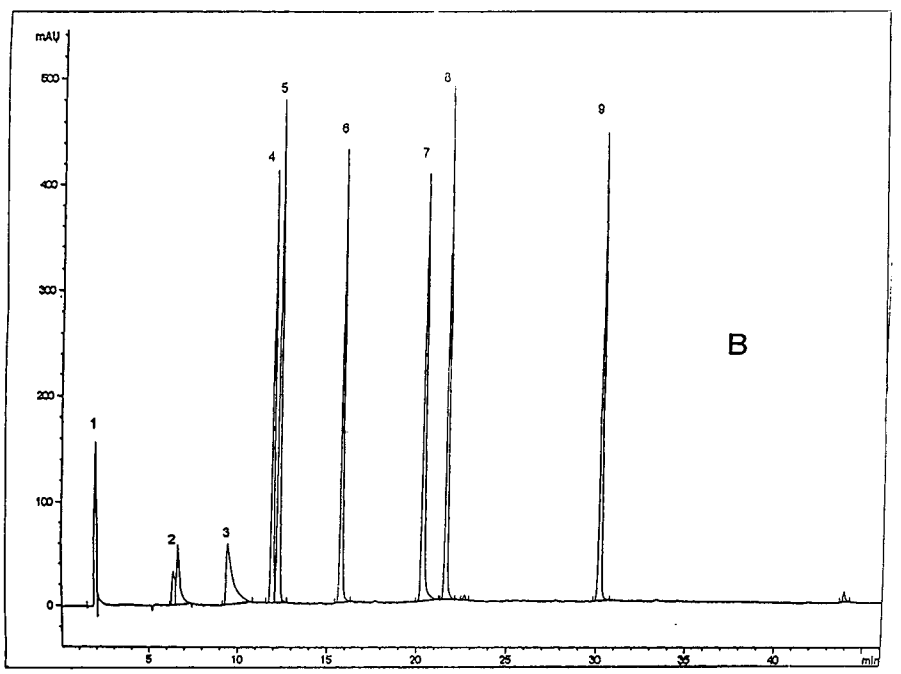
mAU
500
400
300
200
100
0
1
2
3
4
5
6
7
8
9
B
5
10
15
20
25
30
35
40
min

Fig. 1.

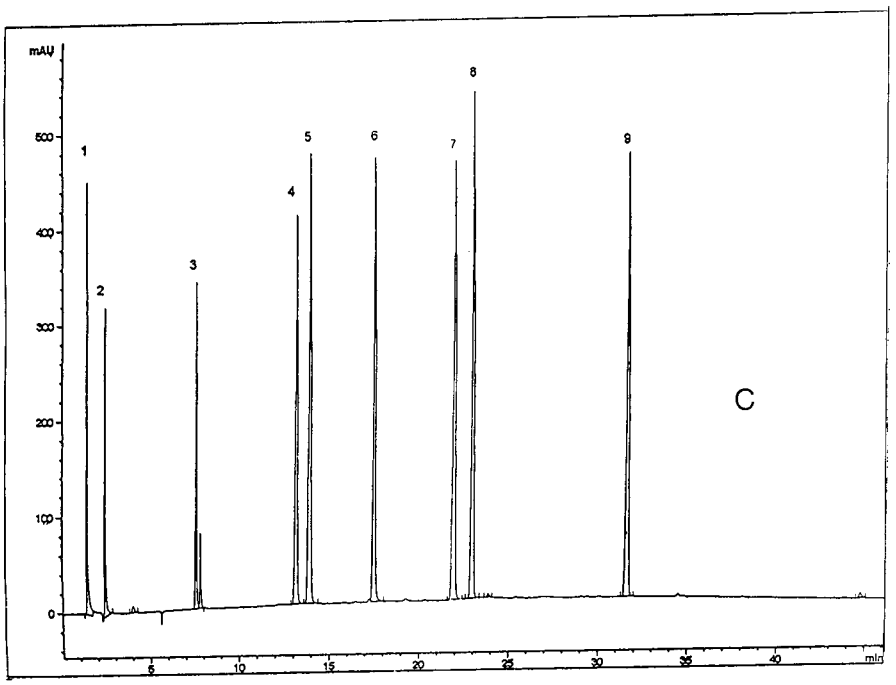

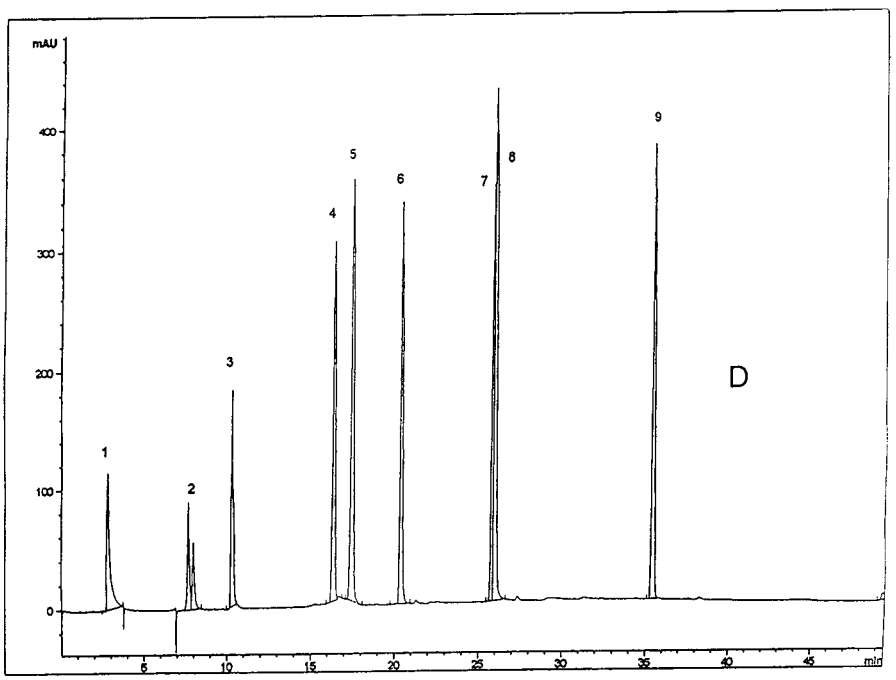

Fig. 1 (*continued on p. 196*).

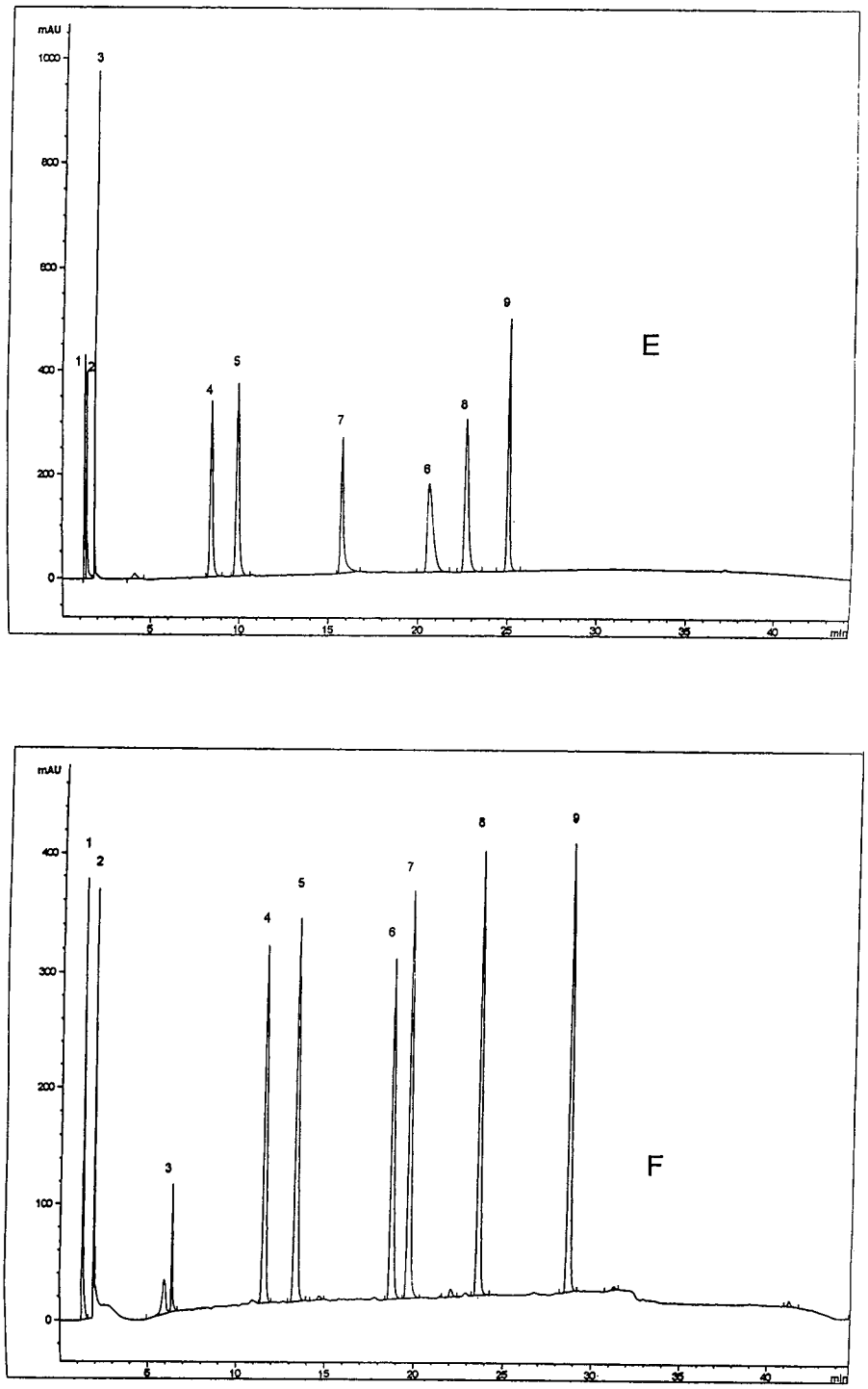
mAU
1000
800
600
400
200
0
1
2
3
4
5
6
7
8
9
E
5
10
15
20
25
30
35
40
min
mAU
400
300
200
100
0
1
2
3
4
5
6
7
8
9
F
5
10
15
20
25
30
35
40
min

Fig. 1.

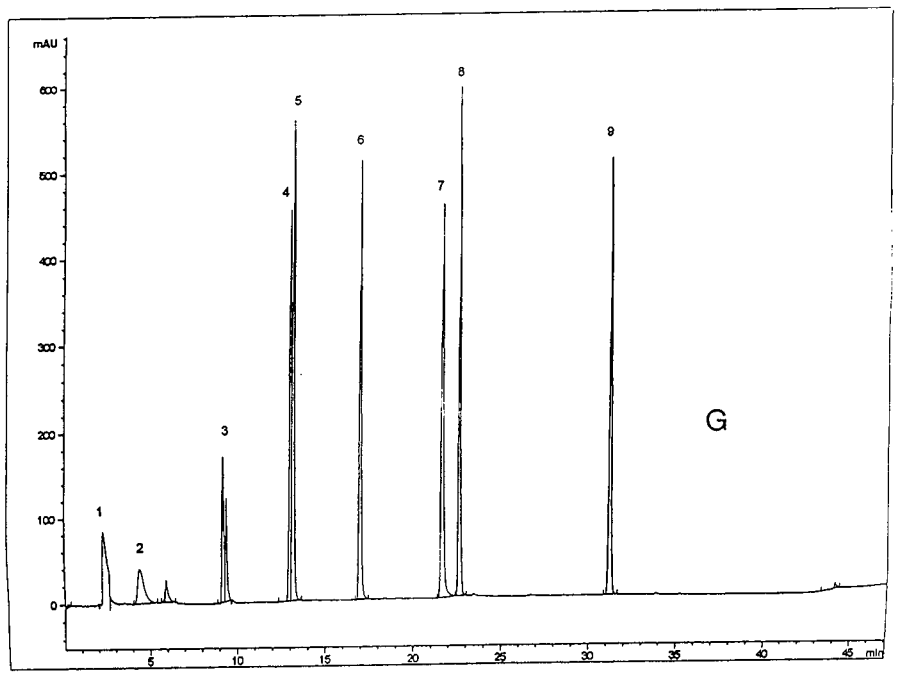

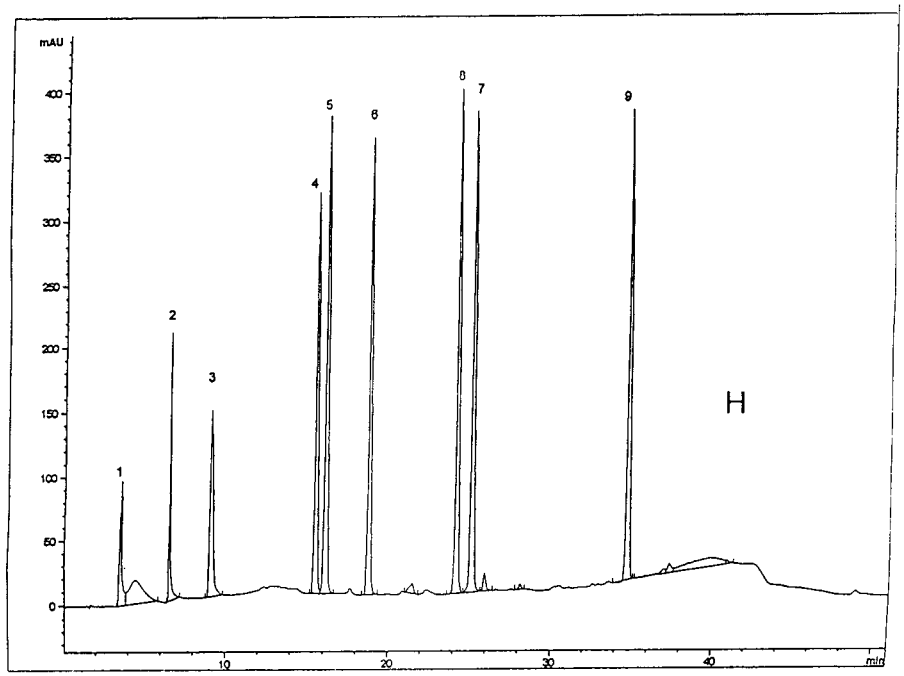

Fig. 1 (*continued on p. 198*).

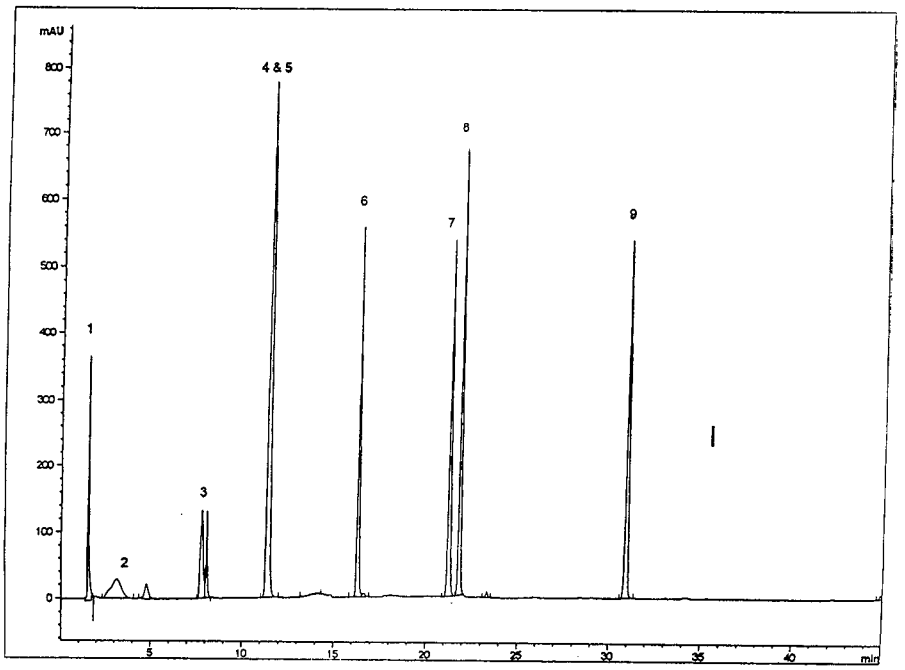

Fig. 1. Chromatograms of the test mix obtained on candidate columns. For conditions see Experimental section. Peak Nos. refer to identities given in Table 1. (A) Spherisorb ODS-2; (B) Hypersil BDS C_{18}; (C) Inertsil ODS-2; (D) Kromasil C_{18}; (E) Suplex pKb-100; (F) Supelcosil ABZ; (G) Ultracarb 5 ODS 20; (H) Ultracarb 5 ODS 30; (I) Zorbax SB-C_{18}. Usually 2 to 4 injections were made to ensure consistent chromatography. Note that generally only one (new) column of each type was tested and that it would be incorrect to infer from these results that any one commercial packing material is necessarily superior to any other.

relevant comparator is resolution per unit CT, and this is almost constant for gradients of 15 to 45 min. The choice of gradient then depends on a subjective judgement of how much resolution can be sacrificed. Fig. 2A and B demonstrate the loss of information content incurred around the major peak when using a 20-min gradient instead of one of 40 min. Comparison with isocratic conditions (Fig. 2C), selected such that the capacity factors exceeded 10, shows that loss of resolution of materials having closely similar retentions is acceptable when GT = 40 min,

Table 2
Comparison of candidate column performances

Column	System	Hits	Mean w_h (±R.S.D., %)	Mean SYM (±R.S.D., %)
Spherisorb ODS-2	1	58	0.089 (± 45)	0.77 (± 71)
Spherisorb ODS-2	2	47	0.101 (± 47)	1.29 (± 145)
Spherisorb ODS-2	3	55	0.094 (± 33)	0.81 (± 56)
Inertsil ODS-2	1	85	0.088 (± 29)	0.89 (± 38)
Inertsil ODS-2	2	45	0.109 (± 31)	0.89 (± 45)
ABZ	1	77	0.081 (± 29)	0.78 (± 32)
ABZ	2	50	0.091 (± 34)	0.97 (± 71)
Kromasil C_{18}	1	85	0.106 (± 21)	0.68 (± 21)

Table 3
Effect of gradient and cycle times on resolution (R_s)

GT	CT	R_s	R_s/GT	R_s/CT
5	18	20	4.1	1.2
15	28	51	3.3	1.8
25	38	68	2.7	1.8
35	48	79	2.2	1.6
45	58	86	1.9	1.5

GT is the time in minutes between 0 and 100% B, CT is the time between injections, allowing 2- and 4-min isocratic periods at the respective extremes of the gradient to ensure representative chromatography of both hydrophilic and lipophilic materials. CT also includes 2 min to return to 0% B, and a 5-min re-equilibration time before each injection.

whereas when GT = 20 min it is not. This point is the more relevant when one considers that the impurities most likely to be present will often be isomers of the parent compound or other closely related compounds.

A GT of 40 min was therefore selected, and isocratic and equilibration times adjusted as detailed in the Experimental section to ensure elution of most lipophiles and to obtain a CT of 1 h.

3.4. Selection of mobile phase system

It is clear from the comparisons made using the compound library that an acidic mobile phase, or possibly one of high ionic content, is necessary to ensure successful chromatography of most routine samples. The mobile phase advocated (system 1) has the advantage over our previously employed standard acidic system (system 3) of allowing high acetonitrile concentrations to be used without causing precipitation of buffer salts. Experience with about 1250 different samples indicates that the vast majority of acidic analytes are ion-suppressed in this buffer system, and that most bases are effectively converted to their conjugate acids.

3.5. Sample stability

A possible source of failure is the stability of the sample, either during storage in the autosampler before the analysis or during the run. These matters are treated separately below.

An extensive evaluation of solution stability was made with a collection of about 200 different samples that represented several distinct synthetic lines and chemical classes. Sets of about 10–15 individual samples were each run twice by immediate repetition of the sequence. No evidence of significant solution instability was found. Currently each sample is analysed once only and the added precaution is taken of cooling the sample solutions to 8°C whilst they await analysis. Potentially unstable solutions are given priority and/or re-analysed after a defined time in solution. No serious problems have occurred; but on three or four occasions samples have precipitated before injection.

Samples with acid-labile protecting groups are quite common. For most compounds studied to date, on-column acid hydrolysis does not seem to represent a problem. Although the mobile phase pH is quite low (around 2), sample solutions are typically 0.1% (m/v) or less, and contact time at 40°C with acid is limited to the retention time since samples are dissolved in non-acidified water–acetonitrile mixtures. If the stability of a particular sample is in doubt, a run using system 2 can be informative. It is also possible to check for acid lability by use of micro-preparative chromatography. This entails injection of a suitable aliquot of a concentrated sample solution and collection of the fraction containing the major component. Re-injection of this fraction then reveals any artefacts due to on-column decomposition. In practice, very few examples of serious incompatibility with system 1 have been identified in cases where there was good a priori reason to question stability towards the conditions used. However, an instrument employing system 2 is available for acid-labiles and to screen potential preparative applications for omission of buffer additives. More rigorous criteria would be required to test candidate pharmaceuticals against specifications applied in, for example, clinical trial work. The system reported here is quite adequate to provide initial impurity profiles of research compounds.

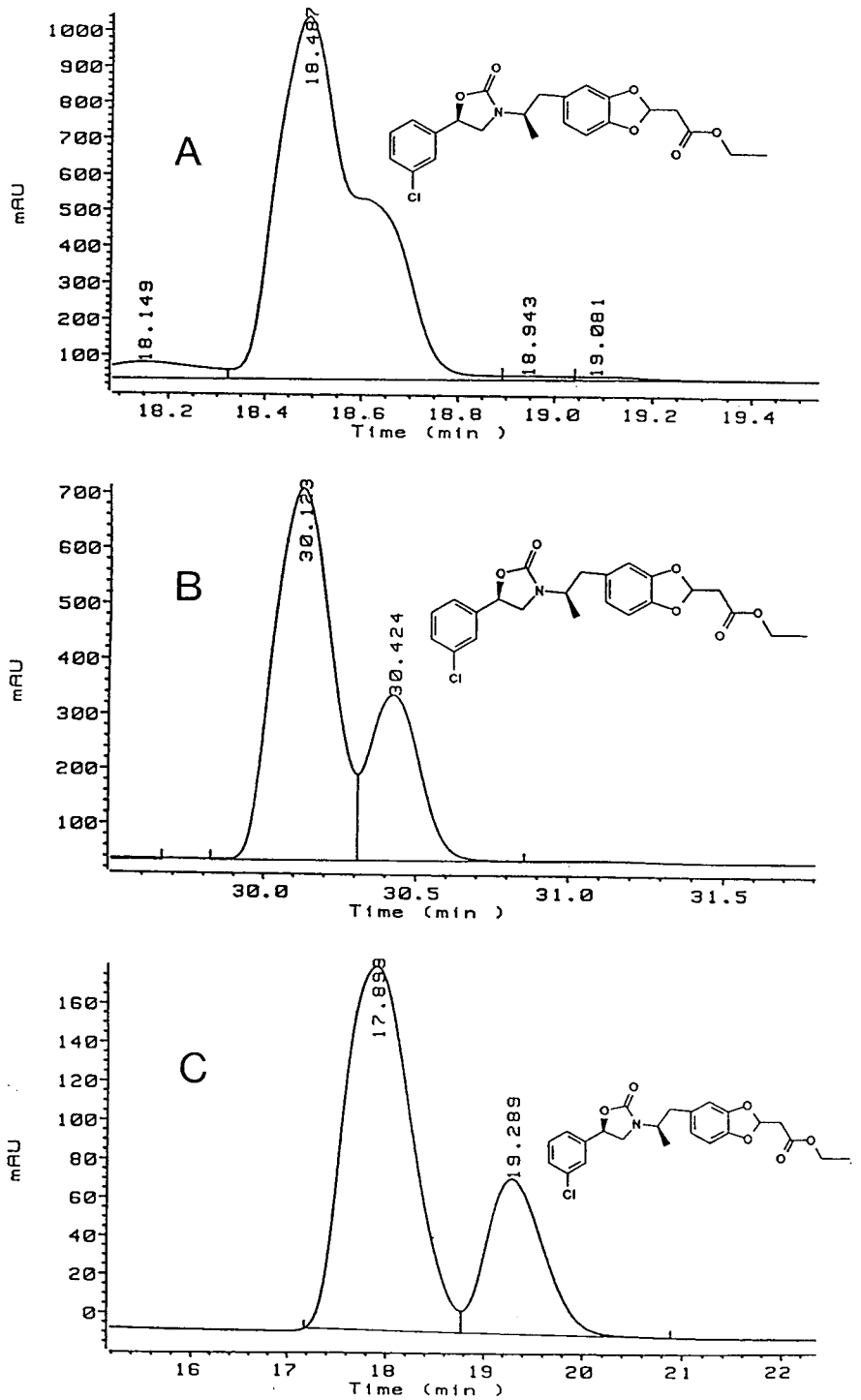

Fig. 2. Analysis of an approximately 2:1 mixture of diastereomers on an Inertsil column. Mobile phase: system 1 with (A) a 20-min gradient; (B) a 40-min gradient; and (C) isocratically with 50% (v/v) acetonitrile.

3.6. Protocol

Current practice is to run two blanks and a sample of the test mix each day. This provides a visual check for artefactual, "system" peaks, and a record of column performance. Monitoring the blank runs helps evaluate different sources of supply of the mobile phase components and hence to further reduce background signals. Mean retention times of benzyl alcohol and phenyl ether had respective R.S.D.s of ± 0.3 and $\pm 0.5\%$ when monitored for a month. Trends in parameters such as retention times, peak areas, w_h and SYM advise the operator to change the either the test mix, precolumn or main column. All our ODS columns, whether Inertsil stock or alternatives under evaluation, are assessed with the test mix and the reported method. It is also intended to use the test mix in a study of minituarised systems.

4. Conclusions

There are many excellent deactivated C_{18} materials commercially available. Examination of several of these materials shows significant differences in their selectivities and activities towards selected probes. Further evaluation of three columns resulted in identification of one that was particularly suitable for routine analysis of many RP-amenable candidate pharmaceuticals and synthetic intermediates.

The selected column has been used in an automated procedure that incorporates performance checks. Successful analysis of about 95% of 1250 compounds was obtained during the preceding year. Rapid provision of high quality impurity profiles enables immediate assessment of the suitability of samples for purposes such as submission to biological screens or use in synthetic schemes. Benefits to the analyst include method simplification, ease of data storage and retrieval, and significant savings of time, solvents and instrumental requirements.

Deactivated, high-purity ODS-silica packing materials are recommended as the initial choice for new reversed-phase applications.

References

[1] R.J.M. Vervoort, F.A. Maris and H. Hendriks, *J. Chromatogr.*, 623 (1992) 207.
[2] *HPLC ChemStation Fact File*, Hewlett-Packard, Waldbronn, 1988.
[3] I. Parr, personal communication, 1994.
[4] D.V. McCalley, *J. Chromatogr.*, 636 (1993) 213.
[5] A.M. Krstulovic and P.R. Brown, *Reversed-Phase High-Performance Liquid Chromatography —Theory, Practice and Biomedical Applications*, Wiley, New York, 1982.
[6] J.W. Dolan, D.C. Lommen and L.R. Snyder, *J. Chromatogr.*, 485 (1989) 91.

ELSEVIER

Journal of Chromatography A, 697 (1995) 203–211

JOURNAL OF CHROMATOGRAPHY A

Automated solid-phase extraction and coupled-column reversed-phase liquid chromatography for the trace-level determination of low-molecular-mass carbonyl compounds in air

P.R. Kootstra*, H.A. Herbold

Laboratory of Organic-analytical Chemistry, National Institute of Public Health and Environmental Protection (RIVM), P.O. Box 1, 3720 BA Bilthoven, Netherlands

Abstract

This study reports the development of a coupled-column RPLC method for the trace level determination of several volatile aldehydes in ambient air. Carbonyls in air are sampled using a ozone scrubber and SPE C_{18} cartridges which are pretreated with 2,4-dinitrophenylhydrazone. The method is used for the separation of 13 different aldehydes and ketones. All analytes are separated without high blanks or ozone interferences. The analytical detection limits for the most important compounds formaldehyde, acetaldehyde, 2-propenal (acroleine), 2-butenal (crotonaldehyde) and benzaldehyde, range from 50 to 150 ng/m^3 (ppt) or 0.5–1.0 pmol/l, with relative standard deviations of 6%. The sampled air volume was 200 l. Due to the high sensitivity of the method, high purity solvents must be used. The analytical method as described below, has high recoveries for all analytes ($>90\%$) and is fully automated. This procedure has been applied in a pilot study with 60 air samples.

1. Introduction

Carbonyl compounds, aldehydes and ketones, are given increased attention as pollutants and possible key compounds in photochemical reactions [1]. Some aldehydes, particularly formaldehyde, are well known for their impact on human health, and therefore require sensitive and selective methods of analysis [2]. A variety of analytical techniques have been developed, most of them focused on formaldehyde. Formaldehyde is a common industrial chemical which is used for example in the manufacturing of glues and resins. In homes, a major source of formaldehyde is particle board.

The derivatisation with 2,4-dinitrophenylhydrazine (DNPH) prior to high-performance liquid chromatography (HPLC) has received widespread acceptance because of its selectivity. Early field applications of the method involves sampling with impingers which contain a DNPH solution [3,4]. Currently, most sampling is done on small DNPH coated C_{18} cartridges as described by Kuwata et al. [5]. However, the drawbacks of this widely used and accepted method are high blanks, ozone interference and long collection times to achieve sub-ppb detection limits [6]. Ozone, usually present in urban air, degrades the hydrazone derivatives [7].

* Corresponding author.

0021-9673/95/$09.50
SSDI 0021-9673(94)00973-2

Some of the problems are the cartridge background levels of formaldehyde, acetaldehyde and acetone which are about 1.1–2.3 nmol (56–70 ng) [8]. Levels of 6 μmol (180 μg) formaldehyde are also reported on uncoated C_{18} cartridges. The actual cause of this background is, however, not known [9].

During the development of the HPLC method, several problems had to be dealt with. The first goal was to improve selectivity and sensitivity for formaldehyde, acetaldehyde, 2-propenal (acroleine), 2-butenal (crotonaldehyde) and benzaldehyde, in order to analyse air samples with a carbonyl concentration of $\pm$ 1 pmol/l ($\pm$ 50 ng/m^3). Secondly, the method must be automated due to the expected high number of samples to be analysed.

Large volume injection on a small precolumn seems to be a possibility for improving sensitivity but unfortunately the excess of unreacted DNPH reagent is difficult to separate from early eluting compounds. Coupled-column reversed-phase liquid chromatography (RPLC) appeared to be very useful for trace-level determination of various compounds in water. Using two highly efficient separation columns, very strong polar analytes such as ethylenethiourea, chloroallylalcohol and methylisocyanate in aqueous samples can be analysed directly to a level of 1 μg/l (ppb) [10,11]. Therefore, this method was adopted for the analysis of aldehydes.

The described procedure involves off-line sampling on two DNPH-coated C_{18} cartridges coupled to an easy to build and effective ozone scrubber and coupled-column RPLC for the automated highly efficient clean-up and analysis of the samples. Due to the sensitivity of the described method, unforeseen impurities in the solvents used caused additional problems.

2. Materials and methods

2.1. Reagents

Bakerbond SPE columns C_{18} (3 ml LD, 200 mg, 40 μm), phosphoric acid, methanol HPLC-grade, acetonitrile HPLC-grade and 'Baker analysed', HPLC-grade water, were purchased from J.T. Baker (Deventer, Netherlands). 2,4-Dinitrophenylhydrazine (DNPH) and potassium iodide were purchased from Fluka Chemie (Buchs, Switzerland). Stock solution of aldehydes, ThetaKit TK-151, and ketones and ThetaKit TK-155 were purchased from Rochrom (Rotterdam, Netherlands). HPLC columns (100 $\times$ 4.6 mm I.D.) packed with 3 μm MicroSphere C_{18} were obtained from Chrompack (Bergen op Zoom, Netherlands). LC-grade water was obtained by purifying demineralised water with a Milli-Q system (Millipore, Bedford, MA, USA). Ozone was produced with a highly efficiency Hg-lamp in a laboratory made ozone generator. SPE columns were first washed twice with 2 ml acetonitrile ('Baker analysed') and once with 2 ml DNPH solution (1 mg DNPH per ml acetonitrile 'Baker analysed', 2% phosphoric acid). The columns were dried for 20 min under a stream of nitrogen (purity 5.0, HoekLoos, Schiedam, Netherlands). The coated columns, with air tight caps on both sides, were stored in a dark and cool place and used within 10 days [11]. Luer caps were purchased from Omnilabo (Breda, Netherlands). Caps for the other side (I.D. 9 mm) of the SPE columns were purchased from Gilson (Villiers-le-Bel, France). A saturated solution of potassium iodide was put in a copper tube (1 m $\times$ 4.6 mm I.D.) for 10 min and dried under a stream of nitrogen (200 ml/min) for 3 h. This tube was used as an ozone scrubber.

2.2. Apparatus

The high-pressure gradient LC-system (Fig. 1) consisted of two Gynkotec (Germening, Germany) dual piston isocratic LC pumps (P-2), a Model 480 programmable and a Model 300 slave pump. A Waters (Millipore, Bedford, MA, USA) Model 6000 solvent delivery system (P-1) was used to condition the first analytical column. All LC solvents were degassed with a Separations GT-103 degasser (Separations, H.I. Ambacht, Netherlands). An ASPEC (Automated Sample Preparation with Extraction Columns, Gilson) system equipped with a Rheodyne (Berkeley, CA, USA) 7010 high-pressure switching

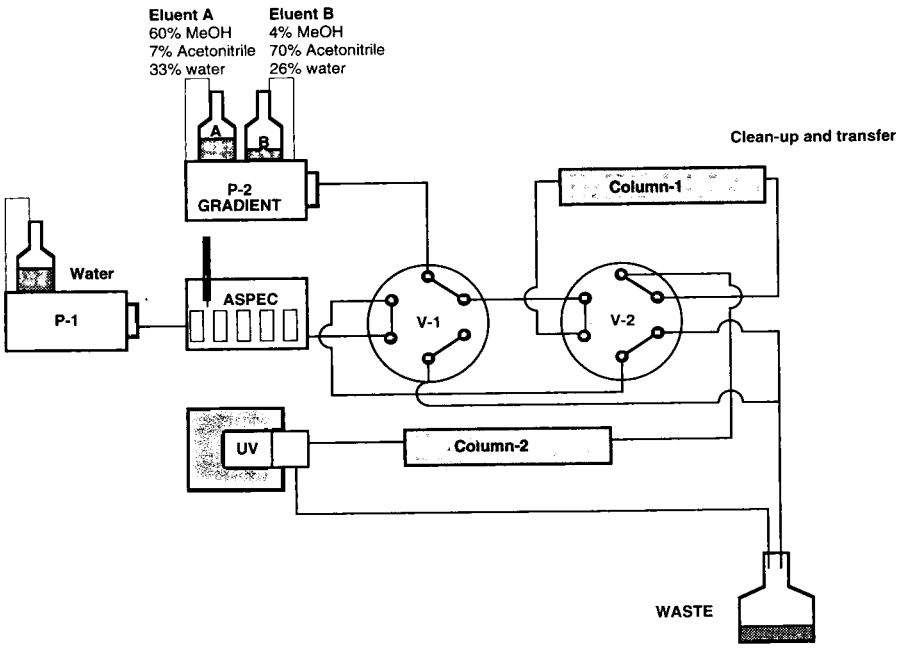

Fig. 1. Schematic setup of the coupled-column HPLC system for the analysis of aldehydes and ketones. ASPEC = Automated sample preparation with extraction columns; V-1 and V-2 = valves; P-1 = isocratic LC pump; P-2 = gradient LC pump; UV = UV–Vis detector.

valve is used for the automated elution and injection of the samples. A multiport stream-switch, MUST (Spark-Holland, Emmen, Netherlands) with two automated Rheodyne 7010 high-pressure six-port switching valves was used for coupled-column chromatography. An ABI 757 UV detector (Applied Biosystems, Foster City, CA, USA) was used at 360 nm. Data were acquired on an HP 3365 Series II ChemStation, running on a HP Vectra personal computer (Hewlett-Packard, Rockville, MD, USA).

2.3. Sampling

Sampling took place with two SPE columns, connected to each other with a polypropylene sealing cap (Gilson) and the ozone scrubber placed before the cartridges. A 200-l air sample was taken with a GAST vacuum pump type DOA-V112-BN (MFG, Benton Harbor, MI, USA) at a flow-rate of 2 l/min. After sampling, SPE columns were capped and stored dark in a refrigerator (5°C).

2.4. HPLC analysis

Mobile phase A consisted of methanol–acetonitrile–water (60:7:33, v/v/v). Mobile phase B consisted of methanol–acetonitrile–water (4:70:26, v/v/v). All flow-rates were 1 ml/min. Before each injection the first column, column-1, was conditioned with water for 10 min.

Cartridges were extracted with 3 ml acetonitrile which was diluted with 7 ml water. From this solution, 2 ml were injected on column-1. After injection, valve V-1 was switched to the gradient LC system (P-2) for a linear gradient from 100% mobile phase A to 100% mobile phase B in 30 min. A clean-up volume of 4 ml was used to separate the first eluting analyte from early eluting interferences, and after 4 min, column-1 and column-2 were coupled by switch-

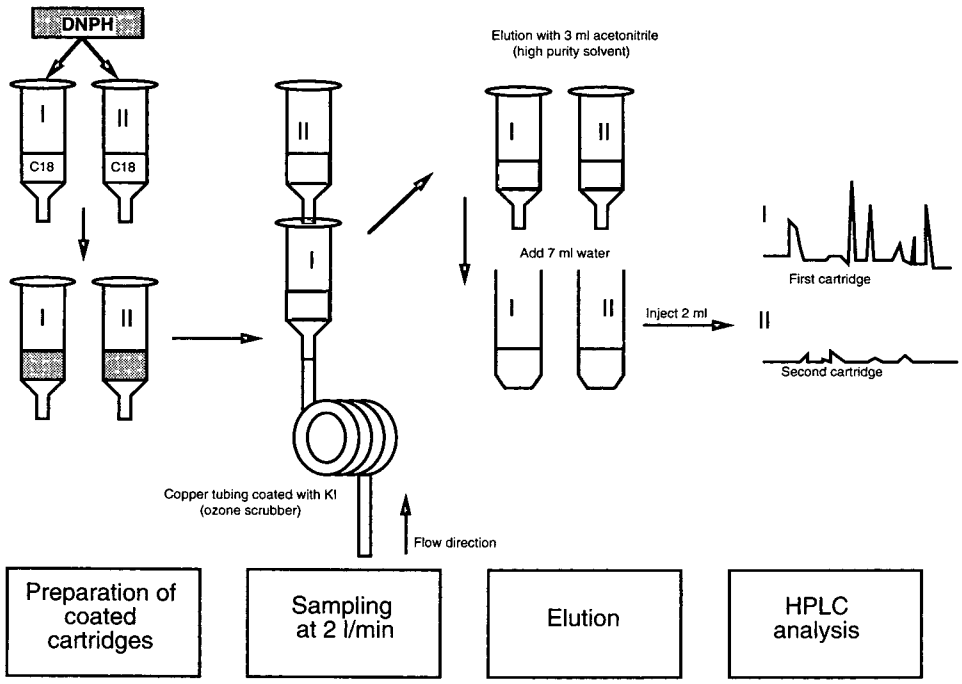

Fig. 2. Procedure for the cartridge preparation, sampling and analysis of carbonyl compounds in air. For details see text.

ing valve V-2 (see also Fig. 1). Compounds were identified by elution. During the method development, on-column derivatisation of the aldehydes and ketones, was checked with FTIR. Blank levels were first obtained by sampling 200 l of nitrogen gas from a cylinder. Afterwards blanks were obtained by eluting an unused DNPH-treated cartridge with acetonitrile.

An ASPEC system was used for the complete automated elution, dilution and injection of the samples.

The procedure is summarised in Fig. 2. Extraction and analysis of the samples must take place within 10 days.

3. Results and discussion

The major problem encountered in the determination of the DNPH-derivatives of both aldehydes and ketones, is the presence of unused DNPH reagent which causes, particularly in the first part of the chromatogram, a large background interference. In order to reduce this interference, the possibility of precolumn switching was investigated. Since C_{18} cartridges are eluted with 3 ml acetonitrile, dilution is necessary in order to increase retention on another C_{18} precolumn. The use of a short precolumn (specificity) did not provide the required selectivity. Unfortunately the excess of unreacted DNPH reagent was difficult to separate from the early eluting compounds (data not shown). Better results were obtained when the precolumn was replaced by an analytical column. As has been shown in other applications by Hogendoorn et al. [10], the use of a first column with high separation power provides more efficient separation of the large excess of the early eluting interferences and the first eluting analytes. In this case dilution with water is also necessary to increase retention on the first RPLC column. The dilution was therefore optimised. Fig. 3 shows the results of the analysis with and without the coupled-column switching technique. As can be seen, early eluting compounds such as form-

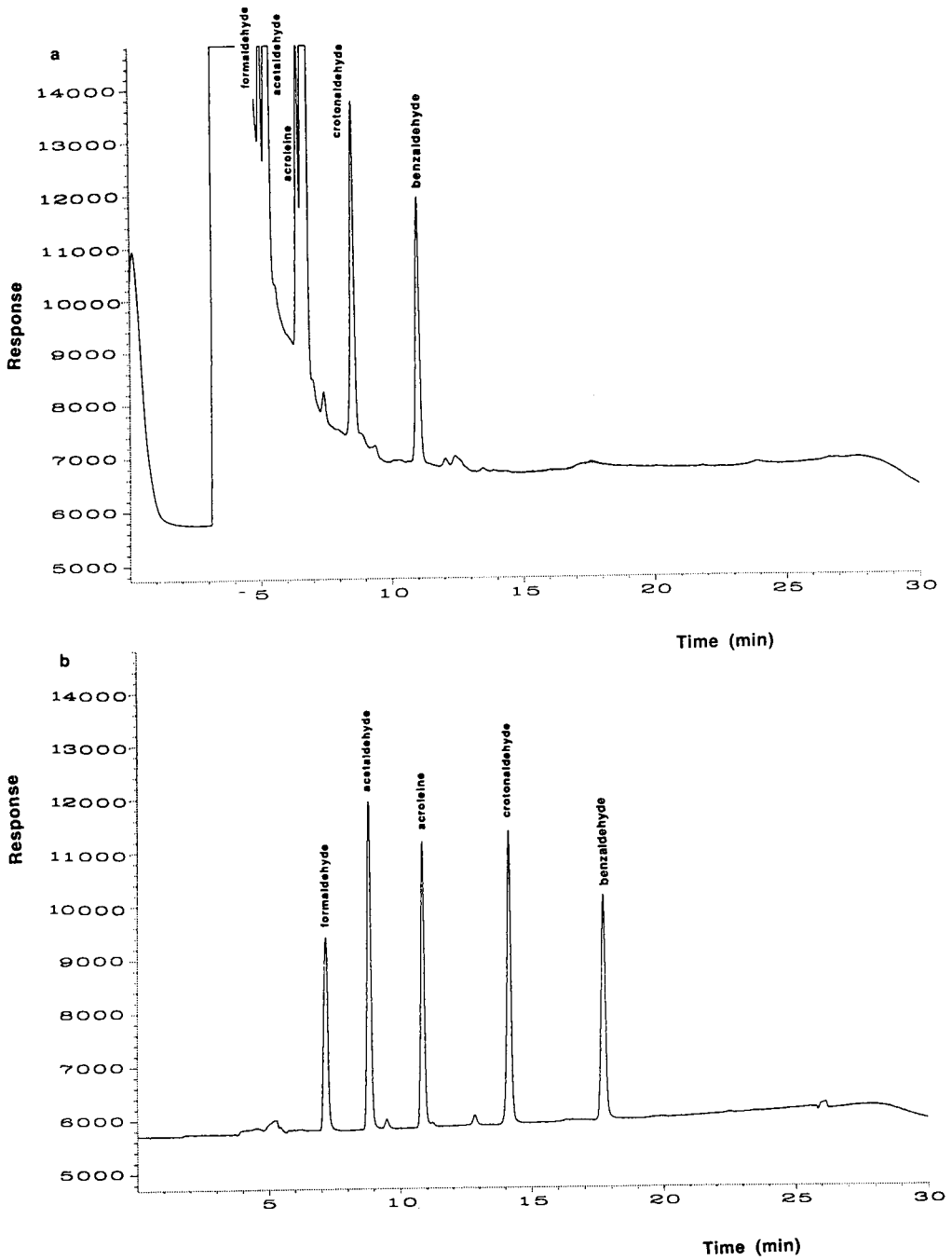

Fig. 3. Results of the clean-up method. Analysis of an air sample (a) with and (b) without column switching. Analytical conditions as described in the text. During the analysis without column-switching, valve-2 in Fig. 1 was not switched. Response of detector in counts.

aldehyde are separated from the large excess of DNPH.

A large air volume with known concentrations of the carbonyl compounds, is very difficult to realise. As the best approach for recovery experiments, standard mixtures were added to an SPE column. All compounds had recoveries above 90%. The minimal detectable amounts range from 0.6 to 3.0 ng (20–40 pmol) carbonyl injected. This means, for a 200 l sample with an injection volume of 2 ml from an extract of 10 ml, a detection limit of 0.5 pmol/l can be realised. This theoretical value has been tested by spiking a DNPH-treated SPE cartridge with ca. 1.0 ng of aldehydes. The cartridge was connected to another, unused, cartridge to check the breakthrough of the aldehydes on the first cartridge. Then, 200 l of nitrogen from a cylinder was led through both cartridges, followed by elution and analysis.

As these levels were easy to analyse (signal-to-noise better than 3, with a relative standard deviation of 6%), the calculated values can be used in practice. From the results from analysed (real) samples, it became clear that the calculated detection limits were realisable. Even lower limits seem possible with larger air volumes.

Concentrations of formaldehyde in the second cartridge are dependent on the relative humidity and ranged from 0.1 to 2.0 $\mu g/m^3$ (3–66 pmol/l) in real air samples.

Because the method should be used for monitoring purposes, the expected number of samples will be high. The method therefore needs to be automated, especially when each air sample produces two cartridges to be analysed. Experiments indicated that extracts of the cartridges cannot be stored for long in an autosampler vial at room temperature. Extracts can be stored at least for one year if stored in the dark and refrigerated [12]. With these restrictions, a procedure was developed for a Gilson ASPEC system which subsequently eluted one cartridge, diluted the extract and injected an amount of 2 ml onto the HPLC system.

Quantification of aldehydes and ketones from ambient air samples is difficult due to ozone interferences. Under chromatographic conditions commonly reported for the aldehydes by HPLC, two of the peaks from the ozone-DNPH decomposition products can readily co-elute with the formaldehyde hydrazone. Smith et al. [13] succeeded in separating ozone DNPH artifacts from formaldehyde. Removal of ozone before its possible reaction with DNPH, is another approach and good results were reported by Dye and Oehme [14]. This latter method was adopted and Fig. 4a shows the results of a 200-l air sample in the presence of 400 ppb ozone with and without using the ozone scrubber. Fig. 4b also shows the compounds one can typically expect in air.

The purity of the acetonitrile used for eluting the hydrazones from the SPE column may cause some unexpected problems, because acetone is a major contamination which will react with the excess DNPH reagent which, in turn, will result in high blanks. Several brands of HPLC-grade acetonitrile were tested. Only high-purity acetonitrile can be used for the elution of the cartridges. One should realise that different batches may contain various concentrations of acetone. Therefore every batch of acetonitrile has to be tested before being used in the procedure. Because acetone is frequently used in a laboratory, high levels can be found in ambient laboratory air which may also cause contamination. These problems can be solved by working in a fume hood, and a laboratory from which acetone is banned.

The method was used for the analysis of formaldehyde, acetaldehyde, 2-propenal (acroleine), 2-butenal (crotonaldehyde) and benzaldehyde in ambient air. The results of these studies will be reported elsewhere. The procedure may be adapted for the separation of additional aldehydes and ketones. Fig. 5 shows the chromatogram of all the aldehydes and ketones which have been separated with the described method. The method proved to be very satisfactory for series of more than 200 air samples. From the analysed air samples it became clear that the calculated detection limits are attainable. The method has also been adapted for the analyses of aldehydes and

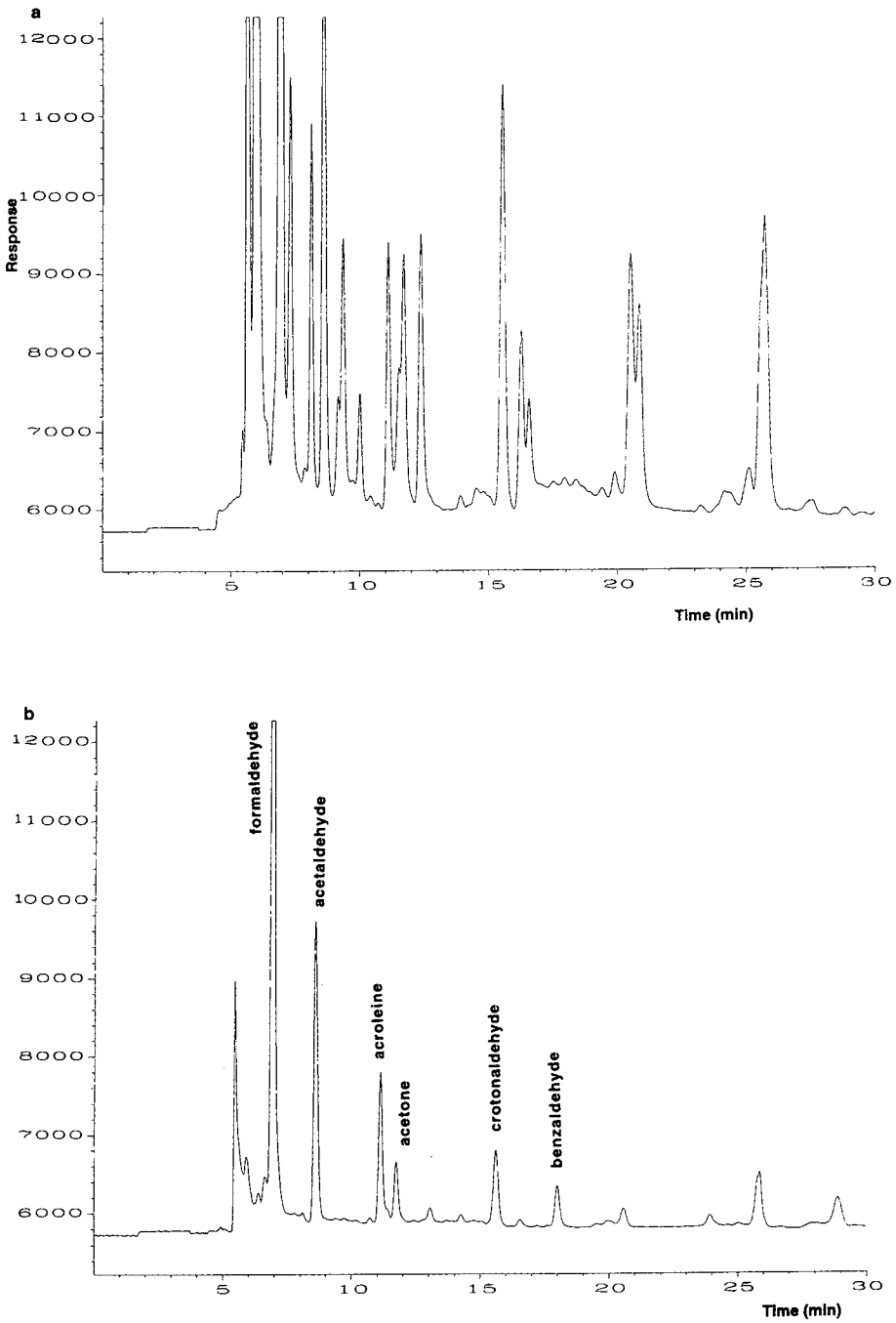

Fig. 4. The effect of an ozone-scrubber on the analysis of carbonyl compounds. Sampling was done in the presence of high concentrations of ozone (400 ppb), (a) without ozone scrubber, (b) with ozone-scrubber. Analytical conditions as described in the text. Response of detector in counts.

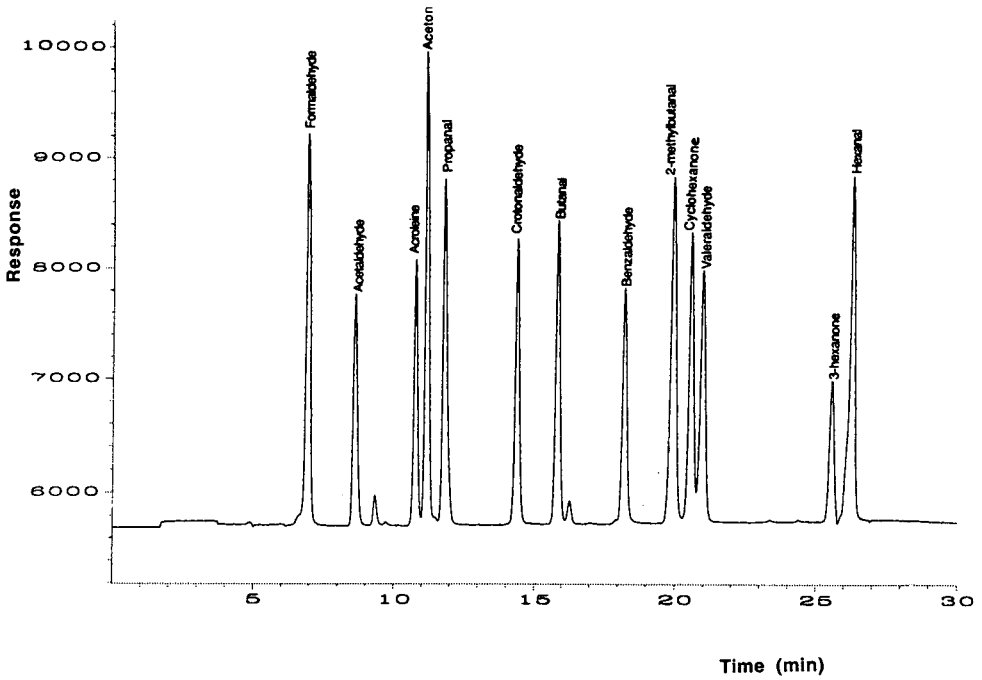

Fig. 5. Analysis of a mixture of 13 different compounds. Analytical conditions as described in the text.

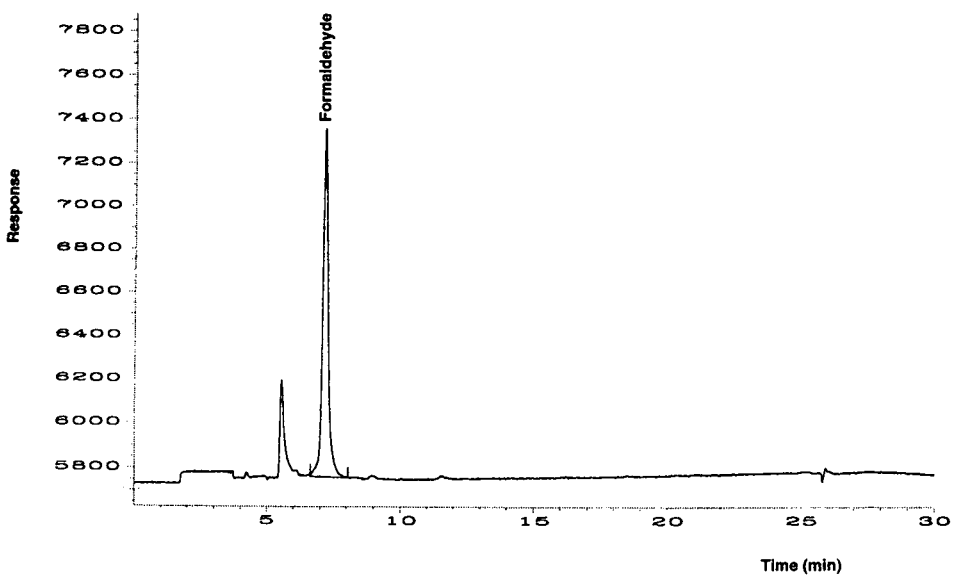

Fig. 6. Analysis of a 100 ml tap water sample preconcentrated on a DNPH-treated SPE-column. Analytical conditions as described in the text.

ketones in water samples. About 100 ml of water can be preconcentrated on the DNPH-pretreated SPE columns. A chromatogram of tap water is shown in Fig. 6. Further extension to other types of water samples are in progress.

4. Conclusions

The combination of chemical derivatisation, selective detection and coupled column RPLC can be used to attain maximum sensitivity and selectivity in the determination of atmospheric carbonyls. This method does not have the usual drawbacks of high blanks and ozone interference. The contamination of acetone in solvents may cause high blanks.

Coupled-column reversed-phase liquid chromatography in combination with chemical derivatisation and selective UV-detection, solves the major problem in the determination of the DNPH derivatives of both aldehydes and ketones. The background system peak, caused by the unused DNPH reagent, is separated from the compounds of interest. Consequently low detection limits of upto 0.5–1.0 pmol/l (50 to 150 ng/m^3) were established.

The use of high-purity solvents is necessary. The purity of acetonitrile used for elution of the derivatives from the SPE column is essential. Because of the excess DNPH reagent, aldehyde and ketone contaminants in acetonitrile will result in high blanks. A major impurity is acetone. The method can easily be adapted for the analysis of aldehydes and ketones in water samples.

References

[1] P. Carlier, H. Hannachi and G. Mouvier, *Atmos. Environ.*, 20 (1986) 2079–2099.
[2] Committee on Toxicology and Environmental Health Hazards, National Research Council, *Formaldehyde and Other Aldehydes*, National Academic Press, Washington, DC, 1981.
[3] D. Grosjean, *Environ. Sci. Technol.*, 16 (1982) 254–262.
[4] R. Kuntz, W. Lonneman, G. Namie and L.A. Hull, *Anal. Lett.*, 13 (1980) 1409–1415.
[5] K. Kuwata, M. Uerobi, H. Yamasaki, Y. Kuge and Y. Kiso, *Anal. Chem.*, 55 (1983) 2013–2016.
[6] A. Vairavamurthy, J.M. Roberts and L. Newman, *Atmos. Environ.*, 26A (1992) 1965.
[7] R.R. Arnts and S.B. Tejada, *Environ. Sci. Technol.*, 23 (1989) 1428–1430.
[8] C.M. Druzik, D. Grosjean, A. van Neste and S.S. Parmar, *Int. J. Environ. Anal. Chem.*, 38 (1990) 495–512.
[9] Å. Larsen, N.A. Jentoft and T. Greibrokk, *Sci. Total. Environ.*, 120 (1992) 261–269.
[10] E.A. Hogendoorn, P. van Zoonen and U.A.Th. Brinkman, *Chromatographia*, 31 (1991) 285–292.
[11] E.A. Hogendoorn, V. Verschraagen, U.A.Th. Brinkman and P. van Zoonen, *Anal. Chim. Acta*, 268 (1992) 205–215.
[12] D. Grosjean, *Environ. Sci. Technol.*, 25 (1991) 710–715.
[13] D.F. Smith, T.E. Kleindienst and E.E. Hudgens, *J. Chromatogr.*, 483 (1989) 433–436.
[14] Ch. Dye and M. Oehme, *J. High Resolut. Chromatogr.*, 15 (1992) 5.

ELSEVIER

Journal of Chromatography A, 697 (1995) 213–217

JOURNAL OF CHROMATOGRAPHY A

Porous graphitic carbon for the chromatographic separation of O-tetraacetyl-β-D-glucopyranosyl isothiocyanate-derivatised amino acid enantiomers

Weng C. Chan*, Ruth Micklewright, David A. Barrett

Department of Pharmaceutical Sciences, University of Nottingham, University Park, Nottingham NG7 2RD, UK

Abstract

Amino acid enantiomers, following facile N-derivatisation with O-tetraacetyl-β-D-glucopyranosyl isothiocyanate, have been separated by high-performance liquid chromatography on a porous graphitic carbon column (Hypercarb S) using a binary 0.1% (v/v) aqueous trifluoroacetic acid–acetonitrile gradient elution profile. Resolution of fourteen pairs of derivatised D,L-amino acid diastereoisomers (apparent $\alpha = 1.02–1.63$) was achieved, including the simultaneous analysis of common protein-derived amino acid enantiomers.

1. Introduction

High-performance liquid chromatographic (HPLC) separation of common amino acid enantiomers has been achieved previously by the use of chiral derivatisation reagents or chiral ligands [1–4] on silica-based stationary phases. To date, one of the most facile chiral derivatisation reagent is O-tetraacetyl-β-D-glucopyranosyl isothiocyanate (GITC), which gives relatively stable diastereomeric glucopyranosyl thiourea derivatives [2,5]. The condensation reaction, outlined in Fig. 1, is most rapid under basic conditions. Efficient separation of these thiourea derivatives (GITC-amino acids) have been demonstrated on reversed-phase silica using a complex ternary solvent system [5]. In addition to the complexity of this elution profile, alkyl-bonded silica stationary phases suffer from a number of drawbacks, including poor stability at extremes of pH and a variety of unwanted interactions due to surface heterogeneity [6].

Porous graphitic carbon (PGC, Hypercarb) was recently introduced as an alternative for HPLC [7,8]. This material, consisting of pure carbon micro-particles, has several advantages, most notably its physical and chemical stability as well as superior selectivity towards diastereoisomers and geometric isomers [9–13]. We now report, for the first time, efficient separation of GITC-D,L-amino acid diastereoisomers on graphitic carbon-HPLC using the commercially available Hypercarb S column.

2. Experimental

2.1. Chemicals

Amino acids, GITC and other reagents were purchased from Sigma (Poole, UK) and Aldrich (Gillingham, UK). HPLC-grade acetonitrile,

* Corresponding author.

0021-9673/95/$09.50
SSDI 0021-9673(94)00937-6

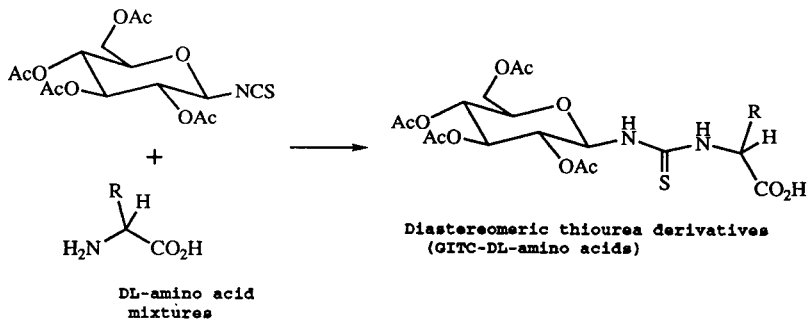

Fig. 1. Derivatisation of amino acids with the isothiocyanate GITC.

purchased from Fisons (Loughborough, UK) and double-distilled water (using Elgastat Spectrum) were used for all sample preparations and chromatographic separations. The pre-packed graphitic carbon column (Hypercarb S, 200 × 4.6 mm, particle diameter 7 μm) was supplied by Shandon HPLC (Runcorn, UK). All experiments were performed at ambient temperature.

2.2. Chromatographic analysis

The HPLC apparatus (Pharmacia LKB, Milton Keynes, UK) was equipped with a binary solvent-delivery system comprised of two 2150 HPLC pumps, a 2152 controller and 2151 variable-wavelength monitor. The eluents used were: (A) 0.1% (v/v) aqueous trifluoroacetic acid (TFA) and (B) 0.1% (v/v) TFA in 90% (v/v) aqueous acetonitrile. The elution step program is as follows: isocratic 30% B for 15 min, followed by linear gradient from 30 to 36% B in 10 min, then 36% B for 3 min, then 36 to 39% B in 5 min, then 39% B for 2 min, then 39 to 45% B in 10 min, then 45% B for 5 min, then 45 to 100% B in 33 min, then 100% B for 10 min, and 100 to 30% B in 3 min (total run time 96 min). The Hypercarb S column was eluted at a flow-rate of 1.10 ml min^{-1} and the eluate was monitored at 250 nm. Using acetone, the t_0 for the column was found to be 2.0 min.

Initially, all the derivatised amino acid enantiomers were analysed separately (in duplicate) to determine the elution order, and subsequently the enantiomer mixtures were analysed. In the latter analysis, including that obtained for the HPLC trace shown in Fig. 2, the mixtures were acquired by mixing freshly prepared respective GITC-amino acids of similar but not identical concentrations. The mean apparent capacity factor (k') and separation factor (α) in gradient elution chromatography were calculated from multiple injections of the enantiomer mixtures. The degree of correlation between the resulting retention data and with previous data on the separation of GITC-derivatised amino acids on an ODS silica column [5] was determined using linear least squares analysis.

2.3. GITC derivatisation of amino acids

To a solution of each amino acid (2.0 μmol; except for Lys whereby 1.0 μmol was used) in 50% (v/v) aqueous acetonitrile (100 μl) was added triethylamine (2 μl) followed by GITC in acetonitrile (20 μl, 40 mg ml^{-1}). The mixture was allowed to stand for about 30 min at room temperature, and was then quenched with 1.0 *M* aqueous hydrochloric acid (50 μl) and 25% (v/v) aqueous acetonitrile (830 μl). An aliquot of 5–20 μl of the resultant mixture was analysed.

Preliminary quantitative analysis using proline confirmed that the GITC-derivatisation reaction is complete within 20 min at room temperature.

3. Results and discussion

GITC has previously been used for derivatisation of both D,L-amino acids and N^{α}-methyl-D,L-

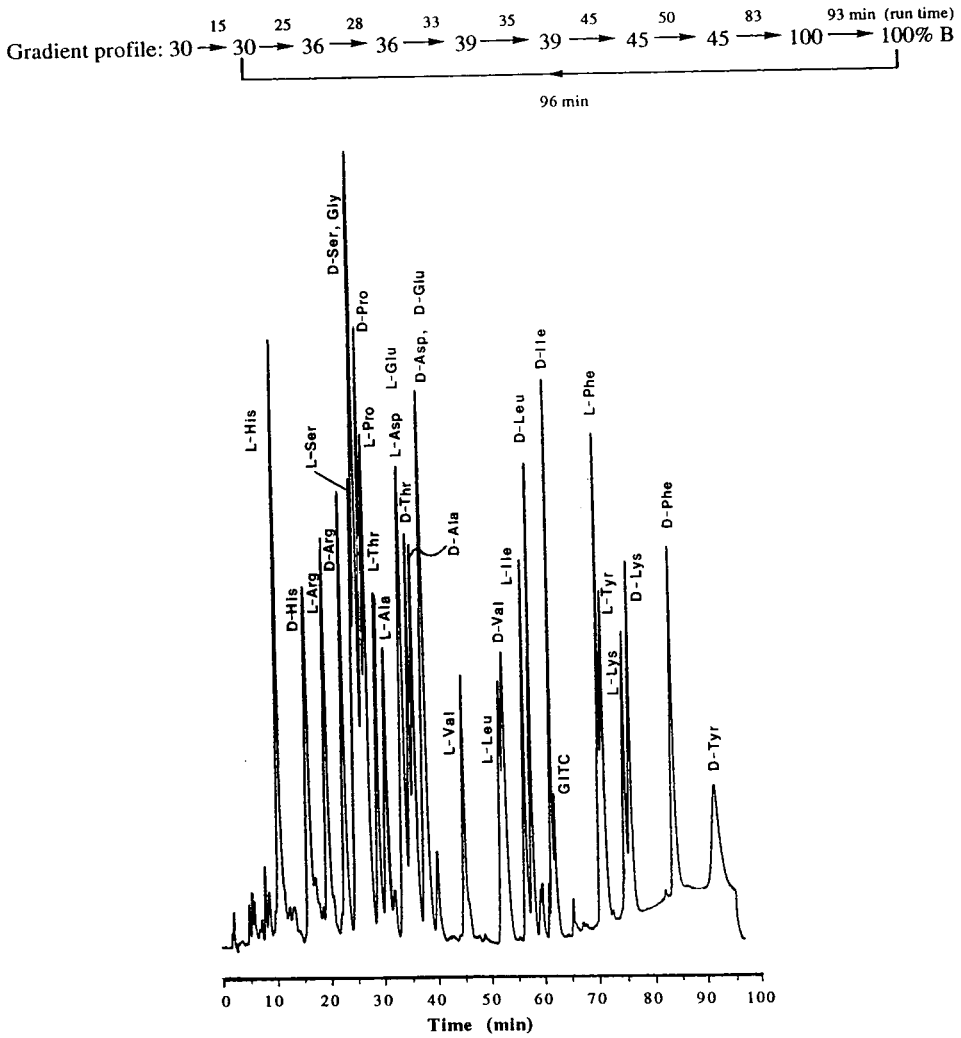

Fig. 2. Elution profile of GITC-D,L-amino acid diastereoisomers. See Experimental section for conditions.

amino acids to give lipophilic thiourea diastereoisomers which are separated by reversed-phase HPLC [5,14]. We have now accomplished similar separations (Fig. 2) of GITC-D,L-amino acids on a recently introduced graphitic carbon HPLC column. In addition, our chromatographic conditions allow simultaneous resolution of thiourea derivatives of all common proteinaceous amino acid enantiomers, except tryptophan (not eluted), obtainable by acid hydrolysis (Fig. 2, Table 1). With the exception of three pairs, excellent baseline resolutions are obtained for all thiourea D,L-amino acid diastereoisomers with apparent α values >1.1. Furthermore, the resolutions for the aromatic amino acid derivatives GITC-D,L-Phe and GITC-D,L-Tyr (apparent α, 1.2 and 1.3 respectively) are notably good. The strong retention of aromatic amino acids by the PGC column was confirmed by the failure to elute GITC-derivatised tryptophan enantiomers, which had an apparent k' value of >50 under the analytical conditions used. This behaviour of the aromatic amino acids is not unexpected since hydrophobic compounds are known to interact

Table 1
Separation of GITC-D,L-amino acids on Hypercarb S column

Amino acid	Apparent capacity factor, k'		
	D-isomer	L-isomer	α
His	7.15	4.38	1.63
Arg	10.54	8.92	1.18
Ser	11.89	11.60	1.03
Pro	12.43	12.78	1.03
Thr	16.67	13.71	1.22
Ala	17.07	14.49	1.18
Asp	17.97	16.03	1.12
Glu	17.97	16.03	1.12
Val	25.52	21.69	1.18
Leu	28.02	25.17	1.11
Ile	29.9	27.41	1.09
Phe	41.0	34.27	1.20
Lys	37.17	36.65	1.02
Tyr	45.04	34.67	1.30

more strongly with the PGC compared to ODS silica materials [9]. The order of elution of the GITC-derivatised enantiomers is consistently L-isomer before D-isomer, with the sole exception of GITC-proline, for which the D-isomer elutes before the L-isomer. The reason for this change of elution order is not known.

A detailed comparison of our data with those obtained using ODS-bonded silica [5], with respect to apparent k' values, revealed a linear correlation ($R^2 = 0.8$; Fig. 3). This suggests that the lipophilic tetraacetylglucopyranosyl moiety

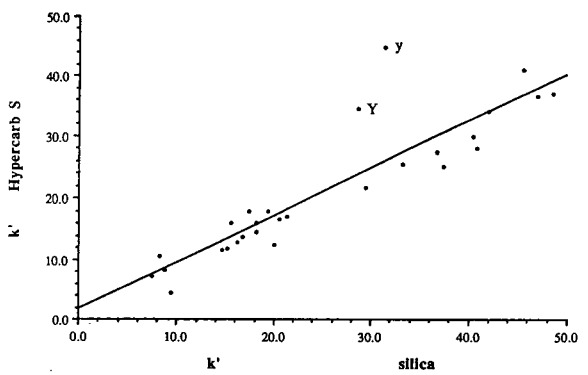

Fig. 3. Correlation between GITC-D,L-amino acids apparent k' obtained on Hypercarb S and on reversed-phase (C_{18}) silica. Reversed-phase silica data re-plotted from Ref. [5]. Y = GITC-L-Tyr; y = GITC-D-Tyr.

of these GITC-D,L-amino acids interacts with the graphitic carbon surface in a manner similar or comparable to the reversed-phase silica. However, for GITC-aromatic amino acids such as tyrosine, this is further enhanced by the stronger hydrophobic interactions with the graphitic carbon, giving comparatively longer retention times.

In conclusion, we have demonstrated a rapid and simple procedure for analysis of amino acid enantiomers in peptides and proteins by graphitic carbon-HPLC. This methodology clearly has broader applications, e.g. for the quality control of starting materials and analysis for racemisation during chemical synthesis of peptides. Since PGC was observed to have improved diastereo-selectivity for aromatic-containing compounds, we are currently exploring the separation of amino acid enantiomers by derivatisation with N^{α}-(2,4-dinitro-5-fluorophenyl)-L-alaninamide [15].

Acknowledgement

We thank Shandon HPLC (Runcorn, UK) for supply of Hypercarb HPLC columns.

References

[1] T. Tamegai, M. Ohmae, K. Kawabe and M. Tomoeda, *J. Liq. Chromatogr.*, 2 (1979) 1229.
[2] T. Kinoshita, Y. Kasahara and N. Nimura, *J. Chromatogr.*, 210 (1981) 77.
[3] E. Gil-Av, A. Tishbee and P.E. Hare, *J. Am. Chem. Soc.*, 102 (1980) 5115.
[4] E. Oelrich, H. Preusch and J. Wilhelm, *J. High Resolut. Chromatogr. Chromatogr. Commun.*, 3 (1980) 269.
[5] N. Nimura, A. Toyama and T. Kinoshita, *J. Chromatogr.*, 316 (1984) 547.
[6] J. Nawrocki and B. Buszewski, *J. Chromatogr.*, 449 (1989) 1.
[7] J.H. Knox and B. Kaur, in P.R. Brown and R.A. Hartwick (Editors), *High Performance Liquid Chromatography*, Wiley, New York, 1989, p. 189.
[8] J.H. Knox and M.T. Gilbert, *UK Pat.*, 7 939 449 (1979); US Pat., 4 263 268 (1979); *F.R.G. Pat.*, P2 946 688-4 (1979).
[9] J.H. Knox, B. Kaur and G.R. Millward, *J. Chromatogr.*, 352 (1986) 3.

[10] B.J. Bassler and R.A. Hartwick, *J. Chromatogr. Sci.*, 27 (1989) 162.
[11] Z. Pawlak, D. Kay and B.J. Clark, *Anal. Proc.*, 27 (1990) 16.
[12] G. Gu and C.K. Lim, *J. Chromatogr.*, 515 (1990) 183.
[13] Q.H. Wan, P.N. Shaw, M.C. Davies and D.A. Barrett, *J. Chromatogr. A*, 697 (1995) 219.
[14] R. Albert and F. Cardinaux, in J.E. Rivier and G.R. Marshall (Editors), *Peptides: Chemistry, Structure and Biology*, ESCOM, Leiden, 1990, p. 437.
[15] P. Marfey, *Carlsberg Res. Commun.*, 49 (1984) 591.

ELSEVIER

Journal of Chromatography A, 697 (1995) 219–227

JOURNAL OF CHROMATOGRAPHY A

Chromatographic behaviour of positional isomers on porous graphitic carbon

Qian H. Wan, P. Nicholas Shaw, Martyn C. Davies, David A. Barrett*

Department of Pharmaceutical Sciences, University Park, University of Nottingham, Nottingham, NG7 2RD, UK

Abstract

Retention characteristics of six sets of ionizable substituted benzene isomers have been measured on a porous graphitic carbon column using buffered aqueous eluents containing 35% acetonitrile. The elution orders varied with the different types of substituents on the benzene ring and were not readily predictable from the known structures of the isomers. Over the range of mobile phase between pH 2 to 9.4, the retention of the solutes was correlated directly with their degree of ionization, with the ionized form being least retained. An interpretation of these data was suggested based on the solute molecular orientation effect induced by the competing interactions of solute with adsorbent and solvent.

1. Introduction

The retention behaviour of positional isomers in liquid chromatography (LC) has been a subject of recurring interest because the separation of such compounds is of primary importance in pharmaceutical analysis. In addition, the investigation of the separation behaviour of isomers can impart some valuable insights into the molecular mechanism of retention as well as providing useful data to test the accuracy of existing retention models. In the case of positional isomers of disubstituted benzenes, the principal factors which determine the elution order of *ortho-*, *meta-*, and *para*-isomers have been extensively studied for both normal- and reversed-phase LC. Elution orders on alumina were first established by Snyder [1] and interpreted in terms of various physicochemical effects, including intramolecular hydrogen bonding, electronic activation, steric repulsion and solute molecular orientation. Studies by Kiselev et al. [2] of retentive behaviour of isomers with polar substituents on hydroxylated silica largely confirmed the observations made by Snyder; that is, the elution orders varied for different sets of isomers, depending upon the nature and position of the substituent groups, their influence on the electron density distribution in the benzene ring, the possibility of the formation of intra- and inter-molecular hydrogen bonds and the orientation of solute molecules relative to the adsorbent surface.

The retentive behaviour of isomeric alkylbenzenes in reversed-phase LC has been studied by several groups and shown to be difficult to predict. Smith [3] showed that the connectivity index, derived from the topology of the molecule, fails to correlate with the relative retentions of isomeric compounds separated on three reversed-phase silica columns. With similar columns, Barman and Martire [4] examined the

* Corresponding author.

0021-9673/95/$09.50
SSDI 0021-9673(94)00813-2

dependence of solute retention on the polarity of the mobile phase, solute dipole moment and column temperature for isomeric xylenes, ethyltoluenes and diethylbenzenes. They found that the elution order of the isomers is consistent with a change in dipole moment. Knox et al. [5] noted that the elution order of isomeric xylenes separated on porous graphitic carbon (PGC) is the opposite to that observed on reversed-phase silica and they attributed this to the unique surface properties of the graphitic carbon.

Being the only LC support with a crystalline surface, PGC can be expected to show improved separation of positional isomers [6]. First, the energy of solute–adsorbent interactions is very much dependent upon the distance between the surface and the force centres in the solute molecule, so the planar surface of graphitic carbon may conveniently be exploited to separate isomers which differ only in geometrical structure [7]. Secondly, unlike bonded reversed-phase silica, which shows persistent residual effects arising from the underivatized silanol groups, PGC possesses an energetically homogeneous surface with minimal active sites on the edges of the graphitic sheets [8]. These properties makes PGC an ideal material for investigation of the retentive behaviour of ionizable compounds and for the further studies of the mechanism underlying the separation of isomers.

This study examines the retention behaviour of isomeric benzenes with ionizable substituents in a reversed-phase liquid chromatographic (RPLC) system consisting of PGC columns and acetonitrile–buffer eluents over a range of pH values. The elution orders of different sets of isomers and the relative retentions at various mobile phase pH values have been examined in order to elucidate the role of solute molecular orientation in determining the elution order of isomers.

2. Experimental

2.1. Chemicals

Orthophosphoric acid of analytical grade was obtained from Sigma (Dorset, UK) and triethylamine (HPLC grade) was purchased from Romil Chemicals (Loughborough, UK). Acetonitrile (HPLC grade), sodium dihydrogenphosphate and disodium hydrogenphosphate were obtained from Fisons (Loughborough, UK). Deionised, purified water was produced in-house with an Elgastat water purification system (Elga, High Wycombe, UK). All mobile phases were carefully degassed by helium purge before use.

The substituted benzenes used as test compounds were of analytical grade or better. Six series of ionizable positional isomers of benzene were selected to include acidic, basic and amphoteric compounds. The cresol isomers were included in order to relate the data to previous studies. The structures of all the test compounds are shown in Table 1.

2.2. Equipment

The chromatographic system consisted of a Gilson 305 pump (Villiers le Bel, France), a Gilson 805 manometric module, a Gilson 231 XL sampling injector, a Gilson 401 diluter and an ABI 759A absorbance detector (Foster City, CA, USA) connected to a Gilson HPLC 715 system controller via a Gilson 506B interface. All pH measurements were carried out with a Corning Model 7 pH meter equipped with automatic temperature compensation. The electrode was calibrated with pH 4.0, 7.0 or 10.0 standard solutions, depending on the range investigated.

2.3. Chromatographic experiments

A Hypercarb column (100 × 4.6 mm I.D., particle diameter 7 μm) was supplied by Shandon HPLC (Runcorn, UK). All separations were performed isocratically at ambient temperature with a flow-rate of 1 ml/min. UV detection at 254 nm was used. The mobile phase consisted of aqueous buffer–acetonitrile in 65:35 volume ratio. The pH value of the buffer was adjusted by adding an appropriate amount of triethylamine or orthophosphoric acid to 0.01 *M* orthophosphoric acid solution. When a change in mobile phase pH was made, equilibration with the new mobile phase was carried out for at least 30 min before the retention data were taken for

Table 1
Retention and selectivity data for disubstituted benzene isomers separated on PGC

Compound	Substituent		k	α	pH
	X	Y			
o-Aminobenzoic acid	H_2N	COOH	7.57	1.96	2.0
m-Aminobenzoic acid	H_2N	COOH	0.28	1.00	2.0
p-Aminobenzoic acid	H_2N	COOH	3.86	13.78	2.0
o-Cresol	CH_3	OH	4.64	1.08	2.0
m-Cresol	CH_3	OH	3.86	1.00	2.0
p-Cresol	CH_3	OH	4.28	1.11	2.0
o-Anisic acid	CH_3O	COOH	7.57	1.00	2.0
m-Anisic acid	CH_3O	COOH	17.28	2.28	2.0
p-Anisic acid	CH_3O	COOH	20.43	2.70	2.0
o-Toluic acid	CH_3	COOH	11.00	1.00	2.0
m-Toluic acid	CH_3	COOH	13.28	1.21	2.0
p-Toluic acid	CH_3	COOH	16.14	1.47	2.0
o-Anisidine	CH_3O	NH_2	1.43	10.21	3.3
m-Anisidine	CH_3O	NH_2	1.93	1.35	3.3
p-Anisidine	CH_3O	NH_2	0.14	1.00	3.3
o-Phenetidine	C_2H_5O	NH_2	4.28	8.50	3.3
m-Phenetidine	C_2H_5O	NH_2	5.07	1.18	3.3
p-Phenetidine	C_2H_5O	NH_2	0.50	1.00	3.3

the next sample. The solute solutions were prepared by dissolving the test compounds in the mobile phase (aqueous buffer–acetonitrile, 65:35) to give a concentration of 1–10 μg/ml. Injections of 1–10 μl of these mixtures produced satisfactory chromatographic peaks. All isomer solutes were analysed separately (in duplicate) to determine the elution order and then the isomer mixtures were analysed. The mobile phase hold-up time, t_M, was taken as the time from injection to the moment when the trace for the solvent disturbance crossed the baseline. The solvent disturbance peak was generated by acetonitrile in which the samples were dissolved. The mean retention factors, k and separation factors, α, were calculated from multiple injections of the isomer mixtures. The effect of the mobile phase on retention of all the isomer mixtures was studied over the pH range from pH 2.0 to pH 9.4.

2.4. Data analysis

The separation factor of a pair of isomers is given as a ratio of the retention factor of the later eluted species to that of the first eluted one, for adjacent peaks.

The retention factor of any ionizable solute as a function of mobile phase pH can be expressed by the general form of Horvath's equation [9]:

$$k = \Sigma x_i k_i$$

where x_i and k_i are the mole fraction and the retention factor of the solute in the ith form, respectively. x_i, as a function of pH, can be readily derived from the known dissociation equilibria. For monoprotic acids and bases, the retention factor is given by

$$k = [k_1 + k_2 \exp(\mathrm{pH} - \mathrm{p}K_{a(1)})]/[1 + \exp(\mathrm{pH} - \mathrm{p}K_{a(1)})]$$

where $pK_{a(1)}$ is the negative logarithm of the acid dissociation constant in the mobile phase and k_1 and k_2 refer to the retention factors of the acidic and basic forms of the solute, respectively.

Similarly, the retention factor of amphoteric substances, such as aminobenzoic acids, is given by

$$k = k_1/[1 + \exp(\mathrm{pH} - \mathrm{p}K_{a(1)}) + \exp(2\mathrm{pH} - \mathrm{p}K_{a(1)} - \mathrm{p}K_{a(2)})] + k_2/[1 + \exp(\mathrm{p}K_{a(1)} - \mathrm{pH}) + \exp(\mathrm{pH} - \mathrm{p}K_{a(2)})] + k_3/[1 + \exp(\mathrm{p}K_{a(2)} - \mathrm{pH}) + \exp(\mathrm{p}K_{a(1)} + \mathrm{p}K_{a(2)} + 2\mathrm{pH})]$$

where k_1, k_2 and k_3 are the retention factors of the cationic, the zwitterionic and the anionic forms of the amphoteric solute and $K_{a(1)}$ and $K_{a(2)}$ are the corresponding dissociation constants, respectively.

The pH and k values are known from the experimental data and the remaining unknown parameters ($\mathrm{p}K_{a(1)}$, $\mathrm{p}K_{a(2)}$, k_1, k_2 and k_3) in the above equations can be found by using a non-linear least squares technique to fit an appropriate model to the data (software package, MINIM 2.0.2 (R.D. Purves, Department of Pharmacology, University of Otago, New Zealand).

3. Result and discussion

3.1. Choice of support material

Consideration of the thermodynamics of chromatographic retention indicates that the interaction energy which is responsible for solute retention is governed by three competing effects: solute–adsorbent interactions, solvent–solute interactions and solvent–adsorbent interactions. As the solute–adsorbent interactions are the only positive contribution to the retention, the surface properties of porous graphitic carbon (PGC) are relevant to this study.

PGC is a spherical microparticulate packing material made by a "template" method invented by Knox and Gilbert [10] in 1979. Spherical silica gel particles are used as a porous template and filled with a polymer. After pyrolysing the polymer in an inert atmosphere, the template silica is dissolved out to leave a porous glassy carbon. The material is then further heated to induce graphitisation. The product thus obtained has the two-dimensional graphitic structure which has been established by an X-ray diffraction analysis [5] and can be considered, at a molecular level, to have a flat, crystalline surface of intertwining graphitic ribbons held together by covalent bonds to form a dense carbon network. It appears that the relatively flat molecular ribbon structure of PGC offers a contrasting selectivity to the "brush like" surface structure of the traditional bonded silica materials used for HPLC analysis.

Thus the PGC material has unique properties as a chromatographic adsorbent and offers outstanding characteristics for the study of the separation of structurally similar compounds by reversed-phase liquid chromatography.

3.2. Effect of substituents

For each series of benzene isomers the mobile phase pH was optimised over the range of pH 2.0 to 9.4 to give the best separation factors and the resulting retention data are listed in Table 1. Figs. 1–3 show the chromatograms of *o*-, *m*- and *p*-isomers of the acidic, basic and amphoteric substituted benzenes obtained at optimum pH values, from which the retention factors, k and separation factors, α, were determined.

Under the optimized chromatographic conditions chosen, all these isomers were separated

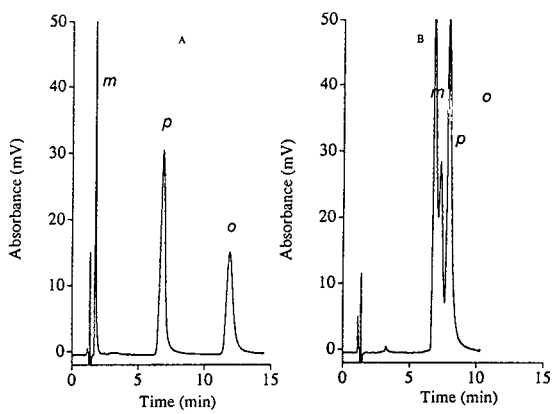

Fig. 1. Separation of disubstituted benzene isomers at pH 2.0. (A) Aminobenzoic acid; (B) cresol.

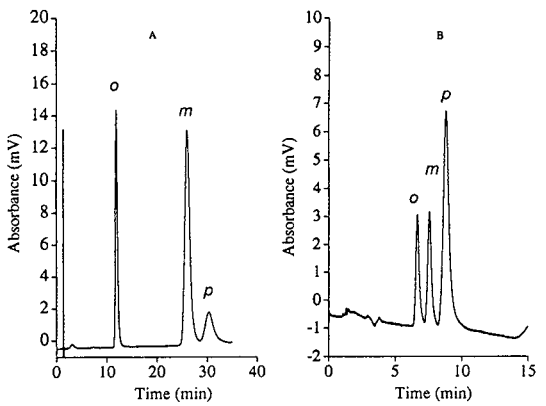

Fig. 2. Separation of disubstituted benzene isomers at pH 2.0. (A) Anisic acid; (B) toluic acid.

with a range of separation factors and elution orders. Of the isomers under examination, the aminobenzoic acid isomers show greatest separability, with the separation factors for the *p*/*m* pair and *o*/*p* pair being 13.78 and 1.96, whereas the cresol isomers were least separated, giving separation factors of 1.11 and 1.08, respectively. These results demonstrate the potential of PGC stationary phases in the separation of positional isomers of either polar or non-polar molecules. Previously, successful isomer separations have been reported for diastereoisomers of an antidepressant, geometrical isomers of cresol [11]; phenol isomers, cephalosporin isomers [12]; geometrical isomers of dothiepin [13]; anionic and cationic compounds of biomedical interest [14] and glucuronide and sulphate metabolites of morphine [15].

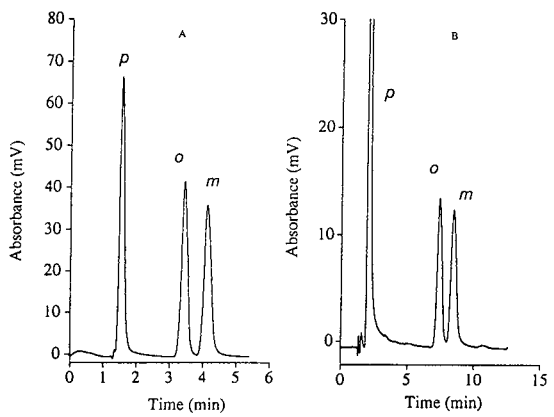

Fig. 3. Separation of disubstituted benzene isomers at pH 3.3. (A) Anisidine; (B) phenetidine.

Three types of elution order were observed for the isomers of differing substituents: $m > p > o$ for aminobenzoic acid and cresol, $o > m > p$ for toluic acid and anisic acid and $p > o > m$ for anisidine and phenetidine. The observation for the first group of isomers that the *m*-isomer elutes before the *p*- and *o*-isomers is consistent with previous results obtained for cresols and xylenes on PGC columns. It has been proposed that the elution order of the cresols was determined by the ability of the solute to undergo charge donor–acceptor interactions with the graphite surface [8]. Of the three isomers, the methyl and hydroxyl groups on the *m*-cresol disturb the electron density the most, resulting in less retention. The elution order for xylenes is accounted for by a different theory [5,7], which is essentially based on the consideration of the number of contact points available to the solute–adsorbent interactions. When *o*- and *p*-xylenes are adsorbed onto the graphite surface, four carbon atoms contact the surface (two from the methyl groups and two from the benzene ring) whereas with *m*-xylene only three carbon atoms contact the surface (two from the methyl groups and one from the benzene ring), thus the *m*-xylene is eluted before *o*- and *p*-xylenes.

However, the above theories cannot provide a satisfactory explanation for the elution orders seen for monoprotic acid and base isomers as neither of them is consistent with the predictions that the *m*-isomer should be eluted before the *o*- and *p*-isomers. Further inspection revealed that these theories assume that the aromatic compound approaches the graphite surface with its flat-side down, thus the direct contact interactions between the solute and the adsorbent surface are the sole factor determining the elution order. The assumption is reasonable in view of a linear relationship between log *k* and carbon number for the *n*-alkylbenzenes [16], but has not been established in the case of aromatic compounds with polar substituents. It is therefore speculated that the strong interaction between the polar substituent and the solvent may have

some significant influence on the alignment of the solute molecule relative to the adsorbent surface. This point will be examined in more detail in the following sections.

3.3. Effect of mobile phase pH

The pH of the mobile phase would be expected to directly influence the retention and selectivity for the separation of ionizable isomers, but the relationship between solute ionization and retention on PGC columns has not been studied in detail. Therefore experiments were carried out to determine the retention factors of the ionizable isomers over the pH range 2.0 to 9.4. In a pure reversed-phase system, with no secondary solute interactions with the stationary phase, the retention of these ionizable compounds should be dependent on the degree of ionization as indicated by the Horvath equation [9]. A PGC stationary phase, which consists predominantly of graphite sheets, might be expected to show ideal behaviour. However, on bonded silica columns it is well known that secondary interactions of residual surface silanols with basic and acidic solutes can cause anomalous retention, and ionized compounds often deviate from ideal chromatographic behaviour.

The experimental data on the ionizable test solutes demonstrated that their retention varied as a function of pH and correlated directly with the degree of ionization of the solutes, with the ionized form being least retained. Figs. 4–9 show the original retention data points for all the isomers over a range of pH 2.0 to 9.4 and a superimposed fitted curve for each individual isomer to show the goodness of fit to the Horvarth model in which solute ionisation alone controls the retention behaviour. In all cases there was an extremely high correlation between the degree of ionization and the retention of the test solutes, indicating that solute ionization is indeed the major factor influencing the retention behaviour of these simple organic acids and bases. As predicted by such a model, a major change in solute retention occurs at pH values close to the isomer pK_a.

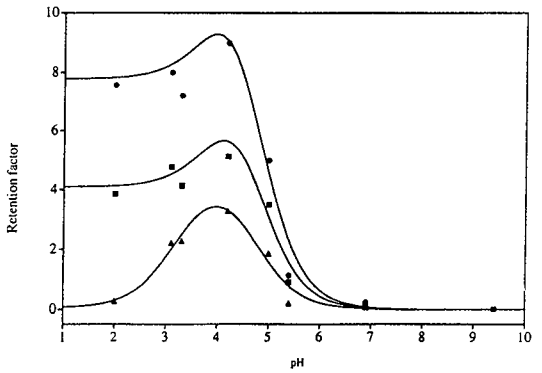

Fig. 4. Effect of pH on the retention of aminobenzoic acid isomers. (●) *ortho*, (▲) *meta*, (□) *para*.

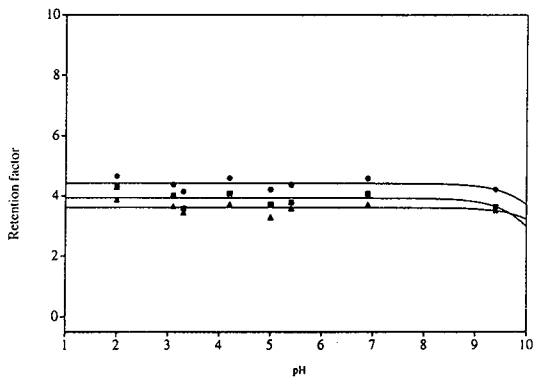

Fig. 5. Effect of pH on the retention of cresol isomers. (●) *ortho*, (▲) *meta*, (□) *para*.

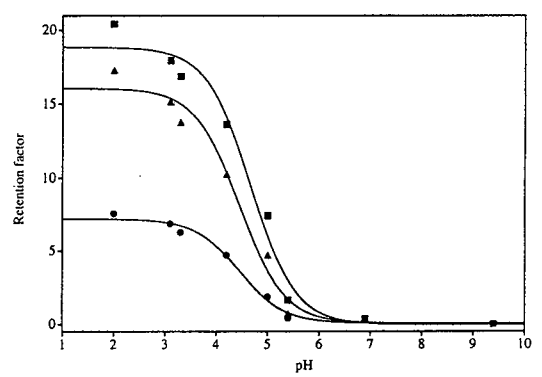

Fig. 6. Effect of pH on the retention of anisic acid isomers. (●) *ortho*, (▲) *meta*, (□) *para*.

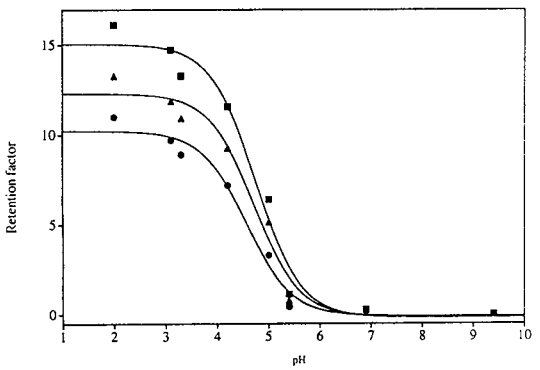

Fig. 7. Effect of pH on the retention of toluic acid isomers. (O) *ortho*, (▲) *meta*, (□) *para*.

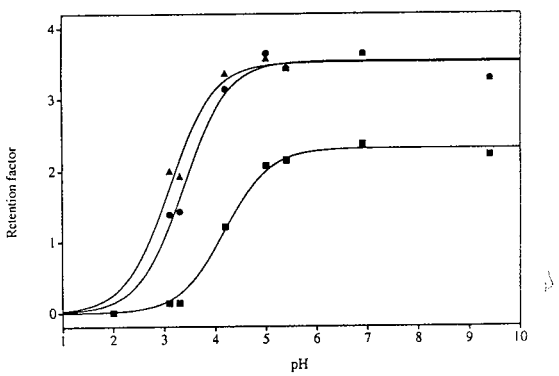

Fig. 8. Effect of pH on the retention of anisidine isomers. (O) *ortho*, (▲) *meta*, (□) *para*.

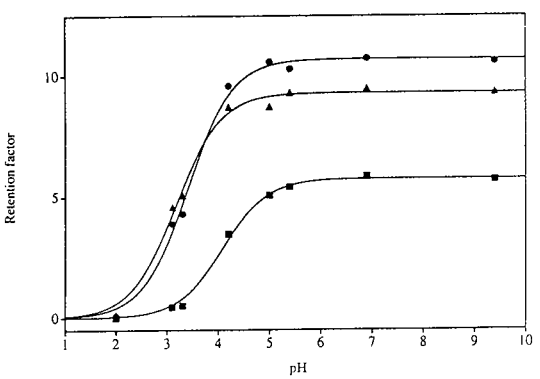

Fig. 9. Effect of pH on the retention of phenetidine isomers. (O) *ortho*, (▲) *meta*, (□) *para*.

Because there appear to be no residual effects with the PGC stationary phase, it is possible to use the curve fitting technique to estimate accurately the pK_a values of each of the isomers. Table 2 lists values of k_1, k_2, k_3, $pK_{a(1)}$ and $pK_{a(2)}$ for substituted benzene isomers, as determined from experimental data presented in Figs. 4–9. The pK_a values thus derived are compared with those in the literature [17]. There is a general agreement between experimental and literature values, with a consistent small shift in the experimental values of pK_a, which is presumably due to the reduced ionization of the solutes resulting from the presence of acetonitrile in the HPLC mobile phase.

These results suggest that the polarity or ionization level of the isomer is important in determining the separation of the isomers, with the most polar isomer eluted first and the least polar last. Using the aqueous pK_a values as an indication of the strength of the acid and basic groups on the isomers, it is possible to observe a direct correlation between order of retention and acid/base strength for the acidic isomers (anisic acid, toluic acid) and the basic isomers (anisidine, phenetidine). Since the acidity/basicity of an organic compound is strongly influenced by its electronegativity and the nature of the solvent, it is likely that both these factors will have a major effect on the order of elution of ionizable isomers.

The high stability of the PGC material over a wide range of pH values makes it feasible to use the mobile phase pH to provide an effective means of varying selectivity and optimizing separation over the pK_a range of the sample. This is best illustrated in the separation of anisidine isomers where a complete separation of three isomers can only be achieved between pH 2 and pH 5, over which range the isomers are all partly ionized. Stronger retention at higher values of pH results in the loss of resolution of *o*- and *m*-isomers. The range of pH stability of PGC columns (pH 1 to 14) will thus allow a greater flexibility in optimising isomer separations compared to the more limited pH range available on conventional bonded silica columns.

Table 2
Values of k_1, k_2, k_3, $pK_{a(1)}$ and $pK_{a(2)}$ for disubstituted benzene isomers, as determined from experimental data in Figs. 4–9

Compound	k_1	k_2	k_3^a	$pK_{a(1)}$ (experimental)	$pK_{a(2)}^a$	$pK_{a(1)}$ (literature)[b]	$pK_{a(2)}^a$
o-Aminobenzoic acid	7.60	12.53	0.00	4.00	4.73	2.108	4.946
m-Aminobenzoic acid	0.05	4.66	0.00	3.23	4.71	[c]	[c]
p-Aminobenzoic acid	4.09	8.17	0.00	4.00	4.78	2.501	4.874
o-Cresol	4.40	0.00		10.73		10.2	
m-Cresol	3.60	0.00		10.95		10.01	
p-Cresol	3.92	0.00		10.50		10.17	
o-Anisic acid	7.20	0.00		4.45		4.09	
m-Anisic acid	16.05	0.00		4.46		4.09	
p-Anisic acid	18.83	0.00		4.67		4.48	
o-Toluic acid	10.23	0.00		4.57		3.91	
m-Toluic acid	12.31	0.00		4.71		4.27	
p-Toluic acid	15.05	0.00		4.74		4.38	
o-Anisidine	0.00	3.53		3.64		4.52	
m-Anisidine	0.00	3.50		3.01		4.23	
p-Anisidine	0.00	2.30		4.14		5.34	
o-Phenetidine	0.00	10.67		3.36		4.43	
m-Phenetidine	0.00	9.25		3.11		4.18	
p-Phenetidine	0.00	5.75		4.05		5.20	

[a] Applies to aminobenzoic acid isomers only (two ionisable groups).
[b] Uncorrected literature values (in water, 25°C) [17].
[c] Data not available in the literature.

3.4. Separation mechanism

One interpretation of these data at a molecular level is offered by considering the orientation of a polar aromatic molecule when approaching the planar graphite surface of the stationary phase. The ionizable or polar side of the solute would be orientated towards the solvent/mobile phase, but the aromatic plane of the solute would tend to interact with the planar graphite surface. Thus it could be envisioned that the polar aromatic solute would not align in a parallel manner to the graphite surface, but rather be orientated at a certain angle, with the polar side of the solute tilting into the bulk of the mobile phase. The degree of the angle formed between the aromatic solute and the graphite surface would be determined by a balance between the adsorptive strength and the solvation force which, as opposed to the former, tends to lift the solute molecule from the substrate surface. From this it follows that the chromatographic resolution of a set of isomers may be improved by exploiting these two competing effects to maximize the difference in solute molecular orientation relative to the graphite surface. If this is the case then the polarity or dipole moment of the solute, which is indicative of the strength of the solvation interaction, should be a key factor along with others determining the elution order. Further experimental work will be necessary to confirm this hypothesis.

4. Conclusions

The preliminary results presented above demonstrate that porous graphitic carbon is an unique packing material which allows the use of a wide range of mobile phase pH values to optimize the separation of polar or ionizable organic isomers. Prediction of the order of elution of the polar isomers cannot be achieved using the previous theories based on solute–stationary phase interactions alone for non-polar

benzene isomers, but the data from this study indicate the major importance of solute–solvent interactions. The type of the substituents (acidic, basic, non-polar) affects the order of elution of the isomers, which appears to be consistent among each of these groups. For the ionizable compounds there is a correlation between retention of the unionized form and acid/base strength, as indicated by the pK_a. The retention behaviour of the ionizable isomers indicated a high correlation between the degree of ionization and the retention, indicating that solute ionization is the major factor determining the retention behaviour of these simple organic acids and bases. The underlying mechanism for the retention of these polar organic isomers has yet to be characterised, but this study indicates the likely importance of the orientation of polar solutes with respect to the planar graphite surface of the stationary phase.

Acknowledgements

Q.H.W. was supported by a BBSRC grant (awarded to D.A.B., M.C.D. and P.N.S.) from the Process Separations Initiative. The authors thank Shandon HPLC (Runcorn, Cheshire, UK) for the provision of materials.

References

[1] L.R. Snyder, *J. Chromatogr.*, 20 (1965) 463.
[2] A.V. Kiselev, A.A. Aratskova, T.N. Gvozdovitch and Ya.I. Yashin, *J. Chromatogr.*, 195 (1980) 205.
[3] R.M. Smith, *J. Chromatogr.*, 209 (1981) 1.
[4] B.N. Barman and D.E. Martire, *Chromatographia*, 34 (1992) 347.
[5] J.H. Knox, B. Kaur and G.R. Millward, *J. Chromatogr.*, 352 (1986) 3.
[6] J.H. Knox and B. Kaur, in P.R. Brown and R.A. Hartwick (Editors), *High Performance Liquid Chromatography*, Wiley, New York, 1989, p. 189.
[7] A.V. Kiselev and Ya.I. Yashin, *Gas Adsorption Chromatography*, J.E.S. Bradley (Translator), Plenum, London, 1969.
[8] Q.H. Wan, *PhD Thesis*, Edinburgh University, 1992.
[9] C. Horvath, W. Melander and I. Molnar, *Anal. Chem.*, 49 (1977) 142.
[10] J.H. Knox and M.T. Gilbert, *U.K. Patent*, 7939449 (1979), *U.S. Patent*, 4263268 (1979), *F.R.G. Patent*, P2946688-4 (1979).
[11] B.J. Bassler and R.A. Hartwick, *J. Chromatogr. Sci.*, 27 (1989) 162.
[12] B.J. Bassler, E. Garfunkel, R.A. Hartwick and R. Kaliszan, *J. Chromatogr.*, 461 (1989) 139.
[13] Z. Pawlak, D. Kay and B.J. Clark, *Anal. Proc.*, 27 (1990) 16.
[14] G. Gu and C.K. Lim, *J. Chromatogr.*, 515 (1990) 183.
[15] D.A. Barrett, M. Pawula, S. Taylor, Q.H. Wan and P.N. Shaw, in preparation.
[16] M.T. Gilbert, J.H. Knox and B. Kaur, *Chromatographia*, 16 (1982) 138.
[17] D.R. Lide (Editor-in-Chief), *CRC Handbook of Chemistry and Physics*, 73rd Edition, CRC Press, Boca Raton, FL, 1992.

ELSEVIER

Journal of Chromatography A, 697 (1995) 229–245

JOURNAL OF CHROMATOGRAPHY A

Liquid chromatographic determination of amino acid enantiomers by derivatization with *o*-phthaldialdehyde and chiral thiols
Applications with reference to food science

H. Brückner[a,*], M. Langer[a], M. Lüpke[a], T. Westhauser[a], H. Godel[b]

[a]*Institute of Food Technology, University of Hohenheim, Garbenstrasse 25, 70593 Stuttgart, Germany*
[b]*Hewlett-Packard GmbH, Waldbronn Analytical Division, 76337 Waldbronn, Germany*

Abstract

Using a fully automated liquid chromatograph, D- and L-α-amino acids (D- and L-AA) were determined in foods and beverages by precolumn derivatization with *o*-phthaldialdehyde (OPA) combined with the chiral thiol N-isobutyryl-L-cysteine (IBLC) or its enantiomer N-isobutyryl-D-cysteine (IBDC) with the structure $(CH_3)_2CHCONHCH(CH_2SH)COOH$. The resulting diastereomeric isoindole derivatives were resolved on an octadecylsilyl stationary phase using a linear gradient formed from sodium acetate buffer (pH 5.95) and methanol–acetonitrile. For the detection of the isoindoles, their fluorescence at 445 nm when excited at a wavelength of 230 nm was used. The suitability of the LC method was demonstrated by the detection of free D-AA as native constituents of grape juice, their determination in alcoholic fermented beverages (beer and wine), fermented dairy products (coumiss, dietary whey drink, hard cheese), lactic acid fermented cabbage juice, a commercial yeast extract and honey. D-AA were detected in all foodstuffs. The results provide further proof that D-AA are common in microbially fermented foods and that microorganisms (bacteria, yeasts) are major, but not exclusive, sources of free D-AA occurring in foodstuffs.

1. Introduction

For the precolumn derivatization of DL-α-amino acids (DL-AA) with chiral reagents followed by the liquid chromatographic (LC) separation of the diastereomeric derivatives formed, the use of various reactive chiral compounds has been reported. Examples are (+)- and (−)-1-(naphthyl)ethyl isocyanate [1], (*R*)-α-methylbenzyl isothiocyanate [2], acetylated β-D-glucopyranosyl isothiocyanates [3,4], dinitroaryl fluorides [5,6], monohalo-*s*-triazines [7], oxycarbonyl chlorides [8], L-α-amino acid carboxy anhydrides [9], and chiral thiols together with *o*-phthaldialdehyde (OPA). In the last instance, the diastereomeric isoindole derivatives formed from DL-AA and OPA together with various chiral thiols such as thio sugars [10,11], N-acetylpenicillamine [12], the chiral drug Captopril [13], D-3-mercapto-2-methylpropionic acid [14] and N-acetylcysteine [15,16] are resolvable by HPLC. In particular, the members of the homologous series N-acetyl- to N-octanoyl-L-cysteine [13,17–19] were systematically investi-

* Corresponding author.

0021-9673/95/$09.50
SSDI 0021-9673(94)01052-8

gated for their suitability as reagents for the so-called indirect approach [20] of separating AA enantiomers as diastereomeric isoindole derivatives. We selected N-isobutyryl-L-cysteine (IBLC) and its enantiomer N-isobutyryl-D-cysteine (IBDC) as the most suitable reagents among the various thiols investigated. In combination with an appropriate ODS stationary phase and optimized gradient elution conditions, we completely and reproducibly separated a multicomponent standard consisting of all protein L-α-amino acids and their corresponding D-enantiomers, DL-cysteic acid, glycine, the non-protein α-aminoisobutyric acid (Aib) and DL-isovaline (Iva) and the internal standard L-*homo*-arginine [21]. The reagents, stationary phase and instrumental set-up are commercially available, and the method has been tested thoroughly with respect to its robustness and reliability in various analytical matrices [21,22–25]. This approach, therefore, is unique among the various HPLC methods proposed for the complete resolution of mixtures of D- and L-AA in realistic samples [26–30].

In continuation of work mainly concerned with the gas chromatographic determination of D- and L-AA in microorganisms [31,32], foodstuffs [23,33–37] and physiological fluids [38,39] by applying the chiral stationary phases Chirasil-Val [40], XE-60-L-Val-(*S*)-α-phenylethylamide and Lipodex E [41], we now show that the HPLC method is also very suitable for the determination of AA enantiomers in food and beverages.

2. Experimental

2.1. Instruments

For HPLC, an instrument that makes possible the fully automated pre-column derivatization of amino acid enantiomers with OPA and chiral thiols was used. It consisted of an HP 1090 Series L chromatograph constructed from a binary DR 5 solvent-delivery system, autoderivatizer and autoinjector (for details, see Ref. [22]), temperature-controlled column compartment and HP 1046 programmable fluorescence detector operated at an excitation wavelength of 230 nm and an emission wavelength of 445 nm (cut-off filter 280 nm). For data processing a Series HP 79994A ChemStation computer, Model 7440A ColorPro plotter and Model 2225B ThinkJet printer were used. All instruments were provided by Hewlett-Packard, Waldbronn Analytical Division (Waldbronn, Germany).

2.2. Chromatography

Columns (250 mm × 4 mm I.D.) and guard columns (20 mm × 2.1 mm I.D.) (Hewlett-Packard) packed with Hypersil ODS of particle size 5 μm (Shandon Scientific, Runcorn, UK) were used. The tested columns are available from Hewlett-Packard, Waldbronn Analytical Division, on request. The columns were kept at 25°C. Eluent A was prepared from 3.13 g (23 mmol) of sodium acetate trihydrate in 990 ml of doubly distilled water adjusted to pH 5.95 by addition of 10% (v/v) acetic acid and made up to 1.0 l. The eluent was filtered through a 0.45-μm filter (Sartorius, Göttingen, Germany). Eluent B consisted of 474 g of methanol and 39 g of acetonitrile (AN). Helium was continuously passed through the eluents. A linear gradient was applied for 75 min at a flow-rate of 1 ml min^{-1} from 0 to 53.5% B and then equilibrated with 100% A for 10 min.

2.3. Automated derivatization procedure

Derivatization of standards and samples was carried out as in previous investigations [21–25]: 260 m*M* IBLC (or IBDC) and 170 m*M* OPA in 1 *M* potassium borate buffer (pH 10.4) (Pierce, Rockford, IL, USA) were used as derivatization reagents (designated OPA–IBLC or OPA–IBDC reagent). Using the unique derivatization device of the instrument [22], amounts of 5 μl of 0.4 *M* sodium borate buffer (pH 10.4) (Hewlett-Packard), 1 μl of OPA–IBLC (or OPA–IBDC) reagent and 2-μl aliquots of the analyte solutions were consecutively drawn up by the autosampler and mixed by the autoderivatizer, programmed for five mixing cycles in the 8-μl mode. The

mixing procedure was completed in ca. 2 min, then the mixture was immediately and automatically injected on to the column. For quantification an external standard consisting of 100 pmol of L-AA and 5 pmol of D-AA in 2 μl of 0.1 *M* HCl was used [25]. The acid-sensitive AA (Gln, Asn and Trp) were dissolved in water and suitable amounts were added to the stock solution between analysis.

2.4. Solvents and chemicals

Solvents and chemicals were of chromatographic or analytical-reagent grade from Merck (Darmstadt, Germany). Dowex 50W-X8 cation exchanger (H^+ form, particle size 0.037–0.075 mm, analytical-reagent grade) and polyamide-6 powder (research grade) were obtained from Serva (Heidelberg, Germany) and were discarded after use. A saturated solution of picric acid (Fluka, Buchs, Switzerland) in water used for the precipitation of proteins is referred to as "picric acid" in the text. L- and D-AA were of the highest available purity and purchased from Sigma (St. Louis, MO, USA), Fluka or Serva. The internal standard L-*homo*-Arg was obtained from Serva and N-isobutyryl-D-cysteine (IBLC) was from Calbiochem–Novabiochem (Läufelfingen, Switzerland). N-Isobutyryl-L-cysteine (IBLC) was synthesized in our laboratory [22] and is also available from Calbiochem–Novabiochem or Calbiochem (La Jolla, CA, USA); IBLC and IBDC are now also available as ChiraSelect reagents from Fluka. The reagents used were of 99.91 ± 0.01% (IBLC) and 99.78 ± 0.02% (IBDC) optical purity.

2.5. Sources of food and beverage samples and treatment for analyses

Grape juice

Freshly harvested and selected ripe grapes *Vitis vinifera* L. (cultivar Trollinger) from a vineyard in the Stuttgart area were carefully washed with 70% ethanol. Grapes (ca. 200 g) were squeezed and the juice was collected using an automated juicer based on the centrifugal principle (Multipress MP 50, Type 4154, from Braun, Frankfurt, Germany). The juice was filtered using a fluted paper filter and centrifuged at 1650 *g*. To 1-ml aliquots of the juice, 31.3 μl of 1.6 m*M* L-*homo*-Arg in 0.1 *M* HCl were added, the pH was adjusted to 2 by addition of 2 *M* HCl and the mixture was transferred to the top of a column containing Dowex 50W-X8 cation exchanger (bed size 5 cm × 1 cm). Amino acids were eluted with 4 *M* aqueous ammonia (30 ml), the eluent was evaporated to dryness using a vacuum evaporator, the residue was dissolved in 0.1 *M* HCl (1 ml) and 2-μl aliquots were analysed.

Wines

Bottled wines [French rosé wine (Rosé d'Anjou, 4 years old) and Madeira wine (Leacocks, 10 years old)] were purchased in a local wine shop. To an aliquot of the rosé wine (10 ml), picric acid (10 ml) and 0.1 *M* HCl (10 ml) were added, the mixture was stirred for 15 min and then centrifuged at 1650 *g*. The clear solution was passed through a column packed with polyamide-6 powder (bed volume 5 cm × 1 cm) and then subjected to Dowex 50W-X8 treatment and analysed as described above. For the Madeira wine, an aliquot (25 ml) was adjusted to pH 2 by addition of 6 *M* HCl and the mixture was subjected to Dowex 50W-X8 treatment and elution of AA as described above. After evaporation to dryness, the residues were dissolved in 0.1 *M* HCl (2 ml) and 2-μl aliquots were used for analysis by HPLC.

Vinegar

Vinegar made from Sherry wine (Old Sherry wine vinegar, from Jerez de la Frontera) was investigated. The vinegar was matured for several years in oak barrels, bottled in Jerez, Spain, and imported and distributed in Germany by Probare, Skandinavien- und Süd-Import, Maisach, Germany. Aliquots of 2 μl were directly analysed after filtration.

Beer

A bottled German Export beer (Das echte Schwabenbräu, Stuttgart), produced with the aid of the bottom-fermenting yeast *Saccharomyces*

carlsbergensis, was investigated. The beer contained 6% (v/v) ethanol and had an original gravity of 13%. To an aliquot (10 ml) picric acid (10 ml) was added and the mixture was stirred for 10 min and centrifuged at 1630 *g* for 10 min. The supernatant was filtered using a fluted paper filter and the filtrate was extracted three times with 20-ml portions of light petroleum (b.p. 50–70°C)–diethyl ether (1:1, v/v). The aqueous phase was evaporated to dryness and the residue was dissolved in 0.01 *M* HCl (20 ml), filtered and subjected to cation exchanger treatment and ammonia elution of AA as described above. The dry residue was dissolved in 0.1 *M* HCl (3 ml) and filtered using a 0.45-μm disposable filter and aliquots of 2 μl were analysed.

Lactic fermented cabbage juice

Bottled and pasteurized lactic fermented (pickled) cabbage juice (Eden Sauerkrautsaft; Eden, Bad Soden, Germany) was purchased in a shop specializing in health food (Reformhaus). An aliquot of the juice was filtered using a Millex GV 13 filter (Millipore, Monheim, France). A 1-ml aliquot was diluted with 4 ml of doubly distilled water and 2-μl aliquots were analysed.

Coumiss

This commercially available product (Kumylac) was provided by Kurgestüt Hoher Odenwald (Waldbrunn, Germany). According to the manufacturer's declaration, this product is produced from the milk of mares by controlled addition of lactobacilli and yeast. To an aliquot (40 ml), acetonitrile (80 ml) was added and the mixture was stirred for 15 min and centrifuged at 1650 *g*. The supernatant was concentrated in vacuo to a volume of ca. 5 ml, then picric acid (5 ml) and 0.1 *M* HCl (10 ml) were added. The mixture was centrifuged at 1650 *g* and the supernatant was extracted with light petroleum (b.p. 50–70°C)–diethyl ether (1:1, v/v) (3 × 20 ml). The supernatant was passed through a Dowex 50W-X8 column and amino acids were eluted as described above. The effluent was evaporated to dryness, the residue was dissolved in 0.1 *M* HCl (2 ml) and 2-μl aliquots were analysed. Analogously, an unfermented mares milk (Equilac) sample, serving as starting material for coumiss, was analysed.

Dietetic whey drink

A 1-l package of heat-treated whey (Heirler Diät Kurmolke; Heirler, Gauting bei München, Germany) was purchased in a shop specializing in dietetic and health food (Reformhaus). According to the manufacturer's declaration, the dietetic whey was made from acidic whey with addition of Sanoghurt starter culture (*Streptococcus lactis* ssp. *lactis* or ssp. *cremoris*). In addition, whey proteins and pectin were added by the manufacturer. To whey (1 ml), solid 5-sulfosalicylic acid (80 mg) was added and the mixture was shaken for several minutes and centrifuged at 4000 *g*. The supernatant was filtered using a Millex GV 13 filter (see above) and 2-μl aliquots were analysed.

Cheese

A French pressed cheese, purchased in a cheese shop in France, of the protected origin (d'origin controllé) Cantal, was investigated. This popular traditional cheese from the Central Massif area of France is made from cow milk with the addition of mixed starter cultures, usually *Lactobacillus lactis* and *Leuconostoc citrovorum*. The cheese had 45% fat in dry matter and 58% dry matter. From the interior an aliquot (1.0 g) was removed, 96% ethanol (30 ml) was added and the mixture was stirred vigorously at 50°C for 45 min. Water (35 ml) was added and stirring was continued for another 15 min. The mixture was centrifuged (1600 *g*, 10 min) and the supernatant was evaporated to a volume of ca. 10 ml in vacuo. The pH was adjusted to 2 by addition of 0.1 *M* HCl and the solution was extracted with light petroleum (b.p. 50–70°C)–diethyl ether (1:1, v/v) and further treated as described for coumiss.

Yeast extract

A dietary yeast extract (Marmite, Burton on Trent, UK), used as a spread or seasoning, was purchased in the UK. According to the declaration, the ingredients were yeast extract, salt, vegetable extract, spices and vitamins. An

aliquot (1 g) was dissolved in doubly distilled water (10 ml). To a 1-ml aliquot, 5-sulfosalicylic acid (50 mg) was added, the mixture was centrifuged and the supernatant was diluted to a final volume of 10 ml. Aliquots of 2 μl were analysed.

Honey

White fir honey (collected in spring 1993 in the Stuttgart area by honey bees, *Apis mellifera carnica*) was kindly provided by Professor Dr. G. Vorwohl, Landesanstalt für Bienenkunde, Universität Hohenheim (Hohenheim, Germany). Samples (1 g) were dissolved in 0.01 *M* HCl (10 ml), evaporated to a volume of ca. 5 ml in vacuo and then subjected to Dowex 50W-X8 treatment as described above. The dry residue was dissolved in 0.1 *M* HCl (1 ml) and 2-μl aliquots were analysed.

3. Results and discussion

The elution profiles of AA (referred to as aminograms) from foodstuffs and derivatized with OPA–IBLC or OPA–IBDC are shown in Figs. 1–11 (for chromatograms of standards we refer to previous publications [21,25]; as IBLC or IBDC has to be used together with the dialdehyde, we omit OPA in the following text). The reversal of the elution order of AA enantiomers is extremely helpful for the certain assignment and quantification of D-AA, in particular when complex matrices are analysed. In order to demonstrate this, aminograms resulting from the use of both reagents are shown, with the exception of beer. The relative percentage values given in parentheses in the text are those determined with IBDC. In cases where no data are given, quantification or reliable assignment of the respective enantiomer was not possible. In the following, the relative amounts of D-AA that have been determined are presented and their relevance is discussed. The absolute amounts of D-AA determined in native, unprocessed grape juice, rosé wine, vinegar made from Sherry wine, juice of pickled cabbage, Cantal cheese, dietary whey drink, honey and edible yeast extract are displayed in Table 1.

3.1. Grape juice

The elution profiles of D- and L-AA determined in a freshly pressed grape juice are shown in Fig. 1a and b. Relative amounts of 0.9% (1.2%) D-Asp, 0.7% (0.5%) D-Glu, 1.2% (1.4%) D-Ser, 1.2% (1.5%) D-Arg and 1.0% (1.2%) D-Ala were determined. As microbial contamination or spoilage is excluded, this result further corraborates that certain D-AA are native constituents of fruit juices [21,25]. Their amount and diversity increase as soon as bacteria

Table 1
Quantification of D-amino acids (D-AA) in foodstuffs

D-AA	Grape juice (μmol l^{-1})	Rosé wine (μmol l^{-1})	Vinegar (μmol l^{-1})	Pickled cabbage juice (μmol l^{-1})	Cheese[a] (μmol kg^{-1})	Dietary whey (μmol l^{-1})	Honey (μmol kg^{-1})	Yeast extract	
								μmol kg^{-1}	mg kg^{-1}
D-Asp	1.6	3.3	10.9	181	337	24	9.8	2153	287
D-Asn	–	–	–	–	–	–	–	2981	394
D-Glu	3.9	6.0	9.1	20	998	20	10.1	1866	275
D-Ser	1.9	–	1.4	49	n.d.	2.3	3.1	1283	135
D-Ala	5.4	6.2	2.3	718	987	29	8.1	3984	355
D-Arg	8.2	–	–	–	–	–	–	–	–
D-Tyr	–	–	–	–	–	–	–	548	99
D-Phe	–	–	–	–	n.d.	–	–	1026	135
D-Leu	–	–	3.5	59	104	–	3.1	–	–
D-Lys	–	–	–	2.4	–	1.0	1.5	–	–

For origin of foodstuffs see Experimental; – = not detected; n.d. = not determined.
[a] D-Pro (122 μmol kg^{-1}), D-*allo*-Ile (32 μmol kg^{-1}) and D-Phe (182 μmol kg^{-1}) determined by GC.

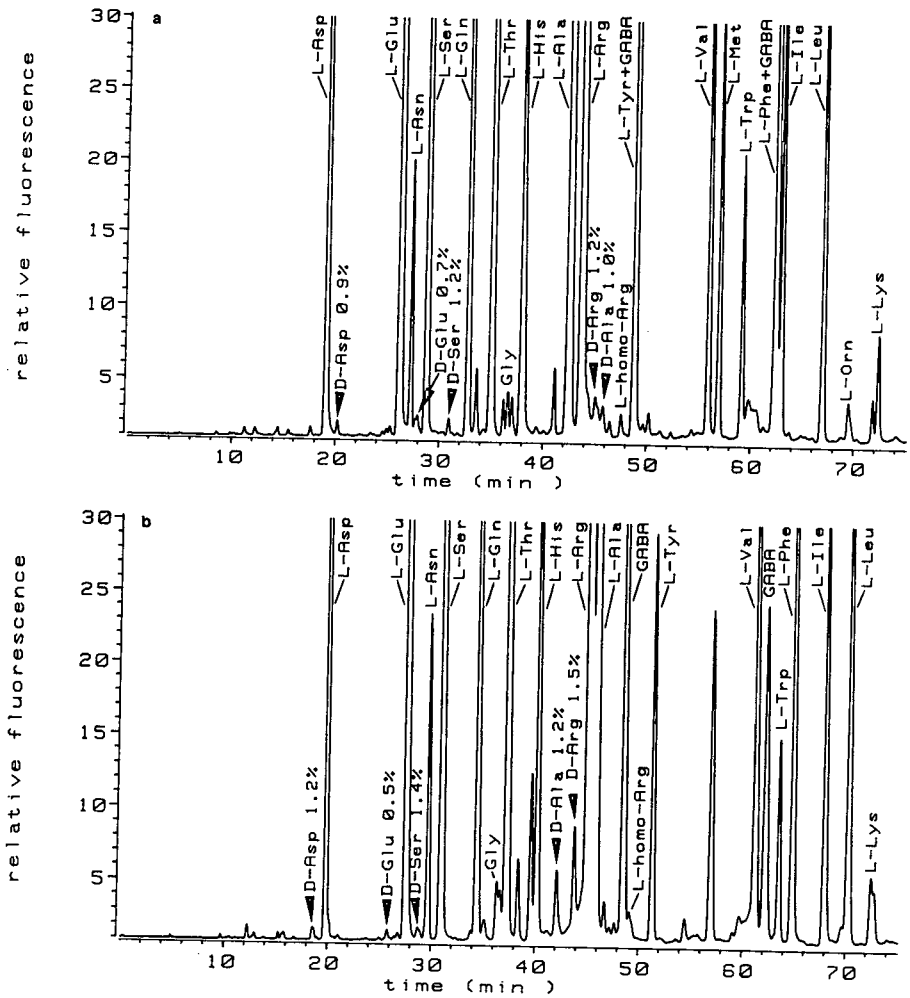

Fig. 1. Aminogram of freshly pressed grape juice derivatized with (a) IBLC and (b) IBDC. Arrows mark positions of D-AA in all aminograms.

are allowed to grow in plant juices (cf. Table 1 and Fig. 6). This might cause spoilage [36] or, if grown under controlled conditions, is used for manufacturing fermented foods or drinks [31] (see also below).

3.2. Wines

The aminograms of a French rosé wine are shown in Fig. 2a and b. Relative amounts of 3.4% (5.8%) D-Asp, 2.4% D-Glu, 2.9% D-Ala and 3.2% D-Tyr were determined. Using IBDC (Fig. 2b), D-Glu, D-Ala and D-Tyr elute together with unknown components, and the assignment of D-Ser and D-Leu is not confirmed by derivatization with IBLC. The total amounts of AA (D + L) in this wine was 901 mg l^{-1} and the sum of D-AA was 2.5 mg l^{-1}.

The chromatograms of a Madeira wine are shown in Fig. 3a and b. Relative amounts of 20.5% (20.5%) D-Asp, 22.5% (20.4%) D-Glu, 17.8% D-Asn, 4.4% (5.3%) D-Arg, 16.9% (17.8%) D-Ala, presence of D-Tyr, 3.2% D-Val and 7.7% (6.7%) D-Leu and, by derivatization with IBDC, 11.4% D-Ser were determined. D-Tyr and D-Phe are detectable using IBLC, but are not quantifiable relative to their L-forms as L-Tyr and L-Phe elute together with derivatives

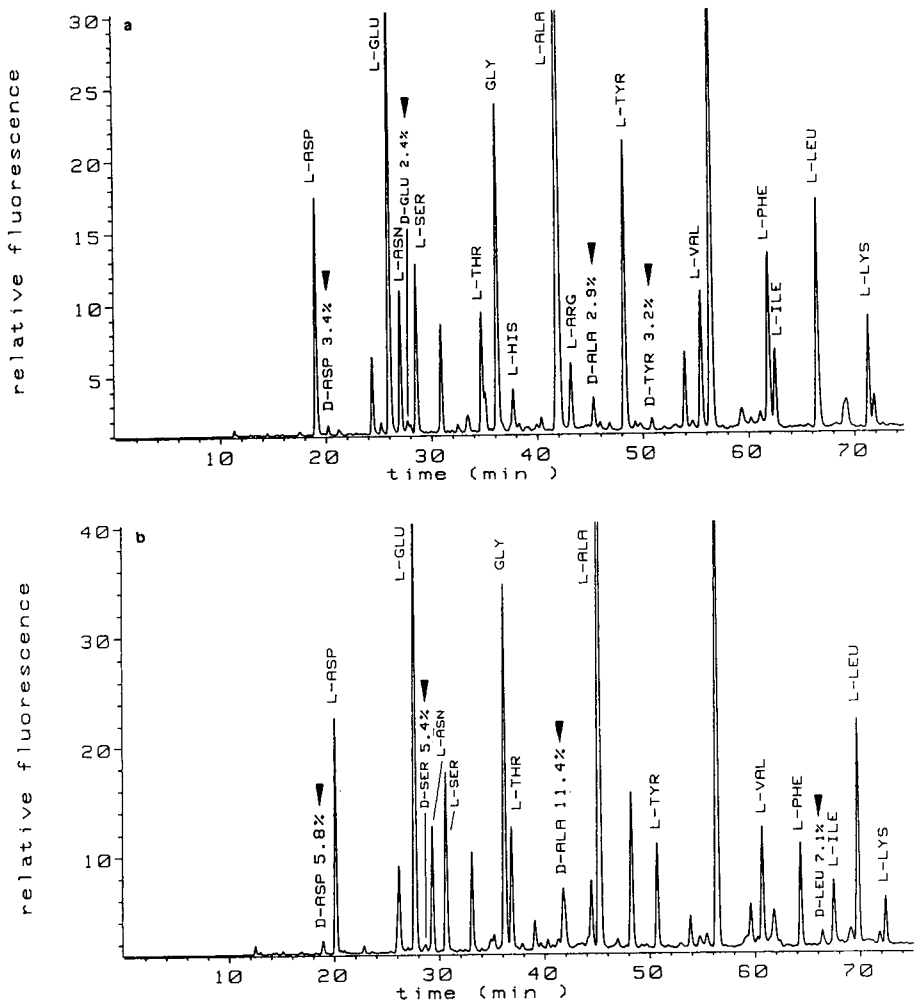

Fig. 2. Aminogram of a bottled rosé wine derivatized with (a) IBLC and (b) IBDC.

formed from GABA, named GABA(1) and GABA(2) (see Fig. 3b). In this wine, D-Ser is not quantifiable using IBLC as its derivative elutes close to an unknown component and D-Asn is not detectable using IBDC. The total amount of AA (D + L) in this wine was 517 mg l^{-1} and the sum of D-AA was 30 mg l^{-1}. In particular, the data show a characteristic difference for the relative amounts of D-AA between wines and fortified wines.

From the large number of white, red and rosé wines which we have investigated [33–35], the presence and the relative amounts of ca. 1–3% of D-Asp, D-Glu and D-Ala are typical (higher amounts of certain D-AA have been reported to occur in Portuguese elementary wines [42]). In fortified wines (Madeira, Sherry, Port), however, in general high amounts of D-Asp, D-Glu and D-Ala and a greater diversity of D-AA are found (see Fig. 3). This is attributed to the manufacturing procedures for fortified wines, where alcohol is added to the vigorously fermenting must in order to stop the fermentation process, followed by curing and maturing of these fortified wines under typical conditions for several years. The raw materials, manufacturing

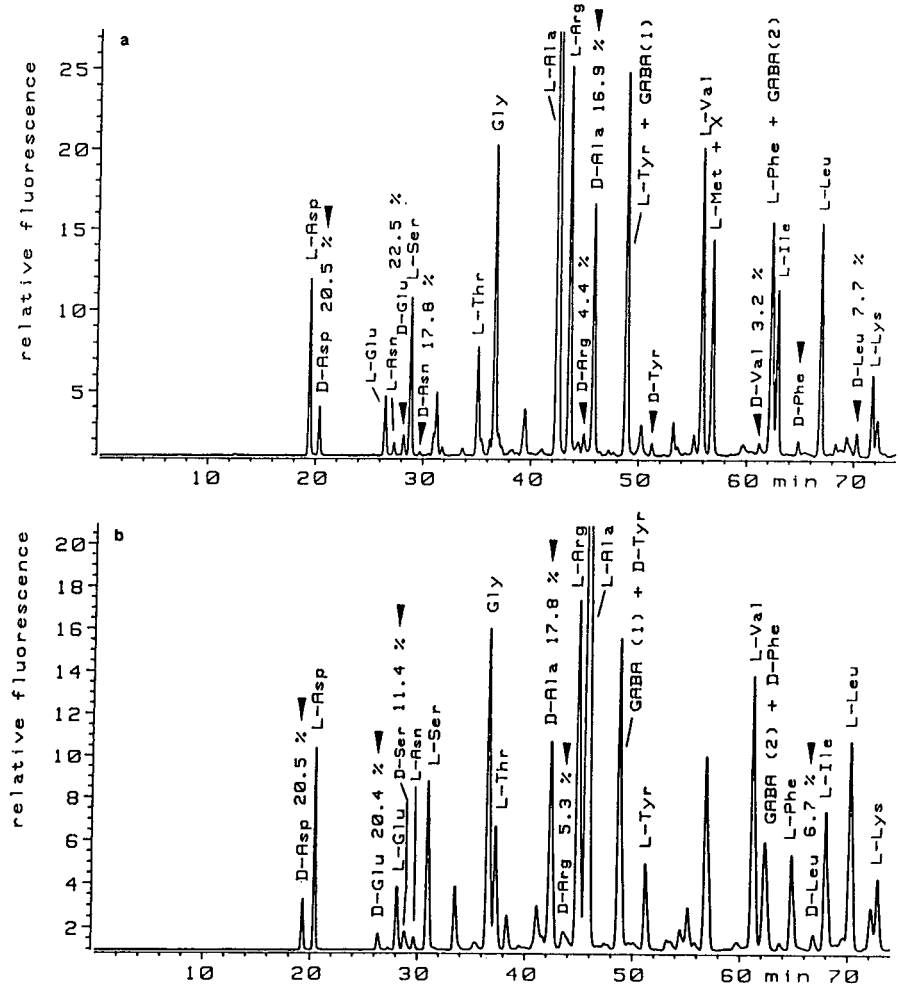

Fig. 3. Aminogram of a 10-year-old Madeira wine derivatized with (a) IBLC and (b) IBDC.

processes, fermentation procedures (including yeasts and bacteria) and maturing conditions of the various wines show a great variety and the blending of fortified wines is also common. In the context of this work, it should briefly be stated that the action of microbial and plant enzymes such as amino acid isomerases and transaminases is assumed to be responsible for the occurrence of D-AA in wines, rather than an acid-catalysed racemization of L-AA.

3.3. Vinegar

The chromatograms of vinegar made from Sherry wine are shown in Fig. 4a and b. Relative amounts of 22.1% (25.4%) D-Asp, 17.9% (13.4%) D-Glu, 6.0% (4.7%) D-Ser, 21.7% (24.4%) D-Ala and 10.0% (9.4%) D-Leu were found. Such high relative amounts of D-AA are also found in other high-quality vinegars such as Italien aceto balsamico [35], which is produced and stored in wooden barrels for several years. As with wine, the formation of D-AA is attributed to the action of microbial enzymes. At the beginning of the fermentation the yeast *Saccharomyces cerevisiae* converts sugars into ethanol, which is then fermented to acetic acid by species of *Acetobacter*. Consequently, D-AA

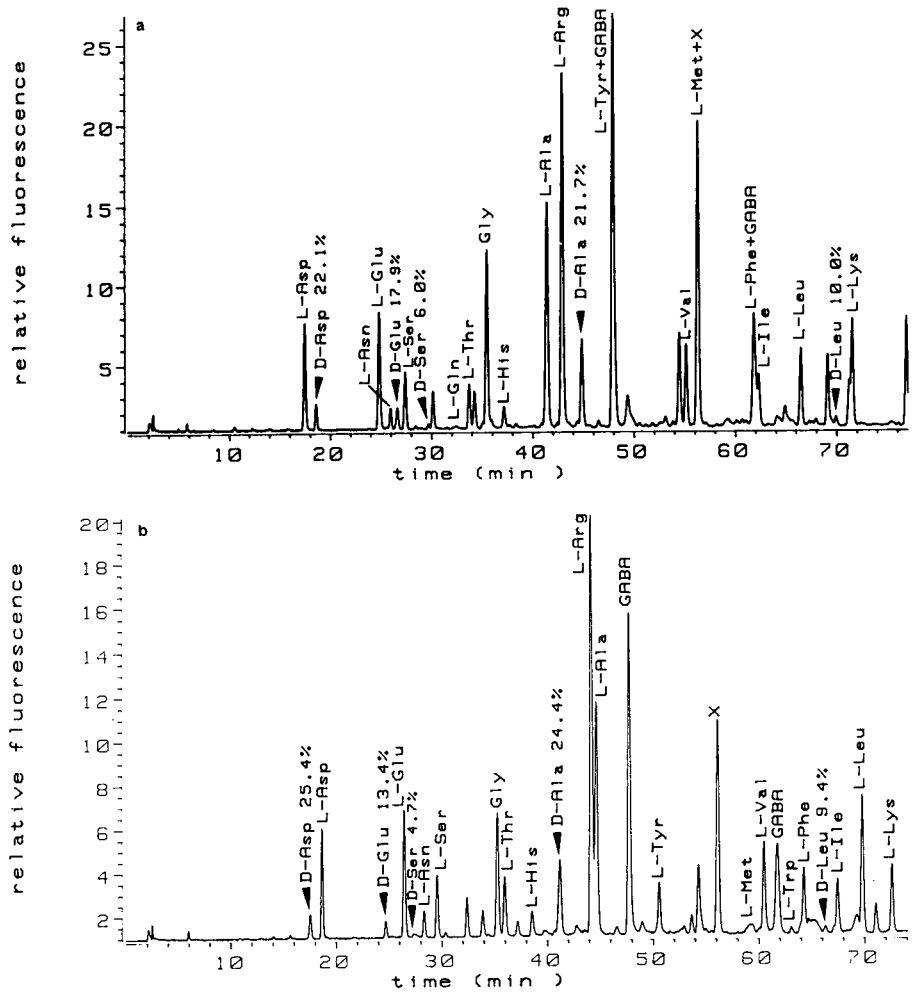

Fig. 4. Aminogram of a vinegar produced from Sherry wine derivatized with (a) IBLC and (b) IBDC.

have also been detected in the acetic acid bacterium *Acetobacter esbia*, which is used as a starter culture for the production of vinegar [31].

3.4. Beer

The elution profile of AA from a beer, derivatized with IBLC, is shown in Fig. 5. Relative amounts of 29.0% D-Asp, 5.9% D-Glu and 3.3% D-Ala were found. The total amount of AA (D + L) was 697 mg l^{-1} and the sum of D-AA was 11 mg l^{-1}. Like wine, beer belongs to the alcoholic fermented beverages and, consequently, D-AA have been detected by GC in all beers which were brewed under various conditions [33–35]. The most abundant D-AA is D-Asp, followed by D-Glu and D-Ala. Although varieties of the yeasts *Saccharomyces cerevisiae* and *Saccharomyces carlsbergensis* play the major role in the brewing process, bacteria are also involved and the possible contribution of the processes of malting, liquating and torrefying on the formation of D-AA, as well as the contribution of plant D-AA [25], still has to be evaluated.

3.5. Lactic acid fermented cabbage

The chromatograms of AA isolated from fer-

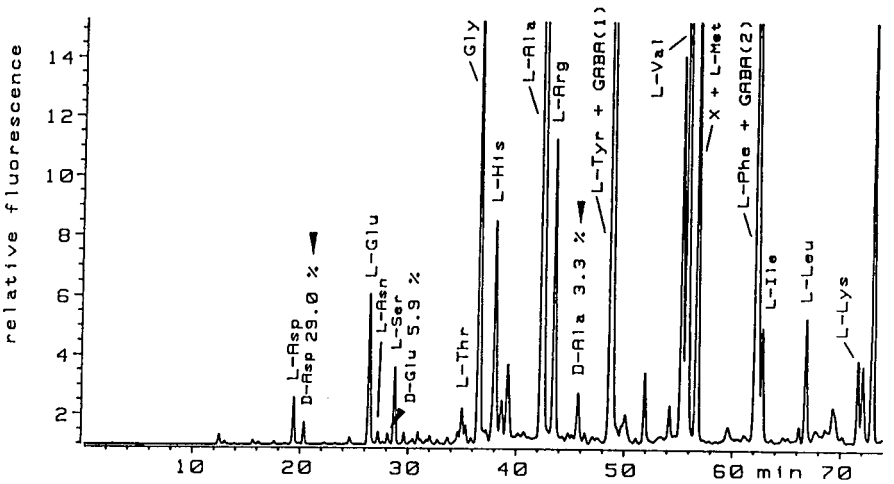

Fig. 5. Aminogram of bottom-fermented beer derivatized with IBLC.

mented cabbage are shown in Fig. 6a and b. Relative amounts of 5.2% (4.7%) D-Asp, 13.5% (12.3%) D-Glu, 3.0% (2.5%) D-Ser, 11.2% (8.2%) D-Ala 7.5% (7.2%) D-Leu and 10.2% (4.9%) D-Lys were found. Fermented (pickled) cabbage juice is used as a dietary drink. The bacterium *Leuconostoc mesenteroides* is involved in the beginning of fermentation, and later *Lactobacillus brevis* and *Lactobacillus plantarum* dominate. Lactobacilli show a high racemase activity [21,31,37] and are responsible for the relatively high amounts of D-AA determined.

3.6. Coumiss

Fig. 7a and b show the AA determined in the fermented milk of mares; 33.4% (34.5%) D-Asp, 9.5% (9.7%) D-Glu, 14.0% (15.3%) D-Ser and 76.1% (73.7%) D-Ala were found. These high amounts of free D-AA are the result of the microbial fermentation of the milk in which, again, amino acid isomerases and racemases are involved. In the fresh milk of mares, serving as a blank, only low amounts of D-Ala (0.9%), D-Glu (0.5%), D-Ser (0.3%) and traces of D-Asp (not quantifiable) were detectable using derivatization with OPA–IBLC.

3.7. Cheese

The AA determined in a ripened cheese are shown in Fig. 8a and b; 6.1% (7.1%) D-Asp, 14.3% (15.4%) D-Glu, 32.7% (32.4%) D-Ala and 0.8% (2.0%) D-Leu were found. With the exception of D-Leu, these values show good agreement, taking the very complex food matrix into account. The higher amount of D-Leu as determined by derivatization with OPA–IBDC is attributed to the co-elution of a background impurity. The total amount of AA (D + L) in the Cantal cheese was 7724 mg kg^{-1} and the sum of D-AA was 435 mg kg^{-1}. Quantitative data for D-AA determined in many cheeses have been reported [24,33–35,37,43] and their amounts and kinds have been rationalized as a result of the concerted action of high microbial protease and racemase activities [37,43].

3.8. Whey

Fig. 9a and b show the chromatograms of AA determined in a dietary whey beverage. Amounts of 23.7% (26.1%) D-Asp, 6.0% (5.7%) D-Glu, 10.0% (10.5%) D-Ser, 22.2% (24.8%) D-Ala and 15.2% (16.5%) D-Lys were found. Whey is milk serum obtained when caseins of milk are precipitated for cheese production by the action of rennet and cheese starter cultures. Depending on the starter cultures used and the manufacturing procedures applied, a high bacterial racemase activity in cheese and whey is observed [37]. In the dietary

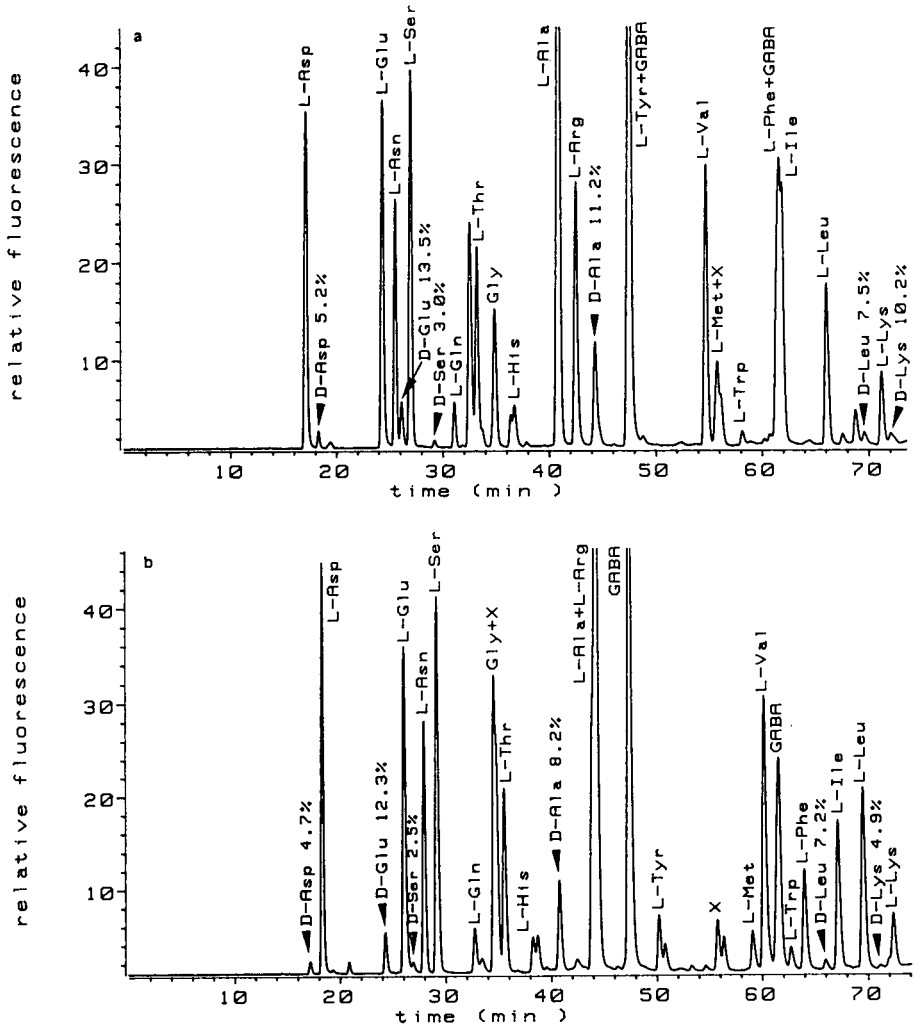

Fig. 6. Aminogram of lactic fermented cabbage juice derivatized with (a) IBLC and (b) IBDC.

whey drink investigated, additional species of *Streptococcus* that show a high racemase activity [31] were added to acid whey.

3.9. Honey

Fig. 10a and b show the aminograms of AA isolated from white fir honey; 5.2% (7.3%) D-Asp, 4.1% (4.2%) D-Glu, 1.8% (1.2%) D-Ser, 3.3% Ala, 1.8% D-Phe and 6.9% (5.7%) D-Leu were determined. D-Ala and D-Phe were not determinable using IBDC as a result of the co-elution with an unknown component (X) and GABA, respectively. Using chiral phase GC with another sample of a commercially available fir honey, 3.3% D-Asp, 5.7% Glx, 5.7% D-Ala and 3.8% D-Phe were detected. No D-Pro (which is not determinable using the method described) was found by GC, although L-Pro is the major AA in both honeys. Although the occurrence of AA in honey is well documented and the ratios between the concentrations of the individual AA have been used to determine the geographic source of honeys [44], the presence of D-AA in honey has not previously been reported. Honey, per se, is not considered to be a fermented food. Concerning the origin of D-AA in honey, clues might be that D-AA have been detected in

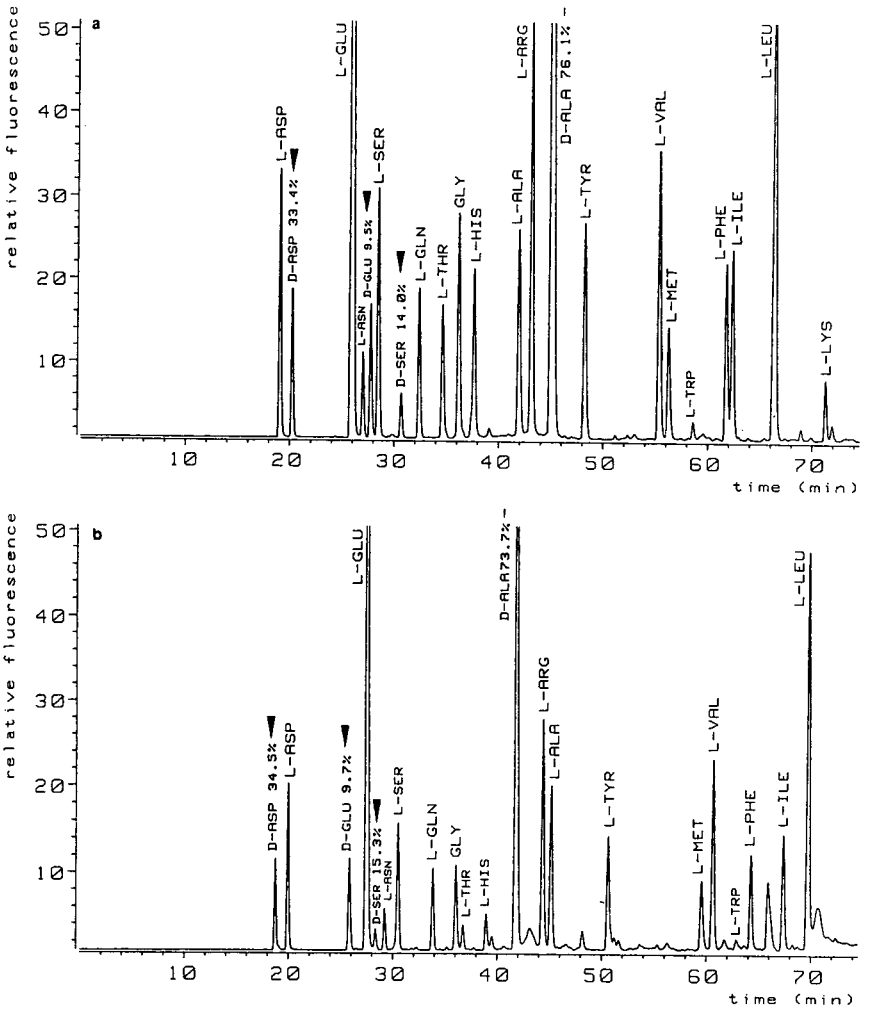

Fig. 7. Aminogram of coumiss derivatized with (a) IBLC and (b) IBDC.

insects [45], in nectar exudates of orchids [46] and in fruits and vegetables [25].

3.10. Yeast spread

In the yeast extract (Fig. 11a and b), amounts of 3.0% (2.7%) D-Asp, 1.8% (2.3%) D-Glu, 5.2% (4.9%) D-Asn, 1.3% (1.2%) D-Ser, 2.3% (2.6%) D-Ala, 1.9% D-Tyr and 1.7% D-Phe were determined (D-Tyr and D-Phe were determinable using the IBLC reagent, but not with the IBDC reagent as a result of the co-elution of the derivatives with the two arising from GABA [21]. It is of interest that dietary yeast also contains D-AA. The high absolute amounts are worth noting: a total of 1.7 g of D-AA in 1 kg of the yeast spread (see Table 1 for amounts of individual D-AA). As yeast extracts are widely used as seasonings in the food industry, these extracts are potential sources of D-AA in foodstuffs. As we have also found ethanol-extractable, free D-AA in baker's yeast, brewer's yeast and wine yeast (relative amounts of 1–2% with respect to the L-enantiomers have been determined by GC for D-Ala, D-Val, D-Ser, D-Asx and

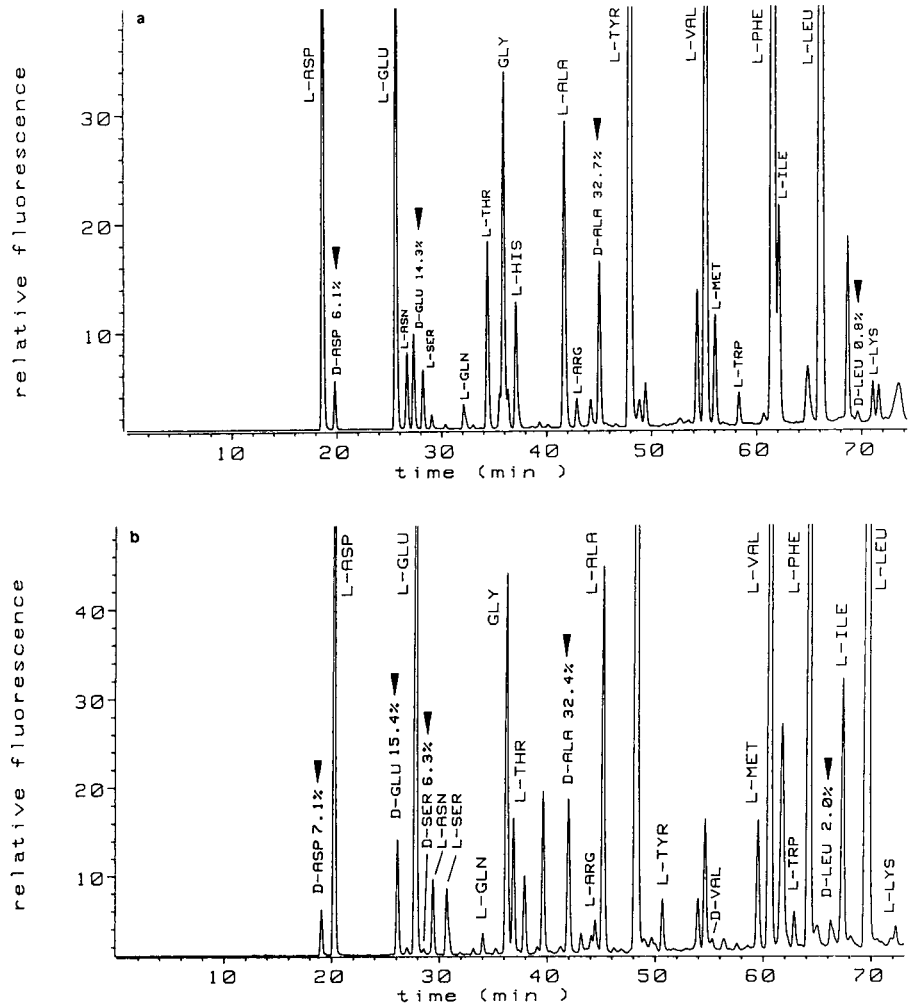

Fig. 8. Aminogram of a French Cantal cheese derivatized with (a) IBLC and (b) IBDC.

D-Glx), it is evident that D-AA also originate from the yeasts used for food production.

3.11. Practical aspects

As with biosamples [21], fully automated pre-column derivatization with OPA and the chiral thiols IBLC or IBDC has proved to be a rapid and reliable method for the indirect determination of the enantiomers of primary AA in foods and beverages. Although in several instances, such as with fruit juices, direct analysis is possible [25], the isolation of food AA using a cation exchanger is advantageous and gives cleaner aminograms and increases the lifetime of the column. Proteins have to be precipitated by addition of 5-sulfosalicylic acid, picric acid or organic additives and fat and other lipophilic compounds should be removed, e.g., by extraction with organic solvents. The suitability of polyamide-6 powder, which leads to partial decolorization of wines and other beverages, has to be further investigated. When low amounts of D-AA have to be determined, precautions with respect to microbial contamination have to be applied [21]. Samples subjected to cation-ex-

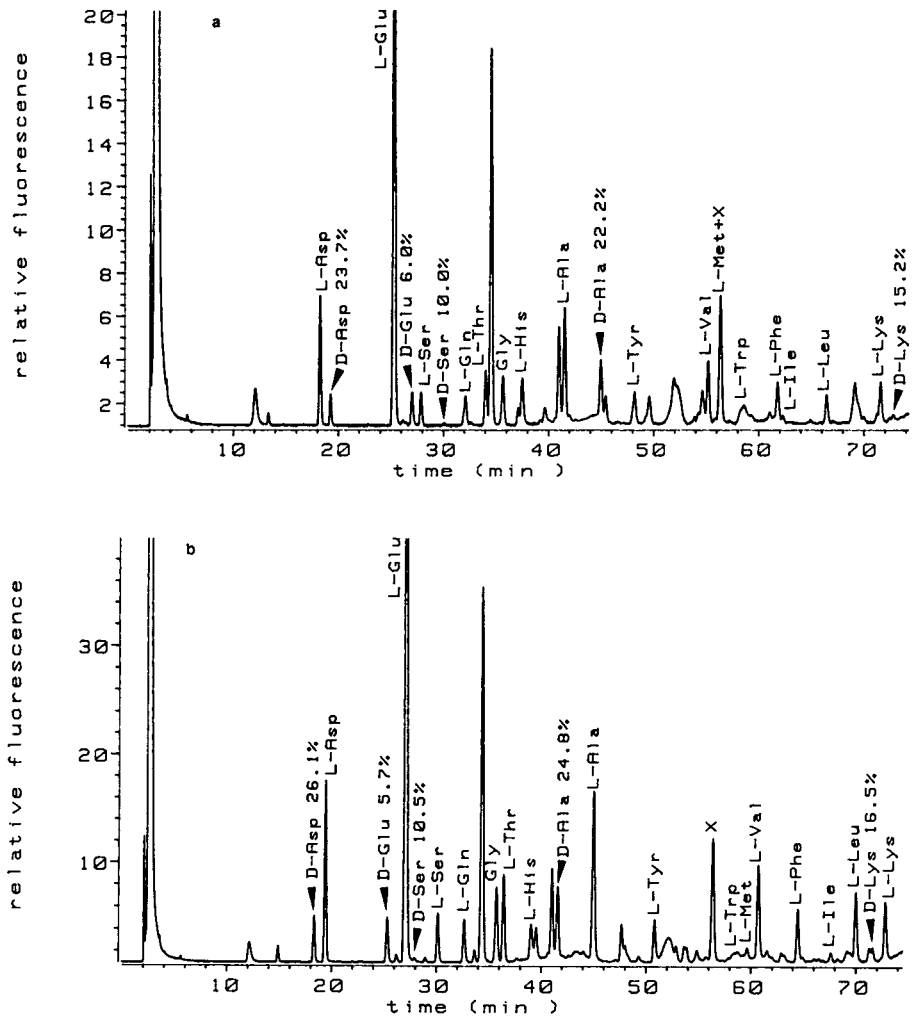

Fig. 9. Aminogram of dietetic whey drink derivatized with (a) IBLC and (b) IBDC.

change treatment should not have a pH value less than 2, as loss of acidic AA has been observed. In some instances low recoveries of the internal standard L-*homo*-Arg were recognized after ion-exchange treatment. This might depend on the food matrix and should therefore be tested. We discarded the ion exchanger after a single use as we have observed a rapid decrease in its capacity and quality, even when thoroughly regenerated, when food and biosamples were applied several times.

An important aspect of this work is that it further supports the thesis that free D-AA are common [34] or ubiquitous [35] constituents of microbially fermented foods and beverages. D-Ala, D-Asx and D-Glx are the D-AA found most frequently in the peptidoglycan [47] of all Eubacteria (i.e., Gram-positive and Gram-negative bacteria) which play a role in food production [31]. These D-AA are the same as those found to be must abundant in foodstuffs. It should be pointed out, however, that the peptidoglycan of several bacteria contains further D-AA such as D-Ser (*Bifidobacterium bifidum*), D-Orn (*Acetobacter woodii*) or D-Lys (*Clostridium innocuum*); these D-AA have also been detected in

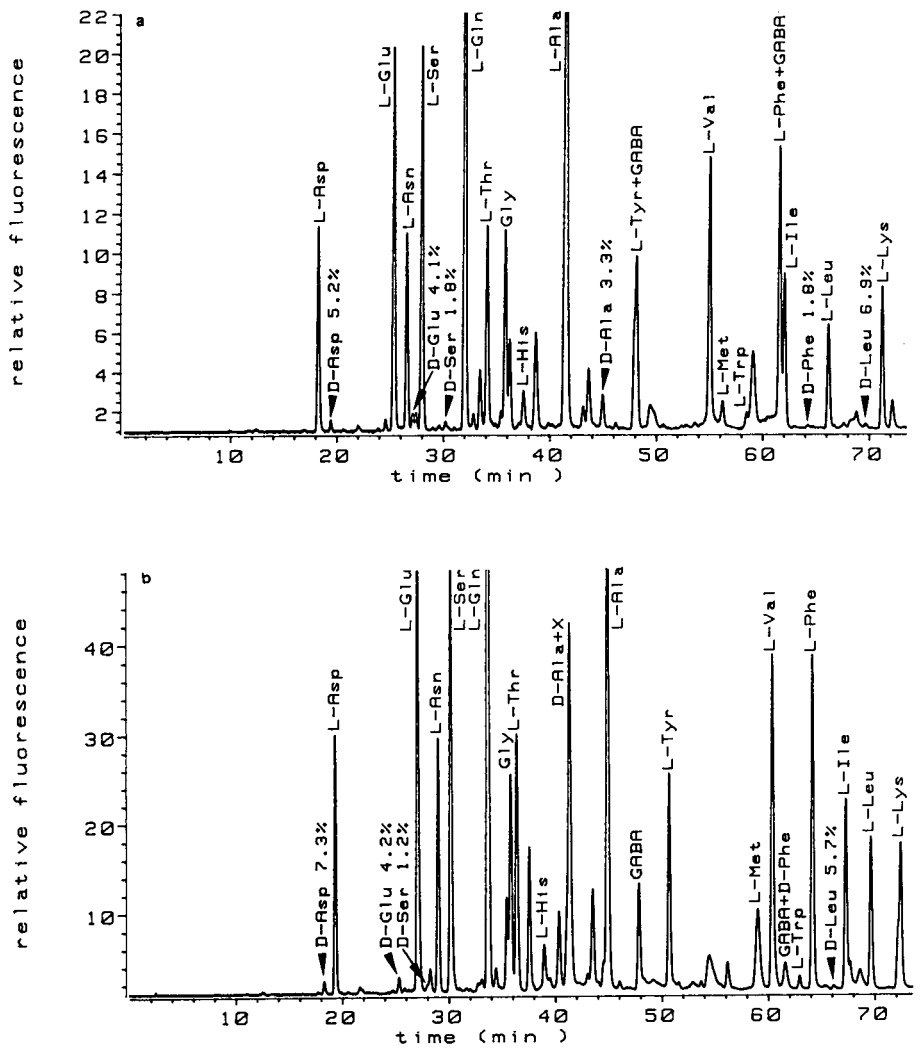

Fig. 10. Aminogram of fir honey derivatized with (a) IBLC and (b) IBDC.

certain foodstuffs. Moreover, a great diversity of D-AA, obviously not involved (or not known to be involved) in the formation of peptidoglycan, such as D-Pro, D-Val, D-Thr, D-Ile, D-*allo*-Ile, D-Leu, D-Phe, D-Tyr and D-Met, has been detected as free AA in the cytoplasm of bacteria used as starters for the production of fermented foods [31]. As shown above, yeasts are also potential sources of D-AA. Remarkably, free D-AA, not directly attributable to microbial activities, have been detected as native constituents of fruits and vegetables [21,25]. From a nutritional point of view, uptake of dietary D-AA is therefore the rule and not the exception as is the case with certain peptide-bonded D-AA that are formed in food proteins when processed severely enough [48–50]. Foods, together with intestinal microorganisms [31], are therefore assumed to be potential sources of the free D-AA that are regularly found in physiological fluids and certain tissues of man and animals (see Ref. [21] and references cited therein).

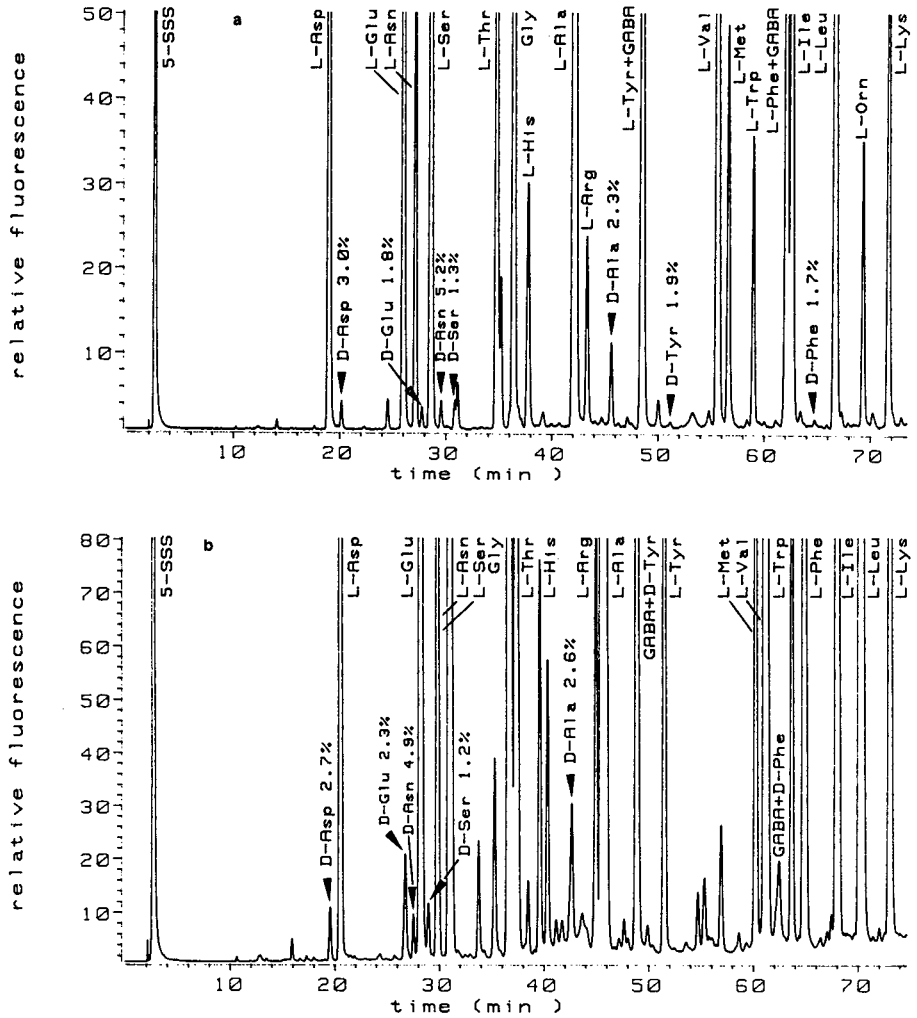

Fig. 11. Aminogram of a yeast spread derivatized with (a) IBLC and (b) IBDC.

Acknowledgements

We thank Mrs. B. Thomé for assistance with part of this work and are in particular obliged to Dr. R.E. Dunmur for drawing our attention to and providing a sample of the yeast spread.

References

[1] D.S. Dunlop and A. Neidle, *Anal. Biochem.*, 165 (1987) 38.
[2] J. Gal and A.J. Sedman, *J. Chromatogr.*, 314 (1984) 275.
[3] T. Kinoshita, Y. Kasahkara and N. Nimura, *J. Chromatogr.*, 210 (1981) 77.
[4] M. Lobell and M.P. Schneider, *J. Chromatogr.*, 633 (1993) 287.
[5] P. Marfey, *Carlsberg Res. Commun.*, 49 (1984) 591.
[6] H. Brückner and C. Gah, *J. Chromatogr.*, 555 (1991) 81.
[7] H. Brückner and B. Strecker, *J. Chromatogr.*, 627 (1992) 97.
[8] S. Einarsson, B. Josefsson, P. Möller and D. Sanchez, *Anal. Chem.*, 59 (1987) 1191.
[9] T. Takaya, Y. Kishida and S. Sakakibara, *J. Chromatogr.*, 215 (1981) 279.
[10] S. Einarsson, S. Folestad and B. Josefsson, *J. Liq. Chromatogr.*, 10 (1987) 1589.

[11] A. Jegorov, V. Matha, T. Trnka and M. Cerny, *J. High Resolut. Chromatogr.*, 13 (1990) 718.
[12] R.H. Buck and K. Krummen, *J. Chromatogr.*, 387 (1987) 255.
[13] H. Brückner, R. Wittner and H. Godel, in G. Lubec and G.A. Rosenthal (Editors), *Amino Acids: Chemistry, Biology and Medicine*, Escom Science, Leiden, 1990, pp. 143–151.
[14] A.L.L. Duchateau, H. Knuts, J.M.M. Boesten and J.J. Guns, *J. Chromatogr.*, 623 (1992) 237.
[15] D. Aswad, *Anal. Biochem.*, 137 (1984) 405.
[16] N. Nimura and T. Kinoshita, *J. Chromatogr.*, 352 (1986) 169.
[17] H. Brückner, R. Wittner and H. Godel, *J. Chromatogr.*, 476 (1989) 73.
[18] M.E. Euerby, L.Z. Partridge and W.A. Gibbons, *J. Chromatogr.*, 483 (1989) 239.
[19] H. Brückner, Ch. Keller-Hoehl and R. Wittner, in D. Brandenburg, V. Ivanov, W. Voelter (Editors), *Chemistry of Peptides and Proteins, Vol. 5/6, Proceedings of the 7th USSR–FRG Symposium on Chemistry of Peptides and Proteins, Dilizhan, USSR, 23–30 September 1989, and of the Eight FRG–USSR Symposium on Chemistry of Peptides and Proteins, Aachen, FRG, 29 September–3 October 1991*, DWI Reports, Deutsches Wollforschungsinstut an der TH Aachen, Vols. 112A + B, Verlag Mainz, Aachen, 1993, Part A, pp. 145–156.
[20] W. Lindner, In M. Zief and L.J. Crane (Editors), *Chromatographic Separations*, Marcel Dekker, New York, 1988, pp. 91–129.
[21] H. Brückner, S. Haasmann, M. Langer, T. Westhauser, R. Wittner and H. Godel, *J. Chromatogr. A*, 666 (1994) 259.
[22] H. Brückner, R. Wittner and H. Godel, *Chromatographia*, 32 (1991) 383, and references cited therein.
[23] M. Langer, R. Wittner, P. Jaek, H. Godel and H. Brückner, in W. Baltes, T. Eklund, R. Fenwick, W. Pfannhauser, A. Ruiter and H.P. Thier (Editors), *Strategies for Food Quality Control and Analytical Methods in Europe, Vol. 1, Proceedings of Euro Food Chem VI, Hamburg, 22–26 September, 1991*, Behr, Hamburg, 1991, pp. 385–390.
[24] H. Brückner, P. Jaek, M. Langer and H. Godel, *Amino Acids*, 2 (1992) 271.
[25] H. Brückner and T. Westhauser, *Chromatographia*, 39 (1994) 419.
[26] A. Dossena, G. Galaverna, R. Corradini and R. Marchelli, *J. Chromatogr. A*, 653 (1993) 229.
[27] G. Palla, R. Marchelli, A. Dossena and G. Casnati, *J. Chromatogr.*, 475 (1989) 43.
[28] D.W. Armstrong, J.D. Duncan and S.H. Lee, *Amino Acids*, 1 (1991) 97.
[29] S. Lam and A. Karmen, *J. Chromatogr.*, 289 (1984) 339.
[30] S. Lam, *J. Chromatogr. Sci.*, 22 (1984) 416.
[31] H. Brückner, D. Becker and M. Lüpke, *Chirality*, 5 (1993) 385.
[32] H. Brückner, D. Becker, M. Lüpke, S. Haasmann and M. Langer, in U. Schlemmer (Editor), *Proceedings of the International Conference Bioavailability '93 —Nutritional, Chemical and Food Processing Implications of Nutrient Availability, 9–12 May 1993, Ettlingen, Germany, Part I*, Berichte der Bundesforschungsanstalt für Ernährung, Karlsruhe, 1993, pp. 28–33.
[33] H. Brückner and M. Hausch, *J. High Resolut. Chromatogr.*, 12 (1989) 680.
[34] H. Brückner and M. Hausch, *Chromatographia*, 28 (1989) 487.
[35] H. Brückner and M. Hausch, in G. Lubec and G.A. Rosenthal (Editors), *Amino Acids: Chemistry, Biology and Medicine*, Escom Science, Leiden, 1990, pp. 1172–1182.
[36] H. Brückner and M. Lüpke, *Chromatographia*, 31 (1991) 123.
[37] H. Brückner and A. Schäfer, in C. Benedito de Barber, C. Collar, M.A. Martinez-Anaya and J. Morell (Editors), *Progress in Food Fermentation, Vol. 2, Proceedings of Euro Food Chem VI, 20–22 September 1993, Valencia, Spain*, IATA, CSIC, Valencia, 1993, pp. 485–491.
[38] H. Brückner and M. Hausch, *J. Chromatogr.*, 614 (1993) 7.
[39] H. Brückner, S. Haasmann and H. Friedrich, *Amino Acids*, 6 (1994) 205.
[40] H. Frank, G.J. Nicholson and E. Bayer, *J. Chromatogr. Sci.*, 15 (1977) 174.
[41] W.A. König, *The Practice of Enantiomer Separation by Gas Chromatography*, Hüthig, Heidelberg, 1989.
[42] H.J. Chaves das Neves, A.M.P. Vasconcelos and M.L. Costa, in B. Holmstedt, H. Frank and B. Testa (Editors), *Chirality and Biological Activity*, Alan R. Liss, New York, 1990, pp. 137–143.
[43] H. Brückner and M. Hausch, *Milchwissenschaft*, 45 (1990) 421.
[44] J.W. White, *Adv. Food Res.*, 24 (1978) 287.
[45] J.J. Corrigan and N.G. Srinivasan, *Biochemistry*, 5 (1966) 1185.
[46] M.S. Pais, H.J. Chaves das Neves and A.M.P. Vasconcelos, *Apidologie*, 17 (1986) 125.
[47] K.H. Schleifer and E. Stackebrandt, *Annu. Rev. Microbiol.*, 37 (1983) 143.
[48] M. Friedman, J.C. Zahnley and P.M. Masters, *J. Food Sci.*, 46 (1981) 127.
[49] L. Liardon and R.F. Hurrell, *J. Agric. Food Chem.*, 31 (1983) 432.
[50] M. Friedman, M.R. Gumbmann and P.M. Masters, in M. Friedman (Editor), *Nutritional and Toxicological Aspects of Food Safety*, Plenum Press, New York, 1984, pp. 367–412, and references cited therein.

ELSEVIER

Journal of Chromatography A, 697 (1995) 247–250

JOURNAL OF CHROMATOGRAPHY A

Short communication

Simple stationary phases derived from gluconolactone for chiral high-performance liquid chromatography

K.M. Maher[a], D.R. Taylor[a,*], H.J. Ritchie[b]

[a]*Chemistry Department, UMIST, P.O. Box 88, Manchester M60 1QD, UK*

[b]*Shandon HPLC, Astmoor, Runcorn, Cheshire WA7 1PR, UK*

Abstract

A new family of chiral stationary phases (CSPs) have been prepared by chemical modification of D-δ-gluconolactone with ring opening. They were chemically bonded to 5-μm microporous silica and evaluated as column packing materials for chiral analysis by HPLC. The best was the CSP in which the hydroxyl groups derived from the ring-opened gluconolactone were converted to carbamate residues using a naphthylethyl isocyanate.

1. Introduction

Lactones have been used in the preparation of chiral stationary phases (CSPs) [1] for HPLC and as chiral analytes [2] in GC. These applications demonstrate their ability to take part in chiral recognition processes with either an open chain or a closed ring system. With the earlier work of Lourenco [3] in mind, a number of novel CSPs for HPLC were synthesised from a cheap and readily available carbohydrate, D-δ-gluconolactone (**I**).

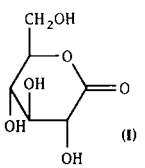

(I)

2. Experimental

2.1. Instrumentation

The HPLC system consisted of a Shimadzu LC-5A single-head pump, Rheodyne 7125 manual injector valve and Cecil Instruments CE 212 variable-wavelength UV monitor (254 nm).

2.2. Materials

HPLC-grade solvents were obtained from Rathburn. N-3,5-Dinitrobenzoyl (DNB) derivatives of various amino acids (Aldrich and Janssen) were synthesised at UMIST using established methods [4]. Hypersil silica (5 μm) was supplied by Shandon HPLC.

2.3. Preparation of CSPs

CSPs 1–5 were prepared according to Fig. 1. The synthesis involved nucleophilic ring opening of the lactone (**I**) with allylamine, followed by acetylation and conversion to an active silane

* Corresponding author.

0021-9673/95/$09.50
SSDI 0021-9673(94)00935-X

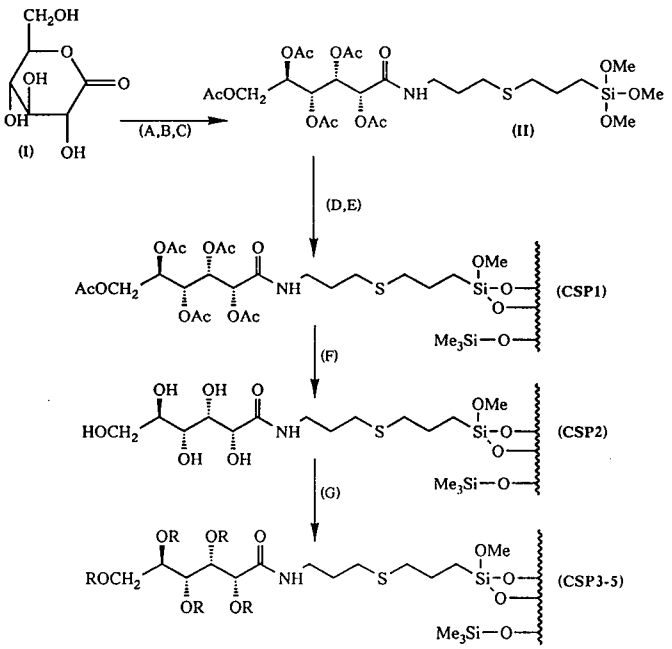

Fig. 1. Synthesis of novel CSP from gluconolactone. RO = Aryl–NH–(CO)–O and HO, according to Table 1. Reagents: A = allylamine; B = Ac_2O; C = $(MeO)_3Si(CH_2)_3SH$; D = silica; E = Me_3SiCl; F = NH_3–MeOH; G = aryl isocyanate.

derivative. The acetylated silane (**II**) was bonded to 5-μm Hypersil silica. Residual silanols on the silica surface were then end-capped with trimethylsilyl (TMS) chloride. This was followed by deacetylation and carbamate formation. The CSPs were then packed into standard steel HPLC columns (15 cm × 4.5 mm I.D.) by Shandon HPLC.

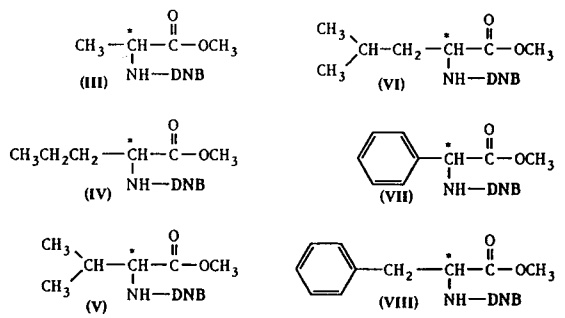

3. Results and discussion

The surface coverages of the phases were estimated from their % carbon contents. CSP 1 contained 237 μmol of chiral selector and 422 μmol of TMS groups per gram of silica. The corresponding values for CSP 2 were 274 and 174 μmol g^{-1}. The chiral selector strands on CSPs 3–5 were not fully carbamated: the ratios of carbamate to hydroxyl groups on these phases are shown in Table 1.

Some reasonable separations were obtained on the acetylated phase, CSP 1. The chromatograms of a series of racemic N-3,5-DNB-amino acid methyl esters (**III–VIII**) on this phase are presented in Fig. 2. The hydroxyl-containing phase, CSP 2, showed very poor enantioselectivity.

The carbamate phases (CSPs 3–5) all afforded better enantioresolutions than CSP 1. Fig. 3 compares the α values for the same amino acid derivatives on the carbamate CSPs. As the carbamate is made more electron-rich from phenyl (CSP 3) to dimethylphenyl (CSP 4) to naphthylethyl (CSP 5), the separation of these electron-deficient analytes improves. This suggests that a π–π interaction is important in the chiral recognition process on these CSPs. Fig. 4 shows the resolution of the racemic samples (**III–VIII**) on the best performing phase, CSP 5.

Table 1
Structures of carbamate CSPs

Phase	OR group on strands of chiral selector	Concentration of strands	Concentration of TMS	OR:OH ratio on chiral strand
CSP 3	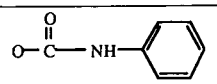	270	170	3.1:1.9
CSP 4	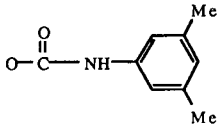	270	170	2.3:2.7
CSP 5	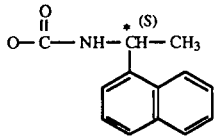	180	70	1.0:4.0

Concentrations are reported as μmol per gram of silica gel. Average ratios of OR:OH groups on the chiral strands are also quoted.

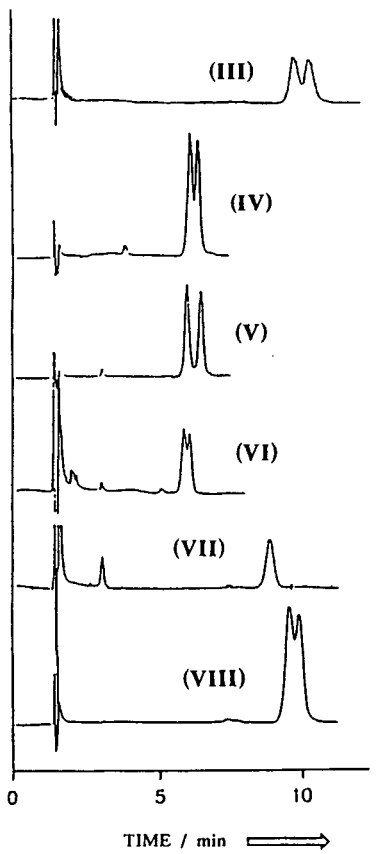

Fig. 2. Chromatograms of racemic N-3,5-DNB-amino acid methyl esters on CSP 1. Mobile phase: tetrahydrofuran (THF)–*n*-hexane (15:85) at 1.0 ml min^{-1}.

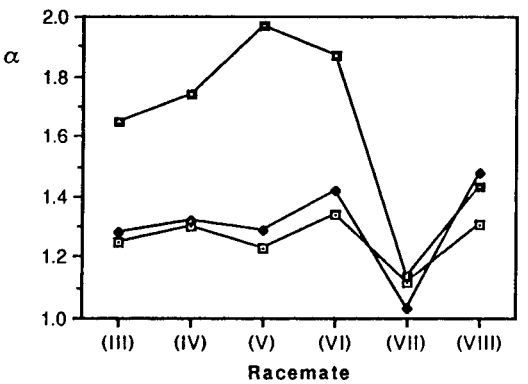

Fig. 3. Comparison of the α values for the racemic N-3,5-DNB-amino acid methyl esters on the carbamate phases CSP 3 (□), CSP 4 (◆) and CSP 5 (■). Mobile phase: THF–*n*-hexane (25:75) at 1.0 ml min^{-1}.

4. Conclusions

A family of simple CSPs for HPLC were prepared from a cheap and readily available starting material, D-δ-gluconolactone. These chiral stationary phases were used to separate the enantiomers of amino acid derivatives that contained the electron-deficient 3,5-DNB group. The phase that shows the most commercial promise (CSP 5) contains the naphthylethyl carbamate functionality.

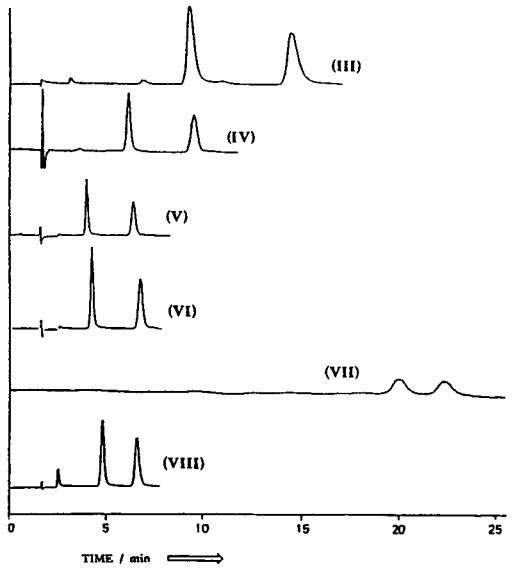

Fig. 4. Chromatograms of racemic N-3,5-DNB-amino acid methyl esters on CSP 5. Mobile phase as in Fig. 3.

Acknowledgements

We gratefully acknowledge the financial assistance provided by Shandon HPLC, a division of Life Sciences International, and also by SERC (for a Total Technology studentship for K.M.M.).

References

[1] D. Lohmann and R. Dappen, *Chirality*, 5 (1993) 168.
[2] S. Brochu et al., *Polymer Bull.*, 30 (1993) 223.
[3] W. Lourenco, *Ph.D. Thesis*, UMIST, Manchester, UK (1989).
[4] W.H. Pirkle and C.J. Welch, *J. Org. Chem.*, 49 (1984) 138.

ELSEVIER

Journal of Chromatography A, 697 (1995) 251–255

JOURNAL OF CHROMATOGRAPHY A

Enantiomeric separation by packed column chiral supercritical fluid chromatography

J. Whatley

Physical Methods Department, Roche Research Centre, Roche Products Limited, Welwyn Garden City, Herts AL7 3AY, UK

Abstract

Supercritical fluid chromatography (SFC), is now a well established chromatographic technique for the separation of a range of compounds both analytically and preparatively. The advantages of SFC over HPLC are lower fluid viscosity and higher efficiencies per unit time. Furthermore, SFC is more convenient than HPLC in operation, because solvent power of the supercritical fluids, an important operational factor, is easily controlled by pressure and temperature. Cellulose and amylose derivatives coated onto a functionalised silica backbone have been used extensively for chiral resolution by HPLC. This article illustrates the preparative separation of several racemic glibenclamide analogues using both OD (tris-3,5-dimethylphenyl carbamate supported on cellulose) and AD (tris-3,5-dimethylphenyl carbamate supported on amylose) chiral phases packed into preparative columns (250 mm × 10 mm I.D.). The effect of loading, throughput and recovery of material are discussed together with the optical purity obtained from preparative chiral SFC. Comparison with chiral HPLC for some of these compounds is shown highlighting several important advantages of SFC over HPLC.

1. Introduction

Glibenclamide is known to be a potent potassium channel blocker active in the heart and pancreas. A series of glibenclamide analogues have been synthesised for assessing their potency and selectivity in the heart versus the pancreas. A preparative chiral method was required to separate the enantiomers of a series of racemic compounds for in vitro testing.

Supercritical fluid chromatography (SFC) is now a well established technique for the separation of a range of compounds both analytically and preparatively [1]. The advantages of SFC over HPLC are lower fluid viscosity and higher efficiencies per unit time. Furthermore, SFC is more convenient than HPLC in operation, because solvent power of the supercritical fluids, an important operational factor, is easily controlled by pressure and temperature [2]. The ability to programme the density or pressure of the mobile phase is unique to SFC. These considerations led to a study of the conditions required to optimise the separation of seven glibenclamide analogues.

Cellulose and amylose derivatives coated onto a functionalised silica backbone have been used extensively for chiral resolution by HPLC [3,4]. This paper describes the preparative separation of seven racemic glibenclamide analogues using Daicel OD (tris-3,5-dimethylphenyl carbamate supported on cellulose) and AD (tris-3,5-dimethylphenyl carbamate supported on amylose) chiral phases packed into both analytical (250 × 4.6 mm I.D.) and preparative columns (250 × 10 mm I.D.).

0021-9673/95/$09.50
SSDI 0021-9673(94)00811-6

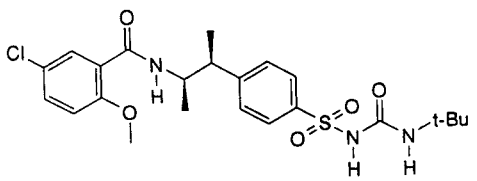

Fig. 1. Structure of a potassium channel blocker, Ro 32-1964.

2. Experimental

Industrial grade carbon dioxide was obtained from British Oxygen Company (London, UK). HPLC grade solvents, ethanol, hexane and isopropanol were purchased from Rathburn Chemicals (Walkerburn, UK). Daicel chiral columns were purchased from J.T. Baker.

Preparative chiral SFC was carried out on a Gilson SFC 3 system (Anachem, UK) equipped with a variable-wavelength UV detector fitted with a flow cell rated to 41.3 MPa. Gradient elution using ethanol–carbon dioxide was used to achieve the desired separation of the enantiomers. The Nupro valve (2 ml volume) supplied with the instrument was replaced with a Rheodyne valve Model 7037 fitted with a 3-μl volume internal loop. This valve situated downstream of the column allowed fractions to be collected as seen from the detector response avoiding any time lag.

For safety reasons a stainless-steel pressure

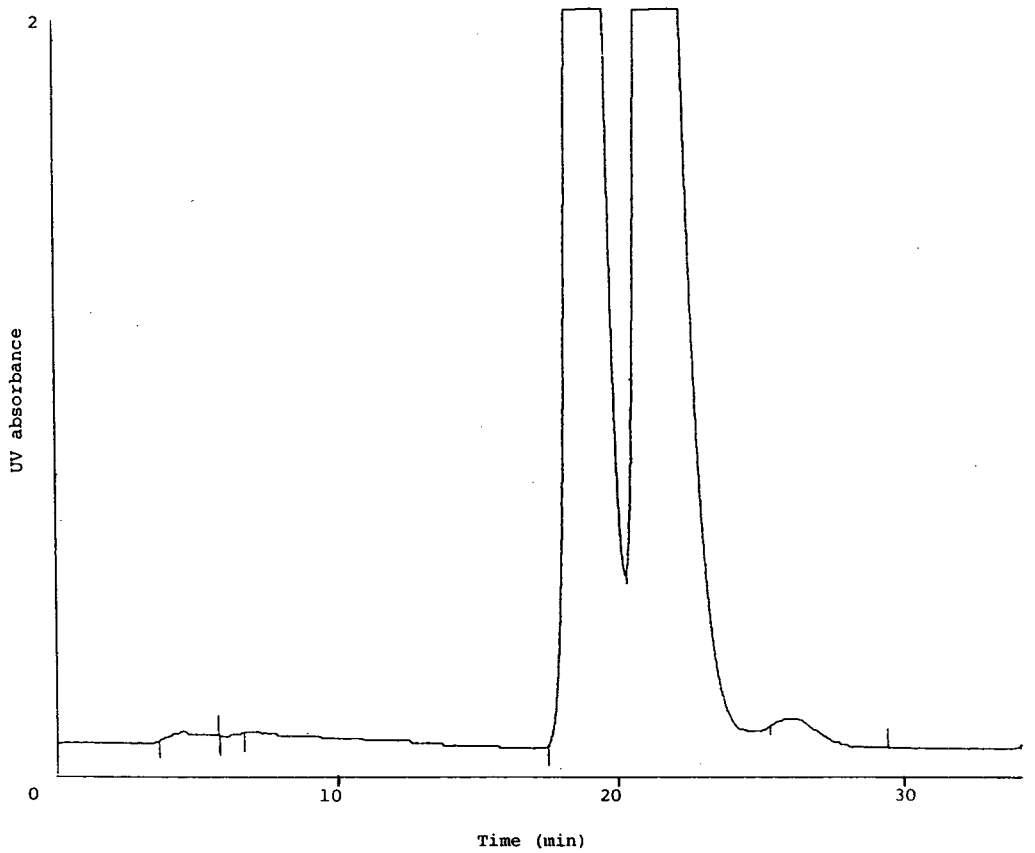

Fig. 2. Chiral SFC separation of Ro 32-1964. SFC conditions: Chiralpak AD column (250 × 10 mm I.D.). Gradient program: 2 ml 20% ethanol–carbon dioxide to 3 ml 60% ethanol–carbon dioxide over 30 min. Pressure program: 13.8 MPa to 20.6 MPa. Temperature: 45°C. UV Detection: λ_{265}, 2.0 a.u.f.s. Loading: 5 mg/0.5 ml ethanol.

guard column was purchased from Lancashire Fittings (Harrogate, UK). It was considered important that due safety precautions be taken to contain any burst that might occur when using high pressures. The guard column is certificated to 55 MPa and will accommodate a column of dimensions 250 × 20 mm I.D.

3. Results and discussion

Fig. 1 represents the typical structure of the racemic glibenclamide analogues separated by packed-column chiral SFC. Fig. 2 is the chiral SFC separation of Ro 32-1964 on a Chiralpak AD column using gradient elution. This separation is representative of the chiral separations achieved for the series of compounds under test.

Separated enantiomers of the glibenclamide analogues were checked for optical purity by chiral HPLC using either a Chiralcel OD column or a Chiralpak AD column. The first eluting enantiomer from each separation had 100% e.e. The second eluting enantiomer varied in optical purity, ranging from 99% e.e. down to 90% e.e.

Previous attempts to separate one of the glibenclamide analogues by preparative HPLC on a Chiralcel OD column using ethanol–hexane had met with limited success, Fig. 3. Low loadings and poor resolution meant that extensive chromatography was required to achieve the desired quantity and purity of enantiomers for biological testing. By contrast, SFC on a Chiralcel OD column allowed higher loadings with better peak symmetry and consequently faster throughput to make preparative SFC the method of choice, Fig. 4.

It is interesting to note that under HPLC conditions one of the racemic compounds could not be resolved on the Chiralpak AD column. However, when a Chiralpak AD column (250 × 4.6 mm I.D.) was installed in the Gilson SFC3 and run under similar SFC conditions to those already used, an acceptable separation was achieved. On scale-up to a preparative Chiralpak AD column (250 × 10 mm I.D.) this separation was maintained to afford milligram quantities of each enantiomer.

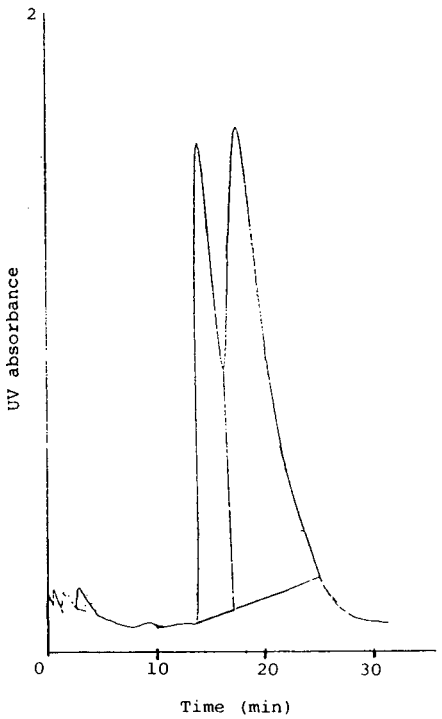

Fig. 3. HPLC separation of glibenclamide analogue. HPLC conditions: Chiralcel OD column (250 × 10 mm I.D.). Mobile Phase: 15% ethanol–hexane. Flow-rate: 20 ml/min. UV Detection: λ_{254}, 2.0 a.u.f.s. Loading: 2 mg/0.5 ml ethanol–hexane.

It is thought that this unexpected resolution under gradient SFC conditions is attributable to the low fluid viscosity and high solute diffusivity of the supercritical carbon dioxide into the pores of the silica. The result is greater permeability and therefore better chiral interaction with the stationary phase.

4. Enantiomeric recovery

It is well known that efficient containment of column eluates under SFC conditions can be difficult since the column effluent is emitted as a fine atomised mist. Before chiral separation of these compounds was undertaken an experiment was set up to investigate the recovery possible by trapping the column eluates in a suitable solvent surrounded by solid carbon dioxide.

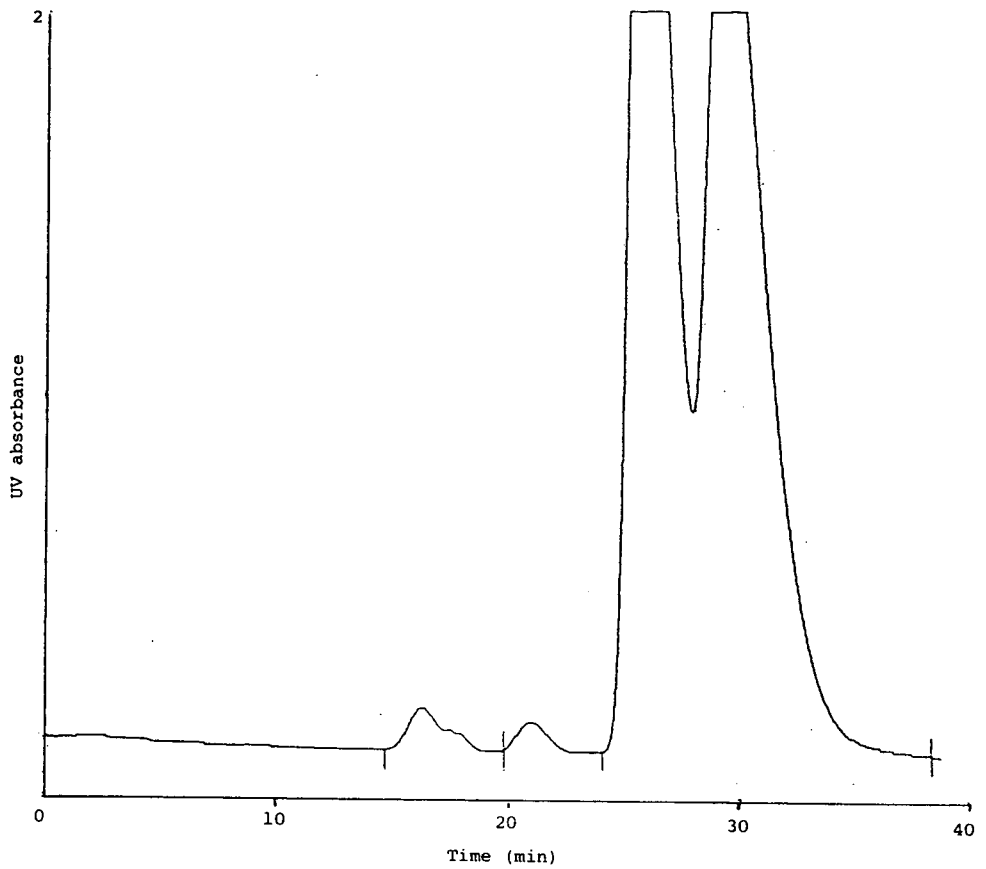

Fig. 4. Chiral SFC separation of glibenclamide analogue. SFC conditions: Chiralcel OD column (250 × 10 mm I.D.). Gradient program: 3 ml 15% ethanol–carbon dioxide to 3 ml 30% ethanol–carbon dioxide over 30 min. Pressure program: 17.3 MPa to 24.2 MPa. Temperature: 45°C. UV Detection: λ_{265}, 2.0 a.u.f.s. Loading: 3.5 mg/0.5 ml ethanol.

The compound Ro 32-2059 was chosen as a model for this exercise. A known amount (6.0 mg) was dissolved in ethanol (0.3 ml) and injected onto the Chiralcel OD column. Both eluted enantiomers were trapped by dipping the column outlet tube into 20 ml ethanol contained in a sealed vial with a small vent hole pierced in the plastic top. The vial was chilled by surrounding it with solid carbon dioxide. After evaporation of the ethanol 5.6 mg was recorded for the total enantiomers. This represented a very favourable recovery of 93%. This procedure of bubbling the column effluent into chilled ethanol contained in semi-sealed vials was adopted for all the compounds chromatographed. Recoveries from processing the other analogues varied, the worse case being 70% yield, which was considered to be quite acceptable. Ideally, the racemic compound being chromatographed should have good solubility in the trapping solvent. The better this solubility, the greater, in general, the recovery of separated isomers.

5. Loading and throughput

Typical loadings of 4 mg per injection were possible on the preparative column and 0.5 mg per injection on the analytical column. It was possible to process up to 8 mg of racemate per hour.

At the start of this work manual injection of

the glibenclamide compounds was made onto the preparative column. Very reproducible chromatography was observed with only small changes in retention time over a 30 min run time. Towards the end of this project the Gilson SFC3 system was upgraded to automatic sample injection and fraction collection controlled by the 232-401 processor.

6. Conclusions

Packed-column chiral SFC using both Chiralcel OD and Chiralpak AD chiral phases has proved to be a quick and convenient method for separating mg quantities of racemic glibenclamide analogues. The high resolving power and better efficiency resulted in superior chromatography compared to chiral HPLC. This was exemplified by the successful separation of a glibenclamide analogue under SFC conditions using the Chiralpak AD column compared to HPLC methodology where the racemate could not be resolved. One distinct advantage over HPLC is the small volume of solvent needed to be removed to recover the enantiomers. The bulk of the mobile phase comprises carbon dioxide which volatilises immediately at atmospheric pressure. Additionally there is no problem with concentration of residues in solvents, as in HPLC, where often several litres of solvent have to be evaporated to recover the isomers.

Environmentally SFC has much to offer since the volume of solvent to be removed is minimal compared to preparative HPLC, where litres of organic solvents have to be disposed of at high cost.

References

[1] K. Anton, J. Eppinger, L. Frederiksen, E. Francotte, T. Berger and A. Wilson, *J. Chromatogr. A*, 666 (1994) 395–401.
[2] P. Petersson and K. Markides, *J. Chromatogr. A*, 666 (1994) 381–394.
[3] N. Bargmann, A. Tambute and M. Caude, *Analusis*, 20 (1992) 189–200.
[4] Y. Kaida and Y. Okamoto, *Bull. Chem. Soc. Jpn.*, 65 (1992) 2286–2288.

ELSEVIER

Journal of Chromatography A, 697 (1995) 257–261

JOURNAL OF CHROMATOGRAPHY A

Rapid method development for the separation of enantiomers by means of chiral column switching

J.A. Whatley

Physical Methods Department, Roche Research Centre, Roche Products Limited, Welwyn Garden City, Herts. AL7 3AY, UK

Abstract

Some of the most extensive and versatile chiral stationary phases (CSPs) are those based on polysaccharide derivatives (cellulose and amylose) coated onto macroporous silica. Each derivative can exhibit subtly different enantioselectivity for a variety of chiral compounds.

Chiral column switching is a very useful analytical tool and ideally suited to these CSPs since they are all used with isopropanol–hexane or ethanol–hexane mixtures, with small additions of acid or base modifiers where appropriate. The technique lends itself to rapid method development where automated overnight runs can be set up to scout for a column and find separation conditions for racemic compounds.

The usefulness and potential of chiral column switching using twelve different CSPs arranged in two banks of six columns is illustrated with several chiral molecules. Examples where peak reversal has occurred are highlighted to show the advantages this presents the analyst in final quantitation and enantiomeric excess determination.

When scale-up is a consideration the main priority is to achieve high selectivity. Chiral column switching can be used to great effect to search for a column that will fulfil this need. This optimised separation can then be translated to a comparable preparative chiral column for isolation of milligram quantities of each enantiomer.

1. Introduction

During the last few years interest in the direct chromatographic resolution of enantiomers has increased dramatically, both analytically and preparatively. The efficiency, speed, wide applicability and reproducibility of HPLC has made it the instrument of choice for enantiomeric separations. Chiral column technology is now a rapidly expanding field in which well over fifty different phases are commercially available, with new ones appearing all the time [1]. This presents the chromatographer with a wide choice but also a difficult one in terms of which chiral stationary phase (CSP) to use for any given separation problem. Attempts to predict interaction mechanisms of chiral compounds with CSPs as a prelude to separation are often thwarted.

One of the most extensive and versatile CSPs are those based on polysaccharide derivatives (cellulose and amylose) coated onto macroporous silica [2]. The separations occur due to a multi-mode mechanism involving hydrogen bonding, $\pi-\pi$ interactions, dipole stacking and inclusion complexes. Each derivative shows subtly different characteristics and a definite enantioselectivity for a variety of compounds.

Chiral column switching is a very useful analytical tool and ideally suited to these CSPs since they are all used with isopropanol–hexane or ethanol–hexane mixtures, with small additions of

0021-9673/95/$09.50
SSDI 0021-9673(94)01030-7

acid or base modifiers where appropriate. The technique lends itself to rapid method development where automated overnight runs can be set up to scout for a column and find separation conditions for racemic compounds. Final optimisation of the best separation can then be undertaken if required.

More recently derivatised cyclodextrins have become available where derivatisation of the secondary hydroxyls has extended the enantioselective interactions not available on native cyclodextrins [3]. These columns can be used in normal-phase modes making them a useful addition to the chiral column switching range.

The Pirkle-type phases [4] and synthetic polymers such as OT(+) are examples of other chiral supports compatible with alcohol–hexane eluents which can be incorporated into column switching. Combination of all these CSPs gives the chromatographer a wide range of chiral columns to resolve racemic compounds.

2. Experimental

Chromatography was performed using a Kontron series 400 liquid chromatograph comprising an autosampler and dual-wavelength detector. Chiral columns were purchased from J.T Baker and Technicol. Hexane, isopropanol and ethanol (HPLC grade) were purchased from Rathburn. Polyether ether ketone (PEEK) tubing and Upchurch fittings were supplied by Anachem.

3. Results and discussion

This paper describes the usefulness and potential of chiral column switching using 12 different CSPs arranged in two banks of 6 columns. The column switching comprises two 6-way Valco valves, each housing 6 columns. The 8-way Valco valve directs the flow of solvent to each bank of 6 columns in turn and similarly directs the column eluent to the detector, via the 6-way zero-volume connectors. The column switching is integrated into the Kontron HPLC system where programming and commands for switching through the 12 columns is controlled via the data system incorporating an RS-232 multiport.

To minimise dead volume and band spreading the column switching was housed between the autosampler and the dual-wavelength detector. PEEK tubing, 1/16 in. × 0.010 in. I.D. (1 in. = 2.54 cm) and Upchurch fingertight fittings were used to make all connections between valves and columns. The flexibility of the PEEK tubing and ease of making connections rated to 4000 p.s.i. (1 p.s.i. = 6894.76 Pa) was seen as an advantage. Any column changes could be made quickly, without the need for spanners, and problems associated with cold welding of stainless-steel ferrules are avoided. All columns used in this configuration were 25 cm × 0.46 cm I.D. with inverted female end fittings.

A typical overnight program would inject one sample sequentially through 12 columns allowing 1 h analysis time per column, plus 20 min equilibration of mobile phase for each column prior to sample injection. This would give a total run time of 16 h, 20 min column conditioning and 60 min assay time. Alternatively, two compounds could be assayed through 6 columns over the same time span. The system is flexible enough to allow the analyst to select specific columns from the 12 to assay the racemic compound. This is made possible via the program file of the Kontron HPLC system whereby commands to initiate contact closures can be made to switch through to the chosen columns.

As an illustration of what can be achieved an intermediate in the potassium channel opener project, Ro 31-6905/000 (Fig. 1) was used as an example.

The sample used for the overnight run was

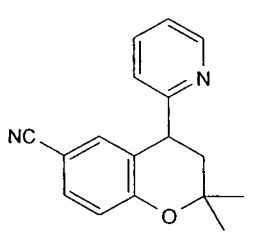

Fig. 1. Structure of potassium channel opener, Ro 31-6905/000.

made up to give an enantiomeric excess of isomers (approximately 2:1, *R*:*S*) to highlight peak reversal. The 12 chiral columns used in this switching program are as follows: Chiralcel OA, Chiralcel OB, Chiralcel OC, Chiralcel OD, Chiralcel OF, Chiralcel OG, Chiralcel OJ, Chiralcel OK, Chiralcel OT(+), Chiralpak AD, Whelk-01(R,R) and Pirkle DNBPG (covalent). Four of the 12 columns showed a separation, Chiralcel OG, Chiralcel OD, Chiralpak AD and Chiralcel OJ using a mobile phase of isopropanol–hexane (10:90) at a flow-rate of 0.7 ml min^{-1}. Fig. 2 compares the enantiomeric separation achieved on these four columns. When this program was repeated with the same racemic mixture using ethanol–hexane (8:92) at 0.7 ml min^{-1} only two columns separated the enantiomers, viz. Chiralcel OD and Chiralcel OJ. The separation factor α was lower using the ethanol–hexane solvent mixture.

Notable points of interest are the inversion of peak elution order of the enantiomers on amylose- and cellulose-derivatised supports and peak reversal on two cellulose-based columns, i.e. Chiralcel OG and Chiralcel OJ.

The significance of peak order reversal of enantiomers merits comment. The chromatographer is often faced with the situation where a trace of the unwanted enantiomer elutes on the tail of the main enantiomer, making accurate quantitation difficult. If a column can be found that will invert the elution order then a much more favourable method is available for quantitation (lower limit of detection) and assay validation. In addition, any preparative clean up is made much easier if the unwanted isomer elutes first. Thus on both these counts column switching can be advantageous in searching quickly for possible peak reversal.

The significance of peak reversal to the chromatographer is best illustrated by the compound Ro 31-8829/000 (Fig. 3), a key intermediate in the synthesis of protein kinase C inhibitors.

It was necessary to determine accurately the optical purity of this compound by chiral HPLC. A reasonable separation had been achieved on a Chiralcel OF column using isopropanol–hexane (1:99) (Fig. 4). However, the undesired enantiomer (*S* enantiomer) eluted on the tail of the required isomer and was not fully resolved, making quantitation difficult. When this compound was chromatographed through 12 chiral columns during an overnight run a better separation was achieved on the Chiralcel OD column, but more importantly the elution order of the enantiomers was reversed (Fig. 5). This enabled the analyst to quantify more accurately the percentage of unwanted isomer since good baseline resolution had been achieved.

When scale-up to preparative HPLC is required the main priority is to obtain high selectivity. Chiral column switching can be used to great effect to search for a column that will achieve this. The optimised separation can then be translated to a comparable preparative chiral column for isolation of milligram quantities of each enantiomer for biological testing. This can save the synthetic chemist many hours of work striving for a homochiral route.

As a starting point racemic compounds are put through the chiral column switching program using 10% isopropanol or ethanol in hexane, with modifiers where appropriate, at a flow-rate of between 0.5 to 0.7 ml min^{-1}. An analysis time of 60 min per column is considered adequate in most cases, combined with a 15-min equilibration period for each column prior to injection.

4. Conclusions

Chiral column switching offers the chromatographer a means of developing quickly separations of racemic compounds routinely and automatically during overnight runs. More often than not at least one column from the twelve will give a separation. Final optimisation of the separation can then be carried out if necessary.

Both isopropanol–hexane and ethanol–hexane mixtures can be used within the constraints of the maximum allowable alcohol percentages recommended by the manufacturers. Indeed when a separation is not obtained using isopropanol as the alcohol modifier, ethanol should also be tried. There are instances where a compound

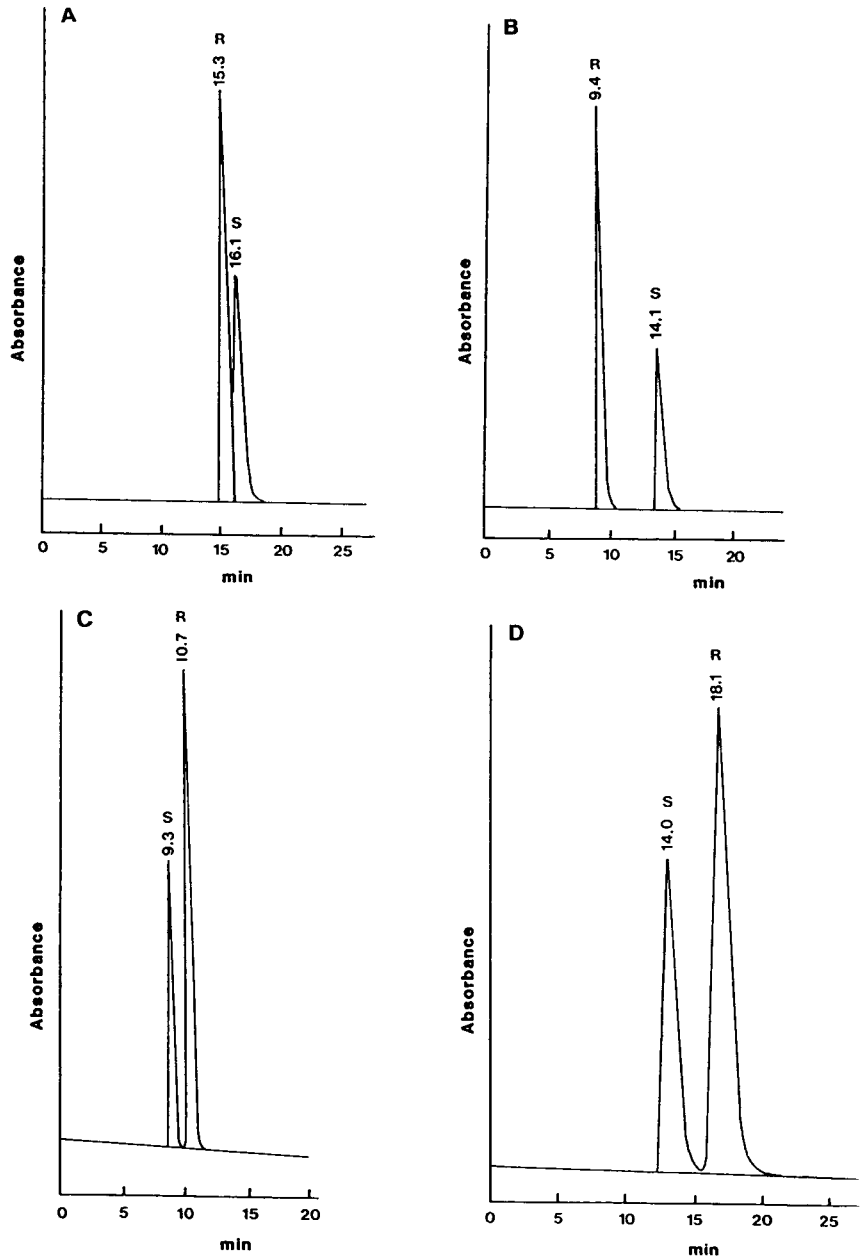

Fig. 2. Separation achieved on 4 out of 12 columns tried. (A) Chiralcel OG, (B) Chiralcel OD, (C) Chiralpak AD, (D) Chiralcel OJ. HPLC conditions: isopropanol–hexane (10:90), 0.7 ml min^{-1}; λ 215 nm, 2.0 AUFS; 1.0 mg ml^{-1}; 10 μl.

will not separate with isopropanol–hexane but will with ethanol–hexane and vice versa.

Over the past few years we have chromatographed a large number of racemic compounds using 12-column chiral switching methodology with a success rate of approximately 90%. A successful separation is one where at least one column has produced a baseline or near-baseline

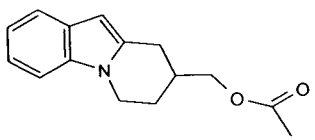

Fig. 3. Structure of protein kinase C inhibitor, Ro 31-8829/000.

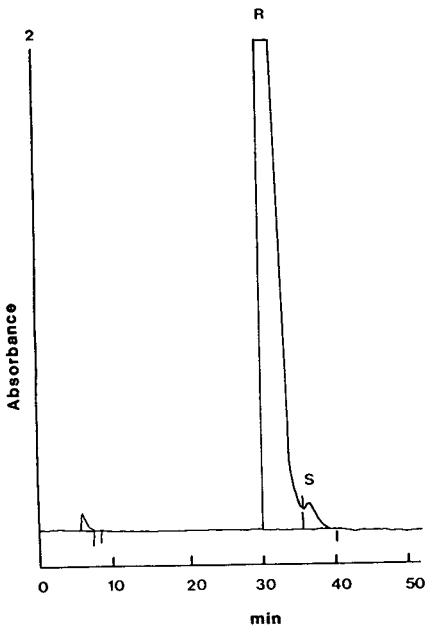

Fig. 4. Enantiomer separation of Ro 31-8829/000. HPLC conditions: Chiralcel OF; isopropanol–hexane (1:99), flow-rate 0.5 ml min^{-1}; λ 220 nm, 1.0 AUFS; 2.0 mg ml^{-1}; 10 μl.

separation. Quite often several columns demonstrate enantioselectivity.

Our experience has shown that in terms of successful applications using polysaccharide columns the Chiralcel OD and Chiralpak AD are by far the most versatile; approximately 75% of racemates could be separated on one or both of these columns. The Chiralcel OJ and Chiralcel

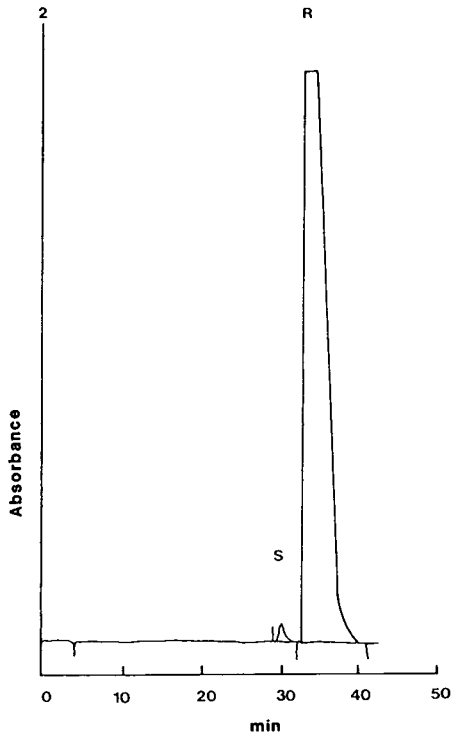

Fig. 5. Enantiomer separation of Ro 31-8829/000, peak reversal. HPLC conditions: Chiralcel OD; isopropanol–hexane (1:99), flow-rate 0.5 ml min^{-1}; λ 220 nm, 1.0 AUFS; 2.0 mg ml^{-1}; 10 μl.

OG follow on as the next most useful columns for our work.

References

[1] I. Wainer, *Trends Anal. Chem.*, 6 (1987) 125.
[2] T. Shibata, I. Okamoto and K. Ishii, *J. Liq. Chromatogr.*, 9 (1986) 313.
[3] D. Armstrong and W. Demand, *J. Chromatogr. Sci.*, 22 (1984) 411.
[4] V.R. Meyer, *Chromatographia*, 24 (1987) 639.

ELSEVIER

Journal of Chromatography A, 697 (1995) 263–269

JOURNAL OF CHROMATOGRAPHY A

Chiral resolution of protein kinase C inhibitors by reversed-phase high-performance liquid chromatography on cellulose tris-3,5-dimethylphenylcarbamate

J.A. Whatley

Physical Methods Department, Roche Research Centre, Roche Products Ltd., Welwyn Garden City, Herts. AL7 3AY, UK

Abstract

Protein kinase C (PKC) inhibitors are under investigation as potential anti-arthritic drugs. Attempts to resolve a lead compound into its respective enantiomers were made using normal chiral phase methodologies, e.g. Chiralcel OD, OG, OJ using isopropanol–hexane mixtures. Although good retention was achieved on some chiral columns, no separation was seen.

Silica-based cellulose tris-3,5-dimethylphenylcarbamate, Chiralcel OD, has been used previously to successfully resolve various drugs by reversed-phase HPLC using aqueous buffer–acetonitrile eluting systems.

This work investigates the direct chiral resolution of a range of PKC inhibitor racemates by reversed-phase chiral HPLC on Chiralcel OD using acetonitrile–phosphate buffer mixtures. The effect on the separation was studied with variables such as acetonitrile concentration, flow-rate, buffer pH and column temperature.

The effect on chromatography at sub-ambient temperature is discussed and examples are given where enhancement on resolution was achieved. In some cases baseline separation was obtained allowing determination of enantiomeric excess down to 0.1% level.

Although an increase in band broadening was observed as the temperature was reduced it did not reach an unacceptable level, even at 0°C.

1. Introduction

Separation of enantiomers by chiral HPLC is now well established with over 50 different chiral phases commercially available. Cellulose and amylose derivatives coated onto a silica backbone have been used extensively for chiral resolution using normal-phase conditions. Protein kinase C (PKC) inhibitors are under investigation as potential anti-arthritic drugs [1,2]. Modelling studies suggested that the individual enantiomers of bisindolylmaleimides such as Ro 31-8830 should have different activities against the enzyme [3].

Attempts to resolve Ro 31-8830 into its respective enantiomers, Ro 32-0432 and Ro 32-0434 were made using normal chiral phase methodologies, e.g. Chiralcel OD, OG, OJ and Pirkle phases with isopropanol–hexane mixtures. Although good retention was achieved on some chiral columns, no separation was seen. Silica-based cellulose tris-3,5-dimethylphenylcarbamate (CDMPC), Chiralcel OD-R, has been used previously to successfully resolve various drugs by reversed-phase HPLC using aqueous buffer–acetonitrile eluting systems [4,5].

This report investigates the direct chiral resolution of Ro 31-8830 and other PKC inhibitor

0021-9673/95/$09.50
SSDI 0021-9673(94)00748-9

racemates by reversed-phase chiral HPLC on Chiralcel OD-R. The effect on separation was studied with variables such as acetonitrile concentration, flow-rate, buffer pH and column temperature.

2. Experimental

Chiral chromatography was carried out on a Chiralcel OD-R column, Daicel (250 × 4.6 mm I.D.) using a Kontron 400 series liquid chromatograph equipped with a dual-wavelength detector operating at wavelengths 215 and 254 nm. Chromatographic data were collected and processed on a Kontron data system 450.

HPLC-grade acetonitrile was obtained from Rathburn. Water used to prepare the buffer was purified by a Milli-Q system. The buffer, triethylammonium phosphate, was prepared by adding triethylamine (Fluka) to 0.05 *M* phosphoric acid (Fluka) until the desired pH was reached. Adjustment of pH was made before addition of the organic modifier.

Compounds were chromatographed by dissolving them in the mobile phase at a concentration of 1 mg/ml. They were filtered through a 2-μm acro-disc and 10-μl injections were made via the auto sampler. A column chiller purchased from Jones Chromatography was used for experiments carried out at sub-ambient temperature.

3. Results and discussion

The structures of the PKC racemic compounds studied in this work are listed in Fig 1.

The results of the chiral separation of the twenty racemates chromatographed at 20°C are summarised in Table 1. The compounds were eluted with acetonitrile–phosphate buffer pH 2.5 (25:75) at a flow-rate of 0.5 ml min^{-1}, where $\alpha \geq 1.20$: baseline separation; $\alpha = 1.15$: near-baseline separation; and $\alpha = 1.05$: enantiomers just separate.

Fig. 2 is an example typical of the separations achieved for the majority of the compounds under test.

3.1. Chromatography at sub-ambient temperature

Retention and selectivity typically are adjusted by modifying the mobile phase composition or by changing the chromatographic column used. Chromatography at sub-ambient temperatures can reduce column efficiency due to poor mass transfer, arising from increased eluent viscosity and decreased solute diffusivity. The use of column cooling in chiral HPLC can be a valuable technique for improving column selectivity for racemates. This report highlights the benefits of sub-ambient temperature to enhance the resolution of racemates. The PKC inhibitor racemates Ro 31-8830 and Ro 31-8425 were used as typical examples to illustrate this effect. Chromatograms for both compounds were run at 5°C intervals from 20 to 0°C. Before each temperature study the column was conditioned for 30 min with mobile phase flowing at 0.5 ml min^{-1}. A plot of retention factor (α) against column temperature was made (Fig. 3). A near-linear relationship was obtained in which baseline separation is achieved at 0°C. The chromatogram of racemate Ro 31-8830 at 0°C (Fig. 4) shows the baseline separation achieved between the enantiomers Ro 32-0432 and Ro 32-0434. This method was used to determine the presence of the unwanted enantiomer Ro 32-0434 in various large-scale samples of Ro 32-0432. Detection down to 0.1% level was possible (Fig. 5).

Good thermal contact between the column and the base of the chiller ensured an even temperature throughout the length of the column. Three thermocouples placed at the beginning, middle and end of the column showed virtually no difference in the set temperature. An appreciable pressure increase was observed as the column was cooled to 0°C, but at the experimental flow-rate of 0.5 ml min^{-1} using acetonitrile–phosphate buffer (25:75) the back pressure did not exceed 2500 p.s.i. (1 p.s.i. = 6894.76 Pa), which therefore was acceptable.

The effect of increasing the pH of the phosphate buffer to 4.0 caused an increase in retention time with little overall effect on the separation. The pK_a of the ionisable amino

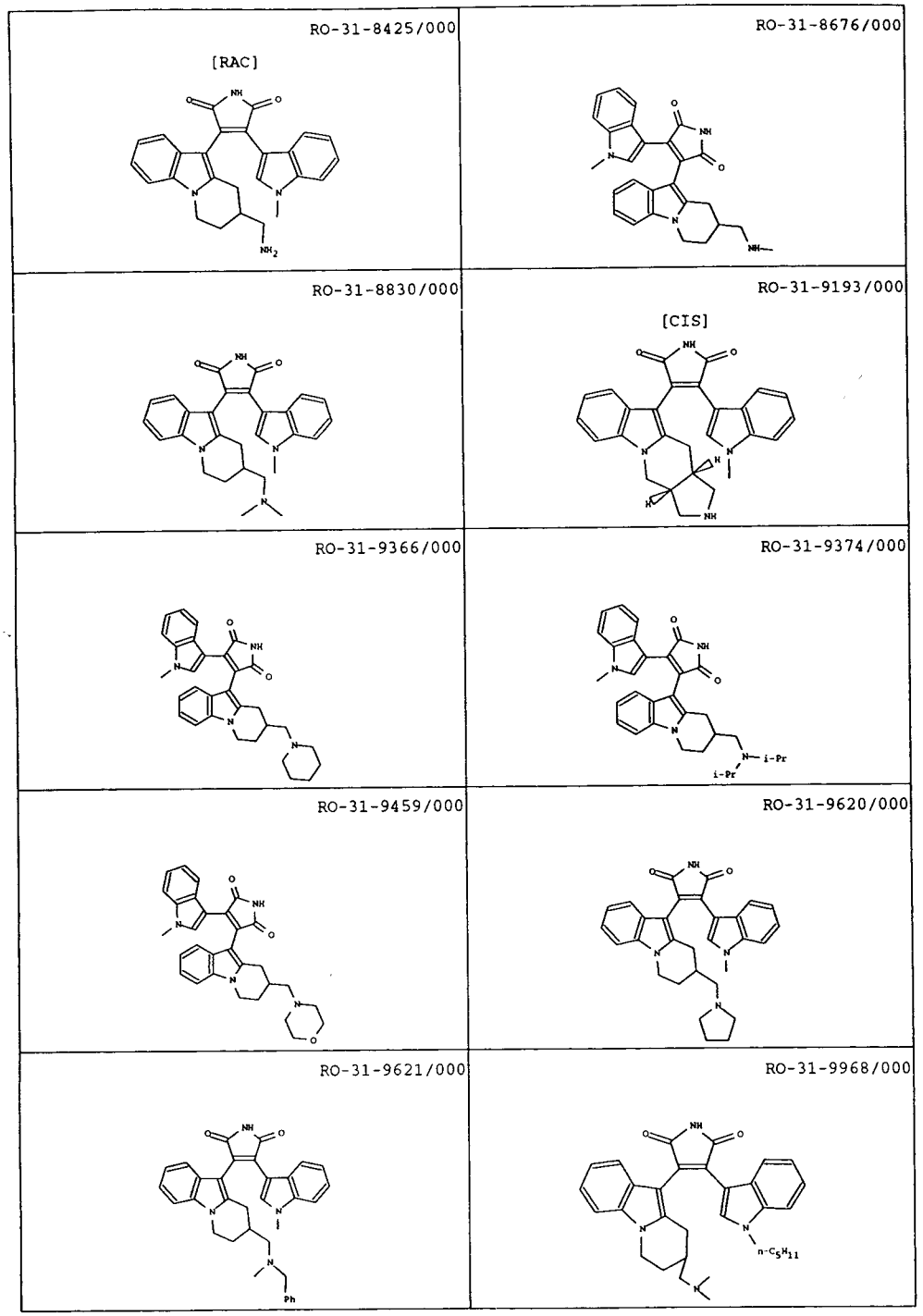

Fig. 1 (*continued on p. 266*).

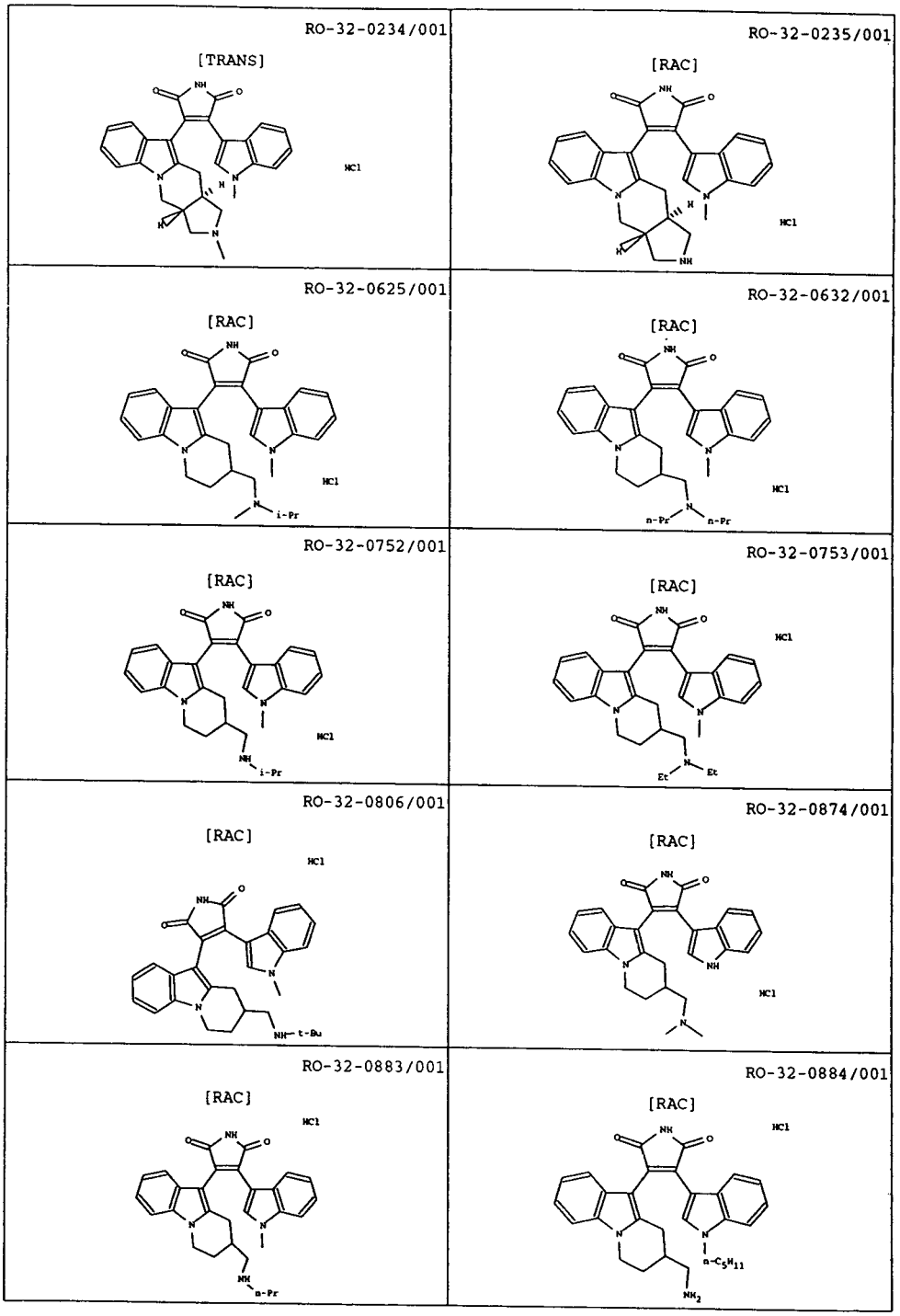

Fig. 1. Structures of racemic compounds under investigation.

Table 1
Comparison of retention of twenty chiral PKC inhibitors

PKC racemate	k_1'	k_2'	α
Ro 31-8830	4.34	4.90	1.13
Ro 31-8425	3.64	4.20	1.15
Ro 31-9366	8.44	9.76	1.16
Ro 31-9459	6.34	7.48	1.18
Ro 31-9620	6.50	7.36	1.13
Ro 31-8676	4.78	5.74	1.20
Ro 31-9193	4.42	4.58	1.04
Ro 31-9374	12.28	15.72	1.28
Ro 31-9621	26.62	29.82	1.12
Ro 31-9968	31.54	33.80	1.07
Ro 32-0625	7.54	8.92	1.18
Ro 32-0753	7.16	8.26	1.15
Ro 32-0874	2.94	3.12	1.06
Ro 32-0234	4.56	5.84	1.28
Ro 32-0235	3.58	4.58	1.28
Ro 32-0632	21.40	25.2	1.18
Ro 32-0752	6.40	8.10	1.27
Ro 32-0806	7.80	10.54	1.35
Ro 32-0883	7.36	9.58	1.30
Ro 32-0884	27.02	28.28	1.05

k_1' = Retention factor of first-eluting enantiomer; k_2' = retention factor of second-eluting enantiomer; α = retention factor.

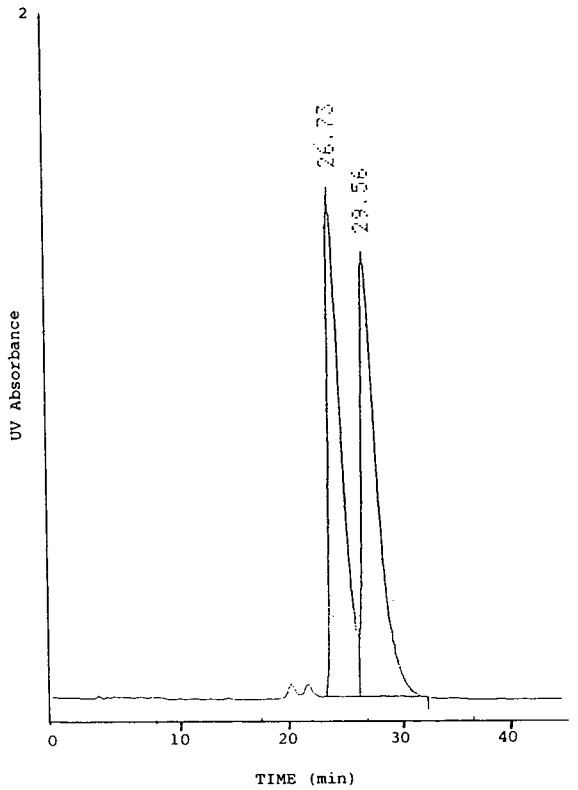

Fig. 2. Optical resolution of Ro 31-8830. HPLC conditions: Chiralcel OD-R; CH_3CN–phosphate buffer (25:75), pH 2.5; 0.5 ml min^{-1}; UV detection at 254 nm; 20°C.

group in the compounds under investigation is approximately 10. Increasing the acetonitrile concentration above 25% decreased the retention time with subsequent loss of resolution. Reducing the organic modifier below 25% increased the retention time with subsequent loss of peak shape and poor efficiency.

Following the success with Chiralcel OD-R in separating PKC inhibitors other chiral phases of similar chemical composition were tried using reversed-phase methodology. Chiral phases OG (cellulose tris-4-methylphenylcarbamate), OC (cellulose tris-phenylcarbamate) and AD (amylose tris-3,5-dimethylphenylcarbamate) were tested as possible candidates. Racemate Ro 31-8830 was used as the test compound. The OG phase showed some chiral recognition but only produced a slight separation. Chiral phase AD retained the racemate on the column without effecting a separation. The pressure on the OC column increased significantly as the mobile phase was passed through the column (acetonitrile–phosphate buffer, 25:75) at 0.5 ml min^{-1} and blockage occurred very quickly.

4. Conclusions

Chiralcel OD-R used in reversed-phase mode has proved to be a useful separation technique for resolving racemic PKC inhibitors. Chromatography at reduced temperature, down to 0°C, has proved effective in separating racemates that are difficult to separate at ambient temperature. Although an increase in band broadening was observed as the column temperature was reduced it did not reach an unacceptable level, even at 0°C.

Low-temperature chiral HPLC has been particularly useful in determining enantiomeric ex-

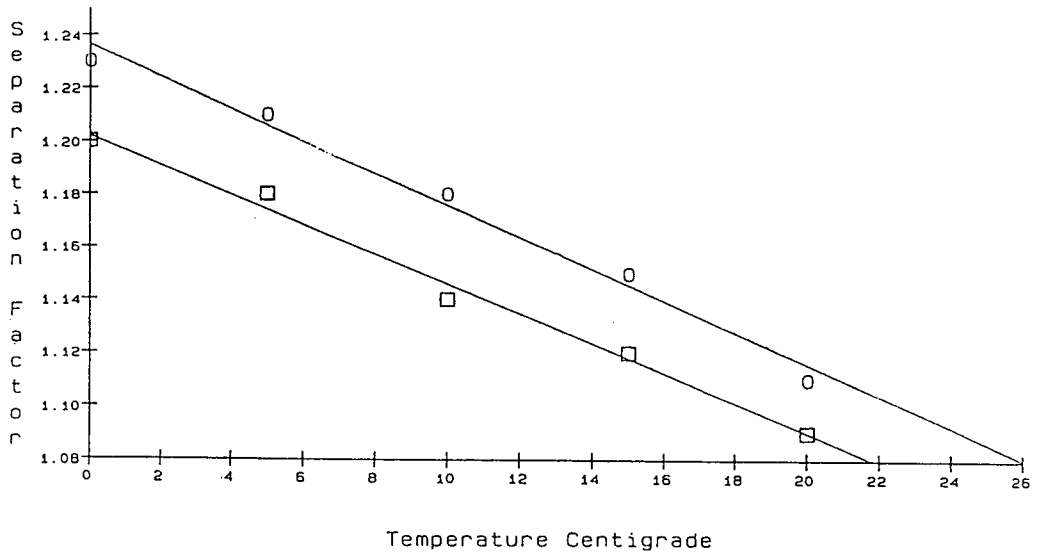

Fig. 3. PKC inhibitors Ro 31-8425 (□) and Ro 31-8830 (○): plot of separation factor vs. column temperature.

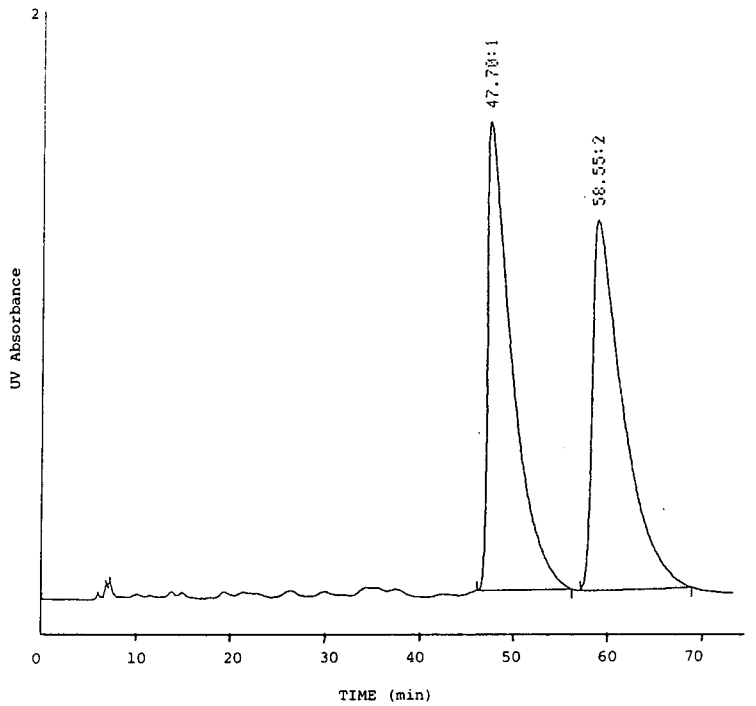

Fig. 4. Optical resolution of Ro 31-8830 at 0°C ($\alpha = 1.23$). HPLC conditions: Chiralcel OD-R; CH_3CN–phosphate buffer (25:75), pH 2.5; 0.5 ml min^{-1}; UV detection at 254 nm; 20°C.

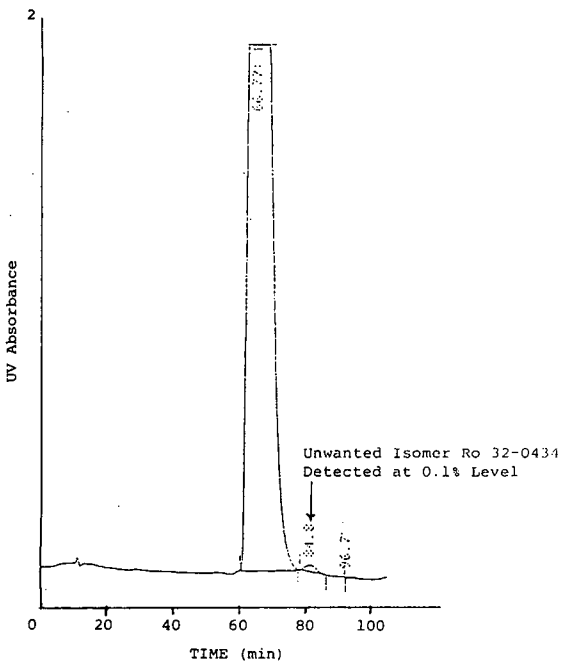

Fig. 5. Determination of the optical purity of Ro 32-0432 down to 0.1% level of unwanted enantiomer, Ro 32-0434. HPLC conditions: Chiralcel OD-R; CH_3CN–phosphate buffer (25:75), pH 2.5; flow-rate reduced to 0.3 ml min^{-1} for improved separation; UV detection at 254 nm; column temperature 0°C.

cesses of racemic compounds at low levels of detection. During this study the methodology was used to determine the presence of the unwanted enantiomer Ro 32-0434 in Ro 32-0432 down to the 0.1% level. The desired enantiomer Ro 32-0432, *S* configuration, eluted first from the column. The IC_{50} vs. PKC was 19 n*M* for the *S*-enantiomer and 90 n*M* for the *R*-enantiomer (Ro 32-0434). Substituting 0.1% trifluoroacetic acid for phosphate buffer would allow small-scale preparative separation of enantiomers for biological testing. Racemic Ro 31-9193 was successfully separated on a semi-preparative OD-R column (25 cm × 1 cm I.D.) using acetonitrile–0.1% aqueous trifluoroacetic acid (25:75) yielding mg quantities of the respective enantiomers. The IC_{50} (the amount of drug required to reduce activity of the enzyme to 50% of the uninhibited control) for the first-eluting enantiomer was 30 n*M* and 6 n*M* for the second-eluting enantiomer. The *trans* fused form of Ro 31-9193 was subsequently pursued as this was found to be more active than the *cis* configuration. Reversed-phase chiral chromatography would be compatible with drug metabolism/pharmacokinetics studies where monitoring of metabolites in aqueous media could be undertaken.

The OD-R column used for this work has been in use for over a year and subjected to various temperature changes and variations in mobile phase composition. Many samples have been assayed with little loss in performance. The separation of the racemate Ro 31-8830 has been used as a test for assessing the efficiency and chiral recognition of the Chiralcel OD-R column. The column is routinely washed with acetonitrile after use and capped off to prevent it drying out.

References

[1] Y. Nishizuka, *Nature*, 308 (1984) 693–698.
[2] A. Farago and Y. Nishizuka, *FEBS Lett.*, 268 (1990) 350–354.
[3] P. Davis, L. Elliott, W. Harris, C. Hill, S. Hurst, E. Keech, H. Kumar, G. Lawton, J. Nixon and S. Wilkinson, *J. Med. Chem.*, 35 (1992) 994–1001.
[4] K. Ikeda, T. Hamasaki, H. Kohno, T. Ogawa, T. Matsumoto and J. Sakai, *Chem. Lett.*, (1989) 1089–1090.
[5] A. Ishikawa and T. Shibata, *J. Liq. Chromatogr.*, 16 (1993) 859–878.

ELSEVIER

Journal of Chromatography A, 697 (1995) 271–278

JOURNAL OF CHROMATOGRAPHY A

Chiral high-performance liquid chromatography with cellulose carbamate-coated phases
Influence of support surface chemistry on enantioselectivity

S.J. Grieb[a], S.A. Matlin[a,*], A.M. Belenguer[b], H.J. Ritchie[c]

[a]*Department of Chemistry, University of Warwick, Coventry CV4 7AL, UK*
[b]*SB Pharmaceuticals, Old Powder Mills, Tonbridge, Kent TN11 9AN, UK*
[c]*Shandon HPLC, Astmoor, Runcorn, Cheshire WA7 1PR, UK*

Abstract

The influence of support surface chemistry on the enantioselectivity and column performance of cellulose tris(3,5-dimethylphenyl carbamate)-coated chiral HPLC phases was investigated. Stable coated phases were produced using underivatised, aminopropylated and octadecylated silica as the support media. For many racemates, underivatised silica at a 20% (w/w) loading was found to be the most efficient phase.

1. Introduction

Polysaccharide tris(aryl carbamate) derivatives coated onto large pore (1000–4000 Å) 7–10 μm aminopropylated spherical silica (APS) have proved to be extremely useful stationary phases. Developed by Okamoto and co-workers [1–3] and marketed by Daicel as Chiralcel and Chiralpak columns, they are renowned for the separation of a wide range of neutral, basic and acidic chiral compounds [1–10]. Recently, we have shown that use of smaller-particle APS (<5 μm) affords significant advantages, including high resolution and rapid separations [11].

APS is widely accepted as a suitable support for the polysaccharide tris(aryl carbamate)s. It is reportedly used [12] to (i) decrease non-stereoselective interactions by deactivating the acidic silanol groups and (ii) increase the stability of the coating by providing sites for hydrogen bond formation with the carbamate. However, to our knowledge, there have been no reported data substantiating either of these claims.

In this paper we report the results of a study using small-particle (3 μm) underivatised (SI), aminopropylated (APS) and octadecylated (ODS) spherical silicas from the Hypersil range to support cellulose tris(3,5-dimethylphenyl carbamate). This work has indicated that both polar (underivatised silica) and non-polar (octadecylated) supports can be used and in many cases, may offer some advantages.

2. Experimental

2.1. Chemicals and solvents

Underivatised, aminopropylated and octadecylated silicas (Shandon HPLC, UK)

* Corresponding author.

0021-9673/95/$09.50
SSDI 0021-9673(94)00868-X

which had the following properties were used: particle size, 3 μm; pore size, 120 Å; surface area, 170–180 m^2/g; pore volume 0.6 ml/g. Elemental analyses, APS: C 1.67, H 0.48, N 0.57; ODS: C 9.50, H 1.84. The cellulose (Sigmacel, degree of polymerisation 400–500) was purchased from Sigma (UK) and 3,5-dimethylphenyl isocyanate from Lancaster (UK). Racemic mixtures and enantiomers were purchased from either Sigma or Aldrich (UK). Solvents (HPLC grade) were obtained from Rathburn (UK).

2.2. Apparatus

Separations were carried out on an HPLC system comprising a Beckman 114 M pump, a Beckman System Gold 166 UV detector and a Promise autosampler. Data were acquired using a Waters 860 Expertease package. A high-pressure slurry packer fitted with a Haskel 780-3 pump was used for column packing. Gel permeation chromatography (GPC) was carried out on a PL Modular System with Caliber software using refractive index (RI) detection. Particle size distributions were determined as dispersions in methanol using a Malvern Mastersizer X.

2.3. Chromatographic conditions

Chromatography was performed at ambient temperature using the mobile phase compositions listed along with the results at the foot of Tables 1–3. Typically, 10-μl samples of 1% (w/v) solutions dissolved in the mobile phase were injected. A flow-rate of 0.5 ml/min was maintained throughout the study and the racemates detected using a suitable wavelength. The dead time (t_0) of each column was determined by injection of 1,3,5-tri-*tert.*-butylbenzene.

2.4. Chromatographic calculations

The separation factor (α) was calculated as $\alpha = k_2'/k_1'$ and capacity factor (k') as $k_1' = (t_1 - t_0)/t_0$ and $k_2' = (t_2 - t_0)/t_0$, where t_1 and t_2 refer to the retention times for the first and second eluting enantiomers, respectively.

The resolution factor (R_s) was calculated by the formula: $R_s = 2(t_2 - t_1)/(w_1 + w_2)$ where w_1 and w_2 are the peak widths for the first and second eluting enantiomer peaks, respectively.

2.5. Preparation of the chiral columns

Cellulose tris(3,5-dimethylphenyl carbamate) (CDMPC) was prepared as previously reported [2]. The dried carbohydrate was refluxed for 24 h in dry pyridine. After cooling 3.5 equivalents of 3,5-dimethylphenyl isocyanate was added and the mixture refluxed for a further 72 h. The cooled solution was poured into 1.5 l methanol and stirred for 1 h. The white solid was filtered, washed well with methanol and dried under vacuum at 50°C to constant mass. Elemental analysis $(C_{33}H_{37}N_3O_3)_n$, calculated: C 65.66, H 6.18, N 6.98; found: C 64.94, H 6.07, N 6.81. GPC analysis [two PL Mixed-C columns in series, elution with tetrahydrofuran (THF)] showed product to have $M_n = 1.01 \cdot 10^5$ and $M_w/M_n = 5.46$, where M_n is number-average molecular mass and M_w is weight-average molecular mass.

Silica, APS or ODS (3 g) was refluxed in THF (30 ml) for 30 min and allowed to cool. An appropriate amount of CDMPC [0.529 g for 15% (w/w), 0.75 g for 20% (w/w)] was dissolved in 20 ml THF–N,N-dimethylacetamide (80:20, v/v) and added to the refluxed silica. The solvent was removed under vacuum to dryness and the material sieved (38 μm) to ensure a free flowing powder suitable for packing. Mean particle size distributions were essentially unchanged from corresponding starting supports. The phase was high-pressure slurry packed (6000 p.s.i.; 1 p.s.i. = 6894.76 Pa) into a stainless-steel column (10 cm × 4.6 mm I.D.) in hexane–2-propanol (50:50, v/v) and equilibrated with hexane–2-propanol (80:20, v/v).

The preparation of columns of this type has been shown to be very reproducible from one batch to another, e.g. several batches of CDMPC-coated APS supports gave very similar α and R_s values for a series of test analytes.

3. Results and discussion

3.1. Influence of support chemistry

Previous studies with small-particle APS [11] have shown that a coating of 15% (w/w) cellulose tris(aryl carbamate) is optimum for the 120 Å pore phase. Therefore, in order to compare their behaviour, each support was coated with 15% (w/w) CDMPC and the influence of support surface chemistry on column performance was investigated.

The enantiomeric resolution of 16 chiral analytes (6 neutral, 5 basic and 5 acidic) can be seen in Tables 1–3.

3.2. Neutral analytes

For all the neutral analytes examined, capacity factors are highest on the coated ODS phase and lowest on the coated SI phase (Table 1). This result may seem surprising, since the test analytes are all relatively polar in nature and would not be expected to interact strongly with the non-polar ODS surface. However, the separation factors also show the same trend, thus there must be more CDMPC interaction sites on the ODS phase than there are on the SI phase. An explanation for this, along with a possible reason for the lower than expected resolution observed on the coated ODS phase, will be given later.

3.3. Basic analytes

A marked difference in chromatographic behaviour can be seen (Table 2) between analytes with a sterically hindered basic group (Trogers base and homatropine) and those in which the basic group is more accessible (orphenadrine, alprenolol and oxprenolol).

The analytes which have the more accessible basic group have high capacity factors on the coated SI phase and low capacity factors on the coated ODS phase. This is consistent with previously reported studies [6,7] suggesting that there are strong interactions between accessible basic amino groups in the analyte and any exposed acidic silanol groups. In the case of the coated SI phase, interactions with the support surface are so strong that the chromatography is extremely poor. The analytes in which the basic group is more sterically hindered are not able interact as strongly with the surface groups and the capacity factors for the three phases are more similar.

For all the basic analytes, the separation factors are highest on the coated ODS phase and, in general, lowest on the coated SI phase. This is consistent with the suggestion that there are more CDMPC interaction sites on the coated ODS phase.

3.4. Acidic analytes

In general, capacity factors are largest when APS is the support (Table 3). This is the counterpart of the effect seen with the basic compounds on the coated SI phase, ie the acidic group appears to be interacting with exposed APS groups. For the majority of analytes, separation factors are slightly higher on the coated ODS phase, but in general are lower than have been described in the literature [8]. Reasons for this are as yet unclear. Suprofen shows a somewhat different pattern of behaviour to the other acidic analytes, presumably as a result of its polyfunctional nature.

3.5. Stability

The stability of each 15% coated column was examined for 170 h under a flow-rate of 1 ml/min (total volume was approx. 10 l) at ambient temperature using hexane–2-propanol (80:20, v/v) as mobile phase. There was no deterioration in column performance, as judged by the lack of change in k', N or R_s for a test mixture.

3.6. General discussion

In order to explain the chromatographic trends seen for the three phases, the effects of introducing a bonded group onto the surface of a small-pored phase need to be considered. A bonded group will not only change the chemical nature of the surface (examples of non-stereospecific interactions between the analyte and the

Table 1
Resolution of neutral racemates on CDMPC-coated supports

Sample	Mobile phase		APS, 15%	ODS, 15%	SI	
					15%	20%
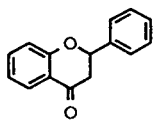 Flavanone	A	k'_1	1.78	2.49	1.62	2.12
		k'_2	2.30	3.15	1.96	2.78
		α	1.29	1.26	1.21	1.31
		R_s	2.46	2.14	1.80	2.53
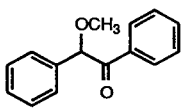 Benzoin methyl ether	A	k'_1	1.49	1.74	1.31	1.59
		k'_2	1.96	2.52	1.68	2.24
		α	1.32	1.44	1.28	1.41
		R_s	2.47	2.91	2.06	2.86
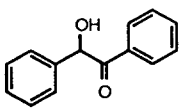 Benzoin	A	k'_1	3.50	4.35	3.17	3.75
		k'_2	4.67	5.97	3.99	5.24
		α	1.33	1.37	1.26	1.40
		R_s	3.04	2.97	2.40	3.27
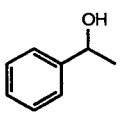 Phenethyl alcohol	B	k'_1	5.04	5.21	4.81	5.80
		k'_2	5.85	6.16	5.25	6.85
		α	1.16	1.19	1.09	1.18
		R_s	1.89	1.65	1.03	1.99
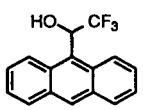 1-(9-Anthryl)-2,2,2-trifluoroethanol	A	k'_1	3.25	3.49	2.22	3.96
		k'_2	7.30	9.09	4.91	9.14
		α	2.25	2.61	2.21	2.31
		R_s	6.89	6.00	7.63	6.56
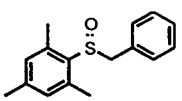 Benzyl mesityl sulphoxide	A	k'_1	3.50	3.93	3.25	3.76
		k'_2	6.65	8.36	5.55	8.17
		α	1.90	2.13	1.71	2.17
		R_s	5.56	4.77	4.96	6.04

Mobile phase: hexane–2-propanol [A = 90:10 (v/v); B = 98:2 (v/v)].

surface group have already been discussed) but will also affect the pore structure.

An aminopropyl or octadecyl group will reduce the pore diameter and thus the pore volume, compared with the underivatised silica. This should lead to an increase in the amount of CDMPC which is prevented from entering the pores, the magnitude of this effect depending to some extent on the spatial arrangement and conformation of the bonded group. In addition,

Table 2
Resolution of basic racemates on CDMPC-coated supports

Sample	Mobile phase		APS, 15%	ODS, 15%	SI	
					15%	20%
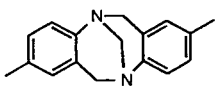 Trogers base	C	k'_1	1.39	1.62	1.59	2.01
		k'_2	1.75	2.27	2.10	2.46
		α	1.25	1.40	1.32	1.22
		R_s	1.71	2.21	2.24	1.49
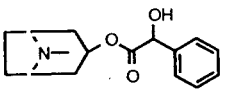 Homatropine	D	k'_1	1.52	1.37	1.27	1.41
		k'_2	2.10	2.21	1.84	2.17
		α	1.38	1.62	1.45	1.54
		R_s	2.65	3.04	2.49	3.20
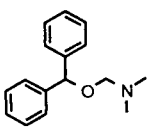 Orphenadrine	C	k'_1	0.90	0.63	2.16	2.00
		k'_2	1.23	1.05	2.49	2.44
		α	1.37	1.67	1.15	1.22
		R_s	2.02	2.18	1.07	1.40
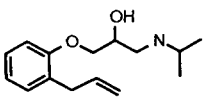 Alprenolol	D	k'_1	1.11	0.41	4.23	3.52
		k'_2	1.70	0.88	4.54	4.27
		α	1.53	2.14	1.07	1.21
		R_s	2.48	2.42	P.R.	1.21
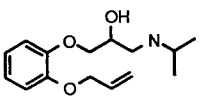 Oxprenolol	D	k'_1	2.26	1.11	6.56	5.27
		k'_2	5.43	3.61	8.54	9.38
		α	2.40	3.26	1.30	1.78
		R_s	5.48	5.40	1.50	3.69

P.R. = Partial resolution (<0.5). Mobile phases: C = hexane–2-propanol–diethylamine (90:10:0.1, v/v/v); D = hexane–2-propanol–diethylamine (80:20:0.1, v/v/v).

whilst the polar SI and APS supports may have an attractive or stabilising effect on the relatively polar CDMPC coating, via hydrogen bonding or dipole interactions, the more lipophilic ODS group may have a repelling or destabilising effect which will further deter the CDMPC from entering the pores.

An insight into how the chromatography is affected when there is a large amount of chiral phase on the outside of the particle was obtained during recent studies to determine the optimum carbamate loading for our small-pored APS supports [11]. At low levels ($<15\%$, w/w), an increase in the carbamate loading was accompanied by an increase in the capacity, separation and resolution factors. This was assumed to be due to an increase in the number of carbamate interaction sites. However, as the loading was further increased, a loading threshold was eventually reached, above which resolution deteriorated and eventually the particles became aggregated and would not pack satisfactorily.

Taking account of the chromatographic results, the support pore model and the observa-

Table 3
Resolution of acidic racemates on CDMPC-coated supports

Sample		APS, 15%	ODS, 15%	SI	
				15%	20%
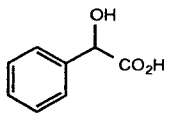 Mandelic acid	k'_1	8.93	5.67	5.46	6.94
	k'_2	9.52	6.94	6.09	7.85
	α	1.06	1.11	1.12	1.13
	R_s	0.72	0.73	1.08	1.29
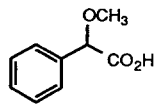 2-Methoxyphenylacetic acid	k'_1	4.82	3.26	3.66	5.09
	k'_2	5.33	3.74	4.05	5.82
	α	1.11	1.15	1.11	1.14
	R_s	1.32	1.17	1.19	1.67
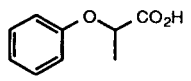 2-Phenoxypropionic acid	k'_1	3.14	2.48	2.67	3.17
	k'_2	4.52	4.51	4.12	4.99
	α	1.44	1.82	1.54	1.57
	R_s	3.89	4.42	4.10	4.34
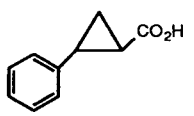 2-Phenyl-1-cyclo-propane carboxylic acid	k'_1	5.48	4.78	4.67	6.45
	k'_2	6.25	5.13	5.35	7.49
	α	1.14	1.07	1.14	1.16
	R_s	1.78	P.R.	1.73	1.93
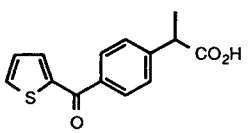 Suprofen	k'_1	11.78	12.34	11.64	12.60
	k'_2	12.83	14.22	12.83	13.91
	α	1.09	1.15	1.11	1.10
	R_s	1.07	1.23	1.56	1.14

P.R. = Partial resolution (< 0.5). Mobile phase: hexane–ethanol–trifluoroacetic acid (96:4:1, v/v/v).

tions from the loading experiments, the following phase descriptions are proposed;

(i) *Coated SI phase*. Owing to its polar nature and relatively large pore volume, the underivatised silica support is able to accommodate the polar CDMPC coating more easily than the other two supports. Therefore it has the least amount of CDMPC coating on the outside of the particles, which reduces the number of chiral interaction sites, leading to the lowest degree of separations. The strong interactions seen with some basic analytes indicate that there are regions where the coverage of accessible silica surface by CDMPC is low.

(ii) *Coated APS phase*. The aminopropyl support appears to have slightly more CDMPC coating on the outside of the particles, demonstrated by higher capacity and separation factors for neutral analytes compared to the coated SI phase. High resolution is observed for many of the analytes and loading experiments confirm that 15% (w/w) CDMPC is close to optimum for

this support. Higher than average interactions with some acidic analytes suggest that, as with the SI support, there are regions where the density of the CDMPC phase is low.

(iii) *Coated ODS phase.* This support, due to its large non-polar bonded group, does not readily accommodate CDMPC into its pore volume. Therefore it has the largest amount of CDMPC on the outside of the particles, which provides the largest number of chiral interaction sites, as demonstrated by the high separation factors observed for the majority of analytes. However, in contrast to the APS coated phase, the amount of CDMPC on the outside of the ODS particles appears to have exceeded the optimum. Whilst the column has still packed satisfactorily, the resolution factors are not as high as might be predicted.

3.7. The use of underivatised silica

It was of particular interest that, contrary to popular belief, the coated SI phase showed good chromatography for many test analytes. It was noted that (i) SI appears to most readily accept the CDMPC coating, due to its polar nature and larger pore volume; and (ii) in previous studies [1–3], wider-pore APS was able to accept loadings of 20–25% (w/w). Consequently, the behaviour of a 20% (w/w) CDMPC coating on SI was investigated.

The underivatised silica readily accepted this higher loading and the results in Tables 1–3 show that the 20% (w/w) coated SI column was significantly more efficient than the 15% (w/w) coated SI column for the majority of racemates tested. The resolution of benzoin methyl ether on the 15 and 20% (w/w) coated SI phases is shown in Fig. 1.

For many analytes the 20% (w/w) coated SI column also gave superior performance to either the ODS or APS 15% (w/w) coated phases. Of remaining concern were the poor results seen with some basic analytes, due to interactions with exposed surface silanol groups. Compared to the 15% (w/w) coated SI phase, an improvement was seen in the capacity and separation factors on the 20% (w/w) coated SI phase, indicating that interactions with Si–OH groups had been reduced by the heavier coating. However, a substantial improvement was made by increasing the amount of diethylamine, a silanol

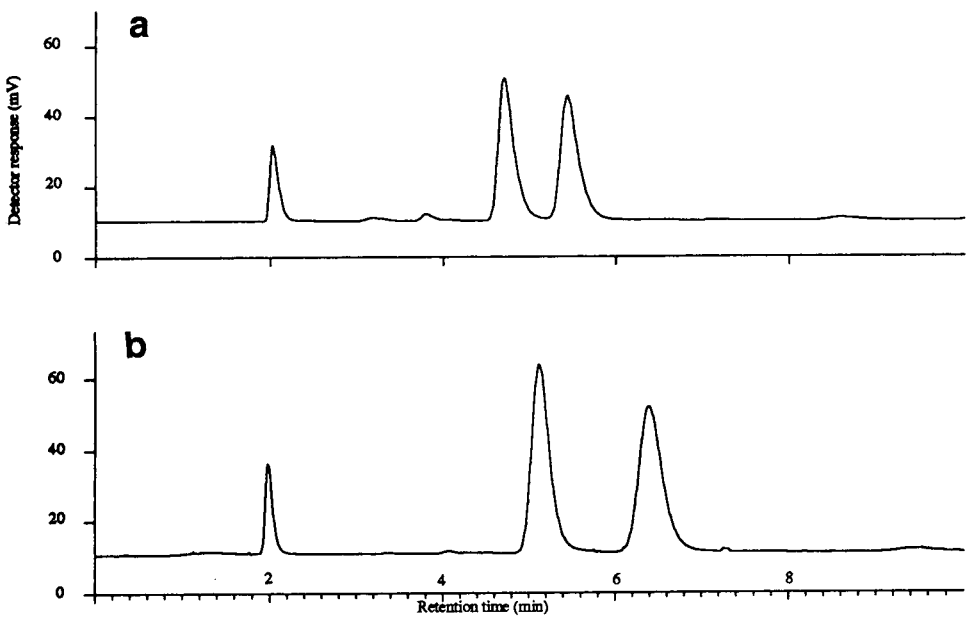

Fig. 1. Resolution of benzoin methyl ether at two loading levels of CDMPC on SI: (a) 15%, (b) 20%.

suppressor, in the mobile phase from 0.1 to 1.0%. For example, for oxprenolol on the 20% (w/w) coated SI phase, the k_1' value decreased from 5.27 to 2.86 and the α and R_s factors increased from 1.78 to 2.48 and 3.69 to 5.30, respectively. The column continued to remain stable with this mobile phase composition for the duration of the study and showed no deterioration in performance after return to standard test conditions.

4. Conclusions

It is possible to produce stable cellulose carbamate-coated phases using supports other than APS. For many compounds, 3 μm Hypersil SI coated with 20% (w/w) CDMPC was the most efficient phase. Further investigations of these phenomena are in progress.

Acknowledgements

This work was supported by EPSRC, SmithKline Beecham Pharmaceuticals and Shandon HPLC.

References

[1] Y. Okamoto, M. Kawashima and K. Hatada, *J. Am. Chem. Soc.*, 106 (1984) 5357.
[2] Y. Okamoto, M. Kawashima and K. Hatada, *J. Liq. Chromatogr.*, 363 (1986) 173.
[3] Y. Okamoto, R. Aburatani, T. Fukumoto and K. Hatada, *Chem. Lett.*, (1987) 1857.
[4] T. Shibata, I. Okamoto and K. Ishii, *J. Liq. Chromatogr.*, 9 (1986) 313.
[5] Y. Okamoto, R. Aburatani, K. Hatano and K. Hatada, *J. Liq. Chromatogr.*, 11 (1988) 2147.
[6] Y. Okamoto, M. Kawashima, R. Aburatani, K. Hatada, T. Nishiyama and M. Masuda, *Chem. Lett.*, (1986) 1237.
[7] H.Y. Aboul-Enein and V. Serignese, *J. Liq. Chromatogr.*, 16 (1993) 197.
[8] Y. Okamoto, R. Aburatani, Y. Kaida and K. Hatada, *Chem. Lett.*, (1988) 1125.
[9] Y. Okamoto, R. Aburatani, Y. Kaida, K. Hatada, N. Inotsume and M. Nakano, *Chirality*, 1 (1989) 239.
[10] S.A. Matlin, E. Tiritan, A.J. Crawford, Q.B. Cass and D. Boyd, *Chirality*, 6 (1994) 135.
[11] S.J. Grieb, S.A. Matlin, J.G Phillips A.M. Belenguer and H.J. Ritchie, *Chirality*, 6 (1994) 129.
[12] G. Felix and T. Zhang, *J. Chromatogr.*, 639 (1993) 141.

ELSEVIER

Journal of Chromatography A, 697 (1995) 279–287

JOURNAL OF CHROMATOGRAPHY A

Preparation of silicas combined with optically active organic compounds: optical resolution of metal chelate complexes on the silica composites

Fujio Mizukami[a,*], Hiroyuki Izutsu[b], Tetsuya Osaka[c], Yoshikatsu Akiyama[c], Naokazu Uiji[c], Kouji Moriya[c], Katsuya Endo[c], Kazuyuki Maeda[a], Yoshimichi Kiyozumi[a], Kengo Sakaguchi[c],

[a]*National Institute of Materials and Chemical Research, 1-1, Higashi, Tsukuba, Ibaraki 305, Japan*
[b]*Taki, Chemical Co., Ltd., 2, Midorimachi, Befu-cho, Kakogawa, Hyogo 675-01, Japan*
[c]*Faculty of Science and Technology, Science University of Tokyo, 2641 Yamazaki, Noda, Chiba 278, Japan*

Abstract

A new type of optically active organic–inorganic composite was prepared by a sol–gel method in which tetraethoxysilane is hydrolysed after replacing the ethoxy group with D-lactose or L-tartaric acid, and compared in the optical resolution of tris(2,4-pentanedionato)metal complexes with conventional silica composites (kneading with L-lactose and impregnation with an L-lactose or L-tartaric acid solution) and the organic compounds themselves. The sol–gel composites showed much higher optical resolution abilities than the conventional materials and, in addition the optically active organic compounds could not resolve the racemate under similar conditions. The high resolution ability of the sol–gel composites was deduced to come from the combined effect of silica and a dispersed optically active organic compound.

1. Introduction

Many composites made up of silica and an optically active organic compound have been prepared and used in chromatography [1–13]. However, they are mostly limited to two classes, one in which an optically active organic compound is covalently coupled to a functional group pendant on the silica surface through C–Si bonds such as aminopropyl-derivatized silica [1–8], and another in which the silica surface is coated with an optically active compound such as cellulose [9–13]. In these composites, silica is used as a support to fix an optically active compound and no further role other than as the support is expected.

We considered that a composite incorporating an optically active compound in the skeleton structure or matrix network of silica should have different properties to a composite bearing an optically active compound on the silica surface, and might show certain synergism of the combined effect of the adsorptive ability of silica and the molecular recognition ability of an optically active compound in separation. Because organic–inorganic composites obtained by combining

* Corresponding author.

0021-9673/95/$09.50
SSDI 0021-9673(94)00751-9

organic and inorganic compounds at a molecular level not only show properties of both the organic and inorganic parts but often also entirely new properties [14].

Here we report the incorporation of optically active organic compounds such as D-lactose, D-glucose, L-tartaric acid and L-malic acid in silica by a sol–gel procedure via the substitution of the ethoxy group of tetraethoxysilane (TEOS) and the optical resolution of tris(2,4-pentanedionato)metal complexes [M(acac)$_3$] with the optically active organic–silica composites obtained by the sol–gel procedure.

2. Experimental

2.1. Preparation of an optically active organic compound–silica composite

D-Lactose–silica (D-lac–SiO_2)

TEOS (0.6 mol) was mixed with D-lactose (0.04–0.2 mol) in ethanol (100 g) in the presence of acetic acid (0.2 mol) at 80°C for 2 h. To the solution, water (1.2–5.6 mol) was added at the same temperature and allowed to stand for 6–8 h to give a gel. The gel was dried at 80°C under reduced pressure.

D-Glucose–silica (D-glu–SiO_2), D-sorbitol–silica (D-sor–SiO_2) and D-fructose–silica (D-fru–SiO_2)

These three composites were prepared in a manner identical with the above, but in all the preparations the saccharide:TEOS and water:TEOS ratios were only 0.2:0.6 and 2.0:0.6 (mol/mol), respectively.

L-Tartaric acid–silica (L-tart–SiO_2), L-malic acid–silica (L-mal–SiO_2) and L-mandelic acid–silica (L-mand–SiO_2)

These composites were also prepared in a manner identical with the above, but the water:TEOS ratio was always 2 (mol/mol), and the hydroxycarboxylic acid:TEOS ratio was 0.1–0.8:0.6 for L-tart–SiO_2, 0.27:0.40 for L-mal–SiO_2 and 0.40:0.80 for L-mand–SiO_2.

Kneading D-lac–SiO_2, impregnation D-lac–SiO_2 and L-tart–SiO_2

For comparison, D-lac–SiO_2 and L-tart–SiO_2 were also prepared by conventional methods such as kneading and impregnation procedures, in which TEOS was first hydrolysed to silica in the presence of acetic acid, and the silica was kneaded with D-lactose or impregnated with a solution of D-lactose or L-tartaric acid.

In all of the silica composites prepared, the content of the optically active compound was checked by thermogravimetric–differential thermal analysis (TG–DTA) and the optically active compound:SiO_2 ratio was found to be almost equal to the optically active compound:TEOS ratio used in the preparation.

2.2. Packing and elution

All the composites were ground to powders below 200 mesh. Each of the composites was slurried with *n*-hexane and packed in a glass tube (6 mm I.D.). A small amount of a benzene solution of a racemic M(acac)$_3$ was placed on a column and eluted with *n*-hexane–benzene, *n*-hexane–benzene–1,4-dioxane or *n*-hexane–benzene–methyl ethyl ketone (MEK).

2.3. Measurement and characterization

The X-ray diffraction (XRD) patterns were recorded on a MAC Science MXP 18 instrument using Cu Kα radiation with a nickel filter. TG–DTA was carried out on a MAC Science TG–DTA 2100 instrument in air. The circular dichroism (CD) spectra were recorded on a JASCO J-600 spectropolarimeter.

3. Results and discussion

3.1. Saccharide–silica composites

Table 1 shows the molecular circular dichroisms ($\Delta\varepsilon$) of the first fractions of Co(acac)$_3$ eluted from the D-lactose monohydrate, kneading, impregnation and sol–gel D-lac–SiO_2 columns with *n*-hexane–benzene–1,4-dioxane

Table 1
Optical resolution of $Co(acac)_3$ with different D-lac–SiO_2 composites and D-lactose monohydrate

	D-lac:SiO_2 (mol/mol)	$\Delta\varepsilon$ (546 nm)[a]	Column length × I.D. (mm)
D-Lactose monohydrate	∞	0.3[b]	900 × 30
		No resolution	380 × 6
Kneading D-lac–SiO_2	0.1:0.3	No resolution	400 × 6
Impregnation D-lac–SiO_2	0.1:0.3	No resolution	400 × 6
Sol-gel D-lac–SiO_2 [c]	0.1:0.3	1.3	370 × 6

Eluent: *n*-hexane–benzene–1,4-dioxane(45:45:10).
[a] The first fraction eluted.
[b] Ref. [15].
[c] H_2O:TEOS = 1.0:0.3.

(45:45:10, v/v/v). Under the conditions used here, kneading and impregnation D-lac–SiO_2 composites and D-lactose monohydrate did not give the optically active complex, and only sol–gel D-lac–SiO_2 partially resolved the racemate into the optically active forms. The resolution ability of sol–gel D-lac–SiO_2 was found to be much higher than those of the others, taking into account the length and diameter of the columns. This suggests that the sol–gel method is suitable for drawing out certain combined effects of organic and inorganic compounds.

The properties of the materials obtained by the sol–gel method are considerably affected by the preparation conditions, especially the amount of water added in preparing a sol and gel. Table 2 shows the effects of the amounts of water and D-lactose used in preparing D-lac–SiO_2 composite sols and gels on the optical resolution of $Co(acac)_3$ with the composites, including the effect of the eluents. When the amount of water added increased, the resolution ability of D-lac–SiO_2 initially increased, but decreased again at H_2O:TEOS ratios over 3.33. As for the amount of D-lactose in the composite, the resolution ability increased with increasing D-lactose:TEOS ratio, but it was very difficult to obtain a D-lac–SiO_2 gel at the ratios over 1:3 when the

Table 2
Optical resolution of $Co(acac)_3$ with sol–gel D-lac–SiO_2 composites

No.	Preparation conditions			Eluent (volume ratio)	$\Delta\varepsilon$ (328 nm)[a]	Flow-rate (ml/r
	Lactose (mol)	TEOS (mol)	H_2O (mol)			
1	0.1	0.3	0.6	*n*-Hexane–benzene–1,4-dioxane (45:45:10)	−1.4	0.008
2	0.1	0.3	1.0	*n*-Hexane–benzene–1,4-dioxane (45:45:10)	−21.6	0.011
3	0.1	0.3	1.4	*n*-Hexane–benzene–1,4-dioxane (45:45:10)	−5.8	0.043
4	0.1	0.3	2.2	*n*-Hexane–benzene–1,4-dioxane (45:45:10)	−6.7	0.025
5	0.1	0.3	2.6	*n*-Hexane–benzene–1,4-dioxane (45:45:10)	No resolution	0.069
6	0.1	0.3	2.8	*n*-Hexane–benzene–1,4-dioxane (45:45:10)	No resolution	0.039
7	0.1	0.3	1.0	*n*-Hexane–benzene–1,4-dioxane (45:45:10)	−21.4	0.009
8	0.08	0.3	1.0	*n*-Hexane–benzene–1,4-dioxane (45:45:10)	−9.8	0.007
9	0.04	0.3	1.0	*n*-Hexane–benzene–1,4-dioxane (45:45:10)	−4.3	0.003
10	0.02	0.3	1.0	*n*-Hexane–benzene–1,4-dioxane (45:45:10)	−3.5	0.001
11	0.1	0.3	1.0	Benezene–1,4-dioxane (90:10)	−9.4	0.005
12	0.1	0.3	1.0	*n*-Hexane–benzene–acetone (45:45:10)	−21.6	0.004
13	0.1	0.3	1.0	*n*-Hexane–Benzene–MEK (45:45:10)	−49.2	0.005
14	0.1	0.3	1.0	*n*-Hexane–benzene–t-BuOH (44:44:12)	−6.2	0.004
15	0.1	0.3	1.0	*n*-Hexane–benzene–diethyl ether (44:44:12)	No resolution	Fast
16	0.1	0.3	1.0	*n*-Hexane–benzene (50:50)	No elution	Very slow

[a] The first fraction eluted.

H_2O:TEOS ratio was kept 3.33. Hence a D-lactose:TEOS:H_2O ratio of 0.1:0.3:1 in the preparation of the composite seems to be the optimum to obtain a D-lac–SiO_2 with high recognition ability for the chirality of $Co(acac)_3$. As for the eluent and its flow-rate, mixed solutions such as *n*-hexane–benzene–1,4-dioxane, *n*-hexane–benzene–acetone and *n*-hexane–benzene–methyl ethyl ketone were suitable as the eluents, and at the flow-rates of the eluents listed in Table 2 it was difficult to find some special relationship between the flow-rate and $\Delta\varepsilon$ or the optical resolution, because the D-lac:TEOS ratio was variable when $\Delta\varepsilon$ increased with an increase in flow-rate.

Table 3 shows the optical resolution of $Co(acac)_3$ with sol–gel D-glu–SiO_2, D-sor–SiO_2 and D-fru–SiO_2 prepared under conditions similar to the optimum preparation conditions for sol–gel D-lac–SiO_2. These three composites could resolve $Co(acac)_3$ partially as well as sol–gel D-lac–SiO_2, but only D-fru–SiO_2 shows opposite chirality recognition.

In the above resolution experiments, the performance of the composites in the optical resolution of $Co(acac)_3$ often varied with the drying conditions before use or the moisture in the composites. This seems to be due to the water in the composites blocking the interaction of $Co(acac)_3$ with the saccharide and silica parts.

Figs. 1 and 2 show the XRD patterns of silica, D-lac–SiO_2, D-lactose monohydrate, D-fru–SiO_2, D-sor–SiO_2 and D-glu–SiO_2. With sol–gel D-lac–SiO_2 composites, as the amounts of D-lactose (Fig. 1b–d) and water (Fig. 1d–f) used increased, the peaks due to D-lactose crystals became stronger and sharper. The XRD peaks of kneading and impregnation D-lac–SiO_2 composites are also as sharp as those of D-lactose monohydrate. These results indicate that the dispersibility of D-lactose in the sol–gel composites decreases with increase in the amounts of D-lactose and water used, and then the dispersibility of D-lactose in the kneading and impregnation composites is basically low, because generally crystals show sharper and stronger XRD peaks with increase in size. As D-lactose dissolves easily in water and slightly in ethanol, it seems strange that the dispersibility of D-lactose decreases with increase in the amount of water used. However, it is in fact natural because the C–O–Si bond formed by replacing the ethoxy group of TEOS with D-lactose is easily hydrolysed with a large amount of water and D-lactose tends to come out of the network of silica. This suggests that sol–gel D-lac–SiO_2 composites prepared with a large amount of water would be similar in properties to impregnation D-lac–SiO_2 composites. Actually, the sol–gel D-lac–SiO_2 composites prepared with a large excess of water (e.g., Nos. 5 and 6 in Table 1) were similar in their XRD and TG–DTA patterns and in the resolution behaviour of $Co(acac)_3$ to the impregnation D-lac–SiO_2 composite, and also to the kneading composite. Impregnation and kneading D-lac–SiO_2 composites showed simple combined patterns of the individual TG–DTA curves of D-lactose and silica, but sol–gel D-lac–SiO_2 composites prepared with H_2O:TEOS ratios below 7 showed different patterns. As for the other saccharide–silica composites, D-glu–SiO_2 composite showed slightly broader XRD peaks, and

Table 3
Optical resolution of $Co(acac)_3$ with sol–gel saccharide–SiO_2 composites

Composite	Eluent (volume ratio)	$\Delta\varepsilon$ (328 nm)[a]
D-lac–SiO_2	*n*-Hexane–benzene–MEK (45:45:10)	−49.2
D-glu–SiO_2	*n*-Hexane–benzene (50:50)	−21.5
D-sor–SiO_2	*n*-Hexane–benzene (50:50)	−19.5
D-fru–SiO_2	*n*-Hexane–benzene (50:50)	+61.7

Saccharide:SiO_2 = 1:3; H_2O:TEOS = 1:0.3; column, 400 mm × 6 mm I.D.
[a] The first fraction eluted.

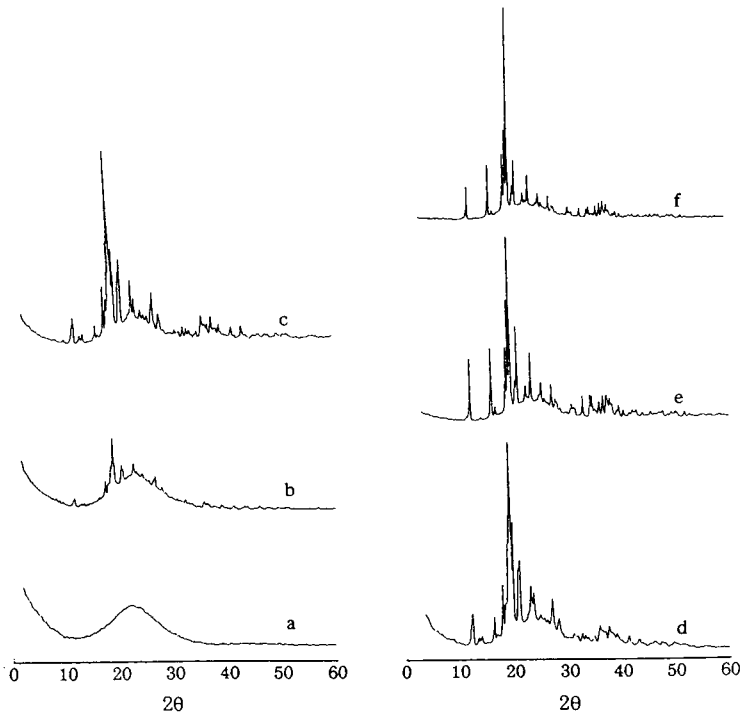

Fig. 1. XRD patterns of sol–gel D-lactose–silica composites and silica. (a) SiO_2. D-lac–SiO_2; (b) lac:TEOS = 0.02:0.3, H_2O:TEOS = 1:0.3; (c) lac:TEOS = 0.08:0.3, H_2O:TEOS = 1:0.3; (d) lac:TEOS = 0.1:0.3, H_2O:TEOS = 1:0.3; (e) lac:TEOS = 1:0.3, H_2O:TEOS = 2.2:0.3; (f) lac:TEOS = 0.1:0.3, H_2O:TEOS = 2.8:0.3.

both D-sor–SiO_2 and D-fru–SiO_2 composites did not show any clear XRD peaks due to the respective saccharide crystals. However, D-sorbitol, D-fructose and D-glucose could be easily extracted from the respective composites by washing them with water. Hence, it is considered that D-sor–SiO_2 and D-fru–SiO_2 composites do not have D-sorbitol and D-fructose crystals of sufficient size to diffract X-rays, and it is found that D-sorbitol, D-fructose and D-glucose are more dispersed than D-lactose in the composites. The dispersion of saccharides in the composites also seems to be closely related to their solubilities in ethanol, because a large amount of ethanol is produced by the hydrolysis of TEOS or in the sol–gel process, and the solubility of the saccharides used here decreases in the order D-sorbitol ≈ D-fructose >> D-glucose >> D-lactose [16].

From the above results, it is roughly concluded that a composite in which a saccharide is highly dispersed shows a higher recognition ability for the chirality of $Co(acac)_3$ and the high dispersion is the reason why, in the optical resolution of $Co(acac)_3$, the sol–gel D-lac–SiO_2 composite is superior to the corresponding kneading and impregnation composites.

3.2. Hydroxycarboxylic acid–silica composites

Table 4 shows the results of the optical resolution of $Co(acac)_3$ with the three sol–gel composites L-tart–SiO_2, L-mal–SiO_2 and L-mand–SiO_2, prepared under similar conditions. Under the conditions used here, L-tart–SiO_2 showed a much higher resolution ability than the other two, as can be seen from the comparison of the $\Delta\varepsilon$ values.

Thus, the preparation conditions for L-tart–SiO_2 were investigated in detail. Table 5 gives

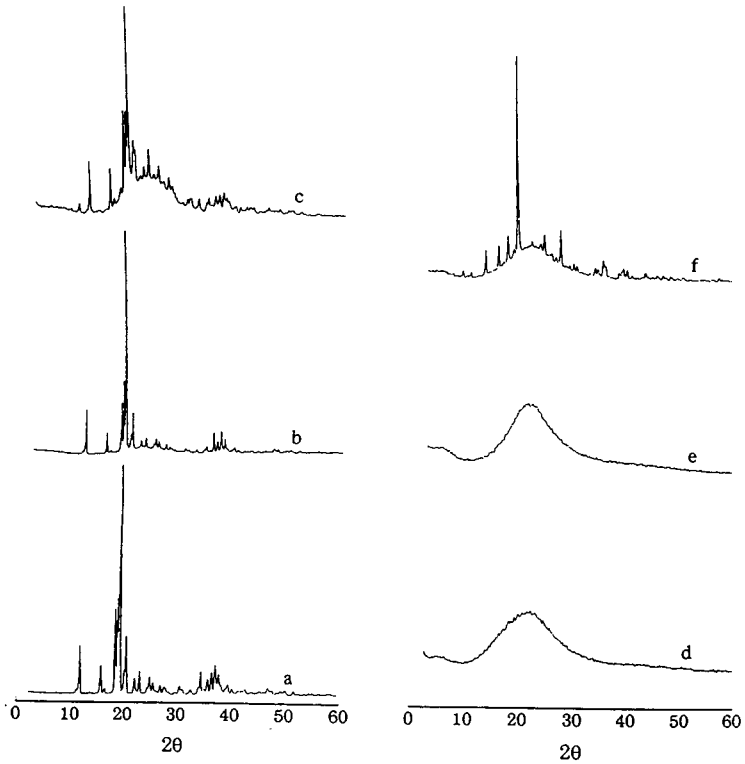

Fig. 2. XRD patterns of saccharide–silica composites and D-lactose monohydrate. (a) D-lactose monohydrate. Saccharide–SiO_2 (saccharide:SiO_2 = 0.1:0.3); (b) kneading D-lac–SiO_2; (c) impregnation D-lac–SiO_2; (d) sol–gel D-fru–SiO_2; (e) sol–gel D-sor–SiO_2; (f) sol–gel D-glu–SiO_2.

the $\Delta\varepsilon$ values of the first fractions of $Co(acac)_3$ eluted from L-tartaric acid and different L-tart–SiO_2 columns with *n*-hexane–benzene (1:1, v/v). With L-tartaric acid itself, the optically active cobalt complex was not obtained. This might be due to the high flow-rate (0.298 ml/min) of the eluent, but the rate is comparable to that of sol–gel 8 in Table 5. As for impregnation L-tart–SiO_2, only the composites with L-tart:SiO_2 ratios of 0.33–0.67 gave fractions with low optical activity, and it was difficult to resolve the racemate of the cobalt complex using the composites with higher L-tartaric acid contents with L-tart:$SiO_2 \geq 1$, even when the flow-rate of the eluent was slow. On the other hand, with sol–gel L-tart–SiO_2, fractions with high optical activity were easily obtained; as the L-tartaric acid content increased, the $\Delta\varepsilon$ of the fractions first increased and then decreased after maintaining high values over a wide range of L-tartaric acid content. In addition, even when the tartaric acid content was very high (L-tart:SiO_2 = 1.33) and the flow-rate of eluent was high (0.270 ml/min), the fraction showed weak optical activity. These

Table 4
Optical resolution of $Co(acac)_3$ with sol–gel L-hydroxycarboxylic acid–silica composites

Composite	$\Delta\varepsilon$[a]	
	328 nm	571 nm
L-tart–SiO_2	58.5	−4.7
L-mal–SiO_2	2.8	−0.1
L-mand–SiO_2	No elution	

L-Hydroxycarboxylic acid:SiO_2 = 0.2:0.6; column, 400 mm × 6 mm I.D.
[a] The first fraction eluted.

Table 5
Effect of the L-tartaric acid content in L-tart–SiO_2 on optical resolution of $Co(acac)_3$ with L-tart–SiO_2

	L-tart:SiO_2 (mol/mol)	Flow-rate (ml/min)	$\Delta\varepsilon$*	
			328 nm	571 nm
Sol–gel 1	0.1:0.6	Very slow	No elution	
Sol–gel 2	0.2:0.6	0.005	58.5	−4.7
Sol–gel 3	0.3:0.6	0.021	50.6	−4.8
Sol–gel 4	0.4:0.6	0.022	61.7	−4.9
Sol–gel 5	0.5:0.6	0.044	64.3	−5.3
Sol–gel 6	0.6:0.6	0.042	61.8	−5.0
Sol–gel 7	0.7:0.6	0.098	28.7	−2.3
Sol–gel 8	0.8:0.6	0.270	4.9	–
Impregnation 1	0.1:0.6	Very slow	No elution	
Impregnation 2	0.2:0.6	0.063	13.7	−1.0
Impregnation 4	0.4:0.6	0.076	4.9	–
Impregnation 6	0.6:0.6	0.110	No resolution	
Impregnation 8	0.8:0.6	0.036	No resolution	
L-Tartaric acid	∞	0.298	No resolution	

Column: 6 mm I.D. × 400 mm; eluent, *n*-hexane/benzene (1:1 v/v).
* The first fraction eluted.

results clearly show that sol–gel L-tart–SiO_2 composites have higher recognition abilities than L-tartaric acid and impregnation L-tart-SiO_2 composites for the chirality of $Co(acac)_3$, and also a synergistic effect appears in the chirality recognition of L-tart–SiO_2 composites if L-tartaric acid and silica are combined by the sol–gel technique.

Fig. 3 shows CD spectra of the fractions of $Co(acac)_3$ and $Cr(acac)_3$ eluted from the columns packed with sol–gel L-tart–SiO_2 (L-tart:SiO_2 = 0.33). Spectra a_1 and b and spectrum a_f show CD patterns characteristic of Δ- and Λ-$Co(acac)_3$, respectively [17,18], and spectrum c also shows the characteristic pattern of Δ-$Cr(acac)_3$ [19,20]. Thus, the Λ configuration of the metal chelate complexes is found to interact more strongly than the Δ configuration with L-tart–SiO_2. Although the maximum $\Delta\varepsilon$ values of the optically pure $Co(acac)_3$ are still unknown, the highest $\Delta\varepsilon$ value at 571 nm which has been reported so far is around 6. On the other hand, the $\Delta\varepsilon$ value at 535 nm of the optically pure Δ-$(+)_{589}$-$Cr(acac)_3$ is known to be −4.5 [19,20] and this value is consistent with that of the first fraction of $Cr(acac)_3$ obtained with the 1400 mm

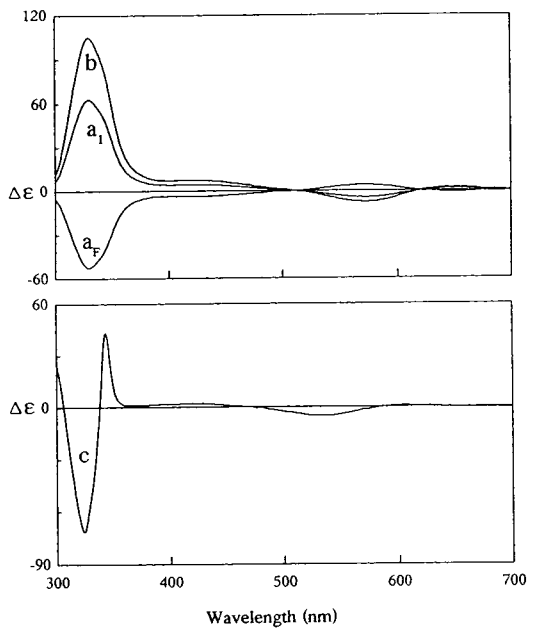

Fig. 3. CD spectra of $M(acac)_3$ eluted from sol–gel L-tart–SiO_2 with L-tart:SiO_2 = 0.33. $Co(acac)_3$: (a_1) first fraction by 400-mm column; (a_F) final fraction by 400-mm column; (b) first fraction by 1400-mm column. $Cr(acac)_3$: (c) first fraction by 1400-mm column.

Table 6
Optical resolution of $M(acac)_3$ with sol–gel L-tart–SiO_2 composite

$Co(acac)_3$ $\Delta\varepsilon$[a]		$Cr(acac)_3$ $\Delta\varepsilon$[a]		
328 nm	571 nm	323 nm	343 nm	535 nm
103.9	−8.6	−72.2	44.1	−4.4

L-tart:SiO_2 = 0.2:0.6; column 1400 mm × 6 mm I.D.
[a] The first fraction eluted.

column of sol–gel L-tart–SiO_2 (Table 6). Hence it is concluded that the 1400 mm column of sol–gel L-tart–SiO_2 can give the optically pure isomer of $Cr(acac)_3$, and deduced that the $\Delta\varepsilon$ values, −8.6 at 571 nm and 103.9 at 328 nm of the first fraction of $Co(acac)_3$ obtained by the 1400 mm column, correspond to the $\Delta\varepsilon$ values of optically pure Δ-$Co(acac)_3$.

Fig. 4 shows the XRD patterns of sol–gel L-mand–SiO_2, L-mal–SiO_2 and L-tart–SiO_2 composites. The first shows weak peaks due to L-mandelic acid crystals, but the last two do not show clear XRD peaks. L-Mandelic acid, L-malic acid and L-tartaric acid crystals were easily extracted from the respective composites by washing them with hot ethanol, although their ethylates were also extracted to a small extent. From these facts, it is concluded that L-malic acid and L-tartaric acid are more dispersed than L-mandelic acid in the silicas. This is in harmony with the results in Table 4.

Fig. 5 shows XRD patterns of L-tartaric acid, impregnation L-tart–SiO_2 and sol–gel L-tart–SiO_2 powders. All impregnation L-tart–SiO_2

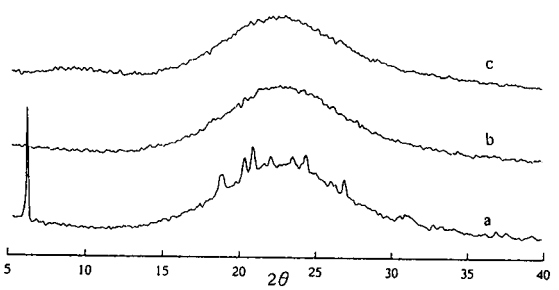

Fig. 4. XRD patterns of sol–gel hydroxycarboxylic acid–silica composites. (a) L-mand–SiO_2; (b) L-mal–SiO_2; (c) L-tart–SiO_2.

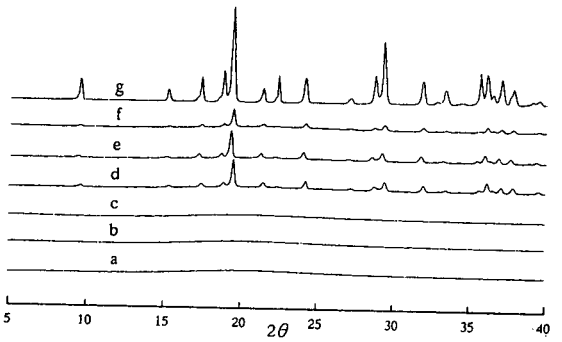

Fig. 5. XRD patterns of L-tartaric acid–silica composites and L-tartaric acid. Sol–gel L-tart–SiO_2: (a) tart:SiO_2 = 0.6:0.6; (b) tart:SiO_2 = 0.4:0.6; (c) tart:SiO_2 = 0.2:0.6. Impregnation L-tart–SiO_2: (d) tart:SiO_2 = 0.6:0.6; (e) tart:SiO_2 = 0.4:0.6; (f) tart:SiO_2 = 0.2:0.6. (g) L-Tartaric acid.

composites listed in Table 5 showed XRD patterns characteristic of L-tartaric acid crystals [21,22] and their TG–DTA curves had an endothermic peak without mass loss around 175°C corresponding to the melting point of L-tartaric acid. In addition, as the L-tartaric acid content in the composites increased, the XRD and TG–DTA peaks became sharper and stronger. These results indicate that, in the impregnation L-tart–SiO_2 composites, L-tartaric acid molecules are easy to aggregate among themselves with order and are dispersed as the crystals. On the other hand, all sol–gel L-tart–SiO_2 composites showed neither clear XRD peaks nor an endothermic peak around 175°C in their TG–DTA curves. This strongly suggests that, in the sol–gel composites, L-tartaric acid is dispersed at the molecular level, because the composites certainly contain a large amount of L-tartaric acid, as stated above. This high dispersion of sol–gel composites would be natural if it is considered that L-tartaric acid bonded to the silicon by substituting the ethoxy group from TEOS is difficult to hydrolyse because L-tartaric acid is a polydentate ligand and can coordinate strongly to a metal ion.

According to the literature [22], L-tartaric acid molecules are held in the crystal structure by a three-dimensional network of O–H–O hydrogen bonds of the usual strength. Thus, when L-tartaric acid is dispersed in the composites as the

crystals, the chance that $Co(acac)_3$ and $Cr(acac)_3$ complexes interact with L-tartaric acid is low and the interaction seems to be loose. This is the reason why L-tartaric acid and impregnation L-tart–SiO_2 cannot resolve the metal chelate complexes. In contrast, if L-tartaric acid is dispersed at the molecular level, the metal complexes interact repeatedly and intimately with L-tartaric acid. Alternatively, L-tartaric acid which is dispersed as molecules or clusters in the composites is effective for the chirality recognition or the optical resolution of the metal chelate complexes. As this kind of L-tartaric acid is much more evident in the sol–gel composite than in the corresponding impregnation composite, the former shows a very high performance in the optical resolution of the metal chelate complexes.

4. Conclusions

Saccharides and hydroxycarboxylic acids can substitute alkoxy groups from metal alkoxides. Thus, composites in which optically active organic compounds such as D-fructose, D-sorbitol and L-tartaric acid are highly dispersed in silica can be obtained by a sol–gel procedure using tetraethoxysilane as the silica source.

The composites obtained by the sol–gel procedure show much higher abilities in the optical resolution of tris(2,4-pentanedionato)metal complexes than those obtained by kneading and impregnation procedures, and optically active saccharides and hydroxycarboxylic acids themselves.

The sol–gel procedure is suitable for drawing out the potential of optically active organic compounds for chirality recognition or certain combined effects of organic and inorganic compounds.

References

[1] H.E. Lee and H.W. Jarrett, *J. Chromatogr.*, 511 (1990) 69.
[2] F. Gasparrini, D. Misiti, C. Villani, F. La Torre and M. Sinibaldi, *J. Chromatogr.*, 457 (1988) 235.
[3] S. Oi, M. Shijo and S. Miyano, *Chem. Lett.*, (1990) 59.
[4] W.H. Pirkle and T.C. Pochapsky, *J. Am. Chem. Soc.*, 108 (1986) 352.
[5] Y. Dobashi and S. Hara, *J. Org. Chem.*, 52 (1987) 2490.
[6] S. Oi, M. Shijo, Y. Yamashita and S. Miyano, *Chem. Lett.*, (1988) 1545.
[7] G. Blaschke, W. Bröker and W. Fraenkel, *Angew. Chem., Int. Ed. Engl.*, 25 (1986) 830.
[8] P. Roumeliotis, A.A. Kurganov and V.A. Davankov, *J. Chromatogr.*, 266 (1983) 439.
[9] Y. Okamoto, S. Honda, I. Okamoto and H. Yuki, *J. Am. Chem. Soc.*, 103 (1981) 6971.
[10] T. Shibata, I. Okamoto and K. Ishii, *J. Liq. Chromatogr.*, 9 (1986) 313.
[11] Y. Okamoto, M. Kawashima, K. Yamamoto and K. Hatada, *Chem. Lett.*, (1984) 739.
[12] T. Shibata, T. Sei, H. Nishimura and K. Deguchi, *Chromatographia*, 24 (1987) 552.
[13] Y. Okamoto, R. Aburatani, T. Fukumoto and K. Hatada, *Chem. Lett.*, (1987) 1857.
[14] H.R. Allcock, *Adv. Mater.*, 6 (1994) 106.
[15] T. Moller and E. Grulyas, *J. Inorg. Nucl. Chem.*, 5 (1958) 245.
[16] *The Merck Index*, Merck, Rahway, NJ, 1968.
[17] R.B. Von Dreele and R.C. Fay, *J. Am. Chem. Soc.*, 93 (1971) 4936.
[18] R.C. Fay, A.Y. Girgis and U. Klabunde, *J. Am. Chem. Soc.*, 92 (1970) 7075.
[19] H. Yoneda, U. Sakaguchi and Y. Nakashima, *Bull. Chem. Soc. Jpn.*, 48 (1975) 1200.
[20] K.L. Stevenson, *J. Am. Chem. Soc.*, 94 (1972) 6652.
[21] F. Stern and C.A. Beevers, *Acta Crystallogr.*, 3 (1950) 341.
[22] Y. Okaya and N.R. Stemple, *Acta Crystallogr.*, 21 (1966) 237.

ELSEVIER

Journal of Chromatography A, 697 (1995) 289–294

JOURNAL OF CHROMATOGRAPHY A

High-performance liquid chromatographic determination of the geometrical isomers of β-carotene in several foodstuffs

Cassia R.L. Carvalho[a,b], Paulo Roberto N. Carvalho[b], Carol H. Collins[a,*]

[a]*Instituto de Química, Universidade Estadual de Campinas, Caixa Postal 6154, 13083-970 Campinas, Brazil*

[b]*Instituto de Tecnologia de Alimentos, Av. Brasil 2880, 13073-001 Campinas, Brazil*

Abstract

To better evaluate the provitamin A content of foodstuffs, an HPLC separation of the geometric isomers of β-carotene was developed. Of the several different stationary phases studied, the best separations of all-*trans*-, 9-*cis*- and 13-*cis*-β-carotene were obtained with calcium hydroxide columns using isocratic elution with *n*-hexane, isooctane or mixtures of these solvents. When xanthophyll pigments are also present, a gradient elution with acetone in isooctane is required. These techniques were used to determine the provitamin A content of squash, peaches, dendê oil (palm tree oil) and orange juice.

1. Introduction

Carotenoids, a class of naturally occurring hydrocarbons (commonly called carotenes) and their oxygenated derivatives (xanthophylls) are ubiquitous in nature. Those carotenoids with at least half of the β-carotene molecule, i.e., an unsubstituted β-ionone ring having an 11-carbon polyene side chain, are classified as metabolic precursors of vitamin A, which is considered important for vision and, possibly, as an anticarcinogenic agent. Thus, quantification of the provitamin A activity of foodstuffs is of primary importance, to access the contribution of the individual carotenoids present.

Traditional analyses of carotene mixtures have involved paper, thin-layer, normal phase gravity-flow column, and both normal- and reversed-phase HPLC [1]. One of the problems common to these chromatographic methods in determining the provitamin A content of foodstuffs is the separation of the different geometrical isomers, which have considerably different provitamin A activities [2]. For example, 13-mono-*cis*-β-carotene has 53% and 9-mono-*cis*-β-carotene has 38% of the activity of *trans*-β-carotene [3]. All *trans*-α, 13-mono-*cis*-α- and 9-mono-*cis*-α-carotene have 37%, 22% and 23%, respectively, of the activity of *trans*-β-carotene [4]. Other authors [5,6] have reported different values but the overall impression is the same: *trans*-β-carotene is an excellent source of provitamin A while the other carotenes contribute significantly lower quantities. Thus separation and quantification of the geometrical isomers is relevant in determining the provitamin A content of foodstuffs.

Currently, HPLC is considered the method of choice for provitamin A determination as it circumvents various analytical difficulties encountered with the classical methods. Most of the HPLC methods reported for provitamin A

* Corresponding author.

0021-9673/95/$09.50
SSDI 0021-9673(94)00752-7

determinations have used reversed-phase (C_{18}) columns [7], since these appear to reduce the risk of pigment degradation attributed to silica columns [8]. The use of alumina [9], magnesium oxide [10,11], calcium hydroxide [12,13], amino [14], and nitrile [15] columns has also been reported. However, most of these columns do not satisfactorily separate the geometrical isomers [16].

The objective of this work is to develop a separation of the geometrical isomers of β-carotene to better evaluate the provitamin A content of several foodstuffs.

2. Experimental

2.1. Chemicals

All reagents and solvents were of analytical or chromatographic grade. All solutions were stored in brown flasks or protected from light by aluminium foil. Pure samples of *trans*-β-carotene were obtained by extracting a carotenoid mixture from appropriate vegetable samples and separating this mixture by gravity-flow liquid chromatography with a mixture of calcium hydroxide and Hyflosupercel as stationary phase and elution with increasing quantities of ethyl ether in petroleum ether [2]. Isomerization, to obtain 9-*cis*- and 13-*cis*-β-carotene, was done by exposure to visible light in the presence of iodine dissolved in ethyl ether. The isomerized samples were also separated by gravity-flow chromatography and identified by UV–visible absorption spectra and appropriate chemical reactions [17]. The standards were used immediately after separation and identification.

2.2. Food samples

Oranges (*Citrus sinensis* Osbeck), yellow squash (*Curcubita maxima*), dendê oil (*Elaeis guineensis*, L.) and fresh peaches (*Prunus persica*) were purchased from supermarkets in Campinas, Brazil. These foods were chosen because of their varying carotenoid composition and their content of possible interfering substances. The squash and peach samples (10–30 g) were finely chopped and then homogenized for three min in a Waring blender containing 100 ml of acetone and 10 g of Hyflosupercel [18]. The resulting suspension was suction-filtered and the acetone extraction of the solids was repeated until complete removal of the pigments. The combined filtrates were partitioned with petroleum ether and this solution was washed with distilled water. The orange juice and dendê oil samples were similarly extracted with acetone, partitioned, and washed. The samples were saponified by treatment with 10% (v/v) methanolic potassium hydroxide overnight, followed by washing with distilled water. The final petroleum ether solution was dried by passing it through a short column containing anhydrous sodium sulfate. This solution was then concentrated on a rotary evaporator for injection into the chromatograph.

2.3. Chromatographic columns

Three commercial and two laboratory-packed columns were evaluated: a 125 × 4 mm I.D. LiChrocart column containing 5 μm LiChrosphere 100-RP-18 (Merck) with a C_{18} precolumn (Merck); a 125 × 4 mm I.D. LiChrocart column containing 5 μm LiChrosphere 100-NH_2 (Merck) with a NH_2 precolumn (Merck); a 250 × 2 mm I.D. column containing 10 μm Micropak-CN (Varian); a 150 × 4 mm I.D. laboratory-packed column containing 5 μm LiChrosorb Alox-T (Merck) and a 250 × 2.2 mm I.D. laboratory-packed column containing $Ca(OH)_2$ (Nakarri Chemicals).

2.4. Equipment

HPLC separations were carried out on a Varian Model 5000 liquid chromatograph equipped with a Rheodyne Model 7125 injection valve with a 10-μl loop and an oven with both heating and cooling capabilities. Detection was with a Varian Model 100 variable-wavelength spectrophotometric detector coupled to an Infralab Model 4290 integrator or with a Shimadzu Model SPDM6A diode array detector coupled to an Acer Model 915 V microcomputer. Absorption spectra were obtained with a VanDen Model PC2500 double beam UV–visible spectropho-

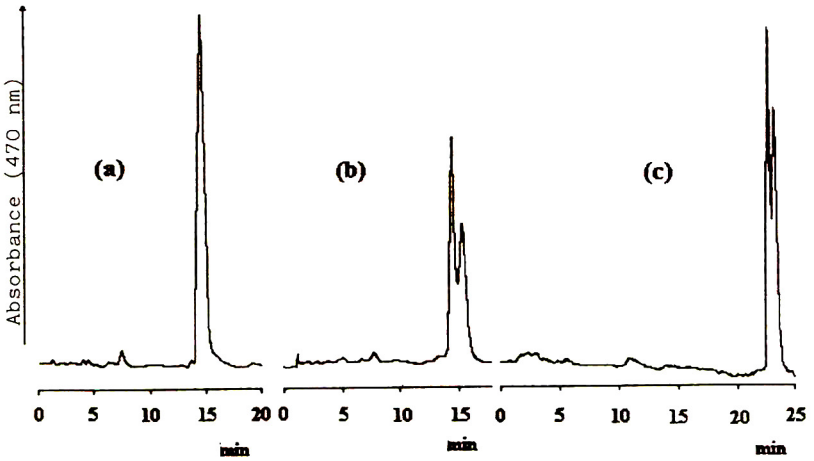

Fig. 1. Chromatograms of *trans*-β-carotene before (a) and after (b,c) isomerization. Column: 125 × 4 mm I.D. with LiChrospher 100 RP-18, 5 μm. Mobile phase: a,b = methanol–acetone (90:10, v/v) at 1.0 ml min^{-1}; c = pure methanol (15 min) then acetone 50% in 5 min, flow-rate 0.7 ml min^{-1}. Detection: absorbance at 470 nm.

tometer using 1 cm silica cells, coupled to an Intralab Model Omega recorder.

2.5. Calculation of the vitamin A value

One retinol equivalent (RE) corresponds to 6 μg of the provitamin A *trans*-β-carotene. The comparative provitamin A activity of the other carotenoids was taken from tabulated values [2,3].

3. Results and discussion

Separations on the C_{18} column were tested using different mixtures of methanol–water; methanol–acetone; methanol–chloroform, and

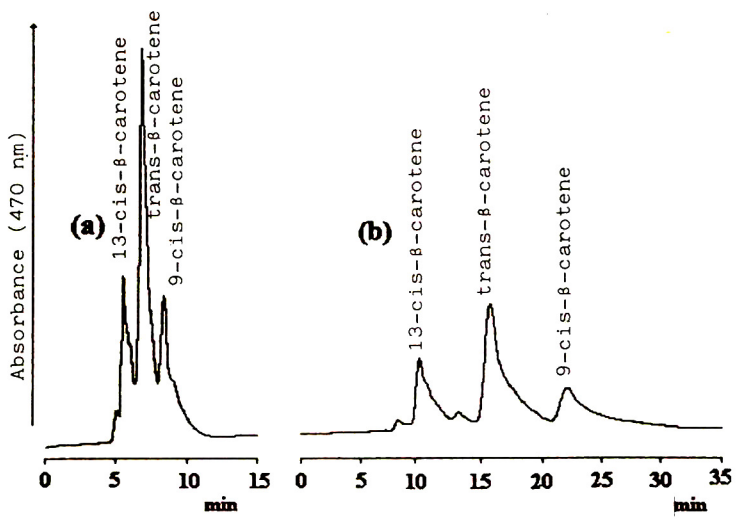

Fig. 2. Chromatograms of isomerized *trans*-β-carotene. Column: 250 × 2.2 mm I.D. with $Ca(OH)_2$. Mobile phase: (a) *n*-hexane; (b) isooctane, at 0.5 ml min^{-1}. Detection: absorbance at 470 nm.

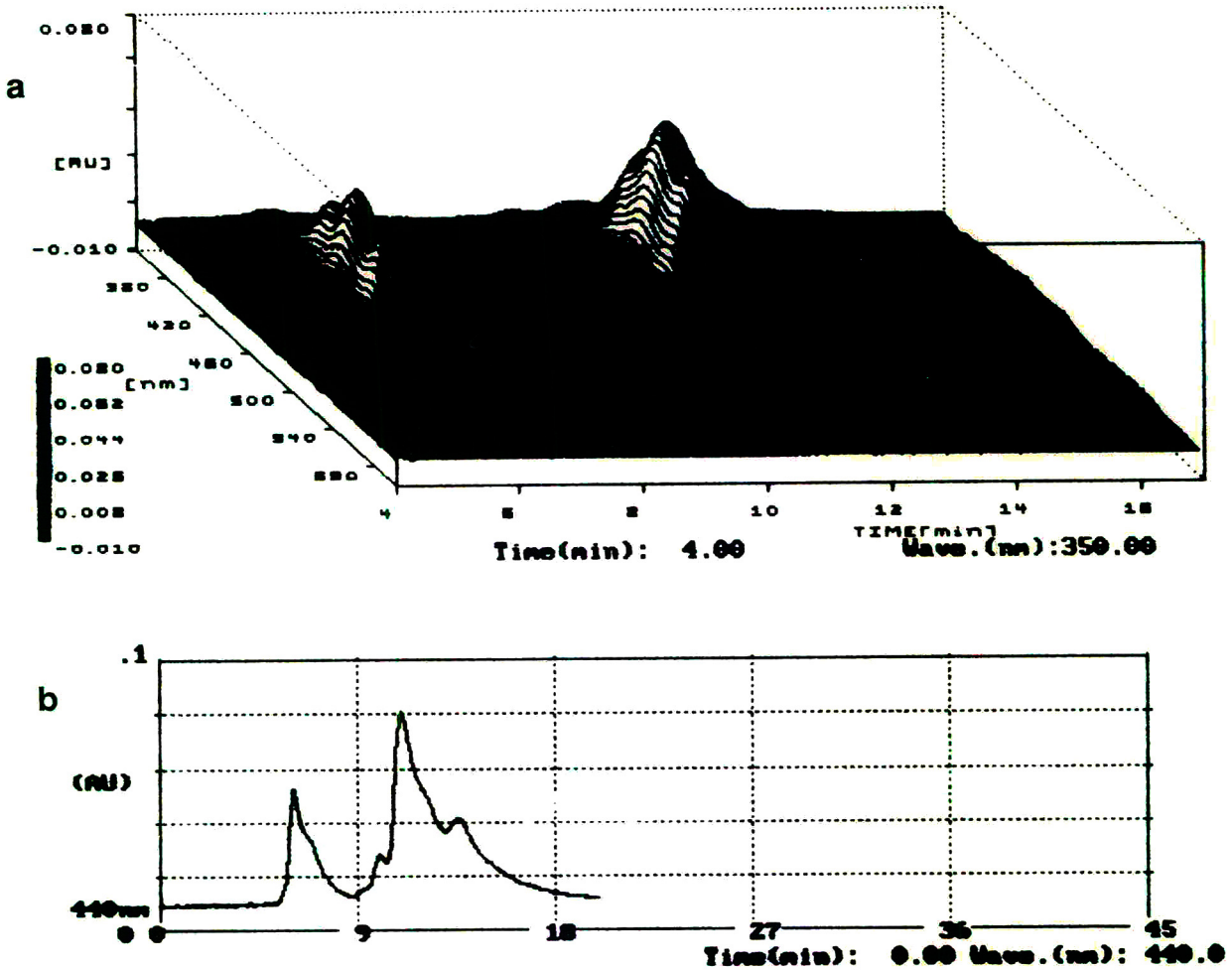

Fig. 3. Chromatograms of the carotenoids extracted from dendê oil. Column: 250 × 2.2 mm I.D. with $Ca(OH)_2$. Mobile phase: isooctane at 0.5 ml min^{-1}. (a) three-dimensional; (b) two-dimensional chromatogram at 440 nm.

ethanol–acetone. Partial separation of the *cis*- and *trans*-isomers was obtained using a 90:10 (v/v) methanol–acetone phase or with gradient elution with the same solvents. However, the two *cis* isomers were not separated under any conditions on this C_{18} phase (Fig. 1).

Separation of *cis* from *trans* isomers was also observed using the CN column with *n*-hexane. Mobile phase mixtures of hexane with dichloromethane, acetone or acetonitrile did not improve this separation. On the other hand, neither the NH_2 nor the Alox-T columns provided any separation of these geometrical isomers.

The best separations of all three geometrical isomers were observed with the calcium hydroxide column (Fig. 2), in agreement with previous literature [12,13]. Variation of the column temperature between −25°C and +40°C did not cause significant changes in the resolution although changes in retention times were observed. Thus, the column was used at room temperature with isooctane at a flow-rate of 0.5 ml min^{-1} for the quantification of the geometrical isomers in yellow squash and dendê oil (Fig. 3). A gradient from 100% isooctane to isooctane–acetone (80:20) in 60 min, also at a

flow-rate of 0.5 ml min^{-1}, was used for the orange and peach samples (Fig. 4) to separate β-cryptoxanthin from the β-carotenes.

Table 1 reports the provitamin A contents of the four foodstuffs studied in this work. The final column of this table lists the retinol equivalents (RE). For yellow squash, where only *trans*-β-carotene is observed, and orange juice, where only traces of the *cis*-β-carotene isomers are found, the RE values are similar to those previously determined [10,11]. The RE values reported here for dendê oil are less than those of the literature [19] since poor resolution of the geometrical isomers resulted in an overestimation of the *trans*-β-carotene content. Several recent studies using HPLC with extracts from peaches [20,21] have reported the separation and identification the β-carotene isomers. In the present work, β-cryptoxanthin was also quantified.

Despite the inconvenience of having to prepare the calcium hydroxide column in the laboratory, the resulting separations confirm this to be an excellent stationary phase for the separation

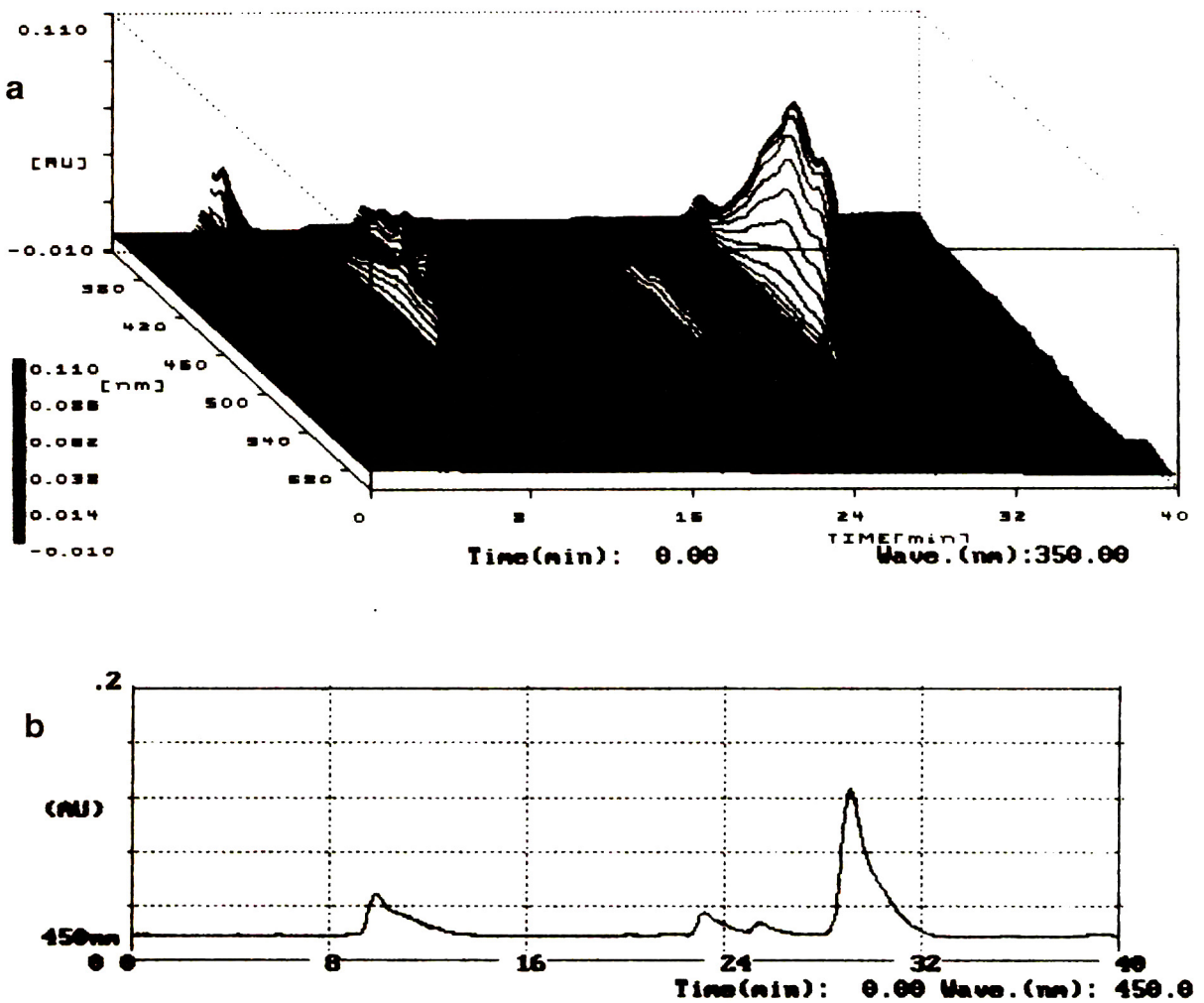

Fig. 4. Chromatogram of the carotenoids extracted from peaches. Mobile phase: gradient from isooctane to isooctane–acetone (80:20, v/v) in 60 min and detection at 450 nm. Other conditions as in Fig. 3.

Table 1
Provitamin A content of several foodstuffs

Foodstuff	Sample	Provitamin A found (mg/100 g)					Average retinol equivalent (RE/100 g)
		α-Carotene	13-*cis*-β-Carotene	*trans*-β-Carotene	9-*cis*-β-Carotene	β-Cryptoxanthin	
Yellow squash	1	–	–	0.93	–	–	
	2	–	–	0.82	–	–	150
	3	–	–	0.94	–	–	
Orange juice	1	0.007	tr[a]	0.011	–	0.016	
	2	0.009	tr	0.014	–	0.020	4.3
	3	0.009	tr	0.011	–	0.019	
Peaches	1	–	tr	0.17	–	0.58	
	2	–	tr	0.16	–	0.53	75
	3	–	tr	0.17	–	0.59	
Dendê oil	1	5.67	1.37	19.6	2.36	–	
	2	5.77	0.77	19.2	1.43	–	3960
	3	5.42	1.45	19.9	2.11	–	

[a] tr = Present at trace levels too low to quantify.

of the β-carotene isomers, permitting better estimation of the true provitamin A content of the foodstuffs tested. In the absence of xanthophylls, isocratic elution with isooctane is effective, however, elution of the more highly retained oxygenated compounds, after the β-carotene isomer separation, requires a gradient with a more polar component.

Acknowledgements

The authors express their appreciation to EMBRAPA for a fellowship to CRLC and to CNPq and FAEP (UNICAMP) for financial support.

References

[1] O.H. Will III and U. Ruddat, *LC Mag.*, 2 (1984) 610.
[2] D.B. Rodriguez-Amaya, *J. Micronutr. Anal.*, 5 (1989) 191.
[3] J.C. Bauerfeind, *J. Agric. Food Chem.*, 20 (1972) 456.
[4] J.P. Sweeney and A.C. Marsh, *J. Nutr.*, 103 (1973) 20.
[5] H.J. Deuel, Jr., C. Johnston, E.R. Meserve, A. Polgas and L. Zechmeister, *Arch. Biochem.*, 7 (1945) 247.
[6] R.M. Johnson and C.A. Baumann, *Arch. Biochem.*, 14 (1947) 361.
[7] P.R.N. Carvalho, C.H. Collins and D.B. Rodriguez-Amaya, *Chromatographia*, 33 (1992) 133.
[8] T. Brauman and L.H. Grimme, *Biochim. Biophys. Acta*, 637 (1981) 8.
[9] S.K. Reeder and G.L. Park, *J. Assoc. Off. Anal. Chem.*, 58 (1975) 595.
[10] I. Stewart, *J. Assoc. Off. Anal. Chem.*, 60 (1977) 132.
[11] I. Stewart, *J. Aric. Food Chem.*, 25(1977) 1132.
[12] K. Tsukida, K. Saiki, T. Takii and Y. Koyama, *J. Chromatogr.*, 245 (1982) 359.
[13] L.A. Chandler and S.J. Schwartz, *J. Food Sci.*, 52 (1987) 669.
[14] R.J. Bushway, *J. Liq. Chromatogr.*, 8 (1985) 1527.
[15] H.T. Gillan and R.B. Johns, *J. Chromatogr. Sci.*, 21 (1983) 34.
[16] F.W. Quackenbush and R.L. Smallidge, *J. Assoc. Off. Anal. Chem.*, 69 (1986) 767.
[17] D.B. Rodriguez, L.C. Raymundo, T.C. Lee, K.L. Simpson and C.O. Chichester, *Ann. Bot. (London)*, 40 (1976) 615.
[18] A.Z. Mercadante and D.B. Rodriguez-Amaya, *Chromatographia*, 28 (1989) 249.
[19] J.A. Trujillo-Quijano, D.B. Rodriguez-Amaya, W. Esteves and G.F. Plonis, *Fat. Sci. Technol.*, 92 (1990) 222.
[20] F.W. Quackenbush, *J. Liq. Chromatogr.*, 10 (1987) 643.
[21] F. Khachik, G.R. Beecher and W.R. Lusby, *J. Agric. Food. Chem.*, 37 (1989) 1465.

ELSEVIER

Journal of Chromatography A, 697 (1995) 295–307

JOURNAL OF CHROMATOGRAPHY A

Use of chromogenic and fluorescent oxycarbonyl chlorides as reagents for amino acid analysis by high-performance liquid chromatography

H. Brückner*, M. Lüpke

Institute of Food Technology, University of Hohenheim, 70593 Stuttgart, Germany

Abstract

The aryloxycarbonyl chlorides 4-phenylazobenzyloxycarbonyl chloride (PAZ-Cl), *p*-nitrobenzyloxycarbonyl chloride (PNZ-Cl), *o*-nitrobenzyloxycarbonyl chloride (ONZ-Cl), 2-naphthoxycarbonyl chloride (NOC-Cl) and 2-(naphthylmethyl)oxycarbonyl chloride (NMOC-Cl) were used for the precolumn derivatization of amino acids. The separations of the derivatives thus formed by reversed-phase (C_{18} or C_8) high-performance liquid chromatography (HPLC) were investigated and compared with those with the established reagent 9-fluorenylmethoxycarbonyl chloride (FMOC-Cl). A robotic autosampler enabled the fully automated mixing of samples with alkaline borate buffers, addition of excess of reagents (and of the scavenger 1-aminoadamantane if required), the final dilution of aliquots of the reaction mixtures with sodium acetate buffers and solvents and injection on to the HPLC column. Derivatives were eluted from the columns at 45°C using gradients made up from sodium acetate buffers and acetonitrile. Derivatives were detected by their UV absorbance (PAZ-, PNZ- and ONZ-amino acids) or by their fluorescence (NOC-, NMOC- and FMOC-amino acids). Hydrolysates of equine myoglobin, bovine β-lactoglobulin A and bovine serum albumin were quantitatively analysed with the reagents NOC-Cl and PNZ-Cl and the results were found to be in good agreement with those obtained by derivatization with FMOC-Cl and with the calculated amino acid composition of the proteins.

1. Introduction

For the precolumn derivatization of mixtures of amino acids (AAs) with UV-absorbing, chromogenic or fluorescent reagents, and separation of the resultant derivatives by reversed-phase high-performance liquid chromatography (HPLC), a relatively large number of reagents have been described [1,2] and, in part, compared with each other [3,4]. A survey of the literature (where possible, newer references or reviews are cited in this paper to provide entries to the respective literature) shows that the currently most frequently used reagents are *o*-phthaldialdehyde together with various thiols [5–7], phenyl isothiocyanate [8–10], 9-fluorenylmethoxycarbonyl chloride (FMOC-Cl) [11,12], 4-dimethylaminoazobenzene-4′-sulfonyl chloride (dabsyl chloride, DABS-Cl) [13,14], 5-(dimethylamino)-naphthalene-1-sulfonyl chloride (dansyl chloride) [15] and Sanger-type reagents [16,17]. Chiral variants of several of these reagents suitable for the HPLC separation of DL-AAs as diastereoisomers have also been described [18–23].

In analogy with FMOC-Cl, substituted aryloxycarbonyl chlorides ("chloroformates" or, more correctly "carbonochloridates") as derivatizing reagents for amines or imines in general deserve

* Corresponding author.

0021-9673/95/$09.50
SSDI 0021-9673(94)00938-4

attention as a result of their high reactivity and structural diversity and the relative easy synthesis of these compounds. Use of an excess of oxycarbonyl chlorides under alkaline conditions for the precolumn derivatization of amino components should allow their quantitative derivatization within a short time and at ambient temperature. Consequently, 2-(9-anthryl)ethyl chloroformate [24] and 2-(1-pyrenyl)ethyl chloroformate [25] have been synthesized and used as fluorescent reagents for the derivatization and liquid chromatographic resolution of biogenic amines; these reagents are also considered to be suitable for the derivatization of AAs.

In this paper, we describe the use of PAZ-Cl, PNZ-Cl, ONZ-Cl, NOC-Cl and NMOC-Cl, which have not been employed before as analytical reagents for the precolumn derivatization of AAs, followed by the liquid chromatographic separation of the resultant derivatives, and compare their suitability with that of FMOC-Cl. The latter reagent [26], together with PAZ-Cl [27] and PNZ-Cl [28], were originally developed as selectively cleavable amino protecting groups in peptide chemistry and are variants of the classical reagent benzyloxycarbonyl chloride [29], usually designated Z-Cl in honour of one of its inventors, L. Zervas. NOC-Cl has been used for labelling amino acids in order to develop an assay for carboxy peptidase [30] and for the derivatization of drugs containing tertiary amino groups [31].

2. Experimental

2.1. Instruments

For HPLC, a LiChroGraph instrument consisting of an L-6200 pump, low-pressure gradient mixture, Model T-6300 thermostat, Model AS-4000 autosampler with freely programmable liquid handling functions and freely programmable sample and reagent racks, Mega D-2500 integrator and F-1050 fluorescence detector (with 12-μl cuvette) or SPD-6A variable-wavelength UV detector (with 8-μl cuvette) were used. Eluents were flushed with helium. Instruments were obtained from Merck–Hitachi (Darmstadt, Germany), with the exception of the UV detector, which was from Shimadzu (Kyoto, Japan).

For recording the absorption and fluorescence spectra shown in Fig. 2, a Hewlett-Packard (HP) LC 1090 Series L liquid chromatograph was used together with an HP 1046 fluorescence detector and an HP photodiode-array detector.

L-Alanine was derivatized by the AS 4000 autosampler, transferred to the HP LC 1090 liquid chromatograph and analysed using a Hypersil ODS column, particle size 5 μm, and gradient elution as described for the respective derivatives.

2.2. Columns

LiChroCART columns (250 mm × 4 mm I.D.) and precolumns (4 × 4 mm I.D.) were used. For analysis with PAZ-Cl the stationary phase was LiChrospher 100 RP-18 (5 μm) (guard column packed with the same material). For analyses with PNZ-Cl, ONZ-Cl and FMOC-Cl the stationary phase was Superspher 60 RP-8 (4 μm) and the respective guard columns were packed with LiChrospher 100 RP-8 (5 μm). For analyses with NOC-Cl and NMOC-Cl, the stationary phase was Superspher 100, RP-18, end-capped (4 μm), and the guard columns were packed with LiChrospher 100, RP-8 (5 μm).

2.3. Solvents, chemicals and reagents

Acetonitrile (MeCN) was of HPLC grade from Baker (Deventer, Netherlands). Tetrahydrofuran (THF) was of chromatography grade, acetic acid, boric acid and sodium hydroxide pellets were of analytical-reagent grade, toluene, dioxane, dichloromethane and dimethylformamide (DMF) were of synthetic grade, DMF being refluxed in the presence of ninhydrin and distilled before use; all these reagents were from Merck (Darmstadt, Germany). 2-Naphthol, 2-naphthylmethanol [(2-hydroxymethyl)napthalene], 2-nitrobenzyl alcohol (*o*-nitrobenzyl alcohol), quinoline and 1-aminoadamantane (1-adamantylamine, ADAM) were purchased from Aldrich (Steinheim, Germany) and 1.93 *M*

(20%) phosgene in toluene from Fluka (Buchs, Switzerland). FMOC-Cl was obtained from Merck.

PAZ-Cl and PNZ-Cl were purchased from Bachem (Bubendorf, Switzerland) and were recrystallized from light petroleum (b.p. 50–70°C). PAZ-Cl had m.p. 78–79.5°C (lit. [27] m.p. 82°C); PNZ-Cl had m.p. 28–30°C (lit. [28] m.p. 33.5–34°C).

NOC-Cl was synthesized in our laboratory from 30 mmol of 2-naphthol and 30 mmol of quinoline in a mixture of 18 g of toluene and 5 g of dichloromethane by treatment with 47 ml of 1.93 *M* phosgene in toluene at 0°C according to the literature [30]; yield 5.1 g (84%); m.p. 45–48°C (lit. [30] m.p. 65–67°C). NMOC-Cl was synthesized analogously from 10 mmol of 2-naphthylmethanol in 15 ml of toluene by treatment with 16 ml of 1.93 *M* phosgene in toluene at 0°C; yield 1.9 g (85%); m.p. 59–62°C (crystals). ONZ-Cl was synthesized from 10 mmol of 2-nitrobenzyl alcohol in 4 ml of dioxane and treatment with 15.5 ml of 1.93 *M* phosgene in toluene; yield 1.7 g (80%) (yellow oil). The oxycarbonyl chloride reagents used were of acceptable purity with regard of the aim of this work but were not of analytical quality.

2.4. Sources and hydrolyses of proteins

Bovine serum albumin (product No. 11920) and lyophilized equine myoglobin from skeletal muscle (product No. 29895) were purchased from Serva (Heidelberg, Germany). The myoglobin had, according to manufacturer's specification, a purity of >95% and consisted mainly of metymyoglobin. β-Lactoglobulin A from bovine milk (product No. L-7880) was obtained from Sigma (St. Louis, MO, USA). For AA determination, amounts of 3–5 mg were hydrolysed in 0.7 ml of 6 *M* HCl at 110°C for 41 h in 1-ml Reacti-vials (Wheaton, Millville, NJ, USA). Samples were evaporated to dryness in a stream of nitrogen (80°C at the beginning and ambient temperature at the end of the evaporation). The residues were dissolved in 700 μl of 0.1 *M* HCl and the solutions were filtered using disposable 0.2-μm ANOTOP membrane filters (Merck). Aliquots were used for analyses by HPLC with NOC-Cl, PNZ-Cl or FMOC-Cl as reagents (see below).

2.5. Amino acid standards

The AA standard mixtures were purchased from Sigma (product No. AA-S-18) or from Pierce (Product No. 20088). The standards were fortified (if required; see chromatograms) by addition of cysteic acid (CyA), Gln, 5-hydroxylysine (Hyl) (all from Sigma), L-*homo*-Arg, γ-aminobutyric acid (GABA) (from Serva), Asn (from Fluka) and ornithine (Orn) (from Merck). The hydrolysis-sensitive amino acids Asn and Gln were freshly added to standards before use.

2.6. Derivatization with oxycarbonyl chloride reagents and elution conditions for amino acid derivatives

Preparation of sodium acetate and sodium borate buffers

A 0.5 *M* sodium acetate (NaOAc) buffer was prepared from 0.5 mol of acetic acid in 950 ml of doubly distilled water, adjusted to pH 4.0 by addition of 20% (w/w) NaOH and made up to a final volume of 1 l by addition of water. We prepared 100 m*M* NaOAc eluent buffers of pH 4.4, 4.6 and 7.0 analogously, and 0.4 and 0.5 *M* sodium borate buffers were prepared similarly from solutions of boric acid, with adjustment of the pH to 8.0, 9.0 and 10.5 by addition of 20% NaOH and final dilution to 1 l.

Derivatization procedures for amino acids with the various reagents, performed by the robotic autosampler at ambient temperature, are described below. The column temperature was 45°C in all instances and the flow-rate of the mobile phases was 1.25 ml min^{-1} for all analyses with the exceptions of derivatization with NOC-Cl and NMOC-Cl, where it was 1.0 ml min^{-1} for analyses and 1.25 ml min^{-1} for equilibration.

PAZ-Cl

Amounts of 100 μl of 0.5 *M* sodium borate buffer (pH 9.0), 20 μl of AA standard mixture or analyte solution and 250 μl of PAZ-Cl solu-

tion (5 m*M* in MeCN) were mixed by the autosampler. After 5 min, 250 μl of ADAM solution [40 m*M* in acetone–water (3:1, v/v)] were added and, after a further 5 min, 320 μl of a mixture of 0.5 *M* NaOAc buffer (pH 4.0) and MeCN (1:1, v/v) were added to 80 μl of the reaction mixture and 20-μl aliquots were injected on to the HPLC column. For gradient elution of the derivatives, eluent A (100 m*M* NaOAc of pH 7.0) and eluent B (100% MeCN) were used. The gradient programme was 22 to 50% B (0–40 min), 50 to 80% B (40–45 min), 80 to 100% B (45–46 min), 100% B (46–55 min). The column was then equilibrated for 12 min with 22% B.

PNZ-Cl and ONZ-Cl

Amounts of 150 μl of 0.5 *M* sodium borate buffer (pH 10.5), 30 μl of AA standard mixture or analyte solution in 0.1 *M* HCl and 300 μl of PNZ-Cl (or ONZ-Cl) solution (50 m*M* in MeCN) were mixed by the autosampler. Then, in the case of derivatization with ONZ-Cl, after 2 min amounts of 300 μl of 40 m*M* ADAM in acetone–water (3:1, v/v) were added. After 2 min, 320 μl of a mixture of 0.5 *M* NaOAc (pH 4.0) and MeCN (1:1, v/v) were added to 80 μl of the reaction mixture and 20-μl aliquots were injected on to the HPLC column. For elution of the PNZ or ONZ derivatives, gradients from eluent A (100 m*M* NaOAc of pH 4.4 for PNZ and of pH 4.6 for ONZ) and eluent B (100% MeCN) were used. The gradient programme was 10 to 25% B (0–10 min), 25 to 30% B (10–20 min), 30 to 45% B (20–30 min), 45 to 100% B (30–35 min) and 100% B (35–40 min). The column was then equilibrated for 14 min with 10% B.

NOC-Cl and NMOC-Cl

Amounts of 100 μl of 0.4 *M* sodium borate buffer (pH 9.0), 20 μl AA standard mixture or analyte solution and 100 μl of NOC-Cl (or NMOC-Cl) solution (10 m*M* in MeCN) were mixed by the autosampler. After 2 min, 250 μl of ADAM solution [40 m*M* in acetone–water (3:1, v/v)] were added. After a further 2 min, 360 μl of a mixture of 0.5 *M* NaOAc (pH 4.0) and MeCN (1:1, v/v) were added to 40 μl of the reaction mixture and 20-μl aliquots were injected on to the HPLC column.

For the elution of the derivatives a ternary gradient from eluent A (100 m*M* NaOAc, pH 7.0), eluent B (100 m*M* NaOAc, pH 4.6) and eluent C (100% MeCN) was used. The gradient programme started with a mixture of 75% A, 15% B and 10% C, changing to 0% A, 70% B and 30% C (0–15 min), 0% A, 40% B and 60% C (15–30 min) and 0% A, 0% B and 100% C (30–35 min), followed by isocratic elution with 100% C (35–43 min). The column was then equilibrated for 13 min. The flow-rate was 1.0 ml min^{-1} during analyses and 1.25 ml min^{-1} for equilibration.

FMOC-Cl

Amounts of 100 μl of 0.4 *M* sodium borate buffer (pH 8.0), 20 μl of AA standard solution and 100 μl of FMOC-Cl solution (3 m*M* in acetone; MeCN is recommended as the solvent with UV detection) were mixed by the autosampler. After 2 min, 100 μl of ADAM solution [40 m*M* in acetone–water (3:1, v/v)] were added. After a further 2 min, 380 μl of a mixture of 0.5 *M* NaOAc (pH 4.0) and MeCN (1:1, v/v) were added to 20 μl of the reaction mixture and 20-μl aliquots were injected on to the HPLC column. For elution of the derivatives, gradients from eluent A [100 m*M* NaOAc of pH 4.6–THF–DMF (90:5:5, w/w/w)] and eluent B (100% MeCN) were used. The gradient programme was 7 to 15% B (0–10 min), 15 to 50% B (10–35 min), 50 to 100% B (35–40 min), isocratic elution with 100% B (40–45 min) and equilibration with 7% B for 10 min.

3. Results and discussion

The structures of the oxycarbonyl chloride reagents are illustrated in Fig. 1. The absorption spectra of L-Ala derivatized with PAZ-Cl and PNZ-Cl are shown in Fig. 2a and b, respectively, and the absorption and fluorescence spectra of L-Ala derivatized with NOC-Cl are shown in Fig. 2c and d, respectively. The spectra were taken under gradient elution conditions using a photo-

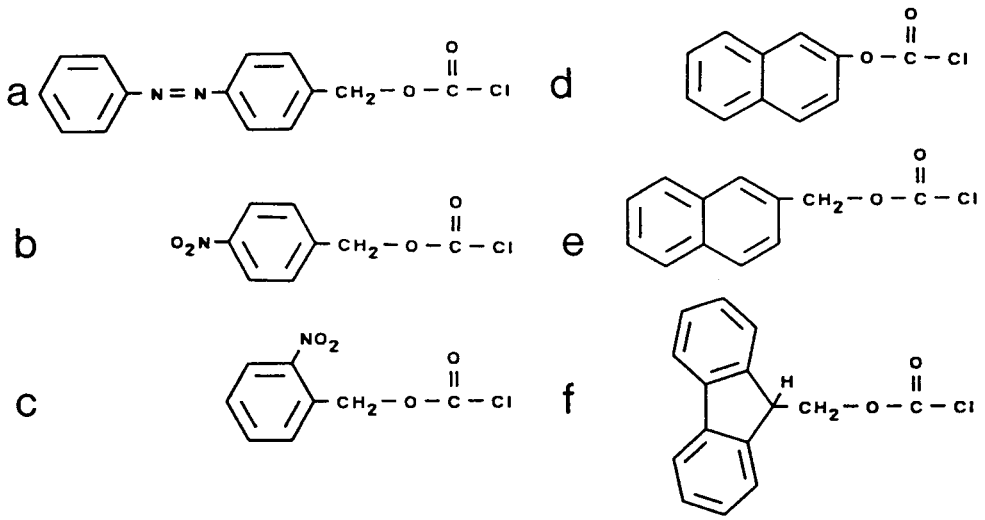

Fig. 1. Structures of (a) *p*-phenylazobenzyloxycarbonyl chloride (PAZ-Cl), (b) *p*-nitrobenzyloxycarbonyl chloride (PNZ-Cl), (c) *o*-nitrobenzyloxycarbonyl chloride (ONZ-Cl), (d) 2-naphthoxycarbonyl chloride (NOC-Cl), (e) 2-(naphthylmethyl)oxycarbonyl chloride (NMOC-Cl) and (f) 9-fluorenylmethoxycarbonyl chloride (FMOC-Cl).

diode-array detector or a fluorescence detector with the stopped-flow method (see Experimental).

The elution profiles of AA standard mixtures derivatized with PAZ-Cl, PNZ-Cl, ONZ-Cl NOC-Cl, NMOC-Cl and FMOC-Cl are shown in figs. 3–8. Chromatograms of analyses of hydrolysates of equine myoglobin with PNZ-Cl are shown in Fig. 4b and c and of bovine serum albumin with NOC-Cl in Fig. 6b.

Data for the analyses of hydrolysates of myoglobin, lactoglobulin and albumin using PNZ-Cl, NOC-Cl and FMOC-Cl are listed in Table 1 and agree satisfactorily with values calculated from the amino acid composition of these proteins.

Derivatization conditions as described under Experimental were investigated and optimized with respect to the pH of derivatization (tested range pH 7–11), derivatization temperature (tested range 4–60°C) and reaction time (tested range 2–20 min). The optimum pH for derivatization was 9.0 for NOC-Cl and PAZ-Cl, 10.5 for PNZ-Cl and 8.0 for FMOC-Cl. As a result of the fast reactions of the reagents, very little influence of temperature on derivatization yields was observed. The derivatization was completed within 2 min at room temperature, with the exception of PAZ-Cl, which needed 5 min. The conditions are a compromise, as the derivatization kinetics of the various AAs are slightly different and the use of larger excesses of reagents is limited by their solubilities. Intensive efforts were undertaken in order to optimize the gradient elution conditions with regard to the separation of AA derivatives on the stationary phases used. It is expected, however, that testing of other stationary phases and eluents will further improve those resolutions which are not completely satisfactory.

In the following we discuss the chromatograms in more detail.

Derivatization of a seventeen-component AA standard with PAZ-Cl (Fig. 3) leads to a satisfactory resolution of the derivatives, with the exception of Pro and Arg, which elute together under the chromatographic conditions used. PAZ-Cl is to some extent comparable to the structurally related DABS-Cl [13,14], which requires, however, derivatization of AA at 70°C for ca. 15 min. The PAZ-AAs, which at high concentration were intensely red, were detected by their absorption at 320 nm; a second absorption maximum was found in the visible range, in agreement with the literature [27] at 440 nm (cf., Fig.

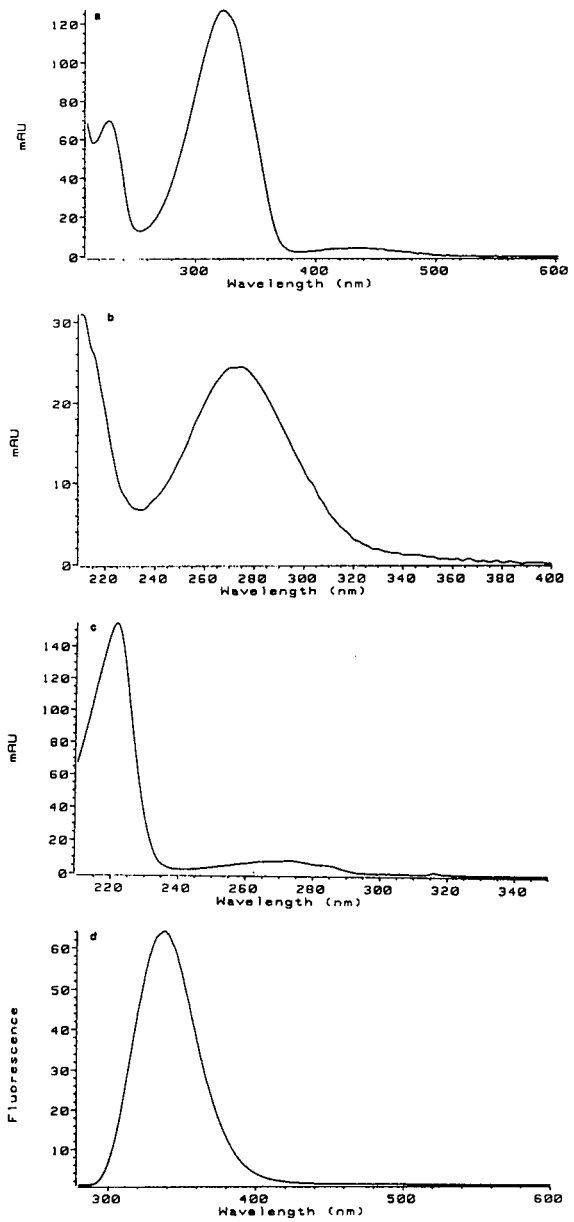

Fig. 2. Absorption spectra of L-Ala derivatized with (a) PAZ-Cl, (b) PNZ-Cl and (c) NOC-Cl, and (d) fluorescence spectrum of NOC-Ala when excited at 274 nm. For conditions see Experimental; mAU = milli-absorption units.

2a). It is worth noting that peaks arising from the hydrolysed reagent (designated A in the chromatograms) and the ammonolysis product of the reagent (designated B) elute at positions in the chromatogram which are not occupied by AAs, with the exception of cystine (designated Cys–Cys), which elutes close to the hydrolysed reagent. The peak designated C in this and the other chromatograms is assumed to be the carbonate formed by reaction of the respective oxycarbonyl chloride with its alcohol, the latter formed by partial hydrolysis of the chloride. Tyr gives rise to both the mono- and the disubstituted product under the derivatization conditions used. Four additional peaks, probably originating from impurities of the reagent (designated X in chromatograms), can be seen in the chromatograms but do not interfere with the AAs eluted. These peaks, and also those arising from impurities of the other oxycarbonyl chlorides used, might disappear if analytical-reagent grade reagents are prepared. The reaction product with the scavenger ADAM elutes with 100% MeCN and is not shown in the chromatograms.

The retention times of AAs measured on one column ($n = 5$) had a reproducibility of 0.11–0.32 min, and relative standard deviation (R.S.D.) of the retention times was 0.18–2.35%, with the exceptions of Glu and Asp, R.S.D.s of 6.16% and 7.21%, respectively; the R.S.D. of peak areas was 1–4% with respect to Val (Tyr >4%); linearity was found in the range 1.3–130 pmol per AA injected, and the correlation coefficient of linearity ($n = 3$ for each concentration, 7–9 calibration points were used in all experiments) was 0.993–0.999 for all AAs; the detection limit was approximately 0.5 pmol per AA.

We found that the resolution of PAZ-AA decreased after injection of a relatively small number (ca. 40) of samples. It appears that the PAZ derivatives are partly irreversibly bonded to the C_{18} stationary phase. It has not yet been investigated whether this phenomenon (which was not observed with the other oxycarbonyl chlorides investigated) can be overcome by changing the stationary phase.

The elution profile of AAs from a seventeen-component AA standard derivatized as described under Experimental with PNZ-Cl is shown in Fig. 4a. For quantification of the AAs in a total hydrolysate of equine myoglobin, the

Table 1
Amino acid (AA) composition of total hydrolysates[a] of proteins determined by HPLC ($n = 5$) and derivatization with NOC-Cl, PNZ-Cl and FMOC-Cl[b] in comparison with calculated (calc.) values [32–35][c]

AA	Equine myoglobin				Bovine β-lactoglobulin A				Bovine serum albumin[c]				
	NOC-Cl	PNZ-Cl	FMOC-Cl	Calc. [32]	NOC-Cl	PNZ-Cl	FMOC-Cl	Calc. [32]	NOC-Cl	PNZ-Cl	FMOC-Cl	Calc.	[33–35]
Asx	10.1	11.5	10.6	10.0	17.0	17.7	16.0	16.0	54.4	58.5	52.3	54.0	54.0
Glx	19.9	21.6	22.5	19.0	27.0	27.0	28.4	25.0	81.2	86.0	87.1	79.0	79.0
Ser	4.6	5.2	5.3	5.0	6.2	6.9	6.3	7.0	24.8	26.5	27.1	28.0	28.0
Gly	14.2	16.9	16.1	15.0	3.0	3.4	3.3	3.0	16.5	17.8	18.9	16.0	16.0
Arg	2.2	1.9	2.5	2.0	3.1	2.7	3.4	3.0	23.4	22.9	25.6	23.0	23.0
Thr	6.9	7.2	7.1	7.0	7.8	7.1	7.7	8.0	32.2	30.9	32.3	34.0	33.0
Ala	15.2	14.0	14.7	15.0	14.8	12.4	13.4	14.0	46.1	42.2	44.0	46.0	47.0
Pro	4.1	4.3	4.5	4.0	8.3	8.5	8.3	8.0	27.6	29.2	28.7	28.0	28.0
Val	7.0	7.4	7.4	7.0	10.5	10.5	10.1	10.0	36.3	37.2	36.5	36.0	36.0
Phe	7.2	7.6	7.8	7.0	4.3	4.4	4.2	4.0	27.7	29.2	27.7	27.0	27.0
Ile	8.4	9.0	9.1	9.0	9.8	9.6	9.7	10.0	13.6	14.6	14.2	14.0	14.0
Leu	17.4	17.6	18.5	17.0	23.8	22.2	23.0	22.0	61.2	61.3	62.6	61.0	61.0
His	10.6	14.5	10.6	11.0	1.7	2.3	1.7	2.0	15.6	19.4	13.7	17.0	17.0
Lys	19.5	20.1	20.0	19.0	15.1	14.4	14.3	15.0	61.3	61.0	58.7	59.0	59.0
Tyr	1.9	1.8	1.7	2.0	3.8	3.5	3.7	4.0	19.3	17.6	18.3	19.0	20.0

[a] Cys, Met and Trp (if present) not determined; Asx = Asp + Glu; Glx = Glu + Gln
[b] For abbreviations of reagents and derivatization conditions, see text.
[c] Suppliers do not provide or guarantee amino acid composition of proteins; in bovine serum albumin a difference is found for classical and DNA-deduced sequences.

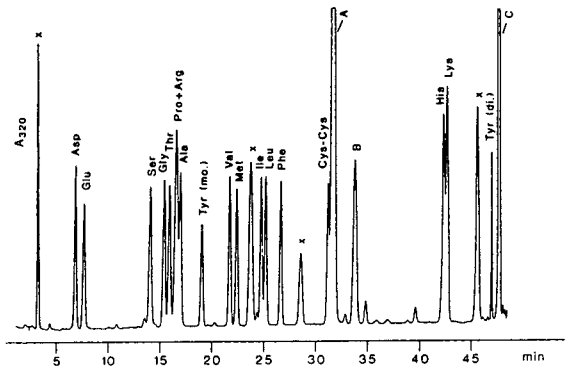

Fig. 3. Chromatogram of an AA standard (injected amounts 65 pmol per AA, cystine 32.5 pmol) derivatized with PAZ-Cl. A_{320} = absorption at 320 nm; peaks designated A, B, C and X in all chromatograms arise from reagents (see text); Cys–Cys = cystine; mo. and di. refer to mono- and disubstituted AA. For stationary phases, derivatization and elution conditions for all chromatograms, see Experimental.

absorption maxima at 265 nm of the weakly yellow derivatives were used (Fig. 4b). The ratios of those AAs that could be determined in the protein hydrolysate are given in Table 1. The AAs are satisfactorily resolved in these chromatograms. It was observed that, using a new stationary phase, Arg and Ala are completely resolved. During use, owing to the ageing of the column, Arg shows a shift in retention time and, finally, elutes together with Ala (Fig. 4c). This age-dependent shift of the retention time on reversed phases is characteristic of Arg and has also been reported for FMOC-Arg [11].

Asp and Ser are acceptably resolved on the column using the chromatographic conditions described for Fig. 4a and c. These AAs are baseline resolved on a new stationary phase using an eluent of pH 3.4, but this resolution occurs at the expense of that of other AAs. His and Tyr form disubstituted derivatives with an excess of reagent (cf., Fig. 4a and b); disubstituted His shows a time-dependent decay forming the monosubstituted derivative (ca. 50% in 24 h). The chromatograms in Fig. 4a and b were recorded directly after derivatization with PNZ-Cl, and therefore no monosubstituted His can be seen. The chromatogram shown in Fig. 4c was recorded ca. 2.5 h after derivatization; the monosubstituted His released at this time elutes close to Thr. Cystine elutes close to the hydrolysed reagent (A), and the ammonolysis product of the reagent (B) is satisfactorily resolved from Val.

The reproducibility of retention times of AA derivatives ($n = 5$), measured on one column, was 0.02–0.08 min, with an R.S.D. of 0.8–1.20% for Glu, Ser and Asp and 0.08–0.34% for the other AAs; The R.S.D. of peak areas ($n = 5$) was 1.5–4.0% (His >4%); linearity was found in the range 6–600 pmol per AA injected, the correlation coefficient of linearity ($n = 3$) was 0.9997–0.9998 for the AAs with the exceptions of cystine (0.9996), His (0.9994) and Tyr (0.9990); the detection limit was ca. 1 pmol per AA, with the exceptions of Met (6 pmol) and cystine (12 pmol).

The elution profile of a seventeen-component AA standard derivatized with ONZ-Cl in the presence of ADAM (which was not used for PNZ-Cl) as scavenger is shown in Fig. 5. The elution conditions are almost identical with those for the derivatives of PNZ-Cl (see Experimental) and the chromatograms look very similar. The position of the nitro group in these derivatives (*para* in PNZ-AAs and *ortho* in ONZ-AAs) therefore has little influence on retention times. Arg and Ala are resolved, but, cystine elutes together with an unknown component (designated X), Val together with X and the ammonolysis product of the reagent and disubstituted Tyr together with peak C. Peaks arising from ADAM and its derivatization product are eluted from the column when eluent B is applied and are not seen in the chromatograms. Acetone, eluting at the beginning of the chromatogram, had been used as the solvent for ADAM, but the use of MeCN is recommended when derivatives are determined by measuring their UV absorbance. As ONZ-Cl has no noticeable advantage over PNZ-Cl, the former reagent was not investigated further.

The elution profile of a 24-component AA standard, including hydrolysate AAs and also CyA, Asn, Gln, GABA, Hyl, Orn and homo-Arg, derivatized with NOC-Cl and followed by addition of the scavenger ADAM, is shown in

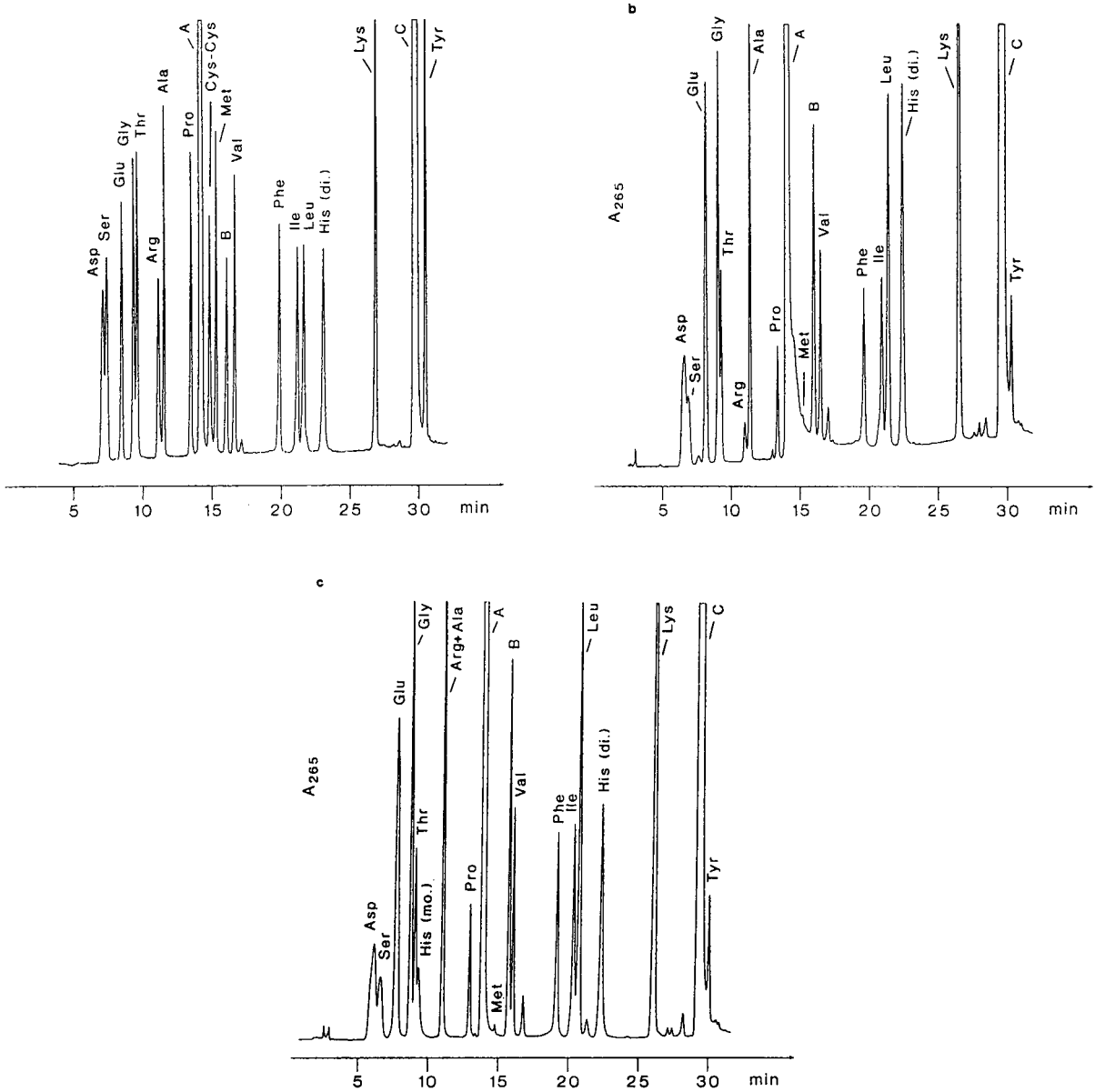

Fig. 4. Chromatograms of (a) AA standard on a new column (injected amounts 5 nmol per AA, cystine 2.5 nmol), (b) total hydrolysate of equine myoglobin (1.5 μg) derivatized with PNZ-Cl and immediately injected on to the column and (c) total hydrolysate of equine myoglobin injected 2.5 h after derivatization on to an aged column A_{265} = absorbance at 265 nm; for details, see text.

Fig. 6a. The fluorescence of the derivatives was measured at an emission of 336 nm with excitation at 274 nm. The AAs of the standard are satisfactorily resolved. Ser and Gln in the standard elute together; this might be a problem in physiological samples; Gln in proteins, however, is hydrolysed to Glu under the conditions of total hydrolysis (cf., Fig. 6b and Table 1). Tyr and His form mono- and disubstituted derivatives under the derivatization conditions used; monosubsti-

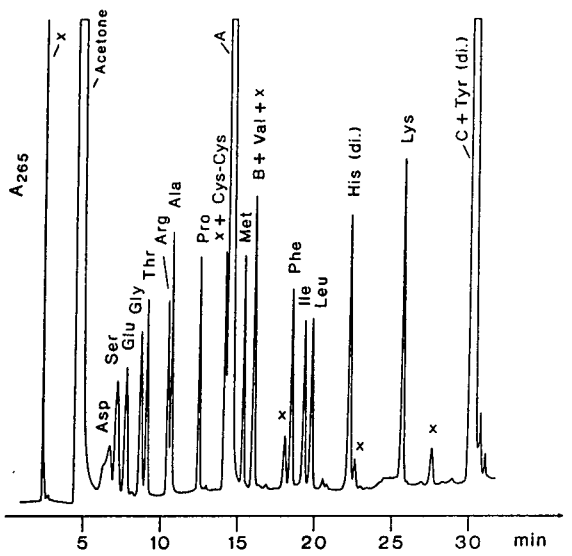

Fig. 5. Chromatogram of an AA standard derivatized with ONZ-Cl (injected amounts 0.4 nmol per AA, cystine 0.2 nmol). The same standard and column were used as in Fig. 4a; for other conditions, see Experimental.

tuted Tyr and His elute together. The disubstituted derivative of His forms ca. 50% monosubstituted His in 5 h. The phenomenon that His apparently forms two monosubstituted derivatives (designated mo. 1 and mo. 2), in addition to the disubstituted derivative (designated di.), requires further investigation (cf., Fig. 6a). For quantification of NOC-AA in Table 1 the disubstituted derivatives of Tyr and His were used.

The reproducibility of the retention times (n = 5) of the derivatives was 0.03–0.07 min; the R.S.D. of peak areas was 3.5–4.5% (monosubstituted His >4.5%); linearity was found in the range 0.9–45 pmol per AA injected, and the correlation coefficients of linearity of AA were 0.9995–0.9998 (Tyr, His and cystine <0.9995); the detection limit was ca. 25 fmol per AA, with the exceptions of mono- and disubstituted His (0.1 pmol) and cystine (0.5 pmol). The hydrolysed reagent (A) and the ammonolysis product (B) of the reagent elute together and do not overlap with the AA. Two additional peaks (X) arise from the reagent.

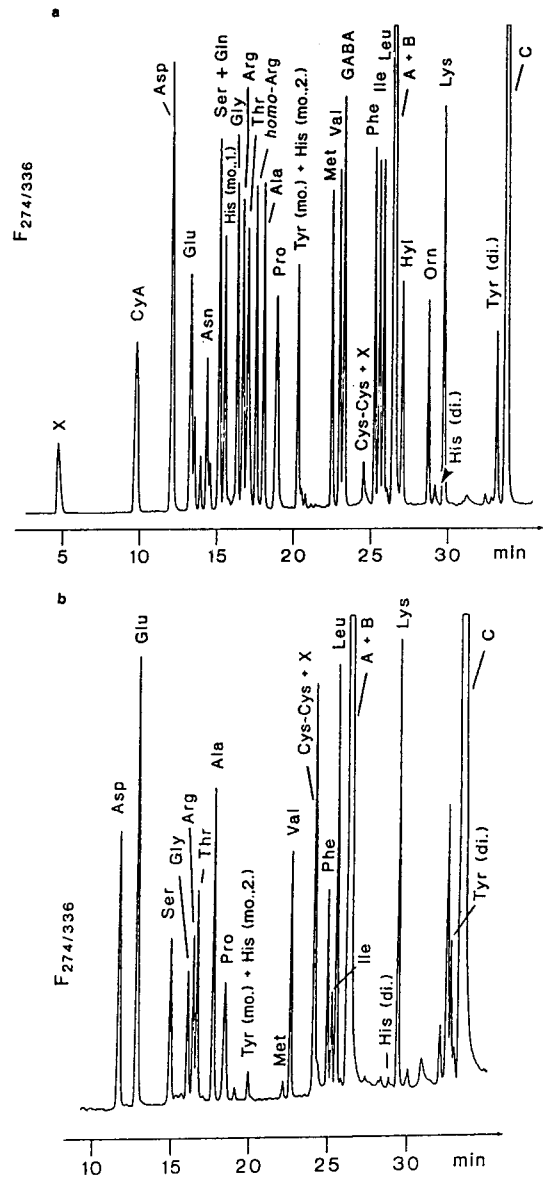

Fig. 6. Chromatograms of (a) an AA standard (injected amounts 10 pmol per AA, His 40 pmol, GABA and Asp 20 pmol, cystine 5 pmol) and (b) bovine serum albumin (3.5 ng total hydrolysate), both derivatized with NOC-Cl. $F_{274/336}$ = relative fluorescence at 274 nm (excitation) and 336 nm (emission).

Investigation of protein hydrolysates by use of NOC-Cl gave satisfactory ratios for AAs with respect to calculated data (cf., Table 1). The chromatogram of AAs from a total hydrolysate

of bovine serum albumin derivatized with NOC-Cl is shown in Fig. 6b. Met and Cys are partly oxidized and Trp is destroyed under the hydrolysis conditions used and therefore cannot be determined. Cystine elutes together with an unknown component and cannot be determined under the chromatographic conditions used; further, Cys also shows strong fluorescence quenching. For the determination of Tyr and His, the disubstituted derivatives were used.

The elution profile of a seventeen-component AA standard derivatized with NMOC-Cl is shown in Fig. 7. Under the chromatographic conditions used, this standard shows an unsatisfactory resolution of AA. Ser and the monosubstituted derivative of His and Pro and the monosubstituted derivative of Tyr are not resolved. Further, neither Val and the hydrolysed reagent (A), nor Phe, cystine and the ammonolysis product (B), nor Phe, cystine and the ammonolysis product (B), nor the disubstituted Tyr and peak C are separated. As the chromatographic conditions, in particular with respect to the selectivity of the stationary phase, can certainly be improved upon, no statistical data are given.

The elution profile of a 24-component AA standard, derivatized with FMOC-Cl, followed by addition of ADAM is shown in Fig. 8. The fluorescence of the derivatives was measured at an emission of 313 nm with excitation at 263 nm. All hydrolysate AAs and CyA are satisfactorily resolved from Asn and Gln and from the unusual AAs *homo*-Arg, GABA, Hyl and Orn, with the exceptions of the pair Val and GABA, which elute almost together. Tyr forms the mono- and disubstituted derivatives and His the disubstituted derivative. The latter is relatively stable and forms ca. 10% of the monosubstituted derivative in 24 h at room temperature.

For the determination of AAs in protein hydrolysates (Table 1), the monosubstituted derivative of Tyr and the disubstituted derivative of His were used. Cysteine, although a component of the standard, cannot be seen in the chromatogram, probably as a result of fluorescence quenching. Cysteine and cystine can be determined, however, by UV detection of derivatives, or after oxidation with formic acid

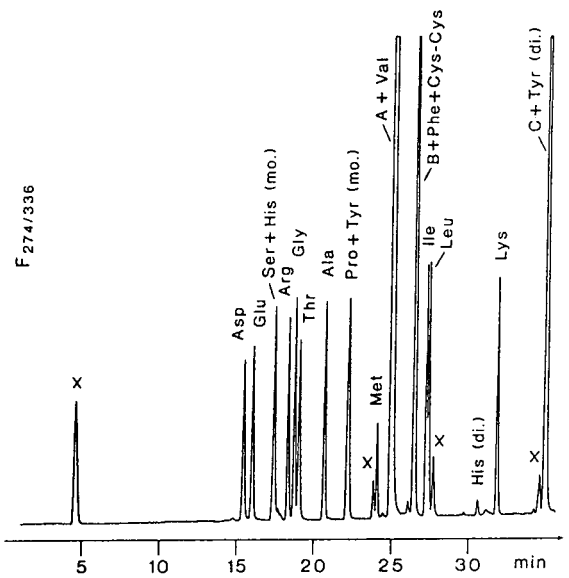

Fig. 7. Chromatogram of AA standard derivatized with NMOC-Cl (injected amounts 20 pmol per AA, cystine 10 pmol). $F_{274/336}$ = fluorescence at excitation 274 nm and emission of 336 nm.

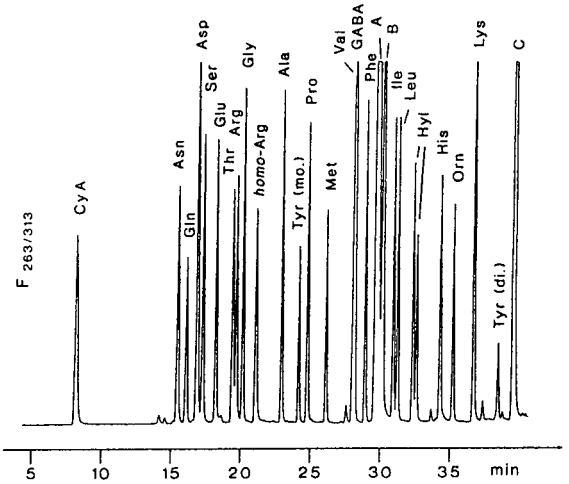

Fig. 8. Chromatogram of standard of AA derivatized with FMOC-Cl (injected amounts 6 pmol per AA, Asp 12 pmol, GABA 15 pmol, His 30 pmol). $F_{263/313}$ = relative fluorescence at 263 nm (excitation) and 313 nm (emission). CyA = Cysteic acid.

peroxide as cysteic acid (CyA) by measuring the fluorescence of the derivative. The hydrolysed reagent (A) and the ammonolysis product (B) of the reagent elute at a position not occupied by the AAs of the standard. Data of the analysis of the hydrolysed test proteins are given in Table 1.

The reproducibility of retention times ($n = 5$) was 0.02–0.10 min; the R.S.D. of peak areas ($n = 5$) was 2.0–5.0%; linearity of the detector response ($n = 3$) for each concentration was found in the range 0.06–6 pmol per AA injected; the correlation coefficient of linearity was 0.9995–0.9998 per AA (Tyr <0.9995). Under the chromatographic conditions used the detection limit is ca. 5 fmol per AA, with the exceptions of Ile and Leu (ca. 30 fmol), and Lys and disubstituted His (ca. 150 fmol). The excellent resolution of the AAs of the standard (which is among the best reported up to now) by derivatization with FMOC-Cl does not necessarily imply that this reagent is far superior to the others, in particular NOC-Cl. The chromatogram shown in Fig. 8 rather reflects the most intensive efforts with respect to the selection of an appropriate stationary phase together with optimum gradient elution conditions.

3.1. General aspects of the use of oxycarbonyl chlorides as derivatizing reagents

Ideally, reagents used for the precolumn derivatization of AAs, followed by the liquid-chromatographic separation of the derivatives formed, should react rapidly and quantitatively with the AAs at room temperature and yield stable derivatives. These should be detectable with high sensitivity by employing UV–visible or fluorescence detectors. The AA derivatives should follow the Beer–Lambert law over several orders of magnitude, and trifunctional AAs such as His, Tyr and Lys should yield uniform derivatives. The derivatization procedure should advantageously be carried out in a fully automated device [36] at room temperature, and the derivatives formed should be completely resolved within a short time on employing standard reverse-phase columns and simple linear gradient elution conditions. The stationary phase should also be stable for a large number of analyses. The method should at least allow the complete resolution of hydrolysate AAs including an internal standard or, ideally, of a mixture of so-called physiological AAs. Peaks necessarily arising from the unreacted or hydrolysed reagents, the carbonate formed therefrom, the ammonolysis product of the oxycarbonyl chloride and the reaction product formed from the scavenger and the excess of reagents should elute at positions away from those of the AAs to be determined, or be eluted last, and completely, from the column. Further, as secondary AAs such as Pro and Hyp, and also cysteine and cystine, are important protein AAs, the reagent should also allow their derivatization and determination. Finally, the reagent should be stable and of high purity and be commercially available at a moderate price. A critical survey of the literature reveals, however, that none of the reagents used for the precolumn derivatization and liquid chromatographic resolution of AAs fulfils all of the above requirements. Analysts agree, therefore, that the method that is finally chosen for AA analysis has to be a compromise depending on the aim of the work.

In comparison with other methods for the precolumn derivatization of AAs, the new reagents show the inherent advantages and disadvantages of oxycarbonyl chlorides, including FMOC-Cl: the reaction proceeds rapidly and quantitatively at room temperature with primary and secondary AAs, thus making derivatization chemistry fully automatable. Derivatives of the new reagents are stable for at least 3 days when stored at room temperature, with the exception of disubstituted His, which forms increasing amounts of monosubstituted His during storage. The necessary use of an excess of reagents and side-reactions lead to the formation of byproducts that interfere in the chromatography of AA derivatives. The ratio of mono- and disubstituted derivatives formed from His and Tyr depends on the structure and excess of reagents used. The latter is difficult to control in real samples and is limited by the solubility of reagents. In practice, an advantage of the oxycarbonyl chlorides de-

scribed is that an instrument designed for automated AA analysis employing automated pre-column derivatization chemistry can be easily used with the new reagents. Thus a change in the elution positions of AAs in chromatograms is possible where no interference by other AAs or certain absorbing components of the analyte occurs. This is of importance when AAs are to be determined in biomatrices, physiological samples or foodstuffs. In these cases the choice among reagents with different spectrophysical properties might also be of advantage. With respect to the overall resolution of derivatives, NOC-AAs are approximately comparable to FMOC-AAs; the simple eluent used for the separation of NOC-AAs, however, does not require addition of DMF and THF. Shortcomings of the chromatography of the derivatives of the other reagents should certainly be circumventable by testing other stationary phases. In conclusion, the availability of a set of highly reactive reagents and the favourable chromatographic properties of the derivatives formed therefrom should contribute to the advancement of AA analysis by HPLC.

References

[1] F. Lottspeich and A. Henschen, in A. Henschen, K.-P. Hupe, F. Lottspeich and W. Voelter (Editors), *High Performance Liquid Chromatography in Biochemistry*, VCH, Weinheim, 1985, pp. 139–216.

[2] C. Lazure, J.A. Rochemont, N.G. Seidah and M. Chrétien, in K.M. Gooding and F.E. Regnier (Editors), *HPLC of Biological Macromolecules: Methods and Applications*, Marcel Dekker, New York, 1990, pp. 263–300.

[3] P. Fürst, L. Pollack, T.A. Graser, H. Godel and P. Stehle, *J. Chromatogr.*, 499 (1990) 557.

[4] G. Sarwar and H.G. Botting, *J. Chromatogr.*, 615 (1993) 1.

[5] G. Georgi, C. Pietsch and G. Sawatzki, *J. Chromatogr.*, 613 (1993) 35.

[6] M.C. García Alvarez-Coque, M.J. Medina Hernández, R.M. Villanueva Camañas and C. Mongay Fernández, *Anal. Biochem.*, 178 (1989) 1.

[7] H. Godel, P. Seitz and M. Verhoef, *LC-GC Int.*, 5 (1992) 44.

[8] S.A. Cohen and D.J. Strydom, *Anal. Biochem.*, 174 (1988) 1.

[9] G. Sarwar and H.G. Botting, *J. Assoc. Off. Anal. Chem.*, 73 (1990) 470.

[10] I. Molnár-Perl, *J. Chromatogr. A*, 661 (1994) 43.

[11] B. Gustavsson and I. Betnér, *J. Chromatogr.*, 507 (1990) 67.

[12] P.A. Haynes, D. Sheumack, J. Kibby and J.W. Redmond, *J. Chromatogr.*, 540 (1991) 177.

[13] V. Stocchi, G. Piccoli, M. Magnani, F. Palma, B. Biagiarelli and L. Cucchiarini, *Anal. Biochem.*, 178 (1989) 107.

[14] D. Drnevich and T.C. Vary, *J. Chromatogr.*, 613 (1993) 137.

[15] M. Simmaco, D. De Biase, D. Barra and F. Bossa, *J. Chromatogr.*, 504 (1990) 129.

[16] R.C. Morton and G.E. Gerber, *Anal. Biochem.*, 170 (1988) 220.

[17] I. Fermo, E. De Vecchi, L. Diomede and R. Paroni, *J. Chromatogr.*, 534 (1990) 23.

[18] H. Brückner, S. Haasmann, M. Langer, T. Westhauser, R. Wittner and H. Godel, *J. Chromatogr. A*, 666 (1994) 259.

[19] J. Gal and A.J. Sedman, *J. Chromatogr.*, 314 (1984) 275.

[20] S. Einarsson, B. Josefsson, P. Möller and D. Sanchez, *Anal. Chem.*, 59 (1987) 1191.

[21] P. Marfey, *Carlsberg Res. Commun.*, 49 (1984) 591.

[22] H. Brückner and C. Gah, *J. Chromatogr.*, 555 (1991) 81.

[23] H. Brückner and B. Strecker, *J. Chromatogr.*, 627 (1992) 97.

[24] A.J. Faulkner, H. Veening and H.-D. Becker, *Anal. Chem.*, 63 (1991) 292.

[25] M.A. Cichy, D.L. Stegmeier, H. Veening and H.-D. Becker, *J. Chromatogr.*, 613 (1993) 15.

[26] L.A. Carpino and G.Y. Han, *J. Org. Chem.*, 37 (1972) 3404.

[27] R. Schwyzer, P. Sieber and K. Zatsko, *Helv. Chim. Acta*, 61 (1958) 491.

[28] F.H. Carpenter and D.T. Gish, *J. Am. Chem. Soc.*, 74 (1952) 3818.

[29] M. Bergmann and L. Zervas, *Ber. Dtsch. Chem. Ges.*, 65 (1932) 1192.

[30] G. Wolf and A.M. Seligman, *J. Am. Chem. Soc.*, 73 (1951) 2080.

[31] G. Gübitz, R. Wintersteiger and A. Hartinger, *J. Chromatogr.*, 218 (1981) 51.

[32] M.O. Dayhoff, *Atlas of Protein Sequence and Structure*, National Biomedical Research Foundation Georgetown University Medical Center, Washington, DC, Vol. 5, 1972, and Suppl. I, 1973.

[33] J.R. Brown, *Proc. FEBS Meet.*, 50 (1977) 1.

[34] R.G. Reed, E.W. Putnam and T. Peters, *Biochem. J.*, 191 (1980) 867.

[35] T. Peters, *Albumin —An Overview and Bibliography*, Miles, Kankakee, IL, 2nd ed., 1992.

[36] W.-D. Beinert, A. Meisner, M. Fuchs, E. Riedel, M. Lüpke and H. Brückner, *GIT Fachz. Lab. (Darmstadt)*, 36 (1992) 1018.

ELSEVIER

Journal of Chromatography A, 697 (1995) 309–315

JOURNAL OF CHROMATOGRAPHY A

Determination of the cysteine derivatives N-acetylcysteine, S-carboxymethylcysteine and methylcysteine in pharmaceuticals by high-performance liquid chromatography

F.Y. Tsai*, C.J. Chen, C.S. Chien

Department of Health, National Laboratories of Foods and Drugs, 161–2 Kuen Yang Street, Nankang, Taipei, Taiwan

Abstract

A high-performance liquid chromatographic method was developed for the determination of three mucolytic agents, N-acetylcysteine (NACS), S-carboxymethylcysteine (SCMCS) and methylcysteine (MCS). Chromatography was performed on an ODS column using an isocratic mobile phase consisting of acetonitrile, methanol and sodium hexanesulfonic acid buffer (pH 2.9) at a flow-rate of 1.0 ml/min, with UV detection at 220 nm. Methionine was used as an internal standard. Good quantitative results were obtained, the recoveries from synthetic mixtures being >98.2% with R.S.D. <1%. Linearity over a concentration range of over one order magnitude was obtained; the correlation coefficients were >0.9997 at concentrations of 0.05, 0.1, 1.0, 2.0 and 3.0 mg/ml. The addition of methanol and acetonitrile to the mobile phase improved the peak shape and retention of the compounds of interest. The selectivity of the method was demonstrated by separating four similar thiol compounds and determination of the analytes in pharmaceuticals.

1. Introduction

The cysteine derivatives N-acetylcysteine (NACS), S-carboxymethylcysteine (SCMCS) and methylcysteine (MCS), amino acid-like compounds, are members of the group of mucolytic agents. They are used to reduce the viscosity of pulmonary secretions [1], to improve chronic bronchitis by reducing coughing and sputum [2], as nebulizers [3] and as aids suppressing coughing in anti-influenza preparations. They can also protect against hepatoxicity of high doses of acetaminophen [4–6].

Numerous methods have been studied for their determination. NACS has been determined by colour development with iron(III) in the presence of 1,10-phenantholine [7], potentiometrical titration of the thiol group with mercury (II) nitrate [8,9] and spectrophotometry [10]. These methods were not specific and were unable to distinguish among thiol-containing compounds. Various advanced methods for NACS have been tested, with postcolumn [11,12] and precolumn [13,14] derivatization with 4-fluoro-7-nitrobenzo-2,1,3-oxadiazole, N-[4-(6-dimethylamino-2-benzofuranyl)phenyl] [maleimide and 2,4-dinitro-1-fluorobenzene, and spectrofluorimetry. A gas chromatographic (GC) method for SCMSC, of high volatility, involved time-consuming sample preparation because it required derivatization with N,O-bis(trimethyl)-trifluoroacetamide–1% trimethylchlorosilane [15], and HPLC with buffered eluents [15–18]. The sample preparation time using GC assay was

* Corresponding author.

0021-9673/95/$09.50
SSDI 0021-9673(94)00959-7

about 3–4 h. No method has been reported for MCS.

This paper describes an HPLC method using sodium hexanesulfonic acid, which can eliminate the interference from other organic thiol-containing compounds, and allows NACS, SCMCS and MCS to be distinguished from each other. It also represents a distinct challenge because of the lack of a UV chromophore in the molecule. The UV detection mode at low wavelength limits the mobile phase modifier that can be used to enhance selectivity and peak shape. For the recovery study, synthetic mixtures were made up with lactose and potato starch. The aim of this work was to establish a routine method and deal with the above problem to provide an assay procedure for the determination of NACS and its analogues in pharmaceuticals, synthetic mixtures or bulk drugs.

2. Experimental

2.1. Materials and reagents

HPLC-grade methanol, acetonitrile and phosphoric acid and analytical-reagent grade sodium hydrogen sulfite were purchased from Merk (Darmstadt, Germany) and sodium hexanesulfonic acid, standard NACS and MCS and the internal standard methionine from Sigma (St. Louis, MO, USA) and SCMCS was donated by Isochem (Philippelbon, Gennevillers, France). Various production forms were purchased commercially. Excipients, lactose and potato starch, used in synthetic formulations, were of reagent grade. Water was of HPLC grade, obtained by passage through a 0.22-μm membrane filter (Waters Milli-Q SP reagent water system).

2.2. Apparatus

A Model 600 E liquid chromatographic dual-pump system controller, Model 700 Satellite WISP autosampler with a loop injection valve, Model 486E tunable UV detector and 745B data module integrator (Waters, Bedford, MA, USA) were employed. The mobile phase was pumped through a reversed-phase column (μBondapak ODS, 30 cm × 3.9 mm I.D.; 10 μm; Waters) with an isocratic flow-rate of 1 ml/min. The detector was set at 220 nm. Chromatography was performed at room temperature. Injections of 10 μl of all solutions at concentrations of 0.05–3.0 mg/ml, synthetic formulations and commercial products were made.

2.3. Mobile phase

A series of mobile phases of 5 m*M* sodium hexanesulfonic acid (pH 2.9) with different percentages of organic modifier were prepared in order to study the effect of solvent strength. Another mobile phase composition of 5 m*M* sodium hexanesulfonic acid (pH 2.9)–acetonitrile–methanol (98.6:0.8:0.6, v/v/v) was prepared, the pH being adjusted with phosphoric acid. This solution was filtered through a membrane of 0.45 μm, degassed under a stream of helium and used to establish the best separation and peak shape.

2.4. Internal standard stock standard solution

Methionine (250 mg) was dissolved in 40 ml of 0.05% sodium hydrogensulfite solution and adjusted to pH 3 with phosphoric acid. The flask was shaken in an ultrasonic bath and diluted to 50 ml with methanol.

2.5. Standard solutions

To prepare each standard solution, the internal standard stock standard solution was added to an accurately weighed 50-mg amount of NACS, SCMCS and MCS, dissolved in 90 ml of 0.05% sodium hydrogen sulfite solution and adjusted to pH 3 with phosphoric acid. The flask was shaken in an ultrasonic bath and the contents were diluted to 100 ml with methanol.

2.6. Sample preparation

To prepare a sample solution, 10 ml of internal standard stock standard solution were added to an accurately weighed homogeneous tablet,

capsule contents or granule dosage equivalent to 50 mg of NACS, SCMCS and MCS and the volume was adjusted to 100.0 by adding 80 ml of 0.05% sodium hydrogensulfite solution and then methanol.

2.7. Solution for linearity response

Five concentrations of NACS, SCMCS and MCS ranging from 0.05 to 3.0 mg/ml, with internal standard stock standard solution added, were prepared. Solutions of each concentration were chromatographed five times.

2.8. Solutions for recovery study of NACS, SCMCS and MCS in synthetic mixtures

Solutions of five synthetic formulations of NACS, SCMCS and MCS were prepared by accurately weighing 50.0-mg amounts. Each solution was made up to 100.0 ml with 0.05% sodium hydrogen sulfite solution, 10 ml of internal standard stock standard solution and methanol, and was chromatographed five times.

3. Results and discussion

The linearity of the peak-area ratio of cysteine derivatives versus the internal standard was verified by injection of five solutions containing NACS, SCMCS and MCS at concentrations of 0.05, 0.1, 1.0, 2.0 and 3.0 mg/ml. A straight line with a good correlation coefficient was obtained for five injections and good R.S.D., as shown in Table 1. The data in Table 1 demonstrate the linearity of the response for standard solutions using the proposed method.

Reproducibilities for these cysteine derivatives, both on the same day and day-to-day, were evaluated. The R.S.D. on the basis of peak-area ratio for five standard injections on the same day for NACS, SCMCS and MCS was between 0.11% and 0.38% for an amount of 10 μg; the day-to-day R.S.D. was 0.43% for same amount. As expected, the same-day R.S.D.s were much lower because they were not affected by as many variables. The mean deviations for NACS, SCMCS and MCS was 0.01, 0.02 and 0.07, respectively. Based on the recovery range, the low R.S.D. and mean deviation, the precision was good.

The results for standard addition recovery studies of NACS, SCMCS and MCS in five synthetic formulations are given in Table 2 and range from 98.8% to 99.2%. Because the average recovery was greater than 98.8% and the R.S.D. was 0.02–0.16%, there was obviously no interference due to the excipients. This indicated that the proposed HPLC method is relatively unaffected by the sample matrix.

Typical chromatograms of NACS, SCMCS and MCS commercial dosage forms are shown in Fig. 1B, C and D. The retention times were 4.1 min for SCMCS, 6.8 min for NACS, 5.2 min for MCS and 11 min. for the internal standard. When compared with that obtained for a standard mixture shown, in Fig. 1A, no additional peak elutes. The results for various pharmaceuticals are given in Table 3, and lie within the official requirement of 90–110% based on the declared concentration. The selectivity of the method was demonstrated by using different pH

Table 1
Linearity results for standard MCS MCS and SCMCS at concentrations of 0.05, 0.1, 1.0, 2.0 and 3.0 mg/ml

Compound	r	y	R.S.D. (%) ($n = 5$)
MCS	0.9998	$1.4955x - 0.0066$	0.05
NACS	0.9997	$2.2113x - 0.0278$	0.02
SCMCS	0.9999	$1.1294x - 0.0054$	0.08

Table 2
Recovery of NACS, SCMCS and MCS from synthetic formulations

Formulation	Component	Added (mg)	Mean found (mg)[a]	Mean recovery (%)[a]	R.S.D. (%)[a]
(A) Granule	NACS	20	19.80	99.0	0.09
	Lactose	440			
	Potato starch	540			
(B) Granule	NACS	40	39.52	98.8	0.16
	Lactose	420			
	Potato starch	520			
(C) Tablet	SCMCS	375	371.62	99.1	0.02
	Lactose	100			
	Potato starch	100			
(D) Tablet	SCMCS	250	248.0	99.2	0.08
	Lactose	100			
	Potato starch	100			
(E) Capsule	MCS	50	49.55	99.1	0.06
	Lactose	124			
	Potato starch	124			

[a] $n = 5$.

values and the four similar thiol compounds were completely resolved, as illustrated in Fig. 1. Excipients from commercial formulations did not affect the resolution.

An organic modifier can be used to control the retentions of the three systeine derivatives. Complete separation using a mobile phase with only an ion-pair reagent as buffer. It was possible to control the separation of the analytes by adding either acetonitrile or methanol alone to adjust the eluent strength, and badly tailing peaks were obtained. The retention and peaks shape were investigated with both methanol and acetonitrile added to the mobile phase. Fig. 2 shows chromatograms obtained as the acetonitrile concentration was increased at the expense of the buffer. With increase in acetonitrile to 0.8%, NACS, SCMCS, MCS and methionine were rapidly separated, and the peak shape improved dramatically.

Plots of retention volume vs. percentage of organic modifier are shown in Fig. 3. The variations in retention and peak shapes of the four analytes were investigated as methanol and acetonitrile were added to the mobile phase. An optimum percentage of acetonitrile was necessary to enhance the peak shape of NACS and the unsymmetrical tailing of methionine. Upto at least 0.7% of acetonitrile added the retention volume of NACS decreased, after which there was hardly any change according to Fig. 3. The plot for SCMCS hardly changed at different percentages of organic solvent.

The buffer concentration was found to be a key parameter in controlling the separation of NACS and its analogues. Peak tailing and long retention were observed in the absence of buffer, and improved with increasing buffer concentration. No further change in retention occurred at buffer concentrations higher than 7 m*M*. At a concentration of 10 m*M*, NACS was eluted after methionine and both retentions were longer than at 5 m*M*.

The dependence of the separation on pH is illustrated by the plot of retention volume vs. pH at constant buffer concentration in Fig. 4. pH values of the mobile phase less than 3.2 were necessary for optimum resolution. A slight increase in pH produced shorter retentions and incomplete resolution. As has been observed

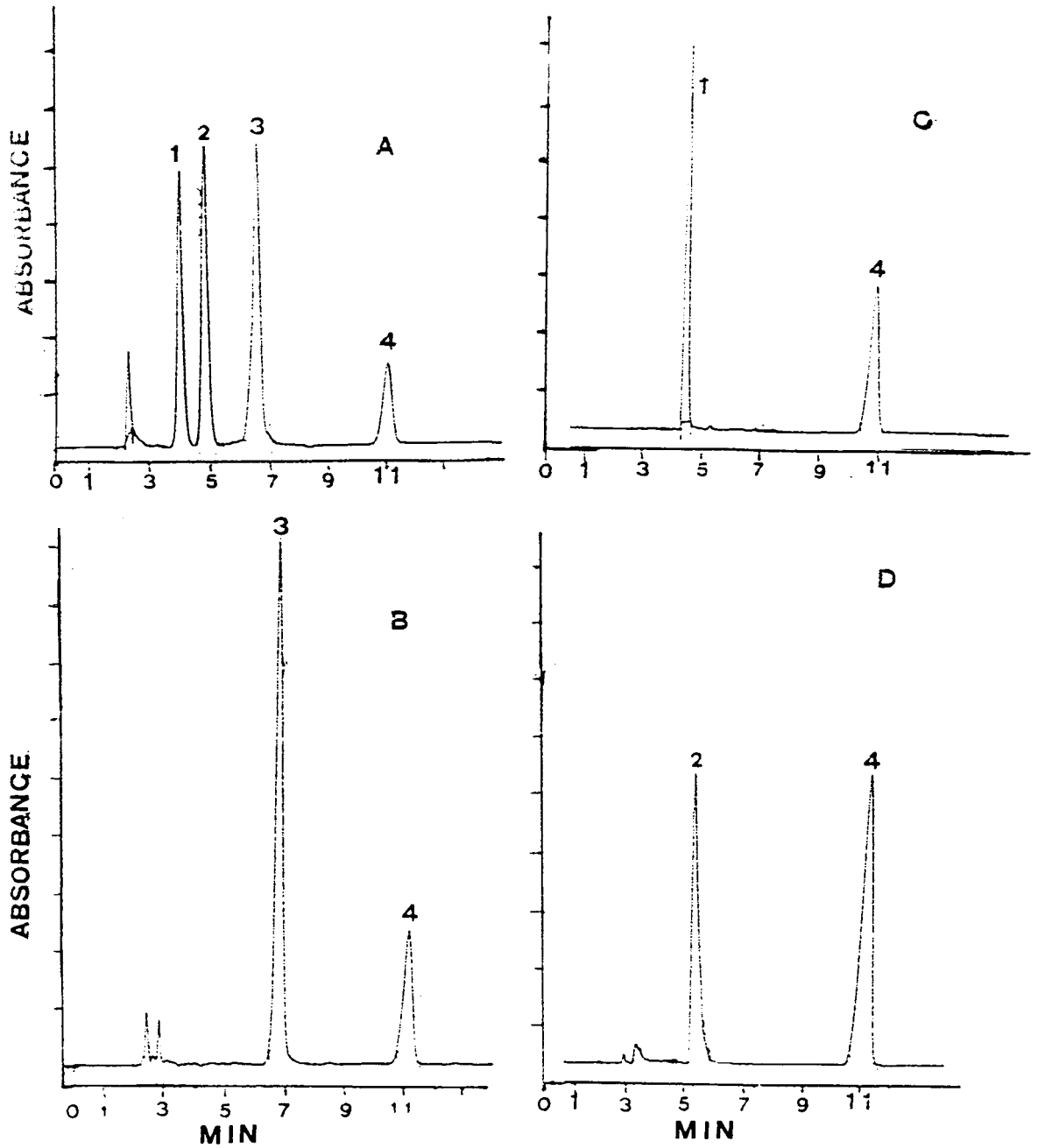

Fig. 1. Chromatograms of N-acetylcysteine, S-carboxymethylcysteine, and methylcysteine in commercial preparations. (A) 1 mg of standard and 0.5 mg/ml internal standard mixture; (B) 40 mg of NACS granule; (C) 50 mg of MCS capsule; (D) 375 mg of SCMCS table. Peaks: 1 = SCMCS; 2 = MCS; 3 = NACS; 4 = methionine (internal standard).

Table 3
Recoveries of NACS, SCMCS and MCS from various commercial formulations

Formulation	Component	Added (mg)	Found (mg)	Recovery (%)
(1) Granule	NACS (5 g)	100	99.40	99.4
(2) Granule	NACS (3 g)	200	197.80	98.9
(3) Tablet	SCMCS	375	372.5	99.8
(4) Capsule	MCS	50	49.55	99.1

with NACS and SCMCS, an increase in high pH produced same retention [11,13]. A better peaks shape was also observed at lower pH for NACS, SCMCS and MCS. As expected, pH prolonged the retention of the internal standard. At pH less than 2.5, three analytes were eluted fast than at pH 2.9 and methionine eluted at 15.2 min with a broad peak, as shown in Fig. 5. From the retention volumes of MCS and SCMCS, no significant change was obtained when the pH was 3.0–3.1. However, the retention volume for NACS was higher in the same pH range.

4. Conclusions

A mobile phase consisting of methanol, acetonitrile and sodium hexanesulfonic acid buffer with a μBondapack ODS reversed-phase column was shown to improve the separation of N-acetylcysteine, S-carboxymethylcysteine, methylcysteine and internal standard methionine. Addition of methanol or acetonitrile alone prolonged the retention time and resulted in

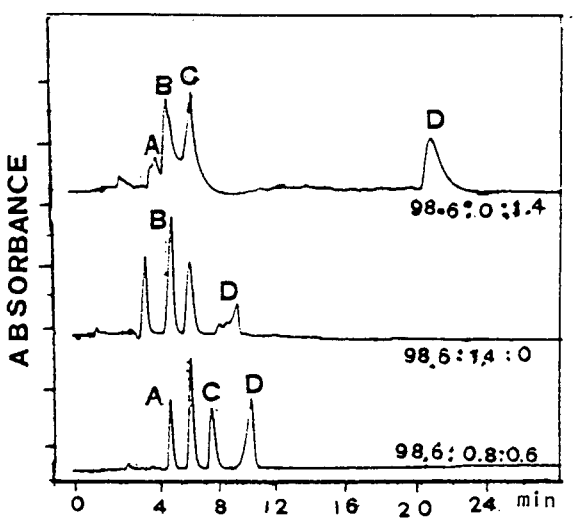

Fig. 2. Effect of methanol and acetonitrile on separation and peak shapes of MCS, NACS and SCMCS. Mobile phase 5 m*M* sodium hexanesulfonic acid (pH 2.9)–acetonitrile–methanol in the ratios indicated. A = SCMCS; B = NACS; C = MCS; D = methionine (in amounts of 2.5 μg).

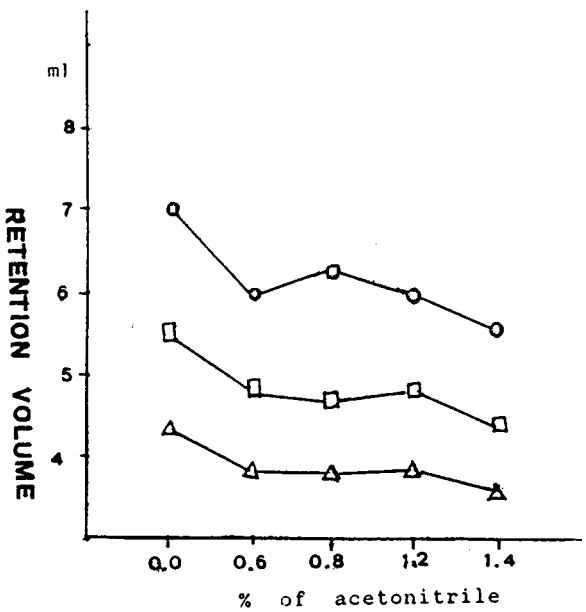

Fig. 3. Effect of solvent strength on retention volumes of (△) SCMCS, (□) MCS and (O) NACS. Mobile phase, 5 m*M* sodium hexanesulfonic acid (pH 2.9)–acetonitrile–methanol; column temperature, room temperature.

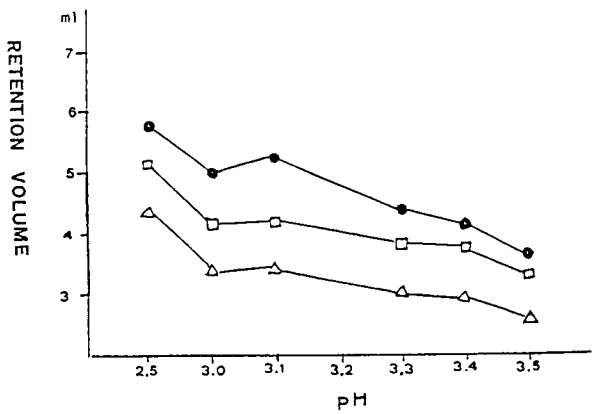

Fig. 4. Effect of pH on retention volumes of (△) SCMCS, (□) MCS, and (●) NACS. Mobile phase, 5 m*M* sodium hexanesulfonic acid (pH 2.9)–acetontrile–methanol (98.6:0.8:0.6); column temperature, room temperature.

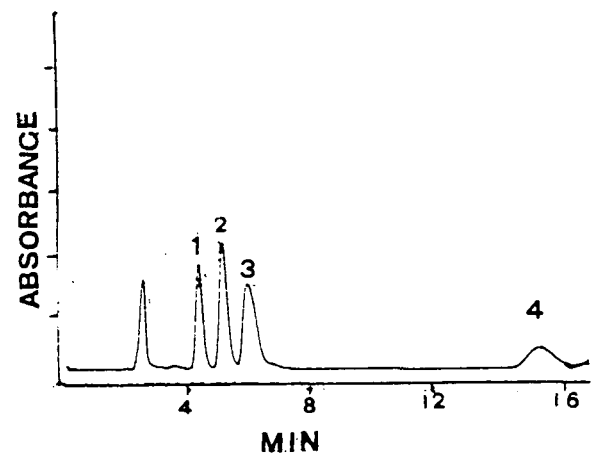

Fig. 5. Chromatogram of N-acetylcysteine, S-carboxymethylcysteine and methylcysteine obtained with 5 m*M* sodium hexanesulfonic acid (pH 2.45)–acetontrile–methanol (98.6:0.8:0.6), 0.5 mg/ml of standard and 0.5 mg/ml internal standard mixture. Peaks: 1 = SCMCS; 2 = MCS; 3 = NACS; 4 = methionine (internal standard).

peak tailing; however, acetonitrile reduced the peak tailing except for methionine. When the concentrations of methanol and acetonitrile are 0.6 and 0.8% (v/v), the peak shape and retention are greatly improved. The proposed method for NACS, SCMCS and MCS successfully separates the analytes within 12 min, provides good precision and is a sensitive and suitable quality control for pharmaceuticals or bulk drugs.

References

[1] N. Paze, et al., *Can. Med. Assoc. J.*, 95 (1966) 522.
[2] K.N.V. Palmer, et al., *Br. Med. J.*, 1 (1962) 280.
[3] J. Liebermann, *Am. J. Med.*, 49 (1970) 1.
[4] L.A. Goodmann and A. Goodman, *The Pharmacological Basis of Therapeuticals*, Macmillan, New York, 6th ed., 1988, p. 702.
[5] L.F. Proscott, R.N. Illingworth, J.M. Critchley, M.J. Steward and A.T. Proud, *Br. Med. J.*, 2 (1979) 1097.
[6] P. Crome, G.N. Volans, J.A. Naile, B. Widdop, R. Goulding and R.S. Williams, *J. Int. Med. Res.*, 4, Suppl. 4 (1976) 105.
[7] M.A. Raggi, V. Carrini and A.M. Di Pietra, *J. Pharm. Sci.*, 71 (1986) 1384.
[8] B.S.R. Muuty, J.N. Kapoor and M.W. Kim, *Am. J. Hosp. Pharm.*, 30 (1977) 526.
[9] *United States Pharmacopeia XXII Revision*, US Pharmacopeial Convention. Rockville, MD, 1985, p. 17.
[10] J.R. Talley, R.A. Magraian and E.B. Sommers, *Am. J. Hosp. Pharm.*, 30 (1973) 526.
[11] N. Kenichiro, U. Chiemi, Y. Hiromi, N. Shin' Ichi and A. Shuzo, *J. Chromatogr.*, 414 (1987) 11.
[12] M. Johansson and S. Lenngren, *J. Chromatogr.*, 432 (1988) 65.
[13] P.A. Lewis, A.J. Woodward and J. Maddock, *J. Chromatogr.*, 327 (1985) 261.
[14] U. Hannestad and B. Sorbo, *Clin. Chim. Acta*, 95 (1979) 189.
[15] C.K. Mulucci, G.W. Lyman, A.D. Bond and R.N. Johnson, *J. Chromatogr.*, 391 (1987) 321.
[16] B. Staffeldt, J. Brockmoller and I. Roots, *J. Chromatogr.*, 571 (1991) 133.
[17] A.R. Buckpitt, D.E. Rollins, S.D. Nelson, R.B. Franklin and J.R. Michell, *Anal. Biochem.*, 83 (1977) 168.
[18] G. Bovis and P. Chiesi, *Boll. Chim. Farm.* 119 (1980) 172.

ELSEVIER

Journal of Chromatography A, 697 (1995) 317–327

JOURNAL OF CHROMATOGRAPHY A

Indirect detection of saccharides in reversed-phase liquid chromatography with highly alkaline mobile phases

Bing Lu, Morgan Stefansson[1], Douglas Westerlund*

Analytical Pharmaceutical Chemistry, Uppsala University Biomedical Centre, P.O. Box 574, S-751 23 Uppsala, Sweden

Abstract

An indirect UV-detection method in the separation of saccharides by reversed-phase LC was developed. Porous graphitic carbon was used as the solid phase and sorbic acid, muconic acid and furanacrylic acid were tested as UV-absorbing markers included in the alkaline sodium hydroxide–methanol mobile phase. The indirect response of the saccharides was in general found to follow earlier developed theories. The most important parameters for optimizing the response were the retention of the solutes relative to the marker, which should be close to 1, and a high loading of the marker on the solid phase. The detection sensitivity can be improved by optimizing the marker and organic solvent concentrations in the mobile phase, the pH as well as the temperature.

The stability of the saccharides was found to be adequate for the alkaline conditions used in the separation systems.

1. Introduction

Research activities on carbohydrates in the biosciences have increased considerably during recent years; especially regarding their role as components in the cell walls and membranes for molecular recognition. It is expected that many future drugs, i.e. antibiotics and diagnostics, will exert their effect by influencing the carbohydrate chemistry in the living cell. In this context it is essential to develop new analytical techniques for carbohydrate analysis regarding content, stability and purity, as well as for studies on biological materials. Gas chromatography is a well established technique in the analysis of carbohydrates, and provides in combination with mass spectrometric detection a reliable analytical technique. A drawback is, however, the necessity to produce derivatives of the analytes in order to improve their chromatographic and detection properties.

Detection is also one of the major obstacles in liquid chromatographic analysis of saccharides. As saccharides do not exhibit absorbance at wavelengths above 200 nm, direct UV detection is not applicable due to low sensitivity and high background interference. Alternatively, refractive index has been used for determination of saccharides but does not allow determination of sugars at trace levels and the use of gradient elution. Another type of detection, pulsed amperometric detection, provides sensitive detection for saccharides [1,2], but the electrode may be fouled by additives in the mobile phase.

* Corresponding author.

[1] Present address: Department of Analytical Chemistry, Institute of Chemistry, Uppsala University, P.O. Box 531, S-751 21 Uppsala, Sweden.

0021-9673/95/$09.50
SSDI 0021-9673(94)00814-0

However, pre- or postcolumn derivatization followed by use of photometric or fluorimetric detection are methods frequently used today and can measure saccharides at the 10 pmol range [3–5]. The time consumption and technical complications, particularly in analysis of non-reducing saccharides that require an initial hydrolysis step, are the drawbacks of such techniques.

An indirect UV-detection method, which is based on the use of a mobile phase marker with detector response, was first applied to determine sugars by Gnanasambandan and Freiser [6]. Xylose, ribose and fructose were detected by using a mobile phase containing an UV-absorbing counter ion, methylene blue. Herné et al. [7] also detected sorbose, fructose and sorbitol by adding arbutin into the mobile phase, but it seemed that sensitivity and selectivity need to be improved.

This paper describes a simple and sensitive method for analysis of saccharides in HPLC through the use of indirect UV detection with sorbic acid as the absorbing ion.

2. Theory

The principles of indirect detection of ionic compounds in reversed-phase systems have been derived earlier [8–10]: a detectable component is included in the aqueous mobile phase and is assumed to distribute to the solid phase. When a solution deviating in composition from the mobile phase is injected the established equilibria in the column are disturbed and the analytes will travel through the column in zones together with mobile phase components in concentrations differing from those of the bulk mobile phase. All mobile phase components that are interacting with an injected analyte will also create migrating zones, so-called system peaks (also called eigenpeaks). It is assumed that the most common interaction between the components is competition for the adsorption sites on the solid phase. The following relationship for the analyte response (R) is generally valid:

$$R = k\phi_s\alpha_s/(\alpha_s - 1) \quad (1)$$

where ϕ_s is the fractional loading of the marker on the solid phase; α_s is the retention of the analyte relative the system peak. In the present study the analytes are present both in charged and uncharged form involving that a correction factor (k) has to be introduced on the right hand side of the equation.

A retention equation can be derived assuming that the ionized sugar (X^-) and the marker (M^-) are distributed as ion pairs with sodium to the stationary phase; sodium hydroxide may also compete for the adsorption sites. It is further assumed that the uncharged sugar (HX) also is distributed to the stationary phase and competing for the same adsorption sites:

$$k'_X = qK^0(K_{HX}a_{H^+} + K_{NaX}[Na^+]) \times [(a_{H^+} + K_{a(HX)})(1 + K_{NaM}[Na^+][M^-] + K_{NaOH}[Na^+][OH^-])]^{-1} \quad (2)$$

where k' is the capacity ratio, q is the phase ratio, K^0 is the adsorption capacity of the solid phase, $K_{a(HX)}$ is the acid dissociation constant for the sugar, and the K values are the equilibrium constants for the different adsorption equilibria. The retention of the sugar can in principle be regulated by the concentrations of sodium, the marker and hydroxide (which also determines the pH in this case), and is furthermore governed by the capacity of the solid phase, and the magnitude of the equilibrium constants including pK_a.

The retention of the marker can be described by a related equation [11]; however, it is not given here since the system peak retention was not studied in detail in this paper.

3. Experimental

3.1. Apparatus

The chromatographic system was set up with an LKB 2150 pump (Bromma, Sweden), a Rheodyne 7125 sample injector with a 20-μl loop and a Tefzel alkaline resistant rotor seal, Spectro-

Monitor III UV detector (LDC, Riviera Beach, FL, USA), and Kipp and Zonen BD 40 recorder. Two porous graphitic carbon Hypercarb columns (100 mm × 4.7 mm I.D.), containing material from the same batch Nos. 0492 and 0498 (Shandon Scientific, Runcorn, UK) were used. The column No. 0498 was probably somewhat contaminated by an unknown substance from previous studies. The test chromatogram showed that solutes were less retained on this column than on column No. 0492, but the efficiency and selectivity were similar. Determinations of molar absorbances for the markers were performed with a Spectrophotometer Model 25 (Beckman, Irvine, CA, USA).

3.2. Chemicals

Sodium hydroxide (1 *M* Titrizol), phenol and methanol were obtained from E. Merck (Darmstadt, Germany) and sorbic acid from Fluka (Buchs, Switzerland). Other chemicals were purchased from Sigma (St. Louis, MO, USA). All chemicals were of analytical-reagent grade.

3.3. Chromatographic conditions

Deionized water (Millipore, Bedford, MA, USA) was used for preparation of mobile phases. Sodium hydroxide dilutions were kept in plastic bottles under protection from carbon dioxide by soda lime tubes. The mobile phases were freshly prepared and degassed prior to use. Flow-rate was 1.0 ml/min and the eluent was monitored at 254, 258 and 294 nm when using sorbic acid (SA), muconic acid (MA) or furanacrylic acid (FA) as UV-absorbing ions, respectively. The temperature of column and injector was maintained constant (22°C), if not otherwise indicated, using a Heto type 02 pt 923 C water-bath (Birkeröd, Denmark).

3.4. Calculations

The capacity ratio, k', was calculated conventionally from: $k' = (V_R - V_m)/V_m$, where V_R is the retention volume and V_m is the interstitial volume of the mobile phase in the column. V_m was obtained from the front disturbance in the chromatogram. The molar absorbances of the markers were determined by static measurements in the relevant mobile phase in a spectrophotometer. The apparent molar absorptivity (ϵ^*) of an analyte was calculated according to the equation [12]:

$$\epsilon^* = \frac{Ysu}{mdb} \quad (3)$$

where Y is peak area, s is sensitivity setting of the detector, u is flow-rate, m is amount of analyte, d is the chart speed and b is the path length in the detector cell.

4. Results and discussion

4.1. Using sorbic acid as the UV-absorbing ion

Our previous work showed that using porous graphitic carbon (PGC) as the solid phase can give fairly high retention of di- and oligosaccharides with sodium hydroxide as the mobile phase [2]. In the same system, SA, which has a high molar absorptivity at 254 nm: $\log \epsilon = 4.46$ (see Table 4), was found to have a retention similar to the disaccharides. These conditions should be applicable for using SA as an UV-absorbing ion for indirect detection of saccharides. With addition of SA to the mobile phase, di- and trisaccharides were detected with relative retention values (k'_{solute}/k'_{SA}) between 0.43 and 2.87 (Fig. 1). SA with pK_a 4.8 is negatively charged, while the saccharides, pK_a 12–14 [11], are partly charged in the highly alkaline mobile phase (pH above 12). Lactose, the retention of which was closest to that of SA, demonstrated the highest detector response (log $\epsilon^* = 5.4$), i.e. about ten times higher apparent molar absorbance than the marker. The response was lower for sugars with both lower and higher retention than the system peak [8–10], but the apparent molar absorbances were higher than ϵ for the marker in all cases. The relationship

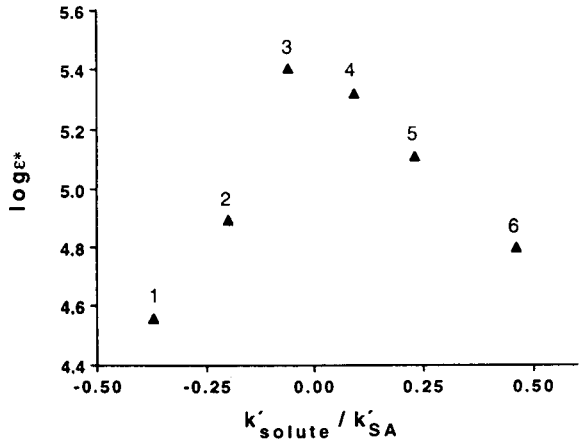

Fig. 1. Response of saccharides with sorbic acid (SA) as UV-absorbing ion. Mobile phase: $2 \cdot 10^{-5}$ *M* SA in 0.1 *M* NaOH and 10% (v/v) methanol. Solid phase: PGC No. 0492. 1 = Melibiose; 2 = sucrose; 3 = lactose; 4 = melezitose; 5 = gentiobiose; 6 = cellobiose.

between detection sensitivities and relative retentions (k'_{solute}/k'_{SA}) for individual sugars were in agreement with earlier developed theories; a graphical illustration of Eq. 1 is given in Fig. 2; a negative response is represented by a negative value of ϵ^*.

4.2. Influence of SA concentration on detector response

The detector responses of four disaccharides were determined using mobile phases that contained different concentrations of SA ($5 \cdot 10^{-6}$–$3 \cdot 10^{-5}$ *M*). The detection sensitivity increased with increasing concentrations of SA, and the logarithm of the apparent molar absorptivity (ϵ^*) of solutes versus the logarithm of the concentration of SA demonstrated linear relationships in this concentration range (Fig. 3). However, the system became less stable as the background absorbance approached the limit of the detector; consequently a SA concentration higher than $3 \cdot 10^{-5}$ *M* was not tested. Generally, a higher concentration of UV-absorbing ion in a mobile phase would give a higher loading (Φ) of the UV-absorbing ion on solid phase, therefore the detection sensitivity would improve according to Eq. 1. However, an increase in marker concentration will also increase noise, and an optimal signal-to-noise ratio will be obtained at an intermediate value.

The retentions of the saccharides were not

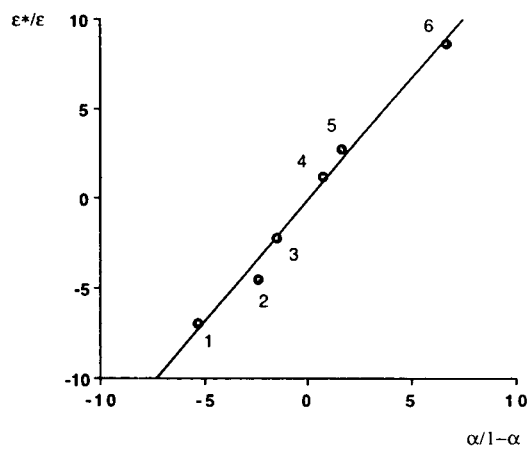

Fig. 2. Graphical computation of the response function (Eq. 1). Chromatographic conditions as in Fig. 1. 1 = Melezitose; 2 = gentiobiose; 3 = cellobiose; 4 = melibiose; 5 = sucrose; 6 = lactose.

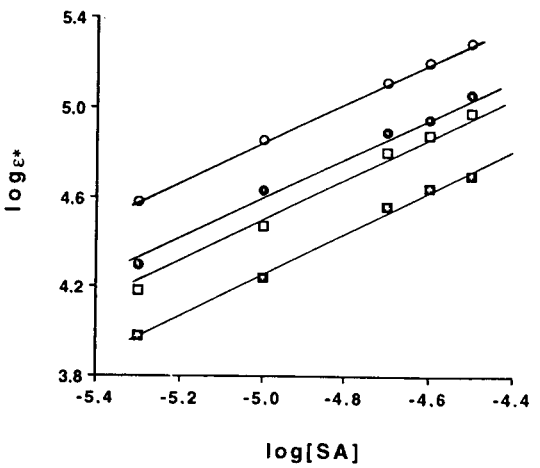

Fig. 3. Influence of sorbic acid concentration on response. Mobile phases: $5 \cdot 10^{-6}$–$3 \cdot 10^{-5}$ *M* SA in 0.1 *M* NaOH and 10% (v/v) methanol. Solid phase: PGC No. 0492. ○ = Gentiobiose; ● = sucrose; □ = cellobiose; ■ = melibiose.

influenced by a variation of the sorbate concentration in the range tested; this means that the term $K_{NaM}[Na+][M-]$ in Eq. 2 is negligible in the concentration range studied. The analyte retentions are then governed mainly by pH, the sodium and hydroxide concentrations.

4.3. Influence of pH on retention and response

Since the pK_a values of the saccharides are ca. 12 or higher a high pH is needed to dissociate the solutes in the mobile phase. When the sodium hydroxide concentration was changed from 0.1 to 0.02 *M*, the retentions of all solutes increased, whereas the SA retention was constant (Fig. 4). The retention behaviour shows that the distribution of the uncharged form of the sugar dominates in the studied pH interval (see Eq. 2). The distribution of the charged form as ion pair with sodium also plays a role, since otherwise there would be a linear relationship between log k' and pH, which is not the case. The change in elution order for melibiose and sucrose with $pK_a = 12.6$ [13] is probably due to a difference in their pK_a values. Sorbic acid ($pK_a = 4.8$) is anionic during the whole pH interval, and its unchanged retention shows that sodium hydroxide, in this concentration interval, does not compete significantly for the adsorption sites with the marker.

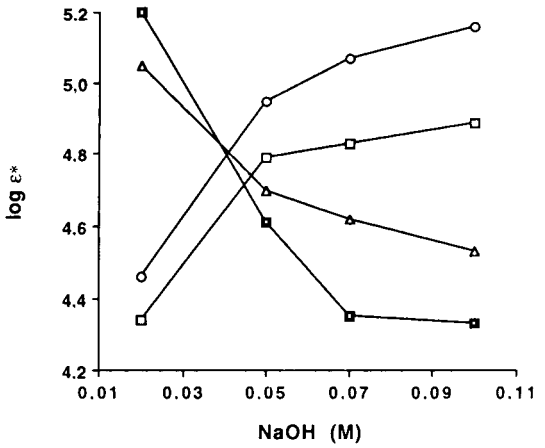

Fig. 5. Influence of pH on response. Chromatographic conditions and symbols as in Fig. 4.

The detector responses increased for melibiose and sucrose, while they decreased for gentiobiose and cellobiose with decreasing pH (Fig. 5). The response for sucrose was smaller than that of melibiose when sucrose eluted earlier than melibiose. These results were caused by the change of relative retentions of solutes to the

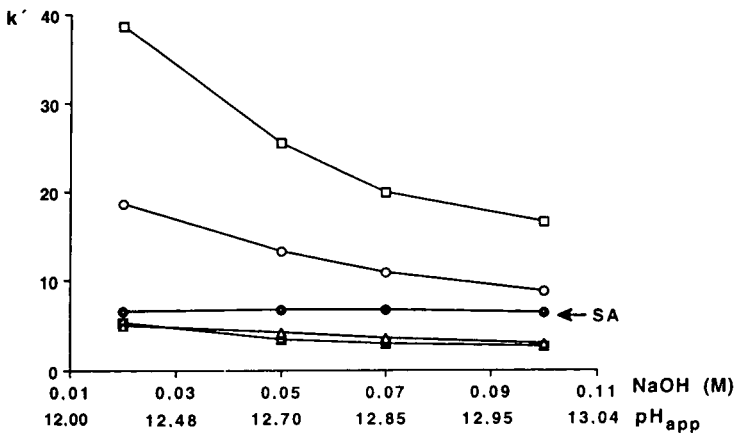

Fig. 4. influence of pH on retention of saccharides. Mobile phases: $2 \cdot 10^{-5}$ *M* SA in $2 \cdot 10^{-2}$–$1 \cdot 10^{-1}$ *M* NaOH, and 8% (v/v) methanol. Solid phase: PGC No. 0498. □ = Cellobiose; ○ = gentiobiose; ● = SA; △ = sucrose; ■ = melibiose.

system peak, Eq. 1 (see Fig. 4), again illustrating that solutes eluting closer to the UV-absorbing compound will have lower detection limits. Since the indirect detection mechanism involves a mutual interaction between the marker and the analyte, it is interesting that the main factor determining the magnitude of the response is the closeness of the analyte and system peaks. As discussed above the change in retention order between sucrose and melibiose is probably due to differences in the pK_a values, and this means that the fraction of uncharged melibiose is larger than that of sucrose at the lowest pH studied. This indicates that the charged marker competes with both the uncharged and charged forms of the sugars for the adsorption sites, which also is an assumption made in the derivation of the retention equation.

4.4. Influence of methanol concentration on detector response

In order to shorten the chromatographic run times and to improve system selectivity, an organic modifier, methanol, was added to the mobile phase. As expected, the capacity ratios of both the system and sample peaks were reduced with increasing concentrations of methanol from 4 to 12%. However, the effect was more pronounced on the analytes, particularly on the highly retained saccharides, than on the marker (SA) (see Table 1). Consequently, gentiobiose eluted closer to the marker, while the peaks of melibiose and sucrose generally became more distant from the system peak with increasing methanol content.

The detection sensitivity varied with increasing concentration of methanol (Table 1). The apparent molar absorbance of melibiose and sucrose decreased significantly, whereas that of gentiobiose showed a considerable increase. In general, addition of an organic modifier to the mobile phase will lead to a decrease in detection sensitivity, as a result of a reduced loading of the UV-absorbing component on the solid phase [14–16]. Furthermore, a change in relative retention (k'_{solute}/k'_{SA}) will also cause an alteration in the detection sensitivity. For melibiose and sucrose, the large decrease in detector response was likely due to the sample peaks becoming more distant from the system peak and a reduction in loading of SA on the solid phase at higher concentration of methanol. However, the relative retention (k'_{solute}/k'_{SA}) of gentiobiose became closer to 1. Consequently, the effect of the decrease in loading of SA on the solid phase was counteracted by an improvement in relative retention.

A typical chromatogram is given in Fig. 6 which shows the separation of some di- and trisaccharides. It clearly demonstrates that sugars eluting close to the system peak have lower detection limits than those eluting more distant to this peak. However, the peak shape of compounds that are eluted close to the system peak may be distorted [e.g. lactose (peak 3 in Fig. 6)],

Table 1
Influence of methanol concentration on the retention and indirect detector responses of sugars

Sugars	Concentration of methanol (%, v/v)							
	4.0		8.0		10.0		12.0	
	α_s	Log ϵ^*	α_s	Log ϵ^*	α_s	Log ϵ^*	α_s	Log ϵ^*
Melibiose	0.76	5.20	0.49	4.79	0.41	4.54	0.37	4.30
Sucrose	0.82	5.48	0.75	5.16	0.59	4.89	0.56	4.68
Gentiobiose	3.36	4.87	2.03	5.17	1.62	5.14	1.41	5.26

Mobile phase: $2 \cdot 10^{-5}$ *M* sorbic acid and methanol in 0.1 *M* NaOH. Solid phase: PGC No. 0492. $\alpha_s = k'_{solute}/k'_{SA}$; ϵ^* = apparent molar absorptivity.

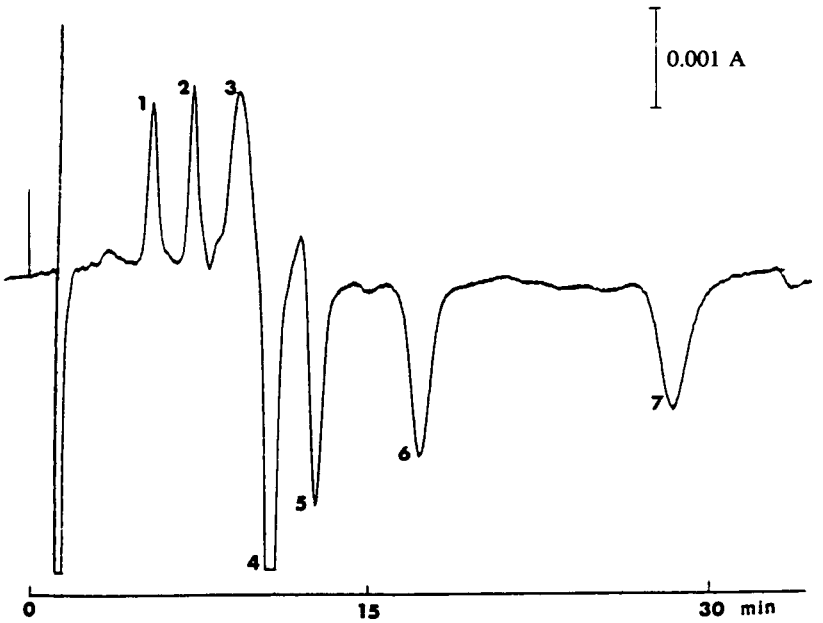

Fig. 6. Separation of di- and trisaccharides. Mobile phase: $2.5 \cdot 10^{-5}$ *M* SA in 0.1 *M* NaOH and 10% (v/v) methanol. Solid phase: PGC No. 0492. Temperature: 22°C. Peaks: 1 = melibiose (1.36 μg); 2 = sucrose (0.68 μg); 3 = lactose (0.34 μg); 4 = system peak (sorbic acid); 5 = melezitose (0.50 μg); 6 = gentiobiose (0.68 μg); 7 = cellobiose (1.36 μg).

since the relative response for the part of the peak coming closer to the system peak will be higher than more distant parts.

4.5. Effect of temperature on detector response

The influence of temperature on the detection sensitivity showed that the detector responses were significantly reduced, when the temperature was raised from 12 to 42°C (Fig. 7). The retentions of sugars decreased at a similar rate to that of SA (see Fig. 8, which is discussed below), hence the retentions of the solutes relative to SA essentially remained constant at different temperatures. The main reason to the decreasing response, in accordance with theory (see Eq. 1), was due to decreased loading of the marker on the solid phase with increasing temperature (Table 2). The decrease in loading from 12 to 42°C was about 2.6 times and the decreases in response for the different analytes were of the same magnitudes. The Van 't Hoff plots (Fig. 8) were linear in the studied temperature interval indicating an unchanged retention mechanism for the saccharides. The thermodynamic parameters calculated from the relationships (Table 3)

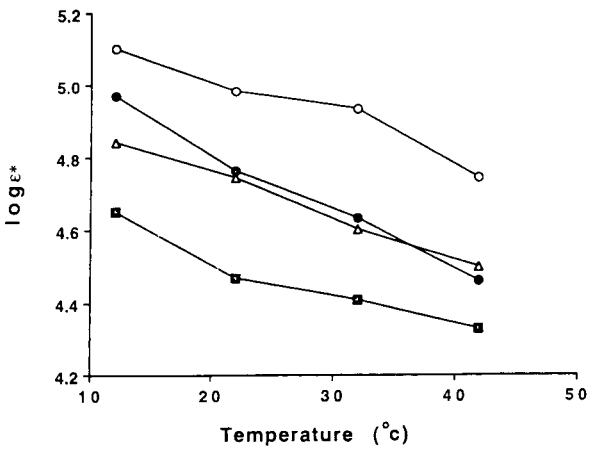

Fig. 7. Effect of temperature on the detector response. Mobile phase: $2 \cdot 10^{-5}$ *M* SA in 0.1 *M* NaOH and 8% (v/v) methanol. Solid phase: PGC. No. 0498. ○ = Gentiobiose; ● = cellobiose; △ = sucrose; □ = melibiose.

Table 2
Influence of temperature on the adsorption of sorbic acid on the solid phase

Temperature (°C)	Amount adsorbed (μg)[a]
12	29.6
22	21.9
32	14.4
42	11.2

Mobile phase: $2 \cdot 10^{-5}$ *M* SA and 8% (v/v) methanol in 0.1 *M* NaOH. Solid phase: PGC No. 0498.
[a] Measured by breakthrough techniques.

indicate that the retention of the carbohydrates is due to the enthalpic factors (bonding to the solid phase), while the bonding results in increasing order in the system (negative entropy values). The magnitude (but not the sign) of the entropy data are uncertain, however, due to the non-accessibility of the phase ratio, which was roughly calculated according to $(V_t - V_m)/V_m$, where V_t = total volume of the column. The results seem to confirm that the retention mechanism of the marker, SA, is the same as for the analytes, which was assumed in deriving the retention equation, Eq. 1.

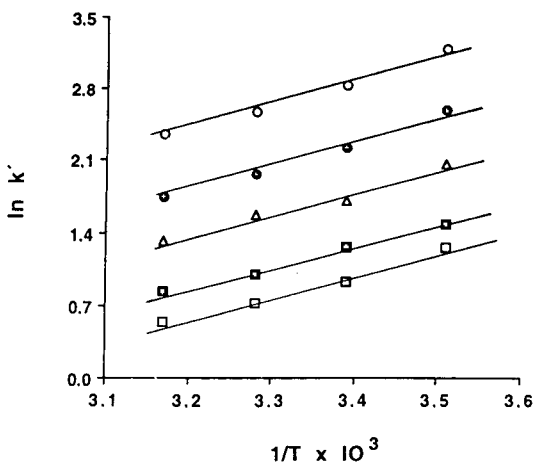

Fig. 8. Indirect detection of sugars in HPLC Van 't Hoff plots. Mobile phase: $2 \cdot 10^{-5}$ *M* sorbic acid in 0.1 *M* NaOH and 8% (v/v) methanol. Solid phase: PGC No. 0498. Solutes: ○ = cellobiose; ● = gentiobiose; ■ = sucrose; □ = melibiose; △ = sorbic acid (marker).

Table 3
Thermodynamic parameters for retention of saccharides on porous graphitic carbon

Solutes	r^{2} [a]	ΔH^0 (kcal/mol)	ΔS^0 (cal/mol·K)	$T\Delta S^{0}$ [b] (kcal/mol)
Melibiose	0.987	−4.23	−10.7	−3.2
Sucrose	0.993	−3.96	−9.3	−2.7
Gentiobiose	0.989	−5.08	−11.0	−3.3
Cellobiose	0.990	−4.96	−9.4	−2.8
Sorbic acid[c]	0.978	−4.27	−9.3	−2.7

Mobile phase: $2 \cdot 10^{-5}$ *M* SA and 8% (v/v) methanol in 0.1 *M* NaOH. 1 cal = 4.184 J.
[a] Correlation coeffient for the linear fit of the Van 't Hoff plot.
[b] At 295 K.
[c] Marker.

Lower column temperature would give rise to higher response, but a disadvantage is an increased zone broadening, on average an almost 3-fold decrease in the number of theoretical plates was obtained in going from 42 to 12°C.

4.6. Responses with different UV-absorbing ions

In addition to SA, MA and FA were tested as potential markers under the same chromatographic conditions. As shown in Table 4, MA, SA and FA exhibited approximately the same molar absorptivities at 258, 254 and 294 nm, respectively. The loading of the individual ions on the solid phase varied depending on differences in their hydrophobic properties. In order to obtain comparable background absorbances, each UV-absorbing ion was added in the same

Table 4
Properties of markers

Marker	ϵ [a]	Amount adsorbed on the solid phase (μg)[b]
MA	$2.55 \cdot 10^4$ (258 nm)	4.5
SA	$2.88 \cdot 10^4$ (254 nm)	21.9
FA	$2.25 \cdot 10^4$ (294 nm)	134.1

[a] Molar absorptivity in the solvent: 8% methanol in 0.1 *M* NaOH.
[b] Measured by breakthrough techniques; chromatographic conditions were the same as in Table 5.

concentration to the mobile phases. The detector was set at the wavelength of maximum absorption of respective marker. Responses and relative retentions for sugars in these systems are summarized in Table 5. The detection sensitivity was shown to be dependent on the retentions of both solutes and UV-absorbing ions. MA, which is a divalent acid, was less retained than the solutes and gave rise to lower and approximately the same response for all actual sugars. This was unexpected and not in accordance with the general theory; a constant response would not be obtained until the relative retentions were >20. It would be of interest to study di- and polyvalent acids further in order to find out whether this is a general phenomenon. Markers of that type would then make the application of indirect detection principles more convenient. In the case of FA, all solutes were eluted earlier than the marker. The loading of FA on the solid phase was considerably higher (see Table 4); the detector responses of individual sugars increased with increasing retention. A very high response was noted for the most retained sugar, cellobiose —an almost 15-fold higher apparent molar absorbance compared to the ϵ of FA. It indicates that FA might be very useful for more retained saccharides, i.e. higher oligo- and polysaccharides. However, as shown in Table 5, using SA, which had about the same retention as that of the solutes, as the marker gave generally the highest detection sensitivity in spite of the fact that the amount of SA adsorbed on the solid phase was 6-fold lower than that of FA in the system. This demonstrates again the importance of choosing a marker that gives retentions relative the solutes close to 1 in order to obtain high detection sensitivities in indirect detection systems.

These systems were not suitable for detection of monosaccharides and amino monosaccharides due to their very low retention; using sorbic or muconic acid as markers the small sugars were unretained on the PGC column. By using the more polar marker phenol as the UV-absorbing ion, three monosaccharides and amino monosaccharides could be separated and detected as shown in Fig. 9.

4.7. Stability of the sugars at alkaline conditions

Since highly alkaline sodium hydroxide solutions were used as the mobile phase, the stability of the sugars under such conditions must be adequately high in order to achieve reliable separations. This was investigated by dissolving each sugar in 0.1 *M* sodium hydroxide solution and analyzing the solutions stored at ambient temperature, about 20°C, by the indirect detection technique developed, at increasing time intervals (see Table 6). The non-reducing sugar, melezitose, was stable during the whole period studied, 2 h. The reducing sugars were degraded slowly; gentiobiose and melibiose being the most sensitive, a slight degradation could be observed after 15 min. Sucrose, cellobiose and lactose

Table 5
Relative retentions and indirect detector responses of sugars with different markers

Sugars	k'_{solute}/k'_{system}			log ϵ*		
	MA	SA	FA	MA	SA	FA
Melibiose	2.2	0.4	0.1	3.93	4.33	4.16
Sucrose	2.8	0.6	0.1	4.10	4.53	4.33
Lactose	3.9	0.8	0.2	4.23	5.06	4.56
Melezitose	4.6	0.9	0.2	3.81	5.24	4.57
Gentiobiose	7.8	1.6	0.3	4.00	5.16	4.81
Cellobiose	13.4	2.8	0.6	3.74	4.83	5.52

Mobile phase: $2 \cdot 10^{-5}$ *M* marker and 8% (v/v) methanol in 0.1 *M* NaOH. Solid phase: PGC No. 0498. UV detection: 258, 254 and 294 nm for MA, SA and FA, respectively.

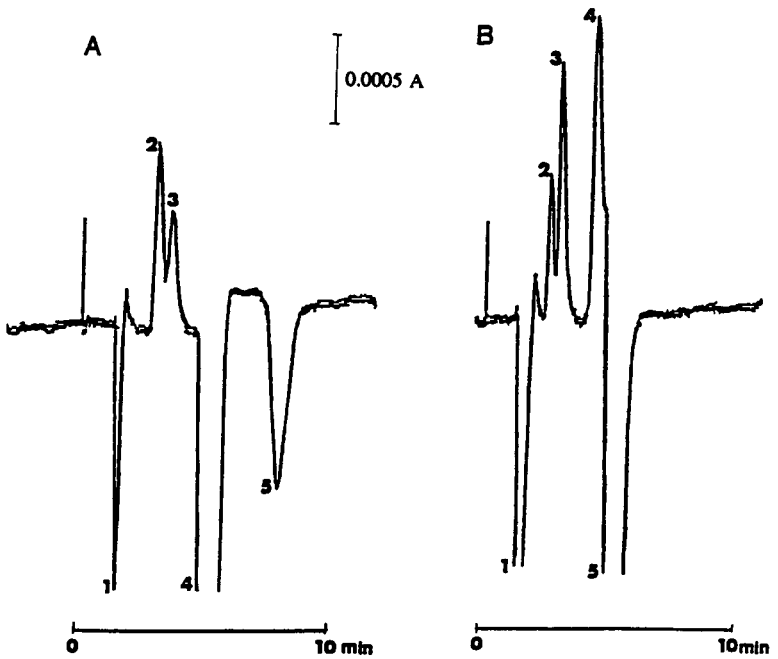

Fig. 9. Separation of amino sugars and monosaccharides with phenol as the UV-absorbing ion. Mobile phase: 0.1 *M* NaOH and $1.5 \cdot 10^{-4}$ *M* phenol. Solid phase: PGC No. 0492. UV detection at 287 nm. (A) 1 = System peak; 2 = glucosamine (0.72 μg); 3 = galactosamine (0.18 μg); 4 = system peak; 5 = N-acetylgalactosamine (0.22 μg). (B) 1 = System peak; 2 = glucose (0.72 μg); 3 = galactose (0.72 μg); 4 = fucose (0.33 μg); 5 = system peak.

were, however, more stable. It is obvious that for some reducing sugars the chromatographic run time should be kept adequately short in order to avoid degradation and to achieve reliable results in quantitative determinations. An advantageous alternative might be to use a lower pH for sensitive sugars, for example gentiobiose. The retention would then be longer (see Fig. 4) and the response somewhat lower (see Fig. 5) using the standard conditions. It is probable, however, that it would be possible to adapt the mobile phase conditions (amount of organic modifier, concentration of marker, temperature) in order to achieve suitable conditions for the analysis also of a pH-sensitive carbohydrate of interest.

Table 6
Stability of saccharides in alkaline solution

Sugars	Relative peak area (%)				
	0 min	15 min	30 min	60 min	120 min
Melezitose	100	100	100	100	100
Sucrose	100	100	100	98.4	92.3
Cellobiose	100	100	100	96.2	93.6
Lactose	100	100	97.8	91.1	84.4
Gentiobiose	100	98.3	94.5	91.6	87.3
Melibiose	100	97.4	93.6	89.4	86.2

Chromatographic conditions as in Fig. 7. Solutes were dissolved in 0.1 *M* NaOH and stored at ambient temperature.

Acknowledgements

The research was supported by grants from the Swedish Research Council of Natural Sciences, and by travel grants (to B.L.) from the Swedish Academy of Pharmaceutical Sciences.

References

[1] R.D. Rocklin and C.A. Pohl, *J. Liq. Chromatogr.*, 6(9) (1983) 1577–1590.
[2] M. Stefansson and B. Lu, *Chromatographia*, 35 (1993) 61–66.
[3] M. Krämer and H. Engelhardt, *J. High Resolut. Chromatogr.*, 15 (1992) 24–29.
[4] A. Coquet, J.-L. Veuthey and W. Haerdi, *J. Chromatogr.*, 553 (1991) 255–263.
[5] Y. Umegae, H. Nohta and Y. Ohkura, *Anal. Sci.*, 5 (1989) 675–680.
[6] T. Gnanasambandan and H. Freiser, *Anal. Chem.*, 54 (1982) 2379–2380.
[7] P. Herné, M. Renson and J. Crommen, *Chromatographia*, 19 (1984) 274–279.
[8] J. Crommen, G. Schill and P. Herné, *Chromatographia*, 25 (1988) 397–403.
[9] J. Crommen, G. Schill, D. Westerlund and L. Hackzell, *Chromatographia*, 24 (1987) 252–260.
[10] G. Schill and E. Arvidsson, *J. Chromatogr.*, 492 (1989) 299–318.
[11] E. Arvidsson, J. Crommen, G. Schill and D. Westerlund, *Chromatographia*, 24 (1987) 460–468.
[12] L. Hackzell and G. Schill, *Chromatographia*, 15 (1982) 437–444.
[13] C. Degani, *Carbohydr. Res.*, 18 (1971) 329–332.
[14] T. Gnanasambandan and H. Freiser, *Anal. Chem.*, 54 (1982) 1282.
[15] J. Crommen and P. Herné, *J. Pharm. Biomed. Anal.*, 2 (1984) 241.
[16] L. Hackzell, T. Rydberg and G. Schill, *J. Chromatogr.*, 282 (1983) 179–191.

ELSEVIER

Journal of Chromatography A, 697 (1995) 329–335

JOURNAL OF CHROMATOGRAPHY A

Soluble glycoproteins from sugar cane juice analysed by high-performance liquid chromatography and fluorescence emission

Maria Estrella Legaz[a,*], Mercedes M. Pedrosa[a], R. De Armas[b], Maritza M. Martinez[b], C. Vicente[a]

[a]*Department of Plant Physiology, Faculty of Biology, Complutense University, 28040 Madrid, Spain*
[b]*Department of Plant Physiology, Faculty of Biology, Havana University, Havana, Cuba*

Abstract

Soluble polysaccharides have been isolated from sugar cane by size-exclusion chromatography using two successive columns of Sephadex G-10 and G-50. Two main fractions of different molecular mass were separated and their homogeneity was tested by HPLC using a Zorbax GF-450 and a Zorbax GF-250 column in series. Whereas the high-molecular-mass soluble polysaccharide (SP) fraction seems to be composed of two different polymers with retention times of about 16.5 and 24.5 min, the mid-molecular-mass carbohydrate (MMMC) fraction is resolved as only one peak with a retention time of about 2.45 min. This implies that Sephadex G-50 is not able to discriminate between the two categories of macromolecules, as SP eluted from Sephadex G-50 is clearly contaminated by MMMC. Fractionation of clarified juice with 80% (v/v) ethanol separates SP as an insoluble fraction and MMMC as an ethanol-soluble macromolecule. The natural fluorescence of both polymers reveals that they are glycoproteins and, in addition, they can clearly be recognized by the degree of tryptophan exposure to its chemical microenvironment.

1. Introduction

Fructans are polyfructosylsucrose polymers that occur widely as storage carbohydrates in vegetative parts of plants [1]. Three main types of fructans occur, depending on plant species [2]:

(i) inulins, which consist of continuous (2→1)-linked β-D-fructofuranosyl units;

(ii) linear fructans of cereal grasses, which are (2→1)-linked β-D-fructofuranosyl units;

(iii) highly branched fructans, consisting of both 1- and 6-linked β-D-fructofuranosyl units with a sucrose unit at the end of the chain. These fructans also contain small proportions of atypical linkages.

On the other hand, sugar cane stalks accumulate heterofructans that are composed of both fructose and galactitol [3]. These fructans occur in two main groups of molecular mass forms: mid-molecular-mass carbohydrates (MMMC), which are [galactitol$_5$: fructose$_4$]$_n$, and high-molecular-mass soluble polysaccharide (SP), which are [galactitol$_3$: fructose$_2$]$_n$ [3,4]. MMMC occurs in at least two forms of M_r about 871 000 and 380 000 [3]. Both SP and MMMC are hydrolysed by a glycosidase system which produces fructose and galactitol from its substrates [3–5].

Both SP and MMMC seem to be produced from structural polymers occurring in the cell

* Corresponding author.

0021-9673/95/$09.50
SSDI 0021-9673(94)00948-1

wall of parenchymatous cells [4], in contrast to fructans synthesized by C3 grasses [6,7], where fructans are produced when the amount of sucrose exceeds that required for transport and metabolism [8]. The structural sugar cane polymer is partially hydrolysed by a glycosidase to liberate mainly SP to the cytosol, where MMMC is produced later [4].

Fructans of the *Gramineae* are usually separated by using strongly alkaline conditions for their elution from anion-exchange columns and pulsed amperometric detection [9]. Oligosaccharides from partially hydrolysed fructans can be separated by HPLC using a Spherisorb-5-NH_2 column and running it with a mobile phase of acetonitrile–water [10]. Gas–liquid chromatography also allows the separation of several oligosaccharides as trimethylsilyl derivatives or methylated alditol acetates [11]. Separation of heterofructans from sugar cane has been carried out by HPLC using a PWSX GO209 column packed with G5000 PWXL [4].

In this work, both SP and MMMC were analysed by HPLC and fluorescence emission in order to obtain some additional information about their chemical nature.

2. Experimental

2.1. Plant material

Saccharum officinarum L., of variety Jaronu 60-5, field-grown, was used throughout.

2.2. Preparation of soluble polysaccharides

Stalks from 12-month-old plants were mechanically crushed, immediately after cutting, and the raw juice was adjusted to pH 8.0 by adding a saturated solution of ammonium carbonate, followed by filtration through filter-paper. Sodium azide was added to the filtrate to obtain a final concentration of 0.02% (w/v) [12].

This clarified juice was then filtered through a 15 cm × 2.5 cm I.D. column of Sephadex G-10 (Pharmacia, Uppsala, Sweden), pre-equilibrated with a saturated solution of ammonium carbonate containing 0.02% sodium azide. The first 20 × 1.0-ml fractions of eluate were discarded. Fractions 21–39 were collected and filtered through a Sephadex G-50 column (30 cm × 2.5 cm I.D.), pre-equilibrated as above. Fractions 40–70 contained the soluble, high-molecular-mass polysaccharides (SP fraction) whereas the mid-molecular-mass carbohydrates (MMMC fraction) eluted from 71 to 120 ml [12]. Carbohydrates were quantitatively measured in the different fractions by the method of Dubois et al. [13]. Both GLC and HPLC analyses [3] showed the absence of sucrose and monosaccharides in fractions from 40 to 120 ml. Clarified juice and soluble polysaccharides were dialysed overnight, at 4°C, against 0.2 *M* phosphate buffer (pH 6.9) using Visking dialysis tubing 27/32 from Serva (Heidelberg, Germany), which retains more than 90% of cytochrome *c* (M_r 12 400).

Alternatively, raw juice was brought to 5% (w/v) trichloroacetic acid or to 80% (v/v) cold ethanol, filtered through a double cheese-cloth and centrifuged for 30 min at 20 000 *g* at room temperature. Pellets were discarded and supernatants were heated at 60°C for 20 min and subjected twice to the same precipitation procedure with 80% (v/v) ethanol [14]. The last supernatants were evaporated to dryness under reduced pressure. Each residue was dissolved in 2.0 ml of 0.2 *M* sodium phosphate buffer (pH 6.9). Finally, solutions were loaded on to the chromatographic column.

The different samples were also assayed for the Folin phenol reaction according to Lowry et al. [15], using bovine serum albumin as a standard.

2.3. HPLC analysis

Approximately 20 μg of soluble polysaccharides were chromatographed on two columns (both 25 cm × 9.4 mm I.D.) Zorbax GF-450 and Zorbax GF-250 (DuPont–Hichrom, Reading, UK), connected in series, according to Pedrosa and Legaz [16], using 0.2 *M* phosphate buffer (pH 6.9) as the mobile phase at a flow-rate of 1 ml min^{-1}. The dead time was determined as 12.3

min, using Blue Dextran 2000 as a standard. The equipment was a Spectra-Physics (Fremont, CA, USA) SP8800 liquid chromatograph equipped with an SP 4290 computer. Detection was performed at 210 and 275 nm by using a Spectra-Physics SP8490 UV–Vis detector.

2.4. Measurements of absorbance and fluorescence spectra

Absorption spectra were recorded using a Varian (Walnut Creek, CA, USA) DMS 90 dual-beam spectrophotometer. Fluorescence spectra of different polysaccharides were determined by using a Kontron (Milan, Italy) SFM-25 spectrofluorimeter equipped with quartz cuvettes of 1-cm path length. The wavelength of the exciting radiation was either 210 or 275 nm.

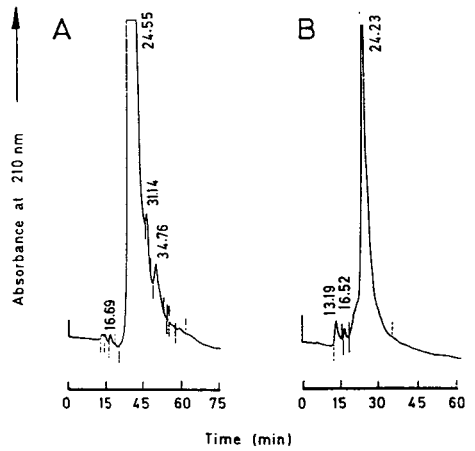

Fig. 1. HPLC elution profiles of (A) filtered raw sugar cane juice and (B) centrifuged and dialysed sugar cane juice. Numbers near the peak represent retention times in minutes.

3. Results

3.1. HPLC separation of water-soluble glycoproteins from sugar cane juice

The conventional procedure for SP and MMMC preparation includes clarification of sugar cane juice by precipitation with ammonium carbonate, filtration through filter-paper and subsequently sequential filtration through successive columns of Sephadex G-10 and G-50. The HPLC traces obtained for clarified sugar cane juice showed a main peak at 24.55 min and secondary peaks at 13.25, 14.42 (traces), 16.69, 31.14 and 34.76 min. This same juice, after dialysis followed by a second centrifugation, produced only three peaks at 13.19, 16.52 and 24.23 min (Fig. 1A and B). As the dialysis membrane retained polymers with molecular masses higher than 10 000, substances eluted at 31.14 and 34.76 min should have molecular masses lower than this value.

SP solution, after dialysis, produced two peaks recorded at 210 nm, with retention times of 16.6 and 23.86 min (Fig. 2A). Only this last peak was also recorded at 275 nm, with a retention time of 23.53 min (Fig. 2B). The ratio of area counts at 210 nm to those at 275 nm was 3.25. However,

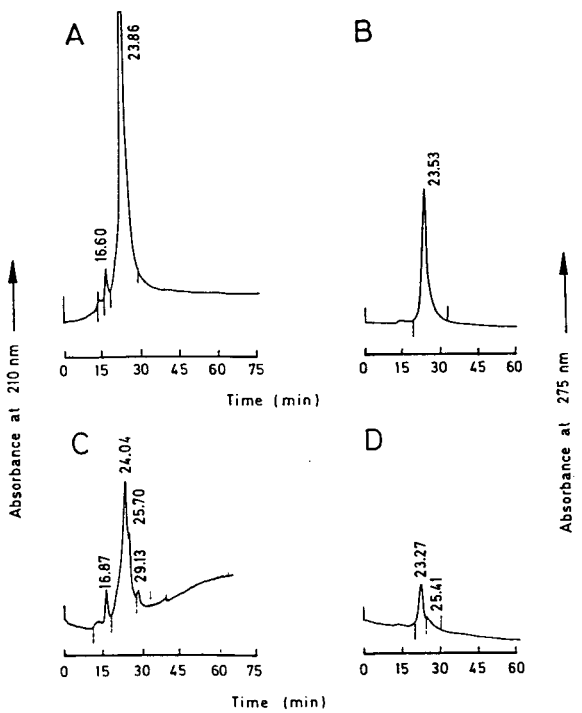

Fig. 2. HPLC elution profiles of (A) and (B) dialysed SP and (C) and (D) SP recently isolated from a Sephadex G-50 column.

SP recently prepared by filtration of sugar cane juice through Sephadex G-10 and G-50 contained two main substances that eluted at 16.87 and 24.04 min, with monitoring of the eluate at 210 nm (Fig. 2C). However, only one peak at 23.27 min was detected at 275 nm (Fig. 2D). The ratio of area counts at 210 nm to that at 275 nm was 4.64. Only one peak in HPLC was detected for MMMC samples filtered through Sephadex or dialysed, with a retention time near 24 min. This substance was detected at 210 and 275 nm, although its absorbance at 210 nm was 3–4 times higher than that observed at 275 nm (Fig. 3).

3.2. HPLC separation of both ethanol-soluble and ethanol-insoluble glycoproteins from sugar cane juice

An alternative procedure for isolating soluble polysaccharides from sugar cane juice was attempted in order to separate proteins from the polysaccharide fraction. Precipitates produced after ethanol extraction were dried for later chromatography. In parallel, juices were first precipitated with 5% (w/v) TCA, the precipitate was discarded and the supernatant extracted with cold 80% (v/v) ethanol as described previously. The different precipitates were dried and subsequently analysed. Finally, the last supernatant was dried and chromatographed. Only the peak with a retention time of about 24.5 min appeared in the last supernatant (Fig. 4), similar in chromatographic behaviour to that shown as the sole component of the MMMC fraction. Chromatographic analysis of the pellets redissolved in distilled water indicated that the substance with a retention time of 16.55 min is completely recovered in these pellets, independently of the previous treatment with TCA.

3.3. Spectral characteristics of soluble glycoproteins from sugar cane juice

The UV absorption spectra of dialysed SP and MMMC showed an absorption maximum at 274 nm and only that of MMMC a shoulder at 250 nm (Fig. 5A). The absorbance at 210 nm was

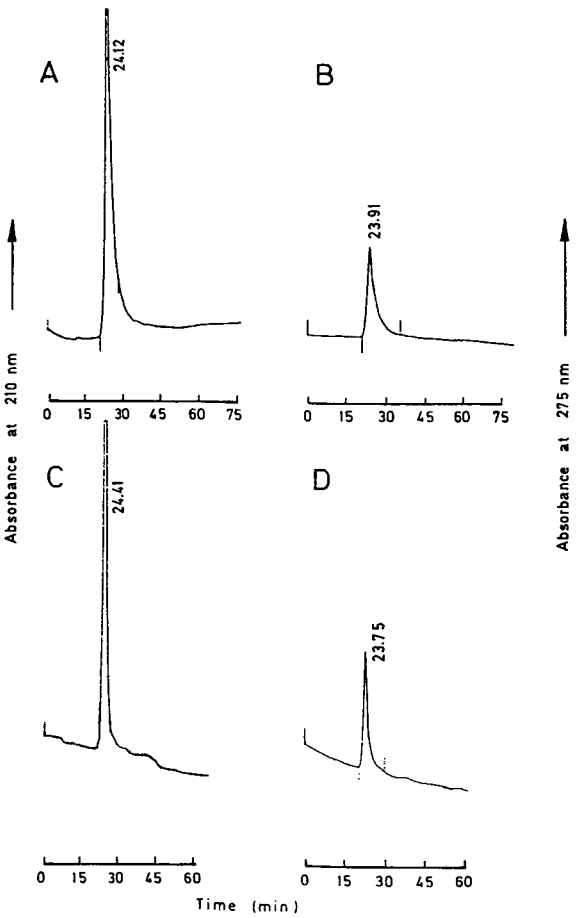

Fig. 3. HPLC elution profiles of (A) and (B) dialysed MMMC and (C) and (D) MMMC recently isolated from a Sephadex G-50 column.

about three times higher than at 274 nm. The UV absorption spectrum of Sephadex filtered SP showed an absorption maximum at 275 nm whereas that of MMMC showed a main maximum at 271 nm and a secondary maximum at 246 nm (Fig. 5B), very similar to that found for the dialysed carbohydrate. The absorbance at 210 nm was 3.5 times higher than at 271–275 nm.

Both preparations of SP, that only filtered through Sephadex G-50 and that dialysed, showed some similarities in their fluorescence spectra when the wavelength of the excitation

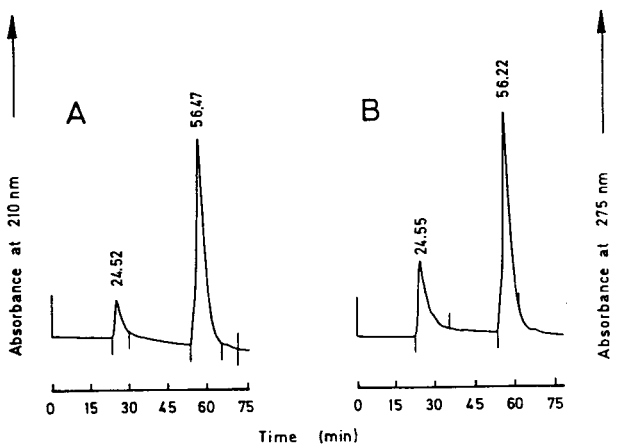

Fig. 4. HPLC elution profiles of the last supernatants after ethanol extraction of raw sugar cane juice monitored at (A) 210 and (B) 275 nm.

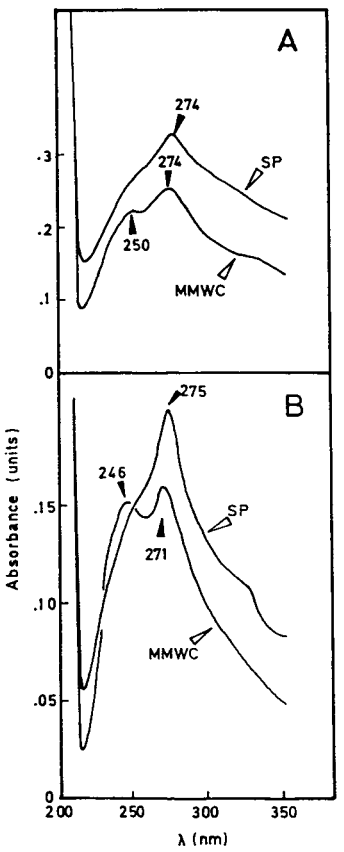

Fig. 5. UV absorption spectra of (A) dialysed SP and MMMC and (B) recently SP and MMMC filtered through Sephadex G-50.

radiation was 210 nm. Whereas SP filtered through Sephadex had a net maximum of fluorescence emission at 422 nm, a secondary maximum at 296 nm and a shoulder at 332 nm (Fig. 6A), dialysed SP had two maxima of fluorescence emission, a secondary maximum at 427 nm and another, the main maximum, at 327 nm, and two shoulders at 380 and 302 nm (Fig. 6B). MMMC showed a net maximum of fluorescence emission at 296–297 nm on using exciting radiation of 210 nm, but only that filtered through Sephadex had a secondary maximum at 347 nm (Fig. 6C and D). By exciting samples with radiation of 275 nm, both forms of SP showed only one maximum of fluorescence emission at 334–336 nm (Fig. 7A and B). However, MMMC filtered through Sephadex showed a maximum of emission at 347 nm (Fig. 7C) whereas dialysed MMMC had a secondary maximum at 346 nm and a main maximum at 320 nm (Fig. 7D).

Results for the determination of different the polysaccharides as glycoproteins, according to Lowry et al. [15], showed that SP was composed of equal proportions of the protein and polysaccharide moieties, whereas MMMC was 20% protein and 80% polysaccharide (data not shown).

4. Discussion

Martínez et al. [4] were able to find that SP, purified by column chromatography on Sephadex from Cuba 374-72 sugar cane juice, was a heteropolymer with a molecular mass of about 1 735 000, whereas MMMC had a molecular mass of about 870 000. Both purified fractions were contaminated with a dextran with a molecular mass of about 9000. Analyses were carried out by HPLC using a PWSX GO209 column packed with G5000 PWXL. However, purification of both SP and MMMC from Jaronu 60-5 sugar can juice using the procedure described in this work did not completely separate the two

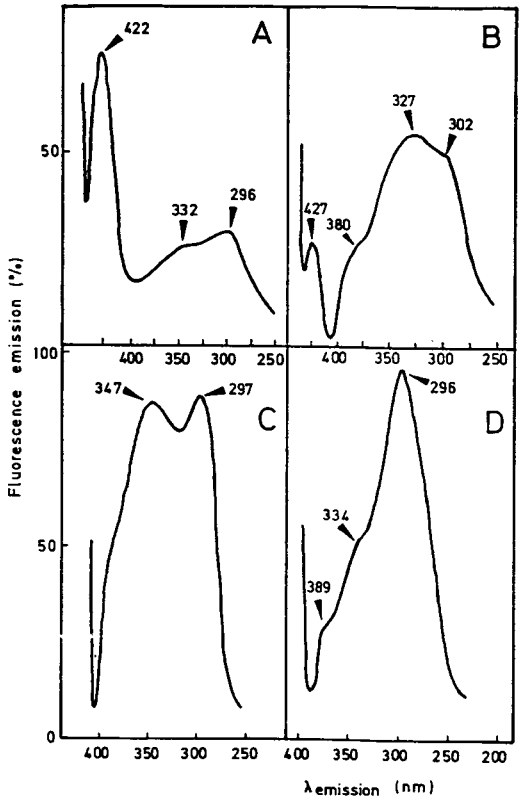

Fig. 6. Fluorescence emission spectra of (A) SP recently filtered through Sephadex G-50, (B) dialysed SP, (C) MMMC recently filtered through Sephadex G-50 and (D) dialysed MMMC, obtained by exciting samples with radiation of 210 nm. Fluorescence emission was recorded from 440 to 250 nm.

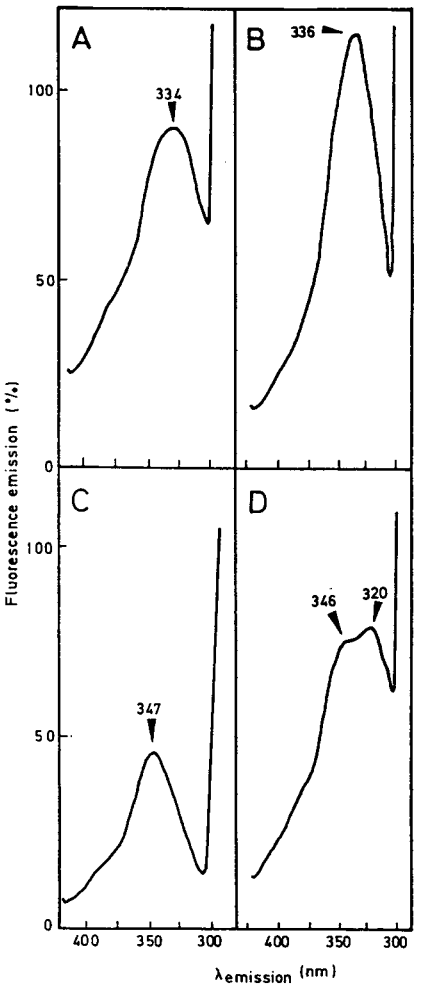

Fig. 7. Fluorescence emission spectra of (A) SP recently filtered through Sephadex G-50, (B) dialysed SP, (C) MMMC recently filtered through Sephadex G-50 and (D) dialysed MMMC, obtained by exciting samples with radiation of 275 nm. Fluorescence emission was recorded from 440 to 280 nm.

forms of heterofructan, as MMMC behaves as a macromolecule purified to homogeneity with a sole peak in HPLC with a retention time of about 24.5 min, and this same peak also appeared in the chromatographic traces of SP analysis in addition to one with a retention time of about 16.5 min (Figs. 2 and 3). The last peak corresponds to a substance largely insoluble in 80% (v/v) ethanol and then the final supernatants after three successive extractions with ethanol do not contain this SP form (Fig. 4). Insolubility in ethanol can be explained as a consequence of the high molecular mass of this polymer [4].

However, some optical properties of these heterofructans reveal that they are not pure polysaccharides but glycoproteins. The fluorescence of both SP and MMMC cannot be explained in terms of polysaccharide excitation and subsequent emission, as this class of macromolecules fluoresces only when they are highly oxidized [17], although the polysaccharide moiety of both SP and MMMC is a heterofructan composed of fructose and galactitol [3] and hence

they are even more reduced than homofructans from grasses [1,8]. However, the possible glycoproteic nature of these soluble molecules could explain several of their fluorescence characteristics. Tryptophan becomes evident in MMMC by the maximum of fluorescence emission at 347–346 nm after exciting the samples with radiation of 275 nm (Fig. 6C and D). However, this maximum displaces towards 334–336 nm for SP (Fig. 6A and B). According to these results, tryptophan seems to be highly exposed in MMMC molecules whereas the amino acid could be placed in a more hydrophobic position in SP, far from the hydrophilic surface of the glycoprotein [18,19]. By exciting the samples with radiation of 210 nm, the same behaviour of fluorescence emission of tryptophan is recorded but, in this instance, tyrosine can also be detected by a net peak of fluorescence at 296–302 nm (Fig. 7).

Acknowledgements

This work was supported by a grant from the Dirección General de Cooperación Internacional (Spain). We are indebted to Miss Raquel Alonso for technical assistance.

References

[1] H.G. Pontis, in P.M. Dey (Editor), *Methods in Plant Biochemistry, Vol. 2. Carbohydates*, Academic Press, London, 1990, p. 353.

[2] N.C. Carpita, J. Kanabus and T.L. Housley, *J. Plant Physiol.*, 134 (1989) 162.

[3] M.E. Legaz, L. Martín, M.M. Pedrosa, C. Vicente, R. de Armas, M. Martínez, I. Medina and C.W. Rodriguez, *Plant Physiol.*, 92 (1990) 679.

[4] M. Martínez, M.E. Legaz, M. Paneque, R. de Armas, M.M. Pedrosa, I. Medina, C.W. Rodriguez and C. Vicente, *Int. Sugar J.*, 92 (1990) 155.

[5] M. Martínez, M.E. Legaz, M. Paneque, R. Domech, R. de Armas, I. Medina, C.W. Rodriquez and C. Vicente, *Plant Sci.*, 72 (1990) 193.

[6] C.W.E. Darwen and P. John, *Plant Physiol.*, 89 (1989) 658.

[7] D. Dubois, M. Winzeler and J. Nösberger, *Crop Sci.*, 30 (1990) 315.

[8] C.J. Pollock, *New Phytol.*, 104 (1986) 1.

[9] N.J. Chatterton, P.A. Harrison, N.R. Thornley and J.H. Bernett, *Plant Physiol. Biochem.*, 27 (1989) 289.

[10] M. Frehner, F. Keller, A. Wiemken and Ph. Matile, *J. Plant Physiol.*, 116 (1984) 197.

[11] C.J. Pollock, M.A. Hall and D.P. Roberts, *J. Chromatogr.*, 171 (1979) 411.

[12] C.W. Rodriguez, P. Valdés and M. Martínez, *Cienc. Agric.*, 22 (1985) 63.

[13] D. Dubois, K.A. Gilles, J.K. Hamilton, P.A. Rebers and F. Smith, *Anal. Biochem.*, 28 (1956) 350.

[14] C. Vicente, J.L. Mateos, M.M. Pedrosa and M.E. Legaz, *J. Chromatogr.*, 553 (1991) 271.

[15] H.O. Lowry, N.H. Rosebrough, A.L. Farr and R.J. Randall, *J. Biol. Chem.*, 193 (1951) 265.

[16] M.M. Pedrosa and M.E. Legaz, *Electrophoresis*, in press.

[17] I.D. Campbell and R.A. Dwek, *Biological Spectroscopy*, Benjamin/Cumming, Menlo Park, CA, 1984, p. 61.

[18] S.M. Green, E. Eisenstein, P. McPhie and P. Hensley, *J. Biol. Chem.*, 265 (1990) 1601.

[19] S.M. Green, A. Ginsburg, M.S. Lewis and P. Hensley, *J. Biol. Chem.*, 266 (1991) 21474.

ELSEVIER

Journal of Chromatography A, 697 (1995) 337–343

JOURNAL OF CHROMATOGRAPHY A

High-performance frontal analysis for the study of protein binding of troglitazone (CS-045) in albumin solution and in human plasma

Akimasa Shibukawa[a,*], Takeshi Sawada[a], Chikako Nakao[a], Takashi Izumi[b], Terumichi Nakagawa[a]

[a]*Faculty of Pharmaceutical Sciences, Kyoto University, Sakyo-ku, Kyoto 606, Japan*

[b]*Product Development Laboratories, Sankyo Co. Ltd., 2-58 Hiromachi 1-chome, Shinagawa-ku, Tokyo 140, Japan*

Abstract

An on-line frontal analysis HPLC system was developed for the determination of the unbound concentration of troglitazone (CS-045), a new oral antidiabetic agent, in human serum albumin (HSA) solution and in human plasma. This system consists of a high-performance frontal analysis (HPFA) column, an extraction column, and an analytical column, which are connected via two switching valves. After the direct injection of the sample solution into the HPFA column, the drug was eluted as a zonal peak with a plateau region. The unbound drug concentration was determined as the drug concentration in the plateau. As low as 0.3 nM unbound CS-045 was determined with good reproducibility. It was found that CS-045 strongly binds with HSA, and the bound fraction in the 550 μM HSA solution was 99.93%, which was very close to that in human plasma (99.89%). The bound fractions were constant within the total drug concentration range of 1–10 μM in the HSA solution and 250 nM–10 μM in human plasma.

1. Introduction

Troglitazone (CS-045, Fig. 1) is a novel oral antidiabetic agent which enhances insulin action at the receptor and postreceptor levels in both peripheral and hepatic tissues, while it does not enhance insulin secretion [1]. CS-045 is now under development for the treatment of non-insulin-dependent diabetes mellitus. CS-045 is highly bound to plasma protein, and the unbound CS-045 concentration could not be determined precisely using any conventional method.

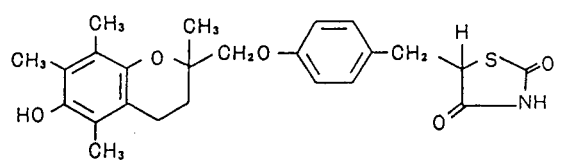

Fig. 1. Molecular structure of troglitazone (CS-045).

The quantitative investigation of drug–protein binding is essential in effective drug development and its safe use in clinical applications, because protein binding plays an important role in the pharmacokinetics and pharmacodynamics of the drug [2–4]. Equilibrium dialysis and ultrafiltration followed by HPLC analysis have been widely used for this purpose. However, these conventional analytical methods are not applicable for the analyses of strongly bound drugs,

* Corresponding author.

0021-9673/95/$09.50
SSDI 0021-9673(94)00929-5

because of the errors caused by drug adsorption onto the membrane and by the leakage of the bound drug from the membrane as well as the difficulty in determining low concentrations of unbound drug. To overcome this problem, we have developed high-performance frontal analysis (HPFA), a chromatographic method which allows simple and easy determination of unbound drug concentrations after direct sample injection [5–13]. HPFA is advantageous for the analysis of strongly bound drugs because (i) HPFA is free from the problems which arise using a membrane (adsorption of drug and leakage of bound drug), and (ii) the bound drug is transformed into the unbound form in the HPFA column, which improves the measurement of low levels of unbound drug [13]. Details of the principle and features of the HPFA method were mentioned previously [6]. The reliability of this method has been confirmed by comparing the analytical results with those obtained by the conventional methods, such as ultrafiltration, using many kinds of drugs (indometacin, salicylate, acetazolamide, diclofenac, carbamazepine, warfarin, ketoprofen and fenoprofen) as model samples.

This paper deals with the development of an on-line frontal analysis HPLC system, in which the HPFA method was incorporated, to determine the unbound CS-045 concentrations in human serum albumin (HSA) solution and in human plasma.

2. Experimental

2.1. Reagent and materials

CS-045 was a product of Sankyo (Tokyo, Japan). Human serum albumin (HSA, fatty acid free) was purchased from Sigma (St. Louis, MO, USA). Human plasma was prepared from fresh human blood.

2.2. Preparation of sample solutions

The stock solution of CS-045 was made up in ethanol. An appropriate volume of the stock solution was transferred to a 10-ml screw-capped glass vial, and the solvent was evaporated under a nitrogen gas stream. An appropriate volume of the HSA solution (in 67 m*M* phosphate buffer, ionic strength 0.17) or human plasma was added to the vial, and was shaken gently for 2 h at 37°C.

2.3. Determination of unbound CS-045 concentration

Fig. 2 shows the schematic diagram of the on-line frontal analysis HPLC system, where the HPFA column (F) (Develosil 100Diol5, 30 cm × 8 mm I.D., Nomura, Seto, Japan), an extraction column (G) (Develosil ODS-10, 1 cm × 4 mm I.D., Nomura), and an analytical column (H) (Cosmosil $5C_{18}$-AR, 15 cm × 4.6 mm I.D., Nacalai Tesque, Kyoto, Japan) were connected via a four-port switching valve (I) and a six-port switching valve (J). The operating conditions are given in Table 1.

The sample solution was directly injected onto the diol-silica column through the injector loop. CS-045 was eluted as a zonal peak with a plateau region, as the drug–protein binding equilibrium in the sample solution was regenerated at the top of the diol-silica column. As a result, the drug concentration in the plateau region represents the unbound drug concentration in the sample

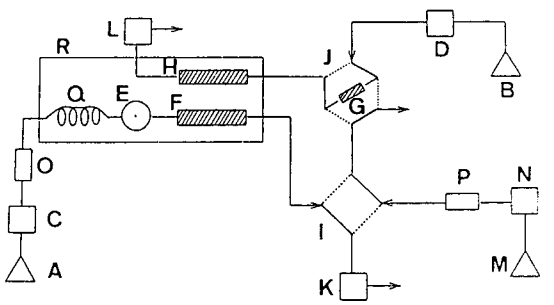

Fig. 2. Schematic diagram of the on-line HPLC system. (A) Mobile phase for HPFA; (B) mobile phase for chiral separation; (C,D) pump; (E) sample injector; (F) column for HPFA; (G) column for extraction; (H) analytical column; (I) four-port switching valve; (J) six-port switching valve; (K,L) UV detector; (M) distilled water to wash extraction column; (N) pump; (O,P) ODS column for mobile phase purification; (Q) 5 ml loop for mobile phase preheating; (R) column oven.

Table 1
Conditions of HPFA–HPLC system

Subsystem		Condition
HPFA	Column	Develosil 100Diol5 (30 cm × 8 mm I.D.)
	Mobile phase	67 m*M* sodium phosphate buffer (pH 7.4, ionic strength 0.17)
	Flow-rate	1.0 ml/min
	Detection	UV 230 nm
	Temperature	37°C
Extraction	Column	Develosil ODS-10 (1 cm × 4 mm I.D.)
Analytical HPLC	Column	Cosmosil $5C_{18}$-AR (15 cm × 4.6 mm I.D.)
	Mobile phase	Water–acetonitrile–acetic acid (500:500:1, v/v)
	Flow-rate	1.2 ml/min
	Detection	UV 230 nm
	Temperature	37°C

solution. While the plateau region was being eluted from the HPFA column, the valve I was switched from the solid line to the broken line for a given period of time. By this heart-cut procedure, a known volume of eluent in the plateau region was transferred into the extraction column G where the drug was adsorbed and concentrated. By switching the valve J, the extracted drug was desorbed and transferred into the analytical column H, and the peak area was measured at UV 230 nm. The extraction column was washed with water for 3 min before the heart-cut procedure and for 1 min after the heart-cut procedure. The 5 ml loop Q was used for preheating the HPFA mobile phase. For the purification of the mobile phase, small ODS columns O and P (Develosil ODS-10, 1 cm × 4.0 mm I.D., Nomura Chemical) were put in the line. A typical time schedule for valve switching is shown in Fig. 3.

The instruments used are as follows: pumps C and D (LC-6A, Shimadzu), pump P (Twincle, Jasco, Tokyo, Japan), UV detectors K and L (SPD-2A and SPD-6A, Shimadzu), injector E (Rheodyne Type 8125, equipped with a 20 μl or 2.5 ml loop) and an integrated data analyzer (Chromatopac C-R6A, Shimadzu).

The calibration line was prepared as follows. The standard solutions of CS-045 were made up in ethanol at the concentrations of 0.415, 1.02, 2.44, 5.06, 10.1, 14.9 and 20.0 μM for the analysis of the CS-045–HSA mixed solutions, and at 0.232, 0.58, 1.16, 2.31, 4.62, 8.06, 11.5 and 16.0 μM for the analysis of the CS-045–plasma samples. The diol-silica column was off-line, and the volume of the injector loop was changed from 2.5 ml to 20 μl. A 5-μl portion of standard solution was injected directly into the extraction column which had been previously washed with water for 3 min. After perfusing the extraction column with water for 1 min, the adsorbed CS-045 was back-flushed into the analytical column by the column switching procedure. The calibration line was prepared by plotting the peak area (average of two runs) vs. the amount of CS-045 (picomole) injected. The

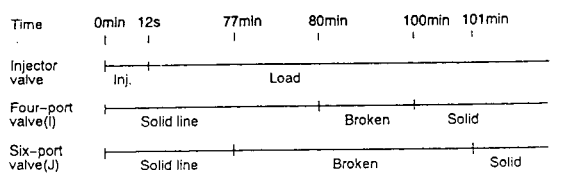

Fig. 3. Typical time program for valve switching. The heart-cut time is 80–100 min.

calibration lines showed good linearity (correlation coefficient, >0.999). The amount of CS-045 calculated from the calibration line was divided by the heart-cut volume to give the unbound drug concentration.

The peak area of CS-045 obtained by injecting a 5-μl portion of 14.9 μM CS-045 solution in ethanol into extraction column G were 96% compared to the direct injection of the same volume of the same CS-045 solution into the analytical column H. This indicates the complete extraction of CS-045 onto column G and the complete transfer of the extracted CS-045 into the analytical column.

3. Results and discussion

3.1. Determination of unbound CS-045 in HSA solution

It is essential that the binding equilibrium in the drug–protein sample solution is regenerated in the HPFA column. In order to maintain the equilibrium state, it is preferable to use an aqueous buffer solution without organic modifier in the mobile phase. However, it is difficult to elute a hydrophobic drug from a restricted-access type stationary phase containing hydrophobic ligands using an aqueous buffer solution. Therefore, a hydrophilic diol-silica column was used in the present study. This column allows the elution of CS-045 by phosphate buffer containing no organic modifier.

Fig. 4 shows the chromatograms of 10 μM CS-045 and 550 μM HSA mixed solution. When 5 μl of the mixed solution were injected into the diol-silica column, CS-045 gave a single peak well separated from the protein peak (Fig. 4A). However, when a 200-μl portion of the mixed solution was injected, CS-045 was eluted as the zonal peak with a plateau region (Fig. 4B), which can be found more clearly from the subtraction chromatogram (Fig. 4D). The plateau height was not changed even when the injection volume of the same solution was decreased to 100 μl. When CS-045 standard solution containing no protein was injected, CS-045

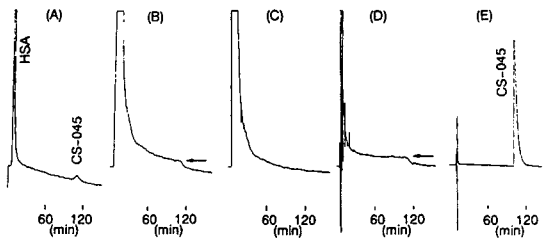

Fig. 4. Elution profile of CS-045 from the diol-silica column. Sample: (A,B) 10 μM CS-045–550 μM HSA solution; (C) 550 μM HSA; (E) 1.39 mM CS-045 in ethanol. Injection volume: (A) 5 μl, (B) 200 μl, (C) 200 μl, (E) 5 μl. Chromatogram (D) is the subtraction of (C) from (B). HPLC conditions, see Table 1. The a.u.f.s. of chromatogram (E) is eight times larger than those of (A)–(D).

was eluted as a single sharp peak (Fig. 4E). This clearly indicates that the protein binding is responsible for the zonal elution of this drug. From this result, the injection volume was determined to be 200 μl.

Preventing diffusion of the sample solution in the injector loop is essential for HPFA, because otherwise the binding equilibrium is disturbed and the plateau region may disappear. The injector-reswitching technique [12] is useful to overcome this problem. In this study, the injector loop was loaded with a 300-μl portion of the CS-045–HSA solution, and connected to the mobile phase flow (1.0 ml/min) for 12 s. This resulted in 200 μl sample injection. By this technique, the sample input could be regarded as an ideal rectangular shape.

Fig. 5 shows the relation between the elution time and the CS-045 concentration in the eluent. The eluent was heart-cut every 5 min, and was subjected to the on-line preconcentration and HPLC analysis. Each point was plotted at the end of the heart-cut time. This result clearly indicates that a wide range of the plateau region appeared between 35–115 min. The unbound concentration, estimated as the average CS-045 concentration in this region (35–115 min, 16 data points), was 7.28 ± 0.187 nM, that is, the bound fraction (bound:total concentration ratio) was 99.93%.

It is interesting that a plateau volume as large as 80 ml was obtained by injecting only a 200 μl portion of the sample volume. This is called

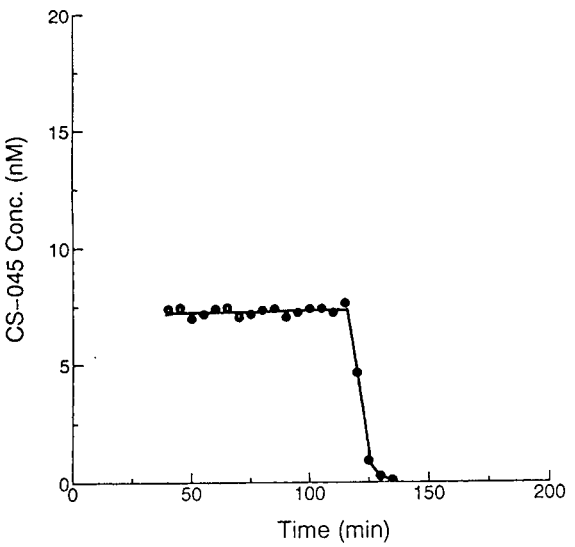

Fig. 5. Relation between the elution time and the CS-045 concentration for human plasma. Sample: 10 μM CS-045–550 μM HSA solution. Injection volume: 200 μl. HPLC conditions, see Table 1. Heart-cut volume, 5 ml. Each point was plotted at the end of the heart-cut time.

'regulation effect' [13]. In HPFA, the bound drug is not separated from the unbound drug, but is converted into the unbound form. Then, the whole (bound and unbound) drug fraction is eluted as a single zonal peak, and the drug concentration in the plateau region is regulated by the protein binding to be the same as the unbound drug concentration. Because of this 'regulation effect', the plateau volume becomes larger than the injection volume. This effect increases when the drug binds more strongly to the protein.

Table 2 lists the unbound CS-045 concentrations in 550 μM HSA solutions determined by the present HPLC system. Fig. 6 shows the

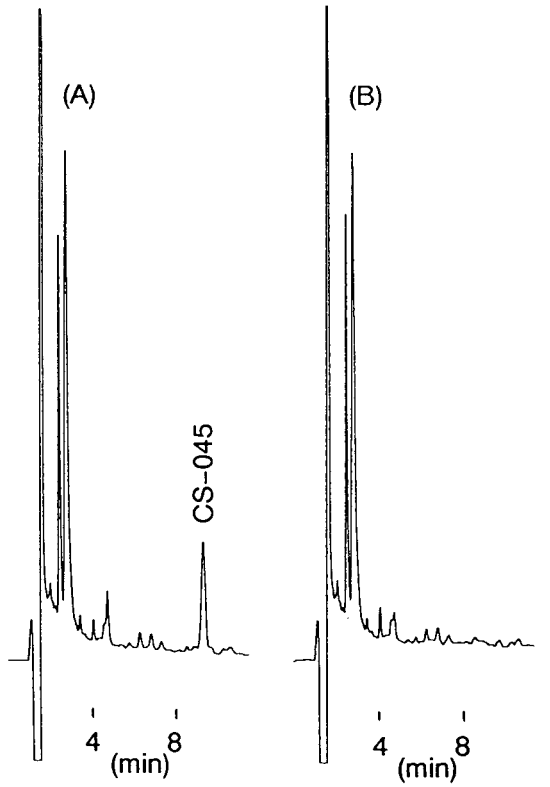

Fig. 6. Analysis of unbound CS-045 in HSA solution on the analytical column. Sample: (A) 1 μM CS-045–550 μM HSA solution; (B) 550 μM HSA solution. HPLC conditions, see Table 1.

chromatogram obtained from the sample solution containing 1 μM CS-045. As low as 0.655 nM of the unbound concentration was determined by UV detection (230 nm), because CS-045 in a large volume (20 ml, heart-cut time 80–100 min) of the plateau region was concentrated in the extraction column. The reproducibility was good (C.V. = 5.10%, $n = 5$). The

Table 2
Unbound CS-045 concentrations in human serum albumin solutions

Sample solution	Unbound concentration (nM)	Bound fraction
1 μM CS-045–550 μM HSA	0.655 ± 0.033	99.93 ± 0.003%
10 μM CS-045–550 μM HSA[a]	7.28 ± 0.187	99.93 ± 0.002%

Mean ± S.D. ($n = 5$).
[a] Determined from the results of Fig. 5 ($n = 16$).

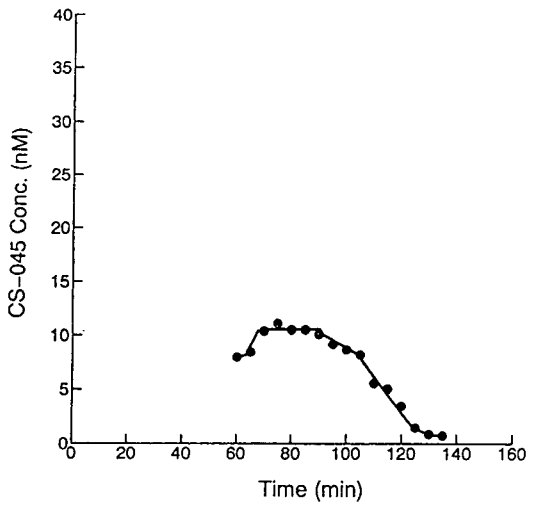

Fig. 7. Relation between elution time and CS-045 concentration in the eluent. Sample: 10 μM CS-045 in human plasma. Injection volume: 1.33 ml. HPLC conditions, see Table 1. Heart-cut volume, 5 ml. Each point was plotted at the end of the heart-cut time.

bound fraction in this sample solution was 99.93%, which was the same as in the 10 μM CS-045–550 μM HSA solution.

3.2. Determination of unbound CS-045 in human plasma

The present system was applied to the analysis of plasma samples. As reported previously, the injection volume for HPFA depends on the unbound drug fraction; a larger injection volume is required if the unbound drug fraction is higher [8]. In the analyses of plasma samples, the sample injection volume was selected to be 1.33 ml, because the unbound fraction in human plasma was higher than that in the 550 μM HSA solution as mentioned later. The injection procedure was as follows. A 2-ml portion of the sample solution was loaded into the injector loop, and the loop was then connected to the mobile phase flow for 80 s. Therefore, the actual injection volume was 1.33 ml. Fig. 7 shows the relation between the elution time and the concentration of CS-045 in the eluent after direct injection of 10 μM CS-045 in human plasma. The CS-045 concentration in each of the eluent fractions between 65 and 90 min was almost the same. That is, the plateau region continued for 25 min. The unbound CS-045 concentration, averaged over 65–90 min (5 data points), was 10.5 ± 0.36 nM, that is, the bound fraction was 99.89%.

Table 3 lists the unbound CS-045 concentrations in human plasma determined by the present system. The chromatograms obtained are shown in Fig. 8. No significant interference by the endogenous plasma components was observed. Very low unbound drug concentrations in the plasma samples containing therapeutic levels of CS-045 (total drug concentration, 250 nM and 1 μM) were determined (heart-cut volume, 10 ml) with good reproducibility (C.V. $< 9.31\%$, $n = 5$). The unbound fractions in the human plasma samples containing 250 nM, 1 μM and 10 μM CS-045 were 0.110%, 0.106% and 0.105%, respectively. These results indicate that the unbound CS-045 concentration in human plasma was proportional to the total concentration ranging from 250 nM to 10 μM. From the results in Table 2, it is obvious that HSA plays a major role in the protein binding of CS-045 in human plasma.

Table 3
Unbound CS-045 concentrations in human plasma

Total concentration	Unbound concentration	Bound fraction
250 nM CS-045	0.274 ± 0.026 nM	$99.89 \pm 0.010\%$
1 μM CS-045	1.06 ± 0.075 nM	$99.89 \pm 0.007\%$
10 μM CS-045[a]	10.5 ± 0.363 nM	$99.90 \pm 0.004\%$

Mean ± S.D. ($n = 5$).
[a] Determined from the result of Fig. 7 ($n = 5$).

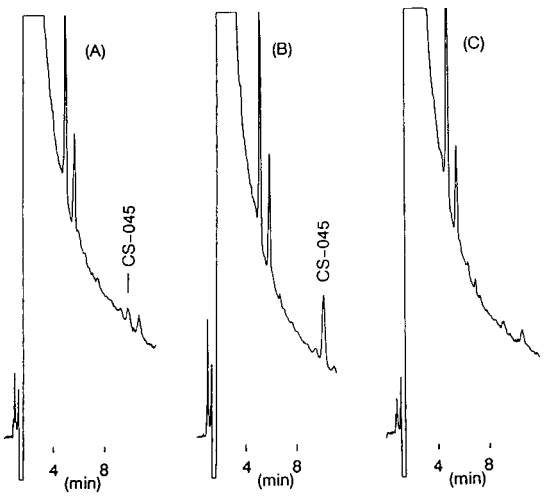

Fig. 8. Analysis of unbound CS-045 in human plasma on the analytical column. Sample: (A) 250 n*M* CS-045 in human plasma; (B) 1 μM CS-045 in human plasma; (C) human plasma. HPLC conditions, see Table 1.

4. Conclusion

The unbound CS-045 concentrations in the 550 μM HSA solution and in human plasma were determined using an on-line frontal analysis HPLC system. CS-045 was strongly bound to plasma protein; the bound CS-045 fraction was 99.89%. The bound CS-045 fraction was constant within a wide range of total drug concentration (250 nM–10 μM). HSA plays a major role in the protein binding of CS-045.

References

[1] T. Fujiwara, S. Yoshioka, T. Yoshioka, I. Ushiyama and H. Horikoshi, *Diabetes*, 37 (1988) 1549–1558.
[2] M.C. Meyer and D.E. Guttman, *J. Pharm. Sci.*, 57 (1968) 895–918.
[3] J.J. Vallner, *J. Pharm. Sci.*, 66 (1977) 447–465.
[4] T.C. Kwong, *Clin. Chim. Acta*, 151 (1985) 193–216.
[5] A. Shibukawa, T. Nakagawa, N. Nishimura, M. Miyake and H. Tanaka, *Chem. Pharm. Bull.*, 37 (1989) 702–706.
[6] A. Shibukawa, N. Nishimura, K. Nomura, Y. Kuroda and T. Nakagawa, *Chem. Pharm. Bull.*, 38 (1990) 443–447.
[7] A. Shibukawa, M. Nagao, Y. Kuroda and T. Nakagawa, *Anal. Chem.*, 62 (1990) 712–716.
[8] N. Nishimura, A. Shibukawa and T. Nakagawa, *Anal. Sci.*, 6, (1990) 355–359.
[9] A. Shibukawa, A. Terakita, J. He and T. Nakagawa, *J. Pharm. Sci.*, 81 (1992) 710–715.
[10] A. Terakita, A. Shibukawa and T. Nakagawa, *Anal. Sci.*, 9, (1993) 229–232.
[11] A. Shibukawa, M. Nagao, A. Terakita, J. He and T. Nakagawa, *J. Liq. Chromatogr.*, 16 (1993) 903–914.
[12] A. Terakita, A. Shibukawa and T. Nakagawa, *Anal. Sci.*, 10 (1994) 11–15.
[13] A. Shibukawa, C. Nakao, T. Sawada, A. Terakita, N. Morokoshi and T. Nakagawa, *J. Pharm. Sci.*, 83 (1994) 868–873.

ELSEVIER

Journal of Chromatography A, 697 (1995) 345–355

JOURNAL OF CHROMATOGRAPHY A

Determination of traces of herbicide mixtures in water by on-line solid-phase extraction followed by liquid chromatography with diode-array detection and multivariate self-modelling curve resolution

S. Lacorte[a], D. Barceló[a,*], R. Tauler[b]

[a]*Department of Environmental Chemistry, CID–CSIC, Jordi Girona Salgado 18–26, 08034 Barcelona, Catalonia, Spain*
[b]*Department of Analytical Chemistry, University of Barcelona, Av. Diagonal 647, 08028 Barcelona, Catalonia, Spain*

Abstract

Multivariate self-modelling curve resolution was applied to the determination of co-eluted alachlor and metolachlor mixtures. Mixture analysis of these two pesticides in the presence of other interferents in real water mixtures was achieved using automated on-line solid-phase extraction coupled with liquid chromatography and diode-array detection (DAD) followed by a recently developed multivariate self-modelling curve resolution method. Two different kinds of water samples were analysed (Milli-Q-purified water and surface river water) using two different analytical columns (Merck and Waters). The proposed approach permitted an improvement in the resolution of the co-eluted herbicides after preconcentration of 100 ml of water samples spiked at the 1.5 μg/l concentration level and also allowed their simultaneous determination independently of the water matrix. Recommendations about further incorporation of the proposed method in liquid chromatographic–diode-array detection methods are given.

1. Introduction

Solid-phase extraction (SPE) coupled on-line with liquid chromatography (LC) is being used for monitoring pesticides in surface and drinking water samples at trace levels (0.1–5 μg/l) in various monitoring programs through Europe [1–5]. The use of automated systems [4–6] or fully automated systems [control of SPE, gradient elution and diode-array detection (DAD) with unique software] [7,8] offers event more advantages for the routine measurement of pesticides at trace levels, since it guarantees good reproducibility and the possibility of analysing a large number of samples routinely. Recently, such systems were validated [6] in interlaboratory exercises in which groundwater samples containing pesticides were analysed and the results were compared with those given by conventional gas chromatographic techniques.

One of the major problems in the on-line determination of pesticides at low levels in different types of waters is the presence of interfering substances, namely humic substances, in the early eluting peaks of the chromatogram. Such interferences are more relevant when analysing surface and estuarine river waters [1,3–5]. The water type is a relevant parameter in the

* Corresponding author.

0021-9673/95/$09.50
SSDI 0021-9673(94)00957-0

determination of pesticides at these low levels, and differences in calibration and quantification have been found depending on the water type [1,5]. A second problem that arises when determining pesticides at these low levels is derived from the co-elution of two compounds in a mixture. Since the LC runs usually involve a mixture of about 30 compounds, is difficult to achieve baseline separation between all the analyte peaks and matrix interferences which appear at this low level of concentration. One co-elution problem in the determination of pesticides in water samples is the co-elution of alachlor and metolachlor [1,9], which is also enhanced by the fact that both compounds elute approximately at 100% organic modifier and also by the presence of interfering compounds.

Recently, our groups [10,11] have been developing software systems for the quantification and deconvolution of chromatographic peaks in different mixtures. Such methods have already been applied to the determination of naphthol and pirimicarb in different eluting mixtures [12]. In the case of alachlor and metolachlor, multivariate self-modelling curve resolution (MSCR) [10–16] is proposed for the resolution and quantification of co-eluted compounds in LC–DAD. In this work, the MSCR method was extended to handle real LC data for herbicides at low concentrations (μg/l) using automated preconcentration techniques.

MSCR will be applied to improve the resolution of co-eluted herbicides metolachlor and alachlor, which have very similar spectra. The determination of these compounds is even more problematic in the case of mixtures at low concentrations (μg/l) when on-line solid-phase preconcentration techniques are used [17]. Then, interferents at very low concentrations and mobile phase effects become more significant than for direct injection analysis of more concentrated samples (mg/l level).

The aim of this work was the application of the most recent chemometric approaches developed by us for the resolution and determination of alachlor and metolachlor at trace levels (1–5 μg/l) in various water samples. The chemometric system developed will be applied in the first instance to (i) direct injection of standard samples of both compounds, (ii) the preconcentration of clean water samples and (iii) the preconcentration of surface river water samples containing both pesticides and the natural interfering substances. The development of such a software system that allows the quantification of peaks at trace levels is particularly relevant since this problem has not been solved in the automated routine measurement of pesticides in water samples by automated SPE methods. The incorporation of such software systems into the DAD software will be a consideration for the future and would be of help for laboratories involved in the routine measurement of pesticides at trace levels using automated systems.

2. Experimental

2.1. Chemicals and reagents

The herbicides alachlor and metolachlor were obtained from Promochem (Wesel, Germany). Pesticide-grade acetonitrile, methanol and water obtained from a Milli-Q purification system (Milli-Q water) were purchased from J.T. Baker (Deventer, Netherlands).

2.2. Chromatographic analysis

Standard solutions of alachlor, metolachlor and a mixture of alachlor and metolachlor were prepared in acetonitrile at a concentration of 20 μg/ml. Each standard was analysed by direct injection using a 20-μl loop and by "on-line" SPE coupled to LC–DAD. When the "on-line" method was used, Milli-Q water was spiked with each standard at a level of 1.5 μg/l. Further, estuarine water samples from the Ebre delta were spiked with the solution containing alachlor and metolachlor.

On-line SPE–LC–DAD was performed with a Prospekt automated preconcentration system (Spark Holland, Emmen, Netherlands). Samples were preconcentrated on 10×2 mm I.D. disposable precolumns prepacked with 15–25-μm PLRP-s styrene–divinylbenzene copolymer,

(Spark, Holland). Precolumns were conditioned via a solvent-delivery unit (SDU) from Spark Holland with 10 ml of acetonitrile, 10 ml of methanol and 10 ml of water at a flow-rate of 2 ml/min. A 100-ml volume of Milli-Q water was percolated through the precolumn at a flow-rate of 2 ml/min. The analytes were desorbed by coupling the precolumn "on-line" with the analytical column and starting the gradient. This method has been validated for some organophosphorus pesticides and was described in a recent paper [6].

The LC analysis was performed with a Waters model (Milford, MA, USA) 600-MS solvent-delivery unit equipped with a Waters model 996 photodiode-array detector. Two cartridge columns were used: (a) a Superspher column (250 × 4 mm I.D.) packed with 4-μm Superspher C_8 (Merck, Darmstadt, Germany) with gradient elution from acetonitrile–water (40:60) to (75:25) in 22 min at a flow-rate of 1 ml/min and then returning to the initial conditions in 3 min and (b) a Novo-Pak cartridge column (15 × 4 mm I.D.) packed with 4–6-μm C_8 (Waters) with gradient elution from acetonitrile–water (30:70) to (80:20) in 8 min, then isocratic for 2 min, at a flow-rate of 1 ml/min, with a return to the initial conditions in 3 min.

The detector was operated at the maximum resolution of 1.2 nm and at one spectrum per second. These conditions were necessary to attain the best spectral resolution.

2.3. Data pretreatment

When the Waters column was used, eight different conditions were studied (matrices W1–W8). When the Merck column was selected, five conditions were studied (matrices M1–M5). A description of each data matrix is given in Table 1.

The selection of the particular elution time

Table 1
Experimental details of different data matrices

Analytical column[a]	Data matrix[b]	Composition[c]		Sample type[d]	Method[e]
		Ala (ng)	Met (ng)		
Waters	W1 (61,51)	404	–	Pure	1
Waters	W2 (41,51)	–	400	Pure	1
Waters	W3 (41,51)	404	400	Pure	1
Waters	W4 (41,51)	–	–	Milli-Q	2
Waters	W5 (41,51)	150	–	Milli-Q	2
Waters	W6 (41,51)	–	151	Milli-Q	2
Waters	W7 (41,51)	150	151	Milli-Q	2
Waters	W8 (34,51)	150	151	River	2
Waters	W9 (34,51)	–	–	River	2
Merck	M1 (81,51)	404	–	Milli-Q	1
Merck	M2 (51,51)	–	400	Milli-Q	1
Merck	M3 (101,51)	404	400	Milli-Q	1
Merck	M8 (66,51)	150	151	River	2
Merck	M9 (66,51)	–	–	River	2

[a] Columns used in each analysis.
[b] Data matrices used in the analysis. In parentheses, the number of rows (elution times every 1 s) and the number of columns (51 wavelengths, between 190 and 251 nm) are given.
[c] Composition of the samples analysed given as total amount of the analytes input to the column; Ala = ng of alachlor and Met = ng of metolachlor injected.
[d] Sample type: Pure = standards prepared in acetonitrile at a concentration of 20 μg/ml; Milli-Q = Milli-Q water spiked with the analytes at a concentration of 1.5 μg/l; River = real water samples taken from the Ebre river spiked or not (see Experimental).
[e] Analytical method used: 1 = direct injection of the standard without preconcentration; 2 = on-line SPE–LC–DAD with the Prospekt preconcentration system.

ranges included in each data matrix is done empirically, choosing those elution times having the desired cluster of peaks (identified from the spectra). Each chromatographic run provides a data array of numbers which are ordered in a data matrix with a number of rows equal to the number of selected elution times and a number of columns equal to the number of wavelengths. Whereas for all the runs the same spectral range is selected (190–251 nm, 51 wavelengths, R_s = 1.2 nm), a different number of elution times is selected for each data matrix depending on the elution of the components of interest. Thus, all data matrices will have the same number of columns but they can have different number of rows (see Table 1). The time resolution in the data analysis is one spectrum per second.

For all data matrices, especially those obtained using preconcentration techniques and for chromatograms at lower wavelengths, a certain amount of background absorption is detected. Most of this background contribution is caused by absorption of the mobile phase, whose composition and relative concentration change during the chromatographic run. To subtract the initial background absorption caused by the mobile phase, the spectrum at the first initial elution time is subtracted from subsequent spectra at all other elution times. Fig. 1A and B show data matrix W8 and W3 after background subtraction was done. In this way all the chromatograms start at zero, but owing to gradient elution a small background contribution is still present.

2.4. Data structure

We assume that K chromatographic runs of different analyte mixtures at different concentrations are analysed. For each chromatographic run a data matrix $\boldsymbol{D}_k$ is obtained:

$$\boldsymbol{D}_k = \boldsymbol{C}_k\boldsymbol{S} + \boldsymbol{D}_{k0}\,, \qquad k = 1, 2, \ldots, N \tag{1}$$

where $\boldsymbol{C}_k$ is the matrix of the concentration profiles of the chemical components eluted during a particular chromatographic run in the analysis of sample k, $\boldsymbol{S}$ is the matrix of the unit or pure spectra of these components and $\boldsymbol{D}_{k0}$ is the background absorption. The analysis can also be performed simultaneously over several chromatographic runs, setting the corresponding data matrices $\boldsymbol{D}_k$ one on top of each other keeping their columns (wavelengths) the same for all of them:

$$\boldsymbol{D} = \begin{bmatrix} \boldsymbol{D}_1 \\ \boldsymbol{D}_2 \\ \vdots \\ \boldsymbol{D}_N \end{bmatrix} = \begin{bmatrix} \boldsymbol{C}_1 \\ \boldsymbol{C}_2 \\ \vdots \\ \boldsymbol{C}_N \end{bmatrix} \boldsymbol{S} + \boldsymbol{D}_0 = \boldsymbol{C}\boldsymbol{S} + \boldsymbol{D}_0 \tag{2}$$

$$\boldsymbol{D} = \boldsymbol{C}\boldsymbol{S} + \boldsymbol{D}_0 \tag{3}$$

The new augmented data matrix $\boldsymbol{D}$ has a number of rows equals to the total number of acquired spectra in the different chromatographic runs (elution times) and has a number of columns equals to the number of wavelengths. In the case of the simultaneous analysis of different samples, the new augmented data matrix will be the product of an augmented concentration matrix $\boldsymbol{C}$ times the unit spectra matrix $\boldsymbol{S}$. The augmented concentration matrix $\boldsymbol{C}$ includes the different concentration submatrices $\boldsymbol{C}_k$ related to each of the data matrices $\boldsymbol{D}_k$ analyzed. $\boldsymbol{S}$ has the unit pure spectra of the components and $\boldsymbol{D}_0$ the background absorption. Multivariate self-modelling curve resolution is applied to this new augmented data matrix using the method previously described [10–16] and also based on other methods previously developed by other workers [18–24].

In the analysis of a single chromatographic run, quantification is possible only if some external information is provided explicitly [25]. When several samples are simultaneously analysed (Eq. 2) using the constrained alternating least squares [10–12], the area of the concentration profiles of the different components in the matrices give the relative amounts of the analytes in each individual data matrix. As under conditions of linearity, the area under the concentration profile of a certain component is proportional to the amount of the analyte, and the ratio between these areas for a particular analyte gives the ratio between the amounts of that particular analyte in the different samples. Absolute concentrations or absolute amounts can be then estimated if for one of the individual data matrices included in

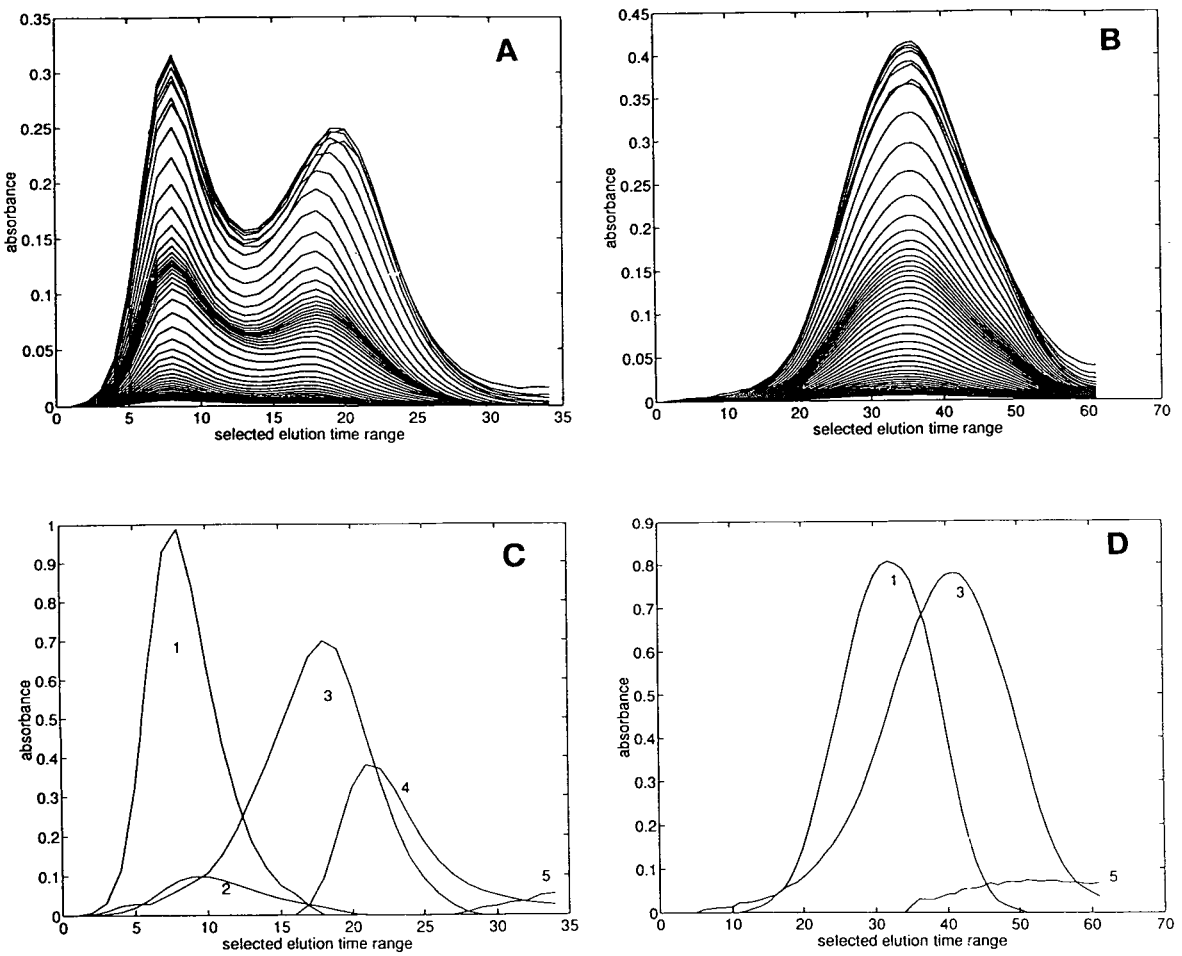

Fig. 1. (A) Elution profile of Ebre delta water sample spiked with alachlor and metolachlor, corresponding to matrix W8 (see Table 1); (B) elution profile of W3 (see Table 1); (C) elution profiles of the five resolved species in the simultaneous analysis of W8 (for identification of species, see Table 2); (D) elution profiles of the three resolved species in the simultaneous analysis of samples W3, W1 and W2 (augmented data matrix W3 + W1 + W2, see Table 4).

the augmented data matrix, the concentration of that analyte, is known in advance, i.e., a standard sample is included in the simultaneous analysis. The amount of this particular analyte in the other data matrices included in the augmented data matrix is easily estimated from

$$m_u = (A_u/A_k)m_k \quad (4)$$

where m_k and m_u are the amounts of the analyte in the known and unknown samples, respectively, and A_u/A_k is the ratio of areas of the resolved elution profiles for the analyte in both known and unknown data matrices which are included in the simultaneous analysis (Eq. 2).

3. Results and discussion

3.1. Individual analysis of each chromatographic run

The number of co-eluted compounds detected in the individual analysis of each data matrix is given in Table 2. A maximum number of five

Table 2
Individual analyses of the eight chromatographic runs

Matrix[a]	No. of components[b]	PCA fit[c]	ALS fit[d]	Species[e]
W1	2	0.34	1.26	3, 5
W2	2	0.19	0.44	1, 5
W3	3	0.16	–	1, 3, 5
W4	3	1.94	3.97	2, 4, 5
W5	4	0.25	0.65	2, 3, 4, 5
W6	4	0.32	0.52	1, 2, 4, 5
W7	5	0.17	1.14	1, 2, 3, 4, 5
W8	5	0.24	2.18	1, 2, 3, 4, 5
W9	3	2.55	2.71	2, 4, 5
M1	2	0.31	0.59	3, 5
M2	2	0.19	0.90	1, 5
M3	3	0.25	0.75	1, 3, 5
M8	4	0.43	4.79	1, 2, 3, 5
M9	4	9.99	1.50	2, 5

[a] Experimental data matrix analysed (see Table 1 for notation).
[b] Number of components found in the principal component analysis (PCA).
[c] Lack of fit by PCA using the selected number of components. It is calculated using the percentage lack of fit by the equation % lack of fit = $[\text{sum}(d_{ij} - d_{ij^*})^2)/\text{sum}(d_{ij})^2] \cdot 100$, where d_{ij} and d_{ij}^* are, respectively, the experimental absorption at elution time i and wavelength j and the reproduced PCA absorption using the selected number of components at the same elution time i and wavelength j.
[d] Lack of fit by ALS optimization of the concentration and spectra profiles. It is calculated using the percentage lack of fit by the equation % lack of fit = $[\text{sum}(d_{ij} - c_{il}s_{lj})^2/\text{sum}(d_{ij})^2] \cdot 100$, where d_{ij}, c_{il} and s_{lj} are, respectively, the experimental absorption at elution time i and wavelength j, the calculated concentration for special l at elution time i and the unit signal (absorption) contribution of species l at wavelength j.
[e] Identification of the species and their elution order: 1 = metolachlor; 2 = interferent found in preconcentration experiments; 3 = alachlor; 4 = interferent found in preconcentration experiments using the Waters column; 5 = mobile phase contribution (see Fig. 1).

components is detected for matrices W7 and W8 (Fig. 1A). Of these five species, the first is the elution of metolachlor, the second species is an unknown contribution always present when preconcentration techniques are used, the third is the elution of alachlor and the fourth and fifth species are minor contributions which have been related to the mobile phase, the gradient elution and/or the subtraction procedure. Matrices W5 and W6 have a maximum of four components because one of the two analytes is not present. Blank data matrices W4 and W9 have a maximum of three components (unknown interferent and mobile phase contributions). Matrix W3 (Fig. 1B) has three components, the two analytes and a low mobile phase contribution. Matrices W1 and W2 have two components, one of the two analytes and a very low mobile phase contribution. Similar results are obtained using Merck column (data matrices M1, M2, M3, M8 and M9 in Table 1) with a better resolution of the analytes, the interferents and the mobile phase. Matrices M8 and M9 give four components (only a mobile phase contribution is detected for the Merck column). Matrices M1 and M2 have only a major contribution and a very low mobile phase contribution; M3 has three components, the two analytes and the mobile phase.

In Table 2, the principal component analysis (PCA) and alternating least squares (ALS) lack of fit as a percentage of residual error are compared for each species in the individual analysis of all the data matrices. Small residuals are always found except for blank matrices W4, W9 and M9, where the PCA lack of fit per-

centage is higher than for the other data matrices, as a consequence of the much lower signal-to-noise ratio in those blank matrices.

Normalized pure spectra of the two analytes, metolachlor and alachlor, are easily estimated from the individual analysis of matrices W1, W2, M1 and M2 (without preconcentration). They are very similar with a correlation coefficient of 0.9992 (Table 3). These two spectra are used as input values in the analysis of the other data matrices and confirmed in the analysis of matrices W5 and W6 (similarly to W1 and W2 with only one of the two analytes but using the preconcentration method). The analysis of the blank data matrices W4, W9 and M9 provided the initial estimations of the spectra of the interference and mobile phase. Once these components has been identified, multivariate self-modelling curve resolution of co-eluted components in the mixture matrices W3, W7 and W8 was attempted. Resolution for both alachlor and metolachlor is achieved in the individual analysis of data matrices W7, W8, M3 and M8 (see Table 2). For matrix W3 (Fig. 1B) however, resolution fails to converge to a reasonable solution, probably because of the higher overlap of these two compounds in this data matrix. In Fig. 2A, the plots of the estimated normalized pure spectra of the five detached co-eluted compounds in the different chromatographic runs are given. Correlations between these unit spectra are also given in Table 3. More detailed plots of the normalized unit spectra for alachlor and metolachlor are given in Fig. 2B. Using the complete set of pure spectra given in Fig. 2A, a good fit of all the individual data matrices (except for W3) is achieved (Table 2).

3.2. *Quantification of simultaneous chromatographic runs*

By using the proposed method of simultaneous analysis of several data matrices, the resolution power is improved with respect to the individual analysis of the different data matrices, the relative quantification of the different analysis being possible [10]. Results of the simultaneous analysis of different chromatographic runs are given in Table 4, and are grouped in accordance with the combination of matrices that have been used as problems or as standards. Each group is identified with roman numerals.

(I) The simultaneous analysis of chromatographic runs W1, W2 and W3 without preconcentration (augmented matrix W1 + W2 + W3) allowed the resolution of the two analytes, alachlor and metolachlor, even for matrix W3 (Fig. 1B), which could not be resolved in the in-

Table 3
Chromatographic resolution between metolachlor and alachlor and correlation between pure spectra of the resolved components

Matrix	Resolution
W3	0.2
W7	0.4
W8	0.5
M3	0.6
M8	0.7

No.[a]	Correlation				
	1	2	3	4	5
1	1.0000	0.9795	0.9992	0.8788	0.8216
2	0.9795	1.0000	0.9876	0.9561	0.9174
3	0.9992	0.9876	1.0000	0.9902	0.9681
4	0.8788	0.9561	0.9902	1.0000	0.9934
5	0.8216	0.9174	0.9681	0.9934	1.0000

[a] Identification of numbers as in Table 2.

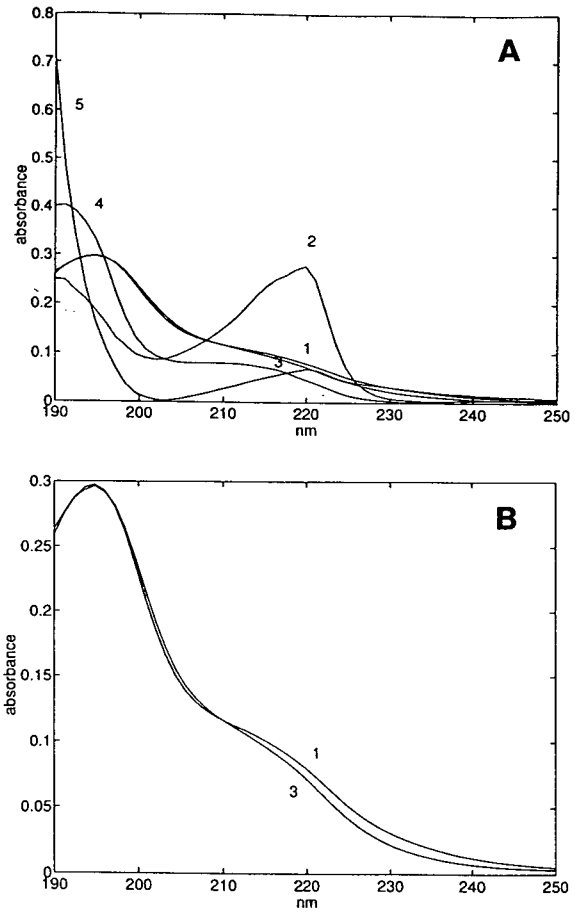

Fig. 2. (A) Normalized spectra of detected species: 1 = metolachlor; 2 = unknown interferent found in preconcentration experiments; 3 = alachlor; 4 = unknown interferent or mobile phase contribution found in the preconcentration experiments mostly with the Waters column; 5 = mobile phase contribution due to gradient and first spectrum subtraction. (B) More detailed plot of the estimated normalized unit spectra of alachlor and metolachlor (the correlation coefficient between these two spectra is 0.9992).

dividual analysis. A small contribution of the mobile phase is also confirmed. In Fig. 1D, the elution profiles of the mixture of alachlor and metolachlor from matrix W3 are given. Even for this unfavourable case of strongly co-eluted (resolution $R_S = 0.2$) and very similar (correlation coefficient 0.9992) compounds (Table 3), a good resolution and quantitative estimation is achieved for the two analytes. The same can be said for matrix M3 when analysed together with matrices M1 and M2 (augmented matrix W3 + W1 + W2), although now (Merck column) the resolution is higher ($R_S = 0.6$). When one of the single analyte matrices is omitted from the analysis (W2 or W1 in the analysis of W3 or M1 or M2 in the analysis of M3) the results permit the determination of both components (see Table 4).

(II) The simultaneous analysis of chromatographic runs of preconcentrated water samples spiked with alachlor and metolachlor at a level of 1.5 μg/l (augmented matrix W7 + W4 + W5 + W6) allowed the resolution of the co-eluted components and their quantification using the set of pure spectra identified in the individual analysis. Samples having only one of the two analytes were taken as standards. Percentage errors in the quantitative estimations are given in Table 4. When one of the single analyte matrices, W5 or W6, is omitted from the augmented matrix, quantitative estimations are still good (see results for the analysis of the augmented matrices W7 + W4 + W5), even when blank information is also omitted (augmented matrices W7 + W5 or W7 + W6).

(III) The simultaneous analysis of preconcentrated Ebre river waters spiked with the two analytes (W8) and blank (W9) together with other water samples (augmented matrix W8 + W9 + W7 + W4 + W5 + W6 + W3 + W2 + W1) gives similar results to those obtained previously. These results are also illustrative of the comparison between preconcentrated water samples and direct injection of standards. In Fig. 1C, the resolved elution profiles of the five co-eluted components present in W8 are given. The chromatographic resolution between metolachlor and alachlor in sample W8 is around 0.5. The error in the determination of the different components is lower than 10%, which is an acceptable value according to the EPA. A relevant question here is whether the area ratios of one specified analyte obtained under the different experimental conditions (direct injection or preconcentration) are reproducible. The results show that the area ratio of the different elution profiles is always between 2.3 and 2.7, showing that the preconcentration factor is independent of the consid-

Table 4
Simultaneous analysis of different chromatographic runs

No. Column	Matrix[a]	ALS fit[b]	Met[c]	Error (%)[d]	Ala[c]	Error (%)[d]
I Waters	W3	1.57	381	5	396	2
	W1		–	–	404	s
	W2		400	s	–	–
	W3	1.60	–	–	392	3
	W1		–	–	404	s
	W3	0.86	396	1	–	–
	W2		400	s	–	–
II Waters	W7	5.09	159	5	151	1
	W4		–	–	–	–
	W5		–	–	150	s
	W6		151	s	–	–
	W7	4.59	–	–	144	4
	W4		–	–	–	–
	W5		–	–	150	s
	W7	2.25	–	–	136	10
	W5		–	–	150	s
	W7	8.41	156	3	–	–
	W6		151	s	–	–
III Waters	W8	3.26	154	2	158	5
	W9		–	–	–	–
	W7		146	3	141	6
	W4		–	–	–	–
	W5		–	–	150	s
	W6		151	s	–	–
	W3		420	5	368	9
	W2		–	–	393	3
	W1		410	2	–	–
	W8	2.31	161	7	152	2
	W1		–	–	404	s
	W2		400	s	–	–
	W8	3.00	–	–	144	4
	W1		–	–	404	s
	W8	1.44	172	13	–	–
	W2		400	s	–	–
	W8	1.85	160	6	154	2
	W3		400	s	404	s
IV Merck	M3	1.54	425	6	400	1
	M1		–	–	404	s
	M2		400	s	–	–
	M3	1.14	–	–	408	1
	M1		–	–	404	s
	M3	1.23	430	7	–	–
	M2		400	s	–	–
	M8	3.09	140	7	149	1
	M9		–	–	–	–
	M3		437	9	387	4
	M1		–	–	404	s
	M2		400	s	–	–
	M8	4.43	–	–	135	10
	M1		–	–	404	s
	M8	2.51	150	1	–	–
	M2		400	s	–	–

(Continued on p. 354.)

Table 4 (*continued*)

No. Column	Matrix[a]	ALS fit[b]	Met[c]	Error (%)[d]	Ala[c]	Error (%)[d]
V Merck	W3	1.70	416	4	385	5
	W1		–	–	404	1
	W2		428	7	–	–
	M3		424	6	427	6
	M1		–	–	404	s
	M2		400	s	–	–
VI Merck	W8	1.90	166	10	–	–
	M2		400	s	–	–

[a] Augmented data matrix analysed (see Table 1 and Eq. 2).
[b] Percentage lack of fit in the ALS optimization. See footnote d in Table 2.
[c] Amount of metolachlor (Met) and alachlor (Ala) recovered from the analysis using Eq. 2; s means that this elution profile has been considered as standard for the quantification of the corresponding analyte using Eq. 4.
[d] Relative error in the prediction of the amounts of analyte in the corresponding chromatographic runs.

ered sample, analyte and/or column. The analysis of real samples with preconcentration can be correlated with a standard injected directly on to the column. This is the case, for instance, for the analysis of the augmented data matrix W8 + W1 + W2. Determination of the two analytes alachlor and metolachlor in W8 was also possible (Table 4).

(IV) Similar results were also obtained in the simultaneous analysis of different chromatographic runs using the Merck column (Table 4).

(V) The simultaneous analysis of chromatographic runs obtained using either the Waters or Merck column (augmented matrix W3 + W1 + W2 + M3 + M1 + M2) showed that standards obtained with one of the two columns can be also used in the determination of the analytes in samples analysed with the other column. This is true because the mobile phase composition, the gradient elution and other physical parameters were kept identical in all the experiments.

(VI) Finally, the determination of metolachlor in the Ebre river water analysed using the Waters column (matrix W8) was performed using as a standard metolachlor injected directly onto the Merck column. Even in this case, a reasonable determination of metolachlor is possible with an error of 10% in the prediction of its concentration.

4. Conclusions

The proposed multivariate self-modelling curve resolution method can be used for the simultaneous determination of herbicides with similar elution times and absorption spectra (e.g., alachlor and metolachlor) at a level of few μg/l in real water samples. The error made is less than 10%, even in cases where the determination of metolachlor in Ebre river water samples was performed using as standard direct injection of metolachlor and both samples analysed with different columns. Quantification at these low levels is of environmental importance, as they are similar to those present in the environment.

The individual analysis of the different data matrices using different columns showed that (1) the analysis was independent of the column used, (2) mobile phase contributions are mostly due to gradient elution and (3) unknown co-eluted contributions can appear when on-line solid-phase preconcentration methods are used.

From all these results, a stepwise recommended chemometric procedure is proposed for data analysis and for the quantification of mixtures of alachlor and metolachlor at low concentrations:

(1) LC analysis of the water sample which has

an unknown amount of alachlor and/or metolachlor. If they are present at very low concentrations, use preconcentration techniques. Storage of data matrix U.

(2) LC analysis of a pure standard of alachlor or metolachlor or of a mixture of both. Storage of data matrix K.

(3) Data pretreatment of matrices U and K. Selection of elution time and wavelength of interest. Background and mobile phase contribution subtraction.

(4) Determination of the number of co-eluted components of matrix U. Multivariate self-modelling curve resolution of matrix U (Eq. 1). Estimation of the elution order.

(5) Multivariate self-modelling curve resolution of the augmented data matrix U + K (Eq. 2). Determination of the concentration profiles and unit spectra of the co-eluted components. Quantification of analytes in the unknown mixture (Eq. 4).

Acknowledgements

This work was supported by the Environment R & D Programme 1991–1994 (Commission of the European Communities) (Contract EV5V-CT92-0105) and by PLANICYT (AMB94-0950-CE). S.L. gratefully acknowledges financial support from CICYT (Grant AMB92-0218). R. Figueras (Waters, Barcelona, Spain) is acknowledged for software assistance.

References

[1] S. Chiron, A. Fernandez Alba and D. Barceló, *Environ. Sci. Technol.*, 27 (1993) 2352.
[2] I. Liska, E.R. Brouwer, A.G.L. Ostheimer, H. Lingeman, U.A.Th. Brinkman, R.B. Geerdink and W.H. Mulder, *Int. J. Environ. Anal. Chem.*, 47 (1992) 267.
[3] R. Reupert, I. Zube and E. Plöger, *LC·GC Int.*, 5 (1992) 43.
[4] J. Slobodnik, E.R. Brouwer, R.B. Geerdink, W.H. Mulder, H. Lingeman and U.A. Th. Brinkman, *Anal. Chim. Acta*, 268 (1992) 55.
[5] V. Pichon and M.C. Hennion. *J. Chromatogr. A*, 665 (1994) 269.
[6] S. Lacorte and D. Barceló, *Anal. Chim. Acta*, 296 (1994) 223.
[7] J. Slobodnik, M.G.M. Groenwegen, E.R. Brouwer, H. Lingeman and U.A.Th. Brinkman, *J. Chromatogr.*, 643 (1993) 359.
[8] U.A.Th. Brinkman, *LC·GC Int.*, 7 (1994) 157.
[9] G. Durand, V. Bouvot and D. Barceló, *J. Chromatogr.*, 607 (1992) 319.
[10] R. Tauler and D. Barceló, *Trends Anal. Chem.*, 12 (1993) 319.
[11] R. Tauler, B.R. Kowalski and S. Flemming, *Anal. Chem.*, 65 (1993) 2040.
[12] R. Tauler, G. Durand and D. Barceló, *Chromatographia*, 33 (1992) 244.
[13] R. Tauler, A.K. Smilde, J.M. Henshaw, L.W. Burgess and B.R. Kowalski, *Anal. Chem.*, 66 (1994) 3337.
[14] R. Tauler, A. Izquierdo-Ridorsa and E. Casassas, *Chemometr. Intell. Lab. Systs.*, 18 (1993) 293.
[15] R. Tauler and E. Casassas, *Anal. Chim. Acta*, 223 (1989) 257.
[16] R. Tauler, E. Casassas and A. Izquierdo-Ridorsa, *Anal. Chim. Acta*, 248 (1991) 447.
[17] M.W.F. Nielen, *Ph.D. Thesis*, Free University, Amsterdam, 1987.
[18] E.V. Dose and G. Guiochon, *Anal. Chem.*, 61 (1989) 2571.
[19] H. Gampp, M. Maeder, Ch. Meyer and A.D. Zuberbuhler, *Talanta*, 32 (1985) 1133.
[20] E.R. Malinowski, *J. Chemometr.*, 6 (1992) 29.
[21] S. Wold, *Technometrics*, 20 (1978) 397.
[22] H.R. Keller, D.L. Massart, Y.Z. Liang and O.M. Kvalheim, *Anal. Chim. Acta*, 263 (1992) 29.
[23] W. Windig and J. Guilment, *Anal. Chem.*, 63 (1991) 1425.
[24] G.H. Golub and Ch.F. Van Loan, *Matrix Computations*, Johns Hopkins, Baltimore, MD, University Press, 2nd ed., 1989.
[25] B.G.M. Vandeginste, M. Gerritsen, J.W. Noor and G. Kateman, *J. Chemometr.*, 1 (1987) 57.

ELSEVIER

Journal of Chromatography A, 697 (1995) 357–362

JOURNAL OF CHROMATOGRAPHY A

Simultaneous determination of 27 phenols and herbicides in water by high-performance liquid chromatography with multi-electrode electrochemical detection

Guido Achilli[a,*], Gian Piero Cellerino[a], Gianvico Melzi d'Eril[b], Sue Bird[c]

[a]*EuroService srl, Piazza Maggiolini 3, 20015 Parabiago, Italy*

[b]*Servizio di Analisi, IRCCS Fondazione "Istituto C. Mondino", Via Palestro 3, 27100 Pavia, Italy*

[c]*ESA Analytical, 7 Cromwell Mews, St. Ives, UK*

Abstract

A sensitive and simple method for the simultaneous evaluation of phenol, 26 substituted phenols and herbicides was developed using HPLC and electrochemical detection. After extraction from the samples on solid-phase cartridges, the compounds were separated on a reversed-phase column by using a combined gradient of organic modifier and counter-ion. The total analysis time was less than 63 minutes. Identification of the compounds was based on retention time comparison with authentic standards. In addition, further confirmation of peak identities and of their purity was determined by comparison of the ratio of the peak's height of each compound across the electrode array, with the similar ratio of the authentic standard. The detection limit was found to be much lower than that indicated by the European Community: for the least sensitive compound (a herbicide, Linuron) it was less than 0.0005 μg/l at signal-to-noise of 3. The method was used to examine the residual levels of phenylurea herbicides, phenol, chloro- and nitro-phenols in tap water, mineral water and spring water from different sources.

1. Introduction

Phenol and substituted phenols are common products of many industrial processes, while substituted phenylureas are selective herbicides used often in agriculture. The leaking of these substances from the soil into local ground water is a common phenomenon. Under environmental conditions phenols and phenylureas can persist at the mg/l level in ground water [1], for a number of days or weeks depending on temperature and pH. Therefore, if such ground waters are to be used as sources of drinking water, it is necessary to screen them for contamination by these organic pollutants, given the high mammalian toxicity of these substances. The high standards for drinking water purity laid down by the European Community give 0.1 μg/l as the admissible concentrations for any individual pesticide, with a limit of up to 0.5 μg/l for the total content of pesticides. The local legislation in Italy (DPR 236/88) allows up to 0.5 μg/l of phenols. As a result, an analytical method which offers high selectivity and sensitivity for both the identification and the quantitation of these substances is needed. This paper describes a procedure for the simultaneous determination of phenols and phenylureas using HPLC and elec-

* Corresponding author.

0021-9673/95/$09.50
SSDI 0021-9673(94)00791-8

trochemical detection. After preconcentration of the samples on solid-phase cartridges, the compounds were separated on a reversed-phase column by using a combined gradient of organic modifier and counter-ion.

2. Experimental

2.1. Chemicals

The mobile phases used in the gradient runs were provided by ESA (Bedford, MA, USA). Mobile phase A was composed of 34.7 μM sodium dodecyl sulphate (SDS)–0.1 M monobasic sodium phosphate–50 nM nitrilotriacetic acid (pH 3.45), while mobile phase B was composed of 173 μM SDS–0.1 M monobasic sodium phosphate–50 nM nitrilotriacetic acid–50% aqueous methanol (pH 3.45).

Solutions A and B were filtered through 0.2 μm PTFE lyophilic filters (Millipore, Bedford, MA, USA) and degassed by sonication under vacuum for 10 min prior to use.

The water used for dilution of the standards and of the samples was purified with a Milli-Q R/O water purification system (Millipore).

2.2. Apparatus

A Coulochem Electrode Array System (CEAS) obtained from ESA was used. The instrument consisted of a refrigerated autosampler which is capable of variable volume injections with a 100-μl loop. A circulating bath was used to maintain sample vials between 0°C to 4°C prior to sample injection. Gradient operation was provided by two HPLC pumps capable of operating from 0.05 to 10 ml/min. The output of the pumps was connected to a dynamic gradient mixer. The analytical column (80 × 4.6 mm I.D.) used was a stainless-steel column packed with 3 μm particles of silica-based C_{18} materials (HR 80, ESA). The detection system consisted of four coulometric array cell modules, each containing four electrochemical detector cells (cat. no. 55-0685 A). The detectors, porous graphite working sensors with palladium reference and counter electrodes, were arranged in series after the analytical column. The detector, the column and a pulse damper were housed in a thermal chamber maintained at 37°C. Two additional pulse dampers were placed before the column and cell compartment. The autosampler, pumps, detectors, temperature controlled box and all associated electronic circuitry were monitored and controlled by CEAS software installed on a Model 386 computer equipped with a 32 Mb hard disk and a 1.2 Mb floppy disk drive. The computer was coupled with a high resolution colour monitor with a "touch screen" interface and to a matrix graphic printer. The computer system also performed data storage, analysis and report generation. An appropriate software package was used for summary reports of the final data (Lotus 1-2-3, Lotus Corp., Cambridge, MA, USA).

2.3. Chromatographic method

A method capable of completely separating the 27 compounds chosen was developed. It consisted of a gradient where the organic modifier and counter-ion were modified during the run. The gradient used in the separation, expressed by percentage of phase B was: 6% isocratic for 4 min, then it reached 100% of phase B at 14 min after the injection; it was isocratic till 54 min after the injection, then the phase B was returned to the initial value of 6%. Nine minutes were allowed for column reequilibration. The flow-rate was 0.8 ml/min and the cell potentials constituted an increasing array: 0 mV at electrode 1, 80 mV at electrode 2, with increments of 80 mV at each subsequent electrode until a value of 1200 mV was reached at electrode 16. The indicated potentials are referred to the solid state palladium reference electrode built in the coulometric cell; their absolute value is about 250 mV lower than the corresponding potential measured by using an Ag/AgCl reference electrode. At the end of each analysis, all cell potentials were increased to 1200 mV for 60 s to prevent long term adsorption of material to the electrode surface. The elec-

trodes were then allowed to stabilize for 9 min before the next injection.

2.4. Standard and sample preparation

The pollutants chosen to be studied were the most ubiquitous species of the aminophenols, nitrophenols, chlorophenols, cresols, phenols (residues of many industrial processes) and Phenylurea herbicides (widely used in agriculture). In fact numerous studies have investigated these particular molecules [2–6].

All standards (Table 1) were purchased from Sigma (St. Louis, MO, USA). The primary stock standard solutions were made by dissolving 10 mg of the component in 10 ml of methanol. These concentrates were then subdivided into 1-ml portions. They were stored at −30°C and thawed when necessary at 4°C. Individual secondary working stock standard solutions were made by diluting each component of the primary solutions with methanol in order to give a concentration of 500 ng/ml (with the exception of phenol and 2-nitrophenol whose concentrations were 250 ng/ml). Injection of these single components was done for the characterization of the chromatographic and electrochemical behaviour of each molecule. A 27-component working standard solution was prepared by combining and diluting with methanol the aliquot of each of

Table 1
Chromatographic and electrochemical characteristics of the 27 external standards

Identif. number	Name[a]	Retention time (min)	Recovery (%)	Detection limit (μg/l)	Within-run R.S.D. (%)	Between-run R.S.D. (%)	Dominant potential (mV)
1	Pyrogallol[5]	4.07	98	0.00008	1.8	2.2	80
2	4-Hydroxy-aniline[1]	5.03	96	0.00045	1.9	2.4	80
3	Benzocatechine[5]	9.73	97	0.00022	2.2	2.9	160
4	2-Hydroxy-aniline[1]	12.58	102	0.00032	2.5	3.5	160
5	Phenol[5]	13.93	105	0.00003	1.2	2.0	640
6	1,2-Phenylendiamine[1]	14.98	98	0.00036	3.1	4.8	160
7	4-Nitrophenol[2]	16.90	101	0.00018	2.8	5.2	880
8	2,4-Dinitrophenol[2]	17.69	96	0.00022	3.5	5.3	1040
9	*o*-Cresol[4]	18.33	97	0.00015	2.9	4.3	560
10	2-Nitrophenol[2]	18.77	100	0.00008	2.8	4.2	880
11	Metoxuron[6]	19.43	96	0.00021	2.6	3.9	560
12	3-Methyl-2-nitrophenol[2]	20.23	102	0.00038	2.2	4.2	720
13	Monuron[6]	20.99	96	0.00030	3.2	4.1	800
14	2,6 Dichlorophenol[3]	23.42	100	0.00031	2.8	3.8	640
15	4,6-Dinitrocresol[4]	23.47	101	0.00035	3.4	4.2	960
16	5-Methylphenol[5]	23.83	98	0.00030	2.5	3.5	640
17	Monolinuron[6]	23.88	96	0.00041	3.3	5.3	880
18	4-Methyl-2-nitrophenol[2]	24.75	98	0.00032	2.7	4.8	720
19	Methobromuron[6]	25.86	102	0.00040	3.2	5.2	960
20	Chlortholuron[6]	26.15	104	0.00043	3.2	4.9	800
21	4-chloro-3-methylphenol[3]	26.50	98	0.00038	2.2	3.2	640
22	Buturon[6]	28.02	96	0.00043	3.5	5.5	800
23	2,4-Dichlorophenol[3]	28.27	98	0.00029	2.9	4.2	720
24	Isoproturon[6]	28.88	102	0.00032	2.1	4.1	640
25	Diuron[6]	29.51	97	0.00028	3.2	5.0	880
26	Linuron[6]	34.92	98	0.00049	3.3	4.9	960
27	2,4,5-Trichlorophenol[3]	46.69	98	0.00042	2.8	3.9	640

[a] The reference made to each compound refers to their classification: 1 = Amino-phenols, 2 = Nitro-phenols, 3 = Chloro-phenols, 4 = Cresols, 5 = Phenols, 6 = Phenylurea herbicides.

the primary stock standard solutions to the concentration of 500 ng/ml (with the exception of phenol and 2-nitrophenol whose concentrations were 250 ng/ml). For recovery studies this 27-component working standard solution was prepared by diluting with water the primary standard solutions to appropriate concentrations. Prior to the injection all standard solutions were filtered through a 0.22-μm membrane (Millipore).

This method was used to measure the compounds in three different samples of water: tap water from an aqueduct of Piacenza (a city in the middle of Val Padana, Italy), water from a spring at 1600 m over sea level and commercial mineral water (Levissima). The samples of water were collected in 1.5-l polyethylene bottles and stored at 4°C prior to extraction.

To increase the sensitivity of the method all the water samples were concentrated by a solid-phase extraction. This was achieved by filtering 1000 ml of sample through the Sep-Pak cartridges C-18, 5 mm (Millipore) at a flow-rate of about 16 ml/min. The percolate was discarded and the cartridge was eluted with 1 ml of methanol.

Of this organic phase 10 μl were injected into the CEAS.

2.5. Assay performance

Assay linearity and detection limit were examined by analysing in triplicate the 27-component standard solution with increasing concentrations of the components. Recovery was examined by analysing the 27-component standard solutions in water treated in the same manner as the samples. The concentration ranges studied were from 10 000 μg/l to 0.1 μg/l with seven concentrations of each analyte. Each sample was analyzed in triplicate. To examine the within-run variability of the assay, 10 replicates of the 27-component standard solution in water (containing 5 ng of each component) were analyzed after having been treated as a sample. Variability between runs was studied by analysing two replicates of the same solution used for the within-run study. This was done on 10 separate days.

3. Results

The 27 standards are listed according to their retention times. Their concentration is 500 μg/l with the exception of phenol and 2-nitrophenol whose concentrations were 250 μg/l (corresponding to 5 and 2.5 ng/10 μl, respectively). The recovery, the detection limit, the within- and between-run precision and their dominant potentials are also reported (the dominant potential is that of the electrode potential where the maximum signal occurs). The peak confirmation was achieved by comparing the matching ratio (R) between a standard and the actual sample (R is the dominant channel/subdominant channel ratio) [7].

Fig. 1 shows the chromatogram of a 10-μl sample containing the 27 components as external standard at the concentration reported above. The total analysis time was 63 min. Retention time reproducibility reported during the precision study (carried out over a 10-day span) of each individual standard was found to be very good (R.S.D. $<2\%$).

This was due to the strict control of the detector and column temperature, mobile phase composition and gradient profile. Assay linearity was found to be good in all the intervals analyzed. In fact with least-squares regression analysis, detector response was directly proportional to standard concentration (10-μl sample injection) and calibration curves were linear in the tested range from 10 000 μg/l to 0.1 μg/l. The detection limit (signal-to-noise ratio = 3) is very low for all the components; for the less sensitive compound (linuron) it is <0.0005 μg/l which is much lower than the limit laid down by the European Community (0.1 μg/l or 0.1 ppb). The analytical recovery is high for all the components, ranging from 96% to 105%. As a result, the use of an internal standard was not taken into consideration. The within-run concentration variability (R.S.D.) ranged from 1.2%

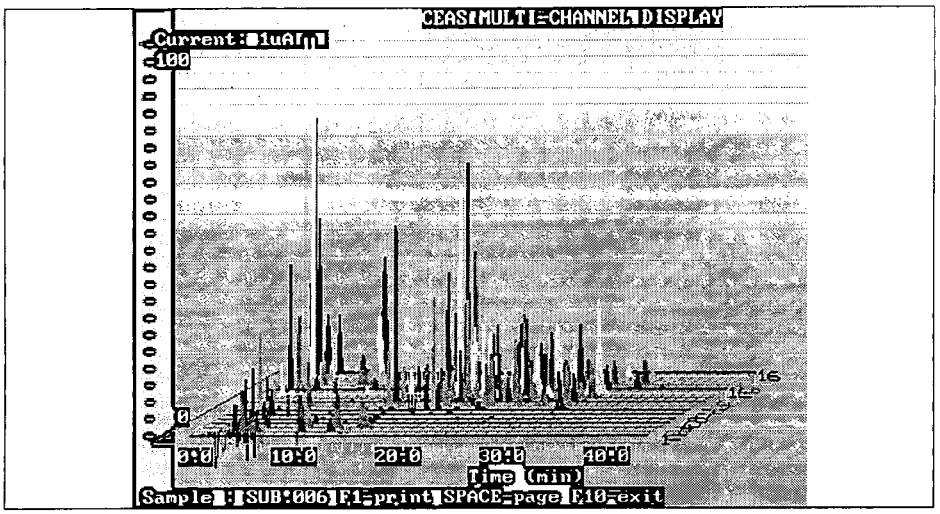

Fig. 1. 16-channel chromatogram of 10 μl of extracted standard mixture containing the 27 compounds.

to 3.5%; the between-run concentration variability ranged from 2.0% to 5.5%.

This method was used to examine the level of 27 different molecules in three different types of water: tap water from an aqueduct of Piacenza, a rural area of the flat Padana region with intensive cultivation; spring water collected at Pian delle Betulle (Alps) at 1600 m above sea level, and an oligomineral water sold commercially in Italy (Levissima). The concentration of the various components found in these samples are reported in Table 2, sorted according their retention time. The 16-channel chromatogram for one of the water samples (Mineral water Levissima) is shown in Fig. 2.

4. Discussion and conclusion

The use of the CEAS for the determination of neurochemicals in tissues and biological fluids has already been reported [7–11]. Recently, it has been used for the determination of 36 phenolic constituents in natural beverages and plant extracts [12]. The coulometric efficiency of each element of the array allows a complete

Table 2
Concentrations of the compounds identified in water samples from the 3 different sources.

Identif. number	Name	Concentration in μg/l		
		Tap water	Spring water	Mineral water
5	Phenol	0.580	0.051	0.161
7	4-Nitrophenol			0.002
8	2,4-Dinitrophenol			0.001
17	Monolinuron	0.009		0.051
18	4-Methyl-2-nitrophenol		0.016	0.087
20	Chlortholuron	0.177		
25	Diuron			0.005

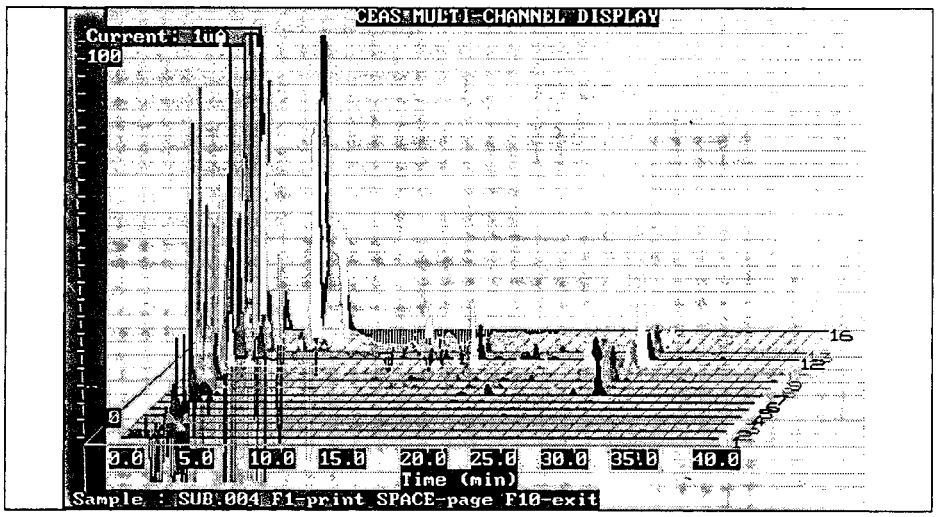

Fig. 2. 16-channel chromatogram of 10 μl of extracted sample of Piacenza tap water.

voltammetric resolution of analytes as a function of their reaction potential. Some peaks can be resolved by the detector even if they are unresolved when they leave the chromatographic column. In this study we have demonstrated that this technique can also be applied to phenols, substituted phenols as well as the phenylurea herbicides found in water. We separated 27 compounds in less than 63 min with this method. The reproducibility of the retention time coupled with the selectivity inherent to this detector allows measurements with high precision of a variety of different compound families in a single sample. For the samples analyzed here, we were able to measure 3 compounds in the tap water of the flat Padana region, 2 in the spring water of the Alps, and 6 in the oligomineral water. Of the three samples of water considered in this study only that from the Alps is below the limits of standards of purity. The tap water contains phenols and chlortholuron, and even the mineral water contains phenols above the limit set by the European Community.

References

[1] M.E. Leon-Gonzalez and A. Townshend, *J. Chromatogr.*, 539 (1991) 47.
[2] A. Di Corcia and M. Marchetti, *J. Chromatogr.*, 541 (1991) 365.
[3] A. Balinova, *J. Chromatogr.*, 643 (1993) 203.
[4] R.B. Geerding, A.M.B. Graumans and J. Viveen, *J. Chromatogr.*, 547 (1991) 478.
[5] Y. Ishli, K. Asakura and T. Sakamoto, *Nippon Noyaku Gakkaishi*, 15 (1990) 435.
[6] S. Yao, A. Meyer and G. Henze, *Fresenius' J. Anal. Chem.*, 339 (1991) 207.
[7] V. Rizzo, G. Melzi d'Eril, G. Achilli and G.P. Cellerino, *J. Chromatogr.*, 536 (1991) 229.
[8] K.J. Swartz and W.R. Matson, *Anal. Biochem.*, 185 (1990) 363.
[9] C.N. Svendsen and E.D. Bird, *Neurosci. Lett. Suppl.*, 35 (1989) 49.
[10] W.R. Matson, P.G. Gamache, M.F. Beal and E.D. Bird, *Life Sci.*, 41 (1987) 905.
[11] P.H. Gamache, M.L. Kingery and I.N. Acworth, *Clin. Chem.*, 39/9 (1993) 1825.
[12] G. Achilli, G.P. Cellerino, P. Gamache and G. Melzi d'Eril, *J. Chromatogr.*, 632 (1993) 111.

ELSEVIER

Journal of Chromatography A, 697 (1995) 363–369

JOURNAL OF CHROMATOGRAPHY A

Improved method for the determination of glyphosate in water

M.P. Abdullah[a], J. Daud[a], K.S. Hong[b,*], C.H. Yew[a]

[a]*Chemistry Department, Universiti Kebangsaan Malaysia, 43600 Ukm Bangi, Selangor, Malaysia*

[b]*Veterinary Diagnostic Laboratory, Veterinary Department, Persiaran Barat, 46630 Petaling Jaya, Selangor, Malaysia*

Abstract

A method for the determination of glyphosate (Glyph) and its metabolite aminomethylphosphonic acid (AMPA) in environmental water was developed with the emphasis on the clean-up procedure. The organic compounds in the environmental water were extracted with dichloromethane and the sample was concentrated by rotary evaporation. The concentrated sample was then passed through a strong anion-exchange (SAX) cartridge with an additional 2 ml of resin in the hydroxide form packed above the SAX packing. Glyph and AMPA were eluted with citrate buffer at pH 5.00 and determined directly by high-performance liquid chromatography with a postcolumn reactor and fluorescence detector. The detection limit and average recovery for both components were <2 μg/l and $>85\%$, respectively.

1. Introduction

Glyphosate, N-(phosphonomethyl)glycine (Glyph), is a very broad spectrum, non-selective, post-emergence herbicide. Glyphosate is the active ingredient in Roundup and Rodeo herbicides produced by Monsanto and is widely used in various applications for weed and vegetation control. Its impact on the environment is becoming more pertinent. The difficulties of obtaining a simple method for the determination of this compound at residue levels are mainly due to its properties: its relatively high solubility in water, its insolubility in organic solvents and its complexing behaviour [1].

Procedures for the determination of Glyph and its metabolite aminomethylphosphonic acid (AMPA) have been reviewed [2]. Although gas chromatographic procedures continue to be of interest, in general they suffer from tedious sample preparation because of the need to convert the analytes into volatile derivatives. Because of the requirement for a better detection limit, liquid chromatographic procedures have been developed [3].

For liquid chromatography procedures, both pre- and post-column derivatization methods have been developed. Precolumn procedures have focused on derivatization with 9-fluorenylmethyloxycarbonyl chloroformate (FMOCCl) with fluorescence detection [4]. However, other derivatization agents such as 1-fluoro-2,4-dinitrobenzene [5] and *p*-toluenesulfonyl chloride [6] have been used to form Glyph and AMPA derivatives that can be detected in the UV–Vis region. Postcolumn derivatization has been commonly used with *o*-phthalaldehyde–mercaptoethanol (OPA–MERC) [2,7]. The direct injection method recommended by the AOAC [7] was found in our initial work to damage the column, sometimes only after five injections, so frequent regeneration is required.

The main objective of this work was to develop a simpler and sensitive method for the

* Corresponding author.

SSDI 0021-9673(94)01161-3

determination of Glyph and its AMPA in the aquatic environment with emphasis on a simple clean-up procedure. The determination of the components is based on high-performance liquid chromatography (HPLC) with a postcolumn reactor and fluorescence detection.

2. Experimental

2.1. Reagents

All reagents were of analytical-reagent grade and used as received. The solvent methanol was of liquid chromatographic grade.

2.2. Preparation of solutions

Mobile phase: 0.005 M KH_2PO_4 buffer

A 1.36-g amount of KH_2PO_4 was dissolved in 2 l of methanol–water (4:96) and the pH was adjusted to 2.1 with H_2PO_4. The solution was filtered through a 0.22-μm membrane and degassed. The flow-rate of this mobile phase was 0.4 ml/min.

Oxidative solution

A 0.5-g amount of $Ca(OCl)_2$ was dissolved in 500 ml of deionized, distilled water using a magnetic stirrer at high speed for 30 min. A solution was prepared by dissolving 1.36 g of KH_2PO_4, 11.6 g of NaCl, 0.4 g of NaOH and 10 ml of the first solution in 1 l of deionized, distilled water, mixed thoroughly and filtered through a 0.22-μm membrane. This solution was delivered at a flow-rate of 0.4 ml/min via a postcolumn reagent system (PCRS) with mixing tees and maintained at 48°C to oxidize the analytes eluted.

o-Phthalaldehyde–mercaptoethanol solution

A 10.0776-g amount of anhydrous disodium tetraborate was dissolved in 900 ml of deionized, distilled water. Solid $Na_2B_4O_7$ was poured in a little at a time to prevent caking. A 0.800-g amount of OPA was dissolved in 10 ml of methanol in a small beaker and the OPA solution was poured into a 1-l beaker. The beaker was rinsed with $Na_2B_4O_7$ solution. The pH of the solution was adjusted to 11.5 using 60% NaOH. The solution was made up to 1 l using deionized, distilled water. The solution was then mixed completely and filtered through a 0.22-μm membrane and degassed prior to the addition of 2 ml of 2-mercaptoethanol. This solution was delivered at 0.3 ml/min to the postcolumn reactor at ambient temperature.

2.3. Instrumentation

A Waters HPLC system was used, consisting of Waters Model 510 and 501 pumps, a reagent-delivery module (RDM), an autoinjector (WISP 712), coils, column heater and Rheodyne valve. The temperature of the column heater was maintained at 48°C with a column heater temperature control module. The postcolumn reactor consisted of a dual-pump derivatization system including two reaction coils, one maintained at 48°C and the other at ambient temperature. Glyph and AMPA derivatives were detected with a Waters Model 470 fluorescence detector with excitation at 340 nm and emission at 455 nm. The system was controlled and data were collected and analysed using a system interface module (SIM), a NEC computer and Waters Maxima 820 software.

The analytical column was a 250 mm × 4.1 mm I.D. PRP-X400 (7 μm) cation-exchange column obtained from Hamilton. The strong anion-exchange (SAX) cartridge used in the clean-up step was Supelclean LC-SAX manufactured by Supelco.

2.4. Procedure

Environmental water samples were taken from Taman Jaya Lake, Petaling Jaya, Selangor. A 250-ml sample was taken and spiked with Glyph and AMPA. The solution was filtered and extracted with 100 ml of dichloromethane to remove organic compounds. The aqueous phase which contained Glyph and AMPA was concentrated to a very small volume by rotary evaporation and the pH was adjusted to ca. 10 with 0.2 *M* NaOH. With the aid of a Supelco vacuum

system, the sample was passed through the Supelclean SAX cartridge with an additional 2 ml of Bio-Rad SAX resin in the hydroxide form packed on top of the Supelclean packing. The cartridge was washed with 20 ml of deionized distilled water to remove interferences. Glyph and AMPA were eluted using 10 ml of 0.4 *M* sodium citrate buffer at pH 5.00.

Glyph and AMPA were determined by HPLC using a cation-exchange column, which provided good separation. Glyphosate was oxidized with calcium hypochlorite in the postcolumn reactor coil at 48°C to form glycine. The glycine was treated with OPA in the presence of mercaptoethanol (MERC) in the second coil to form a fluorophore at ambient temperature, and was detected with a fluorescence detector ($\lambda_{ex} = 340$ nm, $\lambda_{em} = 455$ nm) [7]. AMPA was made to by-pass the oxidizing reagent by a switching valve. It underwent a similar reaction with OPA–MERC reagent to form another fluorophore, which was detected by the fluorescence detector under the same conditions as for Glyph. An example of the separation is shown in Fig. 1.

The efficiency of the system was checked and optimized using glycine running concurrently with Glyph. The amounts of hypochlorite required for Glyph and AMPA were also determined and optimized.

3. Results and discussion

The variables that primarily affect the fluorescence detection include the postcolumn reaction temperature and length of the coil. A series of preliminary experiments designed to establish the qualitative effect of each variable were carefully evaluated over a defined range while all other factors were held constant. The prelimin-

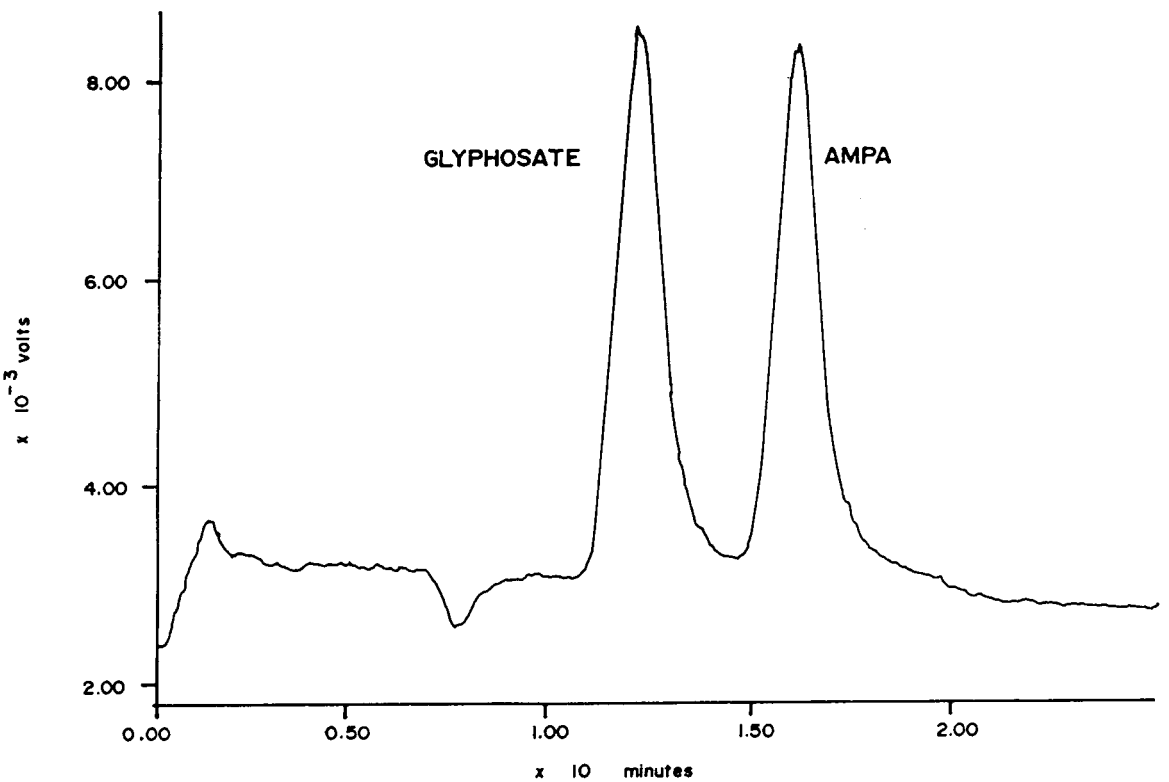

Fig. 1. Typical chromatogram for Glyph and AMPA, both at 1.0 mg/l concentration.

ary experiments demonstrated that a column flow-rate of 0.4 ml/min and the postcolumn flow-rate of 0.3 ml/min each for calcium hypochlorite and OPA–MERC solutions were optimum for Glyph and AMPA.

The purpose in optimizing each variable was to obtain an accurate, reproducible change in fluorescence that would correspond to the best detection limits for Glyph and AMPA. When the mixing coil beyond the mixing tee was increased in length, while other variables were held constant, the reaction of the analyte with calcium hypochlorite was more complete and the fluorescence became larger, as can be seen in Table 1. Table 1 also indicates that a coil length of 15 feet is appropriate for this purpose and it thus used in this work.

Using the same conditions but changing the temperature indicated that the optimum reaction coil temperature for glyphosate was 48°C (Fig. 2). At higher temperatures, the peak area began to decrease because the effectiveness of calcium hypochlorite to produce chlorine and disproportionate in water to form hypochlorous acid decreased [8]. The optimum temperature seems to be critical, as indicated in Fig. 2. However, this effectively poses little difficulty because the temperature control module used can easily and precisely control the required temperature.

The optimum concentration of hypochlorite solution was also investigated. It was found that the fluorescence intensity of AMPA was substantially reduced when passed through the hypochlorite reaction coil (Fig. 3). This phenomenon is unlike the earlier reported findings that AMPA is relatively unreactive towards hypochlorite and undergoes a similar reaction with OPA–MERC reagent [7]. AMPA, a primary amine, reacted directly with OPA–MERC. However, AMPA also reacted with the hypochlorite reagent to form chloramine and small amounts of ammonia. This substantially decreased the ultimate fluorescence response of the AMPA, as shown in Fig. 3. As AMPA does not require hypochlorite, the present postcolumn set-up was modified to incorporate a switching valve so the hypochlorite solution does not enter the reaction coil whenever AMPA is supposed to be in the coil. This is done automatically and is controlled by the Maxima 800 software.

The linear response of the detector was checked using five standard solutions (0.025, 0.050, 0.100, 0.500 and 1.00 μg/l). The concentration of the five standard solutions was plotted on the ordinate against the peak-area response of the respective analyte on the abscissa. The correlation coefficient was 0.999 for both Glyph and AMPA.

Resin in the hydroxide form was chosen and used for a clean-up step in the cartridge because it has the lowest selectivity in anion-exchange chromatography and therefore would be readily exchanged by another anion. However, the commercially available resin in the hydroxide form has a large particle size (20–50 mesh), which produced a fast elution flow-rate, so a resin of smaller mesh size is required. This was achieved by converting the resin in the chloride form into the hydroxide form using 20 volumes of 1 *M* NaOH. The surface area-to-volume ratio of the

Table 1
Percentage conversion of glyphosate to glycine

Concentration of glyphosate (μg/l)	Conversion of glyphosate to glycine (%)	
	10 ft. × 0.02 in. I.D. coil	15 ft. × 0.02 in. I.D. coil
0	0	0
500	85.5	95.2
1000	84.3	95.6
5000	85.6	95.1
10000	85.7	95.7

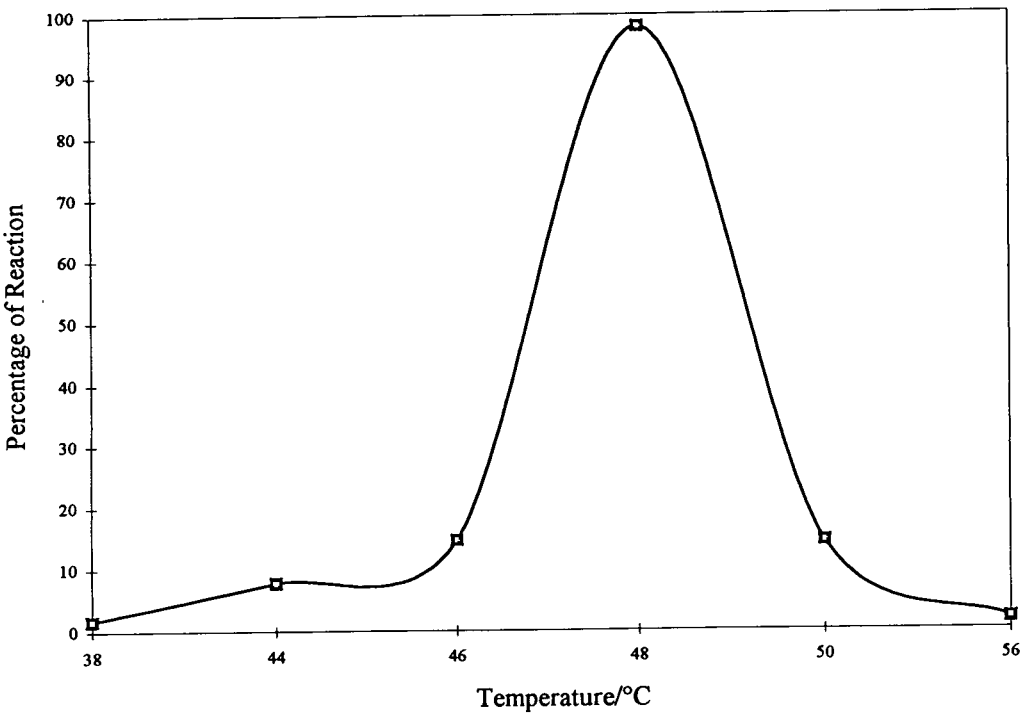

Fig. 2. Effect of temperature on oxidation of Glyph.

small particle resin would be greater than that of the large particle resin. As this resin is packed on top of the Supelclean packing, the flow-rate was controlled by the finer material in the Supelclean packing.

The acid dissociation constants of Glyph were determined to be $pK_1 = 2.32 \pm 0.03$, $pK_2 = 5.86 \pm 0.03$, $pK_3 = 10.86 \pm 0.03$ [9]. During the clean-up procedure, it is very important that the pH of the sample be maintained near the pK_3 value and that the pH of the sample be adjusted to near the pK_3 value before elution in order to obtain adequate recoveries from the SAX cartridge.

It was found that 0.1 *M* KH_2PO_4 buffer solution (pH 1.9) could not elute the analytes from the cartridge [10]. Sodium citrate buffer at 0.4 *M* (pH 5.00) was used as the elution solvent because it shows high relative selectivity in anion-exchange chromatography.

When the clean-up procedure was applied to a standard sample, virtually all the Glyph and AMPA were retained by the cartridge and 10 ml of 0.4 *M* sodium citrate buffer (pH 5.00) could give high recoveries (>95%) for both components.

When the same clean-up procedure was applied to the Taman Jaya Lake water samples, neither Glyph nor AMPA could be detected, which indicates their absence. The recoveries were then assessed by adding known amounts of Glyph and AMPA (in the range 2–40 μg/l) to these water samples. The results in Table 2 were calculated by comparison of the detector response with that for a standard solution containing both analytes at the same concentration as in the eluate. The mean recoveries of Glyph and AMPA were 91.6% and 88.6% with relative standard deviations of 6.2% and 7.4%, respectively. The method detection limit found for both components based on a signal-to-noise ratio of 3:1 is better than 2 μg/l.

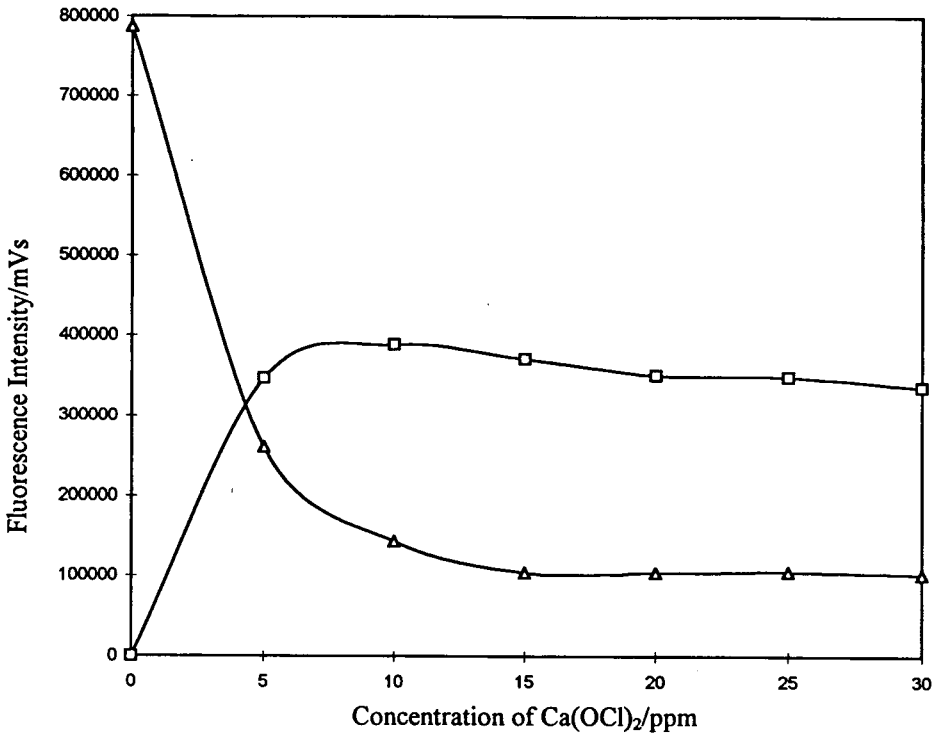

Fig. 3. Effect of $Ca(OCl)_2$ on (□) Glyph and (△) AMPA.

Table 2
Recoveries of Glyph and AMPA from environmental water samples

Analyte	Concentration added ppb (μg/l)	No. of additions	Range of recoveries (%)	Mean (%)	S.D. (%)	R.S.D. (%)
Glyph	2–40	30	81.3–97.8	91.6	5.7	6.2
AMPA	2–40	30	79.6–97.4	88.6	6.6	7.4

4. Conclusion

The sample preparation procedure developed is efficient with a method detection limit of less than 2 μg/l and mean recoveries of more than 85%. The efficiency of the oxidative cleavage in the first reaction coil could be checked and optimized by the simultaneous injection of glycine and glyphosate. Calcium hypochlorite solution was found to decrease the fluorescence intensity of AMPA substantially, which justified the use of a switching valve. This procedure offers a simple, sensitive and reproducible determination of Glyph and AMPA at residue levels in water. The elution order can be reversed depending on whether the separation is carried out on an anion- or cation-exchange column.

Acknowledgements

The financial support of Malaysian Government under an R&D grant, IRPA programme 4-07-03-002, is gratefully acknowledged. The authors also thank the Public Service Depart-

ment (JPA) for the financial support, the Veterinary Department (Petaling Jaya), the Chemistry Department (Ukm Bangi) for the facilities provided and Mr. S.K. Ooi for his technical help.

References

[1] M. Yusof, *Ph.D.* Thesis, University of Glasgow, Glasgow, 1988.
[2] P.C. Bardalaye, W.D. Wheeler and H.A. Moye, in E. Grossbard and D. Atkinson (Editors), *The Herbicide Glyphosate*, 1985, p. 263.
[3] M.J. Lovdahl and D.J. Pietrzyk, *J. Chromatogr.*, 602 (1992) 197.
[4] C.J. Miles, L.R. Wallace and H.A. Moye, *J. Assoc. Off. Anal. Chem.*, 3 (1986) 458.
[5] L.N. Lundgen, *J. Agric. Food Chem.*, 34 (1986) 535.
[6] S. Kawai and M. Tomita, *J. Chromatogr.*, 540 (1991) 411.
[7] M.E. Oppenhuizen and J.E. Cowell, *J. Assoc. Off. Anal. Chem.*, 74 (1991) 317.
[8] C.J. Miles and G. Leong, *LC–GC Mag.*, 10 (1992) 452.
[9] D. Wauchope, *J. Agric. Food Chem.*, 24 (1976) 717.
[10] Y.Y. Wigfield and M. Lanouette, *Anal. Chim. Acta.*, 233 (1990) 311.

ELSEVIER

Journal of Chromatography A, 697 (1995) 371–375

JOURNAL OF CHROMATOGRAPHY A

Sensitive determination of the benzene metabolite S-phenylmercapturic acid in urine by high-performance liquid chromatography with fluorescence detection

T. Einig*, W. Dehnen

Medizinisches Institut für Umwelthygiene, Abteilung Biochemie, Auf dem Hennekamp 50, D-40225 Düsseldorf, Germany

Abstract

A method was developed for the determination of the specific benzene metabolite S-phenylmercapturic acid in urine. The analyte is determined by HPLC with fluorescence detection after solid-phase extraction of urine with C_{18} material and hydrolysis followed by precolumn derivatization. The samples are separate by a column-switching method with a dual column system. As the method is highly sensitive (detection limit ca. 1 μg/l), urinary S-phenylmercapturic acid concentrations for non-exposed persons (e.g., non-smokers) can also be measured precisely.

1. Introduction

Benzene is a natural occurring compound of relatively low acute toxicity [1]. As petrol contains up to 5% of benzene, traffic is the main source of benzene in the environment. It is also an important product in the chemical industry. It has been shown that the main source of non-occupational benzene exposure is cigarette smoke [2]. Despite the low acute toxicity, monitoring of benzene is of great interest in occupational and environmental medicine because it causes cancer in humans [3]. The important pathways of benzene metabolism are well known (Fig. 1) [4].

Several methods for the determination of benzene metabolites as biomarkers for benzene exposure have been published [5–16]. As phenol is also formed by the metabolism of other xenobiotics and by catabolism of proteins, the determination of phenol in urine [5–7] is not a specific biomarker for benzene. Several workers have described methods for the determination of *trans,trans*-2,4-hexadienedioic acid in urine [7–10], S-phenylcysteine bound to albumin [11] or haemoglobin [12] and S-phenylmercapturic acid (S-PMA) in urine [13–16] as biomarkers for benzene exposure. As most methods are not sensitive enough to determine these biomarkers in urine of low-exposed persons (non-smokers), we describe here an improved method to determine S-PMA by HPLC with fluorescence detection with a sufficiently low detection limit. The method is based on a procedure published earlier [13].

* Corresponding author.

0021-9673/95/$09.50
SSDI 0021-9673(94)00788-8

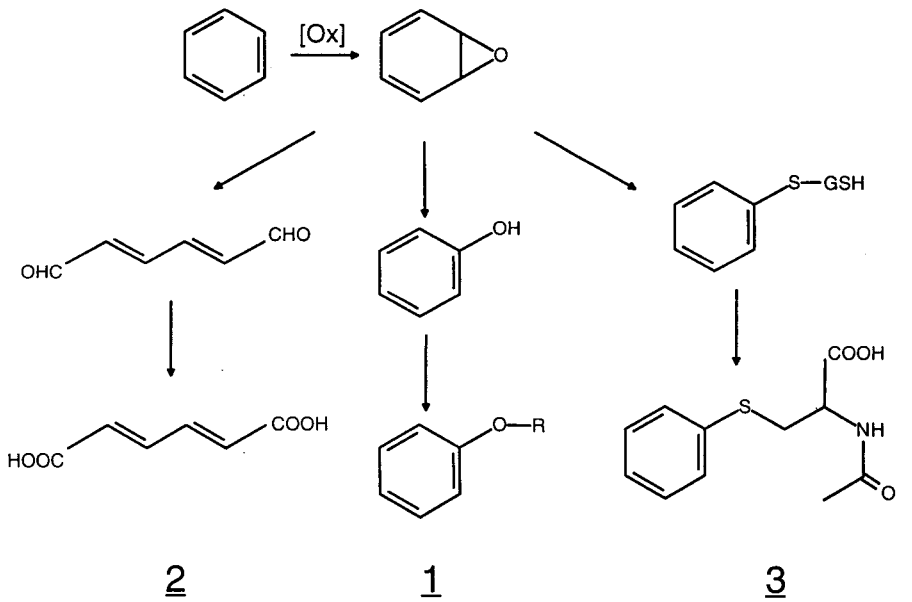

Fig. 1. Important pathways of benzene metabolism (for details see [2]). Most of the benzene uptake is metabolized to phenol (centre), which is excreted as conjugate **1** (R = sulfate or glucuronic acid). Formation of the specific metabolites *trans,trans*-2,4-hexadienedioic acid (**2**) (left) and S-phenylmercapturic acid (**3**) (right) totals only ca. 2%.

2. Experimental

2.1. Chemicals

N-Acetyl-S-phenylcysteine (S-PMA) was supplied by Janssen Chimica (Neuss, Germany), methanol for HPLC by Baker (Bad Soden/Ts., Germany) and monobromobimane by Calbiochem (Gross Gerau, Germany). All other chemicals were obtained from Merck (Darmstadt, Germany) and were the highest purity available. Creatinine determination was carried out according to the Jaffé method with a test kit (Boehringer, Mannheim, Germany).

2.2. Chromatographic equipment

Two Model 114M pumps with an AI 406 interface connected to a personal computer with System Gold Software (version 7.00) (all from Beckman Instruments, Munich, Germany), an M6000 pump (Millipore, Eschborn, Germany), a Model 717 autosampler (Millipore, Eschborn, Germany), Latek HMV-P electric switching valve (purchased from Millipore) and an HP 1046A fluorescence detector (Hewlett-Packard, Waldbronn, Germany) were used. Columns were purchased from Macherey–Nagel (Düren, Germany). The following solid-phase extraction (SPE) cartridges were used: BondElut C_{18} (Analytichem International; obtained from ICT, Frankfurt, Germany), Bakerbond C_{18} (Baker) and Sep-Pak C_{18} (Millipore, Eschborn, Germany).

2.3. Synthesis of the internal standard

S-Acetyl-4-methylthiophenol was synthesized as the internal standard by reaction of 0.5 g of 4-methylthiophenol in 20 ml of acetonitrile with 1 ml of acetic anhydride; 1 ml of N,N-dimethyl-4-aminopyridine in acetonitrole (0.5 mol/l) was added as catalyst. The mixture was refluxed for 60 min and poured in 500 ml of ice–water after cooling to room temperature. The reaction product was extracted three times with 100 ml of dichloromethane. The solvent was evaporated to

dryness and the purity of the product was confirmed by HPLC.

2.4. Solid-phase extraction

For extraction of S-PMA from urine, C_{18} cartridges with 500 mg of sorbent were used. The cartridges were washed with 5 ml of methanol and conditioned with 10 ml of 1% acetic acid. S-PMA was extracted from 2 ml of urine adjusted to pH 1.0 with 25% hydrochloric acid after addition of 50 μl of internal standard in methanol ($15 \cdot 10^{-6}$ mol/l). The cartridges were then washed with 2 ml of 1% acetic acid. S-PMA was eluted with 2 ml of methanol–ammonium acetate buffer (0.1 mol/l, pH 7.0) (80:20).

2.5. Derivatization

A 100-μl volume of NaOH (10 mol/l) was added to the extract. In a 5-ml flack with an 8-cm long narrow neck (Dünges flask [17]), the solution was concentrated to ca. 100 μl at 78°C under nitrogen and hydrolysed for 30 min at 95°C. A 2-ml volume of glycine–NaOH buffer (0.4 mol/l, pH 9.0) was added followed by 350 μl of phosphoric acid [diluted 1:1 (v/v) with water]. The thiophenol (TP) released from S-PMA by the hydrolysis was derivatized by adding 500 μl of monobromobimane (MB) [18] ($1 \cdot 10^{-3}$ mol/l) in acetonitrile–water (1:9, v/v). The reaction is shown in Fig. 2.

2.6. Chromatographic conditions

A 50-μl volume of the above solution was separated under the following conditions. A dual column system was used (see Fig. 3): preseparation of the sample was carried out on a 50 mm × 2 mm I.D. column with an 11 mm × 2 mm I.D. built-in precolumn filled with Nucleosil 120 C_{18} (5 μm) (column 1). Two minutes before elution of the analyte, the eluent from column 1 was directed to a 125 mm × 2 mm I.D. column filled with Nucleosil 120 C_{18} (3 μm) for further separation (column 2). Separation was carried out by gradient elution: column 1 was equilibrated with 10% methanol in 0.1% acetic acid.

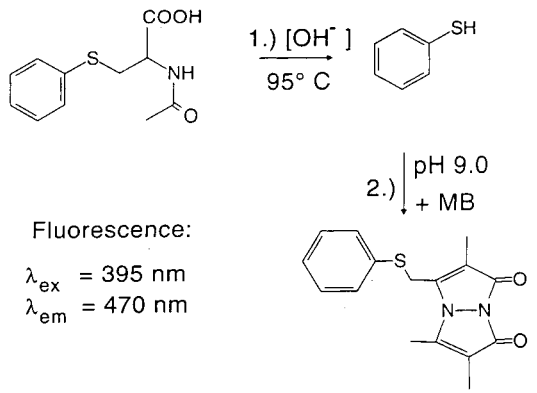

Fig. 2. Precolumn derivatization occurs in two steps: (1) the extract from the Sep-Pak C_{18} cartridge is concentrated, followed by alkaline hydrolysis; (2) the pH is adjusted to 9.0 and the thiophenol released is derivatized with monobromobimane.

After 2 min, the modifier concentration was increased to 50% in 3 min; the flow-rate was 0.2 ml/min. Thiophenol–MB was eluted from column 1 after 24 min under these conditions, and therefore column switching was applied after 22 min. At this time the methanol concentration was increased to 60% and the flow-rate was decreased to 0.1 ml/min to avoid excessively high pressure (both in 1 min). The retention times were 48 and 65 min for thiophenol–MB

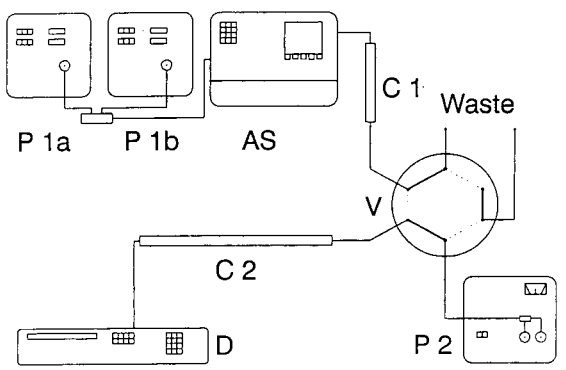

Fig. 3. Diagram for the column-switching procedure. P 1a, P 1b and P2 = pumps; AS = autosampler; C1 and C2 = columns; V = switching valve; D = fluorescence detector. On-column focusing and preseparation are carried out on column 1 with the valve in position 1 (thick lines). Final separation on column 2 occurs after switching to position 2 (dotted lines).

and 4-methylthiophenol–MB, respectively. After elution of the internal standard, the valve was turned back and column 1 was re-equilibrated for 10 min at a flow-rate of 0.2 ml/min, and meanwhile column 2 was flushed with the M6000 pump isocratically with 50% methanol in 0.1% acetic acid (flow-rate 0.1 ml/min). The excitation and emission wavelengths of the detector were set at 395 and 470 nm, respectively.

3. Results and discussion

An HPLC method was established for the determination of the benzene metabolite S-PMA in urine. The formation of S-PMA seems to be specific for benzene, unlike *trans,trans*-2,4-hexadienedioic acid, where interference may occur from the preservative sorbic acid in samples from "non-exposed" persons, as the metabolism of sorbic acid also leads to low levels of *trans,trans*-2,4-hexadienedioic acid [8,19].

For SPE, three different C_{18} materials were tested. Recoveries of the extraction from urine samples spiked with 250 μg/l of S-PMA using the different C_{18} SPE cartridges were 45% (BondElut), 82% (Bakerbond) and 103% (Sep-Pak). As Sep-Pak C_{18} cartridges showed the highest recovery (103%), they were subsequently used for extraction of the urine samples. The internal standard can also be extracted by the procedure described above. The detection limit of the method (signal-to-noise ratio = 3) is below 1 μg/l, which is sufficiently low for the analysis of samples from "non-exposed" persons (for chromatograms, see Fig. 4). The linearity of the calibration graphs indicates a quantifiable range between 1 and 200 μg/l. It was confirmed that no interferences with the internal standard occur on co-elution under the described conditions. The peak shape and bandwidth of the TP–MB peak indicate that no co-elution with the analyte occurs.

The precision of the method was confirmed by repeated analyses of a urine sample with internal standard and standard addition. The reproducibility (R.S.D.) of the method was <5% within-day and <10% day-to-day (measured with a sample containing ca. 15 μg/l). S-PMA in urine samples from non-smokers was determined less accurately (within day reproducibility 20% for a sample containing 2.5 μg/l). A number of urine samples from smokers and non-smokers were analysed, confirming the values obtained previously [13]. The mean results were 2.0 and 7.6 μg/g creatinine for samples from non-smokers and smokers, respectively.

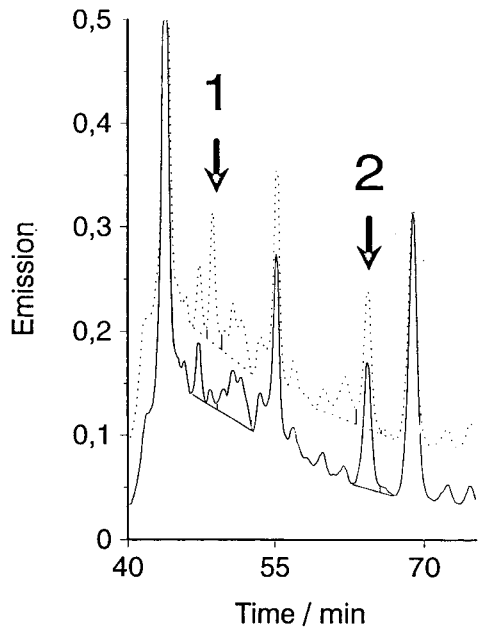

Fig. 4. Chromatogram of a urine sample from a non-exposed person. Peaks: 1 = S-PMA; 2 = internal standard. Straight line = chromatogram of urine without addition of S-PMA; dotted line = chromatogram of the same sample after addition of 40 ng of S-PMA to 2 ml of sample.

References

[1] H.W. Horace, in F.A. Patty (Editor), *Industrial Hygiene and Toxicology*, Vol. II, Interscience, New York, 2nd ed., 1963, p. 1220.
[2] L.A. Wallace, *Cell. Biol. Toxicol.*, 3 (1989) 297.
[3] G.F. Kalf, G.B. Post and R. Snyder, *Annu. Rev. Pharmacol. Toxicol.*, 27 (1987) 399.
[4] G.F. Kalf, *CRC Crit. Rev. Toxicol.*, 18 (1987) 141.
[5] W.E. Bechtold and R.F. Henderson, *J. Toxicol. Environ. Health*, 40 (1993) 377.
[6] J. Angerer, in D. Henschler (Editor), *Analysen in Biologischen Materialien*, VCH, Weinheim, 1983.

[7] H. Schad, F. Schäfer, L. Weber and H. Seidel, *J. Chromatogr.*, 593 (1992) 147.
[8] P. Ducos, R. Gaudin, A. Robert, J.M. Francin and C. Maire, *Int. Arch. Occup. Environ. Health*, 62 (1990) 529.
[9] P. Ducos, R. Gaudin, J. Bel, C. Maire, J.M. Francin, A. Robert and P. Wild, *Int. Arch. Occup. Environ. Health*, 64 (1992) 309.
[10] D. Rauscher, G. Lehnert and J. Angerer, *Clin. Chem.* 40 (1994) in press.
[11] W.E. Bechtold, J.K. Willis, J.D. Sun, W.C. Griffith and T.V. Reddy, *Carcinogenesis*, 13 (1992) 1217.
[12] W.E. Bechtold, J.D. Sun, L.S. Birnbaum, S.N. Yin, G.L. Li, S. Kasicki, G. Lucier and R.F. Henderson, *Arch. Toxicol.*, 66 (1992) 303.
[13] W. Dehnen, *Zbl. Hyg.*, 189 (1990) 441.
[14] G. Müller, W. Popp, A. Bibowsky and K. Norpoth, presented at the *1st International Congress on Environmental Medicine, Duisburg, Germany, 1994.*
[15] P. Stommel, G. Müller, W. Stücker, C. Verkoyen, S. Schöbel and G. Norpoth, *Carcinogenesis*, 10 (1989) 279.
[16] F. J. Jongeneelen, H.A.A.M. Dirven, C.-M. Leijdekkers, P.T. Henderson, R.M.E. Browns and K. Halm, *J. Anal. Toxicol.*, 11 (1987) 100.
[17] W. Dünges, *Prä-Chromatographische Mikromethoden*, Hüthig, Heidelberg, 1979.
[18] G.L. Newton, R. Dorian and R.C. Fahey, *Anal. Biochem.*, 114 (1981) 383.
[19] G. Westöö, *Acta Chem. Scand.*, 18 (1964) 1373.

ELSEVIER

Journal of Chromatography A, 697 (1995) 377–382

JOURNAL OF CHROMATOGRAPHY A

Quantitative estimation of heterocyclic aromatic amines by ion-exchange chromatography and electrochemical detection

M.M.C. Van Dyck[a], B. Rollmann[b], C. De Meester[a,*]

[a]*Laboratoire de Tératogenèse et de Mutagenèse, Université Catholique de Louvain, Avenue E. Mounier 72.37, 1200 Brussels, Belgium*

[b]*Laboratoire d'Analyse Physico-Chimique des Médicaments, Université Catholique de Louvain, Avenue E. Mounier 72.30, 1200 Brussels, Belgium*

Abstract

Conditions for the quantitative determination of three heterocyclic aromatic amines (HAAs), produced by heat processing of protein-rich food products, were established for a HPLC–electrochemical detection system. The separation of 2-amino-3-methylimidazo[4,5-*f*]quinoline (IQ), 2-amino-3,4-dimethylimidazo[4,5-*f*]quinoline (MeIQ) and 2-amino-3,8-dimethylimidazo[4,5-*f*]quinoxaline ($MeIQ_x$) was achieved on an ion-exchange column with acetonitrile–80 m*M* phosphate buffer (30:70) mobile phase at pH 5.6. The figures of merit were calculated. Reproducibility gave a relative standard deviation of 1.6–2.4% when measured by peak area. Detection limits (signal-to-noise ratio 3) ranged from 35 pg for $MeIQ_x$ to 70 pg for MeIQ. The method was applied to the determination of HAAs in a commercial beef extract sample.

1. Introduction

Heterocyclic aromatic amines (HAAs) are formed by condensation of amino acids, sugar and creatinine by a Maillard-type reaction [1]. These products, which can be found at low parts per billion (w/w) range in cooked meat and fish products, possess a high mutagenic activity in the Ames test [2–6]. They induce tumors in the liver, lung, breast, small and large intestine and other sites in rodents [7] and are considered as possible human carcinogens.

Daily human exposure to HAAs varies greatly and is dependent on diet habits and cooking practices [8]. These findings suggest the need to develop analytical techniques able to determine low levels present in meats cooked under industrial conditions as well as in traditional cooking practices. Separation and detection of these compounds require fast, selective and sensitive analytical techniques. Sophisticated and expensive techniques, such as HPLC–MS [9,10], GC–MS [11–13] or enzyme-linked immunosorbent assay (ELISA) [14], have been proposed. Restricted analyses are obtained with techniques such as HPLC with UV and/or fluorescence detection [15,16]. However, electrochemical detection (ED) achieves higher selectivity and sensitivity than classical UV detection and studies using this mode of detection have been recently described [17–20]. Separations of HAAs are commonly achieved on a reversed-phase (C_{18}) column. However, in the acidic conditions needed for the separation of these compounds,

* Corresponding author.

0021-9673/95/$09.50
SSDI 0021-9673(94)00837-X

amino groups are protonated and interact with the free silanols of the stationary phase. Moreover, in the purification scheme described by Gross and Grüter [15,16], HAAs are successfully purified by adsorption on a propylsulfonyl silica gel.

This work aimed to develop a separation procedure on an ion-exchange column. Conditions were established for the determination of three HAAs identified in commercial beef extracts: 2-amino-3-methylimidazo[4,5-*f*]quinoline (IQ), 2-amino-3,4-dimethylimidazo[4,5-*f*]-quinoline (MeIQ) and 2-amino-3,8-dimethylimidazo[4,5-*f*]quinoxaline ($MeIQ_x$) using ion-exchange HPLC with ED. The method was applied to the analysis of these three HAAs in commercial beef extracts.

2. Experimental

2.1. Chemicals

IQ, MeIQ and $MeIQ_x$, whose structures are presented in Fig. 1. were purchased from Toronto Research Chemicals (Toronto, Canada). Stock solutions (1 mg ml^{-1}) were prepared in methanol and used for further dilutions. Extrelut extraction cartridges and refill material were from Merck (Darmstadt, Germany). Bond-Elut propylsulfonyl silica gel (PRS; 500 mg) and C_{18} (100 mg) cartridges were purchased from Analytichem International (ICT, Basle, Switzerland). Acetonitrile (gradient grade), disodium hydrogenphosphate (analytical-reagent grade) and phosphoric acid (analytical-reagent grade) were from Merck. All the solutions were passed through a 0.45-μm filter before being used in the HPLC system. The pH was fixed in the mixture acetonitrile–buffer solution.

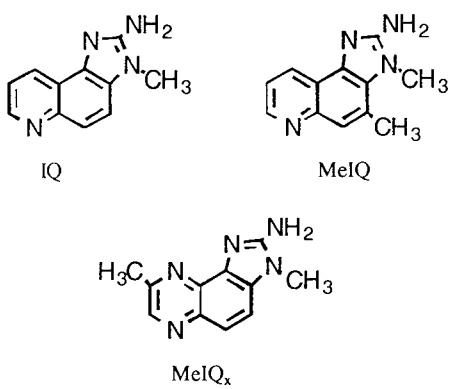

Fig. 1. Chemical structures of the mutagenic heterocyclic amines.

2.2. Extraction scheme

Extraction of the HAAs was carried out using the protocol described by Gross and Grüter [15,16]. Practically, 2 g of beef extract were homogenized in 12 ml of 1 *M* NaOH. The solution was adsorbed to diatomaceous earth (Extrelut cartridge). The Extrelut cartridges were conditioned with 20 ml dichloromethane. The HAAs were eluted with 35 ml dichloromethane and adsorbed to the coupled PRS cartridge. This cartridge was then connected to a peristaltic pump and rinsed at a flow-rate of 1–2 ml min^{-1} with 6 ml 0.1 *M* HCl and 15 ml of methanol–0.1 *M* HCl (4:6), followed by 2 ml water. The PRS cartridge, which contained the polar IQ-type compounds, was then coupled to a Bond-Elut C_{18} cartridge. The HAAs were transferred to the C_{18} cartridges by washing the PRS cartridge with 20 ml of 0.5 *M* ammonium acetate buffer (pH 8.0). The C_{18} cartridge was rinsed with 1 ml water. The solutes were eluted with 0.8 ml methanol–concentrated ammonia solution (9:1). The solvent was evaporated under nitrogen. Solutes were then dissolved with 100 μl methanol before injection. The volume injected in the HPLC system was twofold the loop volume. Solvent evaporation was minimized by conservation of solutions at 4°C and were injected as fast as possible.

2.3. Instruments

HPLC was carried out with a Kontron (Milan, Italy) Model 420 pump. The sample was introduced via a Rheodyne (Cotati, CA, USA) 7125 injector equipped with a loop of 20 μl. A Spherisorb SCX 5U column (5 μm; 250 × 4.6

mm) (Alltech, Deerfield, IL, USA) and a Supelguard LC-8DB precolumn (Supelco, Gland, Switzerland) were used at room temperature. The detection was achieved successively on a UV detector, Kontron Model 432 at a wavelength of 263 nm, and an amperometric detector, BAS (Lafayette, IN, USA) Model LC-4B, equipped with a working electrode (glassy carbon electrode), a reference electrode (Ag/AgCl/KCl 3 *M*) and with an auxiliary electrode. A data processor Softron (Kontron) was used. Acetonitrile–phosphate buffer (30:70, v/v) at different pH values and ionic strengths was used as a mobile phase at a flow-rate of 1.0 ml min^{-1}.

2.4. Calibration

Calibrations were carried out in quadruplicate with 2-g aliquots of beef extract, which were spiked with 100 μl standard solution of the mixture of the three HAAs (0.25, 0.5, 0.75 or 1 μg ml^{-1}) after extraction. For each compound, linear regression analysis was carried out. Recovery of extraction was determined by spiking beef extract sample before extraction. Concentrations were determined from the calibration curve. Extraction efficiency was expressed as the ratio of amount measured and amount added in the sample.

3. Results and discussion

3.1. Optimization of the chromatographic conditions

Separations on an ion-exchange stationary phase were dependent on the ionic strength of the mobile phase and on the ionization state of the different amines. Mobile phase (acetonitrile–phosphate buffer) was tested for different concentrations of salt. The concentration in Na_2HPO_4 varied from 10^{-2} to 10^{-1} *M*. The pH value was fixed at 6.0 by phosphoric acid solution. The capacity factors (k') obtained for each compounds are indicated in Fig. 2. An increase in the ionic strength produces a decrease of k'

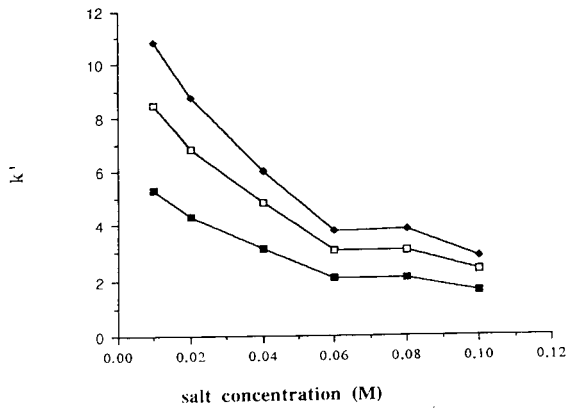

Fig. 2. Effect of concentration in Na_2HPO_4 on the separation of heterocyclic amines. Mobile phase: acetonitrile–phosphate buffer pH 6.0 (30:70). Working potential: +1050 mV vs. Ag/AgCl. □ = IQ; ◆ = MeIQ; ■ = $MeIQ_x$.

due to the competitive interaction of solutes and salt with the ionic sites. A compromise must be found between the analysis time and the resolution of the different peaks. The best separation was obtained at a salt concentration of 80 m*M*.

Separation is also influenced by the pH value of the mobile phase. The capacity factors for the three compounds obtained at different pH values varied from 4.0 to 7.0 and are presented in Fig. 3. The mobile phase was acetonitrile–80 m*M* Na_2HPO_4 (30:70, v/v). An increase in the pH

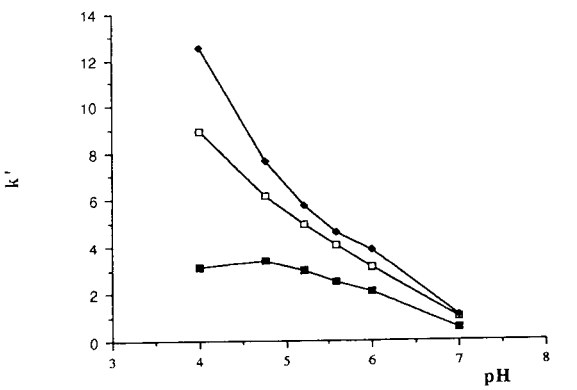

Fig. 3. Effect of mobile phase pH on the separation of heterocyclic amines. Mobile phase: acetonitrile–80 m*M* phosphate buffer (30:70). Working potential: +1050 mV vs. Ag/AgCl. □ = IQ; ◆ = MeIQ; ■ = $MeIQ_x$.

value induces a decrease of k' related to a progressive reduction of amine protonation.

It must be stressed that no gradient in the composition of the mobile phase can be applied with ED. Even very small modifications in the composition carry away a shift of the baseline. It can be concluded that the separation of the three HAAs must be realised with a mobile phase of acetonitrile–80 m*M* aqueous Na_2HPO_4 (30:70, v/v). At pH 5.6, all the compounds can be separated as can be seen in Fig. 4, which shows the chromatogram obtained with a standard solution under the conditions described.

The optimal potential was obtained from the hydrodynamic voltammogram at the separation conditions previously established. The results obtained by variation of potential from + 700 to + 1100 mV are presented in Fig. 5. The highest surface area with the lowest background noise were obtained at a working potential of + 1050 mV which corresponds to a maximum response for the three compounds and is located in the beginning of the plate to limit interferences.

From the voltammogram, it can be observed that the two quinoline derivatives present the same curve aspect whereas the quinoxaline derivative present a reduced tendency to oxidation.

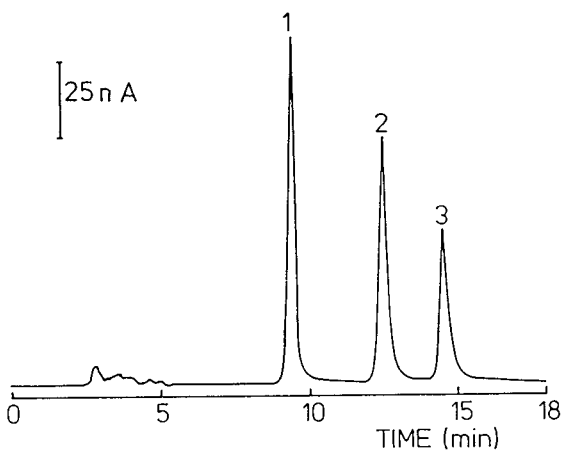

Fig. 4. Chromatogram of standard solution. Mobile phase: acetonitrile–80 m*M* phosphate buffer pH 5.6 (30:70). Working potential: + 1050 mV vs. Ag/AgCl. Peaks: 1 = $MeIQ_x$; 2 = IQ; 3 = MeIQ.

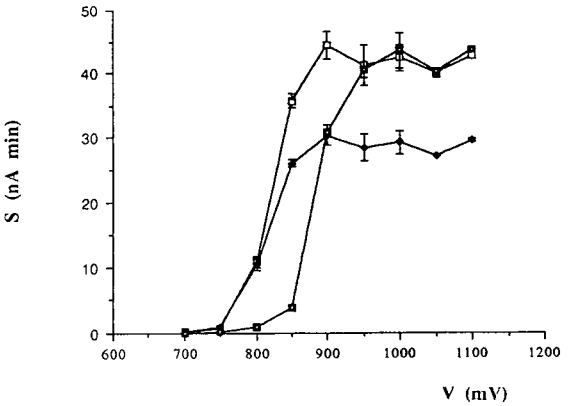

Fig. 5. Hydrodynamic voltammogram. Mobile phase: acetonitrile–80 m*M* phosphate buffer pH 5.6 (30:70). □ = IQ; ◆ = MeIQ; ■ = $MeIQ_x$.

ED can be used for the characterization of these three compounds in a matrix.

3.2. Linearity and limits of detection

Linearity and limits of detection were determined with standard solution diluted in methanol. Peak area was used as the response in the optimal conditions.

Calibrations were carried out with concentrations in the range 10^{-3}–1 μg ml^{-1}; beef extract containing only trace amounts of HAAs (no higher concentration than 20 ng g^{-1} was studied).

Six replicate determinations of 20 ng (1 μg ml^{-1} solution) of each analyte in methanol were carried out to determine the precision of the method. Relative standard deviations (R.S.D.) obtained were in the range 1.66–2.42%. The detection limits for the heterocyclic amines,

Table 1
Figures of merit

Analyte	Range of linearity (ng)	Limits of detection (pg)	Precision (R.S.D., %)
IQ	1.0–20	37	2.20
MeIQ	2.5–20	70	2.42
$MeIQ_x$	2.5–20	35	1.66

Table 2
Analysis of beef extract

Analyte	Recovery (%)	Precision (R.S.D., %)	Results (ng/g)	Precision (R.S.D., %)
IQ	36.14	12,27	9.59	29,48
MeIQ	50.72	11,24	N.D.	
$MeIQ_x$	27.75	19,90	35.91	18,92

N.D. = Not detected.

based on a signal-to-noise ratio of 3 ranged from 35 to 70 pg (Table 1).

Using these experimental conditions, the detection limit was strongly improved in comparison with the results described in the literature [18–20]; this may be attributed to the pH of the solution, and thus the ionization state of analytes, which plays an important role on the electrochemical reaction [20].

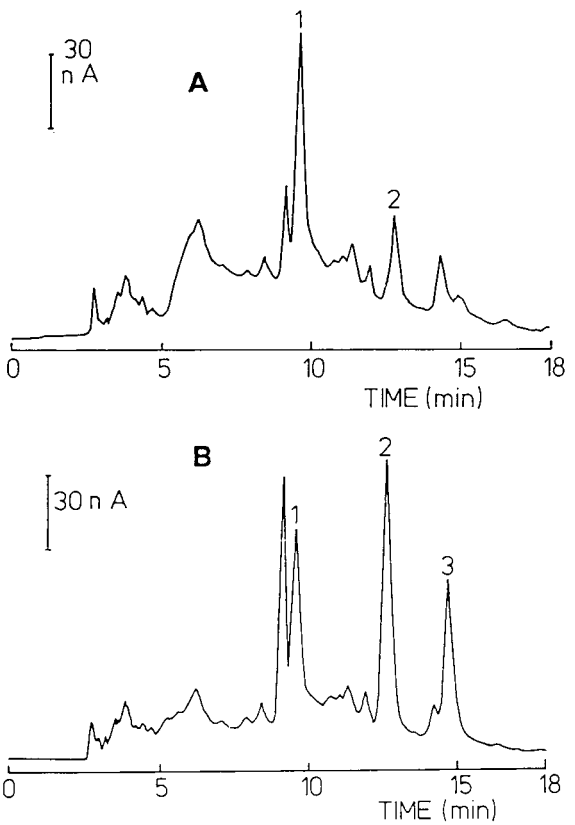

Fig. 6. Chromatogram of a beef extract. Mobile phase: acetonitrile–80 m*M* phosphate buffer pH 5.6 (30:70). Working potential: +1050 mV vs. Ag/AgCl. (A) Extract, (B) extract spiked before the clean-up (100 ng of IQ and MeIQ). Peaks: 1 = $MeIQ_x$; 2 = IQ; 3 = MeIQ.

3.3. Application

After optimization of experimental conditions, commercial beef extract was analyzed. Results presented in Table 2 were obtained from four successive extractions. Peak identification was confirmed by UV detection. The percentage recovery is lower than that presented in the literature [15,16,20], which may result from the clean-up procedure; therefore further investigations are needed to clarify this discrepancy.

Chromatograms of the sample and the spiked sample are presented in Fig. 6. No interferences were observed with impurities of the extract and the different compounds are easily quantified. MeIQ could not be detected in the sample (Fig. 6A). Such observation was reported previously for the beef extract [1].

4. Conclusions

Quantification of mutagenic heterocyclic amines is essential for the determination of risks to human health. In this study, conditions have been established for the separation and the determination by HPLC–ED with an ion-exchange column of three heterocyclic amines. The applicability, linearity and sensitivity of the method have been studied. The method has been applied to the quantification of IQ, MeIQ and

$MeIQ_x$ in commercial beef extract. Research is currently in progress to extend the method to other heterocyclic amines present in beef extract.

Acknowledgements

We thank A. Brams and A. Loukili for technical assistance. This research was supported by the "Services Fédéraux des Affaires Scientifiques, Techniques et Culturelles" of Belgium.

References

[1] J.S. Felton and M.G. Knize, *Mutation Res.*, 259 (1991) 205.
[2] H. Ohgaki, H. Hasegawa, T. Kato, M. Suenaga, M. Ubukata, S. Sato, S. Takayama and T. Sugimura, *Environ. Health Perspect.*, 67 (1986) 129.
[3] J.S. Felton, M. Knize, N. Shen, B. Andersen, L.B. Bjeldanes, F. Hatch and T. Fred, *Environ. Health Perspect.*, 67 (1986) 17.
[4] S. Nishimura, *Environ. Health Perspect.*, 67 (1986) 11.
[5] T. Sugimura, *Trends Pharmacol. Sci.*, 9 (1988) 205.
[6] R. Vikse, A. Knapstad, L. Klungsoyr and S. Grivas, *Mutation Res.*, 298 (1993) 207.
[7] K. Wakabayashi, M. Nagao, H. Esumi and T. Sugimura, *Cancer Res. (Suppl.)*, 52 (1992) 2092s.
[8] J.S. Felton and M.G. Knize, in C.S. Cooper and P.L. Grover (Editors), *Chemical Carcinogenesis and Mutagenesis I*, Springer, Berlin, Heidelberg, New York, 1990, p. 471.
[9] C.G. Edmonds, S.K. Sethi, Z. Yamaizumi, H. Kasai, S. Nishimura and J.A. McClosey, *Environ. Health Perspect.*, 67 (1986) 35.
[10] H. Milon, H. Bur and T. Turesky, *J. Chromatogr.*, 394 (1987) 201.
[11] S. Murray, N.J. Gooderham, V.F. Barnes, A.R. Boobis and D.S. Davies, *Carcinogenesis*, 8 (1987) 937.
[12] S. Murray, N.J. Gooderham, A.R. Boobis and D.S. Davies, *Carcinogenesis*, 9 (1988) 321.
[13] S. Vainiotalo, K. Matveinen and A. Reunanen, *Fresenius' J. Anal. Chem.*, 345 (1993) 462.
[14] M. Vanderlaan, B.E. Watkins, M. Hwang, M. Knize and J.S. Felton, *Carcinogenesis*, 9 (1988) 153.
[15] G.A. Gross, *Carcinogenesis*, 11 (1990) 1597.
[16] G.A. Gross and A. Grüter, *J. Chromatogr.*, 592 (1992) 271.
[17] S. Grivas and T. Nyhammar, *Mutation Res.*, 142 (1985) 5.
[18] M. Takahashi, K. Wakabayashi, M. Nagao, M. Yamamoto, T. Masui, T. Goto, N. Kinae, I. Tomita and T. Sugimura, *Carcinogenesis*, 6 (1985) 1195.
[19] S.M. Billedeau, M.S. Bryant and C.L. Holder, *LC·GC Int.*, 4 (1991) 38.
[20] M.T. Galceran, P. Pais and L. Puignou, *J. Chromatogr. A*, 655 (1993) 101.

ELSEVIER

Journal of Chromatography A, 697 (1995) 383–388

JOURNAL OF CHROMATOGRAPHY A

Use of solvent optimization software for rapid selection of conditions for reversed-phase high-performance liquid chromatography of nicotine and its metabolites

S. Pichini, I. Altieri, A.R. Passa, M. Rosa, P. Zuccaro*, R. Pacifici

Istituto Superiore di Sanità, Viale Regina Elena 299, 00161 Rome, Italy

Abstract

Solvent optimization software was used to develop a reversed-phase HPLC method for nicotine, five of its metabolites and caffeine under isocratic conditions, using UV detection and a LC_8DB reversed-phase column. Starting from a methanol–buffer gradient, the software helped to find a quaternary solvent composition consisting of 2.3% methanol, 4.3% acetonitrile, 0.3% tetrahydrofuran and 93.1% buffer for the separation. The method was applied to human spiked serum and to serum of 12 cigarette smokers using a simple purification treatment before chromatography.

1. Introduction

In recent years, the metabolism of nicotine has been found to be complex, leading to more than twenty metabolites, which differ in structure and polarity [1–3]. At present, high-performance liquid chromatographic (HPLC) methods able to simultaneously quantify more than two metabolites, always require lengthy gradient mobile phases [4–7]. Moreover, different extractions from biological matrices are needed depending on the polarity of the metabolites investigated [4,8].

During the last decade, several schedules have been developed to aid the chromatographer to obtain appropriate separations in the shortest possible period of time [9]. In some cases this has led to the production of commercially available systems, either as complete instruments or as separate software packages [10,11].

We have developed a reversed-phase HPLC method for nicotine and five of its metabolites (Fig. 1) under isocratic conditions, using UV detection. Diamond solvent optimization software (Unicam, Cambridge, UK) [11,12] was used together with the HPLC system to optimize the separation of nicotine, its metabolites and caffeine using N′-ethylnorcotinine as an internal standard. The method was applied to the serum of 12 smokers using a simple purification treatment before chromatography.

2. Experimental

2.1. Materials

Cotinine (COT), nicotine (NIC) and caffeine (CAF) were purchased from Sigma (St. Louis,

* Corresponding author.

0021-9673/95/$09.50
SSDI 0021-9673(94)00865-5

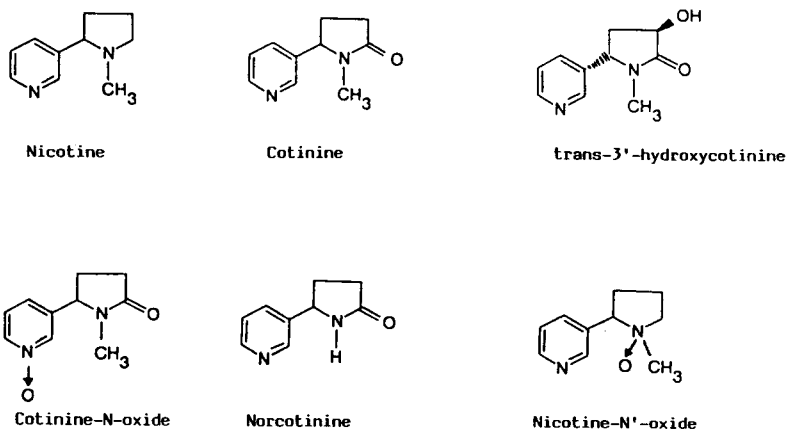

Fig. 1. Structural formulae of nicotine and five of its metabolites.

MO, USA). *trans*-3′-Hydroxycotinine (THOC), cotinine-N-oxide (CNO), nicotine-N′-oxide (NN′O), norcotinine (NCOT) and N′-ethylnorcotinine (NENC) were obtained from Dr. Georg B. Neurath (Hamburg, Germany). All solvents were analytical grade.

2.2. Chromatography

The HPLC system consisted of a Crystal 200 Series HPLC pump (Unicam, Cambridge, UK), a Crystal 240 diode array detector (Unicam), a PU4247 LC Autosampler (Philips Analytical, Cambridge, UK) and a Crystal Integrated Control Software. Both the HPLC control software and the Diamond solvent optimization software were run on a Dell 433/M computer, and were operated under a Windows 3.0 environment. Chromatographic data were collected and stored using the UICS operating software (Unicam). Then, data could be accessed from the Diamond environment, from where they could be displayed and interpreted, following any appropriate manipulation. For biological samples analyses, the HPLC pump was coupled with a Beckman 160 fixed-wavelength detector, set at 254 nm, and a Varian 4290 chromato-integrator.

A Supelcosil LC_8DB column(5 μm particle size, 25 cm × 4.6 mm I.D.; Supelchem, Rome, Italy) was used at room temperature at a flow-rate of 1.4 ml/min. The four solvents were methanol (MeOH), acetonitrile (MeCN), tetrahydrofuran (THF), and a buffer containing triethylamine (2 ml/l), 0.012 *M* each of sodium heptanesulphonate, K_2HPO_4 and citric acid, adjusted to pH 4.7 with citric acid. The injection volume was 20 μl.

2.3. Biomedical applications

Solutions of stock reference standards (1 mg/ml, 10 μg/ml, 1 μg/ml) were prepared in methanol and stored below 0°C. Dilutions were made fresh daily to create serum standards.

Drug-free human sera (1 ml) spiked with different amounts of nicotine, its five metabolites, caffeine and N′-ethylnorcotinine were transferred in a tube and rapidly deproteinized by 100 μl of perchloric acid (70%). The deproteinized samples were centrifuged at 2000 *g* for 10 min, the supernatants were removed, evaporated under nitrogen at 40°C and redissolved in 100 μl of water before chromatography. These spiked sera were used throughout the entire procedure to create calibration curves, and to determine analytical recoveries, intra-day and inter-day variabilities.

Blood samples (5 ml) from 12 smokers were obtained by venipuncture with silicone-coated vacutainers. Samples were collected at 8:00 a.m. after consumption of two cigarettes, the last one 10 min prior to collection. Immediately after collection the samples were centrifuged at 1000 *g*

for 5 min, extracted as described above and injected into the HPLC column.

3. Results and discussion

The HPLC method was developed using a LC_8DB column, used earlier to separate nicotine and four metabolites under gradient mobile-phase conditions [8]. Initially, the analytes mixture was chromatographed using a methanolic gradient consisting of 5% methanol and 95% buffer at the beginning and changed to 30% methanol and 70% buffer in 30 min (Fig. 2). This gradient was extrapolated from previous investigations [8]. Using the retention times of the first and last eluting peaks, the t_0 of the system, the methanolic profile information, and the number of components in the mixture, the software supplied an isocratic aqueous methanolic solvent composition of 14% which should result in elution of the final peak with a k' of approximately 10, as the number of components expected was 8. The mixture was run with this solvent composition and the retention time of the last peak was input to the software program, to check if the prediction was correct. An equivalent acetonitrile binary composition was obtained, the entire process was repeated and a THF binary composition was suggested. Finally, when all three binary solvent compositions had been checked, the software defined an isoeluotropic plane of 10 solvent compositions of approximately equal solvent strength (Fig. 3).

When all 10 chromatographic runs were collected, the one containing most peaks, which was the one with the THF binary solvent composition, was chosen to create a library of reference UV spectra for each of the substances present in the mixture. Then, for each of the 10 chromatograms, the spectrochromatographic data obtained with the diode array detector were interrogated. The chromatograms were divided into segments, the positions of the peaks were de-

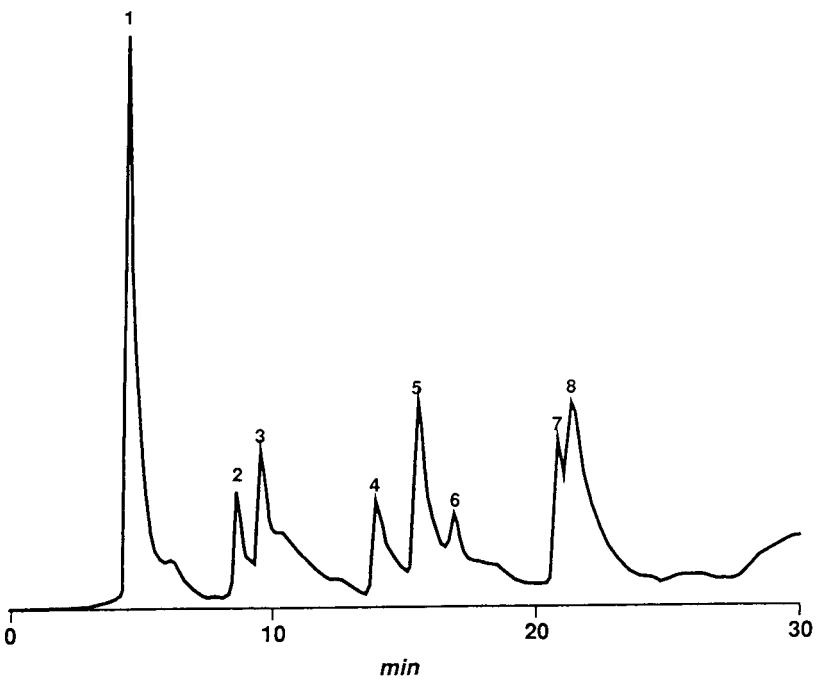

Fig. 2. Chromatogram of a standard mixture using a methanol–buffer gradient. Peaks: 1 = cotinine-N-oxide; 2 = *trans*-3′-hydroxycotinine; 3 = norcotinine; 4 = cotinine; 5 = caffeine; 6 = nicotine-N′-oxide; 7 = nicotine; 8 = N′-ethylnorcotinine.

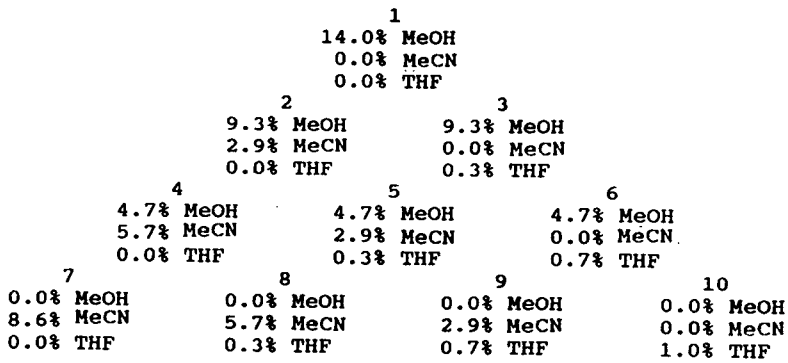

Fig. 3. The ten-solvent compositions used to define the isoeluotropic solvent plane, as determined using the software. The figures represent the percentage of each component in the mobile phase at each point, with buffer making the composition up to 100%.

termined from the second derivative of the chromatogram, and the spectral data of each peak were extracted using deconvolution where two or more peaks overlapped. When the extracted spectra were accepted, they were matched against those in the reference library and the retention times of the components were stored in the database.

Once the retention information for all 10 chromatographic data sets were achieved, the retention maps for each of the components were synthesized as shown in Fig. 4 for nicotine. The retention maps for nicotine, its metabolites, caffeine and NENC were combined to produce the final resolution map, from which the optimal separation conditions were derived (Fig. 5) using the response function ('TNE') for the minimum separation and retention time of the last peak. A quaternary solvent composition consisting of 2.3% methanol, 4.3% acetonitrile, 0.3% tetrahydrofuran and 93.1% buffer was proposed for the separation of nicotine, its metabolites, caffeine and the internal standard.

The chromatographic separation performed using the solvent composition suggested by the software showed to be very similar to the predicted one (Fig. 6).

An example of the method's application was the HPLC determination, using UV fixed-wave-

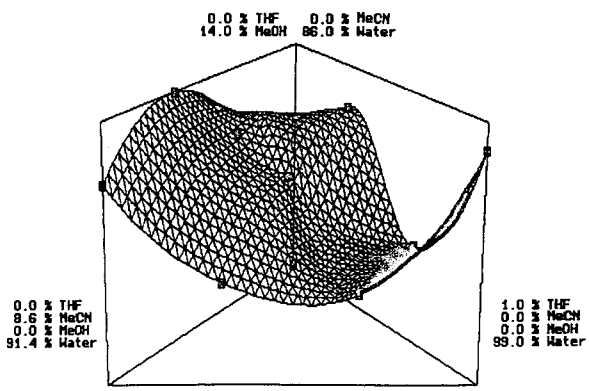

Fig. 4. Retention map for nicotine viewed towards the methanol corner.

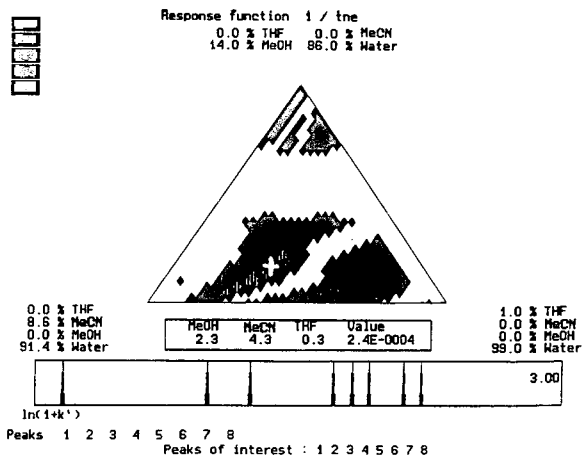

Fig. 5. Final resolution map for the separation of nicotine, five of its metabolites, caffeine and N'-ethylnorcotinine, calculated using the 'TNE' function (see text), presented as a contour plot. The white cross indicates the optimal predicted solvent composition.

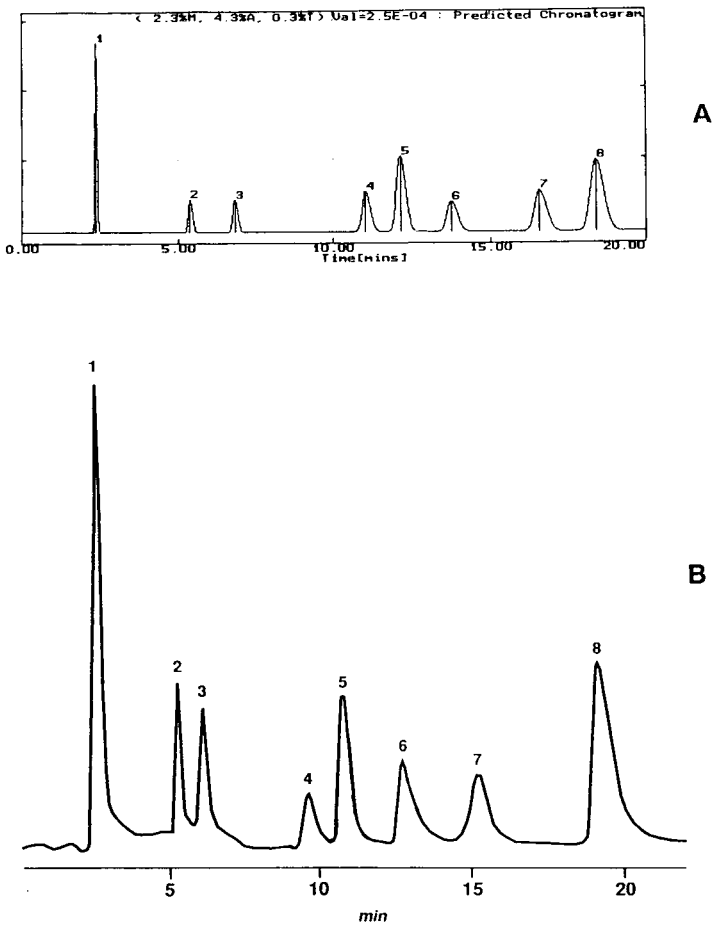

Fig. 6. A comparison of the simulated chromatogram for the optimal separation derived from the software prediction (A), and the actual separation obtained using the predicted optimal mobile phase composition calculated by the software (B). Peaks: 1 = cotinine-N-oxide; 2 = *trans*-3′-hydroxycotinine; 3 = norcotinine; 4 = cotinine; 5 = caffeine; 6 = nicotine-N′-oxide; 7 = nicotine; 8 = N′-ethylnorcotinine.

length detection, of nicotine, its metabolites and caffeine, which is present in 80% of smokers' serum samples [13], in human sera of 12 smokers, who had smoked just prior to blood collection. The results obtained are shown in Table 1.

The limits of detection (signal-to-noise ratio of 3) observed with this method were 10 ng/ml for nicotine and nicotine-N′-oxide, 5 ng/ml for cotinine, *trans*-3′-hydroxycotinine, caffeine and norcotinine, 3 ng/ml for cotinine-N-oxide. The calibration curves of the peak area vs. the amount of analytes (μg/ml) were linear over the range of 10–500 ng/ml for NIC ($y = 0.14x +$

Table 1
Concentrations of nicotine and its metabolites in serum samples of 12 smokers

Compound	Concentration, mean ± S.D. (ng/ml)
NIC	42.2 ± 35.1
COT	307.1 ± 81.6
THOC	96.5 ± 31.0
CNO	3.5 ± 1.3
NCOT	9.1 ± 2.7
NN′O	12.5 ± 1.6[a]

[a] Detected only in three samples.

0.06; $r = 0.99$) and NN'O ($y = 0.16x + 0.10$; $r = 0.98$); over the range of 5–500 ng/ml for COT ($y = 0.01x + 0.14$; $r = 0.90$), THOC ($y = 0.016x + 0.10$; $r = 0.93$), NCOT ($y = 0.03x - 0.13$; $r = 0.99$) and CAF ($y = 0.02x + 0.05$; $r = 0.98$), and over the range of 3–500 ng/ml for CNO ($y = 0.05x + 0.4$, $r = 0.99$). Over the concentration ranges tested in the analysis, recoveries were above 90% for all analytes. The within-day and between-day coefficients of variation were always less than 4 and 6% for 100 and 500 ng/ml analytes, respectively.

In conclusion, solvent optimization software proved to be a versatile and useful tool, simple to use, and interactive with the analyst, thus reducing the time spent in achieving an acceptable separation using a mathematical approach.

References

[1] J.W. Gorrod and P. Jenner, in W.J. Hayes (Editor), *Essays in Toxicology*, Academic Press, New York, Vol. 6, 1975, pp. 35–78.

[2] P. Jacob III, N.L. Benowitz and A.T. Shulgin, *Pharmacol. Biochem. Behav.*, 30 (1988) 249.

[3] K. Rustemeier, D. Demetriou, G. Schepers and P. Voncken, *J. Chromatogr.*, 613 (1993) 95.

[4] G.A. Kyerematen, L.H. Taylor, J.D. deBethizy and E.S. Vesell, *J. Chromatogr.*, 419 (1987) 191.

[5] K.T. Manus and J.D. deBethizy, D.A. Garteiz, G.A. Kyerematen and E.S. Vesell, *J. Chromatogr. Sci.*, 28 (1990) 510.

[6] D. Demetriou, K. Rustemeier, P. Voncken and G. Schepers, *Med. Sci. Res.*, 20 (1992) 873.

[7] G. Schepers, K. Rustemeier, R.A. Walk and U. Hackenberg, *Eur. J. Drug Metab. Pharmacokinet.*, 18 (1993) 187.

[8] P. Zuccaro, I. Altieri, M. Rosa, A.R. Passa, S. Pichini, G. Ricciarello, R. Pacifici, *J. Chromatogr.*, 621 (1993) 257.

[9] P.J. Schoenmakers, *Optimization of Chromatographic Selectivity*, Elsevier, Amsterdam, 1986.

[10] P.J. Schoenmakers, H.A.H. Billiet and L. De Galan. *J. Chromatogr.*, 205 (1981) 13.

[11] P.B. Bowman, J.T. Hann, J.G.D. Marr, D.J. Salvat and B.E. Thompson. *J. Pharm. Biomed. Anal.*, 11 (1993) 1295.

[12] P.B. Bowman, J.G.D. Marr, D.J. Salvat and B.E. Thompson. *J. Pharm. Biomed. Anal.*, 11 (1993) 1303.

[13] S. Pichini, I. Altieri, R. Pacifici, M. Rosa, G. Ottaviani and P. Zuccaro. *J. Chromatogr.*, 577 (1992) 358.

ELSEVIER

Journal of Chromatography A, 697 (1995) 389–396

JOURNAL OF CHROMATOGRAPHY A

Quantitation of phenylbutazone and oxyphenbutazone in equine plasma by high-performance liquid chromatography with solid-phase extraction

M.R. Taylor, S.A. Westwood*

Horseracing Forensic Laboratory Limited, PO Box 15, Snailwell Road, Newmarket, Suffolk CB8 7DT, UK

Abstract

Phenylbutazone (bute) and oxyphenbutazone are non-steroidal anti-inflammatory drugs (NSAIDs) widely used in the equine world. Both substances are prohibited under the British Jockey Club Rules of Racing but are permitted up to a certain threshold level in blood plasma by some other equine governing bodies. There is therefore the requirement for accurate quantitation of these compounds in equine plasma samples.

A quantitative analytical method utilising solid-phase extraction and reversed-phase HPLC was developed and a full validation exercise performed. Additional studies of analyte stability and development of a confirmatory analysis method were also carried out.

A linear calibration over the plasma concentration range of 1–10 μg ml^{-1} for both analytes was achieved using fenclofenac as an internal marker. Inter-assay precision ($n = 6$) testing of plasma samples spiked at 2 μg ml^{-1} with both analytes produced results (R.S.D.) of 5.1% for phenylbutazone and 4.0% for oxyphenbutazone with standard error of the mean 0.0140 and 0.0138, respectively. The analytes were prone to oxidation during extraction and storage and preventative measures were incorporated into the methods. Confirmatory analysis was achieved by GC–MS with on-column derivatisation (methylation) of back extracted residues from the quantitative method.

1. Introduction

Phenylbutazone (4-butyl-1,2-diphenyl-3,5-pyrazolidinedione) (PB) is one of the most widely used drugs in the equine world. It is a non-steroidal anti-inflammatory drug (NSAID) with antipyretic and analgesic activity. Its major use in the horse is in treatment of bone and joint inflammation, laminitis and soft tissue inflammation [1–8]. PB is metabolised in the liver to form oxyphenbutazone (OPB) which is pharmacologically active, and γ-hydroxyphenylbutazone which is presumed inactive [9] (Fig. 1). PB and its two metabolites have been reported to be heavily bound to plasma proteins [10] and excreted in the urine as both the unchanged drug and as the two major metabolites [11,12].

The potential misuse of NSAIDs such as PB has resulted in the banning of their use in the treatment of horses in competition by many equine governing bodies including the British Jockey Club [13,14].

PB and OPB are permitted up to a threshold plasma level by some other equestrian authorities. Therefore there is a requirement for an accurate and fully validated quantitative method for PB and OPB in equine plasma. Numerous quantitative methods for PB and its metabolites

* Corresponding author.

0021-9673/95/$09.50
SSDI 0021-9673(94)00834-5

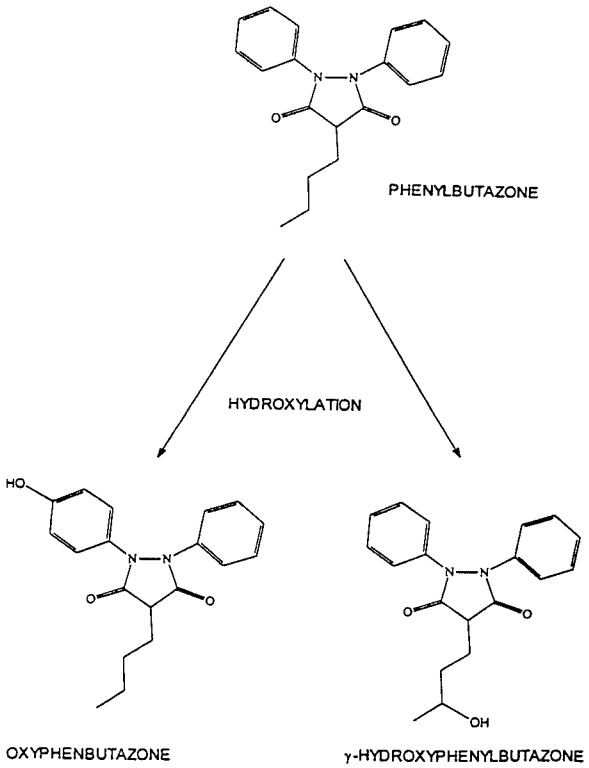

Fig. 1. Metabolism of phenylbutazone in the horse.

have been published using both gas chromatography (GC) [15–18] and high-performance liquid chromatography (HPLC) with UV detection [19–30]. Of these only one [28] addressed the problem of decomposition of PB and OPB during extraction. There is an additional requirement to unequivocally identify the presence of PB or OPB in a positive sample (with a result greater than the threshold limit) and mass spectrometric (MS) data provides this information.

In this article we present results from a simple, fully validated quantitative analytical method for PB and OPB using HPLC with solid-phase extraction (SPE). A study of the degradation of the compounds prior to, during and after extraction has been carried out and preventative measures have been incorporated into the method. A confirmatory analysis method based upon GC–MS with a solid-phase back extraction of the HPLC sample residues is also presented.

2. Experimental

2.1. Materials

Isolute cartridges, C_{18} (non-endcapped, 500 mg, 6 ml reservoir) were obtained from International Sorbent Technology (Hengoed, UK). Bond elut cartridges, Certify (300 mg, 6 ml reservoir) were obtained from Anachem (Luton, UK). Diethylether, dichloromethane, ethyl acetate, hexane and methanol (HPLC grade) were obtained from Rathburn Chemicals (Walkerburn, UK). Sodium dihydrogen orthophosphate, disodium hydrogen orthophosphate and acetic acid (AnalR grade) were obtained from BDH (Poole, UK). Phenylbutazone, oxyphenbutazone hydrate, 1-heptanesulfonic acid, N-methyl-N-(trimethylsilyl)trifluoroacetamide (M-STFA) and alumina were obtained from Sigma (Poole, UK). Fenclofenac {[2-(2,4-dichlorophenoxy)phenyl] acetic acid} was obtained from Reckitt and Colman (Pharmaceuticals Division, Hull, UK). Trimethylanilinium hydroxide (TMAH) (0.2 *M* in methanol) was obtained from Supelco (Poole, UK). Blank equine plasma was obtained from thoroughbred racehorses stabled at the Horseracing Forensic Laboratory.

2.2. Chromatography

The HPLC apparatus consisted of Hewlett Packard HP1090 Series I and Series II instruments with diode-array detectors and a Waters 600E multisolvent delivery system with Waters 990 photodiode-array detector and Waters WISP 712 autosampler. A monitoring wavelength of 240 nm (4 nm bandwidth) was used with reference wavelength of 550 nm (100 nm bandwidth). Peak controlled spectral data acquisition was performed over the wavelength range of 230–350 nm (2 nm step, 640 ms sampling interval). Injection volume was 50 μl.

Separations were performed on a Hypersil C_{18} column (5 μm, 100 × 4.6 mm I.D., Jones Chromatography, Hengoed, UK) under isocratic conditions at a flow-rate of 1.5 ml/min. Mobile phase was methanol (60%) and acetic acid (0.1

M) with heptane sulfonic acid (0.01%) (40%) which was filtered through 0.45 μm glass sinter and helium degassed. Chromatography was carried out at 40°C. Relative peak areas were calculated using the HPLC Chemstation integration software which was calibrated on each assay with extracted standard solutions.

The GC–MS apparatus consisted of a Varian 3400GC fitted with a Finnigan MAT A200S autosampler and Finnigan MAT Incos 50 mass spectrometer. Separations were performed on an SE54 capillary column (30 m × 0.25 mm I.D., film thickness 0.25 μm, Alltech, Carnforth, UK). Injection was made at 250°C, splitless for 70 s. Carrier gas was helium at 15 p.s.i. (103 kPA) head pressure. Temperature programme was isothermal at 100°C for 2 min then ramped at 21°C/min to 320°C then isothermal at 320°C for 7.5 min. Transfer line was maintained at 290°C, ion source at 175°C and scanning at 40–650 amu in one second.

2.3. Sample preparation

Quantitative HPLC method

Mixed standards of PB and OPB were prepared in methanol at 0.4 mg ml^{-1} calibration samples (at 1, 2, 4, 7 and 10 μg ml^{-1}) and control samples (at 2 and 6 μg ml^{-1}) in blank equine plasma. The control samples were prepared by an independent analyst using a separate mixed standard. 2 ml aliquots of calibration, control, unknown and blank plasma samples were pipetted (in duplicate) into tubes and a fenclofenac internal marker solution (0.1 mg ml^{-1} in methanol, 100 μl) were added to all except one of the blank plasma samples. Phosphate buffer (pH 7.2, 0.1 *M*, 1 ml) and de-ionised water (3 ml) was added to all samples before capping and mixing. Samples were drawn through C_{18} cartridges which had been pre-conditioned with methanol (2 ml) and de-ionised water (2 ml) under vacuum. The cartridges were sequentially washed with phosphate buffer (pH 7.2, 0.1 *M*, 1 ml) and hexane (2 ml). The cartridges were dried under vacuum (approximately 20 in. Hg, ca. 68 kPA) for 2 min prior to elution with a mixture of ethylacetate and hexane (1:1, v/v; 2 ml). The eluates were evaporated to dryness (at 40°C) under a stream of oxygen free nitrogen (OFN). The dry residues were reconstituted in methanol (100 μl) and phosphate buffer (pH 7.2, 0.1 *M*, 150 μl) and submitted to HPLC analysis. Low volume (i.e. <4ml) or high concentration (i.e. ≥10 μg ml^{-1}) samples were diluted with blank equine plasma prior to extraction.

Confirmatory GC–MS method

Selected residues from HPLC quantitation were back-extracted for GC–MS (generally the suspicious samples, blanks and a calibration or control sample). The residues were diluted with phosphate buffer (pH 5.5, 0.1 *M*, 6 ml) and drawn through a Certify cartridge which had been preconditioned with methanol (2 ml) and phosphate buffer (pH 5.5, 0.1 *M*, 2 ml). The cartridges were sequentially washed with a methanol–phosphate buffer (pH 5.5, 0.1 *M*) mixture (1:9, v/v; 1 ml), acetic acid (1.0 *M*, 1 ml) and hexane (2 ml). The cartridges were dried under vacuum (ca. 68 kPA) for 5 min before elution with dichloromethane (3 ml). The eluates were evaporated (at 40°C) to dryness under a stream of OFN. The dry residues were reconstituted in 30 μl MSTFA and 30 μl TMAH (0.2 *M* in methanol) for GC–MS analysis.

3. Results

3.1. Linearity

The proportional relationship of HPLC response to analyte concentration over the working range was demonstrated. Peak areas of PB and OPB ratioed to the internal standard were plotted against concentration and subjected to linear regression analysis. The linearity was determined over the concentration range of 1 to 10 μg ml^{-1} using five data points ($n = 6$). For PB the result was $y = 4.00x + 0.0910$ ($r = 0.99$), for OPB $y = 3.29x + 0.201$ ($r = 0.999$).

3.2. Precision

The inter-assay precision, expressed as the R.S.D. was determined for PB and OPB at five concentration levels using four different operators, four different HPLC instruments and two different SPE cartridge batches. The results ($n = 6$) are presented in Table 1.

3.3. Recovery

Drug recoveries were calculated by extracting a set of calibration samples and comparing results with non-extracted standards representing 100% recovery. The ranges found were 53.5 to 63.1% for PB and 43.3 to 47.2% for OPB.

3.4. Selectivity

No significant interference peaks were observed from plasma taken from ten different horses and extracted using the quantitative procedure.

3.5. Matrix effects

Calibration samples were prepared in blank equine plasma which had been previously frozen and thawed. The results were compared to those from samples prepared in fresh (non frozen) plasma and to calibration samples prepared one month earlier and stored frozen. A negative bias in PB results obtained from fresh plasma was seen. Reductions of up to 14% were observed. No loss of either PB or OPB was found in the sample stored frozen for one month.

The use of blank equine plasma and de-ionised water as diluents for high-concentration or low-volume samples (unknowns) was investigated. It was found that when deionised water was used as a diluent the results were negatively biased compared to when blank equine plasma was used. Depressions as high as 18% were observed.

3.6. Stability of standards

The methanolic stock standards (PB, OPB and fenclofenac) were stable for at least 8 weeks with storage at 4°C. Storage at elevated temperatures resulted in decomposition of PB and OPB (Fig. 2).

3.7. Stability during extraction

Degradation of PB and OPB was observed when diethylether was evaluated as an elution solvent in solid-phase extraction. The decomposition was reduced if the diethylether was passed through an alumina column prior to use to remove peroxides. No decomposition was observed when an ethyl acetate–hexane mixture was used as the eluent (Fig. 3).

Degradation of PB and OPB was observed if samples were exposed to acidic conditions or if samples were left dry and open to the atmosphere.

Table 1
Inter-assay precision data ($n = 6$) for quantitation of PB and OPB in equine plasma

Calibration level	Concentration ($\mu g\ ml^{-1}$)	R.S.D. (%)	
		PB	OPB
1	1	8.89	9.73
2	2	5.07	3.96
3	4	4.40	2.97
4	7	4.08	2.27
5	10	4.95	2.23

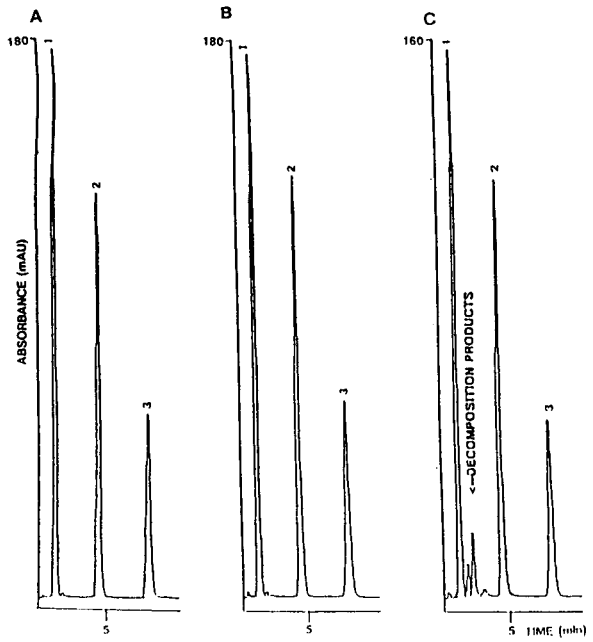

Fig. 2. Chromatograms obtained from methanolic stock standards. (A) Freshly prepared, (B) 8 weeks storage at 4°C, (C) 8 weeks storage at 37°C. 1 = OPB, 2 = PB, 3 = fenclofenac.

3.8. Stability after extraction

Plasma extracts ($n = 6$) from samples spiked at 2 μg ml^{-1} were re-analysed by HPLC after six days storage at 25°C. When results were compared to the original data no significant differences were observed.

3.9. Confirmatory analysis

Back-extracted HPLC residues from a spiked sample (4 μg ml^{-1}) were submitted to GC–MS with on-column derivatisation. The methyl derivatives of PB and fenclofenac and dimethyl derivative of OPB were identified (Fig. 4). A typical result from a post administration sample is shown in Fig. 5.

4. Discussion

The measurement of inter-assay precision during validation of the quantitative procedure is

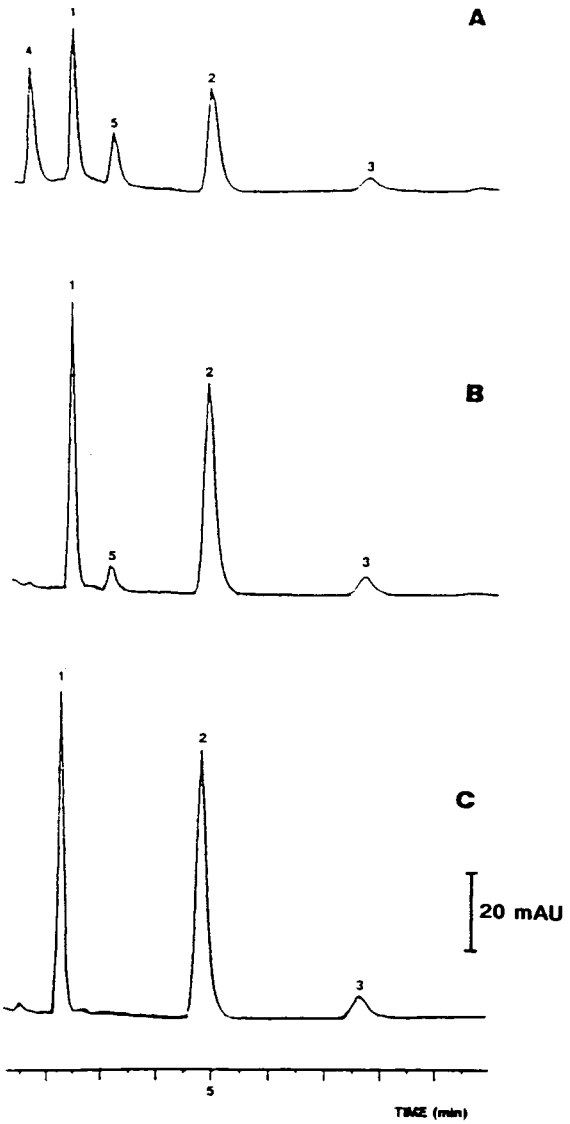

Fig. 3. Chromatograms showing degradation due to peroxide induced autoxidation of PB and OPB. Elution of C_{18} with different solvents. (A) Untreated diethyl ether, (B) alumina treated diethyl ether, (C) ethyl acetate–hexane (1:1). 1 = OPB, 2 = PB, 3 = fenclofenac, 4,5 = decomposition products.

especially important where a maximum permitted (threshold) level is applied. The validation exercise was set up to generate the maximum possible variation of results which could occur in the normal routine use of the quantitative procedure. By the incorporation of as many vari-

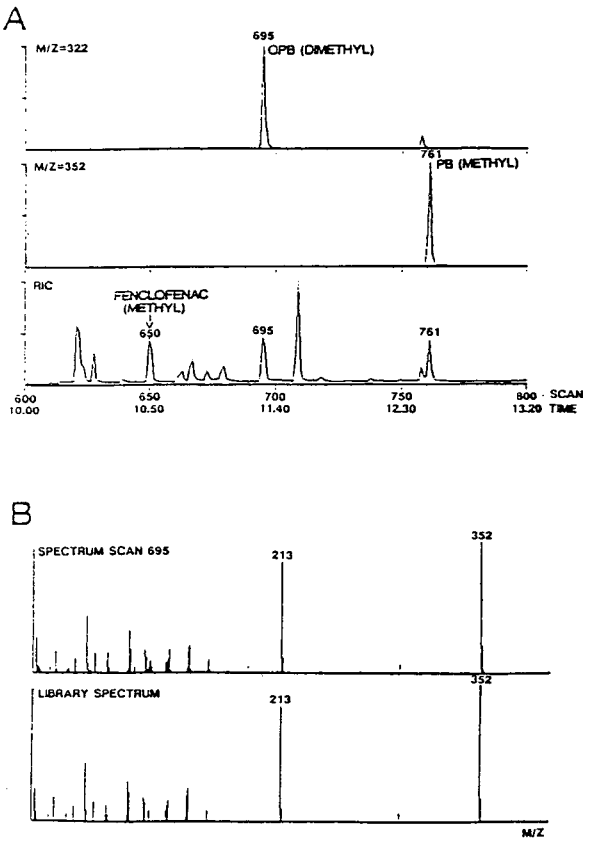

Fig. 4. Confirmatory GC–MS analysis of PB and OPB in equine plasma spiked at 4 μg ml^{-1}. (A) Reconstructed ion chromatogram and ion chromatograms, (B) OPB (dimethyl) mass spectrum with library search result.

ables as possible into the validation, i.e. different operators, HPLC instruments, SPE cartridge batches, etc., a 'worst case scenario' is created. This provides a basis upon which to decide if a result is over or under the threshold limit (within a specified level of confidence) accounting for the maximum expected level of method variation.

The problem of decomposition by oxidation of PB and OPB prior to, during and after extraction has been addressed and preventative measures incorporated into the method. Plasma was spiked with PB and OPB and frozen for 28 days prior to analysis with no indication of instability. This observation is in agreement with those made by Hyde et al. [29] who demonstrated that sample storage and treatment prior to analysis may affect the analytical result. It is recommended that plasma is separated from the red blood cells prior to freezing, as 10–25% losses of PB and OPB may occur on thermocyling in the presence of the red blood cell fraction [29]. Whether the losses are due to drug decomposition or plasma dilution by haemolysis is unknown. We found PB and OPB to be stable in methanolic solutions for 8 weeks at 4°C whereas Carturla and Cusido [28] observed decomposition within one week under identical storage conditions. The use of diethyl ether, presumably contaminated with peroxides, during the extraction of PB and OPB was demonstrated. The authors [28] found little decomposition despite using diethyl ether in their extraction procedure. After extraction a methanol–buffer (pH 7.2) mixture was used as a sample diluent to prevent oxidation of PB and OPB which may occur if the pH is too low.

The negative bias in results from fresh (non-frozen) plasma may possibly be related to protein binding of PB. The majority of plasma samples submitted to the quantitation will have been frozen prior to analysis and thawed if routine drug screening indicated the presence of PB and/or OPB.

The GC–MS procedure was a convenient way of unequivocally identifying PB and OPB after HPLC analysis. The on-column methylation procedure was quick, simple and efficient compared to conventional derivatisation with iodomethane for example, and has been previously used in analysis of diuretics in equine urine samples [31]. The advantage of back-extraction from HPLC residues is that both quantitation and confirmation can be achieved from one aliquot of plasma rather than two separate aliquots. This is important when sample volumes are limited as is often the case when dealing with plasma.

5. Conclusion

An HPLC procedure with SPE has been developed and validated to measure plasma

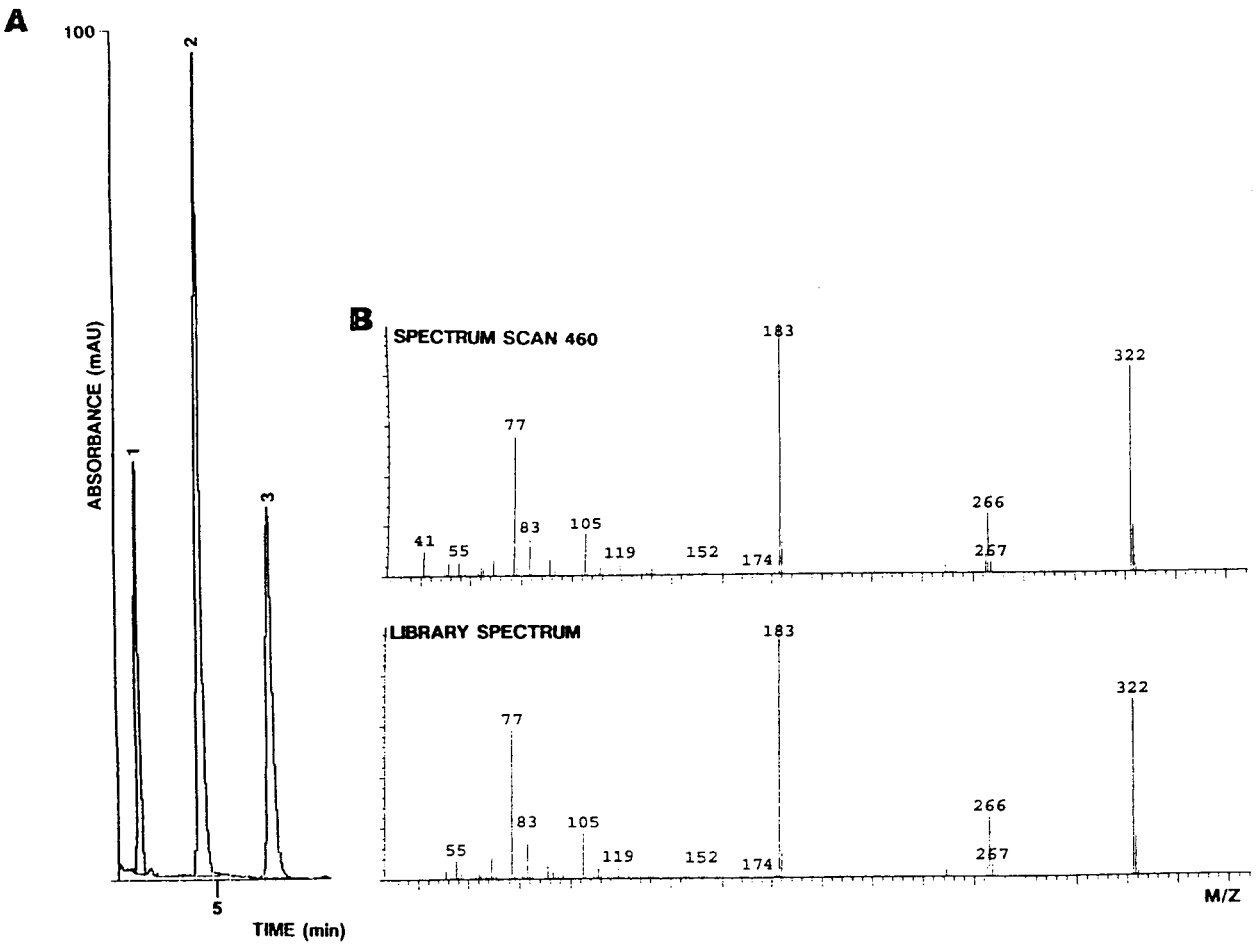

Fig. 5. (A) HPLC chromatogram of a post administration sample. 1 = OPB (1.26 mg ml^{-1}), 2 = PB (4.61 mg ml^{-1}), 3 = fenclofenac internal standard. (B) GC–MS of positive sample and library spectrum confirming the presence of PB.

concentrations of phenylbutazone and oxyphenbutazone in equine samples. The assay is linear over the range of concentrations tested and has a lower limit of quantitation below 1 μg ml^{-1} using 2 ml plasma. The quantitative procedure avoids decomposition of the compounds before, during and after extraction and HPLC.

A GC–MS confirmatory procedure utilising on-column methylation was developed and was successfully applied to the HPLC residues after solid-phase back extraction.

The sample preparation procedures are simple and have potential for automation.

References

[1] K.L. Gabriel and J.E. Martin, *J. Am. Vet. Assoc.*, 140 (1962) 337.
[2] H.A. Gorman, W.A. Wolff, W.W. Frost, W.V. Lumb and A.W. Nelson, *J. Am. Vet. Med. Assoc.*, 152 (1968) 487.
[3] E.J. Finnochio, F.J. Ozog, F.W. Oehme, J.H. Johnson and G.W. Osbaldiston, *J. Am. Vet. Med. Assoc.*, 156 (1970) 454.
[4] A.A. Gabel, T. Tobin, R.S. Ray and G.A. Maylin, *J. Eq. Med. Surg.*, 1 (1977) 221.
[5] L.B. Jeffcot and C.M. Colles, *Equine Vet. J.*, 9 (1977) 105.
[6] K. Hinrichs and E.D. Watson, *Am. J. Vet. Res.*, 52(5) (1991) 678.

[7] A. Le Ninivin and A. Vrins, *Recl. Med. Vet.*, 168(8-9) (1992) 669.
[8] J.M. Denoix and I. Delannoy, *Recl. Med. Vet.*, 168(8-9) (1992) 679.
[9] E.L. Gerring, P. Lees and J.B. Taylor, *Equine Vet. J.*, 13, 3 (1981) 152.
[10] C.P. Gandal, P.G. Dayton, M. Weiner and J.M. Perel, *Cornell Vet.*, 59 (1969) 577.
[11] M.S. Moss and P.E. Haywood, *Vet. Rec.*, 93 (1973) 124.
[12] G.A. Maylin, *Proc. 20th Conv. of Assoc. Am. Equine Pract.*, (1974) 243.
[13] M.S. Moss, *Equine Vet. J.*, 4 (1972) 69.
[14] R. Hopes, *Equine Vet. J.*, 4 (1972) 66.
[15] R. Perego, E. Martinelli and P.C. Vanoni, *J. Chromatogr.*, 54 (1971) 280.
[16] J. McGilveray, K.K. Midha, R. Brien and L. Wilson, *J. Chromatogr.*, 89 (1974) 17.
[17] R.D. Budd, *J. Chromatogr.*, 243 (1982) 368.
[18] L.R. Soma, D.E. Gallis, W.L. Davis, T.A. Cochran and C.B. Woodward, *Am. J. Vet. Res.*, 44(11) (1983) 2104.
[19] N.J. Pound, J. McGilveray and R.W. Sears, *J. Chromatogr.*, 89 (1974) 23.
[20] T. Marunaka, T. Shibatta, Y. Minami and Y. Umeno, *J. Chromatogr.*, 183 (1980) 331.
[21] M. Alvinerie, *J. Chromatogr.*, 181 (1980) 132.
[22] H. Fabre, B. Mandrai and H. Eddine, *J. Pharm. Sci.*, 71 (1982) 120.
[23] B. Weise, K. Martin and J. Harmansson, *Chromatographia*, 15 (1982) 737.
[24] K. Martin, M.I. Stridsberg and B. Weise, *J. Chromatogr.*, 276 (1983) 224.
[25] D.F. Gerken and R.J. Sams, *J. Pharm. Biopharm.*, 13 (1985) 467.
[26] L.G. Tillman and G.E. Hardee, *Anal. Lett.*, 18 (1985) 1987.
[27] M.J.A.M. Franssen, Y. Tan, I. Freij, C.A.M. Van Ginneben and F.W.J. Gribnau, *Pharm. Weekbl. (Sci.)*, 8 (1986) 229.
[28] M.C. Carturla and E. Cusido, *J. Chromatogr.*, 581 (1992) 101.
[29] W. Hyde, K. Ambrisco and J. Stevens, *Proc. of the 9th International Conference of Racing Analysts and Veterinarians, New Orleans*, (1992) 307.
[30] W. Hyde and K. Ambrisco, *Proc. of the 9th International Conference of Racing Analysts and Veterinarians, New Orleans*, (1992) 297.
[31] H.W. Hagedorn and R. Schulz, *J. Anal. Toxicol.*, 16 (1992) 194.

ELSEVIER

Journal of Chromatography A, 697 (1995) 397–405

JOURNAL OF CHROMATOGRAPHY A

Development of an isocratic high-performance liquid chromatographic method for monitoring of ciprofloxacin photodegradation

Kirsti Torniainen[a,*], Eila Mäki[b]

[a]*Turku University Hospital, Hospital Pharmacy, FIN-20520 Turku, Finland*

[b]*Department of Pharmacy, Pharmaceutical Chemistry Division, P.O. Box 15, University of Helsinki, FIN-00014 Helsinki, Finland*

Abstract

An isocratic reversed-phase ion-pair high-performance liquid chromatographic method was developed for monitoring the photodegradation of ciprofloxacin in aqueous solutions. Changes in the chromatographic behaviour of ciprofloxacin and its degradation products under the influence of organic modifiers, anionic and cationic ion-pair reagents and pH were investigated. Baseline separation was achieved with use of an eluent of acetonitrile–phosphoric acid (20 m*M*, pH 2.3) containing 2.5 m*M* 1-heptanesulphonic acid sodium salt. The method was applied to the quantification of ciprofloxacin in irradiated solutions. The calibration graphs were linear from 5 to 150 μg/ml ($r > 0.9999$). Within the same range, the accuracy was 99–102% of the expected values. The intra-assay repeatability of the peak areas and retention times was good (R.S.D. $\leq 0.9\%$). Likewise the intra-day reproducibility of the method was good: R.S.D. values ($n = 6$) were $\leq 2.3\%$ and 1.8% for the lowest and highest concentrations, respectively. The inter-day precision gave a mean R.S.D. of 2.4% for peak areas and R.S.D. of 3.3% for retention times during a working period of three months.

1. Introduction

Ciprofloxacin (1 - cyclopropyl - 6 - fluoro - 1,4-dihydro - 4 - oxo - 7 - (1 - piperazinyl) - 3 - quinolone carboxylic acid) (Fig. 1), a synthetic fluoroquinolone antibiotic with nalidixic acid as progenitor, has a broad spectrum Gram-negative and Gram-positive antibacterial activity [1]. Commercial dosage forms are tablets and infusion fluids containing ciprofloxacin as hydrochloride and lactate salt, respectively.

Ciprofloxacin is a relatively stable molecule, but storage protected from light is recommended [2,3]. A wavelength-dependent loss of antibiotic activity with maximal effect around 320 nm has been observed in irradiated ciprofloxacin solutions [4]. Very few studies have been made on the photochemical stability of fluoroquinolones,

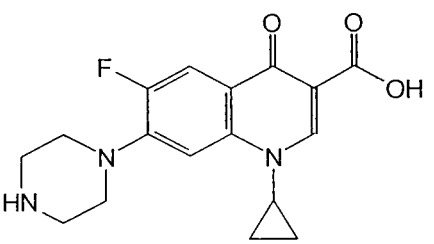

Fig. 1. Structure of ciprofloxacin.

* Corresponding author.

0021-9673/95/$09.50
SSDI 0021-9673(94)00831-0

and most of these have dealt with quinolone drugs in solid state. Ciprofloxacin tablet powder turned yellowish brown after exposure to sunlight for seven days. However, no degradation products were detected by UV, IR or thin-layer chromatography (TLC) [5]. Powdered enoxacin tablets illuminated with fluorescent light at room temperature changed colour, and degradation products were observed [6]. Two pathways have been suggested for the degradation of temafloxacin hydrochloride powder exposed to a high-intensity UV lamp: ring opening followed by cleavage of the piperazine ring, and oxidation of the secondary and tertiary amino groups [7]. Irradiation of ciprofloxacin solutions, with a high-pressure mercury lamp caused degradation of the parent compound, with the product formation depending on the pH of the solutions [8]. In a recent study on the photodegradation of quinolones including ciprofloxacin in UVA-irradiated solutions, Tiefenbacher et al. [9] detected several degradation products by HPLC.

The aim of our study was to develop an isocratic reversed-phase high-performance liquid chromatographic (RP-HPLC) method allowing adequate separation of the degradation products from each other and from ciprofloxacin, and accurate quantification of the parent compound in the presence of its photodegradation products.

2. Experimental

2.1. Chemicals

The identity and purity of ciprofloxacin hydrochloride (Bayer, Leverkusen, Germany) were verified by TLC, by measuring the melting point (Electrothermal digital melting point apparatus, Southend, UK) and by UV and IR spectrometry (Philips PU 8740 UV–Vis spectrometer and Unicam SP3-200 IR spectrometer, both from Pye Unicam, Cambridge, UK).

All chemicals and solvents were of analytical or HPLC grade. Disodium hydrogenphosphate dodecahydrate ($Na_2HPO_4 \cdot 12H_2O$), methanol (MeOH), orthophosphoric acid (H_3PO_4) and acetic acid (CH_3COOH) were purchased from E. Merck (Darmstadt, Germany). Acetonitrile (ACN) was obtained from J.T. Baker (Deventer, Netherlands), tetrahydrofuran (THF) from Rathburn (Walkerburn, UK) and triethylamine (TEA) from Riedel-de Haen (Seelze, Germany). 1-Heptanesulphonic acid sodium salt (Na-HSA) and tetrabutylammonium phosphate (TBAP) were from Sigma (St. Louis, MO, USA). Water was processed with Finn-Aqua H75 Santasalo-Sohlberg (Espoo, Finland).

2.2. Irradiation experiments

Solutions were irradiated with two different high-pressure mercury lamps, TQ 150 and TQ 718, both equipped with a quartz glass cooling mantle (Hanau, Germany). For qualitative experiments, a 1 mg/ml ciprofloxacin solution as hydrochloride salt was prepared in ethanol–0.1 *M* hydrochloric acid (1:1). Aliquots of 2 ml in 10-ml clear glass vials were irradiated for 2 h at a distance of 2 cm from the lamp TQ 150 ($\lambda > 300$ nm).

For quantitative purposes, ciprofloxacin (1 mg/ml) hydrochloride solutions were prepared in 0.001, 0.01 and 0.1 *M* hydrochloric acid and in phosphate buffer pH 3.1. Aliquots of 3 ml were irradiated at ambient temperature in 1 cm I.D. glass cuvettes at a distance of 10 cm from the lamp (TQ 718 at 500 W). A Corning CS-7-54 filter was used to cut off wavelengths longer than 400 nm. During the irradiation the solutions were magnetically stirred (Thermolyne Nuova II stirrer, Dubuque, IA, USA). The lamp was switched off when the samples were taken and restarted after 5 min. At appropriate time intervals, 0.5-ml aliquots of the test solutions were diluted with water to give a concentration of 0.1 mg/ml. Before HPLC runs the samples were filtered through Acrodisc LC 25, Ø 0.22-μm (Gelman, Ann Arbor, MI, USA). The follow up time for the photodegradation was 4 h and all experiments were made in triplicate. A reference sample of ciprofloxacin (1 mg/ml) with the appropriate solvent was prepared for each determination. All the samples were stored in dark after irradiation and after preparation for HPLC runs.

2.3. HPLC systems

The following apparatus from Waters (Milford, MA, USA) was used for the method development: a Model 501 solvent-delivery pump coupled to a 20-μl Rheodyne 7125 manual injector, a Model 484 variable-wavelength UV detector and a Model 741 data module printer. Chromatographic separations were performed at room temperature using a stainless-steel Nova-Pak C_{18} column (4 μm, 15 × 0.39 cm I.D.). The mobile phases (Table 1.) were vacuum filtered with a Waters filtering kit. Helium served for degassing before pumping of the mobile phase at 1.5 ml/min, and the stabilization period after the eluent was changed was 30 min. Detection was at 278 nm. The hold-up time (t_0) for the column was determined with sodium nitrate.

Other Waters equipment was used for the peak purity control: two 501 pumps coupled to an automated gradient controller with the same kind of injector as noted above, a Model 991 diode-array detector with NEC PowerMate 386/25 computer and photodiode array (PDA) software combined with a 5200 printer/plotter. The UV spectra were recorded in the range 210–350 nm. The column was the same as for the first apparatus. The mobile phase for the runs was ACN–phosphoric acid (20 m*M*, pH 2.3) (15:85, v/v) + 2.5 m*M* Na-HSA used at a flow-rate of 1.5 ml/min.

Duplicate injections were used throughout the study.

3. Results and discussion

3.1. Development of the HPLC method

Antimicrobial fluoroquinolones are ampholytic compounds. The pK_a value of the carboxylic group of ciprofloxacin is 6.09 and that of the nitrogen on the piperazinyl ring 8.74 [10]. Near neutral pH, ciprofloxacin is in zwitterionic form and its solubility is at minimum level. The majority of published HPLC applications for ciprofloxacin deal with its separation from other fluoroquinolones [11–13] or its metabolites in body fluids and tissues [14–16]. An HPLC method based on gradient elution with THF–phosphoric acid has been proposed for quantitative determination of ciprofloxacin in irradiated solutions [17]. Gradient elution requires special equipment however, and the total time of analysis may be long due to the need to re-equilibrate the column. With the purpose of developing a simple isocratic method for monitoring of ciprofloxacin photodegradation, we investigated the effect of organic modifiers, ion-pairing agents and pH of the aqueous phase on the retention factor (k) and the peak resolution (R_s).

Effect of organic modifiers

In qualitatively irradiated ciprofloxacin solutions two major degradation products were formed and several minor ones. Method development was started with mixtures of ACN and phosphoric acid (Table 1, eluent 1), which

Table 1
Mobile phases used in the development of an LC method for photodegradation studies on ciprofloxacin

No.	Components	Organic modifier (%, v/v)
1	ACN–H_3PO_4 (20 m*M*, pH 2.3)	10–50
2	MeOH–H_3PO_4 (20 m*M*, pH 2.3)	22–30
3	THF-H_3PO_4 (20 m*M*, pH 2.3)	4–12
4	ACN–H_3PO_4 (20 m*M*, pH 2.3) + Na-HSA (1.0–4.0 m*M*)	15
5	ACN–H_3PO_4 (20 m*M*, pH 2.3) + Na-HSA (2.5 m*M*) + TBAP (0.05–0.25 m*M*)	15
6	THF–H_3PO_4 (20 m*M*, pH 2.3) + Na-HSA (0.125–2.0 m*M*)	6
7	ACN–Na_2HPO_4 (20 m*M*, pH 2.3–7.0, adjusted with H_3PO_4)	15
8	ACN–Na_2HPO_4 (20 m*M*, pH 6.0) + TBAP (0.5–3.0 m*M*)	15

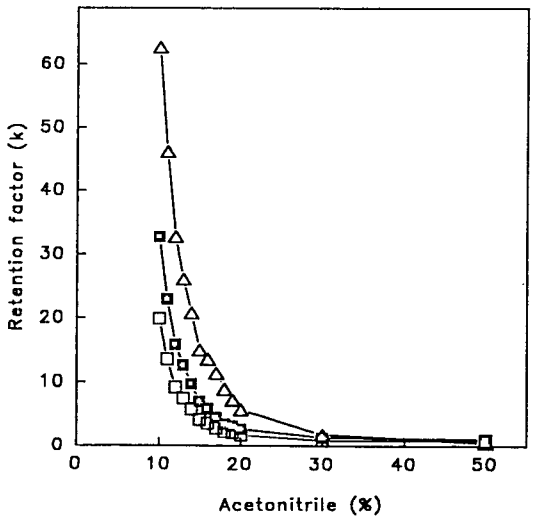

Fig. 2. Effect of the proportion of acetonitrile in the mobile phase (20 m*M* phosphoric acid, pH 2.3) on the retention factor of ciprofloxacin (■), compound I (□) and compound II (△). LC conditions: column, Nova-Pak C_{18} (4 μm, 15 × 0.39 cm I.D.); flow-rate, 1.5 ml/min; detection, UV at 278 nm.

are typical components in HPLC of fluoroquinolones [12–16]. Fig. 2 shows the retention factor of the parent drug and the two major compounds, tentatively named compounds I and II, as a function of the percentage of ACN. When the content of organic modifier was greater than 20%, the compounds eluted partly together with retention time < 4.5 min. With less than 12% ACN, the analysis time for compound II was > 45 min. Best separation was achieved with ACN and 20 m*M* phosphoric acid (pH 2.3) (15:85, v/v), the retention factors being 4.24, 6.98 and 14.99 for compound I, ciprofloxacin and compound II, respectively. A problem arose in the separation of the medium-sized degradation product Ia, which at all ACN concentrations eluted close to compound I (maximum $R_s = 1.0$) without baseline separation, partly due to the peak tailing. Addition of TEA improved the shape of the first peaks, but the resolution between compounds I and Ia then became worse. Amine modifier had no effect on compound II. Addition of acetic acid, which should reduce the interaction of acidic compounds with the silica surface, had similar effects as TEA on the elution of ciprofloxacin and compounds I and Ia. The retention of compound II was strongly reduced, however, suggesting it to have predominantly an acidic character.

MeOH and THF were tested as organic modifiers in place of ACN (Table 1, eluents 2 and 3). Solvent strength equivalent to 15% ACN was approximated by using the nomograph described by Snyder et al. [18]. MeOH gave the worst resolutions. The retention times were increased, but compounds I and Ia were virtually unseparated and eluted partly together with the parent compound in the MeOH concentration range 22–30% (v/v). THF suppressed the peak tailing and strongly decreased the retention of the first eluting peaks. Compounds I and Ia eluted in reversed order relative to the order in ACN and MeOH, but the resolution remained poor.

Effect of ion-pair reagents

Since ciprofloxacin and presumably also some of its degradation products are amphoteric, we studied the effect of both anionic and cationic ion-pair reagents on the retention. Addition of Na-HSA (Table 1, eluent 4) strongly increased the retention of ciprofloxacin and compounds I and Ia, indicating an ion-pair formation (Fig. 3). The increase was most pronounced for ciprofloxacin, which was now the last eluting compound. Na-HSA had no effect on the retention of compound II. The chromatographic behaviour of compound II suggested that it had lost the basic character of the parent drug and the ability for ion-pair formation with an anionic ion-pair reagent. A baseline separation ($R_s = 1.4$) for the poorly resolved peaks of I and Ia was obtained with ACN–20 m*M* phosphoric acid (pH 2.3) (15:85, v/v) containing 2.5 m*M* Na-HSA (Fig. 4). A cationic ion-pair reagent TBAP (Table 1, eluent 5) added to this eluent exerted a similar deteriorating effect as TEA on the retention and resolution of ciprofloxacin and compounds I and Ia. The retention of compound II was not affected.

In a mobile phase containing THF (Table 1, eluent 6), the addition of Na-HSA had a similar effect as in eluents containing ACN. The re-

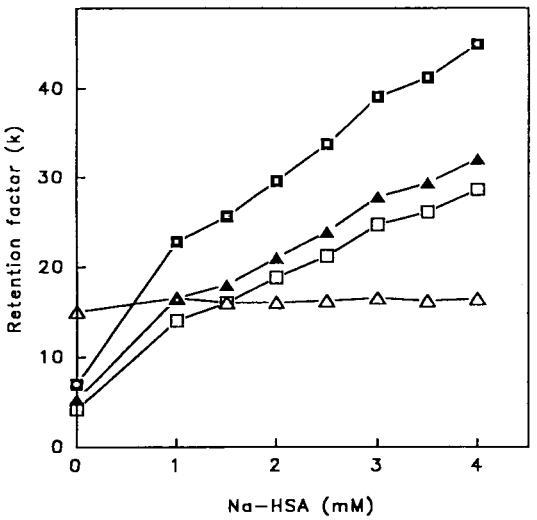

Fig. 3. Effect of the concentration of 1-heptanesulphonic acid sodium salt on the retention factor of ciprofloxacin (■), compound I (□), compound Ia (▲) and compound II (△). LC conditions: mobile phase, acetonitrile–phosphoric acid (20 m*M*, pH 2.3) (15:85, v/v). Other conditions as in Fig. 2.

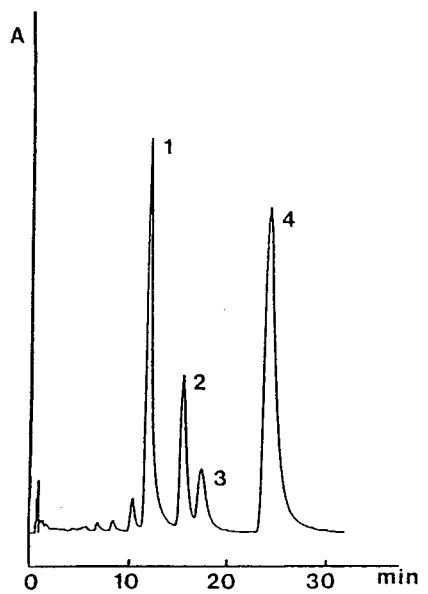

Fig. 4. Chromatogram of a ciprofloxacin hydrochloride solution (ethanol–0.1 *M* hydrochloric acid, 1:1) exposed to Hg lamp TQ 150 for 2 h. LC conditions: mobile phase, acetonitrile–phosphoric acid (20 m*M*, pH 2.3) (15:85, v/v) containing 2.5 m*M* 1-heptanesulphonic acid sodium salt. Other conditions as in Fig. 2. Peaks: 1 = compound II; 2 = compound I; 3 = compound Ia; 4 = ciprofloxacin.

tention of ciprofloxacin and compounds I and Ia increased, while the retention of compound II was unchanged. The peaks were sharp, but satisfactory separation of all compounds was not achieved within a reasonable time. For quantification of ciprofloxacin in irradiated solutions in which compound II was absent, a mixture of THF and 20 m*M* phosphoric acid (pH 2.3) (6:94, v/v) containing 0.25 m*M* Na-HSA provided a good assay method, the retention time of ciprofloxacin being 11.5 min.

Effect of pH

The effect of pH on the retention was tested using a constant proportion of ACN (15%) and phosphate buffer in the range pH 2.3–7 (Table 1, eluent 7). Fig. 5 shows the dependence of the *k* values on the pH of the aqueous phase. There was a marked decrease in the retention of compound II at pH higher than 5, in agreement with the assumption that compound II has only acidic properties. The ionization of the COOH group should become marked near pH 6 if the pK_a value of the degradation product is similar to that of the parent compound ($pK_a = 6.09$).

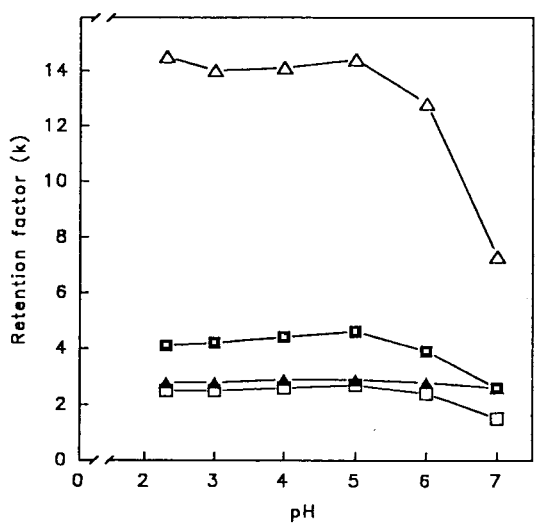

Fig. 5. Effect of the pH of the aqueous phase on the retention factor of ciprofloxacin (■), compound I (□), compound Ia (▲) and compound II (△). LC conditions: mobile phase, acetonitrile–20 m*M* disodium hydrogenphosphate (15:85, v/v). Other conditions as in Fig. 2.

The pH effect was smaller for ciprofloxacin, and also for degradation products I and Ia, which probably have retained their amphoteric character and therefore are in ionized form over a wide pH range. With all mobile phases containing phosphate buffer, the peaks tended to broaden, which further reduced the resolution between amphoteric compounds. Addition of TBAP to the eluent at pH 6 (Table 1, eluent 8), where the carboxyl groups are approximately half ionized, did not improve the separation. A slight increase was observed in the retention of compound II, and a decrease in the retention of the other compounds. Apparently, the TBAP concentrations were too low for a true ion-pair formation.

3.2. Validation of the method

For quantitative analysis of ciprofloxacin, the linearity was tested using two different eluents: ACN–20 m*M* phosphoric acid (pH 2.3) (15:85, v/v) with 2.5 m*M* Na-HSA (eluent A) and THF–20 m*M* phosphoric acid (pH 2.3) (6:94, v/v) with 0.25 m*M* Na-HSA (eluent B). The calibration graphs were constructed by plotting peak areas versus ciprofloxacin concentration, and the linearities were verified on seven (eluent A) and three (eluent B) separate days. The data collected in Table 2 show excellent linearity over the concentration range (5–150 μg/ml) studied.

The equipment with diode-array detector was used to perform the UV spectral analyses and to test the peak purity of ciprofloxacin and its degradation products (Fig. 6). The similarities in spectra of the parent compound and the major degradation products indicated the presence of an unchanged chromophoric system in all compounds. The maximum absorbance of compound II was slightly shifted to lower wavelengths (274 nm) relative to that of the parent compound (278 nm).

The repeatability of the chromatographic systems (eluents A and B) was determined by six replicate injections of solutions containing 5 and 150 μg/ml of ciprofloxacin and six injections of a ciprofloxacin solution that had been irradiated for 2 h (initial concentration 100 μg/ml). At minimum, six replicate samples were used to assess the precision of the whole procedure. Intra-day repeatability was very good, with a mean R.S.D. ≤ 0.9% for both the peak areas and the retention times. Mean R.S.D. values for inter-day determinations were slightly higher: ≤ 1.6% for peak areas and ≤ 3.3% for retention times. The intra-day precision of the whole method was good with R.S.D. values of ≤ 2.3% and 1.8% for concentrations of 5 and 150 μg/ml, respectively. Measurement of the day-to-day precision gave a mean R.S.D. of 2.4% for peak areas and R.S.D. of 3.3% for retention times during a period of three months ($n = 13$, 100 μg/ml, eluent A).

The accuracy of the method was determined with six separate ciprofloxacin solutions at three concentration levels (5, 100 and 150 μg/ml). Samples were diluted using two separate stock solutions (2 and 1.5 mg/ml). The accuracy expressed as percentages of the nominal concentration was 99–102% (R.S.D. ≤ 1.7%, $n = 6$) with eluent A and 102% (R.S.D. = 1.4%, $n = 6$) with eluent B.

Table 2
Calibration graphs for ciprofloxacin

Eluent	Slope (b), $\times 10^7$	Intercept (a), $\times 10^5$	r
ACN–H_3PO_4	9.5235	−1.1813	0.9999
(20 m*M*, pH 2.3)	9.5213	−1.2940	0.9999
+ 2.5 m*M*	9.4410	−1.0127	0.9999
Na-HSA	9.4134	−1.3175	0.9999
	9.4647	−1.3573	0.9999
	9.2068	−0.8482	0.9999
	9.2795	−0.3819	0.9999
THF–H_3PO_4	8.8449	0.4793	0.9999
(20 m*M*, pH 2.3)	8.7661	0.5061	0.9999
+ 0.25 m*M*	8.7595	0.5106	0.9999
Na-HSA	8.7823	0.4007	0.9999
	8.7801	0.4345	0.9999
	8.7727	0.3865	0.9999
	9.1240	−0.0554	0.9999

Ciprofloxacin concentration range 5–150 μg/ml. $y = bx + a$, where x = concentration of the injected substance (μg/ml) and y = peak area of ciprofloxacin. r = correlation coefficient.

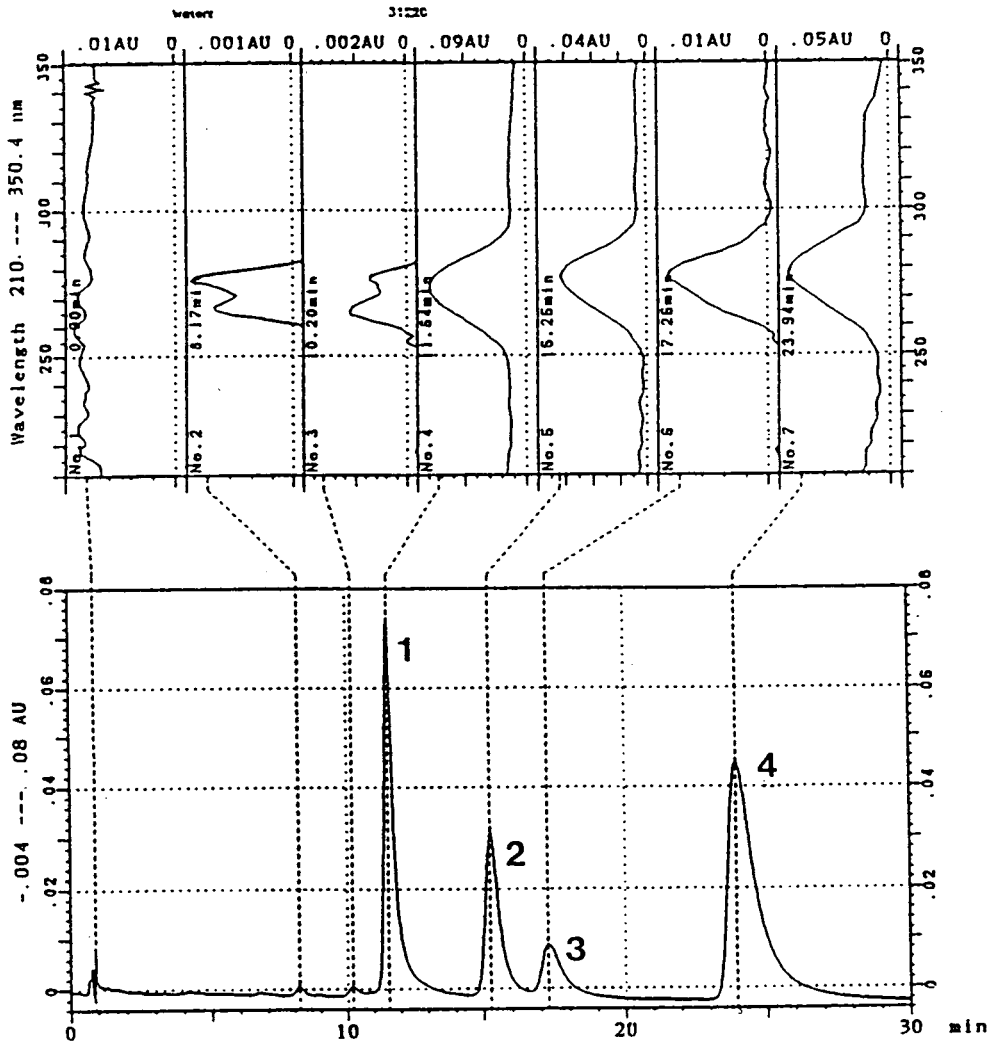

Fig. 6. Chromatogram of a ciprofloxacin hydrochloride solution (ethanol–0.1 *M* hydrochloric acid, 1:1) exposed to Hg lamp TQ 150 for 2 h and UV spectra of ciprofloxacin and its degradation products. LC conditions: photodiode array detector. Other conditions and peak identification as in Fig. 4.

3.3. Application to quantification

The applicability of the method (eluent A) for the quantification of ciprofloxacin was demonstrated by following the disappearance of the drug in solutions irradiated with a high-pressure mercury lamp (TQ 718). The degradation proceeded fastest in 0.1 *M* hydrochloric acid (pH 1.2). After exposure of the solutions for 4 h, about 40% of the initial ciprofloxacin content was left (Fig. 7). Compound II was clearly formed only in this solution. The reaction rate decreased with decreasing concentration of hydrochloric acid. During an irradiation period of 4 h, the ciprofloxacin content decreased about 20 and 10% from the initial value in 0.01 *M* (pH 2.2) and 0.001 *M* (pH 3.1) hydrochloric acid, respectively. It is noteworthy that the degradation proceeded at approximately the same rate in phosphate buffer of pH 3.1 as in 0.01 *M*

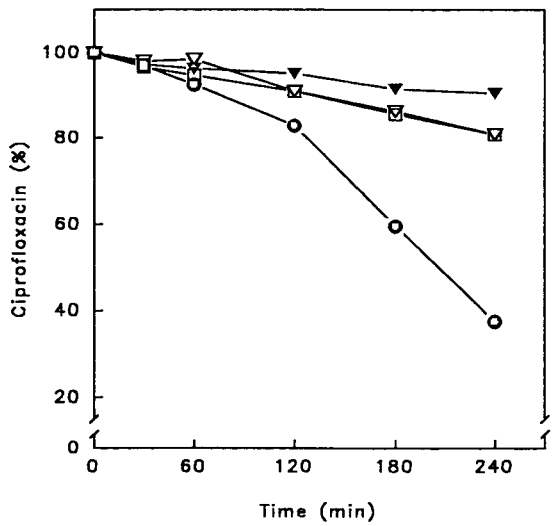

Fig. 7. Time course for the photodegradation of ciprofloxacin hydrochloride in 0.001 *M* hydrochloric acid (pH 3.1) (▼), 0.01 *M* hydrochloric acid (pH 2.2) (▽), 0.1 *M* hydrochloric acid (pH 1.2) (○) and phosphate buffer (pH 3.1) (□). Radiation source: Hg lamp TQ 718.

hydrochloric acid. The possible accelerating effect of buffer species on the reaction remains to be studied. The radiation source had apparently no influence on the product formation. The same photodegradation products were formed in solutions artificially irradiated and exposed to normal daylight. No degradation of ciprofloxacin was observed in solutions kept in the dark, indicating that the reaction was light-induced.

For comparison, the ciprofloxacin concentrations in a photodegraded solution prepared in 0.1 *M* hydrochloric acid were determined by high-performance TLC (HPTLC) with subsequent densitometric measurement [19]. The two methods correlated well. A straight line with a slope 1.05 ($r = 0.998$, $n = 10$) was obtained when ciprofloxacin concentrations (percentages from the initial content) obtained in HPLC were plotted against those obtained in HPTLC.

4. Conclusions

An isocratic HPLC method was developed for monitoring the photodegradation of ciprofloxacin in aqueous solutions. The procedure enables investigations with the kind of basic equipment available in hospital pharmacies, where stability studies of drugs are essential.

Ciprofloxacin and some of its photodegradation products showed very similar chromatographic behaviour. To obtain a baseline separation for the parent compound and its major degradation products in an isocratic run, some peak tailing and a relatively high retention factor of ciprofloxacin ($k = 33.8$) had to be accepted. The method was accurate and precise, and suitable for further studies on the photodegradation kinetics of ciprofloxacin.

Acknowledgement

K.T. is grateful for financial support received from the Finnish Culture Foundation, which made this work possible.

References

[1] S. Norris and G.L. Mandell, in V.T. Andriole (Editor), *The Quinolones*, Academic Press, London, 1988, p. 4.
[2] *United States Pharmacopeia/National Formulary (USP XXII/NFXVII)*, Suppl. 4, USP Convention, Rockville, MD, 1991, p. 2458.
[3] J.E.F. Reynolds (Editor), *Martindale: The Extra Pharmacopoeia*, Pharmaceutical Press, London, 30th ed., 1993, p. 145.
[4] G. Phillips, B.E. Johnson and J. Ferguson, *J. Antimicrob. Chemother.*, 26 (1990) 783.
[5] Y. Hiraki, T. Nomaguchi, T. Kawazoe, Y. Kumamoto, T. Shinohara, K. Kusaka and Y. Syouji, *J. Jpn. Soc. Hosp. Pharm.*, 25 (1989) 1375; *C.A.*, 112 (1989) 42442g.
[6] N. Mizushima, F. Ohuchi and T. Fujii, *Byoin Yakugaku*, 16 (1990) 198; *C.A.*, 114 (1990) 12063h.
[7] L. Elrod, C.L. Linton, B.P. Shelat and C.F. Wong, *J. Chromatogr.*, 519 (1990) 125.
[8] S. Tammilehto, H. Salomies and K. Torniainen, *Abstracts of the XII Helsinki University Course in Drug Research, 17–18 June 1993*, Finnish Pharmaceutical Society, Helsinki, 1993, p. 33.
[9] E.-M. Tiefenbacher, E. Haen, B. Pryzbilla and H. Kurz, *J. Pharm. Sci.*, 83 (1994) 463.
[10] D.L. Ross and C.M. Riley, *Int. J. Pharm.*, 63 (1990) 237.

[11] Zs. Budvari-Barany, Gy. Szasz, K. Takacs-Novak, I. Hermecz and A. Lore, *J. Liq. Chromatogr.*, 14 (1991) 3411.
[12] E. Brunt, J. Limberg and H. Derendorf, *J. Pharm. Biomed. Anal.*, 8 (1990) 67.
[13] K. Tyczkowska, K.M. Hedeen, D.P. Aucoin and A.L. Aronson, *J. Chromatogr.*, 493 (1989) 337.
[14] W.M. Awni, J. Clarkson and D.R.P. Guay, *J. Chromatogr.*, 419 (1987) 414.
[15] C.M. Myers and J.L. Blumer, *J. Chromatogr.*, 422 (1987) 153.
[16] F. Kees, W. Raasch and H. Grobecker, *Arzneim. Forsch.*, 42 (1992) 570.
[17] K. Linden and S. Tammilehto, *Abstracts of the XII Helsinki University Course in Drug Research, 17–18 June 1993*, Finnish Pharmaceutical Society, Helsinki, 1993, p. 34.
[18] L.R. Snyder, J.L. Glajch and J.J. Kirkland, *Practical HPLC Method Development*, Wiley, New York, 1988, p. 32.
[19] S. Tammilehto, H. Salomies and K. Torniainen, *J. Planar Chromatogr.*, in press.

ELSEVIER

Journal of Chromatography A, 697 (1995) 407–414

JOURNAL OF CHROMATOGRAPHY A

Micro high-performance liquid chromatography for the determination of nicarbazin in chicken tissues, eggs, poultry feed and litter

Rosa Draisci*, Luca Lucentini, Pierpaolo Boria, Claudio Lucarelli

Laboratorio Alimenti, Istituto Superiore di Sanità, Viale Regina Elena 299, 00161 Rome, Italy

Abstract

A micro high-performance liquid chromatography (HPLC) method has been developed for the determination of the anti-coccidial drug nicarbazin in chicken tissues, eggs, poultry feeds and litter. The 4,4′-dinitrocarbanilide (DNC) component of nicarbazin was extracted from foods, feeds and litter with acetonitrile. The extracts were purified by liquid–liquid partitioning, evaporated to dryness and taken up in methanol–acetonitrile–water (50:30:20, v/v). Micro HPLC of the 4,4′-dinitrocarbanilide (DNC) portion of nicarbazin is performed isocratically using a small bore column (1 mm I.D.) packed with reversed-phase and a UV detector set at 340 nm.

The average recoveries of nicarbazin added to muscle, liver and egg were 92.8, 84.3 and 85.2%, respectively, 95.9% in poultry feed and 76.8–95.9% in different litters. The limit of detection was 25 pg, based on a detector signal-to-noise ratio of 3. These results were achieved with a simplified step extraction without the solid-phase extraction used by various researchers. This method offers a sensitive, selective, rapid, and less expensive alternative to conventional HPLC for such evaluations.

1. Introduction

In recent years increasing attention has been given to the use of micro HPLC in a variety of food analysis applications [1–5]. This interest is due to several advantages that micro HPLC has compared to conventional HPLC [6–8]. Of these, the most important are low consumption of the mobile and stationary phases, an increase in mass sensitivity, compatibility with small samples and easy coupling to mass spectrometers and secondary chromatographic systems.

Conventional liquid chromatographic analysis of the anti-coccidial drug nicarbazin in poultry and eggs has been investigated by many researchers. Nicarbazin, an equimolar complex of 4,4′-dinitrocarbanilide (DNC) and 2-hydroxy-4,6-dimethylpyrimidine (HDP), is used as a feed additive at a maximum level of 125 mg/kg for the prevention of coccidiosis in poultry [9]. Italian and European law demands a 9-day suspension of nicarbazin treatment prior of slaughter in order to reach a detectable residual level of zero in chicken tissues.

The contamination and persistence of nicarbazin in eggs [10] and in chicken liver [11] has been studied and it has been found that chickens excrete the DNC component more slowly than the HDP component [12]. For this reason most analyses for residues in tissue have focused on

* Corresponding author.

0021-9673/95/$09.50
SSDI 0021-9673(94)00960-0

the DNC component. However, it has also been shown that litter is the main source of DNC contamination for broilers of slaughtering age [13]. Hence, it is of great importance to determine the DNC component in litter.

Almost all the procedures developed to date utilise conventional HPLC with either UV detection in chicken tissues [14–17] and eggs [18,19], electrochemical detection in tissues [20] or thermospray mass spectrometry for confirmation analysis [17,21].

Owing to the advantages of micro HPLC, especially the reduced mobile-phase consumption and obvious economic advantages in routine analysis, we hypothesized and tested the possibility of employing micro HPLC for the separation and quantification of the DNC component of nicarbazin in chicken tissues, eggs and poultry feed. We also tested this method on litter.

2. Experimental

2.1. Reagents and standards

All the solvents were LC grade, unless otherwise stated. Acetonitrile, methanol, *n*-hexane and dichloromethane were obtained from Farmitalia Carlo Erba (Rodano, Italy). Acetic acid glacial, sodium acetate anhydrous, sodium chloride and sodium sulphate anhydrous (p.a. quality) were from Farmitalia Carlo Erba. N,N-dimethylformamide (DMF) was purchased from BDH (Poole, UK). Water was purified with a Milli-Q system (Millipore, Bedford, MA, USA). Standard nicarbazin, a complex of a 1:1 molar ratio of 4,4′-dinitrocarbanilide (DNC) and 2-hydroxy-4,6-dimethylpyrimidine (HDP), was purchased from Merck, Sharp and Dohme Research (Rahway, NJ, USA). The standard purity was 97.4%.

The standard stock solution (1000 μg/ml) in DMF was obtained by dissolving the nicarbazin standard by mixing on a magnetic stirrer with heating at 75°C. The solution is stable for at least 1 month at room temperature.

For the standard curve solutions a series of standard solutions of nicarbazin containing 0.05–20 μg/ml were prepared by dilution of 1000 μg/ml stock solution with methanol–acetonitrile–water (50:30:20, v/v).

Standard fortification solution of nicarbazin containing 20 μg/ml was prepared in the same way as the standard curve solutions.

2.2. Apparatus

Meat grinder/mincer (Farmitalia Carlo Erba, Rodano, Italy), rotary vacuum evaporator VV 2000 (Heidolph-Elektro, Kelheim, Germany), magnetic stirrer (PBI, Milan, Italy), centrifuge 4237 (ALC, Milan, Italy), homogenizer H04 (Büler, Tubingem, Weilheim), S and S filter paper, No. 588 (Sleicher and Schuell, Keene, NH, USA), and FEP-teflon centrifuge tubes (10 ml) (Nalgene, Rochester, NY, USA), were used.

2.3. Chromatographic equipment

An HPLC system with a Model 420 pump equipped with pump head S (flow range 10–2000 μl/min (Kontron, Munich, Germany) and a capillary detector Model 433 equipped with a capillary flow cell of 90 nl (22 mm optical pathlength) (Kontron) were used. The system was interfaced via a Multiport to a Data-450 personal computer (Kontron). Chromatographic software DS-450 (Kontron) was used for data acquisition and instrument control. Samples were injected using a Model 7520 micro sample injector (0.5 μl, Rheodyne, Cotati, CA, USA) and separated on a 300 mm × 1 mm I.D. Supelcosil LC-18 (5 μm particle size) small bore column (Supelco, Bellefonte, PA, USA).

Stainless-steel tubing (0.1 mm I.D. × 1/16 in. O.D.) was employed between the injector and the separation column (4 cm in length). The tubing between the separation column and flow cell of the detector was fused-silica capillary of 50 μm I.D.

2.4. Preparation of samples

The samples of muscle, liver, egg and poultry feed were obtained from a farm under study. The samples of litter were made up of either

straw or wood shavings, used for a period of 28 days in the coops of broilers fed with nicarbazin-free feed.

Before extraction, samples of liver, muscle, feed and litter were carefully minced in a meat grinder/mincer. Samples of whole egg without shell were homogenized by shaking.

2.5. Spiking of liver, muscle, egg, poultry feed and litter samples for recovery

Before recovery all the samples were tested in order to verify the absence of nicarbazin. To determine recovery, 0.1, 0.25, 0.5 and 1 ml of the standard nicarbazin fortification solution (20 μg/ml) were added to 25.0 g of blended tissues (liver, muscle), blended litter and shaken egg. This resulted in samples containing 0.08, 0.2, 0.4 and 0.8 μg/g of nicarbazin in tissue, egg and litter. For poultry feed 1, 2.5, 5 and 12.5 ml of standard nicarbazin fortification solution were added to 5.0 g of blended feed to obtain 4, 10, 20 and 50 μg/g of nicarbazin.

2.6. Extraction of liver, muscle, egg and litter

An amount of 25.0 g of homogenised sample was accurately weighed into a 150-ml glass homogenising cup. Samples were blended at low speed (2–3 min) with 50 ml of acetonitrile. The extract was centrifuged (1000 *g* for 10 min) and the supernatant transferred to a separatory funnel. The sediment in the centrifuge tube was re-extracted with 30 ml of acetonitrile. After centrifugation at 1000 *g* for 10 min, the supernatant was combined with the first extract in the funnel and shaken well. After decanting, the lower layer was discarded and the organic layer was saved in the funnel. To the extract in the funnel 80 ml of dichloromethane and 3 g of sodium chloride were added and shaken well. After decanting, the lower layer was discarded and the organic layer was saved in the funnel. To this 3 g of sodium sulphate anhydrous was added and shaken well. Finally, the extract was filtered through filter paper and transferred to a 250-ml round bottom flask and evaporated to dryness using a rotary vacuum evaporator with a temperature controlled bath (45–50°C).

2.7. Extraction of feed

An amount of 5.0 g of ground sample was accurately weighed into a 50-ml glass homogenising cup. Feed was homogenised at low speed (2–3 min) with 25 ml of acetonitrile. The extract was centrifuged (1000 *g* for 10 min) and the supernatant transferred to a 100-ml round bottom flask. The sediment in the centrifuge tube was re-extracted with 25 ml of acetonitrile. After centrifugation at 1000 *g* for 10 min, the supernatant was combined with the first extract in the funnel. Finally, the extract was filtered through filter paper and transferred to a 100-ml round bottom flask and evaporated to dryness using a rotary vacuum evaporator with a temperature controlled bath (45–50°C).

2.8. Purification of samples

After extraction as described above, the residue was quantitatively transferred from the round bottom flask to a 10-ml centrifuge tube with 2 ml of methanol–acetonitrile–water (50:30:20, v/v) and 1 ml of *n*-hexane. The flask was then rinsed four times with 1 ml portions of acetonitrile. The solution was then evaporated to dryness under nitrogen, using a water bath at 50°C. Finally, the residue in the centrifuged tube was redissolved with 2 ml of methanol–acetonitrile–water (50:30:20, v/v) and 0.5 ml of *n*-hexane. After centrifugation (10 min, 4000 rpm), methanol solution was injected into HPLC. The supernatant was generally the hexanic layer, but it depended on tissue type. For feed samples methanol solution was diluted with methanol–acetonitrile–water to yield peak responses within the range of the standard curve.

2.9. Chromatographic conditions

The mobile phase was acetonitrile–acetate buffer (0.1 *M*, pH 4.8) (70:30, v/v). A flow-rate of 30 μl/min was used and the DNC component

of nicarbazin was detected at 340 nm using a UV capillary detector, sensitivity 0.1 AUFS.

3. Results and discussion

3.1. Extraction and chromatographic separation

Various works that use conventional HPLC with extraction and purification by SPE, have shown the presence of interference in the determination of the DNC component in chicken tissues [20,21] and in eggs [18] deriving from the solvents and/or the solid-phase extraction (SPE) column.

In order to eliminate this type of interference, we cut out clean-up by SPE according to Cortesi et al. [22]. This simplified the extraction procedure and should also avoid losses in recovery [21]. However, we still found interference in the determination of the DNC component both in egg and muscle samples and in litter (straw and wood shavings). This was not eliminated when different mixtures of acetonitrile–water, methanol–water or acetonitrile–methanol–water were used as the mobile phase. To separate the DNC component from the interference found in the various matrixes, it was necessary to use a mixture of acetonitrile and acetate buffer as mobile phase (0.1 *M*, pH 4.8) (70:30, v/v). DNC was retained for 9.5 min in this way. The reproducibility of the retention time was less than 1% for 5 injections.

Representative chromatograms of blank control and fortified liver, muscle, eggs and litter (straw) are shown in Figs. 1 and 2. This micro

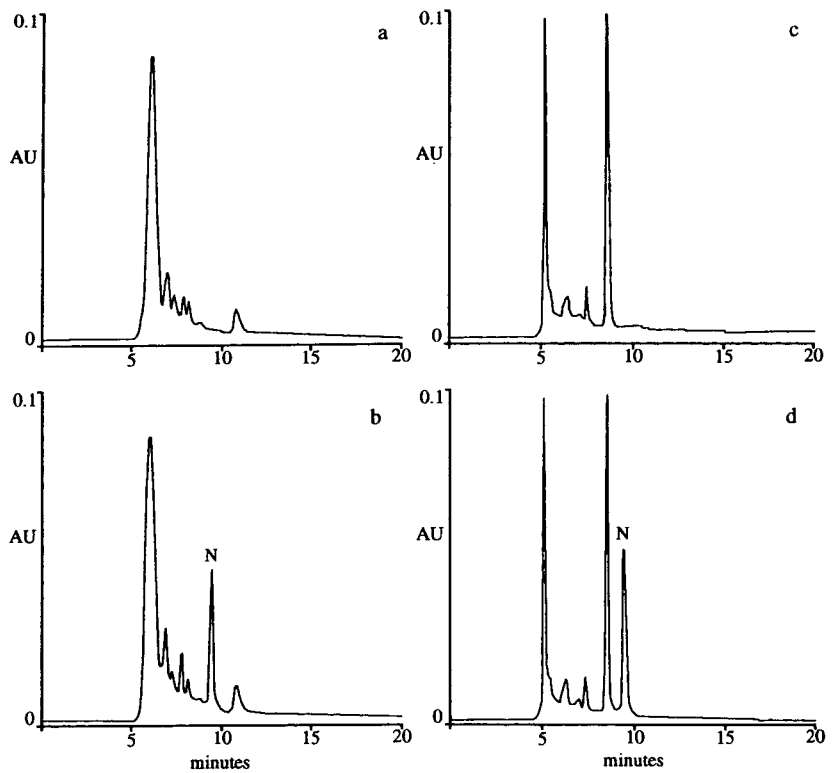

Fig. 1. Micro HPLC chromatograms of: (a) control chicken liver; (b) liver fortified with 0.4 μg of nicarbazin (N) per g sample; (c) control chicken muscle; (d) muscle fortified with 0.4 μg of nicarbazin (N) per g sample. Column, Supelcosil LC-18 (300 × 1 mm I.D., 5 μm). Isocratic elution with mobile phase, acetonitrile–sodium acetate buffer (0.1 *M*, pH = 4.8), (70:30, v/v). Flow-rate, 30 μl/min. Loop, 0.5 μl. UV detection, 340 nm.

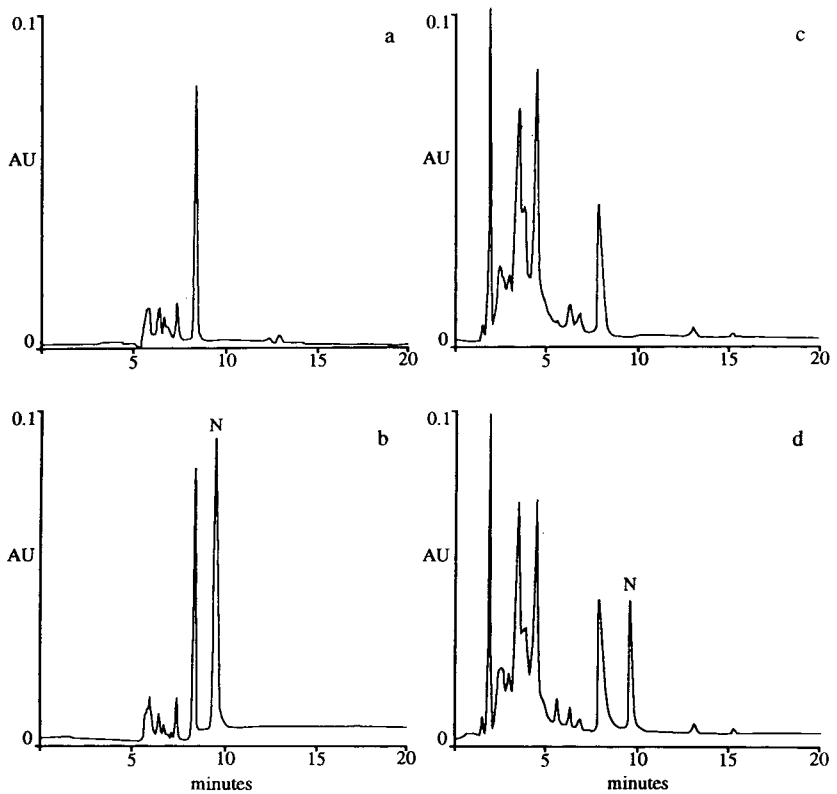

Fig. 2. Micro HPLC chromatograms of: (a) control egg sample; (b) egg fortified with 0.8 μg of nicarbazin (N) per g sample; (c) control chicken litter (straw); (d) litter fortified with 0.4 μg of nicarbazin (N) per g sample. Column, Supelcosil LC-18 (300 × 1 mm I.D., 5 μm). Isocratic elution with mobile phase, acetonitrile–sodium acetate buffer (0.1 *M*, pH = 4.8), (70:30, v/v). Flow-rate, 30 μl/min. Loop, 0.5 μl. UV detection, 340 nm.

HPLC method has also been evaluated for possible interference with certain compounds used in broiler poultry such as narasin.

A chromatogram of poultry feed containing 50 μg/g of nicarbazin with narasin is shown in Fig. 3. No interference was observed around the DNC retention time in blank control tissues (liver and muscle), egg, litter and in poultry feed samples.

3.2. Linearity range and limit of detection

Linearity of the photometric detector response to nicarbazin in standard solution was verified in the range 0.05–20 μg/ml (0.025–10 ng injected). A correlation coefficient of 0.998 was obtained. Nicarbazin concentration can be calculated by assaying DNC and assuming that nicarbazin is a 1:1 molar ratio of the DNC and HDP [15]. The lowest detectable amount of nicarbazin with micro HPLC was found to be 25 pg at a signal-to-noise ratio of 3:1. The limit of detection is about 5 times lower than that found by Vertommen et al. [18] with conventional HPLC. The limit of detection was satisfactory both for monitoring residue for health safety and for checking animal rearing facilities. In fact, the level of nicarbazin found in broiler livers 9 days after the suspension of treatment can often be much higher (ca. 200 ng/g, corresponding to ca. 1.05 ng injected) than the detection level in cases where the litter is not completely changed after treatment. The limit of detection obtained permits the checking of the litter effect, which is the principal cause of nicarbazin residue persistence in chicken tissues [13,23].

3.3. Recovery

The average recoveries and standard deviations for the fortified samples are indicated in Table 1. Recovery and precision data for this method were generated each day for 2 days from the analysis of duplicate control samples which were fortified at 0.08, 0.2, 0.4 and 0.8 μg/g nicarbazin for tissues, egg and litter and 4, 10, 20 and 50 μg/g nicarbazin for poultry feed.

Average recoveries were consistently above 90% for the muscle, feed and litter (wood shavings) with a mean recovery of 92.8% for muscle, 95.9% for poultry feed and 95.9% for litter. Recoveries were above 80% for liver and eggs; only in the litter (straw) sample was the average recovery less than 80% (76.8%).

The precision is also satisfactory at all levels with coefficients of variation less than 3.7% for liver, 3.3 for muscle, 4.5 for eggs and 6.3 for poultry feed. The increased variability (C.V. = 6.8–10.9%) for straw litter is probably due to difficulties in obtaining homogeneous samples.

3.4. Economic considerations

The economic advantages of using micro HPLC was evaluated from two points of view; purchase of a new system already configured for micro HPLC and conversion from conventional

Table 1
Recovery of nicarbazin from fortified chicken tissues, eggs, poultry feed and litter

Sample	Nicarbazin added (μg/g)	Recovery[a] (%)	Standard deviation	C.V. (%)
Liver	0.08	82.7	2.7	3.3
	0.2	86.0	3.2	3.7
	0.4	80.9	2.5	3.1
	0.8	87.5	2.6	3.0
Muscle	0.08	90.7	2.7	3.0
	0.2	93.3	3.1	3.3
	0.4	92.6	2.0	2.2
	0.8	94.7	2.2	2.3
Eggs	0.08	81.9	3.7	4.5
	0.2	86.4	3.9	4.5
	0.4	88.0	1.8	2.0
	0.8	84.5	2.3	2.7
Feed	4	90.7	5.7	6.3
	10	95.5	5.3	5.5
	20	99.8	5.2	5.2
	50	97.7	4.9	5.0
Litter (straw)				
	0.08	75.2	8.2	10.9
	0.2	78.0	5.3	6.8
	0.4	72.0	6.5	9.0
	0.8	81.9	6.9	8.4
Litter (wood shavings)				
	0.08	91.6	4.8	5.2
	0.2	95.9	4.1	4.3
	0.4	98.6	3.5	3.5
	0.8	97.5	3.8	3.9

[a] Each value is the average of 4 extractions.

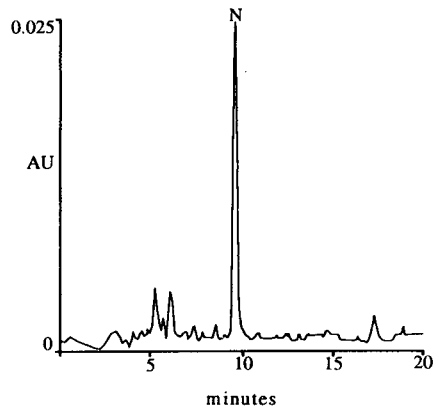

Fig. 3. Micro HPLC chromatogram of poultry feed containing 50 μg of nicarbazin (N) per g sample. Extract was diluted 1:50 before injection. Column, Supelcosil LC-18 (300 × 1 mm I.D., 5 μm). Isocratic elution with mobile phase, acetonitrile–sodium acetate buffer (0.1 *M*, pH = 4.8), (70:30, v/v). Flow-rate, 30 μl/min. Loop, 0.5 μl. UV detection, 340 nm.

HPLC. In either case, the pump and the detector would be the same. The difference in cost would only regard the detector cell, the injection valve, the column and the connecting tubes. These costs were then compared to saving in mobile phase consumption. In our case, we purchased a system already configured for micro HPLC. The additional cost over a conventional HPLC system was ca. US$ 800. On the other hand, if we had converted from a conventional HPLC system, the overall cost of modification would have been ca. US$ 3200. To calculate the saving in mobile phase consumption, we estimated likely conventional HPLC consumption and compared it to ours.

It has been demonstrated that for two columns with the same porosity and different diameters, the ratio between flow-rates required in order to produce the same mobile phase linear velocity is proportional to the square of the ratio of the internal diameters. In our case, the flow-rate of 30 μl/min with the small bore column corresponds to a flow-rate of ca. 0.6 ml/min with a conventional column. This means that with micro HPLC, the daily consumption (8 h) of mobile phase was ca. 14.4 ml compared to ca. 290 ml that would have been necessary with conventional HPLC. This consumption is about 20 times less than that of conventional HPLC. In our laboratory, the saving on mobile phase consumption, calculated on 4000 sample injections (average column lifetime) was ca. US$ 2170. An additional economic advantage is that the quantity of waste solvent is reduced.

In the light of these economic considerations, we calculated that sample injections in excess of 5870 make the cost of conversion viable and that only 1475 injections would cover the relative increase in the cost of a new system.

4. Conclusion

The procedures described represent an easy and relatively inexpensive alternative to conventional HPLC for the determination of nicarbazin in different food samples (liver, muscle, eggs) and also litter and poultry feed.

This method is particularly useful for monitoring involving a large number of samples and for routine checks where repetitive analysis is required. It is a valid procedure for checking animal rearing facilities and food, where residues could have an effect on health. In addition, considering the low flow-rates that make the direct coupling of LC to mass spectrometry possible, the use of small bore columns could be particularly advantageous in LC–MS confirmation analysis, recently tested [17,21] to confirm the presence of nicarbazin in chicken tissues.

References

[1] T. Takeuchi, M. Yamazaky and D. Ishii, *J. Chromatogr.*, 295 (1984) 339.
[2] T. Takeuchi, T. Niwa and D. Ishii, *J. Chromatogr.*, 405 (1987) 117.
[3] T. Takeuchi, K. Murase and D. Ishii, *J. Chromatogr.*, 445 (1988) 139.
[4] E. Brandsteterova', V. Chovancova', E. Matisova, J. Holeckova' and J. Tekel, *J. High. Resolut. Chromatogr.*, 14 (1991) 696.
[5] A.L. Howard, C. Braue and L.T. Taylor, *J. Chromatogr. Sci.*, 31(8) (1993) 323.

[6] R.P.W. Scott and P. Kucera, *J. Chromatogr.*, 125 (1976) 251.
[7] D. Ishii, K. Asai, K. Hibi, T. Jonokuchi and M. Nagaya, *J. Chromatogr.*, 144 (1977) 157.
[8] T. Tsuda and M. Novotny, *Anal. Chem.*, 50 (1978) 271.
[9] Y. Debuf (Editor), *The Veterinary Formulary*, The Pharmaceutical Press, London, 1988, p. 97.
[10] Y. Oishi and T. Oda, *Shokuhin Eiseigaku Zasshi*, 30 (1989) 542.
[11] A. Grassetelli, E. Pierdominici, A. Macrì and S. Castelli, *Ind. Aliment.*, 29 (1990) 237.
[12] C.C. Porter and J.J. GilFillan, *Poultry Sci.*, 34 (1955) 995.
[13] S. Castelli, G.F. Brambilla, A. Riberzani and A. Macrì, *Ind. Alim.*, 28 (1989) 947.
[14] Y. Hori, *Shokuhin Eiseigaku Zasshi*, 24 (1983) 447.
[15] T.D. Macy and A. Loh, *J. Assoc. Off. Anal. Chem.*, 6 (1984) 1115.
[16] R. Malisch, *Z. Lebensm. Unters. Forsch.*, 183 (1986) 253.
[17] J.L. Lewis, T.D. Macy and D.A. Garteiz, *J. Assoc. Off. Anal. Chem.*, 72 (1989) 577.
[18] M.H. Vertommen, A. Van der Laan and H.M. Veenendaal-Hesselman, *J. Chromatogr.*, 481 (1989) 452.
[19] J.A. Tarbin and G. Shearer, *J. Chromatogr.*, 613 (1993) 354.
[20] O.W. Parks, *J. Assoc. Off. Anal. Chem.*, 7 (1988) 778.
[21] Mary G. Leadbetter, J.E. Matusik, *J. Assoc. Off. Anal. Chem. Int.*, 76 (1993) 420.
[22] M.L. Cortesi, F. De Giovanni, G. Catellani and A. Lucisano, *Ind. Aliment.*, 27 (1988) 999.
[23] K.E. Webb and J.P. Fontenot, *J. Anim. Sci.*, 41 (1975) 1212.

ELSEVIER

Journal of Chromatography A, 697 (1995) 415–427

JOURNAL OF CHROMATOGRAPHY A

Chemometric classification of the solvent properties (selectivity) of commonly used gas chromatographic stationary phases

Salwa K. Poole, Colin F. Poole*

Department of Chemistry, Wayne State University, Detroit, MI 48202, USA

Abstract

Abraham's solvation parameter model was used to characterize the solvent properties of 33 stationary phases in terms of their capacity for specific intermolecular interactions at 121.4°C. The capacity of the phases for dispersion, orientation, induction, and hydrogen-bond base interactions, combined with solvent cohesion (ease of cavity formation) were important in defining their behavior. The capacity for π- and n-electron pair acceptor interactions was less important and none of the phases possessed a significant capacity for solvent hydrogen-bond acid interactions. Principal component analysis and hierarchical clustering techniques were used to classify the phases by their similarity for specific intermolecular interactions. These methods provide a visual means of quantitatively comparing the properties of the stationary phases and a mechanism to develop a short list of phases able to represent the range of properties available in the larger data set.

1. Introduction

For many years chromatographers have sought a method to characterize the solvation properties of stationary phases used in gas chromatography with the goal of providing a rational approach for selection of an optimum phase for a given separation and to predict retention of solutes on different phases. Many researchers have contributed to this problem in the past and we will not attempt to review the voluminous literature on the topic in this report; instead we direct the reader to authoritative reviews on the subject [1–4]. If a similar understanding of retention could be developed as currently exists for the kinetic properties of columns, then computer-aided optimization of separations would become a viable alternative to trial-and-error methods development.

Modern approaches to stationary phase characterization are based on the cavity model of solvation [5–8]. This model assumes that the transfer of a solute from the gas phase to solution in the stationary liquid phase involves three factors. Initially a cavity is formed in the stationary phase identical in volume to the solute. The solute is then transferred to the cavity with reorganization of the solvent molecules around the cavity and the set up of solute–solvent interactions. This process can be characterized by the individual free energy terms involved in the transfer process which can

* Corresponding author.

0021-9673/95/$09.50
SSDI 0021-9673(94)00469-P

reasonably be assumed to be additive. The disruption of solvent–solvent interactions to form a cavity is energetically unfavorable for the transfer of a solute from the gas phase to solution and must be less important than the free energy gained from the formation of solute–solvent interactions otherwise the solute will not be retained. The free energy changes associated with reorganization of the solvent molecules around the cavity are likely to be small compared to the changes involved in the other two steps and to a first approximation can be ignored.

The solute in the gas phase can reasonably be assumed to be behaving ideally and solute–solute and solute–gas interactions are essentially negligible. Transfer of the solute to solution in the liquid phase occurs with the creation of additional intermolecular interactions which depend on properties of both the solute and solvent. The solution can reasonably be assumed to be infinitely dilute for the separation conditions employed in analytical gas–liquid chromatography and, therefore, all interactions that are formed in solution are of the solute–solvent type. These interactions can be characterized as dispersion, orientation, induction and complexation. Dispersion interactions are non-selective and are the binding forces that hold all assemblies of non-polar molecules together (they occur, of course, in assemblies of polar molecules were they are augmented by polar interactions). Molecules with a permanent dipole moment can interact with each other by the cooperative alignment of their dipoles (orientation interactions) and by their capacity to induce a temporary complementary dipole in a polarizable molecule (induction interactions). Complexation interactions are selective interactions involving the sharing of electron density or a hydrogen atom between molecules (hydrogen bonding and charge transfer, for example). In gas–liquid chromatography retention will depend on the cohesive properties of the solvent as represented by the energy required to form a cavity in the solvent, the formation of additional dispersion interactions of a solute–solvent type, and on selective solute–solvent polar interactions which depend on the complementary character of the polar properties of the solute and solvent.

The above conceptual picture of retention in gas–liquid chromatography is intuitively sound but must be encoded in a mathematical form to establish the relative importance of the various contributing factors to solvation. As our knowledge exists today this is beyond the scope of computational chemistry. We must seek an empirical solution which combines experimentally accessible information with our overall goal of a quantitative model to express the relative contribution of cavity formation and solute–solvent interactions to the solution process. Two models have been proposed for this process. The solvation parameter model is discussed in this paper. In a companion paper [9] an alternative approach based on the separation of the free energy terms into cavity formation and non-polar and polar interactions with subsequent deconvolution into intermolecular interactions by mutivariate analysis is evaluated.

The master retention equation in the solvation parameter model developed by Abraham [6,7,10,11] can be written as follows:

$$\log K_L = c + rR_2 + s\pi_2^H + a\alpha_2^H + b\beta_2^H + l \log L^{16} \quad (1)$$

where K_L is the gas–liquid partition coefficient, R_2 the solute excess molar refraction [12], π_2^H the effective solute dipolarity/polarizability [13–16], α_2^H the effective solute hydrogen-bond acidity [15,16], β_2^H the effective solute hydrogen-bond basicity [17], and L^{16} the solute gas–liquid partition coefficient on *n*-hexadecane at 25°C [13–15]. The explanatory variables listed above are solvation parameters derived from equilibrium constants or calculated from gas chromatographic measurements and are free energy-related parameters characteristic of the monomeric solute. Values of the solvation parameters for more than 1000 compounds are currently available and in many cases unknown values can be estimated using simple combining rules [7,11]. The solvent properties r, s, a, b and l are unambiguously defined: the r constant refers to the ability of a solvent to interact with solute *n*-

or π-electron pairs; the s constant to the ability of the solvent to take part in dipole–dipole and dipole–induced dipole interactions; the a constant is a measure of the hydrogen-bond basicity of the solvent; the b constant is a measure of the hydrogen-bond acidity of the solvent; and the l constant incorporates contributions from solvent cavity formation and solute–solvent dispersion interactions, and more specifically in gas–liquid chromatography indicates how well the phase will separate members of a homologous series. For an uncharacterized phase the solvent properties r, s, a, b and l are determined from the experimentally derived gas–liquid partition coefficient for a minimum of 15 to 30 varied solutes with known explanatory variables using the statistical analysis technique of multiple linear regression analysis. Abraham and co-workers have used Eq. 1 to characterize the 5 stationary phases in the Laffort data set [12], the 77 stationary phases in the McReynolds data set [18], the 24 stationary phases in the Poole data set [19], to identify impurities in two poly(methylphenylsiloxane)s [20], to characterize a new stationary phase with hydrogen-bond acid properties [21], and to characterize surface interactions on carbonaceous adsorbents [22]. In an analogous fashion Poole and co-workers have used Eq. 1 to characterize the stationary phase properties of 46 liquid organic salts [23,24], to study the influence of temperature on the phase constants of 10 common stationary phases [25], and to estimate the breakthrough volume of a wide range of organic compounds in solid-phase extraction [26,27]. Non-chromatographic applications have included the characterization of chemically selective sensors, the solubility of gases and vapors in organic solvents, the effect of airborne chemicals on the upper respiratory tract irritation in mice, etc., and are reviewed elsewhere [7,17,28].

Carr and co-workers [29–34] have proposed an equation similar to Eq. 1 but different from it in that it uses an empirical polarizability correction factor δ_2 (used in solvatochromic models) in place of R_2 and a new set of explanatory variables derived from chromatographic measurements:

$$\log K_L = c + d\delta_2 + s\pi_2^{*c} + a\alpha_2^c + b\beta_2^c + l \log L^{16} \quad (2)$$

Since the explanatory variables are numerically different from those proposed by Abraham so are the characteristic phase constants derived from them. These differences, however, are generally small and both models yield the same qualitative conclusions [6,11,35]. It is not necessary to summarize the results using both equations for our current purpose and only Eq. 1 will be considered here.

2. Experimental

The name, abbreviation and composition of the stationary phases used in this study are summarized in Table 1. The gas–liquid partition coefficients at 121.4°C were taken from previous studies [23–25,36,37] and are corrected for interfacial adsorption. The experimental protocol for determining the partition coefficients is described in Ref. [38].

Principal component analysis and cluster analysis for data interpretation were performed using Pirouette V1.1 (Infometrix, Seattle, WA, USA) on a Epson Apex 200 computer (Epson America, Torrance, CA, USA). Multiple linear regression analysis was performed using the program SPSS/PC V3.1 (SPSS, Chicago, IL, USA) on an Epson Apex 200 computer. The explanatory variables used for multiple linear regression analysis were taken from the collection by Abraham and co-workers [11–16].

3. Results and discussion

Application of Abraham's solvation parameter model to the phases listed in Table 1 resulted in the characteristic phase constants summarized in Table 2. Initial evaluation reveals that the results are sensible. All coefficients are positive except for the c constant for all phases and the r constant for the fluorine-containing phases. The c constant contains, in part, the contribution from cavity formation, which is always unfavor-

able for solute transfer from the gas phase, so is expected to be negative. The r constant for fluorine-containing solvents is generally negative because of the method used to calculate R_2 and is also reasonable [11,18]. None of the stationary phases are significant hydrogen-bond acids ($b = 0$) at the measurement temperature. Small b constants were observed for the polyester phases EGAD and DEGS as well as for TCEP as shown below.

In each case the b constant is small but statistically significant. Based on the structure of these phases a significant contribution from hydrogen-bond acidity would not be anticipated. Polyester phases, however, are known to be thermally unstable yielding small amounts of the parent acid [1,39] and phases containing cyano groups are easily oxidized to the carboxylic acid [40] providing a possible explanation for the observed weak hydrogen-bond acidity while other phases in Table 1 containing more obvious hydrogen-bond acid functional groups are inert. Force fitting the regression equation to the experimental data with $b = 0$, shown below the best fit to the data summarized above, provides a good fit, with only minor changes (except for b) to the characteristic phase constants. It seems reasonable to conclude that the hydrogen-bond acidity of EGAD, DEGS and TCEP results from a low concentration of acidic impurities generated during use rather than a characteristic property of the stationary phase material itself. Since among common phases used in gas–liquid chromatography none can be identified as possessing significant hydrogen-bond acidity, this suggests an obvious target for the development of new phases with potential to have a significant impact on the practice of gas chromatography, especially since amongst functionalized molecules there are many hydrogen-bond bases. Hydroxyl groups are good hydrogen-bond acids, but as shown by the data in Table 2, hydroxyl groups on alkyl chains (THPED, QTAPSO and QBES) prefer to form solvent–solvent hydrogen-bond

	c	r	s	a	b	l
EGAD	−0.688	0.132	1.394	1.820	0.206	0.429
	(0.035)	(0.024)	(0.036)	(0.063)	(0.048)	(0.005)
	$R = 0.999$	S.E. = 0.026	$F = 1935$	$n = 24$		
	−0.657	0.087	1.471	1.974		0.431
	(0.047)	(0.030)	(0.043)	(0.071)		(0.007)
	$R = 0.998$	S.E. = 0.035	$F = 1291$	$n = 24$		
DEGS	−0.650	0.230	1.572	2.105	0.171	0.407
	(0.004)	(0.003)	(0.004)	(0.007)	(0.005)	(0.001)
	$R = 1.000$	S.E. = 0.004	$F = 119240$	$n = 34$		
	−0.669	0.197	1.668	2.246		0.411
	(0.031)	(0.020)	(0.019)	(0.041)		(0.005)
	$R = 0.999$	S.E. = 0.027	$F = 3045$	$n = 34$		
TCEP	−0.744	0.116	2.088	2.095	0.261	0.370
	(0.029)	(0.017)	(0.025)	(0.038)	(0.031)	(0.005)
	$R = 0.999$	S.E. = 0.025	$F = 4177$	$n = 39$		
	−0.697	0.050	2.215	2.267		0.365
	(0.049)	(0.026)	(0.034)	(0.055)		(0.008)
	$R = 0.998$	S.E. = 0.042	$F = 1742$	$n = 39$		

Table 1
Identification and abbreviations for stationary phases

Number	Abbreviation	Name
1	SQ	Squalane
2	SE-30	Poly(dimethylsiloxane)
3	OV-105	Poly(cyanopropylmethyldimethylsiloxane)
4	OV-3	Poly(dimethylmethylphenylsiloxane) (10 mol% phenyl groups)
5	OV-7	Poly(dimethylmethylphenylsiloxane) (20 mol% phenyl groups)
6	OV-11	Poly(dimethylmethylphenylsiloxane) (35 mol% phenyl groups)
7	OV-17	Poly(methylphenylsiloxane)
8	OV-22	Poly(methylphenyldiphenylsiloxane) (65 mol% phenyl groups)
9	OV-25	Poly(methylphenyldiphenylsiloxane) (75 mol% phenyl groups)
10	OV-330	Poly(dimethylsiloxane)–Carbowax (CW) copolymer
11	OV-225	Poly(cyanopropylmethylphenylmethylsiloxane)
12	OV-275	Poly(dicyanoallylsiloxane)
13	QF-1	Poly(trifluoropropylmethylsiloxane)
14	DDP	Didecylphthalate
15	PPE-5	1,3-bis(3-phenoxyphenoxy)benzene
16	CW 20M	Poly(ethylene glycol)
17	U50HB	Poly(ethylene glycol) (Ucon 50 HB 660)
18	THPED	N,N,N′,N′-Tetrakis(2-hydroxypropyl)ethylenediamine
19	EGAD	Poly(ethylene glycol adipate)
20	DEGS	Poly(diethylene glycol succinate)
21	TCEP	1,2,3-Tris(2-cyanoethoxypropane)
22	QMS	Tetra-*n*-butylammonium methanesulfonate
23	QFMS	Tetra-*n*-butylammonium trifluoromethanesulfonate
24	QBS	Tetra-*n*-butylammonium benzenesulfonate
25	QFBS	Tetra-*n*-butylammonium perfluorobenzenesulfonate
26	QTS	Tetra-*n*-butylammonium 4-toluenesulfonate
27	QACES	Tetra-*n*-butylammonium 2-(2-acetamido)aminoethanesulfonate
28	QTAPSO	Tetra-*n*-butylammonium 3-tris(hydroxymethyl)methylamino-2-hydroxy-1-propanesulfonate
29	QBES	Tetra-*n*-butylammonium N,N-(bis-2-hydroxyethyl)-2-aminoethanesulfonate
30	QPIC	Tetra-*n*-butylammonium picrate
31	QETS	Tetraethylammonium 4-toluenesulfonate
32	QPN	Tetra-*n*-butylphosphonium nitrate
33	QPC	Tetra-*n*-butylphosphonium chloride

complexes to the exclusion of solvent–hydrogen-bond acid solute–hydrogen-bond base interactions [24,36]. Abraham et al. [21] have shown that the phenol-containing phase, bis(3-allyl-4-hydroxyphenyl)sulfone has significant hydrogen-bond acidity. Likewise, Li et al. [31] have demonstrated significant hydrogen-bond acidity for the fluorinated alcohol phase, 4-dodecyl-α,α-bis(trifluoromethyl)benzyl alcohol. Fluorinated alcohols have very low hydrogen-bond basicity which makes them particularly attractive as a structural entity to pursue in the preparation of new phases with hydrogen-bond acid properties [11,21,28]. The magnitude of the characteristic phase constants in Table 2 is a measure of the capacity of a stationary phase for specific intermolecular interactions described by that constant. The various phase constants are only loosely scaled to each other so that changes in magnitude in any column can be read directly but changes in magnitude along rows must be interpreted cautiously. The magnitude of individual intermolecular interactions to the retention of specific compounds are represented by the solute–solvent product terms, some typical examples of which are summarized in Table 3.

Table 2
Abraham's characteristic phase constants at 121.4°C

Stationary phase	c	r	s	a	l	Statistics for fit to Eq. 1[a]	
						S.E.	R
SQ	−0.222	0.129	0.011	0.000	0.583	0.017	1.000
SE-30	−0.194	0.024	0.190	0.125	0.498	0.022	0.999
OV-105	−0.203	0.000	0.364	0.407	0.496	0.024	0.999
OV-3	−0.181	0.033	0.328	0.152	0.503	0.021	0.999
OV-7	−0.231	0.056	0.433	0.165	0.510	0.025	0.999
OV-11	−0.303	0.097	0.544	0.174	0.516	0.029	0.999
OV-17	−0.372	0.071	0.653	0.263	0.518	0.025	0.999
OV-22	−0.328	0.201	0.664	0.190	0.482	0.034	0.998
OV-25	−0.273	0.277	0.644	0.182	0.472	0.042	0.997
OV-330	−0.430	0.104	1.056	1.419	0.481	0.051	0.995
OV-225	−0.541	0.000	1.226	1.065	0.466	0.025	0.999
OV-275	−0.909	0.206	2.080	1.986	0.294	0.036	0.998
QF-1	−0.269	−0.449	1.157	0.187	0.419	0.054	0.996
DDP	−0.328	0.000	0.748	0.765	0.560	0.025	0.999
PPE-5	−0.395	0.230	0.829	0.337	0.527	0.044	0.997
CW 20M	−0.560	0.317	1.256	1.883	0.447	0.032	0.999
U50HB	−0.184	0.372	0.632	1.277	0.499	0.013	1.000
THPED	−0.445	0.000	1.128	2.069	0.477	0.056	0.997
EGAD	−0.688	0.132	1.394	1.820	0.429		
DEGS	−0.650	0.230	1.572	2.105	0.407		
TCEP	−0.744	0.116	2.088	2.095	0.370		
QMS	−0.612	0.334	1.454	3.762	0.435	0.071	0.997
QFMS	−0.552	0.000	1.579	2.135	0.416	0.055	0.998
QBS	−0.924	0.121	1.756	3.507	0.464	0.050	0.996
QFBS	−0.723	−0.088	1.647	2.238	0.459	0.030	0.999
QTS	−0.686	0.156	1.582	3.295	0.459	0.033	0.998
QACES	−0.666	0.283	1.809	3.417	0.329	0.100	0.990
QTAPSO	−0.860	0.266	1.959	3.058	0.317	0.048	0.996
QBES	−0.805	0.253	1.760	3.368	0.382	0.046	0.997
QPIC	−0.542	0.100	1.557	1.424	0.445	0.061	0.994
QETS	−0.762	0.330	2.045	3.429	0.304	0.050	0.998
QPN	−0.758	0.183	1.829	3.538	0.421	0.051	0.996
QPC	−1.009	0.244	1.854	5.418	0.468	0.078	0.993

[a]S.E. = Standard error in the estimate; R = multiple correlation coefficient.

The product term rR_2 is relatively small on all phases, including for iodobenzene, which has the largest R_2 parameter value ($R_2 = 1.188$) of the solutes in the data set. Many phases posses some capacity for π- and n-electron pair interactions, but selectivity for this interaction is all but non-existent amongst the stationary phases in Table 1. Phases containing metal co-ordination centers may have significant capacity for these interactions compared to the phases studied here, but for our present purposes we need not consider the r phase constant further.It is clear from Table 3 that the product term l log L^{16} is always significant. The contribution of cavity formation and dispersion interactions to retention involves at least part of the c constant as well [19,21,25,36]. The $\sum(c + l \log L^{16})$ term is always favorable for transfer of a solute from the gas phase to the stationary phase indicating that the solute–solvent interactions formed by the transfer exceed the energy required to disrupt solvent–solvent interactions in preparing the

Table 3
Contribution of specific solute–stationary phase interactions to retention (log K_L)

Solute	Phase	c	rR_2	$s\pi_2^H$	$a\alpha_2^H$	$b\beta_2^H$	$l \log L^{16}$
Nonan-2-one	OV-17	−0.372	0.008	0.444			2.453
	QF-1	−0.269	−0.053	0.787			1.984
	U50HB	−0.184	0.044	0.430			2.363
	TCEP	−0.744	0.014	1.420		0.133	1.752
	QTS	−0.686	0.019	1.076			2.173
	QPC	−1.009	0.029	1.261			2.216
Nonan-1-ol	OV-17	−0.372	0.014	0.274	0.097		2.654
	QF-1	−0.269	−0.087	0.486	0.069		2.147
	U50HB	−0.184	0.072	0.265	0.472		2.557
	TCEP	−0.744	0.022	0.877	0.775	0.125	1.896
	QTS	−0.686	0.030	0.664	1.219		2.352
	QPC	−1.009	0.047	0.779	2.005		2.398
Iodobenzene	OV-17	−0.372	0.083	0.535			2.332
	QF-1	−0.269	−0.533	0.949			1.886
	U50HB	−0.184	0.442	0.518			2.557
	TCEP	−0.744	0.138	1.712		0.031	1.896
	QTS	−0.686	0.185	1.297			2.066
	QPC	−1.009	0.290	1.520			2.107
Benzonitrile	OV-17	−0.372	0.052	0.725			2.092
	QF-1	−0.269	−0.333	1.284			1.692
	U50HB	−0.184	0.276	0.702			2.015
	TCEP	−0.744	0.086	2.318		0.086	1.494
	QTS	−0.686	0.116	1.756			1.854
	QPC	−1.009	0.181	2.058			1.890
4-Cresol	OV-17	−0.372	0.058	0.568	0.150		2.234
	QF-1	−0.269	−0.369	1.007	0.107		1.807
	U50HB	−0.184	0.306	0.550	0.782		2.152
	TCEP	−0.744	0.095	1.817	1.194	0.081	1.595
	QTS	−0.686	0.128	1.376	1.878		1.979
	QPC	−1.009	0.201	1.613	3.088		2.018

cavity. This we theorize is because cavity formation occurs by displacement retaining some of the solvent–solvent interactions, particularly dispersion interactions, since these are not directional, and the new solute–solvent interactions are simply added to these. The polar solvent–solvent interactions should be the most important in determining the energy required to form a cavity in the solvent. Abraham et al. [19] have shown that the l phase constant is directly proportional to the partial molar Gibbs free energy of solution for a methylene group, $\Delta G(CH_2)$. This conclusion is confirmed by the results obtained in this study (Fig. 1 and Eq. 3).

$$\Delta G(CH_2) = -7.55 - 890\ (l) \quad r^2 = 0.96 \qquad (3)$$

Note, by definition that $\sum(c + l \log L^{16})$ for the n-alkanes is also correlated to $\Delta G(CH_2)$. There is a reasonable correlation between the s phase constant and the c phase constant (Fig. 2 and Eq. 4). Those phases furthest removed from the best straight line generally have extreme values of the phase constants ratio a/s.

$$s = 4.91 \cdot 10^{-4} - 2.29\ (c) \quad r^2 = 0.86 \qquad (4)$$

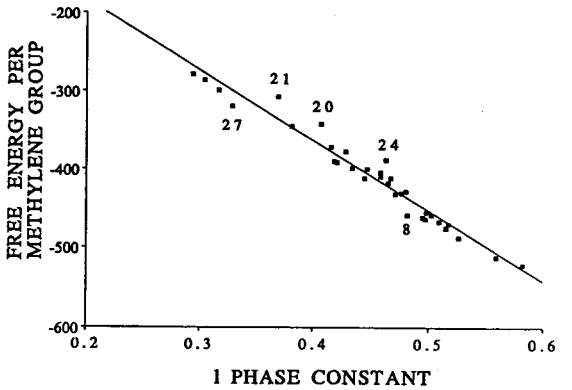

Fig. 1. Plot of the partial molar Gibbs free energy of solution for a methylene group (cal/mol; 1 cal = 4.184 J) against the *l* phase constant. Numbers refer to the phases identified in Table 1.

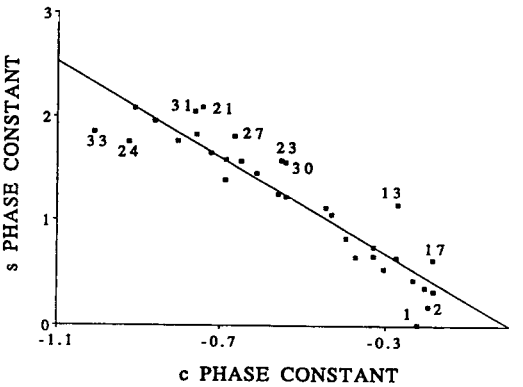

Fig. 2. Plot of the *s* phase constant against the *c* phase constant. Numbers refer to the phases identified in Table 1.

The magnitude of the *c* phase constant is largely determined by polar solvent–solvent interactions which must include other contributions (*a* phase constant in this case) besides those interactions of a dipole type. The general trend in the *c* and *s* phase constants, however, provides convincing evidence that the *c* phase constant is related to the energy required for cavity formation. Unfortunately, at the present time, we have no reliable method to dissect the product $\sum(c + l \log L^{16})$ into precisely defined contributions of cavity formation and dispersion interactions. From an interpretive point of view the *l* phase constant indicates the spacing between members of a homologous series and contains useful information for phase selection. Retention, however, is strongly dependent on the *c* phase constant as well, which is always in opposition to the *l* log L^{16} term, so that phases with similar *l* phase constants exhibit significantly different absolute retention of solutes (Table 4). This is particularly striking in the case of certain of the liquid organic salts which have unusually large *l* phase constants compared to phases of similar polarity but also have characteristically large *c* phase constants. For example, QPC and OV-225 have virtually identical *l* phase constants but very different *c* phase constants, such that log K_L (dodecane) on QPC is 1.657 and on OV-225, 2.113. A large *l* phase constant is desirable for general separations of polar and non-polar compounds. Phases with a small *l* phase constant and large *c* phase constant, such as OV-275, posses high selectivity for the separation of non-polar

Table 4
Contribution of the phase constants to retention (log K_L) of dodecane

Phase	Phase constants		$l \log L^{16}$	$\sum(c + l \log L^{16})$
	c	*l*		
SQ	−0.222	0.583	3.321	3.099
OV-17	−0.372	0.518	2.951	2.579
QPC	−1.009	0.468	2.666	1.657
OV-225	−0.541	0.466	2.654	2.113
QTS	−0.686	0.459	2.614	1.928
CW 20M	−0.560	0.447	2.546	1.986
DEGS	−0.650	0.407	2.318	1.668
OV-275	−0.909	0.294	1.675	0.766

solutes from moderately polar solutes of similar volatility. The stationary phases in Table 2 differ significantly in their capacity for orientation and induction interactions, *s* phase constant, and solvent hydrogen-bond basicity, *a* phase constant. For solutes with complementary properties to the phase constants these interactions make significant contributions to retention (Table 3). The liquid organic salts are all dipolar, $s = 1.4$ to 2.0, and all hydrogen-bond bases, $a = 1.4$ to 5.4. In contrast the non-ionic phases have *s* phase constants from 0 to 2.1 and *a* phase constants from 0 to 2.1. The large *a* and *s* phase constants, and in some cases *l* phase constant as well, are the characteristic features that distinguish the liquid organic salts from non-ionic phases [24]. The identification of selective phases for specific dipolar and solvent hydrogen-bond base interactions will be dealt with subsequently. Principal component analysis and hierarchical clustering methods were applied to the data in Table 2 to classify the phases into groups with similar properties and to identify phases with unique characteristics. Principal component analysis performed with varimax rotation indicated that 99.9% of the variance in the data could be explained by four components (Table 5). The loadings for the principal components (Table 5) are equivalent to the coefficients of the linear equation defining how much each variable (phase constant) contributes to the principal component (interaction) responsible for the solvation mechanism. The output from principal component analysis is displayed in the form of the score plots resulting from the projection of the data vector for the samples (phases) onto the principal components. Principal components (PCs) 1 and 2 are the most important and account for 95.9% of the variance in the data. The score plot, Fig. 3, shows three groups with QF-1, DDP, U50HB, OV-275, TCEP and QPC behaving independently (OV-275 and TCEP are tightly clustered and could be considered as a fourth group with a membership of 2). The loading for PC 1 is heavily weighted towards the *a* phase constant and can be considered as an axis of hydrogen-bond basicity. The loading for PC 2 is weighted towards the *s* phase constant with a significant contribution from the *c* phase constant. Given the approximate correlation of the *c* phase constant with the *s* phase constant (Eq. 4), it is reasonable to associate PC 2 with the capacity of the phases for orientation and induction interactions. That being the case, the phases identified in group 1 (SQ, SE-30, OV-105, OV-3, OV-7, OV-11, OV-17, OV-22, OV-25 and PPE-5) are weak hydrogen-bond bases differentiated by their capacity for modest orientation and induction interactions. QF-1 is loosely associated with this group and differs from them in having a greater capacity for

Table 5
Summary of results from principal component analysis of 33 stationary phases

Principal component	Variance (%)	Cumulative variance (%)	
1	68.1	68.1	
2	27.8	95.9	
3	3.4	99.3	
4	0.7	99.9	
Loadings for principal components			
Phase constant	PC 1	PC 2	PC 3
r	−0.002	−0.011	−0.008
s	−0.007	0.961	−0.027
a	0.999	−0.005	−0.004
l	−0.004	−0.023	0.984
c	−0.043	−0.274	−0.175

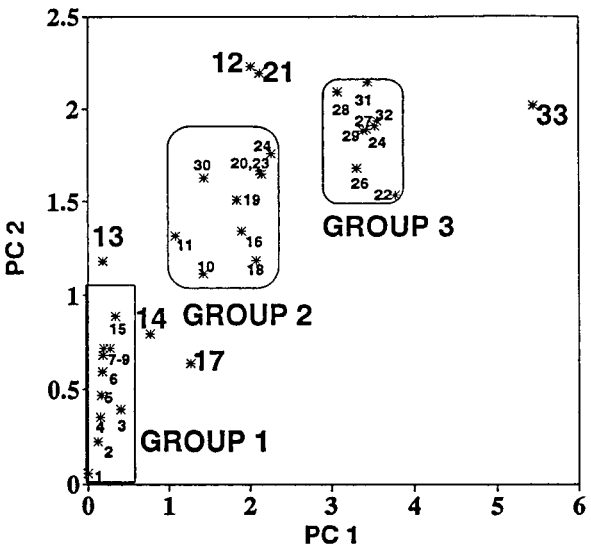

Fig. 3. Score plot for principal component 2 against 1. Numbers refer to the phases identified in Table 1.

orientation and induction interactions with similar hydrogen-bond basicity. DDP and U50HB have a similar capacity for orientation and induction interactions as the group 1 phases but are stronger hydrogen-bond bases. The phases identified in group 2 (OV-330, OV-225, CW 20M, THPED, EGAD, DEGS, QFMS, QPIC and QFBS) are distinguished from the phases in group 1 by their greater capacity for orientation and induction interactions and hydrogen-bond base interactions. They are towards the center of the scale defined by the two principal components so their properties have to be considered as intermediate (this is a diffuse group with respect to orientation and induction interactions and a tight group with respect to hydrogen-bond basicity). Loosely associated with this group are OV-275 and TCEP, which have similar hydrogen-bond basicity but a significantly greater capacity for orientation and induction interactions. OV-275 and TCEP have to be considered as exhibiting unique selectivity. Group 3, which contains only liquid organic salts (QMS, QTS, QBS, QACES, QTAPSO, QBES, QETS and QPN), is characterized by having a strong capacity for orientation and induction interactions and strong hydrogen-bond basicity. QPC to the right of the figure has to be considered exceptional in that it has the largest capacity for solvent hydrogen-bond base interactions with a similar capacity to the other members of group 3 for orientation and induction interactions. The liquid organic salts are unique solvents whose properties cannot be duplicated by any of the non-ionic solvents. The score plot of PC 1 against PC 3, Fig. 4, accounts for 71.5% of the variance in the data. The loading for PC 3 is weighted towards the *l* phase constant with a significant contribution from the *c* phase constant. This component is dominated by the contribution from cavity formation and dispersion interactions to the solvation process. In this plot the phases in group 1 and group 2 in Fig. 3, remain largely intact. Squalane is removed from group 1 as it is significantly easier to form a cavity in this solvent than for the other phases in group 1 (assuming that dispersion interactions are approximately constant as a function of size for all solvents). The group 2 phases have similar cavity forming requirements to the group 1 phases but are more basic. DEGS and QFMS are now removed from group 2 and are distinguished from them by the greater energy required in forming a cavity in the solvent. PC 3 has most influence on group 3 phases which are now widely dispersed on the right-hand side of the figure corresponding to

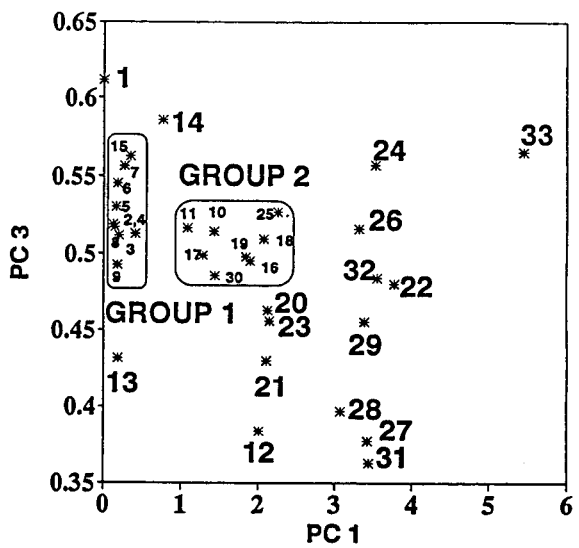

Fig. 4. Score plot for principal component 3 against 1. Numbers refer to the phases identified in Table 1.

similar hydrogen-bond basicity but significantly different requirements for cavity formation. TCEP and OV-275 are similarly separated. Fig. 4 accents an important selection requirement for the group 3 solvents; some of the liquid organic salts provide general retention properties similar to the less basic phases while others can be expected to discriminate against non-polar solutes and yield very low retention (this is true of OV-275 as well). The score plot of PC 2 against PC 3 accounts for 31.2% of the variance in the data. In this plot, Fig. 5, there is a rough general correlation between the capacity of a phase for orientation and induction interactions and for cavity formation and dispersion interactions as demonstrated by the diagonal relationship and the large area of the principal component space that is left empty. The group 1 phases, with the exception of OV-22, OV-25 and SQ lie across the diagonal. Within this group, the poly(siloxane) phases with a high methyl group content have a low capacity for orientation and induction interactions combined with ease of cavity formation while replacing methyl groups with phenyl groups increases both the capacity for orientation and induction interactions and the energy required for cavity formation. The group 2 phases are aligned approximately diagonally in-

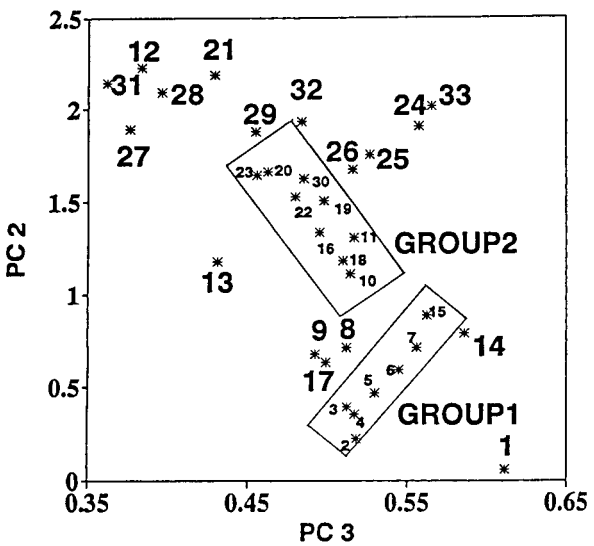

Fig. 5. Score plot for principal component 2 against 3. Numbers refer to the phases identified in Table 1.

dicating that for these phases the increasing energy required to form a cavity is associated with the capacity of the solvent for orientation and induction interactions. The group 3 phases are widely distributed parallel to the horizontal axis as all these phases have a significant capacity for orientation and induction interactions as well as a significant range of energy requirements to form a cavity in the solvent. An alternative classification method to principal component analysis is cluster analysis. In this technique a distance matrix in multivariate space is formed and the Euclidean distance between samples or groups of samples (phases) to each other is used as a measure of the similarity of the samples for all the properties contained in the data matrix. A number of distance metrics can be used as the basis of the cluster algorithm with the final output as a connection dendrogram. The data in Table 2 were analyzed by a number of cluster algorithms with the complete link (farthest neighbor) approach deemed the most appropriate (there was a great deal of similarity in the results obtained for all methods with the single link method showing the greatest variation, but even in this case the differences were small). The complete link dendrogram is shown in Fig. 6. Descendants with a similarity of 1 would be identical and those with a similarity of 0 possessing no properties in common. The major groupings in Fig. 6 agree with the group membership for Fig. 3 with minor differences. The paired descendants indicate the level of similarity between two phases. For example, OV-22 and OV-25 are very similar in their properties and so are OV-275 and TCEP. As a group the liquid organic salts in group 3 have the least in common with the remaining phases. Phases which are singular descendants have properties that differ most of all from the other phases. This includes DEGS, QPIC, THPED, U50HB, PPE-5, DPP, QF-1, SE-30, OV-105, SQ, QMS, QTS, QTAPSO, QETS and QPC. The interesting phases are those that have no descendants and little similarity to their nearest neighbor, as these are the phases that it is most difficult to duplicate their properties by using another phase represented in the data collection. In this sense the most unique solvents are U50HB, QF-1, QMS and QPC. The

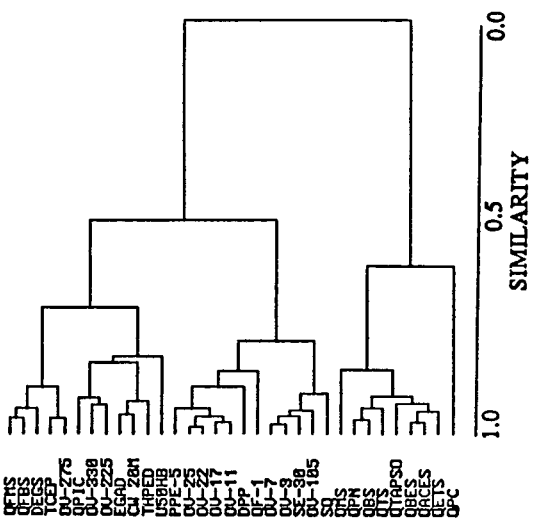

Fig. 6. Complete link dendrogram obtained by cluster analysis of the data in Table 2.

dendrogram is very useful for indicating similarity in a simple visual format but must be used with the group classification to indicate the most useful phases for method development. For example, the fact that OV-275 and TCEP are similar in properties does not mean that neither phase has desirable solvent properties for method development. Rather, either of them is a good candidate as a preferred phase for methods development since they belong to a group whose membership is significantly different to the properties of their neighboring group to which they have most similarity. Thus, it would be sensible based on their solvent properties to select one of the phases QFMS, QFBS, DEGS, TCEP and OV-275 as a preferred phase (the top group in Fig. 6) but a better choice could be made for the next phase to select than to take a second phase from this group.

4. Conclusions

The data in Table 2 combined with the interpretation in Figs. 3–6 allow 9 phases to be identified as representative of the collection of phases studied. This includes phases characteristic of a group as well as phases characteristic of themselves. The list would include squalane (case of cavity formation and dispersion interactions), OV-17 (weak orientation, induction, and hydrogen-bond basicity and ease of cavity formation), QF-1 (intermediate orientation and induction interactions with low hydrogen-bond basicity and ease of cavity formation), U50HB (intermediate hydrogen-bond basicity with weak orientation and induction interactions and ease of cavity formation), CW 20M (intermediate orientation, induction, and hydrogen-bond basicity and ease of cavity formation), QMS (large contribution from hydrogen-bond basicity, intermediate orientation and induction interactions, and intermediate ease of cavity formation), QTS (large orientation, induction and hydrogen-bond basicity, and intermediate ease of cavity formation), QPC (as for QTS except that this phase is an exceptionally strong hydrogen-bond base and is more cohesive with respect to the difficulty of cavity formation), and OV-275 (very cohesive solvent with unfavorable cavity formation, strong orientation and induction interactions, intermediate hydrogen-bond basicity). As discussed previously this list does not contain any phases with a significant capacity for solvent hydrogen-bond acid interactions or strong electron pair donor–acceptor interactions. These interactions are not well represented among the liquid phases commonly used in gas chromatography today. The above discussion has only concerned solvent properties while other practical considerations such as the useful liquid temperature range, coating characteristics, etc., are equally important as selection criteria. Also, those phases characteristic of a group could justifiably be substituted by other phases within the same group. Committees should be left to ponder the question of selecting preferred phases given that other phases than those studied here should also be considered. The above work, we believe, supplies a rational approach for the work of these committees and for those interested in the development of new stationary phases with an expectation of providing different separation characteristics to existing phases. It is important to note that the data in Table 2 were acquired at a common temperature of 121.4°C. It should

provide a reasonable guide to the selection of phases for particular applications in the neighborhood of the reference temperature. Little is known about the change in phase constants as a function of temperature [11,25,33] and what information is available is in conflict. Selectivity changes with temperature, however, are likely to be phase dependent, and it cannot be assumed that the ranking order produced at one temperature will hold at all temperatures. When using Eq. 1 to predict retention on different phases it should be remembered that this equation refers to a gas–liquid partition model and that predictions will be less reliable for separation conditions and phases where interfacial adsorption is a significant retention mechanism [1,2,41].

References

[1] C.F. Poole and S.K. Poole, *Chromatography Today*, Elsevier, Amsterdam, 1991.
[2] C.F. Poole and S.K. Poole, *Chem. Rev.*, 89 (1989) 377.
[3] H. Rotzsche, *Stationary Phases in Gas Chromatography*, Elsevier, Amsterdam, 1991.
[4] K.K. Unger (Editor), *Packings and Stationary Phases in Chromatographic Techniques*, Marcel Dekker, New York, 1990.
[5] M.H. Abraham, P.L. Grellier, I. Hamerton, R.A. McGill, D.V. Prior and G.S. Whiting, *Faraday Disc. Chem. Soc.*, 85 (1988) 107.
[6] C.F. Poole, T.O. Kollie and S.K. Poole, *Chromatographia*, 34 (1992) 281.
[7] M.H. Abraham, *Chem. Soc. Rev.*, 22 (1993) 73.
[8] P.W. Carr, *Microchem. J.*, 48 (1993) 4.
[9] S.K. Poole and C.F. Poole, *J. Chromatogr. A*, 697 (1995) 429.
[10] M.H. Abraham, *Pure Appl. Chem.*, 65 (1993) 2503.
[11] M.H. Abraham, in P. Politzer and J.S. Murray (Editors), *Theoretical and Computational Chemistry, Vol. 2, Solvent Interactions*, Elsevier, Amsterdam, in press.
[12] M.H. Abraham, G.S. Whiting, R.M. Doherty and W.J. Shuely, *J. Chem. Soc., Perkin Trans. 2*, (1990) 1451.
[13] M.H. Abraham, G.S. Whiting, R.M. Doherty and W.J. Shuely, *J. Chromatogr.*, 587 (1991) 213.
[14] M.H. Abraham and G.S. Whiting, *J. Chromatogr.*, 594 (1992) 229.
[15] M.H. Abraham, *J. Chromatogr.*, 644 (1993) 95.
[16] M.H. Abraham, P.L. Grellier, D.V. Prior, P.P. Duce, J.J. Morris and P.J. Taylor, *J. Chem. Soc., Perkin Trans. 2*, (1989) 699.
[17] M.H. Abraham, *J. Phys. Org. Chem.*, 6 (1993) 660.
[18] M.H. Abraham, G.S. Whiting, R.M. Doherty and W.J. Shuely, *J. Chromatogr.*, 518 (1990) 329.
[19] M.H. Abraham, G.S. Whiting, R.M. Doherty and W.J. Shuely, *J. Chromatogr.*, 587 (1991) 229.
[20] M.H. Abraham, G.S. Whiting, J. Andonian-Haftvan, J.W. Steed and J.W. Grate, *J. Chromatogr.*, 588 (1991) 361.
[21] M.H. Abraham, J. Andonian-Haftvan, I. Hamerton, C.F. Poole and T.O. Kollie, *J. Chromatogr.*, 646 (1993) 351.
[22] M.H. Abraham and D.P. Walsh, J. Chromatogr., *J. Chromatogr.*, 627 (1992) 294.
[23] T.O. Kollie and C.F. Poole, *Chromatographia*, 33 (1992) 551.
[24] S.K. Poole and C.F. Poole, *Analyst*, submitted for publication.
[25] C.F. Poole and T.O. Kollie, *Anal. Chim. Acta*, 282 (1993) 1.
[26] M.L. Larrivee and C.F. Poole, *Anal. Chem.*, 66 (1994) 139.
[27] K.G. Miller and C.F. Poole, *J. High Resolut. Chromatogr.*, 17 (1994) 125.
[28] J.W. Grate and M.H. Abraham, *Sensors Actuators B*, 3 (1991) 85.
[29] J. Li, A.J. Dallas and P.W. Carr, *J. Chromatogr.*, 517 (1990) 103.
[30] J. Li, Y. Zhang, A.J. Dallas and P.W. Carr, *J. Chromatogr.*, 550 (1991) 101.
[31] J. Li, Y. Zhang, H. Ouyang and P.W. Carr, *J. Am. Chem. Soc.*, 114 (1992) 9813.
[32] J. Li, Y. Zhang and P.W. Carr, *Anal. Chem.*, 64 (1992) 210.
[33] J. Li, Y. Zhang and P.W. Carr, *Anal. Chem.*, 65 (1993) 1969.
[34] J. Li and P.W. Carr, *J. Chromatogr. A*, 659 (1994) 367.
[35] M.H. Abraham, J. Andonian-Haftvan, C.M. Du, J.P. Osei-Osusu, P. Sakellariou, W.J. Shuelly, C.F. Poole and S.K. Poole, *J. Chromatogr. A*, 688 (1994) 125.
[36] T.O. Kollie, C.F. Poole, M.H. Abraham and G.S. Whiting, *Anal. Chim. Acta*, 259 (1992) 1.
[37] B.R. Kersten, S.K. Poole and C.F. Poole, *J. Chromatogr.*, 468 (1989) 235.
[38] S.K. Poole and C.F. Poole, *J. Chromatogr.*, 500 (1990) 329.
[39] R.F. Kruppa and R.S. Henly, *J. Chromatogr. Sci.*, 12 (1974) 127.
[40] B.E. Richter, J.C. Kuel, J.I. Shelton, L.W. Castle, J.S. Bradshaw and M.L. Lee, *J. Chromatogr.*, 279 (1983) 21.
[41] S.K. Poole, T.O. Kollie and C.F. Poole, *J. Chromatogr. A*, 664 (1994) 229.

ELSEVIER

Journal of Chromatography A, 697 (1995) 429–440

JOURNAL OF CHROMATOGRAPHY A

Application of principal component factor analysis to the cavity model of solvation to identify factors important in characterizing the solvent properties of gas chromatographic stationary phases

Salwa K. Poole, Colin F. Poole*

Department of Chemistry, Wayne State University, Detroit, MI 48202, USA

Abstract

Principal component factor analysis was applied to two sets of data consisting of the gas–liquid partition coefficient for 30 solutes on 22 stationary phases or 67 solutes on 10 stationary phases at 121.4°C. Three or four factors were required to characterize the data and were identified as contributions from cavity formation and dispersion interactions, solvent hydrogen-bond base interactions, and orientation interactions typical of aromatic and aliphatic compounds. None of the stationary phases were identified as significant hydrogen-bond acids. The contribution from cavity formation and dispersion were combined into a single factor while orientation interactions were divided into two contributions representing either the additional polarity of polarizable solutes (aromatic compounds) or a family type behavior resulting from a structural contribution to the number of solute–solvent interactions calculated using the cavity model. There is good general agreement between the assignments made using the principal component factor model and results obtained previously using the solvation parameter model.

1. Introduction

A number of attempts have been made to develop a quantitative scale of solvent selectivity to characterize the retention properties of gas chromatographic stationary phases based on the Gibbs free energy of solution for a series of reference compounds [1–5]. Reference compounds were selected assuming that each compound was retained by a single dominant intermolecular interaction and the stationary phases were ranked in accordance with their capacity to retain the reference compounds. This approach had to be abandoned when it was demonstrated that suitable reference compounds for individual intermolecular interactions did not exist and that the calculated selectivity parameters based on the above approach were dependent on the size of the reference compound as well as its capacity for polar interactions [5–7]. A new approach was required that enabled a separation of molecular size and solute–solvent interactions to be made.

The cavity model of solution is a suitable model for separating the contribution of solute size from specific solute–solvent interactions [8–10]. The size contribution is represented by the cavity term, which accounts for the work that must be done to create a cavity in the solvent of a suitable size to accommodate the solute. This is a solvent property as it depends only on the free

* Corresponding author.

0021-9673/95/$09.50
SSDI 0021-9673(94)00705-5

energy required to disrupt solvent–solvent interactions in preparing the cavity. The magnitude of the cavity term will depend on the cohesive character of the solvent and the size of the solute transferred to the solvent. For transfer of the solute from the gas phase to the stationary phase to be favorable the contribution of solute–solvent interactions set up once the solute is transferred to the solvent must exceed the free energy required to disrupt solvent–solvent interactions in preparing the cavity. This difference in free energy is responsible for the variation in gas–liquid partition coefficients observed for different solutes in the same solvent and the same solute in different solvents. Intuitively, this model provides a reasonable qualitative picture of the solvation process but as a quantitative model it is limited by the lack of an exact method to calculate the contribution of solute–solvent and solvent–solvent intermolecular interactions to the solvation process for conditions typical of gas chromatographic experiments. Semi-empirical solutions are available, however.

The first of these solutions is due to Abraham and co-workers, and in a slightly modified version by Carr and co-workers, as outlined in a companion paper [11]. The general equation for the solvation process in gas–liquid chromatography proposed by Abraham and co-workers is represented by Eq. 1.

$$\log K_L = c + rR_2 + s\pi_2^H + a\alpha_2^H + b\beta_2^H + l \log L^{16} \quad (1)$$

where K_L is the gas–liquid partition coefficient, R_2 the solute excess molar refraction, π_2^H the effective solute dipolarity/polarizability, α_2^H the effective solute hydrogen-bond acidity, β_2^H the effective solute hydrogen-bond basicity and L^{16} the solute gas–liquid partition coefficient on *n*-hexadecane at 25°C. The explanatory variables listed above are solvation parameters derived from equilibrium constants or calculated from gas chromatographic measurements and are free energy related parameters characteristic of the monomeric solute. The solvent properties *r*, *s*, *a*, *b* and *l* are unambiguously defined: the *r* constant refers to the ability of a solvent to interact with solute *n*- or π-electron pairs; the *s* constant to the ability of the solvent to take part in dipole–dipole and dipole–induced dipole interactions; the *a* constant is a measure of the hydrogen-bond basicity of the solvent; the *b* constant is a measure of the hydrogen-bond acidity of the solvent and the *l* constant incorporates contributions from solvent cavity formation and solute–solvent dispersion interactions, and more specifically in gas–liquid chromatography indicates how well the phase will separate members of a homologous series. For an uncharacterized phase the solvent properties *r*, *s*, *a*, *b* and *l* are determined from the experimentally derived gas–liquid partition coefficient for a minimum of 15 to 30 varied solutes with known explanatory variables using the statistical analysis technique of multiple linear regression analysis.

An alternative approach is due to Poole and co-workers [6,9] and results in the following general equation for the solvation process

$$\Delta G_S^{Soln}(X) = \Delta G_S^{Soln}(HC)^V + \Delta G_{SQ}^P(X) + \Delta G_S^{Int}(X) \quad (2)$$

where $\Delta G_S^{Soln}(X)$ is the partial Gibbs free energy of solution for the transfer of solute X from the gas phase to the stationary phase S, $\Delta G_S^{Soln}(HC)^V$ is the partial Gibbs free energy of solution for an *n*-alkane with an identical Van der Waals volume to solute X in the stationary phase S, $\Delta G_{SQ}^P(X)$ is the partial Gibbs free energy of interaction for the polar contribution of solute X in a non-polar reference solvent squalane, SQ, calculated as shown by Eq. 3, and $\Delta G_s^{Int}(X)$ is the partial Gibbs free energy of interaction for the polar contribution of solute X to solvation in solvent S.

$$\Delta G_{SQ}^P(X) = \Delta G_{SQ}^{Soln}(X) - \Delta G_{SQ}^{Soln}(HC)^V \quad (3)$$

Experimentally, evaluation of Eq. 2 requires the determination of the gas–liquid partition coefficient for solute X on the stationary phase S and the reference phase squalane as well as the determination of the gas–liquid partition coefficients for an appropriate number of *n*-alkanes on both phases to construct the linear relationship between the Van der Waals volume of the *n*-

alkanes and the logarithm of their gas–liquid partition coefficient. All the terms in Eq. 2 can then be evaluated. The contribution from cavity formation and dispersion interactions to the solvation process is represented by the sum of the first two terms on the right-hand side of Eq. 2. The $\Delta G_S^{Int}(X)$ parameter represents the sum of the polar interactions such as orientation and hydrogen bond formation to the solvation process. For simple molecules $\Delta G_S^{Int}(X)$ depends on the type of functional group present in a solute and can be treated as an incremental constant for prediction purposes. Poole and co-workers have used Eq. 2 to characterize the properties of 28 common stationary phases [6,9], to compare the solvation properties of 12 analogous alkanesulfonate and perfluoroalkanesulfonate liquid organic salts [12], and to study the influence of temperature on the selectivity of 10 stationary phases [13,14].

A comparison of the two models represented by Eqs. 1 and 2 shows acceptable agreement for the contribution of the sum of cavity formation and dispersion interactions (Eq. 4) and the contribution of polar interactions to the solvation process (Eq. 5) at 121.4°C [9,12,13,15,16]. There is, perhaps, a small numerical difference in the magnitude of the sum of cavity formation and dispersion interactions to solvation estimated by both models but this does not affect the agreement in general trends indicated by both models at a constant temperature. A more detailed comparison of the contributions of individual intermolecular interactions to solvation estimated by both models requires that a method be developed to identify these contributions to the free energy terms indicated in Eq. 2. This should be possible using chemometric techniques, such as principal component factor analysis, which are explored in this paper.

$$\Delta G_S^{Soln}(HC)^V + \Delta G_{SQ}^P(X) = 1.806 \sum (c + l \log L^{16}) \quad (4)$$

$$\Delta G_S^{Int}(X) = 1.806 \sum (rR_2 + s\pi_2^H + a\alpha_2^H + b\beta_2^H) \quad (5)$$

The application of principal component analysis and factor analysis to gas chromatographic data was pioneered by the research groups headed by Wold, Chastrette, Chretien and Howery and is reviewed in detail elsewhere [17–20]. In most cases the retention index data base of McReynolds was used to identify factors able to explain retention and to identify the similarity of solutes and solvents. The relationship between specific factors and fundamental intermolecular interactions was not made in these studies, perhaps in part due to the unreliable nature of some of the McReynolds data as well as the fact that the retention index is a composite term expressing properties of both the individual solutes and the retention index standards on the different stationary phases [4,9]. We have removed these objections in this paper by using the gas–liquid partition coefficients as the characteristic retention parameter.

2. Experimental

The name, abbreviation and composition of the stationary phases used in this study are summarized in Table 1. The gas–liquid partition coefficients at 121.4°C were taken from previous studies and are corrected for interfacial adsorption [3,15]. For data analysis it is necessary that the gas–liquid partition coefficient is accurately known for all phases in that data set. This resulted in the use of two data sets for evaluation purposes containing the results for 30 solutes on 22 phases and 67 solutes on 10 phases (the 10 phases are also contained in the 22-phase set).

To compare results obtained from the solvation parameter model with those obtained by the application of principal component factor analysis to the cavity model represented by Eq. 2, the appropriate gas–liquid partition coefficients equivalent to the Gibbs free energy terms with a molar standard state were used. For computational purposes the following expressions were used:

$$\log K_L(\text{cavity–dispersion}) = \log ([K_L^{NV}(X)]_S \cdot [K_L(X)]_{SQ}) / [K_L^{NV}(X)]_{SQ} \quad (6)$$

where $K_L^{NV}(X)$ is the gas–liquid partition coeffi-

Table 1
Identification and abbreviations for stationary phases

No.	Abbreviation	Name[a]
1	SQ	Squalane*
2	SE-30	Poly(dimethylsiloxane)
3	OV-105	Poly(cyanopropylmethyldimethylsiloxane)*
4	OV-3	Poly(dimethylmethylphenylsiloxane), 10 mol% phenyl groups
5	OV-7	Poly(dimethylmethylphenylsiloxane), 20 mol% phenyl groups
6	OV-11	Poly(dimethylmethylphenylsiloxane), 35 mol% phenyl groups
7	OV-17	Poly(methylphenylsiloxane)*
8	OV-22	Poly(methylphenyldiphenylsiloxane), 65 mol% phenyl groups
9	OV-25	Poly(methylphenyldiphenylsiloxane), 75 mol% phenyl groups
10	OV-330	Poly(dimethylsiloxane)/Carbowax copolymer
11	OV-225	Poly(cyanopropylmethylphenylmethylsiloxane)*
12	QF-1	Poly(trifluoropropylmethylsiloxane)*
13	DDP	Didecylphthalate
14	PPE-5	1,3-bis(3-phenoxyphenoxy)benzene
15	CW-20M	Poly(ethylene glycol)*
16	U50HB	Poly(ethylene glycol) (Ucon 50 HB 660)
17	THPED	N,N,N′,N′-Tetrakis(2-hydroxypropyl)ethylenediamine*
18	EGAD	Poly(ethylene glycol adipate)
19	DEGS	Poly(diethylene glycol succinate)*
20	TCEP	1,2,3-Tris(2-cyanoethoxypropane)*
21	QTS	Tetra-*n*-butylammonium 4-toluenesulfonate*
22	QBES	Tetra-*n*-butylammonium N,N-(bis-2-hydroxyethyl)-2-aminoethanesulfonate

[a] An * indicates membership of the 10-phase data set.

cient for an *n*-alkane with an identical Van der Waals volume to solute X and is derived from the linear relationship between log K_L^{NV} and the Van der Waals volume, V_A, for the *n*-alkanes on each stationary phase.

$$\log K_L^{NV}(X) = m_s V_A + b_s \quad (7)$$

where m_s and b_s are the coefficients obtained by linear regression. Log $K_L(X)$ is the gas–liquid partition coefficient for solute X on stationary phase S or SQ as indicated by the subscript. The contribution of polar interactions is given by

$$\log K_L^{Int}(X) = \log ([K_L(X)]_S \cdot [K_L^{NV}(X)]_{SQ})/([K_L(X)]_{SQ} \cdot [K_L^{NV}(X)]_S) \quad (8)$$

where log $K_L^{Int}(X)$ is the gas–liquid partition coefficient corresponding to the term $\Delta G_S^{Int}(X)$ in Eq. 2.

The Van der Waals volume for the test solutes were calculated with the molecular modeling program MacroModel 2.0 (Department of Chemistry, University of New York, New York, NY, USA) executed on a VAX 11/750 computer (Digital Equipment, Merrimack, NH, USA) [6]. Principal component and cluster analysis for data interpretation was performed using Pirouette V1.1 (Infometrix, Seattle, WA, USA) on a Epson Apex 200 computer (Epson America, Torrance, CA, USA). Raw varimax rotation without additional data preprocessing was used for the principal component factor analysis. The raw rotation method gave consistently better results than any of the weighted or normalized rotation techniques. The characteristic phase constants obtained from application of the solvation parameter model to the data sets discussed in this paper are taken from Ref. [11].

3. Results and discussion

The cavity model of solution provides a reasonable framework for understanding the retention properties of solutes in gas–liquid partition chromatography. It quite reasonably identifies two sets of factors underlying retention attributable to the contributions of solvent–solvent and solute–solvent interactions but does not identify the specific factors involved. These can be fairly confidently identified as dispersion, induction, orientation, hydrogen-bond acid–base, and perhaps electron donor–acceptor interactions (at least for isotropic solvents). The individual importance of these interactions for any system considered is a characteristic property of both the solvent and the solute, and in the absence of explicit information of the solute or solvent contribution, there is no simple approach to establishing the relevant complementary properties of the uncharacterized solvent (or solute) based on the singular observation of retention. One possible solution based on the assignment of characteristic properties to the solute, which are proportional to the specific factors, can be used to isolate the complementary solvent properties by multiple linear regression analysis, as discussed in a companion paper [11]. An alternative approach, based on exploratory data analysis, uses abstract mathematical constraints to reduce the dimensionality of the data to a smaller number of abstract factors retaining the useful information contained in the original data, which are subsequently converted to physically meaningful factors by a factor analytical procedure. There are many approaches to converting the abstract factors to meaningful physical factors as detailed in general texts on factor analysis [20–26], which will not be discussed here. Factor analysis, in general, is performed to acquire a new understanding of a problem and must be judged by logical chemical constraints since, in the end, the answers provided may be true or abstract factors, and the mathematical procedure used in their isolation will not be able to distinguish between the two alternatives.

In this paper we have used the principal component method of data reduction to identify the abstract factors and the method of varimax rotation to convert the abstract factors to terminal factors for interpretation [21,22,25,26]. A characteristic property of the principal component method is that the first principal component will tend to be a weighted average of all the variables present in the data set and the second and succeeding principal components will tend to contain about equal loadings of opposite sign. In the absence of a single dominant general factor this is unlikely to represent a realistic factor solution for most chemical problems. The mathematical operation of rotation is employed to obtain a simpler structure which it is hoped will more closely resemble the true situation. By rotation the principal component axes are relocated within the factor hyperspace such that as many row points as possible lie close to the final factor axes, with only a small number of points remaining between the rotated axes. Varimax rotation is an example of an orthogonal rotation method that seeks simplicity among the factors by maximizing the total variance of the squared loadings. This is the method employed in these studies as implemented in the Pirouette software environment.

Principal component analysis of either the 10 or 22 stationary phase sets indicates that a single component accounts for $>98\%$ of the total variance of the contribution of cavity formation and dispersion interactions to the solvation process. After rotation of the principal components additional factor axis are produced that contain substantial variance (Table 2). All the principal component factors, however, are strongly correlated with each other (both within a rotation set and between different rotation sets), $r^2 > 0.95$. Also, the product of the score and loading coefficients for each solute on all phases are significantly correlated to $\sum(c + l \log L^{16})$ from the solvation parameter model. These and other tests indicate that rotation of the principal components produces phantom factors highly correlated to principal component 1 for the non-rotated factor matrix. It must be concluded that only a single factor can be isolated to describe the contribution of cavity formation and dispersion interactions in the cavity model. This is not

Table 2
Variance extracted by principal component factor analysis applied to the cavity formation and dispersion interaction term of the data set containing 23 solutes and 21 phases

Number of rotations	Principal component	Variance accounted for (%)
0	1	99.83
	2	0.14
	3	0.03
2	1	50.15
	2	49.81
	3	0.03
3	1	20.25
	2	48.15
	3	31.60

Table 3
Variance extracted by principal component factor analysis applied to the polar interaction term for the data set containing 67 solutes on 10 phases

Principal component	Number of factor rotations		
	0	2	3
Complete data set (67 solutes)			
1	97.83	53.68	42.23
2	1.54	45.69	39.12
3	0.54	0.54	18.56
Aliphatic compounds only (38 solutes)			
1	98.56	75.06	75.40
2	1.24	24.74	20.88
3	0.11	0.11	3.64
Aromatic compounds only (28 solutes)			
1	98.55	55.28	54.17
2	1.18	44.45	23.84
3	0.02	0.21	21.93

so surprising since the free energy involved in cavity formation and the free energy resulting from dispersion interactions in solution are both likely to be dependent on solute size.

The larger number of solutes available for the 10 stationary phase set allowed a greater level of flexibility in assigning the number of factors for the contribution of the polar interaction term to the cavity solution model. Principal component analysis indicated that about 98% of the variance could be accounted for by a single component which after rotation suggested that up to three principal component factors were significant (Table 3). Detailed evaluation of the factor loadings and deletion of certain solute types from the solute set was used to preliminary establish the identity of the factor axes. For the complete data set with three factor rotations the first principal component factor was heavily weighted towards aliphatic solutes capable of strong orientation interactions with dipolar aromatic solutes in an intermediate position and weakly dipolar aromatic and all solutes with a capacity to function as hydrogen-bond acids weakly loaded (Table 4). The second principal component factor was heavily weighted towards solutes with a capacity for hydrogen-bond acid interactions with all other solutes lightly loaded. The third principal component factor was heavily weighted towards aromatic solutes and weakly weighted towards aliphatic and aromatic hydrogen-bond acid solutes. There are two possible assignments for this factor. The characteristic factor used to represent the cavity is the Van der Waals volume. The solvent accessible surface area of the cavity would be a more logical term to account for the number of solute–solvent interactions but this term can not be calculated in a straightforward manner for the types of solvent involved in these studies. The shape of the cavity for aromatic and other cyclic compounds is likely to be different from that for straight-chain aliphatic compounds and the cancellation of interactions proposed in the model for aliphatic compounds by an *n*-alkane of identical Van der Waals volume a better approximation than is obtained for the aromatic and cyclic compounds. Factor three, therefore, could arise in an artificial way to compensate for differences in the capacity of straight chain aliphatic compounds and aromatic (possibly also aliphatic cyclic compounds) to enter into solute–solvent intermolecular interactions. An alternative explanation is to assign principal component factor 3 to a capacity to enter into induction interactions based on the greater polarizability of aromatic compounds compared to aliphatic compounds. Deleting the aromatic compounds from the data set and repeating the principal com-

ponent factor analysis shows that factor three is substantially reduced in the percentage of the variance it contains (3.64% in the 3 factor rotation) and is heavily weighted to the single compound 1,1,2,2-tetrachloroethane. Considering just the aromatic compounds in the original data set then the principal component factor 3 is responsible for a significant fraction of the total variance (21.93% in the 3 factor rotation). In this case the identity of factors 1 and 2 are switched. Of course the variance represented in a data set is not independent of either the identity or the number of solutes in the data set so that the data entries cannot be directly compared in any quantitative sense. The changes are so large in this case that they can safely be used as a qualitative indication of the features involved.

Confirmation of the above indications was sought by comparison to the contributing factors isolated with Abraham's solvation parameter model (see [11]). The comparison was made using the data set for 22 phases and 30 solutes. Principal component factor 1 is well correlated to the product term $s\pi_2^H$ (Fig. 1), with a correlation coefficient $r^2 = 0.92$. The quality of the fit is influenced by the poor agreement of PPE-5 and DDP with the other phases. Principal component factor 2 is correlated to the product term $a\alpha_2^H$ (Fig. 2), with a correlation coefficient $r^2 = 0.96$. Principal component factor 3 is correlated to the sum $\Sigma(s\pi_2^H + rR_2)$ (Fig. 3), $r^2 = 0.81$ with QF-1 considerably removed from the best line through the other phases (eliminating QF-1, $r^2 = 0.95$). The product term $s\pi_2^H$ is also well correlated to factor 3 but not rR_2 by itself. Inspection of the plots shows that combining $s\pi_2^H$ and rR_2 improves the fit of CW-20M, OV-22, OV-25 and U50HB with the best line through the data but

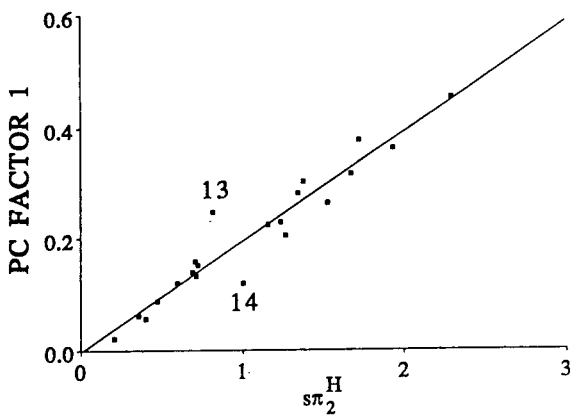

Fig. 1. Plot of principal component (PC) factor 1 extracted from the polar interaction term of the cavity model against the solvation parameter model parameter for dipole–dipole and dipole–induced dipole interactions for nitrobenzene. The numbered stationary phases are identified in Table 1.

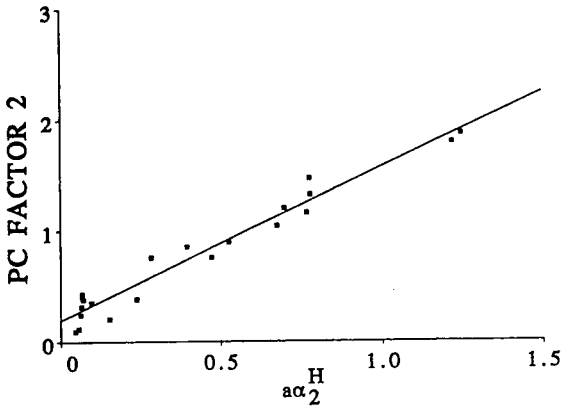

Fig. 2. Plot of principal component factor 2 extracted from the polar interaction term of the cavity model against the solvation parameter model parameter for solvent hydrogen-bond base interactions for octanol.

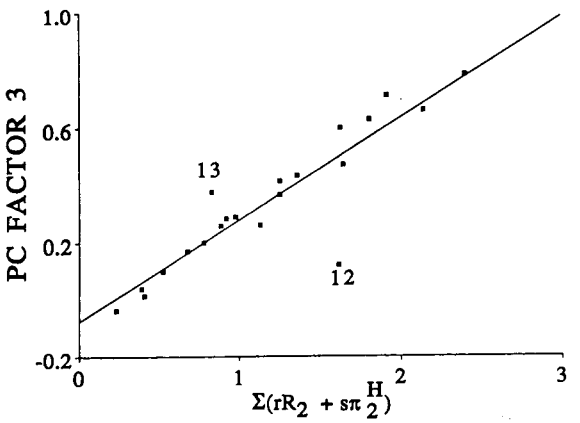

Fig. 3. Plot of principal component factor 3 extracted from the polar interaction term of the cavity model against the sum of the terms representing dipole–dipole, dipole–induced dipole and electron-pair interactions in the solvation parameter model for benzonitrile. The numbered stationary phases are identified in Table 1.

Table 4
Principal component factor loadings for the data set containing 67 solutes on 10 phases

Loading for factor 1		Loading for factor 2		Loading for factor 3	
Component	Loading	Component	Loading	Component	Loading
Dimethyl sulfoxide	0.3165	2-Chlorophenol	−0.4278	Iodobenzene	0.3212
Dimethylacetamide	0.2418	Phenol	−0.3636	2,6-Dimethylaniline	0.2578
Dimethylformamide	0.2348	4-Methylphenol	−0.3408	N,N-Dimethylaniline	0.2550
Dibutylformamide	0.2263	3,5-Dimethylphenol	−0.3363	Bromobenzene	0.2332
Methyl hexadecanoate	0.2030	2,5-Dimethylphenol	−0.3122	Benzodioxane	0.2285
Methyl tetradecanoate	0.1939	2,6-Dimethylphenol	−0.2192	1,2-Dichlorobenzene	0.2197
Dodecan-2-one	0.1904	Octan-1-ol	−0.2042	Anisole	0.2083
Methyl dodecanoate	0.1839	Nonan-1-ol	−0.1979	Benzene	0.2057
Nitrohexane	0.1815	Heptan-1-ol	−0.1957	*n*-Butylbenzene	0.2017
Methyl undecanoate	0.1774	Butan-1-ol	−0.1901	Chlorobenzene	0.1969
Undecan-2-one	0.1753	Hexan-1-ol	−0.1889	Benzaldehyde	0.1964
Methyl decanoate	0.1735	Pentan-1-ol	−0.1886	Acetophenone	0.1962
Methyl octadecanoate	0.1705	1,1,2,2-Tetrachloroethane	−0.1226	2,4,6-Trimethylpyridine	0.1914
Nonan-2-one	0.1695	Aniline	−0.1211	Ethylbenzene	0.1881
Decan-2-one	0.1693	2-Methyl-2-pentanol	−0.1198	Aniline	0.1838
Methyl nonanoate	0.1686	N-Methylaniline	−0.0918	N-Methylaniline	0.1835
Octan-2-one	0.1637	Dimethyl sulfoxide	−0.0455	Toluene	0.1713
Methyl octanoate	0.1629	2,6-Dimethylaniline	−0.0362	Pyridine	0.1697
Nitropentane	0.1627	Dodec-1-yne	−0.0346	Dioxane	0.1667
Nitropropane	0.1599	Nitrobenzene	−0.0327	*cis*-Hydrindane	0.1436
Heptan-2-one	0.1581	Benzonitrile	−0.0324	1,1,2,2-Tetrachloroethane	0.1313
Methyl heptanoate	0.1554	Nitrocyclohexane	−0.0289	Nitrobenzene	0.1305
Hexan-2-one	0.1532	Nitrohexane	−0.0273	Oct-2-yne	0.1265
Methyl hexanoate	0.1516	Dimethylformamide	−0.0165	Methyl octanoate	0.1105
Pentan-2-one	0.1460	1,2-Dichlorobenzene	−0.0158	2,6-Dimethylphenol	0.1040
Nonanal	0.1404	Dimethylacetamide	−0.0138	Benzonitrile	0.0940
Butan-2-one	0.1389	Nitropropane	−0.0111	Dihexyl ether	0.0683
Benzonitrile	0.1239	Dibutylformamide	−0.0102	Nitrocyclohexane	0.0560
Nitrocyclohexane	0.1111	Nitropentane	−0.0091	Butan-2-one	0.0559

Nitrobenzene	0.0845	Benzodioxane	−0.0066	2,5-Dimethylphenol	0.0483
Dioxane	0.0810	Methyl octadecanoate	−0.0066	Pentan-2-one	0.0430
Acetophenone	0.0631	Chlorobenzene	−0.0045	Dodec-1-yne	0.0397
2-Methyl-2-pentanol	0.0563	Iodobenzene	0.0006	Nitropropane	0.0342
Butan-1-ol	0.0562	Benzaldehyde	0.0023	Nitropentane	0.0296
Benzaldehyde	0.0560	Bromobenzene	0.0044	Hexan-2-one	0.0278
Pyridine	0.0539	Acetophenone	0.0081	3,5-Dimethylphenol	0.0235
Octan-1-ol	0.0480	Pyridine	0.0104	Methyl heptanoate	0.0222
Nonan-1-ol	0.0454	Ethylbenzene	0.0121	4-Methylphenol	0.0189
Dihexyl ether	0.0369	Toluene	0.0134	Methyl hexanoate	0.0157
2,4,6-Trimethylpyridine	0.0363	Nonanal	0.0137	Heptan-2-one	0.0150
Heptan-1-ol	0.0348	Dodecan-2-one	0.0147	Nonanal	0.0149
Hexan-1-ol	0.0339	Methyl tetradecanoate	0.0156	Dimethylformamide	0.0137
Pentan-1-ol	0.0290	Methyl hexanoate	0.0159	Dimethylacetamide	0.0101
Benzodioxane	0.0252	Undecan-2-one	0.0186	Octan-2-one	0.0065
Dodec-1-yne	0.0241	Methyl dodecanoate	0.0200	Phenol	0.0053
N,N-Dimethylaniline	0.0168	Nonan-2-one	0.0202	Methyl nonanoate	0.0008
Anisole	0.0137	*cis*-Hydrindane	0.0213	Decan-2-one	−0.0048
Aniline	0.0123	Decan-2-one	0.0214	Nonan-2-one	−0.0052
2-Chlorophenol	0.0091	Methyl undecanoate	0.0224	Methyl decanoate	−0.0086
2,6-Dimethylaniline	0.0078	Oct-2-yne	0.0237	2-Methyl-2-pentanol	−0.0163
N-Methylaniline	0.0006	Octan-2-one	0.0239	Undecan-2-one	−0.0166
Toluene	0.0006	Methyl decanoate	0.0244	Methyl undecanoate	−0.0170
Phenol	−0.0003	Heptan-2-one	0.0256	Dimethyl sulfoxide	−0.0205
Oct-2-yne	−0.0027	Methyl nonanoate	0.0266	Nitrohexane	−0.0209
n-Butylbenzene	−0.0077	2,4,6-Trimethylpyridine	0.0280	Dibutylformamide	−0.0224
4-Methylphenol	−0.0091	Methyl octanoate	0.0284	Methyl dodecanoate	−0.0289
3,5-Dimethylphenol	−0.0152	Hexan-2-one	0.0295	2-Chlorophenol	−0.0318
2,6-Dimethylphenol	−0.0209	Benzene	0.0299	Hexan-1-ol	-0.0336
Benzene	−0.0226	Methyl heptanoate	0.0300	Dodecan-2-one	−0.0383
Ethylbenzene	−0.0244	Anisole	0.0302	Heptan-1-ol	−0.0444
1,1,2,2-Tetrachloroethane	−0.0252	Methyl hexanoate	0.0313	Methyl octadecanoate	−0.0446
Chlorobenzene	−0.0254	Butan-2-one	0.0325	Methyl tetradecanoate	−0.0485
2,5-Dimethylphenol	−0.0284	Pentan-2-one	0.0332	Butan-1-ol	−0.0506
1,2-Dichlorobenzene	−0.0315	Dihexyl ether	0.0332	Nonan-1-ol	−0.0616
Bromobenzene	−0.0347	*n*-Butylbenzene	0.0395	Methyl hexadecanoate	−0.0679
cis-Hydrindane	−0.0516	N,N-Dimethylaniline	0.0437	Octan-1-ol	−0.0698
Iodobenzene	−0.0761	Dioxane	0.0485	Pentan-1-ol	−0.2852

QF-1 is still in poor agreement with the other phases. Numerically, rR_2 is generally small compared with $s\pi_2^H$ so that its ability to significantly influence the correlation is not very great. Its inclusion with the properties of factor 3 seems reasonable but is not essential in defining the meaning of factor 3. The π_2^H parameter is a dipole/polarizability parameter and its correlation with properties of factor 1 and 3 is not inconsistent with factor 1 representing the properties of dipolar aliphatic compounds and factor 3 the dipolar and polarizability properties of aromatic compounds. For example benzene and cyclohexane are not considered to have significant dipole character but benzene is significantly more polarizable than cyclohexane and this is reflected in their π_2^H parameters of 0.52 for benzene and 0.10 for cyclohexane. The correlation coefficients are independent of the solute's identity. There is good agreement between the product of the scores and loading coefficients for the 22-phase data set and the 10-phase data set for the solutes they have in common that are highly loaded on the individual factor axes. The score coefficients correlate with the phase constants of Abraham's model for both data sets but the absolute value of the score coefficients depends on the number of data entries and, for this reason, we have made the comparison using the product terms in both models. Thus the original assignments that factor 1 is determined by the capacity for orientation type interactions, factor 2 for solvent hydrogen-bond base interactions, and factor 3 for either induction interactions or aromatic character are reasonable.

Based on these solutions a ranking of stationary phases by their capacity for different intermolecular interactions can be given (Table 5). The relative contributions are scaled within a column but not across rows. The phase QF-1 has significantly different contributions for orientation interactions for aromatic and aliphatic compounds and is omitted to avoid using two scales for this interaction. The score coefficients for principal component factor 1 and principal component factor 3 for the polar interactions obtained from the cavity model are otherwise highly correlated, $r^2 = 0.96$, and differences in

Table 5
A ranking of stationary phases by their capacity for specific interactions based on the score coefficients obtained by principal component factor analysis

Stationary phase	Cavity and dispersion	Stationary phase phase	Orientation	Stationary phase	Hydrogen-bond basicity
DDP	10.39	TCEP	3.94	QBES	3.10
U50HB	10.03	DEGS	3.26	QTS	2.96
OV-105	9.89	QBES	3.14	TCEP	2.42
OV-3	9.87	QTS	2.74	DEGS	2.18
OV-7	9.79	CW-20M	2.62	CW-20M	1.98
SE-30	9.79	OV-225	2.44	THPED	1.91
OV-11	9.55	EGAD	2.28	EGAD	1.72
OV-17	9.38	DDP	2.15	OV-330	1.48
PPE-5	9.14	THPED	1.98	OV-225	1.40
OV-22	8.99	OV-330	1.94	DDP	1.25
OV-25	8.85	OV-25	1.38	U50HB	1.24
THPED	8.68	OV-22	1.31	OV-25	0.72
OV-330	8.59	U50HB	1.20	OV-22	0.64
OV-225	7.69	OV-17	1.15	PPE-5	0.64
QTS	7.57	OV-11	1.04	OV-17	0.59
EGAD	7.57	PPE-5	1.03	OV-11	0.53
CW-20M	7.31	OV-7	0.76	OV-7	0.42
QBES	5.70	OV-3	0.53	OV-105	0.34
DEGS	5.48	OV-105	0.48	OV-3	0.20
TCEP	5.00	SE-30	0.18	SE-30	0.16

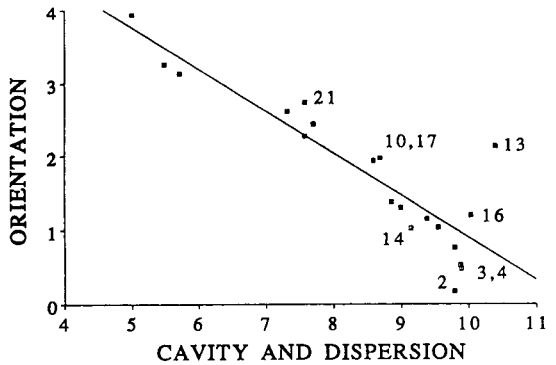

Fig. 4. Plot of the score coefficients representing orientation against the cavity and dispersion contribution from the cavity model. The numbered stationary phases are identified in Table 1.

the ranking are restricted to minor changes in order between coefficients with similar values.

Selectivity differences between phases can be illustrated by plotting the various score coefficients against each other. The plot of orientation against the cavity and dispersion contribution to solution (Fig. 4), indicates the general correlation between the cohesive character of the solvent and its propensity for orientation interactions. TCEP, DEGS and QBES are cohesive solvents with the least favorable contributions for cavity formation. Solutes with a limited capacity for polar interactions will be retained weakly compared to the other phases. DDP is

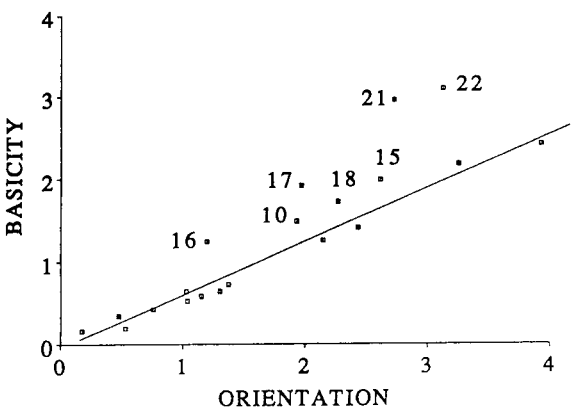

Fig. 5. Plot of the score coefficients representing hydrogen-bond basicity against orientation contributions from the cavity model. The numbered stationary phases are identified in Table 1.

unique in that it has modest demands for cavity formation compared to other solvents of similar polarity. The plot of hydrogen-bond basicity against orientation contributions to solution (Fig. 5) indicates that QBES, QTS, THPED, U50HB, OV-330, CW-20M and EGAD are more basic than other phases of similar orientation capacity. In particular, the two liquid organic salts, QTS and QBES, are strong hydrogen-bond bases. This is expected since they are the only ionic phases present in the data set. As would be anticipated there is no general correspondence between the capacity of a phase to function as a hydrogen-bond base and the cavity and dispersion properties of the same phase. The cohesive character of the solvent will be little influenced by its capacity for hydrogen-bond basicity unless it is simultaneously a hydrogen-bond acid. Since none of the phases were identified as significant hydrogen-bond acids by principal component factor analysis this should not be the general case. The absence of significant hydrogen-bond acidity among the phases studied at the measurement temperature is consistent with other approaches to characterizing the properties of these phases [11].

For the series of poly(methylphenyl)siloxane phases in Table 5 some correspondence between the polar solvent properties of the stationary phases and its composition would be anticipated. This is the general case as illustrated by Eqs. 9–11 below. The individual solvent contributions represented by the score coefficients are well fitted to a second order polynomial function with mol% phenyl groups [P] as the independent variable over the range 0 mol% phenyl groups (SE-30) to 75 mol% phenyl groups (OV-25).

Cavity and dispersion

$$\text{Score} = 9.84 - 1.17 \cdot 10^{-3}[\text{P}] - 1.69 \cdot 10^{-4}[\text{P}]^2$$
$$n = 7,\ r^2 = 0.984 \qquad (9)$$

Orientation

$$\text{Score} = 0.22 + 2.94 \cdot 10^{-2}[\text{P}] - 1.91 \cdot 10^{-4}[\text{P}]^2$$
$$n = 7,\ r^2 = 0.992 \qquad (10)$$

Hydrogen-bond basicity

$$\text{Score} = 0.14 + 1.29 \cdot 10^{-2}[\text{P}] - 7.39 \cdot 10^{-5}[\text{P}]^2$$
$$n = 7,\ r^2 = 0.966 \qquad (11)$$

Principal component factor analysis is a valuable technique for providing insight into the factors affecting the characteristic solvent properties of gas chromatographic stationary phases. Its main limitation is that the solutions provided may not be real in the chemical sense and it is difficult or impossible to distinguish between qualitative factors correlated to a significant extent with real factors. Within these confines the factor solutions extracted from the cavity model seem to be realistic and useful for interpretative purposes. Compared to previous studies where principal component analysis alone was used for interpretation [9,12–16] the factors obtained by rotation are more sensible and are to be preferred.

References

[1] C.E. Figgins, T.H. Risby and P.C. Jurs, *J. Chromatogr. Sci.*, 14 (1976) 453.
[2] R.V. Golovnya and T.A. Misharina, *J. High Resolut. Chromatogr. Chromatogr. Commun.*, 3 (1980) 51.
[3] B.R. Kersten, S.K. Poole and C.F. Poole, *J. Chromatogr.*, 468 (1989) 235.
[4] C.F. Poole and S.K. Poole, *Chem. Rev.*, 89 (1989) 377.
[5] T.O. Kollie and C.F. Poole, *J. Chromatogr.*, 550 (1991) 213.
[6] T.O. Kollie and C.F. Poole, *J. Chromatogr.*, 556 (1991) 457.
[7] M.H. Abraham, G.S. Whiting, R.M. Doherty and W.J. Shuely, *J. Chromatogr.*, 587 (1991) 229.
[8] M.H. Abraham, P.L. Grellier, I. Hamerton, R.A. McGill, D.V. Prior and G.S. Whiting, *Faraday Discuss. Chem. Soc.*, 85 (1988) 107.
[9] C.F. Poole, T.O. Kollie and S.K. Poole, *Chromatographia*, 34 (1992) 281.
[10] P.W. Carr, *Microchem. J.*, 48 (1993) 4.
[11] S.K. Poole and C.F. Poole, *J. Chromatogr. A*, 697 (1995) 415.
[12] T.O. Kollie and C.F. Poole, *Chromatographia*, 33 (1992) 551.
[13] C.F. Poole and T.O. Kollie, *Anal. Chim. Acta*, 282 (1993) 1.
[14] S.K. Poole, T.O. Kollie and C.F. Poole, *J. Chromatogr. A*, 664 (1994) 229.
[15] T.O. Kollie, C.F. Poole, M.H. Abraham and G.S. Whiting, *Anal. Chim. Acta*, 259 (1992) 1.
[16] M.H. Abraham, J. Andonian-Haftvan, I. Hamerton, C.F. Poole and T.O. Kollie, *J. Chromatogr.*, 646 (1993) 351.
[17] D.L. Massart and H.L.O. De Clercq, *Adv. Chromatogr.*, 16 (1978) 75.
[18] J.R. Chretien, *Trends Anal. Chem.*, 6 (1987) 275.
[19] J.R. Chretien, M. Righezza, A. Hassani and B.Y. Meklati, *J. Chromatogr.*, 609 (1992) 261.
[20] E.R. Malinowski, *Factor Analysis in Chemistry*, Wiley, New York, 1991.
[21] R.R. Reyment and K.G. Joreskog, *Applied Factor Analysis in the Natural Sciences*, Cambridge Univ. Press, Cambridge, UK, 1993.
[22] A.L. Comrey and H.B. Lee, *A First Course in Factor Analysis*, Lawrence Erlbaum Associates, Hillsdale, NJ, 2nd ed., 1992.
[23] J.E. Jackson, *A User's Guide to Principal Components*, Wiley, New York, 1991.
[24] I.T. Jolliffe, *Principal Component Analysis*, Springer, New York, 1986.
[25] H.H. Harman, *Modern Factor Analysis*, University of Chicago Press, Chicago, IL, 1976.
[26] M. Forina, S. Lanteri and R. Leardi, *Trends Anal. Chem.*, 6 (1987) 250.

ELSEVIER

Journal of Chromatography A, 697 (1995) 441–451

JOURNAL OF CHROMATOGRAPHY A

New equation for specific retention volumes in capillary column gas chromatography

Rosa Lebrón-Aguilar, Jesús Eduardo Quintanilla-López, Ana María Tello, Alberto Fernández-Torres, José Antonio García-Domínguez*

Instituto de Química Física "Rocasolano", CSIC, Serrano 119, E-28006 Madrid, Spain

Abstract

The evaluation of specific retention volumes in gas chromatography is subject to several sources of error. The use of wall-coated open-tubular columns should yield better values for specific retention volumes. However, on scaling down the flow-rate of the carrier gas, mass of stationary phase and column head pressure, new sources of error are introduced. A careful consideration of the possible sources of error is presented. It was found that, for the use of capillary columns, the classical equation describing the specific retention volume may be modified so that no flow-rates, column head and outlet pressures or mass of stationary phase in the column are necessary in order to obtain correct specific retention volumes.

1. Introduction

Although most often gas–liquid chromatography (GLC) is involved in analytical separations of substances, sometimes it is used for other purposes that involve the evaluation of the specific retention volume (V_g) of solutes, e.g., in thermodynamic studies by inverse gas chromatography (IGC). The parameter V_g is of the greatest importance in chromatography. It is related to the interactions of the solute with the stationary phase (SP). It may be used for identification purposes, although relative retention parameters, such as retention indices or relative retentions, are usually preferred because they are more reproducible and easier to determine. However, it is the key parameter in any work involving thermodynamic studies (such as in the characterization of stationary phases for GC or in the study of relationships between solvents and polymers or polymer–polymer interactions). The accurate determination of V_g values is of great importance in the theory and practice of GLC.

The value of V_g (expressed at 0°C) for a given solute in a particular SP at temperature T_c is given by the equation

$$V_g = \frac{F_c}{W_S} \cdot j(t_R - t_M) \cdot \frac{273.15}{T_c} \quad (1)$$

where

V_g = specific retention volume (ml/g);
F_c = volumetric flow-rate of the dry carrier gas at the column outlet, at the column temperature and ambient pressure (ml/min);
W_S = mass of SP in the column (g);
j = James and Martin's correction factor [1];

* Corresponding author.

0021-9673/95/$09.50
SSDI 0021-9673(94)00806-X

t_R = experimental retention time of the solute (min);

t_M = retention time of a gas which is not retained by the SP (gas hold-up time) (min);

T_c = absolute temperature of the column (K); with symbols used throughout following the recommendations of IUPAC [2].

Retention times, temperatures and pressures are easily measured with the appropriate instruments. In order to have reliable values of V_g, two other magnitudes must be known if Eq. 1 is to be used: the flow-rate of the dry carrier gas at the column outlet (F_c) and the mass of SP in the column, W_S. Most often, a soap-bubble flow meter, capable of a precision of the order of 1% or better for flow-rates of about 5 ml/min or higher, is used to measure the flow of the carrier gas. There are commercial flow meters of various kinds claiming better precision even for lower flow-rates. The amount of SP in a packed column is easily determined using some extraction method [3]. However, when capillary columns are used, both F_c and W_S are very small and, therefore, the precision of the final value of V_g will normally be lower than that obtained on packed columns. With values of flow-rates which might be as low as 0.15 ml/min and amounts of stationary phase of the order of $5 \cdot 10^{-3}$ g, the errors involved may be considerable.

In the course of a study involving the determination of V_g values using capillary columns, we found important variations in the calculated specific retention volumes. Different values were obtained for the same solute in the same column at different flow-rates. Results obtained for the same solute and SP, at the same temperature on different columns, often differing only slightly in length, internal diameter or film thickness, were also different. A careful consideration of the various factors that may affect the precision of the values obtained for both the flow-rate and the mass of Sp in the column led us to establish an equation that is subject to lower experimental errors than the measure of the parameters involved in Eq. 1, when specific retention volumes are determined using capillary columns.

2. Experimental

2.1. Apparatus

Two Hewlett-Packard (HP) 5890A gas chromatographs and a Varian Model 3300 apparatus were used for the experiments with capillary columns. All three gas chromatographs were fitted with a split-type injection system and a flame ionization detector. The HP chromatographs had the standard back-pressure regulator to adjust the carrier gas flows, whereas the Varian apparatus was fitted with the normal pressure regulator placed upstream of the injection port. A few experiments with packed columns were run on an HP 5890 Series II apparatus fitted with a mass flow regulator. All inlet pressures were checked with pressure transducers (Wika Tronic 891.13.500; Alexander Wiegland, Klingenberg, Germany) and numeric displays (Model PM-2900; Félix Mateo, Barcelona, Spain). The pressure readings had a precision of ±67 Pa. Experiments were run isothermally at different temperatures and inlet pressures. Experiments involving mass spectrometry were carried out on a KNK 2000-C Series gas chromatograph (Konik, S. Cugat del Vallés, Spain) coupled to a modified AEI-MS-30 double-focusing mass spectrometer (ionization source, pumping system and detector from VG Analytical, Manchester, UK; electronic console and data system from Mass Spectrometric Services, Manchester, UK).

2.2. Chromatographic columns

Three glass WCOT columns were used in the collection of most of the results reported in this paper. One stainless-steel packed column was used in some experiments. The capillary columns were prepared in our laboratories from borosilicate glass tubes, drawn on a Shimadzu GDM-1B glass drawing machine. The length of the columns was calculated from the diameter of the coils, and the internal diameter was checked with a Nikon microcomparator. The tube walls were leached, washed and dehydrated following the

Table 1
Characteristics of the chromatographic columns

Parameter	Column[a]			
	1	2	3	4
Stationary phase (SP)	PS-255	TFPS35	TFPS35	OV-25
Type	WCOT	WCOT	WCOT	Packed
Length (m)	30.0	23.6	23.6	2.0
I.D. (mm)	0.238	0.225	0.226	2.2
Mass of SP (mg)	6.53	4.92	5.34	2600
Percentage of SP in the packing				15.66
Filling solution of SP (mg/ml)[b]	4.89	5.24	5.64	
Film thickness (μm)	0.29	0.30	0.32	
Deactivation agent	HDMS	TFPMCS	TFPMCS	None
Immobilization agent	DCUP	None	None	None

[a] PS-255 = Polydimethylsiloxane containing 1–3% vinyl groups (Petrarch); TFPS35 = poly(3,3,3-trifluoropropylmethylsiloxane) with 35% substitution of trifluoropropyl group (synthesized in our laboratories [7]); WCOT = wall-coated open-tubular; HDMS = hexamethyldisilazane; TFPMCS = 3,3,3-trifluoropropylmethylcyclosiloxane; OV-25 = polymethylsiloxane with 75% substitution of phenyl groups (Ohio Valley Specialty Chemicals); DCUP = dicumyl peroxide.
[b] Concentration of the solution of SP used to prepare the capillary column.

method described by Grob [4]. The tube was then silanized (see Table 1) according to Blomberg's or Grob's procedures [4–6]. The static method was followed to coat the inner walls of the tube. The amount of SP in the column was calculated from the concentration data of the filling solution and an estimation of the column volume. The packing of the packed column was prepared by evaporation of the mixture of solid support with a solution of the SP in an appropriate solvent, and the percentage of coating was deduced by extraction [3]. The characteristics of the columns are given in Table 1.

2.3. Flow meters

The flow meters used belong to the soap-film type. They were constructed using commercial precision tubes from pipettes. The full scale volumes were 1, 2 and 10 ml. All were made with a water–jacket surrounding the tube. A glass bubble containing part of the soap solution was also fitted inside the water jacket, so that the temperatures of the flow-meter scale and the solution were the same. The volumes of gas monitored in the flow meter were dependent on the actual flow-rate, but they were adjusted so that the time reading was kept at ca. 1 min, in order to minimize errors due to the monitoring of too short times or a different time for each value of the flow-rate. Flow-rates were measured by connecting a rubber tube of the polysiloxane type (I.D. ca. 2 mm) to the flame ionization detector jet (see later for other materials).

2.4. Chromatograms

Chromatograms obtained on capillary columns were measured isothermally at different temperatures from 80 to 160°C, with nitrogen or argon as the carrier gas and with inlet pressures ranging from about 107 to 193 kPa (column outlet pressures ca. 93 kPa). Ambient pressure was checked several times during the day with a mercury barometer (precision 13 Pa). Electronic integrators were used to compute retention times. A mathematical gas hold-up time method [8], based on the retentions of at least four *n*-alkanes, was used to calculate adjusted retention times (t'_R). Once the conditions of the experiment had been established (temperature, column head pressure, etc.), sufficient time was

allowed to elapse to reach equilibrium (see Results for details).

3. Results

3.1. Preliminary results

Specific retention volumes are independent of the chromatographic conditions, with the exception of temperature and the nature of the solute and stationary phase. Therefore, in our preliminary experiments we paid little attention to column length, flow-rate (its effect on column efficiency), film thickness, etc. Our preliminary results for values of V_g obtained with capillary columns for the same solute–SP pair, at the same temperature but at different carrier gas (nitrogen) head pressures for the same column, or values obtained on different columns, were disappointing, with variations (which seemed systematic) as large as 15% (Fig. 1).

3.2. Effect of the various parameters on V_g

An examination of the various factors in Eq. 1 led to the conclusion that, for any one column, errors should not lie on either $T_c(\pm 0.2$ K), $p_i(\pm 67$ Pa), $t_R(\pm 0.1$ s) or W_S (which could be erroneous, but would have the same value for different chromatograms). The factors to be examined more closely are p_o (affecting the values of both j and F_c), t_M (which might give erroneous adjusted retention times) and F_c, for a single column, and also W_S if two or more columns are to be compared. A few checks on the different parameters were carried out with the following results.

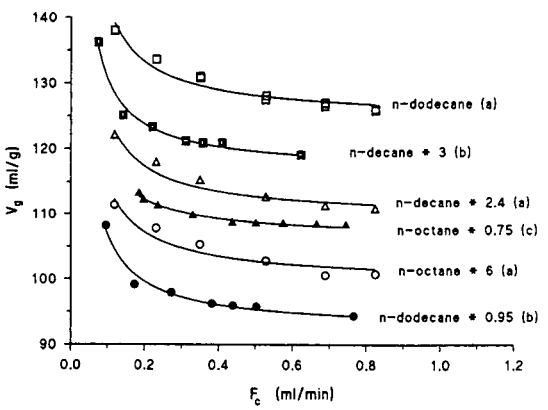

Fig. 1. Specific retention volumes of a few solutes at different flow-rates. Preliminary results. (a) Column 3 (Table 1), 120°C; (b) column 1, 160°C; (c) column 1, 80°C. Carrier gas, nitrogen. *n*-Decane * 3, for example, means that the value of V_g of *n*-decane shown in the plot is three times the correct value.

Gas hold-up time (t_M)

If our method to calculate t_M was erroneous, the values of t'_R would carry larger errors in the early-eluting peaks than for the higher *n*-alkanes. Table 2 gives results for three different columns for various flow-rates. Errors, expressed as a percentage of the lowest value, are roughly independent of the retention time of the solute, indicating that there is no significant error in the gas hold-up time method used to calculate t_M.

Column head and outlet carrier gas pressures (p_i, p_o)

An error of 67 Pa in the value of p_i will produce an error in j below 0.1%. The ambient pressure was measured with a precision of 13 Pa. However, the narrow jet tip of the flame ionization detector, bearing in mind the addition of about 35 ml/min of H_2, 30 ml/min of make-up gas (N_2) and the high temperature of the detector (viscosity of gases increases with temperature), might produce an appreciable pressure drop, with an effect on p_0 (and hence j) and also on the real value of the flow-rate, governed by Poiseuille's law, which for capillary columns is given [9] by the expression

$$F_c = \frac{\pi r_c^4}{16\eta L} \cdot \frac{p_i^2 - p_o^2}{p_o} \qquad (2)$$

were r_c is the column radius, η is the viscosity of the gas, L is the column length and p_i and p_o are the inlet and outlet carrier gas pressures respectively. Considering the effect of p_o on both F_c and j, an unobserved increase of 1.3 kPa in p_o would produce an experimental value of V_g 1.1% higher than the real value, for a head pressure of

Table 2
Calculated specific retention volumes

p_i (kPa)	F_c (ml/min)	Specific retention volume (ml/g)						
		n-Hexane	*n*-Heptane	*n*-Octane	*N*-Nonane	*n*-Decane	*n*-Undecane	*n*-Dodecane
Column 1, 80°C								
117	0.186	35.88	73.33	150.9	310.4	639.4	1307	2650
120	0.198	35.53	72.89	149.5	307.5	632.8	1295	2649
135	0.331	34.38	70.26	146.3	303.7	625.7	1280	2618
147	0.438	34.47	70.53	144.9	297.8	611.6	1250	2552
153	0.502	34.47	70.53	144.7	297.3	610.5	1248	2547
160	0.577	34.47	70.53	144.6	297.1	609.8	1246	2543
175	0.745	34.38	70.35	144.4	296.1	607.8	1242	2533
$\Delta V_g(\%)$[a]		4.4	4.1	4.5	4.8	5.2	5.3	4.6
Column 1, 160°C								
107	0.090	7.10	11.23	17.98	28.60	45.44	71.93	113.9
120	0.174	6.58	10.44	16.58	26.31	41.67	65.96	104.4
133	0.273	6.58	10.35	16.40	25.96	41.14	65.18	103.1
147	0.382	6.40	10.18	16.14	25.53	40.44	64.04	101.3
153	0.439	6.40	10.09	15.96	25.44	40.26	63.77	101.0
160	0.503	6.40	10.09	16.05	25.44	40.26	63.68	100.8
186	0.766	6.31	10.00	15.79	25.00	39.74	62.81	99.32
$\Delta V_g(\%)$[a]		12.7	12.0	13.9	14.4	14.4	14.5	14.7
Column 3, 120°C								
107	0.119	6.77	11.14	18.57	30.74	50.78	83.78	138.0
119	0.232	–	–	17.97	29.67	49.10	80.94	133.6
131	0.350	6.40	10.60	17.55	29.03	47.97	79.32	130.9
147	0.368	6.26	10.20	17.14	28.34	46.86	77.44	127.9
160	0.479	6.05	10.04	16.77	27.90	46.28	76.61	126.8
171	0.573	6.10	10.12	16.81	27.85	46.11	76.22	126.0
$\Delta V_g(\%)$[a]		12.3	11.2	11.1	10.6	10.2	10.0	9.6

[a] ΔV_g is the percentage error calculated as $100(V_{gl} - V_{gh})/V_{gh}$, where V_{gl} and V_{gh} are the V_g calculated at low (l) and high (h) flow-rates, respectively.

200 kPa, and an increase of 3.4% when the head pressure is 133 kPa. Experiments carried out with jet tips of large I.D., with and without make up gas, produced values of V_g that differed by only about 0.3% from those obtained with the normal narrow jet tip.

Flow-rate

The last factor to be considered for measurements corresponding to a single column is the flow-rate, which, according to the previous discussion, should be the source of the observed errors. The flow-rate measured is the volumetric flow-rate of the carrier gas in the flow meter, F, saturated with water vapour in the case of the soap-film type. Its relationship to the flow-rate at the column outlet is

$$F_c = F\left(1 - \frac{p_w}{p_a}\right)\frac{T_c}{T_a} \quad (3)$$

where p_w is the calculated vapour pressure of the water at the temperature of the flow meter, p_a is the ambient pressure and T_a is the absolute temperature of the flow meter.

An important point that is sometimes overlooked is the time needed to reach stable conditions after a change of column, head carrier gas pressure or column temperature. Our experience is as follows: whenever a column is installed in the gas chromatograph, a minimum

of 12 or even 24 h are needed to reach stable conditions. Retention times measured after 6 h are larger than those obtained on the following and subsequent days. This long period of time does not depend on the temperature of the column, which can be left cold overnight. Once retention times are reproducible after this long period, a change of inlet pressure produces reproducible retention times in little more than 1 h, and they remain constant for hours or days. Finally, our experience with a change of temperature is that reproducibility is reached in only a few minutes.

The various factors involved in Eq. 3 will not affect the value of F_c in the same way. T_a, p_a and T_c can be measured very accurately, and the errors would never justify the observed variations in V_g for one solute and column. The value of p_w is known, but it might happen that the gas in the flow meter was not saturated with water vapour. If this was the case, the experimental V_g values would be higher for the high flow-rates. The tendency observed in Fig. 1 is the opposite, so this could not be the cause of the errors in V_g.

Other possibilities were considered: diffusion of gas through the soap film, evaporation of water from the soap solution and diffusion of the gas through the walls of the tube connecting the gas chromatograph to the flow-meter.

If an appreciable diffusion of nitrogen through the soap film takes place, it is reasonable to consider that the effect should be less evident with a heavier gas [10]. In order to check this further, argon was used as the carrier gas. Again, errors that seem to be associated to the flow rate were found, but in this case the variations observed have the opposite sign to that with nitrogen: V_g values corresponding to low flow-rates are low. Fig. 2 shows the two curves obtained with N_2 and Ar for the same substance. The curves seem to converge on a value at high flow-rates, suggesting that errors are smaller for the higher flow-rates.

Water could evaporate from the walls of the flow meter if the gas was not saturated with water vapour. Passing several bubbles through the tube before the actual reading is taken should minimize this effect [11]. Even so, the

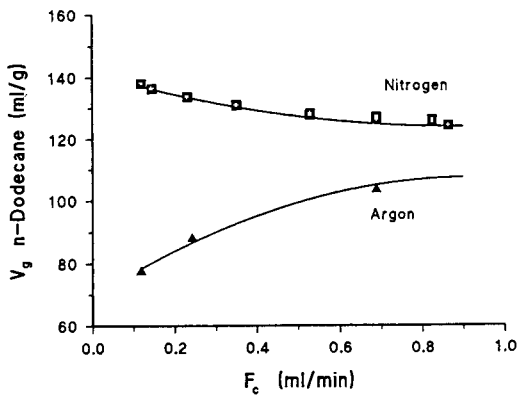

Fig. 2. Experimental specific retention volumes of *n*-dodecane on column 3 (TFPS35) at 120°C, with nitrogen and argon as carrier gases.

effect, if present, could be more evident if a larger volume is used to monitor flow-rates. Table 3 shows that above, say, 0.3 ml (a reading of about 60 s) the error of the flow reading does not depend on the actual volume monitored.

The last possibility to be considered is that gas passes through the walls of the tube that connects the gas chromatograph to the flow meter in a sufficient amount to affect the low flow-rates used in connection with capillary columns. To this end, different tube lengths were used to monitor a given flow-rate, confirming that the ratio of the V_g values obtained with low and high flow-rates were roughly proportional to the tube length used, for both nitrogen and argon (Fig. 3). This might explain why the experimental points in Fig. 1 are slightly scattered round each curve: we did not always use the same length of rubber tubing in our preliminary experiments. Considering that all checks had been carried out using the normal polysiloxane tubing often found in laboratories, other tube materials were used: copper, stainless steel, PTFE and nylon. Table 4 shows that the flow-rate measured does not seem to depend on the material of the connecting tube, with the exception of polysiloxane, which gives high values with nitrogen and low values with argon. Experiments carried out at higher flow-rates (packed column) showed that the errors involved with the use of the polysiloxane material are insignificant for flow-rates above

Table 3
Effect of the volume used in the flow meter to monitor flow-rates

Parameter	Volume in the flow meter meter (ml)					
	0.1	0.2	0.3	0.4	0.6	0.8
F (ml/min)	0.309	0.310	0.312	0.314	0.314	0.313
R.S.D.[a] (%)	0.6	0.5	0.4	0.2	0.3	0.4

Each point is the average of five measurements. p_i = 153 kPa; column 1, 160°C.
[a] Relative standard deviation.

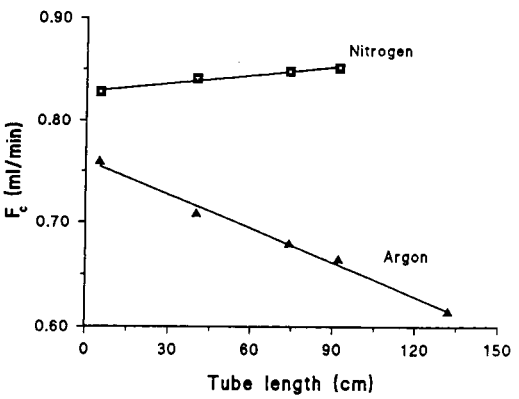

Fig. 3. Effect of the length of the polysiloxane connecting tube (chromatographic column–flow meter) on the experimentally measured flow-rate. Column 3, 120°C; inlet pressure for N_2, 173 kPa; inlet pressure for Ar, 186 kPa.

about 3 ml/min (ambient pressure). Table 5 shows that the specific retention volumes do not depend on the nature of the carrier gas or the flow-rate if the latter is measured using a copper connecting tube. The small difference between low and high flow-rates is probably due to the fact that the copper tube was connected to the gas chromatograph and to the flow meter using a very short length of polysiloxane tubing.

The last experiments described seem to indicate that air (or oxygen) could diffuse through the walls of the polysiloxane tube (when nitrogen is the carrier gas) in sufficient amount to increase the flow-rate reading. In other words, the flow through the column is lower than the flow through the flow meter, and the difference is constant but more evident at low flow-rates. When argon is used as the carrier gas, the argon, with a higher atomic mass, diffuses through and out of the walls at a higher rate than the air diffuses through into the tube, so the reading at the flow meter is lower than the value at the end of the column, and this is more evident at low flow-rates.

In order to check the validity of this argument, two series of experiments involving a mass spec-

Table 4
Experimental flow-rates measured using different connecting tubes between the chromatograph and the flow-meter

Material	Column 3 (capillary)			Column 4 (packed)		
	Nitrogen		Argon	Nitrogen		
Polysiloxane	0.153	0.714	0.687	1.07	2.49	9.20
Copper	0.142	0.689	0.787	1.04	2.46	9.18
Nylon	0.141	0.689	0.786	1.05	2.46	9.18
Stainless steel	0.142	0.689	0.789	–	–	–
PTFE	0.142	0.691	0.787	1.05	2.46	9.18
p_i(kPa)	98	162	186	101	110	146

Column temperature, 120°C.

Table 5
Experimental specific retention volumes of *n*-alkanes using copper tubing to connect the gas chromatograph to the flow-meter

Alkane	V_g(ml/g)			
	Nitrogen		Argon	
n-Hexane	6.16	6.08	6.16	5.94
n-Heptane	10.17	10.03	10.35	9.79
n-Octane	16.77	16.50	16.75	16.27
n-Nonane	27.78	27.30	27.64	27.01
n-Decane	45.87	45.01	45.61	44.59
n-Undecane	75.81	74.20	75.25	73.66
n-Dodecane	124.91	122.09	123.79	121.28
p_i(kPa)	112	163	130	187
F_c(ml/min)	0.141	0.689	0.249	0.787

Column 3, 120°C.

trometer were performed. In the first series, the gas leaving the chromatographic column (helium) was fed directly into the ionization source of a mass spectrometer through a direct line of fused-silica tubing of 0.06 mm I.D. The column–direct line connection was done using various tubes of different materials. The mass peaks of air (*m/z* 28 and 32) in the carrier gas increased for the different materials in the order copper <nylon <PVC <PTFE <polysiloxane. Taking the nitrogen level in the carrier gas when a copper tube is used as the background value of the mass spectrometer, the effect of the air intake on V_g would be that an inlet pressure of about 113 kPa would give approximate errors as follows: nylon, +0.03%; PVC, +0.1%; PTFE, +1%; and polysiloxane, +10%. In the second series of experiments, the polysiloxane tube (4 mm O.D.) that connects the GC column to the fused-silica tubing, was surrounded with a nylon tube (6 mm I.D.). Helium was passed through both tubes, and the gas leaving the outer tube was fed to the mass spectrometer to check the presence of a peak at a nominal mass of 40. Later, the gas in the inner tube was changed to argon, and a few minutes later the presence of a mass peak at a nominal value of 40 could be detected in the gas leaving the outer tube, at a concentration that was independent of the flow-rate in the inner tube. These two experiments confirm that the permeability of the polysiloxane tube is sufficient to invalidate any reading of low flow-rates such as those used in capillary column gas chromatography.

3.3. New equation for V_g

The above discussion makes it clear that measuring specific retention volumes of solutes in capillary columns is subject to serious sources of error. The precise determination of low flow-rates is such a case, even if attention is paid to the tube material used to connect the chromatographic column to the flow-meter. To know the exact amount of SP in the column, which involves a precise knowledge of both its length and its internal diameter, and the values of both head and ambient pressures with sufficient precision are other sources of error that should be eliminated if a reliable value of V_g is to be expected. In order to eliminate some of the sources of error, Eq. 1 must be modified. Some of the magnitudes in Eq. 1 can be expressed as follows:

$$F_c = V_M/t_M = V_M^0/t_M j \quad (4)$$

$$V_M^0 = (L\pi/4)(d_c - 2d_f)^2 \quad (5)$$

$$W_S = CL\pi d_c^2/4 \quad (6)$$

where

F_c = flow-rate of carrier gas expressed at am-

bient pressure and column temperature, T_c(ml/min);
V_M = hold-up volume (cm^3);
V_M^0 = corrected gas hold-up volume (cm^3);
d_c = I.D. of the column tube (cm);
d_f = SP film thickness (cm);
L = length of the column (cm);
C = concentration of the SP in the solution used to fill the capillary tube in the preparation of the chromatographic column (g/ml).

Bearing in mind that the retention factor (also called capacity factor) k is equal to $(t_R - t_M)/t_M$, Eq. 1 may be rewritten as

$$V_g = \frac{k}{C} \cdot \frac{(d_c - 2d_f)^2}{d_c^2} \cdot \frac{273.15}{T_c} \quad (7)$$

The magnitudes k, C and T_c are easily measured, but both the I.D. of the column and the film thickness are more difficult to estimate. If a microcomparator or other magnifying device is available, the I.D. of the column may be measured, but with the uncertainty about the homogeneity or consistency of the column diameter along its length. We have no experience about the precision with which the commercial fused-silica tubes are sold.

The uncertainty in the estimation of V_g through Eq. (7) stems from the term $(d_c - 2d_f)^2/d_c^2$, which can be expressed in a different form. The film thickness, d_f, is a function of both the mass, W_S, and the density, ρ of the SP, and the internal surface of the column ($L\pi d_c$):

$$d_f = \frac{1}{\rho} \cdot C \cdot \frac{L\pi d_c^2}{4} \cdot \frac{1}{L\pi d_c} = \frac{Cd_c}{4\rho} \quad (8)$$

hence

$$\frac{(d_c - 2d_f)^2}{d_c^2} = \left(1 - \frac{C}{2\rho}\right)^2 \quad (9)$$

and therefore

$$V_g = \frac{k}{C}\left(1 - \frac{C}{2\rho}\right)^2 \frac{273.15}{T_c} \quad (10)$$

With this equation, neither d_c nor d_f is needed. The main uncertainty that remains in Eq. 10 lies in the value of the density of the SP, ρ, at the column temperature. The densities of the polymers or other substances normally used as SPs in GC or substances used in IGC experiments may vary [12] from 0.8 to 1.25 at 50°C and from 0.7 to 1.1 at 250°C. Table 6 summarizes the percentage error involved in the estimation of V_g, if a fixed value of 0.9 or 1.0 g/ml is selected for the density of the SP. Considering the small effect that the value of ρ has on the final value of V_g calculated according to Eq. 10, and bearing in mind that its determination involves a careful experimental set-up, it seems reasonable to use the following simplified expression:

$$V_g = \frac{k}{C}\left(1 - \frac{C}{2}\right)^2 \frac{273.15}{T_c} \quad (11)$$

This equation should be reasonably safe for temperatures up to about 100 or 150°C, whereas for higher temperatures (150–250°C) a density of 0.9 for the SP might be selected for a safer estimation of V_g.

The use of Eq. 10 or 11 has several important advantages over Eq. 1. Determination of specific retention volumes with capillary columns is reduced to the careful preparation of the solution of the SP in an appropriate solvent, the making of the column by the static method and the measure of retention times in a chromatograph in which the temperature of the column oven should be homogeneous, and known with a certain precision. No flow-rates, head and ambient pressures (allowing for detector pressure drop) or mass of stationary phase in the column are needed in order to obtain reliable specific retention volumes with errors not larger than those involved in the evaluation of the concentration of SP in the filling solution if Eq. 10 is used, or an additional 0.20% or less if Eq. 11 is preferred.

Table 7 shows values of V_g calculated with Eq. 11 using the same set of chromatograms that served to plot some of the points shown in Fig. 1 (*n*-octane, *n*-decane and *n*-dodecane at 120°C). It may be observed that the specific retention volumes obtained for the same solute do not depend on the inlet pressure or the nature of the

Table 6
Percentage errors in the specific retention volumes calculated with Eq. 10 for stationary phases of different densities if a density of 0.9 or 1.0 is assumed

Real density of SP	Concentration of the filling solution, C (g/ml)					
	0.004		0.005		0.006	
	Value taken for ρ		Value taken for ρ		Value taken for ρ	
	0.9	1.0	0.9	1.0	0.9	1.0
0.7	0.13[a]	0.17	0.16	0.21	0.19	0.25
0.8	0.06	0.10	0.07	0.13	0.08	0.15
0.9	0.00	0.05	0.00	0.06	0.00	0.07
1.0	−0.04	0.00	−0.06	0.00	−0.07	0.00
1.1	−0.08	−0.04	−0.10	−0.05	−0.12	−0.05
1.2	−0.11	−0.07	−0.14	−0.08	−0.17	−0.10
1.3	−0.14	−0.09	−0.17	−0.12	−0.21	−0.14
d_f (μm)[b]	0.25		0.31		0.38	

[a] 0.13, for example, means that the value obtained is 0.13% higher than the correct value.
[b] Thickness of the stationary phase film for a hypothetical column of 0.25 mm I.D. and a value of ρ of 1 g/ml.

carrier gas. For any one column, the small variations, which decrease as the number of carbon atoms of the alkane increases, suggest that they are due to small errors in the measurement of the corresponding retention times. The systematic difference observed between columns (below 2%) is due to errors in the preparation of the solution of the SP. Fig. 4 shows the result of applying Eq. 11 to the experimental results which served to create Fig. 2. The broken horizontal line represents the average value of the specific retention volume of *n*-dodecane obtained with Eq. 11. It may be observed that the new experimental V_g values are independent of the nature of the carrier gas or flow-rate (pressure drop).

4. Conclusions

Many of the errors involved in the determination of specific retention volumes in GC using

Table 7
Values of specific retention volume obtained with Eq. 11 (mean values ± standard deviation of between five and fourteen experiments)

Column	p_i (kPa)	Gas	V_g(ml/g)						
			n-Hexane	*n*-Heptane	*n*-Octane	*n*-Nonane	*n*-Decane	*n*-Undecane	*n*-Dodecane
2	115	N_2	5.97 ± 0.03	9.84 ± 0.04	16.23 ± 0.06	26.87 ± 0.04	44.34 ± 0.04	73.13 ± 0.07	120.34 ± 0.17
	130	Ar	5.98 ± 0.05	9.85 ± 0.09	16.27 ± 0.09	26.88 ± 0.08	44.39 ± 0.12	73.18 ± 0.15	120.39 ± 0.24
	161	N_2	5.97 ± 0.06	9.83 ± 0.11	16.26 ± 0.06	26.89 ± 0.09	44.44 ± 0.10	73.26 ± 0.10	120.54 ± 0.13
	186	Ar	6.09 ± 0.10	10.02 ± 0.17	16.45 ± 0.17	27.08 ± 0.16	44.53 ± 0.20	73.22 ± 0.23	120.38 ± 0.27
3	112	N_2	5.90 ± 0.05	9.74 ± 0.08	16.08 ± 0.09	26.60 ± 0.09	43.94 ± 0.10	72.60 ± 0.19	119.62 ± 0.37
	130	Ar	5.93 ± 0.05	9.79 ± 0.09	16.15 ± 0.05	26.65 ± 0.07	43.99 ± 0.02	72.57 ± 0.08	119.41 ± 0.21
	163	N_2	5.91 ± 0.11	9.76 ± 0.18	16.07 ± 0.19	26.56 ± 0.20	43.83 ± 0.19	72.29 ± 0.32	118.98 ± 0.47
	187	Ar	5.80 ± 0.01	9.56 ± 0.01	15.90 ± 0.01	26.39 ± 0.08	43.57 ± 0.06	71.98 ± 0.16	118.50 ± 0.19

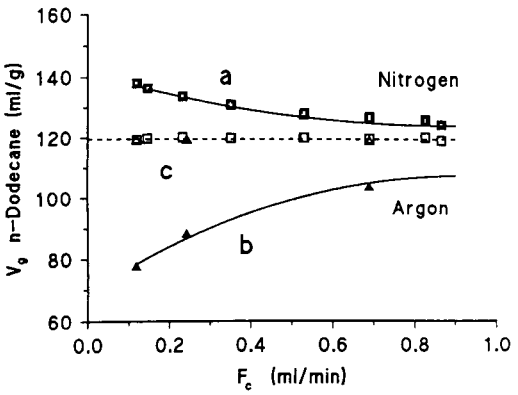

Fig. 4. Experimental specific retention volumes of *n*-dodecane on column 3 (TFPS35) at 120°C, with nitrogen and argon as carrier gases, obtained by applying Eq. 1 (curves a and b), and values obtained by applying Eq. 11 to the same set of experimental results using (△) argon and (□) nitrogen. Line c represents the average value of the specific retention volumes obtained with Eq. 11.

capillary columns are eliminated by the use of the new equation proposed here (Eq. 10 or its simplified version, Eq. 11). Reliable values of V_g will be obtained from data from the chromatogram and the concentration of the solution that served to prepare the chromatographic column. The experimental set-up is also simplified by the elimination of the need for measuring carrier gas pressures or flow-rates. Good pressure regulation and temperature control of the column oven is all that is required of the gas chromatograph.

Acknowledgement

This work was performed with the financial assistance of the Dirección General de Investigación Científica y Técnica of Spain, under Project PB91-0077.

References

[1] A.T. James and J.P. Martin, *Biochem. J.*, 50 (1952) 679.
[2] L.S. Ettre, *Pure Appl. Chem.*, 65 (1993) 819.
[3] E. Fernández-Sánchez, J.A. García-Domínguez, J. García-Muñoz and M.J. Molera, *J. Chromatogr.*, 299 (1984) 151.
[4] K. Grob, *Making and Manipulating Capillary Columns for Gas Chromatography*, Hüthig, Heidelberg, 1986.
[5] L. Blomberg, K. Markides and T. Wännman, *J. High Resolut. Chromatogr. Chromatogr. Commun.*, 3 (1980) 527.
[6] L. Blomberg, J. Buijten, K. Markides and T. Wännman, *J. Chromatogr.*, 239 (1982) 51.
[7] Q. Dai, R. Lebrón-Aguilar, E. Fernández-Sánchez, J.A. García-Domínguez and J.E. Quintanilla-López, *J. High Resolut. Chromatogr.*, 16 (1993) 721.
[8] J.A. García-Domínguez, J. García-Muñoz, E. Fernández-Sánchez and M.J. Molera, *J. Chromatogr. Sci.*, 15 (1977) 520.
[9] W.E. Harris and H.W. Habgood, *Programmed Temperature Gas Chromatography*, Wiley, New York, 1966.
[10] S. Wičar, *J. Chromatogr.*, 295 (1984) 395.
[11] A.E. Bolvari, T.C. Ward, P.A. Koning and D.P. Sheehy, in D.R. Lloyd, T.C. Ward and H.P. Schreiber (Editors), *Inverse Gas Chromatography (ACS Symposium Series)*, American Chemical Society, Washington, DC, 1989, Ch. 2, p. 12.
[12] B.R. Kersten, S.K. Poole and C.F. Poole, *J. Chromatogr.*, 468 (1989) 235.

ELSEVIER

Journal of Chromatography A, 697 (1995) 453–459

JOURNAL OF CHROMATOGRAPHY A

Identification of furan fatty acids in human blood cells and plasma by multi-dimensional gas chromatography–mass spectrometry

Hans Günther Wahl[a,*], Anke Chrzanowski[a], Christiane Müller[a], Hartmut M. Liebich[a], Andreas Hoffmann[b]

[a]*Medizinische Universitätsklinik, Abt. IV, 72076 Tübingen, Germany*

[b]*Gerstel GmbH, Aktienstrasse 232–234, 45473 Mülheim an der Ruhr, Germany*

Abstract

The separation and determination of low-concentration furan fatty acids in complex sample matrices, such as oils, tissue lipids or blood, previously required time-consuming pre-analytical separation steps in order to obtain sufficient resolution in single-column gas chromatography. By using a multi-dimensional GC–MS system, it is now possible to identify directly the methyl esters of furan fatty acids without any further pre-analytical separations. The Folch method was used to isolate the lipids from the different blood components and transesterification of total lipids was carried out by sequential saponification and esterification. Individual lipid classes were isolated by preparative TLC separation and transesterified into their methyl esters by a one-step reaction using acetyl chloride as catalyst. Furan fatty acids were found in all blood samples in differing relative amounts. 12,15-Expoxy-13,14-dimethyleicosa-12,14-dienoic acid (F6) and 12,15-epoxy-13,14-dimethyloctadeca-12,14-dienoic acid (F4) were detected in both red blood cells and in plasma; in platelets, only F6 was found. In serum, furan fatty acids were detected only in the phospholipid fraction, and not in cholesterol esters or triglycerides.

1. Introduction

As one of the first furan fatty acids (F-acids, Fig. 1), disubstituted 9,12-epoxyoctadeca-9,11-dienoic acid was found in the seed oil of *Exocarpus cupressiformis* in 1966 [1]. A series of tri- and tetrasubstituted propyl- and pentyl-side-chain F-acids were later demonstrated to be present in different species of fish [2–8], soft corals [9], different plants [10,11], vegetable oils [12,13], amphibians [14], reptilians [14] and mammals [15,16], including man [17]. Elaborate studies on hepatopancreatic lipids of the crayfish *Procambarus clarkii* revealed a total of 30 F-acids [14].

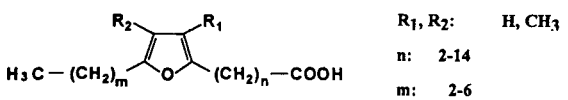

Fig. 1. Structure of furan fatty acids.

The presence of dibasic furanpropionic acids in human urine [18] and blood [19] led to further metabolic studies in which the F-acids were regarded as possible precursors [20–23]. Supporting this theory is the fact that hyperlipidaemic patients treated with fish oil showed an increase in the serum concentration of 3-

* Corresponding author.

SSDI 0378-4347(94)01083-8

carboxy-4-methyl-5-propyl-2-furanpropionic acid soon after treatment had stated [22]. Later it was shown that the fish oil used contained fourteen different furan fatty acids [24]. 3-Carboxy-4-methyl-5-propyl-2-furanpropionic acid, as one of the two major furanpropionic acids, proved to be a metabolite with several adverse biochemical and physiological effects [25,26], especially in connection with chronic renal failure, where it is found at highly elevated levels in plasma [27–30]. The origin, metabolism and possible physiological role of furan acids are not yet clearly understood and the success of further clinical studies will also depend strongly on the quality of the analytical techniques applied.

In order to obtain sufficient resolution in single-column gas chromatography, several pre-analytical steps were applied in the past for the analysis of furan fatty acids in complex matrices. After extraction and transesterification, various conditions for hydrogenation were used, which affected only the unsaturated fatty acids and left the furan ring unchanged [2,3,14,16,31]. F-acids have also been separated from polyunsaturated fatty acids by argentation TLC [1,3–7,11–13], in which the methyl esters of furan fatty acids migrate closely behind the saturated and monoene acids. Following hydrogenation or argentation TLC, F-acids were separated from saturated straight-chain fatty acids by urea fractionation, as the F-acid methyl esters do not form urea inclusion complexes [2,3,5–7,14,16,31].

Yet another method is hydrogenation with 5% rhodium on aluminium oxide in hexane under a 150 kPa hydrogen pressure for 2 h, which will attack the furan ring, thus yielding isomeric tetrahydrofuran derivatives [10,17]. According to the *syn*-addition of hydrogen, the all-*cis* configurations in amounts up to 88% of the four isomers were formed [17]. After separation by TLC the tetrahydrofuran derivatives were identified and quantified by single-column GC–MS [10,17].

This paper describes a method for the identification of furan fatty acids in different blood components. After lipid extraction and transesterification, the methyl esters can directly be identified by the use of a multi-dimensional GC–MS system without any further pre-analytical separations. This technique should also be applicable to any other minor component fatty acid in complex sample matrices.

2. Experimental

2.1. Chemicals

All solvents and reagents used were of the highest grade available. The reference lipids for the TLC separation were purchased from Sigma Chemie (Deisenhofen, Germany). TLC plates (20 cm × 20 cm glass plates precoated with a 0.25-mm layer of silica gel 60) were obtained from Merck (Darmstadt, Germany).

2.2. Sample preparation

Red blood cells, platelets and plasma were obtained from the local blood bank in a very high purity separation. Lipids from blood samples (20 ml) were extracted by the method of Folch et al. [32]. For red blood cells, both total cells and membranes [33] were used. The lipid extracts were transesterified by sequential saponification and esterification [34,35]. The reaction was carried out under a nitrogen atmosphere to avoid oxidation of polyunsaturated fatty acids. Individual lipid classes of cholesterol esters, triglycerides and phospholipids were isolated by preparative TLC separation [36] and transesterified by a modified one-step reaction [36,37] as reported by Lepage and Roy [38,39].

2.3. GC–MS system

Electron impact ionization was performed with a Hewlett-Packard (Avondale, PA, USA) HP 5890/5971 GC–MS system equipped with an HP 7673 automatic sampler and a 25 m × 0.2 mm I.D. × 0.33 μm HP-1 (dimethylpolysiloxane) column. The column head pressure was set to 60 kPa and the injection volume was 1 μl with a splitting ratio of 1:10. The injector and the transfer line temperatures were 280 and 300°C, respectively; after injection, the column temperature was programmed at 2°C/min from 130

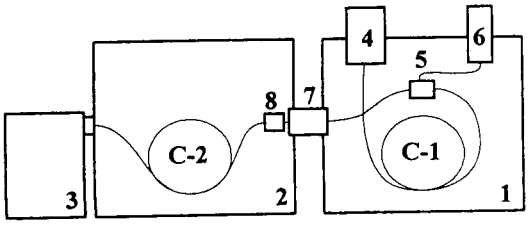

Fig. 2. Schematic diagram of the multi-dimensional system applied. 1 = GC oven with precolumn C-1; 2 = GC oven with analytical column C-2; 3 = mass-selective detector; 4 = cold injection system CIS-3; 5 = column-switching device; 6 = flame ionization detection (FID) monitor; 7 = cryotrap; 8 = second switching device.

to 300°C, the final temperature being held for 20 min.

2.4. Multi-dimensional GC–MS

Fig. 2 shows schematically the various components used to configure the system employed for this work. The apparatus consists of a temperature-programmable cold injection system with a septumless sampling head (CIS-3; Gerstel, Mülheim an der Ruhr, Germany), two HP 5890 GC ovens (Hewlett Packard, Avondale PA, USA), connected via a heated transferline incorporating a cryotrap (CTS-1, Gerstel, Mülheim an der Ruhr, Germany). The second oven is equipped with an HP 5971 A mass-selective detector (Hewlett Packard).

For column switching and transfer of cuts, the cryotrap is cooled with liquid nitrogen from its normal temperature of 200°C to −150°C 2 min before the cut, followed by heating at 12°C/s to 280°C for "reinjection" of the focused cut to the second column and to the MS detector.

2.5. Analytical conditions

The following conditions were used:

Columns:	
Precolumn C-1	HP 1 (Hewlett-Packard), 25 m × 0.32 mm I.D. × 1.05 μm
Analytical column C-2	Stabilwax (Restek) 30 m × 0.25 mm I.D. × 0.25 μm
Pneumatics:	
Carrier gas (He)	p_i = 130 kPa, split 1:20 p_c = 40 kPa, 10 ml/min, p_{c1} = 35 kPa
FID	H_2, 30 ml/min; air, 300 ml/min; N_2, 30 ml/min
Temperatures:	
CIS	80°C $\xrightarrow[5°C/min]{12°C/s}$ 300°C
GC oven 1	200°C $\xrightarrow{5°C/min}$ 300°C
GC oven 2	180°C $\xrightarrow{12°C/s}$ 240°C
CTS	280°C $\xrightarrow{12°C/s}$ −150°C −150°C ⟶ 280°C
FID	320°C
MS	280°C

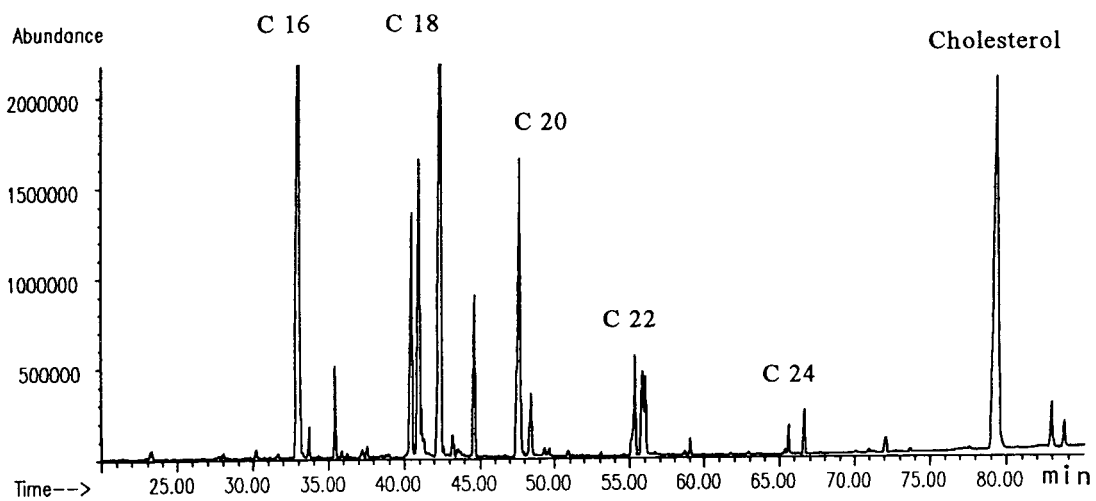

Fig. 3. Total ion chromatogram of red blood cells.

Detectors:

Monitor detector in GC 1	FID
Main detector in GC 2	MSD, scan 50–450 u

3. Results and discussion

After transesterification of the lipid extracts, the samples were analysed by single-column GC–MS (see Fig. 5a) in order to determine the retention times used later for the cuts in multi-dimensional GC–MS (see Fig. 5b) together with the FID monitor's chromatogram. It was also used to characterize the fatty acid compositions of red blood cells, platelets and plasma.

3.1. Single-column chromatography

The major fatty acid components found in the blood samples were palmitic (C16:0), linoleic (C18:2, ω6), oleic (C18:1, ω9), stearic (C18:0) and arachidonic acid (C20:4, ω6). In plasma linoleic acid showed the highest relative concentration (26% of total fatty acids), followed by palmitic and oleic (21–24%), stearic (8%) and arachidonic acid (5%). The five major fatty acid

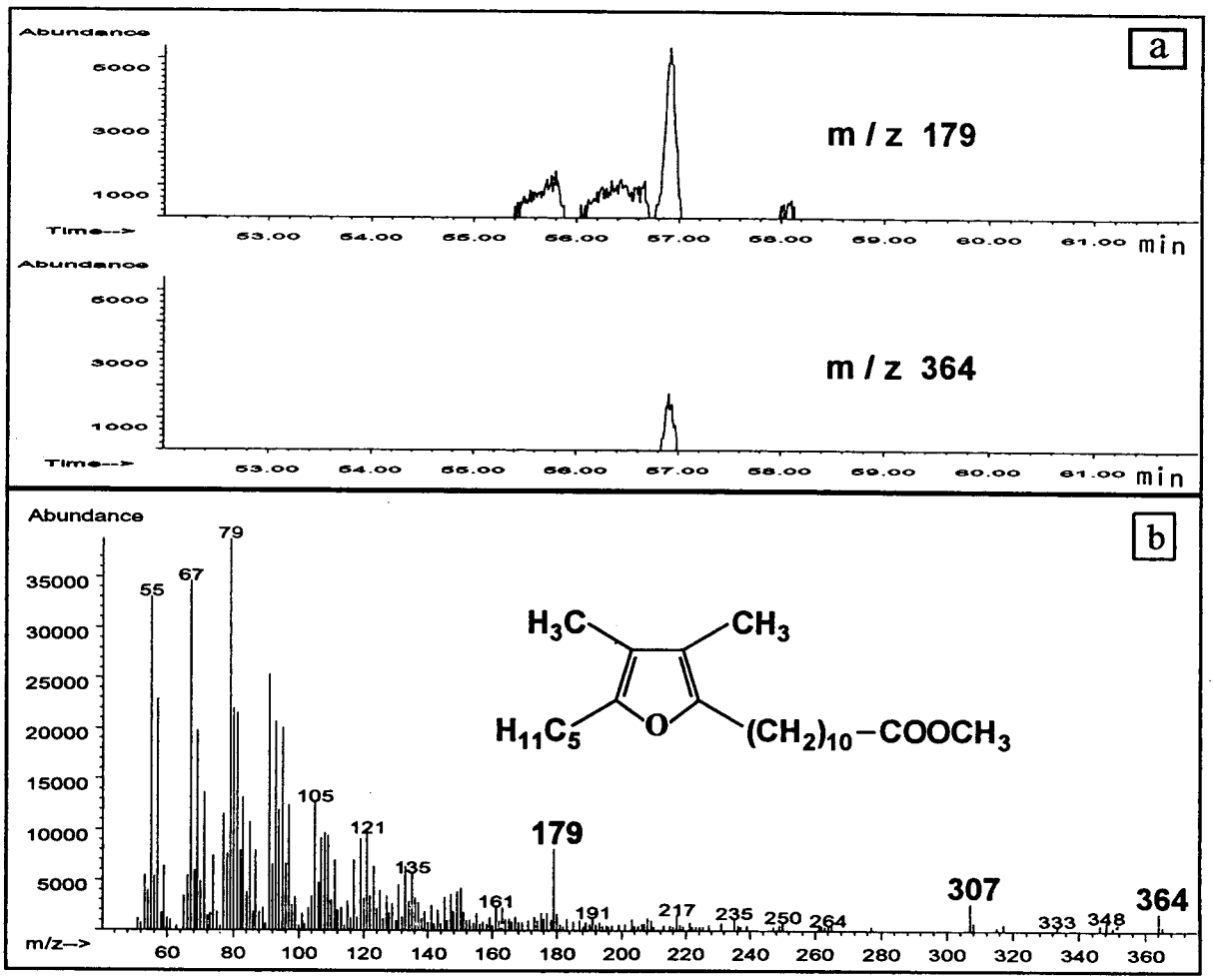

Fig. 4. (a) Ion chromatogram and (b) mass spectrum of furan fatty acid F6 obtained by single-column GC–MS (TIC Fig. 5a).

constituents in red blood cells were palmitic and stearic (17–20%), followed by arachidonic, oleic and linoleic acid with a similar distribution range of 10–14%. Finally, platelets revealed the highest relative amount of arachidonic acid (24% of total fatty acids), followed by palmitic (17%), stearic (14%), linoleic (14%) and oleic acid (10%). These relative amounts are in agreement with those reported in the literature [40,41]. Fig. 3 shows a typical chromatogram of a red blood cell sample.

Only furan fatty acid F6 (Fig. 4b) could be detected in all blood samples by single-column GC–MS when using single-ion monitoring. After injection of a larger volume of concentrated samples with the mass spectrometer operating in full-scan mode, it was possible to identify F6 in the ion chromatogram (Fig. 4a) by its mass spectrum. However, even after background subtraction there are many ions left in the mass spectrum of F6 due to unseparated substances, especially in the lower mass region (Fig. 4b).

3.2. Multi-dimensional GC–MS

By choosing the right cut times in the total ion chromatogram of the precolumn (Fig. 5) for the described configuration of the multi-dimensional

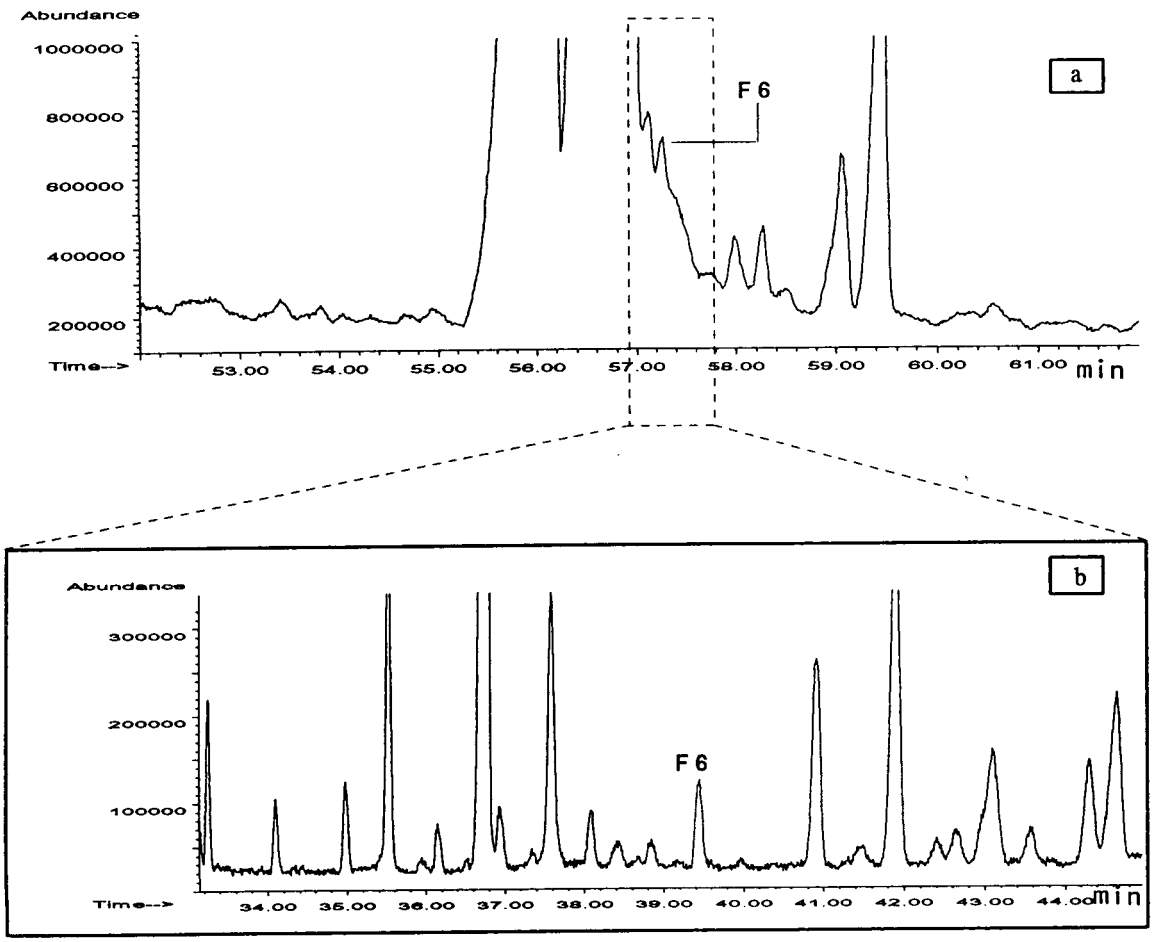

Fig. 5. Multi-dimensional GC–MS: TIC of (a) precolumn and (b) analytical column (red blood cells).

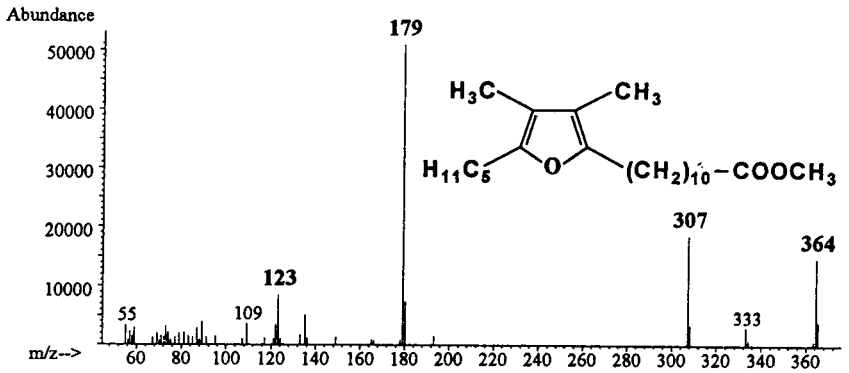

Fig. 6. Mass spectrum of furan fatty acid F6 obtained by multi-dimensional GC–MS.

GC–MS system, the methyl esters of furan fatty acids become well separated on the second column, as shown for the identification of F6 in red blood cells (Fig. 5). The mass spectrum of F6 (Fig. 6) is now free of any ions due to interfering substances. After furan fatty acid F6, which was found in all blood components, F4 (Fig. 7) was found in red blood cells and plasma. For red blood cells there was no significant difference observed when whole red blood cells were used instead of the isolated membranes. The analysis of serum samples led to variable results: in most instances furan fatty acids could be detected, but not in all. As furan fatty acids have also been found in red blood cells and platelets, there might be an exchange taking place depending on the time the serum stays in contact. In serum furan fatty acids were detected only in the phospholipid fraction, and not in cholesterol esters or triglycerides. This is in agreement with an earlier report by Puchta et al. [17].

4. Conclusions

The identification of minor component furan fatty acids in blood lipids has been achieved by using a multi-dimensional GC–MS system. Except for transesterification there is no need for any further pre-analytical separation or concentration steps. This method should also be applicable to the identification of any other minor component fatty acid in complex sample matrices.

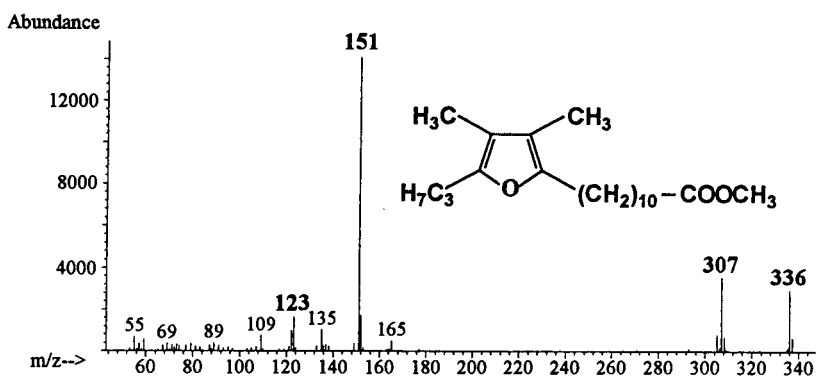

Fig. 7. Mass spectrum of furan fatty acid F4 obtained by multi-dimensional GC–MS.

References

[1] L.J. Morris, M.O. Marshall and W. Kelly, *Tetrahedron Lett.*, (1966) 4249.
[2] R.L. Glass, T.P. Krick and A.E. Eckhardt, *Lipids*, 9 (1974) 1004.
[3] R.L. Glass, T.P. Krick, D.M. Sand, C.H. Rahn and H. Schlenk, *Lipids*, 10 (1975) 695.
[4] R.L. Glass, T.P. Krick, D.L. Olson and R.L. Thorson, *Lipids*, 12 (1977) 828.
[5] F.D. Gunstone and R.C. Wijesundera, *J. Chem. Soc. C*, (1976) 630.
[6] F.D. Gunstone, R.C. Wijesundera and C.M. Scrimgeour, *J. Sci. Food Agric.*, 29 (1978) 539.
[7] C.M. Scrimgeour, *J. Am. Oil. Chem. Soc.*, 54 (1977) 210.
[8] K. Ishii, H. Okajima, Y. Okada and H. Watanabe, *J. Biochem.*, 103 (1988) 836.
[9] A. Groweiss and Y. Kashman, *Experientia*, 34 (1978) 299.
[10] K. Hannemann, V. Puchta, E. Simon, H. Ziegler and G. Spiteller, *Lipids*, 24 (1989) 296.
[11] H. Hasma and A. Subramaniam, *Lipids*, 13 (1978) 905.
[12] H. Guth and W. Grosch, *Fat. Sci. Technol.*, 7 (1991) 249.
[13] H. Guth and W. Grosch, *Z. Lebensm.-Unters.-Forsch.*, 194 (1992) 360.
[14] K. Ishii, H. Okajima, T. Koyamatsu, Y. Okada and H. Watanabe, *Lipids*, 23 (1988) 694.
[15] C.P. Gorst-Allman, V. Puchta and G. Spiteller, *Lipids*, 23 (1988) 1032.
[16] R. Schödel and G. Spiteller, *Liebigs Ann. Chem.*, (1987) 459.
[17] V. Puchta, G. Spiteller and H. Weidinger, *Liebigs Ann. Chem.*, (1988) 25.
[18] M. Spiteller and G. Spiteller and G.-A. Hoyer, *Chem. Ber.*, 113 (1980) 699.
[19] J. Pfordt, H. Thoma and G. Spiteller, *Liebigs Ann. Chem.*, (1981) 2298.
[20] D.M. Sand, H. Schlenk, H. Thoma and G. Spiteller, *Biochim. Biophys. Acta*, 751 (1983) 455.
[21] R. Schödel, P. Dietel and G. Spiteller, *Liebigs Ann. Chem.*, (1986) 127.
[22] H.G. Wahl, H.M. Liebich and B. Tetschner, *J. High Resolut. Chromatogr.*, 15 (1992) 815.
[23] S. Bauer and G. Spiteller, *Helv. Chim. Acta*, 68 (1985) 1635.
[24] H.G. Wahl, H.M. Liebich and A. Hoffmann, in P. Sandra (Editor), *Fifteenth International Symposium on Capillary Chromatography, Riva, 1993*, p. 730.
[25] H. Mabuchi and H. Nakahashi, *Ther. Drug Monit.*, 10 (1988) 261.
[26] H. Mabuchi and H. Nakahashi, *Nephron*, 49 (1988) 281.
[27] T. Niwa, T. Yazawa, T. Kodama, Y. Uehara, K. Meada and K. Yamada, *Nephron*, 56 (1990) 241.
[28] H.M. Liebich, J. Bubeck, A. Pickert, G. Wahl and A. Scheiter, *J. Chromatogr.*, 500 (1990) 615.
[29] H.M. Liebich, A. Reichenmiller, H.G. Wahl, B. Tetschner, T. Risler and M. Eggstein, *J. High Resolut. Chromatogr.*, 15 (1992) 601.
[30] H. Mabuchi and H. Nakahashi, *J. Chromatogr.*, 415 (1987) 110.
[31] H. Okajima, K. Ishii and H. Watanabe, *Chem. Pharm. Bull.*, 32 (1984) 3281.
[32] J. Folch, M. Less and G.H.S. Stanley, *J. Biol. Chem.*, 226 (1957) 497.
[33] F. De Venuto, T.F. Zuck, A.I. Zegna and W.Y. Moores, *J. Lab. Clin. Med.*, 89 (1977) 509.
[34] D.R. Knapp, *Handbook of Analytical Derivatization Reactions*, Wiley, New York, 1979, p. 164.
[35] H.G. Wahl, H.M. Liebich and A. Hoffman *J. High Resolut. Chromatogr.*, 17 (1994) 308.
[36] H.M. Liebich, B. Jakober, C. Wirth, A. Pukrop and M. Eggstein, *J. High Resolut. Chromatogr.*, 14 (1991) 433.
[37] H.M. Liebich, C. Wirth and B. Jakober, *J. Chromatogr.*, 572 (1991) 1.
[38] G. Lepage and C.C. Roy, *J. Lipid Res.*, 29 (1988) 227.
[39] G. Lepage and C.C. Roy, *J. Lipid Res.*, 27 (1986) 114.
[40] H.M. Liebich, J. Schoppet, S. Hillinger, C. Wirth, M. Pfohl, D. Wendler, H.G. Wahl and M. Eggstein, in P. Sandra and M.L. Lee (Editors), *Proceedings*, Foundation for the International Symposium on Capillary Chromatography, Miami, FL, 1992, p. 252.
[41] J.J. van Doormaal, F.A. Muskiet, E. van Ballegooie, W.J. Sluiter and H. Doorenbos, *Clin. Chim. Acta*, 144 (1984) 203.

ELSEVIER

Journal of Chromatography A, 697 (1995) 461–468

JOURNAL OF CHROMATOGRAPHY A

Simultaneous determination of glycerol, and mono-, di- and triglycerides in vegetable oil methyl esters by capillary gas chromatography

Christina Plank*, Eberhard Lorbeer

Institute of Organic Chemistry, University of Vienna, Währingerstrasse 38, A-1090 Vienna, Austria

Abstract

A gas chromatographic procedure for the simultaneous determination of glycerol, mono-, di- and triglycerides in vegetable oil methyl esters has been developed. Quantitative information about this group of organic contaminants is very important for the quality of these oleochemical products when used as automotive diesel fuel substitutes.

Trimethylsilylation of glycerol, mono- and diglycerides, followed by GC using a 10-m capillary column coated with a 0.1-μm film of DB-5 allows the determination of all analytes in a single GC run. Calibration is performed by analysis of standard solutions containing glycerol, mono-, di- and triolein as well as two internal standards, 1,2,4-butanetriol and tricaprin. The recovery of the procedure at different concentration levels and the repeatability of the quantitative results are evaluated.

1. Introduction

Vegetable oil methyl esters (VOMEs), obtained by alkali-catalyzed transesterification of vegetable oils with methanol, can be significantly contaminated with glycerol, mono-, di- and triglycerides due to incomplete transesterification and insufficient purification. For the use as automotive diesel fuel substitutes, now the most important field of application, the presence of these minor components can lead to serious engine problems and hazardous emissions [1]. Limits for the permissible levels of glycerol, mono-, di- and triglycerides have therefore been introduced by existing standard specifications [2] and will be also included in future standard specifications. As a consequence, continuous quality control of these oleochemical products is essential.

During the last few years, several analytical procedures have been developed for both the determination of glycerol as well as for mono-, di- and triglycerides in VOMEs. Methods, based on the extraction of glycerol from VOMEs into an aqueous phase and its subsequent gas chromatographic (GC) analysis, were described by Bondioli et al. [3] and Hödl and Schindlbauer [4]. An enzymatic determination of glycerol in an aqueous extract of fatty acid methyl esters was described by Bailer and De Hueber [5]. Mittelbach analyzed glycerol after derivatization with N,O-bis(trimethylsilyl)trifluoroacetamide (BSTFA) directly in the VOME sample [6].

Capillary GC is normally used for the analysis of mono-, di- and triglycerides in VOMEs.

* Corresponding author.

0021-9673/95/$09.50
SSDI 0021-9673(94)00867-1

Freedman et al. [7] applied capillary GC for studying transesterification of soybean oil to fatty esters. Mariani et al. [8] described a GC method for the determination of fatty acid methyl esters together with mono-, di- and triglycerides in vegetable oil derivatives. Recently, we reported on a GC method for the determination of mono-, di- and triglycerides in VOMEs, which was developed especially for quantitative analysis of these compounds in VOMEs used as diesel fuel substitutes [9]. Isocratic HPLC–gel permeation chromatography (GPC) with density detection was applied by Trathnigg and Mittelbach for the analysis of triglyceride methanolysis mixtures [10]. For kinetic studies, Freedman et al. analyzed reaction mixtures of transesterified soybean oil by thin-layer chromatography with flame ionization detection (TLC–FID) [11].

All methods, reported so far, were designed to determine the content of either free glycerol or of mono-, di- and triglycerides in VOMEs. In this work, we have developed a rapid and reliable GC procedure for the simultaneous determination of glycerol, mono-, di- and triglycerides in VOMEs, predominantly consisting of C_{18}-fatty acid methyl esters, such as rapeseed oil methyl ester, sunflower oil methyl ester, soybean oil methyl ester and used frying oil methyl ester. This method can be used for both the routine quality control of VOMEs in the course of production and the inspection of their compliance with the required specifications.

Trimethylsilylation of the free hydroxyl groups of glycerol, mono- and diglycerides, followed by GC using a short thin film capillary column allows the determination of all analytes, varying considerably in polarity and volatility, in a single GC run. By the use of two internal standards, 1,2,4-butanetriol and tricaprin, reliable quantitative analysis of glycerol, mono-, di- and triglycerides can be carried out within a run time of 30 min. Calibration is performed by analysis of standard solutions containing glycerol, mono-, di- and triolein and both internal standards. The recovery of the procedure at different concentration levels and the repeatability of the quantitative results are carefully evaluated.

2. Experimental

2.1. Chemicals

The reference substances used in this study, glycerol, (*S*)-(−)-1,2,4-butanetriol, 1-mono[*cis*-9-octadecenoyl]-*rac*-glycerol (monoolein), 1,3-di-[*cis*-9-octadecenoyl]glycerol (diolein), 1,2,3-tri-[*cis*-9-octadecenoyl]glycerol (triolein) and 1,2,3-tridecanoylglycerol (tricaprin), were purchased from Sigma (Deisenhofen, Germany) and were chromatographically pure (>99%). N-Methyl-N-trimethylsilyltrifluoroacetamide (MSTFA) was obtained from Fluka (Buchs, Switzerland). Analytical grade *n*-heptane and pyridine were supplied by Loba Feinchemie (Fischamend, Austria).

2.2. Preparation of samples and standard solutions

Stock solutions of glycerol (0.5 mg/ml), monoolein (4.0 mg/ml), diolein (4.0 mg/ml), triolein (5.0 mg/ml), 1,2,4-butanetriol (3.0 mg/ml) and tricaprin (8.0 mg/ml) in pyridine were used to prepare standard solutions at 5 different concentration levels. The concentration of glycerol in the standard solutions varied from 0.001 to 0.006 mg/ml, of mono- and diolein from 0.005 to 0.063 mg/ml, and of triolein from 0.007 to 0.110 mg/ml; the concentration of the internal standards was 0.022 mg/ml for 1,2,4-butanetriol and 0.090 mg/ml for tricaprin in all standard solutions. Appropriate amounts of the stock solutions of glycerol, mono-, di- and triolein, 70 μl of butanetriol stock solution and 100 μl of tricaprin stock solution were transferred into 10 ml screw-cap vials.

For preparation of samples, butanetriol stock solution (70 μl) and tricaprin stock solution (100 μl) were added as internal standards to 100.0–110.0 mg of VOME in a 10 ml screw-cap vial. MSTFA (100 μl) was added to the standard and to the sample material. After 15 min at room temperature, the silylated mixtures were dissolved in *n*-heptane and diluted to 9 ml.

2.3. Instrumentation

GC analyses were performed with a Fisons Instruments GC 8000 gas chromatograph (Milan, Italy). The instrument was equipped with an on-column injector and a flame ionization detector, and was fitted with a 2 m × 0.53 mm I.D. uncoated, deactivated fused-silica pre-column (Carlo Erba) connected in series with a 10 m × 0.32 mm I.D. fused-silica capillary column coated with a 0.1-μm film of DB-5 (J&W Scientific, Folsom, CA, USA) by means of a butt connector. Acquisition and processing of data was performed with a Chromcard (Fisons Instruments) in combination with an IBM compatible personal computer.

Samples (1 μl) were injected on-column by an AS 800 automatic sampler (Fisons Instruments) at an oven temperature of 50°C. After an isothermal period of 1 min, the GC oven was heated at 15°/min to 180°C, at 7°/min to 230°C and ballistically to 370°C (held for 10 min). Hydrogen was used as carrier gas at a flow-rate of 3 ml/min measured at 50°C. Detector temperature was 370°C; nitrogen served as detector make up gas at an inlet pressure of 0.5 bar. Run time was 30 min.

3. Results and discussion

This GC method for the simultaneous determination of glycerol, mono-, di- and triglycerides was developed especially for rapeseed oil methyl ester (RME). The reference substances were selected with respect to the fatty acid composition of rapeseed oil. Temperature programming was adjusted to obtain group-type separation of glycerol, mono-, di- and triglycerides, typically occuring in RME. VOMEs with fatty acid compositions or chain lengths similar to that of RME, such as sunflower oil methyl ester, soybean oil methyl ester and used frying oil methyl ester, can be analyzed by the outlined method without any adjustment of conditions. However, this GC method can not be applied to methyl esters obtained by transesterification of lauric oils without modifications, because superimpositions of peaks of long-chain fatty acid methyl esters and short-chain monoglycerides make a reliable quantitative analysis impossible.

3.1. Derivatization

In principle, glycerol, mono-, di- and triglycerides can be analyzed on highly inert columns coated with apolar stationary phases without derivatization. The inertness of the column, required to obtain good peak shapes and satisfactory recoveries, cannot be easily maintained in routine analysis. Trimethylsilylation of the free hydroxyl groups of glycerol, mono- and diglycerides, however, ensures excellent peak shapes, good recoveries and low detection limits, and enormously improves the ruggedness of the procedure.

For complete silylation of glycerol and partial glycerides, the conditions of the derivatization reaction have to be controlled carefully. Extensive studies on the silylation of partial glycerides, previously carried out in our laboratory, showed that complete silylation can be obtained under the following conditions [12]: (i) BSTFA as silylating agent, addition of pyridine or dimethylformamide and heating to 70°C for 15 min; (ii) BSTFA + 1% trimethylchlorosilane as silylating agent, addition of pyridine and a reaction time of 15 min at room temperature; (iii) MSTFA as silylating agent, addition of pyridine and a reaction time of 15 min at room temperature; (iiii) MSTFA as silylating agent and heating to 70°C for 15 min. With the mentioned conditions, the degrees of conversion were determined by GC analysis of the corresponding reaction mixtures to be higher than 98% for monoglycerides and 100% for glycerol and diglycerides. This method employs derivatization conditions according to (iii), as the consumption of silylating agent is reduced when using MSTFA instead of BSTFA, and as heating is not necessary when pyridine is added as a catalyst.

The internal standard 1,2,4-butanetriol serves as a very sensitive indicator of incomplete derivatization. In case of insufficient silylation (not

all of the three hydroxyl groups are silylated), the peak of 1,2,4-butanetriol appears splitted and drastically reduced in height.

3.2. Qualitative analysis

A gas chromatogram of silylated rapeseed oil methyl ester with 1,2,4-butanetriol and tricaprin as internal standards (as trimethylsilyl derivatives) is shown in Fig. 1. Separation of compound classes only is required, not of compounds within a class. Peak identification was achieved by analysis of samples spiked with reference substances or by comparison with reference chromatograms.

Glycerol and 1,2,4-butanetriol elute in advance of the fatty acid methyl esters at column temperatures lower than 100°C. The enlargements in Fig. 1b show the regions of the gas chromatogram, where the peaks of mono-, di- and triglycerides appear. On 5% phenyl polydimethylsiloxane, mono-, di- and triglycerides are mainly separated according to carbon numbers (CN).

For monoglycerides, the peak with the relative retention time (RRT) of 0.78 with respect to the internal standard tricaprin (t_R = 19.7 min) clearly dominates and corresponds to the signals of monoolein, monolinolein and monolinolenin. The asymmetric peak shape is due to the superimposition of these monoglyceride peaks with equal carbon number (CN = 18) but different number of double bonds. In addition, the signals of monopalmitin (CN = 16; RRT = 0.70) and monostearin (CN = 18; RRT = 0.79) could be identified.

The diglycerides are also primarily separated according to carbon number and appear in groups of peaks corresponding to 1,2- and 1,3-isomers or to diglycerides with equal carbon number but different number of double bonds. The individual diglyceride peaks could not be reliably identified. Nevertheless, the signals with relative retention times from 1.09 (t_R = 21.4 min) to 1.17 (t_R = 23.0 min) could clearly be assigned to diglycerides with carbon numbers of 34, 36 and 38 by comparison of chromatograms of samples with high and low degrees of transesterification and reference chromatograms.

At the end of the chromatogram, the triglycerides form a group of peaks separated only according to carbon number. Signals with relative retention times from 1.35 (t_R = 26.6 min) to 1.47 (t_R = 29.2 min) corresponding to triglycerides with carbon numbers of 52, 54, 56 and 58 were included in quantitation.

3.3. Calibration

For the quantitative determination of free glycerol, mono-, di- and triglycerides in VOMEs a calibration with the reference substances glycerol, mono-, di- and triolein was carried out. Due to structural differences between the individual analyte classes and to partial thermal degradation observed for the high boiling di- and triglycerides, calibration is of great importance for a reliable quantification.

Freshly prepared standard solutions (5 concentration levels), containing known amounts of the reference substances glycerol, mono-, di- and triolein and both internal standards were analyzed three times each by capillary GC. A corresponding gas chromatogram is shown in Fig. 2. Table 1 summarizes the regression data of the linearly fitted calibration functions, which show excellent linearity for glycerol, mono- and diolein and acceptable linearity for triolein in the concentration range of interest.

3.4. Quantitative results

For the quantitative determination of monoglycerides, the corresponding peaks were integrated separately, and the concentrations were calculated according to the calibration function obtained for monoolein based on the internal standard tricaprin. The total concentration was then calculated by summing up the concentrations of the individual monoglycerides. Di- and triglycerides were quantified analogously. The concentration of glycerol was calculated according to its calibration function based on the internal standard 1,2,4-butanetriol.

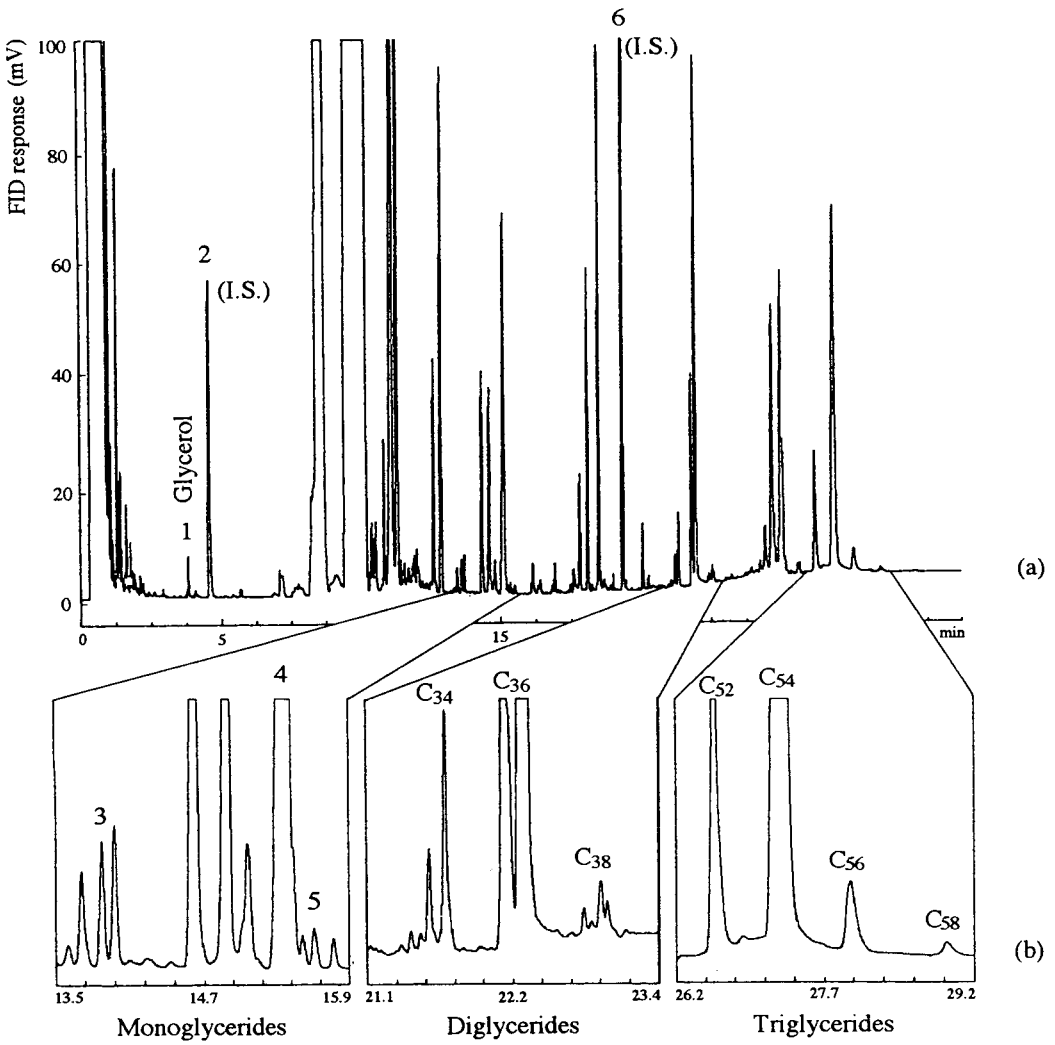

Fig. 1. (a) Gas chromatogram of silylated rapeseed oil methyl ester with 1,2,4-butanetriol and tricaprin as internal standards. (b) Enlargements of the regions, where the signals of mono-, di- and triglycerides appear in the upper gas chromatogram. GC column: 10 m × 0.32 mm I.D. fused-silica capillary column coated with DB-5 (0.1 μm film thickness), equipped with a 2 m × 0.53 mm I.D. uncoated, deactivated pre-column. GC temperature programme: 50°C (1 min), at 15°/min to 180°C, at 7°/min to 230°C, ballistically to 370°C (10 min). Peak assignment: 1 = glycerol; 2 = 1,2,4-butanetriol, I.S.; 3 = monopalmitin; 4 = monoolein, monolinolein, monolinolenin; 5 = monostearin; 6 = tricaprin, I.S.; C_{34}–C_{38} = diglycerides with carbon numbers of 34, 36 and 38; C_{52}–C_{58} = triglycerides with carbon numbers of 52, 54, 56 and 58.

For the evaluation of the recovery, reference samples and spiked RME samples containing known amounts of standard substances at different concentration levels were analyzed. The reference samples contained glycerol, mono-, di- and triolein at concentrations, typical of authentic VOME samples. Distilled RME (containing small amounts of glycerol and monoglycerides but no detectable amounts of di- and triglycerides) was spiked with the standard substances mentioned. By comparing the quantitative results obtained by GC analysis and the

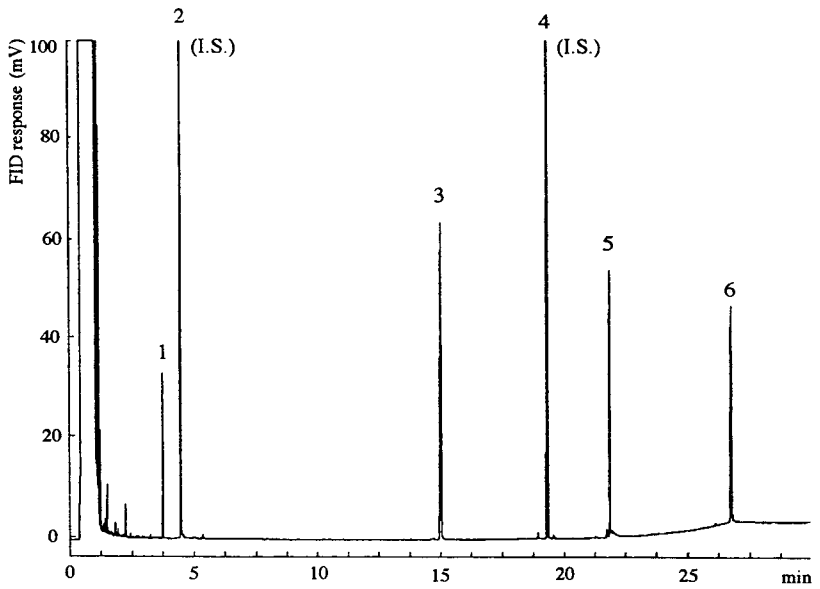

Fig. 2. Gas chromatogram of a standard solution containing the trimethylsilyl derivatives of glycerol, 1,2,4-butanetriol, monoolein and diolein, as well as tricaprin and triolein. Conditions as in Fig. 1. Peak assignment: 1 = glycerol; 2 = 1,2,4-butanetriol, I.S.; 3 = monoolein; 4 = tricaprin, I.S.; 5 = diolein; 6 = triolein.

actual concentrations of the standard substances, the percentage recoveries were calculated and are given in Table 2. Except for triolein in the lowest concentration level (5 μg/ml), the recovery of all solutes of interest is excellent.

In order to check the precision of the method, a sample of RME was prepared and consecutively analyzed seven times. The quantitative results for glycerol, mono-, di- and triglycerides are given in Table 3.

Additionally, seven samples of the same RME specimen were prepared and analyzed by GC. The results are summarized in Table 4. The data in Tables 3 and 4 indicate the excellent repeatability of the quantitative results obtained by the method outlined. Due to simple sample preparation (comprising sample weighing, the addition of the internal standards, derivatization and dilution), the reproducibility of the quantitative results obtained by repeated complete analy-

Table 1
Calibration functions for glycerol, monoolein, diolein and triolein: $W_c/W_{st} = b \cdot A_c/A_{st} + a$ ($n = 5$)

	b	a	Standard error	r^2
Glycerol	0.937 ± 0.005	-	0.002	0.999
Monoolein	0.748 ± 0.004	-	0.005	0.999
Diolein	0.819 ± 0.012	0.019 ± 0.005	0.007	0.999
Triolein	1.213 ± 0.052	0.085 ± 0.027	0.039	0.995

Abbreviations: W_c, weight of component; W_{st}, weight of internal standard; A_c, peak area of component; A_{st}, peak area of internal standard; r, correlation coefficient.

Table 2
Average recovery ($n = 3$) for glycerol, mono-, di- and triglycerides at three concentration levels

	Recovery (%)					
	Reference sample			Spiked RME		
Conc. (μg/ml)	1	2	4	1	2	4
Glycerol	104	103	100	106	103	101
Conc. (μg/ml)	5	50	100	5	50	100
Monoolein	95	101	101	103	101	101
Diolein	98	100	102	129[b]	101	102
Triolein	148[a]	95	98	201[a,b]	109	110

[a] The calibration function for triolein shows a higher error in this low concentration range.
[b] Distilled RME contains di- and triglycerides at concentrations below the detection limits which effect the recovery of di- and triolein in this low concentration range.

sis is as good as that obtained by consecutive injection of the same sample.

4. Conclusion

In a single GC run, the proposed method provides qualitative and quantitative information about glycerol, mono-, di- and triglycerides, the most important organic contaminants of vegetable oil methyl esters. High reliability of results, simple instrumentation and sample preparation, short analysis time and the possibility of complete automation make this method well suited for the quality control of these oleochemical products, gaining steadily in importance for technical applications, especcially as diesel fuel substitutes.

Table 3
Repeatability of the quantitative results for glycerol, mono-, di- and triglycerides, obtained by consecutive GC injections ($n = 7$)

Analysis	Concentration (weight%) in RME			
	Glycerol	Monoglycerides	Diglycerides	Triglycerides
1	0.009	0.355	0.505	1.152
2	0.009	0.357	0.510	1.168
3	0.009	0.365	0.509	1.162
4	0.009	0.363	0.509	1.169
5	0.009	0.358	0.510	1.173
6	0.009	0.350	0.510	1.174
7	0.009	0.364	0.513	1.171
Mean	0.009	0.359	0.509	1.167
S.D.	<0.001	0.005	0.002	0.007
R.S.D. (%)	1.3	1.4	0.4	0.6

Table 4
Repeatability of the quantitative results for glycerol, mono-, di- and triglycerides obtained by repeated complete analysis including sample preparation ($n = 7$)

Analysis	Concentration (weight%) in RME			
	Glycerol	Monoglycerides	Diglycerides	Triglycerides
1	0.009	0.362	0.512	1.176
2	0.009	0.366	0.516	1.179
3	0.009	0.365	0.514	1.170
4	0.009	0.358	0.514	1.183
5	0.009	0.367	0.511	1.170
6	0.009	0.360	0.508	1.168
7	0.009	0.359	0.513	1.173
Mean	0.009	0.362	0.513	1.174
S.D.	<0.001	0.003	0.002	0.005
R.S.D. (%)	1.3	0.9	0.5	0.5

Acknowledgement

Financial support by the Austrian Federal Ministry of Agriculture and Forestry is gratefully acknowledged.

References

[1] M. Mittelbach, M. Wörgetter, J. Pernkopf and H. Junek, *Energy Agric.*, 2 (1983) 369.
[2] *ÖNORM C 1190: Fuels - Diesel Engines, Rape Seed Oil Methyl Ester; Requirements*, Österreichisches Normungsinstitut, Vienna, 1991.
[3] P. Bondioli, C. Mariani, A. Lanzani, E. Fedeli and S. Veronese, *Riv. Ital. Sostanze Grasse*, 69 (1992) 7.
[4] P. Hödl and H. Schindlbauer, in Research Institute for Chemistry and Technology of Petroleum Products, *Handbook of Analytical Methods for Fatty Acid Methyl Esters Used as Diesel Fuel Substitutes*, University of Technology, Vienna, 1994, ch. 2, p. 27.
[5] J. Bailer and K. De Hueber, *Fresenius' Z. Anal. Chem.*, 186 (1991) 340.
[6] M. Mittelbach, *Chromatographia*, 37 (1993) 623.
[7] B. Freedman, W.F. Kwolek and E.H. Pryde, *J. Am. Oil Chem. Soc.*, 63 (1986) 1370.
[8] C. Mariani, P. Bondioli, S. Venturini and E. Fedeli, *Riv. Ital. Sostanze Grasse*, 68 (1991) 549.
[9] Ch. Plank and E. Lorbeer, *J. High Resolut. Chromatogr.*, 15 (1992) 609.
[10] D. Trathnigg and M. Mittelbach, *J. Liq. Chromatogr.*, 13 (1990) 95.
[11] B. Freedman, E.H. Pryde and T.L. Mounts, *J. Am. Oil Chem. Soc.*, 61 (1984) 1638.
[12] Ch. Plank and E. Lorbeer, unpublished results.

ELSEVIER

Journal of Chromatography A, 697 (1995) 469–474

JOURNAL OF CHROMATOGRAPHY A

Monitoring of lipase-catalyzed cleavage of acylglycerols by high-temperature gas chromatography

Thomas L. Bereuter*, Eberhard Lorbeer

Institute for Organic Chemistry, University of Vienna, Währingerstrasse 38, 1090-Vienna, Austria

Abstract

High-temperature gas chromatography was applied to assay the activity and selectivity of lipases, and to test various reaction conditions. This technique is capable to analyze mixtures of fatty acids and acylglycerols simultaneously and, therefore, to monitor the hydrolysis of acylglycerols. Lipases can catalyze the hydrolysis of acylglycerols in aqueous solution. The reaction conditions employed are milder than those of conventional chemical hydrolysis. In practice, this method was used in the sample preparation procedure for the quantitative analysis of γ-linolenic acid in triacylglycerols.

1. Introduction

Modification of fats and oils is a special area of enzyme technology which can be used for analytical purposes. Esters can be synthesized, rearranged and hydrolyzed by lipase enzymes (E.C. 3.1.1.3). Sometimes it is sufficient to observe the appearance or disappearance of free fatty acids (FAs) in order to monitor the course of these reactions. However, if complex mixtures have to be transformed, it is advisable to profile the complete lipid pattern. Unwanted or changed substrate specificities of the enzymes could cause problems in the case of non-quantitative transformations. The results of the experiments are strongly influenced by the way reactions are carried out.

Various analytical methods have been developed to follow, e.g., the lipase-catalyzed hydrolysis of wax esters [1], esterification and interesterification of lipids by TLC [2], hydrolysis of triacylglycerols by HPLC [3,4], enantioselective transesterification with allylic alcohols [5] and interesterification of cholesteryl esters by capillary GC [6]. Zhang and Wainer [7] developed an enzyme reactor with immobilized lipase coupled on-line to an HPLC-column. Berg et al. [8] also used an immobilized lipase for the on-line supercritical fluid extraction–supercritical fluid chromatography approach.

In our investigations, high-temperature GC was used to monitor the hydrolysis of acylglycerols by lipases. Control of the conversion rates was carried out by analysis of FAs and acylglycerols in a single GC run following methylation of the acids by diazomethane.

According to the IUPAC method [9] FA methyl esters of $(n-3)$ and $(n-6)$ oils are prepared by alkali-catalyzed transesterification of the triacylglycerols with methanol. The deficiencies of this method are the following: (i) free FAs are saponified but not esterified, and will not be detected in the subsequent analysis; (ii) reaction conditions for the transesterification

* Corresponding author.

0021-9673/95/$09.50
SSDI 0021-9673(94)00866-3

need to be anhydrous because water would lead to saponification and, therefore, to a loss in recovery of FAs; (iii) the basic reaction conditions applied may result in isomerisation of the double bonds of unsaturated FAs [10,11]. Other ways to produce FA methyl esters, including the boron trifluoride method which is also accepted as a standard procedure [12,13], are discussed by Shantha and Napolitano [10].

For quantitative determination of γ-linolenic acid (γLn) in triacylglycerols of borage oil and a corresponding water-in-oil emulsion (produced as a galenical preparation) the lipase from *Candida cyclindracea* was applied in the sample preparation procedure. By using standard GC equipment and commercially available capillary columns, this method is applicable in routine laboratories. The method demonstrates its benefits especially in the analysis of samples containing water.

2. Experimental

2.1. Chemicals

Buffer components

Sodium hydroxide (0.1 *M*) and 0.1 *M* hydrochloric acid, Titrisol, were obtained from Merck (Darmstadt, Germany); calcium chloride ($CaCl_2$) and disodium EDTA (purum) and Tris (BioChemika) from Fluka (Buchs, Switzerland); deionized water from own deionization plant.

Derivatizing reagents

1-Methyl-1-nitroso-3-nitroguanidine, 97%, was obtained from Aldrich (Steinheim, Germany); N-methyl-N-nitroso-*p*-toluenesulfonamide (Diazald) from Merck; N-nitroso-N-methylurea synthesized according to [14]. Ethereal diazomethane was prepared from these reagents (see Section 3.2).

Enzymes

Lipase (E.C. 3.1.1.3) type VII (from *Candida cyclindracea*) was obtained from Sigma (Deisenhofen, Germany); lipase from *Candida cyclindracea*, 22%, lipase from *Candida cyclindracea* My, 13%, and lipase from *Candida cyclindracea*, immobilised on Gulsenit, from Chemie Linz (Linz, Austria).

Reference substances

Triheptadecanoin, triolein and γLn, 99%, were obtained from Sigma; heptadecanoic acid, 99%, from Fluka.

Solvents

Hexane and diethyl ether, analytical-reagent grade, were obtained from Loba (Fischamend, Austria).

2.2. Sample preparation

To the lipid sample [10 mg of the water-in-oil emulsion or 6 mg of the borage oil; for the preparation of stock solutions the emulsion is dissolved in dichloromethane–hexane–methanol (2:2:1), the oil as well as the I.S. in *n*-hexane] and the I.S. (1.5 mg of triheptadecanoin) were added the lipase (approximately 2 mg), *n*-hexane (0.1 ml), and the buffer (1 ml of a 10 m*M* Tris buffer —adjusted to a pH of 7.5 with Titrisol— containing 40 m*M* $CaCl_2$ and 1 m*M* EDTA). The mixture was stirred over night in a closed vial under nitrogen atmosphere by a magnetic stirrer at 37 ± 1°C. The solution was acidified with hydrochloric acid (5%, w/w) prior to the extraction of the free FAs with *n*-hexane (three times with 2 ml each) by shaking vigorously on a vortex shaker. Phase separation and settling of suspended matter were accelerated by centrifugation. The combined extracts were concentrated to a small volume (about 10 μl) under a flow of nitrogen gas at ambient temperature.

The samples were derivatized by freshly prepared or distilled ethereal solution of diazomethane at room temperature and 1 h reaction time. Diethyl ether and non-reacted diazomethane were evaporated under a flow of nitrogen gas. The lipids were then dissolved in *n*-hexane (5 ml) and ready for GC analysis.

2.3. Chromatographic conditions

The gas chromatograph used was an HRGC 5300 Mega series (Fisons Instruments, Milan, Italy) equipped with a flame ionization detector and optional split- or cold-on-column injection. Data acquisition was done by a PE Nelson Interface 900 series (Perkin-Elmer Nelson Systems, Cupertino, CA, USA), and injection of 1-μl sample with a 10-μl syringe.

Screening procedure

A Pyrex glass capillary column, 25 m × 0.32 mm I.D., was coated (0.15 μm film thickness) with OV-1701 OH (7% cyanopropyl-, 7% phenyl- and 86% methylpolysiloxane) [15]. The injection mode employed was cold-on-column and the inlet pressure of hydrogen, the carrier gas, 100 kPa. The oven temperature was programmed from 70 to 170°C at 25°C/min, then from 170 to 380°C at 10°C/min, and isothermal at 380°C for 15 min. The temperature of the detector was 380°C.

Quantification procedure

A fused-silica capillary column (J & W, Folsom, CA, USA), 20 m × 0.32 mm I.D., with a DB-1 phase (100% methylpolysiloxane, 0.1 μm film thickness) and cold-on-column injection was used. The inlet pressure of hydrogen was 50 kPa and the temperature programmed from 70 to 140°C at 25°C/min, from 140 to 200°C at 7°C/min, then from 200 to 260°C at 30°C/min, and isothermal at 260°C for 5 min. The temperature of the detector was held at 280°C.

3. Results and discussion

3.1. Optimization of reaction conditions

Lipase-catalyzed hydrolysis of acylglycerols in aqueous medium followed by esterification with diazomethane is advantageous in comparison to conventional sample preparation procedures, especially for the cleavage of triacylglycerols present in water-in-oil emulsions. The free FAs are not lost by this procedure. Reaction conditions are mild and the water content of the sample does not reduce the recoveries of FAs.

The buffer compositions proposed in the literature for lipase catalysis and tested for our application were: 25 m*M* borate (adjusted to pH 8.4) containing 33% methanol, 10 m*M* and 100 m*M* phosphate (adjusted to pH 7.0), and 10 m*M* Tris (adjusted to pH 8.0 and 7.45, respectively) [16]. These buffer systems have been used in combination with different lipase preparations for the hydrolysis of a mixture of triacylglycerols with triolein as a major constituent. Borate buffer containing methanol has been most promising because the reaction products, glycerol and FAs, are removed from the equilibrium. Borate complexes glycerol and methyl alcohol should react with FAs by lipase catalysis to the corresponding methyl esters. In a single high-temperature GC run we separated the acylglycerols from the FAs and determined the conversion rates. Our experiments showed that triacylglycerols were not hydrolyzed quantitatively when borate buffer containing methanol was used. Instead, partial acylglycerols and soaps have been formed in considerable amounts.

The best results we obtained with the Tris buffer (pH 7.45) and lipase from *Candida cyclindracea* (type VII and My). Hydrolysis of triacylglycerols was quantitative (Fig. 1). $CaCl_2$ and EDTA were added to the Tris buffer for the following reasons [16]: the calcium ions in the buffer protect the enzyme against product inhibition. According to the literature calcium may be considered as a co-reactant leading to calcium soaps. In order to prevent losses of free FAs by soap formation, the aqueous solution was acidified (pH 4) with hydrochloric acid prior to extraction with *n*-hexane. EDTA has been added to the buffer as a masking reagent that complexes heavy metal ions which catalyze autoxidation reactions. The cleavage of the triacylglycerols was performed additionally under nitrogen atmosphere.

The lipase from *Candida cyclindracea* shows no discrimination of the 1- and 2-position of triacylglycerols. Its specificity towards different types of FA residues (e.g. oleic acid is set free at higher rates than stearic acid [16]) results only in

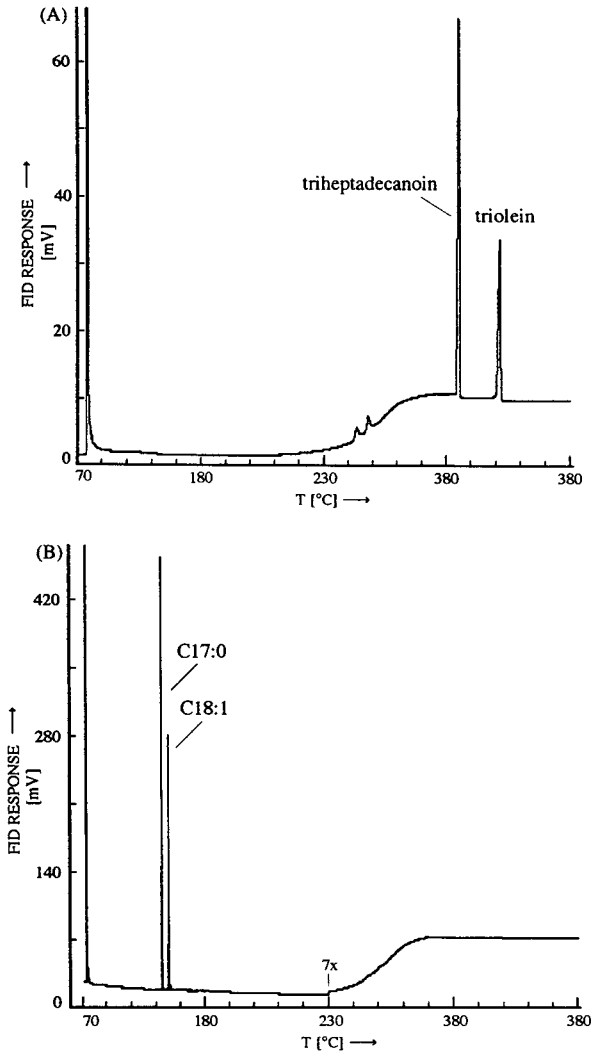

Fig. 1. High-temperature GC separation of (A) triolein and triheptadecanoin, and (B) their cleavage products oleic acid ($C_{18:1}$) and heptadecanoic acid ($C_{17:0}$) as their esters, For conditions, see Section 2.3, *Screening procedure*. FID = Flame ionization detection.

a kinetic discrimination and can be overcome by quantitative cleavage of the ester bonds. We observed no difference between the hydrolysis of triolein and triheptadecanoin (Fig. 1). Triheptadecanoin is, therefore, suitable as an internal standard for the quantitative analysis of unsaturated FAs released from acylglycerols.

The enzymatic reaction carried out by the lipase involves a water-soluble enzyme in the aqueous phase and a water-insoluble substrate in the organic hexane phase. This is an example of heterogeneous catalysis in which the catalytic events occur at a lipid-water surface. The addition of *n*-hexane improved the activity of the enzyme, but was also essential for the dissolution of triheptadecanoin and the ointment base (a water-in-oil emulsion with hydrocarbons as major constituents).

3.2. Derivatization of FAs

The free FAs produced by cleavage of the triacylglycerols were methylated for GC analysis by diazomethane at room temperature. Different procedures were tested for the diazomethane production. Consistently good results have been achieved with N-nitroso-N-methylurea [14], which is of advantage if large amounts of diazomethane are needed. The ethereal solution of diazomethane is stable in the freezer but has to be distilled before use. For freshly prepared diazomethane in small amounts Diazald [17] was employed. N-Nitrosoguanidine [18] gave unsatisfactory low yields of diazomethane. This may be a storage problem of the starting product [19].

3.3. GC analysis

Screening procedure

The screening by high-temperature GC used a fast temperature program. Only the total percentage of each lipid class (FAs as the products, mono- and diacylglycerols as intermediates, and triacylglycerols as unreacted starting material of the transformation) without separating them into individual components was of interest. The OV-1701 OH stationary phase is thermally very stable and has, therefore, a long lifetime. This makes the phase suitable for the development of methods for lipase catalysis which demands a large number of GC runs. Besides, this phase can be used to separate mixtures of *trans*- and *cis*-FAs containing, for example, elaidic and oleic acid by modified temperature programming. The cold-on-column injection is of advantage as the constituents of the sample have a broad range of boiling points.

Quantification procedure

Cold-on-column injection, but also split injection and a commercially available fused-silica capillary column coated with DB-1 were used in the quantification procedure so that this method can be employed in normal routine laboratories with conventional auto sampler equipment. More polar stationary phases than DB-1 are proposed for the separation of FAs but for our application the methyl polysiloxane phase was satisfactory.

Peak assignment for the quantitative analysis of γLn was done by spiking the sample solution with the methyl ester of γLn. Calibration was carried out by analysis of standard samples containing reference substance γLn and the internal standard heptadecanoic acid. The linearity of the detector response was checked. The recoveries of FAs comparing cold-on-column injection and split injection were the same.

Representative chromatograms for the quantitative analysis of γLn are presented in Fig. 2. The results showed that this method is well suited for the quantitative determination of polyunsaturated FAs which are released by cleavage of acylglycerols. This method should also be applicable for the analysis of triacylglycerols containing labile or reactive FAs.

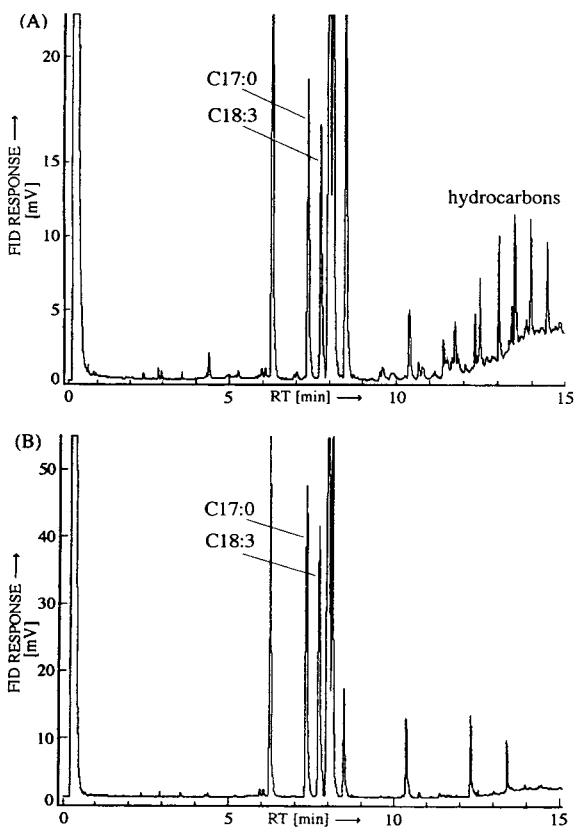

Fig. 2. Quantitative GC analysis of γLn ($C_{18:3}$) in (A) galenical preparation, and (B) borage oil by using an I.S. (heptadecanoic acid, $C_{17:0}$) as methyl ester. For conditions, see Section 2.3, *Quantification procedure*.

Acknowledgements

The lipases were provided by A. Köpf, Institute for Biochemistry and Molecular Cell Biology, University of Vienna. The borage oil and the ointment were provided by H.P. Thomi, Schering-Plough.

References

[1] S. Misra, A. Choudhury, A.K. Dutta, A. Ghosh and J. Dutta, *J. Chromatogr.*, 280 (1983) 313.
[2] R. Schuch and K.D. Mukherjee, *J. Chromatogr.*, 450 (1988) 488.
[3] F. Ergan and G. André, *Lipids*, 24 (1989) 76.
[4] H. Uzawa, H. Ohrui, H. Meguro, T. Mase and A. Ichida, *Biochim. Biophys. Acta*, 1169 (1993) 165.
[5] U. Bornscheuer, S. Schapöhler, T. Scheper, K. Schügerl and W.A. König, *J. Chromatogr.*, 606 (1992) 288.
[6] P. Kalo, J. Rinne, H. Huotari and M. Antila, *Fat Sci. Technol.*, 95 (1993) 58.
[7] X.-M. Zhang and I.W. Wainer, *Tetrahedron Lett.*, 34 (1993) 4731.
[8] B.E. Berg, E.M. Hansen, S. Gjørven and T. Greibrokk, *J. High Resolut. Chromatogr.*, 16 (1993) 358.
[9] *IUPAC Method 2.301*, Part 5, International Union of Pure and Applied Chemistry, Oxford, 1992.
[10] N.C. Shanta and G.E. Napolitano, *J. Chromatogr.*, 624 (1992) 37.
[11] O.W. Thiele, *Lipide, Isoprenoide mit Steroiden*, Georg Thieme Verlag, Stuttgart, 1979.
[12] *Official Methods of Analysis of the Association of Official Analytical Chemists*, Association of Official Analytical Chemists, Washington, DC, 1990.
[13] *German Standard Methods for the Analysis of Fats and Other Lipids*, German Society for Fat Sciences (DGF), Münster, 1994.

[14] K. Schwetlick, *Organikum*, VEB Deutscher Verlag der Wissenschaften, Berlin, 1976, pp. 665 and 672.
[15] W. Blum and R. Aichholz, *Hochtemperatur Gas-Chromatographie*, Hüthig, Heidelberg, 1991.
[16] R.S. Schifreen and R.W. Carr, *Anal. Lett.*, 12 (1979) 47.
[17] M. Hudlicky, *J. Org. Chem.*, 45 (1980) 5377.
[18] H.M. Fales, T.M. Jaouni and J.F. Babashak, *Anal. Chem.*, 45 (1973) 2302.
[19] G. Lorbeer, personal communication.

ELSEVIER

Journal of Chromatography A, 697 (1995) 475–484

JOURNAL OF CHROMATOGRAPHY A

Enantiomer separation of α-campholene and fencholene derivatives by capillary gas chromatography on permethylated cyclodextrin phases
I☆. Compounds separable with single columns

R. Reinhardt[a], A. Steinborn[b], W. Engewald[b,*], K. Anhalt[c], K. Schulze[c]

[a]*Institute of Pharmacology and Toxicology, Department of Medicine, University of Leipzig, Härtelstrasse 16–18, D-04107 Leipzig, Germany*

[b]*Institute of Analytical Chemistry, Department of Chemistry, University of Leipzig, Linnéstrasse 3, D-04103 Leipzig, Germany*

[c]*Institute of Organic Chemistry, Department of Chemistry, University of Leipzig, Liebigstrasse 18, D-04103 Leipzig, Germany*

Abstract

α-Campholene and fencholene derivatives are compounds with interesting odour properties, e.g. sandalwood and woody notes. They have one (derived from the initial product, α-pinene) or several stereogenic centres. The stereoisomers of these compounds may have different odour properties; therefore, analysis methods are developed for the complete separation of the diastereomers and enantiomers. It is shown that the alcohols with one stereogenic centre as well as of the esters and ethers of α-campholene and fencholene derivatives with two stereogenic centres can be separated on permethylated α- und β-cyclodextrins dissolved in polysiloxanes. Factors influencing the separation are discussed.

1. Introduction

Apart from the characteristic functional groups, the typical odour note of a compound is determined especially by the molecular size and form [1]. Accordingly, different diastereomers as well as enantiomers may have different odour notes or even completely different types of odour [2–4].

One of the odorous substances which have been popular for more than 4000 years is the East Indian sandalwood oil. Originally, for the main substances α- and β-santalol, equal odour tones were given for all the diastereomers and enantiomers [5], but more recent studies deny this [6].

As the demand for sandalwood fragrances for a long time could not be covered by natural resources, synthetic sandal perfumes were introduced in 1940. The α-campholene [6] and fencholene compounds [7,8] found in Leipzig, which can be easily obtained from α-pineneoxide via α-campholene (**1**) or fencholene aldehyde (**2**), are suitable sandal and woody odourants. Also other substances which can be synthesized from **1** and **2**, for example **3–28**, have typical flowery, earthy, woody notes (e.g. **28**) as well as sandal

* Corresponding author.

☆ For Part II, see Ref. [31].

0021-9673/95/$09.50
SSDI 0021-9673(94)01072-2

notes (e.g. **10** and **27**). All α-campholene and fencholene compounds have one stereogenic centre corresponding to the configuration of the C-5 atom in the starting α-pinene (Fig. 1); some have several stereogenic centres due to condensation in the side chain. For the exact determination of the odour notes, also in dependence on diastereomers and enantiomers, methods are necessary for the exact differentiation of stereomers. Because all the stereomer mixtures were volatile, analysis was carried out by means of gas chromatography on chiral stationary phases.

From structurally similar classes of substances, numerous studies on furanes [9,10] are known. Likewise, lactones were analyzed on permethylated [11,12] or on different substituted alkyl derivatives [13] as well as on alkyl/acyl derivatives of the cyclodextrins [14–17]. However, the results did not permit any conclusion that the α-campholene and fencholene derivatives are separable. The first results for this class of compounds were recently presented by us [18]. In order to include also intermediate synthetics, a considerable extension of these studies was necessary. Moreover, the investigations into the connection between structure and retention for α-campholene and fencholene compounds on chiral phases fell well into line with more comprehensive studies [19] carried out on this problem.

Part I deals with the analysis of substances with one stereogenic centre. Here, mainly alcohols, but partially also compounds with other functional groups (ester, ether) are described. In Part II [31], the analysis of α-campholene and fencholene derivatives with two and more stereogenic centres is described. Often, a complete separation of all stereoisomers of such mixtures is only possible after coupling of columns.

2. Experimental

2.1. Investigated substances

The initial compounds α-campholene (**1**) and fencholene aldehyde (**2**) are obtained from α-pinene via α-pinene oxide (**i**): the $ZnBr_2$-catalyzed camphane rearrangement of the α-pinene oxide (Fig. 1) supplies α-campholene aldehyde (**1**) [7,20].

Fencholene aldehyde (**2**) is formed by fenchane rearrangement of the trans-pinocarveol (**ii**), which can be obtained from α-pinene oxide (**i**) with aluminiumisopropylate, with subsequent hydrobromination and dehydrobromination [7,8]. By analogy, the 3-ethyl compounds (**7–11**) can be obtained from ethylapopinene [21]. The configuration of the used α-pinene determines the configuration of the C-1 atom in the five-membered ring of the campholene and fencholene compounds (see Fig. 1). The configura-

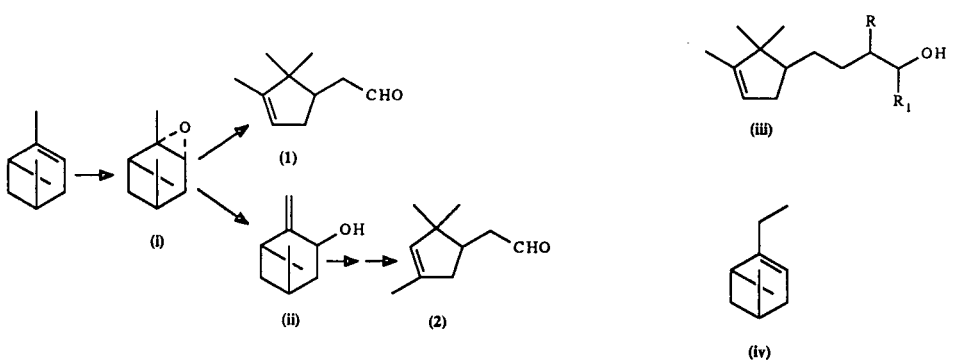

Fig. 1. Reaction scheme of the α-campholene and fencholene derivatives (**1**) and (**2**); α-pinene oxide (**i**); *trans*-pinocarveol (**ii**); fragrance compounds (**iii**) and ethylapopinene (**iv**).

tion of further stereogenic centres in compounds of the type **iii** results in the course of the condensation and reduction reactions.

The individual structures of substances investigated in Part I are shown in Fig. 2.

2.2. Instrumentation

The GC–MS analyses were carried out on a Hewlett-Packard HP 5890 II gas chromatograph–HP 5971A mass-selective detector. Elec-

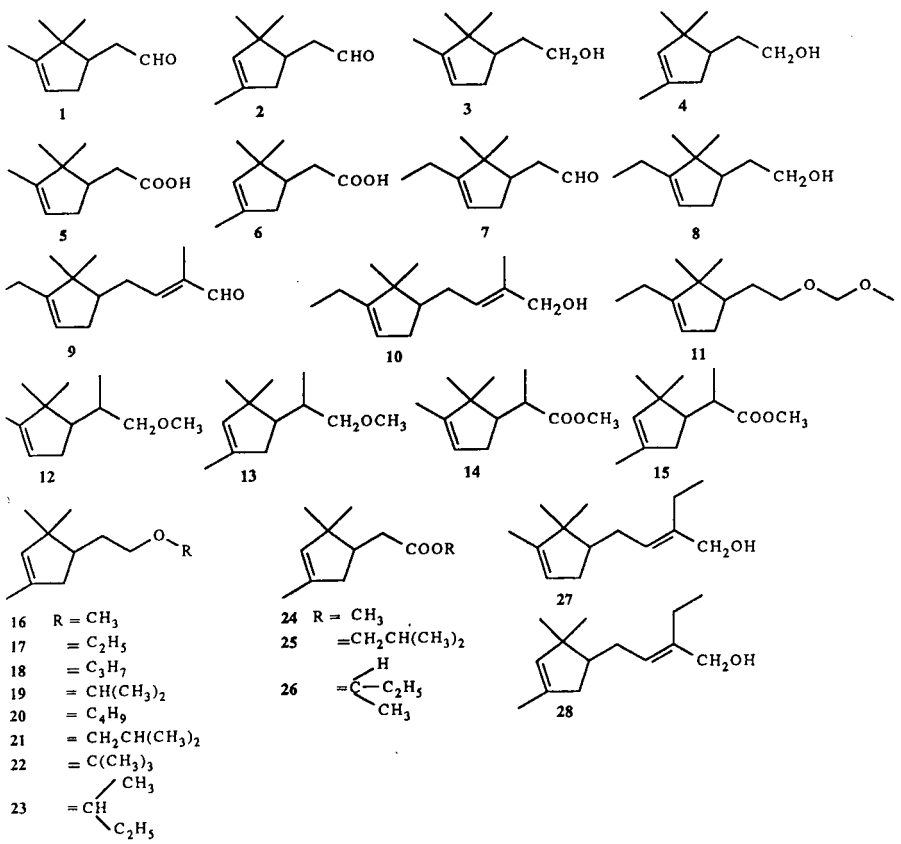

Fig. 2. Investigated substances. **1** = 2-(2,2,3-Trimethyl-3-cyclopentenyl)ethanal (α-campholene aldehyde); **2** = 2-(2,2,4-trimethyl-3-cyclopentenyl)ethanal (fencholene aldehyde); **3** = 2-(2,2,3-trimethyl-3-cyclopentenyl)ethanol; **4** = 2-(2,2,4-trimethyl-3-cyclopentenyl)ethanol; **5** = 2-(2,2,3-trimethyl-3-cyclopentenyl)acetic acid; **6** = 2-(2,2,4-trimethyl-3-cyclopentenyl)acetic acid; **7** = 2-(3-ethyl-2,2-dimethyl-3-cyclopentenyl)ethanal; **8** = 2-(3-ethyl-2,2-dimethyl-3-cyclopentenyl)ethanol; **9** = 2-methyl-4-(3-ethyl-2,2-dimethyl-3-cyclopentenyl)but-2-enal; **10** = 2-methyl-4-(3-ethyl-2,2-dimethyl-3-cyclopentenyl)but-2-enol; **11** = methoxymethyl-[2-(3-ethyl-2,2-dimethyl-3-cyclopentenyl)ethyl] ether; **12** = methyl-[2-(2,2,3-trimethyl-3-cyclopentenyl)propyl] ether; **13** = methyl-[2-(2,2,4-trimethyl-3-cyclopentenyl)propyl] ether; **14** = methyl-2-(2,2,3-trimethyl-3-cyclopentenyl)propionate; **15** = methyl-2-(2,2,4-trimethyl-3-cyclopentenyl)propionate; **16** = methyl-[2-(2,2,4-trimethyl-3-cyclopentenyl)ethyl] ether; **17** = ethyl-[2-(2,2,4-trimethyl-3-cyclopentenyl)ethyl] ether; **18** = [2-(2,2,4-trimethyl-3-cyclopentenyl)ethyl]propyl ether; **19** = isopropyl-[2-(2,2,4-trimethyl-3-cyclopentenyl)ethyl] ether; **20** = butyl-[2-(2,2,4-trimethyl-3-cyclopentenyl)ethyl] ether; **21** = 2-(2,2,4-trimethyl-3-cyclopentenyl)ethyl-(2-methylpropyl) ether; **22** = *tert.*-butyl-[2-(2,2,4-trimethyl-3-cyclopentenyl)ethyl] ether; **23** = but-2-yl-[2-(2,2,4-trimethyl-3-cyclopentenyl)ethyl] ether; **24** = 2-(2,2,4-trimethyl-3-cyclopentenyl)acetic acid methyl ester; **25** = 2-(2,2,4-trimethyl-3-cyclopentenyl)acetic acid (2-methylpropyl) ester; **26** = 2-(2,2,4-trimethyl-3-cyclopentenyl)acetic acid but-2-yl ester; **27** = 2-ethyl-4-(2,2,3-trimethyl-3-cyclopentenyl)but-2-enol; **28** = 2-ethyl-4-(2,2,4-trimethyl-3-cyclopentenyl)but-2-enol.

Table 1

No.	Column	Length (m)	Basic phase	Supplier
1	FS-CYCLODEX alpha I/P	50	OV-1701	CS-Chromatographie Service
2	CP-CD-β-2,3,6 M19	50	OV-1701	Chrompack
3	β-DEX 110	60	SPB 35	Supelco
4	γ-DEX 110	60	SPB 35	Supelco

tron impact ionization (70 eV) was used; the spectra were obtained in scan mode (mass range 35–400) by using helium as carrier gas. For all other analyses, a Hewlett-Packard 5890 II gas chromatograph, equipped with flame ionization detector and split/splitless injector, was available. As carrier gas, hydrogen with a split ratio of 1:100 was chosen.

The chiral resolution cR_s given in the tables was calculated according to Eq. 1.

$$cR_S = 1.177 \cdot \frac{t_{R(2)} - t_{R(1)}}{w_{h(1)} + w_{h(2)}} \quad (1)$$

where the indices 1 and 2 refer to the first- and second-eluting enantiomers, respectively.

The capacity factors k' given in the tables were calculated from the retention times of the stereoisomers and the dead time which was estimated by coinjection of methane.

2.3. Capillary columns

The columns used are shown in Table 1. All capillaries were 0.25 mm I.D. and have the film thickness $d_f = 0.25$ μm.

3. Results and discussion

In order to distinguish the target compounds from any possible impurities and by-products, all mixtures were investigated by GC–MS on chiral and non-chiral columns. The determination of the separation and capacity factors and of the chiral resolution cR_s took place by subsequent analyses by GC–flame ionization detection (FID) at different column temperatures after optimization of the chromatographic conditions. All the substances were analyzed within a temperature interval of about 50°C. In the tables, the separation and capacity factors for the individual compounds are given only at the temperature at which the resolution was highest.

The results of the initial substances used for the separation are shown in Table 2.

Several reports are known on the separation of the two enantiomers of α-pinene [22–25] (but not the α-pinene oxide) by means of capillary GC. Permethylated α-cyclodextrin dissolved in OV-1701 shows the highest enantioselectivity (Table 3) for the simple reduction and oxidation products of α-campholene and fencholene aldehyde with only short side chains (**1–6**).

The separation of the non-derivatized and

Table 2
Separation of initial substances

Compound	First enantiomer	Separation factor, α	Conditions
α-Pinene	(1*S*)-(−)	1.050	Column 2/70°C
α-Pinene oxide	(1*R*)-(−)	1.091	Column 2/100°C
Ethylapopinene	*R*-(+)	1.018	Column 3/120°C
Ethylapopinene oxide	*S*-(+)	1.042	Column 3/120°C

Table 3
Separation factors (α), capacity factors (k') and chiral resolution (cR_s) on permethylated α-, β- and γ-cyclodextrins for **1–8** at column temperature T

No.	α-CD (column 1)				β-CD (column 2)				β-CD (column 3)				γ-CD (column 4)			
	α	k'	T (°C)	cR_s	α	k'	T (°C)	cR_s	α	k'	T (°C)	cR_s	α	k'	T (°C)	cR_s
1	1.025	17.31 17.75	78	1.46	1.00	17.23	80	0.00	1.006	18.62 18.74	80	0.69	1.00	10.40	90	0.00
2	1.034	13.78 14.25	78	2.80	1.00	11.39	88	0.00	1.00	9.36	90	0.00	1.00	7.65	88	0.00
3	1.021	24.87 25.39	90	1.62	1.00	32.24	90	0.00	1.00	9.57	110	0.00	1.00	10.28	110	0.00
4	1.023	21.72 22.22	88	1.41	1.008	8.99 9.07	110	0.64	1.009	7.91 7.98	110	0.82	1.00	7.61	107	0.00
5	1.030	34.18 35.21	110	1.52	1.013	48.60 49.22	110	0.96	1.013	39.60 40.13	110	1.09	1.00	25.70	120	0.00
6	1.045	20.47 21.39	115	2.24	1.059	27.86 29.51	115	2.99	1.062	16.85 17.89	120	4.63	1.016	19.08 19.38	120	1.16
7	1.00	41.78	80	0.00	1.00	21.71	110	0.00	1.00	19.40	110	0.00	[a]			
8	1.00	32.23	100	0.00	1.011	29.85 30.18	105	1.29	1.010	24.56 24.80	120	1.58	[a]			

[a] No values determined.

highly polar acids **5** and **6** is remarkable, especially because as a rule the analysis of carbonic acids on cyclodextrin derivatives took place after the derivatization to esters [26,27]. Only occasionally separations of non-derivatized compounds are reported [4]. Resolution is satisfactory, also on permethylated β-cyclodextrin (Fig. 3).

However, on non-polar stationary phases (OV-1), basically asymmetric peaks appear for these compounds, irrespective of their sample concentration and chromatographic conditions. The good separability on the cyclodextrin phases used should be due to the fact that the non-polar chiral selector is dissolved in medium-polar polysiloxanes.

As in the conditions for enantiomer separation, the retention time becomes very long for the carbonic acids (for the α-campholene acid **5** especially) it should be reduced by shortening the columns accordingly, as recommended earlier [28]. Therefore **5** and **6** were analyzed on a 25-m capillary with permethylated β-cyclodextrin dissolved in polysiloxane.

The results from a comparison with the 50-m capillary (Table 4) show that the chiral resolution decreases with shorter columns. If the enantioselectivity of the chiral selector is small, a separation of the enantiomers is not possible (**5** on the short column). A simultaneously decrease of the column temperature to obtain a higher separation factor [29] also cannot be recommended, because the difference in retention times on the long and the short columns would be negligible small. Therefore we employ a shorter column only if the separation factor is higher than 1.04 (see also [30]).

As the synthesized compounds were obtained from (−)- or (+)-α-pinene with a great enantiomeric excess, it was possible to ascertain the elution order of the enantiomers. With the exception of **1** on column 3, the (1*R*)-enantiomers elute before the (1*S*)-enantiomers on all the columns.

The separation of the α-campholene compounds **9**, **10** and **27** on permethylated cyclodextrin phases is not possible. This is remarkable because the respective fencholene compound

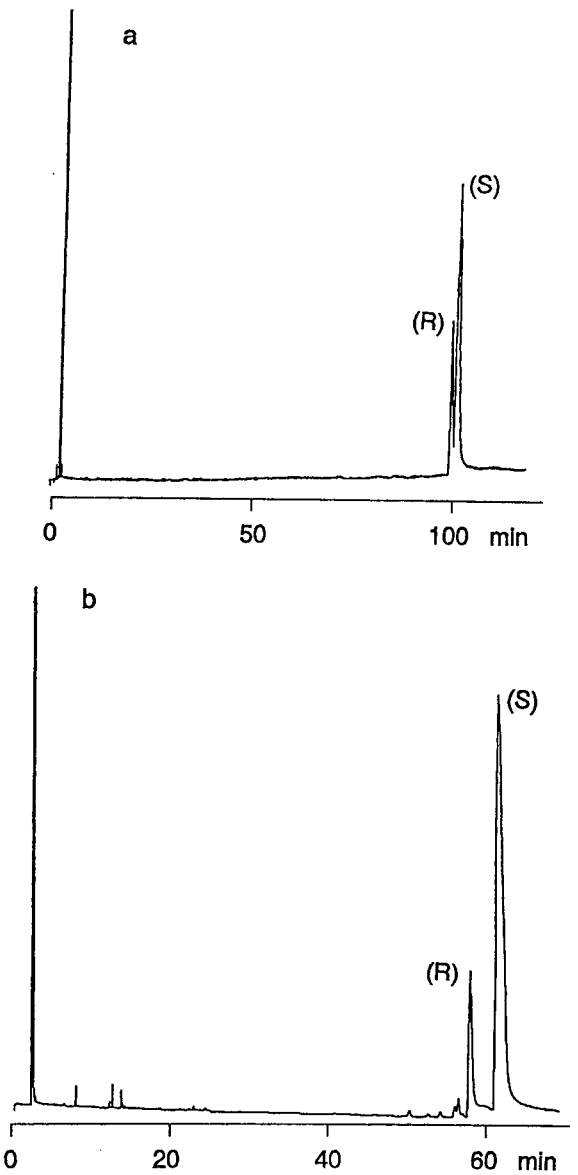

Fig. 3. Chromatograms of (a) α-campholenic acid (**5**) and (b) fencholenic acid (**6**) on permethylated β-cyclodextrin (column 2). Column temperature: 110°C (a) or 115°C (b); injection and FID temperatures: 275 and 250°C, respectively; carrier gas: hydrogen; split ratio 1:100.

(**28**) is separated in the same way as α-campholene derivatives with alkyl chains comparable with **9** and **10** (see [31]). Accordingly, the position of substituents on the five-membered ring and the conformative mobility as well as the

Table 4
Separation factors (α), capacity factors (k') and chiral resolution (cR_s) on capillaries with different length coated with permethylated β-cyclodextrin for α-campholene acid (**5**) and fencholene acid (**6**)

No.	50-m Capillary				25-m Capillary			
	α	k'	T (°C)	cR_s	α	k'	T (°C)	cR_s
5	1.009	19.36 19.53	125	0.78	1.00	19.70	125	0.00
	1.013	48.60 49.22	110	0.96	1.011	49.68 50.29	110	0.55
6	1.050	15.09 15.84	125	3.11	1.047	15.30 16.03	125	2.35
	1.059	27.86 29.51	115	2.99	1.059	28.74 30.45	115	2.58

distance of functional groups from the stereogenic centre in the ring have an influence on the separability of the enantiomers of α-campholene and fencholene derivatives.

The results for the ethers **12**, **13** and **16–23**, and esters **14**, **15** and **24–26** are given in Table 5. For better comparison, ethers and esters with several stereogenic centres are not discussed in Part II but already here.

The polarity of the compounds decreases from

Table 5
Separation factors (α), capacity factors (k') and chiral resolution (cR_s) on permethylated α- and β-cyclodextrins for esters and ethers of α-campholene and fencholene derivatives at column temperature T

No.		α-CD (column 1)				β-CD (column 2)			
		α	k'	T (°C)	cR_s	α	k'	T (°C)	cR_s
12	D1[b]	1.00	29.50	70	0.00	1.00	28.64	70	0.00
	D2	1.025	32.47 33.28	70	1.29	1.00	32.57	70	0.00
13	D1	1.00	21.95	70	0.00	1.00	20.28	70	0.00
	D2	1.00	24.19	70	0.00	1.009	23.79 24.01	70	0.72
14	D1	1.00	28.31	85	0.00	1.00	26.69	85	0.00
	D2	1.018	30.60 31.15	85	1.05	1.009	29.31 29.58	85	0.74
15	D1	1.00	21.46	85	0.00	1.00	19.22	85	0.00
	D2	1.00	22.42	85	0.00	1.00	21.57	85	0.00
16		1.00	28.85	60	0.00	1.011	29.04 29.36	60	0.85
17		1.017	32.89 33.46	65	0.94	1.025	31.46 32.26	65	1.59
24		1.016	22.62 22.98	80	0.90	1.030	22.47 23.14	80	1.18
25			[a]		1.015		21.80 22.13	105	1.38
26	D1		[a]		1.022		24.07 24.61	100	2.20
	D2		[a]		1.012		24.33 24.61	100	1.09

[a] No values determined.
[b] The marking of the individual diastereomers was done schematically by D1 and D2, with D1 corresponding to the diastereomers eluating first on the polar stationary phases (Carbowax) and D2 corresponding to the diastereomer eluating last.

the corresponding alcohols via the esters to the ethers. Connected with this a decrease is found in the enantioselectivity of permethylated α- and β-cyclodextrin both for the α-campholene and the fencholene derivatives. The results show that dipole interactions between the alcohols (or the esters and ethers derived from it) and the chiral selector of the stationary phase contribute to the enantiomer differentiation on permethylated cyclodextrins but they are not their sole cause.

In comparison with **13** and **15**, the separation factors for **16** and **24** are, as expected, slightly larger both on permethylated α- and on β-cyclodextrin. Because this is also the case for α-campholene and fencholene derivatives with two stereogenic centres [31], the better separation must be due to the smaller steric hindrance of the geminal methyl groups on the five-membered ring by the α-positioned methyl substituent in the alkyl side chain.

From the methyl ether **16** to the ethyl ether **17**, the enantioselectivity increases initially on both phases, but gets completely lost with the further extension of the side chain so that **18–23** cannot be separated into the enantiomers. In contrast, the "chiral separation power" will change only slightly in the case of the polar esters **25** and **26**. Also the acetates of the α-campholene and fencholene alcohols **3** and **4** are excellently separated into the enantiomers.

With the increasing space requirement of the alkyl substituents, the ether oxygen of the compounds is sterically more shielded so that for interactions with cyclodextrin it is available only to a limited extent, whereas one free oxygen atom is further available for interactions in the esters. These results also are in favour of a contribution to the enantiomer differentiation from polar interactions.

In the separation of **16** and **17** as well as **24** and **25**, the *R*-enantiomers elute before the *S*-enantiomers in each case. It is remarkable that this elution sequence for **17** and **24** reverses on permethylated α-cyclodextrin (Fig. 4).

Even before, Armstrong et al. [32] and Bicchi et al. [33] had found an inversion of the elution sequence on α- and β-cyclodextrin when using similar cyclodextrin derivatives for selected

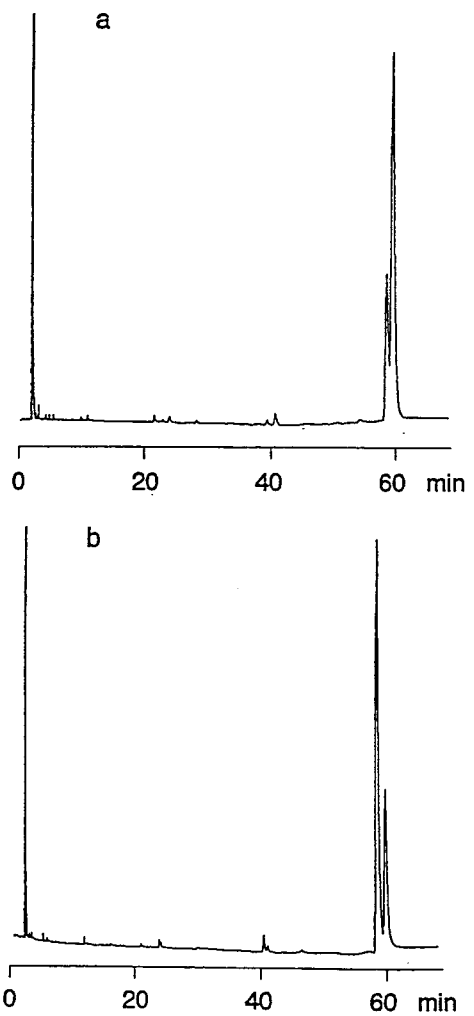

Fig. 4. Chromatograms of **17** on (a) permethylated α-cyclodextrin (column 1) and (b) permethylated β-cyclodextrin (column 2). Column temperature: 65°C; injection and FID temperature: 250°C; carrier gas: hydrogen; split ratio 1:100.

species. Consequently, by selecting the respective stationary phase, it can be made sure that an enantiomer present in excess will elute as second peak in each case. Furthermore, errors that might occur in the determination of the enantiomeric ratio or of the enantiomeric excess will be reduced in this way, for example by the peak area of a component with a small share being influenced by the tailing of the respective surplus component.

Table 6
Separartion factors (α), capacitiy factors (k') and chiral resolution (cR_s) on permethylated β-cyclodextrin for α-campholene and fencholene derivatives with longer alkyl side chains (flavour compounds)

No.	β-CD (column 2)				β-CD (column 3)			
	α	k'	T (°C)	cR_s	α	k'	T (°C)	cR_s
27	1.00	22.19	130	0.00	1.00	21.25	130	0.00
28	1.019	16.44 16.76	130	1.69	1.016	15.60 15.85	130	1.65

α-Campholene and fencholene derivatives with woody and sandal notes (e.g. **10**, **27**, **28**) can only be separated on permethylated β-cyclodextrin phases. Separation factors for two selected representatives are given in Table 6. In all cases, the *R*-enantiomer elutes before the *S*-enantiomer.

Different odour notes of α-campholene and fencholene compounds correlate with the different separability of the two derivatives. Obviously, the conformation differences which are due to the different position of the vinylic methyl group in the five-membered ring influence both odour notes and enantiomer separation.

4. Conclusions

Beginning with the starting substances for the synthesis of woody and sandal wood fragrances of α-campholene and fencholene types all obtained compounds can be separated very well into their enantiomers by using permethylated cyclodextrins dissolved in medium-polar polysiloxanes. For aldehydes, alcohols and acids with short alkyl side chains we employ permethylated α-cyclodextrin; for compounds with longer alkyl chains permethylated β-cyclodextrin can be recommended.

The separation is slightly dependent on the polarity of the compounds and the position of methyl substituents to each other. If there is a steric hindrance of the methyl groups on the five-membered ring, the separation will deteriorate.

Acknowledgement

We wish to thank Supelco, Bad Homburg, Germany for capillary columns 3 and 4. The financial support for this work by the Deutsche Forschungsgemeinschaft and the Fonds der Chemischen Industrie is gratefully acknowledged.

References

[1] P. Schreier and A. Mosandl, *Chem. Unserer Zeit*, 19 (1985) 22–30.
[2] P. Werkhoff, S. Brennecke and W. Brettschneider, *Chem. Mikrobiol. Technol. Lebensm.*, 13 (1991) 129–152.
[3] A. Mosandl, *J. Chromatogr.*, 624 (1992) 267–292.
[4] A. Mosandl, *Kontakte (Darmstadt)*, 3 (1992) 38–48.
[5] E.J. Brunke and E. Klein, in E.T. Theimer (Editor), *Fragrance Chemistry: The Science of the Sense of Smell*, Academic Press, New York, 1982, pp. 397–431.
[6] G. Buchbauer, personal communication.
[7] H. Uhlig, M. Mühlstädt and K. Schulze, *Miltitzer Ber.*, (1985) 23–40.
[8] K. Schulze and H. Uhlig, *Monatsh. Chem.*, 120 (1989) 547–559.
[9] A. Mosandl, G. Bruche, C. Askari and H.-G. Schmarr, *J. High Resolut. Chromatogr.*, 13 (1990) 660–662.
[10] A. Dietrich, B. Maas, W. Messer, G. Bruche, V. Karl, A. Kaunzinger and A. Mosandl, *J. High Resolut. Chromatogr.*, 15 (1992) 590–593.
[11] V. Schurig, D. Schmalzing, U. Mühleck, M. Jung, M. Schleimer, P. Mussche, C. Duvekot and J.C. Buyten, *J. High Resolut. Chromatogr.*, 13 (1990) 713–717.
[12] E. Guichard, A. Hollnagel, A. Mosandl and H.-G. Schmarr, *J. High Resolut. Chromatogr.*, 13 (1990) 299–301.
[13] W.A. König, R. Krebber and G. Wenz, *J. High Resolut. Chromatogr.*, 12 (1989) 641–644.

[14] H.-P. Nowotny, D. Schmalzing, D. Wistuba and V. Schurig, *J. High Resolut. Chromatogr.*, 12 (1989) 383–392.
[15] W.A. König, S. Lutz, C. Colberg, N. Schmidt, G. Wenz, E. von der Bey, A. Mosandl, C. Günther and A. Kustermann, *J. High Resolut. Chromatogr. Chromatogr. Commun.*, 11 (1988) 621–625.
[16] H.-G. Schmarr, A. Mosandl and K. Grob, *Chromatographia*, 29 (1990) 125–130.
[17] C. Bicchi, G. Artuffo, A. D'Amato, G. Pellegrino, A. Galli and M. Galli, *J. High Resolut. Chromatogr.*, 14 (1991) 701–704.
[18] R. Reinhardt, A. Steinborn, W. Engewald, K. Schulze and K. Beutmann, in P. Sandra (Editor), *Proceedings of the 15th International Symposium on Capillary Chromatography, Riva del Garda, May 1993*, Hüthig, Heidelberg, pp. 337–344.
[19] R. Reinhardt, *Thesis*, University of Leipzig, Leipzig, 1993.
[20] B. Arbusov, *Ber. Dtsch. Chem. Ges.*, 68 (1935) 1430–1435.
[21] K. Schulze, K. Beutmann, A.-K. Habermann and U. Himmelreich, *J. Prakt. Chem.*, 335 (1993) 445–448.
[22] V. Schurig, M. Jung, D. Schmalzing, M. Schleimer, J. Duvekot, J.C. Buyten, J.A. Peene and P. Muschee, *J. High Resolut. Chromatogr.*, 13 (1990) 470–474.
[23] G. Takeoka, R.A. Flath, T.R. Mon, R.G. Buttery, R. Teranishi, M. Güntert, R. Lautamo and J. Szejtli, *J. High Resolut. Chromatogr.*, 13 (1990) 202–206.
[24] W.A. König, R. Krebber, P. Evers and G. Bruhn, *J. High Resolut. Chromatogr.*, 13 (1990) 328–332.
[25] A. Mosandl, U. Hener, P. Kreis and H.-G. Schmarr, *Flavour Frag. J.*, 5 (1990) 193–199.
[26] W.A. König, R. Krebber and P. Mischnick, *J. High Resolut. Chromatogr.*, 12 (1989) 732–738.
[27] P. Fischer, R. Aichholz, U. Bölz, M. Juza and S. Krimmer, *Angew. Chem.*, 102 (1990) 439–441.
[28] M. Lindström, *J. High Resolut. Chromatogr.*, 14 (1991) 765–767.
[29] I. Hardt and W.A. König, *J. Microcol. Sep.*, 5 (1993) 35–40.
[30] C. Bicchi, G. Artuffo, A. D'Amato, A. Galli and M. Galli, *J. High Resolut. Chromatogr.*, 15 (1992) 655–658.
[31] A. Steinborn, R. Reinhardt, W. Engewald, K. Wyssuwa and K. Schulze, *J. Chromatogr. A*, 697 (1995) 485–494.
[32] D.W. Armstrong, W. Li and J. Pitha, *Anal. Chem.*, 62 (1990) 214–217.
[33] C. Bicchi, G. Artuffo, A. D'Amato, G.M. Nano, A. Galli and M. Galli, *J. High Resolut. Chromatogr.*, 14 (1991) 301–305.

ELSEVIER

Journal of Chromatography A, 697 (1995) 485–494

JOURNAL OF CHROMATOGRAPHY A

Enantiomer separation of α-campholene and fencholene derivatives by capillary gas chromatography on permethylated cyclodextrins
II☆. Compounds separable with coupled techniques

A. Steinborn[a], R. Reinhardt[b], W. Engewald[a,*], K. Wyssuwa[c], K. Schulze[c]

[a]*Institute of Analytical Chemistry, Department of Chemistry, University of Leipzig, Linnéstrasse 3, D-04103 Leipzig, Germany*
[b]*Institute of Pharmacology and Toxicology, Department of Medicine, University of Leipzig, Härtelstrasse 16–18, D-04107 Leipzig, Germany*
[c]*Institute of Organic Chemistry, Department of Chemistry, University of Leipzig, Liebigstrasse 18, D-04103 Leipzig, Germany*

Abstract

Odoriferous substances, such as sandal and woody notes of the α-campholene and fencholene type with two and more stereogenic centres, were analyzed by capillary gas chromatography on permethylated cyclodextrins dissolved in polysiloxanes. From enantiomer-enriched α-pinene compounds, received as non-racemic mixtures, the theoretically possible number of stereoisomers were determined after the introduction of additional stereogenic centres. The derivatives with two stereogenic centres were separated on single columns. In the case of substances with three stereogenic centres a serial coupling of non-chiral and chiral columns partially connected with a mass selective detector was necessary for the separation and reliable identification. For optimizing the selectivity of the serially coupled system the principle of selectivity tuning was used. This discussion also deals with the retention behaviour and the factors influencing the enantiomer separation of the α-campholene and fencholene compounds.

1. Introduction

After the introduction of derivated cyclodextrins as chiral stationary phases for capillary gas chromatography (GC) [1–6] there are various cyclodextrin derivatives for routine analysis of chiral substances nowadays known and used. However, only in the last few years attempts have been made to investigate the separation mechanism on the basis of thermodynamic data [7–9], NMR investigations [10], molecular modelling experiments [11,12], and by comparing the separation of structurally similar compounds [13,14]. The latter method was also used for the investigation of α-campholene and fencholene derivatives in this study, as described in Parts I and II of this article.

α-Campholene and fencholene aldehyde, which are easily made available by camphane or fenchane rearrangement from α-pinene via α-pineneoxide, are suitable initial substances for the synthesis of odoriferous compounds, such as wood and sandalwood notes. The α-campholene and fencholene compounds are stereoisomeric

* Corresponding author.
☆ For Part I, see Ref. [15].

0021-9673/95/$09.50
SSDI 0021-9673(94)01073-0

mixtures; one stereogenic centre is transmitted by α-pinene, others are formed by alkylations, aldol reactions and reductions. In Part I [15] we reported on the GC separation of α-campholene and fencholene derivatives with one stereogenic centre. In this part we are describing the separation of α-campholene and fencholene alcohols with two and more chiral centres.

For compounds whose separation or assignment of the enantiomers was difficult on chiral stationary phases serially coupled column systems were used. For several years this method, also known as multidimensional gas chromatography (MDGC), has been used successfully by some teams for the analysis of multicomponent mixtures [16–20]. The separation of the diastereomers takes place on an non-chiral precolumn, after which they are transmitted onto a chiral column and are separated into the enantiomers. Because of the sometimes not easily separable by-products and impurities in the stereoisomer mixtures mass selective detection was indispensable. For this purpose a commercial MDGC device with a gas chromatography–mass spectrometry (GC–MS) system was coupled via a heatable transfer line.

By means of MDGC the assignment of the pairs of enantiomers to the diastereomers was also possible beyond any doubt for compounds with three stereogenic centres .

2. Experimental

2.1. Investigated substances

α-Campholene and fencholene derivatives with two or more stereogenic centres were synthesized according the scheme given in Part I and as described earlier [21–24]. The individual structures of the substances investigated in Part II are shown in Fig. 1.

2.2. Instrumentation

A double oven GC from Siemens (Sichromat 2-8) with two flame ionization detectors (FIDs) and split injector was available for the MDGC analyses. Mass selective detection took place by coupling the Sichromat with a conventional HP 5890 II GC/HP 5971A MSD system via a heatable transfer line (laboratory made). The temperature of the transfer line was 250°C. The ionization took place by electron impact (70 eV). For the acquisition of spectra in the scan mode (mass range 35–400) helium was used as carrier gas. For all further analyses a Hewlett-Packard 5890 II gas chromatograph, equipped with FID and split/splitless injector was used. As carrier gas hydrogen with a split ratio of 1:100 was chosen.

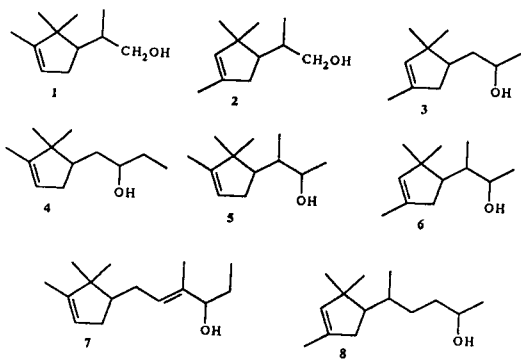

Fig. 1. Investigated Substances. **1** = 2-(2,2,3-Trimethyl-3-cyclopentenyl)propanol; **2** = 2-(2,2,4-trimethyl-3-cyclopentenyl)propanol; **3** = 1-(2,2,4-trimethyl-3-cyclopentenyl)-2-propanol; **4** = 1-(2,2,3-trimethyl-3-cyclopentenyl)-2-butanol; **5** = 3-(2,2,3-trimethyl-3-cyclopentenyl)-2-butanol; **6** = 3-(2,2,4-trimethyl-3-cyclopentenyl)-2-butanol; **7** = 4-methyl-6-(2,2,3-trimethyl-3-cyclopentenyl)-hex-4-en-3-ol; **8** = 5-(2,2,4-trimethyl-3-cyclopentenyl)-2-hexanol.

The chiral resolution cR_s and the capacity factors k' given in the tables were calculated as given in Part I [15]. The dead times were measured by injection of methane.

2.3. Capillary columns

The internal diameter of all capillaries was 0.25 μm, the film thickness (d_f) 0.25 μm (column 7 $d_f = 0.2$ μm). The specifications of the columns are given in Table 1.

2.4. Description of the laboratory-made MDGC–MS coupling

The coupling of the Sichromat with the GC–MS system took place via a transfer line heatable

Table 1

No.	Column	Length (m)	Basic phase	Supplier
1	FS-CYCLODEX alphaI/P	50	OV-1701	CS-Chromatographie Service
2	CP-CD-β-2,3,6 M19	50	OV-1701	Chrompack
3	β-DEX 110	60	SPB 35	Supelco
4	γ-DEX 110	60	SPB 35	Supelco
5	Supelcowax	30		Supelco
6	DB-5	60		Chrompack
7	SB-11	60		IAS

in the temperature range from 30 to 380°C. It consists of a 1.25-m long steel tube (I.D. = 1 mm) through which an uncoated deactivated fused-silica capillary (Chrompack, non-polar, deactivated) runs from the second column of the Sichromat to the interface of the MSD. In order to enlarge the outside diameter and to ensure a better heat transmission a copper tube is placed on the steel tube holding the heater winding. The temperature is controlled by means of two thermo elements arranged at the two ends and an external thermo regulator (control tolerance ± 1%).

The system was tested for differently polar, high-boiling test substances (*n*-alkanes, alcohols, dimethylnaphthalene, cyclopentenyl derivatives) for a possible dependence of the peak form or the retention on the temperature of the transfer line. Any significant changes in the peak symmetry, tailing or differences in the retention times can not be proved if the temperature is equal to or higher than the one in the GC oven. By using well deactivated fused-silica no signs of adsorption effects were observed.

3. Results and discussion

3.1. Solution of difficult separation problems

With the exception of **3** and **7** the separation of the enantiomers with two stereogenic centres on the columns used was possible without any problems. The marking of the individual diastereomers was done schematically by D1 to D4, with D1 corresponding to the diastereomers eluting first on the polar stationary phases (Carbowax) and D4 corresponding to the diastereomer eluting last.

The analysis of **3** proved to be particularly difficult. On non-polar non-chiral phases the two diastereomers could only be partially separated and on medium and strong polar phases not at all. In preliminary experiments on a 25-m capillary with permethylated β-cyclodextrin (dissolved in OV-1701) a separation into two peaks took place. As enantiomer-enriched α-pinene was used in the synthesis a comparison of peak areas obtained on chiral and non-chiral phases showed that not the diastereomers were separated but the enantiomers, with each the diastereomers *RR* and *RS* as well as *SS* and *SR* overlapping in one peak. If a 50-m column with the same stationary phase (column 2) was used, all stereoisomers were able to be separated at different temperatures (Fig. 2).

Also **7** has two asymmetric centres, and because of the double linkage in the side chain the possibility of *Z*/*E* isomerism is theoretically given. However, the formation of the *Z*-isomer on the reaction path used is unlikely [25]. Accordingly, two diastereomeric pairs of enantiomers are to be expected. On columns 2–4 altogether 3 peaks were registered for the compound, which cannot be assigned by means of peak area comparison because the separation is incomplete. Only a preseparation of the diastereomers and a subsequent transfer of single diastereomers onto a second chiral column showed that the enantiomers of the first eluting

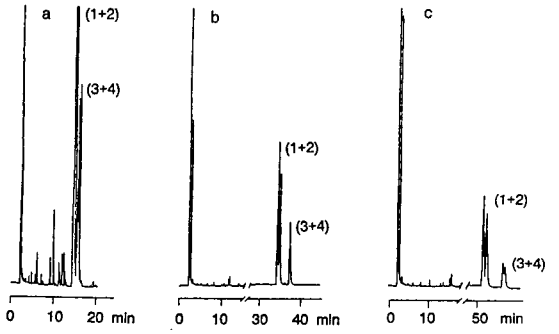

Fig. 2. Chromatogram of **3** on permethylated β-cyclodextrin (column 2). Column temperature: (a) 115°C, (b) 95°C, (c) 90°C; injection/FID: 300°C/250°C; carrier gas: hydrogen; split ratio 1:80; Peak (1) and (2): *SS*- and *SR*-stereoisomers; Peak (3) and (4): *RR*- and *RS*-stereoisomers.

diastereomer are separated but not those of the second diastereomer.

The compounds 3-(2,2,3-trimethyl-3-cyclopentenyl)-2-butanol (**5**), 3-(2,2,4-trimethyl-3-cyclopentenyl)-2-butanol (**6**) and 5-(2,2,4-trimethyl-3-cyclopentenyl)-2-hexanol (**8**) each have three stereogenic centres so that eight stereoisomers can be expected. A complete separation of all components was also not possible on a single column. The fundamental approach is explained by the example of **5**.

The chromatogram of **5** (Fig. 3a) on a non-chiral column shows a great number of peaks and those marked were identified by GC–MS as diastereomers of **5**.

A subsequent GC–MS analysis of this compound on column 4 shows seven peaks whose mass spectra are in accordance with 3-(2,2,3-trimethyl-3-cyclopentyl)-2-butanol (**5**). As eight components were expected in this mixture a co-elution of two stereoisomers was taken place in one peak, or one of the diastereomers was not separated into the optical antipodes. A complete separation was possible only when columns 4 and 5 were coupled in series. A double oven system was necessary because the temperatures of the non-chiral and the chiral column are different.

In principle it is possible in such a system to transfer individual peaks as well as groups of peaks to the second column after a preseparation on the first column. The individual peak transfer

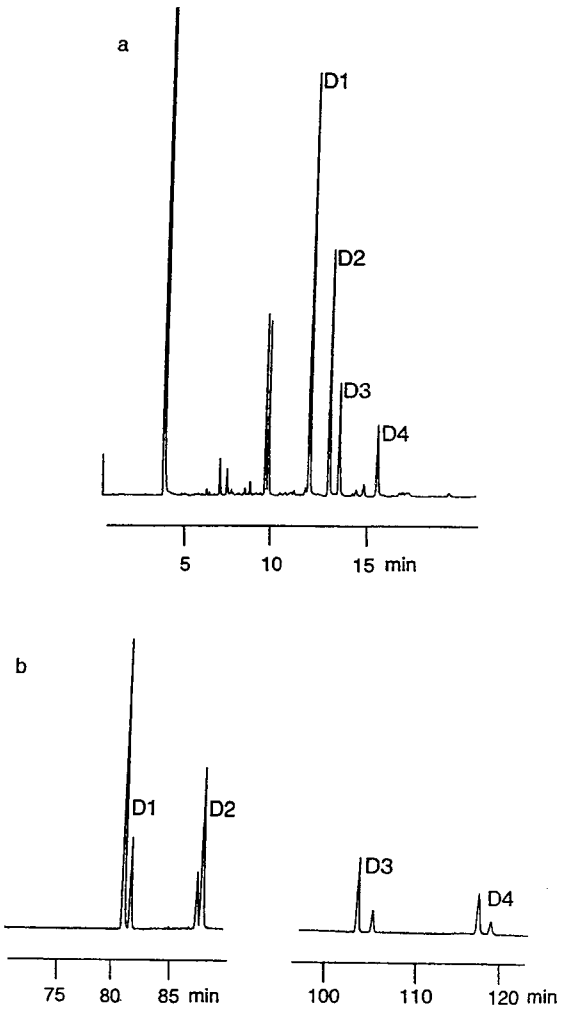

Fig. 3. (a) Separation of **5** on Carbowax (column 5). Column temperature: 160°C; injection/FID: 250°C; 55 kPa helium; split 1:30. (b) Separation of diastereomers D_1–D_4 on column 4. Column temperature: 120°C; 120 kPa Helium.

corresponds to a genuine multidimensional GC and has the advantage that any peak overlapping are to the greatest possible extent excluded; however, the analysis of mixtures needs a rather long time. Generally, an optimization of the column system is also necessary in the case of a single-peak transfer because the separation on the overall system is influenced by both columns in which the share of cyclodextrin should be as large as possible. For optimizing the selectivity in serially coupled systems the principle of selectivi-

ty tuning can be used (for theory, see Refs. [26,27]; for applications, see Refs. [28,29]). The system allows to calculate capacity factors k' for various medium pressures from the k' values for the individual columns.

The relative share, Φ, of a column used (often named relative retentivity) is expressed as ratio of the dead time of the column to the dead time of the total system. In Fig. 4 we show the relative retention of the 8 stereoisomers (related to stereoisomer **8**) calculated for different shares, Φ_2, of the cyclodextrin phase in the total system.

Here $\Phi_2 = 1$ correspond to the poor cyclodextrin phase; $\Phi_2 = 0$ to the poor Carbowax phase. For the diastereomers **2** and **3** the most favourable separation is possible at very small Φ_2 values (0.1–0.3) or at relatively large Φ_2 values (0.6–0.8). However, not all the Φ values can be realized by experimental procedures. Investigations have shown that by using this column system, selectivity tuning is only possible for Φ_2 values between 0.45 and 0.70. The chromatogram (Fig. 3) shows the separation of the diastereomers **1** and **2** as well as **3** and **4** of 3-(2,2,3-trimethyl-3-cyclopentenyl)-2-butanol (**5**) in 2 cuts at $\Phi_2 = 0.61$.

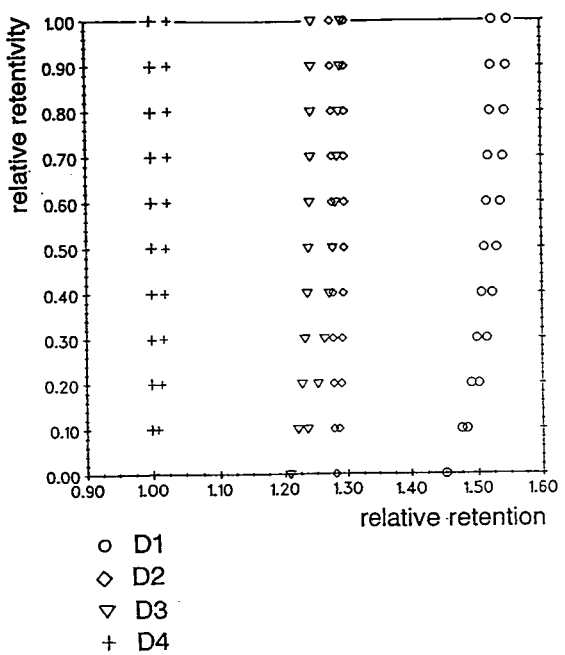

Fig. 4. Selectivity change in dependence on the share of columns.

In the case of **6** also eight stereoisomers can be expected. The chromatogram on non-chiral column (Fig. 5a) shows a coelution of the fourth diastereomer and impurities of the mixture. Therefore by coupling the non-chiral and chiral columns a mass selective detection was necessary for complete identification (Fig. 5b).

3.2. Discussion of retention behaviour

The separation factors make clear that only in few cases permethylated α-cyclodextrin is suitable as chiral selector. Having in mind the number of separable stereoisomers and the chiral resolution the best results are clearly obtained by the use of permethylated β-cyclodextrin. This was also found for the compounds investigated in Part I [15].

The results of the studies with the four permethylated cyclodextrin phases are shown in Table 2.

With growing size of the alkyl side chains also the enantioselectivity of permethylated γ-cyclodextrin will be higher, i.e. with increasing statistical space requirements of the investigated derivatives the cyclodextrin derivative with the larger cavities is more suitable. This fact underlines the importance of inclusion effects for enantiomer separation. On the other hand, permethylated α-cyclodextrin shows a certain enantioselectivity for a few stereoisomers of the larger molecules. Consequently, besides the formation of host–guest inclusion complexes also other interactions should be of importance for enantiomer differentiation, for example electrostatical ones.

In the following it is shown that the enantiomer differentiation of the α-campholene and fencholene derivatives is influenced by the structure of the compound, i.e. by steric effects. On all cyclodextrin phases the fencholene compounds are better separated than their analogous α-campholene derivatives although they differ from each other only in the position of the methyl group on the cyclopentenyl ring (α-cam-

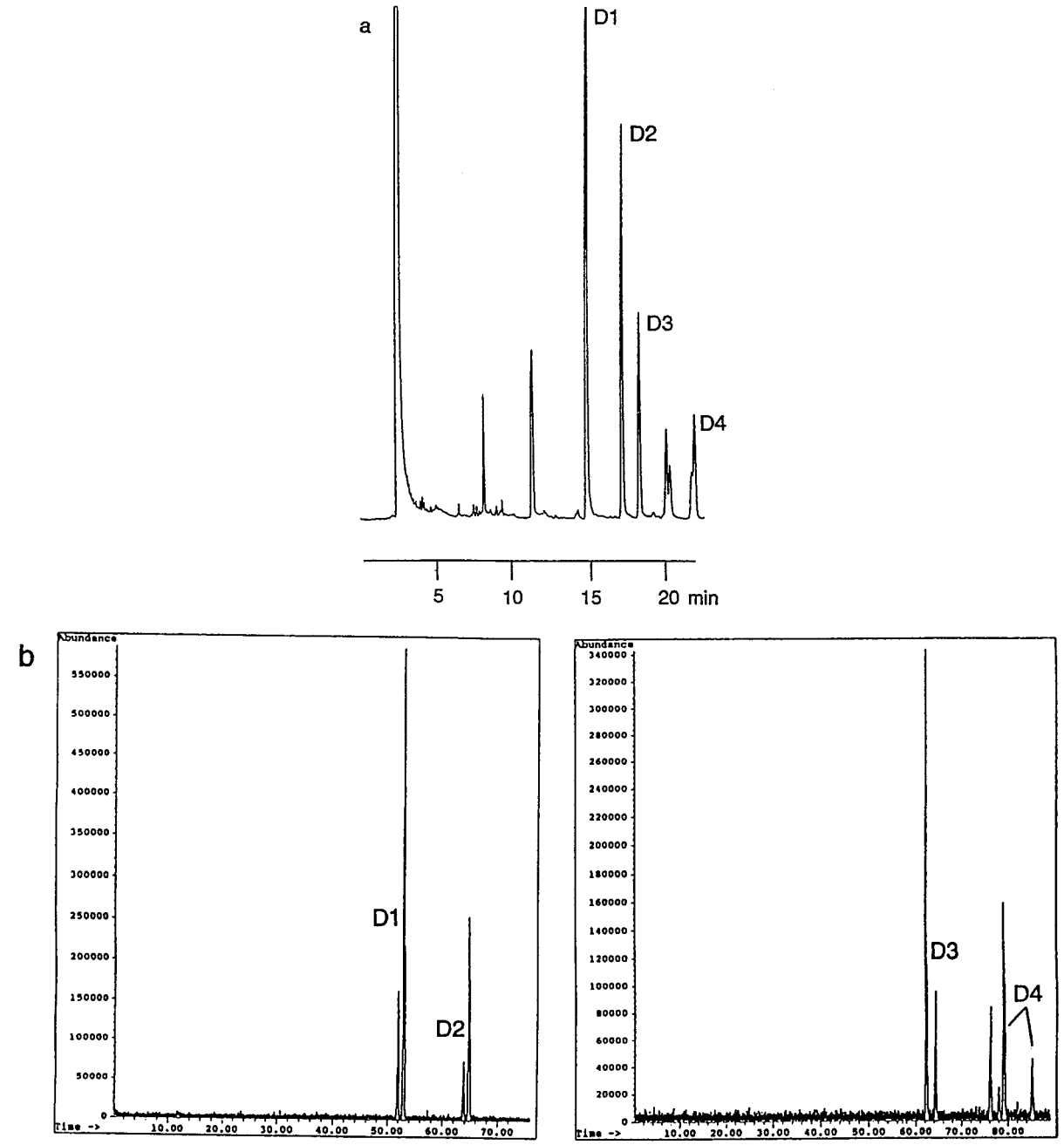

Fig. 5. Analysis of **6** with MDGC–MS. (a) Chromatogram of the diastereomers on column 5. Column temperature: 140°C; injection/FID: 300°C; 50 kPa helium; split 1:30. (b) Separation of the four diastereomers after peak transfer onto column 3. Column temperature: 120°C; 150 kPa helium; detector: MS, transferline: 280°C.

pholene = 3-methyl; fencholene = 4-methyl). If the five-membered ring enters the cyclodextrin cavity, the methyl group in the 4-position is possibly capable of additional dispersive interactions within the cyclodextrin because they are sterically less influenced by the geminal methyl substituents on the ring. Obviously, for α-campholene derivates such interactions are not that typical.

The results for the alcohols **1** and **2** are remarkable. The diastereomers of the α-campholene compounds are partially separated on permethylated α-cyclodextrin but not those of the fencholene analogue. On permethylated β-cyclodextrin, however, it are only the diastereomers of the fencholene compounds that are better separable, those of the α-campholene derivate can only be partially separated. In the case of these substances they hinder each other by the methyl group in the side chain which is in the α-position of the five-membered ring and the two geminal methyl substituents on cyclopentene, or they cause a different conformation of the side chain. Additionally, another steric hin-

Table 2
Separation factors, α, capacity factors, k' and chiral resolution, cR_S, on permethylated α-, β- and γ-cyclodextrins dissolved in polysiloxanes

No.		α-CD (column 1)				β-CD (column 2)			
		α	k'	T (°C)	cR_S	α	k'	T (°C)	cR_S
1	D1	1.017	27.87 28.34	95	0.94	1.030	15.20 15.66	110	2.14
	D2	1.017	30.80 31.32	95	0.94	1.00	16.66	110	0.00
2	D1	1.00	21.10	95	0.00	1.045	12.25 12.80	110	3.46
	D2	1.00	23.40	95	0.00	1.021	13.04 13.31	110	1.57
3	D1	1.00	18.16	90	0.00	1.059	9.65 10.22	105	5.37
	D2	1.00	18.16	90	0.00	1.054	9.75 10.28	105	3.29
4	D1	1.00	12.84	115	0.00	1.021	25.06 25.59	100	1.79
	D2	1.00	13.08	115	0.00	1.025	26.14 26.79	100	1.79
5	D1	1.00	28.73	95	0.00	1.00	14.13	110	0.00
	D2	1.015	33.79 34.28	95	0.89	1.015	17.05 17.30	110	1.50
	D3	1.032	34.84 35.94	95	1.84	1.013	17.42 17.65	110	0.94
	D4	1.00	44.10	95	0.00	1.053	22.16 23.34	110	4.34
6	D1	1.00	12.55	105	0.00	1.043	10.06 10.49	110	3.49
	D2	1.00	15.11	105	0.00	1.069	12.83 13.72	110	5.99
	D3	1.016	15.51 15.76	105	0.90	1.030	13.46 13.86	110	2.37
	D4	1.017	18.48 18.79	105	0.93	1.143	17.62 20.14	110	10.99

(*Continued on p. 492*)

Table 2 (*continued*)

No.		β-CD (column 3)				γ-CD (column 4)			
		α	k′	T (°C)	cR$_s$	α	k′	T (°C)	cR$_s$
1	D1	1.024	14.01 14.35	110	2.21	1.021	15.78 16.12	110	2.03
	D2	1.00	15.47	110	0.00	1.00	16.80	110	0.00
2	D1	1.038	10.97 11.39	110	3.39	1.021	11.46 11.70	110	1.86
	D2	1.023	11.71 11.98	110	2.16	1.00	12.70	110	0.00
3	D1	1.042	8.39 8.75	105	3.29	1.00	17.68	100	0.00
	D2	1.061	8.39 8.90	105	4.48	1.013	18.10 18.36	100	0.95
4	D1	1.031	21.82 22.50	100	3.01	1.00	18.03	105	0.00
	D2	1.014	22.96 23.27	100	1.26	1.00	18.68	105	0.00
5	D1	1.009	13.18 13.30	110	0.87	1.026	14.69 15.07	110	2.71
	D2	1.015	15.72 15.95	110	1.39	1.015	17.77 18.04	110	1.73
	D3	1.011	16.52 16.71	110	1.13	1.044	17.77 18.55	110	4.39
	D4	1.052	20.87 21.96	110	4.31	1.030	22.62 23.30	110	3.96
6	D1	1.040	9.24 9.61	110	3.74	1.009	10.51 10.61	110	0.88
	D2	1.066	11.59 12.36	110	6.25	1.048	12.99 13.61	110	4.38
	D3	1.031	12.36 12.74	110	2.86	1.048	12.99 13.61	110	4.38
	D4	1.143	15.99 18.27	110	13.01	1.015	17.13 17.39	110	[a]
8	D1	1.019	30.04 30.62	110	1.47		[a]		
	D2	1.012	30.68 31.04	110	1.23				
	D3	1.013	33.88 34.30	110	1.21				
	D4	1.011	34.69 35.07	110	1.20				

[a] No values determined.

drance of this methyl group takes place with the one in 3-position on the five-membered ring. On the basis of this the steric effects for **1** and **2** as compared with **3** and **4** in [15] should have a stronger influence on the enantiomer differentiation. This assumption is in agreement with the measured values on all cyclodextrin phases used. The changes on the two permethylated β-cyclodextrin phases being the largest.

If a compound is a mixture of two or more independent diastereomers with very similar chemical and physical properties (e.g. **2/3**) only a very narrow temperature range will exist for an optimum resolution of all the stereoisomers

present in the mixture. If there are deviations from this optimum column temperature by only 5°C there will be peak overlapping (Fig. 6) or an inversion of the elution sequence, as was observed for **3** (Fig. 2).

The cause for this behaviour is the different temperature dependence of the retention of the diastereomers and the enantiomers. With the change of the column temperature the difference in the retentions of both the diastereomers and the enantiomers will be changing. Both changes neither need to be equal in their extent nor need the retention difference of two (neighbouring) stereoisomers become altogether bigger in the case of a change in the column temperature. The probability of overlapping or of elution sequence inversion of various stereoisomers due to the change in the column temperature is the higher, the smaller the selectivity of the stationary phase used is against the diastereomers, and the more independent stereogenous centres are included in the compound. By analogy with the iso-enantioselective temperature [30–32] at which two enantiomers are overlapping this point could be called the pseudo-iso-enantioselective temperature.

As the compounds were stereoisomer mixtures no clear configuration assignment was possible for the various peaks. However, the following can be derived from the path of synthesis. The α-pinene used for the synthesis showed a clear excess of (*R*)-(+)-enantiomers (40% ee). As neither epoxidation nor camphane and fenchane rearrangement will change the ratio of the enantiomers, α-campholene and fencholene aldehyde are received with 40% ee of the resulting (*S*)-(−) enantiomers. The subsequent Grignard reaction to alcohol **3** leads to the formation of a new stereogenic centre which is not diastereoselectively influenced by the one already existing.

Because of the non-racemic ratio of the enantiomers in the pinene the ratio of the enantiomers in the alcohol **3** can therefore not be expected to be racemic. According to this, the stereoisomers *SS*/*SR* to *RR*/*RS* must behave like *R* to *S* in the pinene used (*S* to *R* in the α-campholene aldehyde).

As there is no change in the priority of the substituents on the asymmetric carbon of the five-membered ring beginning with the aldehyde it can be deduced from the peak area ratios that for **3** the *SS* elutes before the *RR* and, likewise, the *SR* elutes before the *RS* enantiomers. By analogy to this an assignment was made for **2** in Fig. 6, and for **7** in Fig. 3.

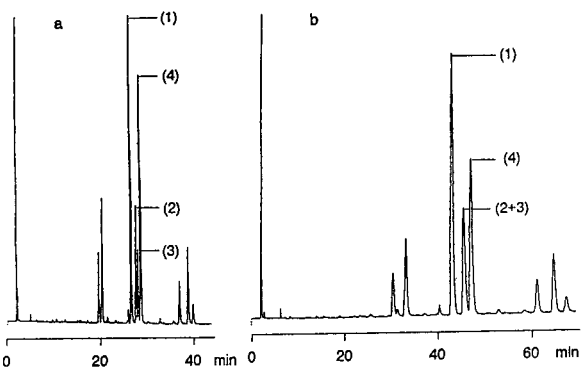

Fig. 6. Chromatogram of **2** on permethylated β-cyclodextrin (column 2). column temperature: (a) 110°C, (b) 105°C; injection/FID: 300°C/250°C; carrier gas: hydrogen; split ratio 1:80; Peak (1) and (4): *SS*- and *SR*-stereoisomers; Peak (2) and (3): *RR*- and *RS*-stereoisomers.

4. Conclusion

On permethylated α-, β- and γ-cyclodextrins dissolved in polysiloxanes it is possible to separate stereoisomer mixtures of α-campholene and fencholene derivatives with up to three stereogenic centres into the enantiomers in an excellent way.

For compounds with two stereogenic centres the separation is possible on single columns. It needs to be considered that the diastereomer selectivity of the basic phases and the enantiomer selectivity of the chiral selector are temperature-dependent to a different extent so that peak overlapping and elution sequence inversions were often observed.

Especially the steric structure of the compounds has an influence on the enantiomer

separation. If methyl substituents of the substances hinder each other the separation is clearly impaired. This effect was also found for the ethers and esters discussed in Part I.

For compounds with three stereogenic centres couplings of the non-chiral precolumn and the chiral main column are necessary in order to guarantee a complete separation of the mixture. For a reliable identification of the derivatives with two asymmetric centres and for separation of impurities it is helpful — and for the derivatives with three stereogenic centres absolutely necessary — that the considerably better separation by column coupling is combined with the advantages of mass selective detection. Such coupling is easily realized between commercial instruments.

Acknowledgement

We wish to thank Supelco Deutschland/Bad Homburg for capillary columns 3 and 4. The financial support for this work by the Deutsche Forschungsgemeinschaft and the Fonds der Chemischen Industrie is gratefully acknowledged.

References

[1] V. Schurig and H.-P. Nowotny, *J. Chromatogr.*, 441 (1988) 155–163.
[2] W.A. König, S. Lutz, and G. Wenz, *Angew. Chem.*, 100 (1988) 989–990.
[3] D.W. Armstrong, W. Li, and J. Pitha, *Anal. Chem.*, 62 (1990) 214–217.
[4] D.W. Armstrong, W. Li, C.D. Chang and J. Pitha, *Anal. Chem.*, 62 (1990) 914–923.
[5] Z. Juvancz, G. Alexander and J. Szejtli, *J. High Resolut. Chromatogr. Chromatogr. Commun.*, 10 (1987) 105.
[6] A. Venema and P.J.A. Tolsma, *J. High Resolut. Chromatogr. Chromatogr. Commun.*, 12 (1989) 32.
[7] A. Berthod, W. Li and D.W. Armstrong, *Anal. Chem.*, 64 (1992) 873–879.
[8] V. Schurig, D. Schmalzing and M. Jung, *J. Chromatogr.*, 552 (1991) 43–57.
[9] R. Reinhardt, W. Engewald, G. Haufe and O. Goj, *Chromatographia*, 39 (1994) 192–199.
[10] W. Meier-Augenstein, B.V. Burger, H.S.C. Spies and W.J.G. Burger, *Z. Naturforsch.*, 47b (1992) 877–886.
[11] F. Kobor, K. Angermund and G. Schomburg, *J. High Resolut. Chromatogr.*, 16 (1993) 299–311.
[12] N. Koen de Vries, B. Coussens, R.J. Meier and G. Heemels, *J. High Resolut. Chromatogr.*, 15 (1992) 499–504.
[13] A. Venema, H. Hendriks and R. v. Geest, *J. High Resolut. Chromatogr. Chromatogr. Commun.*, 14 (1991) 676–680.
[14] I.D. Smith and C.F. Simpson, *J. High Resolut. Chromatogr.*, 15 (1992) 800–806.
[15] R. Reinhardt, A. Steinborn, W. Engewald, K. Anhalt and K. Schulze, *J. Chromatogr. A*, 697 (1995) 475–484.
[16] P. Werkhoff, S. Brennecke and W. Brettschneider, *Chem. Mikrobiol. Technol. Lebensm.*, 13 (1991) 129–152.
[17] A. Mosandl, *J. Chromatogr.*, 624 (1992) 267–292.
[18] A. Bernreuther and P. Schreier, *Phytochem. Anal.*, 2 (1991) 167–170.
[19] P. Kreis and A. Mosandl, *Flavour Frag. J.*, 7 (1992) 187–193.
[20] S. Nitz, H. Kollmannsberger and F. Drawert, *Chem. Mikrobiol. Technol. Lebensm.*, 12 (1989) 75–80.
[21] B. Arbusov, *Ber. Dtsch. Chem. Ges.*, 68 (1935) 1430–1435.
[22] H. Uhlig, M. Mühlstädt and K. Schulze, *Miltitzer Ber.*, (1985) 23–40.
[23] M. Mühlstädt, G. Feustel, M. Hermann and W. Dollase, *DD-Pat.*, 68936 (1969), *C.A.* 72 (1969) P125008.
[24] E.-J. Brunke and E. Klein, *DBP*, 2827957 (1978), *C.A.*, 93 (1980) P137899.
[25] K. Schulze and H. Uhlig, *Monatsh. Chem.*, 120 (1989) 547–559.
[26] J.V. Hinshow and L.S. Ettre, *Chromatographia*, 21 (1986) 561–572.
[27] J.V. Hinshow and L.S. Ettre, *Chromatographia*, 21 (1986) 669–680.
[28] T. Maurer, W. Engewald and A. Steinborn, *J. Chromatogr.*, 517 (1990) 77–86.
[29] A. Steinborn, W. Engewald and R. Reinhardt, in P. Sandra (Editor), *Proceedings of the 15th International Symposium on Capillary Chromatography, Riva del Garda, May 1993*, Hüthig, Heidelberg, 1993, pp. 892–900.
[30] B. Koppenhöfer and E. Bayer, *Chromatographia*, 19 (1984) 123–130.
[31] K. Watabe, R. Charles and E. Gil-Av, *Angew. Chem.*, 101 (1989) 195–197.
[32] V. Schurig, J. Ossig and R. Link, *Angew. Chem.*, 101 (1989) 197–198.

ELSEVIER

Journal of Chromatography A, 697 (1995) 495–499

JOURNAL OF CHROMATOGRAPHY A

Computerized capillary gas chromatographic identification and determination of Siberian fir oil constituents

A. Orav*, K. Kuningas, T. Kailas

Institute of Chemistry, Estonian Academy of Sciences, Akadeemia tee 15, EE-0026 Tallinn, Estonia

Abstract

A method for the computer-assisted identification of peaks on a chromatogram on the basis of their retention indices on two capillary columns of different polarity was developed and applied to the identification and determination of Siberian fir oil components

1. Introduction

High-resolution capillary gas chromatography is still the most suitable technique available for the separation and identification of complex mixtures of volatile aroma compounds. This work is a part of our efforts to develop a rapid and simple, but reliable, method for a food and perfumery control system in Estonia. The purpose of this particular study was to develop a computerized capillary GC method with two columns of different polarity for analysing fir oil samples for terpenoic compounds.

The volatile constituents of conifer needles and oleoresins have been studied by different GC methods by several groups [1–3]. Siberian fir oil is produced by steam distillation from needles, twigs and sprouts of the plants *Abies sibirica* Ledeb. Average yields of the oil are 1.2–3%.

2. Experimental

Experiments were performed on a Chrom-5 gas chromatograph (Laboratórní Přístroje, Prague, Czech Republic) equipped with a flame ionization detector. Helium was used as the carrier gas with a splitting ratio of about 1:150. A Hewlett-Packard Model 3390A integrator and IBM 286 personal computer were applied for data processing.

Table 1 specifies the columns used and the conditions of analysis.

Characteristic properties of industrial Siberian fir oil samples were as follows: origin, Krasnoyarsk Region, Siberia; colour, light-yellow, clear liquid; odour, specific coniferous odour; density (ρ^{20}), 0.902–0.903 g/cm^3; refractive index (n_D^{20}), 1.469–1.470; and acid value, 0.102–0.123 mg KOH/g. Five samples of the oil (0.2–0.4 μl) were analysed by GC without any preliminary separations. All analyses were performed in triplicate.

The individual terpenoic compounds in the fir oil were identified by comparison of their retention indices (I) determined on the two capil-

* Corresponding author.

0021-9673/95/$09.50
SSDI 0021-9673(94)01059-5

Table 1
Capillary columns used and operating conditions

Parameter	Bonded stationary phase	
	Polydimethyl siloxane OV-101	Polyethylene glycol 20M PEG 20M
Column length (m)	50	60
Column I.D. (mm)	0.20	0.32
Stationary phase film thickness (μm)	0.50	0.25
Plate number for *n*-decane at 90°C	145 000	300 000
Retention factor for *n*-decane at 90°C	1.45	0.32
Injector temperature (°C)	250	250
Helium flow-rate, (ml/min)	0.25–0.28	0.87–1.00
Column temperature (°C)	70–180	7 min at 70, then 70–180
Programming rate (°C/min)	1	2

lary columns with authentic data either determined in our laboratory or obtained from the literature [4,5]. The temperature-programmed I was calculated with the following equation [6]:

$$I = 100 \cdot \frac{t_{R(x)} - t_{R(z)}}{t_{R(z+1)} - t_{R(z)}} + 100z$$

where t_R = retention time, x = substance of interest and z and $z + 1$ = *n*-alkanes with z and $z + 1$ carbon atoms emerging before and after substance x, respectively. The reproducibility of I expressed in terms of the standard deviation was 0.1–2.5 index units.

A program written in BASIC was used to calculate the I value for each chromatographic peak on both columns. Then the I on PEG 20M of each component present in the sample was compared with data obtained for standards on PEG 20M existing in the library, and possible identifications were made. In the next step the program looked up in the library the data for the same standard compound on OV-101 and made a comparison with the I values for each chromatographic peak obtained on OV-101. When a match was obtained, the component contents determined with the two columns were compared. The possibility of peak overlapping on OV-101 was also taken into account. A tolerance of 0.2% was selected for each I and 8% for the component concentration in a sample.

A flow diagram of the computer program is shown in Fig. 1; a listing of the program is available from the authors on request.

3. Results and discussion

The retention indices of terpenoic compounds on OV-101 and PEG 20M identified in Siberian fir oil are reported in Table 2. Typical gas chromatograms of a fir oil sample analysed on the two columns are presented in Figs. 2 and 3. All terpenoic compounds investigated were completely separated on the OV-101 and PEG 20M columns except *p*-cumene, β-phellandrene and limonene on OV-101.

The quantitative composition of fir oil was determined by using the internal normalization method and checked by the internal standard method. *n*-Dodecane for OV-101 and *n*-tetradecane for PEG 20M column were used as standard markers. The purity of the standards was higher than 98%. The relative calibration coefficients for oxygen compounds were obtained from the literature [7].

The concentrations of the individual terpenoic compounds of a typical fir oil sample determined with the internal normalization and the internal standard methods are given in Table 3. Comparison of the two methods showed good agreement in component composition. The relative deviation between the results of two methods did not exceed 5%.

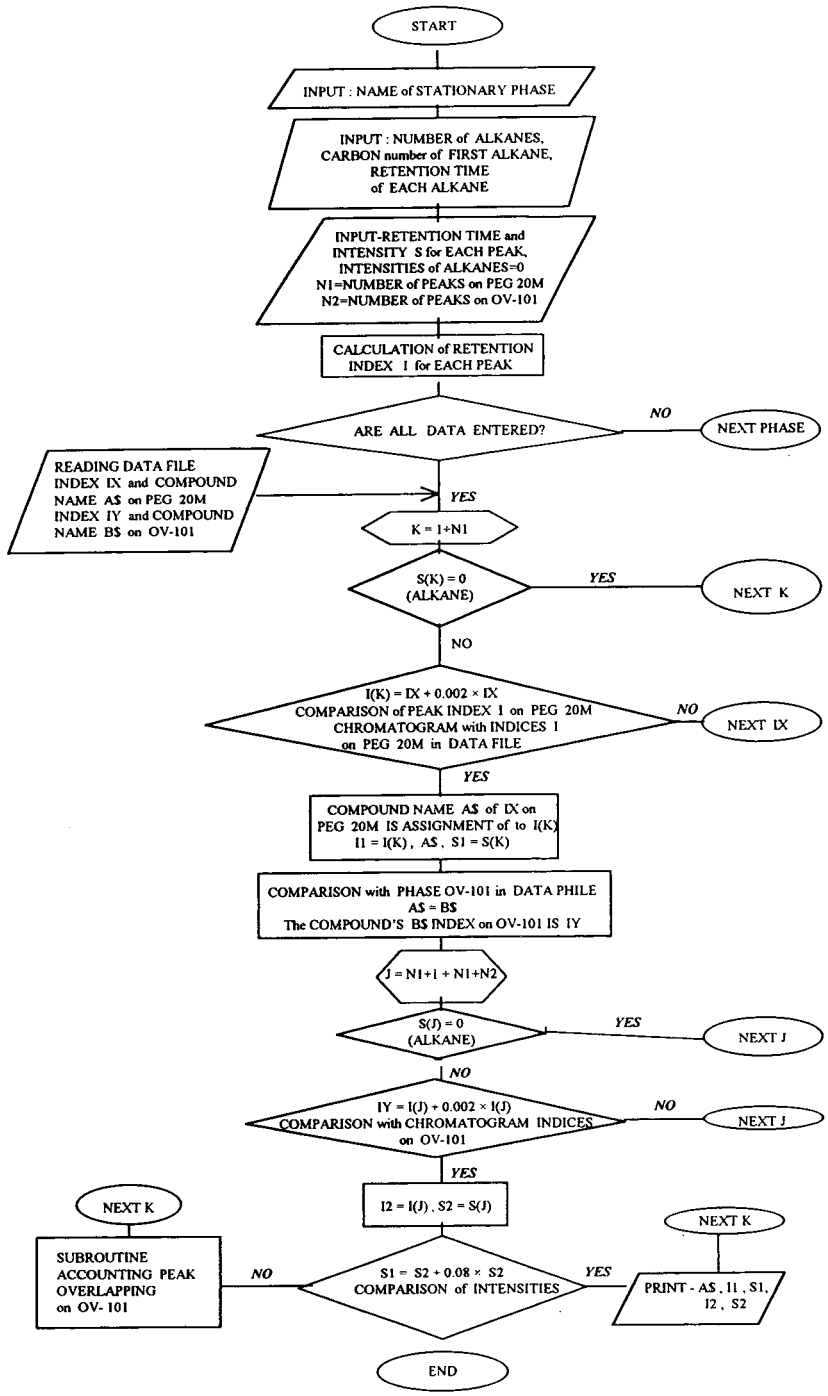

Fig. 1. Flow diagram of computer program.

Table 2
Retention indices of terpenoic compounds on OV-101 and PEG 20M columns with temperature programming

Peak no.	Compound	*I*	
		OV-101	PEG 20M
1	Santene	880	1000
2	Tricyclene	919	1020
3	α-Pinene	930	1033
4	Camphene	943	1083
5	β-Pinene	967	1118
6	Myrcene	979	1167
7	α-Phellandrene	995	1172
8	Δ^3-Carene	1005	1158
9	α-Terpinene	1009	1186
10	*p*-Cumene	1016	1277
11	β-Phellandrene	1018	1218
12	Limonene	1020	1209
13	γ-Terpinene	1045	1253
14	Terpinolene	1076	1290
15	Terpinen-4-ol	1120	1634
16	Camphor	1130	1524
17	Borneol	1152	1705
18	Bornyl acetate	1268	1591
19	Geranyl acetate	1361	1765
20	β-Caryophyllene	1406	1604
21	α-Humulene	1438	1673

The reproducibility of GC analysis determined as the standard deviation with a 95% probability was 0.001–1.1. The relative standard deviation (R.S.D.) was 0.5–4% for compounds with oil contents more than 0.2% and up to 8% for the minor components (<0.2%). As can be seen from Table 3, the reproducibility of the results

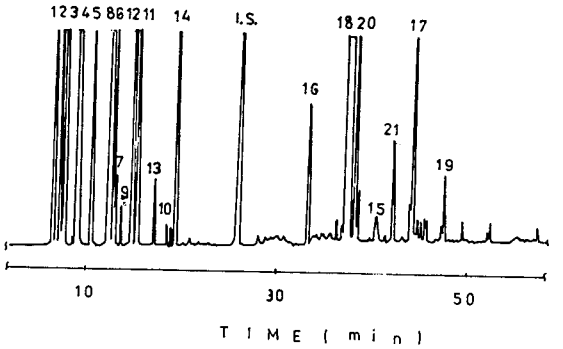

Fig. 3. Chromatogram of Siberian fir oil obtained on PEG 20M column. Peak numbers refer to the compounds listed in Table 2. I.S. = internal standard (*n*-tetradecane).

was better using the internal normalization method (<4%).

The results obtained demonstrated the possibility of using the simpler and rapid internal normalization method for the GC analysis of fir oil.

In the five Siberian fir oil samples studied, bornyl acetate (30–34%), camphene (22–24%), α-pinene (10–12%) and Δ^3-carene (11–13%) were identified as major components, constituting about 80% of oil composition. The total content of santene, tricyclene, β-pinene, limonene, β-phellandrene, terpinolene, β-caryophyllene and borneol amounted for over 16% of oil composition.

In comparison with fir oils of other *Abies* species (European *A. alba* and *A. balsamifera* Mich.) [8], bornyl acetate occurred in higher

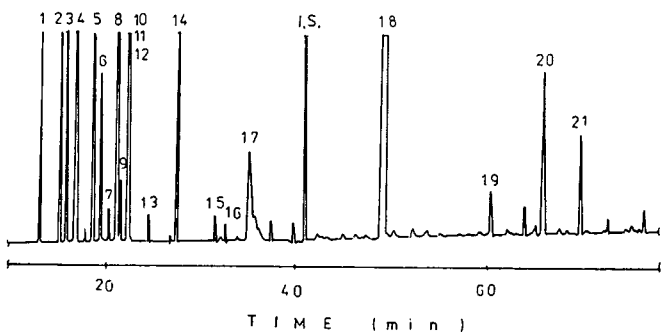

Fig. 2. Chromatogram of Siberian fir oil obtained on OV-101 column. Peak numbers refer to the compound listed in Table 2. I.S. = internal standard (*n*-dodecane).

Table 3
Composition of the fir oil

Peak no.	Compound	Internal standard method		Internal normalization method	
		Content (%, w/w)	R.S.D. (%)	Content (%, w/w)	R.S.D. (%)
1	Santene	2.51 ± 0.11	1.8	2.52 ± 0.05	0.8
2	Tricyclene	2.37 ± 0.07	1.2	2.38 ± 0.04	0.7
3	α-Pinene	13.67 ± 0.42	1.2	13.74 ± 0.56	1.6
4	Camphene	24.16 ± 0.72	1.2	24.27 ± 0.62	1.0
5	β-Pinene	1.57 ± 0.08	2.1	1.57 ± 0.08	2.1
6	Myrcene	0.68 ± 0.02	1.2	0.69 ± 0.02	1.2
7	α-Phellandrene	0.12 ± 0.01	3.4	0.12 ± 0.005	1.7
8	Δ^3-Carene	12.15 ± 0.49	1.6	12.23 ± 0.16	0.5
9	α-Terpinene	0.10 ± 0.01	4.0	0.10 ± 0.005	2.0
10	p-Cumene	0.14 ± 0.02	6.2	0.15 ± 0.01	2.7
11	β-Phellandrene	2.36 ± 0.15	2.6	2.47 ± 0.09	1.5
12	Limonene	3.98 ± 0.15	1.5	4.08 ± 0.08	0.8
13	γ-Terpinene	0.14 ± 0.02	5.8	0.14 ± 0.01	2.9
14	Terpinolene	1.10 ± 0.05	1.8	1.12 ± 0.02	0.7
15	Terpinen-4-ol	0.15 ± 0.02	5.4	0.14 ± 0.01	2.9
16	Camphor	0.05 ± 0.01	8.0	0.05 ± 0.005	4.0
17	Borneol	1.56 ± 0.20	5.2	1.66 ± 0.08	2.0
18	Bornyl acetate	30.81 ± 1.10	1.4	30.96 ± 0.45	0.6
19	Geranyl acetate	0.18 ± 0.01	2.2	0.17 ± 0.01	2.2
20	β-Caryophyllene	0.58 ± 0.03	2.0	0.59 ± 0.03	2.0
21	α-Humulene	0.33 ± 0.02	2.4	0.33 ± 0.02	2.4
Total		98.71		99.42	

concentrations in the Siberian fir oil samples investigated.

4. Conclusions

The computerized capillary GC method described here is simple and convenient for the identification and determination of terpenoic compounds in fir oils. This method may be applied to the quality control of commercial fir oils and also other essential oils, whereas other analytical procedures, e.g., spectroscopy and refractometry, do not allow the determination of the composition of individual components.

References

[1] L.A. Smedman, K. Snajberk, E. Zavarin and T.R. Mon, *Phytochemistry*, 8 (1969) 1471.
[2] T.F. Titova, V.A. Han, V.I. Bolshakova, L.I. Demenkova, Z.V. Dubovenko and V.A. Pentegova, *Khim. Prirod. Soyed.*, 2 (1980) 195.
[3] J.A. Corkill, *J. High Resolut. Chromatogr. Chromatogr. Commun.*, 11 (1988) 211.
[4] N.W. Davies, *J. Chromatogr.*, 503 (1990) 1.
[5] P. Sandra and C. Bicchi (Editors), *Capillary Gas Chromatography in Essential Oil Analysis*, Hüthig, Heidelberg, 1987, p. 270.
[6] H. van den Dool and P. Kratz, *J. Chromatogr.*, 11 (1963) 463.
[7] E. Leibnitz and H.G. Struppe, *Rukovodstvo po Gazovoi Khromatografii*, Vol. II, Mir, Moscow, 1988.
[8] S.D. Kustova, *Spravotshnik po Efirnom Maslam*, Food Industry, Moscow, 1978.

ELSEVIER

Journal of Chromatography A, 697 (1995) 501–513

JOURNAL OF CHROMATOGRAPHY A

Comparative study of Colombian citrus oils by high-resolution gas chromatography and gas chromatography–mass spectrometry

C. Blanco Tirado, E.E. Stashenko*, M.Y. Combariza, J.R. Martinez

Phytochemistry Laboratory, Chemistry Department, Industrial University of Santander, A.A. 678, Bucaramanga, Colombia

Abstract

Essential oils from fruit peel and leaves of colombian lemon (*Citrus volkameriana*), mandarin (*C. reticulata*) and orange (*C. sinensis*) were obtained by steam distillation and/or cold pressing. The extracts were analysed by high-resolution gas chromatography using either a flame ionization detector or a mass selective detector (electron impact ionization, 70 eV). The oil constituents were identified according to their mass spectra and Kováts retention indices determined on both polar and non-polar stationary phase capillary columns. The concentration of volatile secondary metabolites was maximum when the citrus fruits were at an intermediate maturation stage characterized by a greenish yellow coloration (45–75% green). While citrus peel oils contained from 94.01 to 98.66% of monoterpenes ($C_{10}H_{16}$), limonene as a major component and from 0.82 to 5.84% of oxygenated compounds, the extracts from citrus leaves contained only 65.26, 31.23 and 79.43% of monoterpenes ($C_{10}H_{16}$) in lemon, mandarin and orange, respectively. Oxygenated compounds in these oils represented 33.08, 68.47 and 16.38%, respectively.

1. Introduction

Citrus oils constitute the largest sector of the world production of essential oils. The study of the dependence of citrus oil composition on variables that affect the raw plant material, such as freshness, climate, location and harvest time, is a necessary step in the development of their production on a large scale [1–6]. We recently established that the concentration of volatile compounds in lemon (*Citrus volkameriana*) peel was maximum when fruits were at their intermediate maturation stage [7]. We now report a comparative high-resolution (HR) GC and GC–MS study of the incidence of maturation on the composition of oils extracted from the leaves and fruit peels of Colombian lemon (*C. volkameriana*), mandarin (*C. reticulata*) and orange (*C. sinensis*).

2. Experimental

2.1. Plant material

The various citrus fruits were gathered from the same plantation, situated 30 km north of Bucaramanga (Santander, Colombia). Oil extractions used lemon, mandarin and orange peels chopped manually into ca. 4-cm^2 pieces. Fruits belonging to different harvesting periods (December 1993, February 1994 and April 1994) had

* Corresponding author.

0021-9673/95/$09.50
SSDI 0021-9673(94)00955-4

different colorations, which were used as a ripeness indicator. Thus, the plant materials were classified as completely green (I), 45–75% green (intermediate maturity stage) (II) and yellow-orange, fully ripe fruits (III). The leaves used for oil extraction from lemon, mandarin and orange trees were collected at the same time as the respective fruits. Fresh plant material was employed in all extractions.

2.2. Essential oil extraction

Essential oils from citrus fruit peels were isolated by both steam distillation (A) and cold pressing (B). Secondary metabolites from the citrus leaves were obtained only by steam distillation. Cold pressing was used to isolate the essential oils from 2.0–2.5 kg of lemon, mandarin or orange fruit peel in different stages of ripeness (IB, IIB and IIIB). Steam distillation was carried out by passing steam (1 kg/h; 96–100°C) at 1.1 atm (1 atm = 101 325 Pa) for 3 h through a 5-*l* round-bottomed flask containing 1.0–1.5 kg of chopped lemon, mandarin or orange fruit peel in different stages of maturity (IA, IIA and IIIA), or 500–700 g of the respective leaves cut into small pieces. The condensed volatile oils were decanted from brine and dried over anhydrous Na_2SO_4. Three extractions were performed for each type of plant material.

The yields for lemon, mandarin and orange essential oils obtained by steam distillation and cold pressing were 0.19, 0.21, 0.17% and 0.60, 0.71 and 0.79%, respectively. The yields of volatile oils obtained from citrus leaves were 0.18, 0.54 and 0.34% for lemon, mandarin and orange, respectively. The reported data are averages of three extractions for each type of plant material.

2.3. Instrumental analysis

HRGC analysis of the samples was performed on a Hewlett-Packard (HP) (Palo Alto, CA, USA) 5890A Series II gas chromatograph equipped with a split–splitless injector (250°C, splitting ratio 1 : 30) and a flame ionization detector operated at 250°C. Chromatographic data were processed with an HP ChemStation 3365-II. The columns used were a DB-1 (J&W Scientific, Folsom, CA, USA) cross-linked fused-silica capillary column (60 m × 0.25 mm I.D.) coated with polydimethylsiloxane (0.25-μm phase thickness) and a DBWAX (J&W Scientific) fused-silica capillary column (60 m × 0.25 mm I.D.) coated with Carbowax 20M (0.25-μm phase thickness). The oven temperature was programmed from 50°C (10-min hold) to 150°C (20-min hold) at 2°C min^{-1} for the DBWAX column and from 70°C (5-min hold) to 270°C at 2.5°C min^{-1} for the DB-1 column. Helium (AGA, 99.995%) was used as the carrier gas (inlet pressure 152 kPa) with linear velocity 19 cm s^{-1} for both columns. Air and hydrogen flow-rates were maintained at 300 and 30 ml min^{-1}, respectively. Nitrogen was used as a make-up gas at 30 ml min^{-1}. The injection volume was 0.5 μl of a 20% (v/v) solution of citrus oil in dichloromethane (chromatography-grade reagent, Merck), using *n*-tetradecane (reference substance for gas chromatography, Merck) as an internal standard. Peak areas from different chromatograms were compared after they had been normalized with this standard.

An HP 5890A Series II gas chromatograph interfaced to an HP 5972 mass-selective detector with an HP MS ChemStation data system was used for identification of the GC components. The column used was a DB-1 (J&W Scientific) cross-linked fused-silica capillary column (30 m × 0.25 mm I.D.) coated with polydimethylsiloxane (0.25-μm phase thickness). The oven temperature was programmed from 50°C (5-min hold) at 3.5°C min^{-1} to 250°C. The helium inlet pressure was 78 kPa, with a linear velocity of 20 cm min^{-1} (splitting ratio 1 : 10). The injector temperature was kept at 250°C and the volume injected was 0.5 μl. The temperatures of the ionization chamber and of the transfer line were 180 and 280°C, respectively. The electron energy was 70 eV. Mass spectra and reconstructed total ion chromatograms were obtained by automatic scanning in the mass range m/z 30–350 at 2.2 scans s^{-1}. Chromatographic peaks were checked for homogeneity with the aid of the mass chromatograms obtained for the

characteristic fragment ions (e.g., m/z 136, 121 for monoterpenes; m/z 154, 139 for monoterpenols; m/z 204, 189 for sesquiterpenes). A C_7–C_{19} hydrocarbon mixture (Bio-Rad, Sadtler Division) was used to determine Kováts retention indexes.

3. Results and discussion

3.1. Citrus peel essential oils

A typical profile of citrus essential oils from lemon, mandarin and orange isolated by steam distillation is shown in Fig. 1. Table 1 gives the compositions found for citrus oils extracted by steam distillation (A) and cold-pressing (B) from fruits at different stages of ripeness (I, II and III). The various compounds were identified by comparison of their Kováts retention indices [8], determined utilizing a non-logarithmic scale on both polar (DBWAX) and non-polar (DB-1) stationary phase columns, and by comparison of the mass spectra of each GC component with those of standard and reported data [9–11].

Thirty components were detected in the orange peel extracts and the volatile mixtures isolated from mandarin and lemon peels were composed of 35 and 41 compounds respectively. Using both chromatographic (retention indices) and spectroscopic (mass spectra) criteria, 90, 97 and 90% of the detected compounds were fully identified in lemon, mandarin and orange peel oils, respectively.

Whereas the essential oils extracted by either steam distillation or cold pressing from lemon, mandarin and orange fruit peel differed considerably both qualitatively and quantitatively, the oils extracted from the fruits at different stages of maturity changed only quantitatively (Table 1). Limonene was the main component in all samples, with a mass concentration that varied in the ranges 77.27–79.36, 83.45–84.29 and 91.03–92.57% for lemon, mandarin and orange oils obtained by steam distillation, respectively. These values for mandarin and

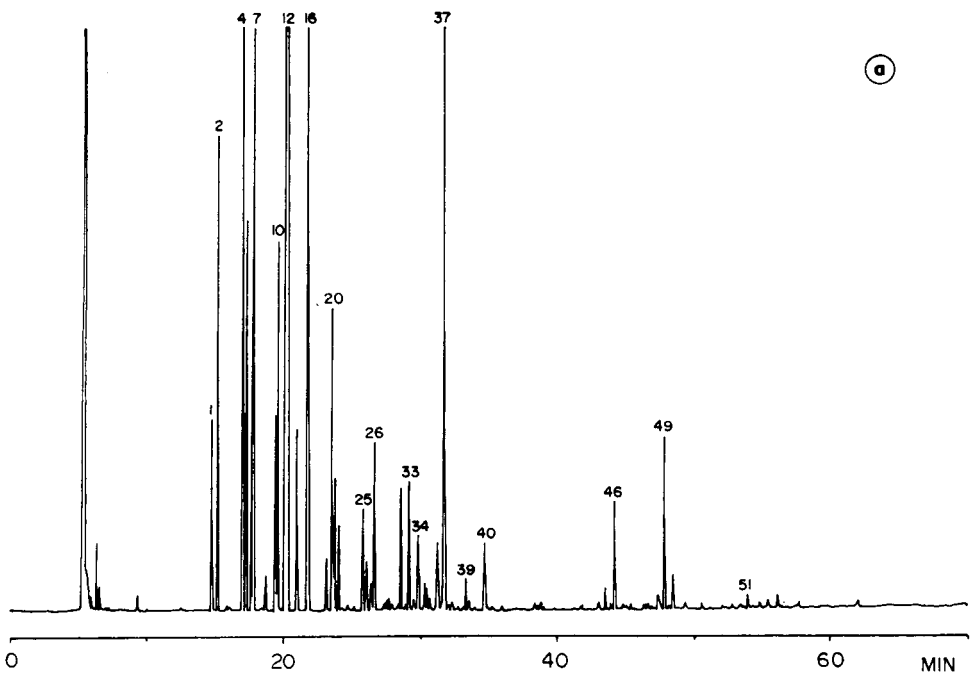

Fig. 1 (*continued on p. 504*).

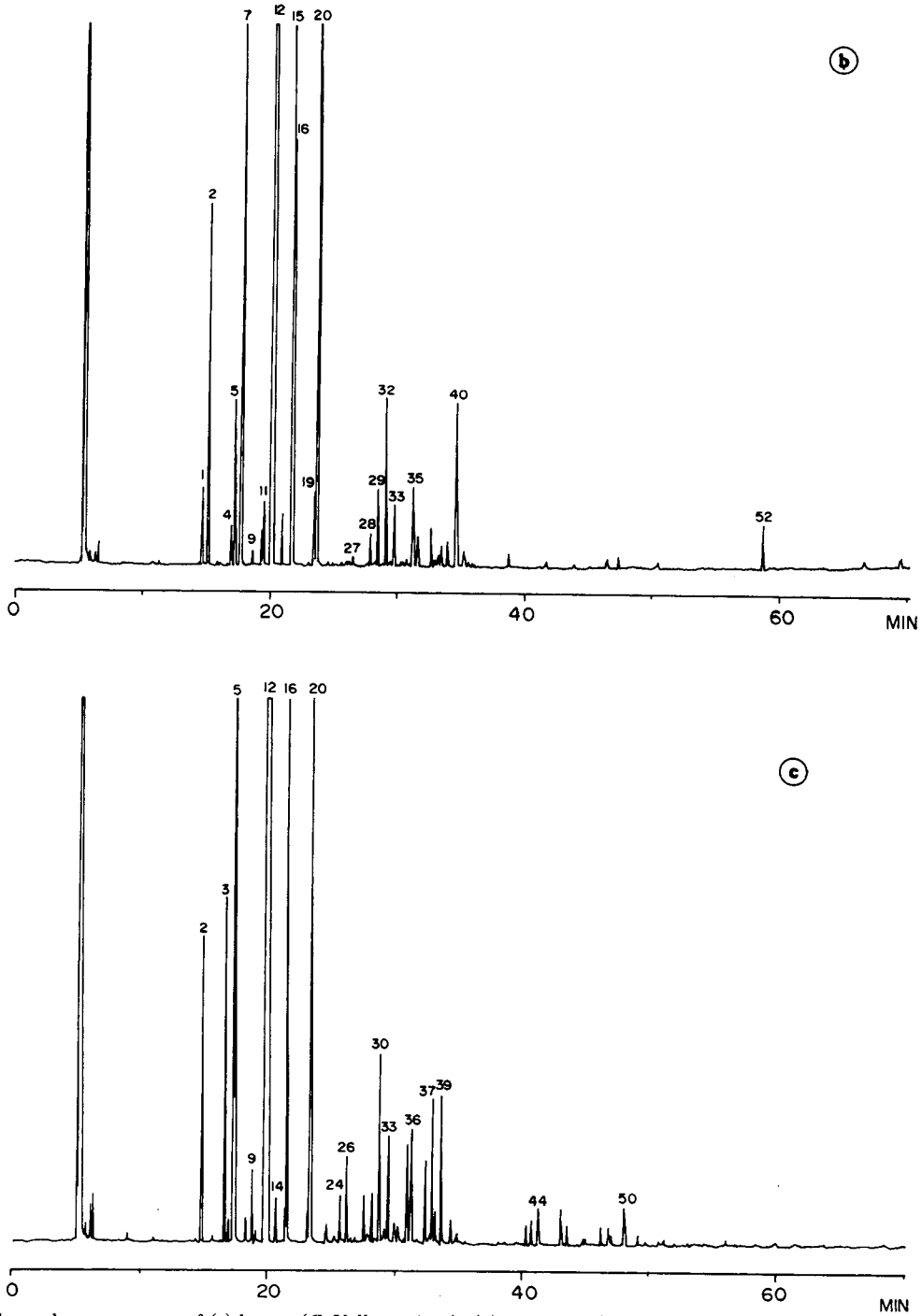

Fig. 1. Typical gas chromatograms of (a) lemon (*C. Volkameriana*), (b) mandarin (*C. reticulata*) and (c) orange (*C. sinensis*) peel oils obtained by steam distillation on a DB-1 cross-linked fused-silica column (60 m × 0.20 mm I.D.) coated with polydimethylsiloxane (0.25-μm phase thickness). Column temperature programmed from 70°C (5-min hold) to 270°C at 2.5°C min^{-1}. Splitting ratio, 1 : 30. Flame ionization detector. Carrier gas, helium; inlet pressure, 152 kPa. See Table 1 for peak identification.

Table 1
Chemical compositions of citrus peel essential oils from fruits at different stages of maturity

Peak No. (DB-1)	Compound	I_K[a]		GC peak area (%)[b]																	
		DB-1	DBWAX	Lemon						Mandarin						Orange					
				I	S.D.	II	S.D.	III	S.D.	I	S.D.	II	S.D.	III	S.D.	I	S.D.	II	S.D.	III	S.D.
1	α-Thujene	924	1025	0.32[c]	$8\cdot10^{-2}$	0.31	$3\cdot10^{-2}$	0.34	$3\cdot10^{-2}$	0.12	$2\cdot10^{-2}$	0.11	$2\cdot10^{-2}$	0.19	$1\cdot10^{-1}$	–	–	–	–	–	–
				0.47[d]	$3\cdot10^{-2}$	0.33	$2\cdot10^{-1}$	0.36	$2\cdot10^{-1}$	0.19	$3\cdot10^{-3}$	0.17	$1\cdot10^{-2}$	0.16	$1\cdot10^{-2}$	–	–	–	–	–	–
2	α-Pinene	932	1021	1.00	$2\cdot10^{-1}$	0.80	$8\cdot10^{-2}$	0.90	$6\cdot10^{-2}$	0.54	$1\cdot10^{-1}$	0.53	$1\cdot10^{-1}$	0.39	$2\cdot10^{-1}$	0.28	$2\cdot10^{-2}$	0.32	$1\cdot10^{-2}$	0.32	$2\cdot10^{-2}$
				1.53	$3\cdot10^{-2}$	1.50	$3\cdot10^{-3}$	1.42	$3\cdot10^{-2}$	0.93	$9\cdot10^{-3}$	0.86	$4\cdot10^{-2}$	0.87	$3\cdot10^{-2}$	0.53	$1\cdot10^{-2}$	0.29	$2\cdot10^{-1}$	0.52	$1\cdot10^{-2}$
3	Comphene	962	1083	–	–	–	–	–	–	–	–	–	–	–	–	0.27	$2\cdot10^{-1}$	0.36	$1\cdot10^{-4}$	0.35	$1\cdot10^{-2}$
				–	–	–	–	–	–	–	–	–	–	–	–	0.52	$2\cdot10^{-2}$	0.46	$6\cdot10^{-2}$	0.42	$1\cdot10^{-2}$
4	Sabinene	967	1120	3.55	$3\cdot10^{-1}$	1.39	$3\cdot10^{-1}$	1.15	$6\cdot10^{-1}$	0.11	$5\cdot10^{-3}$	0.17	$9\cdot10^{-2}$	0.15	$6\cdot10^{-2}$	0.02	$1\cdot10^{-2}$	0.02	$6\cdot10^{-4}$	0.02	$6\cdot10^{-4}$
				4.87	$9\cdot10^{-1}$	3.40	$1\cdot10^{-1}$	2.25	$4\cdot10^{-1}$	0.15	$1\cdot10^{-3}$	0.14	2.103	0.14	$2\cdot10^{-3}$	0.03	$1\cdot10^{-3}$	0.02	$1\cdot10^{-3}$	0.03	$6\cdot10^{-4}$
5	β-Pinene	973	1107	0.80	$4\cdot10^{-2}$	0.65	$7\cdot10^{-2}$	0.73	$3\cdot10^{-2}$	0.30	$3\cdot10^{-2}$	0.46	$2\cdot10^{-1}$	0.29	$4\cdot10^{-3}$	0.63	$4\cdot10^{-1}$	1.05	$2\cdot10^{-1}$	0.89	$9\cdot10^{-2}$
				0.99	$3\cdot10^{-2}$	0.94	$5\cdot10^{-4}$	0.90	$4\cdot10^{-2}$	0.36	$4\cdot10^{-3}$	0.33	$1\cdot10^{-2}$	0.32	$2\cdot10^{-2}$	0.63	$1\cdot10^{-1}$	0.76	$6\cdot10^{-2}$	0.72	$2\cdot10^{-2}$
6	n-Octanal	977	1270	0.20	$1\cdot10^{-1}$	0.22	$2\cdot10^{-2}$	0.25	$1\cdot10^{-1}$	0.83	$6\cdot10^{-1}$	0.39	$3\cdot10^{-1}$	1.05	$3\cdot10^{-1}$	1.50	$1\cdot10^{-2}$	1.60	$4\cdot10^{-2}$	1.64	$3\cdot10^{-2}$
				0.12	$6\cdot10^{-4}$	0.17	$6\cdot10^{-3}$	0.14	$3\cdot10^{-2}$	0.49	$3\cdot10^{-1}$	0.28	$1\cdot10^{-2}$	0.26	$3\cdot10^{-2}$	1.55	$5\cdot10^{-1}$	1.87	$1\cdot10^{-2}$	1.89	$1\cdot10^{-2}$
7	β-Myrcene	982	1162	1.74	$1\cdot10^{-1}$	1.68	$5\cdot10^{-2}$	1.65	$4\cdot10^{-2}$	1.49	$2\cdot10^{-1}$	1.49	$7\cdot10^{-2}$	1.45	$9\cdot10^{-2}$	0.01	$9\cdot10^{-3}$	–	–	–	–
				2.00	$1\cdot10^{-2}$	1.96	$2\cdot10^{-2}$	1.55	$5\cdot10^{-1}$	1.86	$7\cdot10^{-3}$	1.84	$4\cdot10^{-3}$	1.86	$3\cdot10^{-3}$	–	–	–	–	–	–
8	α-Phellandrene	994	1177	0.08	$3\cdot10^{-2}$	0.07	$5\cdot10^{-3}$	0.07	$4\cdot10^{-3}$	0.04	$7\cdot10^{-4}$	0.04	$2\cdot10^{-3}$	0.04	$9\cdot10^{-4}$	0.02	$1\cdot10^{-2}$	0.04	$2\cdot10^{-3}$	0.04	$1\cdot10^{-4}$
				0.06	$7\cdot10^{-4}$	0.06	$2\cdot10^{-3}$	0.06	$3\cdot10^{-4}$	0.04	$3\cdot10^{-4}$	0.04	$2\cdot10^{-3}$	0.04	$1\cdot10^{-3}$	0.04	$2\cdot10^{-3}$	0.05	$1\cdot10^{-2}$	0.04	$3\cdot10^{-4}$
9	3-Carene	1000	1150	–	–	–	–	–	–	–	–	–	–	–	–	0.04	$3\cdot10^{-2}$	0.08	$1\cdot10^{-2}$	0.08	$7\cdot10^{-3}$
				–	–	–	–	–	–	–	–	–	–	–	–	0.05	$1\cdot10^{-2}$	0.07	$2\cdot10^{-2}$	0.07	$7\cdot10^{-3}$
10	1,4-Cineole	1009	1177	0.33	$7\cdot10^{-2}$	0.36	$5\cdot10^{-2}$	0.34	$2\cdot10^{-2}$	0.11	$2\cdot10^{-2}$	0.09	$1\cdot10^{-2}$	0.11	$7\cdot10^{-3}$	0.02	$6\cdot10^{-4}$	–	–	–	–
				0.19	$8\cdot10^{-3}$	0.13	$9\cdot10^{-2}$	0.20	$5\cdot10^{-3}$	0.09	$1\cdot10^{-2}$	0.08	$8\cdot10^{-3}$	0.08	$2\cdot10^{-4}$	–	–	–	–	–	–
11	p-Cymene	1013	1284	1.28	$3\cdot10^{-1}$	0.65	$1\cdot10^{-1}$	0.92	$3\cdot10^{-1}$	0.20	$4\cdot10^{-2}$	0.24	$8\cdot10^{-2}$	0.36	$2\cdot10^{-1}$	–	–	–	–	–	–
				0.59	$2\cdot10^{-2}$	0.50	$7\cdot10^{-2}$	0.55	$1\cdot10^{-1}$	0.08	$1\cdot10^{-2}$	0.18	$1\cdot10^{-1}$	0.24	$9\cdot10^{-2}$	–	–	–	–	–	–
12	d-Limonene	1026	1201	77.27	$8\cdot10^{-1}$	79.36	$7\cdot10^{-1}$	78.78	$8\cdot10^{-1}$	84.29	$2\cdot10^{+0}$	83.71	$2\cdot10^{+0}$	83.45	$2\cdot10^{+0}$	91.63	$9\cdot10^{-1}$	91.03	$6\cdot10^{-1}$	92.57	$4\cdot10^{-1}$
				77.10	$9\cdot10^{-1}$	78.90	$1\cdot10^{-1}$	78.21	$6\cdot10^{-1}$	89.25	$2\cdot10^{-1}$	89.54	$3\cdot10^{-1}$	90.05	$3\cdot10^{-1}$	94.55	$1\cdot10^{-1}$	93.77	$6\cdot10^{-1}$	94.42	$2\cdot10^{-1}$
13	cis-β-Ocimene	1028	1235	tr[e]		tr		tr		tr		tr		tr		–	–	–	–	–	–
				tr		tr		tr		tr		tr		tr		–	–	–	–	–	–
14	trans-β-Ocimene	1035	1252	0.32	$6\cdot10^{-2}$	0.24	$5\cdot10^{-2}$	0.21	$4\cdot10^{-2}$	0.14	$2\cdot10^{-2}$	0.14	$3\cdot10^{-2}$	0.13	$1\cdot10^{-2}$	0.02	$2\cdot10^{-2}$	0.03	$9\cdot10^{-3}$	0.03	$3\cdot10^{-3}$
				0.32	$1\cdot10^{-2}$	0.21	$4\cdot10^{-2}$	0.18	$1\cdot10^{-2}$	0.13	$1\cdot10^{-2}$	0.13	$2\cdot10^{-2}$	0.10	$2\cdot10^{-2}$	0.02	$5\cdot10^{-4}$	0.02	$7\cdot10^{-4}$	0.02	$8\cdot10^{-4}$
15	Not identified	1045	–	–	–	–	–	–	–	–	–	–	–	–	–	0.01	$1\cdot10^{-2}$	0.02	$9\cdot10^{-3}$	0.01	$6\cdot10^{-3}$
			–	–	–	–	–	–	–	–	–	–	–	–	–	0.02	$3\cdot10^{-3}$	0.01	$9\cdot10^{-4}$	0.02	$1\cdot10^{-3}$
16	γ-Terpinene	1051	1248	7.81	$9\cdot10^{-2}$	8.85	$2\cdot10^{-1}$	8.75	$3\cdot10^{-1}$	4.27	$2\cdot10^{-1}$	3.85	$4\cdot10^{-1}$	3.63	$2\cdot10^{-1}$	0.41	$3\cdot10^{-1}$	1.09	$4\cdot10^{-1}$	0.64	$4\cdot10^{-2}$
				7.32	$1\cdot10^{-1}$	7.87	$3\cdot10^{-1}$	7.92	$2\cdot10^{-1}$	3.87	$4\cdot10^{-2}$	3.64	$2\cdot10^{-1}$	3.35	$1\cdot10^{-2}$	0.02	$2\cdot10^{-3}$	0.04	$7\cdot10^{-3}$	0.03	$3\cdot10^{-4}$
17	trans-Sabinene hydrate	1054	1463	0.06	$5\cdot10^{-2}$	0.01	$8\cdot10^{-3}$	0.04	$2\cdot10^{-2}$	0.11	$6\cdot10^{-4}$	0.33	$3\cdot10^{-1}$	0.19	$1\cdot10^{-1}$	–	–	–	–	–	–
				0.16	$2\cdot10^{-2}$	0.08	$5\cdot10^{-2}$	0.08	$4\cdot10^{-2}$	–	–	–	–	–	–	–	–	–	–	–	–
18	n-Octanol	1074	1507	0.12	$4\cdot10^{-2}$	0.08	$2\cdot10^{-2}$	0.10	$2\cdot10^{-2}$	–	–	–	–	–	–	0.02	$1\cdot10^{-2}$	0.03	$4\cdot10^{-3}$	0.03	$5\cdot10^{-4}$
				0.06	$1\cdot10^{-3}$	0.05	$6\cdot10^{-3}$	0.06	$5\cdot10^{-3}$	–	–	–	–	–	–	0.02	$3\cdot10^{-3}$	0.04	$8\cdot10^{-4}$	0.02	$1\cdot10^{-3}$

Table 1 *(continued)*

Peak No. (DB-1)	Compound	I_K[a]		GC peak area (%)[b]																	
		DB-1	DBWAX	Lemon						Mandarin						Orange					
				I	S.D.	II	S.D.	III	S.D.	I	S.D.	II	S.D.	III	S.D.	I	S.D.	II	S.D.	III	S.D.
19	Not identified	1078	–	–	–	–	–	–	–	0.22	$3\cdot10^{-2}$	0.18	$2\cdot10^{-2}$	0.21	$9\cdot10^{-3}$	–	–	–	–	–	–
			–	–	–	–	–	–	–	0.20	$2\cdot10^{-3}$	0.19	$7\cdot10^{-3}$	0.17	$3\cdot10^{-3}$	0.06	$1\cdot10^{-4}$	0.04	$2\cdot10^{-2}$	0.07	$1\cdot10^{-3}$
20	Terpinolene	1080	1291	0.53	$1\cdot10^{-2}$	0.55	$4\cdot10^{-2}$	0.54	$2\cdot10^{-2}$	4.55	$8\cdot10^{-1}$	5.95	$1\cdot10^{+0}$	5.96	$1\cdot10^{+0}$	2.61	$6\cdot10^{-1}$	2.54	$4\cdot10^{-1}$	1.83	$2\cdot10^{-1}$
				0.42	$7\cdot10^{-3}$	0.43	$4\cdot10^{-3}$	0.42	$6\cdot10^{-3}$	1.46	$1\cdot10^{-1}$	1.57	$5\cdot10^{-2}$	1.41	$2\cdot10^{-1}$	0.58	$4\cdot10^{-1}$	0.78	$5\cdot10^{-2}$	0.75	$9\cdot10^{-3}$
21	Nonanal	1082	1382	0.08	$4\cdot10^{-2}$	0.12	$2\cdot10^{-2}$	0.12	$5\cdot10^{-2}$	–	–	–	–	–	–	–	–	–	–	–	–
				0.09	$8\cdot10^{-3}$	0.13	$1\cdot10^{-3}$	0.11	$3\cdot10^{-2}$	–	–	–	–	–	–	–	–	–	–	–	–
22	Linalool	1083	1553	0.43	$3\cdot10^{-1}$	0.16	$1\cdot10^{-1}$	0.24	$1\cdot10^{-1}$	–	–	–	–	–	–	–	–	–	–	–	–
				0.28	$3\cdot10^{-2}$	0.23	$2\cdot10^{-2}$	0.18	$6\cdot10^{-2}$	–	–	–	–	–	–	–	–	–	–	–	–
23	*cis*-Sabinene hydrate	1088	–	0.05	$3\cdot10^{-2}$	0.16	$3\cdot10^{-2}$	0.18	$7\cdot10^{-2}$	–	–	–	–	–	–	–	–	–	–	–	–
				0.07	$9\cdot10^{-2}$	0.10	$5\cdot10^{-2}$	0.21	$6\cdot10^{-2}$	–	–	–	–	–	–	–	–	–	–	–	–
24	*cis*-Epoxylimonene	1118	–	0.07	$6\cdot10^{-2}$	0.25	$5\cdot10^{-2}$	0.31	$1\cdot10^{-1}$	–	–	0.02	$3\cdot10^{-3}$	0.02	$7\cdot10^{-3}$	0.04	$4\cdot10^{-2}$	0.04	$1\cdot10^{-2}$	0.02	$3\cdot10^{-3}$
				0.12	$2\cdot10^{-1}$	0.17	$8\cdot10^{-2}$	0.38	$9\cdot10^{-2}$	–	–	–	–	–	–	0.02	$6\cdot10^{-3}$	0.37	$5\cdot10^{-3}$	–	–
25	1,2-Dihydrolinalool	1121	1449	0.04	$1\cdot10^{-2}$	0.08	$1\cdot10^{-2}$	0.10	$3\cdot10^{-2}$	–	–	–	–	–	–	–	–	–	–	–	–
				0.03	$4\cdot10^{-2}$	0.05	$2\cdot10^{-2}$	0.10	$1\cdot10^{-2}$	–	–	–	–	–	–	–	–	–	–	–	–
26	Not identified	1127	–	0.06	$9\cdot10^{-3}$	0.05	$1\cdot10^{-2}$	0.05	$4\cdot10^{-3}$	–	–	–	–	–	–	0.02	$1\cdot10^{-2}$	0.06	$3\cdot10^{-2}$	0.03	$8\cdot10^{-4}$
				0.05	$2\cdot10^{-3}$	0.04	$3\cdot10^{-3}$	0.04	$2\cdot10^{-3}$	–	–	–	–	–	–	0.09	$1\cdot10^{-1}$	0.02	$6\cdot10^{-4}$	0.02	$1\cdot10^{-3}$
27	Citronellal	1131	1472	0.40	$2\cdot10^{-1}$	0.30	$1\cdot10^{-2}$	0.33	$1\cdot10^{-1}$	0.08	$4\cdot10^{-2}$	0.07	$2\cdot10^{-2}$	0.13	$2\cdot10^{-2}$	–	–	–	–	–	–
				0.36	$5\cdot10^{-3}$	0.41	$8\cdot10^{-3}$	0.40	$3\cdot10^{-2}$	0.06	$2\cdot10^{-2}$	0.04	$7\cdot10^{-3}$	0.06	$4\cdot10^{-3}$	–	–	–	–	–	–
28	Isopulegol	1146	1565	0.40	$2\cdot10^{-1}$	0.27	$2\cdot10^{-2}$	0.29	$2\cdot10^{-2}$	–	–	0.05	$2\cdot10^{-2}$	0.02	$8\cdot10^{-3}$	0.03	$2\cdot10^{-2}$	0.05	$9\cdot10^{-4}$	0.05	$4\cdot10^{-4}$
				0.03	$5\cdot10^{-3}$	0.03	$1\cdot10^{-3}$	0.03	$5\cdot10^{-3}$	–	–	–	–	–	–	–	–	–	–	–	–
29	Nonanol	1161	–	–	–	–	–	–	–	0.09	$9\cdot10^{-3}$	0.13	$4\cdot10^{-2}$	0.10	$3\cdot10^{-2}$	–	–	–	–	–	–
			–	–	–	–	–	–	–	–	–	–	–	–	–	–	–	–	–	–	–
30	Terpinen-4-ol	1168	1610	–	–	–	–	–	–	–	–	–	–	–	–	0.11	$9\cdot10^{-2}$	0.18	$4\cdot10^{-2}$	0.13	$2\cdot10^{-2}$
				–	–	–	–	–	–	–	–	–	–	–	–	0.23	$2\cdot10^{-1}$	0.07	$2\cdot10^{-2}$	0.06	$7\cdot10^{-4}$
31	Not identified	1173	–	0.46	$2\cdot10^{-1}$	0.31	$5\cdot10^{-2}$	0.35	$9\cdot10^{-2}$	–	–	–	–	–	–	–	–	–	–	–	–
				0.29	$3\cdot10^{-2}$	0.23	$2\cdot10^{-2}$	0.18	$7\cdot10^{-2}$	–	–	–	–	–	–	–	–	–	–	–	–
32	α-Terpineol	1179	1740	0.05	$3\cdot10^{-2}$	0.02	$3\cdot10^{-3}$	0.03	$8\cdot10^{-3}$	0.26	$4\cdot10^{-2}$	0.35	$5\cdot10^{-2}$	0.35	$1\cdot10^{-1}$	–	–	–	–	–	–
				0.04	$3\cdot10^{-3}$	0.03	$5\cdot10^{-3}$	0.03	$3\cdot10^{-3}$	0.10	$2\cdot10^{-3}$	0.09	$4\cdot10^{-3}$	0.09	$1\cdot10^{-3}$	–	–	–	–	–	–
33	Decanal	1183	1482	0.34	$2\cdot10^{-1}$	0.19	$9\cdot10^{-3}$	0.21	$8\cdot10^{-2}$	0.14	$8\cdot10^{-2}$	0.13	$6\cdot10^{-3}$	0.10	$8\cdot10^{-2}$	0.11	$8\cdot10^{-2}$	0.25	$1\cdot10^{-1}$	0.35	$3\cdot10^{-2}$
				0.30	$1\cdot10^{-3}$	0.28	$2\cdot10^{-2}$	0.26	$3\cdot10^{-2}$	0.14	$3\cdot10^{-3}$	0.17	$2\cdot10^{-2}$	0.17	$8\cdot10^{-3}$	0.26	$4\cdot10^{-2}$	0.39	$7\cdot10^{-3}$	0.38	$2\cdot10^{-2}$
34	Methylthymol	1196	–	0.05	$2\cdot10^{-2}$	0.05	$9\cdot10^{-3}$	0.05	$1\cdot10^{-2}$	–	–	–	–	–	–	–	–	–	–	–	–
				0.01	$8\cdot10^{-3}$	0.01	$4\cdot10^{-3}$	0.00	$6\cdot10^{-3}$	–	–	–	–	–	–	–	–	–	–	–	–
35	Citronellol	1203	1751	0.04	$0\cdot10^{+0}$	0.08	$3\cdot10^{-2}$	0.08	$2\cdot10^{-2}$	0.14	$5\cdot10^{-2}$	0.23	$9\cdot10^{-2}$	0.19	$8\cdot10^{-2}$	–	–	–	–	–	–
				0.02	$2\cdot10^{-2}$	0.03	$2\cdot10^{-2}$	0.06	$3\cdot10^{-3}$	–	–	–	–	–	–	–	–	–	–	–	–
36	Nerol	1208	1832	0.24	$1\cdot10^{-1}$	0.23	$9\cdot10^{-2}$	0.27	$2\cdot10^{-1}$	0.08	$4\cdot10^{-4}$	0.07	$8\cdot10^{-3}$	0.10	$6\cdot10^{-3}$	0.07	$5\cdot10^{-2}$	0.13	$3\cdot10^{-2}$	0.10	$1\cdot10^{-2}$
				0.05	$4\cdot10^{-3}$	0.06	$1\cdot10^{-3}$	0.07	$5\cdot10^{-3}$	–	–	–	–	–	–	–	–	–	–	–	–
37	Neral	1215	1705	2.11	$6\cdot10^{-1}$	1.83	$4\cdot10^{-1}$	1.85	$3\cdot10^{-1}$	0.28	$1\cdot10^{-1}$	0.13	$4\cdot10^{-2}$	0.18	$1\cdot10^{-2}$	0.12	$9\cdot10^{-2}$	0.15	$4\cdot10^{-4}$	0.12	$2\cdot10^{-2}$
				1.19	$2\cdot10^{-2}$	0.98	$1\cdot10^{-1}$	0.99	$2\cdot10^{-2}$	0.10	$2\cdot10^{-3}$	0.08	$2\cdot10^{-2}$	0.08	$4\cdot10^{-3}$	0.08	$9\cdot10^{-3}$	0.08	$2\cdot10^{-4}$	0.08	$2\cdot10^{-3}$

Table 1 *(continued)*

Peak No. (DB-1)	Compound	I_K[a]		GC peak area (%)[b]																			
		DB-1	DBWAX	Lemon						Mandarin						Orange							
				I	S.D.	II	S.D.	III	S.D.	I	S.D.	II	S.D.	III	S.D.	I	S.D.	II	S.D.	III	S.D.		
38	Geraniol	1237	1789	–	–	–	–	–	–	0.17	$1\cdot10^{-1}$	0.12	$6\cdot10^{-3}$	0.13	$3\cdot10^{-2}$	0.14	$1\cdot10^{-1}$	0.17	$6\cdot10^{-3}$	0.14	$2\cdot10^{-2}$		
				–	–	–	–	–	–	–	–	–	–	–	–	0.11	$1\cdot10^{-2}$	0.11	$1\cdot10^{-3}$	0.10	$2\cdot10^{-3}$		
39	Geranial	1248	1735	0.11	$7\cdot10^{-2}$	0.08	$2\cdot10^{-2}$	0.07	$4\cdot10^{-2}$	0.12	$5\cdot10^{-2}$	0.05	$3\cdot10^{-2}$	0.12	$5\cdot10^{-2}$	0.15	$1\cdot10^{-1}$	0.21	$4\cdot10^{-2}$	0.23	$3\cdot10^{-3}$		
				0.06	$6\cdot10^{-3}$	0.04	$1\cdot10^{-2}$	0.03	$6\cdot10^{-3}$	0.05	$5\cdot10^{-3}$	0.04	$4\cdot10^{-3}$	–	–	0.02	$1\cdot10^{-3}$	0.02	$8\cdot10^{-4}$	0.02	$3\cdot10^{-4}$		
40	Perillaldehyde	1265	–	0.18	$1\cdot10^{-1}$	0.11	$2\cdot10^{-2}$	0.13	$2\cdot10^{-2}$	0.43	$7\cdot10^{-2}$	0.36	$6\cdot10^{-2}$	0.36	$1\cdot10^{-1}$	0.01	$1\cdot10^{-2}$	0.03	$2\cdot10^{-3}$	0.02	$5\cdot10^{-3}$		
				0.08	$2\cdot10^{-2}$	0.06	$2\cdot10^{-2}$	0.05	$2\cdot10^{-2}$	0.11	$2\cdot10^{-2}$	0.09	$2\cdot10^{-2}$	0.08	$5\cdot10^{-3}$	–	–	–	–	–	–		
41	Decanol	1270	1729	0.04	$3\cdot10^{-2}$	0.03	$6\cdot10^{-3}$	0.04	$1\cdot10^{-2}$	0.07	$1\cdot10^{-2}$	0.09	$2\cdot10^{-3}$	0.10	$2\cdot10^{-2}$	–	–	–	–	–	–		
				0.03	$8\cdot10^{-3}$	0.03	$1\cdot10^{-3}$	0.03	$4\cdot10^{-3}$	–	–	–	–	–	–	–	–	–	–	–	–		
42	Thymal	1286	2100	0.02	$1\cdot10^{-2}$	0.02	$2\cdot10^{-2}$	0.03	$2\cdot10^{-2}$	–	–	–	–	–	–	–	–	–	–	–	–		
				0.03	$2\cdot10^{-4}$	0.05	$2\cdot10^{-3}$	0.04	$9\cdot10^{-3}$	–	–	–	–	–	–	–	–	–	–	–	–		
43	Citronellyl acetate	1335	1645	–	–	–	–	–	–	0.10	$5\cdot10^{-2}$	0.07	$9\cdot10^{-4}$	0.05	$6\cdot10^{-3}$	–	–	–	–	–	–		
				–	–	–	–	–	–	0.09	$5\cdot10^{-3}$	0.07	$7\cdot10^{-3}$	–	–	–	–	–	–	–	–		
44	δ-Elemene	1384	1475	–	–	–	–	–	–	0.10	$6\cdot10^{-3}$	0.05	$8\cdot10^{-3}$	0.02	$9\cdot10^{-4}$	0.07	$5\cdot10^{-2}$	0.09	$3\cdot10^{-2}$	0.09	$5\cdot10^{-3}$		
				–	–	–	–	–	–	–	–	–	–	–	–	0.03	$1\cdot10^{-3}$	0.07	$1\cdot10^{-2}$	0.08	$4\cdot10^{-3}$		
45	β-Caryophyllene	1424	1654	0.07	$3\cdot10^{-2}$	0.04	$1\cdot10^{-2}$	0.04	$0\cdot10^{+0}$	0.11	$7\cdot10^{-4}$	0.04	$5\cdot10^{-4}$	0.04	$3\cdot10^{-3}$	0.01	$1\cdot10^{-2}$	0.02	$3\cdot10^{-3}$	0.02	$7\cdot10^{-4}$		
				0.06	$5\cdot10^{-3}$	0.03	$6\cdot10^{-3}$	0.03	$2\cdot10^{-3}$	–	–	–	–	–	–	–	–	–	–	–	–		
46	α-Bergamotene	1435	1589	0.22	$4\cdot10^{-2}$	0.20	$3\cdot10^{-2}$	0.19	$3\cdot10^{-2}$	–	–	–	–	–	–	–	–	–	–	–	–		
				0.21	$2\cdot10^{-3}$	0.18	$2\cdot10^{-2}$	0.20	$9\cdot10^{-3}$	–	–	–	–	–	–	–	–	–	–	–	–		
47	Germacrene D	1477	1714	–	–	–	–	–	–	0.08	$4\cdot10^{-2}$	0.06	$7\cdot10^{-3}$	0.03	$2\cdot10^{-3}$	0.02	$1\cdot10^{-2}$	0.02	$2\cdot10^{-3}$	0.15	$9\cdot10^{-4}$		
				–	–	–	–	–	–	0.08	$2\cdot10^{-3}$	0.07	$6\cdot10^{-3}$	0.05	$2\cdot10^{-3}$	0.02	$1\cdot10^{-3}$	0.02	$7\cdot10^{-4}$	0.02	$6\cdot10^{-4}$		
48	β-Bisabolene	1495	1770	0.09	$4\cdot10^{-2}$	0.04	$1\cdot10^{-2}$	0.04	$3\cdot10^{-3}$	0.09	$4\cdot10^{-2}$	0.06	$1\cdot10^{-2}$	0.05	$5\cdot10^{-3}$	–	–	–	–	–	–		
				0.07	$2\cdot10^{-2}$	0.02	$8\cdot10^{-3}$	0.03	$1\cdot10^{-3}$	0.06	$5\cdot10^{-3}$	0.06	$7\cdot10^{-3}$	0.05	$8\cdot10^{-3}$	–	–	–	–	–	–		
49	α-Muurolene	1502	1730	0.33	$8\cdot10^{-2}$	0.12	$2\cdot10^{-1}$	0.29	$6\cdot10^{-2}$	–	–	–	–	–	–	–	–	–	–	–	–		
				0.28	$3\cdot10^{-3}$	0.24	$3\cdot10^{-2}$	0.26	$1\cdot10^{-2}$	–	–	–	–	–	–	–	–	–	–	–	–		
50	δ-Cadinene	1511	1766	–	–	–	–	–	–	–	–	–	–	–	–	0.04	$3\cdot10^{-2}$	0.04	$4\cdot10^{-3}$	0.03	$4\cdot10^{-3}$		
				–	–	–	–	–	–	–	–	–	–	–	–	0.03	$2\cdot10^{-3}$	0.03	$1\cdot10^{-3}$	0.03	$1\cdot10^{-3}$		
51	Sesquiterpenol	1650	–	0.02	$8\cdot10^{-3}$	0.02	$1\cdot10^{-2}$	0.03	$4\cdot10^{-3}$	–	–	–	–	–	–	–	–	–	–	–	–		
				0.03	$2\cdot10^{-3}$	0.01	$7\cdot10^{-3}$	0.02	$1\cdot10^{-2}$	–	–	–	–	–	–	–	–	–	–	–	–		
52	α-Sinensal	1725	–	–	–	–	–	–	–	0.23	$1\cdot10^{-1}$	0.15	$3\cdot10^{-2}$	0.13	$2\cdot10^{-2}$	–	–	–	–	–	–		
			–	–	–	–	–	–	–	0.20	$7\cdot10^{-3}$	0.20	$2\cdot10^{-2}$	0.18	$3\cdot10^{-2}$	–	–	–	–	–	–		
53	Sesquiterpenol	1780	–	0.02	$5\cdot10^{-3}$	0.02	$1\cdot10^{-2}$	0.03	$7\cdot10^{-3}$	–	–	–	–	–	–	–	–	–	–	–	–		
			–	0.03	$6\cdot10^{-3}$	0.03	$2\cdot10^{-3}$	0.03	$6\cdot10^{-3}$	–	–	–	–	–	–	–	–	–	–	–	–		

[a] Experimentally determined Kováts retention indices.
[b] Percentages were calculated from the peak areas on the DB-1 column (flame ionization detector).
[c] Steam distillation.
[d] Cold pressing.
[e] Traces.

orange oils are slightly higher in the extracts isolated by cold pressing (Table 1).

Nonanal (0.08–0.13%), linalool (0.16–0.43%), *cis*-sabinene hydrate (0.05–0.21%), 1,2-dihydrolinalool (0.03–0.10%), thymol (0.02–0.05%), methylthymol (0.01–0.05%), α-bergamotene (0.18–0.22%) and α-muurolene (0.12–0.33%) were found only in lemon oils. Among characteristic secondary metabolites, nonanol (0.10–0.13%), citronellyl acetate (0.05–0.10%) and α-sinensal (0.13–0.23% were present only in mandarin oil and camphene (0.27–0.52%), 3-carene (0.04–0.08%) and δ-cadinene (0.03–0.04%) only in orange oil.

In order to appreciate the influence of fruit maturity on the chemical composition of the essential oils obtained, the results from Table 1 were grouped into compound families, as shown in Fig. 2. For quantitative evaluation, all GC peak areas were compared relative to the internal standard. Monoterpenes ($C_{10}H_{16}$) represented the main compound family in all extracts. Their abundance varied in the oils isolated by steam distillation (cold pressing) in the ranges 94.01–94.40% (94.19–96.36%) in lemon, 95.92–97.01% (98.43–98.66%) in mandarin and 95.94–96.72% (96.25–97.03%) in orange.

Mandarin fruits possessed the highest content of monoterpenes ($C_{10}H_{16}$) when at their intermediate (II) and full (III) maturation stages. At any stage of fruit ripeness, lemon and mandarin essential oils had 1.5–2 times more oxygenated compounds than the respective distilled or cold-pressed orange oils. The sesquiterpene ($C_{15}H_{24}$) contents were found to be 2–3 times higher in lemon than in mandarin and orange essential oils, respectively.

The generation of the total volatile secondary metabolites grew initially during the fruit maturation and achieved the highest concentration at the intermediately matured stage (II, 45–75% green), but then decreased as the fruits ripened completely (III) and their peel colaration turned yellow-orange (Fig. 2).

3.2. *Citrus leaf essential oils*

Fig. 3 shows typical gas chromatograms of the oils extracted by steam distillation from lemon, mandarin and orange leaves. Kováts retention indices calculated for chromatographic peaks on both polar (DBWAX) and non-polar (DB-1) columns were used together with the mass spectra in the identification of the essential oil components. Table 2 contains the results of the triplicate analysis of lemon, mandarin and orange leaf oils. The chemical composition of these extracts differed more sharply than for those isolated from the respective citrus peels (Table 1 and 2).

Whereas only 37 compounds (97% positively identified) were detected in mandarin leaf oil, 50 and 52 constituents (96% positively identified in both oils) were found in the extracts distilled

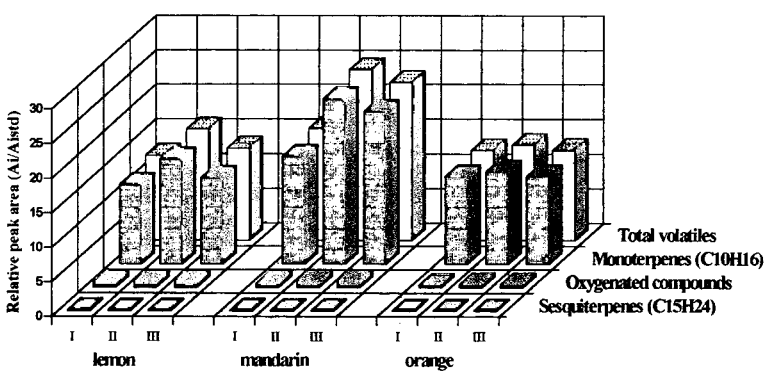

Fig. 2. Compositional variation of citrus peel oils obtained by steam distillation from fruits at different stages of ripeness (I = 100% green; II = 45–75% green; III = fully matured, yellow-orange fruits).

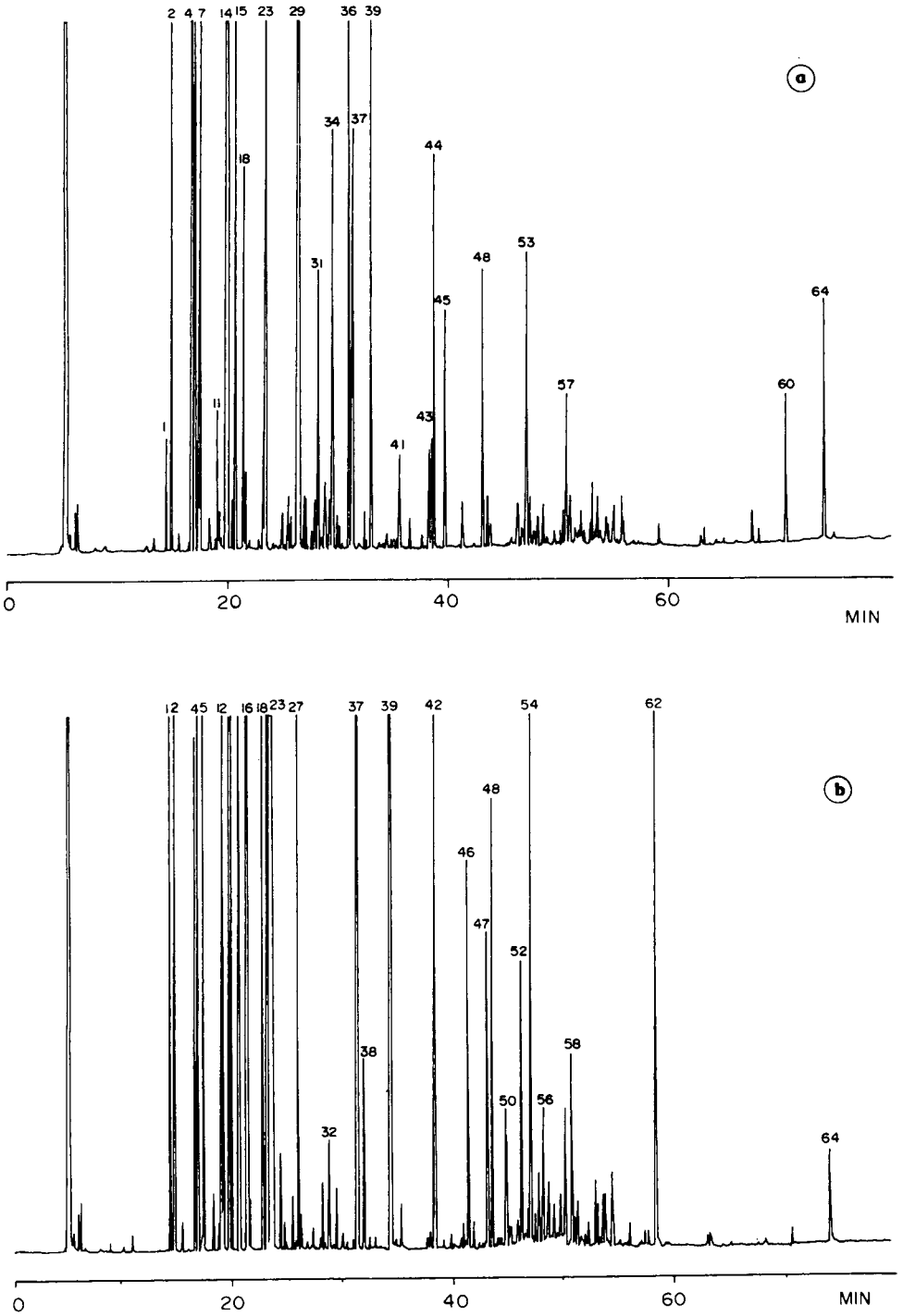

Fig. 3 (*continued on p. 509*).

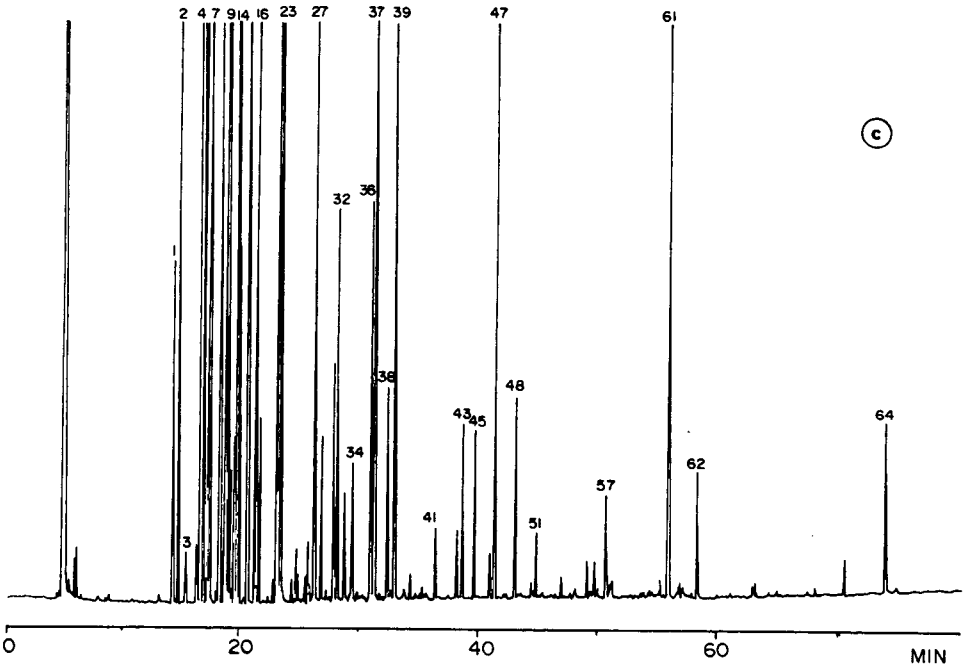

Fig. 3. Typical gas chromatograms of (a) lemon (*C. Volkameriana*), (b) mandarin (*C. reticulata*) and (c) orange (*C. sinensis*) leaf oils obtained by steam distillation on a DB-1 cross-linked fused-silica column (60 m × 0.20 mm I.D.) coated with polydimethylsiloxane (0.25-μm phase thickness). See Fig. 1 for GC conditions. See Table 2 for peak identification.

from lemon and orange leaves, respectively. The second most abundant compound in lemon leaf oil was citronellal (22.21%) (limonene was the most abundant, 41.74%), followed by sabinene (16.16%), *trans*-β-ocimene (3.88%) and linalool (3.12%). In the mandarin leaf oil linalool (52.66%) was found to be the major compound, together with limonene (8.32%), *trans*-β-ocimene (7.87%), neral (6.05%) and geranial (7.45%), which were presented in large amounts. Orange leaf oil possessed sabinene (47.68%) as the main compound, followed by *trans*-β-ocimene (8.31%), 3-carene (7.38%), limonene (5.95%) and linalool (4.38%). Whereas citrus peel oils were constituted mainly by $C_{10}H_{16}$ monoterpenes (94.01–98.66%), the essential oils distilled from lemon, mandarin and orange leaves contained 65.26, 31.23 and 79.43% of monoterpenes, respectively.

Fig. 4 shows comparative chemical compositions of citrus leaf oils, based on the compound group classification. Mandarin leaf oil contained 2 and 3.5 times more oxygenated compounds than oils distilled from lemon and orange leaves, respectively. Based on the high content of linalool, neral and geranial (total 66.16%), mandarin leaf essential oil could be developed as an important raw material for the flavour and fragrance industries.

Fig. 5 shows the comparative chemical compositions of oxygenated compounds found in the citrus leaf oils analysed. Aldehydes were 2 and 3.5 times more abundant in lemon leaf oil (27.59%) than in mandarin and orange leaf oils, respectively. Alcohols were the predominant (70%) oxygenated compounds in mandarin leaf oil and prevailed almost six times over the total alcohol concentration in lemon and orange leaf oils.

4. Conclusions

The various constituents of the essential oils from Colombian lemon (*C. volkameriana*), mandarin (*C. reticulata*) and orange (*C. sinensis*) were isolated by cold pressing or/and by steam distillation from the fruit peel and leaves, and

Table 2
Chemical compositions of citrus leaf essential oils

Peak No. (DB-1)	Compound	I_K[a]		GC peak area (%)[b]					
		DB-1	DBWAX	Lemon	S.D.	Mandarin	S.D.	Orange	S.D.
1	α-Thujene	924	1025	0.11	$6 \cdot 10^{-2}$	1.26	$1 \cdot 10^{-2}$	0.30	$1 \cdot 10^{-2}$
2	α-Pinene	932	1021	0.53	$1 \cdot 10^{-1}$	2.66	$7 \cdot 10^{-2}$	0.55	$6 \cdot 10^{-1}$
3	Camphene	962	1083	0.04	$1 \cdot 10^{-2}$	0.37	$7 \cdot 10^{-2}$	0.02	$7 \cdot 10^{-4}$
4	Sabinene	967	1120	16.16	$3 \cdot 10^{+0}$	2.81	$1 \cdot 10^{-1}$	47.68	$2 \cdot 10^{+0}$
5	β-Pinene	973	1107	0.69	$1 \cdot 10^{-1}$	0.86	$9 \cdot 10^{-2}$	2.00	$7 \cdot 10^{-2}$
6	*n*-Octanal	977	1270	0.13	$6 \cdot 10^{-3}$	–	–	0.04	$5 \cdot 10^{-3}$
7	β-Myrcene	982	1162	1.56	$3 \cdot 10^{-1}$	0.05	$6 \cdot 10^{-3}$	3.73	$2 \cdot 10^{-1}$
8	α-Phellandrene	994	1177	0.06	$6 \cdot 10^{-3}$	–	–	0.69	$3 \cdot 10^{-2}$
9	3-Carene	1000	1150	–	–	0.04	$4 \cdot 10^{-3}$	7.38	$3 \cdot 10^{-1}$
10	1,4-Cineole	1009	1177	–	–	0.27	$8 \cdot 10^{-3}$	0.48	$3 \cdot 10^{-2}$
11	α-Terpinene	1012	1183	0.11	$4 \cdot 10^{-2}$	1.95	$3 \cdot 10^{-1}$	0.12	$1 \cdot 10^{-2}$
12	*p*-Cymene	1013	1284	–	–	2.35	$3 \cdot 10^{-1}$	0.02	$1 \cdot 10^{-3}$
13	1,8-Cineole	1018	1228	–	–	0.70	$2 \cdot 10^{-1}$	0.16	$6 \cdot 10^{-3}$
14	*d*-Limonene	1026	1201	41.74	$2 \cdot 10^{+0}$	8.32	$2 \cdot 10^{+0}$	5.95	$2 \cdot 10^{-1}$
15	β-Phellandrene	1027	1213	–	–	–	–	0.33	$3 \cdot 10^{-2}$
16	*trans*-β-Ocimene	1035	1252	3.88	$4 \cdot 10^{-1}$	7.87	$9 \cdot 10^{-1}$	8.31	$4 \cdot 10^{-1}$
17	Not identified	1045	–	–	–	–	–	0.13	$6 \cdot 10^{-3}$
18	γ-Terpinene	1051	1248	0.27	$8 \cdot 10^{-2}$	1.20	$2 \cdot 10^{-1}$	0.65	$4 \cdot 10^{-2}$
19	*trans*-Sabinene hydrate	1054	1463	0.07	$3 \cdot 10^{-2}$	–	–	0.16	$7 \cdot 10^{-3}$
20	*n*-Octanol	1074	1507	–	–	–	–	0.27	$1 \cdot 10^{-2}$
21	Terpinolene	1080	1291	0.11	$1 \cdot 10^{-2}$	1.49	$2 \cdot 10^{-1}$	1.57	$7 \cdot 10^{-2}$
22	Nonanal	1082	1382	0.16	$3 \cdot 10^{-2}$	–	–	–	–
23	Linalool	1083	1553	3.12	$7 \cdot 10^{-1}$	52.66	$3 \cdot 10^{+0}$	4.38	$2 \cdot 10^{-1}$
24	*cis*-Sabinene hydrate	1088	–	–	–	0.08	$9 \cdot 10^{-3}$	0.02	$2 \cdot 10^{-3}$
25	Myrcenol	1104	1581	–	–	–	–	0.05	$2 \cdot 10^{-3}$
26	Methyl *n*-octanoate	1106	1372	–	–	–	–	0.12	$1 \cdot 10^{-1}$
27	*cis*-Epoxylimonene	1118	–	0.07	$3 \cdot 10^{-2}$	0.59	$1 \cdot 10^{-1}$	0.05	$3 \cdot 10^{-3}$
28	1,2-Dihydrolinalool	1121	1449	0.05	$1 \cdot 10^{-2}$	0.03	$8 \cdot 10^{-3}$	0.02	$9 \cdot 10^{-4}$
29	Citronellal	1131	1472	22.21	$3 \cdot 10^{+0}$	–	–	2.83	$1 \cdot 10^{-1}$
30	Isopulegol	1146	1565	0.04	$1 \cdot 10^{-2}$	–	–	0.13	$2 \cdot 10^{-2}$
31	Isoborneol	1157	1654	0.18	$1 \cdot 10^{-1}$	–	–	0.20	$2 \cdot 10^{-2}$
32	Nonanol	1161	–	0.17	$1 \cdot 10^{-2}$	0.19	$6 \cdot 10^{-2}$	0.37	$1 \cdot 10^{-2}$
33	α-Terpineol	1179	1740	0.13	$2 \cdot 10^{-2}$	0.06	$5 \cdot 10^{-3}$	0.10	$4 \cdot 10^{-3}$
34	Decanal	1183	1482	0.96	$1 \cdot 10^{-1}$	–	–	0.15	$6 \cdot 10^{-3}$
35	Methylthymal	1196	–	0.02	$2 \cdot 10^{-2}$	–	–	–	–
36	Citronellol	1203	1751	1.43	$5 \cdot 10^{-1}$	–	–	0.53	$2 \cdot 10^{-2}$
37	Neral	1215	1705	0.91	$6 \cdot 10^{-1}$	6.05	$1 \cdot 10^{+0}$	1.87	$7 \cdot 10^{-2}$
38	Geraniol	1237	1789	0.04	$2 \cdot 10^{-3}$	0.16	$1 \cdot 10^{-2}$	0.21	$8 \cdot 10^{-3}$
39	Geranial	1248	1735	1.26	$5 \cdot 10^{-1}$	7.45	$1 \cdot 10^{-1}$	2.61	$1 \cdot 10^{-1}$
40	Linalyl acetate	1264	1519	0.02	$8 \cdot 10^{-3}$	–	–	0.03	$2 \cdot 10^{-3}$
41	Thymol	1286	2100	0.07	$4 \cdot 10^{-2}$	–	–	0.07	$3 \cdot 10^{-3}$
42	Citronellyl acetate	1335	1645	0.11	$2 \cdot 10^{-2}$	0.43	$3 \cdot 10^{-1}$	0.06	$2 \cdot 10^{-3}$
43	Neryl acetate	1340	1729	0.13	$3 \cdot 10^{-2}$	–	–	0.17	$7 \cdot 10^{-3}$
44	Not identified	1341	–	0.60	$1 \cdot 10^{-1}$	–	–	–	–
45	Geranyl acetate	1357	1746	0.37	$8 \cdot 10^{-2}$	–	–	0.16	$6 \cdot 10^{-3}$
46	Longifolene	1380	1642	0.07	$3 \cdot 10^{-3}$	0.23	$1 \cdot 10^{-1}$	0.04	$2 \cdot 10^{-3}$
47	δ-Elemene	1384	1475	0.05	$2 \cdot 10^{-3}$	0.22	$1 \cdot 10^{-1}$	0.63	$2 \cdot 10^{-2}$
48	β-Caryophyllene	1424	1654	0.36	$1 \cdot 10^{-2}$	0.24	$2 \cdot 10^{-1}$	0.21	$8 \cdot 10^{-3}$

(*Continued on p. 512.*)

Table 2 (*continued*)

Peak No. (DB-1)	Compound	I_K[a]		GC peak area (%)[b]					
		DB-1	DBWAX	Lemon	S.D.	Mandarin	S.D.	Orange	S.D.
49	Isoeugenol	1431	–	0.06	$1 \cdot 10^{-2}$	–	–	–	–
50	α-Bergamotene	1435	1589	0.06	$2 \cdot 10^{-3}$	0.11	$2 \cdot 10^{-2}$	–	–
51	α-Humulene	1452	1676	0.04	$1 \cdot 10^{-3}$	0.08	$3 \cdot 10^{-2}$	0.06	$3 \cdot 10^{-3}$
52	Germacrene D	1477	1714	0.04	$2 \cdot 10^{-2}$	0.17	$1 \cdot 10^{-1}$	–	–
53	β-Bisabolene	1495	1770	0.31	$9 \cdot 10^{-2}$	–	–	0.03	$2 \cdot 10^{-3}$
54	β-Selinene	1500	1756	0.08	$1 \cdot 10^{-2}$	1.01	$4 \cdot 10^{-1}$	–	–
55	α-Muurolene	1502	1730	–	–	0.08	$5 \cdot 10^{-2}$	–	–
56	δ-Cadinene	1511	1766	0.03	$2 \cdot 10^{-3}$	0.08	$1 \cdot 10^{-2}$	–	–
57	Germacrene D	1564	1550	0.15	$6 \cdot 10^{-2}$	0.10	$4 \cdot 10^{-2}$	0.12	$5 \cdot 10^{-3}$
58	α-Bisabolol	1570	2022	–	–	0.29	$5 \cdot 10^{-2}$	–	–
59	δ-Cadinol	1615	2150	0.03	$8 \cdot 10^{-3}$	0.06	$8 \cdot 10^{-3}$	–	–
60	Sesquiterpenol	1650	–	0.05	$2 \cdot 10^{-2}$	0.09	$1 \cdot 10^{-2}$	0.03	$6 \cdot 10^{-3}$
61	Not identified	1672	–	–	–	–	–	0.75	$4 \cdot 10^{-2}$
62	α-Sinensal	1725	–	–	–	0.50	$2 \cdot 10^{-1}$	0.13	$8 \cdot 10^{-3}$
63	$C_{20}H_{40}O$	1918	–	0.03	$3 \cdot 10^{-3}$	–	–	–	–
64	Phytol	2066	–	0.66	$2 \cdot 10^{-1}$	0.13	$1 \cdot 10^{-2}$	0.22	$9 \cdot 10^{-3}$

[a] Experimentally determined Kováts retention indices.
[b] Percentages were calculated from the peak areas on the DB-1 column.

were identified and quantified by means of HRGC with flame ionization or mass spectrometric detection. DB-1 and DB-WAX fused-silica capillary columns (both 60 m × 0.25 mm I.D.) were successfully applied to resolve completely all volatile compounds present in the extracts. Thus, under the conditions employed in this work, prefractionation of the citrus essential oils was not required for their complete GC analysis. The highest concentration of the volatile secondary metabolites was observed in the extracts isolated either by steam distillation or cold pressing from the citrus peel (*lemon, mandarin or orange*) at the intermediate stage of fruit maturity (45–75% green). No pronounced qualitative or quantitative differences in composition were detected between the expressed and distilled citrus peel oils studied. In the Colombian citrus peel oils, the total mass concentration of citral (neral + geranial) and linalool, which are considered to be the most potent aroma compounds in citrus oils [12], did not exceed 3.0%

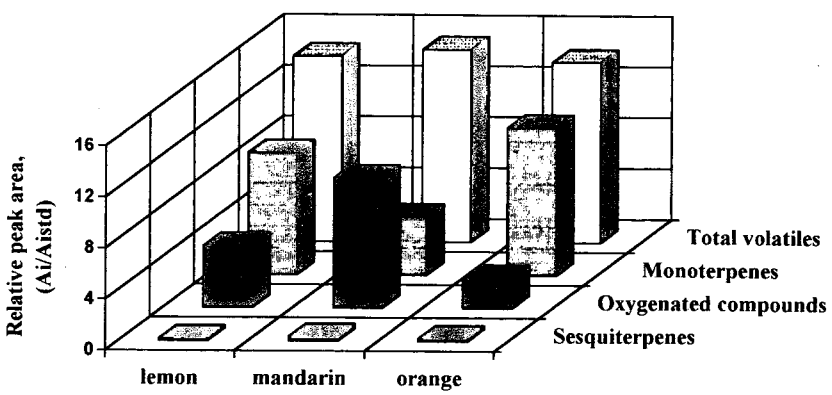

Fig. 4. Comparative chemical compositions of citrus leaf oils obtained by steam distillation.

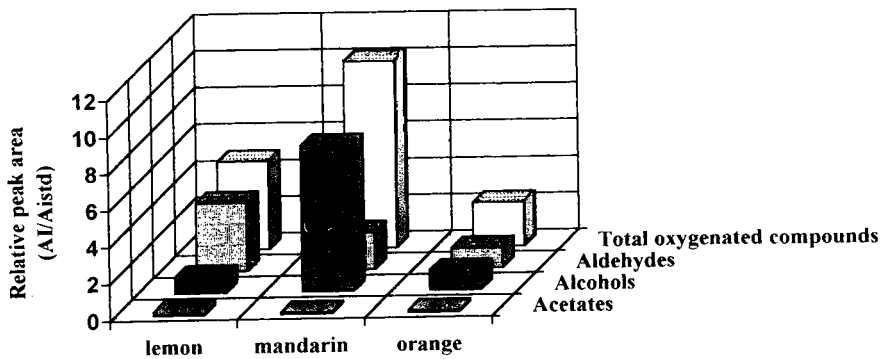

Fig. 5. Comparative chemical composition of the oxygenated compounds in the oils distilled from citrus leaves.

(lemon), 0.4% (mandarin) and 0.35% (orange). The content of limonene, suggested to be more important than citral to convey the fresh lemon aroma [13], reached 78.90, 90.05 and 94.55% in lemon, mandarin and orange peel oils, respectively. The high mass concentrations of citronellal (22.21%), linalool (52.66%) and citral (13.50%) in the steam-distilled lemon and mandarin leaf oils, respectively, make these oils very attractive raw materials for the flavour industry.

Acknowledgements

Financial support to the laboratory from Colciencias (Grant 1102-18) is highly appreciated. The authors thank Casa Cientifica, representatives of Hewlett-Packard in Colombia, for their continuing technical assistance.

References

[1] P.E. Shaw, *J. Agric. Food Chem.*, 27 (1979) 246.
[2] G. Mazza, *Sci. Aliment.*, 7 (1987) 459.
[3] M.H. Boelens and R. Jimenez, *J. Essent. Oil Res.*, 1 (1989) 151.
[4] F.M. Lanças and M. Cavicchioli, *J. High Resol. Chromatogr.*, 13 (1990) 207.
[5] A. Cotroneo, A. Verzera, G. Lamonica and G. Dugo, *Flavour Fragrance J.*, 1 (1986) 69.
[6] R.E. Berry, P.E. Shaw, J.H. Tatum and C.W. Wilson, III, *Food Technol.*, 12 (1983) 88.
[7] Y. Combariza, C. Blanco T., E.E. Stashenko and T. Shibamoto, *J. High Resolut. Chromatogr.*, 17 (1994) 643.
[8] E. Kováts, *Adv. Chromatogr.*, 1 (1965) 229.
[9] W. Jennings and T. Shibamoto, *Qualitative Analysis of Flavor and Fragrance Volatile by Glass Capillary Gas Chromatography*, Academic Press, New York, 1980.
[10] S.K. Ramaswami, P. Briscese, R.J. Gargiullo and T. van Geldern, in B.M. Lawrence, B.I. Mookherjee and B.J. Willis (Editors), *Flavors and Fragrances: a World Perspective, Proceedings of the 10th International Congress on Essential Oils, Flavors and Fragrances, Washington, DC, 1986*, Elsevier, Amsterdam, 1988, p. 51.
[11] N.W. Davies, *J. Chromatogr.*, 503 (1990) 1.
[12] P. Schieberle and W. Grosch, *J. Agric. Food Chem.*, 36 (1988) 797.
[13] F. Drawert and N. Christoph, in P. Schreier (Editor), *Analysis of Volatiles*, Walter de Gruyter, Berlin, 1984, p. 269.

ELSEVIER

Journal of Chromatography A, 697 (1995) 515–523

JOURNAL OF CHROMATOGRAPHY A

Aerobic bacterial degradation of selected polyaromatic compounds and *n*-alkanes found in petroleum

E. Šepič[a], H. Leskovšek[a,*], C. Trier[b]

[a]*"Jožef Stefan" Institute, Jamova 39, 61111 Ljubljana, Slovenia*

[b]*University of Plymouth, Department of Environmental Sciences, Drake Circus, Plymouth, UK*

Abstract

Biodegradation in vitro studies were carried out on selected aromatic and aliphatic hydrocarbons in aqueous medium. Biotic and abiotic samples were analysed by GC and/or GC–MS. It was clearly shown that abiotic losses for selected compounds were much higher than might have been expected from the literature. The experiments were undertaken using the higher-relative-molecular-mass compounds; e.g. phenanthrene, chrysene, benzo[*a*]pyrene and a series of *n*-alkanes. Although *n*-C_{17} proved too volatile, *n*-C_{22} and *n*-C_{30} were shown to be extensively biodegraded, and these *n*-alkanes were degraded preferentially to the polyaromatic compounds. Chrysene and benzo[*a*]pyrene were less affected by abiotic losses but did not biodegrade significantly during a four-month incubation. A similar experiment with diesel oil confirmed the above findings.

1. Introduction

Widespread and already frequent contamination by toxic organic chemicals in water, soil and sediment ranges from industrial chemical waste contamination [1–3] to halogenated hydrocarbons and pesticides in ground water [4,5] and oil spills [6,7]. In situ biodegradation processes are focusing attention on the role that microorganisms may play in alleviating environmental pollution [8–13].

Biodegradation is a form of biotransformation which by simplification of an organic compound's structure through the breaking intramolecular bonds, alters its toxicity and transport properties [14]. The simplification may be subtle, involving merely a substituent functional group, or severe, resulting in mineralisation. The process of biotic reactions is accompanied by abiotic reactions, which include all of the reactions not encompassed by biotic reactions, i.e. inorganic, organic, photolytic, surface-catalysed, sorptive and transport processes. Abiotic contribution to the losses of organic compounds, especially those with lower relative molecular mass, have been underestimated in the past.

Several laboratory-based studies have been undertaken to assess the fate of polycyclic aromatic hydrocarbons (PAHs) in the soil [15–18]. These indicate that biodegradation is the key process leading to the loss of most PAHs in the soil system when abiotic losses are controllable. Generally, low-molecular-mass compounds are reported to be affected by volatilisation and/or

* Corresponding author.

0021-9673/95/$09.50
SSDI 0021-9673(94)01032-3

abiotic degradation processes [18]. A broadly inverse relationship has been shown between the rate of biodegradation and the number of benzene rings [15], probably due to changes in solubility, bioavailability and stability of PAHs depending on their molecular structure [17]. Low-molecular-mass PAHs such as naphthalene have higher aqueous solubilities and are less lipophilic than the higher-molecular-mass compounds and can act as a sole carbon/energy source for some soil microbes [16]. The polyringed species cannot act as a sole source of carbon/energy, but may be degraded by co-oxidation processes [19].

It has been shown that PAH mineralisation can be accelerated in soils and sediments that have previously been contaminated; this implies that an adapted microbial population has been developed [16,20]. PAH degradation may also be enhanced by the addition of organic supplements that stimulate the general level of biomass activity. Many other factors are important for the process of bacterial degradation. The presence of the microorganisms in the soil is fundamental. One way to enhance biodegradation of organic compounds is to inoculate the environment with microorganisms, which are known to readily metabolise these chemicals. The rate of microbial decomposition of organic compounds in soils is a function of three variables: (a) the availability of the chemicals to the microorganisms that can degrade them, (b) the quantity of these microorganisms and (c) the activity level of these organisms. Factors such as organic matter and clay content, moisture level, temperature, pH, aeration and nutrient status, are of importance as moderators and driving factors [21].

In the present study, in vitro biodegradation experiments were carried out on both, single compound and mixtures of aromatic and aliphatic hydrocarbons. In addition as a real sample biodegradation of diesel oil (DO) was examined. Single bacterial species *Pseudomonas putida* and *Pseudomonas fluorescens* Texaco were used. Known concentrations of hydrocarbons were added to mineral media paying attention not to exceed the limit of solubility in water.

2. Experimental

2.1. Experimental design

Mineral media and standard compounds of interest were added to a series of Erlenmeyer flasks. Bacterial broth was added only to biotic samples. Hg_2Cl_2 (Aldrich, Dorset, UK) was added to the remaining samples to ensure that only abiotic conditions prevailed. The concentrations of each hydrocarbon in aqueous solution (0.8 mg/l) was kept below the limit of solubility of one of the common PAHs in water samples —phenanthrene. Such high concentration levels are expected in case of fuel spills where we wish to apply our results. For that reason we did not use lower concentration levels, although biodegradation has been mainly studied at these lower levels [22,23]. All the compounds, that is phenanthrene (Ph), chrysene (Chr), benzo[*a*]pyrene (BaP), *n*-C_{17}, *n*-C_{22} and *n*-C_{30} from Aldrich and BaP from Sigma, Dorset, UK, except the internal standard stock solution [2-methylphenanthrene (2MPh) for aromatics and *n*-C_{25} for aliphatics, Aldrich] were added to the mineral media solution on day 0. Internal standards were injected to the sample on the day of analysis prior to extraction. The selected hydrocarbons were chosen because they can be found abundantly in petroleum.

Flasks, stoppered with non-adsorbent cotton wool, were then incubated aerobically in the absence of the light on a shaker, at room temperature and at a lower temperature (4–5°C) for up to four months. Control abiotic flasks containing mineral salts, hydrocarbons, but no bacterial inoculum, were incubated under the same conditions to monitor abiological losses (e.g. evaporation). The experiments were carried out in duplicates. During incubation on each day of analysis, two biotic and two abiotic samples were extracted three times with 10 ml of dichloromethane (all the solvents were purchased at Rathburn, Peebleshire, UK) from the salt solution, dried with anhydrous Na_2SO_4 (Aldrich) for 60 min and filtered. After transferring the samples into separation funnels, the flasks were

rinsed three times with dichloromethane (DCM) to avoid any compound left in the flask due to the adsorption to glass walls. The volume was reduced (nitrogen) to 1 ml prior to analysis by capillary gas chromatography.

Initial experiments were set up with compounds (benzene, naphthalene) that were proved as too volatile for such a kind of experiment. Therefore following studies were performed using single compounds phenanthrene and n-C_{17} and mixtures of three aromatic (Ph, 2MPh and BaP) and three aliphatic (n-C_{17}, n-C_{22} and n-C_{30}) hydrocarbons. As a real sample DO (Plinsko olje D2; Petrol, Koper, Slovenia) was tested. DO was separated into aromatic and aliphatic fraction by wet column chromatography. The column was filled with dried (450°C, 24 h) and activated silica. For 1 g of sample 25 g of silica were required. Aliphatic fraction was eluted first with hexane. Aromatics were eluted with hexane–diethyl ether (10:1).

P. putida and *P. fluorescens* Texaco [24] were chosen for this study because of their known ability to degrade hydrocarbons even at low temperatures [25]. They are also common in the soil contaminated with petroleum products. Cultures were prepared in an OXOID nutrient broth (1.3%) for 24 h at 20°C before use.

All glassware and mineral media were sterilised by autoclaving (120°C, 20 min). Bacterial broth (1 ml, approx. 10^7 bacteria) was added to a conical flask (250 ml) containing 100 ml of sterilised salt solution where 5‰ NH_4Cl, 1‰ NH_4NO_3, 2‰ Na_2SO_4; 3‰ K_2HPO_4; 1‰ KH_2PO_4 and 0.1‰ $MgSO_4 \cdot 7H_2O$ (Aldrich) were dissolved in 1000 ml of deionised water [22].

A set of experiments to prove evaporation losses was undertaken (evaporation test). Three samples containing examined hydrocarbons and mineral media were incubated under different conditions. One sample was refrigerated and the other two were observed at room temperature; one on a bench top and the other in the fume cupboard. It was suspected that high abiotic losses resulted from a higher air flow in the fume cupboard where experiments were set up at the beginning. All the samples were extracted after 5 days of incubation. Despite the higher air flow in the fume cupboard, no significant difference was revealed between with cotton wool stoppered samples carried out at room temperature. The comparison between the samples incubated at room temperature and the refrigerated one showed clearly that abiotic losses were diminished greatly at lower temperature.

The problem of evaporation was confirmed with Soxhlet extraction of non-absorbent cotton wool used for stoppering conical flasks. Discernible amount (about 10%) of observed compound was found in the cotton wool after extraction. Reference cotton wool did not contain this compound. The head space analysis of the same sample also confirmed the above findings.

The bacteria in the samples were tested to ascertain if they were alive prior to analysis by spreading an agar plate with a loopful of sample. The count of the bacteria was performed on the day of analysis by the Miles and Misra drop counts method with serial of dilutions of the organisms [26]. It was shown that experiments with higher biodegradation losses gave higher counts in general. The bacteria incubated in the cold room had visibly lower counts, but the chosen bacteria did grow and multiply.

A quick agar plate test was performed in order to determine the biodegradation potential of selected compounds with chosen bacterial species. Agar plates were prepared especially for this experiment with nutrient agar with no usable carbon substrate for bacterial growth. These plates were spread with the culture. A thin layer of the compound was sprayed over the surface of the inoculated plate using an aerosol spray [27]. The plates were left to dry before being incubated at 30°C. Blanks included an inoculated plate without compounds, a plate with compounds and no bacteria and an empty plate. No growth of bacteria was observed on any of the blanks, even after 10 days of incubation. Only plates sprayed with the n-docosane, n-eicosane and DO gave visible growth of bacteria within the incubation time. This proved that only simple short chain aliphatic hydrocarbons are readi-

ly degraded in a single compound and single culture degradation experiment without any other organic carbon present.

2.2. Gas chromatography

Gas chromatography was performed using a Carlo Erba (Milan, Italy) 4160 gas chromatograph with on-column injector and flame ionisation detector. Separation was achieved using a 30 m × 0.32 mm I.D. phenyl silica column (1 μm film thickness) DB 5 (J & W Scientific, Loughborough, UK). Oven temperature was programmed from 65 to 300°C at 5°C/min and held for 10 min. Hydrogen was used as the carrier gas at a flow-rate of 1.5 ml/min. The flame ionisation detector's temperature was 330°C. Quantitation of individual hydrocarbons was made by measurement of GC peak areas with a Shimadzu (Kratos Analytical, Manchester, UK) CR3-A integrator and a comparison of these with the responses of known concentrations of internal standards, 2MPh for aromatic hydrocarbons and n-C_{25} for aliphatic ones. In case of DO a mixture of internal standards (squalane and BaP) was used. Compounds were identified by co-chromatography with authentic compounds. For confirmation some samples were run on GC–MS (HP 5890 series II gas chromatograph coupled to 5970 series mass-selective detector) (Hewlett-Packard, Waldbronn, Germany) using HP1 column (12 m × 0.32 mm I.D.), splitless injection and head pressure of 36 kPa. Biological degradation was calculated from differences between biotic and abiotic losses.

3. Results and discussion

Biodegradation studies of selected aromatic and aliphatic compounds showed that the abiotic losses amounted to 78% of the starting concentration within 17 days of incubation when working at room temperature with a single compound (Ph and n-C_{17} separately) under the limit of solubility. This discernible diminished the purely biotic degradation to about 4% only. One possible explanation was evaporation, and this was clearly proven by the evaporation test. An experiment which was set up in the dark (to avoid possible photodegradation) in a cold room (4–5°C) showed lower abiotic losses at lower temperature. The results of the biodegradation were in this case visibly higher —up to 29% within 20 days of incubation. These experiments clearly showed that evaporation plays a decisive role when working with low concentrations and a single compound. It should be born in mind that even if the limit of solubility is exceeded the quantity of the compound available to the microorganism does not increase.

The abiotic losses were examined at room temperature with the mixture of three aromatic and three aliphatic compounds. The effect of evaporation on the compounds with different vapour pressures was clearly shown. The abiotic losses were very high for the compounds with lower molecular mass (n-C_{17} and Ph). These reached 92 ± 5% within 61 days of incubation at room temperature and affected the others according to their molecular mass (Fig. 1). Of all the compounds tested, n-C_{22} was proven to be the best for biodegradation studies. As an aliphatic compound it was readily degradable —89 ± 4% of the compound was biodegraded— and it was less affected by abiotic losses than n-C_{17} and Ph; abiotic factors resulted in only 9 ± 2% losses overall. n-C_{30} was slightly less degraded (81 ± 5%) than n-C_{22} under the same conditions, but its abiotic losses were diminished to 2 ± 1%. Aromatic compounds experienced lower biotic degradation in general. Ph, the lowest-molecular-mass aromatic compound tested, was found to have only 3 ± 1% losses due to biological degradation and extended abiotic losses to 92 ± 6%. PAHs with higher molecular masses were only slightly affected from both abiotic and biotic losses. This proved that bacteria of the genus *Pseudomonas* utilised alkanes more intensively than PAHs [28] and this was manifested by higher plate counts, higher metabolic activity and hydrocarbon degradation rate. In general all kinds of bacteria would oxidise compounds with a lower molecular mass more easily. Between aliphatic and aromatic compounds they would degrade aliphatic hydrocar-

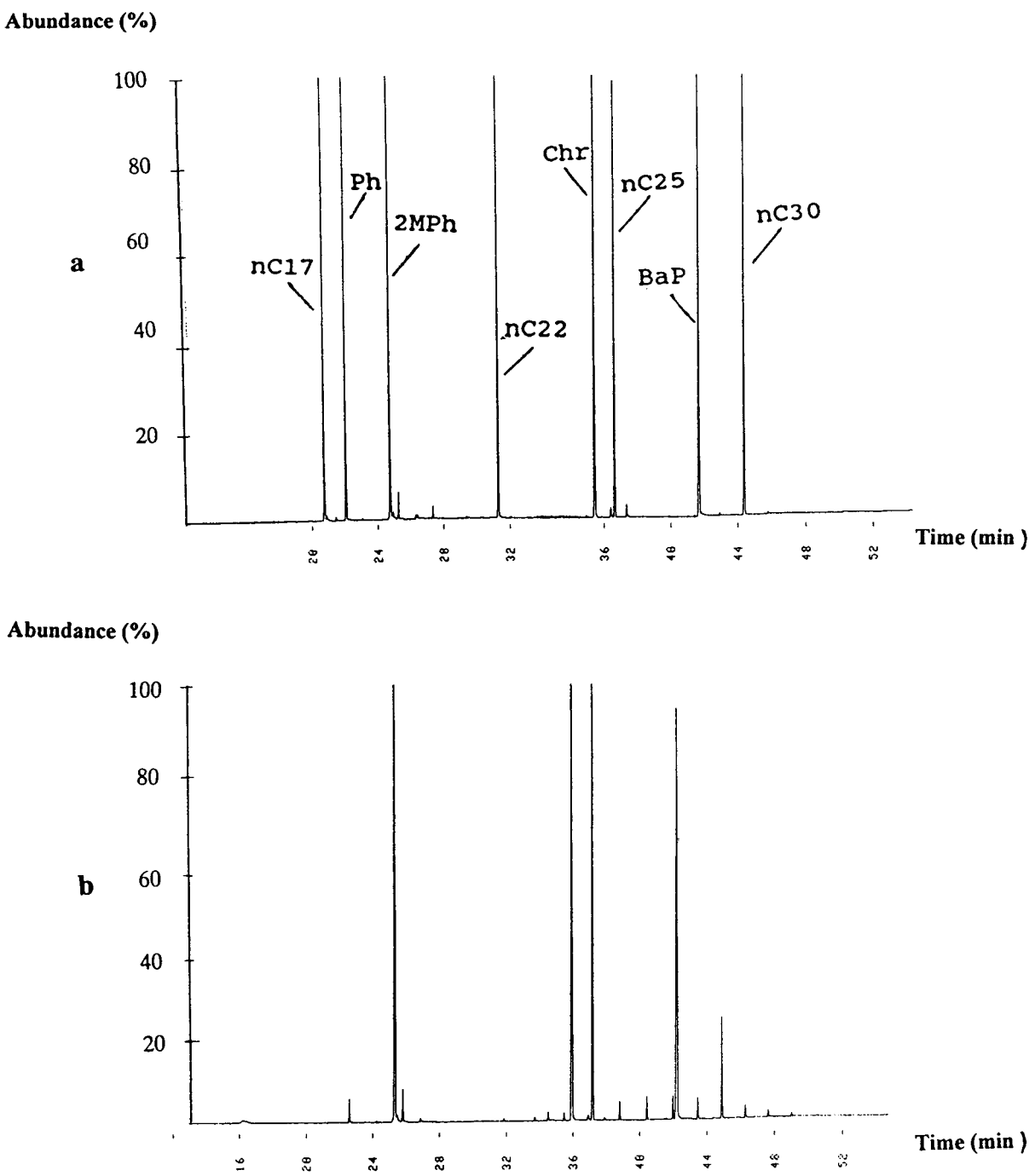

Fig. 1 (*continued on p. 520*).

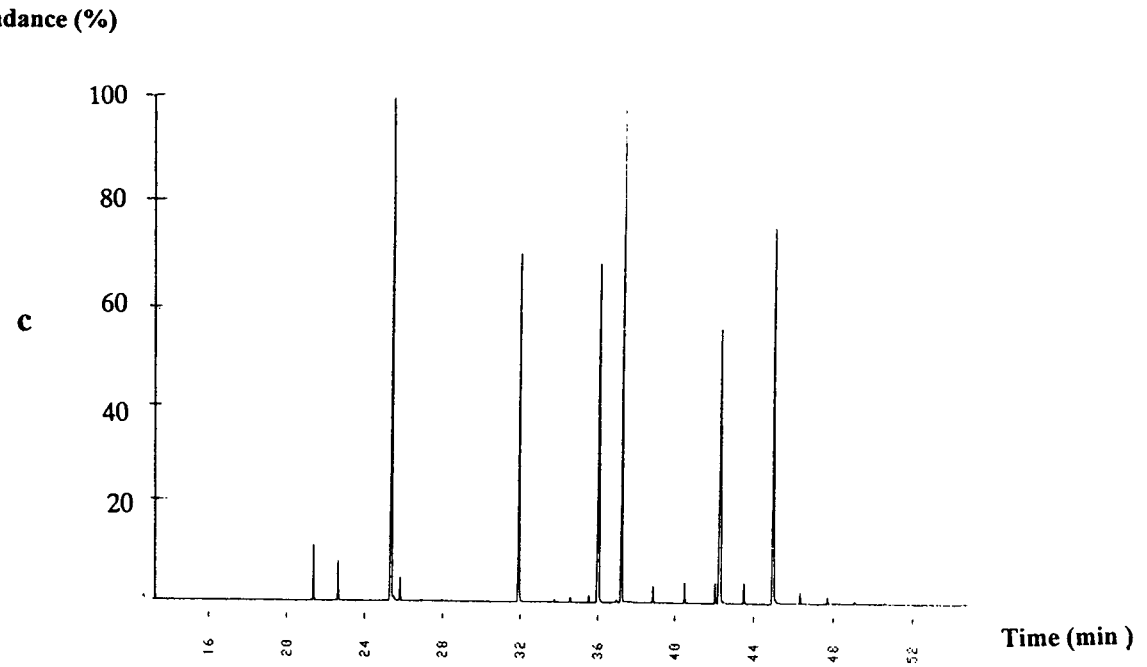

Fig. 1. Biodegradation of selected aromatic and aliphatic hydrocarbons. (a) Gas chromatogram of the mixture of hydrocarbons on day 0; (b) biotic and (c) abiotic samples after 61 days of incubation.

bons first. Bacteria will use compounds that are more difficult to degrade only if they are incubated for long enough and an adopted microbial population is developed.

It has been shown that hydrocarbons, which can not be used for growth by many soil organisms, can be oxidised if present as co-substrates in a system in which another substrate is available for growth [29]. It seems likely that bacteria become modified after attacking lower-molecular-mass compounds in a way so that they are able to oxidise even higher, less degradable compounds. When bacteria are exposed straight away to the heavy less degradable compounds, they quite possibly will not be able to oxidise them. A very interesting study has been reported very recently about a conditional-suicide containment system for bacteria which mineralise aromatic hydrocarbons [30].

The study of a real sample DO showed more effective biodegradation than its separated aromatic fraction. This was expected and proved the above conclusions. Abiotic losses were much lower in the real sample and the biological degradation more efficient. Fig. 2 represents the total ion chromatograms of the complex DO on day 0 of incubation (a) and its biotic (b) and abiotic (c) sample after 48 days of incubation. It is noticeable that as a result of evaporation all the light compounds disappeared in both biotic and abiotic samples. Disappearance of several heavier compounds was a result of biological degradation.

4. Conclusions

Results from this study proved that abiotic losses can play more important role than has previously been reported in the literature. Very recently similar findings have been obtained with PAHs only [31,32]. Compounds which are particularly affected are those with lower molecular masses, e.g. PAHs with less than four benzene rings and straight-chain alkanes with less than 20 C atoms. It was shown that higher concentra-

tions of hydrocarbons reduce the abiotic losses, but the availability of those compounds to the biota is then questionable. Abiotic losses in real samples such as DO are much lower. The abiotic losses are expected to be significantly diminished when working in a soil–water system because of

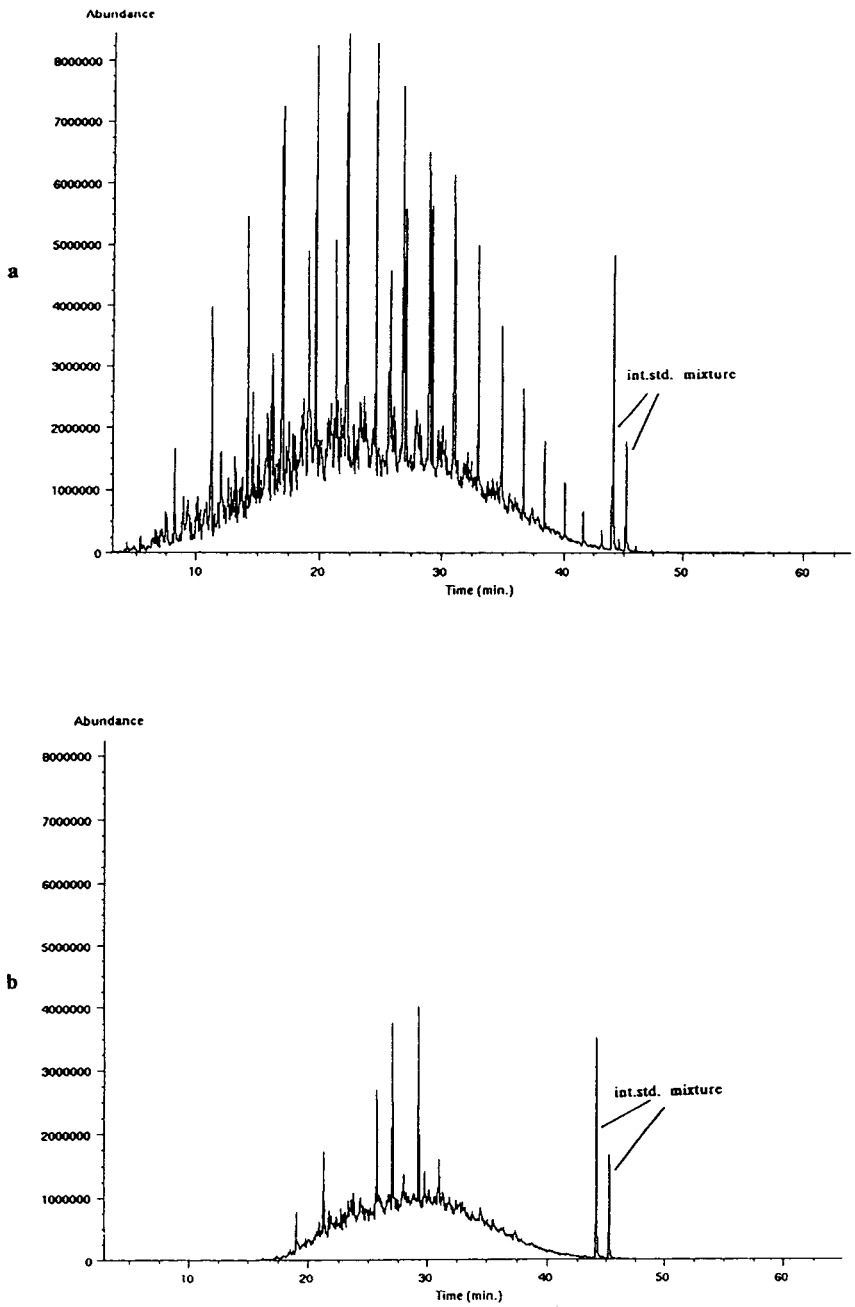

Fig. 2 (*continued on p. 522*).

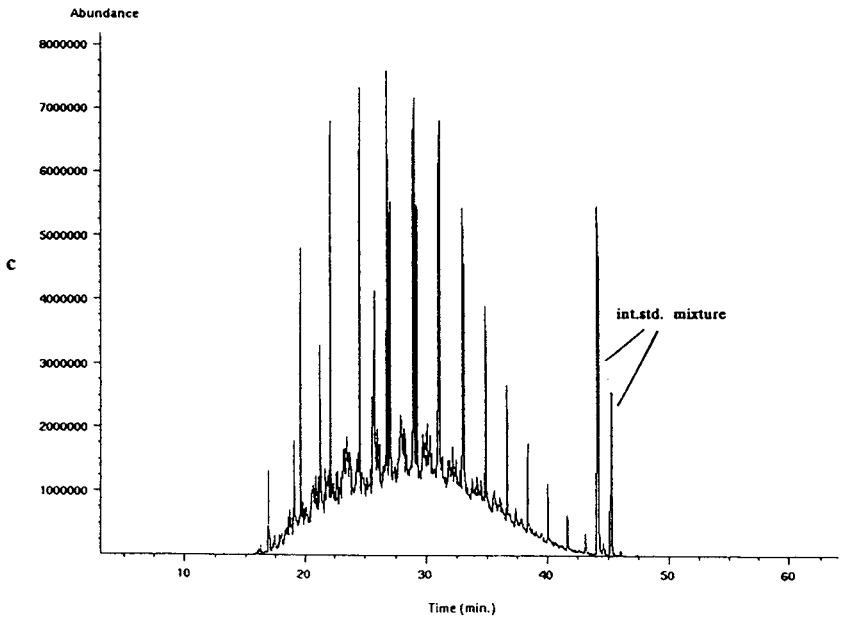

Fig. 2. Biodegradation of diesel oil. (a) Total ion chromatogram of diesel oil on day 0 of incubation; (b) biotic and (c) abiotic samples after 48 days of incubation.

the adsorption processes present. Care should be taken when relating laboratory-based observations concerning hydrocarbon losses to the losses occurring in the field.

In addition to in vitro biodegradation studies it is usually suggested to use chemical and microbiological measurements on samples from a contaminated site. The majority of biodegradation investigations that utilise environmental samples (water, soil and sediments from contaminated and uncontaminated sites) in laboratory flask assays demonstrate biodegradation potential, not in situ biodegradation. A laboratory approach allows the testing of a large number of controlled environment parameters within a relatively short time. But it is necessary to be aware of the limitations of such studies in reproducing field situations. For example, important parameters such as tillage and soil texture cannot be meaningfully tested in a laboratory system. It also remains to be determined whether temperature fluctuations around a daily mean during a 24-h cycle can be equated with a constant incubation temperature. Consequently, laboratory findings need validation and possible adjustment when compared to field studies. Nevertheless, laboratory studies can greatly reduce and simplify any subsequent field tests. The reason for performing the laboratory studies is clear —the control over mass balances and ability to distinguish biotic from abiotic reactions allow definite conclusions to be drawn.

Acknowledgement

Nearly all the experiments were performed during the stay of E.Š. at the University of Plymouth in the Department of Environmental Sciences. We thank Professor Les Ebdon to enable us to carry out this research and Professor Steve Rowland for helpful discussions during this investigation. Our thanks are also expressed to the technical staff of University of Plymouth, most notably to Mr. Ian Doidge, Mr. Roger Srodzinsky (Chemistry), Mrs. Jo Carter and Ms. Nicola Wilson (Biology). Bacterial broth was a kind donation of Biology Department, Universi-

ty of Plymouth, UK. We would also like to sincerely thank Professor Jože Marsel from the University of Ljubljana for his helpful comments.

E.Š. wishes to thank the Ministry of Science and Technology of Slovenia for a studentship.

References

[1] A.G. Levine, *Love Canal: Science, Politics and People*, Lexington Books, Lexington, MA, 1982.
[2] R.F. Lewis, *Air Waste*, 43 (1993) 503.
[3] S.R. Wild, K.C. Jones, *J. Environ. Qual.*, 21 (1992) 217.
[4] B.H. Keswick, in G. Bitton and C.P. Gerba (Editors), *Groundwater Pollution Microbiology*, Wiley, New York, 1984, Ch. 3.
[5] S. Pacenka et al., *J. Contam. Hydrol.*, 2 (1987), 73.
[6] J.F. Piatt et al., *Auk*, 107 (1990) 387.
[7] P.H. Pritchard and C.F. Costa, *Environ. Sci. Technol.*, 25 (1991) 372.
[8] M.D. Lee et al., *Crit. Rev. Environ. Control*, 18 (1988) 29.
[9] P. Morgan and R.J. Watkinson, *FEMS Microbiol. Rev.*, 63 (1989) 277.
[10] J.M. Thomas and C.H. Ward, *Environ. Sci. Technol.*, 23 (1989) 760.
[11] S.R. Hutchins, G.W. Sewell, D.A. Kovacs and G.A. Smith, *Environ. Sci. Technol.*, 25 (1991) 68.
[12] T.A. Anderson, E.A. Guthrie and B.T. Walton, *Environ. Sci. Technol.*, 27 (1993) 2630.
[13] D.H. Zitomer and R.E. Speece, *Environ. Sci. Technol.*, 27 (1993) 227.
[14] E.L. Madsen, *Environ. Sci. Technol.*, 25 (1991) 1662.
[15] I.D. Bossert and R. Bartha, *Bull. Environ. Contam. Toxicol.*, 37 (1986) 490.
[16] M.A. Heitkamp and C.E. Cerniglia, *Environ. Toxicol. Chem.*, 6 (1987) 535.
[17] G. Stucki and M. Alexander, *Appl. Environ. Microbiol.*, 53 (1987) 292.
[18] K.S. Park, R.C. Sims, R.R. Dupont, W.J Doucette and J.E. Matthews, *Environ. Toxicol. Chem.*, 9 (1990) 187.
[19] J. Keck, R.C. Sims, M.P. Coover, K.S. Park and B. Symons, *Water Res.*, 23 (1989) 1467.
[20] R.J.F. Bewley and P. Theile, in K. Wolf, W.J. van der Brink and F.J. Colon (Editors), *Contaminated Soil '88*, Kluwer, Hingham, MA, 1988, p. 739.
[21] E. Šepič, H. Leskovšek and C. Trier. in preparation.
[22] J.N. Robson and S.J. Rowland, *Org. Geochem.* 13 (1988) 691.
[23] M. Alexander, *Env. Sci. Technol.*, 18 (1985) 106.
[24] I.B. Beech and C.C. Gaylarde, *J. Appl. Bacteriol.*, 67 (1989) 201.
[25] C.E. Cerniglia, in R.M. Atlas (Editor), *Petroleum Microbiology*, Collier Macmillan Publ., London, 1984, Ch. 3, p. 99.
[26] C.H. Collins and P.M. Lyne, *Microbiological Methods*, Butterworths, London, 5th ed., 1984, Ch. 9, p. 128.
[27] H. Kiyohara, K. Nagao and K. Yana, *Appl. Env. Microbiol.*, 2 (1982) 454.
[28] B. Tržilova and E. Horska, *Biologia (Bratislava)*, 43 (1988) 209.
[29] R.L. Raymond, V.W. Jamison and J.O. Hudson, *Lipids*, 6 (1971) 453.
[30] A. Contreras, S. Molin and J.L. Ramos, *Appl. Environ. Microbiol.*, 57 (1991) 1504.
[31] S.R. Wild and K.C. Jones, *Environ. Toxicol. Chem.*, 12 (1993) 5.
[32] R. Leduc, R. Samson, B. Al-Bashir, J. Al-Hawari and T. Cseh, *Wat. Sci. Tech.*, 26 (1992) 51.

ELSEVIER

Journal of Chromatography A, 697 (1995) 525–532

JOURNAL OF CHROMATOGRAPHY A

Optimization of the gas stripping and cryogenic trapping method for capillary gas chromatographic analysis of traces of volatile halogenated compounds in drinking water

Dj. Djozan*, Y. Assadi

Department of Analytical Chemistry, Faculty of Chemistry, University of Tabriz, Tabriz, Iran

Abstract

A simple laboratory-made gas stripping and cryogenic trapping system coupled to a gas chromatograph with flame ionization detector as a universal detector has been developed for the determination of traces of volatile halogenated compounds (VHCs) in drinking water. The effects of inert gas velocity, stripping time, temperature and salting out on the extraction efficiency and the efficacy of different adsorbents for water vapour elimination were studied. The VHCs were trapped in a stainless-steel coil (50 cm × 1.5 mm I.D.) placed in liquid nitrogen. The trapped compounds were released by thermal desorption and injected in the capillary column. To prevent peak tailing arising from the injection of the sample spread in a large volume of the carrier gas, VHCs were retrapped in the beginning of the capillary column with a cryofocusing system. The chromatographic analyses were run with a suitable temperature program.

The present method allows the determination of 0.1–10 ppb of each VHC. The relative standard deviation of 5–10% ($n = 5$) was obtained at 2 ppb for different VHCs. The detection limits (signal-to-noise ratio 3) were 0.01–0.05 ppb for the studied compounds which are comparable with US Environmental Protection Agency method 502.2.

1. Introduction

Volatile organic compounds (VOCs) such as volatile halogenated compounds (VHCs) are found virtually in all homes and workplaces in our modern technological society. Chlorine reacts with organic matter during water disinfection, produces VHCs and increases our exposure to these compounds [1,2], and numerous studies have confirmed the mutagenic effects of these compounds [3–7]. The combination of ubiquitous exposure and possible serious health effects makes VHCs a public health concern [8]. As a result of the possible risk to health, the World Health Organization has recommended a limit of 30 ppb for chloroform [9] and USA legislation has established a limit of 100 ppb for total VHCs [10].

Gas chromatography is often used for the analysis of these compounds [11–15]. However, due to the very low concentration of VHCs in drinking water, a preextraction and preconcentration step is needed. So far several techniques have been used for this purpose: liquid–liquid extraction [12,16–18], adsorption onto solid phase [15,19], permeability through membranes

* Corresponding author.

0021-9673/95/$09.50
SSDI 0021-9673(94)00980-5

[20,21], head-space [21–23], closed-loop stripping [24], cryofocusing [25] and spray extraction [26,27]. These methods are subjected to the solvent, airborne or solid-phase contaminations, which often gives high background and different interferences [11].

The purge-and-trap technique is free from these problems because it uses a purified inert gas to extract VHCs from water; once introduced to the system it is never in contact with the atmosphere and the relatively high concentrating factor obtained by this method allows analysis of very-low-concentration samples [28,29].

This paper describes a new analytical method for the trace analysis of some VHCs using a simple laboratory-made gas stripping and cryogenic trapping system coupled to gas chromatography (GSCT–GC) with flame ionization detection (FID) as a universal detector.

2. Experimental

2.1. Chemicals and reagents

Helium 99.999% was purchased from Air Products (Middle East), Dubai, U.A.E.; chloroform, carbon tetrachloride, dibromochloromethane, 1,2-dichloroethane, trichloroethylene, tetrachloroethylene, 1,1,2-trichloroethane, 1-chloro-2-bromoethane, dibromomethane, KBr, NaCl, LiCl, $CaCl_2$, Na_2SO_4, $MgSO_4$ and all other reagents were from E. Merck (Germany).

Stock solutions of VHCs were prepared by dissolving 1 mg of each in 5 ml methanol (200 ppm); stock solution of internal standard was prepared by dissolving 1 mg of dibromomethane in 5 ml methanol. Model aqueous solutions at 2 ppb level were prepared by adding 2.5 μl of stock solutions of each VHC into 250 ml doubly distilled and stripped water. $MgSO_4$, $CaCl_2$ and alkali metal salts were activated in 400°C for 60 min and used as dryer for the elimination of water vapour from released VHCs.

2.2. Apparatus

The GC apparatus consisted of a Shimadzu (Japan) GC-15 A, equipped with a FID system, a data processor Model C-R4 A Chromatopac, hydrogen generator Model OPGU-1500 S and split/splitless injector. A Shimadzu Hicap CBP10-S25-050 (OV-1701) capillary column was used.

2.3. Stripping and trapping process

A general view of the laboratory-made GSCT–GC system is shown in Fig. 1. In this system, impurities in the helium gas are eliminated in cryogenic trapping interface (1) kept at −196°C with liquid nitrogen; the pure He is then passed via a stainless-steel filter (2) into the stripping column (100 × 2 cm I.D. glass tube) containing 250 ml of the water sample (3) kept at 80°C; the released VHCs accompanying water vapour are passed through the dryer column packed with activated adsorbents (4), in which the water vapour is retained; dried VHCs are trapped in a cold trapping coil (50 cm × 1.5 mm I.D. stainless-steel tube) kept at −196°C with liquid nitrogen (5). When the stripping process is completed (75 min), the liquid nitrogen is removed and the trapping coil is warmed with hot air, hence the analytes are thermally desorbed and introduced into the GC system (6); to prevent peak tailing arising from the injection of the sample in a large volume, the VHCs are cryofocused in the beginning of the capillary column (the first 50 cm of the column is placed in liquid nitrogen) (7); after 2 min the liquid nitrogen is removed and the GC analysis is started with a suitable temperature program.

2.4. Quantitative analysis

For quantitative analysis by GSCT–GC, the internal standard method was used. This approach is less attentive and offers better precision than other calibration methods [30,31]. To 250 ml model aqueous solution containing 0.1–10 ppb of each VHC are added 2.5 μl of stock

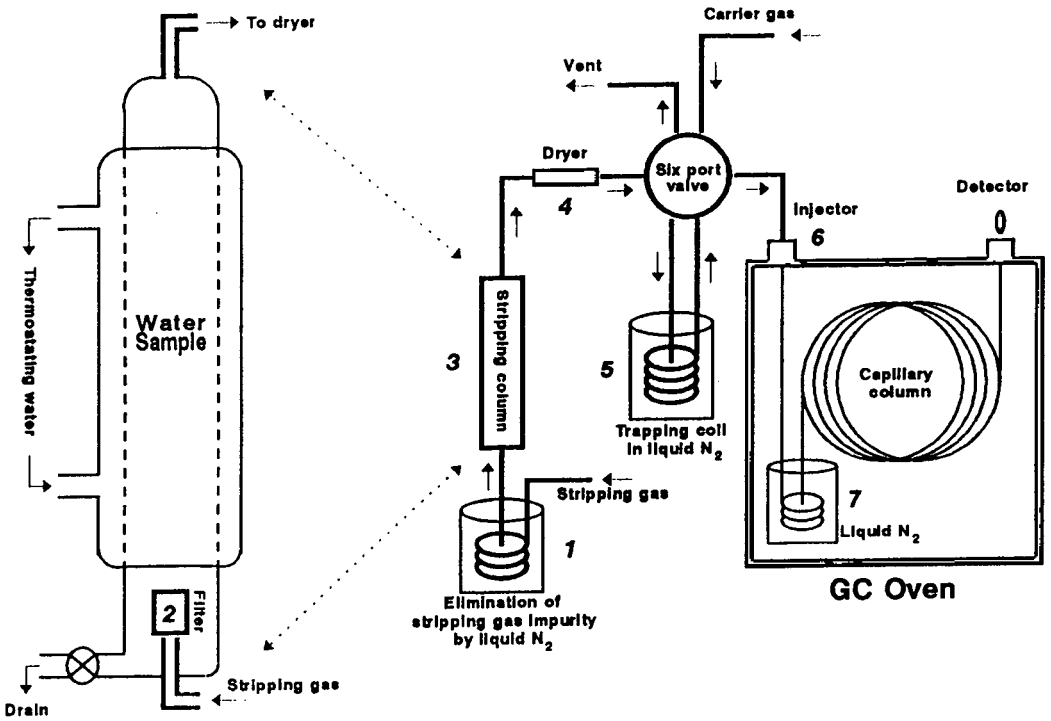

Fig. 1. Schematic diagram of on-line gas stripping and trapping system coupled with GC. See text.

dibromomethane solution rendering an internal standard concentration of 2 ppb.

3. Results and discussion

3.1. Optimization of chromatographic conditions

In order to optimize the chromatographic conditions a 1-μl portion of the VHC mixture was directly injected at a split ratio of 80:1. The best capillary column, suitable oven temperature program, optimum carrier and makeup gas flow-rates and injector temperature were determined on the basis of peak resolutions and reproducibility of the retention times. A typical chromatogram obtained under optimized conditions is shown in Fig. 2. The observed resolution (R_s) for chloroform and carbon tetrachloride was 1 and for other VHCs the R_s value was >1.5. The calculated standard deviation for the retention times of 0.03–0.08 for various VHCs show that under the selected conditions, a good separation and identification of VHCs seem possible.

3.2. Analysis of model aqueous solution

Under the optimized GC conditions, 250 ml of the model aqueous solution were analysed using GSCT–GC. Fig. 3 shows that a good identification of the studied VHCs can be achieved.

3.3. Effect of stripping time on stripping efficiency

The stripping efficiencies of the studied VHCs in model aqueous solutions were determined over the time range 30–105 min, in 15-min intervals. The results obtained are shown in Fig. 4. Since the stripping curve of each compound

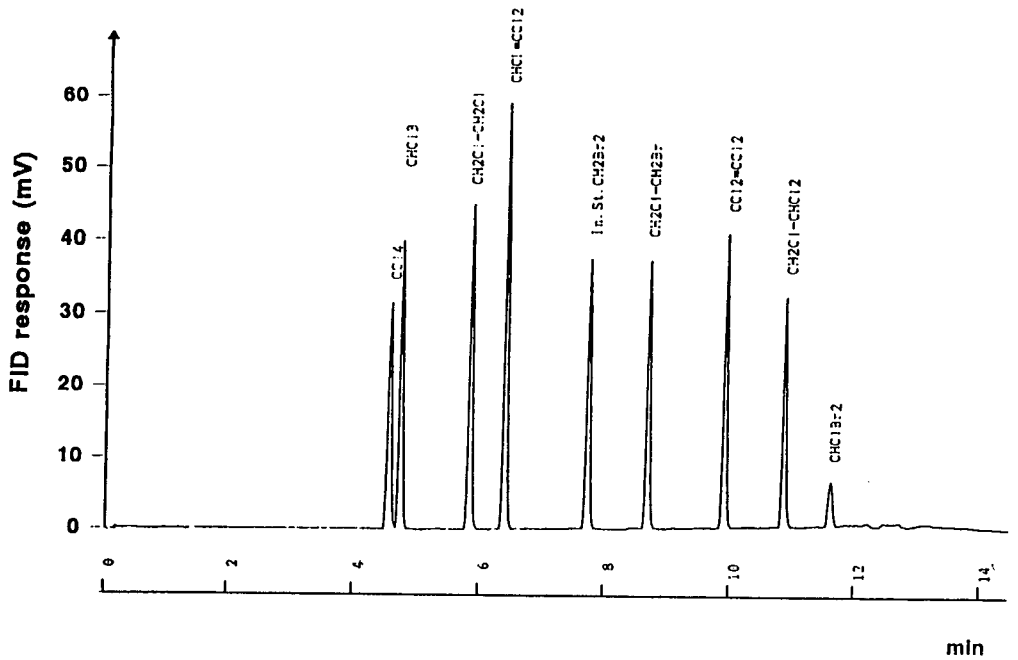

Fig. 2. Typical chromatogram of VHCs. Column CBP-10 (OV-1701), 25 m × 0.33 mm I.D., film thickness 0.5 μm; carrier gas velocity 25 cm/s; split ratio 80:1; injection volume 1 μl; injector temperature 150°C; oven temperature program 30°C with a 5-min hold rising at 7°C/min to 120°C, and hold 5 min; makeup gas 25 ml/min; FID temperature 150°C.

reaches a quasi plateau over 75 min, we can accept 75 min stripping as optimum stripping time.

3.4. Effect of stripping temperature on stripping efficiency

For this study, the stripping was carried out for the same model aqueous solution at 75 min and various temperatures (20–80°C). Representative plots of the peak areas against temperature for each VHC are shown in Fig. 5. It can be seen that the stripping efficiencies of all studied compounds increase with temperature. However, due to the inconvenient interference of water molecules in the cold trap device, increasing the temperature over 80°C is not practically suitable. Therefore we took the stripping temperature of 80°C as the optimum.

3.5. Effect of salting out on stripping efficiency

For this investigation we have studied the effect of various amount of Na_2SO_4 on the stripping efficiency of VHCs. Fig. 6 plots the peak area versus Na_2SO_4 quantities in water. We observe that the addition of 30–40 g Na_2SO_4 in 250 ml model aqueous solution increases the stripping efficiency of VHCs two-fold.

3.6. Study of the drying device efficiency

Since the stripping temperature is relatively high, some quantity of the water vapour is transferred along with VHCs which freezes in the cold trap coil and clogs this device. For this reason the elimination of water before entering the cold trapping device is necessary. Therefore we have investigated the usefulness of various inorganic salts such as NaCl, LiCl, KBr, $CaCl_2$,

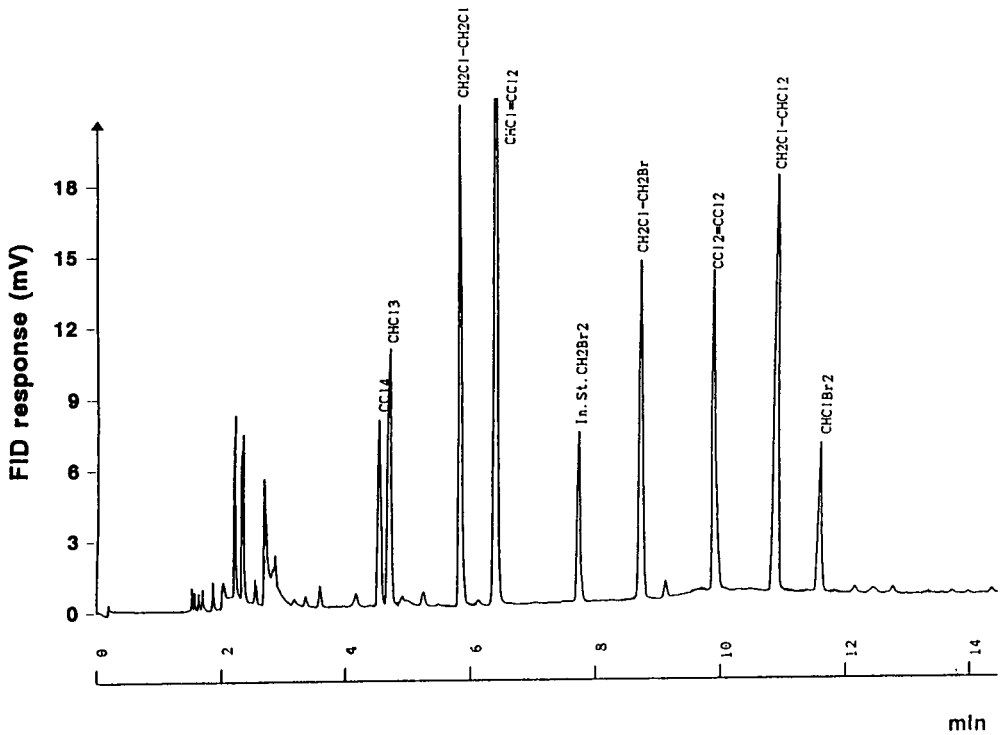

Fig. 3. Typical chromatogram of model aqueous solution. Chromatographic conditions as in Fig. 2; sample volume 250 ml containing 2 ppb of each VHC in which 30 g Na_2SO_4 was dissolved; stripping time 75 min; stripping temperature 80°C.

Na_2SO_4 and $MgSO_4$ as dryers. The investigations show that KBr and Na_2SO_4 have not much affinity towards water molecules. The others are very effective for water elimination, but they can also adsorb VHCs. Table 1 shows the adsorption strength of water and VHCs using various dryers. The results obtained from this study, reveal that activated NaCl and $CaCl_2$ have a

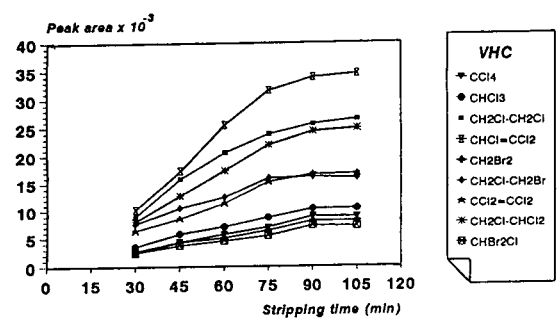

Fig. 4. Effect of time in stripping efficiency. Conditions as in Fig. 3. Dryer $CaCl_2$.

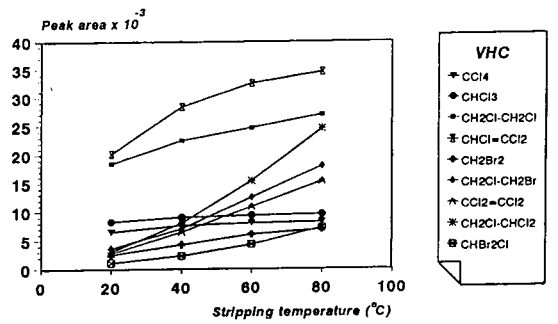

Fig. 5. Effect of temperature in stripping efficiency. Conditions as in Fig. 3. Dryer $CaCl_2$.

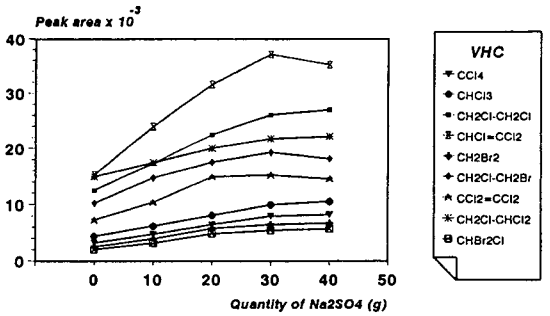

Fig. 6. Effect of salting out in stripping efficiency. Conditions as in Fig. 3. Dryer $CaCl_2$.

Table 1
Adsorption strength of water and VHCs onto various adsorbents

Dryer	Water adsorption strength	VHC adsorption strength
LiCl	VL	VL
KBr	VS	S
NaCl	M	VS
$CaCl_2$	L	S
$MgSO_4$	L	L
Na_2SO_4	M	M

VL = Very large; VS = very small; L = large; M = medium; S = small.

relatively good affinity for water and adsorb very little and negligible quantities of the VHCs; therefore they are suitable dryers in these experiments.

3.7. Recovery study

Five replicates of 2-μl portions of diluted standard solution in *n*-pentane containing 500 ng of each VHC were analysed by direct splitless injection (split valve opened at 1 min) and five replicates of 250-ml portions of model aqueous solution containing the same quantities of VHCs were analysed by GSCT–GC. With comparing the peak areas of each VHC in two sets of experiments, recoveries of 75–86% were obtained (Table 2).

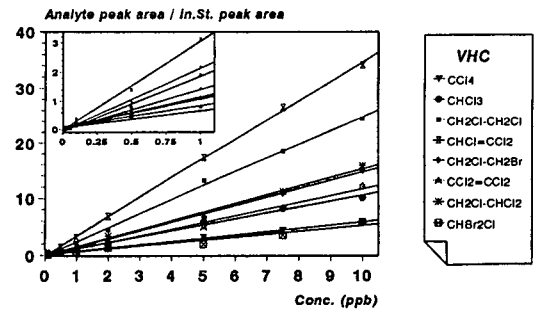

Fig. 7. Calibration graphs of VHCs. Internal standard (CH_2Br_2) 2 ppb. Conditions as in Fig. 3. Dryer $CaCl_2$.

Table 2
Recoveries of tested compounds with GSCT–GC method

Formula	Peak area, mean ± S.D. ($n = 5$)[a]	Peak area, mean ± S.D. ($n = 5$)[b]	Recovery (%), mean ± S.D.
CCl_4	10 400 ± 150	8 600 ± 450	83 ± 4.6
$CHCl_3$	13 100 ± 210	10 200 ± 720	78 ± 5.6
$CH_2Cl–CH_2Cl$	31 700 ± 410	26 000 ± 1300	82 ± 4.2
$CHCl=CCl_2$	40 700 ± 670	35 000 ± 1700	86 ± 4.4
CH_2Br_2	8 800 ± 170	7 100 ± 460	80 ± 5.4
$CH_2Cl–CH_2Br$	22 700 ± 430	17 000 ± 1000	75 ± 4.6
$CCl_2=CCl_2$	19 000 ± 250	15 000 ± 1300	79 ± 6.9
$CH_2Cl–CHCl_2$	29 300 ± 480	24 000 ± 1800	82 ± 6.3
$CHClBr_2$	9 200 ± 220	6 900 ± 690	75 ± 7.7

[a] The peak area of VHCs from direct injection of 2 μl standard solution in *n*-pentane with 500 ng of each compound.
[b] The peak area of VHCs after extraction from 250 ml standard water with 2 ppb of each compound.

Table 3
Characteristic parameters of the calibration graphs and analytical features of the determination of VHCs

Formula	Retention time (min)	LOD (ppb)[a]	D.r. (ppb)[b]	Regression equation[c]	r^2[d]	R.S.D. (%) ($n = 5$)
CCl_4	4.60 ± 0.06	0.04	0.1–10	$y = 0.077 + 0.58x$	0.999	5.3
$CHCl_3$	4.75 ± 0.06	0.04	0.1–10	$y = 0.110 + 1.04x$	0.997	7.1
$CH_2Cl–CH_2Cl$	5.90 ± 0.08	0.02	0.1–10	$y = -0.141 + 2.48x$	0.999	5.0
$CHCl=CCl_2$	6.44 ± 0.07	0.01	0.1–10	$y = -0.143 + 3.47x$	0.999	4.9
$CH_2Cl–CH_2Br$	8.71 ± 0.05	0.04	0.1–10	$y = -0.120 + 1.47x$	0.999	5.9
$CCl_2=CCl_2$	9.94 ± 0.04	0.04	0.1–10	$y = -0.113 + 1.17x$	0.996	8.5
$CH_2Cl–CHCl_2$	10.86 ± 0.03	0.03	0.1–10	$y = 0.010 + 1.51x$	0.995	7.6
$CHBr_2Cl$	11.65 ± 0.04	0.05	0.1–10	$y = 0.085 + 0.52x$	0.973	10

[a] Limit of detection ($S/N = 3$).
[b] Dynamic range; internal standard = CH_2Br_2 (2 ppb).
[c] y = Analyte peak area/internal standard peak area; x = analyte concentration (ppb).
[d] Correlation coefficient.

Table 4
Comparison of LOD in GSCT–GC with LOD in EPA method 502.2

Formula	EPA 502.2 (ppt)	GSCT–GC (ppt)
CCl_4	20	40
$CHCl_3$	10	40
$CH_2Cl–CH_2Cl$	ND	20
$CHCl=CCl_2$	60	10
$CH_2Cl–CH_2Br$	ND	40
$CCl_2=CCl_2$	20	40
$CH_2Cl–CHCl_2$	40	30
$CHBr_2Cl$	ND	50

ND = Not detected.

3.8. Quantitative analysis

The calibration graphs of the studied VHCs representing the ratios of analyte peak area to internal standard peak area versus concentration in ppb are shown in Fig. 7. Some statistical data for these curves and five replicate analyses are illustrated in Table 3. From the results obtained the quantitative analysis of the VHCs can be carried out with a good precision and accuracy. Data in Table 4 illustrate the LOD of this method and US Environmental Protection Agency (EPA) method 502.2 [32]. The results show that the proposed method using FID is comparable to the EPA method. Table 5 shows

Table 5
Measured VHCs in Tabriz drinking water

Formula	Drinking water, mean ± S.D. (ppb, $n = 5$)	Added (ppb)	Found, mean ± S.D. (ppb, $n = 5$)
CCl_4	0.51 ± 0.03	1.0	1.45 ± 0.11
$CHCl_3$	3.90 ± 0.20	1.0	4.72 ± 0.28
$CH_2Cl–CH_2Cl$	< 0.05	1.0	1.03 ± 0.05
$CHCl=CCl_2$	0.29 ± 0.02	1.0	1.21 ± 0.08
$CH_2Cl–CH_2Br$	0.30 ± 0.02	1.0	1.32 ± 0.09
$CCl_2=CCl_2$	0.49 ± 0.04	1.0	1.40 ± 0.13
$CH_2Cl–CHCl_2$	< 0.1	1.0	0.96 ± 0.07
$CHBr_2Cl$	0.70 ± 0.07	1.0	1.85 ± 0.17

the measured quantity of some VHCs in Tabriz drinking water.

4. Conclusions

The results show that the GSCT method is very convenient for sensitive analysis of trace amounts of dissolved VHCs in water. The concentration factor is very high and the method is free from airborne, solvent and solid-phase contaminations. Minute amounts of contaminants of the stripping gas (helium) can also be eliminated completely.

Acknowledgement

We thank the Research Office of Tabriz University for funding.

References

[1] A.V. Nero, Jr., *Sci. Am.*, 258 (1988) 42–48.
[2] R. Olson, E.E. Doyle, D.T. Williams and P.D. Bothwell, *Bull. Eviron. Contam. Toxicol.*, 31 (1983) 222–229.
[3] J.J. Rook, *Water Treat. Exam.*, 23 (1974) 234.
[4] J. Symons, T.A. Bellar, J.K. Carswell, J. DiMarco, K.L. Kropp, G.G. Robek, D.R. Seeger, C.J. Slocum, B.L. Smith and A.A. Stevens, *J. Am. Water Works Assoc.*, 67 (1975) 634.
[5] J.W. Hayden, E.G. Comstock and B.S. Comstock, *Clin. Toxicol.*, 9 (1976) 169–184.
[6] J.D. Ramsey and R.J. Flanagan, *J. Chromatogr.*, 240 (1982) 423–444.
[7] T.A. Bellar and J.J. Lichtenberg, *J. Am Water Works Assoc.*, 66 (1974) 739.
[8] D.L. Ashley, M.A. Bonin, F.L. Cardinali, J.M. McCraw, J.S. Holler, L.L. Needham and D.G. Patterson, Jr., *Anal. Chem.*, 64 (1992) 1021–1029.
[9] *Guidelines for Drinking Water Quality, Recommendations*, Vol. 1, World Health Organization, Geneva, 1984, p. 77.
[10] *National Interim Primary Drinking Water Regulations; Control of Trihalomethanes in Drinking Water; Fed. Reg.*, 44, No. 231 (Nov. 1979) 68624.
[11] L. Lepine and J.F. Archambault, *Anal. Chem.*, 64 (1992) 810–814.
[12] C. Garcia, P.G. Tiedra, A. Ruano, J.A. Gomez and R.J. Garcia Villanova, *J. Chromatogr.*, 605 (1992) 251–255.
[13] K. Abrahamsson and A. Ekdahl, *J. Chromatogr.*, 643 (1993) 239–248.
[14] W. Janicki, L. Wolska, W. Wardencki and J. Namiesnik, *J. Chromatogr. A*, 654 (1993) 279–285.
[15] S. Mitra and C. Yun, *J. Chromatogr.*, 648 (1993) 415–421.
[16] K. Abrahamsson and S. Klick, *J. Chromatogr.*, 513 (1990) 39.
[17] R. Otson and D.T. Williams, *J. Chromatogr.*, 212 (1981) 187–197.
[18] G. Castello, T. Gerbino and S. Kanitz, *J. Chromatogr.*, 351 (1986) 165–175.
[19] A.L. Sunesson, C.A. Nilsson, B. Andersson and R. Carlson, *J. Chromatogr.*, 623 (1992) 93–103.
[20] R.D. Blanchard and J.K. Hardy, *Anal. Chem.*, 58 (1986) 1529.
[21] D. Gryder-Boutet and J. Kennish, *J. Am. Water Works Assoc.*, 80 (1988) 52.
[22] B. Colb, M. Auer and P. Pospisil, *J. Chromatogr.*, 279 (1983) 341–348.
[23] M.E. Comba and K.L.E. Kaiser, *Int. J. Environ. Anal. Chem.*, 16 (1983) 17–31.
[24] J.E. Smith, W.R. Hewitt and J.B. Book, *Toxicol. Appl. Pharmacol.*, 79 (1985) 166.
[25] T. Kohno and K. Kuwata, *J. Chromatogr.*, 587 (1991) 338–342.
[26] G. Baykut and A. Voigt, *Anal. Chem.*, 64 (1992) 677–681.
[27] G. Matz and P. Kesners, *Anal. Chem.*, 65 (1993) 2366–2371.
[28] M. Mehran, M. Nickelsen, N. Golkar and W.Cooper, *J. High Resolut. Chromatogr.*, 13 (1990) 429.
[29] H.C. Hu and P.H. Weiner, *J. Chromatogr. Sci.*, 18 (1980) 333–342.
[30] B. Colby, P. Ryan and J. Wilkinson, *J. High Resolut. Chromatogr. Chromatogr. Commun.*, 6 (1983) 72–76.
[31] P. Olynyk, W. Budde and J. Eichelberger, *J. Chromatogr. Sci.*, 19 (1981) 377–382.
[32] J.S. Ho, *US EPA Method 502.2, Revision 2.0*, Environmental Monitoring System Laboratory, Office of Research and Development, US Environmental Protection Agency, Cincinnati, OH, 1989.

ELSEVIER

Journal of Chromatography A, 697 (1995) 533–540

JOURNAL OF CHROMATOGRAPHY A

Chromatographic separation of continuous mixtures in distributed pores

Benjamin J. McCoy

Department of Chemical Engineering and Materials Science, University of California, Davis, CA 95616, USA

Abstract

Complex multi-component mixtures are conveniently modeled with frequency distribution functions that are continuous functions of a molecular property, e.g., molecular radius. Size-exclusion chromatographic separations can be simulated by accounting for the partitioning of the species in the pores of the stationary phase. The mathematical theory in this paper describes the separation of solutes based on relative sizes of pores and molecules. Linear partition coefficients are represented for continuous distributions of molecular sizes in either continuous or discrete distributions of cylindrical pores. Fractal distributions of pores also illustrate the partitioning behavior. The mass balance equation that governs the frequency distribution of the spherical molecules can be solved exactly when axial dispersion is the only rate process. This equilibrium-dispersive model yields temporal moment expressions that are also useful for interpreting chromatographic data.

1. Introduction

Size-exclusion chromatography (SEC) allows the separation into size fractions of a mixture of different-sized solutes by their partitioning into pores of different radii [1,2]. This defining statement suggests that a complete analysis of SEC requires consideration of the distributions of both solutes and pores. Both discrete and continuous distributions may be contemplated, but many realistic systems will have essentially continuous distributions of both pores and solutes.

Continuous-mixture theories [3,4] of complex multi-component systems are based on the concept of the concentration frequency distribution function (FDF), $C(x)$, which is defined so that the concentration in the property range $(x, x + dx)$ is $C(x)\,dx$. When integrated over the entire range of the property x, the FDF becomes the lumped concentration, c. This approach explains chromatographic separations based on molecular properties of mobile complex mixtures that interact with an immobile phase [5,6]. Goto et al. [7] applied the concept to multi-component leaching or extraction from porous particles in a continuous-flow system. Desorption from the solid matrix and partitioning between the extraction fluid and an immiscible fluid in the pores of the matrix were included.

The earlier works laid a foundation for understanding and extending the approach, but much remains to be done to explore fully the possibilities of this theory. The models for single-sized pores have not yet been extended to the more realistic case of distributed pores. Hence it is the objective of this paper to examine in greater detail the nature of the partitioning of molecules in porous chromatographic media. Specifically, we consider here the effect of a distribution of cylindrical pore sizes on the separation of a

0021-9673/95/$09.50
SSDI 0021-9673(94)01087-0

mixture of distributed spherical molecules. Fractal pore-size distributions illustrate the behavior of the partitioning coefficient for discrete distributions. The combined influences of the single-particle partition coefficient for spheres in cylinders, the distribution of pore sizes and the distribution of spherical molecule sizes yield results of mathematical and practical interest.

2. Chromatographic theory

Assuming that the concentration frequency distribution is $C(x, z, t)$, we can write the total, or lumped, concentration, $c(z, t)$, as the integral over x;

$$c(z, t) = \int_0^\infty C(x, z, t)\, dx \tag{1}$$

The mechanism for size-exclusion separation in chromatography is partitioning of the solutes in pores of the immobile phase. The frequency distribution of the partitioned species can be defined such that the concentration in the interval $(x, x + dx)$ is $Q(x)\, dx$. The lumped partitioned concentration, which is a function of position and time, is the integral

$$q(z, t) = \int_0^\infty Q(x, z, t)\, dx \tag{2}$$

In the present treatment we consider only linear relationships between Q and C, i.e.,

$$Q(x) = K(x)C(x) \tag{3}$$

where for chromatography Q and C will also depend on position z and time t, but $K(x)$ is considered uniform and constant (independent of z and t).

2.1. Equilibrium-dispersive model

In the absence of chemical reactions, the molecular properties of the different chemical species are unchanged. Then the mass balance equations that apply for the concentration also govern the frequency distributions, $C(x, z, t)$ and $Q(x, z, t)$:

$$\varepsilon\, \partial C/\partial t + (1 - \varepsilon)\, \partial Q/\partial t + v\, \partial C/\partial z = D\, \partial^2 C/\partial z^2 \tag{4}$$

in terms of the superficial velocity v, the void fraction ε and the axial dispersion coefficient D. The axial dispersion coefficient, which can be assumed to incorporate other mass transfer resistances, is considered constant.

For an impulse input to the chromatographic column the initial and boundary conditions are

$$C(x, z, t = 0) = 0 \tag{5}$$

$$C(x, z = \infty, t) = 0 \tag{6}$$

$$C(x, z = 0, t) = C_0(x)\, \delta(t)\tau \tag{7}$$

where $\tau = z/v$.

2.2. Exact solution

When the linear adsorption isotherm is Eq. (3), the chromatographic equation can be written as

$$A(x)\, \partial C/\partial t + v\, \partial C/\partial z = D\, \partial^2 C/\partial z^2 \tag{8}$$

where

$$A(x) = \varepsilon + (1 - \varepsilon)K(x) \tag{9}$$

The solution [8,9] that satisfies the initial and boundary conditions is

$$C(x, z, t) = [C_0/(4\pi Dt/Az^2)^{1/2}] \exp[-(1 - vt/Az)^2/(4Dt/Az^2)] \tag{10}$$

which is valid for $t \geq 0$ and $z \geq 0$. The asymptotic solution for $D/vz \to 0$ is

$$C(x, z, t) = [C_0/(4\pi D/vz)^{1/2}] \exp[-(1 - vt/Az)^2/(4D/vz)] \tag{11}$$

which is Gaussian in t.

2.3. Moment solution

When other mass transfer or adsorption rate processes are incorporated into the chromatographic model, an exact solution is usually not feasible. In such cases one can apply moment methods, which provide moment expressions that allow the interpretation of experimental

observations of chromatographic output. Moreover, the moments can be used to construct an approximate solution to the chromatographic equation. We next solve the partial differential Eq. 11 by applying the temporal moment method, which entails computing limits of the derivatives of Laplace transform solutions. The expressions for the moments are readily derived from

$$M_n(x, z) = \lim_{s\to 0} (-1)^n \, \mathrm{d}^n C/\mathrm{d}s^n \tag{12}$$

where $C(x, z, s)$ is the Laplace transform of $C(x, z, t)$. The zero, first and second temporal moments [5] of the frequency distributions, when we use the isotherm Eq. 3, are

$$M_0(x, z) = M_0(x, z = 0) = M_0(x) = C_0(x)A(x)z/v \tag{13}$$

$$M_1(x, z) = M_0(x)A(x)z/v \tag{14}$$

$$M_2(x, z) = M_0(x)[A(x)z/v]^2(1 + D/2v) \tag{15}$$

These moment expressions determine the pulse response for any value of the property x.

The temporal moments of the lumped concentration, $c(z, t)$, according to Eq. 1, are the integrals over x:

$$m_n(z) = \int_0^\infty M_n(x, z)\, \mathrm{d}x \tag{16}$$

where n is the order of the moment, i.e., 0, 1 or 2. The reduced first moment is defined as

$$\mu_1' = m_1/m_0 \tag{17}$$

and the variance as

$$\mu_2 = m_2/m_0 - (\mu_1')^2 \tag{18}$$

The results for the lumped moments are as follows [5]:

$$\mu_1' = \langle A\rangle z/v \tag{19}$$

$$\mu_2 = 2Dz\langle A^2\rangle/v^3 + (z/v)^2[\langle A^2\rangle - \langle A\rangle^2] \tag{20}$$

where

$$\langle A^n\rangle = \int_0^\infty A(x)^n C_0(x)\, \mathrm{d}x \Big/ \int_0^\infty C_0(x)\, \mathrm{d}x \tag{21}$$

is the average over x of the nth power of $A(x)$. If the parameter $K(x)$ has only one value, namely $K_0\,\delta(x - x_0)$, then $\langle A^n\rangle = \langle A\rangle^n$ and the usual moments for a single component system are recovered. However, since in general $\langle A^2\rangle - \langle A\rangle^2 = \langle (A - \langle A\rangle)^2\rangle$, the variance of the lumped concentration of the continuous mixture is greater than the variance of the single-component system. Thus the lumped HETP, defined as $z\mu_2/(\mu_1')^2$, would be greater than that for a single-component system. Expressions for the third moment indicating asymmetry were also discussed by McCoy [5].

To portray the time dependence of the frequency distributions at any position z, one can represent $C(x, z, t)$ as a Gaussian function [10,11]:

$$C(x, z, t) = [M_0/(2\pi\sigma^2)^{1/2}] \times \exp[-(t - M_1/M_0)^2/(2\sigma^2)] \tag{22}$$

where

$$\sigma^2 = M_2/M_0 - (M_1/M_0)^2 \tag{23}$$

is the variance of the frequency distribution. By substituting the moment expressions, Eqs. 13–15, one can show that the moment solution is equivalent to the asymptotic solution, Eq. 11. For relatively long columns, high velocities or small dispersion, the approximate solution is satisfactory.

The HETP for each value of x can be defined as

$$H(x) = z\sigma^2/(M_1/M_0)^2 \tag{24}$$

which yields on substitution of Eqs. 13–15 and 23

$$H(x) = 2D/v \tag{25}$$

The HETP for a continuous mixture that obeys the model of Eq. 8 is thus independent of x unless dispersion and mass transfer provide for $D(x)$.

The chromatographic behavior of a continuous mixture was illustrated for examples of the partition coefficient, $K(x)$, and the feed distribution, $C_0(x)$, in Ref. [6]. The input to the chromatographic column was assumed to be Gaussian:

$$C_0(x) = G \exp[-(x - 2)^2] \tag{26}$$

The partition coefficient, for $x \leq r$, was taken as

$$K(x) = (1 - x/r)^2 \tag{27}$$

thus smaller molecules are more strongly retained than larger molecules. The consequent behavior is reflected in the concentration contours plotted on t versus x, where the contours slope downward to the right [6]. For the linear adsorption isotherm, larger molecules are retained longer in the column, and the contours slope upward.

3. Partitioning in distributed pores

The single-pore partition coefficient accounts for exclusion of the spherical solute from an annular region of the cylindrical pore, or from the pore itself if the sphere is larger than the pore,

$$\Phi(x, r_j) = (1 - x/r_j)^2 \qquad \text{for } x < r_j$$
$$\Phi(x, r_j) = 0 \qquad \text{for } x \geq r_j \tag{28}$$

Consider the case when the pores are not simply of one size, but are distributed in radius according to a given continuous or discrete function. Denote the normalized frequency distributions by n_j and $n(r)$ for discrete and continuous cases, respectively:

$$1 = \sum_j n_j \qquad \text{and} \qquad 1 = \int n(r)\, dr \tag{29}$$

For the discrete distribution the actual partitioned concentration, $Q(x)$, is the sum over all size pores, and we obtain Eq. (3), $Q(x) = K(x)C(x)$, where

$$K(x) = \sum_j n_j \Phi(x, r_j) \tag{30}$$

is the distributed-pore partition coefficient. For the continuous distribution, we have the integral expression for $K(x)$:

$$K(x) = \int n(r)\Phi(x, r)\, dr \tag{31}$$

Thus, when local equilibrium applies for all z and t, we can always write the distribution coefficient as $K(x)$. The discontinuous nature of $\Phi(x, r)$ calls for special attention in the summation or integration to obtain $K(x)$. The dependence of K on x is required to connect the limiting values $K(x = 0) = 1$ (vanishingly small solutes are totally partitioned in the pores), and $K(x \geq r_{max}) = 0$ (solutes larger than the largest pore are totally excluded from the pores).

To illustrate the behavior of a continuous pore-size distribution, we first consider a distribution of single-size pores, $n(r) = \delta(r - r_0)$. When integrated according to Eq. 31 one obtains

$$K(x) = \Phi(x, r_0) \tag{32}$$

which is pictured in Fig. 1 for $r_0 = 1$, 0.5 and 0.1. The maximum value of r is r_0, and as r_0 becomes vanishingly small, $K(x)$ goes to zero since all solutes are excluded from infinitesimally small pores.

Next, consider the normalized rectangular distribution

$$n(r) = 1/(r_2 - r_1) \tag{33a}$$

for $r_1 \leq r \leq r_2$ and

$$n(r) = 0 \tag{33b}$$

otherwise. The partition coefficient $K(x)$ has the three different values depending on the value of x:

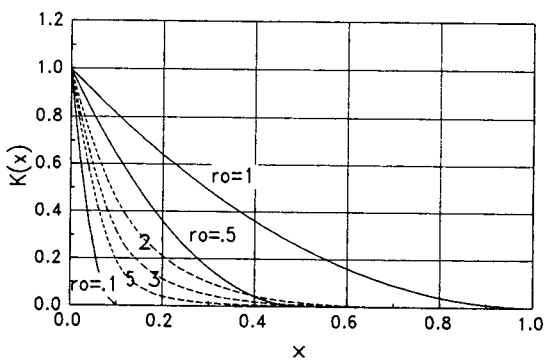

Fig. 1. The distributed-pore partition coefficient, $K(x)$, plotted versus the solute radius, x, for a distribution of single-size pores, $n(r) = \delta(r - r_0)$, with $r_0 = 1$, 0.5, 0.1 (solid lines), and for fractal media with cylindrical pores ($\Omega = \pi$, $\sigma = 1.5$, $a = 1$) and $h = 2$, 3 and 5 (dashed lines).

$$\text{if } x > r_2, \quad \text{then } K(x) = 0$$

$$\text{if } x < r_1, \quad \text{then } K(x) = 1 + 2x \ln(r_1/r_2)/(r_2 - r_1) + x^2/r_1 r_2$$

$$\text{if } r_1 \leq x \leq r_2, \quad \text{then } K(x) = 2x \ln(x/r_2)/(r_2 - r_1) + (r_2^2 - x^2)/r_2(r_2 - r_1) \tag{34}$$

$K(x)$ is plotted in Fig. 2, where $r_2 = 1.0$ and $r_1 = 0.5$, and the values at $K(x = r_1)$ match smoothly as required.

A continuous power-law distribution of pore sizes is defined by

$$n(r) = (b + 1)r^b \tag{35}$$

Integrating $n(r)\Phi(x, r)$ over r between x and 1 (i.e., $x \leq r \leq 1$) yields

$$K(x) = 1 - x^{b+1} - 2x(b + 1)(1 - x^b)/b + x^2(1 - x^{b-1})(b + 1)/(b - 1) \tag{36}$$

which is plotted in Fig. 2 for several values of b. As b increases, $K(x)$ approaches $(1 - x)^2$. These pore-size distributions demonstrate cut-off behavior for solutes larger than r_{max}.

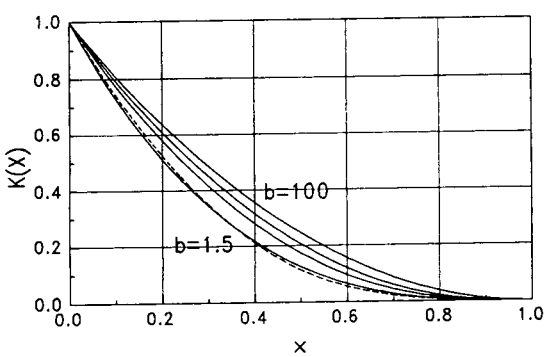

Fig. 2. The distributed-pore partition coefficient, $K(x)$, plotted versus the solute radius, x, for a rectangular distribution of pores (Eq. 33) with $r_1 = 0.5$ and $r_2 = 1.0$ (dashed line), and for a power-law distribution (Eq. 35) with $b = 1.5$, 5 10 and 100 (solid lines).

4. Fractal pore-size distributions

Discrete pore-size distributions can sometimes be represented by a fractal power relationship [12]. A model of a porous membrane with a deterministic fractal distribution of pores can be developed by a conceptual process of making non-intersecting holes of equal length in the immobile phase. Adler [13], in a study of flow in a porous medium, suggested that such fractals could be applied to diffusion and conduction (thermal or electrical), but did not introduce mixtures of different-sized molecules. The benefit of the fractal approach is that simple mathematical equations describe the fractal properties.

We first consider a pore distribution based on the fractal known as the Sierpinski carpet [14], and then generalize the concept to consider holes of different numbers, shapes and sizes. Fig. 3 shows the steps $j = 1, 2, 3$ in the construction of a periodic porous medium from a unit square of area a^2. At step 1 a square hole of edge $a/3$ is formed, and in each of the remaining eight squares a hole of size $(a/3^2)^2$ is formed. This process is repeated indefinitely for every square. The edge length of a square at step j is $r_j = a/3^j$ and its cross-section has area $a^2/9^j$. The number and volume of pores of length L formed at the jth step are

$$n_j = 8^{j-1} \quad \text{and} \quad V_j = L(8/9)^j a^2/8 \tag{37}$$

respectively. The cumulative pore-volume distribution up to the jth step can be shown to be $La^2[1 - (8/9)^j]$, which becomes La^2 if $j \to \infty$, meaning that the volume La^2 is eventually removed by making square holes in the membrane. The discrete pore-volume distribution as the fractal property that it can be represented by a non-integer power, or fractal dimension, D:

$$V_j/La^2 = B^D(r_j/a)^{2-D} \tag{38}$$

where

$$D = \ln 8/\ln 3 \text{ and } B = 8^{-1/D} \tag{39}$$

The fractal pore distribution can be generalized by considering pores of cross-sectional area Ωr_j^2 where $\Omega = 1$ for squares, π for circles or

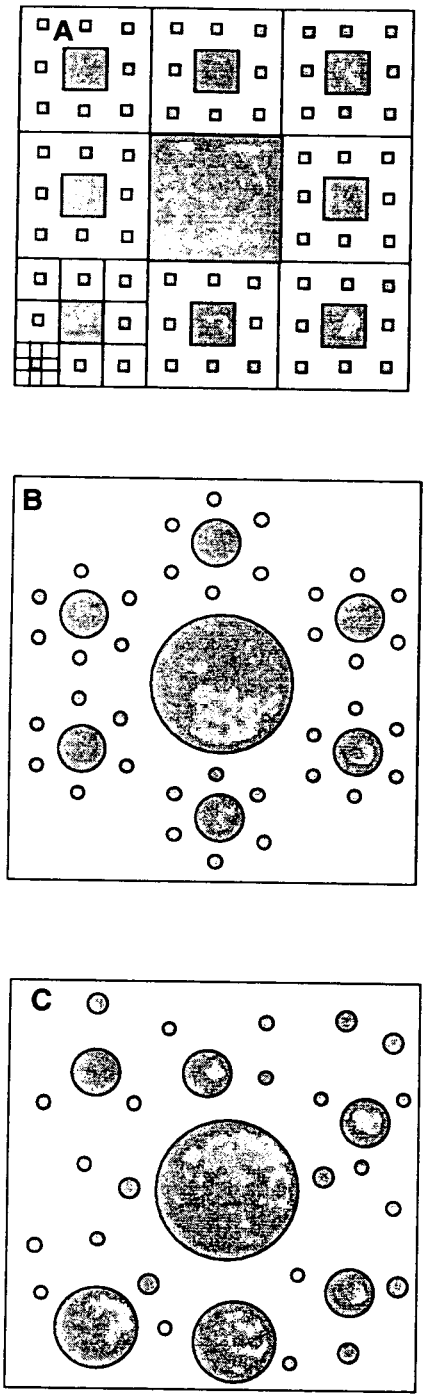

Fig. 3. Steps in the construction of fractal pores in a spatially periodic medium: (A) Sierpinski medium, i.e., $\Omega = 1$, $\sigma = 3$, $h = 8$, $j = 1$–3; (B) $\Omega = \pi$, $\sigma = 3$, $h = 6$, $j = 1$–3; (C) $\Omega = \pi$, $\sigma = 1.5$, $h = 2$, $j = 1$–5.

other constants for other cross-section shapes. Even though the pores are positioned randomly over the solid, the underlying fractal order of pore size applies. The relative size (e.g., radius) of the pores formed at two subsequent steps is defined as the constant σ:

$$\sigma = (\text{size of pore formed at step } j)/(\text{size of pore formed at step } j+1) \quad (40)$$

The relative number of pores formed at subsequent steps is also a constant:

$$h = (\text{number of pores formed at step } j+1)/(\text{number of pores formed at step } j) \quad (41)$$

A similar generalization of the Sierpinski carpet was suggested by Pfeifer and Obert [15]. The size of pores removed at step j is $r_j = a/\sigma^j$, and the volume of a pore is $L\Omega(a/\sigma^j)^2$. The volume removed at the jth step is $L(\Omega a^2/h)(h/\sigma^2)^j$, and the cumulative volume removed is $[L\Omega a^2/(\sigma^2 - h)][1 - (h/\sigma^2)^j]$. When the cumulative volume of pores at the jth step is La^2, the structure possesses fractal properties in a finite range of pore sizes. The fractal dimension D and the premultiplier B in the equation

$$V_j/La^2 = B^D(r_j/a)^{2-D} \quad (42)$$

can be shown to be

$$D = \ln h/\ln \sigma \quad \text{and} \quad B = (\Omega/h)^{1/D} \quad (43)$$

For the Sierpinski pores $\Omega = 1$, $\sigma = 3$ and $h = 8$, and the expressions reduce appropriately to Eqs. 39. If $h = \sigma^2$ then the distribution is rectangular and discrete.

Examples of fractal constructions are pictured in Fig. 3. The Sierpinski carpet (A) shows the first three steps in making the square holes of size ratio $\sigma = 3$ and number ratio $h = 8$. A medium with circular cross-section pores is shown (B) with $\sigma = 3$ and $h = 6$. The random positioning of the pores (C) with $\sigma = 1.5$ and $h = 2$ does not affect the separation process.

Fig. 4 shows the pore volume distribution versus r/a for various values of the parameters. The fractal media display pore-volume distributions that may either increase or decrease with pore size. One may utilize such power-law dis-

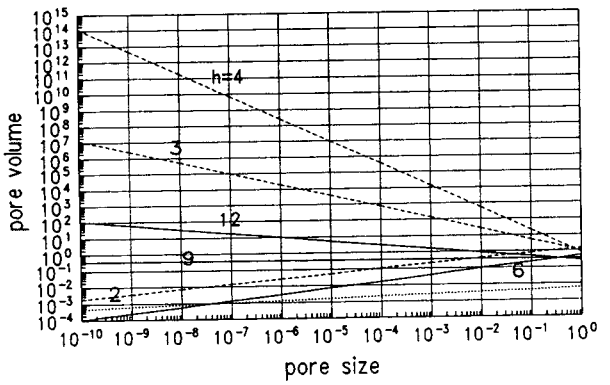

Fig. 4. Log–log plot of the pore-volume distribution: reduced volume, V_j/La^2, versus pore size, r_j/a, for fractal media with cylindrical pores ($\Omega = \pi$), $\sigma = 1.5$ (dashed lines) and $\sigma = 3$ (solid line), and several values of h. The dotted line is the Sierpinski medium ($\Omega = 1$, $\sigma = 3$, $h = 8$).

tributions as continuous distributions. For the discrete distribution, values of r_j are spaced evenly on the logarithmic axis by the amount $\log \sigma$. The line for the square-pore Sierpinski medium would be parallel to the cylindrical-pore case for $\sigma = 3$ and $h = 8$ (not plotted). For a given value of σ, lines for different h intersect at $r = 1/\sigma$.

Table 1 shows values of r_j and $n(r_j)$ for several values of h. If the smallest value of x is 0.1, then $j = 5$ is the smallest pore that will partition the solute. The partition coefficients for these discrete fractal distributions are plotted in Fig. 1. As the largest pore is $r_1 = 0.6667$, $K(x \geq r_1) = 0$ shows the pore cut-off. The partitioning behavior reflected in the integration procedure ensures that $K(x)$ is a continuous function for x in the interval $(0, 1)$. The development of quantitative expressions for temporal moments or contour plots of the concentration frequency distribution is straightforward, and provides the same conclusions summarized above from McCoy [5] and McCoy and Goto [6]. The specific task addressed here, to construct the partition coefficient given a pore-size distribution, provides the essential information needed for the retention time (first moment). Development of expressions showing how the rate processes, e.g., intraparticle diffusion in distributed pores, influence the band broadening (second moment) remains an assignment for the future.

Table 1
Pore size and pore volume fraction in a fractal distribution of five pore sizes ($\sigma = 1.5$, $\Omega = \pi$, $a = 1$)

j	r_j/a	n_j		
		$h = 2$	$h = 3$	$h = 5$
1	0.6667	0.250	0.104	0.023
2	0.4444	0.222	0.138	0.051
3	0.2963	0.197	0.184	0.113
4	0.1975	0.175	0.246	0.252
5	0.1317	0.158	0.328	0.560

5. Conclusions

The distributed-pore partition coefficient, $K(x)$, for a continuous mixture, denoted as a distribution in the solute radius, x, is the key parameter investigated here for size-exclusion chromatography in distributed pores. The function is calculated for continuous and discrete pore distributions. The partitioning of the spherical solute molecules in the cylindrical pores makes use of the single-pore partition factor, $\Phi(x, r)$, to exclude the spherical solute from an annular region of the pore, and to exclude totally solutes larger than a pore. Once $K(x)$ is known, then the exact solution to the equilibrium-dispersive model can be found. Temporal moments can also be computed in order to provide information about how the distribution of solutes is separated in the column. In addition to continuous pore-size distributions, we have examined how fractal distributions of pores can be constructed and integrated to determine $K(x)$. The current theory incorporating size distributions of both solutes and pores thus invites further study of chromatographic and other separation processes involving porous media.

Symbols

$A(x)$ $= \varepsilon + (1 - \varepsilon)K(x)$
$C(x)$ concentration frequency distribution

$C_0(x)$	input concentration frequency distribution
c	lumped concentration
D	axial dispersion coefficient
G	parameter in inlet concentration frequency distribution
HETP	height equivalent to a theoretical plate
$H(x)$	HETP for the concentration frequency distribution
$K(x)$	partition coefficient
$M_0(x)$	zeroth moment of the concentration frequency distribution $C(x)$
$M_1(x)$	first moment of $C(x)$
$M_2(x)$	second moment of $C(x)$
$M_n(x)$	nth moment of $C(x)$
m_n	nth moment of the lumped concentration c
$Q(x)$	concentration frequency distribution of adsorbed species
q	lumped concentration of adsorbed species
t	time
v	superficial column velocity
x	molecular property
z	position coordinate in the chromatographic column

Greek letters

ε	column void fraction
δ	Dirac delta distribution function
μ_1'	$= m_1/m_0$, reduced first moment of the lumped concentration c
μ_2	$= m_2/m_0 - (\mu_1')^2$, variance of the lumped concentration c
σ^2	$= M_2/M_0 - (M_1/M_0)^2$, variance of the frequency distribution

References

[1] R. Tijssen and J. Bos, in F. Dondi and G. Guiochon (Editors), *Theoretical Advancement in Chromatography and Related Separation Techniques* (*NATO ASI Series*, Vol. C383), Kluwer, Dordrecht, 1992.

[2] J.C. Giddings, *Unified Separation Science*, Wiley-Interscience, New York, 1991, pp. 31–35.

[3] G. Astarita and S.I. Sandler (Editors), *Kinetic and Thermodynamic Lumping of Multicomponent Mixtures*, Elsevier, Amsterdam, 1991.

[4] A.V. Sapre and F.J. Krambeck (Editors), *Chemical Reactions in Complex Mixtures*, Van Nostrand Reinhold, New York, 1991.

[5] B.J. McCoy, *Chem. Eng. Sci.*, 44 (1989) 993.

[6] B.J. McCoy and M. Goto, *Chem. Eng. Sci.*, 49 (1994) 2351.

[7] M. Goto, T. Hirose and B.J. McCoy, *J. Supercrit. Fluids*, 7 (1994) 61.

[8] O. Levenspiel and W.K. Smith, *Chem. Eng. Sci.*, 6 (1957) 227.

[9] S. Golshan-Shirazi and G. Guiochon, in F. Dondi and G. Guiochon (Editors), *Theoretical Advancement in Chromatography and Related Separation Techniques*, (*NATO ASI Series*, Vol. C383), Kluwer, Dordrecht, 1992, p. 61.

[10] E. Kucera, *J. Chromatogr.*, 19 (1965) 237.

[11] R.V. Mehta, R.L. Merson and B.J. McCoy, *J. Chromatogr.*, 88 (1974) 1.

[12] P.M. Adler, *Porous Media–Geometry and Transport*, Butterworth-Heinemann, Boston, 1992.

[13] P.M. Adler, in D. Avnir (Editor), *The Fractal Approach to Heterogeneous Chemistry*, Wiley,Chichester, 1989, p. 341.

[14] B.B. Mandelbrot, *The Fractal Geometry of Nature*, Freeman, San Francisco, 1977.

[15] P. Pfeifer and M. Obert, in D. Avnir (Editor), *The Fractal Approach to Heterogeneous Chemistry*, Wiley, Chichester, 1989, p. 35.

ELSEVIER

Journal of Chromatography A, 697 (1995) 541–548

JOURNAL OF CHROMATOGRAPHY A

Freeze-thaw flow management: a novel concept for high-performance liquid chromatography, capillary electrophoresis, electrochromatography and associated techniques

C.D. Bevan*, I.M. Mutton

Structural Chemistry Department, Glaxo Research and Development Limited, Greenford Road, Greenford, Middlesex UB6 0HE, UK

Abstract

A new method for managing flow in capillaries or narrow channels is described. The fluid is made to act as its own shut-off valve by freezing the contents of a small section of the tube. In particular flow can thereby be diverted to further tube(s), forming the basis of an innovative flow switching device that requires no moving parts and contributes no dead volume. The principle of the method is demonstrated, and it is shown that full exploitation of the technique will require the development of junctions with very low dead volumes. Some advantages of this advance are discussed.

1. Introduction

Sequential chromatographic techniques are used widely and their advantages have been documented thoroughly [1]. These benefits derive primarily from the very high specificity and information content obtained with coupled orthogonal methods [2]. In addition to the sequential approach, coupled techniques such as liquid chromatography–mass spectrometry (LC–MS) and liquid chromatography–nuclear magnetic resonance spectroscopy (LC–NMR) have also contributed to the development of highly selective and sensitive analytical methods [3].

Advantages of performing separations in open tubular columns have been apparent for many years, and indeed capillary gas chromatography has been employed with great success for over three decades [4]. However, significant transfer of capillary technology to liquid chromatography and electrophoresis had to await the appropriate developments in instrumentation and in column chemistries. Many important advances have been made in the last decade and as a result, both capillary LC and capillary electrophoresis (CE) are well established.

Despite the successes of sequential chromatography and capillary separation science, the potential inherent in their combination has yet to be exploited fully. Again, considerable technological barriers impede further progress. One constraint is the design of conventional switching valve technology. The need to handle nanolitre volumes of analyte solutions imposes severe limitations on the specifications of switching devices. For example, the best commercial rotary valves have effective dead volumes no smaller than about 40 nl and it is unlikely that

* Corresponding author.

0021-9673/95/$09.50
SSDI 0021-9673(94)00954-6

this type of design can furnish the order of magnitude scale of improvements that are necessary to maintain the resolution obtainable with capillary technology. Some aspects of this general problem have been encountered by several workers [5–10].

Lemmo and Jorgensen documented the severe limiting restrictions encountered when using a combined size exclusion–CE system [5] and have described the construction of a transverse flow gating interface that enables coupling of micro-column LC with CE [6].

Fraction collection at the micro- and nano-scales further highlights the problems associated with the management of very small volumes. Nashabeh et al. [7] designed a post-column multi-capillary device to address this issue.

Fluids used in electrophoresis can be directed into specified channels by voltage control and this principle has been applied in the design of miniaturised CE systems micro-machined on chips of silicon or glass [8–10]. Reduction of convective leakage in these devices requires independent control of the potential of all buffer reservoirs connected to the intersection. Furthermore, it may not always be convenient to control the potential at the end of each limb of an electrically driven sequential system. Hence alternative means of switching merit consideration.

In 1991, we were studying unnatural oligonucleotides that contained multiple chiral phosphoramidate bridges. In an extreme case a sample comprising a set of 512 possible diastereoisomers gave a broad envelope of incompletely resolved peaks when subjected to micellar electrokinetic chromatography (MEKC) [11,12]. The potential problems involved in the identification, isolation and quantification of any single one of these components prompted us to consider means of achieving higher resolution than that obtained by MEKC. This in turn prompted our interest in sequential CE.

We now introduce an idea that represents a radical departure from conventional switching using valves or voltage control. The fluid control method described in this report appears to be particularly well suited to solving the problems outlined above, and should also prove to have a widespread utility in areas other than separation science. We show that the idea of using the fluid as its own shut-off valve to control and divert flow can simply and elegantly be realised by freezing and thawing. The advantages of freeze-thaw control (FTC) and freeze-thaw switching (FTS) will be discussed. Integrated use of FTC and FTS is termed freeze-thaw flow management (FTFM).

2. Experimental

2.1. Apparatus

Electrophoresis was performed using an Applied Biosystems (ABI, Warrington, UK) Model 270A capillary electrophoresis system. The column compartment was normally air thermostatted at 30°C. Various voltages between 10 kV and 30 kV were employed. Samples were introduced by applying a vacuum of 127.0 mm Hg (ca. 16.9 kPa) to the cathodic end of the column. The UV spectrophotometric detector was used at wavelengths indicated in the text.

Polyvinylchloride (PVC) tubing (0.25 mm I.D. × 2.8 mm O.D) was obtained from Ormantine International (Winchester, UK). Fused-silica capillaries (720 mm × 50 μm I.D. × 375 μm O.D.) were obtained from ABI. New capillaries were conditioned by flushing for 30 min with 1.0 *M* sodium hydroxide, rinsing with deionised water for 10 min, 0.1 *M* sodium hydroxide for 30 min and the electrophoretic buffer for 30 min. Capillaries used for the analysis of fractions had an effective length of 500 mm from injection point to detector window. Capillary assemblies were constructed as indicated schematically in Fig. 1, using this tubing or UV-transparent 75 μm I.D. × 375 μm O.D. fused-silica tubing (Supelco, Bellefonte, PA, USA).

The individual silica limbs were connected using a 'Y'-piece of either fused-silica (Composite Metal Services, UK) or glass (Supelco) and cemented in place with epoxy resin glue. This construction resulted in an estimated total dead volume between the three capillary ends of about 200 nl. The assembly (Fig. 1) was installed

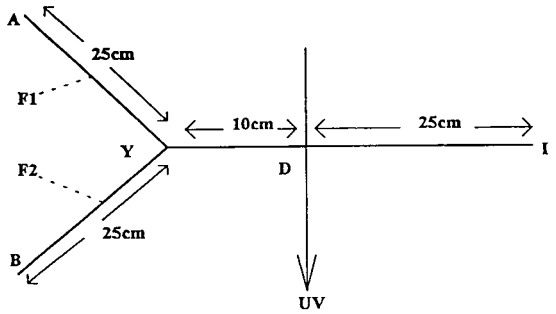

Fig. 1. Schematic diagram of the capillary assembly used to demonstrate FTS. I = Injection end (anode); A and B = cathodic limbs; D = detector; Y = Y-piece; F1 and F2 = freeze points, arbitrarily located approximately 10 cm from Y.

into the electrophoretic instrument such that both limbs AY and BY were dipped into the cathodic buffer and the detector D was located between the Y-piece and the anodic buffer at I. Freezing of capillary contents at points F1 and F2 was achieved by controlled direction of a carbon dioxide jet from a cylinder of the compressed liquid. The jet was a mixture of liquid and gaseous carbon dioxide fluids, and was delivered through 0.5 mm I.D. polyether ether ketone (PEEK) tubing.

2.2. Materials

Reagents used in preparation of buffers were of Analytical Reagent or Electrophoresis Purity grades. Crocein Orange G and *m*-Cresol Purple were obtained from Aldrich (Gillingham, UK). Reagents and chemicals were used without further purification. Water was purified by passage through an Elgastat Spectrum system (Elga, High Wycombe, UK). The electrophoretic buffer was 50 m*M* sodium dodecyl sulphate (SDS) in a solution obtained by adjusting the pH of 50 m*M* disodium tetraborate to 7.0 with 50 m*M* sodium dihydrogenphosphate. Buffers and rinsing solutions were filtered using disposable 0.45 μm syringe filter units (Anachem, Luton, UK) and degassed with helium before use.

3. Results and discussion

3.1. Freeze-thaw control

Hydraulically driven flow is usually controlled and switched by valves that require moving parts to block or divert the fluid. Valve components may contribute to dead volume and potentially be subject to abrasion and corrosion, resulting in leaks and contamination. These defects become worse as the internal diameter of the tube decreases. However, the advantages of using the flowing liquid as its own shut-off valve increase with decreasing tube I.D. because it becomes more practicable to rapidly freeze the contents of a short section of narrow tubing. The blockage produced may be expected to stop instantaneously all liquid flow inside tubing of suitable dimensions until thawing is allowed to occur. Managed cycles of freezing and thawing will control the presence or absence of flow in a narrow tube (FTC). It will be possible to divert or switch flow into specified tubes (FTS) by using FTC to block a tube or channel selected from within a system of interconnected tubes.

To test the feasibility of this idea, it was necessary to select an experimentally convenient device capable of rapidly freezing small flows of liquid. We chose to use liquid carbon dioxide to produce a fine spray of cold fluids. This cold spray was directed onto the outer wall of the tubing at the point where freezing was required. Clearly other methods, for example devices using thermoelectric means of heat transfer such as Peltier [13] devices, are also attractive. We were able almost instantaneously to stop hydraulically driven flows of water–acetonitrile (100:0 to 40:60 by volume) of up to at least 1.0 ml/min by using cold fluids sprayed from a nozzle of I.D. 0.5 mm, onto 1.6 mm O.D. stainless steel tubes having I.D.s of 0.7–1.1 mm. Smaller flows of up to about 90% (v/v) acetonitrile could also be halted, as could mixtures of up to about 20% (v/v) methanol in water. The technique is also applicable to fluids in fused-silica capillaries, but is less effective when used with tubes of PEEK, which is a good thermal insulator. The potential to halt flow can be

gauged by the fact that the temperature of the jet of fluids was found to be around −65°C. Using published [14] values of the respective thermal capacities of quartz and water of 0.74 J g^{-1} K^{-1} and 4.22 J g^{-1} K^{-1} (at 0°C), thermal conductivity of vitreous silica of 1.20 W m^{-1} K^{-1} (at −50°C), and enthalpy of fusion of water of 334 J g^{-1}, calculation shows that the 20 nl of water contained at 30°C in a 1 cm section of 50 μm I.D. × 375 μm O.D. fused-silica tubing will be frozen in a few tenths of a second by rapidly flowing carbon dioxide fluids at −65°C. The frozen plug of ice weighs about 20 μg and so only releases about 10 mJ on formation from water at 30°C. About 200 mJ more are required if it is assumed that the silica wall and ice cool to −65°C.

Freezing also proved effective when used to halt mass transport in electrically driven systems. Fig. 2 shows the trace produced by electrophoresis of a synthetic mixture in a 720 mm fused-silica column, through the detector zone and past a freeze point. After 5.9 min, the column contents at this point were frozen. The loss of current indicates the instantaneous formation of an insulating plug of ice. Freezing was maintained for 5 min, during which period the voltage was reversed. On subsequent thawing, rapid restoration of current was recorded, as was a 'mirror image' of the 'frozen' electropherogram of the components passing in reversed order through the detector zone. Very little evidence of diffusive resolution loss can be seen. Freezing halts the flow as effectively as does removal of electromotive force as illustrated in Fig. 3.

3.2. Freeze-thaw switching

We next performed a simple demonstration of the ability of FTC to switch analytes (FTS) to a second capillary via a fused-silica Y-piece (Fig. 1). First, a solution of Cresol Purple (10 mg/ml) was sampled into the assembly and allowed to electrophorese into limb IY for 1 min. Power was then turned off and limb BY was blocked by sleeving it with 0.25 mm I.D. PVC tubing plugged with copper wire. Section AYI was then flushed with electrophoretic buffer (ca. 10 μl) into an Eppendorf tube using gentle pressure from a syringe attached at A. The contents of the tube were blown gently to dryness and reconstituted in deionised water (10.0 μl). This solution served as a reference standard and was

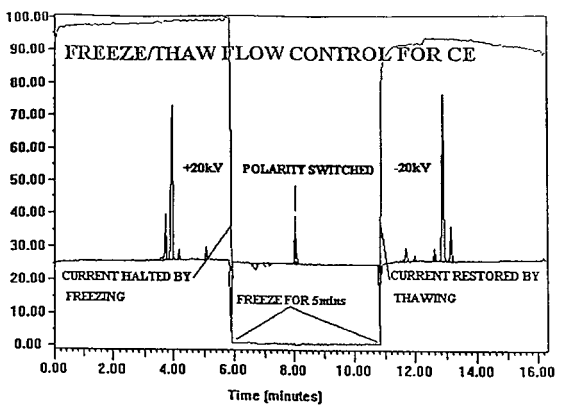

Fig. 2. A demonstration of the effect of freezing and thawing on the process of capillary electrophoresis. Sample: synthetic mixture in deionised water, vacuum injection (1.5 s). Column: 720 mm (500 mm to detector), 50 μm I.D. × 375 μm O.D. fused-silica. Electrolyte: 50 m*M* SDS in pH 7.0, 50 m*M* phosphate–borate buffer. Detection at 220 nm; response shown in arbitrary units. Voltage: between + and −20 kV as described in the text.

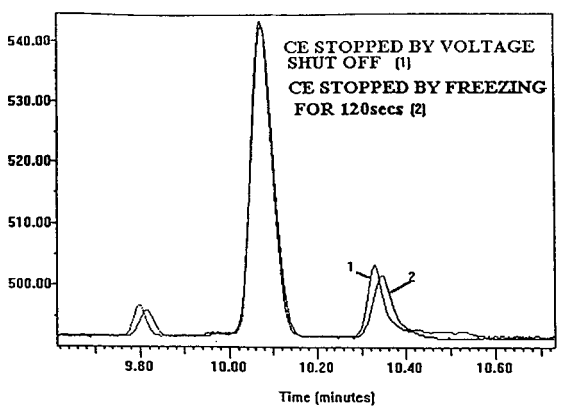

Fig. 3. Comparison of peak profiles produced when electrophoresis was halted for 120 s by (1) voltage shut-off and (2) freezing whilst maintaining −20 kV across the column. Sample and conditions as for Fig. 2. Response in arbitrary units. Note: migration time is 3 min shorter than in Fig. 2 because electrophoresis was interrupted for a correspondingly shorter time.

analysed (3.0 s injection, detection at 210 nm) using a 720 mm column operated at 30 kV as indicated above. To demonstrate FTS, a second aliquot of the Cresol Purple solution was sampled at I and electrophoresis allowed to continue until the sample zone was in section DY, when limb AY was frozen after 7.1 min with a jet of cold carbon dioxide fluids. Freezing was maintained until the sample zone was judged to be several centimetres into limb BY, when AY was allowed to thaw (t = 12.7 min). Fig. 4 shows the electropherogram obtained; note the reduction in current that occurred when only one of the limbs AY and BY (i.e. the latter) was open circuit. Limbs AY and BY were simultaneously flushed with electrophoretic buffer from a syringe at I into separate Eppendorf tubes at A and B. The contents of both tubes were dried, reconstituted and analysed as before. The experiment was repeated and the mean relative peak areas (reference standard peak area defined as 100%) were 10.4% in frozen limb AY and 64.5% in open limb BY. Thus 75% of the dye was recovered and had been split at Y with a ratio of 86:14. Although this result is a demonstration of the validity of the FTS concept, recovery was incomplete and totally clean switching was not obtained. Both these effects can be directly attributed to the use of a Y-piece of relatively large dead volume and with a potential for stagnant zones. It is difficult to take full advantage of having a shut-off valve (i.e. the frozen plug) that contributes no effective dead volume, because the internal volume of the Y-piece used (ca. 200 nl between column ends) is much greater than the volume occupied by a typical analyte zone.

Fig. 5 illustrates the peak broadening due to the Y-piece. This trace was produced by injection of a mixture of two dyes, Cresol Purple (1.0 mg/ml) and Crocein Orange (0.1 mg/ml) and allowing Cresol Purple to pass through Y into the limbs AY and BY. Power was turned off after 8.5 min, i.e. after the Crocein Orange zone had passed the detector but before it had reached Y. The voltage was reversed after 8.8 min and the power restored, driving the Crocein Orange zone back through the detector. The Cresol Purple peak shows gross broadening following two passages through the Y-piece. Note that on its second passage through the detector, the Crocein Orange peak had narrowed slightly and its area had decreased by about 7%. These observations both indicate a small Poiseuille flow towards I. After allowing

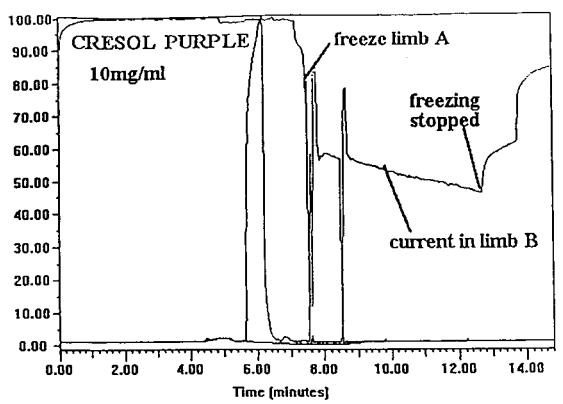

Fig. 4. Freeze-thaw switching. Sample: Cresol Purple, 10 mg/ml in deionised water, vacuum injection for 1.5 s. Column: construction shown in Fig. 1 (UV-transparent tubing and fused-silica Y-piece). Electrolyte as in Fig. 2. Detection at 300 nm; response in arbitrary units. Voltage: 17 kV applied continuously. Other details as given in the text.

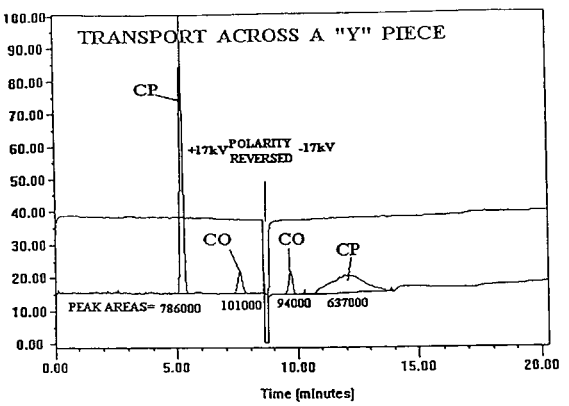

Fig. 5. The effect of the Y-piece on bandwidths and recoveries in the absence of freezing. Sample: Cresol Purple (1.0 mg/ml) (CP) and Crocein Orange (0.1 mg/ml) (CO) both in deionised water. Vacuum injection for 0.5 s. Column construction, electrolyte and detection as in Fig. 4. Voltage: 17 kV, reversed at 8.5–8.8 min. Response in arbitrary units.

for this effect, the loss of Cresol Purple in the Y-piece was estimated at 13%. This result confirms that the Y-piece caused substantial losses and peak broadening.

As expected, the experimental conditions employed here do not help to confine the analyte zone [15]. The Y-piece will cause more peak dispersion in hydraulically driven systems. Clearly, the design of the connector is critical. Conventional means of forming capillary junctions incur considerable void volume arising from the abuttal of three or more capillary walls (e.g. ca. 30 nl contained in the void between three tubes of 375 μm O.D. abutting at 120° to each other as shown in Fig. 6). We have therefore designed a connector of minimal void volume that we believe will help to realise fully the potential of FTS. This device is currently under development.

3.3. Advantages of freeze-thaw flow management

Controlling and switching flow in this manner affords a number of significant advantages of

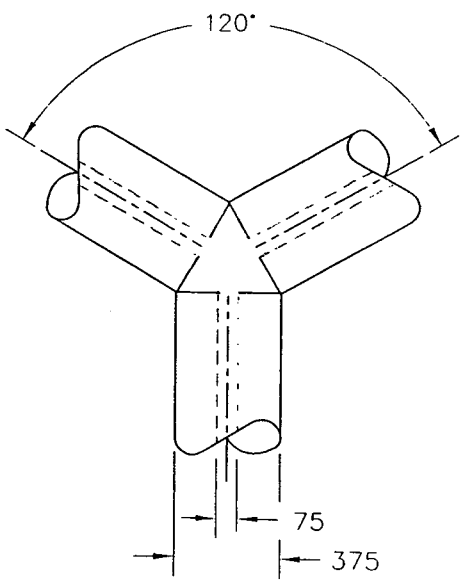

Fig. 6. Illustration of the void volume produced by abutting three columns at 120° to each other. Dimensions in μm.

relevance to micro-column separation technology:

(i) Freezing is extremely rapid due to the very small thermal capacities of the tubing and its contents. There is potential for 'fine-tuning' by automated remote control of both the flow of the cryogen and of warm gas for thawing.

(ii) Control is non-invasive. This is a direct consequence of using the liquid in the tubing as its own shut-off valve. Therefore there are no moving parts to contribute to peak dispersion arising from extra dead volume or turbulence. This is especially relevant in packed columns where there is inevitably extra void volume upstream of any conventional valve owing to the need for an in-situ sinter barrier. Similarly, FTFM should be suited to liquids containing suspended solids. Elimination of moving parts removes the possibility of the shut-off mechanism altering the chemical composition of the liquid stream, whether by mechanical abrasion, adsorptive losses and carry-over, contamination by valve components or lubricants, or by attack by corrosive liquids.

(iii) Carbon dioxide is economical, effective and safe to use, being both non-flammable and an electrical insulator. It can achieve temperatures of below −50°C on evaporation; if liquids freezing below this temperature are to be controlled, then suitable alternative cryogens could be substituted.

(iv) The FT principle has no inherent requirement for precision engineering and can be expected to work on any fluid that can be frozen.

(v) The shut-off unit (the frozen plug) has no extra-column connections and so external leakage at this point is impossible. With aqueous systems, the water will expand to ice and self-seal against any internal creep leakage. This sealing, which utilises friction between the plug and the internal wall, will become increasingly effective with decreasing column I.D.

(vi) Column coatings should remain unaffected by FTFM.

(vii) FTFM offers further advantages when the liquid is driven electrically. During the separation process, electroosmosis and ion transport are maintained across what is essentially a shut-

off valve in the open configuration. There is no electrical contact between column and switch, so the high voltages cannot be earthed through the switch. Additionally, the insulating properties of carbon dioxide and ice should be noted; the former maintains safety and the latter instantaneously halts electroosmosis and electrophoresis in the column both upstream of and downstream from the freeze point The minute size of the ice plug ensures rapid thawing with concomitant restoration of current.

There would appear to be considerable scope for the application of FTFM to the separation sciences. Briefly, any valve in conventional chromatographic and electrophoretic systems is in principle replaceable with an FTS device in the corresponding miniaturised systems. We believe the technique is applicable to many areas and therefore we demonstrated its principles by construction of an elementary switching device. FTC and FTS should facilitate heart-cutting, sequential and coupled techniques, in-line reactions and derivatisation schemes, and preparative applications on a miniaturised scale. The latter would be achieved by switching fractions into the desired limb which would then function as a microstorage vessel. A particular area that interests us is the potential of the technique for expanding the range of mobile phases and buffers compatible with a mass spectrometer. An example of this would be an in-line micellar CE–MS interface. Such a device is currently under development. FTFM becomes increasingly attractive with diminishing column dimensions. Therefore we anticipate use of this technology in the design of miniaturised separation systems such as CE devices incorporated within single plastic [16], silicon or glass [8–10] micro-chips. Electrothermal (e.g. Peltier) cooling is an attractive possibility in this context.

FTFM should also find applications in other areas of analytical chemistry (for example flow injection analysis) and in technologies where there is a requirement for remote control of fluids in narrow channels.

We have not attempted to define the practical limitations of this approach since clearly these will depend on the sizes, flows and physical properties of the materials used. Whilst in principle it is possible to freeze eluant from a 50 mm I.D. preparative column for example, there is in this case no advantage in replacing a conventional valve with an FTFM device. On the other hand, FTS would seem to be a method of choice for sequential micro-column separations.

4. Conclusions

We have introduced here a novel means of managing fluid flow in narrow tubes and channels. The method, termed freeze-thaw flow management, appears to have wide applicability. This paper has demonstrated freeze-thaw control and freeze-thaw switching, outlined some of their advantages, and discussed some potential applications. FTFM is an advance applicable not only to micro-liquid chromatography, electrochromatography, capillary electrophoresis, sequential and coupled techniques, but also to other areas of science and technology.

Acknowledgement

We would like to thank Andrew Hansell for his excellent technical assistance.

References

[1] H.J. Cortes (Editor), *Multidimensional Chromatography. Techniques and Applications (Chromatographic Science Series*, Vol. 50), Marcel Dekker, New York, 1990.
[2] J.C. Giddings, *J. High Resolut. Chromatogr. Chromatogr. Commun.*, 10 (1987) 319–323.
[3] C.F. Poole and S.K. Poole, *Chromatography Today*, Elsevier, Amsterdam, 1991, Ch. 9, p. 948.
[4] M.J.E. Golay, in D.H. Desty (Editor), *Gas Chromatography: Proceedings of the 2nd Symposium, Amsterdam, May, 1958*, Butterworth, London, 1958, p. 36.
[5] A.V. Lemmo and J.W. Jorgenson, *J. Chromatogr.*, 633 (1993) 213–220.
[6] A.V. Lemmo and J.W. Jorgenson, *Anal. Chem.*, 65 (1993) 1576–1581.
[7] W. Nashabeh, J.T. Smith, and Z. El Rassi, *Electrophoresis*, 14 (1993) 407–416.

[8] A. Manz, D.J. Harrison, E. Verpoorte and H.M. Widmer, *Adv. Chromatogr.*, (1993) 1.
[9] Z.H. Fan and D.J. Harrison, *Anal. Chem.*, 66 (1994) 177–184.
[10] S.C. Jacobson, R. Hergenröder, L.B. Koutny and J.M. Ramsey, *Anal. Chem.*, 66 (1994) 1114–1118.
[11] C.D. Bevan, W.P. Blackstock, K. Brinded, R.J. Dennis, T. Haley, H. Muenster and E. Schroeder, in R.M. Caprioli (Editor), *Proceedings of the 39th ASMS Conference on Mass Spectrometry and Allied Topics, Nashville, TN, May 1991*, ASMS, East Lansing, MI, 1991, pp. 983–984.
[12] C.D. Bevan, I.M. Mutton and A.J. Pipe, *J. Chromatogr.*, 636 (1993) 113–123.
[13] J. Bardeen, in E.U. Condon and H. Odishaw (Editors), *Handbook of Physics*, Mcgraw-Hill, New York, 2nd ed., 1985, p. 4–83.
[14] D.R. Lide (Editor), *Handbook of Chemistry and Physics*, CRC Press, Boca Raton, FL, Ann Arbor, Boston, MA, 72nd ed., 1991–1992.
[15] W.G. Kuhr, L. Licklider and L. Amankwa, *Anal. Chem.*, 65 (1993) 277–282.
[16] B. Ekström, G. Jacobson, O. Öhman and H Sjödin, *Int. Pat.*, WO 91/16966 (1990).

ELSEVIER

Journal of Chromatography A, 697 (1995) 549–560

JOURNAL OF CHROMATOGRAPHY A

Enantioselective capillary electrophoresis of amino acid derivatives on cyclodextrin Evaluation of structure–resolution relationships

Wolfgang Lindner[a,*], Barbara Böhs[a], Volker Seidel[b]

[a]*Institut für Pharmazeutische Chemie, Karl-Franzens-Universität Graz, Schubertstrasse 1, A-8010 Graz, Austria*

[b]*Hafslund Nycomed, St. Peter Strasse 25, A-4020 Linz, Austria*

Abstract

In this work a strategy for enantioselective separations of α-amino acid derivatives in cyclodextrin (CD)-modified capillary zone electrophoresis (CZE) is presented and the effects of various experimental parameters such as temperature, pH, applied voltage and the use of organic modifiers (methanol, *tert.*-butyl methyl ether, carnitin) have been studied in detail. For the modification of α-amino acids, also helpful in order to improve sensitivity by UV or fluorescence detection, well known derivatives such as dinitrobenzoyl, dinitrophenyl, dimethylaminonaphthylsulfonyl, carboxybenzyl and 9-fluorenylmethoxycarbonyl and the new 6-aminoquinolyl-N-hydroxysuccinimidylcarbamoyl derivatives have been prepared, and the chiral derivatives have been tested with respect to their resolvability in CZE using different cyclodextrins (α-, β-, γ-CDs and CD derivatives) as chiral additives to the electrophoretic buffer system. In general the selector–selectand interactions could be improved by using amino acid derivatives containing nitro- or dimethylamino groups in combination with extended (methylated or hydroxypropylated) CDs. Further enhancement of enantiomeric resolution was achieved by the addition of organic modifiers and/or lowering the temperature down to 5°C. At temperatures above 40°C a non-linear relationship of the decrease of resolution as function of $1/T$ was noticed.

1. Introduction

Capillary zone electrophoresis (CZE), introduced in the early 1980s [1], is one of the most rapidly developing separation techniques and stands for a high-efficiency non-stereoselective analytical separation method in free solution. By the addition of chiral additives to the electrophoretic buffer system it is possible to create diastereomeric associates, which should be resolvable due to their different conformation and thus electrophoretic mobilities [2]. Various additives have been used as chiral selectors in CE such as D-campher-10-sulfonate, L-menthoxyacetic acid [3], chiral micelle-forming detergents [4–6], chiral metal complexes [7–9], chiral crown ether [10,11], proteins [12], maltoheptaose [13], oligosaccharides [14] and most frequently cyclodextrins (CDs) [15–26] alone, and in combination with others [3,27,28]. CDs are non-ionic cyclic oligosaccharides consisting of six (α), seven (β) or eight (γ) α-(1,4)-linked D-(+)-glucopyranose units. The resulting geometrical structure has been characterized as a hollow truncated cone with a relatively hydrophobic cavity and a hydrophilic external surface. Chiral

* Corresponding author.

SSDI 0021-9673(94)01240-7

recognition seems predominantly be based on the inclusion of an aromatic or alkyl functionality into the cavity and additional electrostatic hydrogen bonding interactions between secondary hydroxyl groups around the cone opening and substituents of the guest molecule. Consequently, the formation of the inclusion complex depends on spatial factors, hydrophobic interactions, hydrogen bonding and solvation effects. The chiral discrimination mechanism using CDs is based on the differential electrophoretic mobilities as a result of the different conformation and stability of inclusion-type complexes between CD and enantiomer moieties [29–31].

In this paper a general strategy for the direct enantiomeric separation of selected α-amino acid derivatives is presented and an attempt is made to elucidate the complexity of structure–resolution relationships. Derivatization of amino acids is of general use in terms of improved sensitivity by UV or fluorescence detection and to enhance chiral discrimination mechanisms. The utility for CE application of recently developed amino acid derivatization methods, e.g. 6-aminoquinolyl-N-hydroxysuccinimidylcarbamoyl (AQC) [32], and several amino acid derivatization reagents [e.g. carboxybenzyl (CBZ), dinitrobenzoyl (DNB), dinitrophenyl (DNP), 5-dimethylaminonaphthylsulfonyl (Dns), 9-fluorenylmethoxycarbonyl (FMOC); for chemical formulas see Fig. 1], which have already been widely used for enantiomeric separations with alternative separation techniques, was studied.

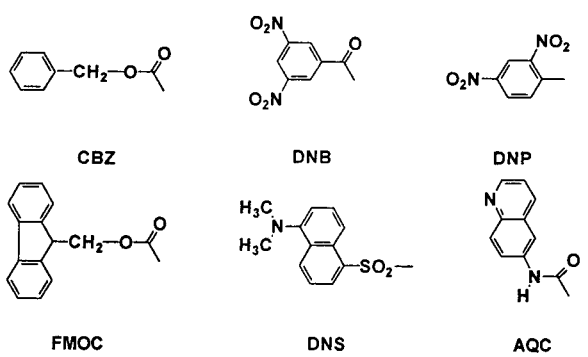

Fig. 1. Molecular structures of amino acid N-derivatives tested for their potential of amino acid enantiomeric separations by CD-modified CZE.

The chemical/spatial structure–inclusion/interaction relationship is discussed and evaluated with respect to size of the aromatic group, substitution, electronic density properties, distance from aromatic moiety to center of chirality, additional hydrogen-bonding facilities etc.

The influence of other experimental CE parameters such as pH, temperature, applied voltage, concentration and type of electrolyte buffer and CD has been extensively studied and will be presented. The effect of organic buffer modifiers (e.g. methanol) was found to be a crucial parameter in terms of lowering electroosmotic flow (EOF) and hence facilitating enantiomeric separations.

2. Experimental

2.1. Reagents and materials

All chemicals were of analytical-reagent grade unless stated otherwise. All cyclodextrins: α-CD, β-CD, γ-CD, 2-hydroxypropyl (HP)-β-CD (substitution degree 0.9), 2,3,6-methyl (Me)-β-CD (substitution degree 1.8), HP-γ-CD, Me-γ-CD were purchased from Wacker Chemie (Salzburg, Austria), sodium hydroxide and all electrolyte buffer solutions (sodium phosphate, sodium tetraborate decahydrate, sodium citrate, 20 m*M* each, pH range 3–9) were obtained from Fluka (Buchs, Switzerland). L-Carnitin hydrochloride [$HOOC–CHOH–(CH_2)_2–N^+(CH_3)_3 \cdot HCl$], mesityloxide, the derivatizing agents 2,4-dinitrofluorobenzene (DNFB, Sanger's reagent), 3,5-DNB chloride (DNB-Cl), benzyloxycarbonylchloride (CBZ, Z), fluorenylmethylchloroformate (FMOC-Cl) and the final DNP-, DNB-, CBZ-, Dns and FMOC derivatives of different α-amino acids were purchased from Aldrich (Steinheim, Germany). The new AQC, trade name AccQ·Fluor) reagent was provided by Millipore, Waters Chromatography (Milford, MA, USA). Deionized water was prepared with a Milli-Q system (Millipore, Vienna, Austria). Water of 18 MΩ was used for the preparation of

all the solutions, electrolyte buffer and standards.

2.2. Apparatus

All CE separations were performed using a HP^{3D} CE system [Hewlett-Packard (HP), Vienna, Austria], equipped with 50–70 cm × 50 μm I.D. uncoated fused-silica capillary with "bubble cell" (3 times extended optical path length). Hydrodynamical injection was achieved by applying a controlled pressure profile at 100 mbar for 3 s. A Peltier element allowed forced-air (10 m/s air velocity) temperature controlling of the capillary cassette down to 5°C (± 0.1°C). Peak detection was accomplished by diode-array detection (DAD, 190–600 nm). Data processing was performed on a HP Vectra personal computer (486/66) with a HPCE ^{3D}ChemStation.

2.3. Methods

The capillary was prewashed via maximum pressure application using a standardized washing procedure with 1.0 *M* NaOH for 5 min, 0.1 *M* NaOH for 3 min, water for 5 min and running buffer for 10 min at the beginning of each working day, and further with 0.1 *M* NaOH for 1 min and running buffer for 7 min prior to each analysis. Sample injections were followed by a 1.0-s injection of water in order to wash the electrode and the outside of the fused-silica capillary. After the final analysis of a sequence running overnight the capillary was washed with 0.1 *M* NaOH for 1 min, water for 15 min and air for 1 min.

3. Results and discussion

3.1. Effect of inclusion interaction between different amino acid derivatives and CD types

There is a direct relation between spatial extension (aromatic size) of the amino acid N-protection group and the inner diameter of the CD cavity (Table 1). Voluminous fluorescent derivatives (Dns, FMOC) showed best resolution with γ-CDs, whereas the smaller chromophores of DNP, DNB, CBZ and AQC could be efficiently separated with β-CD derivatives.

In addition, aromatic substitution with dinitro or dimethylamino functionalities increased chiral discrimination, presumably by the reduced or changed immersion into the CD cavity, thus facilitating additional hydrogen bonding of amino acid moieties (amino and carboxyl groups) towards the secondary hydroxyl groups of the CD rim. The importance of this effect besides hydrophobic inclusion is also made evident by the improved resolution using HP-CDs (Fig. 2) and by the general decrease in separation per-

Table 1
Possible host–guest inclusion interactions between various CDs and α-amino acid derivatives depending on the relationship of the spatial extension of the amino acid N-protection group and the inner diameter of the CD cavity

CD type (cavity diameter at the CD rim in Å)	Amino acid derivative (min. × max. spatial extension in Å)					
	DNB (5.9 × 6.8)	DNP (5.9 × 6.8)	AQC (4.3 × 7.1)	FMOC (5.0 × 8.9)	Dns (7.0 × 8.0)	CBZ (5.0 × 6.7)
α-CD (5.7 nm)						
β-CD (7.8 nm)	+	+			+	
Me-β-CD (7.8 nm)	+	+		+		
HP-β-CD (7.8 nm)	+ +	+ +	+ +			+
γ-CD (9.5 nm)			+	+ +	+ +	+
Me-γ-CD (9.5 nm)						
HP-γ-CD (9.5 nm)					+	

+ = Separation possible; + + = baseline separation achieved.

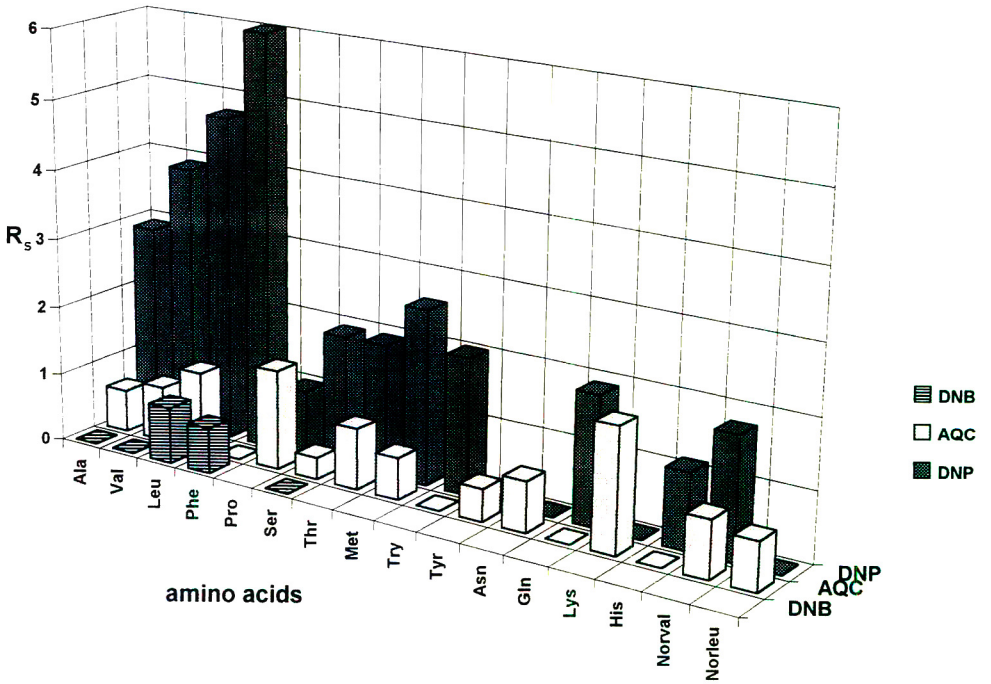

Fig. 2. Resolution (R_s) in CD CZE enantiomeric separation of several amino acid derivatives (100 ppm solutions in methanol) using HP-β-CD (30 mM) as a chiral selector. The background electrolyte was 20 mM sodium tetraborate pH 9.2 for DNB- and DNP-amino acid separations and 70 mM sodium phosphate pH 7 for AQC-amino acids with a methanol content of 10% as an organic modifier. CE separations were performed at 20 kV and 10°C capillary temperature for DNP- and AQC-amino acids and 25°C for DNB-amino acids. Blank cells have not been tested, yet.

formance when using Me-CDs. These facts also prove the recently postulated chiral recognition model of CD CZE [33] assuming a three-point interaction mechanism (aromatic inclusion plus two hydrogen bonding interactions), which was first proposed in HPLC on β-CD bonded stationary phase [34]. However, the restriction of this general approach, when separating DNB, DNP and AQC derivatives of various amino acids using HP-β-CD is also demonstrated in Fig. 2.

3.2. Effect of CD concentration on separation

The effect of CD concentration on the separation, reported as an essential parameter in CD-modified CZE by several authors [12–16], was investigated for DNP- and DNB-amino acids over the concentration range 15–100 mM of HP-β-CD (Fig. 3). Optimum separations for the model substances DNP-Pro and DNB-Phe were achieved at a concentration of 50 mM HP-β-CD, whereas DNP-Leu separation required 100 mM of the selector. However, when rising the CD concentration up to an optimum level, the increase in separation factor α and in resolution was insignificant (mean increase of α ca. 2%), but it has to be paid for by prolonged separation time of about 35%. According to the theoretical model, first introduced by Wren and Rowe [29,30], we deduced that the investigated amino acid derivatives show very high affinity to the CD. The difference in apparent mobility between the two enantiomers ($\Delta\mu$) can be derived from the equation

$$\Delta\mu = \frac{C(\mu_1 - \mu_2)(K_B - K_A)}{1 + C(K_A + K_B) + K_A K_B C^2}$$

(where μ_1 = mobility of the enantiomers, μ_2 = mobility of the complexes, K_A and K_B =

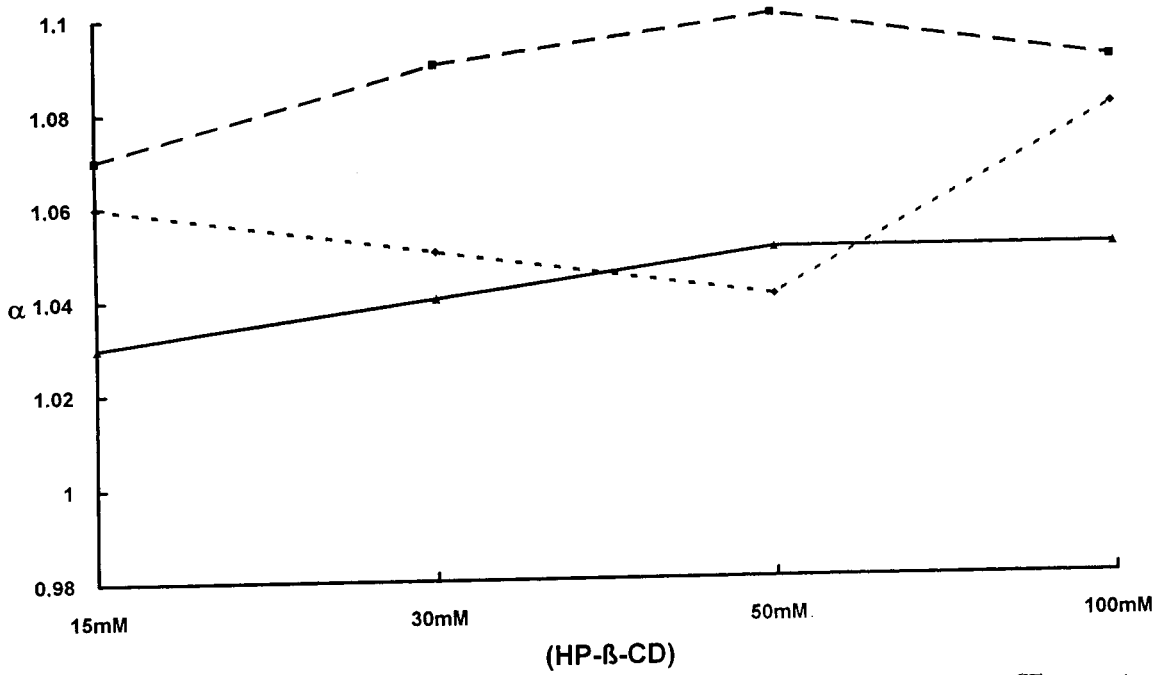

Fig. 3. Influence of HP-β-CD concentration on the separation factor α of selected α-amino acid derivatives. CE parameters: 10 kV electrode voltage, 15°C capillary temperature, electrolyte buffer was sodium tetraborate 20 mM, pH 9.2, analyte concentration 100 ppm in methanol. ◆ = DNP-Leu; ▲ = DNP-Pro; ◘ = DNB-Phe.

formation constants of the enantiomer–CD complex and C = CD concentration), whereby a maximum mobility difference is obtained at

$$C = \frac{1}{\sqrt{(K_A K_B)}}$$

However, the influence of this term is diminished for great values of the equilibrium constants K_A and K_B, which has been proved by the CD CZE separation results of amino acid derivatives shown in Fig. 3. Consequently the optimum selector concentration can be very low, when the affinity of the enantiomers to the CD is high.

3.3. Effect of pH on separation

pH Effects were studied over the range of pH 5–9.2 for DNB-, DNP- and AQC-amino acids using sodium phosphate 70 mM as background electrolyte and HP-β-CD 30 mM as chiral selector (Fig. 4). As a result, all separations of DNB, DNP, Dns and FMOC derivatives showed enhanced resolution at pH values 7–9, since the resulting anionic analytes run counter to the EOF and the "pseudo-stationary" CD phase. AQC derivatives required a low pH setting (5–7) resulting in a reduction of the EOF, presumedly due to a slow kinetics of complex formation, otherwise the EOF may be too rapid, resulting in elution of solute before separation has occurred. However, Fig. 4 also demonstrates the exception of the rule with DNP-Phe showing best separation efficiency at pH 6.

3.4. Effect of the type and concentration of the running buffer

The use of sodium phosphate buffer showed slightly better resolution in CD CZE enantiomeric separation of amino acid derivatives as compared with borate buffer. This can be attributed to a possible complexation of borate anions

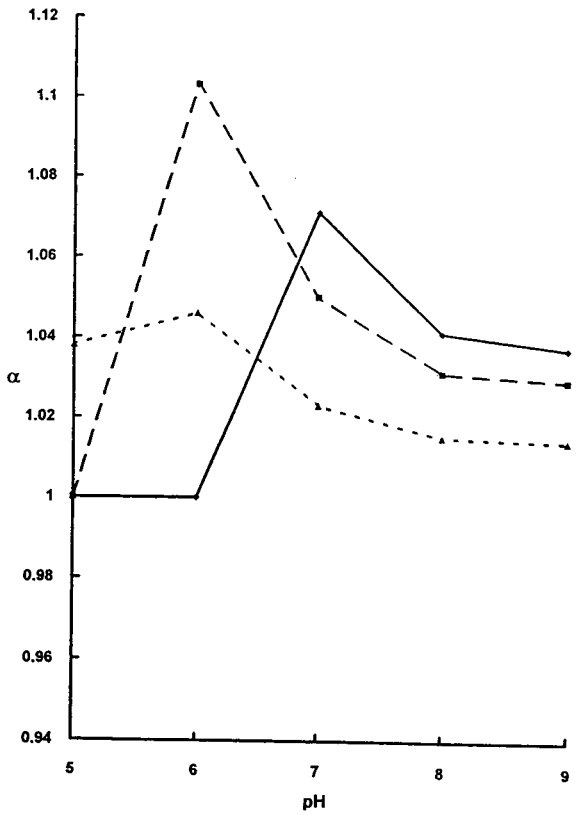

Fig. 4. Effect of electrolyte buffer pH on the separation factor α of selected amino acid derivatives using HP-β-CD (30 mM) as a chiral selector. CE parameters: 20 kV electrode voltage, 10°C capillary temperature, electrolyte buffer was sodium phosphate 70 mM with a modifier content of 20% methanol. The analyte concentration was 100 ppm in methanol. ▲ = AQC-Leu; ■ = DNP-Phe; ◆ = DNB-Phe.

to the vicinal hydroxyl groups in positions 2 and 3 of the CD rim [35]. The optimum ionic strength, studied in a range from 10 to 100 mM, was found to be 20 mM for borate buffer and 70 mM for phosphate buffer.

3.5. Effect of applied voltage

The effect of the applied voltage in the range of 5–30 kV on the EOF and consequently on migration time as well as on separation was studied at a phosphate buffer system (70 mM) with HP-β-CD (30 mM) as chiral selector and DNB-Phe, DNP-Phe and AQC-Leu as model substances. Good enantiomeric separations were achieved by setting the voltage at 30 kV, which is also the limit of most CE devices. But, high analysis speed under elevated voltage setting had to be paid for by a slight decrease in the separation factor α of about 3%, due to the increased Joule heating of the capillary, revealing higher diffusion velocities and peak broadening. However, this effect could be kept to a minimum as a result of the highly sufficient forced-air cooling within the capillary cartridge. Even though, a voltage setting of 15–20 kV seems to be a good compromise of sufficient resolution with acceptable speed of analysis.

3.6. Effect of temperature

Since the host–guest complexation mechanism is a kinetically driven process and there is potential Joule heating within the capillary under usual voltage settings of 5–30 kV, temperature effects are supposed to be a crucial parameter for CD-modified CZE. Joule heating mainly depending on the power, capillary dimensions, conductivity of the running buffer and applied voltage was limited by using an active temperature control (a Peltier element allowing forced-air temperature controlling of the capillary cassette), moderate voltage of 20 kV as well as moderate running buffer concentration of 20 mM and by using capillaries with a narrow inner radius and a large outer radius.

Accordingly our temperature study ranging from 5 to 60°C on enantiomeric separations of DNB-Phe, DNP-Phe and AQC-Leu revealed a significant but not Van 't Hoff-type (linear relation of ln μ or ln α versus $1/T$) relationship of increased migration and resolution versus decreasing temperature down to 5°C (Figs. 5 and 6A and B).The electropherograms of the separation of the DNB-Phe enantiomers as shown in Fig. 5 can be regarded as very useful, because especially DNB-derivatized amino acids showed good resolution results without any organic modifier addition (see Fig. 8). Therefore the possible additional effect of modifier on interaction with capillary wall, with the selector and/or the analyte could be neglected.

Once again, referring to the potential Joule

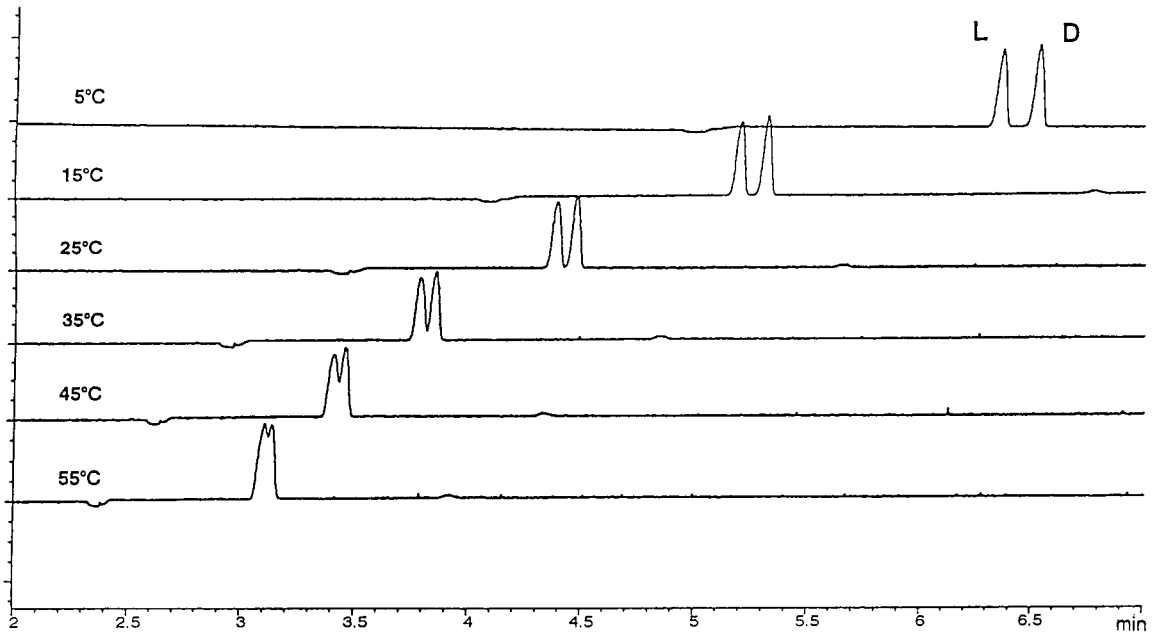

Fig. 5. Electropherogram of the CD CZE separation of DNB-Phe enantiomers (100 ppm racemate in methanol) using HP-β-CD (30 mM) as a chiral selector. CE parameters: fused-silica capillary 70 cm × 50 μm I.D., 20 kV electrode voltage, electrolyte buffer was sodium tetraborate 20 mM, pH 9.2, UV detection at 214 nm.

heating, it has been shown by Knox and McCormack [36] that the temperature rise ΔT in the capillary during electrophoresis, the so-called Joule heating, is proportional to a good approximation to the power dissipated, that is

$$\Delta T = aEI$$

where E = field strength (i.e. the applied voltage per unit length, V/L), I = current and a = power temperature coefficient depending on the cooling and the outer diameter.

Concerning this direct proportionality, the non-linear relationship of ln k' (capacity factor) versus reciprocal of absolute temperature cannot be attributed to the so-called "unstable and undefined" temperatures in the separation system, because whenever there exists Joule heating, it would not result in such sudden non-linearity.

The relationship of enantiomeric separation, complex formation and temperature is given by the Gibbs–Helmholz equation:

$$-\Delta\Delta G = RT \ln \alpha$$

where R is the general gas constant (8.31 J K^{-1} M^{-1}), T is the temperature in K and $\Delta\Delta G$ is the difference in the molar Gibbs energy of the two diastereomeric complexes. The separation factor α was calculated by the quotient of the migration times $[\alpha(\mu) = \mu_B/\mu_A]$ or alternatively by the quotient of capacity factors $[\alpha(k') = k'_B/k'_A)$ in order to compensate the influence of EOF. k' was calculated as $(\mu_{analyte} - \mu_{EOF})/\mu_{EOF}$, where μ_{EOF} is the migration time of mesityloxide used as a neutral marker.

Usually the Gibbs energy is known to be mainly dependent on the enthalpy of the complex formation revealing a linear relationship of ln μ or ln α versus $1/T$. But the formation of inclusion complexes with CDs is also influenced by entropy-controlled factors, e.g. the disarrangement of the solvation status of the CD and the loss of translational and rotational degrees of freedom during complex formation as has been postulated by Kuhn et al. [37] for a chiral 18-crown-6 ether. Consequently α is dependent on the enthalpy difference ($\Delta\Delta H$) and the entropy

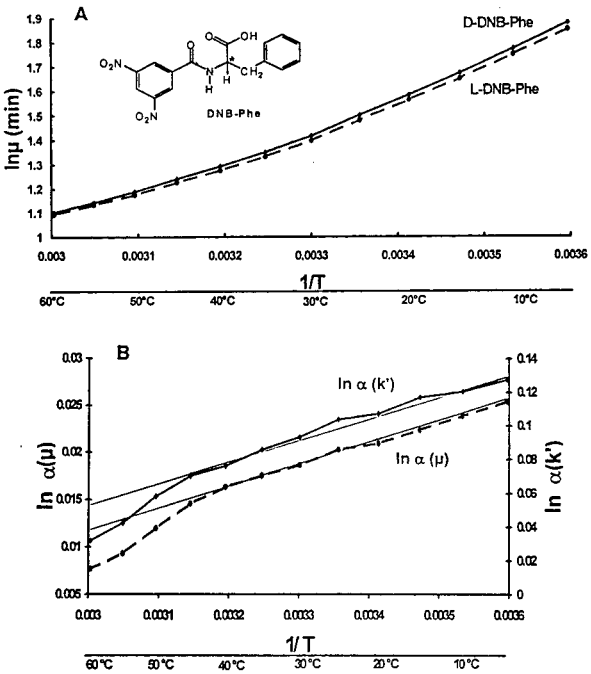

Fig. 6. Van 't Hoff plots showing the non-linear behavior of temperature on the separation of DNB-Phe enantiomers (100 ppm racemate in methanol) using HP-β-CD (30 mM) as a chiral selector. CE parameters: fused-silica capillary 70 cm × 50 μm I.D., 20 kV electrode voltage, electrolyte buffer was sodium tetraborate 20 mM, pH 9.2. (A) Relationship of migration behavior as ln μ versus $1/T$. (B) Relationship of discrimination behavior as ln α versus $1/T$. The separation factor α was calculated as quotient of the two migration times or alternatively to compensate for the EOF as quotient of k' values. The linearity regions are presented by the parallel linear lines.

difference ($\Delta\Delta S$) of the inclusion interaction following the equation:

$$\ln \alpha = -\frac{\Delta\Delta H}{RT} + \frac{\Delta\Delta S}{R}$$

From the non-linear relationship of ln μ versus $1/T$ of our results (Fig. 6A) one might conclude that the migration behavior of the diastereomeric complexes is also significantly influenced by the contribution of entropy to the CD-complex formation with our model amino acid derivatives. A Van 't Hoff plot of ln α versus $1/T$ (Fig. 6B) shows an approximately linear relation in the temperature range from 5 to 40°C. Exceeding this temperature range to higher temperatures resulted in a significant change in the migration behavior and consequently separation of the diastereomeric complexes as a result of additional, predominantly entropy-controlled, effects.

The unusual temperature dependency of these entropy factors might mainly be attributed to temperature-controlled changes in the bulk liquid structure and viscosity thus affecting the rotational and translational degrees of freedom of the host–guest associates and/or to a significantly changed mechanism of interaction (e.g. inclusion-type complex formation is replaced by electrostatic hydrogen bonding at the exterior CD surface). Calculation or prediction of these effects, however, remains difficult. Consequently, the calculation of thermodynamic parameters ($\Delta\Delta H$, $\Delta\Delta S$), as reported for HPLC-type separation using covalently bonded β-CD chiral stationary phase [38], via extrapolation of the linear part of the curve appears to be questionable.

Recently, Lamparczyk and co-workers [39–41] found a non-linear relationship of capacity factor (ln k') versus reciprocal of absolute temperature using β-CD modified mobile phase for the separation of estradiol and other stereoisomers by HPLC. According to this work the mentioned phenomenon seems to be more complex but without any doubt relevant.

Undoubtedly, this non-linear relationship of ln k' versus $1/T$ is the result of many temperature-dependent parameters i.e. expansion of the liquid, resistance due to the change in the conductivity of the running buffer, which itself arises from the change in the viscosity of the buffer, the electroosmotic and the electrophoretic mobilities and the complexation constants of the reversible diastereomerical enantiomer–CD complex.

Further, recent computational studies on the dynamical features of CDs brought into light that CDs can no longer be seen as a rigid cone, but more likely as a flexible, twisting basket [42], which also allows an induced fit of the guest molecule. Obviously, these dynamical features are strongly temperature controlled and may also enhance the contribution of the complexation

entropy to the molar Gibbs energy and consequently to the separation factor α.

However, dynamical features of CD and changes of the interaction from host–guest type to electrostatic hydrogen bonding of the exterior CD surface have been thoroughly discussed before on the basis of molecular modelling (MM) calculations [43] and results from MM have to be applied precautiously in CE, regarding the aqueous system of CE.

The influence of temperature on chiral separation in modified capillaries using CD or CD derivatives as chiral selectors could be studied in more detail, concerning the fact that the performance of chiral separations is strongly influenced by alteration of surface coating [44,45] referring not only the chiral separation of bases but also of organic acids.

However, these results stand in contrast to the experiments by Nielen [23] where hardly any differences and certainly no improvements with a C_{18}-coated capillary could be achieved by separating racemic drugs by CD and CZE.

3.7. Effect of modifiers on separation

Organic modifiers added to the electrolyte buffer system are in many cases reported to facilitate a "finetuning" of enantiomeric separations. We have studied this effect on the enantiomeric separations of DNP-, DNB- and AQC-amino acids adding 20% (v/v) methanol alone and in combination with 1% (v/v) *tert.*-butyl methyl ether or alternatively 5 m*M* carnitin to a sodium tetraborate (20 m*M*, pH 7–9) background electrolyte system with 30 m*M* HP-β-CD as chiral selector at a capillary temperature of 10°C.

The influence of methanol on the enantiomeric separation of DNP, DNB and AQC derivatives of the model amino acid phenylalanine is depicted in Figs. 7 and 8. There was a significant increase in migration time of DNB- and DNP-amino acids of ca. 40%, which could be attributed to the decreased EOF, probably via interaction of the modifier with the capillary wall thus altering charge and hydrophobicity, and consequently changing ζ potential as a driving force of EOF.

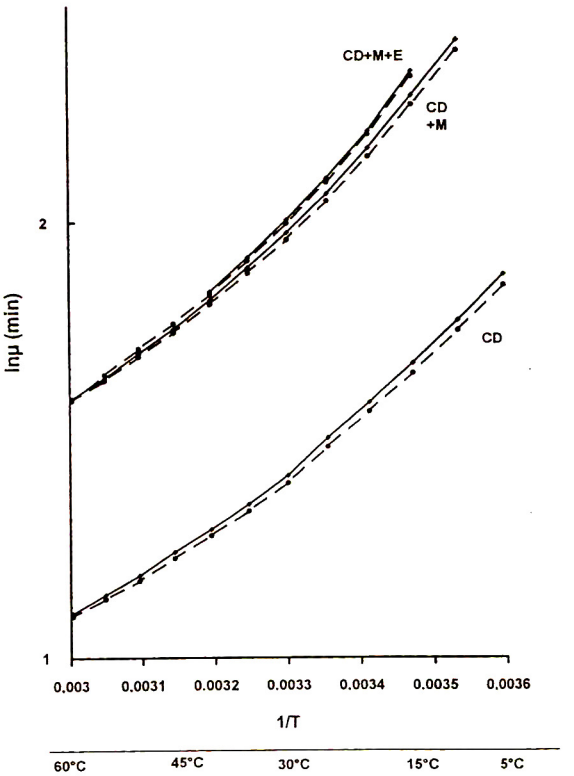

Fig. 7. Van 't Hoff plots showing the influence of different modifiers at variable temperatures on migration and on the separation of DNB-Phe enantiomers (100 ppm racemate in methanol) using HP-β-CD (30 m*M*) as a chiral selector. CE parameters: fused-silica capillary 70 cm × 50 μm I.D., 20 kV electrode voltage, electrolyte buffer was sodium tetraborate 20 m*M*, pH 9.2, without modifier (CD), or alternatively with addition of 20% (v/v) methanol (CD + M) or alternatively with addition of 20% (v/v) methanol and 1% (v/v) *tert.*-butyl methyl ether in combination (CD + M + E).

Moreover the addition of methanol enabled enantiomeric separations of DNP-Asp, DNP-Phe, DNP-Pro, DNP-His and DNP-Try, which could not be accomplished without the modifier. Accordingly, the modifier effect cannot be simply reduced to the influence on EOF. An additional effect on chiral recognition mechanism via interaction with the selector and/or the analyte can be assumed. Also, the change in bulk liquid viscosity and consequently diffusion velocity

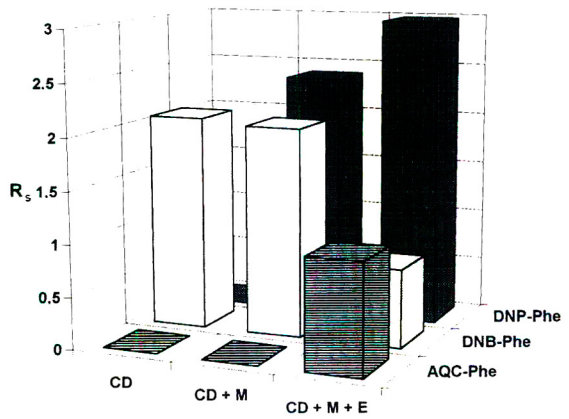

Fig. 8. Modifier effects on the CZE separation of different (*R*)- and (*S*)-Phe derivatives (100 ppm racemate in methanol) using HP-β-CD (30 m*M*) as a chiral selector. CE parameters: fused-silica capillary 70 cm × 50 μm I.D., 20 kV electrode voltage, 10°C capillary temperature, electrolyte buffer was sodium tetraborate 20 m*M*, pH 9.2 for DNB-Phe and DNP-Phe and pH 7 for AQC-Phe. The additives used were 20% (v/v) methanol (M) or 1% (v/v) *tert.*-butyl methyl ether (E).

and/or interaction kinetics should not be neglected.

The additive *tert.*-butyl methyl ether did not significantly improve resolution of DNP- and DNB-amino acids, with DNP-Phe as a single exception of the rule (Fig. 8).

As to the enantiomeric separation of AQC-amino acids the methanol effect on EOF was negligible, due to the lower pH revealing a priori low EOF conditions. But, as shown in this contribution, the combination of methanol and *tert.*-butyl methyl ether rendered possible enantiomeric separations of AQC-Phe, AQC-His, AQC-Cit and AQC-Ser, which have not been accomplished with methanol or without any modifier.

As a result, organic additives proved to be a useful tool to increase resolution and sometimes even to make a separation possible, which always has to be paid for by prolonged analysis time due to the lower EOF.

The use of 5 m*M* L-carnitin as an organic modifier improved resolution of DNP-Phe and AQC-Leu, whereas resolution of DNB-Phe was decreased. The assumed interaction of the zwitterionic and quaternary amine type compound L-carnitin with the silanol groups of the fused-silica capillary, consequently altering the direction of EOF, was obviously overlaid by other interaction equilibria between the CD selector, the electrolyte system, the modifier and the analyte. Further studies are planned to elucidate the complex mechanism of interactions with this unusual modifier.

In general, the prediction of modifier effects seems to be hampered by the high complexity of the various equilibria involved. Consequently, the successful application of organic modifiers for resolution enhancement in CD CE relies still on "trial and error".

4. Conclusions

CDs of different cavity size (α-, β-, γ-CD) have proved to be effective chiral selectors for the enantiomeric separation of various α-amino acid derivatives by CZE. Their potential for the separation of a wide range of chemical different structures was even enhanced by the use of chemical modified (HP and Me) CDs showing improved solubility in aqueous electrolyte buffer systems and facilitating chiral recognition mechanism. This work also demonstrates the influence of several experimental conditions on enantiomeric separations, such as type of buffer, electrolyte pH, CD concentration, organic modifiers, applied voltage and capillary temperature. Table 2 is an attempt to give a general guideline for sufficient enantiomeric separation of various α-amino acids by CE using suitable derivatization methods, appropriate types of CD, different modifiers and optimized CE parameters. However, the prediction of optimum conditions based on the chemical structures of the analytes remains difficult.

Acknowledgements

We gratefully acknowledge Hewlett-Packard (Vienna, Austria) for the instalment of their

Table 2
General guideline for sufficient enantiomer separation of α-amino acids by CD CZE using suitable derivatization methods, appropriate types of CD, different modifiers and optimized CZE parameters

Amino acid	AQC	DNP	DNB	Dns	CBZ	FMOC
Ala	HP-β-CD + M + E	HP-β-CD + M	–		γ-CD	Me-β-CD
Val	HP-β-CD + M + E	HP-β-CD + M		γ-CD		γ-CD + M
Nva	HP-β-CD + M + E	HP-β-CD + M + E				
Leu	HP-β-CD + M + E	HP-β-CD + M	HP-β-CD + M	HP-γ-CD, β-CD	HP-β-CD	γ-CD + M
Ile	–	HP-β-CD + M				
Nle	HP-β-CD + M + E	–				
Phe	HP-β-CD + M + E	HP-β-CD + M	HP-β-CD, β-CD	–		γ-CD + M
Pro	HP-β-CD + M	HP-β-CD + M	–			
Ser	HP-β-CD + M + E	HP-β-CD + M	–	–		
Thr	HP-β-CD + M	HP-β-CD + M				
Cys	–	–				
Met	HP-β-CD + M	HP-β-CD + M		γ-CD		
Trp	–	HP-β-CD + M				
Tyr	HP-β-CD + M + E	–				
Asn	HP-β-CD + M + E	–				
Gln	–	HP-β-CD + M				
Asp	–	–				
Glu	–	–				
Lys	HP-β-CD + M + E	–				
Arg	–	–				
His	HP-β-CD + M + E	HP-β-CD + M				
GABA	–	–		γ-CD		

CE parameters: uncoated fused-silica capillary 70 cm × 50 μm I.D., 20 kV electrode voltage, 10°C capillary temperature, electrolyte buffer was sodium tetraborate 20 m*M*, pH 9.2, and for DNP and AQC derivatives sodium phosphate 70 m*M*, pH 7, the concentration of the chiral selector (CD) was 30 m*M* except for β-CD (max. solubility 15 m*M*), analyte concentration 100 ppm in methanol, UV detection at 214 nm and at 280 nm for AQC. GABA = γ-aminobutyric acid; HP-CD = hydroxypropylated cyclodextrin; Me-CD = methylated cyclodextrin; + M = addition of 20% (v/v) methanol; + E = addition of 1% (v/v) *tert.*-butyl methyl ether; – = no results due to derivatization, solubility or separation problems; blank cells not tested, yet.

HP^{3D} CE system in our laboratories for a limited time.

Further acknowledgement is made to the Austrian Fonds zur Förderung der wissenschaftlichen Forschung, project No. P-8898-CHE for the support of this project and the scholarship of B.B.

References

[1] J.W. Jorgenson and K.D. Lukacs, *Anal. Chem.*, (1981) 1298–1302.
[2] S. Terabe, K. Otsuka and H. Nishi, *J. Chromatogr. A*, 666 (1994) 295–319.
[3] H. Nishi, T. Fukuyama and S. Terabe, *J. Chromatogr.*, 553 (1991) 503–516.
[4] S. Terabe, M. Shibata and Y. Miyashita, *J. Chromatogr.*, 480 (1989) 403–411.
[5] K. Otsuka and S. Terabe, *J. Chromatogr.*, 515 (1990) 221–226.
[6] A. Dobashi, T. Ono and S. Hara, *Anal. Chem.*, 61 (1989) 1986–1988.
[7] P. Gozel, E. Gassmann, H. Michelsen and R.N. Zare, *Anal. Chem.*, 59 (1987) 44–49.
[8] E. Gassmann, J.E. Kuo and R.N. Zare, *Science*, 230 (1985) 813–814.
[9] S. Fanali, L. Ossicini, F. Foret and P. Boček, *J. Microcol. Sep.*, 1 (1989) 190–194.
[10] R. Kuhn, F. Stoecklin and F. Erni, *Chromatographia*, 33 (1992) 32–36.
[11] J. Snopek, H. Soini, M. Novotny, E. Smolkova-Keulemansova and I. Jelínek, *J. Chromatogr.*, 559 (1991) 215–222.
[12] S. Birnbaum and S. Nilsson, *Anal. Chem.*, 64 (1992) 2872–2874.

[13] S. Terabe, Y. Miyashita, Y. Ishihama and O. Shibata, *J. Chromatogr.*, 636 (1993) 47–55.
[14] A.D. Hulst and N. Verbeke, *J. Chromatogr.*, 608 (1992) 275–287.
[15] S. Terabe, H. Ozaki, K. Otsuka and T. Ando, *J. Chromatogr.*, 332 (1985) 211–217.
[16] S. Fanali, *J. Chromatogr.*, 545 (1991) 437–444.
[17] S. Fanali, *J. Chromatogr.*, 474 (1989) 441–446.
[18] S. Fanali and P. Boček, *Electrophoresis*, 11 (1990) 757–760.
[19] A. Pluym, W. Van Ael and M. de Smet, *Trends Anal. Chem.*, 11 (1992) 27–32.
[20] T.L. Bereuter, *LC · GC*, 12 (1984) 748–766.
[21] T.E. Peterson and D. Towbridge, *J. Chromatogr.*, 603 (1992) 298–301.
[22] M.E. Swartz, *J. Liq. Chromatogr.*, 14 (1991) 923–938.
[23] M.W.F. Nielen, *Anal. Chem.*, 65 (1993) 885–893.
[24] H. Nishi, Y. Kokusenya, T. Miyamoto and T. Sato, *J. Chromatogr. A*, 659 (1994) 449–457.
[25] T. Schmitt and H. Engelhardt, *Chromatographia*, 37 (1993) 475–481.
[26] T.E. Peterson, *J. Chromatogr.*, 630 (1993) 353–361.
[27] J. Prufionosa, R. Obach, A. Diez-Cascón and L. Gouesclou, *J. Chromatogr.*, 574 (1992) 127–133.
[28] T. Ueda, F. Kitamura, R. Mitchell, T. Metcalf, T. Kuwana and A. Nakamoto, *Anal. Chem.*, 339 (1991) 63–64.
[29] S.A.C. Wren and R.C. Rowe, *J. Chromatogr.*, 603 (1992) 235–241.
[30] S.A.C. Wren and R.C. Rowe, *J. Chromatogr.*, 609 (1992) 363–367.
[31] S.A.C. Wren, *J. Chromatogr.*, 636 (1993) 57–62.
[32] S.A. Cohen and D.P. Michaud, *Anal. Biochem.*, (1993) in press.
[33] C. Quang and M. Khaledi, *Anal. Chem.*, 65 (1993) 3354–3358.
[34] D.W. Armstrong, T.J. Ward, R.D. Armstrong and T.E. Beesley, *Science*, 232 (1986) 232–235.
[35] P.J. Oefner, A.E. Vorndran, E. Grill, C. Huber and G.K. Bonn, *Chromatographia*, 34 (1992) 308–316.
[36] J.H. Knox and K.A. McCormack, *Chromatographia*, 38 (1994) 279–282.
[37] R. Kuhn, F. Erni, T. Bereuter and J. Häusler, *Anal. Chem.*, 64 (1992) 2815–2820.
[37] K. Cabrera and D. Lubda, *J. Chromatogr. A*, 666 (1994) 433–438.
[38] H. Lamparczyk and P.K. Zarzycki, presented at the *5th International Symposium on Chiral Discrimination, Stockholm, 25–28 September 1994.*
[40] D. Sybilska, M. Asztemborska, A. Bielejewska, J. Kowalczyk, H. Dodziuk, K. Duszczyk, H. Lamparczyk and P. Zarzycki, *Chromatographia*, 35 (1993) 637–642.
[41] H. Lamparczyk, P.K. Zarzycki and J. Nowakowska, *J. Chromatogr. A*, 668 (1994) 413–417.
[42] K.B. Lipkowitz, *J. Chromatogr. A*, 694 (1995) 15.
[43] D.G. Durham and H. Liang, *Chirality*, 6 (1994) 239–244.
[44] D. Belder and G. Schomburg, *J.Chromatogr. A*, 666 (1994) 351–365.
[45] D. Belder and G. Schomburg, *J. High Resolut. Chromatogr.*, 15 (1992) 686.

ELSEVIER

Journal of Chromatography A, 697 (1995) 561–570

JOURNAL OF CHROMATOGRAPHY A

Optimization of enantiomeric separations in capillary electrophoresis by reversal of the migration order and using different derivatized cyclodextrins

Thomas Schmitt*, Heinz Engelhardt

Institute for Applied Physical Chemistry, University of the Saarland, 66123 Saarbrücken, Germany

Abstract

In CE it is easy to optimize the elution order of enantiomeric pairs by reversal of the migration order. Several methods to achieve migration reversal for cationic as well as anionic enantiomers have been investigated. In principle three different approaches can be used. Firstly, electroosmotic flow can be reversed using different additives in the electrolyte buffer. Secondly, selecting different cyclodextrins as chiral additives can also reverse the migration order because of different separation and complexation mechanisms. Especially derivatized cyclodextrins have a great potential for this application and additionally contribute to the number of chiral selectors available in CE. In the third case, chargeable cyclodextrins offer the possibility for migration order reversal by varying the pH value.

1. Introduction

The separation of enantiomers has been a challenging area of research in the field of separation science. Nowadays many analytical methods are available for the separation of enantiomers such as HPLC, supercritical fluid chromatography (SFC), GC and recently CE. CE has already been established for chiral analysis. This is reflected by many reviews and applicative work in this field [1–5]. The reasons for the fast breakthrough are certainly low analysis costs, fast method development and easy handling of ionic or ionogenic analytes without previous derivatisation. In order to expand the applicability of the analysis of chiral compounds by CE the search for new types of chiral selectors is still a main area of research. Terabe et al. [6] introduced micelle forming detergents for the separation of enantiomers. Fanali and co-workers [3,7] employed derivatized neutral and cationic cyclodextrins as chiral selectors. Smith [8] and Schmitt and Engelhardt [9,10] used derivatized anionic cyclodextrins for the separation of neutral and cationic enantiomers. Bile salts were introduced by Nishi et al. [11]. Birnbaum and Nillson [12] and Valtcheva et al. [13] focused on proteins as chiral additives. Aiken and Huie [14] used small chiral compounds incorporated into a micelle to generate a chiral selector. Dextrins were introduced by D'Hulst and Verbecke [15] for the separation of enantiomers. Chiral stationary phases bound to the capillary wall were investigated by Meyer and Schurig [16].

The reversal of the migration order of enantiomers is also an important issue, especially when

* Corresponding author.

0021-9673/95/$09.50
SSDI 0021-9673(94)00838-8

impurities have to be detected and the mobility differences to the main peak are small. As in HPLC, SFC and GC the main component can disturb the analysis of the minor component in the case of overloading of the system or because of tailing peaks. Therefore it is advantageous to detect impurities as the first migrating peak in a chromatogram. With chromatographic methods this can only be achieved by choosing another stationary phase i.e. preparing another column with the other enantiomer which might be tedious and expensive. Asymmetrical peaks in CE are a result of two different mechanisms. The first one is based on slow adsorption–desorption equilibria of the analyte and the capillary wall resulting always in a tailing peak. The second one is due to electrodispersion coming from conductivity-mismatch between the sample zone and the surrounding buffer. This results in triangular fronting or tailing analyte peaks because the mobility of the buffer electrolyte does not match to the mobility of the analyte. Also the concentration of the buffer can be too low and the observed peak shape is a result of overloading. Triangular peaks generated by a non-optimized background electrolyte (buffer) will only be briefly discussed. So it is very important in the determination of optical purity to change easily the elution order to have the trace component on the asymmetric side of the peak.

One elegant way for reversal of the migration order for any analyte is to reverse the electroosmotic flow (EOF). Many different ways have been described in literature so far. Huang et al. [17], Jones and Jandik [18] and Yao et al. [19] used long-chained cationic surfactants for the reversal of the EOF via formation of a double layer on the capillary surface. Adsorbed cationic polyamines were employed by Beck [20], and immobilized cationic coatings on the inner capillary wall were introduced by Towns and Regnier [21] and Huang et al. [22]. Also the application of a second external electric field outside the capillary has been described by Lee and coworkers [23,24]. The last two methods are somewhat critical. So far charged coatings on the capillary wall seem not to be stable over a long time. The use of a second external electric field needs a more difficult instrumental set-up and is still not available in any commercial instrument. The latter method works only at low pH values with low ionic strength of the running buffer.

Micellar electrokinetic chromatography (MEKC) is also a suitable tool for the reversal of the migration order as long as detergents of derivatized amino acids are used. These chiral selectors were introduced by Terabe and coworkers [25,26] and later improved by Mazzeo et al. [27]. Employing the pure (+) or the pure (−) detergent as micelle-forming agents, the migration order can easily be changed. As in HPLC, this method corresponds to the reversal of the chiral environment, and requires both types of enantiomeric detergents.

In this paper we will discuss the application possibilities of spermine, spermidine and cetyltrimethylammonium bromide (CTAB) as potential flow reversal agents together with cyclodextrins (CDs) as chiral selectors for the separation of anionic enantiomers. Furthermore, different derivatized CDs at different pH values were used for the separation of cationic enantiomers. In some cases the nature of the derivatisation as well as the buffer pH was found to revers the migration order of some enantiomers. Since many new types of CDs have been introduced here the nature of this paper is not only focused on the reversal of the migration order but also to expand the number of selectors in CE. The reversal of the migration order with the CD concentration has been already described elsewhere [10].

2. Experimental

Fused-silica capillaries (75 μm I.D.) were obtained from Polymicro Technologies (Phoenix, AZ, USA) and coated with 4% T [T = (g acrylamide + g N,N′-methylenebisacrylamide)/100 ml solution] linear polyacrylamide following a procedure described by Hjertén [28]. For coating the capillary was treated overnight with a 50% (v/v) methacryloxypropyl–trimethoxysilane solution in methanol. Afterwards a degassed solution of 4% (w/v) T acrylamide in 0.1 *M* Tris–boric acid (2 m*M* EDTA) pH 8.2 containing 5 μl of a 10% (w/v) ammonium persul-

Table 1
Characteristics of the cyclodextrins used

Type of cyclodextrin	Degree of derivatisation (molecules per CD ring)	Average M_r (g/mol)	Average formula
Hydroxypropylated β-CD	6.3	ca. 1500	$C_{61}H_{108}O_{41}$
Heptakis (di-O-methyl) β-CD	14	1331	$C_{56}H_{98}O_{35}$
Carboxymethylated β-CD	3.6	ca. 1340	$C_{49}H_{77}O_{42}$
Carboxymethyl β-CD-polymer		ca. 8700	$C_{49}H_{77}O_{42}$
Carboxyethylated β-CD	ca. 6	ca. 1570	$C_{60}H_{94}O_{47}$
Succinylated β-CD	3.5	ca. 1490	$C_{56}H_{84}O_{46}$

fate solution and 5 μl of a N,N,N′,N′-tetraethylmethylendiamine solution per ml acrylamide solution was filled into the capillary. After polymerisation the formed gel inside the column was pressed out leaving a coating at the inner capillary wall. As long as buffers up to pH 7 were used this coating was stable for several months. The stability of the coating was determined by the absence of a significant EOF. The CD derivatives employed in this paper are summarized in Table 1. The data with the degree of modification were obtained from the manufacturer. The hydroxypropyl CDs were obtained from Wacker Chemie (Germany). All other CDs were bought from Cyclolab (Budapest, Hungary). The enantiomers used (Fig. 1) were kind gifts of Professor Knabe and Dr. Dorfmüller from the Pharmaceutical Department and of Dr. Maurer from the Clinical Department of our university. Deionised water from a Milli-Q system (Millipore) was used for buffer preparation. Chemicals such as spermine tetrahydrochloride [$H_2N(CH_2)_3NH(CH_2)_4NH(CH_2)_3NH_2 \cdot 4HCl$], spermidine trihydrochloride [$H_2N(CH_2)_4NH(CH_2)NH2 \cdot 3HCl$] and CTAB were obtained from different suppliers and were all of analytical grade. The experiments were performed on a P/ACE system 2000 (Beckman Instruments, Fullerton USA) and a HP^{3D} CE system (Hewlett-Packard, Waldbronn, Germany).

3. Results and discussion

The possibility to detect cations as well as anions in one electrophoretic run is due to the presence of a strong EOF in an untreated fused-silica capillary. Since a regular EOF is directed towards the cathode all cations are detected in front of the EOF (the fastest ions first) while the anions migrating slower than the EOF are detected behind the EOF (the fastest anions last) in an electropherogram. This means that reversing the EOF, and also reversing the polarity of the electrodes should result in a reversed migration pattern of the analyte, i.e. the fastest anions are first and the fastest cations are detected last in an electropherogram. Long-chained tetraalkylammonium compounds with a chain length of C_{10} to C_{20} are well known in CE as additives for the reversal of the EOF. CTAB was tested here as a potential flow reversal agent together with β- and hydroxypropyl β-CD. As demonstrated in Fig. 2 CTAB is not able to change the direction of the EOF when β-CDs and their derivatives are present in the running buffer. A similar behaviour was found by Quang and Khaledi [29] for basic cationic enantiomers at low pH values using β-CD and CTAB. In our case anions were separated at high pH values (pH 8.3). Fig. 2A shows the separation obtained without any CTAB added to the buffer. All anions migrate behind the EOF and were separated using hydroxypropyl β-CD. The same buffer system with a concentration of 0.5 m*M* CTAB, which is a very suitable concentration for an EOF reversal, does not give the expected result. The EOF is still directed towards the cathode. Increasing the CTAB concentration results only in a decrease of the velocity of the EOF and therefore longer analysis time. Without any cyclodextrin in the buffer, 0.5 m*M* CTAB is sufficient to revers the EOF and all analytes are detected in the reversed migration order (not

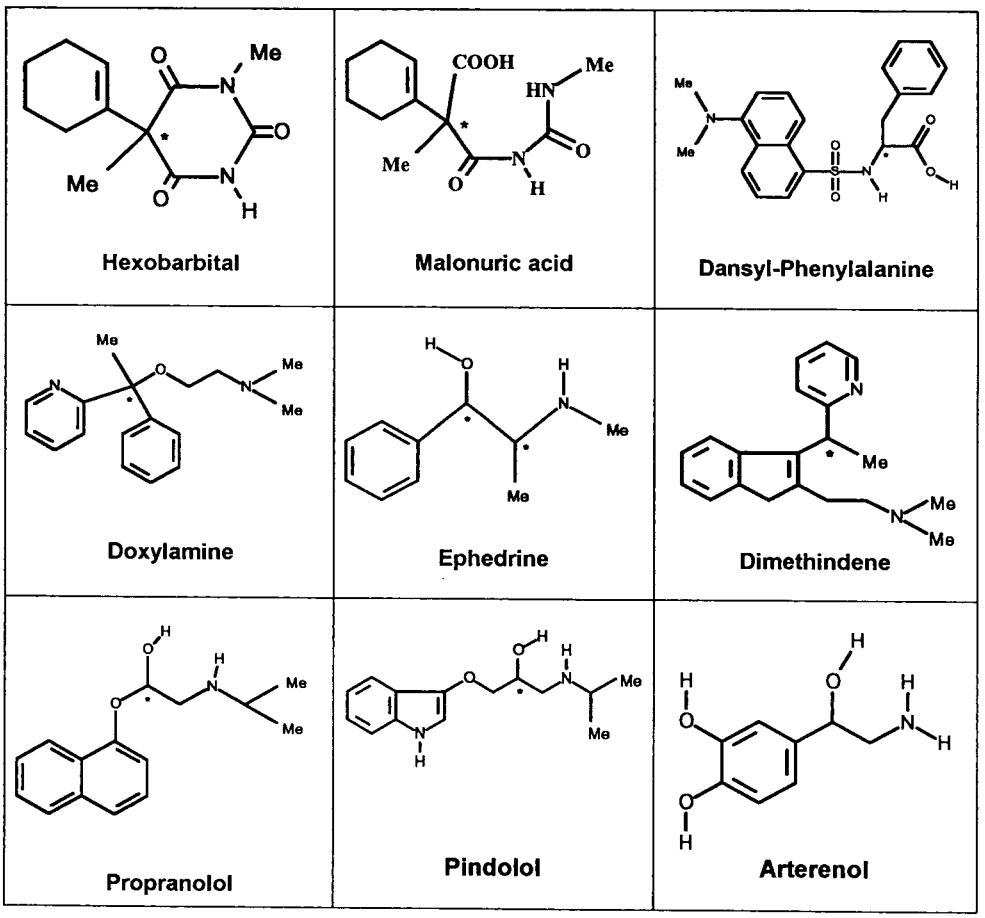

Fig. 1. Structures of the samples.

shown here) but without chiral resolution because no chiral selector is added. Even at a concentration of 1 m*M* CTAB which is above the critical micellar concentration (CMC) of CTAB the EOF is still not reversed (Fig. 2C). The faster migrating analytes [last in an electropherogram (peak 3)] are no longer detected in the given time because the EOF is too slow under these conditions. This clearly indicates that there is a mechanism preventing the CTAB from forming a double layer at the inner surface of the capillary wall. This can be explained by the inclusion of the long alkyl chain of CTAB into the cavity of the CD which results in a lower effective concentration in free solution and therefore increasing the CMC of the detergent and also hindering the formation of the double layer at the capillary wall.

Peak 3 in Fig. 2A and B represents a degradation product of hexobarbital (peak 1) which comes from alkaline hydrolysis of this urea derivative. During hydrolysis of (−)-hexobarbital the optical rotation is changing from the (−)-form to (+)-malonuric acid [30]. Although the steric configuration around the asymmetric carbon atom stays the same during the hydrolysis the complexing properties for the hydrolysis product to the CD have changed dramatically. Ring hydrolysis of the (−)-hexobarbital and the generation of additional functional groups with high hydrogen-bonding capabilities (carboxylic groups and amid groups) result in stronger bind-

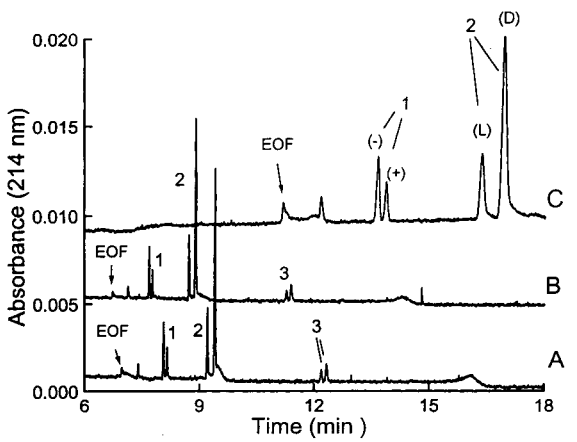

Fig. 2. Influence of CTAB as an EOF flow modifier on the migration direction of the analyte. Run conditions: 67 cm (60 cm to detector) × 75 μm I.D. uncoated capillary, 370 V/cm, 100 m*M* Tris–boric acid pH 8.35. Sample: hexobarbital spiked with (−)-hexobarbital (1), dansyl-phenylalanine spiked with D-dansyl-phenylalanine (2), hydrolysis product of hexobarbital (3), detection at the cathodic end (cathodic EOF in all cases). Instrument: P/ACE 2000. (A) buffer contains 1% (w/v) hydroxypropyl β-CD without CTAB; (B) as (A) but with 0.5 m*M* CTAB; (C) as (A) but with 1 m*M* CTAB.

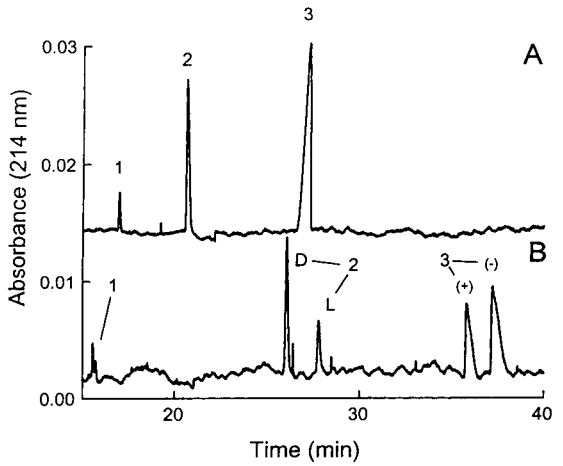

Fig. 3. Influence of spermidine as a flow modifier on the migration direction of the analytes. Run conditions: 67 cm (60 cm to detector) × 75 μm I.D. capillary, 25°C, buffer: 100 m*M* Tris, 100 m*M* boric acid pH 8.3 containing 5 m*M* spermidine hydrochloride, detection at 214 nm. Sample: hydrolysis product of hexobarbital (1) (from alkaline hydrolysis of hexobarbital), dansyl-phenylalanine spiked with D-dansyl-phenylalanine (2), hexobarbital spiked with (−)-hexobarbital (3). Instrument: P/ACE 2000. (A) Applied voltage: 20 kV, no cyclodextrin added to the buffer, detection at the anodic end (anodic EOF); (B) applied voltage: 25 kV, 0.7% (w/v) of hydroxypropyl β-CD added to the buffer, detection at the anodic end (anodic EOF).

ing of the (+)-malonuric acid to the CD. This also demonstrates that small changes in the spacial configuration away from the chiral center as well as the rotation freedom around the same asymmetric carbon atom can have a very strong effect on the stability of the CD–analyte complex. As a result the separation of this analyte may stay the same, or being lost, or even reversed although the absolute configuration on the chiral center stays the same.

Employing a concentration of 5 m*M* spermidine in the running buffer without CD added, the EOF as well as the migration order of the analyte could be reversed (towards the anode). This is shown in Fig. 3A. In Fig. 3B, hydroxypropyl β-CD was added to the same buffer as used in Fig. 3A. It can be seen that enantiomeric separation is achieved and the migration order of all enantiomers is reversed compared to the electropherogram shown in Fig. 2A. Although the buffers were filtered and all reagents were of analytical grade the baseline was found increasingly noisy with analysis time. This baseline noise could be reduced by exchanging spermidine with spermine as a flow modifier in the running buffer. Fig. 4A shows the EOF in direction to the cathode without spermine while in Fig. 4B the EOF is oriented towards the anode after addition of this amine to the buffer. The migration order of the enantiomers has been changed under these conditions; however, including the appearance of the EOF, analysis time has doubled. The advantages of the flow reversal in CE can be seen in Fig. 5. It shows the separation of impurities of hexobarbital with (left electropherogram) and without (right electropherogram) reversal of the EOF. It is shown that the migration order of all analytes is reversed when reversing the EOF. Beside the hydrolysis products other impurities which may be residues from the manufacturing process are also detectable. The sum of peak areas of these impurities are in the 0.1% range compared to the main peaks. Employing the regular mode

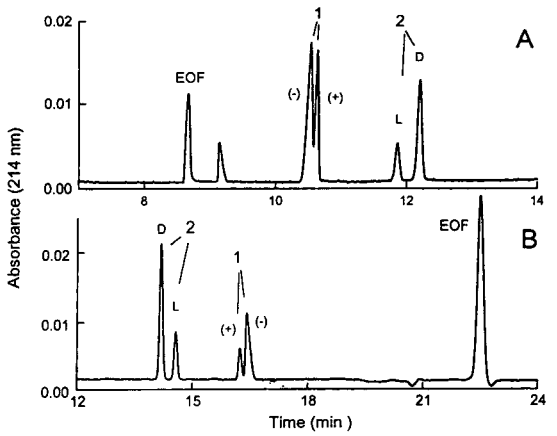

Fig. 4. Influence of spermine as a flow modifier on the migration direction of the analytes. Run conditions: 67 cm (60 cm to detector) × 75 μm I.D. capillary, 25°C, applied voltage: 20 kV, buffer: 100 m*M* Tris, 100 m*M* boric acid pH 8.3 containing 5 m*M* spermine hydrochloride, 0.7% (w/v) of hydroxypropyl β-CD added to the buffer, detection at 214 nm. Sample: hexobarbital spiked with (−)-hexobarbital (1), D,L-dansyl-phenylalanine spiked with D-dansyl-phenylalanine (2). Instrument: P/ACE 2000. (A) Detection at the cathodic end (cathodic EOF), no EOF flow modifier added; (B) buffer containing 5 m*M* spermine hydrochloride, detection at the anodic end (anodic EOF).

[anodic EOF (Fig. 5 on the right)] a further increase of the injected amount leads to distortion of all minor components and the components labelled as a, b, c comigrate with the main peak and cannot be analysed any more which would of course be possible if they are migrating in front of the main components.

Because the EOF has a very low anodic mobility when spermine and spermidine are employed, the analysis of fast moving cationic enantiomers cannot be achieved. For these analytes a very fast anodic EOF with the same velocity as the regular EOF would be appropriate. Therefore, in the following other methods are described for the reversal of the migration order. A mixture of 6 basic aromatic enantiomeric drugs have been used here to demonstrate and examine the separation capabilities of the different CDs as well as their selectivities in terms of changing the migration order. Fig. 6 shows the separation of the test mixture employing heptakis(2,6-di-O-methyl)-β-CD which is a widely used chiral selector so far. This selector was able to resolve four out of the six compounds. The (+)-ephedrine isomer was found

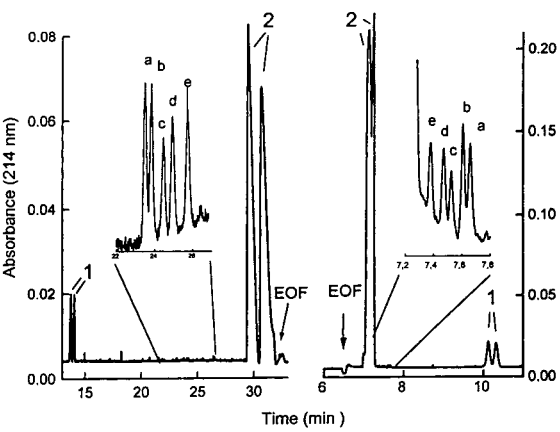

Fig. 5. Detection of impurities with cathodic and anodic electroosmotic flow. Run conditions: 57 cm (50 cm to detector) × 75 μm I.D. uncoated capillary, detection at 214 nm. Peaks: 1 = (±) hydrolysis product; 2 = (±)-hexobarbital; a, b, c, d, e = impuities. Instrument: P/ACE 2000. (A) 430 V/cm, buffer: 0.1 *M* TBE (Tris–boric acid–EDTA) pH 8.3, 1.56% (w/v) β-CD, cathodic EOF; (B) 170 V/cm, buffer: 0.1 *M* TBE pH 8.3, 1.56% (w/v) β-CD, 5 m*M* spermine · HCl, reversed polarity, anodic EOF.

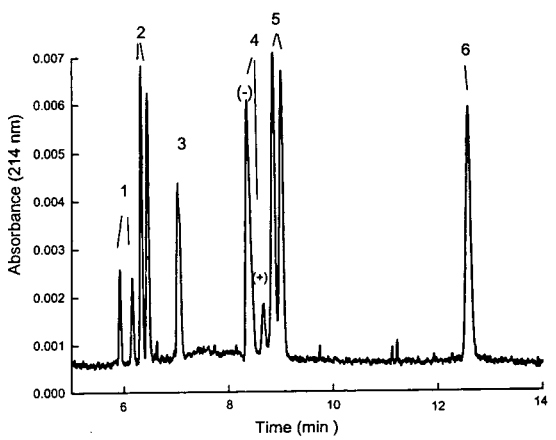

Fig. 6. Separation of basic amines using heptakis(di-O-methyl)-β-CD. Run conditions: 27 cm (20 cm to detector) × 75 μm I.D. coated capillary (linear polyacrylamide), 370 V/cm, 20 m*M* phosphate buffer pH 2.2 (adjusted with HCl and Tris), 30 m*M* heptakis(di-O-methyl)-β-CD. Instrument: P/ACE 2000. Peaks: 1 = arterenol; 2 = doxylamine; 3 = dimethindene; 4 = ephedrine, spiked with (−)-ephedrine; 5 = pindolol; 6 = propranolol.

to migrate behind the (−)-enantiomer [31]. Under the same experimental conditions the determination of optical impurities is hardly possible because the efficiencies in CE strongly depend on the sample loading of the column and the selectivity is not high enough to compensate for this. Therefore resolution is decreasing when higher sample amounts are injected. Employing the carboxymethylated β-CD, baseline resolution of all enantiomers could be achieved with much higher sample load (Fig. 7). Surprisingly, with this chiral selector the (+)-enantiomer of ephedrine migrates faster. This shows clearly that the affinity of enantiomers to CDs strongly depends on the type and degree of derivatisation on the CD. Also there is no need to reverse the migration order with CDs built of D-(−)-glucose instead of D-(+)-glucose units.

As discussed above trace analysis of optical impurities should be done in front of the main component especially when wall effects are observed. Since this is the case for (+)-ephedrine using the carboxymethylated β-CD, the overloading capability and the detection limit was studied for this compound in this buffer system. Furthermore a short coated column was used here to maintain high electric field strength, to speed up the analysis and reduce wall adsorption for these basic analytes [32]. As can be seen in Fig. 8 the detection of 0.3% of the (+)-ephedrine was possible beside the main component. Applying a longer capillary and therefore increased resolution should allow to increase the overloading of the column and achieve higher signals for both the main component and its optical impurity. By doing this the buffer capacity must be consequently increased to minimize electrodispersion due to high conductivity in the sample zones. In the reversal experiment the determination of the (−)-ephedrine in excess of the (+)-ephedrine was only possible in the 1–2% range under identical run conditions. Also a capillary with a three times extended light path at the detection point (75 μm I.D., 225 μm I.D.

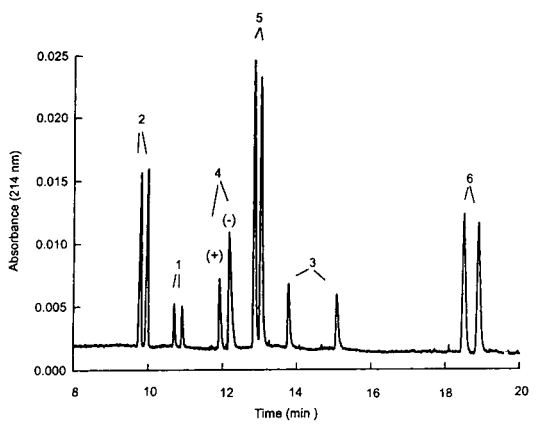

Fig. 7. Separation of basic amines using carboxymethyl β-CD. Run conditions: 67 cm (60 cm to detector) × 75 μm I.D. capillary, 340 V/cm, 20°C, 20 m*M* citric acid pH 2.5 containing 2% (w/v) of the CD. Instrument: P/ACE 2000, racemic mixtures of: doxylamine (2), arterenol (1), ephedrine (4) spiked with (−)-ephedrine, pindolol (5), dimethindene (3) and propranolol (6).

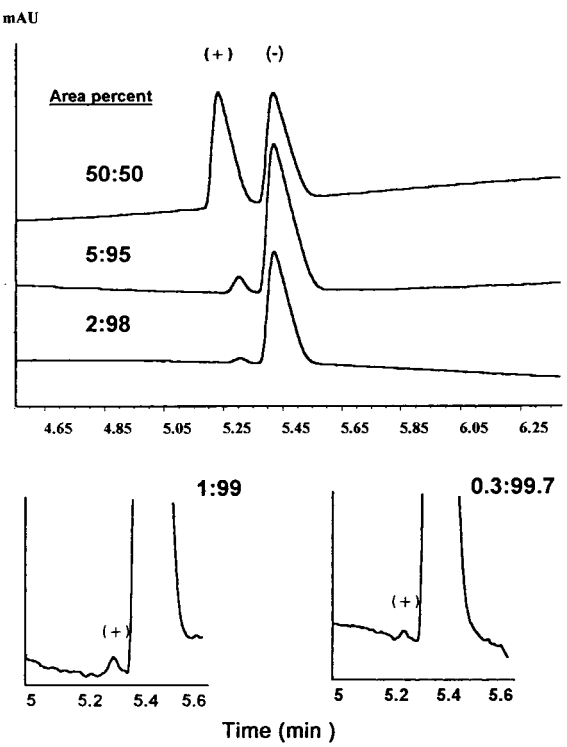

Fig. 8. Determination of the enantiomeric excess of (−)-ephedrine. Run conditions: 32.5 cm (32 cm to detector) × 75 μm I.D. fused-silica capillary with three times extended light path, 470 V/cm, capillary coated with 4% T linear polyacrylamide, pressure injection 10 mbar for 3 s each, 20 m*M* citric acid buffer pH 2.5 containing 2% (w/v) carboxymethylated β-CD. Instrument: HP^{3D} system.

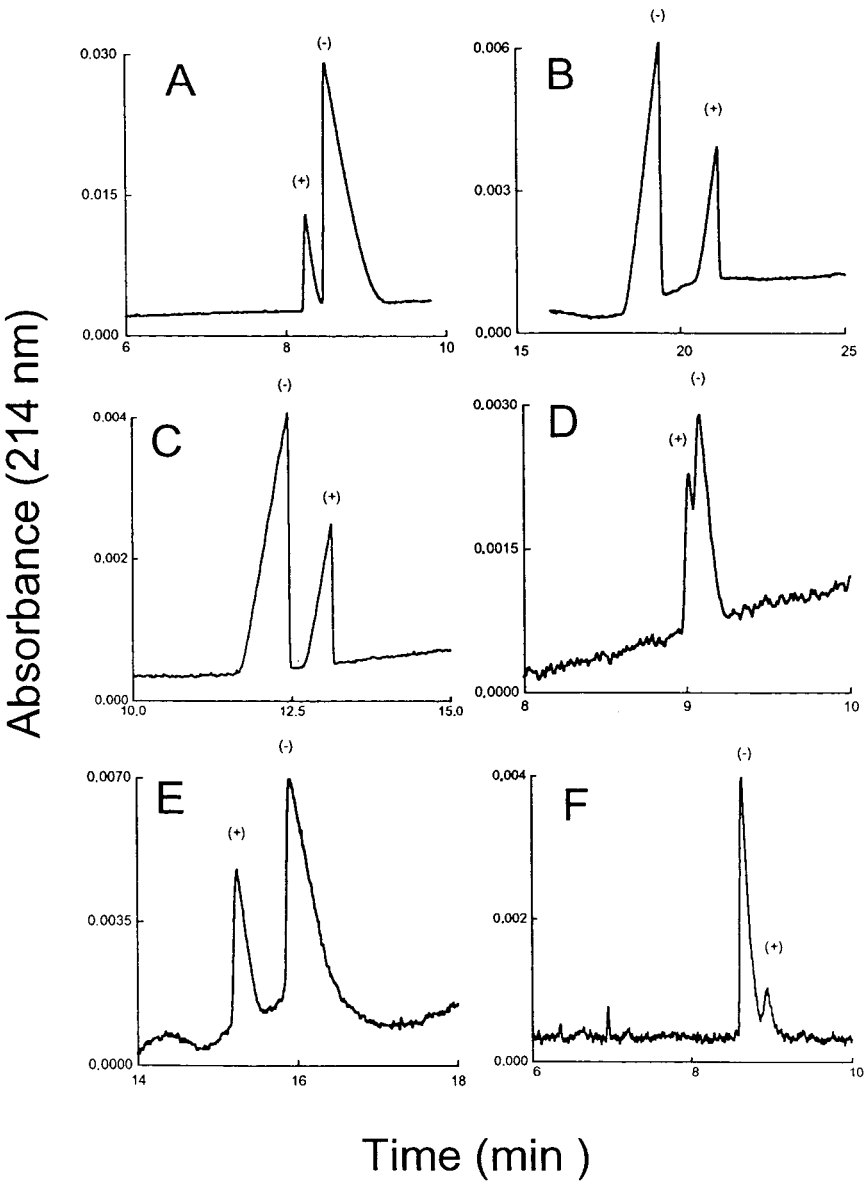

Fig. 9. Reversal of the migration order of enantiomers with pH. Run conditions: sample: ephedrine spiked with (−)-ephedrine, Instrument: P/ACE 2000, detection at 214 nm. (A) 27 cm (20 cm to detector) × 75 μm I.D. coated capillary, 370 V/cm, 25°C, buffer: 20 m*M* citric acid pH 2.8 containing 2% (w/v) carboxymethyl β-CD, detection at the kathodic end. (B) 37 cm (30 cm to detector) × 75 μm I.D. coated capillary, 270 V/vm, 20°C, buffer: 1.5% (w/v) carboxymethyl β-cyclodextrin adjusted to pH 7.2 with Tris, detection at the anodic end. (C) 27 cm (20 cm to detector) × 75 μm I.D. coated capillary, 370 V/cm, 20°C, buffer: 1% (w/v) carboxyethyl β-cyclodextrin adjusted to pH 6.2 with Tris, detection at the anodic end. (D) 37 cm (30 cm to detector) × 75 μm I.D. coated capillary, 540 V/cm, 25°C, buffer: 20 m*M* citric acid pH 2.2 containing 1.55% (w/v) succinyl β-cyclodextrin, detection at the cathodic end. (E) 37 cm (30 cm to detector) × 75 μm I.D. coated capillary, 270 V/cm, 25°C, buffer: 1% (w/v) succinyl β-cyclodextrin adjusted to pH 5.7 with Tris, detection at the cathodic end. (F) 27 cm (20 cm to detector) × 75 μm I.D. coated capillary, 370 V/cm, 25°C, buffer: 20 m*M* phosphate buffer pH 2.2 (adjusted with Tris and HCl) containing 2% (w/v) heptakis(2,6-di-O-methyl)-β-cyclodextrin, detection at the cathodic end.

at the detection point ("bubble cell") was used in this experiment giving a 3–5 times better signal-to-noise ratio compared to a non-expanded capillary.

Another way for reversal of the migration order is the use of charged CDs, where the charge can be altered by changing pH. CDs with carboxylic functions are deprotonated at pH values above pH 5 and the charge of the carboxylic group leads to an own mobility of the CDs. On the other hand at pH values below 3 the CD is no longer charged and behaves like a regular CD. At these pH values the enantiomer with the highest affinity to the chiral selector will be retarded longer and thus will show the slowest mobility. In the charged mode at higher pH values the CD can act as a carrier for the analytes with opposite charges and the stronger binding enantiomer will be detected first. These effects can be observed only if the introduced charge on the CD ring does not affect the enantiomeric selectivity. Also a higher number of charges are necessary on the CD to compensate for the analyte charges because neutral CD complexes are not transported to the detector. This would implicate a kind of ion-pairing mechanism. The strength of interaction of the solute with the CD is then responsible for the migration direction of the enantiomers.

Table 2 summarizes the possibilities of separation and the migration order of ephedrine with different CDs as chiral selectors at different pH values. All charged CDs show a different selectivity dependence on the pH value. Beside β-CD-phosphate (which is always charged) and heptakis(2,6-di-O-methyl)-β-CD (which is not charged at usual pH values) all other CDs show dramatic changes when going from the charged to the uncharged mode of these CDs. Carboxymethyl β-CD was able to resolve (±)-ephedrine as well in the uncharged (below pH 3) as in the charged mode (above pH 5). The reversal of the migration order can be explained as already discussed. Carboxyethyl β-CD is not able to resolve this solute under acidic conditions (pH 2.5) in the uncharged mode. At pH values above 5 the anionic carboxyethyl β-CD groups can act as a carrier (like carboxymethyl β-CD) and transports the enantiomeric cations to the anode, where the detector has to be placed. Only in the charged mode this CD allows the separation of the enantiomers. The succinylated β-CD also shows resolution for ephedrine in the charged and in the uncharged mode. Although higher concentrations had to be used at low pH values in order to obtain resolution, in the charged mode higher resolutions are achieved with lower CD concentrations. Because the binding of the analyte is not strong enough, the anionic CD does not form ion pairs and cannot act as a carrier for the cationic enantiomers. The migration direction of the ephedrine is here still towards the cathode. However the (−)-ephedrine migrates first with this CD. Using the phosphated β-CD and the carboxymethyl β-CD polymer no resolution could be observed for

Table 2
Resolution and migration order of (+)-ephedrine with different cyclodextrins

Cyclodextrin	Resolution (low pH) (uncharged mode)	Resolution (high pH) (charged mode)	Migration order reversal
Carboxymethyl β-CD	(+) First[a]	(−) First[a]	Yes
Carboxyethyl β-CD	No resolution	(−) First[a]	No
Succinyl β-CD	(+) First[a]	(+) First[a]	No
Carboxymethyl β-CD-polymer	No resolution	No resolution	No
β-CD Phosphate	Always charged	No resolution	No
Heptakis(2,6-di-O-methyl)-β-CD	(−) First[a]	Not charged	No

[a] Coated column (suppressed EOF) and polarity must be reversed when going from the charged to the uncharged mode of the cyclodextrin.

ephedrine neither at low nor at high pH values. Triangular peaks were a result of high mass load and therefore overloading of the buffer capacity.

In this study (±)-ephedrine was used as a test compound. This implicates that for other solutes the migration order reversal may be observed using other CDs than the carboxymethylated β-CD.

4. Conclusions

It has been demonstrated that detergents with quaternary ammonium groups are not suitable for reversal of the EOF when β-CD derivatives are present as chiral selector in the running buffer. Polyamines were found to be very suitable for this purpose although the mobility of the EOF is very slow towards the anode. This hinders their application in the reversal of the migration order of cationic enantiomers as well. It is demonstrated that the analysis of impurities of anionic enantiomers can be achieved when overloading the column.

Since a slow reversed EOF cannot be used for the separation of fast cationic enantiomers other methods have been described here in order to achieve a reversal of the migration order. Different derivatized CDs are potential candidates for this goal. A very elegant method is the use of chargeable CDs which can be ionized depending on the pH used in the running buffer. With these CDs a change in pH can reverse the migration order as well. As demonstrated with ephedrine, the determination of the optical impurity in the 0.1% range is possible in CE when the minor compound is migrating in front of the main component.

Acknowledgement

T.S. gratefully appreciates a Landesgraduiertenstipendium of the Saarland.

References

[1] R. Kuhn and S. Hoffstetter-Kuhn, *Chromatographia*, 34 (1992) 505.
[2] I.E. Valko, H.A.H. Billiet, H.A.L. Corstjens and J. Frank, *LC·GC Int.*, 6 (1993) 420.
[3] S. Fanali, *J. Chromatogr.*, 545 (1991) 437.
[4] K.D. Altria, A.R. Walsh and N.W. Smith, *J. Chromatogr.*, 645 (1993) 193.
[5] K.D. Altria, R.C. Harden, M. Hart, J. Hevizi, P.A. Hailey, J.V. Makwana and M.J. Portsmouth, *J. Chromatogr.*, 641 (1993) 147.
[6] S. Terabe, H. Ozaki, K. Otsuka and T. Ando, *J. Chromatogr.*, 332 (1985) 211.
[7] A. Nardi, A. Eliseev, P. Boček and S. Fanali, *J. Chromatogr.*, 638 (1993) 247.
[8] N.W. Smith, *J. Chromatogr. A*, 652 (1993) 259.
[9] T. Schmitt and H. Engelhardt, *Chromatographia*, 37 (1993) 475.
[10] T. Schmitt and H. Engelhardt, *J. High Resolut. Chromatogr.*, 16 (1993) 35.
[11] H. Nishi, T. Fukuyama, M. Matsuo and S. Terabe, *J. Chromatogr.*, 515 (1990) 233.
[12] S. Birnbaum and S. Nillson, *Anal. Chem.*, 64 (1992) 2872.
[13] L. Valtcheva, J. Mohammad, G. Petterson and S. Hjertén, *J. Chromatogr.*, 638 (1993) 263.
[14] J.H. Aiken and C.W. Huie, *Chromatographia*, 35 (1993) 448.
[15] A. D'Hulst and N. Verbeke, *J. Chromatogr.*, 608 (1992) 275.
[16] S. Meyer and V. Schurig, *J. High Resolut. Chromatogr.*, 15 (1992) 129.
[17] X. Huang, J.A. Luckey, M.J. Gorden and R.N. Zare, *Anal. Chem.*, 61 (1989) 767.
[18] W.R. Jones and P. Jandik, *US Pat.*, 5 104 506 (1992).
[19] X.-W. Yao, D. Wu and F.E. Regnier, *J. Chromatogr.*, 636 (1993) 21.
[20] W. Beck, *Dissertation*, University of the Saarland, Saarbrücken, 1993.
[21] J.K. Towns and F.E. Regnier, *J. Chromatogr.*, 516 (1990) 69.
[22] M. Huang, G. Yi, J.S. Bradshaw and M.L. Lee, *J. Microcol. Sep.*, 5 (1993) 205.
[23] C.S. Lee, W.C. Blanchard and C.-T. Wu, *Anal. Chem.*, 62 (1990) 1550.
[24] C.S. Lee, D. McManigill, C.-T. Wu and B. Patel, *Anal. Chem.*, 63 (1991) 1519.
[25] K. Otsuka and S. Terabe, *J. Chromatogr.*, 515 (1990) 221.
[26] K. Otsuka, J. Kawahara, K. Takekawa and S. Terabe, *J. Chromatogr.*, 559 (1991) 209.
[27] J. Mazzeo, E. Grover, M. Swartz and J. Peterson, Waters Chromatography Division of Millipore, Milford, MA, unpublished results.
[28] S. Hjertén, *J. Chromatogr.*, 347 (1985) 191.
[29] C. Quang and M.G. Khaledi, *Anal. Chem.*, 65 (1993) 3354.
[30] J. Knabe, W. Rummel, H.P. Büchi and N. Franz, *Arzneim.-Forschung/Drug Res.*, 28 (1978) 1048.
[31] S. Fanali and P. Boček, *Electrophoresis*, 11 (1990) 757.
[32] D. Belder and G. Schomburg, *J. High Resolut. Chromatogr.*, 15 (1992) 686.

ELSEVIER

Journal of Chromatography A, 697 (1995) 571–578

JOURNAL OF CHROMATOGRAPHY A

Analysis of the quaternary structure of catalase by capillary zone electrophoresis

Mercedes M. Pedrosa[a], A. Reyes[b], C. Vicente[a,*], María Estrella Legaz[a]

[a]*Department of Plant Physiology, The Lichen Team, Faculty of Biology, Complutense University, 28040 Madrid, Spain*

[b]*Department of Genetics, Faculty of Biology, Complutense University, 28040 Madrid, Spain*

Abstract

Analysis of the subunit composition of catalase was achieved by capillary zone electrophoresis. Denaturation of catalase with 34.7 m*M* sodium dodecyl sulfate (SDS) before electrophoretic analysis reveals that the protein is composed by two different classes of subunits. These results were confirmed by polyacrylamide gel electrophoresis. Micellar electrokinetic capillary chromatography also confirmed the occurrence of two classes of subunits when native catalase was injected into the capillary, although a significant decrease in efficiency was observed. However, very low efficiency and resolution were obtained when SDS was included in the running buffer as a modifier.

1. Introduction

High-performance capillary electrophoresis (HPCE) is a relatively new tool for the determination of biologically active molecules. In addition to the capability of attaining separation efficiencies higher than those obtained with high-performance liquid chromatography (HPLC) or isolectrofocusing in a pH gradient (IPG), it has the potential to overcome several of the problems associated with slab gel electrophoresis systems [1]. Molecules such as amino acids, small peptides, proteins and oligonucleotides have been separated under conditions that provide numbers of theoretical plates in the hundreds of thousands and more.

Numerous efforts have been made to separate proteins by free solution capillary electrophoresis (FSCE) as they show potential adsorption to the capillary walls. Such adsorption leads to considerable peak broadening and asymmetry, making it difficult to attain the efficiencies predicted by theory. Optimized separation methods include coating the capillary surface [2,3], addition of modifiers [4,5] and changes in the pH and composition of the electrolyte [6,7].

In a previous paper [7], we demonstrated the importance of the temperature, voltage and ionic strength of the electrolyte buffer in the separation of acidic proteins from a solution mixture by FSCE. Depending on the separation problem, it may be desirable to work at low pH (below the isoelectric point of the proteins) in a cationic regime or, conversely, it may at times be advantageous to work at pH values above the isoelectric point of the proteins, rendering them negative and migrating against the electroosmotic flow (EOF).

A question to be resolved consists in the application of CZE to separate different protomers of a polymeric protein, such as catalase [8], in a way similar to conventional sodium dodecyl

* Corresponding author.

0021-9673/95/$09.50
SSDI 0021-9673(94)00947-3

sulfate polyacrylamide gel electrophoretic (SDS-PAGE) separations. Catalase has an M_r of 250 000 and a pI of 5.4 [8] and it is composed of four protomers. In this work, we tried to analyse the protomer separation of catalase by CZE and PAGE by using SDS as a modifier of the running buffer or, alternatively, as a dissociative agent.

2. Experimental

2.1. Apparatus

A Hewlett-Packard (Waldbronn, Germany) three-dimensional capillary electrophoresis system was used. Fused-silica capillaries (50 μm I.D.) were obtained from Hewlett-Packard.

2.2. Chemicals

All chemicals used for the preparation of the buffers were of analytical-reagent grade (Merck, Darmstadt, Germany) and were used as received. Catalase (M_r 250 000) was purchased from Serva (Heidelberg, Germany), carbonic anhydrase (M_r 29 000), ovoalbumin (M_r 45 000), bovine serum albumin (M_r 66 000), SDS, and acrylamide and N,N′-methylenebis(acrylamide) from Sigma (St. Louis, MO, USA) and the neutral marker, benzene, was from Merck.

2.3. Sample preparation

Catalase solutions containing 0.8 g of catalase purified from bovine liver were prepared with deionized water and filtered through Millipore (Bedford, MA, USA) GS filters of 0.22-μm pore diameter. When indicated, samples were boiled for 10 min with 17.35 or 34.7 mM SDS before analysis.

2.4. Capillary electrophoresis

The conditions for electrophoretic analysis were as follows: uncoated fused-silica capillaries, total length 72 cm and separation length 64 cm × 50 μm I.D.; electrolytes, sodium borate–phosphoric acid buffer (pH 7.2) containing, when indicated, 3.47 or 50 mM SDS; temperature, 20°C; applied voltage, 25 kV; on-line diode-array detection at 200 nm with 16-nm bandwidth; and injection, hydrodynamic by application of 50 mbar for 30 s at the end of the capillary. Benzene at a concentration of 4% (v/v) in the same diluted buffer was used as a neutral marker [7].

2.5. Polyacrylamide gel electrophoresis

To test the homogeneity of catalase preparation and the dissociation of subunits, 150 μl of the corresponding solution, containing about 6.0 μg protein, were mixed with 75 μl of aqueous glycerol and applied on to 12% polyacrylamide gels [9]. The running buffer was 50 mM Tris–glycine (pH 8.3) and at this pH the current generated at 180 mV was about 25 mA at 4°C after equilibration. Staining was performed by using $AgNO_3$ [10]. Carbonic anhydrase (M_r 29 000), egg albumin (M_r 45 000) and bovine serum albumin M_r (66 000) were used as standards.

3. Results

3.1. CZE analysis of native and dissociated catalase

By selecting conditions near those which produced the highest efficiency in the separation of acidic proteins [7], native catalase was resolved as only one peak with a migration time of 6.71 min (Fig. 1A and B). The spectrum of the substance producing this peak showed an absorbance maximum at 280 nm and a secondary peak at 410 nm (Fig. 1C), which revealed the occurrence of the haem iron in the chromoprotein molecule. No dissociation of the protein and no modification of its spectral characteristics were observed when catalase solution was previously boiled with 17.35 mM SDS for 10 min before electrophoretic analysis, although the migration time was delayed to 10.48 min (data not shown). However, two different peaks with migration times of 12.18 and 12.29 min were

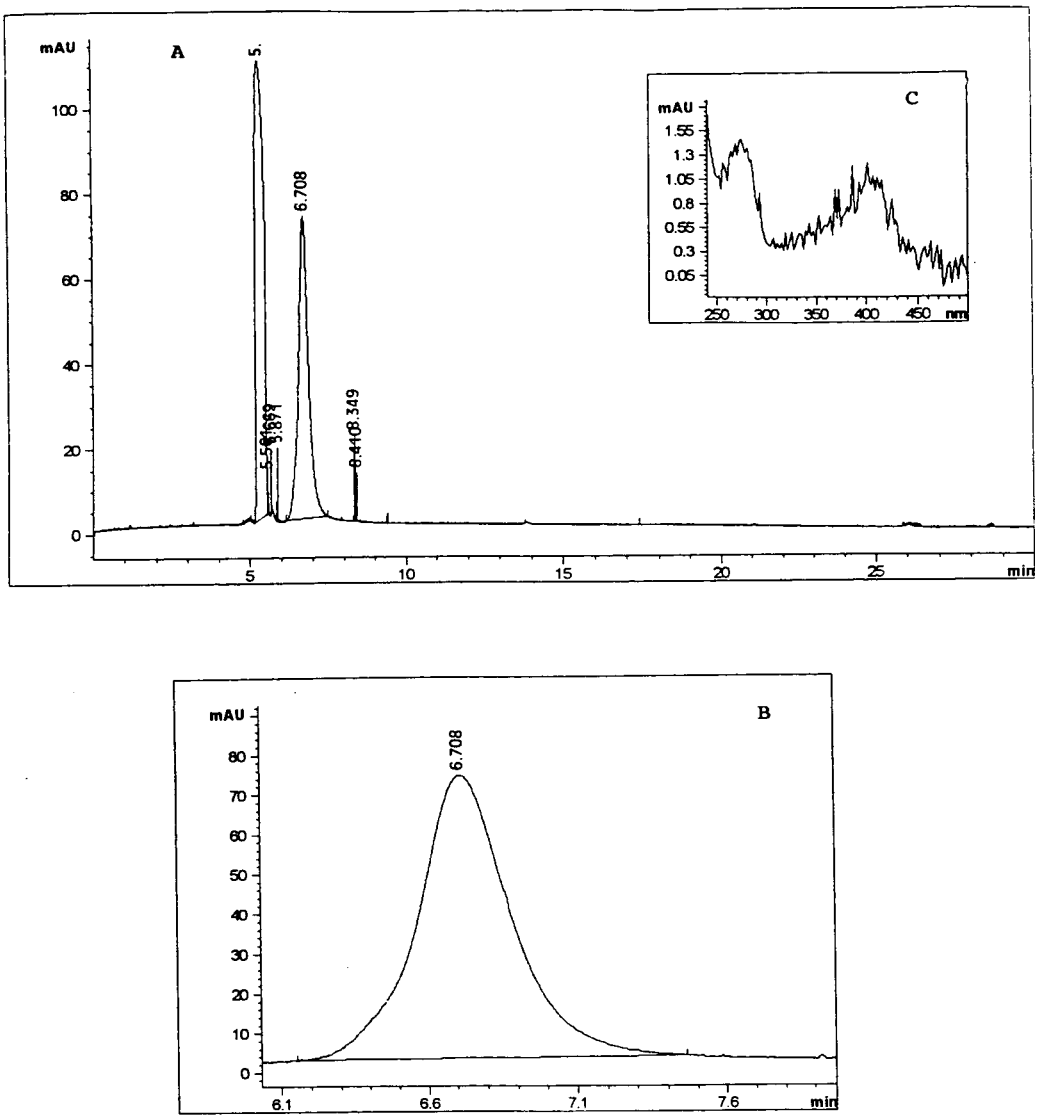

Fig. 1. (A) Normal and (B) amplified capillary electrophoretic profiles of catalase using benzene as neutral marker. (C) Automated absorption spectrum of the protein which moves with a migration time of 6.71 min.

revealed when analysis was performed by using a catalase solution previously boiled with 34.7 m*M* SDS for 10 min (Fig. 2A and B). Absorption maxima at 280 and 410 nm were found for the two peaks, revealing that catalase dissociated into two subunits retaining the haem group after separation (Fig. 2C).

3.2. Effect of modifier and catalase analysis by micellar electrokinetic chromatography

No significant modifications of this elution pattern were effected by including 3.47 m*M* SDS as a modifier in the running buffer (data not shown), although this modifier clearly affected

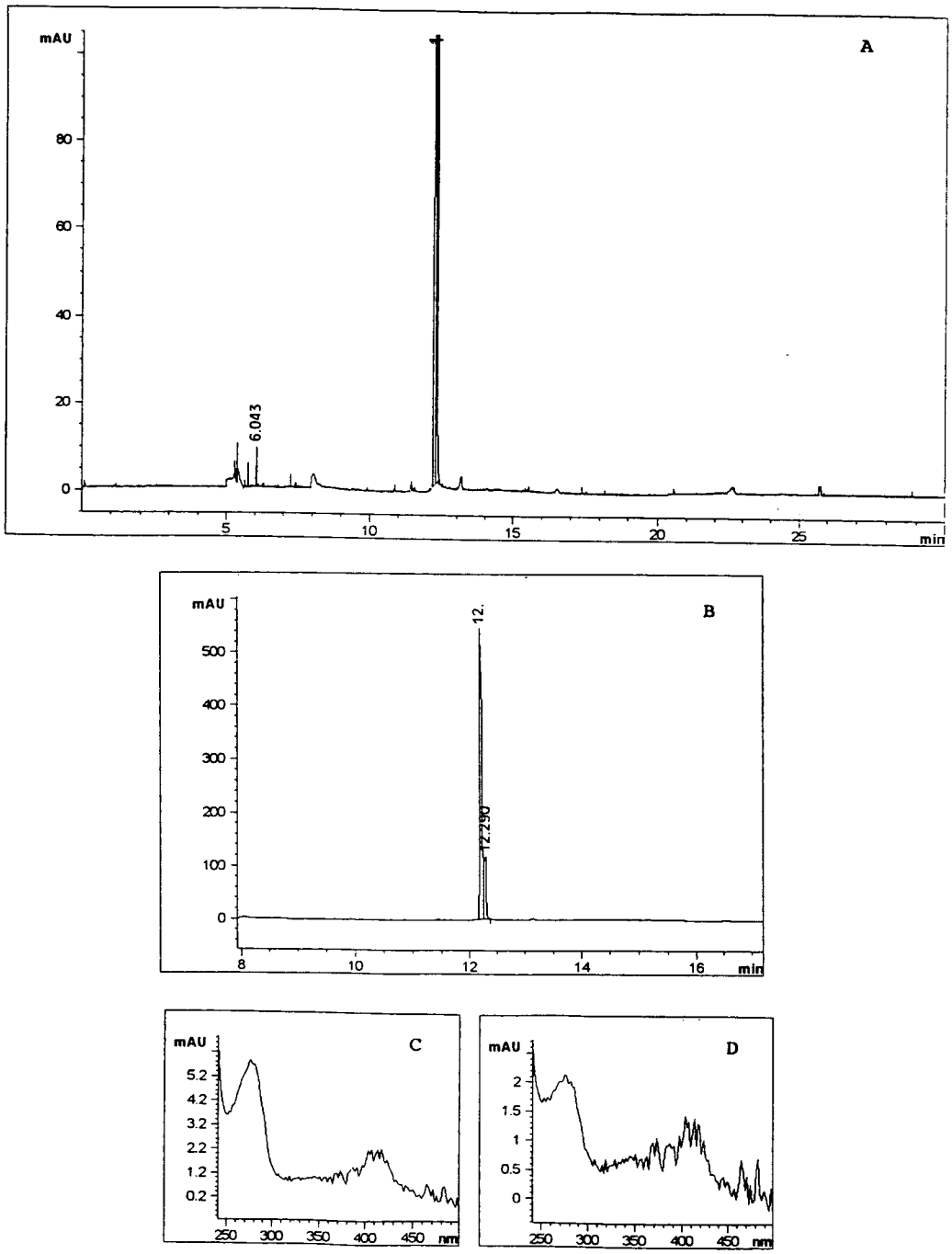

Fig. 2. (A) Normal and (B) amplified capillary electrophoretic profiles of catalase boiled with 34.7 m*M* SDS before analysis, using benzene as neutral marker. (C), (D) Automated absorption spectra of proteins that move with migration times of 12.18 and 12.29 min, respectively.

the broadening of the solute zones on the capillary. However, concentrations of SDS in the range defined for a micellar electrokinetic separation (50 m*M* SDS) added to the running buffer produced two main peaks which separated with an efficiency lower than that shown in absence of the surfactant in the running electrolyte (Fig. 3A and B). Absorption spectra corresponding to these two electrophoretic peaks were characterized by a maximum at 280 nm, although that which should have revealed the haem group appeared considerably distorted (Figs. 3C and D). This maximum was completely lost when catalase was boiled with 17.35 or 34.7 m*M* SDS before the electrokinetic process and, in addition, no separation of the subunits was achieved (Fig. 4). Several peaks different from electric spikes showed spectral characteristics corresponding to degraded protein with maxima displaced towards 265 nm.

3.3. PAGE and SDS-PAGE of catalase

Electrophoretic analysis of native catalase in polyacrylamide produced only one band, which dissociated into two well defined bands after boiling the protein with 34.7 m*M* SDS before analysis (Fig. 5, lanes a and b). When separation was carried out using a gel containing 3.47 m*M* SDS, native catalase dissociated into two main bands (lane c) which was repeated when the protein was previously boiled with 34.7 m*M* SDS (lane d) before analysis. The M_r values of these two bands were estimated as about 57 000 and 50 000, respectively. Several minor bands appeared in a similar way to the small peaks in capillary electrophoresis which showed modified spectral characteristics. On this basis, these bands could be interpreted as small peptides derived from protein degradation during SDS treatment.

4. Discussion

The experiments described here demonstrate that CZE can be used to separate different subunits of a polymeric protein avoiding erroneous interpretations about the nature of minor bands that usually appear in conventional SDS-PAGE. Native, non-dissociated catalase has an M_r value of 250 000 and, according to Glauser and Rossmann [11] and Rossmann and Labaw [12], the enzyme is composed of four identical protomers with an M_r of about 60 000. However, capillary electrophoresis separates two different classes of subunits after protein denaturation with 34.7 m*M* SDS (Fig. 2), both containing their corresponding haem group, as revealed from the absorption spectrum obtained from each peak. These results have been confirmed by conventional PAGE of the denatured protein and, in addition, SDS-PAGE reveals that the M_r of these subunits was 57 000 and 50 000, respectively (Fig. 5).

Separation of two classes of catalase subunits has been achieved by denaturing the protein before analysis with 34.7 m*M* SDS (Figs. 1 and 2) or using the surfactant as a modifier in the electrolyte. Although electroosmosis should not, in principle, affect the broadening of solute zones on the capillary [13], electroosmotic flow can modify the time a solute resides in the capillary [7] and then the efficiency and resolution can also be modified as they are related to the flow-rate. In relation to this, adding a surfactant to the background electrolyte can effectively suppress or change the direction of the electroosmotic flow [14] and then modify the efficiency [15]. Indeed, catalase migrates slower in the presence of SDS and the modifier produces significant broadening of the electrophoretic peak (Fig. 3). However, conditions implying micellar electrokinetic chromatography [16], which include 50 m*M* SDS in the running buffer, do not improve the separation of subunits (Fig. 4). As the hydrophobic tails of the surfactant are oriented towards the centre of the micelles, catalase, behaving as a polyanion at pH 7.2 (p*I* 5.4) [8], is probably rejected from the hydrophilic surface of the anionic surfactant and included inside the micelles. Then, protein migrates as an internalized micellar aggregate, without discrimination between different subunits, in the opposite direction to the electroosmotic flow. This effect could be avoided by

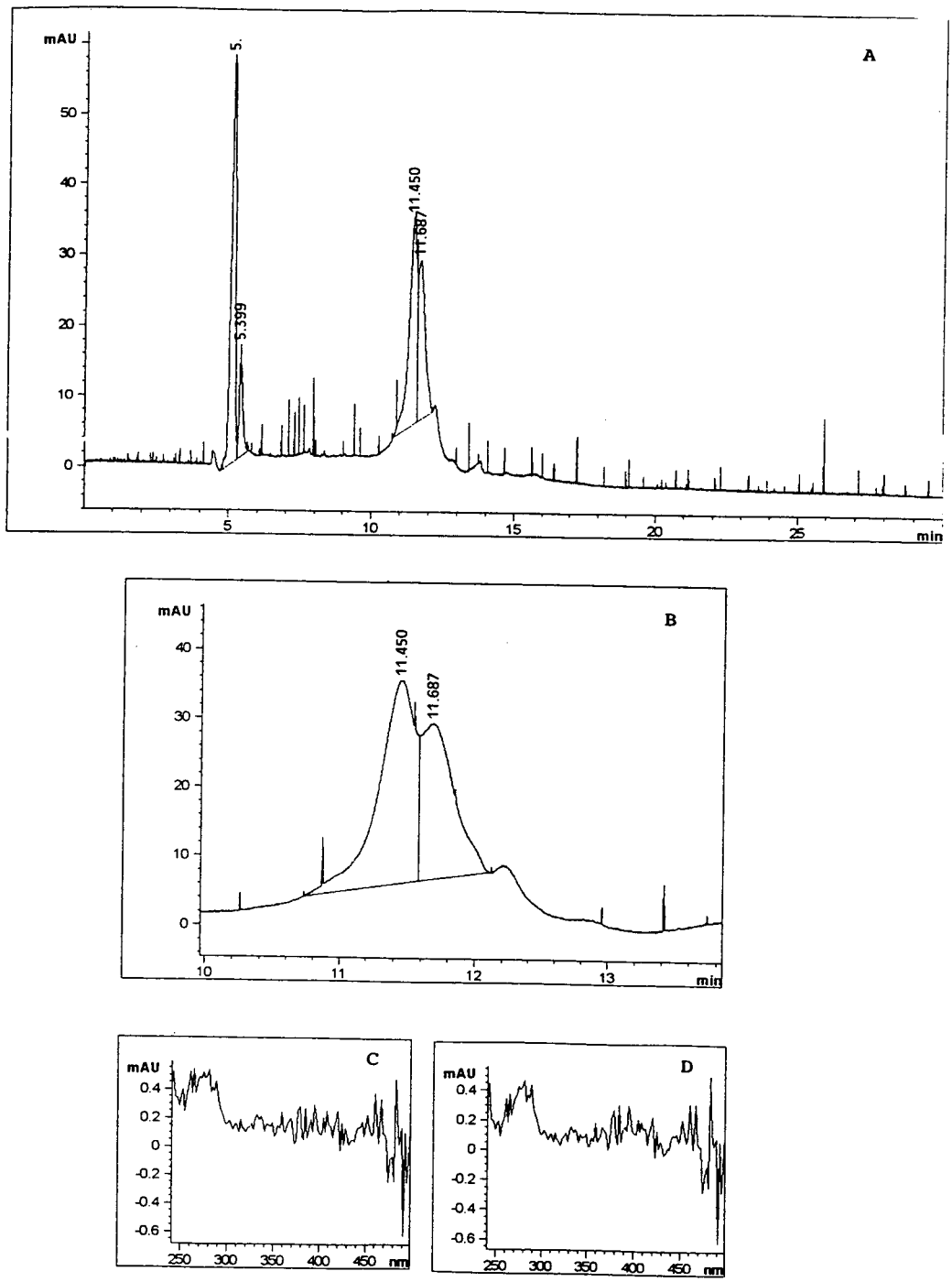

Fig. 3. (A) Normal and (B) amplified capillary electrophoretic profiles of native catalase using benzene as neutral marker and 3.47 m*M* SDS as a modifier in the running buffer. (C), (D) Automated absorption spectra of proteins that move with migration times of 11.45 and 11.69 min, respectively.

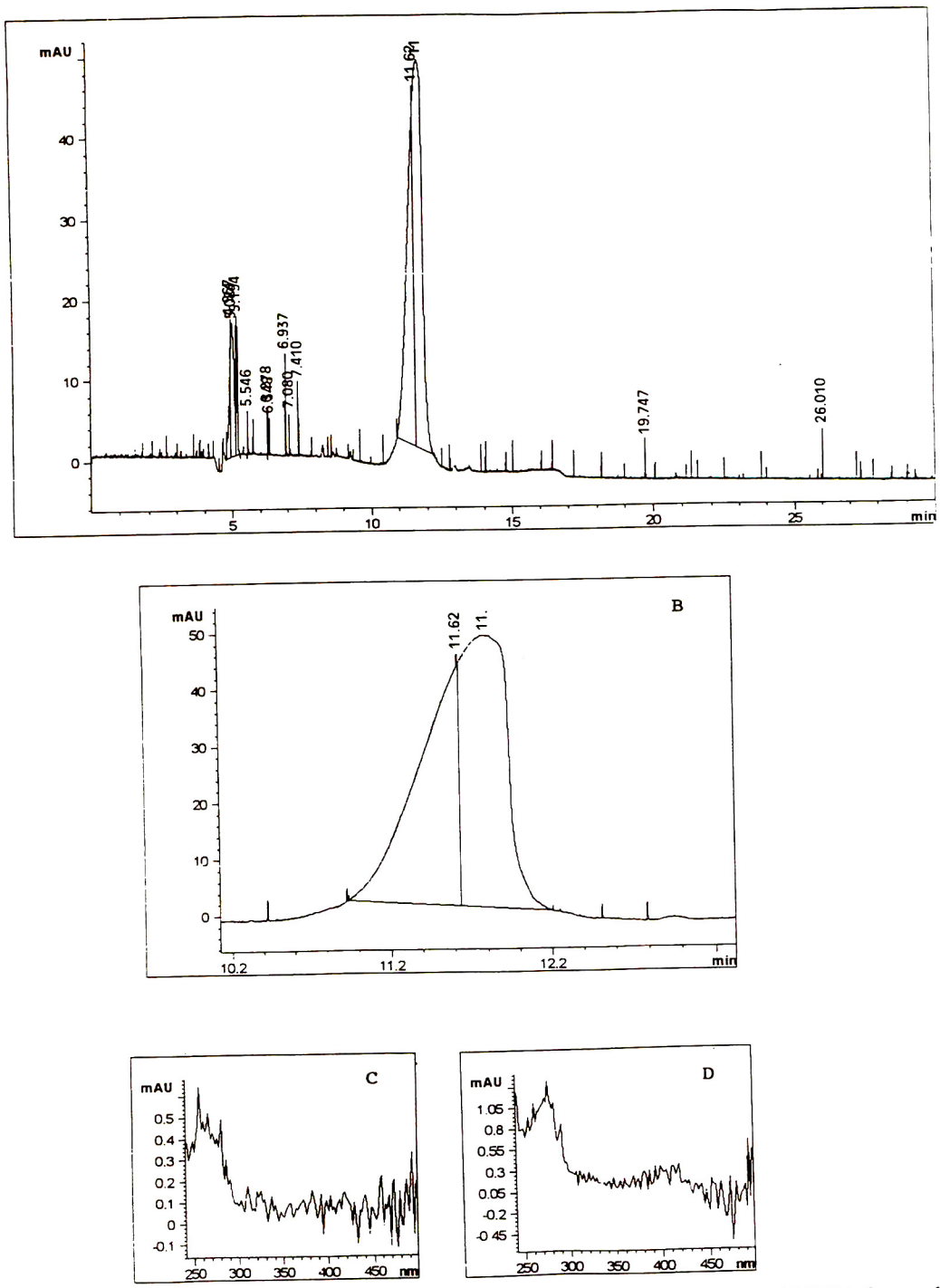

Fig. 4. (A) Normal and (B) amplified capillary electrophoretic profiles of catalase boiled with 34.5 m*M* SDS before analysis using benzene as neutral marker and 3.47 m*M* SDS as a modifier in the running buffer. (C), (D), (E), (F) Automated absorbance spectra of the two zones in which the broadening peak of catalase has been divided.

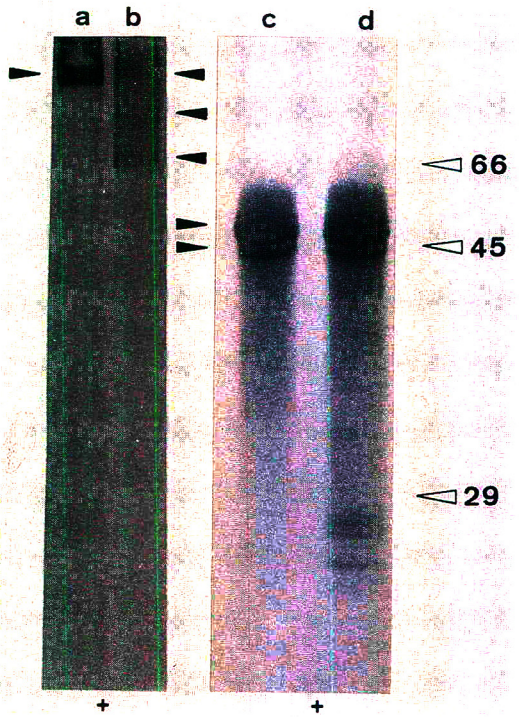

Fig. 5. PAGE of native catalase (lane a) and catalase boiled with 34.7 m*M* SDS (lane b), and SDS-PAGE of native catalase (lane c) and denatured enzyme with 34.7 m*M* SDS (lane d). In SDS-PAGE, the gel contained 3.47 m*M* SDS. Molecular masses of standards, carbonic anhydrase (29 000), egg albumin (45 000) and bovine serum albumin (66 000), are indicated with white arrowheads and catalase and its subunits are indicated with black arrowheads.

using a non-ionic surfactant, such as octylglucoside, complexing with borate [17], but this treatment does not produce a convenient dissociation of catalase.

5. Conclusions

CZE seems to be a very accurate technique for analysing protomers composing polymeric enzymes, such as catalase, when they are previously denatured with SDS. This technique permits the correct identification of the separated subunits and provides arguments to discard some artifactual, degraded subunits which usually appeared in SDS-PAGE analysis. However, MECC with SDS micellar phases exhibits increased retention and a decrease in the efficiency of separation.

Acknowledgements

The generous support and continuous help of Hewlett-Packard España is gratefully acknowledged. We are also indebted to Miss Raquel Alonso for technical assistance. This work was supported by a grant from the Comunidad Autónoma de Madrid (Spain), No. 243/91.

References

[1] T. Tadey and W.C. Purdy, *J. Chromatogr.*, 583 (1992) 111–115.
[2] M. Zhu, R. Rodriguez, T. Wehr and C. Siebert, *J. Chromatogr.*, 608 (1992) 225–237.
[3] J.P. Landers, R.P. Oda, B.J. Madden and T.C. Spelsberg, *Anal. Biochem.*, 205 (1992) 115–124.
[4] A. Vinther, J. Petersen and H. Soeberg, *J. Chromatogr.*, 608 (1992) 205–210.
[5] A. Guttman, A. Arai and K. Magyar, *J. Chromatogr.*, 608 (1992) 175–179.
[6] N.A. Guzman, J. Moschera, K. Iqbal and A.W. Malick, *J. Chromatogr. A*, 608 (1992) 197–204.
[7] M.E. Legaz and M.M. Pedrosa, *J. Chromatogr. A*, 655 (1993) 21.
[8] M.T. Solas, C. Vicente, L. Xavier and M.E. Legaz, *J. Biotechnol.*, 33 (1994) 63.
[9] U.K. Laemmli, *Nature*, 227 (1970) 680.
[10] W. Takeuchi, H. Takahashi and M. Kojima, *Biosci. Biotechnol. Biochem.*, 56 (1992) 1134.
[11] S. Glauser and M.G. Rossmann, *Acta Crystallogr.*, 21 (1966) 175.
[12] M.G. Rossmann and L.W. Labaw, *J. Mol. Biol.*, 29 (1967) 315.
[13] J.W. Jorgenson and K.D. Lukas, *J. Chromatogr.*, 218 (1981) 209.
[14] T. Kaneta, S. Tanaka and H. Yoshida, *J. Chromatogr.*, 538 (1991) 385.
[15] H.-T. Chang and E.S. Yeung, *J. Chromatogr.*, 608 (1992) 65.
[16] S. Terabe, *Trends Anal. Chem.*, 8 (1989) 129.
[17] J. Cai and Z. El Rassi, *J. Chromatogr.*, 608 (1992) 31.

ELSEVIER

Journal of Chromatography A, 697 (1995) 579–585

JOURNAL OF CHROMATOGRAPHY A

Preparative-scale supercritical fluid chromatography

Keith D. Bartle[a], Christopher D. Bevan[b], Anthony A. Clifford[a,*], Saad A. Jafar[a], Naila Malak[a], Michael S. Verrall[c]

[a]*School of Chemistry, University of Leeds, Leeds LS2 9JT, UK*
[b]*Glaxo Group Research Ltd., Greenford Road, Greenford, Middlesex UB6 0HE, UK*
[c]*SmithKline Beecham Pharmaceuticals, Brockham Park Research Centre, Betchworth, Surrey RH3 7AJ, UK*

Abstract

An apparatus for the study of preparative supercritical fluid chromatography (SFC) has been built and used to study the separation of a model system [a 1:1 (w/w) mixture of fluorene and phenanthrene] and a more real system (a mixture of milbemycins containing also other extracted material). The principles of preparative SFC are given and applied to these studies, and some conclusions about the optimisation of preparative SFC drawn.

1. Introduction

Because solubility and diffusion can be optimised by controlling both pressure and temperature, chromatography using a supercritical fluid as the mobile phase (SFC) can achieve better and more rapid separations than liquid chromatography. It is now being used preparatively to separate high-value materials, such as pharmaceuticals, where preparative high-performance liquid chromatography (HPLC) is difficult. Because peaks are narrower in SFC, and for these difficult separations very little overloading can be done so that advantage can be taken of the narrow peaks obtained, the maximum amount of material obtained in a run is of the order of 100 mg in SFC compared with the 1-g amounts obtainable sometimes in HPLC. The equipment described in the next section was built in the laboratory, but commercial systems on a preparative and larger scale are being developed. A number of reports [1–11] of preparative SFC have appeared. The studies described here are aimed at understanding the principles and optimisation of preparative SFC.

2. Experimental

Fig. 1 shows the preparative system, which consists of a pumping system; a core chromatographic section, containing an injection loop, column and detector; and a trapping system followed by a back-pressure regulator to maintain the pressure of the whole system.

2.1. Pumping system

The pumping system is capable of delivering a mixed fluid (e.g. carbon dioxide modified with

* Corresponding author.

0021-9673/95/$09.50
SSDI 0021-9673(94)01058-7

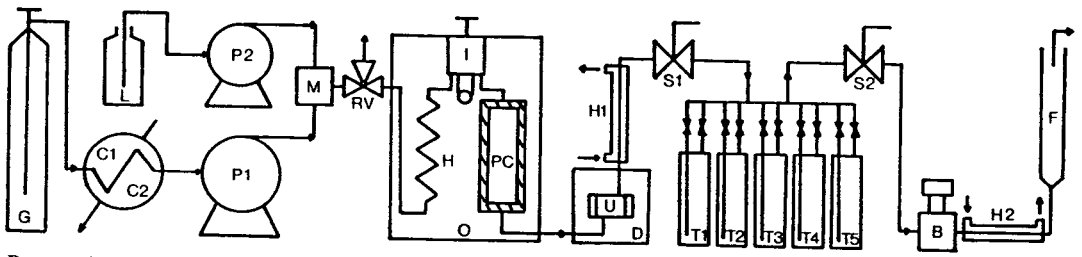

Fig. 1. Preparative SFC system. G = CO_2 cylinder; C1, C2 = condensers; P1 = dual-head reciprocating pump; P2 = liquid pump; M = dynamic mixer and damper; RV = pressure-release valve; O = oven; H = preheater; I = injection valve; PC = preparative column; D = UV detector; U = UV cell; H1 = heat exchanger for cooling; S1, S2 = 7-port valves for switching between traps; T1–T5 = traps; B = back-pressure regulator; H2 = heat exchanger; F = bubble flow meter.

methanol) at a flow-rate of 25 ml CO_2/min and 5 ml/min of modifier at a pressure of 300 bar. Such a system requires judicious choice of pump and efficient cooling of CO_2 before entering the pump and in the pump head to ensure that the CO_2 is pumped as a liquid. CO_2, supplied from a cylinder with a siphon tube, is passed a Nupro filter and cooled in two condensers, C1 and C2. C1 is a 75-ml sample cylinder (Whitey, Manchester Valve and Fitting Co.) fitted inside a coiled copper tube and insulated with polystyrene foam. C2 is constructed from a 5 m length of stainless-steel tubing (6 mm nominal O.D. and 2.16 mm I.D.), which is coiled and placed inside a copper jacket. The CO_2 pump, P1, is a dual-head reciprocating type (Varex, P.S. Instruments) as is the modifier pump, P2 (Gilson). The condensers, C1 and C2, and the CO_2 pump head are cooled by a refrigerated circulating bath (Julabo, Jencons Scientific) to −4°C. A dynamic mixer and damper (Gilson) are used to provide the even flow and composition needed for efficient SFC. A pressure-relief valve, RV, is placed in the line between the pumping system and chromatographic section, set to 300 bar, to which a Bourdon pressure gauge, 0–400 bar, is connected (Rheodyne).

2.2. Chromatographic section

After passing through a preheater, H, consisting of a 5 m length of stainless-steel tubing of 1.5 mm O.D. and 0.5 mm I.D., to bring it to supercritical conditions, the fluid then passes through an injection valve, I, (Rheodyne) with a 1-ml sample loop. A preparative column designed for HPLC, 250 mm × 20 mm I.D. (Phase Separations) is enclosed in a pressure-safety vessel, made in the laboratory. The preheater, injection valve and column are installed in an HPLC oven, O (Dupont), controllable between ambient and 100°C. The temperature of the oven is measured using a type K thermocouple connected to a digital display unit (Ametek). Temperature stability of the oven is ± 0.5°C. Pressures at the inlet and outlet of the column are measured using pressure transducers and control units (Thorn-EMI Datatech, Model SE42 and Lintronic, Model Setra 205-2), not shown. Pressure drops of 10–60 bar across the column and the data referred to the average column pressure. A UV detector, D, containing a high-pressure front-loading cassette cell, U, of 4 μl volume and 5 mm path length (Jasco, Model 875), is used to follow the separation.

2.3. Trapping system

After leaving the chromatographic section, the eluent is cooled in a coil in a water bath to ambient temperature. Trapping of fractions of the peaks is thus done at room temperature where the mobile phase is liquid. The five traps, T1–T5, made in the laboratory, are 60 ml in volume and are connected sequentially into the flow via the 7-port valves, S1 and S2 (Rheodyne 7060) at times indicated by the chromatogram received by the detector. Of the seven ports on each of these valves, five connect via each of the traps, one connects the two valves directly together for use before and after collection, and one goes to vent. The traps are each fitted with

two isolating valves (SSI, Scientific Glass Engineering). The traps are filled with the liquid CO_2 before the separation is carried out and during collection not more than 50% of liquid CO_2 is displaced. At the end of the separation, the traps are frozen in liquid nitrogen and opened to the atmosphere, when the mobile phase slowly evaporates. This type of trapping system is not necessarily the most suitable for routine preparative SFC, but gives quantitative collection and is suitable for the studies described in this paper. After the solid CO_2 has evaporated, the solute is then collected from the traps using an organic solvent and analysed. The back-pressure regulator, B, heated mechanical (GO, Model BP-66) or electromechanical (Jasco, Model 880-81) maintains the required pressure in the system and a bubble flow meter is installed, to check the flow-rates indicated on the pumps, following a simple heat-exchanger to bring the emerging gas up to room temperature, H2.

3. Principles of preparative SFC

For a discussion of principles, a 1:1 (w/w) mixture of two compounds is considered. If their two peaks are well separated, a plot of purity versus the fraction of total material collected will appear as curve A in Fig. 2. The first half

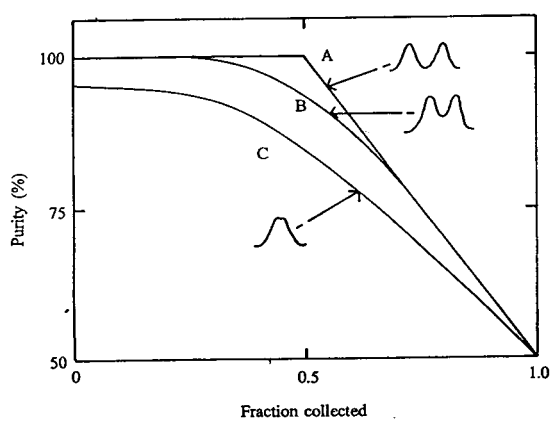

Fig. 2. Schematic plot of purity versus fraction collected for qualities of separation decreasing A to B to C. See text.

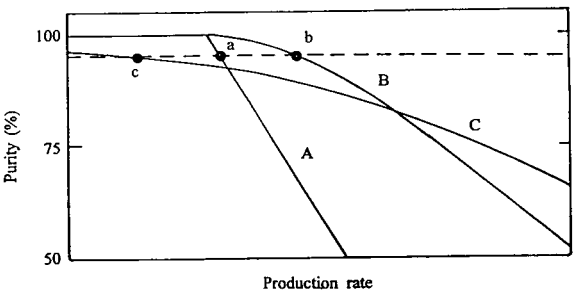

Fig. 3. Schematic plot of purity versus production rate for various qualities of separation decreasing A to B to C, due to increasing loading or flow-rate. See text.

collected will be one pure compound, which will progressively contaminated by the second compound as it is added in to the material collected. If the separation is worse, curve B will be obtained, with the second compound emerging before all the first compound has been collected. If separation is poor, curve C is obtained, with some of the second compound emerging initially.

For a given separation under a given set of other conditions, worse separation is obtained if either the flow-rate or loading is increased. At the same time, however, the production rate is increased. Thus, if purity is plotted against production rate, the curves A, B and C of Fig. 2 will become spread out as in Fig. 3. This is the form in which data are commonly presented, for example in the next section. The horizontal dashed line in Fig. 3 represents a purity of 90% and it cuts the curves A, B and C at the points a, b and c. These points are also shown on Fig. 4 as a schematic plot of production rate versus loading or flow-rate for a purity of 90%. Fig. 4 thus

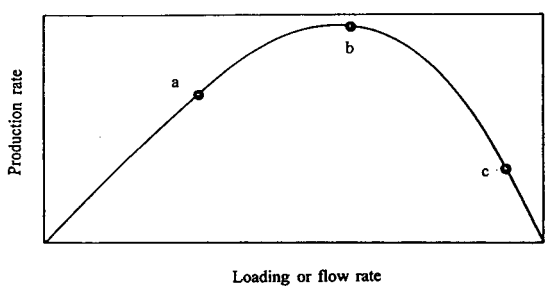

Fig. 4. Schematic plot of production rate versus loading or flow-rate for a given required purity. See text.

shows how an optimum loading or flow-rate arises for a given required purity.

4. Studies using the experimental system

Studies were carried out initially on a 1:1 (w/w) mixture of phenanthrene and fluorene, chosen because they elute close together in SFC. Phenanthrene (BDH) and fluorene (Aldrich) were checked for purity using GC and found to be 98.8 and 97% pure, respectively. After the traps were filled and the system had reached equilibrium, 1 ml of solution of various loadings was injected. Chromatography was carried out using a preparative column designed for HPLC, 250 mm × 20 mm I.D., packed with 10-μm diameter silica particles bonded with octadecylsilyl groups (Phase Separations, type ODS2). In the experiments described here, chromatography was carried out at 40°C and 250 bar. Pure CO_2 (BOC 99.98% purity) and CO_2 modified with up to 20% methanol (v/v at the pumps) was used at CO_2 flow-rates up to 25 ml/min and at loadings of up to 250 mg of the mixture. Removal of the fractions from the traps was done using dichloromethane (FSA Labs., 99.8% quoted purity) and analysis of the five fractions collected was done by UV absorption at 295 and 302 nm for phenanthrene and fluorene, respectively. In a small number of cases, where the concentrations were too small for UV analysis, GC determinations were made. After analysis of the fractions, results from individual fractions and theoretical combinations of the fractions enabled plots of purity versus production rate to be drawn. Such plots for fluorene recovery (the second peak eluted) are shown both for increasing loading in Fig. 5 and increasing flow-rate in Fig. 6. The plots are seen to be of the form of Fig. 4 for both loading and flow-rate.

Studies were then carried out on a more real system; the separation of milbemycin α_2 from a toluene extract of microbial cells. This extract contained only ca. 2.5% of milbemycin α_2 (eluted first), other milbemycins and other compounds. The maximum production of milbemycin α_2 of 90% purity obtained in a single

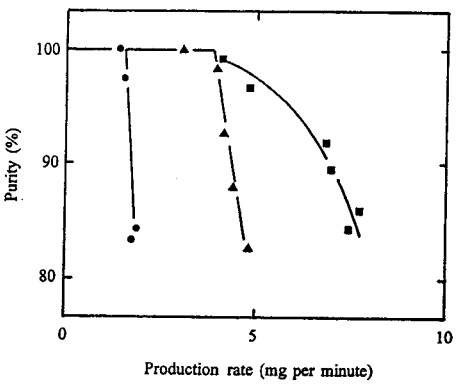

Fig. 5. Purity versus production rate of fluorene for the preparative SFC of phenanthrene–fluorene (1:1, w/w) at loadings of: ○ = 30 mg; ▲ = 75 mg; □ = 108 mg. Column, 250 mm × 20 mm I.D. containing octadecylsilyl-bonded 10-μm silica particles; temperature, 40°C; pressure, 250 bar; mobile phase, pure CO_2; flow-rate of CO_2, 20 ml/min.

run was 10 mg. Initial conditions were sought on an analytical scale, using the same system with analytical columns, 250 mm × 4.6 mm I.D. (Phase Separations). Best separation was ob-

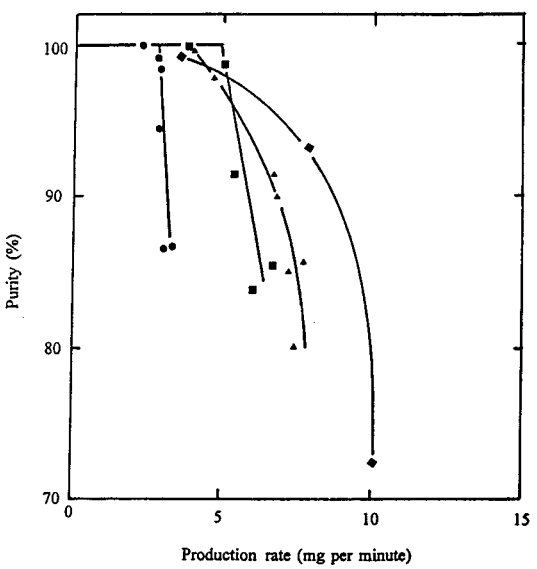

Fig. 6. Purity versus production rate of fluorene for the preparative SFC of phenanthrene–fluorene (1:1, w/w) at flow-rates of: ○ = 10 ml/min; □ = 15 ml/min; ▲ = 20 ml/min; ◆ = 25 ml/min. Column, 250 mm × 20 mm I.D. containing octadecylsilyl-bonded 10-μm silica particles; temperature, 40°C; pressure, 250 bar; mobile phase, pure CO_2; loading 108 mg.

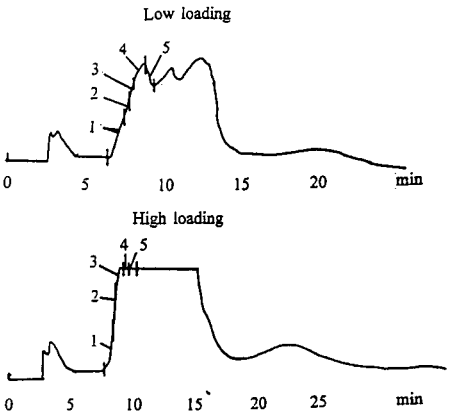

Fig. 7. Chromatograms obtained from the detector of the preparative SFC system for the separation of milbemycin α_2 at low (0.1 g) and high (0.5 g) loadings of crude extract. Column, 250 mm × 20 mm I.D. containing cyanopropyl-bonded 5-μm silica particles; temperature, 47°C; pressure, 120 bar; mobile phase, 5% methanol in CO_2 (v/v at pumps); flow-rate of CO_2, 20 ml/min.

tained using a column packed with cyanopropyl bonded 5-μm silica particles, a temperature of 47°C and a pressure of 120 bar using a mobile phase of 5% methanol in CO_2 (v/v at the pumps). Preparative chromatography was then carried out on a column of 250 mm × 20 mm I.D. containing the same packing (Phase Separations) and under the same conditions. Analysis of samples was carried out by HPLC. Examples of chromatograms obtained from the detector of the preparative SFC system at low (0.1 g) and high (0.5 g) loadings of crude extract, using a 20 ml/min flow-rate of CO_2 are given in Fig. 7. This figure also shows the fractions collected, from which curves of purity versus production rate were obtained and shown in Fig. 8.

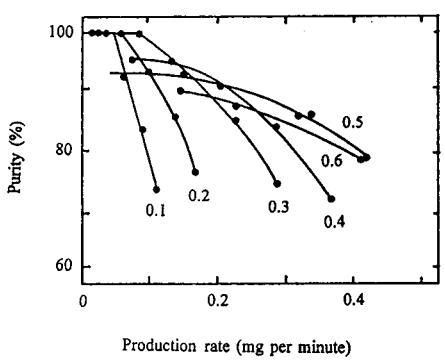

Fig. 8. Purity versus production rate for the preparative SFC of milbemycin α_2 at various loadings of crude extract, shown in grams on the figure. Other chromatographic conditions as in Fig. 7.

5. Optimising preparative SFC

The parameters to be optimised during preparative SFC are column type, temperature, pressure, modifier concentration, flow-rate and loading. The initial search for conditions is carried out by observing the chromatogram obtained, without trapping. It is more economical if at least some of this work is carried out on an analytical-scale SFC, particularly column, pressure, temperature and modifier concentration, as in the milbemycin study, described above. The initial aim of this study was to look for methods of optimising all parameters, but the experience obtained with the experiments described and others is that further optimisation of column type, pressure and temperature is not worthwhile and that further optimisation of modifier concentration (discussed further below) is of questionable worth. However, for further refinement of flow-rate and loading conditions, trapping experiments as described in the last section can be carried out to obtain curves of purity versus production rate for different conditions. These curves can then be further analysed, as is now described for the effect of loading on the isolation of milbemycin α_2. Below 100% purity, the curves of Fig. 8 are fitted to a quadratic and the equations obtained are used to calculate values of the production rate at a given purity for the various loadings. Curves can then be drawn of production rate versus loading for a given purity and this is shown in Fig. 9 for the milbemycin data. As can be seen, there is an optimum loading, for a certain required purity. Similar curves can be obtained for the effect of flow-rate.

Theoretically, a two-dimensional optimisation for both loading and flow-rate could be carried out, and although we have had some success in this, errors in the experimental data make this

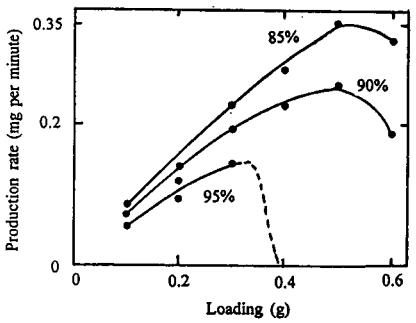

Fig. 9. Production rate versus purity for the preparative SFC of milbemycin α_2 for various required purities, shown on the figure. Column, temperature, pressure and flow-rate as in Fig. 7. A purity of 95% was not obtainable at loadings of 0.4 g and above and so a schematic dashed line is shown.

difficult and the results are not worth reporting. It appears to be better to choose an optimum flow-rate from observation of the chromatograms, obtain an optimum loading by the procedure outlined above and then refine flow-rate by the same procedure. Further iterative optimisations are possible.

As far as modifier concentration is concerned, optimisation by observation of the chromatograph is probably the only viable method, but more quantitative optimisation may be possible for some systems. Good separation of milbemycin α_2 could not be obtained with pure CO_2, improved significantly with 5% added methanol, but did not improve further with greater addition of methanol. For the phenanthrene–fluorene system, quantitative optimisation of modifier concentration was attempted as, although modifier is not needed to affect the separation, it is known that added modifier reduces the tailing of peaks in SFC caused by unbonded sites on the packing and therefore might improve the purities achieved. Experiments were carried out at high loadings and flow-rates. However, as seen in Fig. 10, the effect of modifier, if any, is less than the experimental scatter, which is greater than previously because of more rapid elution, and no improved separation is achieved.

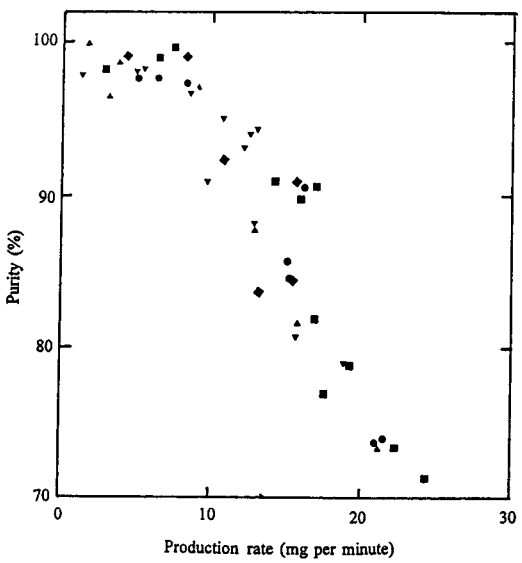

Fig. 10. Purity versus production rate of fluorene for the preparative SFC of phenanthrene–fluorene (1:1, w/w) using CO_2 containing methanol at: ○ = 0%; ◆ = 2%; ▽ = 5%; □ = 10%; ▲ = 20% (v/v). Column, 250 mm × 20 mm I.D. containing octadecylsilyl-bonded 10-μm silica particles; temperature, 40°C; pressure, 250 bar; mobile phase modified CO_2; flow-rate of CO_2, 20 ml/min; loading 250 mg.

6. Conclusions

It is concluded that of the parameters that can be varied in preparative SFC, those of column type, pressure and temperature probably modifier concentration are best chosen by observations of separation on the chromatograms obtained. Further, more quantitative, optimisation can be carried out on flow-rate and loading separately, and perhaps iteratively, by a procedure described above. This procedure involves carrying out trapping experiments at different conditions of loading or flow-rate, plotting curves of purity versus production rate, and fitting these curves to obtain plots of production rate versus loading or flow-rate to obtain optima for a given desired purity. Optimisation along the lines suggested is worthwhile for a preparative SFC that is likely to carried out often and especially for a system which may be taken up to production scale.

Acknowledgements

The authors wish to thank the Engineering and Physical Sciences Research Council (UK) for financial support and Phase Separations for donations of equipment.

References

[1] R.E. Jentoft and T.H. Gouw, *Anal. Chem.*, 44 (1972) 681.
[2] M. Perrrut and P. Jusforgues, *Entropie*, 132 (1986) 107.
[3] M. Saito, Y. Yamauchi, T. Hondo and M Senda, in M. Perrut (Editor) *Proc. 1st Int. Symp. Supercritical Fluids*, Institut National Polytechnique de Lorraine, Nancy, 1988, p. 381.
[4] M. Alkio, T. Harvala and V. Komppa, in M. Perrut (Editor) *Proc. 1st Int. Symp. Supercritical Fluids*, Institut National Polytechnique de Lorraine, Nancy, 1988, p. 389.
[5] T. Gorner and M. Perrut, *LC·GC*, 7 (1989) 36.
[6] M. Saito, Y. Yamauchi, K. Inomata and W. Kottkamp *J. Chromatogr. Sci.*, 27 (1989) 79.
[7] C. Berger and M. Perrut, *J. Chromatogr.*, 505 (1990) 37.
[8] Y. Yamauchi and M. Saito, *J. Chromatogr.*, 505 (1990) 237.
[9] M. Saito and Y. Yamauchi, *J. Chromatogr.*, 505 (1990) 257.
[10] Y. Yamauchi, M Kuwajima and M. Saito, *J. Chromatogr.*, 515 (1990) 285.
[11] L. Wunscher, U. Keller and I Flament, *J. Chromatogr.*, 552 (1991) 539.

ELSEVIER

Journal of Chromatography A, 697 (1995) 587–590

JOURNAL OF CHROMATOGRAPHY A

Short communication

Enantiomer separations by supercritical fluid chromatography on a chiral stationary phase physically anchored to porous graphitic carbon

S.M. Wilkins[a], D.R. Taylor[a,*], R.J. Smith[b]

[a]*Chemistry Department, UMIST, P.O. Box 88, Manchester M60 1QD, UK*

[b]*SmithKline Beecham Pharmaceuticals, Coldharbour Road, Harlow, Essex CM19 5AD, UK*

Abstract

A chiral anthrylamine derivative was prepared and adsorbed on the surface of pre-packed porous graphitic carbon, and was evaluated as a chiral stationary phase in packed-column supercritical (and sub-critical) fluid chromatography. It successfully separated the enantiomers of two commercial anti-inflammatory agents and also a series of racemic tropic acid derivatives.

1. Introduction

Porous graphitic carbon (PGC) is a new packing for chromatographic columns that has been developed in the last decade [1,2]. Its main advantage over silica is its pH stability across the whole range 0–14. The order of retention on PGC is not governed by the order of solute polarity and, as supercritical fluids with polar modifiers are able to solvate many polar species, it is believed that the use of PGC in supercritical fluid chromatography (SFC) may expand the scope of applications in SFC [3]. Good efficiency, peak shapes and selectivity have been demonstrated on PGC in SFC but there is also one major drawback, namely that of the high affinity of the packing for large, planar molecules.

Chiral separations have been effected on such a packing in HPLC but only when a chiral additive is used in the mobile phase [4,5]. It is the high affinity of PGC for large, planar molecules that provides a possible means of producing a carbon-based chiral stationary phase (CSP). In this study, anthracene was used to anchor a chiral selector (**I**), derived from (*R*, *R*)-(+)-tartaric acid, to the carbon surface.

2. Experimental

2.1. Instrumentation

The SFC instrumentation consisted of a Gilson SFC2 cooler, a Gilson Model 305 CO_2 pump, a Gilson model 306 modifier pump, a Gilson Model 805S manometric module, a Gilson Model 811B dynamic mixer, a Rheodyne Model 7125 manual injector valve, a Pye Unicam Model 740592 oven, an Applied Biosystems Model 757 absorbance detector and a Tescom Series 26-1700 back-pressure regulator. The UV instru-

* Corresponding author.

0021-9673/95/$09.50
SSDI 0021-9673(94)00787-X

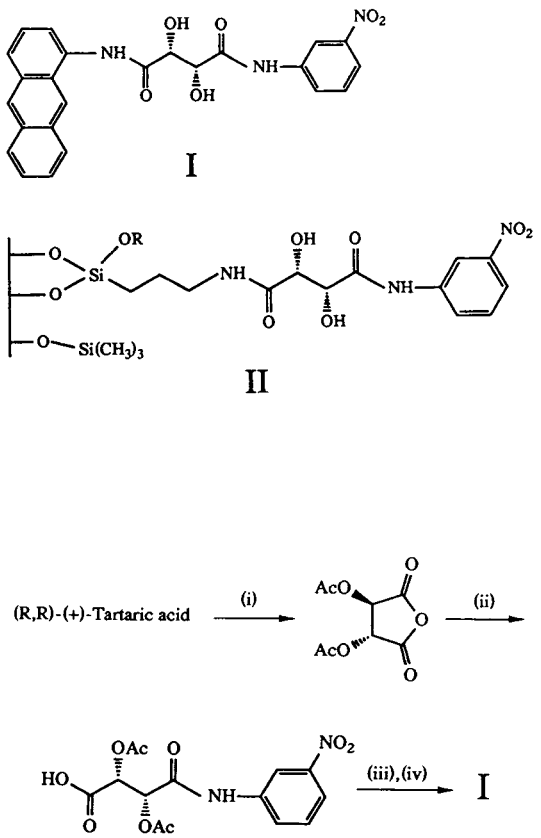

Fig. 1. Synthesis of chiral selector **I**. Reagents: (i) Ac_2O, H_2SO_4; (ii) 3-$NO_2C_6H_4NH_2$; (iii) 1-aminoanthracene, peptide coupling; (iv) $NaHCO_3$, CH_3COCH_3.

mentation consisted of a Shimadzu (UV-2101PC) UV–Vis scanning spectrophotometer.

2.2. Materials

The solvents used included methanol, 2-propanol (Rathburn, HPLC grade) and carbon dioxide with liquid offtake dip-tube (Air Products). The porous graphitic carbon was purchased in the form of a Hypercarb HPLC column (10 cm × 3 mm I.D.; Shandon No. 59863752). The silica-based CSP (25 cm × 4.5 mm I.D.) and tropic acid amides were synthesized at UMIST. Ibuprofen and flurbiprofen were purchased from Sigma and benzoin from Fisons.

2.3. Preparation of chiral selector

The chiral selector **I** chosen for the carbon-based CSP was designed to be analogous to the selector in the silica-based CSP **II**, previously prepared at UMIST [6]. A comparison of the performance of the same selector on these two packings would then be possible. In order to anchor the chiral selector to the Hypercarb, anthracene was directly attached to the tartaric acid moiety via an amide linage. The procedure for the synthesis of **I** is shown in Fig. 1.

Table 1
Analysis of achiral compounds on uncoated and coated PGC

Compound	Uncoated PGC			Coated PGC		
	t_R (min)	N (plates/m)	A_S	t_R (min)	N (plates/m)	A_S
Phenol	1.11	4740	3.3	0.87	4193	1.9
p-Nitrophenol		not eluted		40.50	1850	3.0
p-Cresol	1.95	4350	5.0	1.15	6055	2.4
Naphthalene	5.99	10750	4.0	0.63	4098	4.3
Acetophenone	1.06	12710	1.7	0.58	3982	2.5
Benzoic acid	5.60	2720	0.2	3.08	1073	6.1
Aniline	0.68	5230	2.5	0.59	1594	9.4

Conditions: 1% MeOH–CO_2, 3 ml/min, 200 atm (1 atm = 101 325 Pa) 20°C, 254 nm.

2.4. Coating of chiral selector onto PGC

A solution (5 mg/ml) of **I** in tetrahydrofuran (THF) was pumped and recycled through the column and the decrease in concentration in the reservoir was monitored off-line-by UV spectrophotometry over a 7-day period, after which little further uptake appeared to occur.

3. Results and discussion

The surface coverage of the selector on Hypercarb, determined from the measured uptake of the selector, was 80 mg (400 μmol/g). If the molecular area of anthracene is taken to be 0.202 nm^2, this result suggests a 50% complete monolayer coverage.

Table 1 shows the SFC analysis of some achiral compounds on the coated PGC and a separate uncoated PGC column. Coating PGC with the chiral selector evidently resulted in a decrease in both retention and column efficiency. There is no general trend observed for asymmetry values (A_S) [7] from uncoated to coated PGC and the decrease in efficiency obtained for similar or lower A_S values has been attributed to a relative increase in peak width (values not given). Benzoic acid and aniline were eluted fairly quickly but the peak shapes were poor, presumably owing to strong hydrogen bonding interactions with the selector.

A series of tropic acid amides (Fig. 2a) were resolved by SFC on both the carbon and silica-based CSP. Although the two columns are not of identical dimensions, CSP **II** being used in a longer column, 25 cm × 4.5 mm I.D., similar trends for retention (k'_2) and selectivity values (α) were obtained (see graphs in Fig. 2). The greater values of α obtained on the shorter PGC CSP are promising and should encourage further study of this approach to chiral separations on porous graphitic carbon.

Even more promising are the separations of benzoin, ibuprofen and flurbiprofen (Fig. 3). The last two demonstrate the successful separation of unprotected acid substances under normal-phase conditions. Peak tailing is evident, however, resulting in decreased resolution of the enantiomers. Again, this is thought to be due to hydrogen bonding interactions with the selector.

After continuous use of the CSP, a decrease in retention and resolution was noted. At first this

a

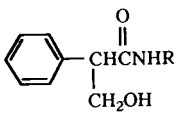

Compound	R
1	$-C_6H_5$
2	$-CH_2C_6H_5$
3	$-CH_2CH_2CH_3$
4	$-CH_2CH{=}CH_2$
5	$-CH(CH_3)_2$
6	$-C(CH_3)_3$

b

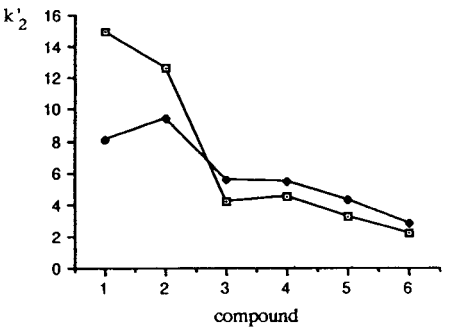

c

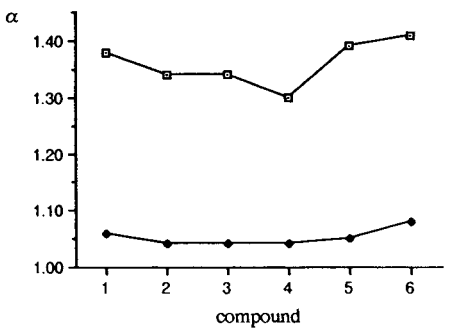

Fig. 2. Comparison of (□) PGC with (▲) silica. (a) Structures of tropic acid amides; (b) retention (k'_2) and (c) selectivity values (α) of compounds **1–6**. Conditions: 6% 2-propanol–CO_2, 3 ml/min, 200 atm, 20°C, 217 nm.

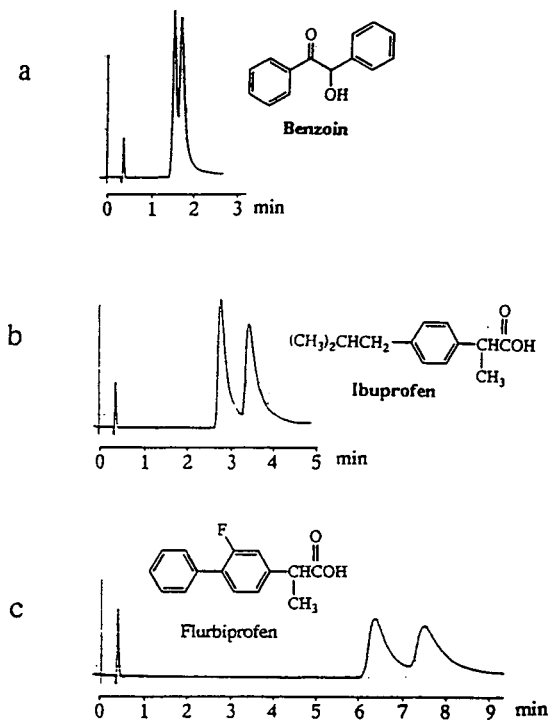

Fig. 3. Separations of (a) benzoin, (b) ibuprofen and (c) flurbiprofen. Conditions: 2% 2-propanol–CO_2, 3 ml/min, 200 atm, 20°C, 217 nm.

was believed to be due to the leaching of the chiral selector from the column. Flushing the column with a mobile phase of 20% THF–CO_2 at room temperature, however, reproduced the original separation. This suggests that the decrease in retention and resolution could be due to the masking of attractive interaction sites by substances highly retained on the column, which can subsequently be washed from the column, leaving the chiral selector undisturbed. Although we have not yet completed a thorough study of the durability and ruggedness of this anthracene-anchored Hypercarb-supported CSP, we have found that the selector is rapidly removed by washing the column with THF.

4. Conclusions

Anthracene has proved to be successful in anchoring the chiral selector **I** to PGC, yielding a satisfactory carbon-based CSP. Superior chiral separations have been demonstrated on this PGC-based CSP than on the corresponding silica-based CSP **II** in SFC and the resolution of unprotected, acidic drugs, e.g., ibuprofen, has been achieved.

Acknowledgements

The authors thank SmithKline Beecham Pharmaceuticals for the purchase of SFC equipment and the SERC for financial support (CASE award to S.M.W.).

References

[1] M.T. Gilbert, J.H. Knox and B. Kaur, *Chromatographia*, 16 (1982) 138.
[2] J.H. Knox, B. Kaur and G.R. Millward, *J. Chromatogr.*, 352 (1986) 3.
[3] T.M. Engel and S.V. Olesik, *Anal. Chem.*, 62 (1990) 154.
[4] B.J. Clark and J.E. Mama, *J. Pharm. Biomed. Anal.*, 7 (1989) 1883.
[5] A. Karlsson and C. Pettersson, *J. Chromatogr.*, 543 (1991) 287.
[6] G. Bridger, *Ph.D. Thesis*, UMIST, Manchester, 1987.
[7] L.R. Snyder, J.L. Glajch and J.J. Kirkland, *Practical HPLC Method Development*, Wiley-Interscience, New York, 1988, Ch. 3.

ELSEVIER

Journal of Chromatography A, 697 (1995) 591–596

JOURNAL OF CHROMATOGRAPHY A

Temperature dependence of chiral discrimination in supercritical fluid chromatography and high-performance liquid chromatography

R.J. Smith[a], D.R. Taylor[b,*], S.M. Wilkins[b]

[a]*SmithKline Beecham Pharmaceuticals, Harlow, UK*

[b]*Chemistry Department, University of Manchester, Institute of Science and Technology, PO Box 88, Manchester, M60 1QD, UK*

Abstract

Chiral separations of related compounds within a series of potassium channel activator (KCA) analogues were compared by supercritical fluid chromatography (SFC) and high-performance liquid chromatography (HPLC) at several temperatures between 0° and 52°C. Mobile phases as close as possible in performance were selected for the two modes of analysis, and the same chiral stationary phase (CSP) was used, namely, cellulose tris(3,5-dimethylphenyl-carbamate) (Chiralcel-OD). Two of the compounds, which differed only by replacement of a benzoyl group by a *n*-pentanoyl group, showed quite strikingly different temperature dependencies. These indicate that one compound is above, and the other below, its isoenantioselective temperature (T_{iso}), at which separation of enantiomers is not possible. The thermodynamic parameters for these chiral discriminations support the conclusion that, in spite of their very similar structures, quite different chiral recognition factors operate for these two racemic mixtures.

1. Introduction

Chiral separations are increasingly important in the development and production control of pharmaceutical compounds, but the way in which temperature should be controlled when developing a new chiral analysis procedure is not well understood, although it is well established that temperature effects are important in chiral selectivity. Recently, several authors [1–4] have reported ways in which temperature variations may alter chiral selectivities. We therefore embarked on a comparison of the role of temperature variation on chiral selectivity in supercritical fluid chromatography (SFC) and high-performance liquid chromatography (HPLC), to determine whether any distinctive differences between the role of temperature in these two modes of chiral analysis might emerge.

The compounds selected for this study are a set of analogues of Cromakalim™ (**1**), a SmithKline Beecham potassium channel activator [5]. For the purposes of this report, only two members of the series are considered, namely compounds **2** and **3**, in which the ex-ring amide function changes from a benzamide in (**2**) to a *n*-pentanoylamide in (**3**): all other structural features remain the same.

* Corresponding author.

0021-9673/95/$09.50
SSDI 0021-9673(94)00934-1

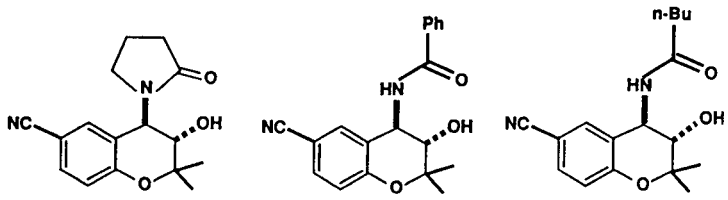

(1) (2) (3)

2. Equipment

For SFC, a Gilson packed-column system was used, comprising a Model SFC2 Cooler, Model 305 carbon dioxide pump, Model 306 organic modifier pump, a Model 811B Dynamic Mixer, and a Model 805S Manometric Module and a Tescom Series 26-1700 back-pressure regulator to provide outlet pressure restriction. Injection was via a manually operated 20 μl Model 7125 Rheodyne loop injector, and detection was achieved using an Applied Biosystems Model 757 SFC UV detector. The 25 cm × 4 mm I.D. stainless-steel column contained Diacel Chiralcel-OD stationary phase on a silica support, and was housed in a modified Pye Unicam Model 740592 GC oven. Pure dry liquid carbon dioxide was supplied via a dip-tube from a pressure regulated cylinder.

For HPLC experiments below 32°C, a Waters Model 6000A pump, Rheodyne 7125 injector and Perkin-Elmer Model LC75 UV absorption detector was used. For HPLC experiments above ambient temperature, an integrated Perkin-Elmer Model 4000 HPLC system fitted with a photodiode array UV detector was used. HPLC grade solvents (Rathburn) were used throughout the work, and the 25 cm × 4 mm I.D. stainless-steel column was identical to that used for SFC, containing the same chiral stationary phase (CSP) (Chiralcel-OD).

3. Experimental procedure

The HPLC conditions for each analyte were chosen initially, working at ambient temperature and using *n*-hexane containing propan-2-ol (IPA). The amount of IPA was determined such that the mean k' of the two enantiomers was between 3.0 and 3.5; it was then kept constant for a given analyte as the temperature was varied. This procedure ensured that although the % IPA differed for the different analytes, their k' values remained very close.

For SFC, since supercritical carbon dioxide resembles *n*-hexane in solvent strength, an appropriate amount of IPA modifier was then sought, starting at 15% and successively reducing it by 1%, until the observed k' values were closely similar to those obtained in HPLC. Since t_m in SFC is less than in HPLC for a comparable flow-rate, the retention times we obtained by SFC are lower than those for HPLC by a factor of ca. 2 (this, one of the main advantages of SFC, has been well documented [6]). The outlet pressure was set at 200 atm (ca. 20 MPa) and the temperature of the SFC column was then varied between 22 and 52°C, without other changes of operating conditions. Subcritical conditions apply below 31°C, but it is not likely that there is any discontinuity of behaviour below the critical value [4].

4. Discussion of results

As can be seen from the chromatograms in Figs. 1 and 2, the HPLC analyses at a series of temperatures in the range 0–42°C show that compounds **2** and **3** behave quite differently. In the case of compound **2**, the selectivity deteriorates somewhat as the temperature is decreased, but this process is accompanied by such a large degree of peak-broadening that baseline resolution is lost below ambient temperature. In con-

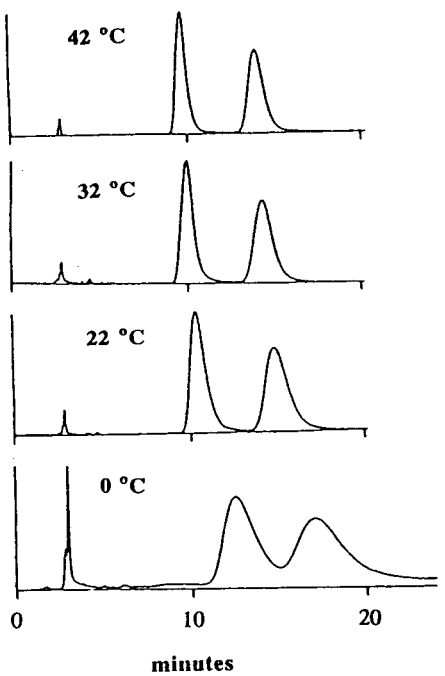

Fig. 1. Chromatograms showing temperature dependence of chiral separation on Chiralcel-OD of compound **2** in HPLC. Mobile phase: *n*-hexane containing 10% IPA.

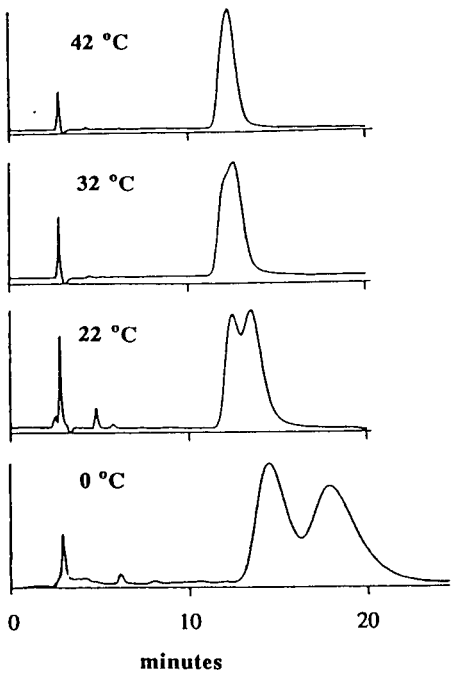

Fig. 2. Chromatograms showing temperature dependence of chiral separation of compound **3** on Chiralcel-OD in HPLC. Mobile phase: *n*-hexane containing 5% IPA.

trast, compound **3** is completely unresolved at the highest temperature used, but approaches a separation factor of 50% at the lowest temperature (0°C). Plots of $\ln(k')$ for both enantiomers of these two compounds (Figs. 3 and 4) explain these observations by showing that compound **2** is well above, whereas compound **3** is at or just below, the temperature at which the two lines intersect.

The temperature at which the enantiomers' $\ln(k')$ vs. $1/T$ lines cross corresponds to the temperature at which the selectivity (α) is 1 (i.e. when $k'_R = k'_S$). This temperature is termed the isoenantioselective temperature (T_{iso}), a parameter of chiral separations well known in gas chromatography as a result of the work of Schurig and co-workers [7–9], but less well documented in HPLC or SFC. Using the $\ln(k')$ vs. $1/T$ plots, or the corresponding graph of $\ln(\alpha)$ vs. $1/T$, we were able to measure, albeit without great precision, not only the isoenantioselective temperatures of compounds **2** and **3** in HPLC on Chiralcel-OD, but also the partial molar excess thermodynamic parameters $\Delta\Delta H^\circ$ and $\Delta\Delta S^\circ$, and hence could determine at any temperature the value of $\Delta\Delta G^\circ$, using the relationships shown below.

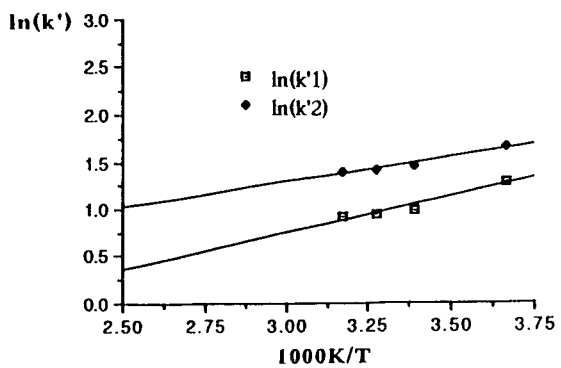

Fig. 3. Plot of $\ln(k')$ vs. $1/T$ for compound **2** in HPLC on Chiralcel-OD.

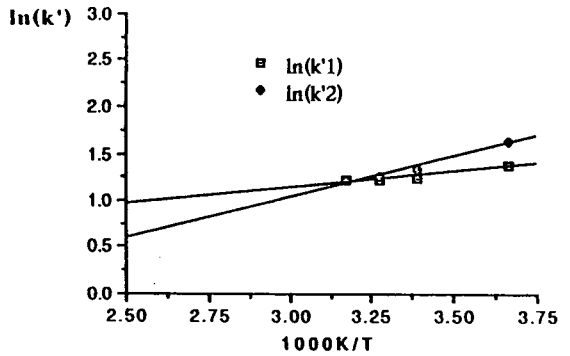

Fig. 4. Plot of $\ln(k')$ vs. $1/T$ for compound **3** in HPLC on Chiralcel-OD.

Since

$$\Delta\Delta G^\circ = \Delta\Delta H^\circ - T\Delta\Delta S^\circ \text{ and } \Delta G^\circ = -RT\ln(K)$$

$$\ln(k')_R = -\Delta H^\circ_R/RT + \Delta S^\circ_R/\mathrm{R} + \ln(\beta) \quad (1)$$

where

$$\beta = \text{phase ratio} = V_s/V_m \text{ and } k' = \beta K$$

$$\ln(k')_S = -\Delta H^\circ_S/RT + \Delta S^\circ_S/R + \ln(\beta) \quad (2)$$

whence

$$\ln(\alpha) = -\Delta\Delta H^\circ/RT + \Delta\Delta S^\circ/R \quad (3)$$

where

$$\Delta\Delta H^\circ = \Delta H^\circ_R - \Delta H^\circ_S$$

and

$$\Delta\Delta S^\circ = \Delta S^\circ_R - \Delta S^\circ_S$$

The resulting values are shown in Table 1, along with the corresponding values of $\Delta\Delta G^\circ$ at the lowest and highest temperatures used (0 and 42°C). Note that the change of sign of $\Delta\Delta H^\circ$ and $\Delta\Delta S^\circ$ between compound **2** and compound **3** can be ignored, since it arises because the value for the more retained isomer is generally given preference over the less retained isomer when calculating selectivity α. Since compound **2** is above, and compound **3** below, its isoenantioselective temperature, and there has necessarily been an invertion of elution order as the T_{iso} temperature is passed, this change of sign can be ignored.

The most striking feature of this data is the very large difference (127°C) between their respective T_{iso} values. This temperature, at which $\Delta\Delta H^\circ = T\Delta\Delta S^\circ$, is reached more quickly, on heating from absolute zero, for compound **2** than for compound **3**, because its $\Delta\Delta H^\circ$ is much smaller (1929 J mol^{-1}) than for compound **3** (4265 J mol^{-1}); their $\Delta\Delta S^\circ$ values (10.3 and 13.6 J mol^{-1} K^{-1}) are not so different. Enthalpy changes in this context arise mainly due to heats of adsorption during retention, and as a consequence of partial bonding to the selector, since for two enantiomers solvation enthalpies must be identical. They determine the slopes of the enantiomers' $\ln(k')$ vs. $1/T$ graphs. When two enantiomers reveal large $\Delta\Delta H^\circ$ values (which may be considered as very temperature dependent differences in their ΔH° values), one possible conclusion is that hydrogen bonding, a very temperature dependent phenomenon, is involved in their chiral discrimination. In the case of compound **3**, which has an ex-ring alkylamide function, this is understandable, since chiral discrimination must reflect to some extent the degree to which the enantiomers form or disrupt hydrogen bonds while retained in the CSP. In the case of compound **2**, chiral recognition may depend critically upon the additional arene com-

Table 1
Thermodynamic parameters for compounds **2** and **3** on Chiralcel-OD in HPLC

Compound	$\Delta\Delta H^\circ$ (J mol^{-1})	$\Delta\Delta S^\circ$ (J mol^{-1} K^{-1})	$\Delta\Delta G^\circ_0$ (J mol^{-1})	$\Delta\Delta G^\circ_{42}$ (J mol^{-1})	T_{iso} (°C)
2	1929	10.3	−883	−1316	−86
3	−4265	−13.6	−552	19	41

ponent, and H-bonding may be less important than $\pi-\pi$ interactions which are, evidently, less temperature dependent.

An important objective of this research was the comparison of chiral SFC separations of the same analytes on the same CSP, to see if the factors in their chiral recognition were affected by the change of solvent system and phase. As the chromatograms (Figs. 5 and 6), $\ln(k')$ vs. $1/T$ graphs (Figs. 7 and 8) and tabulated data (Table 2) clearly show, the results are strikingly similar. Compound **2** is again better resolved at higher temperature, and compound **3** at lower temperature, because compound **2** is above, and compound **3** at or below, its T_{iso} value. Both compounds are, as expected, eluted more rapidly in SFC under comparable conditions with comparable k' values. This arises, as previously

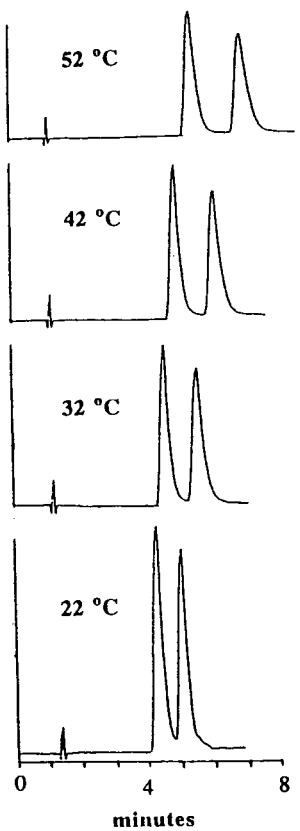

Fig. 5. Chromatograms showing temperature dependence of chiral separation on Chiralcel-OD of compound **2** in SFC. Mobile phase: carbon dioxide containing 12% IPA.

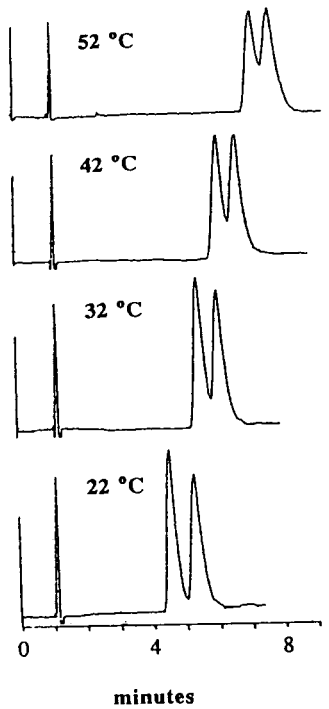

Fig. 6. Chromatograms showing temperature dependence of chiral separation of compound **3** on Chiralcel-OD in SFC. Mobile phase: carbon dioxide containing 7% IPA.

stated, because of the lower value of t_m in SFC, and is a major advantage SFC provides for chiral analyses, which often require long retentions in HPLC.

The effect of temperature on retention in SFC differs from HPLC: at constant column outlet

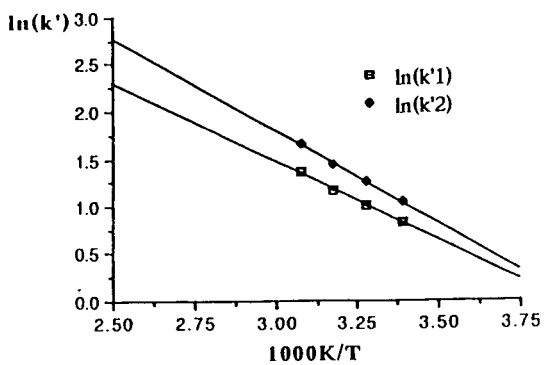

Fig. 7. Plot of $\ln(k')$ vs. $1/T$ for compound **2** in SFC on Chiralcel-OD.

Table 2
Thermodynamic parameters for compounds **2** and **3** on Chiralcel-OD in SFC

Compound	$\Delta\Delta H^\circ$ (J mol^{-1})	$\Delta\Delta S^\circ$ (J mol^{-1} K^{-1})	$\Delta\Delta G^\circ_0$ (J mol^{-1})	$\Delta\Delta G^\circ_{42}$ (J mol^{-1})	T_{iso} (°C)
2	2102	9.0	−544	−813	−39
3	−2654	−7.5	−444	−220	81

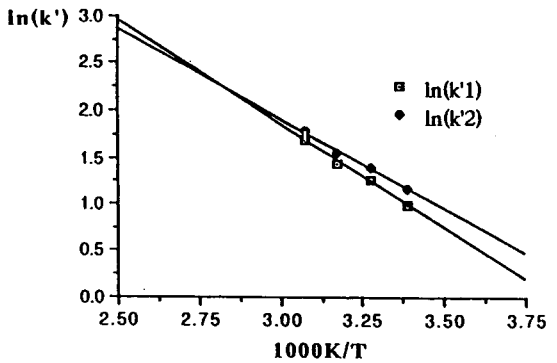

Fig. 8. Plot of $\ln(k')$ vs. $1/T$ for compound **3** in SFC on Chiralcel-OD.

pressure in SFC, increasing temperature makes for a less dense, lower eluent strength, mobile phase. The normal pattern of behaviour in SFC is, therefore, that retention increases initially on heating, but eventually reaches a maximum and then decreases at substantially higher temperatures. In our experiments, at just above ambient temperature, the graphs of $\ln(k')$ vs. $1/T$ have opposite signs of slopes to those observed in HPLC, and do not reach a maximum. The behaviour is similar to HPLC, however, in that there is still a difference of 120°C in their isoenantioselective temperatures, and compound **2** still has the lower value; π–π interactions are still apparently more important than H-bonding, since the discrimination is less temperature dependent and $\Delta\Delta H^\circ$ is much smaller for compound **2**.

In practical terms, since compound **2** is always above its T_{iso} and compound **3** always below its T_{iso}, in our experiments using either HPLC or SFC, the correct use of temperature in the optimization of their chiral resolution is completely different. One should heat the column to improve the enantioselectivity in the case of compound **2** and any racemic mixture which, at the expense of H-bonding factors, involve more π–π interactions. By contrast, one should cool the column to improve the resolution of the enantiomers of compounds such as **3**, which are, we presume, more dependent upon H-bonding.

Acknowledgements

We gratefully acknowledge the financial assistance provided by SmithKline Beecham Pharmaceuticals for the purchase of SFC instrumentation, and also by SERC (for a CASE studentship for S.M.W.).

References

[1] W.H. Pirkle, *J. Chromatogr.*, 558 (1991) 1–6.
[2] D.T. Witte, J-P. Franke, F.J. Bruggeman, D.D. Dijkstra and R.A. De Zeeuw, *Chirality*, 4 (1992) 389–394.
[3] E. Papadopoulou-Mourkidou, *Anal. Chem.*, 61 (1989) 1149–1151.
[4] P. Macaudiere, M. Caude, R. Rosset and A. Tambute, *J. Chromatog. Science.*, 27 (1989) 583–591.
[5] V.A. Ashwood, R.E. Buckingham, F. Cassidy, J.M. Evans, E.A. Faruk, T.C. Hamilton, D.J. Nash, G. Stemp and K. Willcocks, *J. Med. Chem.*, 29 (1986), 2194–2201.
[6] M.L. Lee and K.E. Markides, *Analytical Supercritical Fluid Chromatography and Extraction*, Chromatography Conferences Inc., Provo, UT, 1990.
[7] V. Schurig and R. Link, in D. Stevenson and I.D. Wilson (Editors), *Chiral Separations*, Plenum Press, New York, 1988, pp. 91–114.
[8] V. Schurig, J. Ossig and R. Link, *Angew. Chem. Int. Ed.*, 289 (1989) 194–196.
[9] V. Schurig and M. Jung, in D. Stevenson and I.D. Wilson (Editors), *Recent Advances in Chiral Separations*, Plenum Press, New York, 1990.

ELSEVIER

Journal of Chromatography A, 697 (1995) 597–601

JOURNAL OF CHROMATOGRAPHY A

High-performance thin-layer chromatographic method to determine sorption of propofol to infusion containers

H. Salomies[a,*], P. Lautala[a], M. Toppila[b]

[a]*Department of Pharmacy, Pharmaceutical Chemistry Division, P.O. Box 15, University of Helsinki, FIN-00014 Helsinki, Finland*

[b]*Orion-Farmos Pharmaceuticals, FIN-90650 Oulu, Finland*

Abstract

A stability-indicating HPTLC method developed for the determination of propofol was used to monitor the effect of different infusion containers on the stability of propofol in 5% glucose. According to the results, the new polypropylene-lined bags and glass bottles can safely be used for administration of propofol by i.v. infusion, but polyvinyl chloride bags are not recommended.

1. Introduction

Propofol (2,6-diisopropylphenol) is an intravenous anesthetic agent used for the induction and maintenance of anesthesia during surgical procedures. The drug is only slightly soluble in water and is used as an oil in water emulsion. In addition to propofol, the formulation contains soybean oil, glycerol and egg lecithin, with sodium hydroxide added to adjust the pH. Anesthesia can be maintained by intermittent administration of propofol or by continuous infusion of the drug after it has been diluted, with 5% glucose for example, to a concentration of not less than 2 mg/ml. The sorptive loss of propofol to poly(vinyl chloride) (PVC) plastic materials during i.v. administration has been demonstrated earlier [1].

Existing methods to assay propofol include high-performance liquid chromatographic (HPLC) determination using direct UV [2–4], fluorimetric [5] or electrometric detection [6], or UV detection after precolumn derivatization with Gibb's reagent [7]. Second-derivative UV spectroscopy [4] and gas chromatography [8] have also been used to assay propofol.

The object of the study was to evaluate the stability of propofol in new polypropylene-lined infusion bags (Softbags) and, in comparison, in glass bottles and PVC bags. For the purpose, a simple, rapid and stability-indicating high-performance thin-layer chromatographic (HPTLC) method was developed to determine the concentrations of propofol in samples. To test the reliability of the method, measurements were also made with a modification of the HPLC method described by Bailey et al. [1,4].

2. Experimental

2.1. Materials

Propofol was kindly supplied by ICI Pharma (Helsinki, Finland). The identity and purity of

* Corresponding author.

0021-9673/95/$09.50
SSDI 0021-9673(94)00946-5

the substance were verified by TLC and HPLC, and by UV and IR spectrometry. Diprivan (ICI Pharma, lots C1065A and C1049A), Glucosteril 50 mg/ml, 100-ml glass bottle (Medipolar, Orion-Farmos Pharmaceuticals, lot SHL20AA), Glucos 50 mg/ml, 100-ml PVC bag (Baxter, lots 92D22G52 and 9229G50) and Glucosteril 50 mg/ml, 100-ml Softbag (Medipolar) were kindly supplied by Orion-Farmos Pharmaceuticals, Medipolar. All reagents were of analytical grade and methanol for HPLC was of HPLC grade.

2.2. Chromatographic instrumentation and conditions

The HPTLC assay was developed using glass plates (10×20 cm HPTLC plates 60 F_{254}; Merck, Darmstadt, Germany) and a horizontal chamber (Camag, Muttenz, Switzerland). Before use, the plates were washed with methanol to ensure a sufficiently low background for the photometric measurements. Plates were air-dried at room temperature and used immediately. Solutions were applied at opposite ends of the plates by the Linomat spray-on technique (Linomat IV, Camag). Toluene was used for plate development and the development distance was 40 mm.

Photometric measurements were performed in the absorbance/reflectance mode with a Camag TLC scanner connected to a computer running CATS version 3.14 software. The reflection absorption spectrum of propofol was scanned in situ and wavelength 276 nm was chosen for quantitation.

Stock solution containing 25 mg/ml of propofol was prepared in methanol. For calibration, either different volumes (1–5 μl) of the standard solution (2 mg/ml), or identical volumes (4 μl) of different concentrations (0.25–2.5 mg/ml) diluted from the stock solution, were applied as bands (length 4 mm, distance apart 6 mm) to the plates. The chromatography was performed as described above. The calibration curve was constructed by plotting peak height against the concentration of propofol, using Michaelis–Menten regression 1.

2.3. Validation of the HPTLC method

To validate our HPTLC method, we determined the retention factor (R_F) of propofol, the asymmetry factor (A_s) of the peak and the resolution (R_s) in the Diprivan sample solutions (propofol versus excipients and propofol versus eluent front). The specificity of the method for quantifying propofol in the presence of excipients in Diprivan was studied by comparing the in situ spectra of propofol in standard solution and in Diprivan sample solution, in the wavelength range 190–440 nm.

Repeatability of the sample application was studied by applying the standard solution (2 mg/ml) in amounts of 1, 3 and 5 μl six times each, as 5 mm bands. Diprivan (10 mg/ml propofol) was diluted with 5% glucose solution to 1.0, 1.5 and 2.0 mg/ml and each solution was applied six times in the amount of 4 μl, as 4 mm bands.

Repeatability of the total method was studied by diluting six samples of 1.0 ml, six samples of 1.5 ml, and six samples of 2.0 ml Diprivan to 10.0 ml with 5% glucose solution, and applying to HPTLC plates 4 μl of each sample, in duplicate, as 4 mm bands.

The accuracy of the method was studied by using duplicate samples with theoretical contents of 1.0, 1.5 and 2.0 mg/ml of propofol. Two bands were applied from each solution to HPTLC plate.

Stability of propofol on the sorbent was studied before and after development. Duplicate application of 3 μl of standard solution (2 mg/ml) was made to the same plate 120, 60, 45, 30, 15 and 2 min before development. During this time the plate was stored on a laboratory bench without protection from light. The plate was then developed and the heights of the chromatographic peaks of propofol were immediately compared. In studies on the stability after development of the plate, the heights of two standards, applied 2 min before development were measured immediately after drying the plate, and after 0.5, 2, 4 and 24 h. Between measurements the plate was stored, protected from light, at room temperature.

The stability-indicating nature of the HPTLC

assay was tested with solutions containing intact propofol and propofol that had been degraded in four different ways: in 2 *M* hydrochloric acid or 2 *M* sodium hydroxide at 85°C for 48 h, in 5% glucose while exposed to a high-pressure mercury lamp (original Hanau TQ 150) for 1 h, or in 5% glucose while exposed to daylight on a sunny window sill for two weeks. Samples (4 μl) were studied on the plate.

2.4. HPLC method

The HPLC analyses were performed with an instrument consisting of an LKB 2150 pump, LKB 2151 variable-wavelength monitor (LKB, Bromma, Sweden), D-2000 chromato-integrator (Hitachi, Tokyo, Japan) and a 20-μl loop injector. Propofol was chromatographed on a phenyl column (Novapak, 15 × 0.39 cm, 5 μm). The mobile phase was an isocratic mixture of methanol–30 m*M* ammonium dihydrogenphosphate (30:70, v/v) and the flow-rate was 0.95 ml/min. Propofol was monitored at a wavelength of 276 nm.

A five-point calibration curve was prepared for the range 25–125 μg/ml of propofol, and under the conditions described above propofol eluted from the column at 3.5 min. The other components of the emulsion eluted with the solvent. The calibration curve was linear with a correlation coefficient of 0.9997 ($n = 6$).

2.5. Preparation of admixtures and samples

A 20-ml volume of fluid was withdrawn from each of three 100-ml glass bottles, PVC bags and Softbag bags containing 5% glucose infusion, and replaced by 20 ml of Diprivan solution, producing a nominal concentration of 2 mg propofol/ml. After mixing by gentle agitation, solutions were stored at room temperature (21 ± 2°C), one bottle or bag of each triplicate without protection from light, and two with protection. During the study, the glass containers were kept upright to minimize contact between drugs and the rubber stoppers. The plastic containers were hung from their support ring.

At 0, 1, 2, 4, 6 and 24 h, the admixtures of propofol were visually inspected for clarity and color change; accurately measured samples of 2 ml were then transferred from the infusion bottles and bags. The pH of the solution was measured (at 0 and 24 h) in samples of 5.0 ml (PHM 83 Autocal pH meter; Radiometer, Copenhagen, Denmark). The amount of propofol was determined by HPTLC and, for comparison, by a previously described and validated HPLC method with UV detection [1,4]. Sample pretreatment was unnecessary in the case of HPTLC whereas samples for HPLC had to be filtered before injection.

3. Results and discussion

Among the many mobile phases tested, toluene proved to be the eluent of choice for the HPTLC assay. The R_F value of propofol was 0.7 and propofol could be separated both from its degradation products and from the excipients in Diprivan (Fig. 1). The application of standards in methanol and samples in aqueous emulsions caused some difficulty: the bands of standards were narrow, whereas those of samples dried slowly and were broadened in all directions. Different solutions to the problem were investigated, among others solid-phase extraction, but the best results were obtained when the sample solutions were applied as 4 mm bands and the standards as 5 mm bands.

Baseline resolution ($R_s = 2.44$) was achieved between the peaks of propofol and excipients, and the asymmetric factor of the propofol peak

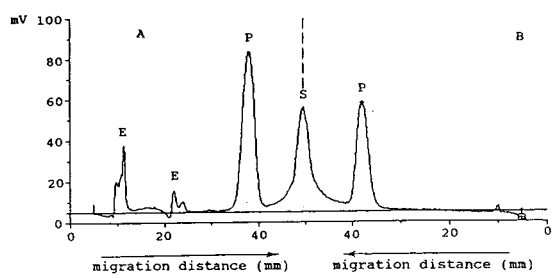

Fig. 1. A scan from the plate developed horizontally from the opposite ends. (A) Scan of diprivan, (B) scan of propofol standard. E = Excipients; P = propofol; S = solvent front.

Table 1
Repeatability of the application according to the heights of the chromatographic peaks of propofol ($n = 6$)

Solution studied	Amount applied (μl)	R.S.D. ($\pm$ %)
Standard 2.0 mg/ml	2	1.68
Standard 2.0 mg/ml	6	1.77
Standard 2.0 mg/ml	10	1.20
Sample 1.0 mg/ml	4	1.11
Sample 1.5 mg/ml	4	1.52
Sample 2.0 mg/ml	4	0.82

was 1.33. When the in situ spectra of propofol in standard solution and in Diprivan sample solution were superimposed, the spectra were seen to be identical, with a correlation factor of 0.9980. It was concluded that the excipients in Diprivan do not interfere with the measurement of propofol. The resolution between propofol and the solvent front was 0.96.

The calibration curve used in the quantitation of propofol was Michaelis–Menten regression 1 [$y = 129.04x/(6.068 + x)$]. Because of the better standard deviation of the calibration curve, different volumes of the standard solution were applied to the plate rather than identical volumes of different concentrations diluted from the stock solution (standard deviation $< \pm 2$ and $< \pm 4$, respectively). The repeatability of the application is presented in Table 1, which shows the relative standard deviation (R.S.D.) values to be less than 3%, the limit value recommended in the literature [9]. R.S.D.s measuring the repeatability of the whole method were 1.5, 1.8 and 1.8% for samples of concentration 1.0, 1.5 and 2.0 mg/ml, respectively. The accuracy of the method was good enough to monitor the sorption of propofol to different infusion containers. The mean value was 99.56% of the true value of propofol, and the R.S.D. was 2.9%. Propofol proved to be stable after application to the HPTLC plate, for at least 120 min before development, and for at least 24 h after development and before densitometric measurement.

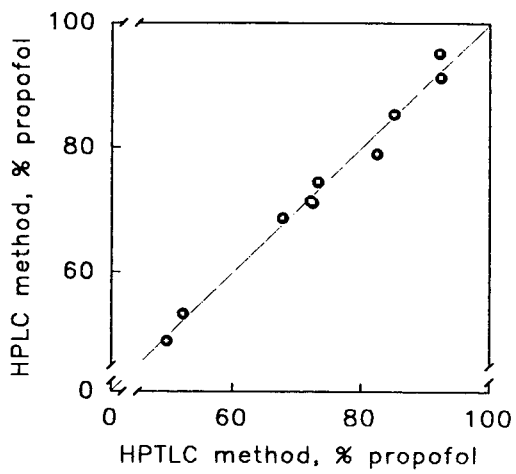

Fig. 2. Results for propofol assayed by HPTLC and by HPLC (slope 0.9962).

The reliability of our results obtained by HPTLC assay was checked by comparison with a published HPLC method. No significant difference was found in the results (Fig. 2). A paired t-test was carried out on the results obtained by the two methods, and the accuracy of the HPTLC method was found acceptable at a confidence level of 95%.

There was no decrease in the concentration of propofol in 5% glucose infusion when stored in glass or new polypropylene-lined Softbag containers for 24 h (Fig. 3). In a recent sorption study, Softbag containers also were shown to be safe for diazepam, nitroglycerine and warfarin sodium [10]. The concentration of propofol rapidly decreased in the PVC containers, however, being about 53% at 24 h (Fig. 3). This value was consistent with the results of a recent report on a static study which at 120 min a 31.54–34.74% loss of propofol had occurred to the plasticized PVC i.v. administration set [1].

The pH values of infusion solutions at 0 and 24 h were 7.2 in glass bottles and Softbag containers, whereas in PVC bags pH 5.1 was measured at 0 and pH 4.9 at 24 h. At no time was there notable discoloration or visual precipitation of sample solution. There was no sign of extra peaks in the chromatograms, confirming that the loss of propofol was caused by an absorptive process rather than degradation.

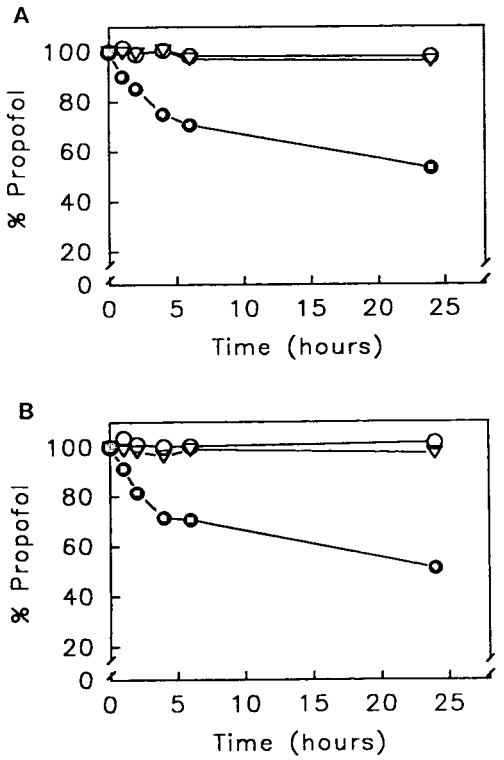

Fig. 3. Concentration of propofol, as a function of time, in glass bottles (○) and in Softbag (▽) and PVC (●) infusion bags. Values expressed as means of six measurements. (A) HPTLC; (B) HPLC.

4. Conclusions

The HPTLC method proved to be reliable and suitable for determining propofol and monitoring its sorption to infusion containers. The advantages of the developed assay over the HPLC method are: sample pretreatment is unnecessary, toluene alone forms the mobile phase which is needed only few milliliters, and the method is rapid because numerous samples can be measured on the same plate simultaneously. According to the results, the new polypropylene-lined containers (Softbags) can safely be used clinically for the administration of propofol in 0.5% glucose by intravenous infusion. Admixtures do not loose their potency when stored at room temperature with or without protection from light for 24 h.

References

[1] L.C. Bailey, K.T. Tang and B.A. Rogozinski, *Am. J. Hosp. Pharm.*, 48 (1991) 2627.
[2] T.B. Vree, A.M. Baars and P.M.R.M. de Grood, *J. Chromatogr.*, 417 (1987) 458.
[3] I. Pavan, E. Buglione, M. Massiccio, C. Gregoretti, L. Burbi and M. Berardino, *J. Chromatogr. Sci.*, 30 (1992) 164.
[4] L.C. Bailey, K.T. Tang and B.A. Rogozinski, *J. Pharm. Biomed. Anal.*, 9 (1991) 501.
[5] G.F. Plummer, *J. Chromatogr.*, 421 (1987) 171.
[6] G. Mazzi and M. Schinella, *J. Chromatogr.*, 528 (1990) 537.
[7] H.K. Adam, E.J. Douglas, G.F. Plummer and M.B. Cosgrove, *J. Chromatogr.*, 223 (1981) 232.
[8] H.-Y. Yu and J.-K. Liau, *J. Chromatogr.*, 615 (1993) 77.
[9] K. Ferenczi-Fodor, Z. Végh and Z. Pap-Sziklay, *J. Planar Chromatogr.*, 6 (1993) 198.
[10] H. Salomies, R. Heinonen and M. Toppila, *Int. J. Pharm.*, 110 (1994) 197.

Author Index

Analytical Applications of Circular Dichroism

Edited by **N. Purdie** and **H.G. Brittain**

Techniques and Instrumentation in Analytical Chemistry Volume 14

Circular dichroism is a special technique which provides unique information on dissymmetric molecules. Such compounds are becoming increasingly important in a wide variety of fields, such as natural products chemistry, pharmaceutics, molecular biology, etc. The content of this book has been selected in order to feature the unique aspects of circular dichroism, and how these strengths can be of assistance to workers in the field.

Substantial discussions have been provided regarding the particular phenomena associated with dissymmetric compounds which give rise to the circular dichroism effect. Reviews are also given of the type of instrumentation available for the measurement of these effects. A number of chapters cover the wide range of applications illustrating the power of the method.

Owing to its broad appeal, the book will be of interest to workers in all areas of chemistry and pharmaceutical science.

Contents:

© 1994 360 pages Hardbound
Price: Dfl. 355.00 (US $ 202.75)
ISBN 0-444-89508-6

ORDER INFORMATION

For USA and Canada
ELSEVIER SCIENCE INC.
P.O. Box 945
Madison Square Station
New York, NY 10160-0757
Fax: (212) 633 3880

In all other countries
ELSEVIER SCIENCE B.V.
P.O. Box 330
1000 AH Amsterdam
The Netherlands
Fax: (+31-20) 5862 845

US$ prices are valid only for the USA & Canada and are subject to exchange rate fluctuations; in all other countries the Dutch guilder price (Dfl.) is definitive. Customers in the European Community should add the appropriate VAT rate applicable in their country to the price(s). Books are sent postfree if prepaid.

ELSEVIER SCIENCE B.V.

Trace Element Analysis in Biological Specimens

Edited by **R.F.M. Herber** and **M. Stoeppler**

Techniques and Instrumentation in Analytical Chemistry Volume 15

The major theme of this book is analytical approaches to trace metal and speciation analysis in biological specimens. The emphasis is on the reliable determination of a number of toxicologically and environmentally important metals. It is essentially a handbook based on the practical experience of each individual author. The scope ranges from sampling and sample preparation to the application of various modern and well-documented methods, including quality assessment and control and statistical treatment of data. Practical advice on avoiding sample contamination is included.

In the first part, the reader is offered an introduction into the basic principles and methods, starting with sampling, sample storage and sample treatment, with the emphasis on sample decomposition. This is followed by a description of the potential of atomic absorption spectrometry, atomic emission spectrometry, voltammetry, neutron activation analysis, isotope dilution analysis, and the possibilities for metal speciation in biological specimens. Quality control and all approaches to achieve reliable data are treated in chapters about interlaboratory and intralaboratory surveys and reference methods, reference materials and statistics and data evaluation.

The chapters of the second part provide detailed information on the analysis of thirteen trace metals in the most important biological specimens. The following metals are treated in great detail: Aluminium, arsenic, cadmium, chromium, copper, lead, selenium, manganese, nickel, mercury, thallium, vanadium and zinc.

The book will serve as a valuable aid for practical analysis in biomedical laboratories and for researchers involved with trace metal and species analysis in clinical, biochemical and environmental research.

Contents: Part 1. Basic Principles and Methods.
1. Sampling and sample storage (A. Aitio, J. Järvisalo, M. Stoeppler). 2. Sample treatment of human biological materials (B. Sansoni, V.K. Panday). 3. Graphite furnace AAS (W. Slavin). 4. Atomic absorption spectrometry. Flame AAS (W. Slavin). 5. Atomic emission spectrometry (P. Schramel). 6. Voltammetry (J. Wang). 7. Neutron activation analysis (J. Versieck). 8. Isotope dilution mass spectrometry (IDMS) (P. de Bièvre). 9. The chemical speciation of trace elements in biomedical specimens: Analytical techniques (P.H.E. Gardiner, H.T. Delves). 10. Interlaboratory and intralaboratory surveys. Reference methods and reference materials (R.A. Braithwaite). 11. Reference materials for trace element analysis (R.M. Parr, M. Stoeppler). 12. Statistics and data evaluation (R.F.M. Herber, H.J.A. Sallé).

Part 2. Elements. 13. Aluminium (J. Savory, R.L. Bertholf, S. Brown, M.R. Wills). 14. Arsenic (M. Stoeppler, M. Vahter). 15. Cadmium (R.F.M. Herber). 16. Chromium (R. Cornelis). 17. Copper (H.T. Delves, M. Stoeppler). 18. Lead (U. Ewers, M. Turfeld, E. Jermann). 19. Manganese (D.J. Halls). 20. Mercury (A. Schütz, G. Skarping, S. Skerfving). 21. Nickel (D. Templeton). 22. Selenium (Y. Thomassen, S.A. Lewis, C. Veillon). 23. Thallium (M. Sager). 24. Vanadium (K.-H. Schaller). 25. Zinc (G.S. Fell, T.D.B. Lyon). Subject index.

©1994 590 pages Hardbound
Price: Dfl. 475.00 (US$ 279.50)
ISBN 0-444-89867-0

ELSEVIER
An imprint of Elsevier Science

ORDER INFORMATION

ELSEVIER SCIENCE B.V.
P.O. Box 330
1000 AH Amsterdam
The Netherlands
Fax: +31 (20) 485 2845

For USA and Canada:
P.O. Box 945
New York, NY 10159-0945
Fax: +1 (212) 633 3680

US$ prices are valid only for the USA & Canada and are subject to exchange rate fluctuations; in all other countries the Dutch guilder price (Dfl.) is definitive. Customers in the European Union should add the appropriate VAT rate applicable in their country to the price(s). Books are sent postfree if prepaid.

PUBLICATION SCHEDULE FOR THE 1995 SUBSCRIPTION

Journal of Chromatography A and *Journal of Chromatography B: Biomedical Applications*

MONTH	1994	J	F	M	A	M[a]	J	
Journal of Chromatography A	Vols. 683–688	689/1 689/2 690/1 690/2	691/1 + 2 692/1 + 2 693/1 693/2	694/1 694/2 695/1 695/2	696/1 696/2 697/1 + 2 698/1 + 2	699/1 + 2 700/1 + 2 702/1 + 2 703/1 + 2	704/1 704/2 705/1 705/2	The publication schedule for further issues will be published later.
Bibliography Section				713/1			713/2	
Journal of Chromatography B: Biomedical Applications		663/1 663/2	664/1 664/2	665/1 665/2	666/1 666/2	667/1 667/2	668/1 668/2	

[a] Vol. 701 (Cumulative Indexes Vols. 652–700) expected in October.

INFORMATION FOR AUTHORS

(Detailed *Instructions to Authors* were published in *J. Chromatogr. A*, Vol. 657, pp. 463–469. A free reprint can be obtained by application to the publisher, Elsevier Science B.V., P.O. Box 330, 1000 AH Amsterdam, Netherlands.)

Types of Contributions. The following types of papers are published: Regular research papers (full-length papers), Review articles, Short Communications and Discussions. Short Communications are usually descriptions of short investigations, or they can report minor technical improvements of previously published procedures; they reflect the same quality of research as full-length papers, but should preferably not exceed five printed pages. Discussions (one or two pages) should explain, amplify, correct or otherwise comment substantively upon an article recently published in the journal. For Review articles, see inside front cover under Submission of Papers.

Submission. Every paper must be accompanied by a letter from the senior author, stating that he/she is submitting the paper for publication in the *Journal of Chromatography A* or *B*.

Manuscripts. Manuscripts should be typed in **double spacing** on consecutively numbered pages of uniform size. The manuscript should be preceded by a sheet of manuscript paper carrying the title of the paper and the name and full postal address of the person to whom the proofs are to be sent. As a rule, papers should be divided into sections, headed by a caption (*e.g.*, Abstract, Introduction, Experimental, Results, Discussion, etc.). All illustrations, photographs, tables, etc., should be on separate sheets.

Abstract. All articles should have an abstract of 50–100 words which clearly and briefly indicates what is new, different and significant. No references should be given.

Introduction. Every paper must have a concise introduction mentioning what has been done before on the topic described, and stating clearly what is new in the paper now submitted.

Experimental conditions should preferably be given on a *separate* sheet, headed "Conditions". These conditions will, if appropriate, be printed in a block, directly following the heading "Experimental".

Illustrations. The figures should be submitted in a form suitable for reproduction, drawn in Indian ink on drawing or tracing paper. Each illustration should have a caption, all the *captions* being typed (with double spacing) together on a *separate sheet*. If structures are given in the text, the original drawings should be provided. Coloured illustrations are reproduced at the author's expense, the cost being determined by the number of pages and by the number of colours needed. The written permission of the author and publisher must be obtained for the use of any figure already published. Its source must be indicated in the legend.

References. References should be numbered in the order in which they are cited in the text, and listed in numerical sequence on a separate sheet at the end of the article. Please check a recent issue for the layout of the reference list. Abbreviations for the titles of journals should follow the system used by *Chemical Abstracts*. Articles not yet published should be given as "in press" (journal should be specified), "submitted for publication" (journal should be specified), "in preparation" or "personal communication".

Vols. 1–651 of the *Journal of Chromatography*; *Journal of Chromatography, Biomedical Applications* and *Journal of Chromatography, Symposium Volumes* should be cited as *J. Chromatogr.* From Vol. 652 on, *Journal of Chromatography A* (incl. Symposium Volumes) should be cited as *J. Chromatogr. A* and *Journal of Chromatography B: Biomedical Applications* as *J. Chromatogr. B.*

Dispatch. Before sending the manuscript to the Editor please check that the envelope contains four copies of the paper complete with references, captions and figures. One of the sets of figures must be the originals suitable for direct reproduction. Please also ensure that permission to publish has been obtained from your institute.

Proofs. One set of proofs will be sent to the author to be carefully checked for printer's errors. Corrections must be restricted to instances in which the proof is at variance with the manuscript.

Reprints. Fifty reprints will be supplied free of charge. Additional reprints can be ordered by the authors. An order form containing price quotations will be sent to the authors together with the proofs of their article.

Chiral HPLC Column

Application Guide for Chiral HPLC Column Selection

SECOND EDITION!

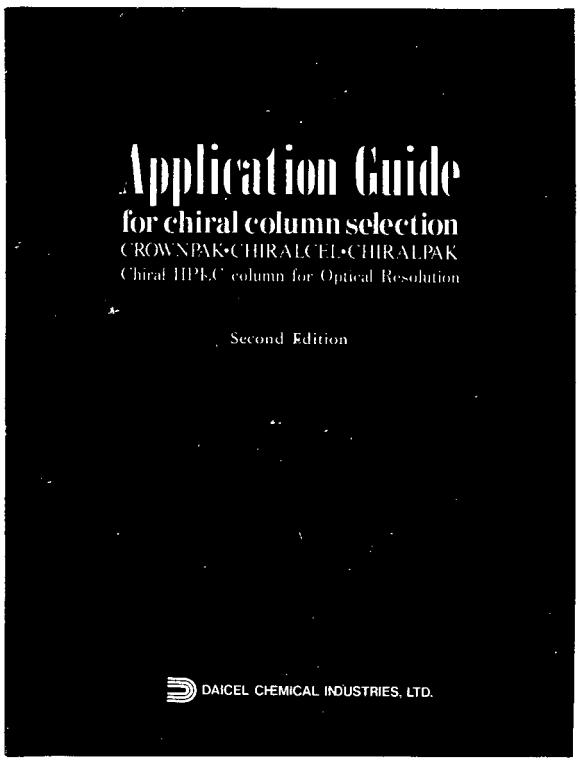

FREE OF CHARGE

The 112-page green book contains chromatographic resolutions of over 350 chiral separations, cross-indexed by chemical compound class, structure, and the type of chiral column respectively. This book also lists chromatographic data together with analytical conditions and structural information. A quick reference guide for column selection from a wide range of DAICEL chiral HPLC columns is included.

To request this book, please let us know by fax or mail.

DAICEL CHEMICAL INDUSTRIES, LTD.

AMERICA

CHIRAL TECHNOLOGIES, INC.

730 Springdale Drive, P.O. Box 564
Exton, PA 19341
Phone: 800-624-4725
Facsimile: 610-594-2325

EUROPE

DAICEL (EUROPA) GmbH

Oststr. 22
D-40211 Düsseldorf, Germany
Phone: +49-211-369848
Facsimile: +49-211-364429

ASIA/OCEANIA

DAICEL CHEMICAL INDUSTRIES, LTD.
CHIRAL CHEMICALS NDD
8-1, Kasumigaseki 3-chome,
Chiyoda-ku, Tokyo 100, JAPAN
Phone: +81-3-3507-3151
Facsimile: +81-3-3507-3193

484 a